

INTERNATIONAL CONFERENCE ON RESEARCH IN EDUCATION & SCIENCE

 **ICRES2018**

April 28 - May 1, 2018

Marmaris/TURKEY

PROCEEDING BOOK

EDITORS

PROF. DR. MACK SHELLEY
PROF. DR. MEHMET OZASLAN
DR. WENXIA WU

Volume II



<http://www.icres.net>

INTERNATIONAL CONFERENCE ON RESEARCH IN EDUCATION & SCIENCE

ICRES2018

April 28 - May 1, 2018

Marmaris/TURKEY

PROCEEDING BOOK

EDITORS

PROF. DR. MACK SHELLEY
PROF. DR. MEHMET OZASLAN
DR. WENXIA WU



www.ijemst.com



www.ijres.net



www.jeseh.net



<http://www.icres.net>

INTERNATIONAL CONFERENCE ON RESEARCH IN EDUCATION & SCIENCE

Editors: Mack Shelley, Mehmet Ozaslan, Wenxia Wu

This book was typeset in 10/12 pt. Times New Roman, Italic, Bold and Bold Italic.

Copyright © by ISRES Publishing.

All rights reserved. No part of this book may be reproduced in any form, by photostat, microfilm, retrieval system, or any other means, without prior written permission of the publisher.

International Conference on Research in Education and Science (ICRES) Published by ISRES Publishing, International Society for Research in Education and Science (ISRES).

Includes bibliographical references and index.

ISBN : 978-605-67951-8-3

Date of Issue: October 01, 2018

Address: Prof. Dr. Mack Shelley, Iowa State University, 509 Ross Hall,
Ames, IA 50011-1204, U.S.A.

E-mail: isresoffice@gmail.com

www.isres.org



<http://www.icres.net>

INTERNATIONAL CONFERENCE ON RESEARCH IN EDUCATION & SCIENCE

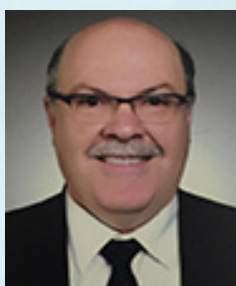
Keynote Speakers



Dr. David Treagust

Curtin University

"The Importance of Multiple Representations for Teaching and Learning Science"



Dr. Mustafa Hilmi Colakoglu

Republic of Turkey Ministry of National Education

"Smart Schools and STEM Education"



Dr. Amy Hutchison

George Mason University

"Digital Possibilities in STEM Education"



INTERNATIONAL CONFERENCE ON RESEARCH IN EDUCATION & SCIENCE

Panels

Panel I: Inquiry-based Learning: International Perspectives

Moderator

Dr. Hakan Akcay

Panelists

Dr. David Treagust, Dr. Ayse Oguz Unver, Dr. Irina Lyublinskaya
(Australia) (Turkey) (Russia)

Panel II: STEM Reasoning and Learning

Moderator

Dr. Hakan Akcay

Panelists

Dr. Amy C. Hutchison, Dr. Mustafa Colakoglu, Dr. Kathy Malone
(U.S.A.) (Turkey) (Kazakhstan)

Panel III: A Teacher and Explainer Professional Development Model to Increase the Effectiveness of Science Centers in Science and Society Communication and Science Education

Moderator

Dr. Mustafa Colakoglu

Panelists

*Dr. Fitnat Köseoğlu, Dr. Uygur Kanlı, Dr. Semra Mirici, Dr. Yasemin Özdem Yılmaz,
Dr. Ceyhan İpekçioğlu, Dr. Alev Çetin*
(Turkey)



INTERNATIONAL CONFERENCE ON RESEARCH IN EDUCATION & SCIENCE

Workshops

Workshop I: The Importance of 21st Skills and Industry 4.0 in STEM Education

Dr. Sahin Idin

Scientix STEM Education Ambassador (Turkey)

Workshop Description: In the Workshop, it is going to be mentioned the relationship between 21st skills and Industry 4.0 in STEM Education. It will also be emphasized 21st skills and their importance for both STEM Education and Industry 4.0. Participants will be able to learn some significant points and the relationship between STEM Education and Industry 4.0 via some real exams within the scope of STEM Education.

Workshop II: STEM Education Applications with 3-D Printers

*Dr. S. Ahmet Kiray, Mustafa Tevfik Hebebcı, Ersah Akgul
(Turkey)*

Workshop Description: In the Workshop, STEM Education Applications will be shown with 3-D printers.

Workshop III: Playing with Mathematics in the Classroom

*Dr. Cara D. Williams
(United Arab Emirates)*

Workshop Description: Tired of assessing students with worksheets in the math classroom? Then this workshop is for you! Participants will participate in demonstrations of how to make math classrooms more student-centered. Differentiating instruction by learning styles will be addressed for various grade levels. The workshop will be engaging, practical, and applicable for all K-12 math teachers.



INTERNATIONAL CONFERENCE ON RESEARCH IN EDUCATION & SCIENCE

Public Talks

The Public Talk: Sexuality Knowledge of University Students



Plenary Speaker: Dr. Sinan Erten

Participating Countries



INDEX

Preparation and Characterization of Biocomposite Polylactic Acid/Coconut Fibre <i>Leong KOK SENG</i>	1
Preparation and Characterization of Solid Polymer Electrolyte Based on Carboxymethyl Chitosan, Ammonia Nitrate and Ethylene Carbonate <i>Leong KOK SENG</i>	10
The Preparation of Controlled Release Fertilizer Based on Gelatin Hydrogel Including Ammonium Nitrate and Investigation of its Influence on Vegetable Growth <i>Mehlika PULAT</i>	17
Preparation of Sodium Carboxymethyl Cellulose Hydrogels for Controlled Release of Copper Micronutrient <i>Gulen Oytun AKALIN</i>	25
Antagonistic of some Trichoderma against Fusarium Oxysporum sp. f. cubense Tropical Race 4 (FocTR4) <i>Laith Khalil Tawfeeq AL-ANI</i>	35
New Fused Heterocyclic Compounds: Synthesis of Some 1,4-di[1,2,4-Triazoles[3,4-b]5-phenyl/aryl-1,3,4-thiadiazole] Benzene <i>Mohanad Yakdhan SALEH</i>	39
Theoretical Investigation of Spectroscopic and Thermodynamic Properties of 1-Acetyl-3-methyl-4-[3-(3-methoxybenzoyloxy)benzylideneamino]-4,5-dihydro-1H-1,2,4-triazol-5-one by 6-311G(d) and 3-21G HF/DFT(B3LYP) Methods <i>Hilal MEDETALIBEYOGLU</i>	49
Antioxidant and Antimicrobial Activities of Some Newly Synthesized 4-[1-(2,6-Dimethylmorpholin-4-yl-methyl)-3-alkyl(aryl)-4,5-dihydro-1H-1,2,4-triazol-5-on-4-yl-azomethine]-2-methoxyphenyl benzoates <i>Yonca YILMAZ</i>	72
Study of the Physical and Structural Properties of Some Local Mineral Clays and Effect of Doping with Chromium Oxide <i>Regab A. BUKER</i>	81
Experimental Investigation of the Time Effect of Pressure Fluctuations in Steady Turbulent Pipe Flows <i>Hasan DUZ</i>	90
Numerical Investigation of the Transition Length at the Entrance Region of Pipe Flows <i>Ahmet Beyzade DEMIRPOLAT</i>	101
Organization of Practical-Research Works with "Black Box" Method <i>Nurgul SHUYUSHBAYEVA</i>	111
Influence of Inclined Bed Channel on Characteristic of Flow for Step Broad-Crested Weirs <i>Saleh Jaafar SULEIMAN</i>	118
Investigation of Biological Properties of New 1-(2,6-Dimethylmorpholin-4-yl-metil)-3-alkyl(aryl)-4-[3-ethoxy-(4-benzenesulfonyloxy)-benzylideneamino]-4,5-dihydro-1H-1,2,4-triazol-5-ones <i>Gul OZDEMIR</i>	128
Synthesis and Antioxidant Activities of Some Novel 1-(Morpholine-4-yl-methyl)-3-alkyl(aryl)-4-(3-methoxy-4-isobutyryloxy)benzylideneamino-4,5-dihydro-1H-1,2,4-triazol-5-ones <i>Sevda MANAP</i>	135
Synthesis and Potentiometric Titrations of 3-Alkyl(Aryl)-4-[3-ethoxy-4-(4-methoxybenzenesulfonyloxy)-benzylideneamino]-4,5-dihydro-1H-1,2,4-triazol-5-ones <i>Ozlem AKTAS YOKUS</i>	143

Study of Some Biochemical Parameters and Fatty Acids Composition in Blood Serum of Women with Polycystic Ovary Syndrome	
<i>Abd-Alkream H.ISMAIL</i>	151
Urea Containing Coated Cu and Zn: A Suitable Fertilizer for Healthier Growth of Rice and N-Uptake	
<i>Saima Kalsoom BABAR</i>	159
Dormancy Breaking Studies of Dodder (<i>Cuscuta</i> spp.) was Problem in Greenhouse Tomato	
<i>Tamer USTUNER</i>	167
Investigation of a New Post Emergence Herbicide, Diquat Dipromide 200 g/l Against to Weeds in Peach Orchards in Black Sea Region	
<i>Ummet DIRI</i>	179
Compact Wideband Lowpass Filter Based on Inverted Cascading Stubs	
<i>Emad S. AHMED</i>	186
The Preliminary Results for Atmospheric Parameters of the Candidate Ap Stars HD 90763 and HD 92728	
<i>Asli ELMASLI</i>	192
Synthesis and Characterization of Osmium (III) Complexes with Substituted Nitrones	
<i>Khalaf I. KHALLOW</i>	196
Effects of Light on Egg Performance and Behaviour in Japanese Quails (<i>coturnix coturnix japonica</i>)	
<i>Gokce Irem DEMIRCI DEMIRBAS</i>	201
Modeling Clustered Scale-free Networks by Applying Various Preferential Attachment Patterns	
<i>Gokhan KUTLUANA</i>	209
Optimization the Combined Heat and Power Economic Dispatch problem using Harmony Search Algorithm	
<i>Fatima Zohra BENAYED</i>	216
Voice Controlled Home Automation Design	
<i>Ahmet VATANSEVER</i>	225
A Comparison of the Performance of Classification Methods and Artificial Neural Networks for Electricity Load Forecasting	
<i>Gurkan TUNA</i>	233
Molecular Investigation of Metallo- β -lactamase Encoding Gene in Nosocomial Carbapenem-Resistant Enterobacteriaceae in Iraqi Hospitals	
<i>Ahmed S. K. AL-KHAFAJI</i>	239
Olive Pomace and Cherry Stones used as Biofuels	
<i>Andreja MARZI</i>	244
Determination of Morphology and Allergenic Proteins of Pistachio (<i>Pistachia vera L.</i>) Pollens in Gaziantep	
<i>Gulay KASOGLU</i>	250
Molecular Characterization of Yogurt Bacteria Isolated from Beans and Lentils	
<i>Mesut CAY</i>	254
Manifestation of Ankylosing Spondylitis and Crohn`s Disease	
<i>Olena SULIMA</i>	259
Treatment of Arthritis with Ulcerative Colitis	
<i>Volodymyr SULYMA</i>	262
Cytotoxic Activity Against Cancer Cells of <i>Pistacia vera</i>	
<i>Basak SIMITCIOGLU</i>	265

Determination of Potential Allergenic Proteins and Morphogenic Proteins and Morphology of Linden (<i>Tilia cordata</i>), Anatolian oak (<i>Quercus ithaburensis</i>) and Birch (<i>Betula alba</i>) Pollens in Gaziantep	
<i>Ozlem ONMAN</i>	270
Detection of Eczema DISEASE by using Image Processing	
<i>Yasir Salam Abdulghafoor AL-KHAFAJI</i>	273
Central Automorphism Groups for Semidirect Product of p-Groups	
<i>Ozge OZTEKIN</i>	288
Synthesis of Some Novel 3-Alkyl(Aryl)-4-[3-(2-furylcarbonyloxy)-4-methoxy-benzylidenamino]-4,5-dihydro-1H-1,2,4-triazol-5-one Compounds	
<i>Onur AKYILDIRIM</i>	290
Gaussian Calculations of 3-(p-Chlorobenzyl)-4-(3,4-Dihydroxybenzylidenamino)-4,5-Dihydro-1H-1,2,4-Triazol-5-One and N-Acetyl Derivative using B3lyp and HF Basis Sets	
<i>Gul KOTAN</i>	295
Supplier Selection with Quality Function Deployment	
<i>Bahar OZYORUK</i>	307
Adsorption of Heavy Metals using Banana Peels in Wastewater Treatment	
<i>Leong KOK SENG</i>	312
UDC 662.33 Experimental Determination of the Sulfur Content in the Shubarkol Coal	
<i>Tateyeva A.B.</i>	318
Numerical Flow Analysis of The Variation of Central Axial Velocity Along The Pipe Inlet	
<i>Hasan DUZ</i>	323
Fuzzy Approaches to the Risk Assesment Methods for the Occupational Health and Safety	
<i>Murat GULBAY</i>	334
Possible Problems in the Introduction in Ukraine of Medical Reform and the Practice of a Family Medicine Doctor	
<i>Volodymyr SULYMA</i>	338
First Results Surgical Treatment of Patients with Chronic anal Fissure Through Electric Welding of Biological Tissue	
<i>Volodymyr SULYMA</i>	342
A Design of Hybrid Expert System for Diagnosis of Breast Cancer and Liver Disorder	
<i>Aysegul ALAYBEYOGLU</i>	345
Investigation the Performance of Stream Water Wheel Turbines using CFD Techniques	
<i>Mohammad A. AL-DABBAGH</i>	354
Evaluation of Flow behavior over Broad-Crested Weirs of a Triangular Cross-Section using CFD Techniques	
<i>Sulaiman D. AL-ZUBAIDY</i>	361
Determination of the Morphological Characteristics of Scandaroon Pigeon Grown in the Central of Hatay Province (<i>Columba livia domestica</i>)	
<i>Hakan YILDIRIM</i>	368
A Critical Review of Major Nature-Inspired Optimization Algorithms	
<i>Julius Beneoluchi ODILI</i>	376
Implementation Strategies for the Cuckoo Search and the African Buffalo Optimization for the Benchmark Rosenbrock Function	
<i>Radzi AMBAR</i>	395

Notes to the Question of Presenting the Theme of Special Solutions of Ordinary Differential Equations in a University Course	
<i>Irina ANDREEVA</i>	403
A Literature Survey on Green Supplier Selection	
<i>Bahar OZYORUK</i>	407
Development of A Diagnostic Expert System (FDD-Expert) for Woven Fabric Defects	
<i>Berkay BARIS</i>	412
Lean Innovation Approach in Industry 5.0	
<i>Banu OZKESER</i>	422
Extraction of Heavy Metals using Dithizone Method on Seawater	
<i>Leong KOK SENG</i>	429
On the Solution of the Generalized Symmetric Woods-Saxon Potential in the Dirac Equation	
<i>Bekir Can LUTFUOGLU</i>	435
Investigation Methods for a Family of Cubic Dynamic Systems	
<i>Irina ANDREEVA</i>	439
Importance of Smart Energy Management Algorithm in Renewable Energy Sources Integrated Energy Storage Unit	
<i>Yagmur KIRCICEK</i>	447
A Reliability Test Track Assessment of a Light Commercial Vehicle by Index Method	
<i>Arif Senol SENER</i>	454
Analysis of Thinning Zones and Pres Parameters of A Car Exhaust to be Produced by Deep Drawing of Sheet Metal	
<i>Erdal OZTURK</i>	464
Artistic Reflections of Urban Wastes in Contemporary Turkish Pictures	
<i>Ayşe ŞAHİN ÖZTÜRK, Ömer Tayfur ÖZTÜRK</i>	47272
Interpainting As A Creating Method in Digital Illustration: Reinterpretations from Movie Scenes	
<i>Erdinç ÇAKIR, Mahmut Sami ÖZTÜRK, Mevlüt ÜNAL, Mehmet SUSUZ</i>	47878
Presence of Semiotics in The Current Curricula of Institutions Providing Art Education	
<i>Mehmet SUSUZ, Mahmut Sami ÖZTÜRK, Mine Ülkü ÖZTÜRK</i>	487
Graphic Designer Profile and Professional Competence Analysis	
<i>Mustafa KINIK, Mahmut Sami ÖZTÜRK</i>	493
Researching of Using Konya Ladik Red Clay as A Raku Glaze. International Conference on Research In Education and Science	
<i>Azize Melek ÖNDER, Mine Ülkü ÖZTÜRK</i>	49999
Contributions of Archaeological Site Findings to Art Education and Art Practices	
<i>Mine Ülkü ÖZTÜRK</i>	506
Existing Aesthetic Problems Based on The Restorations of Stone Works of The Ancient Period in The Side Museum	
<i>Ömer Tayfur ÖZTÜRK</i>	512

Preparation and Characterization of Biocomposite Polylactic Acid/Coconut Fibre

Leong KOK SENG

Polytechnic Tun Syed Nasir Syed Ismail

Abstract: In this research, biocomposite was prepared by using coconut fiber as filler and polylactic acid (PLA) as matrix. Coconut fiber undergo three different treatments which are sodium hydroxide, bleaching and maleic anhydride. Biocomposite was produced by varied composition of coconut fiber into 2%, 4% and 6% to be added into PLA. Characterization of coconut fiber was carried out by using infrared spectroscopy analysis (FTIR) analysis in order to study the changes in functional groups and degree of crystallinity of coconut fiber after treatment. Characterization of the biocomposite produced was carried out by using mechanical test to study the mechanical properties of biocomposites. Based on the results from FTIR analysis, certain functional group in original coconut fibre structure disappeared after chemical treatment. XRD analysis also showed that bleached coconut fibre has the highest crystallinity. Overall, the result from tensile test showed that maximum load and the modulus Young of biocomposite increase with increase composition of coconut fiber until an optimum point which is at 2% coconut fiber. While elongation at break decreased with increasing composition of coconut fiber.

Keywords: Biocomposite, Tensile

Introduction

The petrochemicals derived from synthetic polymers cause environmental pollution because of its biological disintegration. It is not only cost-effective, but it also poses a waste problem. This has prompted researchers to find solutions to address this problem. Composite is a material that results from mixing two or more materials (fillers or reinforcing elements with a matrix compatible) to form a specific character or characteristic. In the composites, fibers and matrices will maintain their physical and chemical properties in order to produce a combination of unreachable properties if only one component exists (Alemdar & Sain 2008). Fiber-reinforced composite polymers are produced when the fibers are mixed into a polymer matrix. The matrix will act as a binder to hold fibers, transfer the burden imposed on fibers, and protect against damage (Agarwal Bhagawan 1980). Fiber is generally a load bearing part, where the matrix around it maintains the fiber in a particular location and orientation. Biocomposites are defined as composites that incorporate the original fibers so like sisal, jut and kenaf with the same polymer where there is biodegradable or non-biodegradable. The biocomposite is composed of a matrix which may undergo the process of biodegradation and the original fibers act as a filler or a reinforcing agent. The development of biocomposites rather than the original biodegradable and fiber polymers has been of interest in the field of composite science because biocomposites justify the perfect decomposition in the soil by not releasing any harmful or toxic components (Lee & Wang 2006). Biocomposites that use biodegradable polymers are reinforced with the original gentian which help to reduce the surrounding natural problems and solve the problem of non-fixed petroleum sources. Examples of biopolymers based on the original source are poly (lactic acid) (PLA), plastic starch, cellulose plastic and plastic soya.

Synthetic polymers undergo slow decomposition processes due to the high molecular mass and have hydrophobic properties. In recent years biodegradable polymers with appropriate mechanical and physical properties have been given attention to replace petrochemical-based synthetic polymers (Iovino et al. 2008). Hence renewable and cheaper natural fibers have been introduced to be a substitute for synthetic fibers (Lee & Wang 2006). Synthetic polymers are widely used in daily life because they are easy to process, have constant

- This is an Open Access article distributed under the terms of the Creative Commons Attribution-Noncommercial 4.0 Unported License, permitting all non-commercial use, distribution, and reproduction in any medium, provided the original work is properly cited.

- Selection and peer-review under responsibility of the Organizing Committee of the Conference

stability, low cost and antibacterial properties (Satyanarayana et al. 2009). In this research, both raw materials namely PLA and coconut fiber were used to produce biocomposite materials. PLA provides high mechanical strength and PLA processing method is simple in most devices but its cost is high and fragile properties have limited its application. The best method to handle this problem is the addition of natural fibers that are bioserrated. The advantages of using natural fibers in composites are low cost, good thermal properties and low density. Therefore, the addition of natural fibers into the PLA polymer can reduce the overall cost by not destroying the biodegradation performance of the polymer matrix (Yussuf et al. 2010).

Research Methodology

In the study, all the chemicals and raw materials used for the preparation of the samples are as follows: Coconut fiber is supplied by MTS Fibromat (M) Sdn. Bhd while the PLA (lactic acid) PLA is from E Sun. Acetic acid and solid sodium hydroxide (NaOH) are supplied by System Chem AR. Solid sodium chloride (NaClO_2) used as a bleach is derived from Agros Organics while malic anhydride (MA) is from Merck Schuchardt. In addition, silicon oils supplied by System ChemAR are also used throughout the investigation.

Mitutoyo Measuring Tool

These measures are used to determine the thickness of the cut samples in the form of dumbbell. Measurement of sample thickness was taken on three different parts and the average readings obtained were recorded with ± 0.1

mm error.

Hollow Die Punch

This cutting tool is used to make a dumbbell shape on a 0.3mm thick sheet according to the 6051/000 standard. Mixer Machine

The mixing machines used to provide matrices and composites are the PL 2 / Brabender Plasti-Coder model internal mixer. Measurement parameters such as temperature, rotor speed and time are set beforehand before blending takes

Strength Machine

The strain machine used is a mechanical testing machine (UTM) type Instron Universal model 5567 based on ASTM D 882/91.

Hydraulic Heat Press

The hydraulic heat suppressor used in the preparation of sample sheets is Carver Model 2697. The temperature and time are set before hand before the sample suppression begins.

Results and Discussion

Fourier Transform Infrared Spectroscopy (FTIR)

FTIR analysis is used to perform analysis on coconut fiber without treatment, alkaline treated coconut fiber, coconut fiber treated with bleach and coconut fiber treated MA. FTIR spectroscopy is used to examine any changes in the structure of the cellulose fibers that arise after chemical treatment is performed on the fibers. Identified types of bonds make sure to produce one infrared spectrum absorption. FTIR spectrum of fiber is shown in Figure 1.

There is a peak at about 3200 cm^{-1} to 3500 cm^{-1} on all the four absorption spectra shown. Based on Rout et al. (2001) the peak appearance of 3400 cm^{-1} in the four samples was due to the strain of O-H from hydrogen bonding of cellulose in the fibers. Additionally, from the spectrum shown peak at about 2906 cm^{-1} up to 2920

cm^{-1} are found in all samples. The peak is related to strain and vibrations by group-bonding (-CH₂-) on cellulose and hemicellulose (Lopattananon et al. 2006). In addition there are two peaks around 898 cm^{-1} and 1059 cm^{-1} on all four absorption spectra. Based on Chen et al. (2009) the peak appearance of about 898 cm^{-1} and 1054 cm^{-1} is related to strain on C-O bonds and C-H vibrations within the cellulose structure.

A peak located at about 1734 cm^{-1} which distinguishes coconut fiber without treatment and with treated coconut fiber. Based on Alemdar et al. (2008), the peak at about 1737 cm^{-1} was due to the carbonyl bond. The appearance of this peak on untreated coconut fiber is due to the group of acetyl and ionic ester groups in the hemicellulose or ester chain for the carboxyl group in the lignin or hemicellulose. This peak is lost in treated coconut fiber because most lignin and hemicellulose have been removed. In addition, there is a loss of a peak around 1510-1513 cm^{-1} for the spectrum of coconut fiber treated with bleach, where this peak can distinguish coconut fiber treated with bleach and with other treatments or without treatment. Based on Alemdar et al. (2008) states that the summit around 1507 cm^{-1} is related to aromatic strain C = C for aromatic rings in the lignin. The loss of peak intensity is considered to be due to removal of lignin after coconut fiber is treated with bleach.

From the FTIR spectrum obtained, the extracted malachite extracts of anhydride, there is a unique peak that is absent in the other fiber FTIR spectrum of approximately 1706 cm^{-1} . Based on Chen et al. (2009), the peak of the wavelength range around 1700 cm^{-1} is related to the carbonyl bond (C = O). The peak appearance in the maleic anhydride (MA) treated sample is due to the formation of an ester chain between the MA and the hydroxide group from the fibers and this peak is completely lost in alkali-treated fibers and bleach. In addition, there is a pathway change at the peak of approximately 3700-3000 cm^{-1} on the spectrum that distinguishes the maleic anhydride with the other. The top change in this coconut fiber sample is due to the change in the OH bond ratio between molecules and intramolecules (Cantero et al. 2003).

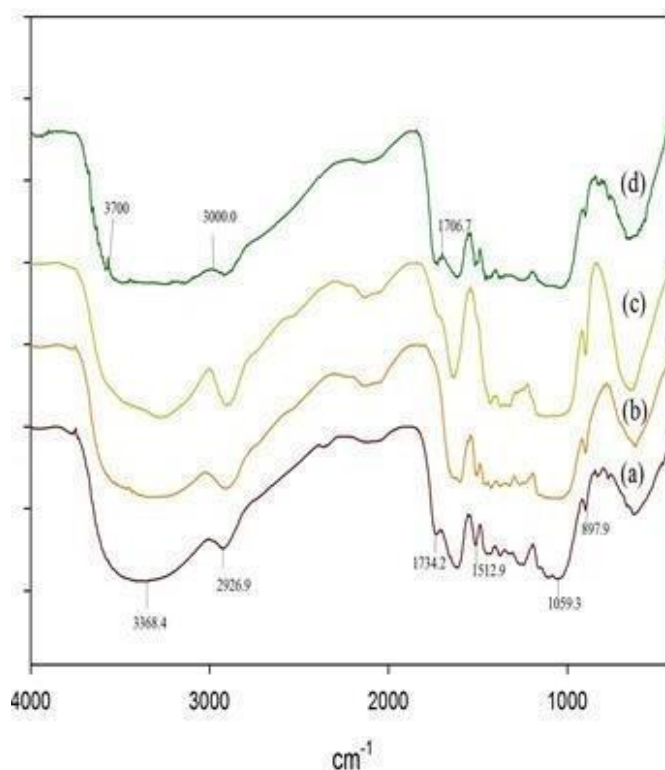


Figure 1 FTIR spectrum for (a) coconut fiber without treatment, (b) alkaline treated coconut fiber, (c) coconut fiber treated with bleach, (c) coconut fiber treated MA

Maximum Stress Test

Maximum stresses for PLA biocomposites enhanced by 0%, 2%, 4%, 6% non-treated coconut fiber, NaOH treated, bleached and treated with MA are presented in Figure 2 and the maximum stress value of each biocomposite is shown in Table 1. From the results obtained, the maximum stress value of biocomposite reinforced by coconut fiber without treatment, treatment with NaOH, treatment with bleach and treatment with

MA is increasing until the optimum value of the 2% composition of coconut fiber and decreased steadily. The good distribution and the interface between the matrix and the fibers are critical factors for determining the mechanical properties of the resulting composites (Arrakhiz et al. 2012). Therefore, the treated coconut fiber has a higher maximum stress than the non-treatment of coconut fiber.

The maximum stress value decreases after the 2% content of the coconut fiber may be due to the addition of the filler which may interfere with the continuity of the polymer matrix. In addition, the decline in stress strength after an optimum level of achievement may also be due to the presence of large filler fibers that result in molding. Thus, the load transfer is not uniform because agglomeration occurs in the matrix (Liu et al. 2009). In addition, the increased composition of coconut fiber will increase the exposure of the interface area and weaken the interaction between the matrix and the filler. This resulted in a decrease in stress strength (Haque et al. 2009).

Based on the maximum stress value of the coconut fiber without treatment is 28.1 MPa while the maximum stress value of coconut fiber with NaOH treatment is 32.1 MPa. The increase in coconut fiber without treatment with NaOH treated coconut fiber was 4.0 MPa at 14%. This explanation is supported by Gu (2009) that compressive stress strength reinforced by alkaline treated coconut fiber increased after alkaline treatment was performed. This is because most fats, lignins and pectin covering the surface of the fibers will be removed and enhanced the interface bonding between the matrix and the filler. Alkaline treatment also reduces the diameter of the fibers and increases the aspect ratio and thereby enhances the mechanical properties of the composite (Mohanty et al. 2000).

In addition, from the results, the maximum stress value for treated fibers treated with bleach is higher than the maximum stress value of the untreated coconut fiber. The maximum stress value for the unmanaged coconut fiber is 28.1 MPa while the maximum stress value for the coconut fiber treated with bleach is 34.2 MPa. The increase in coconut fiber without treatment and with coconut fiber with bleach treatment was 6.1 MPa of 22%. Rosa et al. (2009) states that coconut fiber treated with bleach will produce a smooth surface by removing the wax coating and increasing the interaction between the matrix and filler based on the mechanic test. In addition, the removal of hemicellulose and lignin in natural fibers during treatment with bleach will result in good interaction between the matrix and the enhanced fiber (Mustata et al. 2012).

In addition, the maximum stress value of MA treatment treated with MA is higher than the maximum stress value of the untreated coconut fiber. From the maximum stress value of the unmanaged coconut fiber is 28.1 MPa while the maximum stress value for MA treated coconut fiber is 34.8 MPa. The increase in coconut fiber without treatment with coconut fiber with MA treatment was 6.7 MPa at 24%. Natural fiber treatment with MA will show the better mechanical properties is due to the reduction of wetting process by the formation of covalent bonds between MA molecules and fibers (Avella et al. 1995).

Table 1. Maximum stress value against the composition of coconut fiber

Composition of coconut fibre (%)	Maximum stress (MPa)			
	Without treatment	Treatment alkaline	Treatment bleach	Treatment MA
0	26.1	26.1	26.1	26.1
2	28.1	32.1	34.2	34.8
4	26.8	28.4	30.0	34.4
6	24.5	25.6	26.5	30.7

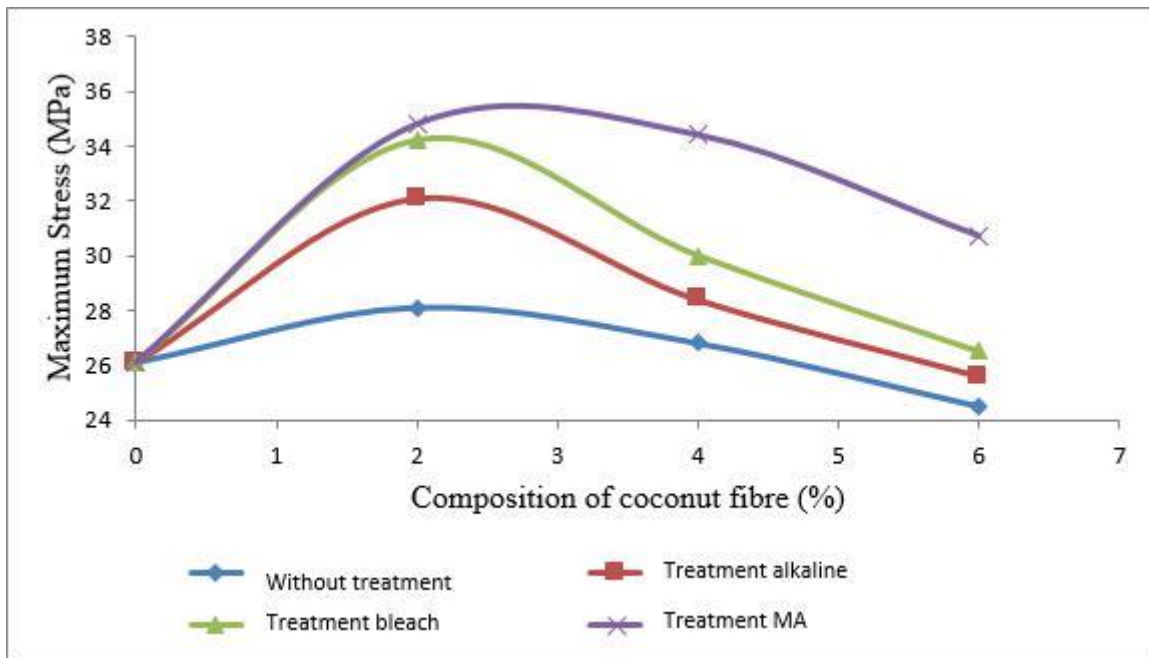


Figure 2 Maximum stress value against the composition of coconut fiber

Young Modulus

Young Modulus of PLA biocomposites enhanced by 0%, 2%, 4%, 6% non-treatment of treated, preserved NaOH coconut fiber, treated bleach and treated with MA is shown in Figure 3 and the results of Young modulus values for each biocomposite are shown in Table 2. From the results obtained, the value of Young's modulus of biocomposite reinforced by coconut fiber without treatment, treatment with NaOH, treatment with bleach and treatment with MA is increasing until the optimum value of the 2% composition of coconut fiber and decreased steadily. It is believed that the enhancement of filler content is aimed at enhancing the properties of rigidity and material stiffness (Ishak Ahmad & Abdullah 2009) and the high filler content is the cause of decreased composite mechanical properties caused by agglomeration process (Pickering et al. 2003)

Unprocessed coconut fiber has a lower Young modulus than the Young modulus value of NaOH treated coconut fiber. From the results of Young's modulus values of non-treatment of coconut fiber is 2278.7 MPa while Young's modulus value of coconut fiber with NaOH treatment is 2320.9 MPa. The increase in coconut fiber without treatment with coconut fiber with NaOH treatment was 42.2 MPa which was 1.85%. The increase in Young modulus of alkaline treated coconut fiber is due to the removal of non-cellulose components on the surface of the fibers. Removal of non-cellulose components will reduce the density of the fibers and the rigidity of the interfibrillar area and then make the microfibrillar better able to rearrange the structure. Therefore, when a strain test is carried out a better load transfer is available (Arrakhiz et al. 2012). In addition, Mohanty et al. (2000) states that alkaline treatment will increase the interaction between the matrix and the filler due to the removal of natural impurities, thus affecting the natural fibers mechanical treatment and increasing the value of the modulus of the resulting composite sample.

Unprocessed coconut fiber has a lower Young modulus than the Young modulus value of treated bleached fibers. From the results of Young's modulus values of non-treatment of coconut fiber is 2278.7 MPa while the Young modulus value of treated bleached coconut fiber is 2346.6MPa. The increase in coconut fiber without treatment with coconut fiber with bleach treatment was 47.9 MPa, which was 3.0%. The increase in Young modulus values after bleaching is due to the removal of hemicellulose, lignin and pectin will enhance the mechanical properties of the composites and reinforce the properties of composite voltages. MA treatment of coconut fiber has a higher Young modulus than the Young Modulus value without treatment. From the results of Young's modulus value of non-treatment of coconut fiber is 2278.7 MPa while the Young modulus value of MA treated coconut fiber is 2390.0 MPa. The increase in coconut fiber without treatment with coconut fiber with MA treatment was 111.3 MPa which was 4.9%. Natural fiber treatment with MA has increased the wetness with the matrix and enhances the mechanical properties of the composite (Ma 2009).

Table 2. Young modulus values against the composition of coconut fiber

Composition of coconut fibre (%)	Young Modulus (MPa)			
	Without treatment	Treatment NaOH	Treatment bleach	Treatment MA
0	2107.5	2107.5	2107.5	2107.5
2	2278.7	2320.9	2346.6	2390.0
4	2250.3	2312.0	2326.4	2330.2
6	2164.9	2216.6	2231.0	2220.3

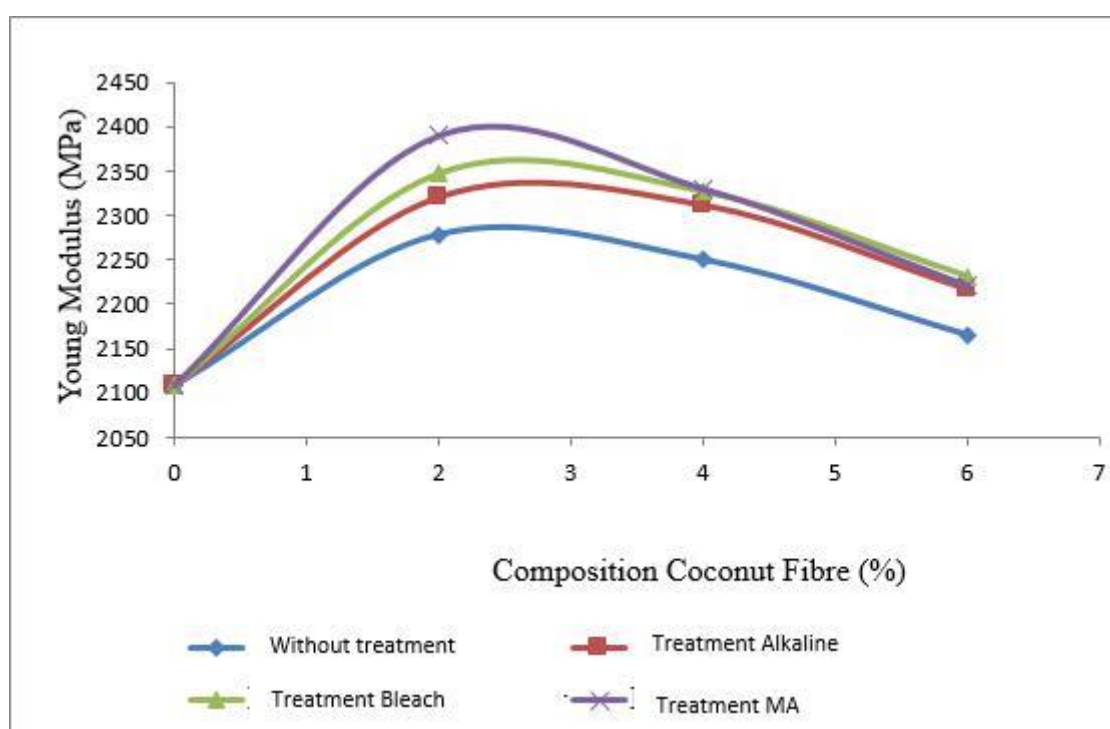


Figure 3. Young modulus values against the composition of coconut fiber

Strain on Backpoint

Strong strain of PLA biocomposites strengthened by 0%, 2%, 4%, 6% on non-treatment of treated, treated NaOH, treated with bleaching and MA treatment are shown in Figure 4 and the result of strain value at break point for each biocomposites are shown in Table 3. From the results obtained, the strain value at break point for biocomposite reinforced by coconut fiber without treatment, treatment with NaOH, bleach treatment and treatment with MA was reduced by the addition of the percentage of coconut fiber. Increased composition of filler will cause composite to become more rigid and hard. This has indirectly reduced the composite resistance and caused resistance to break down to become lower (Ismail et al. 2001). Based on Liu et al. (2009), The addition of fibers will result in a weak bond between the fibers and the biodegradation polymer and causes the formation of microcorrelation between the phases, resulting in a faster crack than the pure biodegradation polymer film.

The strain value at the breaking point of coconut fiber treated by chemical treatments has decreased. Decreased strain value is also due to uneven fiber agglomeration. Uneven fiber spread can cause some areas to have fibers only. Thus, the only fiber having the simpler micro-fracture and the only matrix will be weak (Din 2007).

K.Mohanty et al. (2005) states that alkaline treatment will reduce the diameter of the fibers and increase the aspect ratio thus improving the mechanical properties of the composites. The stiffness increase for natural fibers is due to crystallization (cellulose fibers). Overall, from Figure 4, the strain value at the breaking point of the non-treatable PLA-enhanced PLA biocomposites was the lowest and the treated MA with strain values at the highest breaking point. This is a chemical treatment solution that will increase the strain at the breaking point of the fiber. The strain on the breaking point of the unharmed fibers is low due to the three-dimensional cross-linking of cellulose and lignin. Chemical treatment will break the network structure and increase the strain at the breaking point (Kalia et al. 2009).

Coconut fiber treated with bleach has a strain value at dropping point which decreases overall. The decline in strain values at the breaking point is probably due to the agglomeration and the nonheterogenic size of the fiber in biocomposites (Averous & Boquillon 2004)

Coconut fiber treated with MA indicates inconsistent decline. From the graphs obtained, the strain value at the breaking point is increased to an optimum point of 2% of the coconut fiber treated with MA. However, the strain value at the breaking point is high, this can be explained by the treatment of the bonding of fibers that will cause the fibers to be more hydrophobic because the MA will react with the hydroxide group in the cellulose molecule and cause the hydrogen bond to break down and produce a strong bond between the cellulose molecule and the MA. Therefore, good attachment between matrix and filler can be produced (Mohanty et al. 2000).

Table 3. Strain value at the breaking point against the composition of the coconut fiber

Composition of coconut fibre (%)	Strain at break point(MPa)			
	Without treatment	Treatment alkaline	Treatment bleach	Treatment MA
0	2.6	2.6	2.6	2.6
2	2.3	2.4	2.5	3.1
4	2.2	2.3	2.3	3.7
6	2.1	2.0	2.1	2.5

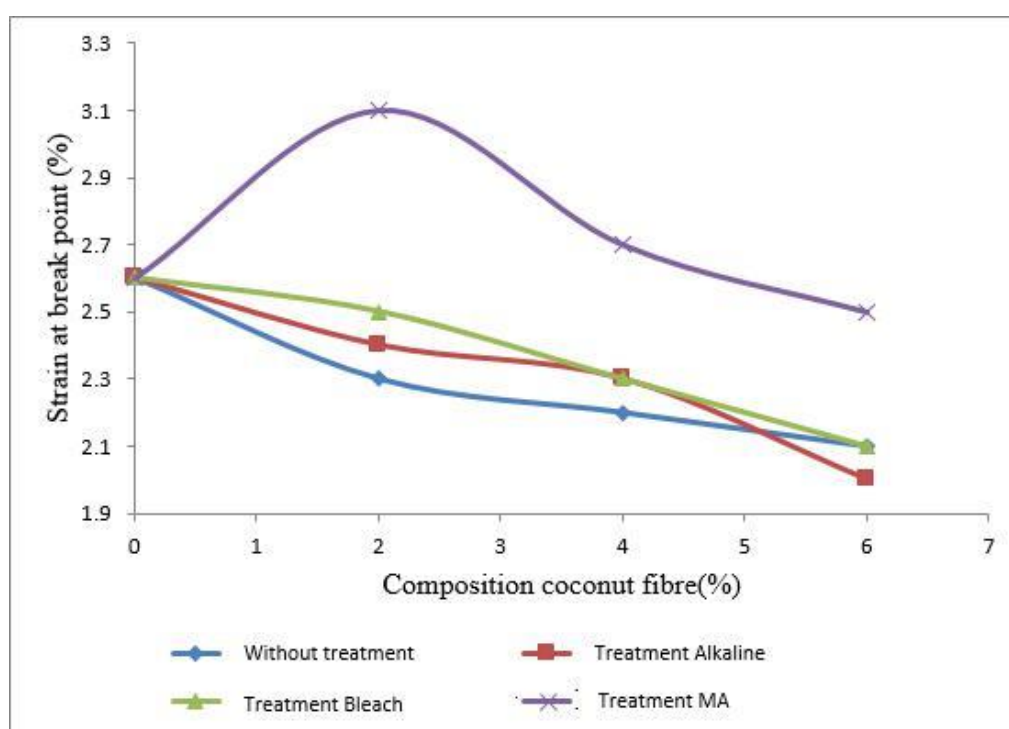


Figure 4. Strain value at the breaking point against the composition of the coconut fiber

Conclusion

This study was carried out for the preparation and characterization of poly-based biocomposites (lactic acid) which is reinforced by coconut fiber. Coconut fiber is treated with three types of treatments NaOH alkaline treatment, bleaching and anhydride treatment. The treatment composition of coconut fiber without treatment with certain treatment was varied to 2%, 4% and 6% to be added to the poly (lactic acid) matrix to produce biocomposites. FTIR infrared spectroscopy analysis was performed to characterize coconut fiber without treatment with certain treatments. Whereas the biocomposites produced will perform mechanical properties tests.

Overall, tensile tests, FTIR and morphological tests give a good result that the addition of coconut fiber fillers can improve the mechanical properties of biocomposites. In addition, chemical treatments carried out by coconut fiber will also increase the interaction between matrix with filler and improve mechanical properties of biocomposite.

FTIR analysis has been used to carry out analysis on coconut fiber without treatment, coconut fiber treated by NaOH, bleaching agents and MA. FTIR analysis is used to detect functional groups from Fourier Transform infrared spectrum records based on visible wave value. Through the analysis, increased cellulose content and removal of hemicellulose and lignin contents can be observed after alkaline treatment and bleaching process is carried out. Certain treatments will provide the removal of certain substances and provide changes in the structure of coconut fiber after chemical treatment.

The strain test results are to show the effectiveness of load transfer from matrix to fiber. The tensile test has three parameters discussed in the stress test, Young modulus and strain at break point. Overall, coconut fiber which treats with chemistry has the highest stress and modulus value as compared to the treatment without coconut fiber. This is because chemical treatments have removed lignin, hemicellulose and other foreign substances, increasing the coconut fiber bonding properties with the PLA matrix. Whereas the strain at the breaking point of the PLA-enhanced, non-treatment of biodegradable PLA showed a decline by the addition of coconut fiber composition.

References

- Agarwal Bhagawan, D. B. L. 1980. Analysis and preparation of fiber composites Ed.: Wiley-Interscience Publication.
- Alemdar, A. & Sain, M. 2008. Biocomposites from wheat straw nanofibers: Morphology, thermal and mechanical properties. *Composites Science and Technology* 68(2): 557-565.
- Arrakhiz, F. Z., El Achaby, M., Kakou, A. C., Vaudreuil, S., Benmoussa, K., Bouhfid, R., Fassi-Fehri, O. & Qaiss, A. 2012. Mechanical properties of high density polyethylene reinforced with chemically modified coir fibers: Impact of chemical treatments. *Materials & Design* 37(0): 379-383.
- Avella, M., Bozzi, C., dell'Erba, R., Focher, B., Marzetti, A. & Martuscelli, E. 1995. Steam-exploded wheat straw fibers as reinforcing material for polypropylene-based composites. Characterization and properties. *Die Angewandte Makromolekulare Chemie* 233(1): 149-166.
- Averous, L. & Boquillon, N. 2004. Biocomposites based on plasticized starch: thermal and mechanical behaviours. *Carbohydrate Polymers* 56(2): 111-122.
- Cantero, G., Arbelaz, A., Llano-Ponte, R. & Mondragon, I. 2003. Effects of fibre treatment on wettability and mechanical behaviour of flax/polypropylene composites. *Composites Science and Technology* 63(9): 1247-1254.
- Chen, Y., Liu, C., Chang, P. R., Anderson, D. P. & Huneault, M. A. 2009. Pea starch-based composite films with pea hull fibers and pea hull fiber-derived nanowhiskers. *Polymer Engineering & Science* 49(2): 369-378.
- Din, R. H. 2007. Komposit Lignoselulosa-Polimer Ed.: Universiti Sains Malaysia.
- Gu, H. 2009. Tensile behaviours of the coir fibre and related composites after NaOH treatment. *Materials & Design* 30(9): 3931-3934.
- Haque, M. M., Hasan, M., Islam, M. S. & Ali, M. E. 2009. Physico-mechanical properties of chemically treated palm and coir fiber reinforced polypropylene composites. *Bioresource Technology* 100(20): 4903-4906.
- Iovino, R., Zullo, R., Rao, M. A., Cassar, L. & Gianfreda, L. 2008. Biodegradation of poly(lactic acid)/starch/coir biocomposites under controlled composting conditions. *Polymer Degradation and Stability* 93(1): 147-157.

- Ishak Ahmad, M. S. J. & Abdullah, I. 2009. *Rice Husk and Clay Loadings into High Density Polyethylene-Natural Rubber-Liquid Natural Rubber Matrix* 38(3): 381-386.
- Ismail, H., Nizam, J. M. & Abdul Khalil, H. P. S. 2001. The effect of a compatibilizer on the mechanical properties and mass swell of white rice husk ash filled natural rubber/linear low density polyethylene blends. *Polymer Testing* 20(2): 125-133.
- K.Mohanty, A., Misra, M. & T.Drazal, L. 2005. *Natural Fibers, Biopolymer, and Biocomposites* Ed.: Taylor & Francis Group.
- Kalia, S., Kaith, B. S. & Kaur, I. 2009. Pretreatments of natural fibers and their application as reinforcing material in polymer composites—A review. *Polymer Engineering & Science* 49(7): 1253-1272.
- Lee, S.-H. & Wang, S. 2006. Biodegradable polymers/bamboo fiber biocomposite with bio-based coupling agent. *Composites Part A: Applied Science and Manufacturing* 37(1): 80-91.
- Liu, L., Yu, J., Cheng, L. & Qu, W. 2009. Mechanical properties of poly(butylene succinate) (PBS) biocomposites reinforced with surface modified jute fibre. *Composites Part A: Applied Science and Manufacturing* 40(5): 669-674.
- Lopattananon, N., Panawarangkul, K., Sahakaro, K. & Ellis, B. 2006. Performance of pineapple leaf fiber-natural rubber composites: The effect of fiber surface treatments. *Journal of Applied Polymer Science* 102(2): 1974-1984.
- Ma, A. 2009. Impacts of Maleic Anhydride and Sodium Hydroxide on Interfacial Properties of Wheat Straw Low Density Linear Polyethylene(LLDPE).Tesis Department of Chemistry Four Years Thesis Project Course
- Mohanty, A. K., Misra, M. & Hinrichsen, G. 2000. Biofibres, biodegradable polymers and biocomposites: An overview. *Macromolecular Materials and Engineering* 276-277(1): 1-24.
- Mustata, F., Tudorachi, N. & Rosu, D. 2012. Thermal behavior of some organic/inorganic composites based on epoxy resin and calcium carbonate obtained from conch shell of *Rapana thomasiana*. *Composites Part B: Engineering* 43(2): 702-710.
- Pickering, K. L., Abdalla, A., Ji, C., McDonald, A. G. & Franich, R. A. 2003. The effect of silane coupling agents on radiata pine fibre for use in thermoplastic matrix composites. *Composites Part A: Applied Science and Manufacturing* 34(10): 915-926.
- Rosa, M. F., Chiou, B.-s., Medeiros, E. S., Wood, D. F., Williams, T. G., Mattoso, L. H. C., Orts, W. J. & Imam, S. H. 2009. Effect of fiber treatments on tensile and thermal properties of starch/ethylene vinyl alcohol copolymers/coir biocomposites. *Bioresource Technology* 100(21): 5196-5202.
- Rout, J., Tripathy, S. S., Nayak, S. K., Misra, M. & Mohanty, A. K. 2001. Scanning electron microscopy study of chemically modified coir fibers. *Journal of Applied Polymer Science* 79(7): 1169-1177.
- Satyanarayana, K. G., Arizaga, G. G. C. & Wypych, F. 2009. Biodegradable composites based on lignocellulosic fibers—An overview. *Progress in Polymer Science* 34(9): 982-1021.
- Yussuf, A., Massoumi, I. & Hassan, A. 2010. Comparison of Polylactic Acid/Kenaf and Polylactic Acid/Rise Husk Composites: The Influence of the Natural Fibers on the Mechanical, Thermal and Biodegradability Properties. *Journal of Polymers and the Environment* 18(3): 422-429.

Author Information

Leong Kok Seng

Polytechnic Tun Syed Nasir Syed Ismail

Malaysia

Contact: kokseng@ptsn.edu.my

Preparation and Characterization of Solid Polymer Electrolyte Based on Carboxymethyl Chitosan, Ammonia Nitrate and Ethylene Carbonate

Leong KOK SENG

Polytechnic Tun Syed Nasir Syed Ismail

Abstract: Research is conducted that related to the preparation and characterization of solid polymer electrolyte based on carboxymethyl chitosan, ammonia nitrate and ethylene carbonate. The potential of carboxymethyl chitosan as a green polymer electrolyte has been explored. Chitosan is a natural biopolymer which can be obtained from partially deacetylated derivative of chitin. Chitosan react with monochloroacetic acid to form carboxymethyl chitosan. The solid films were prepared by solution casting technique with ammonia nitrate and ethylene carbonate. Characterization of carboxymethyl chitosan – 30% wt. ammonia nitrate – ethylene carbonate at the weight percentage of different plasticizers were carried out by using infrared spectroscopy analysis (FTIR) analysis in order to study the changes in functional groups and structural of carboxymethyl chitosan. The changes in shifting of wavenumbers confirmed that there is an interaction between the ion of ammonia nitrate and ethylene carbonate. Scanning electron microscope are used to study the morphology of the film samples. Morphological observation determine whether the blends were homogenous and no phase separation occurred. The presence of amorphous and crystalline structure of the film samples can be determined by X- ray diffraction. The conductivity in the film samples can be calculated through electron impedance spectroscopy (EIS). Solid polymer electrolyte based on carboxymethyl chitosan as host polymer and ammonium nitrate (NH_4NO_3) as a complexing salt and ethylene carbonate were prepared by solution casting technique. The highest ionic conductivity value achieved by carboxymethyl chitosan – 30% wt. ammonia nitrate salt – 25% wt. ethylene carbonate in room temperature was $3.86 \times 10^{-3} \text{ S cm}^{-1}$ which characterized by AC impedance spectroscopic analysis.

Keywords: Polymer

Introduction

Synthetic polymers are polymers made from human using chemicals. Most synthetic polymers are non-biodegradable polymer where synthetic polymers are not easy to decompose. When plastic materials are burned, releases of toxic gases will occur and cause depletion of ozone layer. This causes environmental pollution to occur. This situation has prompted researchers to find solutions to address this problem. Fossil fuel pollution on the environment has resulted in the production of environmentally friendly based products. The use of biodegradable polymers such as natural polymers derived from living things as environmentally friendly materials has grown rapidly to address environmental pollution problems (Luc Averous & Eric Pollet 2012). Materials with independent ions and capable of forming conductive electrical materials are known as electrolytes. The main function of the electrolyte is acting as a medium for transfer of charge occurs between electrons (Rahman et al. 2011). According to Stephen et al. (2006), the polymer electrolyte is known as a membrane having a charge carrier which is comparable to conventional liquid electrolytes. Among the materials that can be used for the production of electrolyte membranes is the polymer in which the polymer is known as polymer electrolyte. The ionic conductivity of a polymer electrolyte is very important for the purpose of its use in an electronic device. Polymers with electron-contributors are suitable as the main polymer (Anon 2005). Electrolyte polymeric materials should have properties such as good mechanical strength, good electrode interaction, and good conductivity values (Agrawal & Pandey 2008). Fenton et al. (1973) was among the first researchers to discover the potential of polymer to be applied as an electrolyte in an electrochemical device system.

- This is an Open Access article distributed under the terms of the Creative Commons Attribution-NonCommercial 4.0 Unported License, permitting all non-commercial use, distribution, and reproduction in any medium, provided the original work is properly cited.

- Selection and peer-review under responsibility of the Organizing Committee of the Conference

Studies on polyethylene oxide using lithium salts have been applied in solid electrolyte polymers especially for battery use in 1979 (Agrawal & Pandey 2008). The very high ionic conductivity properties of the solid electrolytic polymers (SPE) systems have attracted considerable attention as the most suitable option for fabricating full solid state electrochemical devices, ie batteries, detectors and fuel cells (Reddy et al. 2002). This condition led to the development of the study involving electrolyte polymers. Solid polymer electrolytes are a solution capable of electrifying the electrons in which the solution contains salts that are soluble in the polymer matrix. Solid polymer electrolytes used in comparison with liquid electrolytes have some unresolved weaknesses such as toxic liquids that cause flammable and leakage due to corrosion caused by the reaction between strong solvent and container (Armand et al 1978). In addition, solid polymer electrolyte has low volatility, high energy density and easy to form (Rahman et al. 2011). The development of polymer electrolytes was initiated by Fenton et al. (1973) found that poly-poly (ethylene oxide) polymer film (PEO) thin film can be used as a condensing material after dissolving it with lithium salts in the polymer matrix. However, Fenton and Wright faced a low ionic conductivity problem at room temperature during the conduct of electrolyte polymer studies in 1973. One of the steps to improve the ionic conductivity value is the addition of plasticizers and polymeric materials such as polyvinylalcohol. The addition of plasticizers allows the movement of polymer chains to be more flexible and increases the value of conductivity. The use of plasticizers is an efficient and effective way in which plasticizers can reduce crystalline properties and enhance amorphous properties in composite electrolyte polymers (Ramesh & Ong 2010).

Addition of salt such as lithium also helps to improve ionic conductivity (Rahman et al. 2011). In this study, natural polymeric materials such as chitosan have been used to produce carboxymethyl chitosan. Chitosan is a biodegradable material in which chitosan is easily disposed off and does not pollute the environment. Chitosan has a hydroxyl and amine functional group where these functional groups have isolated electrons and are suitable for the preparation of solid electrolyte polymers (Yahya et al. 2003). The addition of salt to the carboxymethyl chitosan helps increase ionic conductivity in the electrolyte. Ammonia nitrate has low lattice energy in which the decomposition of salts and solubility in polymer matrices is easier in electrolytes. The choice of ethylene carbonate as a plasticizer is better than polypropylene carbonate plasticizers because ethylene carbonates have a high dielectric constant and a high boiling temperature range compared to polypropylene carbonate (Ramesh & Ong 2010).

Method

Preparation of membrane

Carboxymethyl chitosan had been prepared according to Sun et al.'s method. In order to prepare polymer electrolyte film, carboxymethyl chitosan was dissolved in 1% acetic acid solution and was continuously stirred with a magnetic bar for 24 hours. Various weight percentage of ethylene carbonate with 30% wt. NH_4NO_3 were dissolved separately in 1% acetic acid solution before added in to the dissolved carboxymethyl chitosan solution. The solutions were further stirred for 24 hours to achieve a homogenous mixture. The solution was cast on petri dishes and allowed it to dried completely at room temperature until a film was obtained. The samples were stored in a desiccator for further use.

Sample characterization

The alternating current (AC) impedance measurement was carried out using a high frequency response analyzer (HFRA; Solartron 1260, Schlumberger) and an electrochemical interface (SI 1286) in the frequency range of 1Hz–10 MHz with 10 mV amplitude at room temperature. The polymer electrolyte was sandwiched between the stainless steel blocking electrodes with a contact surface area of 2.0 cm^2 . The bulk resistance (R_b) was determined from the equivalent circuit analysis by using the Zview analyzer software. Transference number of electrolytes films were determined by the application of D.C. potential (0.1 V) across the sample using stainless steel electrodes at 303K using Zive mp2 multichannel electrochemical workstation. X-ray diffraction model D5000 Siemens was used to determine the amorphous and crystalline properties of the prepared samples. The data was collected in the range of diffraction angle 2θ from 3° to 35° at the rate of 0.05 s^{-1} at room temperature.

Results and Discussion

FTIR analysis

The existence of various groups working on chitosan allows chitosan to be used in the development of composite materials. The chitosan mixes based on the polymer electrolytes have been used in electrochemical devices such as solar cells. Infra-red spectroscopy is used to verify the complexity and ionization mechanisms (Kadir et al. 2010). This is because absorption peaks identified in the infra-red vibrational environment will give different frequency values for specific bonding types (Pavia et al. 2001). The interactions between cations and anions interacting in a polymer electrolyte matrix can be detected through changes in wave numbers in functional groups that interact besides the emergence of new peaks. The polymer mixture of carboxymethyl chitosan binder doped with ammonia nitrate and ethylene carbonate plasticizers will show a waveform shift in the amine and hydroxyl functional groups (Kadir et al. 2010).

Figure 1 shows the FTIR sample carboxymethyl chitosan-30% wt. ammonia nitrate - ethylene carbonate at the weight percentage of different plasticizers. Peaks highlighted after blending are the emergence of C = O peaks at the 1775cm^{-1} and 1807cm^{-1} waves confirmed that there was an interaction between ethylene carbonate and the host polymer. Peak (C = O) without the addition of ethylene carbonate plasticizer gives peak at wave number 1772cm^{-1} . Peak C = O decreases and goes to 1720cm^{-1} wave number when plasticizer is added at 10% wt., 15% wt., 20% wt. and 25% wt. The peak of C = O on the 1775cm^{-1} and 1807cm^{-1} wave numbers was also observed to 1773cm^{-1} and 1802cm^{-1} and the peak of this C = O was increasingly widening after the addition of ammonia nitrate salt. This indicates that no chemical reaction which occurs between the plastics packet and the plastics, and between the plastics and the plasticizers only act physically with the polymer (Alias et al. 2005).

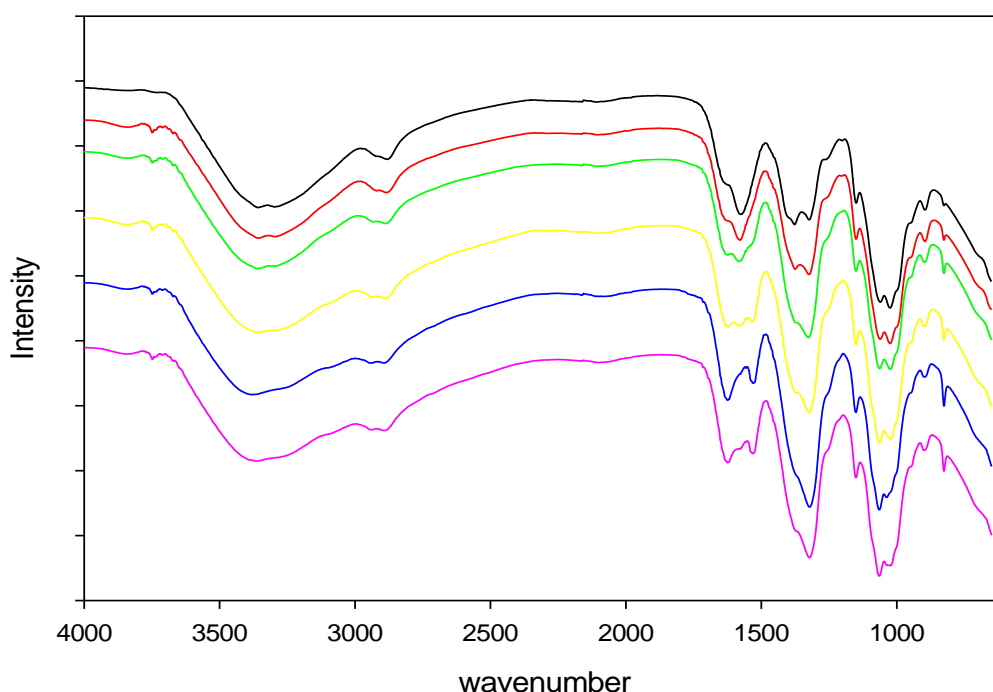


Figure 1. FTIR Analysis carboxymethyl chitosan - 30% wt. ammonia nitrate - ethylene carbonate at the weight percentage of different plasticizers

X-ray Diffraction Analysis

Determination of structural and crystalline properties can be determined by analyzing the X-ray diffraction by observing the presence of amorphous and crystalline phase in the polymer electrolyte film. The amorphous phase shows the intensity of the peaks that are increasingly horizontal while the crystalline phase shows sharp peaks that have high intensities (Wang et.al 2006). Figure 2 shows diffractogram of carboxymethyl

chitosan – 30% wt. ammonia nitrate – ethylene carbonate at the weight percentage of different plasticizers. With the addition of ammonia nitrate salt of 30 wt.% and different weight percentages of ethylene carbonate, the high-peaked prime peaks are reduced and almost invisible. From this study, the semi-crystalline phase that exists in carboxymethyl chitosan has decreased and is increasingly amorphous with the addition of salt and ethylene carbonate at optimum levels. High-density reducer and widening of the hump shows the structure of semi-crystalline carboxymethyl chitosan has changed to amorphous due to the presence of salts allowing polymer chain movement occurs in polymer electrolyte systems (Shin et al.2002).

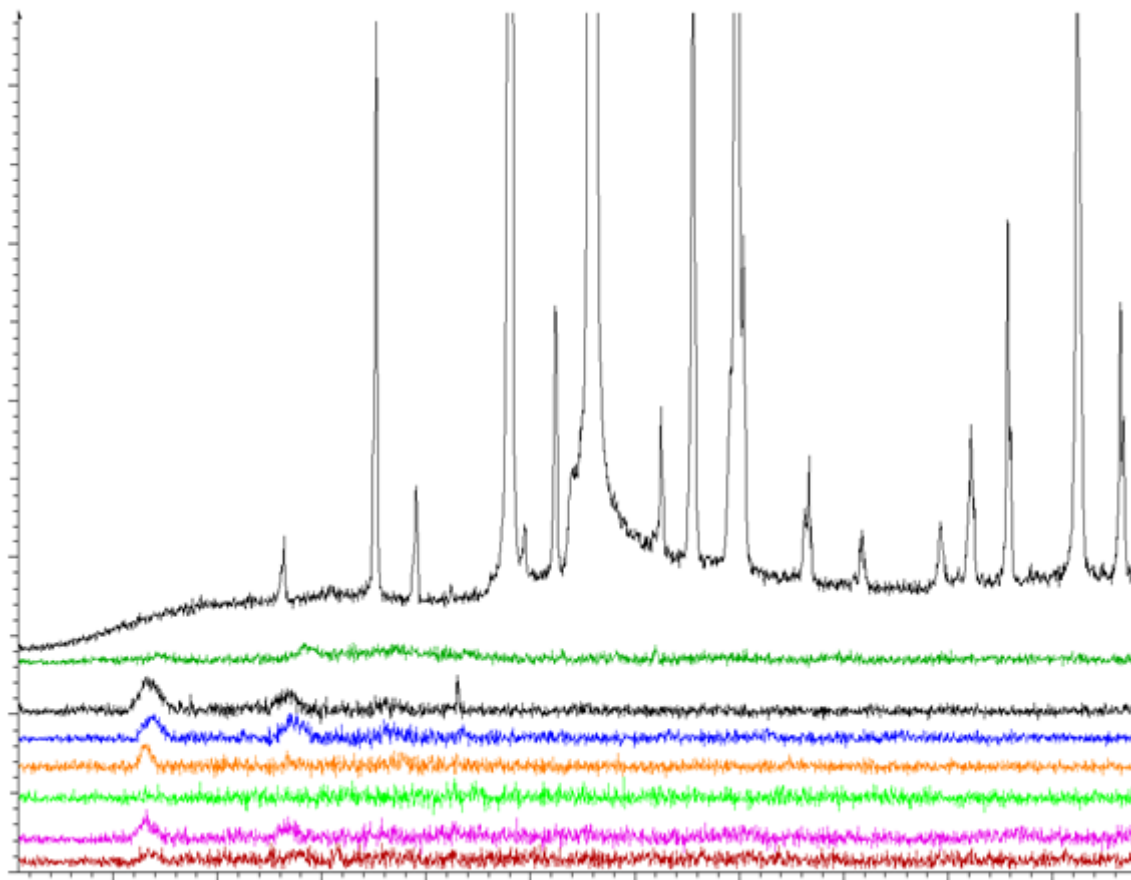


Figure 2: XRD Analysis carboxymethyl chitosan - 30% wt. ammonia nitrate - ethylene carbonate at the weight percentage of different plasticizers

Ionic Conductivity Analysis

The complex impedance plot shows that there are semi-circular areas within the frequency range which will contribute to the conductivity of polymer electrolytes (Jacob et al. 1997, Rajendran et al. 2002, Su'ait et al. 2009) while linear linear areas are contributed by electrode effects in low frequency range (Kim et al. 1999, Rajendran et al. 2002, Su'ait et al. 2009). The conductivity of the carboxymethyl chitosan sample with the addition of 30% wt. salt ammonia nitrate is $1.60 \times 10^{-3} \text{ Scm}^{-1}$. The ionic conductivity showed an increase to $3.63 \times 10^{-3} \text{ Scm}^{-1}$ with an addition of 10% wt. ethylene carbonate plasticizers. The increase in ionic conductivity occurs due to the presence of NH_4^+ which serves as a charge carrier in the electrolyte system. The optimum conductivity, $3.86 \times 10^{-3} \text{ Scm}^{-1}$ obtained by adding 25% wt. ethylene carbonate plasticizers. The conductivity values are gradually increased with the addition of plasticizers to the optimum conductivity achieved at the weight of the plasticizer percentage by 25% wt. This indicates that the polymer electrolyte system of carboxymethyl chitosan dough and 30% wt. salts of ammonia nitrate with the presence of ethylene carbonate plasticizers produce higher ionic conductivity than without ethylene carbonate. The increase in the conductivity of ions with the addition of plasticizers is due to the high acidity dielectric constant which can increase the number of moving ions by weakening the coulombic force between cation and salt anion (Mohamed et al. 2008). Hence, more NH_4^+ ions can be produced and the solubility of salts into the system can also be improved. Additionally, an increase in ion conductivity occurs when the reduction of electrolyte polymer viscosity occurs

after the addition of the material plasticizers and thus facilitating charge carriers to the electrolyte system (Ahmad et al. 2006, Idris et al. 2001, Wang & Kim 2007). This increase was due to the composition of the ammonia nitrate salt decomposed into ion species NH_4^+ and NO_3^- . There are various factors that affect ionic conductivity such as the number of charge carriers and ionic movement. The existence of a charge carrier species occurs when an ionization occurs which helps to increase the value of the ionic conductivity (Wang et al. 2006). According to reports (Buraidah et al. 2009; Choi & Shin 1996; Subban 2003), an initial increase in conductivity was due to an increase in the number of car ions after the addition of plastic materials. The plasticizer, ethylene carbonate acts as an agent in which the process of decomposition of the salt occurs more easily.

Scanning Electron Microscope Analysis

Morphological examination on the surface of the polymer electrolytic film was performed to see the effect of plasticizer on surface morphology and topographic texture of the sample. Figure 3 shows the SEM micrograph of carboxymethyl chitosan sample -30% wt. ammonia nitrate - ethylene carbonate on addition (a) 0% wt. (b) 10% wt. (c) 15% wt. (d) 20% wt. (e) 25% wt. (f) 30% wt. (g) 35% wt. ethylene carbonate plasticizer. Based on the pictures, it is found that the distribution of plasticizers in the carboxymethyl chitosan matrix is uneven but gives a smoother surface compared to the carboxymethyl chitosan surface of 30% wt. ammonia nitrate without addition of ethylene carbonate. The addition of ethylene carbonate plasticizers also reveals darker areas where phase separation occurs between polymer and ethylene carbonate matrices. Figure 3(e) shows the smoothest, uniform and homogeneous surfaces as compared to the other percent weight of ethylene carbonate. A homogeneous surface is usually associated with a reduction in the crystallization phase and an increase in the amorphous phase. The increase in the movement of ions in polymer electrolytes usually occurs in the amorphous phase and causes an increase in ionic conductivity. The ions move freely in the electrolyte with a smooth surface and this leads to the increased ionic conductivity of the polymer electrolyte (Mobarak et al. 2012). However, high concentrations of salt will affect the ionic species for aggregation and associate with each other (Ahmad et al. 2010; Wickham et al. 2007). This will lead to a reduction in the number of species and the mobility of the ion inhibit the migration of ions in the polymer chain segment. Low conductivity of the polymer electrolytic system will occur due to the digression of polymer chain process travel in polymer electrolyte systems (Su'ait et al. 2011).

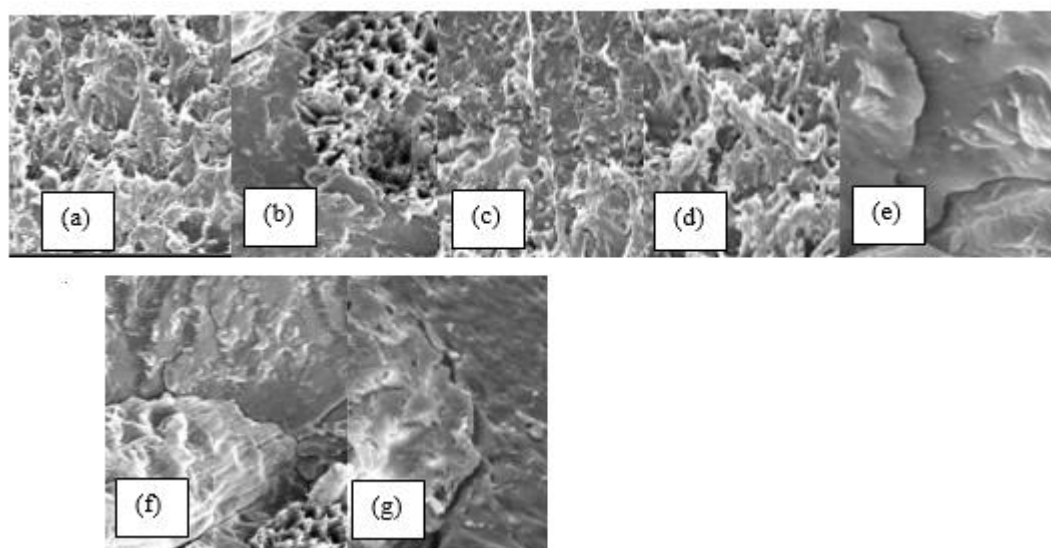


Figure 3: SEM Analysis carboxymethyl chitosan - 30% wt. ammonia nitrate - ethylene carbonate at the weight percentage of different plasticizers

Conclusion

This study was carried out for the preparation and characterization of polymer electrolytes based on the carboxymethyl chitosan blend of chitosan, ammonia nitrate and ethylene carbonate. Solid polymer electrolytes based on the carboxymethyl chitosan mix, ammonia nitrate at 30% wt. of the composition and ethylene

carbonate at different ratios are provided. The effect of different percentage of ethylene carbonate weight ratio and ammonia nitrate doped salt on composition of 30% wt. by weight on the properties of ion conductivity, chemical interactions and morphological surfaces of solid polymeric electrolyte film was successfully analyzed.

In this study, the effect of the addition of ethylene carbonate plasticizers was shown to indicate the overall ionic conductivity. The increase in the ratio of ethylene carbonate plasticizers in the carboxymethyl blend of chitosan-ammonia nitrate contributes to an increase in the value of the ionic conductivity to the optimum level. However, ionic conductivity decreases after one optimum and this occurs due to the recrystallization of ammonia nitrate salt as evidenced in the x-ray diffraction analysis. The addition of low-quantity plasticizers has the ability to reduce the cohesion between the withdrawal of the polymer bond. The plasticizer with a small molecular size compared with the polymer molecule is easier to dissolve to the polymer matrix and the formation of the attraction between the plasticizer and the bonding segment will occur. The reduction of cohesion power between polymer bonds will occur when the attraction occurs and thus increases the segment mobility and ionic conductivity in solid electrolyte polymers. The ionic species will decompose from the ammonia nitrate salt composition when the salts are dissolved in the polymer matrix. When ion decomposition occurs, the charge carrier species will exist and help to increase the value of the ionic conductivity.

References

- Averous, L., & Pollet, E. 2012. Biodegradable Polymers. *Environmental Silicate Nano Biocomposites, Green Energy And Technology Springer-Verlag*: London.
- Rahman, M. Y. A., Ahmad, A., Lee, T. K., Farina, Y. & Dahlan, H. M. 2011. LiClO₄ Salt Concentration Effect on the Properties of PVC-Modified Low Molecular Weight LENR50-Based Solid Polymer Electrolyte. *Journal of Applied Polymer Science*, Vol. 124: 2227–2233.
- Stephan, A. M. 2006. Review On Polymer Electrolytes For Lithium Batteries. *European Polymer Journal* 42: 21-42.
- Agrawal, R. C. & Pandey, G. P. 2008. Solid polymer electrolytes: materials designing and all-solid-state battery applications: an overview. *Applied Physics* 41: 223001.
- Fenton, D. E., Parker, J. M., & Wright, P. V. 1973. Complexes of Alkali Metal Ions with PEO. *Polymer* 14: 589.
- Reddy, C. V. S., Sharma, A. K. & Rao, V. V. R. N. 2002. Effect of plasticizer on electrical conductivity and cell parameters of PVP+ PVA + KClO₃ blend polymer electrolyte system. *Journal of Power Sources* 111: 357–360.
- Armand. 1978. In Extended Abstract Of Second Int. Meeting on Solid Electrolytes. Scotland: St. Andrew.
- Ramesh, S., & Ong, P. L. 2010. Effect of ethylene carbonate on the ionic conduction in poly(vinylidene fluoride-hexafluoropropylene) based solid polymer electrolytes. *Polymer Chemistry* 1: 702–707.
- Yahya, M.Z.A. & Arof, A. K. 2003. Conductivity and X-ray photoelectron studies on lithium acetate doped chitosan films. *Carbohydrate Polymers* 55: 95-100.
- Kadir, M. F. Z., Aspanut, Z., Majid, S. R. & Arof, A. K. 2010. FTIR studies of plasticized poly(vinyl alcohol)–chitosan blend doped with NH₄NO₃ polymer electrolyte membrane. *Spectrochimica Acta Part A* 78: 1068–1074.
- Pavia, D. L., Lampman, G. M., & Kriz, G. S. 2001. Introduction to Spectroscopy 3rd Ed. Brooks/Cole Publishing.
- Alias, Y., Ling, I. & Kumutha, K. 2005. Structural and electrochemical characteristics of 49% PMMA grafted polyisoprene (MG49)-LiCF₃SO₃-PC based polymer electrolytes. *Ionics* 11: 414.
- Wang, H. X., Wang, Z. X., Li, H., Meng, Q. B. & Chen, L. Q. 2006.. Ion transport in small molecule electrolyte based Lil/3-hydroxypropionitrile with high salt contents. *Journal of Electrochimica Acta* 52: 2039-2044.
- Shin, J. H., Lim, Y. T., Kim, K. W., Ahn, H. J. & Ahn, J. H. 2002. Effect of ball milling on structural and electrochemical properties of (PEO)_n LiX (LiX = LiCF₃SO₃ and LiBF₄) polymer electrolytes. *Journal of Power Sources* 107: 103-109.
- Jacob, M. M. E., Prabakaran, S. R. S. & Radakrishna, S. 1997. Effect of PEO in addition on the electrolytic and thermal properties of PVdF-LiClO₄ polymer electrolytes. *Solid State Ionics* 11: 472-476.
- Rajendran, S., Mahendran, O. & Kannan, R. 2002. Characterisation of (1-x)PMMA- xPVdF polymer blend electrolyte with Li⁺ ion. *Journal of Fuel* 81: 1077-1081.
- Su'ait, M. S., Ahmad, A. & Rahman, M. Y. A. 2009. Ionic conductivity studies of 49% poly(methyl metacrylate)-grafted natural rubber - based solid polymer electrolyte. *Ionics* 15: 497-500.
- Kim, W. S., Jeong, Y. C., Park, J. K., Shin, C. W. & Nam-Kim. 2007. Diffraction efficiency behaviour of photopolymer based on P(MMA-co-MAAA) copolymer matrix. *Optical Materials* 29: 1736-1740.

- Mohammad, A. A., Haliman, H., Sulaiman M. A., Yahya, M. Z. A. & Ali, A. M. M. 2008. Conductivity studies of plasticized anhydrous PEO-KOH alkaline solid polymer electrolytes. *Ionics* 14: 59-62.
- Ahmad, A., Isa, K. B. M. & Osman, Z. 2011. Conductivity and Structural Studies of Plasticized Polyacrylonitrile (PAN) –Lithium Triflate Polymer Electrolyte Films. *Sains Malaysiana* 40(7): 691–694.
- Idris, R., Glasse, M. D., Latham, R. J., Linford, R. G. & Schlindwein, W. S. 2001. Polymer electrolytes based on modified NR for the use in rechargeable lithium batteries. *Journal of Power Sources* 94(2): 206-211.
- Wang, Y. J. & Kim, D. 2007. Crystallinity, morphology, mechanical properties and conductivities study of in situ formed PVdF/LiClO₄/TiO₂ nanocomposite
- Buraidah, M. H., Teo, L. P., Majid, S. R. & Arof, A. K. 2008. Ionic conductivity by correlated barrier hopping in NH₄I doped chitosan solid electrolyte. *Physica B* 404: 1373–1379.
- Chen, L., Xiao, G. S. & Sheng, D. 2012. Crosslinked gel polymer electrolytes based on polyethylene glycol methacrylate and ionic liquid for lithium ion battery applications. *Electrochimica Acta* 87: 889–894.
- Subban, R. H. Y., & Arof, A. K. 2003. Experimental investigation on PVC-LiCF₃SO₃-SiO₂ composite polymer electrolytes. *Journal of New Materials for Electrochemical System* 61: 97-203.
- Mobarak, N. N., Ahmad, A., Abdullah, M. P., Ramli, N. & Rahman, M. Y. A. 2012. Conductivity enhancement via chemical modification of chitosan based green polymer electrolyte. *Electrochimica Acta* 92: 161–167.
- Ahmad, A., Pow, C. L. & Su'ait, M. S. 2010. Solid Polymer Electrolyte 49% Poly(Methyl Methacrylate - Grafted Natural Rubber-Lithium Tetrafluoroborate. *Sains Malaysiana* 39(1): 65–71.
- Wickham, J. R., Mason, R. N. & Rice, C. V. 2007. Solid state NMR studies of the crystalline and amorphous domains within PEO and PEO:LiTf systems. *Journal of Solid State Nuclear Magnetic Resonance* 31: 184-192.
- Su'ait, M. S., Ahmad, A., Hamzah, H. & Rahman, M. Y. A. 2011. Effect of lithium salt concentrations on blended 49% poly(methyl methacrylate)- grafted natural rubber based solid polymer electrolyte. *Electrochimica Acta*.

Author Information

Leong Kok Seng

Polytechnic Tun Syed Nasir Syed Ismail
Malaysia
Contact: kokseng@ptsn.edu.my

The Preparation of Controlled Release Fertilizer Based on Gelatin Hydrogel Including Ammonium Nitrate and Investigation of its Influence on Vegetable Growth

Mehlika PULAT
Gazi University

Nese YOLTAY SAGLAM
Akdağmadeni Anadolu İmam Hatip High School

Abstract: A controlled release fertilizer (CRF) systems based on gelatin hydrogel was prepared to improve fertilizer use efficiency and minimize its negative impact on environment. Gelatin hydrogel was synthesized by using glutaraldehyde (GA) as crosslinker and its swelling/degradation behaviors were investigated. Ammonium nitrate (AN) was loaded into the gelatin hydrogel and its releasing was followed. Release of AN from gelatin beads versus time was followed, and it is found that the release gently increased at first and then complied between 40-50 h. The releasing date shows that the prepared AN/gelatin hydrogel system could be named as a CRF. The efficiency of gelatin hydrogel beads including AN were examined on the vegetable growing using cucumber seeds. Plant growth and stem elongations measurements presents the formed hydrogel beads could be successfully used as a CRF system. It can be concluded that the CRF system produced in this study is much promising in utilizing a natural resource like gelatin in the production of matrix material, which could significantly reduce the production costs and offer a quite environmental friendly alternative technique.

Keywords: Gelatin, Controlled release fertilizer, Ammonium nitrate, Plant growth, STEM elongation

Introduction

Fertilizer and water are essential factors that limit agricultural production. The main purpose of fertilizer application is to provide nutrients to plants in order to increase the yields. So it is very important to improve the utilization of water resources and fertilizer nutrients [Ni et al., 2007]. However, about 40-70% of nitrogen and 80-90% of phosphorus of the applied normal fertilizers cannot be absorbed by plants. They are released to the environment which causes not only large economic and resource losses but also a very serious environmental pollution [Corradini et al., 2010].

Researchers and fertilizer producers have attempted to discover advanced techniques for fertilizer usage that can improve nutrient use efficiency and minimize environmental impacts. One possible way to overcome this problem is controlled released fertilizer (CRF) usage. CRFs are broadly defined as products that release nutrients to soil for plant uptake at a pre-determined time and rate (Trenkel, 2007). Compared to the conventional type, CRFs have many advantages such as (1) decreasing fertilizer loss rate, (2) supplying nutrients sustainable, (3) lowering application frequency and (4) minimizing potential negative effects associated with over dosage [Al-Zahrani, 1999].

CRFs can be divided into 3 categories based on their coating and nutrient composition. (1) Uncoated, nitrogen-based fertilizers are the oldest class of CRF that consist of chemically-bound urea and the release rate is determined by particle size, available water, and microbial decomposition e.g. (2) Coated, nitrogen-based fertilizers – Sulphur-coated urea is one of the first CRF. Thickness of sulphur coating controls the nitrogen discharge. (3) Polymer-coated or polymer matrix multi-nutrient fertilizers. All principal classes of polymers, i.e.

- This is an Open Access article distributed under the terms of the Creative Commons Attribution-Noncommercial 4.0 Unported License, permitting all non-commercial use, distribution, and reproduction in any medium, provided the original work is properly cited.

- Selection and peer-review under responsibility of the Organizing Committee of the Conference

plastics, coatings, elastomers, fibers and soluble polymers are presently utilized in applications that include the controlled release of nutrients [Chandra and Rustgi, 1998]. In this type of CRF, thicknesses, porosities and swelling behaviors of polymers control the release of nutrients.

Hydrogels have been extensively studied and preferred for a large number of applications in much kind of industrial fields [Pulat and Asil, 2009; Pulat et al., 2011]. Because of their excellent characteristics, hydrogels can also be used for controlled release of agrochemicals and nutrients in agricultural and horticultural applications [Rafaat et al, 2012].

Most of the synthetic polymers used to prepare hydrogels causes some problems because of their long degradation times and degradation products. Natural polymers are a good choice to overcome this issue. Gelatin is a biodegradable natural polymer with extensive industrial, pharmaceutical, and biomedical uses that has been employed for coatings and microencapsulating various drugs, and for preparing biodegradable hydrogels [Pulat and Akalin, 2013]. Since it is soluble in aqueous solutions, the materials for long-term applications must be submitted to crosslinking, which improves both thermal and mechanical stability of gelatin. Among the chemical crosslinking agents, glutaraldehyde (GA) is by far the most widely used due to its high efficiency of collagenous materials stabilization [Bigi et al, 2001].

In recent years, our studies focused on gelatin hydrogels as a controlled-release material. Based on our pervious works about hydrogels and controlled-release systems, in this study it is intent to develop a CRFs based on gelatin hydrogel (Pulat et al., 2014). The swelling/degradation behaviors of the hydrogel were determined and ammonium nitrate (AN) was chosen as fertilizer to be controlled of release. The objective of this study was to investigate the effect of AN loaded gelatin hydrogels on the germination rate and early development of tomato and cucumber seedlings.

Methods

Preparing and Characterization of Gelatin Hydrogel

In this study, gelatin (Fluka, Type B, 280-Bloom, from pig skin) hydrogel was prepared by mixing 10% of aqueous gelatin solutions with 25% of GA (Aldrich, 25% aqueous solution). Gelatin/GA mass ratio is arranged as 1/0.5. Crosslinking reaction was preceded for 24 h at room temperature in a glass tube. The fresh hydrogel rods were taken from the tube and were cut into pieces 0.5 cm long. After the discs were left overnight at room conditions, they were washed several times with distilled water to remove unreacted chemicals.

Gravimetric tests were carried out, and the formula given below was used to determine hydrogel formation (HF) percentage [Chen et al, 2005]. Dried and weighed samples were placed in water for 48 h to extract the unreacted monomers and then dried.

$$\text{HF (\%)} = \frac{m}{m_0} \times 100 \quad (1)$$

where m and m_0 are the weights of the dried hydrogel after and before extraction, respectively.

Swelling test of hydrogel sample was gravimetrically carried out. First, the dried hydrogel sample were left to swell in the Britton-Robinson buffer (BRB) (pH = 7.0) at 30°C. Swollen gel was taken from the swelling medium at regular intervals, and dried with filter paper, weighed, and placed into the same bath. Measurements were performed to constant weight and the percentage swelling (S%) values were calculated using the equation given below [Chen et al, 2005]:

$$S (\%) = \frac{mw - md}{Md} \times 100 \quad (2)$$

where mw is the wet weight of the sample, and md the dry weight of the sample before swelling.

Degradation test of hydrogel samples were carried out at pH 7.0 and 30°C. Dried hydrogel discs were left to swell in BRB solution. At the end of 48 h, swollen gels were dried and weighed. Then the hydrogels placed into the same bath and the procedure was repeated until they completely degraded. The degradations were determined using the following formula:

$$\text{Degradation (\%)} = \frac{M_m - M_t}{M_m} \times 100 \quad (3)$$

where M_m and M_t are the weights of hydrogel at the maximum swollen stage and at time t .

Loading of AN and Release Studies

In this study, fertilizer-entrapped hydrogel samples were prepared by adding particular amounts of AN (Merck) (53 mg per disc) into the gelatin-GA mixture during crosslinking reactions (Bajpai and Giri, 2002). AN release was followed spectrophotometrically at a wavelength of 305 nm for 60 h. AN-entrapped samples were placed into 100 mL of water. At different times, aliquots of 0.2 mL were drawn from the medium to follow the AN release: a maximum of 30 aliquots were taken, so the volume could be considered constant. The AN release always maintained sink conditions. The cumulative release of AN was calculated by using the equation given below:

$$\text{Release (\%)} = \frac{W_t}{W_{\text{total}}} \times 100 \quad (4)$$

where W_t is the weight of the released fertilizer in the releasing medium at any time, and W_{total} represents the initial total weight of the fertilizer entrapped into the gel system.

Effects of AN loaded Discs on Vegetable Growth

Effect of the hydrogels containing AN on vegetable growth was investigated by following germination and shooting periods. The test conditions were summarized into Table 1.

Healthy and uniformly sized tomato and cucumber seeds were selected and sown into the prepared soil pots. Seeding depth was 3 cm. Seed germination experiments were carried out with 4 sets. First pot set doesn't contain any AN disc. 3, 6 and 9 discs were placed in other pot sets at 1.5 cm depth. Watering schedule is given in Table 1. A series of photographs were taken during experiment days. The seed germination percentage (SG) was calculated from the following formula (Jayarambabu et al. 2016):

$$\text{SG (\%)} = \frac{S_g}{S} \times 100 \quad (5)$$

Where, S_g is number of germinated seeds and S is total number of seeds.

Height of stems was measured using ruler starting from the base to the tip of the plant. Stem elongation yields (E%) were calculated using following formula:

$$\text{E (\%)} = \frac{H_s - H_c}{H_c} \times 100 \quad (6)$$

Where, H_s and H_c are the stem height of the sample and control.

Table 1. Growing test procedure

Sets	AN-3 : 3 discs in one pot AN-6 : 6 discs in one pot AN-9 : 9 discs in one pot C : Control, not includes fertilizer.
Specification of Soil	Torf (Gertengold), 4 L per pot. pH: 6 - 7 ; %0.4-1.0 N; 150-300 ppm of F; 600-1200 ppm of K.
Seeds	Cucumber (<i>Cucumis sativus</i> L., Fento Tohumculuk) Tomato (<i>Solanum lycopersicum</i> , Fento Tohumculuk)
Seeding procedure	4 L torf per pot. 50 tomato seeds per pot 10 cucumber seeds per pot, seeding depth are 3 cm.

	Depth of hydrogel discs are 1.5 cm.
Watering schedule	0.5 L per pot every other day during first 15 days (germination period). After two weeks, same amounts for each day (growing period).

Results and Discussion

Characterization of Gelatin Hydrogel

Gelatin hydrogel discs were produced as described in the methods. HF was calculated via Equation 1 and the result was given in Table 2. The primary purpose of this study is to obtain high efficiency for hydrogel preparing. 94% value is a very satisfactory result.

Swelling behavior was followed at a regular temperature 30 °C and calculated via Equation 2. S% increased with time initially, and then remained constant at close to 48 h. and the maximum value was reached as 218%. Swelling profile of a hydrogel is an important parameter and directly affects the release behavior. On the other hand, degradation time should be compatible cumulative fertilizer release. The time of 100% degradation of prepared hydrogel was found as 60 days. The results presented in Table 2 are very satisfying.

Table 2. HF, maximum swelling (MS) and time of 100% degradation (DT)

HF (%)	MS (%)	DT (day)
94	218	60

AN Release

The release profile of AN from gelatin hydrogel is calculated via Equation 4 and presented in Figure 1. As seen from this figure, AN release gently increased at first and then complied near 50 h. Full of the loaded fertilizer were released at the end of the release time. Release behavior of the hydrogel was similar to swelling profiles.

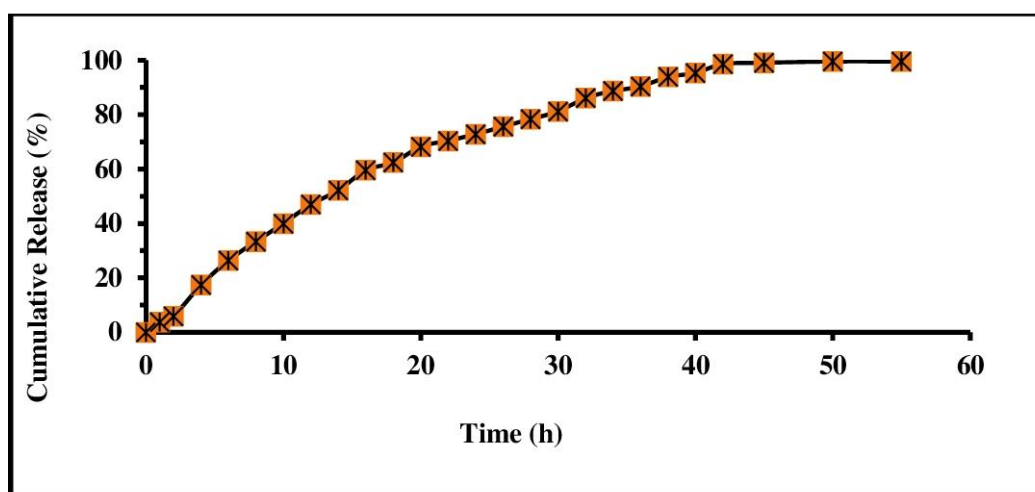


Figure 1. Cumulative release of AN through gelatin hydrogel

The results of the present work indicate that the gelatin hydrogels are good support materials for controlled release of AN with their excellent swelling/degradation capability.

Effects of AN loaded Hydrogel Discs on Vegetable Growth

Seed germination and plant growth of vegetables were followed as described above by taking photographs. As seen from Figures 2-3, the maximum growth was observed for the samples containing 9 hydrogel discs per pot. The less germination and elongation were obtained for control groups.

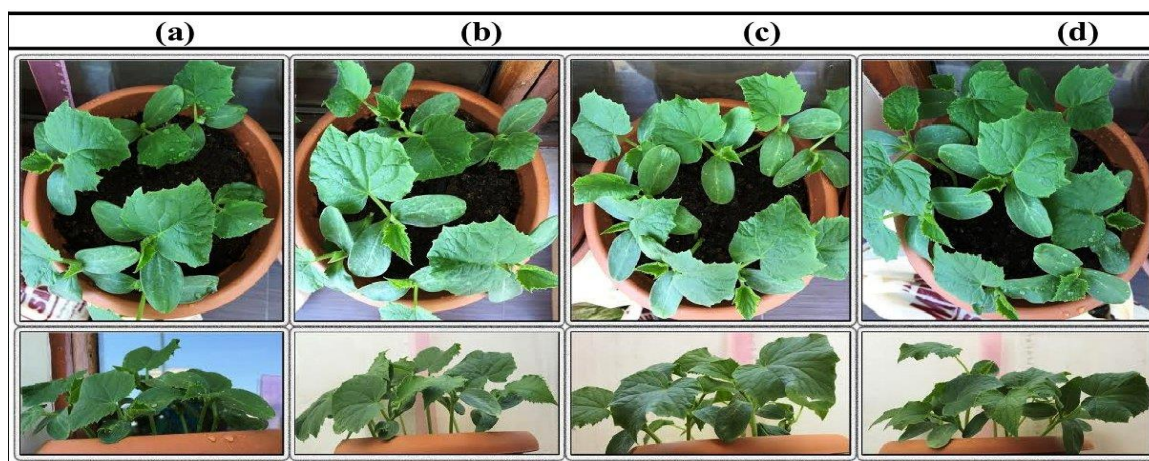


Figure 2. Cucumber growths at 35th day. (a) Control (b) AN-3 (c) AN-6 (d) AN-9

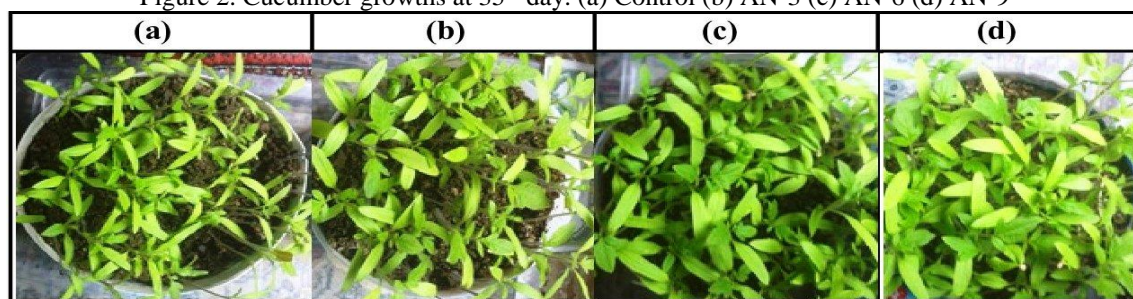


Figure 3. Tomato growths at 35th day. (a) Control (b) AN-3 (c) AN-6 (d) AN-9

The variations of vegetable germination by time were presented in the Figures 4-5. As seen from these figures, the germination was nearly completed at 15 days. The less value was obtained for control groups. The maximum germination was reached for the sample containing 9 hydrogel discs.

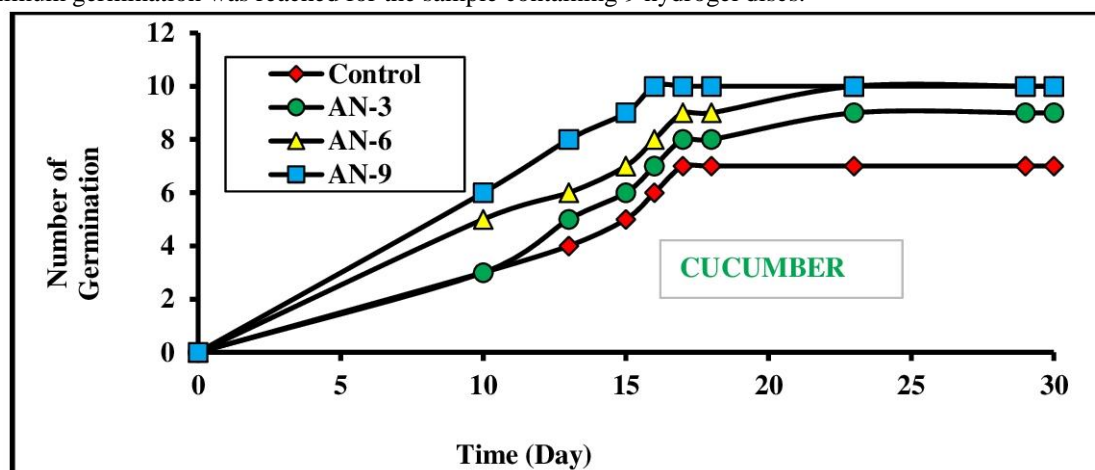


Figure 4. Variation of cucumber germination by day

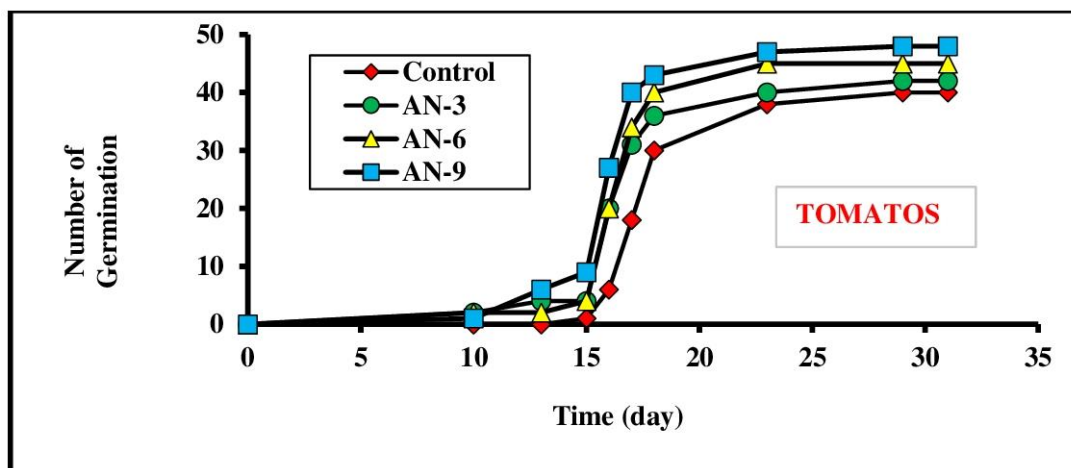


Figure 5. Variation of tomato germination by day

SG (%) values were calculated using Equation 5 and presented in Table 3. The percentage values changed from 70 to 100 for cucumber and from 76 to 94 for tomatos. It is clear that AN included hydrogel discs positively affect the seed germination for all samples.

Table 3. SG (%) and E (%) values of vegetables

Seed	SG (%) at 23 th day				E (%) at 35 th day			
	Control	AN-3	AN-6	AN-9	Control	AN-3	AN-6	AN-9
CUCUMBER	70	100	100	90	-	7	29	42
TOMATOS	76	90	94	80	-	8	25	41

Stem elongation of cucumber and tomato were followed in every day and the variations were presented in Figure 6-7. As seen from these graphs, stem elongation of control groups is less than the samples included AN/hydrogel discs.

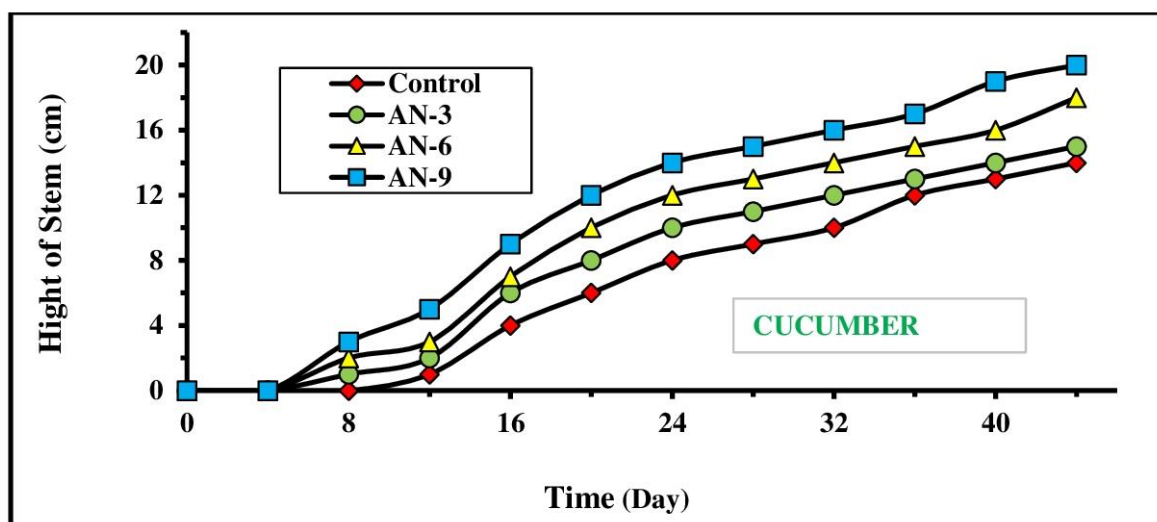


Figure 6. Stem elongation of cucumber

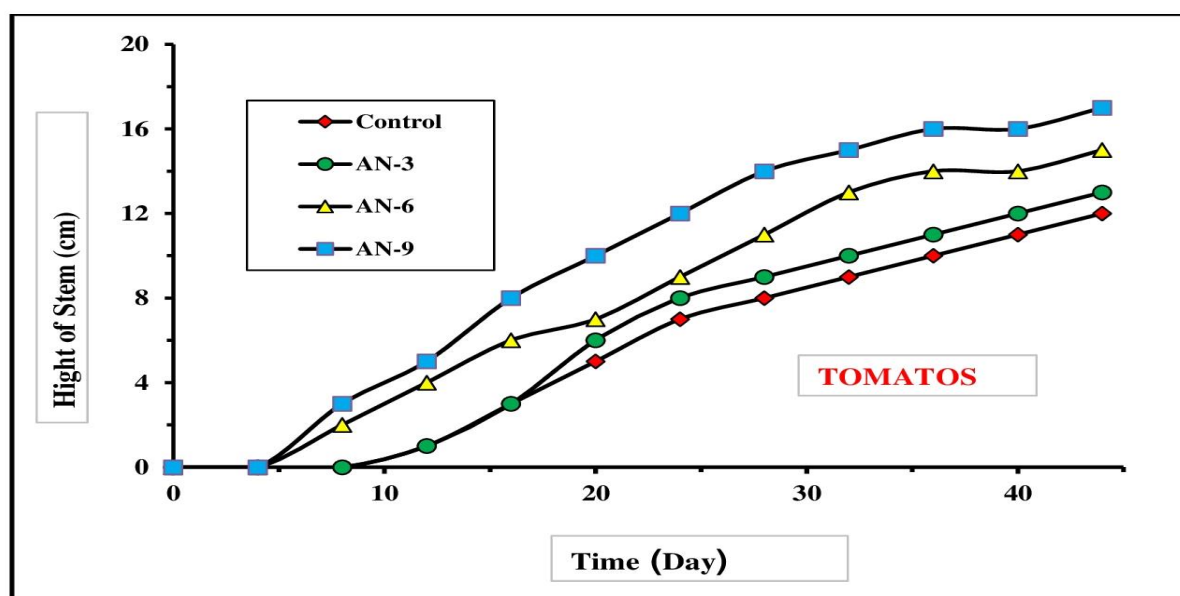


Figure 7. Stem elongation of tomato

Conclusion

It can be concluded that the CRF system produced in this study is much promising in utilizing a natural resource like gelatin in the production of matrix material, which could significantly reduce the production costs and offer a quite environmental friendly alternative technique.

References

- Al-Zahrani S.M. (1999). Controlled-release of fertilizers: modelling and simulation. *Int. J. Eng. Sci.* 37, 1299-1307.
- Bajpai A.K., Giri A. (2002). Swelling dynamics of a macromolecular hydrophilic network and evaluation of its potential for controlled release of agrochemicals. *React. Func. Polym.* 53, 125-141.
- Bigi A., Cojazzi G., Panzavolta S., Rubini K., Roveri N. (2001). Mechanical and thermal properties of gelatin films at different degrees of glutaraldehyde crosslinking. *Biomater.* 22, 763-768.
- Chandra R., Rustgi R. (1998). Biodegradable polymers. *Prog. Polym. Sci.* 23, 273-1335.
- Chen K., Ku Y., Lin H., Yan T., Sheu D., Chen T., Lin F. (2005). Preparation and characterization of pH-sensitive poly (N-vinyl 2-pyrrolidone/itaconic acid) copolymer hydrogels. *Mat. Chem. Phys.* 91, 484-489.
- Corradini E., De Moura M.R., Mattoso L.H.C. (2010). A preliminary study of the incorporation of NPK fertilizer into chitosan nanoparticles. *Exp. Polymer Lett.* 4, 509-515.
- Jayarambabu N, Siva Kumari B, Venkateswara Rao K, Prabhu YT. (2016). Enhancement of growth in maize by biogenic- synthesized mgo nanoparticles, *International Journal of Pure and Applied Zoology*, 4, 3: 262-270.
- Ni B., Liu M., Lu S. (2007). Multifunctional slow-release urea fertilizer from ethylcellulose and superabsorbent coated formulations. *Chem. Eng. J.* 155, 892-898.
- Pulat M., Asil D. (2009). Fluconazole release through semi-ipn hydrogels based on chitosan, AA, and citraconic acid. *J. Appl. Polym. Sci.* 113, 2613-2619.
- Pulat M., Tan N., Onurdağ F.K. (2011). Swelling dynamics of IPN hydrogels including acrylamide-acrylic acid-chitosan and evaluation of their potential for controlled release of piperacillin-tazobactam. *J. Appl. Polym. Sci.* 120, 441-450.
- Pulat M., Akalın G.O. (2013). Preparation and characterization of gelatin hydrogel support for immobilization of *C. Rugosa* lipase. *Artif. Cells Nanomed. Biotechnol.* 41, 145-151.
- Pulat M., Akalın G.O, Demirkol Karahan N. (2014). Lipase release through semi-interpenetrating polymer network hydrogels based on chitosan, acrylamide, and citraconic acid. *Artif. Cells Nanomed. Biotechnol.* 42, 121-127.
- Rafaat A.I, Eid M., El-Arnaouty M.B. (2012). Radiation synthesis of superabsorbent CMC based hydrogels for agriculture applications. *Nucl. Instr. Meth. Phys. Res. B* 283, 71-76.

Trenkel M.E. (2007). Controlled release fertilizers: trends and technologies. *Pharmaceutica*. 5, 1-15

Author Information

Mehlika Pulat

Gazi Üniversitesi, Fen Fakültesi, Kimya Bölümü–
Teknikokullar, Ankara/Türkiye
Contact e-mail: mpulat@gazi.edu.tr

Nese Yoltay Sağlam

Akdağmadeni Anadolu İmam Hatip Lisesi, Akdağmadeni
Yozgat/Türkiye

Preparation of Sodium Carboxymethyl Cellulose Hydrogels for Controlled Release of Copper Micronutrient

Gulen Oytun AKALIN
Aksaray University

Mehlika PULAT
Gazi University

Abstract: In this study, a series of nanoporous sodium carboxymethyl cellulose (NaCMC) hydrogels were synthesized using FeCl_3 ionic-crosslinker by changing the amounts of the components. Hydrogel formation percentages of the samples were determined and the highest value was obtained as 96% for the hydrogel containing the most amounts of polymer and crosslinker. Swelling/degradation behaviors of the hydrogels were studied by changing time, temperature and pH and it was determined that the swelling percentages regularly decreased with increasing the amounts of polymer and crosslinker. S% values were determined to be 102% for the least swollen hydrogel. In general, NaCMC hydrogels much more swelled in basic medium than acidic medium. Releasing of copper micronutrient from NaCMC hydrogels were investigated by Atomic Absorption Spectrometer measurements. Kinetic in vitro release parameters, the release rate factor K and the release exponent n of micronutrients in hydrogel system were calculated. It can be concluded that the produced hydrogel system having controllable release values is useful for agricultural applications.

Keywords: Sodium carboxymethyl cellulose, Hydrogel, Micronutrient, Controlled-release

Introduction

Plant Nutrients

All plants must obtain a number of inorganic elements from their environment to ensure successful growth and development of both vegetative and reproductive tissues. At least 17 elements are known to be base nutrients for plants. There are four types of nutrients that fall into two broad categories: macronutrients and micronutrients. The nutrients which are required by plants in large quantities are called macronutrients. Macronutrients play a very important role in plant growth and development. Their functions range from being structural units to redox-sensitive agents.

Micronutrients are essential elements required by plant organisms in small quantities and play an important role in balanced crop nutrition. They are as important to plant nutrition as primary and secondary macronutrients, though plants don't require as much of them. A lack of any one of the micronutrients in the soil can limit growth, even when all other nutrients are present in adequate amounts. The classification of micro nutrients presented in Table 1.

Table 1. Classification and some important properties of plant micro nutrients

Micronutrients	Mobility	Amount (aver., %)	Functions in the plant
Fe	Fe ⁺² , Fe ⁺³	2.10 ⁻²	Component of many enzymes
Zn	Zn ⁺²	5.10 ⁻³	High crop yields
Mn	Mn ⁺²	5.10 ⁻³	Plays a direct role in photosynthesis
B	BO ₃ ⁻³ , B ₄ O ₇ ⁻²	2.10 ⁻³	Affecting membrane stability
Cu	Cu ⁺²	6.10 ⁻⁴	Activates enzymes and catalyzes reactions
Mo	MoO ₄ ⁻²	1.10 ⁻⁵	Vital for the process of symbiotic N fixation

As a Micronutrient Copper

Copper is necessary for carbohydrate and nitrogen metabolism and, inadequate copper results in stunting of plants. Cu activates enzymes and catalyzes reactions in several plant-growth processes. The presence of copper is closely linked to Vitamin A production, and it helps ensure successful protein synthesis. Copper also is required for lignin synthesis which is needed for cell wall strength and prevention of wilting. Deficiency symptoms of copper are dieback of stems and twigs, yellowing of leaves, stunted growth and pale green leaves that wither easily. Copper uptake decreases as soil pH increases. Increased phosphorus and iron availability in soils decreases copper uptake by plants.

Controlled Release Fertilizers

The traditional fertilization methods cause serious environmental pollution, large economic and resource losses. In recent years, researchers and fertilizer producers have attempted to discover advanced techniques for fertilizer usage that can improve nutrient use efficiency and minimize environmental impacts (Trenkel, 2007) . One possible way to overcome this problem is controlled released fertilizer (CRF) usage. A literature review reveals that the history of CRFs development is based on 1960's. CRFs are broadly defined as products that release nutrients to soil for plant uptake at a pre-determined time and rate. Compared to the conventional type, CRFs have many advantages such as (1) decreasing fertilizer loss rate, (2) supplying nutrients sustainable, (3) lowering application frequency and (4) minimizing potential negative effects associated with over dosage.

CRFs can be divided into 3 categories based on their coating and nutrient composition. (1) Uncoated, nitrogen-based fertilizers are the oldest class of CRF that consist of chemically-bound urea and the release rate is determined by particle size, available water, and microbial decomposition e.g. (2) Coated, nitrogen-based fertilizers – Sulphur-coated urea is one of the first CRF. Thickness of sulphur coating controls the nitrogen discharge. (3) Polymer-coated or polymer matrix multi-nutrient fertilizers.

All principal classes of polymers, i.e. plastics, coatings, elastomers, fibers and soluble polymers are presently utilized in applications that include the controlled release of nutrients. In this type of CRF, thicknesses, porosities and swelling behaviors of polymers control the release of nutrients.

Hydrogels

Hydrogels are three dimensional crosslinked networks depend on hydrophilic polymers that can absorb or retain water without dissolution. The hydrophilic property is due to presence of chemical residues such as –OH, -COOH, -NH₂, -CONH₂, -SO₃H and others with in molecular structure. Hydrogels have been extensively studied and preferred for a large number of applications in much kind of industrial fields (Pulat and Asil, 2009). Because of their excellent characteristics, hydrogels can also be used for controlled release of agrochemicals and nutrients in agricultural and horticultural applications (Pulat and Yoltay, 2016).

Most of the synthetic polymers used to prepare hydrogels causes some problems because of their long degradation times and degradation products. Natural polymers are a good choice to overcome this issue (Pulat Uğurlu, 2016).

In recently hydrogels formed from natural polymers such as NaCMC, carrageenan, gelatin, chitosan etc. have been studied extensively due to biodegradable, biocompatible, nontoxic.

NaCMC

Sodium carboxymethyl cellulose (NaCMC) is a representative cellulose derivative, which is water soluble cellulose ether, manufactured by reacting sodium monochloroacetate with cellulose in alkaline medium. NaCMC is a polysaccharide polymer with excellent bioadhesive, biodegradability and biocompatibility.

It is also known that NaCMC is a polyelectrolyte, and thus this 'smart' cellulose derivative presents sensitivity to pH and ionic strength variations. It is easy to form NaCMC hydrogels because of the large number of reactive hydroxyl groups on the polymer chains (Rafaat, Eid M and El-Arnaouty, 2012).

Besides, the presence of carboxylate groups in the macromolecular chain enables to bond the chains to bond each other via multivalent ionic crosslinking. Several kinds of ions can be used to form ionic hydrogels. As an eco-friendly and nontoxic crosslinking agent, trivalent iron (Fe^{3+}) is a suitable ion to prepare NaCMC hydrogels. Indeed, the presence of NaCMC in a cellulose-based hydrogel enhances electrostatic charges in network, which have a double effect on the swelling capability.

NaCMC is widely used in several applications such as cosmetics, food and wound care industries, medicine and agriculture etc. for gelling, thickening agent, stabilizer and suspending agent (Barbucci, Magnani, and Consumi, 2000).

AIM: The aim of this study was to obtain a system that provides the controlled release of plant micronutrient. The matrices structure was prepared using NaCMC, a natural- biodegradable polymer and copper as micronutrient. Characterization of the synthesized fertilizer system was performed by investigating their swelling/degradation behaviors. Release studies were also carried out in water and soil.

Method

Preparation of NaCMC Hydrogel Beads

As schematically given in Figure 3, four different types of NaCMC hydrogel beads were prepared via ionic crosslinking reaction using $FeCl_3$ (Akalın and Pulat, 2018). 7% of NaCMC solution was drop-wisely added into 25.0 mL of $FeCl_3$ solution at different concentrations by using a 26-gauge needle. The obtained spherical hydrogel beads were mixed with a mechanical stirrer (200 rpm) for 3 h. They were filtered and washed several times with distilled water to remove unreacted $FeCl_3$ on the surface of beads and dried under room temperature for 24 h. The amounts of polymer (P) and crosslinker (C) and the relative ratios were summarized in Table 2.

Table 2. Preparation of hydrogels

Hydrogel	NaCMC (%)	$FeCl_3$ (%)	C/P	<u>Mechanical properties</u>
NaCMC-1	7	4	0.57	Brittle
NaCMC-2	7	6	0.86	Durable, steady
NaCMC-3	7	8	1.14	Durable, steady
NaCMC-4	7	10	1.43	Durable, steady

Hydrogel Formation

Gravimetric tests were carried out, and the formula given below was used to determine hydrogel formation (HF) percentage. Dried and weighed samples were placed in water for 48 h to extract the unreacted monomers and then dried (Chen *et al.*, 2005).

$$HF (\%) = \frac{m}{m_0} \times 100 \quad (1)$$

where m and m_0 are the weights of the dried hydrogel after and before extraction, respectively.

Swelling Behaviors

Swelling tests of hydrogel beads were gravimetrically carried out in three steps. In the first step, the weighed dried hydrogels were immersed in 100 mL of swelling medium Britton-Robinson buffer (BRB) solutions at

pH=7.0, 30°C. Swollen gels removed from the swelling medium at regular intervals. Then, they were dried superficially with a filter paper, weighed, and placed into the same bath. The tests were performed until constant weight was reached. The swelling percentages of hydrogels were calculated from Equation 2:

$$\text{Swelling (\%)} = \frac{(W_2 - W_1)}{W_1} \times 100 \quad (2)$$

Where W_1 is the dry weight of the sample before swelling, W_2 is the swollen mass of sample in every 24 h. In second step, the dried hydrogels were swollen in BRB solution (pH= 7.0) at different temperatures ranging from 10 to 60°C to determine the effect of temperature on swelling behaviors. In the third step, dried hydrogels were immersed in different BRB solutions at various pH values (from 2.0 to 12.0) to investigate the effect of pH on the swelling behaviors. At the end of 24 h incubation, the swollen hydrogels were taken out from swelling medium, dried and weighed (Pulat and Asil, 2009).

Degradation Test

Degradation test of hydrogel beads were performed at pH= 7.0, 30°C (Pulat and Akalın, 2013). Dried samples were left to swell in BRB. At the end of 24 h, swollen gels were removed from solution and weighed. This mass (W_m) recorded as the maximum swollen state of hydrogels. Then, they placed into the same medium and the weighing was continued at regular intervals until hydrogel completely degraded. The degradation was determined in terms of weight loss (%) from Equation 3:

$$\text{Weight loss (\%)} = \frac{(W_m - W_t)}{W_m} \times 100 \quad (3)$$

where W_m is the weight of hydrogel at most swollen stage and W_t is the weight of hydrogel at time t.

SEM Observation

Depending on the swelling/degradation behaviors, NaCMC-4 hydrogel was chosen for release studies. Therefore, the morphological structure of NaCMC-4 was investigated via SEM observations. The hydrogel sample, swollen to equilibrium in water at room temperature, were removed and placed in a deep freezer at -20°C for 24 h and then transferred into a freeze dryer (Christ-Alfa 2-4 Model, Martin Christ GmbH, Germany) at -85°C for 1 week. The dried and swollen straps were coated with 200 Å Au. The surface micrographs of the samples were obtained with a scanning electron microscope (JEOL, JSM 6060A, Japan).

Preparation of the Copper Loaded Hydrogel

Copper loaded NaCMC-4 hydrogel was prepared by soaking method. 0.2 g of beads was left into copper solution (1.0 g/1 mL) for 4 h. Then, they were left to dry first in air and then in a vacuum oven at 40°C. So, each bead contains 0.5 mg of Cu.

Release Studies

In vitro release studies were carried out by using Atomic Absorption Spectrometer (AAS, Perkin Elmer A4000). Cu-loaded hydrogels were transferred in 100 mL distilled water. 0.5 mL of aliquot distilled water was with drawn at different time intervals. This process continued until the equilibrium in vitro release degree was reached (Pulat, Akalın and Demirkol, 2014).

Reproducible results were obtained with triplicate measurements. The cumulative release (%) of the Cu^{+2} was calculated with the following equation:

$$\text{Cumulative release (\%)} = \frac{W_t}{W_{\text{total}}} \times 100 \quad (4)$$

where W_t is the weight of the released Cu in the releasing medium at any time and W_{total} is the initial total weight of Cu^{+2} entrapped into the gel system.

A semi-empirical equation is introduced to represent the substance release process of the swelling polymer (Pulat, Tan and Onurdağ, 2011).

$$F = \frac{M_t}{M_1} \times kt^n \quad (5)$$

where F is fractional solute release, M_t and M_∞ are the amounts of u released at time t and the maximum released amount of MA, respectively. k is a characteristic constant related to the structure of the hydrogel network, and n is a swelling exponent.

Release Studies in Soil

Release studies were also performed in soil. 1of Cu-loaded bead was put into permeable chiffon package to preserve the sample from soil sticking. The packages were placed into the pots containing 5 L of dry torf at 2.0 cm depth. All pots were irrigated daily with 150 mL of water. Each day one package was removed from the pot and the bead was taken to be placed into 100 mL of distilled water. Cu^{+2} nutrient was extracted from the beads into the water and the Cu^{+2} diffusion was measured by AAS. So the amount of released Cu^{+2} into the soil had been calculated. This process was continued until the equilibrium soil release value was reached.

Results and Discussion

Hydrogel Formation

NaCMC hydrogel discs were produced as described in the methods. HF was calculated via Equation 1 and the result was given in Table 3. The lowest hydrogel formation was found as 94% for NaCMC-1 hydrogel. The gel content of NaCMC hydrogel beads that was given in Table 2 are verifying with HF, Ms and DT values. While the concentration of $FeCl_3$ was increased from 4% to 10%, the gel content of the samples also increased. The highest value was found 98% for NaCMC-4 hydrogel. The higher density improved the network binding forces of the polymers, which led to the increase of gel content. It is well known that polymer and crosslinker amounts promote the gel content, so the results are satisfying (Akalin and Pulat, 2018).

Table 3. HF, maximum swelling (MS) and time of 100% degradation (DT)

Hydrogel	HF (%)	MS (%)	DT (day)
NaCMC-1	94	292	36
NaCMC-2	96	213	37
NaCMC-3	97	135	36
NaCMC-4	98	102	38

Swelling results

All swelling percentages calculated from Equation 2. The photographs of dry and swollen hydrogels were presented in Figure 1.

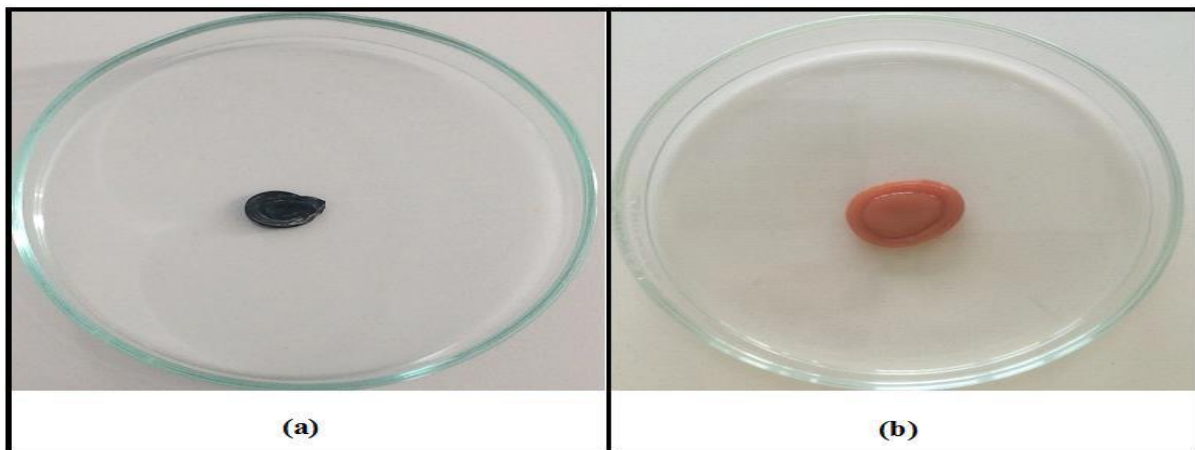


Figure 1. Dry and swollen NaCMC hydrogels

The variations of swelling values with time at pH 7.0 and 30°C were shown in Figure 2. The swelling increased with time initially and then remained constant at close to 24 h. S% values were determined to be 292% for the most swollen hydrogel NaCMC-1, and 102 % for the least swollen hydrogel NaCMC-4. Swelling values were directly connected with composition, monomer ratio, ionic charge content, polymerization route, type and density of cross-linker, and so forth (El-Sherbiny *et al.*, 2005). As C/P ratio increased, S% values decreased. This behavior is attributed to the fact that the network chains became inflexible at higher crosslinker density and thus, fewer amounts of water molecules penetrated the hydrogel structure.

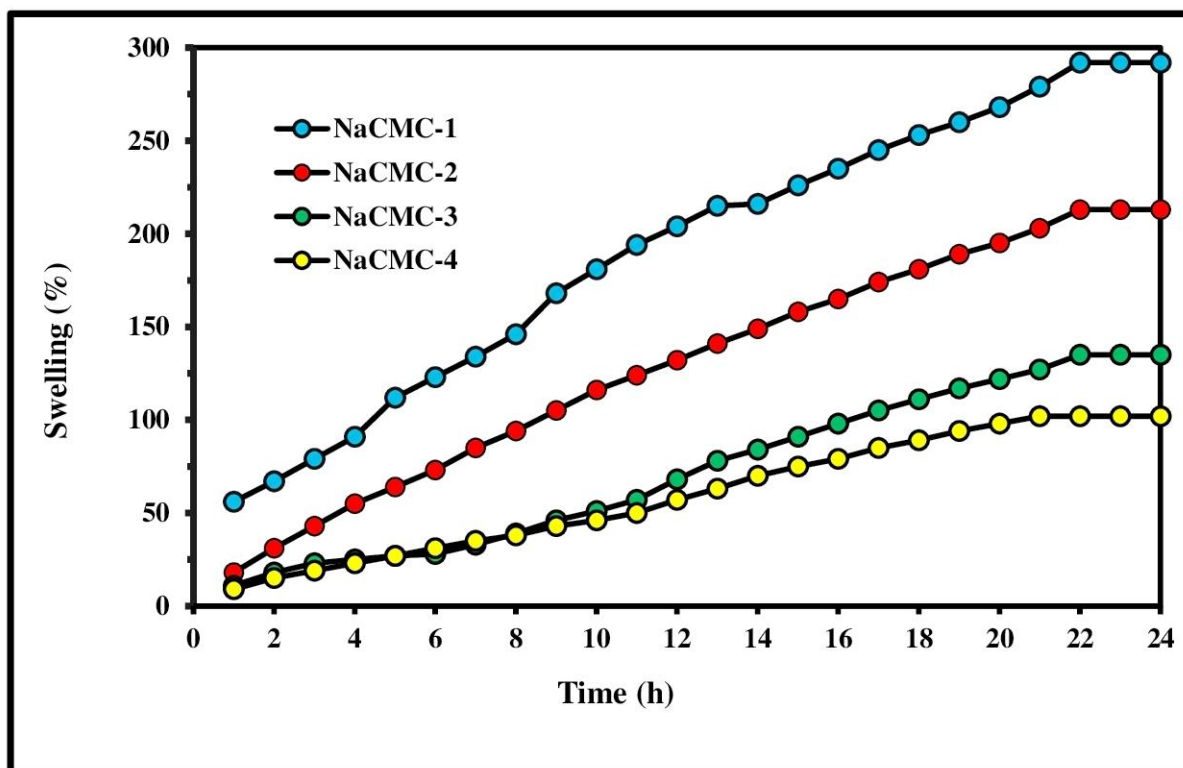


Figure 2. The variation of S% values with time at 30°C, pH = 7.0

The variations of swelling values with temperature at pH 7.0 and 24 h are presented in Figure 3. Swelling percentages slightly increased with temperature. As the temperature increases, thermal mobility of the polymer chains increases and H-bonds were broken, and hydrogels can easily swell. Because of their high stabilities, NaCMC hydrogels are suitable for using in wide temperature ranges.

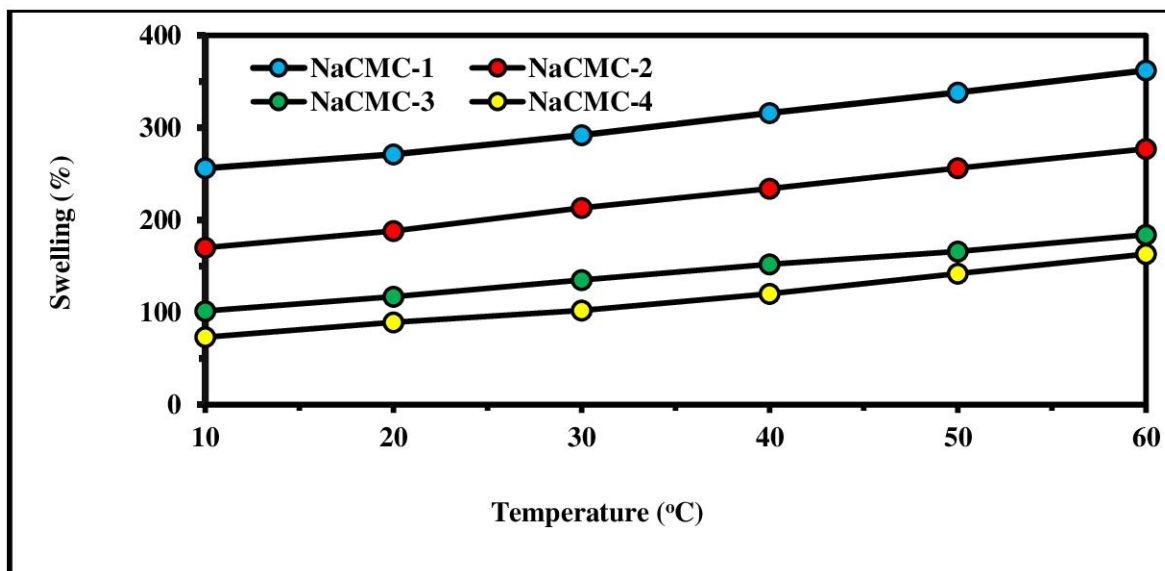


Figure 3. The variation of S% values with temperature at pH = 7.0 and 24 h

Figure 4 presents the variation of S% values of hydrogels with pH at 30°C and 24 h. As the pH is increased from 2 to 7, swelling values kept near constant and then a sharp increment was observed. . This result can be explained by the fact that the pKa of carboxylic acid groups containing in the polymer is about 4.5. These groups were ionized to the COO⁻ form since the pH of the environmental solution raised above its pKa value. The ionized negatively charged pendant groups on the polymer chains caused repulsion leading to swelling. As swelling pressure increased, hydrogel expanded and thereby maximizes the repulsion between the ionized groups.

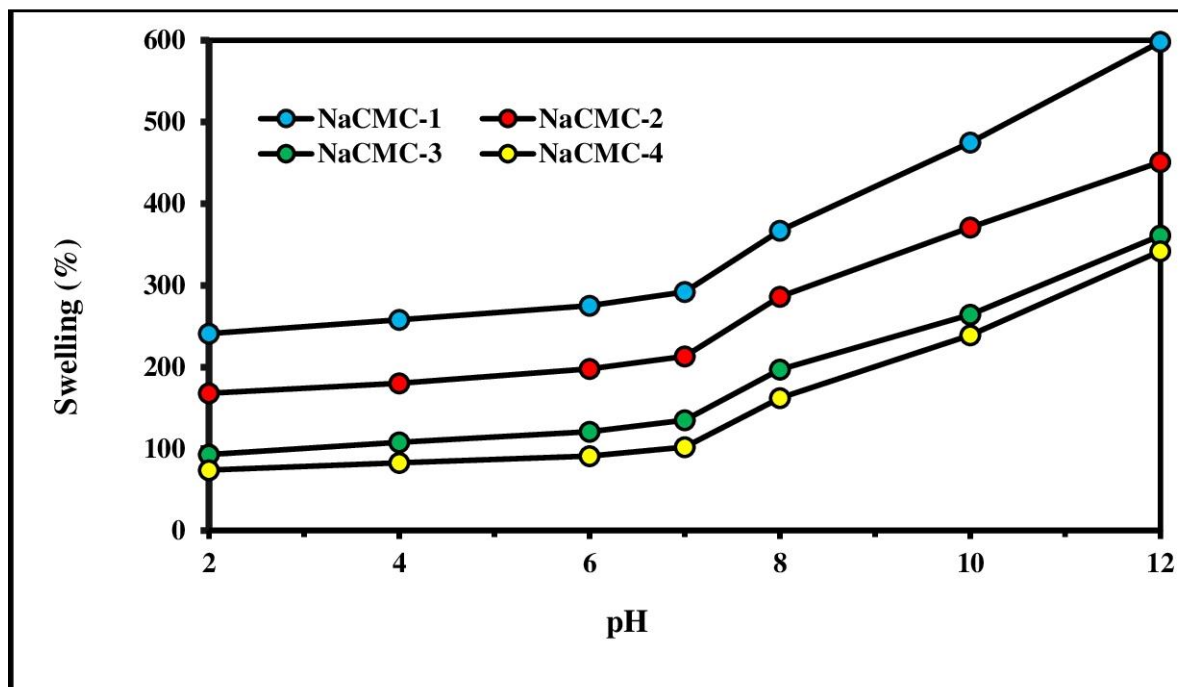


Figure 4. The variation of S% values with pH at 30°C, 24 h

Degradation

In this study, degradation values were calculated using Equation 3 and the degradation profiles were presented in Figure 5. All of the NaCMC hydrogels degraded in approximately 33-38 days. The fastest degradation was observed for NaCMC-1 hydrogel as 33 days. In general, crosslinking density is very effective on the degradations of the hydrogels. The high crosslinked hydrogel degraded slower than the lower crosslinked

hydrogels, since the number of intermolecular bonds enhanced with increasing crosslinking density. NaCMC hydrogels can be suitable for long-term applications because of their good stabilities.

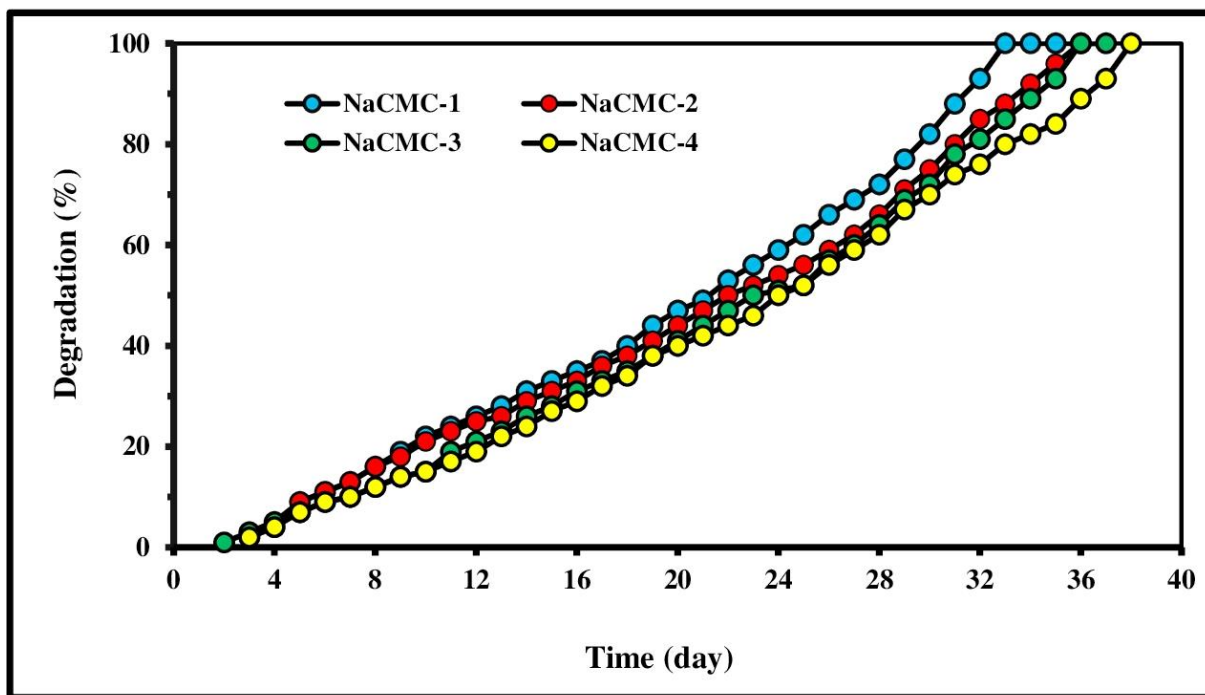


Figure 5. The degradation profiles of hydrogels at 30°C

SEM Analysis

The morphological differences between swollen hydrogels can be clearly observed from SEM micrographs given in Figure 10. The dried surface exhibited smooth and nonporous structure, in contrary the surface of swollen hydrogels had a granule structure. This situation can be explained that the ionic crosslinking occurred intensively on the surface. Polymer chains bound to crosslinker from large number of points, so a granulated view was appeared on the surface. The cross-section images of swollen hydrogels possessed a spongy structure with pores in different sizes from micro- to nano-scale, so this porosity enabled easy diffusion and absorption of water into the structure.

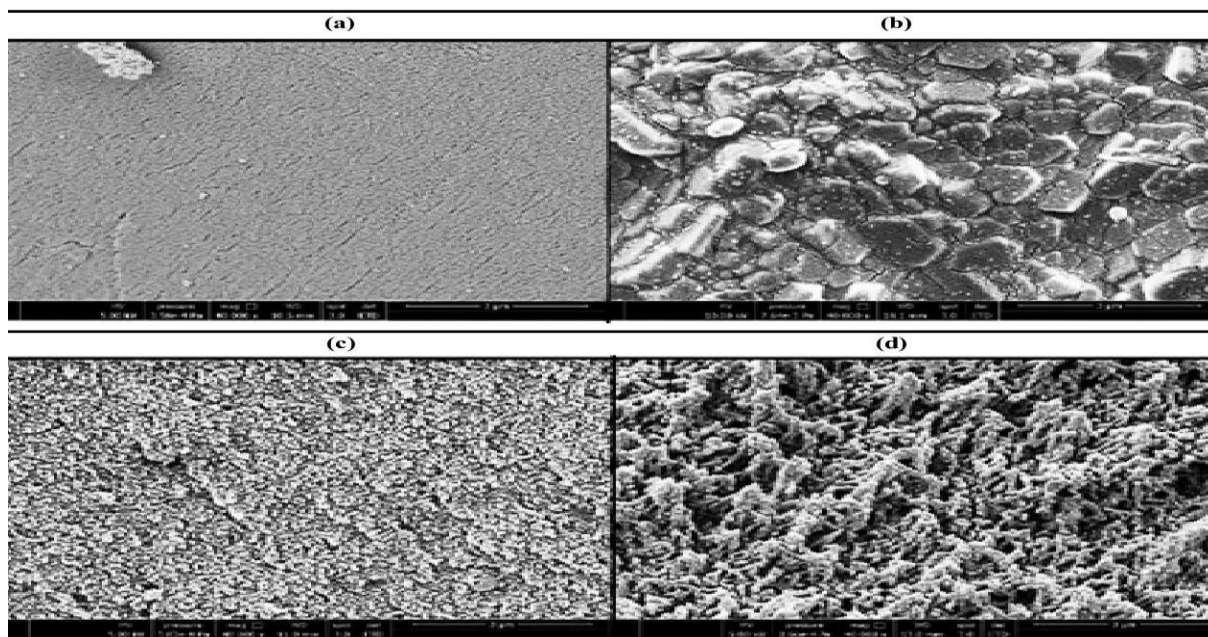


Figure 6. SEM micrographs of dry (a) surface (b) cross-section and swollen hydrogels (c) surface (d) cross-section (X 40000)

Micronutrient Release Kinetics

The release profile of copper micronutrients from NaCMC-4 is presented in Figure 7. The cumulative release (%) increased rapidly and then complied at near 25 h. Kinetic release parameters were calculated using Equation 4. 0.98 and $93,5 \times 10^{-3}$ were found for n and k, respectively. As n value of the hydrogel was found close to 1.0, it can be mentioned about zero order kinetic for this hydrogel. The meaning of this is release rate of Cu are nearly constant during release.

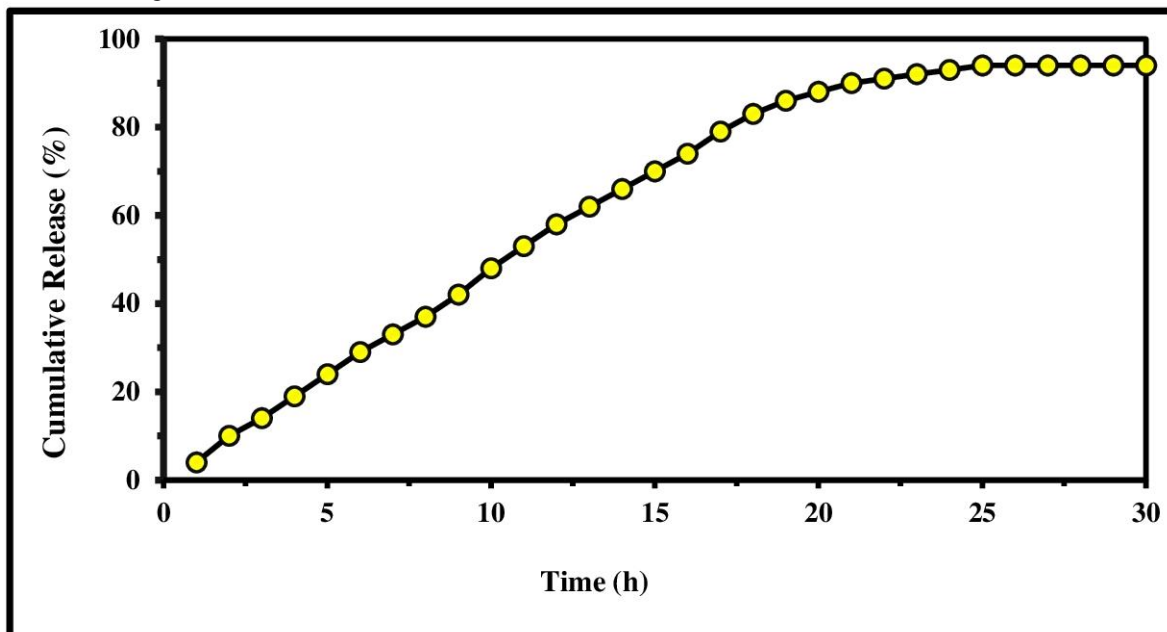


Figure 7. Cu+2 release in water from NaCMC-4 hydrogel

Soil Release

The Cu release through NaCMC-4 hydrogel in soil was also investigated and the profile was given in Figure 8. The maximum release value was reached as 83% at near about 16 days. Release in water 15 times faster than in soil. It could be concluded that this prepared micronutrient-loaded hydrogel system can be effective for a long time uses.

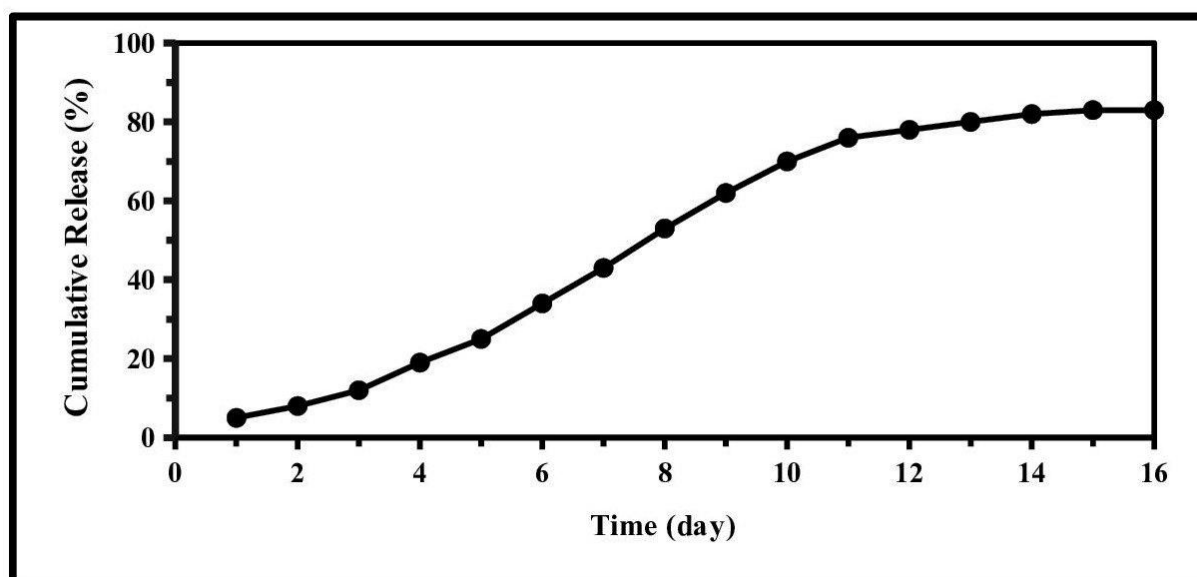


Figure 8. Cu+2 release in soil from NaCMC-4 hydrogel hydrogel

Conclusion

The results of the present work indicate that the NaCMC hydrogels are good support materials for controlled releasing Cu micronutrient with their excellent swelling/degradation capability. It can be concluded that the CRF system produced in this study is much promising in utilizing a natural resource like CMC in the production of matrix material which could significantly reduce the production costs and offering a quite environmental friendly alternative technique.

References

- Akalin G.O., Pulat M. (2018). Preparation and Characterization of Nanoporous Sodium Carboxymethyl Cellulose Hydrogel Beads, *Journal of Nanomaterials*, Article ID 9676949, 12 pages.
- Barbucci, R., Magnani, A., and Consumi, M. (2000). Swelling behavior of carboxymethylcellulose hydrogels in relation to crosslinking, pH, and charge density,” *Macromolecules*, 33:20, 7475–7480.
- Chen K., Ku Y., Lin H., Yan T., Sheu D., Chen T., Lin F. (2005). Preparation and characterization of pH-sensitive poly (N-vinyl 2-pyrrolidone/itaconic acid) copolymer hydrogels. *Mat. Chem. Phys.* 91, 484-489.
- El-Sherbiny I.M., Lins R.J., Abdel-Bary E.M., Harding D.R.K.(2005). Preparation, characterization, swelling and in vitro drug release behaviour of poly(N-AG-chitosan) interpolymeric pH and therm.-responsive hydrogels. *Europ. Polym. J.* 41, 2584-2591.
- Pulat M., Akalin G.O. (2013). Preparation and characterization of gelatin hydrogel support for immobilization of *C. Rugosa* lipase. *Artif. Cells Nanomed. Biotechnol.* 41, 145-151.
- Pulat M., Akalin G.O, Demirkol Karahan N. (2014). Lipase release through semi-interpenetrating polymer network hydrogels based on chitosan, acrylamide, and citraconic acid. *Artif. Cells Nanomed. Biotechnol.* 42, 121-127.
- Pulat M., Asil D. (2009). Fluconazole release through semi-ipn hydrogels based on chitosan, AA, and citraconic acid. *J. Appl. Polym. Sci.* 113, 2613-2619.
- Pulat M., Tan N., Onurdağ F.K. (2011). Swelling dynamics of IPN hydrogels including acrylamide-acrylic acid-chitosan and evaluation of their potential for controlled release of piperacillin-tazobactam. *J. Appl. Polym. Sci.* 120, 441-450.
- Pulat M. & Uğurlu N. (2016). Preparation and characterization of biodegradable gelatin-PAAm-based IPN hydrogels for controlled release of maleic acid to improve the solubility of phosphate fertilizers, *Soft Materials*, , 14:4, 217–227.
- Pulat M., Yoltay N. (2016). Smart fertilizers: preparation and characterization of gelatin-based hydrogels for controlled release of MAP and AN fertilizers, *Agrochimica*, 60:4, 249-261.
- Rafaat A.I, Eid M., El-Arnaouty M.B. (2012). Radiation synthesis of superabsorbent CMC based hydrogels for agriculture applications. *Nucl. Instr. Meth. Phys. Res. B*, 283, 71-76.
- Trenkel M.E. (2007). Controlled release fertilizers: trends and technologies. *Pharmaceutica.* 5, 1-15

Author Information

Mehlika Pulat

Gazi Üniversitesi, Fen Fakültesi, Kimya Bölümü–
Teknikokullar, Ankara/Türkiye
Contact e-mail: mpulat@gazi.edu.tr

Gulen Oytun Akalin

Scientific and Technological Application and Research
Center, Aksaray University, Aksaray/Turkey

Antagonistic of some *Trichoderma* against *Fusarium Oxysporum* sp. f. *cubense* Tropical Race 4 (FocTR4)

Laith Khalil Tawfeeq AL-ANI
University of Baghdad

Shaymaa Fadhel Abbas ALBAAYYIT
University of Baghdad

Abstract: *Fusarium* wilt of banana is a very important fungus that caused the destruction of banana trees in the tropical countries. Biological control is an alternative method to control *Fusarium* wilt diseases such as *Trichoderma* has been known to be particularly active in the control of the plant pathogens. This study aimed to evaluate the ability *Trichoderma* isolates from suppressive soils in Malaysia to suppress *Fusarium* wilt of banana *in vitro*. Thirty one of *Trichoderma* isolates were tested their ability to inhibit the growth of FocTR4 LJ27 strain. The isolates were screened *in vitro* by volatile compounds tested of *Trichoderma* isolates against LJ27 strain. Then eight *Trichoderma* spp. strains (TR10, T10v1, T1, Tveg2, TR102, TL5, Tveg1, T26) was produced the high toxic metabolites with strong activity against LJ27 strain, inhibiting the mycelia growth by 50.33%, 51.33%, 51.67%, 69%, 70.67%, 71.33%, 78%, 96% respectively. The result indicated to a high efficacy of *T. parareesei* T26 for inhibiting the growth of FocTR4. But five isolates of *Trichoderma* such as *T. brevicompactum* (TL7), *T. reesei* (T658, TL102, and TL13552), and *T. harzianum* (TL21) were showing the very low effect on FocTR4. The volatile compounds can produce for the inhibiting of developing of FocTR4 *in vitro*. This improves the high efficacy of *Trichoderma* to use as alternative methods in reducing the synthetic chemicals that are causing a toxic pollution for our environment.

Keyword: FocTR4, *Trichoderma*, Biocontrol, Banana, *Fusarium* wilt

Introduction

Fusarium wilt of banana is a very important fungus that caused the destruction of banana trees in the wide world. This strain is forming high dangerous on the banana *Farming* in many tropical and subtropical countries such as Australia, Malaysia, Jordan, Oman, and Africa (Ploetz, 2006; Ploetz *et al.*, 2015). *Fusarium* wilt could not be controlled effectively, since its discovery. Many other groups of microorganisms have been proposed in the suppression of *Fusarium* wilts on other plants such as *Pseudomonas fluorescens* (Mohammed *et al.*, 2011; Al-Ani 2017), and *Trichoderma* spp. Many reports have indicated that *Trichoderma* spp. can suppress *Fusarium* wilt pathogens effectively (Calvet *et al.*, 1990) including *Fusarium* wilt of banana (Kidane and Laing, 2010). The biocontrol mechanisms of *Trichoderma* can be divided into mycoparasitism, competition, antibiosis, induced resistance, and action of cell wall degrading enzymes (Benítez *et al.*, 2004; Al-Ani 2018). Some of *Trichoderma* spp. have been described as having the ability to inhibit the growth of plant fungal pathogens by producing the volatile compounds (Raza *et al.*, 2013). *T. harzianum* T15 was able to inhibit growth the soil-borne plant pathogens including *Fusarium moniliforme*, *F. culmorum*, and *Gaeumannomyces graminis* var. *tritici* *in vitro* (Kucuk and Kivanc, 2004). Many strains of *Trichoderma* spp. produced the secondary metabolites having the toxic effect on the pathogen-host directly (Vinale *et al.*, 2014). *T. harzianum* was secreting volatile compounds showing high inhibition for the growth of *Fusarium oxysporum* f. sp. *melongenae* (Cherkupally *et al.*, 2017). Therefore, this study is very interesting to evaluate the efficiency of *Trichoderma* spp. in suppressing FocTR4 by producing volatile metabolites.

Methods

Isolate *F. oxysporum* f. sp. *ubense* Tropical race 4

The isolate of *Foc*TR4 LJ27 strain was collected from Dr. Laith K.T. Al-Ani (School of Biological Science, Universiti Sains Malaysia, Malaysia), and re-cultured on Potato dextrose agar.

Isolates *Trichoderma* spp.

Thirty one *Trichoderma* spp. were collected from Dr. Laith K.T. Al-Ani (School of Biological Science, Universiti Sains Malaysia, and Malaysia) and re-cultured on Potato dextrose agar.

Volatile metabolites test

In vitro inhibitory effects of *Trichoderma* spp. isolates against pathogenic LJ27 by the production of volatile metabolites were evaluated using the inverted plate method (Dennis and Webster, 1971) with some modifications. The plugs (5 mm in diameter each) of 31 isolates of *Trichoderma* were testing against plugs (5 mm) of LJ27 individually. A plug LJ27 of Petri dish inverted on fungal-free agar media using as a control factor. Three replicates were prepared for each npF. Colony diameters of the pathogen were measured at 7 days post incubation. Growth inhibition percentage was calculated as follows:

$$\text{PIRG}\% = \left[\frac{\text{Fp} - \text{Tt+p}}{\text{Fp}} \right] \times 100$$

Where:

PIRG, percent of growth inhibition;

FP, growth rate of pathogenic LJ27 control;

Tt+P, a growth rate of pathogenic LJ27 in treatment were combined with each the biocontrol factor of 31 *Trichoderma* isolates (El-Katatny *et al.*, 2011).

Results and Discussion

For evaluation and efficacy of *Trichoderma* spp. could confront and produce the volatile compounds affecting on the growth of *Foc*TR4. *Foc*TR4 was isolated from banana rhizosphere samples which were collected from random banana fields in Terong-Perak-Malaysia. All *Trichoderma* spp. were isolated from the rhizosphere and root and soil samples of the healthy banana plant. In this study, a total 31 strains of *Trichoderma* spp. are including *T. harzianum* (TL21, TL22, TL4, TL5, TL6, Tveg1, Tveg2, TR1031, TR1032 and T3), *T. reesei* (TL1, T31, T658, TL1355, TL13552, TL1322, TL101, T1 and TL102), *T. parareesei* (T6581, TL13551, TL261, T26, TL262, T10v1 and T2), *T. brevicompactum* (TL7), *T. koningii* (TR102), *T. atroviride* (TR10), *T. erinaceum* (TL3), and *T. capillare* (TL2), that isolated from banana healthy were testing against *Foc*TR4 both of dual culture and volatile compound tests. For volatile metabolites test, thirty one isolates of *Trichoderma* spp. showed different antagonistic effects against LJ27. The antagonism of the growth inhibition of the pathogen colony varied among strains of *Trichoderma* spp. The eight strains of *Trichoderma* spp. such as (TR10, T10v1, T1, Tveg2, TR102, TL5, Tveg1, and T26) was produced the high toxic metabolites with strong activity against *Foc*TR4, inhibiting the mycelia growth by 50.33%, 51.33%, 51.67%, 69%, 70.67%, 71.33%, 78%, and 96% respectively (Fig. 1).

The result shows the high role of *Trichoderma* in control the fusarium wilt disease and ability to parasite on hyphae of *Foc*TR4 that lead to degrading the full colony for this pathogen. Several *Trichoderma* spp. are having the ability to produce the antifungal compound that effects indirectly on fungal growth (Al-Ani, 2018). The volatile compounds are produced for the inhibiting of developing of *Foc*TR4 *in vitro*. The cell wall of *Foc*TR4 that contain chitin may possibly be as inducer factor for *Trichoderma* to produce the analysis metabolites that high affect on the fungal cell wall. Kucuk and Kivanc (2004) indicated for the ability of *Trichoderma* to produce the important metabolites that inhibit the mycelium growth. *Trichoderma* is secreting the secondary metabolites that related to the host. *Foc*TR4 may produce some secondary compounds that induce *Trichoderma* to attack *Foc*TR4 indirectly by producing several antifungal compounds. Therefore, they found some isolates of

Trichoderma producing the secondary metabolites very effect on the *Foc*TR4 growth but other did not affect on *Foc*TR4. Vinale *et al.*, (2009) indicated for the presence a relation between productions the secondary metabolites by *Trichoderma* with the pathogen-host.

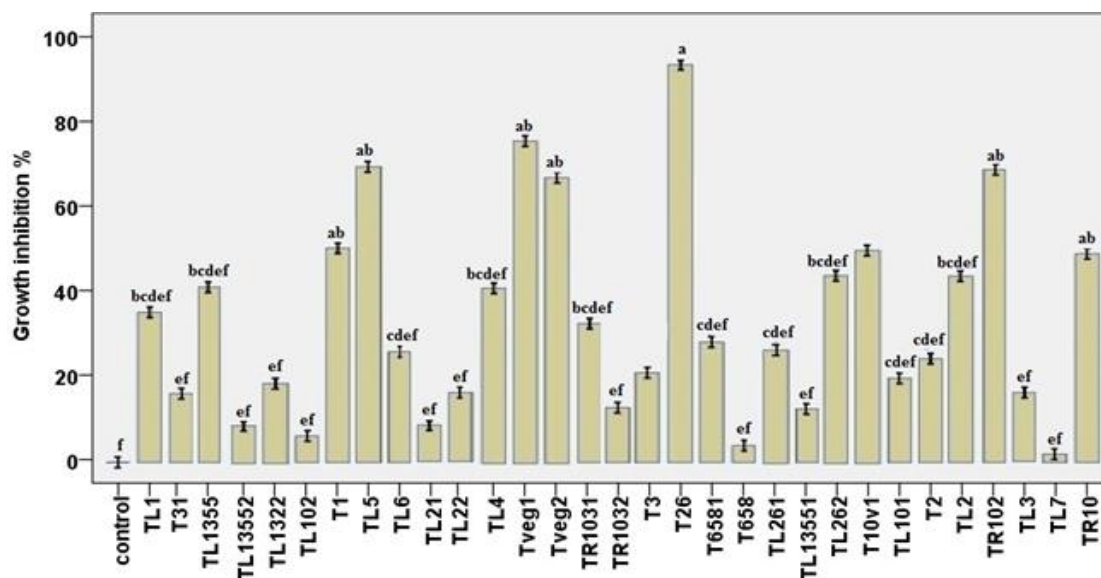


Figure 1. Effect of volatile metabolites produced by *Trichoderma* isolates towards LJ27 on PDA expressed as percentage of inhibition of LJ27 mycelia daily growth rate after 5 days of incubation. a) LSD = 0.055, b) LSD = 0.072, c) LSD = 0.063, d) LSD = 0.050, e) LSD = 0.051, f) LSD = 0.073, (Appendix E)

Conclusion

There are many methods useful for control the plant pathogens. Biological factor as *Trichoderma* is very important agent. It showed high efficacy in control *Foc*TR4. It could affect on the growth of pathogen *Foc*TR4 from distance. The T26 isolate of *T. parareesei* was showed high inhibition for the growth of *Foc*TR4 at 96%. But three species of *Trichoderma* spp. such as *T. harzianum* (Tveg1 and TL5) and *T. koningii* (TR102) showed a middle ability in growth inhibition of *Foc*TR4 at 70.67%, 71.33%, 78%. While, five isolates of *Trichoderma* spp. such as *T. brevicompactum* (TL7), *T. reesei* (T658, TL102, and TL13552), and *T. harzianum* (TL21) didn't effect on mycelium growth of *Foc*TR4 that decrease the growth at range between 2% to 9%. It indicated for the high trait of some strains of *Trichoderma* in control of *Foc*TR4 by producing many secondary metabolites and inhibits the mycelium growth without contact between them. This result indicates that some those of secondary metabolites have the ability in degrading the hyphae of *Foc*TR4 as the antifungal.

Recommendations

This study is useful for controlling on *Foc*TR4 without using chemical pesticides. *Trichoderma* could produce the secondary metabolites impacting on the mycelium growth without contact between them. In additional, *Trichoderma* spp. were different in effect on the growth of *Foc*TR4. Therefore, it can detect the kinds of secondary metabolites that have antifungal activity against *Foc*TR4 in further future.

Acknowledgements

Thank you for funding supports from the fusarium lab – school of Biology Science – Universiti Sains Malaysia. Thank you for all the collaborative efforts between individuals from school of Biology Science.

References

- Al-Ani, L.K.T. (2017). PGPR: A Good Step to Control Several of Plant Pathogens. In: Singh, H.B., Sarma, B.K. and Keswani, C. (Eds), Advances in PGPR Research. CABI, UK, pp.398-410.
- Al-Ani, L.K.T. (2018). *Trichoderma*: beneficial role in sustainable agriculture by plant disease management. In: Egamberdieva D., Ahmad P. (eds) Plant Microbiome: Stress Response. Microorganisms for Sustainability, vol. 5. Springer, Singapore, pp. 105-126.
- Benítez, T., Rincón, A.M., Limón, M.C. and Codón, A.C. (2004). Biocontrol mechanisms of *Trichoderma* strains. *International Microbiology*, 7:249-260.
- Calvet, C., Pera, J. and Bera, J.M. (1990). Interaction of *Trichoderma* spp. with *Glomus mossae* and two wilt pathogenic fungi. *Agricultural Ecosystem and Environment*, 29: 59-65.
- Cherkupally, R., Amballa, H. and Reddy, B.N. (2017). In vitro antagonistic activity of *Trichoderma* species against *Fusarium oxysporum* f. sp. *melongenae*. *International Journal of Applied Agricultural Research*, 12(1):87-95.
- Dennis, C. and Webster, J. (1971). Antagonistic properties of species- group of *Trichoderma* II. Production of volatile antibiotics. *Transactions of the British Mycological Society*, 57: 41-48.
- El-Katatny, M.H., El-Katatny, M.S., Fadi-Allah, E.M. and Emam, A.S. (2011). Antagonistic effect of two isolates of *Trichoderma harzianum* against postharvest pathogens of tomato (*Lycopersicon esculentum*). *Archives of Phytopathology and Plant Protection*, 44(7): 637-654.
- El-Katatny, M.H., El-Katatny, M.S., Fadi-Allah, E.M. and Emam, A.S. (2011). Antagonistic effect of two isolates of *Trichoderma harzianum* against postharvest pathogens of tomato (*Lycopersicon esculentum*). *Archives of Phytopathology and Plant Protection*, 44(7): 637-654.
- Kidane, E.G. and Laing, M.D. (2010). Integrated Control of *Fusarium* Wilt of Banana (*Musa* spp.). *Acta Horticulturae*, 879: 315-321.
- Kucuk, C. and Kivanc, M. (2004). *In vitro* antifungal activity of strains of *Trichoderma harzianum*. *Turkish Journal of Biology*, 28:111-115
- Mohammed, A.M., AL-Ani, L.K.T., Bekbayeva, L. and Salleh, B. (2011). Biological Control of *Fusarium oxysporum* f. sp. *cubense* by *Pseudomonas fluorescens* and BABA *in vitro*. *World Applied Sciences Journal*, 15(2):189-191.
- Ploetz, R., Freeman, S., Konkol, J., Al-Abed, A., Naser, Z., Shalan, K., Barakat, R. and Israeli, Y. (2015). Tropical race 4 of Panama disease in the Middle East. *Phytoparasitica*, 43: 283-293.
- Ploetz, R.C. (2006). *Fusarium* wilt of banana is caused by several pathogens referred to as *Fusarium oxysporum* f. sp. *cubense*. *Phytopathology*, 96: 653-656.
- Raza, W., Faheem, M., Yousaf, S., Rajer, F.U. and Yameen, M. (2013). Volatile and non-volatile antifungal compounds produced by *Trichoderma harzianum* SQR-T037 suppressed the growth of *Fusarium oxysporum* f. sp. *niveum*. *Science Letters*, 1(1): 21-24.
- Vinale, F., Ghisalberti, E.L., Sivasithamparam, K., Marra, R., Ritieni, A., Ferracane, R., Woo, S. and Lorito, M. (2009). Factors affecting the production of *Trichoderma harzianum* secondary metabolites during the interaction with different plant pathogens. *Letters in Applied Microbiology*, 48:705-711.
- Vinale, F., Sivasithamparam, K., Ghisalberti, E.L., Woo, S. L., Nigro, M., Marra, R., Lombardi, N., Pascale, A., Ruocco, M. and Lanzuise, S. (2014). Manganiello, G.; Lorito, M. *Trichoderma* secondary metabolites active on plants and fungal pathogens. *The Open Mycology Journal*, 8:127-139.

Author Information

Laith Khalil Tawfeeq Al-Ani

University of Baghdad

Baghdad/Iraq

Contact e-mail: laith.kt77@gmail.com

Shaymaa Fadhel Abbas Albaayit

University of Baghdad

Baghdad/Iraq

New Fused Heterocyclic Compounds: Synthesis of Some 1,4-di[1,2,4-Triazoles[3,4-b]5-phenyl/aryl-1,3,4-thiadiazole] Benzene

Mohanad Yakhdan SALEH
University of Mosul

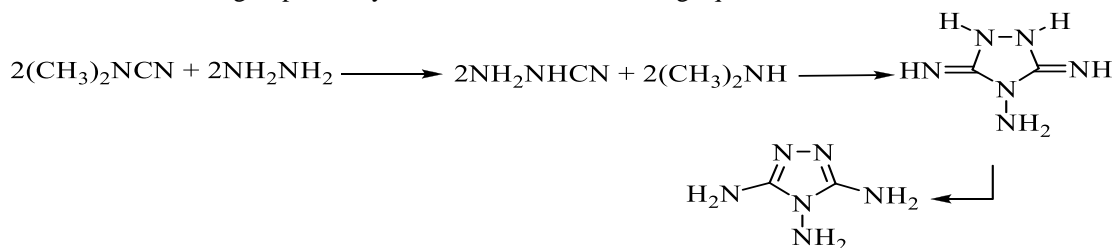
Abstract: In this paper the synthesis of some substituted di – 1,2,4-triazoles and its conversion to multi nuclear heterocyclic compounds ; described Terphthalic acid was esterified to its ethyl ester(1) by its reaction with absolute ethanol , concentrated sulfuric acid , the ethyl ester (1) was treated with hydrazine hydrate in ethanol to give the acid hydrazide (2). the hydrazide (2) then treated with ammonium thiocyanate to give thiosemicarbazide (3) , reaction of thiosemicarbazide (3) with hydrazine hydrate gave 1,4-bis(3-thiol-4-amino-1,2,4-triazole-5-yl) benzene (4). Compound (4) treatment with three type substituted benzaldehyde gave 1,4-di hydrazones phenyl (5,6 and 7). Cyclization hydrazones compounds (5,6,7) with phosphorous oxychloride in xylene to gave bicyclic system 1,4-bis[1,2,4-triazole[3,4-b]-5-substituted – 1,3,4-thiadiazole] benzene (8,9 and 10) . On the other hand some physical parameters of compounds (4 -10) under investigation such as the Mullikan charge at the active atoms, HOMO and LUMO energy levels , hardness (η) , electronic chemical potential (μ) and global electrophilicity index (W) were theoretically calculated using (Gaussian program). The antibacterial activity some of the synthesis compounds was studied. The structures of the synthesized compounds were confirmed by physical and spectral methods.

Keyword: Heterocyclic, Triazoles , Thiadiazole, Terphthalic acid

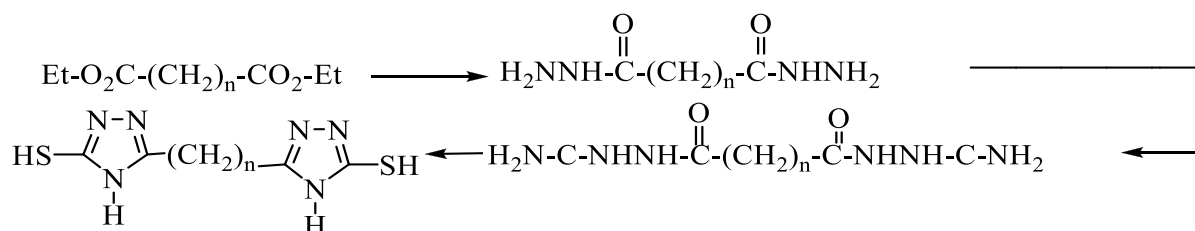
Introduction

Substituted 1,2,4- triazoles possess various biological activities and acts in some cases as a drugs⁽¹⁾ , 1,2,4-triazoles have aromatic properties⁽²⁾ and stable against high temperature⁽³⁾.

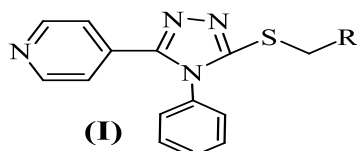
1,2,4- triazole was first synthesized from benzoyl isocyanate and phenyl hydrazine⁽⁴⁾. Quanzine 1,2,4- triazole contains three amino groups was synthesized as in the following equation is⁽⁵⁾:



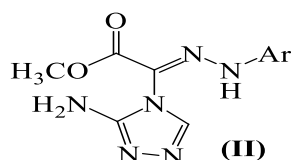
Bicyclic 1,2,4- triazole compounds were synthesized from ethyl succinate , ethyl glutarate⁽⁶⁾ and ethyl butyrate⁽⁷⁾.by conversion to acid hydrazide , the hydrazide was treated with ammonium thiocyanate to give thiosemicarbazide which cyclized to the product as follows :



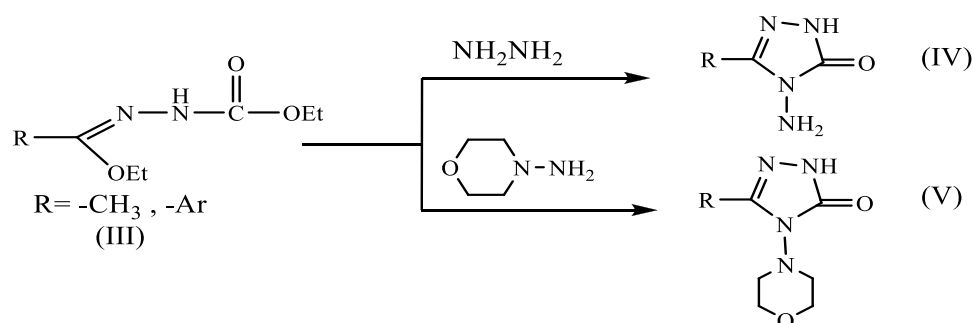
Which show a biological and medical importance⁽⁷⁾. Substituted 1,2,4-triazoles were synthesized from dithiocarbazide salt⁽⁸⁾ and substituted thiosemicarbazide⁽⁹⁾. Some novel 1,2,4-triazole compounds containing pyridine moiety were synthesized under microwave assistant conditions by multi-step reaction, as compound (I).



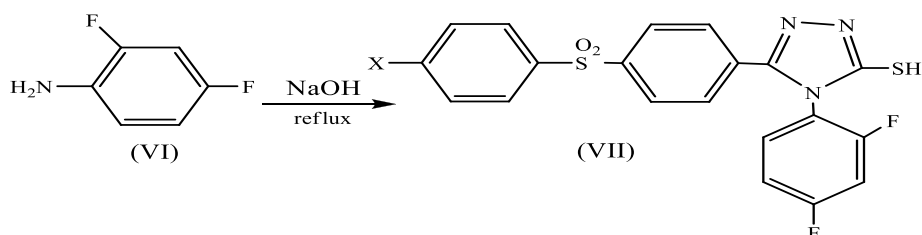
Theoretical calculation of compound (I) was carried out with B3LYP/6-31G the full geometry optimization was carried out using 6-31G(d,p) basis set and the frontier orbital energy, atomic net charge was discussed⁽¹⁰⁾. The reaction of hydrazonoyl halide with 3-aminotriazole in tetrahydrofuran / triethyl amine produce methyl-2-[3-amino-4H-1,2,4-triazol-4-yl]-2-[2-(4-chlorophenyl) hydrazone] acetate (II)⁽¹¹⁾.



Some antimicrobial 1,2,4-triazole derivative (IV,V) were synthesized from the reaction of ester ethoxycarbonyl hydrazone (III) with primary amine⁽¹²⁾.

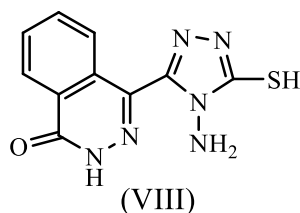


Recently some 1,2,4-triazole compounds (VII) showed good antioxidant activity. These compounds were synthesized by the reaction of hydrazinecarbothioamides (VI) with sodium hydroxide⁽¹³⁾.



The azo dyes containing 1,2,4-triazole ring were synthesized and was found that it may exist in three tautomeric forms specially when para substituted aniline coupling compound was used. 3-ethylthio-5-cyanomethyl-4-phenyl-1,2,4-triazole was treated with diazotized aniline derivatives⁽¹⁴⁾.

The synthesis of 4-(4-amino-5-mercapto-1,2,4-triazol-3-yl)phthalazin-1-(2H)-one was achieved (VIII), from the reaction of 4-oxo-3,4-dihydrophthalazine-1-carbohydrazide with potassium hydroxide in ethanol followed by the addition of carbon disulfide and the mixture than stirred at room temperature to give the potassium salt, its reaction with hydrazine hydrate give final product (VIII)⁽¹⁵⁾.



In this paper the synthesis of fused ring system 1,3,4-thiadiazole - triazole is studied.

Experimental

All chemicals were purchased from Flucka and BDH Chemical Ltd. The melting points were measured on an Electrothermal 9300 Engineering LTD and were uncorrected. IR spectra were recorded on Infrared Spectrophotometer Model Tensor 27, Bruker Co., Germany, using KBr discs. UV spectra were recorded on Shimadzu Double-Beam Spectrophotometer UV-210 A using ethanol as a solvent.

Synthesis of Diethyl terphthalate (1)⁽¹⁶⁾ :

To terphthalic acid (0.025 mole) in absolute ethanol (50 ml), concentrated sulfuric acid (5 ml) was added with cooling, the mixture was refluxed for (8 hours) the solvent was evaporated and the residue then neutralized with 20% sodium bicarbonate, the ester was precipitated as white solid, filtered and recrystallized from ethanol – water, m.p.(214°C), yield (80%).

Synthesis of Terphthalic aced hydrazide (2)⁽¹⁷⁾ :

A mixture of diethyl terphthalate (1) (0.01 mole) and hydrazine hydrate (5 ml, 0.1 mole) in ethanol (30 ml) was refluxed for (10-12) hours the solvent was condensed under reduced pressure a pale brown crystals hydrazide was formed, filtered and recrystallized from ethanol. m.p.(283°C), yield (86%).

Synthesis of Dithiosemicarbazides (3)⁽¹⁸⁾:

Hydrazide (2) (0.1 mol) in ethanol absolute was added to a mixture of carbon disulfide (0.15 mole) and potassium hydroxide (0.15 mole) in absolute ethanol (100 ml) the mixture was refluxed for (16 hours), after the mixture was cooled, dry ether (150 ml) was added the product precipitated, filtered under suction, the greenish yellow salt m.p.>(310°C), yield (58%)

Synthesis of 1,4- (3-thiol-4-amino-1,2,4-triazole-5-yl) benzene (4)⁽¹⁹⁾:

The salt (3) (0.02 mole) was dissolved hydrazine hydrate (0.04 mole) and water (2ml). the mixture was refluxed with stirring for (2 hours) the mixture was cooled, pale green crystals washed with water (100ml), dried and recrystallized from ethanol to give pale brown crystals, m.p.(211-213°C), yield (62%)

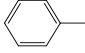
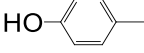
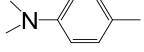
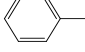
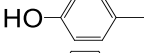
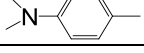
Synthesis of Hydrazones: 1,4-bis (3-thiol-4-substituted-benzylideneamino) -1,2,4-triazol-5-yl) benzene (5-7)⁽²⁰⁾:

A mixture of (4) (0.01 mole) substituted benzaldehyde (0.02 mole), hydrochloric acid (0.5 ml) in ethanol (25 ml) was refluxed for (2) hours the product was cooled and filtered. tables (1,3).

Synthesis of 1,4-di[1,2,4-triazole[3,4-b]-5-substituted – 1,3,4-thiadiazole] benzene (8, 9, 10)⁽²¹⁾:

Compound (5,6 or 7) (0.0025 mol) was dissolved in dry xylene (50 ml) phosphorus oxychloride (10 ml) was added and the mixture refluxed for (6-8) hours. The reduced pressure, cold water was added and the precipitate filtered and recrystallized from ether – pet. ether, tables (1,3).

Table 1. Physical data of compounds (5-10)

Comp. no.	Ar	M.P. °C	Yield %	Color
5		91	74	Pale yellow
6		68	72	Pale yellow
7		79	81	White
8		139	76	Dark brown
9		153	64	Brown
10		161	83	Pale brown

Theoretical Calculation

By use (chem. Office V11) counting Gaussian program is very important and good work advance calculator and give the way for researcher to conduct theoretical and support applied research.

In this paper calculate theoretical some parameter for compound (4-10) by :

1. Draw the figure by (Chem. 3D).
2. Make loser energy by (MM2).
3. Calculate HOMO & LUMO energy .
4. By used equation 1 , 2 , 3 calculate (η) hardness , (μ) electron chemical potential , (W) Global electrophilicity Index .

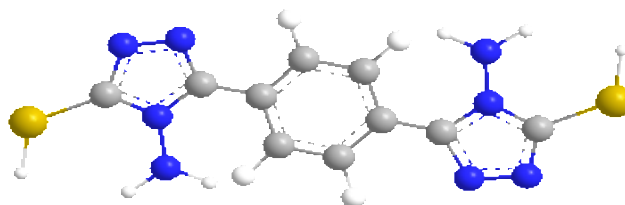
$$\eta = 1/2 (E_{LUMO} - E_{HOMO}) \dots\dots(1)$$

$$\mu = 1/2 (E_{HOMO} + E_{LUMO}) \dots\dots(2)$$

$$W = \frac{\mu^2}{2\eta} \dots\dots(3)$$

Result and Discussion

In this paper the synthesis of some substituted fused ring 1,2,4-triazoles is reported . and draw 3D for compounds (4-10) figure (1):



4

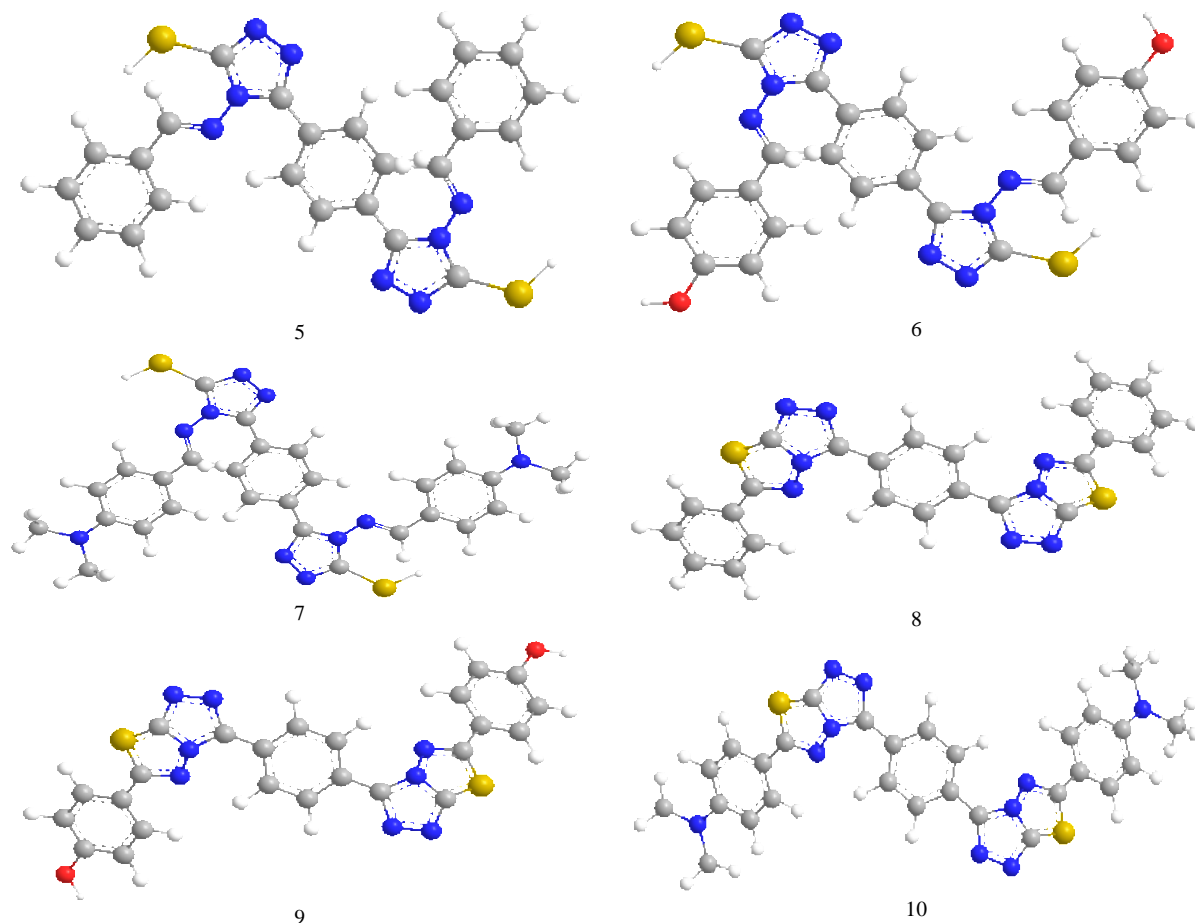


Figure 1. Structure 3D synthesis compounds (4-10)

The structure shows the compounds is not planar and gives an idea as to state energy for surface and according to calculation of energy of HOMO, highest occupied molecular orbital; LUMO, lowest unoccupied molecular orbital theory in table 3, that's important factors that affect bioactivity. HOMO has the priority to provide electrons, while LUMO can accept electrons first⁽²²⁾. The geometry of frame compounds (4-10) is hardly influenced by the introduction of, either the triazole ring, benzene ring or fused ring (figure 2). This also implies that the orbital interaction between the title heterocyclic compound and the aromatic ring or some other side of residue chains of receptors is dominated by π - π or hydrophobic interaction among the frontier molecular orbitals.

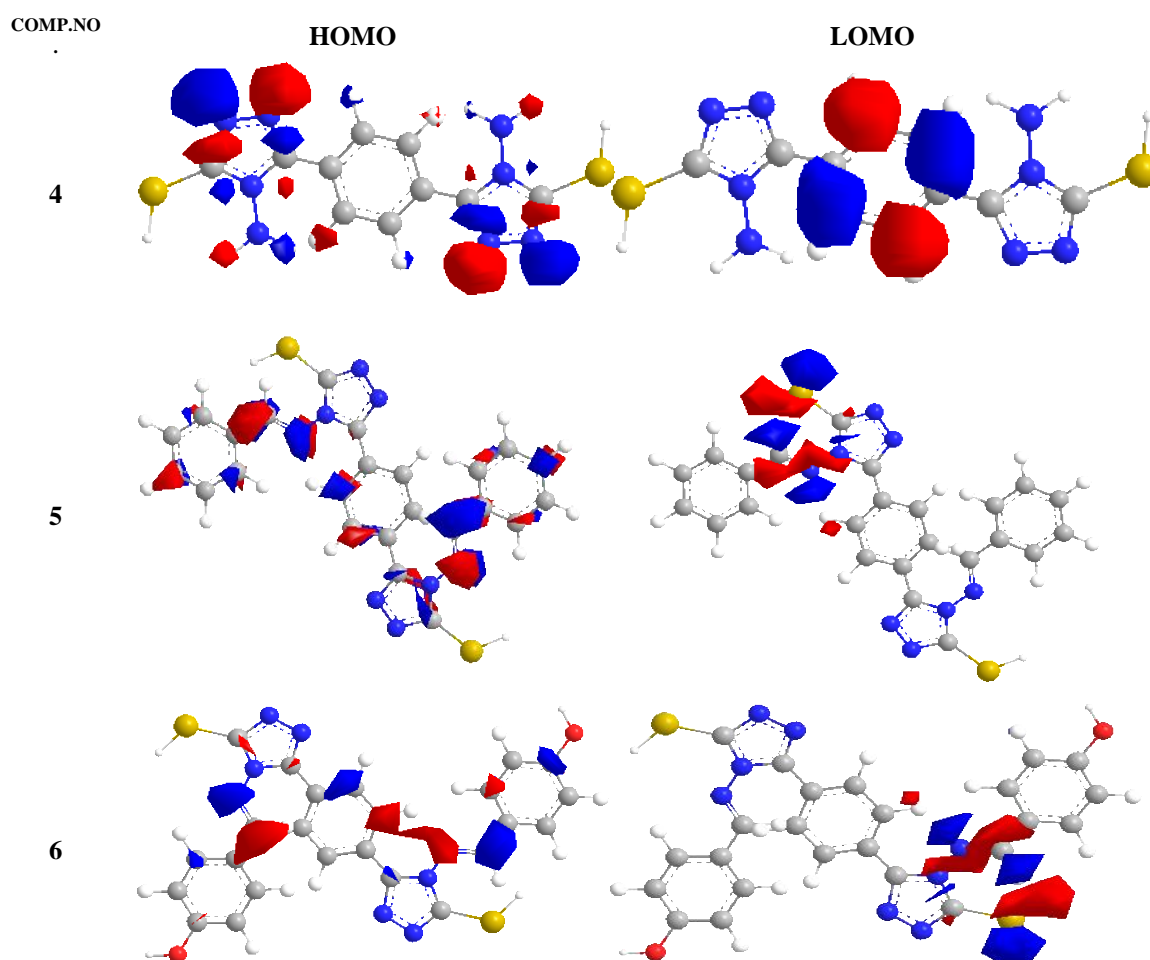
Terephthalic acid was used as starting material which was esterified to its ethyl ester (1) ester by its reaction with absolute ethanol and concentrated sulfuric acid, the IR spectra of ester show absorption at 1728 cm^{-1} for C=O ester. Then converted to acid hydrazide (2) with hydrazine hydrate in ethanol, the C=O absorption for hydrazide at 1642 cm^{-1} , the hydrazide (2) was treated with ammonium thiocyanate and concentrated hydrochloric acid in ethanol to give thiosemicarbazide (3), the IR spectra show 1718 cm^{-1} C=O and 1275 cm^{-1} C=S, thiosemicarbazide (3) was treated with hydrazine hydrate in ethanol to give substituted 1,2,4-triazole (4), IR spectra show no absorption for C=O the C=N absorption at 1627 cm^{-1} and C-H aromatic at 3030 cm^{-1} substituted 1,2,4-triazole (4) was treated with substituted benzaldehyde and concentrated hydrochloric acid in ethanol to give hydrazones (5-7), the NMR spectra compound(5) show sign of multi-at (7.15-8.33) δ back to 14 protons aromatic, single sign at (5.65) δ back to SH group and single sign at (8.9) δ back to N=CH. the IR spectra for compound (5) show absorption at 1669 - 1620 cm^{-1} for C=N, 3190 cm^{-1} for SH and 3050 cm^{-1} C-H aromatic. the NMR spectra compound(6) show sign of multi-at (7.11-8.19) δ back to 12 protons aromatic, single sign at (5.59) δ back to SH group, single sign at (9.01) δ back to O-H phenol and single sign at (8.82) δ back to N=CH. the NMR spectra compound(7) show sign of multi-at (6.93-8.02) δ back to 12 protons aromatic, single sign at (5.59) δ back to SH group, single sign at (2.4) δ back to two methylene group substituted on benzene ring and single sign at (8.42) δ back to N=CH. the hydrazones (5-7) were treated with phosphorus oxychloride or with glacial acetic acid to give bicyclic substituted benzene (8-10), the NMR spectra compound(8) show sign of multi-at (7.57-8.63) δ back to 14 protons aromatic. the IR spectra for compound (8) show 1651 cm^{-1} C=N and 978 , 1166 cm^{-1} C-S-C and no absorption for S-H. the NMR spectra compound

(9) show sign of multi-at (7.11-8.19) δ back to 12 protons aromatic , and single sign at (8.93) δ back to O-H phenol . the NMR spectra compound (10) show sign of multi-at (6.93-8.02) δ back to 12 protons aromatic and single sign at (2.4) δ back to tow methylene group substituted on benzene ring Table (3).

The vibration analysis showed that the optimized structure was in accordance with the point on the potential minimum energy surface.

Table 2. energy of HOMO , highest occupied molecular orbital ; LOML , lowest unoccupied molecular orbital , compounds (4-10) (theory)

Comp.no.	E _{HOMO} e.v.	E _{LOMO} e.v.	H	μ	W
4	-6.277	0.419	3.348	-2.929	1.28121
5	-2.141	-1.231	0.455	-1.686	3.12373
6	-1.658	-1.230	0.214	-1.444	4.87181
7	-1.229	-0.912	0.158	-1.0705	3.62648
8	-5.666	-0.030	2.818	-2.848	1.43915
9	-5.666	0.360	3.013	-2.653	1.16800
10	-5.665	0.429	3.039	-2.618	1.12821



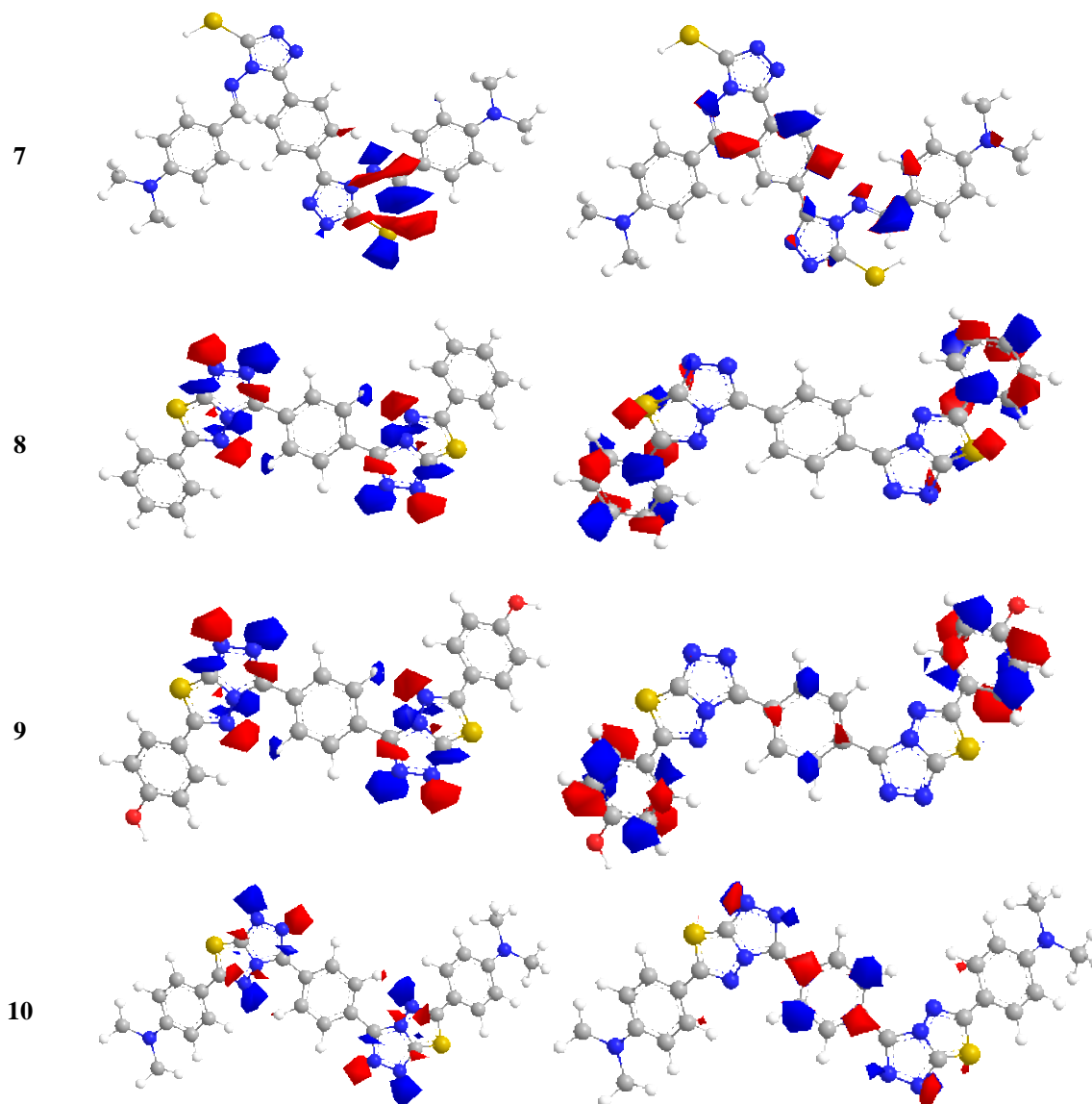


Figure 2. HOMO , highest occupied molecular orbital ; LOML , lowest unoccupied molecular orbital , compounds (4-10)

Note:(Red area mean positive homo energy ,blue area mean negative lumo energy)

Homo,Lumo (5,6,7) & (8,9,10)

The energies of HOMO,LUMO values increase with decreasing viability of donor, and increased disability of stereochemistry, the compounds (5,8) that is not substituted in phenyl ring is less values in HOMO,LUMO energy comparing with other compounds synthesis, although the compound (7,10) is set (Dimethyl Amin) larger than the hydroxyl group in compound (6,9), but the electronegativity of an atom of oxygen increases the donor capacity Comparing with the nitrogen atom in the compound (7,10) as Table (2).

Hardness (η) (5,6,7) & (8,9,10)

Molecular hardness values decrease when there are groups large substituted ring benzene, and then return to its relationship gap energy between Homo and Lumo, where the change of homo , lumo values lead to decrease of different energy between the tow levels , that is lead to decrease of involve energy to transfer of electron (Excitation energy),that is lead to decrease of hardness (decrease of molecular hardness of the compound (7)

comparator with compound(5) and (6) , while the compounds (8-10) show increase values cause the compounds do not contain factional groups only heterocyclic ring as Table(2) .

Electron chemical potential (μ) (5,6,7) & (8,9,10)

Show that increase in electron potential for chemical compounds with decreased susceptibility donor as Table 2.

Global Electrophilicity Index (w) (5,6,7) & (8,9,10)

Show that increased the value of Global electrophilicity index with the decrease susceptibility Donor with compounds (5-7) the hydrogen atoms in (N=CH & -SH) well be acidic make compounds behavior electrophilic that's see in W values theoretical calculated . The increase in electron potential chemical spin Global electrophilicity index is the latest proof of the stability of the prepared compounds as Table 2.

compounds (8-10) contains double bonds between (C=N) behavior nuophilic ; that's see in W values theoretical calculated .The structure of the synthesized compounds were confirmed by UV , IR , NMR and physical methods .

Table 3. UV & IR spectra

Comp. no.	UV	IR ν cm^{-1} , KBr						
		C=O	C=N	-NH	-SH	C-H _{alph}	C-H _{arm}	Others
1	250,324	1728	--	--	--	2944	3060	--
2	241,342	1642	--	3418	--	--	3070	--
3	225,318	1718	--	3400	--	--	3030	C=S 1275
4	234,346	--	1627	3406 , 3292	3206	--	3030	--
5	288,390	--	1669 , 1620	--	3190	2960	3050	--
6	299,401	--	1656 , 1622	--	3172	3000	3060	O-H _{phenol} 3367
7	256,345	--	1670	--	3200	2925	3050	--
8	278,377	--	1651	--	--	--	3071	C-S-C 978,1166 O-H _{phenol} 3422
9	305,412	--	1698	--	--	--	3064	C-S-C 993,1159
10	267,349	--	1653	--	--	2924,2853	3007	C-S-C 1016,1171

Biological Active

The biological studies of compounds (5,6,7,8,9 &10) were evaluated against (*Eschershia Coli* , *Staphylococcus Epidermidis* , *Staphylococcus Aureus*) table (4) the results showed that these compounds (5,6,7,8) have a good activity against (*Eschershia Coli* and *Staph Epidermidis*) .

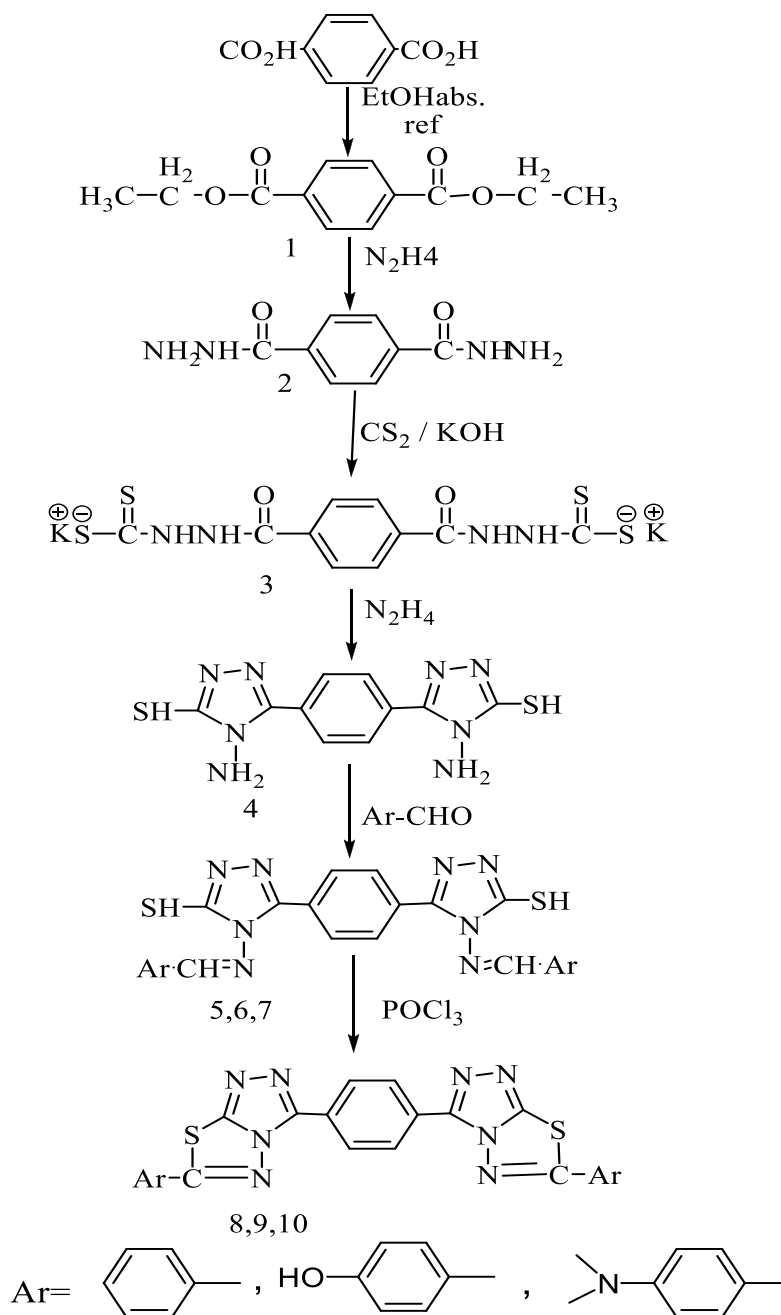
Table 4. Biological active compounds (5-10)

Compound no.	<i>Staph Epidermidis</i>	<i>E. Coil</i>	<i>Staph Aureus</i>
5	19	14	17
6	15	16	11
7	22	18	9
8	14	12	18
9	11	9	15
10	16	11	14
Ciprofloxacin 5mg/disk	-	15	-
Chloramphenicol 30mg/disk	16	14	17

Compounds (5,6,7) were tested against *E.coli* shows a good activity against with compare to standard controls , compounds (8,9,10) were tested against shows a less activity against *E.coli* with respect to standard controls .

Compounds (5,7,10) were tested against *Staph Epidermidi* shows a good activity against with compare to standard controls , compounds (6,8,9) were tested against shows a less activity against *Staph Epidermidi* with respect to standard controls .

Compound (8) were tested against *Staph Aureus* shows a good activity against with compare to standard controls , compounds (6,7,9,10) were tested against shows a less activity against *Staph Aureus* with respect to standard controls , compound (5) give same activity standard control with against *Staph Aureus* .Table 3.



Scheme 1

Conclusion

In conclusion, we have synthesis a simple and efficient method for the synthesis of new triazole fuse ring derivatives and characterized by spectral studies. The newly synthesized compounds (5-10) were evaluated for antibacterial activities. energy for surface calculation of energy of HOMO & LUMO theory . The compounds synthesized have a good activity against .

Acknowledgement

The authors are thankful to Head, Department of Chemistry in Education for pure science college Mosul University, We are also thankful to Head, Department of Biology, Mosul University for providing laboratory facilities.

References

- I.L. Finar, (1964), "Organic Chemistry, Stereochemistry and the Chemistry of Natural Products", 3rd Edn. Longmans Green and Co Ltd., Vol.2, p. 430.
- M.R. Atkinson and J.B. Polya, (1954), J. Chem. Soc. Part I, 141.
- A.R. Katritzky and C.W. Rees, (1984), "Comprehensive heterocyclic Chemistry; Synthesis and Uses of Heterocyclic Compounds", Pergamon Press Ltd., England, Vol. 5, p. 744.
- T.B. Johnson and L.H. Chernoff, (1912), J. Am. Chem. Soc., 34, 167; Chem. Abstr.,(1912),Vol. 6, p.1156.
- R.G. Ghild, (1965), Organic Chemical Research Section, Lederle Laboratories, 2, 98.
- K.M. Daoud and H.A. Aziz, (2003), Raf. J. Sci., 15, 2, 52-57.
- J.B. Hendrickson, D.J. Cram and S.G. Hamond, (1970), "Organic Chemistry", 3rd Edn. McGraw-Hill Inc., Japan, p. 967.
- I.L. Finar, (1975), "Organic Chemistry, Stereo Chemistry and the Chemistry of Natural Products", 5th Ed., Longman Press Ltd., Vol. 2, pp. 433.
- M.Y. Shandala, M.T. Ayob and M.S Noori, (1998), Raf. J. Soc., 9, 2, 39.
- Guo-Xiang sun , Ming-Yan Yang , Yan-Xia Shi , Zhao-Hui Sun , Xing-Hai Liu , Hong-Ke Wu , Bao-Ju Li and Yong-Gang Zhang , (2014) , Int. J. Mol. Sci. , 15 , 8075-8090 .
- Rami Y. Morjan , Basam S. Qeshta , Hussein T. Al-shayyah , John M. Gardiner , Basam A. Abo-Thaaher , Adel M. Awadallah , (2014) , International Journal of Organic Chemistry , 4 , 201-207 .
- Hakan Bakas , Nesrin Karaali , Deniz Sahin , Ahmet Demirbas , Sengul Alpay Karaoglu and Neslihan Demirbas , (2010) , Molecules , 15 , 2427-2438 .
- Stefania-Felicia Barbuceanu , Diana Carolina Ilies , Gabriel Saramet , Valentina Uivarosi , Constantin Draghici and Valeria Raulescu , (2014) , Int. J. Mol. Sci. , 15 , 10908-10925 .
- Mariam Al-sheikh , Hanadi Y. Medrasi , Kamal Usef Sadek and Ramadan Ahmed Mekheimer , (2014) , Molecules , 19 , 2993-3003.
- Mahmoud R. Mahmoud , Wael S.I. Abou-Elmagd , Manal M. El-Shahawi and Mohamed H. Hekal , (2014) , World Journal of Chemistry , 9 , (2) , 24-32 .
- E.R. Bochman, C.M. Mc-Closkey and J.A. Seneker, (1947), J. Am. Chem. Soc., 69, 380.
- H.L. Yale, K. Losee, J. Martins, M. Holsing, F.M. Perry and J. Bernstein, (1953) , J. Am. Chem. Soc., 75, 1933.
- B.S. Holla, M.K. Shivanada, P.M. Akberali, S. Balige and S. Safeer, (1996), Farmaco., 51(12), 785.
- U. Misra, A. Hitkari, A. Saxena, S. Gurtu and K. Shanker, (1996), Eur. J. Med. Chem., 31, 629-634.
- A.K. Sen-Gupta and K. Hajela, (1981), J. Indian Chem. Soc., LVIII, 690.
- K.T. Potts and R.M. Huseby, (1966), J. Org. Chem., 31, 9, 3528.
- Liu , X.H. ; Chen , P.Q. ; Wang , B.L. ; Wang S.H.; Li, Z.M., (2007), Bioorg. Med. Chem. Lett., 17 , 3784-3788.

Author Information

Mohanad Yakdhan Saleh

University of Mosul

Mosul/Iraq

Contact e-mail: mohanadalallaf@uomosul.edu.iq

Theoretical Investigation of Spectroscopic and Thermodynamic Properties of 1-Acetyl-3-methyl-4-[3-(3-methoxybenzoxy)benzylidenamino]-4,5-dihydro-1*H*-1,2,4-triazol-5-one by 6-311G(d) and 3-21G HF/DFT(B3LYP) Methods

Hilal MEDETALIBEYOGLU

Kafkas University

Haydar YUKSEK

Kafkas University

Abstract: In this study, theoretically spectral and thermodynamic values of 1-acetyl-3-methyl-4-[3-(3-methoxybenzoxy)-benzylidenamino]-4,5-dihydro-1*H*-1,2,4-triazol-5-one was calculated and compared with experimental values. For this purpose, firstly, this compound has been optimized using 6-311G(d) and 3-21G HF/DFT(B3LYP) basis sets. ¹H-NMR and ¹³C-NMR spectral values were calculated according to the method of GIAO using Gaussian G09W Software program. Theoretical and experimental values were plotted according to $\delta_{\text{exp}}=a+b \cdot \delta_{\text{calc}}$. The standard error values were found via the Sigma plot with regression coefficient of a and b constants. Furthermore, the vibrational frequency of title compound have been calculated by using 6-311G(d) and 3-21G HF/DFT(B3LYP) basis sets and these values are multiplied with appropriate adjustment factors. In the identification of calculated IR data was used the veda4f program. Also, the molecular structure, the highest occupied molecular orbital-lowest unoccupied molecular orbital (HOMO-LUMO), electronic transition, Natural Bonding Orbital (NBO) analysis, total static dipole moment (μ), the mean polarizability ($\langle\alpha\rangle$), the anisotropy of the polarizability ($\Delta\alpha$), the mean first-order hyperpolarizability ($\langle\beta\rangle$), electronegativity(χ), hardness(η), molecular electrostatic potential maps (MEP) and Mulliken atomic charges of 1-acetyl-3-methyl-4-[3-(3-methoxybenzoxy) benzylidenamino]-4,5-dihydro-1*H*-1,2,4-triazol-5-one molecule have been investigated by using DFT(B3LYP) and HF levels with 6-311G(d) and 3-21G basis sets.

Keywords: 4,5-Dihydro-1*H*-1,2,4-triazol-5-on, Gaussian 09W, GIAO, B3LYP, HF, 6-311G(d), 3-21G basis sets

Introduction

4,5-dihydro-1*H*-1,2,4-triazol-5-one and its derivatives constitute one of the most biologically active classes of compounds having a wide spectrum of activities such as antifungal, antimicrobial (Zhang et al., 2014), anti-HIV, antihypertensive (Ali, Ragab, Farghaly, & Abdalla, 2011), analgesic (Uzgören-Baran et al., 2012), antiviral, hypocholesteremic, anti-inflammatory (El-Serwy, Mohamed, Abbas, & Abdel-Rahman, 2013), antitumor (Chen et al., 2016), antioxidant properties. Some researchers have reported theoretical the electronic, structural properties and spectroscopic (IR, NMR, UV) parameters of 4,5-dihydro-1*H*-1,2,4-triazol-5-one derivatives (Jin et al., 2014; Al-tamimi, 2016; Gatfaoui et al., 2017; Pokharia et al., 2017; Süleymanoğlu et al., 2017)

The quantum-chemical calculation methods have been extensively used to predict the theoretical spectroscopic, thermodynamic and electronic properties of molecule systems. The quantum-chemical calculation methods have been widely used to predict the theoretical, structural, spectroscopic (IR, NMR, and UV) and electronic properties of molecular systems. The quantum chemical methods provide support experimental methods. In addition, many theoretical properties such as vibrational spectroscopy, molecular geometry, electronic and

- This is an Open Access article distributed under the terms of the Creative Commons Attribution-NonCommercial 4.0 Unported License, permitting all non-commercial use, distribution, and reproduction in any medium, provided the original work is properly cited.

- Selection and peer-review under responsibility of the Organizing Committee of the Conference

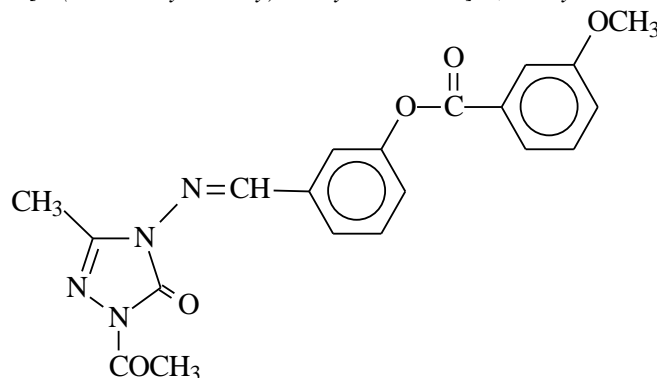
thermodynamic properties, ^{13}C and ^1H NMR chemical shifts, Mulliken atomic charges and HOMO-LUMO energies can be examined by using some theoretical methods. The electronic spectroscopy provides important information on electron transitions and electronic properties in molecular systems. The ^1H and ^{13}C NMR chemical shifts of molecule in solvent and in the gas phase can be calculated by using the DFT/B3LYP and Hartree Fock (HF) methods. Also, the geometric parameters (dihedral angles, bond angles and bond lengths), vibrational frequencies, Mulliken atomic charges, electronic properties, the highest occupied molecular orbital (HOMO) and the lowest unoccupied molecular orbital (LUMO) of the calculated optimized molecule can be determined by using the DFT/B3LYP and Hartree Fock (HF) methods. All structural electronic and thermodynamic calculations were performed by using Gaussian G09W program (Frisch et al., 2009) and GaussView 5.0 program package (Frisch, Nielson, & Holder, 2003)

In this paper, theoretically spectral and thermodynamic values of 1-acetyl-3-methyl-4-[3-(3-methoxybenzoyloxy)-benzylidenamino]-4,5-dihydro-1H-1,2,4-triazol-5-one was calculated and compared with experimental values [hilal tez]. For this purpose, firstly, this compound has been optimized using 6-311G(d) and 3-21G HF/DFT(B3LYP) basis sets. ^1H -NMR and ^{13}C -NMR spectral values were calculated according to the GIAO method (Wolinski, Hilton, & Pulay, 1990). Theoretical and experimental values (Medetalibeyoğlu, & Yüksek 2018) were plotted according to $\delta_{\text{exp}}=a+b \cdot \delta_{\text{calc}}$. The standard error values were found via the Sigma plot with regression coefficient of a and b constants. Furthermore, the vibrational frequency of title compound have been calculated by using 6-311G(d) and 3-21G HF/DFT(B3LYP) basis sets and these values are multiplied with appropriate adjustment factors. In the identification of calculated IR data was used the veda4f program (Jamróz, 2004). Also, the molecular structure, the highest occupied molecular orbital-lowest unoccupied molecular orbital (HOMO-LUMO), electronic transition, Natural Bonding Orbital (NBO) analysis, total static dipole moment (μ), the mean polarizability ($\langle\alpha\rangle$), the anisotropy of the polarizability ($\Delta\alpha$), the mean first-order hyperpolarizability ($\langle\beta\rangle$), electronegativity(χ), hardness(η), molecular electrostatic potential maps (MEP) and Mulliken atomic charges of 1-acetyl-3-methyl-4-[3-(3-methoxybenzoyloxy) benzylidenamino]-4,5-dihydro-1H-1,2,4-triazol-5-one molecule have been investigated by using DFT(B3LYP) and HF levels with 6-311G(d) and 3-21G basis sets.

Result and Discussion

Geometry of title molecule was optimized at the HF and B3LYP levels of theory along with standard 6-311G(d) and 3-21G basis sets. The vibrational frequencies were calculated by HF and B3LYP methods. The ^1H -NMR and ^{13}C -NMR shielding values were calculated according to GIAO (Gauge Including Atomic Orbital) method. (Wolinski, Hilton, & Pulay, 1990; Dodds, McWeeny, & Sadlej, 1980). Time-dependent density functional theory (TD-DFT) was used to compute oscillator strengths, excitation energies for electronic transitions from ground to excited states (Bauernschmitt, & Ahlrichs, 1996; Casida et al., 1998; Stratmann et al., 1998). Some quantum chemical descriptors (bond lengths, bond angles, UV-Vis values, dipole moments, Mulliken atomic charges, HOMO-LUMO energies and total energy) are calculated at the DFT/6-311G(d) and DFT/3-21G, HF/6-311G(d) and HF/3-21G levels. All the calculations were carried out with the Gaussian 09W software (Frisch et al., 2009).

1-Acetyl-3-methyl-4-[3-(3-methoxybenzoyloxy)-benzylidenamino]-4,5-dihydro-1H-1,2,4-triazol-5-one



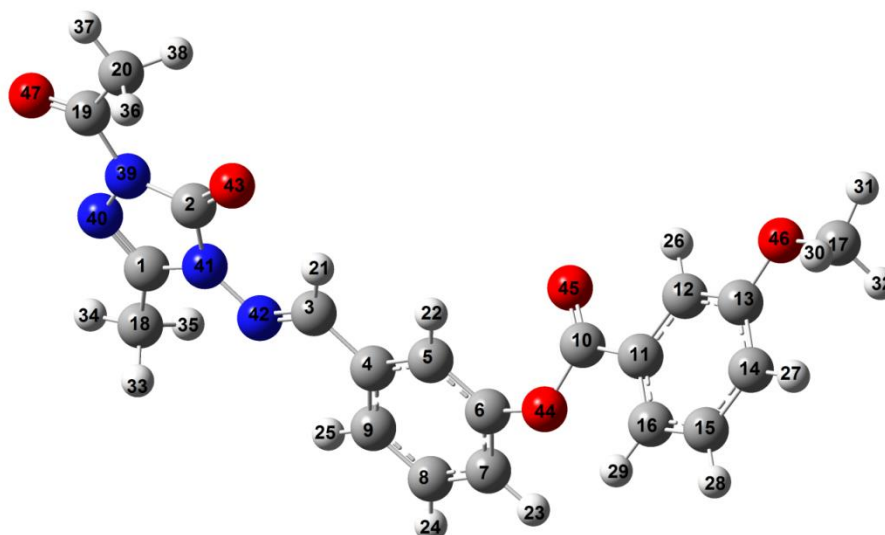


Figure 1. The optimized molecular structure of 1-acetyl-3-methyl-4-[3-(3-methoxybenzyloxy)benzylideneamino]-4,5-dihydro-1H-1,2,4-triazol-5-one

Table 1. The calculated ^1H and ^{13}C NMR isotropic chemical shifts of title compound (with respect to TMS, all values in ppm) (6-311G(d))

	$\delta_{\text{Exp.}}$	$\delta_{\text{cal.}}$ HF (Vacuum)	$\delta_{\text{cal.}}$ HF (DMSO)	Differe nt	Differe nt (DMSO)	$\delta_{\text{cal.}}$ B3LYP (Vacuum)	$\delta_{\text{cal.}}$ B3LYP (DMSO)	Differe nt	Differe nt (DMSO)
C1	146.7 1	150.20	153.41	-3.49	-6.70	139.83	143.55	6.88	3.16
C2	151.0 7	154.29	154.84	-3.22	-3.77	142.67	143.22	8.40	7.85
C3	147.8 1	153.55	154.39	-5.74	-6.58	143.16	144.04	4.65	3.77
C4	134.7 1	139.26	138.85	-4.55	-4.14	125.87	125.57	8.84	9.14
C5	126.2 5	130.22	129.66	-3.97	-3.41	120.14	120.05	6.11	6.20
C6	154.4 5	157.84	157.43	-3.39	-2.98	142.43	141.51	12.02	12.94
C7	125.4 7	126.42	127.68	-0.95	-2.21	117.50	118.35	7.97	7.12
C8	130.0 3	131.76	133.15	-1.73	-3.12	120.71	121.61	9.32	8.42
C9	120.2 4	123.58	124.19	-3.34	-3.95	114.46	115.21	5.78	5.03
C10	164.3 3	166.45	167.95	-2.12	-3.62	151.38	153.22	12.95	11.11
C11	130.3 6	134.36	133.50	-4.00	-3.14	122.62	121.69	7.74	8.67
C12	122.1 5	124.75	122.84	-2.60	-0.69	115.25	113.24	6.90	8.91
C13	159.4 3	165.22	165.40	-5.79	-5.97	149.57	149.42	9.86	10.01
C14	114.3 9	115.28	117.95	-0.89	-3.56	104.12	106.59	10.27	7.80
C15	130.1	131.71	133.27	-1.53	-3.09	120.83	122.37	9.35	7.81

5	8								
C1	120.5	124.11	124.29	-3.54	-3.72	113.33	113.72	7.24	6.85
6	7								
C1	55.47	53.54	54.08	1.93	1.39	35.30	35.77	20.17	19.70
7									
C1	11.21	12.35	12.44	-1.14	-1.23	0.49	0.70	10.72	10.51
8									
C1	166.0	164.44	168.07	1.56	-2.07	151.44	155.51	14.56	10.49
9	0								
C2	23.43	24.57	24.86	-1.14	-1.43	11.43	11.76	12.00	11.67
0									
H2	9.67	9.56	9.54	0.11	0.13	8.94	8.95	0.73	0.72
1									
H2	7.64	7.21	7.26	0.43	0.38	6.62	6.82	1.02	0.82
2									
H2	7.52	6.86	7.10	0.66	0.42	6.65	6.90	0.87	0.62
3									
H2	7.62	7.12	7.38	0.50	0.24	6.85	7.12	0.77	0.50
4									
H2	7.84	7.74	7.86	0.10	-0.02	7.57	7.72	0.27	0.12
5									
H2	7.82	7.57	7.39	0.25	0.43	7.43	7.23	0.39	0.59
6									
H2	7.35	6.33	6.70	1.02	0.65	6.06	6.47	1.29	0.88
7									
H2	7.56	7.03	7.29	0.53	0.27	6.79	7.09	0.77	0.47
8									
H2	7.76	7.45	7.56	0.31	0.20	7.18	7.31	0.58	0.45
9									
H3	3.88	3.19	3.37	0.69	0.51	2.51	2.71	1.37	1.17
0									
H3	3.88	3.69	3.76	0.19	0.12	3.08	3.14	0.80	0.74
1									
H3	3.88	3.18	3.36	0.70	0.52	2.51	2.71	1.37	1.17
2									
H3	2.37	2.00	2.17	0.37	0.20	1.52	1.72	0.85	0.65
3									
H3	2.37	1.83	1.87	0.54	0.50	1.46	1.43	0.91	0.94
4									
H3	2.37	2.00	2.16	0.37	0.21	1.51	1.70	0.86	0.67
5									
H3	2.50	2.14	2.26	0.36	0.24	1.56	1.70	0.94	0.80
6									
H3	2.50	1.60	1.64	0.90	0.86	1.14	1.16	1.36	1.34
7									
H3	2.50	2.17	2.28	0.33	0.22	1.57	1.70	0.93	0.80
8									

Table 2. The calculated ^1H and ^{13}C NMR isotropic chemical shifts of title compound (with respect to TMS, all values in ppm) (3-21G)

	$\delta_{\text{Exp.}}$	$\delta_{\text{cal.}}$ HF (Vacuum)	$\delta_{\text{cal.}}$ HF (DMSO)	Difference	Difference (DMSO)	$\delta_{\text{cal.}}$ B3LYP (Vacuum)	$\delta_{\text{cal.}}$ B3LYP (DMSO)	Difference	Difference (DMSO)
C1	146.7	115.89	118.01	30.82	28.70	112.50	115.35	34.21	31.36
C2	151.0	117.47	117.63	33.60	33.44	115.33	115.50	35.74	35.57

	7								
C3	147.8 1	118.63	119.15	29.18	28.66	116.07	116.63	31.74	31.18
C4	134.7 1	100.14	99.57	34.57	35.14	92.70	92.11	42.01	42.60
C5	126.2 5	90.74	90.19	35.51	36.06	84.32	83.77	41.93	42.48
C6	154.4 5	120.91	120.89	33.54	33.56	111.04	110.87	43.41	43.58
C7	125.4 7	88.41	89.38	37.06	36.09	84.08	84.94	41.39	40.53
C8	130.0 3	93.76	94.93	36.27	35.10	88.87	89.99	41.16	40.04
C9	120.2 4	87.52	87.90	32.72	32.34	83.16	83.63	37.08	36.61
C10	164.3 3	133.24	133.85	31.09	30.48	128.53	129.30	35.80	35.03
C11	130.3 6	96.43	95.69	33.93	34.67	90.09	89.27	40.27	41.09
C12	122.1 5	88.40	86.89	33.75	35.26	85.49	83.70	36.66	38.45
C13	159.4 3	124.42	124.48	35.01	34.95	115.72	115.40	43.71	44.03
C14	114.3 9	83.18	85.14	31.21	29.25	78.28	80.36	36.11	34.03
C15	130.1 8	94.30	95.55	35.88	34.63	88.97	90.44	41.21	39.74
C16	120.5 7	88.15	88.20	32.42	32.37	83.96	84.43	36.61	36.14
C17	55.47	31.56	31.19	23.91	24.28	15.60	16.19	39.87	39.28
C18	11.21	-6.41	-6.56	17.62	17.77	-17.72	-17.73	28.93	28.94
C19	166.0 0	127.55	129.97	38.45	36.03	125.39	128.54	40.61	37.46
C20	23.43	4.34	4.44	19.09	18.99	-7.78	-7.60	31.21	31.03
H21	9.67	9.24	9.21	0.43	0.46	8.68	8.65	0.99	1.02
H22	7.64	7.78	7.70	-0.14	-0.06	7.37	7.28	0.27	0.36
H23	7.52	5.81	6.10	1.71	1.42	5.74	6.06	1.78	1.46
H24	7.62	6.10	6.42	1.52	1.20	5.90	6.26	1.72	1.36
H25	7.84	6.86	6.99	0.98	0.85	6.78	6.96	1.06	0.88
H26	7.82	6.66	6.48	1.16	1.34	6.81	6.56	1.01	1.26
H27	7.35	5.25	5.68	2.10	1.67	4.95	5.44	2.40	1.91
H28	7.56	6.03	6.34	1.53	1.22	5.75	6.13	1.81	1.43
H29	7.76	6.63	6.78	1.13	0.98	6.49	6.70	1.27	1.06
H30	3.88	2.74	2.98	1.14	0.90	1.74	2.03	2.14	1.85
H31	3.88	3.39	3.51	0.49	0.37	2.73	2.82	1.15	1.06

1									
H3									
2	3.88	2.74	2.98	1.14	0.90	1.74	2.03	2.14	1.85
H3									
3	2.37	1.53	1.71	0.84	0.66	0.82	1.04	1.55	1.33
H3									
4	2.37	1.14	1.18	1.23	1.19	0.59	0.62	1.78	1.75
H3									
5	2.37	1.53	1.71	0.84	0.66	0.82	1.04	1.55	1.33
H3									
6	2.50	1.96	2.05	0.54	0.45	1.17	1.29	1.33	1.21
H3									
7	2.50	0.99	1.05	1.51	1.45	0.42	0.45	2.08	2.05
H3									
8	2.50	1.96	2.05	0.54	0.45	1.17	1.29	1.33	1.21

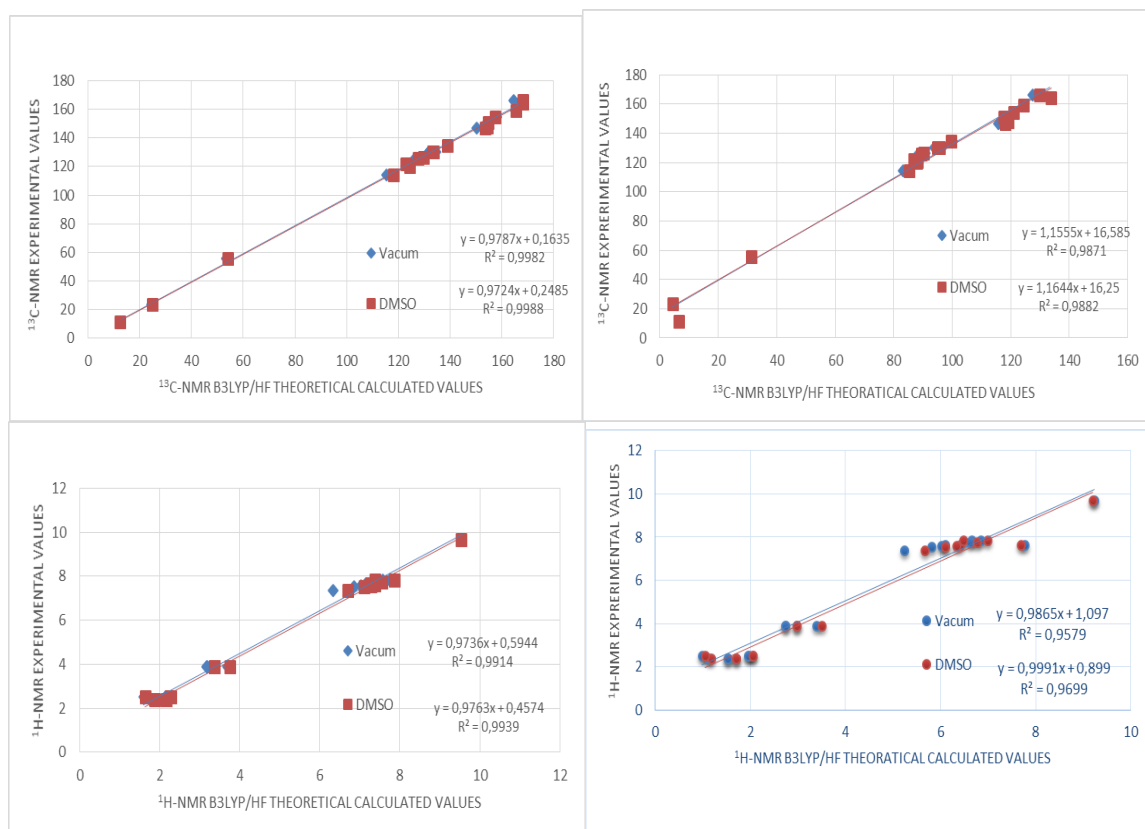


Figure 2. Comparison of experimental/theoretical ^{13}C - and ^1H -NMR chemical shifts values of title compound with 6-311G(d)(a)/B3LYP, HF, B3LYP(DMSO) ve HF(DMSO) ve 3-21G(b)/B3LYP, HF, B3LYP(DMSO) ve HF(DMSO) methods

Table 3. The calculated IR frequencies of title compound (6-311G)

	Vibration Frequencies	HF	B3LYP
1	τ COCC(51), τ NCCC(37), τ CNNC(10)	5	14
2	τ CCCC(14), τ COCC(27), τ CCCN(14), τ CNNC(12), τ NCCN(10)	12	17
3	τ CCOC(65), τ NCCC(13), τ COCC(29), τ CCCC(20)	16	18
4	τ NCNN(30), τ CCNN(18), τ NCCN(38)	35	36
5	τ CCCC(28), τ COCC(19)	37	40
6	δ COC(22), δ CCO(12), τ COCC(19), τ CCNC(15)	52	51
7	τ CCNC(60)	65	67
8	δ CCN(18), δ CNN(10), δ NCC(10), τ COCC(25), τ CCCC(10)	67	74
9	τ COCC(65), τ HCOC(11)	70	84

10	τ CCCN(18), τ CNNC(15), τ CCNN(23), τ NNCN(10), τ NCNN(11)	91	94
11	δ COC(15), δ CCC(13), τ CCNN(27), τ CNNC(19)	130	128
12	δ CCO(13), τ CNNC(12), τ CCNN(18)	140	137
13	δ NCC(10), δ NCN(13), δ NNC(10), δ CCC(12)	161	157
14	τ HCCN(55), τ CNNC(12), τ NCNN(21)	172	161
15	τ CCCC(12), τ NCNN(13)	176	166
16	τ HCCN(69)	185	171
17	τ CNNC(28), τ NNCN(11), τ HCCN(56)	192	177
18	δ CCC(12), δ COC(19)	196	199
19	δ NCN(10), δ CCC(14), τ HCOC(12), τ COCC(13), τ OCCC(24), τ CCCC(18)	225	215
20	δ CCC(12), δ COC(19), δ CCN(14), τ HCOC(12), τ CCCC(18), τ OCCC(12)	226	219
21	τ CCCC(15), τ NCNN(14), τ CCCN(33), τ NCCN(22)	228	237
22	ν CC(13), δ NCN(15), δ CCO(10)	250	244
23	δ COC(28), τ CCCN(14)	270	264
24	τ COCC(10), τ HCOC(45), τ CCCC(25)	292	280
25	δ COC(21), δ OCO(15)	307	296
26	δ CCN(37)	339	327
27	τ NCNN(11), τ CNNC(16), τ NNCN(14), τ CCCN(10), τ CCNN(34), τ NCCN(10)	365	350
28	τ CNNC(35), τ CCNN(11)	375	364
29	δ CCO(19), δ CNN(15), δ OCN(23), δ CCN(29)	391	371
30	δ CCN(25), δ OCN(18)	396	377
31	δ CCC(38), δ COC(10), δ OCO(10), τ CCCC(12)	439	426
32	δ CCN(10), τ CCCC(30)	457	437
33	ν NC(10), δ CCN(11), τ CCCC(18)	468	444
34	τ CCCC(12), τ HCCC(15), τ CCOC(11), τ CCCN(10)	480	457
35	δ CCC(12), δ NNC(13), δ CCO(13)	496	467
36	δ CCC(21), δ COC(10)	507	496
37	δ COC(12), δ CCC(13), τ OCCC(37), τ OCOC(12), τ HCCC(11)	581	551
38	δ COC(20), δ CCC(14), τ CCCC(12), τ OCCC(29)	583	567
39	τ HCCN(11), τ ONNC(24)	600	583
40	δ CCC(10), τ ONNC(15)	612	583
41	δ CCC(11), τ HCCN(16), τ ONNC(32)	613	592
42	δ OCO(10), τ CCOC(26), τ CCCN(19), τ COCC(13), τ CCCC(15)	624	598
43	ν CC(26), δ OCC(32), τ NNCN(21)	629	606
44	ν CC(17), δ CCC(11), δ NNC(16), τ NNCN(11)	675	654
45	τ NNCN(21), τ CNNC(31), τ NCNN(16), τ CNNC(13)	690	655
46	δ NCC(11), δ CNN(11), δ CCN(11), δ OCN(18), δ CCC(10)	699	675
47	δ CCC(14), τ CCCC(18), τ HCCC(18)	711	683
48	δ CCC(18), τ CCCC(18), τ OCCC(10), τ HCCC(27)	716	686
49	τ CCCC(15), τ HCCC(37), τ CCOC(20)	725	691
50	ν CC(10), δ CCC(13), τ ONNC(41)	796	739
51	τ OCOC(45), τ HCCC(24)	808	753
52	ν NN(13), τ NCNN(11), τ ONNC(41)	816	769
53	δ OCO(12), τ HCCC(30)	830	789
54	τ OCOC(23), τ HCCC(50)	848	802
55	τ OCOC(29), τ HCCC(49)	861	809
56	τ HCCC(15)	874	826
57	ν OC(20), τ HCCC(19)	926	875
58	ν CC(22), ν NN(11), τ HCCC(42)	955	891
59	ν OC(11), τ HCCC(49)	966	896
60	ν CC(15), ν NC(11), ν NN(10), δ NNC(10), τ HCCC(25)	967	913
61	τ HCCC(39)	982	917
62	τ HCCC(39)	985	918
63	ν OC(10), ν CC(13), δ CCC(11), τ HCCC(42)	998	957
64	ν CC(19), δ HCH(11), τ HCCN(29), τ HCCC(55)	1020	961
65	ν CC(30), δ CCC(32), δ HCH(10), τ HCCN(25)	1027	968
66	ν CC(21), δ CCC(21), τ HCCC(56)	1034	968

67	v CC(25), δ CCC(23), τ HCCC(46)	1044	1002
68	τ HCCC(59), τ HCNN(85)	1051	1006
69	v CC(17), δ CCC(23), δ HCH(19), τ HCCN(47)	1077	1008
70	δ HCH(17), τ HCCC(39), τ HCNN(89)	1082	1022
71	δ HCH(19), τ HCCN(53)	1114	1059
72	v OC(60), δ HCH(21), τ CNNC(10), τ HCCN(57)	1117	1061
73	v CC(19), δ HCC(22), δ HCH(21), τ HCCN(58)	1124	1067
74	v CC(10), v OC(48), δ HCH(26), δ NNC(11), τ HCCN(10), τ HCOC(26)	1126	1079
75	v OC(11), v CC(14), δ HCC(20)	1137	1084
76	v CC(18), δ HCC(23)	1142	1099
77	v CC(11), v NC(21), δ HCC(21), δ NNC(13)	1144	1111
78	v CC(21), v NN(26), τ HCCN(17)	1156	1136
79	v CC(25), δ HCC(40)	1168	1167
80	v NN(18), δ HCC(14), δ HCH(26), τ HCOC(26), τ HCCN(16)	1204	1172
81	δ HCC(33)	1219	1181
82	δ HCC(26), δ HCH(25), τ HCOC(26)	1232	1185
83	v NC(15), v NN(11), δ OCC(12), δ HCC(20), τ HCOC(11)	1251	1197
84	v CC(15), δ HCC(19), δ HCH(11), τ HCOC(18)	1262	1199
85	v OC(11), v CC(11), δ HCC(12), τ HCOC(11)	1266	1222
86	v NN(22), v NC(13), δ NCN(12)	1296	1246
87	v OC(17), v CC(20), δ NCN(11)	1310	1276
88	v CC(16), v OC(42)	1325	1286
89	v NN(13), v NC(32), δ OCN(10)	1361	1303
90	v OC(17), δ HCC(20)	1368	1311
91	δ HCC(30)	1373	1313
92	v CC(22), δ HCC(78)	1376	1343
93	v CC(24), v NC(17), δ HCC(17), δ CNN(12), δ HCH(13)	1413	1349
94	v NC(11), δ HCN(37), δ NNC(10), δ HCH(11)	1440	1370
95	δ HCH(92), δ HCN(10)	1477	1407
96	δ HCH(64), δ HCN(15)	1481	1417
97	v CC(16), δ HCH(14)	1500	1435
98	δ HCH(72), τ HCCN(23)	1516	1458
99	v CC(14), δ HCC(10), δ HCH(50), τ HCCN(15)	1524	1459
100	v CC(13), δ HCH(24), δ HCC(12)	1528	1465
101	δ HCH(76), τ HCCN(22)	1530	1475
102	δ HCH(76), τ HCCN(24)	1534	1475
103	δ HCH(61)	1546	1480
104	δ HCH(55), δ HCN(10), τ HCCN(19)	1549	1486
105	δ HCH(72), δ HCN(37), τ HCOC(12)	1562	1498
106	δ HCH(71), τ HCOC(10)	1570	1509
107	δ HCC(40), δ HCH(16), δ CCC(12)	1574	1511
108	δ HCC(27), δ CCC(14)	1577	1515
109	v CC(32), δ HCC(10), δ CCC(17)	1691	1610
110	v CC(32), δ HCC(11), δ CCC(15)	1698	1611
111	v CC(21), δ HCC(14)	1717	1628
112	v CC(31)	1718	1638
113	v NC(64), v CC(12)	1796	1647
114	v NC(64)	1802	1663
115	v OC(40)	1859	1772
116	v OC(88)	1904	1786
117	v OC(50)	1921	1811
118	v CH(91)	3030	2982
119	v CH(92)	3059	3025
120	v CH(97)	3070	3036
121	v CH(50)	3086	3041
122	v CH(100)	3117	3078
123	v CH(100)	3135	3095
124	v CH(46)	3149	3117

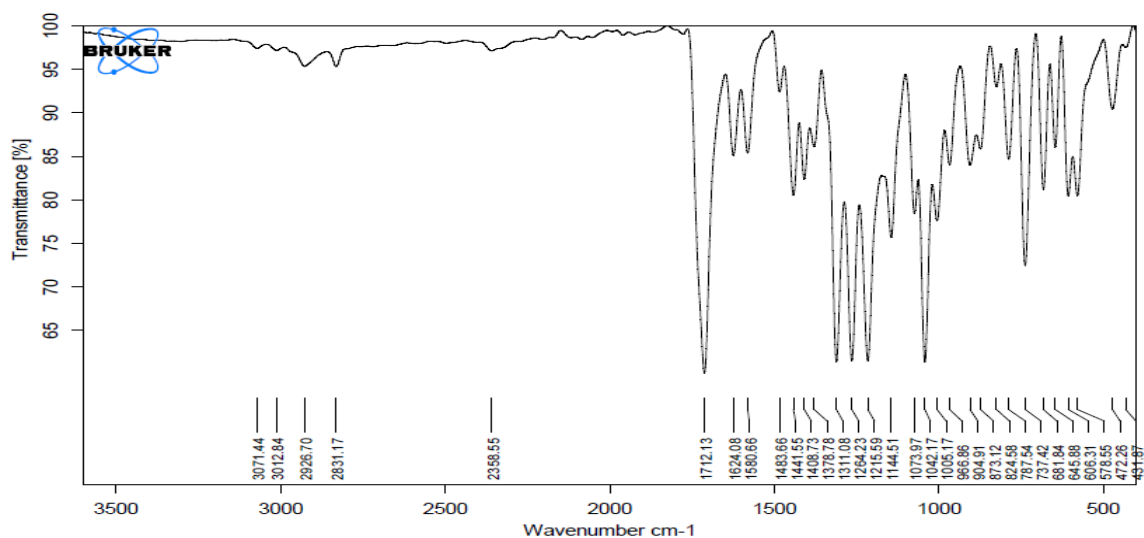
125	v CH(92)	3152	3122
126	v CH(97)	3159	3131
127	v CH(52)	3188	3142
128	v CH(54)	3191	3145
129	v CH(34)	3202	3147
130	v CH(42)	3211	3169
131	v CH(67)	3220	3176
132	v CH(46)	3222	3180
133	v CH(57)	3227	3185
134	v CH(56)	3236	3187
135	v CH(48)	3238	3193

Table 4. The calculated IR frequencies of title compound (3-21G)

Vibration Frequencies		HF	B3LYP
1	τ NCNC(16), τ CCCC(12), τ CNNC(25), τ COCC(17)	13	14
2	τ CCCC(13), τ COCC(34), τ CCOC(24)	17	17
3	δ NCC(18), δ CCO(12), δ CCC(22), δ COC(22), δ NNC(17)	25	24
4	τ CNNC(11), τ COCC(41), τ CCOC(34)	30	32
5	τ NCNN(32), τ CCNC(14), τ NNCC(23)	40	38
6	τ CCNC(65)	62	59
7	δ CCC(13), δ COC(28), δ NNC(16), τ HCOC(10), τ COCC(57)	66	68
8	δ COC(15), δ CCO(17), δ NNC(15), τ CCCC(10), τ COCC(48)	67	80
9	τ COCC(31), τ CCCC(22)	87	94
10	τ NCNC(10), τ NNCC(11), τ CCNN(18), τ CCCC(15)	102	98
11	δ CCC(11), δ COC(13), δ CCO(12), τ HCCN(29), τ NCNC(12), τ CNNC(14), τ CCNN(13)	124	123
12	δ CCO(12), δ CCC(17), δ COC(12), τ NCNC(18), τ CNNC(13), τ CCNN(22)	141	124
13	δ NCC(11), δ CNN(15), τ HCCN(48)	157	141
14	δ CNN(15), δ NCC(11), τ HCCN(50), τ CCNN(10)	167	157
15	τ HCCN(16), τ NCNC(11), τ CCNN(11), τ CCCC(27)	173	160
16	τ CCCC(15), τ HCCN(62)	179	169
17	τ NCNC(16), τ CNNC(19), τ CCNN(10)	185	183
18	δ COC(32)	194	196
19	τ HCOC(45), τ COCC(14), τ OCCC(18), τ CCCC(13)	210	209
20	δ CNN(22), δ CCN(22)	219	216
21	v CC(14), δ COC(12), δ CCN(10)	248	247
22	τ CCCC(22)	263	257
23	δ COC(34), τ HCOC(21), τ CCCC(23)	270	269
24	δ CCO(10), δ CCC(11), δ COC(30), τ HCOC(11), τ CCCC(30)	273	272
25	τ CNNC(26), τ CCCC(17)	281	285
26	δ OCO(11), δ COC(16), δ CCN(23)	325	323
27	δ OCO(11), δ CCO(12), δ CNN(18), δ COC(13)	353	348
28	δ OCN(28), δ CCN(27), τ NCNN(17), τ NNCC(17), τ CNNC(20)	371	352
29	δ OCN(23), δ CCN(27), τ NCNN(17), τ NNCC(21), τ CCNN(37), τ CNNC(20)	372	363
30	δ OCN(23), δ CCN(27), τ NCNN(11), τ NNCC(10), τ CCNN(40)	375	364
31	δ OCC(13), δ CCN(12)	419	409
32	δ CCC(32), δ COC(10)	434	428
33	δ CCC(17), δ NNC(12)	454	446
34	τ CCCC(49)	464	447
35	τ HCCC(20), τ CCCC(42), τ CCOC(14), τ OCCC(10)	485	467
36	δ CCC(18)	495	488
37	δ CCC(16), δ COC(18), τ HCCC(13), τ CCCC(11), τ OCOC(15), τ OCCC(39)	557	550
38	δ CCC(16), δ COC(20), τ CCOC(34), τ CCCC(17), τ HCCC(12), τ OCOC(13), τ OCCC(21)	573	553
39	v NN(10), v CC(15), δ OCC(15), δ CNN(23), δ CCC(14)	581	570

40	v NC(16), v CC(29), δ OCC(34)	585	575
41	δ COC(19), δ CCC(28), δ CCO(14)	594	584
42	τ HCCN(14), τ ONNC(41)	614	595
43	v CC(23), δ CCN(12), τ CCCC(17), τ CCOC(34)	634	608
44	v CC(21), δ CCN(13), τ OCCC(23), τ CCCC(27)	637	626
45	δ OCN(12), δ NCC(13), δ CCC(14)	672	655
46	τ NCNC(19), τ ONNC(10), τ CNNC(12)	693	656
47	v CC(14), δ CCC(28), τ ONNC(43), τ CCNN(13)	694	682
48	τ HCCC(31), τ CCCC(19)	727	702
49	τ HCCC(42), τ CCCC(30)	737	710
50	δ NCN(21)	749	730
51	τ ONNC(43), τ CCNN(13), τ HCCC(13), τ OCOC(55)	784	737
52	δ OCO(17), τ HCCC(12), τ OCOC(52)	790	743
53	v OC(11), δ OCO(27)	801	770
54	δ NCC(11), δ NCN(12), τ ONNC(42), τ CCNN(15)	804	782
55	τ HCCC(34), τ CCCC(13)	862	810
56	τ HCCC(63), τ OCOC(10)	865	812
57	v CC(11), v OC(15), δ OCO(11), τ HCCC(54)	871	850
58	v CC(13)	882	862
59	v CC(23), v OC(11), δ CCC(14), δ NCN(17), τ HCCN(14)	933	912
60	v CC(21), δ NCN(13), τ HCCN(14), τ HCCC(46)	943	919
61	v CC(10), v OC(15), τ HCCC(54)	996	926
62	v CC(14), v OC(11), τ HCCC(33)	998	926
63	v CC(28), δ CCC(10), τ HCCC(28)	1002	945
64	v CC(13), δ CCC(22), τ HCCC(26)	1011	978
65	v CC(32), v OC(24), δ CCC(10), τ HCCC(34)	1017	985
66	v NC(14), δ HCH(12), τ HCCN(31), τ HCCC(60), τ CCCC(14)	1040	995
67	v NC(10), τ HCCC(51), τ HCNN(15)	1041	996
68	v OC(55), v NC(10), δ CCC(22), τ HCCC(51)	1050	996
69	v NC(12), δ CCC(17), τ HCCN(14), τ HCCC(62)	1074	999
70	v OC(34), δ CCC(22), τ HCCC(47)	1078	1012
71	v NC(14), τ HCNN(82), τ HCCN(11)	1087	1044
72	δ CNN(12), δ HCC(18), δ CCC(12), τ HCCN(15)	1090	1047
73	δ HCH(20), τ HCCN(54)	1094	1065
74	v CC(18), v OC(13), δ HCC(17), δ CCC(12)	1099	1068
75	v CC(18), δ HCC(15), δ CNN(14), τ HCNN(21)	1100	1073
76	δ HCH(21), τ HCCN(55), τ HCNN(24)	1100	1075
77	v CC(12), δ HCC(19), τ HCNN(48), τ HCCN(21)	1107	1086
78	v CC(18), δ NCN(12), τ HCCN(19), δ HCC(21)	1121	1091
79	v CC(31), v NC(10), v NN(10), δ HCH(24), τ HCOC(25), τ HCCN(13)	1148	1120
80	v NC(10), v NN(10), v CC(31), δ HCH(24), δ OCC(11), τ HCOC(26)	1155	1121
81	v OC(13), v CC(31), δ HCC(13), δ HCH(24), τ HCOC(26)	1156	1137
82	v CC(10), δ HCC(12), δ HCH(15), τ HCOC(27)	1166	1150
83	v CC(10), v OC(12), δ HCC(14)	1171	1172
84	v NN(13), v CC(18), v OC(13), δ HCC(17), δ HCH(13), τ HCOC(25)	1184	1180
85	δ HCC(39)	1218	1188
86	v CC(14), v OC(10), δ HCC(41)	1219	1202
87	v CC(19), v OC(13), δ HCC(12)	1243	1240
88	v NC(42), v NN(15)	1258	1250
89	v CC(18), v OC(36), δ HCH(13), τ HCOC(25)	1279	1257
90	v CC(27), v OC(23), δ HCC(10)	1294	1280
91	v CC(27), v NC(33), δ HCC(26), δ CNN(15)	1323	1294
92	v CC(15), δ HCC(41)	1334	1309
93	δ HCN(10), δ HCC(50)	1348	1321
94	v NC(14), δ HCN(19), δ HCC(28)	1363	1333
95	δ HCN(38)	1417	1384
96	δ HCH(95)	1436	1407
97	v CC(16), δ HCC(11), δ HCH(98)	1445	1417

98	δ HCH(95), δ HCN(17), δ HCC(10)	1453	1419
99	ν CC(12), δ HCC(15)	1458	1431
100	δ HCH (72), τ HCCN(24)	1470	1453
101	δ HCC(10), δ HCH(72)	1483	1453
102	δ HCH(66), τ HCCN(25)	1488	1472
103	δ HCC(27), δ HCH(76), τ HCCN(24)	1497	1482
104	δ HCC(20), δ CCC(10), δ HCH(74), τ HCCN(26)	1504	1483
105	δ HCH(76), δ HCC(47), τ HCCN(23), δ CCC(10)	1508	1488
106	ν CC(19), δ HCC(24), δ HCH(74), τ HCCN(26)	1513	1493
107	δ HCH(76), τ HCOC(11)	1525	1503
108	δ HCH(74)	1534	1514
109	ν CC(26), ν NC(39), δ HCC(10), δ CCC(10)	1598	1537
110	ν CC(41), ν NC(13), δ HCH(14), δ HCC(17)	1600	1557
111	ν CC(24), δ HCC(20), δ CCC(10)	1613	1557
112	ν CC(34), δ HCC(16), δ CCC(10)	1623	1567
113	ν NC(43), ν CC(30), δ CCC(17)	1649	1572
114	ν CC(21), ν NC(45), δ HCC(11)	1671	1585
115	ν OC(83)	1726	1676
116	ν OC(85)	1744	1684
117	ν OC(46)	1777	1713
118	ν CH(91)	2907	2924
119	ν CH(92)	2933	2967
120	ν CH(96)	2946	2977
121	ν CH(94)	2957	2978
122	ν CH(100)	2985	3016
123	ν CH(100)	3003	3032
124	ν CH(46)	3016	3051
125	ν CH(92)	3018	3060
126	ν CH(96)	3029	3071
127	ν CH(51)	3062	3080
128	ν CH(52)	3064	3093
129	ν CH(36)	3083	3096
130	ν CH(67)	3091	3121
131	ν CH(66)	3092	3123
132	ν CH(29)	3097	3126
133	ν CH(56)	3108	3134
134	ν CH(48)	3119	3152
135	ν CH(26)	3138	3168



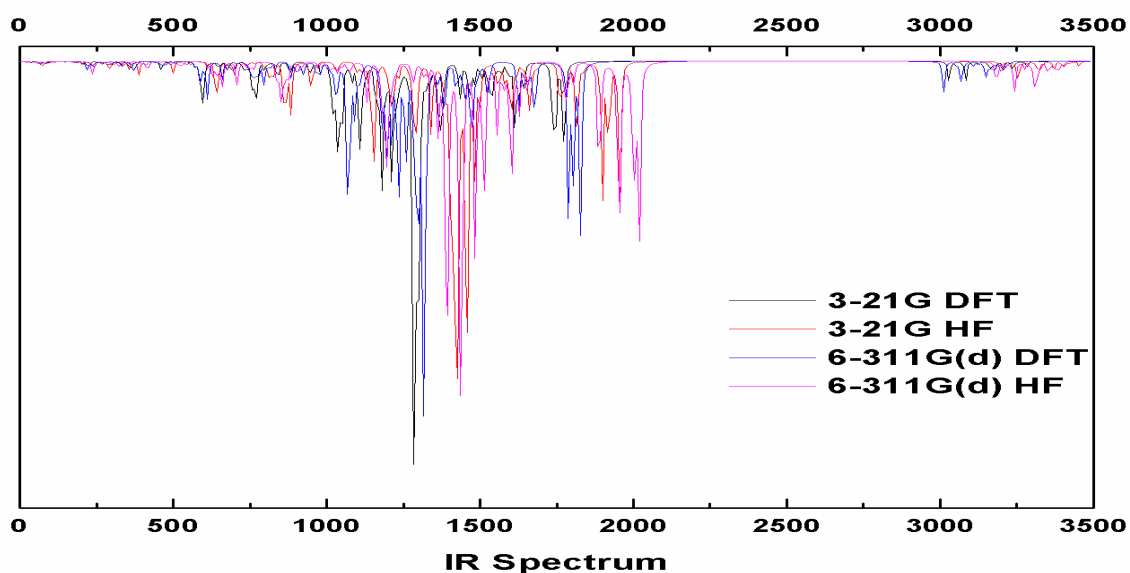
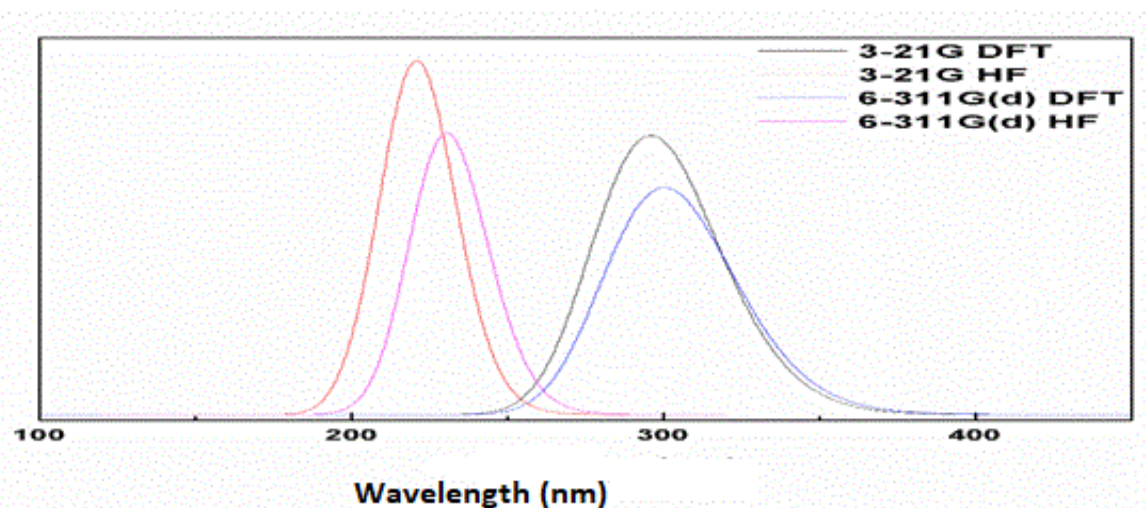
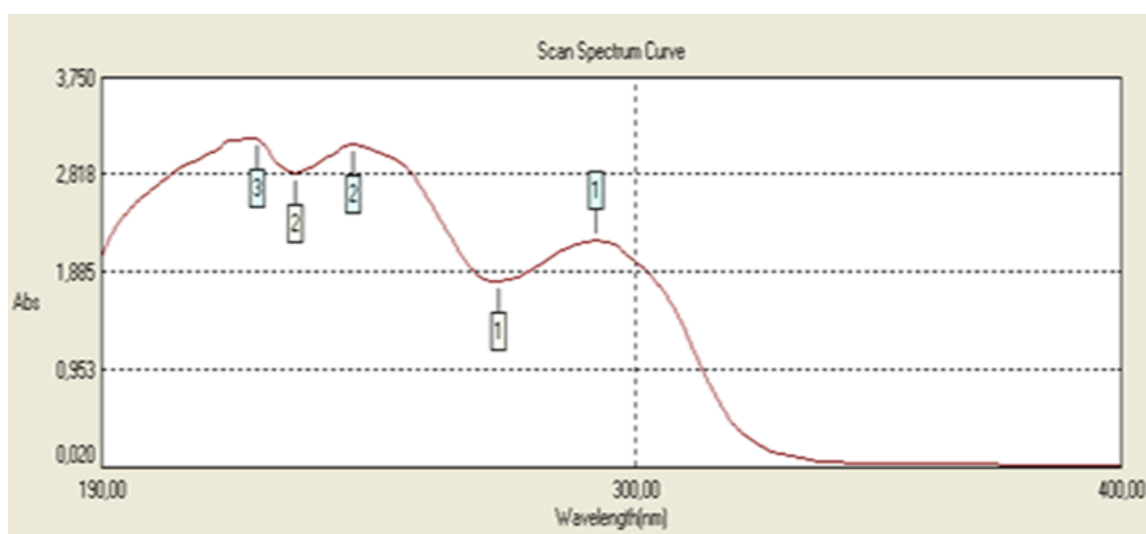


Figure 3. Experimental (a) and theoretical (6-311G(d)/3-21G DFT/HF) IR spectra of title compound



Experiment tal (nm)	λ (nm)	λ (nm)	Excitation Energy (eV)	Excitation Energy (eV)	f (osillatör strengths)	f (osillatör strengths)
	HF/B3LYP 6-311G(d)	HF/B3LYP 3-21G	HF/B3LYP 6-311G(d)	HF/B3LYP 3-21G	HF/B3LYP 6-311G(d)	HF/B3LYP 3-21G
292.00	233.56/305.	223.27/306.	5.3086/4.05	5.5532/4.04	0.5635/0.01	0.4944/0.02
	68	25	60	85	33	89
242.00	230.11/300.	218.45/296.	5.3881/4.13	5.6756/4.18	0.1160/0.61	0.2256/0.41
	10	12	15	70	82	98
222.00	216.34/295.	206.15/293.	5.7311/4.20	6.0143/4.22	0.0905/0.01	0.1064/0.14
	01	56	26	35	86	08

Figure 4. The experimental and calculated UV-vis spectrums (B3LYP/HF 6-311G(d), 3-21G) of title compound

Table 5. The calculated bond angles ($^{\circ}$) of title compound (6-311G(d) HF/B3LYP, 3-21G HF/B3LYP)

Bond Angles	HF	B3LYP	HF	B3LYP	
	6-311G(d)	6-311G(d)	3-21G	3-21G	
1	C(1)-N(40)-N(39)	105.770	105.508	104.543	103.744
2	C(1)-N(41)-N(42)	120.975	121.129	120.272	120.488
3	C(1)-N(41)-C(2)	108.151	108.209	109.246	109.227
4	C(1)-C(18)-H(33)	110.538	110.982	110.099	110.302
5	C(1)-C(18)-H(34)	108.517	108.681	108.875	108.805
6	C(1)-C(18)-H(35)	110.542	110.980	110.099	110.302
7	H(33)-C(18)-H(35)	107.879	107.292	108.036	107.700
8	H(34)-C(18)-H(33)	109.678	109.435	109.862	109.861
9	H(34)-C(18)-H(35)	109.678	109.446	109.862	109.862
10	N(40)-C(1)-N(41)	111.683	111.914	112.041	112.710
11	N(40)-N(39)-C(19)	119.251	119.033	118.857	118.595
12	N(39)-C(19)-O(47)	119.737	119.732	120.513	120.642
13	N(39)-C(19)-C(20)	116.694	115.798	115.264	114.021
14	O(47)-C(19)-C(20)	123.569	124.470	124.223	125.337
15	C(19)-C(20)-H(36)	111.197	111.480	110.990	110.991
16	C(19)-C(20)-H(37)	107.039	107.378	107.237	107.378
17	C(19)-C(20)-H(38)	111.216	111.485	110.990	110.995
18	H(36)-C(20)-H(37)	110.194	110.173	110.299	110.523
19	H(36)-C(20)-H(38)	107.029	106.204	107.056	110.526
20	H(37)-C(20)-H(38)	110.197	110.151	110.299	106.468
21	O(47)-C(19)-N(39)	119.737	119.732	124.223	120.642
22	C(19)-N(39)-C(2)	128.974	128.716	129.765	129.251
23	N(39)-C(2)-N(41)	102.622	102.118	102.792	102.165
24	N(39)-C(2)-O(43)	129.540	129.924	129.598	129.891
25	O(43)-C(2)-N(41)	127.838	127.957	127.611	127.944
26	C(2)-N(41)-N(42)	130.865	130.654	130.483	130.284
27	N(41)-C(1)-C(18)	123.094	123.131	122.180	122.098
28	N(40)-C(1)-C(18)	125.223	124.955	125.779	125.192
29	N(41)-N(42)-C(3)	120.423	119.566	119.242	117.363
30	N(42)-C(3)-H(21)	122.541	122.228	122.716	122.661
31	N(42)-C(3)-C(4)	120.346	120.205	120.114	119.751
32	H(21)-C(3)-C(4)	117.113	117.567	117.170	117.588
33	C(3)-C(4)-C(5)	117.977	117.869	119.062	117.901
34	C(3)-C(4)-C(9)	122.434	122.452	121.682	121.666
35	C(4)-C(5)-H(22)	120.849	120.256	120.988	121.126
36	C(4)-C(5)-C(6)	119.732	119.536	119.062	119.170
37	H(22)-C(5)-C(6)	119.418	120.203	119.949	119.704
38	C(5)-C(6)-O(44)	119.960	122.614	124.875	125.412
39	C(5)-C(6)-C(7)	121.092	120.949	120.767	120.573
40	O(44)-C(6)-C(7)	118.872	116.320	114.357	114.016
41	C(6)-C(7)-H(23)	119.636	119.179	118.702	118.525
42	C(6)-C(7)-C(8)	119.145	119.372	119.741	119.877

43	H(23)-C(7)-C(8)	121.219	121.449	121.557	121.597
44	C(7)-C(8)-H(24)	119.521	119.482	119.587	119.508
45	C(7)-C(8)-C(9)	120.530	120.512	120.328	120.341
46	H(24)-C(8)-C(9)	119.949	120.006	120.085	120.150
47	C(8)-C(9)-H(25)	120.549	120.832	121.108	121.532
48	C(8)-C(9)-C(4)	119.911	119.952	119.517	119.605
49	H(25)-C(9)-C(4)	119.540	119.216	119.374	118.864
50	C(9)-C(4)-C(5)	119.589	119.678	120.584	120.434
51	C(6)-O(44)-C(10)	119.544	120.971	128.197	125.440
52	O(44)-C(10)-O(45)	123.206	123.551	123.387	124.068
53	O(44)-C(10)-C(11)	111.970	111.140	111.477	110.193
54	O(45)-C(10)-C(11)	124.824	125.308	125.136	125.739
55	C(10)-C(11)-C(16)	122.163	122.627	122.037	122.553
56	C(10)-C(11)-C(12)	117.234	117.038	116.957	116.611
57	C(11)-C(12)-H(26)	120.477	120.192	120.635	120.160
58	C(11)-C(12)-C(13)	120.278	120.321	120.064	120.238
59	H(26)-C(12)-C(13)	119.245	119.486	119.301	119.602
60	C(12)-C(13)-O(46)	115.786	115.730	116.040	115.833
61	C(12)-C(13)-C(14)	119.418	119.515	119.348	119.181
62	C(13)-O(46)-C(17)	119.962	118.632	120.977	118.208
63	O(46)-C(13)-C(14)	124.796	124.755	124.612	124.986
64	O(46)-C(17)-H(30)	111.452	111.517	111.298	111.584
65	O(46)-C(17)-H(31)	106.183	105.741	105.458	104.862
66	O(46)-C(17)-H(32)	111.454	111.538	111.298	111.584
67	H(30)-C(17)-H(31)	109.109	109.251	109.624	109.692
68	H(30)-C(17)-H(32)	109.442	109.447	109.459	109.335
69	H(31)-C(17)-H(32)	109.106	109.249	109.624	109.692
70	H(26)-C(12)-C(13)	119.245	119.486	119.301	119.602
71	C(13)-C(14)-C(15)	119.798	119.685	119.348	120.142
72	C(13)-C(14)-H(27)	121.107	121.011	120.690	120.613
73	H(27)-C(14)-C(15)	119.096	119.303	119.171	119.246
74	C(14)-C(15)-C(16)	121.130	121.135	120.796	120.904
75	C(14)-C(15)-H(28)	119.030	119.065	119.260	119.183
76	H(28)-C(15)-C(16)	119.839	119.800	119.944	119.913
77	C(15)-C(16)-H(29)	120.745	120.821	121.386	121.644
78	C(15)-C(16)-C(11)	118.773	119.007	118.647	118.700
79	H(29)-C(16)-C(11)	120.482	120.172	119.967	119.657
80	C(16)-C(11)-C(12)	120.603	120.336	121.006	120.836

Table 6. The calculated bond lengths (\AA) of title compound (6-311G(d) HF/B3LYP, 3-21G HF/B3LYP)

Bond Lengths	HF	HF	B3LYP	B3LYP	
	6-311G(d)	3-21G	6-311G	3-21G	
1	C(1)-N(41)	1.3843	1.3809	1.3907	1.3932
2	C(1)-N(40)	1.2751	1.2614	1.2898	1.3077
3	C(1)-C(18)	1.4836	1.4873	1.4849	1.4857
4	C(18)-H(33)	1.0823	1.0826	1.0925	1.0947
5	C(18)-H(34)	1.0792	1.0796	1.0889	1.0909
6	C(18)-H(35)	1.0823	1.0827	1.0926	1.0947
7	N(41)-C(2)	1.3847	1.3775	1.4070	1.4163
8	C(2)-O(43)	1.2166	1.1924	1.2137	1.2372
9	N(39)-C(2)	1.3762	1.3734	1.3978	1.4032

10	N(39)-N(40)	1.4353	1.3806	1.3917	1.4506
11	N(39)-C(19)	1.4046	1.4122	1.4314	1.4265
12	C(19)-C(20)	1.5080	1.5061	1.5081	1.5149
13	C(19)-O(47)	1.2017	1.1775	1.2000	1.2234
14	C(20)-H(36)	1.0809	1.0813	1.0913	1.0934
15	C(20)-H(37)	1.0784	1.0792	1.0884	1.0901
16	C(20)-H(38)	1.0809	1.0813	1.0914	1.0934
17	N(41)-N(42)	1.4008	1.3642	1.3716	1.4143
18	N(42)-C(3)	1.2670	1.2574	1.2845	1.2969
19	C(3)-H(21)	1.0699	1.0737	1.0863	1.0846
20	C(3)-C(4)	1.4709	1.4763	1.4661	1.4648
21	C(4)-C(5)	1.3883	1.3854	1.4006	1.4033
22	C(4)-C(9)	1.3864	1.3937	1.4036	1.4035
23	C(5)-H(22)	1.0656	1.0746	1.0820	1.0778
24	C(5)-C(6)	1.3807	1.3815	1.3909	1.3949
25	C(6)-O(44)	1.3949	1.3782	1.3922	1.4087
26	C(6)-C(7)	1.3816	1.3746	1.3897	1.3975
27	C(7)-H(23)	1.0693	1.0741	1.0840	1.0817
28	C(7)-C(8)	1.3817	1.3895	1.3955	1.3949
29	C(8)-H(24)	1.0712	1.0746	1.0848	1.0833
30	C(8)-C(9)	1.3811	1.3777	1.3868	1.3917
31	C(9)-H(25)	1.0695	1.0726	1.0829	1.0819
32	O(44)-C(10)	1.3579	1.3782	1.3739	1.3955
33	C(10)-O(45)	1.2049	1.1781	1.2019	1.2276
34	C(10)-C(11)	1.4782	1.4916	1.4885	1.4800
35	C(11)-C(12)	1.3773	1.3802	1.3927	1.3925
36	C(11)-C(16)	1.3885	1.3934	1.4027	1.4029
37	C(12)-H(26)	1.0687	1.0722	1.0828	1.0812
38	C(12)-C(13)	1.3859	1.3903	1.3973	1.3986
39	C(13)-O(46)	1.3686	1.3452	1.3608	1.3822
40	C(13)-C(14)	1.3821	1.3851	1.3988	1.4000
41	C(14)-H(27)	1.0695	1.0726	1.0827	1.0815
42	C(14)-C(15)	1.3879	1.3902	1.3965	1.3990

43	C(15)-H(28)	1.0714	1.0749	1.0850	1.0836
44	C(15)-C(16)	1.3769	1.3770	1.3871	1.3901
45	C(16)-H(29)	1.0673	1.0713	1.0815	1.0793
46	O(46)-C(17)	1.4370	1.3979	1.4195	1.4604
47	C(17)-H(30)	1.0830	1.0849	1.0953	1.0967
48	C(17)-H(31)	1.0772	1.0784	1.0881	1.0900
49	C(17)-H(32)	1.0830	1.0849	1.0954	1.0967

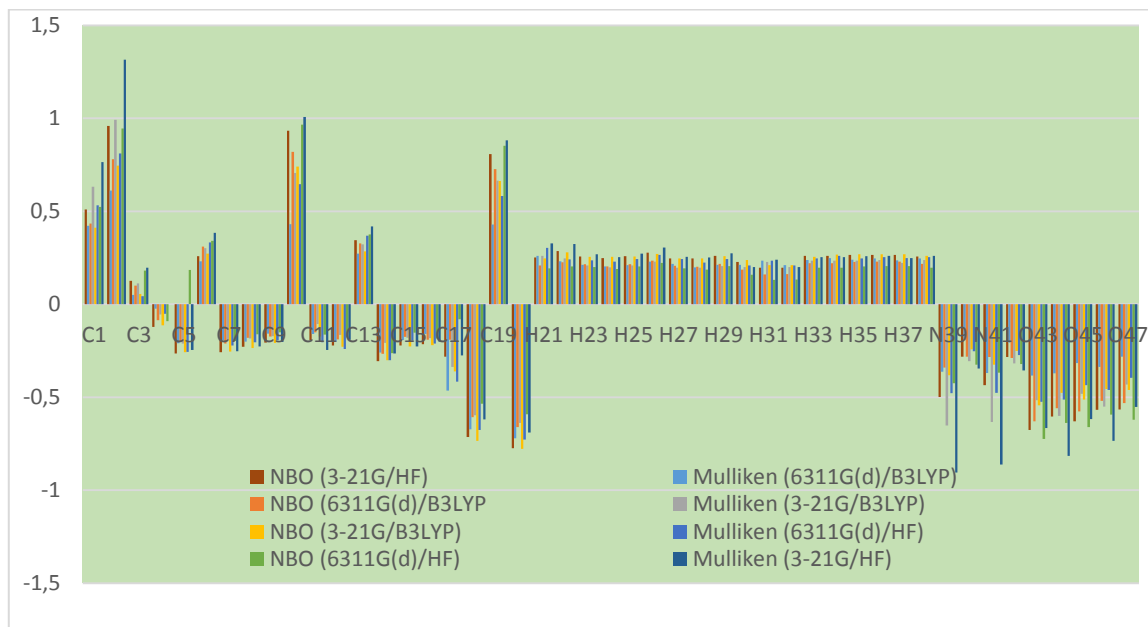
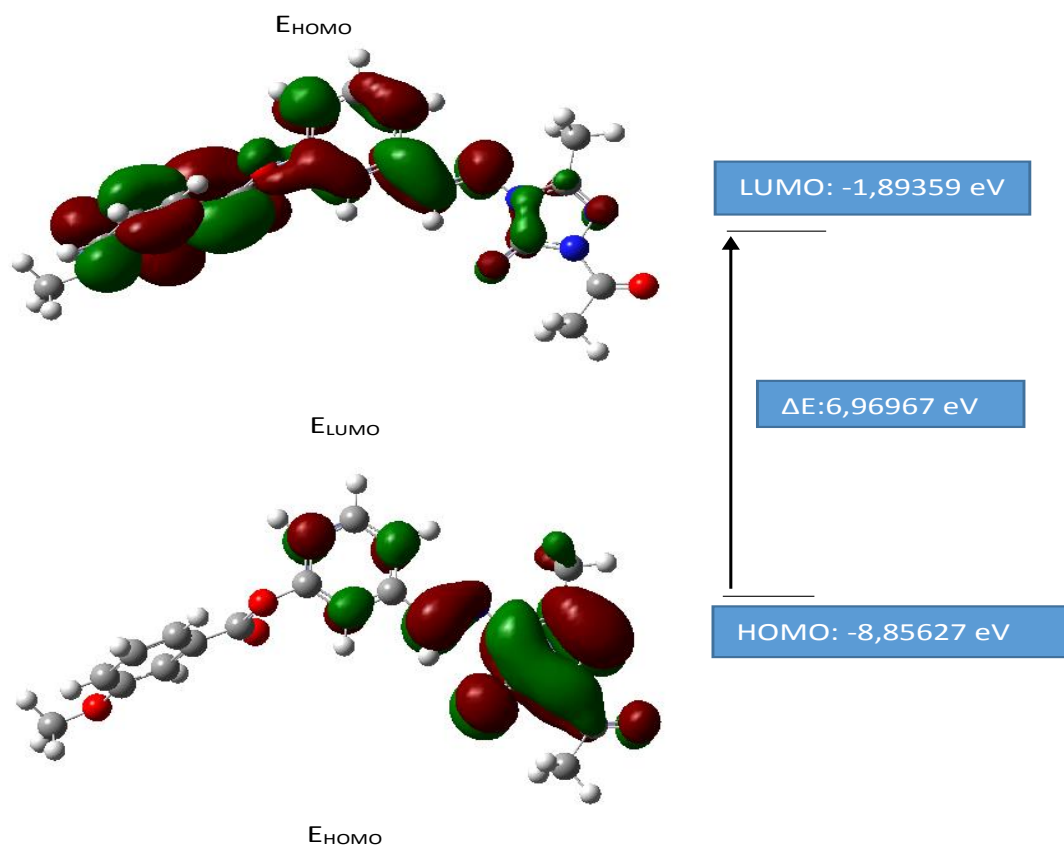
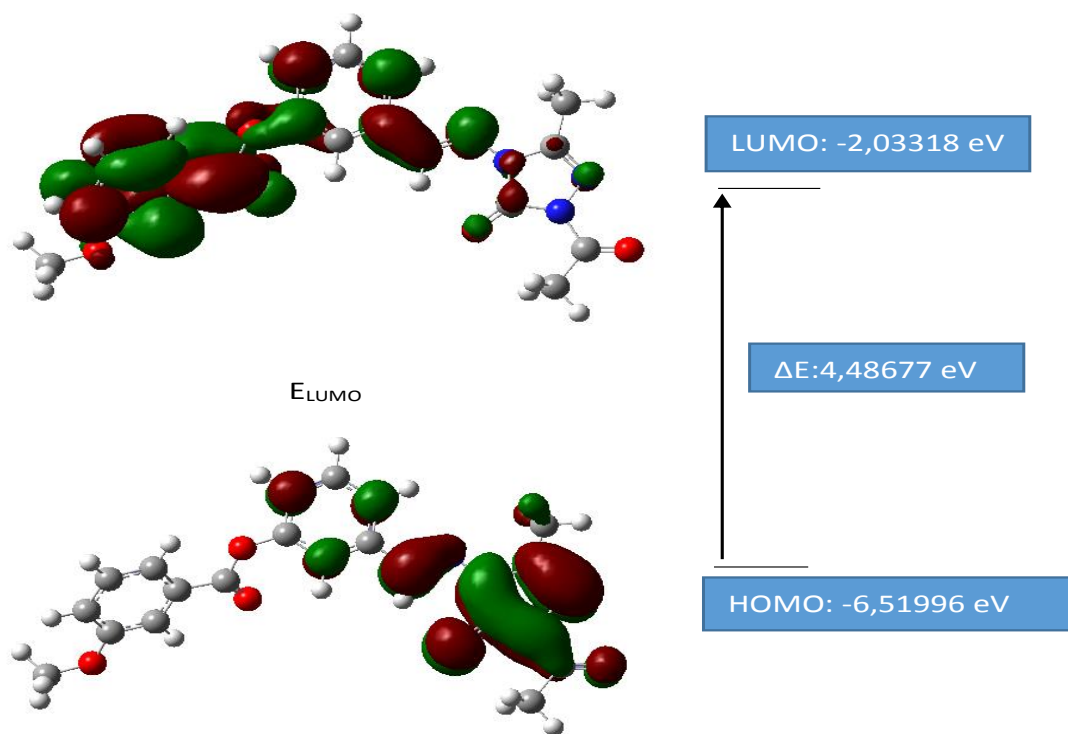


Figure 5. Graphics of the calculated Mulliken atomic charges and NBO values of title compound



B3LYP (3-21G)

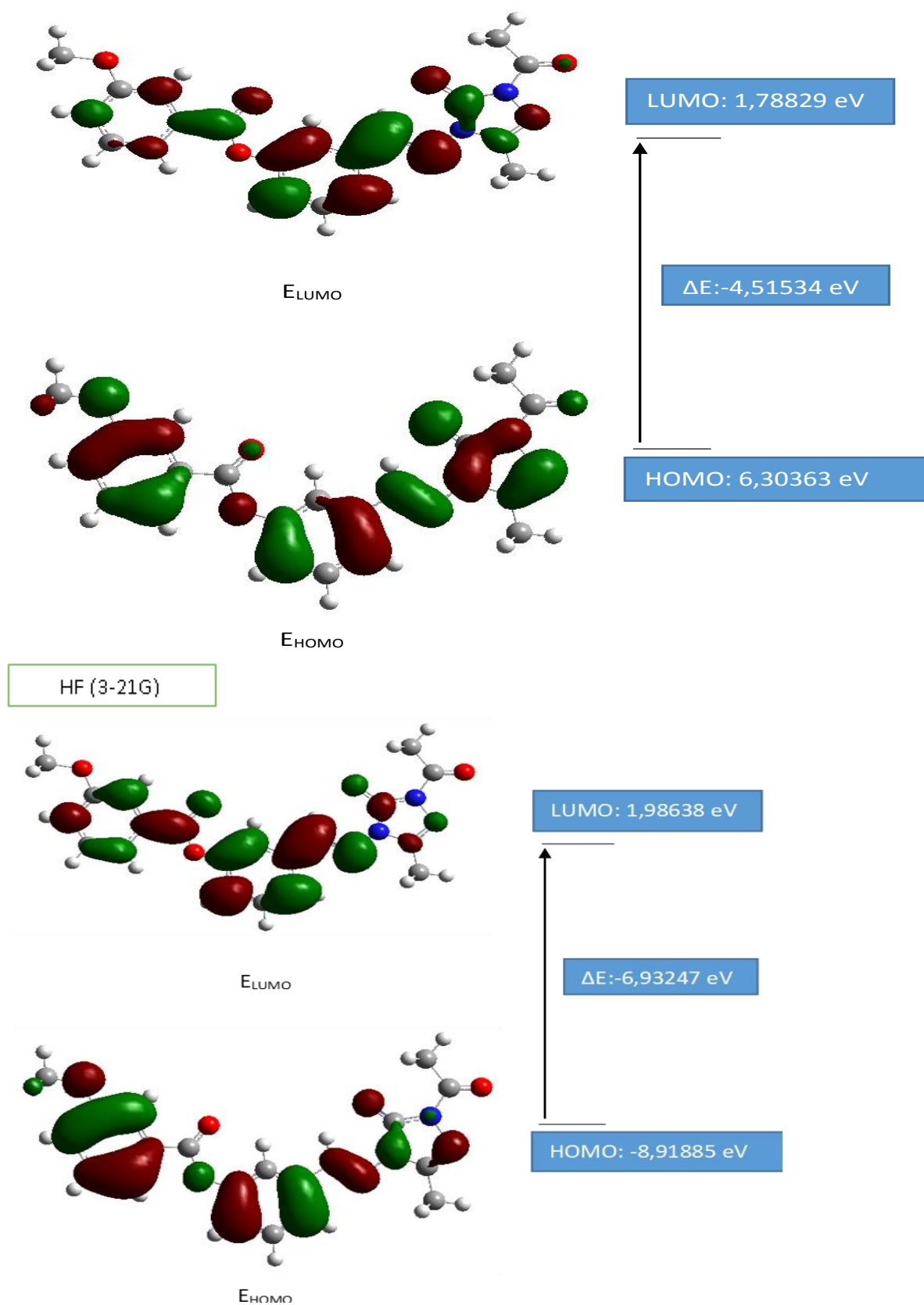


Figure 6. 3D plots of HOMO-LUMO energies of title compound at the HF/B3LYP 6-311G(d) and 3-21G levels

Table 7. The calculated electronic properties of title compound (6-311G(d) HF/B3LYP, 3-21G HF/B3LYP)

	B3LYP (6-311G(d))	Hartree	Ev	Kcal/mol	Kj/mol
	LUMO	-0,07472	-2,03318	-46,887	-196,177
	HOMO	-0,23961	-6,51996	-150,356	-629,096
A	Electron Affinity	0,07472	2,03318	46,887	196,177
I	Ionization Potential	0,23961	6,51996	150,356	629,096
ΔE	Energy Gap	0,16489	4,48677	103,469	432,919
χ	Electronegativity	0,157165	4,27657	98,6215	412,637
Pi	Chemical Potential	-0,157165	-4,27657	-98,6215	-412,637
ω	Electrophilic Index	0,00101823	0,02771	0,63894	2,67336
IP	Nucleophilic Index	-0,01295747	-0,35258	-8,13085	-34,0198
S	Molecular Softness	12,1293	330,047	7611,17	31845,5
η	Molecular Hardness	0,082445	2,24339	51,7345	216,459
	HF (6-311G(d))	Hartree	Ev	Kcal/mol	Kj/mol
	LUMO	-0,06959	-1,89359	-43,6679	-182,709
	HOMO	-0,32547	-8,85627	-204,233	-854,521
A	Electron Affinity	0,06959	1,89359	43,6679	182,709
I	Ionization Potential	0,32547	8,85627	204,233	854,521
ΔE	Energy Gap	0,25588	6,96267	160,565	671,813
χ	Electronegativity	0,19753	5,37493	123,951	518,615
Pi	Chemical Potential	-0,19753	-5,37493	-123,951	-518,615
ω	Electrophilic Index	0,002495988	0,06792	1,56624	6,55322
IP	Nucleophilic Index	-0,02527199	-0,68767	-15,8582	-66,3516
S	Molecular Softness	7,8162	212,683	4904,67	20521,3
η	Molecular Hardness	0,12794	3,48134	80,2827	335,906
	B3LYP (3-21G)	Hartree	Ev	Kcal/mol	Kj/mol
	LUMO	0,06572	1,78829	41,2395	172,548
	HOMO	0,23166	6,30363	145,367	608,223
A	Electron Affinity	-0,06572	-1,78829	-41,2395	-172,548
I	Ionization Potential	-0,23166	-6,30363	-145,367	-608,223
ΔE	Energy Gap	-0,16594	-4,51534	-104,128	-435,675
χ	Electronegativity	-0,14869	-4,04596	-93,3034	-390,386
Pi	Chemical Potential	0,14869	4,04596	93,3034	390,386
ω	Electrophilic Index	-0,00091718	-0,02496	-0,57553	-2,40806
IP	Nucleophilic Index	-0,01233681	-0,33569	-7,74138	-32,3903
S	Molecular Softness	-12,0525	-327,958	-7563,01	-31644
η	Molecular Hardness	-0,08297	-2,25767	-52,0639	-217,838
	HF (3-21G)	Hartree	Ev	Kcal/mol	Kj/mol
	LUMO	0,073	1,98638	45,8077	191,662
	HOMO	0,32777	8,91885	205,677	860,56
A	Electron Affinity	-0,073	-1,98638	-45,8077	-191,662
I	Ionization Potential	-0,32777	-8,91885	-205,677	-860,56

ΔE	Energy Gap	-0,25477	-6,93247	-159,869	-668,899
χ	Electronegativity	-0,200385	-5,45262	-125,742	-526,111
Π	Chemical Potential	0,200385	5,45262	125,742	526,111
ω	Electrophilic Index	-0,00255752	-0,06959	-1,60485	-6,71476
IP	Nucleophilic Index	-0,02552604	-0,69458	-16,0177	-67,0186
S	Molecular Softness	-7,8502	-213,61	-4926,04	-20610,7
η	Molecular Hardness	-0,127385	-3,46624	-79,9345	-334,449

Table 8. The mean polizability ($\langle\alpha\rangle$), the anisotropy of the polarizability ($\Delta\alpha$), the mean first-order hyperpolarizability ($\langle\beta\rangle$) values of title compound

	B3LYP (6-311G(d))	B3LYP(3-21G)	HF(6-311G(d))	HF(3-21G)
μ_x	5.990 Debye	5.1631 Debye	7.0546 Debye	6.3365 Debye
μ_y	-4.973 Debye	-4.2226 Debye	-6.5512 Debye	-6.0344 Debye
μ_z	-1.143 Debye	-1.0421 Debye	-1.4866 Debye	-1.5253 Debye
μ_{Toplam}	7.869 Debye	6.7508 Debye	9.7414 Debye	8.8821 Debye
α_{xx}	62,93 a.u.	62,00 a.u.	51,04 a.u.	49,55 a.u.
α_{yy}	42,44 a.u.	25,78 a.u.	34,08 a.u.	36,49 a.u.
α_{zz}	21,95 a.u.	15,69 a.u.	24,02 a.u.	11,60 a.u.
α	42,440x10 ⁻²⁴ esu	42,176x10 ⁻²⁴ esu	36,389x10 ⁻²⁴ esu	33,394x10 ⁻²⁴ esu
$\Delta\alpha$	35,489x10 ⁻²⁴ esu	34,491x10 ⁻²⁴ esu	23,648x10 ⁻²⁴ esu	32,547x10 ⁻²⁴ esu
β_x	667 a.u.	20608 a.u.	739 a.u.	-2094 a.u.
β_y	2036 a.u.	-2544 a.u.	1181 a.u.	-794 a.u.
β_z	-170 a.u.	1310 a.u.	369 a.u.	-0,0948 a.u.
β_{xxx}	48,83 a.u.	-2361,57 a.u.	31,97 a.u.	-249,90 a.u.
β_{xxy}	243,85 a.u.	-125,85 a.u.	130,25 a.u.	-52,66 a.u.
β_{xyy}	67,75 a.u.	-9,83 a.u.	90,77 a.u.	-81,40 a.u.
β_{yyy}	-40,59 a.u.	-137,91 a.u.	-26,40 a.u.	-14,45 a.u.
β_{xxz}	-145,33 a.u.	76,32 a.u.	-43,56 a.u.	0,000193 a.u.
β_{xyz}	-44,33 a.u.	-13,01 a.u.	-34,44 a.u.	-0,00221 a.u.
β_{yyz}	71,44 a.u.	17,38 a.u.	38,91 a.u.	-0,00985 a.u.
β_{xzz}	-36,87 a.u.	-90,96 a.u.	-21,68 a.u.	81,02 a.u.
β_{yzz}	40,03 a.u.	-40,21 a.u.	37,25 a.u.	-27,86 a.u.
β_{zzz}	53,50 a.u.	62,80 a.u.	48,73 a.u.	-0,00166 a.u.
β	2,149x10 ⁻³⁰ esu	20,806x10 ⁻³⁰ esu	1,441x10 ⁻³⁰ esu	2,241x10 ⁻³⁰ esu

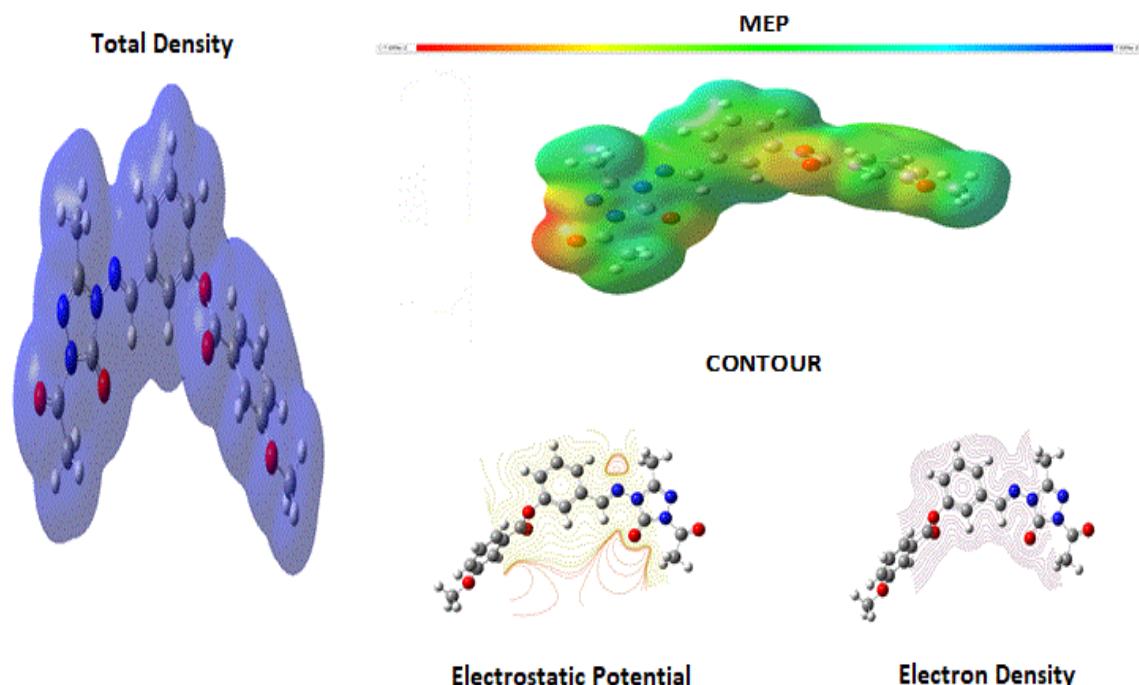


Figure 7. The calculated molecular surfaces of title compound

Table 9. The calculated dipole moment values of title compound (6-311G(d) HF/B3LYP, 3-21G HF/B3LYP)

Dipole Moment	HF	HF	B3LYP	B3LYP
	6-311G(d)	3-21G	6-311G(d)	3-21G
μ_x	7.0546	6.3365	5.9903	5.1631
μ_y	-6.5512	-6.0344	-4.9729	-4.2226
μ_z	-1.4866	-1.5253	-1.1429	-1.0421
μ_{Toplam}	9.7414	8.8821	7.8689	6.7508

Conclusion

In this paper, the spectroscopic, geometric and electronic parameters of 1-acetyl-3-methyl-4-[3-(3-methoxybenzoyloxy)benzylideneamino]-4,5-dihydro-1H-1,2,4-triazol-5-one have been calculated by using DFT (B3LYP) and HF methods with the 6-311G(d) and 3-21G basis sets and compared with the experimental parameters. The IR, ^1H - and ^{13}C - NMR spectra have been recorded and analyzed. The theoretically computed spectra were found good agreement with experimental IR, UV-vis, ^1H - and ^{13}C - NMR spectra. The Mulliken atomic charges, NBO, HOMO and LUMO energy of 1-acetyl-3-methyl-4-[3-(3-methoxybenzoyloxy)benzylideneamino]-4,5-dihydro-1H-1,2,4-triazol-5-one in the ground state have been calculated by using DFT/6-311G(d) and DFT/3-21G, HF/6-311G(d) and HF/3-21G levels. The value of the energy gap between the HOMO-LUMO energies were determined. Geometric parameters; bond angles and bond lengths were compared with experimental values obtained from literature. All results showed that the calculated spectroscopic, geometric and electronic parameters obtained by B3LYP/6-311G(d) method had a better agreement with the experimental values than 3-21G and HF method.

References

- Ali, K. A., Ragab, E. A., Farghaly, T. A., & Abdalla, M. M. (2011). Synthesis of new functionalized 3-substituted [1,2,4]triazolo [4,3-a]pyrimidine derivatives: potential antihypertensive agents. *Acta Poloniae Pharmaceutica*, 68(2), 237-47. Retrieved from <http://www.ncbi.nlm.nih.gov/pubmed/21485297>

- Al-Tamimi, A. S. (2016). Electronic structure, hydrogen bonding and spectroscopic profile of a new 1,2,4-triazole-5(4H)-thione derivative: A combined experimental and theoretical (DFT) analysis. *Journal of Molecular Structure* 1120, 215-227.
<http://dx.doi.org/10.1016/j.molstruc.2016.05.029>
- Bauernschmitt R., & Ahlrichs, R. (1996). Treatment of electronic excitations within the adiabatic approximation of time dependent density functional theory. *Chemical Physics Letters*, 256, 454-464.
[https://doi.org/10.1016/0009-2614\(96\)00440-X](https://doi.org/10.1016/0009-2614(96)00440-X)
- Casida, M.E., Jamorski, C., Casida, K.C, Salahub D.R. (1998). Molecular excitation energies to high-lying bound states from time-dependent density-functional response theory: characterization and correction of the time-dependent local density approximation ionization threshold. *Journal Chemical Physics*. 1998; 108, 4439–4449.
- Chen, X., Shi, Y. M., Huang, C., Xia, S., Yang, L. J., & Yang, X. D. (2016). Novel dibenzo[b,d]furan-1H-1,2,4-triazole derivatives: Synthesis and antitumor activity. *Anti-Cancer Agents in Medicinal Chemistry*, 16(3), 377–386. <http://doi.org/10.2174/1871520615666150817115913>
- Dodds, J.L., McWeeny, R., Sadlej, A.J. (1980). *Molecular Physics*. 41, 1419–1430.
- El-Serwy, W. S., Mohamed, N. A., Abbas, E. M., & Abdel-Rahman, R. F. (2013). Synthesis and anti-inflammatory properties of novel 1,2,4-triazole derivatives. *Research on Chemical Intermediates*, 39(6), 2543–2554. <http://doi.org/10.1007/s11164-012-0781-9>
- Frisch, A., Nielson, A.B., Holder, A.J. (2003). Gaussview User Manual, Gaussian Inc. Wallingford, CT.
- Frisch, M.J., Trucks, G.W., Schlegel, H.B., Scuseria, G.E., Rob, b M.A., Cheeseman, J.R., Scalmani, G., Barone, V., Mennucci, B., Petersson, G.A., Nakatsuji, H., Caricato, M., Li X., Hratchian, H.P., Izmaylov, A.F., Bloino, J., Zheng, G., Sonnenberg, J.L., Hada, M., Ehara, M., Toyota, K., Fukuda, R., Hasegawa, J., Ishida, M., Nakajima, T., Honda, Y., Kitao, O., Nakai, H., Vreven, T., Montgomery, J.A., Jr. Vreven, T., Peralta, J.E., Ogliaro, F., Bearpark, M., Heyd, J.J., Brothers, E., Kudin, N., Staroverov, V.N., Kobayashi, R., Normand, J., Raghavachari, K., Rendell, A., Burant, J.C., Iyengar, S.S., Tomasi, J., Cossi, M., Rega, N., Millam, J.M., Klene, M., Knox, J.E., Cross, J.B., Bakken, V., Adamo, C., Jaramillo, J., Gomperts, R., Stratmann, R.E., Yazyev, O., Austin, A.J., Cammi, R., Pomelli, C., Ochterski, J.W., Martin, L.R., Morokuma, K., Zakrzewski, V.G., Voth, G.A., Salvador, P., Dannenberg, J.J., Dapprich, S., Daniels, A.D., Farkas, O., Foresman, J.B., Ortiz, J.V., Cioslowski, J., Fox, D.J. (2009). Gaussian Inc. Wallingford, CT.
- Gatfaoui, S., Issaoui, N., Mezni, A., Bardak, F., Roisnel, T., Atac, A., Marouani, H. (2017). Synthesis, structural and spectroscopic features, and investigation of bioactive nature of a novel organic-inorganic hybrid material 1H-1,2,4-triazole-4-ium trioxonitrate. *Journal of Molecular Structure*, 1150, 242-257.
<http://dx.doi.org/10.1016/j.molstruc.2017.08.092>
- Jamróz, M.H. (2004). Vibrational Energy Distribution Analysis: VEDA 4 program. Warsaw.
- Jin, R.Y., Sun, X.H., Liu, Y.F., Long, W., Lu, W.T., Maa H.X. (2014). Synthesis, crystal structure, IR, ¹H NMR and theoretical calculations of 1,2,4-triazole Schiff base. *Journal of Molecular Structure*, 1062, 13–20.
<http://dx.doi.org/10.1016/j.molstruc.2014.01.010>
- Pokharia, M., Yadav, S. K., Mishra, H., Pandey, N., Tilak, R., Pokharia, S. (2017). Synthesis, spectroscopic characterization, biological activity and theoretical studies of (E)-N3-(2-chlorobenzylidene)-H-1,2,4-triazole-3,5-diamine. *Journal of Molecular Structure*, 1144, 324-337.
<http://dx.doi.org/10.1016/j.molstruc.2017.05.030>
- Süleymanoğlu, N., Ünver, Y., Ustabas, R., Direkel, Ş., Alpaslan, G. (2017). Antileishmanial activity study and theoretical calculations for 4-amino-1,2,4-triazole derivatives. *Journal of Molecular Structure*, 1144, 80-86.
<http://dx.doi.org/10.1016/j.molstruc.2017.05.017>
- Stratmann, R.E., Cuseria, S.G.E., Frisch, M.J. (1998). An efficient implementation of time-dependent density-functional theory for the calculation of excitation energies of large molecules. *Journal Chemical Physics*. 109, 8218–8224.
<http://doi.org/10.1063/1.477483>
- Uzgören-Baran, A., Tel, B. C., Sargöl, D., Öztürk, E. I., Kazkayas, I., Okay, G., Ertan, M., Tozkoparan, B. (2012). Thiazolo[3,2-b]-1,2,4-triazole-5(6H)-one substituted with ibuprofen: Novel non-steroidal anti-inflammatory agents with favorable gastrointestinal tolerance. *European Journal of Medicinal Chemistry*, 57, 398–406. <http://doi.org/10.1016/j.ejmech.2012.07.009>
- Medetalibeyoğlu, H., Yüksek, H. (2018). Theoretical Investigation of Spectroscopic and Thermodynamic Properties of 1-acetyl-3-methyl-4-[3-(3-methoxybenzoxy)benzylidenamino]-4,5-dihydro-1H-1,2,4-triazol-5-one by 6-311G(d) and 3-21G HF/DFT(B3LYP) Methods. *International Conference on*

Research in Education and Science (ICRES), 141.

Wolinski, K., Hinton, J.F., Pulay, P. (1990). Efficient implementation of the gauge-independent atomic orbital method for NMR chemical shift calculations. *Journal of American Chemical Society*. 112, 8251-8260. <http://doi.org/10.1021/ja00179a005>

Zhang, F., Wen, Q., Wang, S. F., Shahla Karim, B., Yang, Y. S., Liu, J. J., Zhang, W. M., Zhu, H. L. (2014). Design, synthesis and antibacterial activities of 5-(pyrazin-2-yl)-4H-1,2,4-triazole-3-thiol derivatives containing Schiff base formation as FabH inhibitory. *Bioorganic & Medicinal Chemistry Letters*, 24(1), 90–95. <http://doi.org/10.1016/J.BMCL.2013.11.079>

Author Information

Hilal Medetalibeyoglu

Kafkas University,
Department of Chemistry,
Kars, Turkey

Contact e-mail: hilalmedet@gmail.com

Haydar Yuksek

Kafkas University,
Department of Chemistry,
Kars, Turkey

Antioxidant and Antimicrobial Activities of Some Newly Synthesized 4-[1-(2,6-Dimethylmorpholin-4-yl-methyl)-3-alkyl(aryl)-4,5-dihydro-1H-1,2,4-triazol-5-on-4-yl-azomethine]-2-methoxyphenyl benzoates

Yonca YILMAZ
Kafkas University

Ahmet HARMANKAYA
Kafkas University

Sevda MANAP
Kafkas University

Haydar YUKSEK
Kafkas University

Ozlem GURSOY KOL
Kafkas University

Muzaffer ALKAN
Kafkas University

Abstract: In this study, 4-(3-alkyl/aryl-4,5-dihydro-1H-1,2,4-triazol-5-one-4-yl-azomethine)-2-methoxyphenyl benzoates were treated with 2,6-dimethylmorpholine in the presence of formaldehyde according to the Mannich reaction to synthesize six novel 4-[1-(2,6-dimethylmorpholin-4-yl-methyl)-3-alkyl(aryl)-4,5-dihydro-triazol-5-on-4-yl-azomethine]-2-methoxyphenyl benzoates. The structures of synthesized six novel heterocyclic compounds were characterized by IR, ^{13}C -NMR and ^1H -NMR spectroscopic methods. The novel 4-[1-(2,6-dimethylmorpholin-4-yl-methyl)-3-alkyl(aryl)-4,5-dihydro-triazol-5-on-4-yl-azomethine]-2-methoxyphenyl benzoates were investigated *in vitro* antioxidant properties by using reducing power, free radical scavenging and metal chelating activity. For the measurement of the reductive ability, Fe^{3+} - Fe^{2+} transformation was investigated in the presence of compound using by the method of Oyaizu (1986). The hydrogen atoms or electrons donation ability of the synthesized compound was measured by DPPH \cdot using the method of Blois (1958). The chelating effect of ferrous ions by the compound was determined according to the method of Dinis, Madeira & Almeida (1994). BHT, BHA, EDTA and α -tocopherol were used as reference antioxidant compounds. The new compounds were examined *in-vitro* antimicrobial properties against 6 different microorganisms (*Bacillus subtilis* (ATCC11774), *Bacillus Cereus* (ATCC11778), *Staphylococcus aureus* (ATCC6538), *Escherichia coli* (ATCC25922), *Pseudomonas aeruginosa* (ATCC27853) and *Klebsiella pneumonia* (ATCC4352)) by the agar well method and the obtained results were evaluated.

Keywords: Mannich base, 4,5-dihydro-1H-1,2,4-triazol-5-one, Antioxidant, Antimicrobial

Introduction

Mannich bases have applications the field medicinal chemistry, the product synthetic polymers, the petroleum industry, as products used in water treatment, cosmetics, the dyes industry, etc (Tramontini & Angiolini, 1994). Moreover, Mannich bases have some biological activities such as anticancer (Savariz et al., 2010), antibacterial

- This is an Open Access article distributed under the terms of the Creative Commons Attribution-Noncommercial 4.0 Unported License, permitting all non-commercial use, distribution, and reproduction in any medium, provided the original work is properly cited.

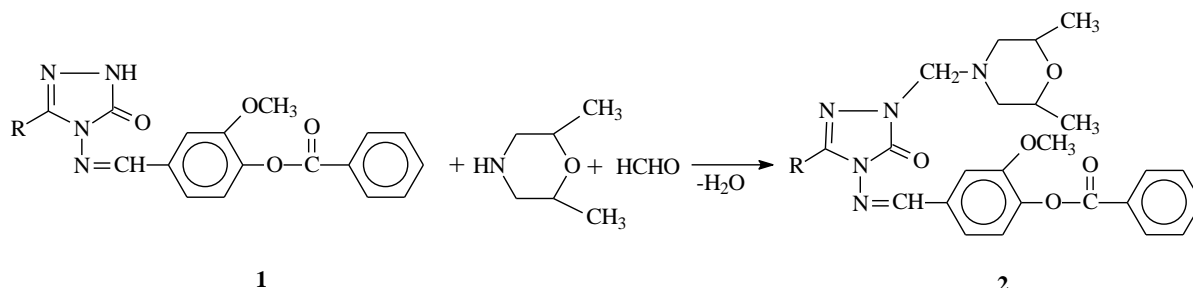
- Selection and peer-review under responsibility of the Organizing Committee of the Conference

(Maddila & Jonnalagadda, 2012), anti-inflammatory (Liu, Yu, Li, Pang, & Zhao, 2013), anti-HIV (Sriram, Yogeewari, Dinakaran, & Sowmya, 2008), analgesic (Nithinchandra, Kalluraya, Aamir, & Shabaraya, 2012), antiviral (Chen et al., 2010), antifungal (Ozkan-Daguyan, Sahin, & Koksak, 2013), antitumor (Pati et al., 2008), antidepressant (Köksal & Bilge, 2007) and antioxidant activities (Hamama, Zoorob, Gouda, & Afsah, 2011).

Antioxidants are extensively studied for their capacity to protect organism and cell from damage that is induced by the oxidative stress. A great deal of research has been devoted to the study of different types of natural and synthetic antioxidant. A large number of heterocyclic compounds, containing the 1,2,4-triazole ring, are associated with diverse biological properties such as antioxidant, anti-inflammatory, antimicrobial and antiviral activity. External chemicals and internal metabolic processes in human body or in food system might produce highly reactive free radicals, especially oxygen derived radicals, which are capable of oxidizing biomolecules by resulting in cell death and tissue damage. Oxidative damages play a significantly pathological role in human diseases. Cancer, emphysema, cirrhosis, atherosclerosis and arthritis have all been correlated with oxidative damage. Also, excessive generation of reactive oxygen species (ROS) induced by various stimuli and which exceeds the antioxidant ability of the organism leads to variety of pathophysiological processes like inflammation, diabetes, genotoxicity and cancer (McClements & Decker, 2000).

Triazoles are heterocyclic compounds that contain three nitrogen atoms. 1,2,4-Triazole and 4,5-dihydro-1H-1,2,4-triazol-5-one derivatives are reported to possess a broad spectrum of biological activities such as analgesic, antibacterial, antioxidant and antiparasitic properties (Aktas-Yokus, Yuksek, Gursoy-Kol, & Alpay-Karaoglu, 2015; Chidananda et al., 2012). Considering about the development of new hetero moieties by combining potential biological active scaffolds, an attempt was made here to obtain 1,2,4-triazoles bearing piperidine ring and to evaluate their antioxidant activity.

In the present paper, 4-(3-alkyl/aryl-4,5-dihydro-1H-1,2,4-triazol-5-one-4-yl-azomethine)-2-methoxyphenyl benzoates (**1**) (Koca, Yıldız, & Köçek, 2010) were treated with 2,6-dimethylmorpholine in the presence of formaldehyde according to the Mannich reaction to synthesize six novel 4-[1-(2,6-dimethylmorpholin-4-yl-methyl)-3-alkyl(aryl)-4,5-dihydro-triazol-5-on-4-yl-azomethine]-2-methoxyphenyl benzoates (**2**).



Scheme 1

Method

Chemicals and Apparatus

Chemical reagents used in this paper were bought from Merck AG, Aldrich and Fluka. Melting points were recorded in open glass capillaries using a Stuart SMP30 melting point apparatus and were not corrected. The infrared spectra were recorded on an Alpha-P Bruker FT-IR Spectrometer. ¹H and ¹³C NMR spectra were determined in deuterated dimethyl sulfoxide with TMS as internal standard using a Bruker Avance III spectrophotometer at 400 MHz and 100 MHz, respectively.

Synthesis of 4-[1-(2,6-dimethylmorpholin-4-yl-methyl)-3-alkyl(aryl)-4,5-dihydro-triazol-5-on-4-yl-azomethine]-2-methoxyphenyl benzoates: The General Procedure

4-(3-alkyl/aryl-4,5-dihydro-1H-1,2,4-triazol-5-one-4-yl-azomethine)-2-methoxyphenyl benzoates (**1**) were obtained according to the literature (Koca, Yıldız, & Köçek, 2010). Then, to solution of this compound (**1**) (5 mmol) in absolute ethanol was added 2,6-dimethylmorpholine (6 mmol). The reaction mixture was refluxed for 4 hours. The mixture was left at room temperature for overnight. After cooling the mixture in the refrigerator,

the solid formed was obtained by filtration, washed with cold ethanol and recrystallized from ethanol. Several recrystallizations of the residue from the same solvent gave pure compounds **2** as colourless crystals.

4-[1-(2,6-dimethylmorpholin-4-yl-methyl)-3-methyl-4,5-dihydro-triazol-5-on-4-yl-azomethine]-2-methoxyphenyl benzoate (2a)

Yield: 70.58%, m.p. 90°C. IR (KBr, ν , cm^{-1}): 1741, 1695 (C=O), 1595 (C=N), 1259 (COO), 753 and 705 (monosubstituted benzenoid ring). ^1H NMR (400 MHz, DMSO- d_6): δ 21.05-1.15 (m, 6H, 2CH₃), 3.87 (s, 3H, OCH₃); 4.58 (m, 4H, NH₂N), 2.3-2.08, 2.33-2.37,-2.56-2.78,2.81-3.56(m, 6H), 7.43 (d, 1H, ArH $J=8.40\text{Hz}$), 7.55-7.57 (m, 1H, ArH), 7.63-7.69 (m, 3H, ArH), 7.77 (m, 1H, ArH), 8.15-8.17 (m, 2H, ArH), 9.76(s, 1H, N=CH). ^{13}C NMR (100 MHz, DMSO- d_6): δ 10.98 (CH₃), 17.90 and 18.93 (2CH₃), 55.02 and 55.60 (2CH₂), 56.06 (OCH₃), 65.26 (NCH₂N), 71.03 (2CH), 111.66 (CH), 120.68 (CH); 123.69(CH),128.43(C), 129.04(2CH), 129.85(2CH), 132.49(C), 134.17(CH),141.92(C), 150.28 (C) (ArC), 143.14 (Triazole C₃), 151.39 (Triazole C₅), 153.60 (N=CH), 163.78 (COO).

4-[1-(2,6-dimethylmorpholin-4-yl-methyl)-3-ethyl-4,5-dihydro-triazol-5-on-4-yl-azomethine]-2-methoxyphenyl benzoate (2b)

Yield: 70.14%, m.p. 122°C. IR (KBr, ν , cm^{-1}): 1741, 1695 (C=O), 1595 (C=N), 1259 (COO), 753 and 705 (monosubstituted benzenoid ring). ^1H NMR (400 MHz, DMSO- d_6): δ 1.05-1.15 (m, 6H, 2CH₃), 1.26 (t, 3H, CH₂CH₃; $J=7.20$ Hz), 2.79 (q, 2H, CH₂CH₃; $J=7.20$ Hz), 3.86 (s, 3H, OCH₃), 4.57-4.60 (m, 2H, NCH₂N), 2.02-2.06, 2.25-2.28, 2.61-2.64, 2.80-2.82, 3.51-3.56 (m, 6H), 7.43 (d, 1H, ArH; $J=8.00$ Hz), 7.54-7.56 (m, 1H, ArH), 7.63-7.67 (m, 3H, ArH), 7.77-7.79 (m, 1H, ArH), 8.15-8.17 (m, 2H, ArH), 9.75 (s, 1H, N=CH). ^{13}C NMR (100 MHz, DMSO- d_6): δ 10.05 (CH₂CH₃), 17.90 (CHCH₃), 18.40 (CH₂CH₃), 18.94 (CHCH₃), 55.03 and 55.63 (2CH₂), 56.05 (OCH₃), 66.29 (NCH₂N), 71.04 (2CH), 111.67; 120.57; 123.69; 128.43; 129.04 (2CH); 129.86 (2CH); 132.52; 134.18; 141.91; 150.38 (ArC), 146.87 (Triazole C₃), 151.39 (Triazole C₅), 153.64 (N=CH), 163.78 (COO).

4-[1-(2,6-dimethylmorpholin-4-yl-methyl)-3-benzyl-4,5-dihydro-triazol-5-on-4-yl-azomethine]-2-methoxyphenyl benzoate (2c)

Yield: 70.31%, m.p. 147°C. IR (KBr, ν , cm^{-1}): 1739, 1706 (C=O), 1592 (C=N), 1254 (COO), 750 and 714 (monosubstituted benzenoid ring). ^1H NMR (400 MHz, DMSO- d_6): δ 1.06-1.15 (m, 6H, 2CH₃), 3.86 (s, 3H, OCH₃), 4.15 (s, 2H, CH₂Ph), 4.63 (s, 2H, NCH₂N), 2.03-2.08, 2.24-2.28, 2.60-2.64, 2.81-2.83, 3.51-3.56 (m,6H), 7.26-7.28 (m, 1H, ArH), 7.33-7.41 (m, 5H, ArH), 7.47-7.48 (m, 1H, ArH), 7.59-7.66 (m, 3H, ArH), 7.77-7.79 (m, 1H, ArH), 8.14-8.17 (m, 2H, ArH), 9.71 (s, 1H, N=CH). ^{13}C NMR (100 MHz, DMSO- d_6): δ 17.89 and 18.93 (2CH₃), 31.02 (CH₂Ph), 55.07 and 55.67 (2CH₂), 56.02 (OCH₃), 65.78 (NCH₂N), 71.02 (2CH), 110.87; 121.23; 123.64; 126.80; 128.42; 128.50 (2CH); 128.83 (2CH); 129.04(2CH); 129.86 (2CH); 132.46; 134.18; 135.76; 141.95; 150.27 (ArC), 144.92 (Triazole C₃), 151.36 (Triazole C₅), 153.00 (N=CH), 163.78 (COO).

4-[1-(2,6-dimethylmorpholin-4-yl-methyl)-3-p-methylbenzyl-4,5-dihydro-triazol-5-on-4-yl-azomethine]-2-methoxyphenyl benzoate (2d)

Yield: 70.31%, m.p. 129°C. IR (KBr, ν , cm^{-1}): 1741, 1706 (C=O), 1579 (C=N), 1252 (COO), 868 (1,4-disubstituted benzenoid ring), 748 and 711 (monosubstituted benzenoid ring). ^1H NMR (400 MHz, DMSO- d_6): δ 1.06-1.10 (m) and 1.15 (d, $J=6.40$ Hz) (6H, 2CH₃), 2.27 (s, 3H, PhCH₃), 3.87 (s, 3H, OCH₃), 4.09 (s, 2H, CH₂Ph), 4.62 (s, 2H, NCH₂N), 2.02-2.07, 2.25-2.28, 2.60-2.64, 2.81-2.83, 3.50-3.56 (m,6H), 7.15 (d, 2H, ArH; $J=8.00$ Hz), 7.26 (d, 2H, ArH; $J=7.60$ Hz), 7.41 (d, 1H, ArH; $J=8.00$ Hz), 7.48-7.50 (m, 1H, ArH), 7.59-7.67 (m, 3H, ArH), 7.78-7.80 (m, 1H, ArH), 8.15-8.17 (m, 2H, ArH), 9.70 (s, 1H, N=CH). ^{13}C NMR (100 MHz, DMSO- d_6): δ 17.89 and 18.93 (2CH₃), 20.56 (PhCH₃), 30.63 (CH₂Ph), 55.08 and 55.68 (2CH₂), 56.01 (OCH₃), 65.76 (NCH₂N), 71.02 (2CH), 110.87; 121.24; 123.64; 128.42; 128.54 (2CH); 129.05(2CH) (2CH); 129.86 (2CH); 132.48; 132.63; 134.18; 135.91; 141.94; 150.26 (ArC), 145.07 (Triazol C₃), 151.36 (Triazol C₅), 152.95 (N=CH), 163.78 (COO).

4-[1-(2,6-dimethylmorpholin-4-yl-methyl)-3-p-methoxybenzyl-4,5-dihydro-triazol-5-on-4-yl-azomethine]-2-methoxyphenyl benzoate (2e)

Yield: 74.60%, m.p. 113°C. IR (KBr, ν , cm^{-1}): 1740, 1706 (C=O), 1595 (C=N), 1247 (COO), 868 (1,4-disubstituted benzenoid ring), 747 and 7134 (monosubstituted benzenoid ring). ^1H NMR (400 MHz, DMSO- d_6): δ 1.05-1.07 (m) and 1.15 (d) (6H, 2CH₃), 3.87 (s, 3H, OCH₃), 4.07 (s, 2H, CH₂Ph), 4.62 (s, 2H, NCH₂N), 2.02-2.07, 2.28-2.32, 2.60-2.64, 2.80-2.83, 3.54-3.58 (m, 6H), 6.90 (d, 2H, ArH; $J=8.80$ Hz), 7.30 (d, 2H, ArH; $J=8.40$ Hz), 7.42 (d, 1H, ArH; $J=8.00$ Hz), 7.49-7.51 (m, 1H, ArH), 7.61-7.67 (m, 3H, ArH), 7.78-7.79 (m, 1H, ArH), 8.15-8.17 (m, 2H, ArH), 9.71 (s, 1H, N=CH). ^{13}C NMR (100 MHz, DMSO- d_6): δ 17.89 and 18.93 (2CH₃), 30.16 (CH₂Ph), 56.03 (OCH₃), 65.76 (NCH₂N), 71.02 (2CH), 110.95; 113.96 (2CH), 121.19; 123.65; 127.49; 128.43; 129.04 (2CH); 129.73 (2CH); 129.86 (2CH); 132.49; 134.48; 141.95; 150.27; 158.16 (ArC), 145.22 (Triazole C₃), 151.37 (Triazole C₅), 153.02 (N=CH), 163.79 (COO).

4-[1-(2,6-dimethylmorpholin-4-yl-methyl)-3-p-chlorobenzyl-4,5-dihydro-triazol-5-on-4-yl-azomethine]-2-methoxyphenyl benzoate (2f)

Yield: 72.13%, m.p. 127°C. IR (KBr, ν , cm^{-1}): 1740, 1705 (C=O), 1596 (C=N), 1252 (COO), 868 (1,4-disubstituted benzenoid ring), 746 and 711 (monosubstituted benzenoid ring). ^1H NMR (400 MHz, DMSO- d_6): δ 1.05-1.14 (m, 6H, 2CH₃), 3.86 (s, 3H, OCH₃), 4.17 (s, 2H, CH₂Ph), 4.62 (s, 2H, NCH₂N), 2.02-2.07, 2.28-2.32, 2.62-2.66, 2.80-2.85, 3.54-3.57 (m, 6H), 7.40-7.42 (m, 5H, ArH), 7.48-7.50 (m, 1H, ArH), 7.58 (m, 1H, ArH), 7.63-7.67 (m, 2H, ArH), 7.78-7.79 (m, 1H, ArH), 8.14-8.17 (m, 2H, ArH), 9.72 (s, 1H, N=CH). ^{13}C NMR (100 MHz, DMSO- d_6): δ 17.88 and 18.93 (2CH₃), 30.34 (CH₂Ph), 55.05 and 55.65 (2CH₂), 56.03 (OCH₃), 65.81 (NCH₂N), 71.02 (2CH), 110.95; 121.22; 123.65; 128.44; 129.04(2CH); 129.86 (2CH); 130.59 (2CH); 130.76 (2CH), 131.51; 132.41; 134.18; 134.77; 141.98; 150.26 (ArC), 144.61 (Triazole C₃), 151.37 (Triazole C₅), 153.16 (N=CH), 163.77 (COO).

Antioxidant Activity

Chemicals

Butylated hydroxytoluene (BHT), ferrous chloride, DPPH, α -tocopherol, 3- butylated hydroxyanisole (BHA), (2-pyridyl)-5,6-bis(phenylsulfonic acid)-1,2,4-triazine (ferrozine) and trichloroacetic acid (TCA) were obtained from E. Merck or Sigma.

Reducing Power

The reducing power of the compounds **2a-i** was determined using the method of Oyaizu (1986). Different concentrations of the samples (50-250 $\mu\text{g/mL}$) in DMSO (1 mL) were mixed with phosphate buffer (2.5 mL, 0.2 M, pH = 6.6) and potassium ferricyanide (2.5 mL, 1%). The mixture was incubated at 50°C for 20 min. after which a portion (2.5 mL) of trichloroacetic acid (10%) was added to the mixture, which was then centrifuged for 10 min at 1000 x g. The upper layer of solution (2.5 mL) was mixed with distilled water (2.5 mL) and FeCl₃ (0.5 mL, 0.1%), and then the absorbance at 700 nm was measured in a spectrophotometer. Higher absorbance of the reaction mixture indicated greater reducing power.

Free Radical Scavenging Activity

Free radical scavenging effect of the compounds **2a-f** was estimated by DPPH, by the method of Blois (1958). Briefly, 0.1 mM solution of DPPH in ethanol was prepared, and this solution (1 mL) was added to sample solutions in DMSO (3 mL) at different concentrations (50-250 $\mu\text{g/mL}$). The mixture was shaken vigorously and allowed to stand at room temperature for 30 min. Then the absorbance was measured at 517 nm in a spectrophotometer. Lower absorbance of the reaction mixture indicated higher free radical scavenging activity. The DPPH concentration (mM) in the reaction medium was calculated from the following calibration curve and determined by linear regression (R: 0.997):

$$\text{Absorbance} = 0.0003 \times \text{DPPH} - 0.0174$$

The capability to scavenge the DPPH radical was calculated using the following equation:

$$\text{DPPH. scavenging effect (\%)} = (A_0 - A_1/A_0) \times 100$$

where A_0 is the absorbance of the control reaction and A_1 is the absorbance in the presence of the samples or standards.

Metal chelating activity

The chelating of ferrous ions by the compounds **2a-f** and references was measured according to the method of Dinis et al., (1994). Briefly, the synthesized compounds (30–60 $\mu\text{g/mL}$) were added to a 2 mM solution of FeCl_2 (0.05 mL). The reaction was initiated by the addition of 5 mM ferrozine (0.2 mL), and then the mixture was shaken vigorously and left standing at room temperature for 10 min. After the mixture had reached equilibrium, the absorbance of the solution was measured at 562 nm in a spectrophotometer. All tests and analyses were run in triplicate and averaged. The percentage of inhibition of ferrozine– Fe^{2+} complex formation was given by the formula: % inhibition = $(A_0 - A_1 / A_0) \times 100$, where A_0 is the absorbance of the control, and A_1 is the absorbance in the presence of the samples or standards. The control did not contain compound or standard.

Antimicrobial Activity

All bacterial and yeast strains were obtained from the company of Microbiological Environmental Protection Laboratories (France) and were as follows: *Bacillus Subtilis* (ATCC 11774), *Bacillus Cereus* (ATCC 11778), *Pseudomonas aeruginosa* (ATCC 27853), *Klebsiella pneumonia* (ATCC 4352), *Staphylococcus aureus* (ATCC 6538) and *Escherichia coli* (ATCC 25922). Simple susceptibility screening test using agar well diffusion method was used (Perez, Pauli, & Bazerque, 1990, Ahmad, Mehmood, & Mohammed, 1998). All the newly synthesized compounds were weighed and dissolved in dimethylsulphoxide (DMSO) to prepare extract stock solution of 1 mg/ml.

Each microorganism was suspended in Mueller-Hinton Broth and diluted to 106 colony forming unit (cfu) per ml. They were “flood-inoculated” onto the surface of Mueller Hinton Agar and then dried. Five-millimeter diameter wells were cut from the agar using a sterile cork-borer, and 250–5000 $\mu\text{g}/50 \mu\text{l}$ of the chemical substances were delivered into the wells. The plates were incubated for 18 h at 35 °C. Antimicrobial activity was evaluated by measuring the zone of inhibition against the test organism. Ampicillin, neomycin and streptomycin were standard antibacterial and antifungal agents, DMSO was used as solved control.

Results and Discussion

In this study, the structures of six new 4-[1-(2,6-dimethylmorpholin-4-yl-methyl)-3-alkyl(aryl)-4,5-dihydro-1,2,4-triazol-5-on-4-yl-azomethine]-2-methoxyphenyl benzoates (**2a-f**) were characterized with IR, ^1H NMR and ^{13}C NMR spectral data.

Antioxidant Activity

The antioxidant capacities of nine newly synthesized compounds **2a-f** were determined. Different processes have been used to identify antioxidant capacities. The processes used in the paper are clarified below:

Reducing Power

The reducing power of the compounds **2** was determined. The reductive capabilities of compounds are assessed by the extent of conversion of the Fe^{3+} /ferricyanide complex to the Fe^{2+} /ferrous form. The reducing powers of the compounds were observed at different concentrations, and results were compared with BHA, BHT and α -

tocopherol. The reducing capacity of a compound may serve as a significant indicator for its potential antioxidant activity (Meir, Kanner, Akiri, & Philosoph-Hadas, 1995). The antioxidant activity of a putative antioxidant has been attributed to various mechanisms, among which are prevention chain initiation, binding of transition metal ion catalyst, decomposition of peroxides, prevention of continued hydrogen abstraction, reductive capacity and radical scavenging (Yildirim, Mavi, & Kara, 2001). In this study, all of the amounts of the compounds showed lower absorbance than blank. Hence, no activities were observed to reduce metal ions complexes to their lower oxidation state or to take part in any electron transfer reaction. In other words, compounds did not show the reductive activities.

DPPH Radical Scavenging Activity

Free radical scavenging effect of the compounds **2** was estimated by DPPH radical model. The effect of antioxidants on DPPH radical scavenging was thought to be due to their hydrogen donating ability (Baumann, Wurn, & Bruchlausen, 1979). DPPH is a stable free radical and accepts an electron or hydrogen radical to become a stable diamagnetic molecule (Soares, Dinis, Cunha, & Almeida, 1997). The reduction capability of DPPH radicals was determined by decrease in its absorbance at 517 nm induced by antioxidants. BHT, BHA and α -tocopherol were used as a reference to antioxidant compounds. Compounds **2a-f** did not show any ability.

Iron Binding Capacity

The chelating of ferrous ions by the compounds **2** and references was measured. Ferrozine can quantitatively form complexes with Fe^{2+} . In the presence of chelating agents, the complex formation is disrupted with the result that the red colour of the complex is decreased. Measurement of colour reduction therefore allows estimation of the chelating activity of the coexisting chelator (Yamaguchi, Ariga, Yoshimura, & Nakazawa, 2000). The transition metals ions play an important role as catalysts of oxidative process, leading to formation of hydroxyl radicals and hydroperoxide decomposition reaction via Fenton chemistry (Halliwell, 1996). The production of these radicals may lead to lipid peroxidation, protein modification and DNA damage. Chelating agents are effective as secondary antioxidants because they potentially inhibit the metal-dependent processes thereby stabilizing the oxidized form of the metal ion (Finefrock, Bush, & Doraiswamy, 2003). Iron binding activities of the compounds **2**, BHT, BHA and α -tocopherol are shown in Figure 2.

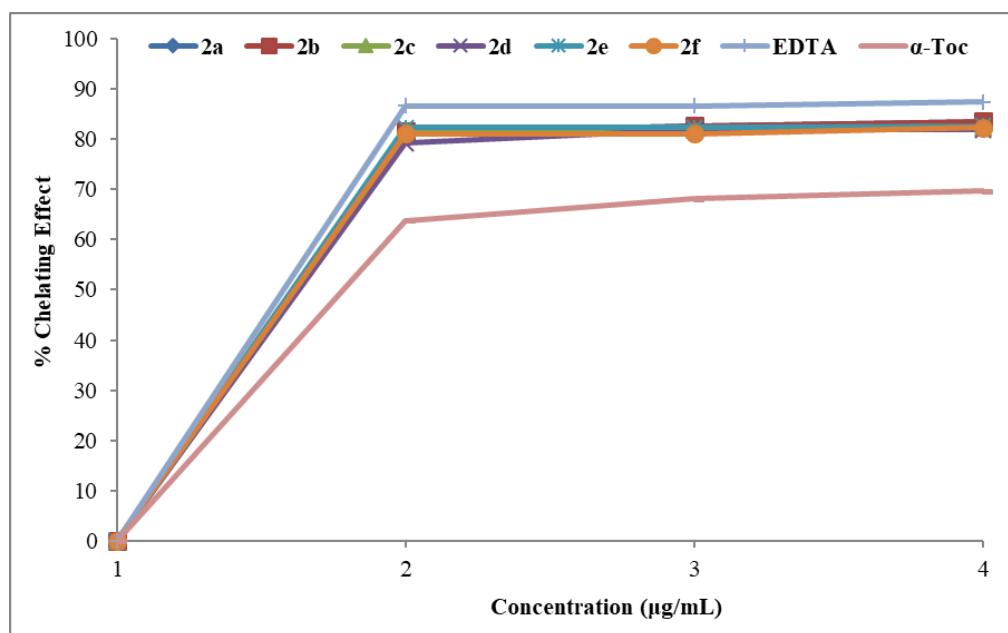


Figure 1. Metal chelating effect of the compounds 2a-f, EDTA and α -tocopherol on ferrous ions

In the current paper, high iron binding capacity of synthesized compounds would be beneficial in retarding metal-chelating oxidation. The data acquired from Figure 1 disclose that the metal chelating effects of all the

compounds (**2**) were significant and concentration-dependent. The metal chelating effect of the compounds and references decreased in order of EDTA > 2a > 2b = 2e > 2c = 2d > 2f > α -tocopherol which were 86.6, 82.7, 82.3, 82.3, 81.9, 81.9, 81.1, 68.1 (%), at the 30 μ g/mL, respectively.

Antimicrobial Activity

The microbiological results are summarized in Table I. Microbiology results are promising; all the compounds showed very good antimicrobial activity against to *Bacillus subtilis* (ATCC-11774) and *Bacillus cereus* (ATCC-11778). However, not all compounds showed any activity against other microorganisms.

Table 1. Antimicrobial activity of the compounds 2.

Code	Compounds	Bs	Bc	Pa	Kp	Sa	Ec
1	2a	18	21	-	-	-	-
2	2b	21	23	-	-	-	-
3	2c	22	20	-	-	-	-
4	2d	18	16	-	-	-	-
5	2e	19	17	-	-	-	-
6	2f	21	20	-	-	-	-
A	Ampicillin X3261	33	36	36	35	37	34
N	Neomycin X3385	17	17	17	16	13	16
S	Streptomycin X3385	12	12	12	11	21	10

Bs: *Bacillus subtilis* (ATCC-11774), Bc: *Bacillus cereus* (ATCC-11778), Pa: *Pseudomonas aeruginosa* (ATCC-27853), Kp: *Klebsiella pneumoniae* (ATCC-4352) Sa: *Staphylococcus aureus* (ATCC-6538), Ec: *Escherichia coli* (ATCC-25922), Amp.: Ampicillin (X3261), Neo.: Neomycin (X3360), Str.: Streptomycin (X3385).

Conclusion

In the present study, new Mannich bases derivatives with 1,2,4-triazole moiety (**2a-f**) were designed and synthesized. Their structures were identified using IR, ^1H NMR and ^{13}C NMR spectral data. The entire target compounds were also investigated for their antioxidant and antimicrobial potential. All of the compounds demonstrate a marked ability for metal chelating activity. The data reported with regard to the observed metal chelating activities of the studied compounds could prevent redox cycling. The results may also give several advices for the improvement of new triazole-based therapeutic target. Also, The synthesized compounds showed very good antimicrobial activity against to *Bacillus subtilis* and *Bacillus cereus*.

References

- Ahmad I., Mehmood Z., & Mohammed F., (1998). Screening of some Indian Medicinal Plants for Their Antimicrobial properties. *Journal of Ethnopharmacology*, 62, 183-193.
- Aktas-Yokus, O., Yuksek, H., Gursoy-Kol, O., & Alpay-Karaoglu, S. (2015). Synthesis and biological evaluation of new 1,2,4-triazole derivatives with their potentiometric titrations. *Medicinal Chemistry Research*, 24(7), 2813–2824. doi: 10.1007/s00044-015-1334-8
- Baumann, J., Wurn, G., & Bruchlausen, V. (1979). Prostaglandin synthetase inhibiting O_2 – radical scavenging properties of some flavonoids and related phenolic compounds. *Naunyn-Schmiedeberg's Archives of Pharmacology*, 308, R27.
- Blois, M. (1958). Antioxidant determinations by the use of a stable free radical. *Nature*, 181(4617), 1199–1200. <http://doi.org/10.1038/1811199a0>
- Chen, D., Zhai, X., Yuan, Q. H., Luo, J., Xie, S. C., & Gong, P. (2010). Synthesis and in vitro anti-hepatitis B virus activity of 1H-benzimidazol-5-ol derivatives. *Chinese Chemical Letters*, 21(11), 1326-1329. doi: 10.1016/j.ccl.2010.05.011
- Chidananda, N., Poojary, B., Sumangala, V., Kumari, N. S., Shetty, P., & Arulmoli, T. (2012). Facile synthesis, characterization and pharmacological activities of 3,6-disubstituted 1,2,4-triazolo[3,4-b][1,3,4]thiadiazoles and 5,6-dihydro-3,6-disubstituted-1,2,4-triazolo[3,4-b][1,3,4]thiadiazoles. *European Journal of Medicinal Chemistry*, 51, 124–136. <http://doi.org/10.1016/j.ejmech.2012.02.030>

- Dinis, T. C. P., Madeira, V. M. C., & Almeida, L. M. (1994). Action of phenolic derivatives (acetaminophen, salicylate, and 5-aminosalicylate) as inhibitors of membrane lipid peroxidation and as proxyl radical scavengers. *Archives of Biochemistry and Biophysics*, 315(1), 161–169. <http://doi.org/10.1006/abbi.1994.1485>
- Finefrock, A. E., Bush, A. I., & Doraiswamy, P. M. (2003). Current status of metals as therapeutic targets in Alzheimer's disease. *Journal of the American Geriatrics Society*, 51(8), 1143–1148. <http://doi.org/10.1046/j.1532-5415.2003.51368.x>
- Halliwell, B. (1996). Antioxidants: The Basics-what they are and how to evaluate them. *Advances in Pharmacology*, 38(C), 3–20. [http://doi.org/10.1016/S1054-3589\(08\)60976-X](http://doi.org/10.1016/S1054-3589(08)60976-X)
- Hamama, W. S., Zoorob, H. H., Gouda, M. A., & Afsah, E. M. (2011). Synthesis and antimicrobial and antioxidant activities of simple saccharin derivatives with N-basic side chains. *Pharmaceutical Chemistry Journal*, 45(2), 118–124. doi: 10.1007/s11094-011-0573-3
- Koca E., Yıldız Ç., & Köçek N. (2010). 3-m-Klorobenzi1-4-amino-4,5-dihidro-1H-1,2,4-triazol-5-on ve Bazı Türevlerinin Sentezi. Bitirme Tezi, Kakkas Üniv. Fen Edebiyat Fakültesi Kimya Bölümü, Kars.
- Köksal, M., & Bilge, S. S. (2007). Synthesis and antidepressant-like profile of novel 1-aryl-3-[(4-benzyl)piperidine-1-yl]propane derivatives. *Archiv Der Pharmazie*, 340(6), 299–303. doi: 10.1002/ardp.200700028
- Liu, D., Yu, W., Li, J., Pang, C., & Zhao, L. (2013). Novel 2-(E)-substituted benzylidene-6-(N-substituted aminomethyl)cyclohexanones and cyclohexanols as analgesic and anti-inflammatory agents. *Medicinal Chemistry Research*, 22(8), 3779–3786. doi: 10.1007/s00044-012-0362-x
- Maddila, S., & Jonnalagadda, S. B. (2012). New class of triazole derivatives and their antimicrobial activity. *Letters in Drug Design & Discovery*, 9(7), 687–693. doi: 10.2174/157018012801319526.
- Meir, S., Kanner, J., Akiri, B., & Philosoph-Hadas, S. (1995). Determination and involvement of aqueous reducing compounds in oxidative defense systems of various senescing leaves. *Journal of Agricultural and Food Chemistry*, 43(7), 1813–1819.
- McClements, D., & Decker, E. (2000). Lipid oxidation in oil-in-water emulsions: Impact of molecular environment on chemical reactions in heterogeneous food systems. *Journal of Food Science*, 65(8), 1270–1282. <http://doi.org/10.1111/j.1365-2621.2000.tb10596.x>
- Nithinchandra, Kalluraya, B., Aamir, S., & Shabaraya, A. R. (2012). Regioselective reaction: Synthesis, characterization and pharmacological activity of some new Mannich and Schiff bases containing sydnone. *European Journal of Medicinal Chemistry*, 54, 597–604. doi: 10.1016/j.ejmech.2012.06.011
- Oyaizu, M. (1986). Studies on products of browning reaction. Antioxidative activities of products of browning reaction prepared from glucosamine. *The Japanese Journal of Nutrition and Dietetics*, 44(17), 307–315. <http://doi.org/10.5264/eiyogakuzashi.44.307>
- Ozkan-Daguyan, I., Sahin, F., & Koksai, M. (2013). Synthesis, Characterization and Antimicrobial Activity of Novel 3,5-Disubstituted-1,3,4-oxadiazole-2-ones. *Revista de Chimie -Bucharest- Original Edition-*, 64(5), 534–539.
- Pati, H. N., Das, U., Kawase, M., Sakagami, H., Balzarini, J., De Clercq, E., & Dimmock, J. R. (2008). 1-Ary1-2-dimethylaminomethyl-2-propen-1-one hydrochlorides and related adducts: A quest for selective cytotoxicity for malignant cells. *Bioorganic & Medicinal Chemistry*, 16(10), 5747–5753. doi: 10.1016/j.bmc.2008.03.060
- Perez C., Pauli M., & Bazerque P., (1990). An Antibiotic Assay by the Well Agar Method. *Acta Biologia et Medicine Experimentalis*, 15,113-115.
- Savariz, F. C., Formagio, A. S. N., Barbosa, V. A., Foglio, M. A., Carvalho, J. E. de, Duarte, M. C. T., ... Sarragiotto, M. H. (2010). Synthesis, antitumor and antimicrobial activity of novel 1-substituted phenyl-3-[3-alkylamino(methyl)-2-thioxo-1,3,4-oxadiazol-5-yl] β -carboline derivatives. *Journal of the Brazilian Chemical Society*, 21(2), 288–298. doi: 10.1590/S0103-50532010000200014.
- Soares, J. R., Dinis, T. C. P., Cunha, A. P., & Almeida, L. M. (1997). Antioxidant activities of some extracts of *Thymus zygis*. *Free Radical Research*, 26(5), 469–478. <http://doi.org/10.3109/10715769709084484>
- Tramontini, M., & Angiolini, L. (1994). *Mannich Bases: Chemistry and Uses*. CRC Press.
- Sriram, D., Yogeewari, P., Dinakaran, M., & Sowmya, M. (2008). Synthesis, anti-HIV and antitubercular activities of nelfinavir diester derivatives. *Biomedicine and Pharmacotherapy*, 62(1), 1–5. doi: 10.1016/j.biopha.2007.08.002
- Yamaguchi, F., Ariga, T., Yoshimura, Y., & Nakazawa, H. (2000). Antioxidative and anti-glycation activity of garcinol from *Garcinia indica* fruit rind. *Journal of Agricultural and Food Chemistry*, 48(2), 180–185. <http://doi.org/10.1021/jf990845y>
- Yildirim, A., Mavi, A., & Kara, A. A. (2001). Determination of antioxidant and antimicrobial activities of *Rumex crispus* L. extracts. *Journal of Agricultural and Food Chemistry*, 49(8), 4083–4089.

<http://doi.org/10.1021/jf0103572>

Author Information

Yonca Yilmaz

Kafkas University,
Department of Chemistry,
Kars, Turkey

Ahmet Harmankaya

Kafkas University,
Department of Chemistry,
Kars, Turkey
Contact e-mail: *ahmetharmankaya5@gmail.com*

Sevda Manap

Kafkas University,
Department of Chemistry,
Kars, Turkey

Haydar Yuksek

Kafkas University,
Department of Chemistry,
Kars, Turkey

Ozlem Gursoy Kol

Kafkas University,
Department of Chemistry,
Kars, Turkey

Muzaffer Alkan

Kafkas University,
Faculty of Education,
Kars, Turkey

Study of the Physical and Structural Properties of Some Local Mineral Clays and Effect of Doping with Chromium Oxide

Regab A. BUKER
Mosul University

Zena M. SHABAN
Ministry of education

Abstract: Chemical composition, physical properties and structural characterization of local natural clays which have been collected from Aski Mosul village, area around Mosul city/ Iraq, were studied. The study approach is based on using x-ray diffraction, x-ray florescence, atomic absorption, thermal gravimetric analysis, differential scanning calorimetry, infrared spectroscopy, instrumental and classical chemical analysis techniques. Chemical composition studies of the natural sample clearly indicating the presence of large amounts of silica and calcium oxide in addition to aluminum oxide and other minor oxides. Moreover, it is shown that such sample yields (~5%) amorphous silica on treating with basic medium. The results were compared with those obtained from acidically treated and chromium oxide doped clay samples. On comparison the physical properties (e.g density, porosity, water absorption, pore size, and capillary action), it seems that the treated clay sample has low density and high porosity and permeability. Moreover, the doped samples are more dens than others. Such variation because of the elimination of carbonate compounds on treating and doping processes. Four samples were prepared in order to be more active and selective adsorbent materials. Soxhlate fractionating techniques were set for all the above types of adsorbents using four eluants gradually increased in polarity. The fractionation results showed significant variations in the fractions isolated according to their polarities as indicated by percentage results.

Keywords: Mineral clays, Virgin olive oil, Soxhlate

Introduction

Many types of mineral clays, which are natural resources, located in massive deposits around the Governorates of Nineveh ^[1]. Such mineral clays have not been utilized yet, inspite of their possibility usage as catalysts in industry in general and especially in fractionation processes. This consideration arises from the fact that such materials accompanied in their locations with heavy crude oil resources as well as local virgin olive oil ^[2,3]. The demand for all kinds of naturally sources of foods and drugs such as olive oil have been the subject for many workers ^[4-6]. Such materials contain a mixture of complex hydrocarbon compounds that can easily be separated by fractionation processes to their major components which are triglycerides and other minor components phenolic and volatile compounds such as aldehydes ^[3].

Meanwhile, locally mineral clays and their manufactured compounds are proposed to be good adsorbents and catalysts in the above refining processes. Recently, Buker and Taher applied ninevite silica gel doped with chromium oxide in solid phase extraction to separate Iraqi virgin olive oil into their simple components ^[3].

As a continuation of these studies very recent investigations were reported applying some local ninevites doped with some complexes in order to be more active and selective adsorbent material in chromatographic columns ^[7].

- This is an Open Access article distributed under the terms of the Creative Commons Attribution-Noncommercial 4.0 Unported License, permitting all non-commercial use, distribution, and reproduction in any medium, provided the original work is properly cited.

- Selection and peer-review under responsibility of the Organizing Committee of the Conference

The present study covers an investigation into the application of Aski-Mosul (a suburb of the Governorate of Nineveh) mineral clays after acidic and basic treating and doping them with chromium oxide in soxhlate technique. They have to be employed as a catalyst in adsorption chromatography to fractionate some Iraqi virgin olive oils.

Experimental

A. Source, collection and preparation of samples:

Natural clay samples were collected from Aski Mosul village, area around Mosul city/ Iraq. These samples are bearing some scemite mineral clays in addition to silica and other non-mineral clays^[8]. The solubility of the clay samples in both the acidic and basic medium was studied and the treated samples as well as the natural one were doped by chromium oxide, Cr₂O₃, applying the impregnation methods^[9] to prepare four samples. Cr₂O₃ was mixed with clay samples in a ratio 1:8 mole respectively, stirred with distilled water and small amount of ethanol for several hours, filtered, dried at 110°C, and heated at 260°C for 2 hours. All samples were physically studied using several techniques including powder x-ray diffraction, thermal gravimetric analysis, differential scanning calorimetry, and infrared spectroscopy, in order to obtain active and selective adsorption material. Moreover, those samples were chemically formulated following several chemical analysis methods^[10] in addition to x-ray fluorescence technique.

B. X-ray powder diffraction and fluorescence:

Powder x-ray diffraction studies were carried out using Cu K α radiation and diffraction patterns were recorded using Shimadzu X-ray Diffraction 7000, 2009, fitted with a vertical goniometry. The phase contributing to the x-ray diffraction patterns were identified by reference to the Joint Committee on Powder Diffraction Standards Powder Diffraction File. Meanwhile, x-ray fluorescence data were obtained using Oxford, X-MET 7500 fluorescence analyzer.

C. Thermal analysis:

Thermogravimetric analysis and differential scanning calorimetry were recorded between 25 and 380°C on METTLER TOLEDO, TGA/ DSC STAR[®] SW 9.30 thermal analysis. The heating rate was 5°C min⁻¹ and α -Al₂O₃ was used as standard reference. The measurement was carried out in AL-Al-Bait University/ Jourdan Kingdom.

D. Infrared Spectra

The absorption spectra of samples under investigation were recorded on SHIMADZO, IR Affinity-1 spectrophotometer using KBr pellets and NaCl cell^[11].

E. Application:

Four adsorption fractionating soxhlate techniques were prepared which were packed applying natural, treated, natural and doped and treated and doped clay samples as adsorbent materials. All samples were of chromatographic grade (300-425 μ m) and activated to be employed in the processes. A known weight (2g) of Iraqi virgin olive oil was fractionated into four isolated samples according to their adsorption polarities using four eluants of different polarities which are petroleum ether, toluene, chloroform and ethanol. IR, ¹H NMR, GC-MS investigation will be presented in future article very soon^[12] in order to study the chemical composition of the eluted stuff and to evaluate the adsorption activity and selectivity of the investigated samples.

Result and Discussion

A- Physical and chemical characterization:

Physical properties (e.g. density, porosity, water absorption, pore size and capillary action) have been measured following the methods described in the literature^[13]. Table (1) shows such data related to the four clay samples under investigation. The capillary action, Figure (1) revealed the rising of water level as monitored with time is taken as the measurement of this action. It is clear that physical properties of these samples show notable difference. It seems that the treated clay sample has low density and high porosity and permeability. Moreover, the doped samples are more dens than others. Such variation because of the elimination of carbonate compounds on treating and doping processes. Meanwhile, the low capillary action at natural sample on comparison with the rest samples may explain the fact that natural clay sample contain large number of small pores which are well connected by an extremely narrow channels^[2]. Furthermore, it seems that doping with chromium oxide affects creating much more permeable new catalysts with different physical properties. As a result, it looks that treating and doping clay samples appeared to be generally the best, regarding adsorption activity^[14].

X-ray fluorescence and instrumental chemical analyses such as atomic absorption and flam photometry, have been used to study the chemical composition of the four clay samples under investigation and the data of these analyses are shown in Table (2). It is clear that natural sample contain large amounts of silica and calcium oxide in addition to aluminum oxide and other minor oxides. Moreover, it is shown that such sample yields (~5%) amorphous silica on treating with basic medium^[7]. On the other hand, the treated sample data reflect the less values of carbonate compounds because of the elimination processes. On doping of those samples, the results of analysis however, improve the doping factor molar ratio 1:8 of chromium to clay material.

B- Structural studies:

Rocks and mineral clays occurred naturally and there is a difficulty in finding a sample consisting 100% of a single phase compound. Therefore, the natural mineral clay samples indeed compose of so many other minor compounds in addition to the primitive one which is for example smectite mineral clay. Careful x-ray powder diffraction studies reveal the presence of these mixed layer structures and frequently indicate their nature and relative abundance^[15].

Accordingly, x-ray powder diffraction for natural clay sample was carried out. Figure (2) shows the sample pattern which contains reflections typical to quartz in addition to montmorillonite, illite and kaolinite. The amorphous silica may also be defined as a broad hump between 2θ (18-22). However, the interplanar spacings of the all contributing phases might be presented in Table (3).

On treating the clay sample and doping with chromium oxide followed by calcination at 700°C, it seem that good crystalline phases were obtained. Furthermore, it looks that calcite and dolomite compounds were eliminated in addition to the destruction of montmorillonite and kaolinite crystal structures. X-ray diffraction chart of these samples are modified to the data presented in Table (4). This presentation clearly indicates the interplanar spacing of the contributing phases present in the above sample. Therefore, all samples under investigation were avoided from heating above 260°C to be active adsorbents whenever they were employed.

The aim of the present study is to prepare a modified mineral clay samples which contain the doped chromium oxide. Such goal to be achieved differential scanning calorimetry technique might be employed, followed by thermogravimetric degradation in order to obtain an activated catalyst. Figure (3) shows DSC curve of chromium doped natural clay sample which contains three endothermic peaks representing the three types of hydration water molecules. The first at 90°C related to the free water molecules on the surface and between the intermolecular planar of the clay. While the second one at 160°C corresponded to the water molecular which are connected to the clay via hydrogen bonding. Finally, the third peak represent the type of molecules which are coordinated to the clay sample^[16]. Meanwhile, DSC curves of the rest of samples were noted to be similar to the above one except in a small variation in the position of the hydration peaks. To interpret such foundation, TGA of the investigated samples were performed and Figure (4) represent one of such analysis. It is clear that losses of 54, 19 and 27% of the whole water molecules weight were observed which correspond to the dehydration phenomena^[17].

Finally, it is of interest to study the migration and elimination of the above water molecules from clay samples on increasing the temperature, in addition to the clay mineralogy by infrared spectroscopy. Therefore, a range of (400-4000) cm^{-1} in frequency was applied and the spectra show several absorption bands including those between (1024-1093) cm^{-1} which may be attributed to the (Si-O) stretching vibration^[18]. Also there are absorption bands at (796-694) cm^{-1} which are related to Si-O-M groups, and those at 877, 468 which correspond to Al-O and Fe-O respectively. Finally, the bands at (3618-3546) cm^{-1} and at (1456-1431) cm^{-1} which represent the structural OH groups and CO_3^{2-} respectively. Such absorptions show a significant variation in the position and sharpness of the vibrations upon treating and heating the samples in the range of (90-500) $^\circ\text{C}$. This may be related to the elimination of carbonate compounds and the dehydration phenomenon.

C- Soxhlate extraction of Iraqi virgin olive oil components:

The above results obtained for four clay samples in the present study show a significant variation in their chemical composition, physical properties, and especially in their structural components. It is therefore, of interest to get benefit of such findings in evaluating the studied clay samples in order to be applied as good adsorbents in fractionation processes.

The clay samples are suitable for the separation of majority of substances or for the separation of complex mixtures into groups of compounds.

Accordingly, four fractionating soxhlates were packed with the chromatographic grade (425-300 μm), already activated at 260 $^\circ\text{C}$, clay samples. They were employed to extract Iraqi virgin olive oil using four eluants increased gradually in their polarities. The oil sample were fractionated into four chemically simple components according to their polarities which created upon using, petroleum ether, toluene, chloroform, and ethanol solvents. The results of such separation are presented in Table (5). The results revealed the percentages of the fractions eluted according to their adsorption polarities.

In general, it is clear that adsorption and desorption of olive oil materials on clay samples has strongly occurred and as a result separated into four components. However, on referring to the previous studies in this field^[2,3,7]. It seems that the best separation and fractionation occurred in case of using the treated clay sample. This suggestion depends on the values of fractions percentage, therefore, to prove such proposed results more investigation was needed. For example chemical characteristic nature of the eluted fractions should be studied via IR, ^1H NMR and GC-MS techniques and it will be hopefully presented very soon in a future article^[12].

References

- M. Dahbia, Al-Muchtuma (2006), Al-Arabi publishing company, Amman, Jordan. pp. 173.
- R. Buker and S. Al-Mallah, (2005), J. Edu. Sci., Vol. 17, No. 4, pp. 42-53.
- R. Buker and N. Taher, Dirasat, (2006), Pure Sciences, Vol. 33, No. 2, pp. 158-167.
- J. Quiles, M. Carmen and P. Yaqoob, (2006), CAB International, London, UK, pp. 46, 49, 51.
- A. Koidis and D. Boskou, (2006), Eur. J. Lipid Sci. Technol. Vol. 108, pp. 323-328.
- C. Lazzerini and V. Domenici, (2017), Journal of Foods, Vol. 6, No. 25, pp. 1-11.
- R. Buker and A. Al-Botani, (2009), J. Raf. Sci., Vol. 20, No. 2, pp. 52-64.
- A. Meunier, (2005), Clay, Springer-Verlag, Germany, pp. 1,9,11.
- J. Anderson and M. Garcia, (2012), Supported Metals in Catalysis, 2nd. Ed., Imperial College Press, London, UK, p. 4.
- P. Jeeferly and D. Hutchison, (1981), Chemical Methods of Rock Analysis, 3rd. Ed., Pergamon Press, New York, pp. 18-22, 30-39, 222.
- B. Schrader, (1995), Infrared and Raman Spectroscopy, VCH, Inc., New York, USA, p. 224.
- R. Buker, S. Ahmad and Z. Shaban, (to be published in 2018).
- J. Kozel, (1975), Text Book on Density and Porosity of Rocks, Academic Press, New York, USA, pp. 155-170.
- R. Vartak, (2001), Resonance, Vol. 6, No. 5, pp. 83-91.
- C. Klein, (2002), Mineral Science, 22nd. Ed., John Wiley and Sons, Inc., USA, P. 407.
- F. Wypych and K. Satyanaryana, (2004), Clay Surfaces: Fundamentals and Applications, Elsevier Ltd., p. 10.
- P. Staszczuk, (1998), Thermochimica Acta, Vol. 308, No. 1, pp. 147-157.

Tyagi, C. Chudasama and R. Jasra, (2006), *Spectrochimica Acta Part A*, Vol. 64, pp. 273-278.

Author Information

Regab A. Buker

Department of chemistry/ College of Education/ Mosul
University, Mosul / Iraq
alinafia22@yahoo.com

Zena M. Shaban

Ministry of education

Appendices

Table 1. Physical properties of clay samples

sample	Density g/cm ³	Porosity %	Pore size cm ³ /g	Water absorption %	PH
Natural	2.3	31.16	1.87	154	8.1
Treated	2.14	36.5	2.19	76.4	4.95
Doped natural	2.1	47	2.82	225	7.8
Doped treated	1.8	50.5	3.03	238	6.3

Table 2. Chemical composition of clay samples

Sample Oxides%	Natural	Treated	Doped natural	Doped treated
Na ₂ O	1.07	0.02	1.04	0.06
K ₂ O	3.13	1.91	3.11	2.15
CaO	1.11	27.20	1.40	30.80
MgO	0.26	7.18	0.16	7.50
Fe ₂ O ₃	1.02	5.60	1.95	6.35
Al ₂ O ₃	7.32	8.19	9.25	10.38
SO ₃	0.08	0.40	0.10	0.20
SiO ₂	78.50	35.70	79.00	36.00
L.O.I	7.51	13.80	3.99	6.56

Table 3. Interplanar spacings of contributing phases in natural clay sample

Crystalline phase	2θ	d-spacing (Å ^o)	hkl
Montmorillonite	6.1	14.47	001
Montmorillonite	19.8	4.48	110
Montmorillonite	27.7	3.02	005
Montmorillonite	36.5	2.50	200
Illite	8.7	10.2	002
Illite	17.8	5.03	004
Illite	22.9	3.88	113
Illite	45.6	1.99	010
Kaolinite	12.4	7.13	001
Kaolinite	21.1	4.18	111
Kaolinite	35.1	2.57	201
Kaolinite	38.5	2.34	202
Quartz	20.9	4.26	100
Quartz	26.6	3.34	101
Quartz	39.4	2.28	102
Quartz	49	1.82	112
Calcite	29.4	3.03	104
Calcite	36	2.49	110
Calcite	43.1	2.09	202
Calcite	47.5	1.91	018
Dolomite	31	2.89	104
Dolomite	37.5	2.40	110
Dolomite	41.1	2.19	113
Dolomite	44.9	2.02	202
Hematite	24.3	3.66	012
Hematite	33.4	2.69	104
Hematite	43.9	2.08	202
Hematite	49.5	1.84	024

Table 4. Interplanar spacings of contributing phases in doped treated clay sample

Crystalline phase	2θ	d-spacing (Å ^o)	hkl
Montmorillonite	6.3	13.94	001
Montmorillonite	19.8	4.48	110
Montmorillonite	27.7	3.02	005
Montmorillonite	34.7	2.58	200
Illite	8.7	10.2	002
Illite	17.8	5.03	004
Illite	22.9	3.88	113
Illite	45.6	1.99	010
Quartz	20.9	4.26	100
Quartz	26.6	3.34	101
Quartz	36.2	2.48	110
Quartz	42.3	2.13	200
Chromatite	24.4	3.64	012
Chromatite	33.6	2.67	104
Chromatite	39.4	2.28	006
Chromatite	41.4	2.17	113
Calcite	29.4	3.03	104
Calcite	43.1	2.09	202
Calcite	47.5	1.91	018
Calcite	49.2	1.87	116
Dolomite	24.1	3.69	012
Dolomite	31	2.89	104
Dolomite	37.5	2.40	110
Dolomite	44.1	2.06	021

Table (5): Soxhlate extractions (%) of 2g Iraqi virgin olive oil using different adsorbents.

Polarity constant Sample	Solvents				Loss %
	Petroleum ether 0.0	Toluene 2.38	Chloroform 4.81	Ethanol 24.6	
Natural	70	14.5	3	3.5	9
Treated	64.5	24.5	4	4.5	2.5
Doped natural	77.5	18	1.5	2.5	0.5
Doped treated	79	15	2	3	1

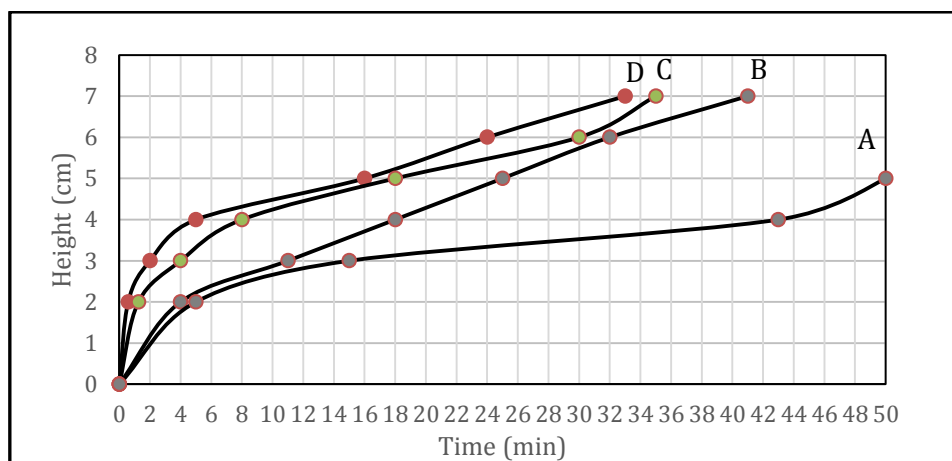


Figure 1. Capillary action curves of (A) natural clay (B) treated clay (C) doped natural clay (D) doped treated clay sample

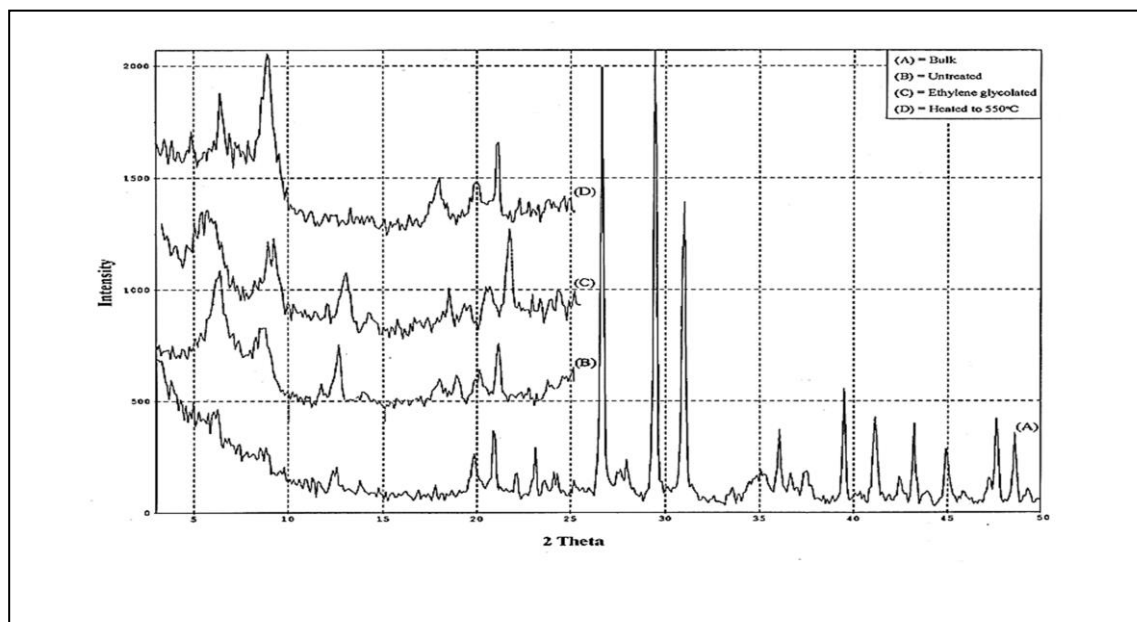


Figure 2. Powder X-ray diffraction pattern of natural clay sample

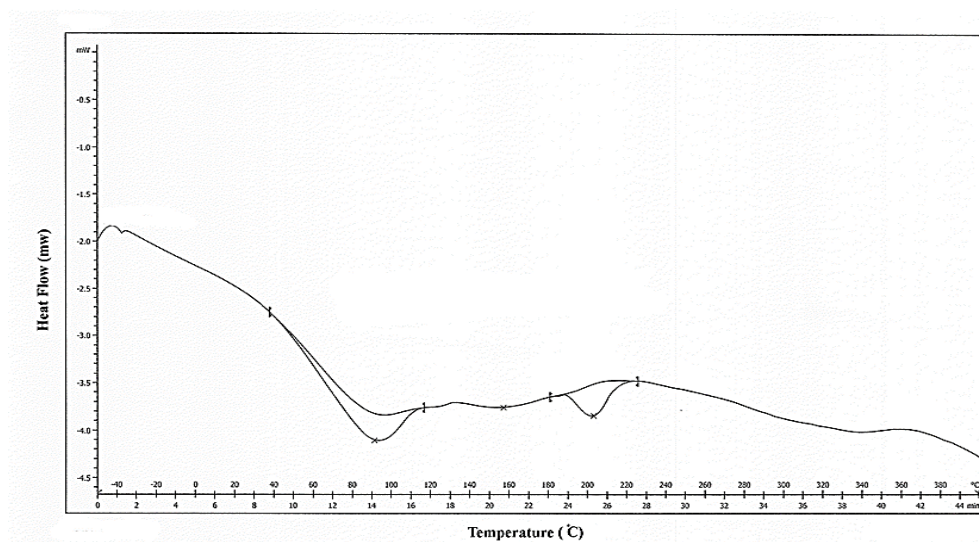


Figure 3 .Differential scanning calorimetry curve of chromium doped clay sample.

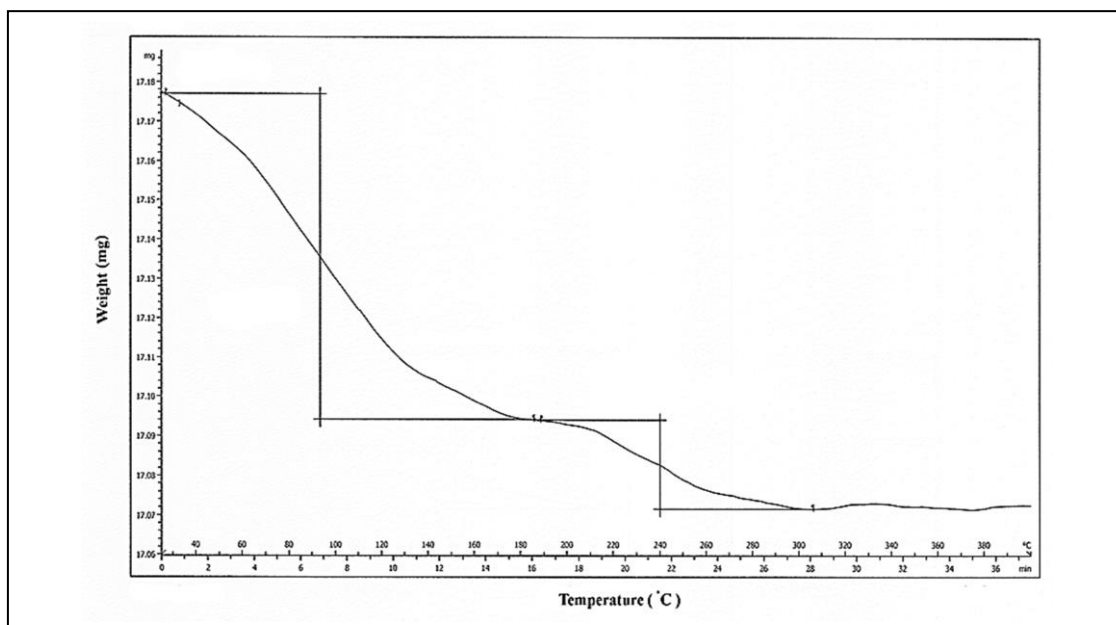


Figure 4. Thermogravimetric analysis curve of chromium doped clay sample

Experimental Investigation of the Time Effect of Pressure Fluctuations in Steady Turbulent Pipe Flows

Hasan DUZ

Batman University

Ahmet Beyzade DEMIRPOLAT

Firat University

Abstract: In the study, which performed experimentally, the behavior of time variation of the static pressure in pipe water flows has been investigated in terms of pipe diameter, flow rate and pipe roughness. In the experiments, five pipe types in different materials and in different roughness were used. In the steady and horizontal pipe water flows, which performed at low Reynolds numbers, the static pressure at different tap locations which is longitudinally placed have been measured. The water heights in the piezometer hoses, which is inserted on pressure taps, has been recorded with a camera for three minutes for each flow rates. A total of 21 snapshots were obtained from each camera recordings at equal time intervals and the pressures were determined from that snapshot images through water height readings. The snapshots of any flow rate has shown that all pressures at the tap locations fluctuate together over the time in the same phase, frequency and amplitude. When RMS values, which shows the pressure fluctuation in mean intensity over the time, was examined, it was observed that the fluctuation amplitudes is independent of pipe roughness but has a relation with velocity of the pipe flow.

Keywords: Pipe flows, Pressure fluctuations

Introduction

Osborne Reynolds (1842-1912) has discovered laminar and turbulent flow behavior by injecting ink into glass-tubular flow in his experiments. At low flow velocities the ink followed a uniform flow path and not mixed to the flow along, while at high flow velocities the ink mixed to the flow over the entire cross section of the pipe flow as the ink moving downstream. In the laminar flows, due to the low flow velocity, fluid particles follows a smooth flow path, for this reason the laminar flows is smooth. Whereas in the turbulent flow, the instabilities in the flow cause the flow to get mixed in so that the fluid particles do not follow a uniform flow path. In general, all flows must be laminar, however some factors that degrade the flow stability, such as surface roughness, upstream turbulence, and heat transfer in the flow, force the flow to be turbulent. For this reason, if precise flow conditions are provided, all flows will remain laminar (Özışık, 1985). Turbulent flows include fluid clusters that are formed continuously and moved along the flow while spinning its around. These moving fluid clusters are called turbulent structures or swirl motions. These vortex structures form continuously, move, divide and disperse in the flow and eventually turn into sensible heat in the flow then disappears. They are responsible of the conversion of some of the mechanical energy into sensible heat energy. This describe why the energy loss is greater in turbulent flows. For example, especially for flows over a solid surface (flow through aircraft, turbine, and compressor blades) the flow being turbulent not only increases energy loss but also gain the vibration and noise to the flow. As a result, in addition to the viscous forces in the turbulent flow, there are also additional drag forces, so that the energy losses in turbulent flows are much higher than laminar flows which viscous forces are dominated.

The flow over a flat surface first becomes laminar and after a certain flow distance, the flow stability is degraded then it becomes turbulent flow. Fig. 1 shows the steps of a flow as being laminar, transition and

- This is an Open Access article distributed under the terms of the Creative Commons Attribution-Noncommercial 4.0 Unported License, permitting all non-commercial use, distribution, and reproduction in any medium, provided the original work is properly cited.

- Selection and peer-review under responsibility of the Organizing Committee of the Conference

turbulence, over the pipe inner surface. The distance from inlet to where the flow first undergo a turbulent state is called transition length, L_t . After the transition length a transitional flow establishes, which is an intermittent flow between laminar and turbulent states. After the transitional flow the flow becomes full turbulent. Some detailed experimental and theoretical progresses for the laminar to turbulent transition in pipe flows have been reported by Kerswell (2005) and recently by Willis a.e (2008). Factors such as inlet smoothness, inlet geometry type, surface roughness, upstream turbulence, mixing the flow at inlet and heating-cooling applications are highly influential on triggering the flow to a turbulent state (Ghajar & Tam, 1995). The smooth velocity profile at pipe inlet starts to change along the downstream and after a certain critical flow distance the velocity profile no longer change. The pipe flow region where the velocity profile changes is called developing flow and where the velocity profile is constant is called fully developed flow. In the fully developed pipe flow region, pressure drop is linear and due to has a relation with it, the wall shear stress is constant also. The measured pipe distance from inlet to where the flow start to fully developed is called entrance length L_e . In general, the flow are assumed to be fully developed when time-averaged flow quantities (velocity and pressure field) and turbulence quantities (turbulence velocities $u' v'$) no longer changes, (Zagarola & Smits, 1998).

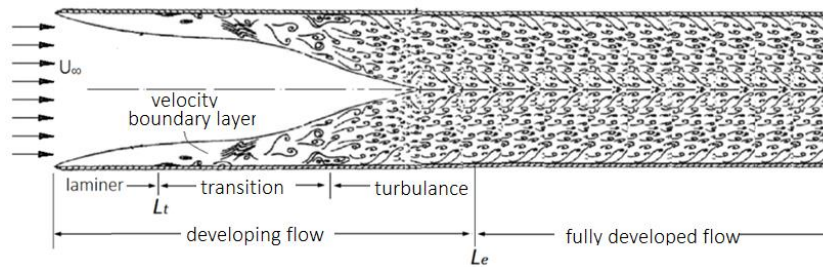


Figure 1. Developing and fully developed flow at pipe entrance

Osborne Reynolds has discovered the dimensionless Reynolds numbers so to specify the flow state. Through his experiments, he has observed that the pipe flow remained as laminar until a Reynolds number of 13000 when the sensitive flow conditions was provided by him and a turbulent state also has reached after a Reynolds number of 2300 when disturb the flow at pipe inlet. For that reason it is hard to mention about a definitely Reynolds number where turbulent pipe flow is established. In general, pipe flows are accepted as laminar for $Re < 2300$ and otherwise are accepted as turbulent (White F.M., 2003).

The flow properties measured at any point in a turbulent flow field shows fluctuating values over the time. As shown in Fig 2, the turbulence flow exhibits non-periodic statistical wavy flow characteristics.

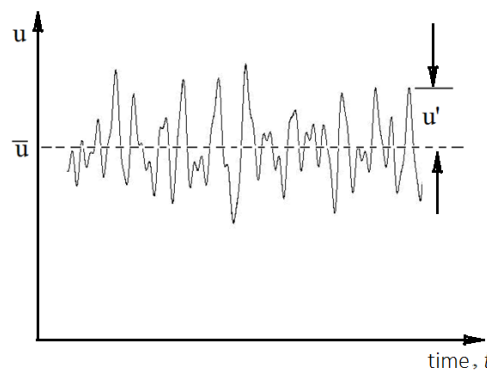


Figure 2. Variation of the instant velocity over the time at at any point in the turbulent flow field

Because the turbulent flows changes with time and position, it requires analytically time dependent and three dimensional flow solution. Therefore it is so difficult to solve the turbulent flows theoretically. One simplification to the solution is to evaluate the turbulent flow over the time average effects. The flow properties can be separated into two parts as the time average value and the fluctuation value, which is the amount of deviation from the mean value, as shown in the instantaneous velocity graph.

$$u = \bar{u} + u' \quad P = \bar{P} + P'$$

u' : velocity fluctuation or amplitude value u : instantaneous velocity \bar{u} : time mean velocity value
 P' : pressure fluctuate or amplitude value P : instantaneous pressure \bar{P} : time mean value

Time mean value can be found by integrating the instantaneous value over the time as shown in Equ.1

$$\bar{u} = \frac{1}{\Delta t} \int_t^{t+\Delta t} u dt$$

In turbulent flows, Reynolds average Navier Stokes equations (RANS), which include mean flow effects, are formed by substituting the flow properties into the basic flow equations, separated as mean and fluctuate values. RANS equations consists of continuity and momentum conservation equations which are called also time-mean basic flow equations. A RANS equation, that define a Newtonian and an incompressible turbulent flow field is given below which shows a momentum equation in x direction also.

$$\rho \left(\frac{\partial \bar{u}}{\partial t} + \bar{u} \frac{\partial \bar{u}}{\partial x} + \bar{v} \frac{\partial \bar{u}}{\partial y} + \bar{w} \frac{\partial \bar{u}}{\partial z} \right) = - \frac{\partial \bar{P}}{\partial x} + \rho g_x + \mu \nabla^2 \bar{u} - \rho \left(\frac{\partial \overline{u'^2}}{\partial x} + \frac{\partial \overline{u'v'}}{\partial y} + \frac{\partial \overline{u'w'}}{\partial z} \right)$$

(2)

While the time mean flow characteristics can be known in a turbulent flow, the time mean effects of the turbulence fluctuation quantities shown in Equ.1 ($-\rho \overline{u'v'}$, $-\rho \overline{u'w'}$ and $\rho \overline{u'^2}$) are not known. The terms formed in the differential flow equation represent the time mean effects of the turbulence in the flow field. These terms are called turbulent stresses or Reynolds stresses. For the solution of Reynolds stresses, many empirical turbulent models are developed. Through this way, turbulent flows are solved in a simple way using RANS equations.

Due to turbulent flows are complex type flows, even though many studies performed it is still exactly not solved with all mystery so it is still of interest in many researchers. In this study, which was aimed to gain a contribution to the solution of turbulent flows, an experimental study of turbulent pipe flows was carried out. In the experimental work, steady and circular pipe water flows were carried out to cover laminar, transition and turbulence flow regimes. In the experiments, time-dependent static pressure measurements were made at different downstream locations of flow field. The pressures measured in each flow rate are analyzed by time-dependent graphs. As a result, in a given flow rate, the static pressures values at all pressure tap locations is fluctuated in the same phase, frequency and amplitude.

If the following sections are summarized, in section 2 the experimental set up, flow conditions and properties are presented. In section 3, the whole study are concluded by analysing the time-dependent variations and the time averages of the experimental results with graphics.

Experiment Set Up and Flow Properties

In order to carry out the experiments, the experimental setup shown in Fig. 3 is prepared. The test setup consists of a pump, a flow rate measurement tank, a rectangular board which the piezometer tubes are attached, a flow control valve, test tubes and a camera for recordings. Water were used in pipe flow experiments. Pressure tappings were welded on the test pipes at regular intervals to measure the static pressures of the flow. The plastic piezometer hoses inserted on pressure taps are glued on the rectangular board and a tape meter is glued next to it to indicate the water height. As can be seen in Fig. 3, different flow rates were carried out by regulating the flow control valve. However the flow rates was measured through weighting tank shown in the test setup.

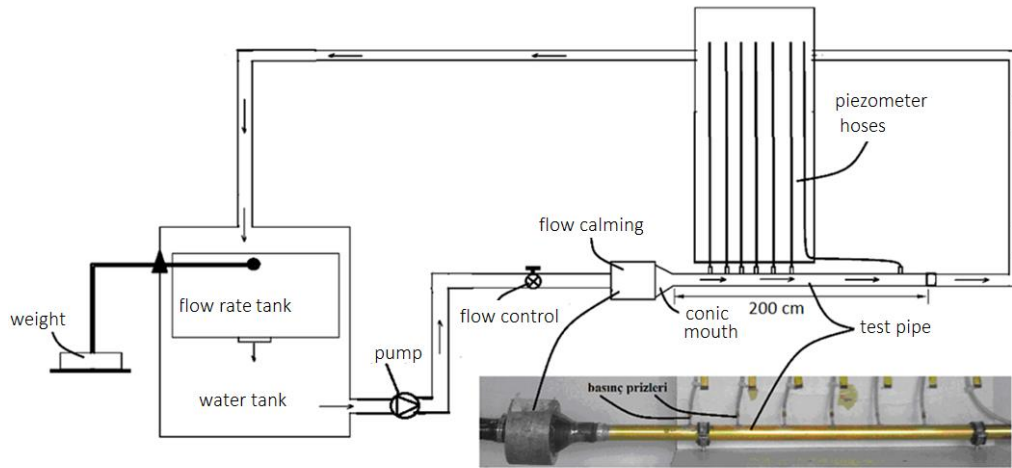


Figure 3. Two dimensional scheme of the experimental set up and test pipe details

To measure the static pressures over the time, the rectangular board which the piezometer hoses were attached was recorded with a camera for three minutes for each flow rate. Snapshots were taken at five second intervals from the camera recording. A total of 21 instantaneous pictures were captured from each flow recordings. The water heights in the piezometer hoses were read from these images and the values were tabulated.

The test tube is connected to a flow calming conic element. In this way it was desired that the fluid enter to the test tube with a low turbulence and a uniform velocity profile. Several studies have reported that the upstream turbulence flow to the test tube is effective on triggering the flow to turbulence (Özışık 1985, Nikuradse, 1932). The test pipe and the pressure taps sequenced on the pipe has shown in Fig. 4. A pipe length of 4 m were used in experiments which correspond to a flow distance of 72D. In most experimental studies reported in the literature, it has been reported that fully developed flow generally occurs at flow distances between 30D and 50D (Laufer (1953), Sarpkaya (1975), Haung ve Chen (1974), Patel ve Head (1974)). These reported entrance lengths were found at locations by observing the mean cross sectional velocity profiles where no longer change observed along the flow. Barbin and Jones (1963) has reported that fully developed flow was observed at distances between 10D and 20D when the pressure gradient reaching the constant values along the flow. According to that information supplied, the length of the test pipe is long enough to cover some of the fully developed flow. Pressure taps are welded on pipe at seven diferent stations. The distances between taps are shown on Fig. 4. According to Fig. 4, the 7th tap is placed on the pipe with a distance of 1.7 m away from the pipe inlet and 1 m away from 6th tap. As depicted on Fig. 4, the first six taps were placed on the pipe with equal intervals. The five pipe types used in the experiment are not the new manufactured ones, they are pipes that were dismantled from the old piping systems. Therefore the surface roughness of these pipes were found through the pipe flow measurements. Since the last two taps are in the fully developed flow section, the pressure differences between them were measured and the relative roughness of each tube was found through. In this method, the relative roughnesses were found by comparing the variation of the fully developed Darcy friction factors with Reynolds numbers, which were calculated from that pressure differences, to the Colebrooke equation. The pipe types, diameters and relative roughness found in the experiment are given in Table 1.

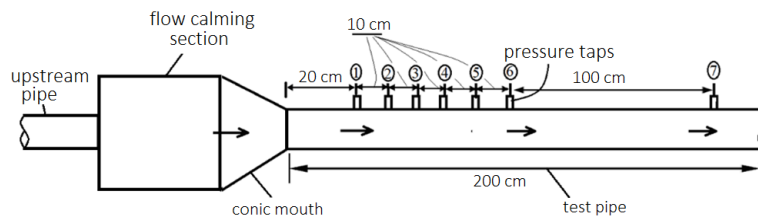


Figure 4. Calming section, test pipe and distances between pressure taps

Table 1. The roughness values found from the experimental measurements for five pipe types

	Aluminium pipe	Copper pipe	Steel pipe	Galvanized pipe	Plastic pipe boru
D (mm)	26	26	28	28	21
Relative roughness: ϵ/D	0.00159	0.000163	0.00236	0.00256	0.000331

Static Pressure Fluctuations

In a steady experimental water flows, which is carried out in a horizontal and circular pipe, variation of static pressures in the entrance and fully developed flow regions of a pipe was investigated in this section. In each pipe flow, water heights in piezometer pipes were recorded for a three minutes with a camera. The pressure at the tap locations are found from the water column heights in piezometer pipes through correlation of $P = \rho gh$. Here “ h ” is the water column height in piezometer pipe. As can be mentioned above, a total of 25 snapshots were recorded at 5-second intervals from the camera recording of each pipe flow. The water heights in the piezometer pipes were read from these snapshots. Through this way, the time-dependent values of pressure values at each tap location has been obtained. For example, Fig.5 has shown the time-dependent variation of the static pressures in the first six pressure taps for close Reynolds numbers of two pipes. When the pressure variations across time are examined, it is seen that the pressures at all tap locations is fluctuated in the same phase, frequency and amplitude as depicted in Fig.5.

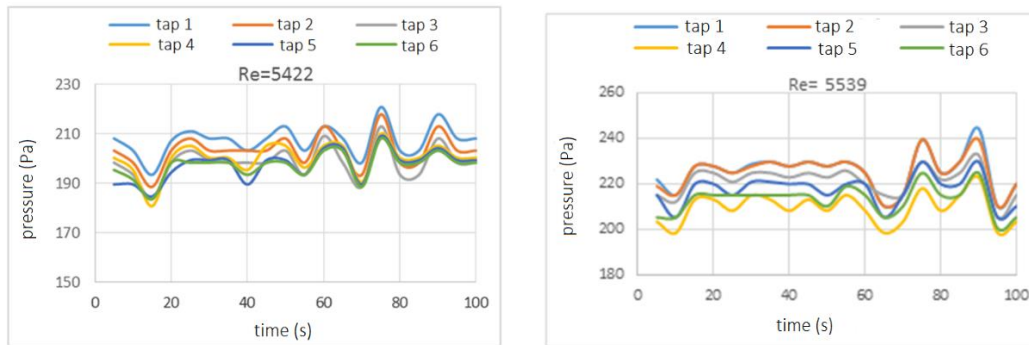


Figure 5. The time-dependent variations of pressure values at each tap at low Reynolds numbers of two pipes



Figure 6. Time dependent variation of pressures at each taps location in different Reynolds numbers

Fig. 6 also shows the time-dependent variations of the pressures at the taps at different Reynolds numbers for two pipes. As can be seen from the figure, the pressure fluctuations are not observed in the lowest Reynolds numbers, but are observed in bigger Reynolds numbers. It is also seen that all pressure taps have pressure fluctuations in the same phase, frequency and amplitude for all Reynolds numbers. Pressure fluctuations in the taps indicate that the friction resistance of the flow increases and decreases over the time also. The variation of the flow resistance over the time indicate that the flow rate fluctuates in time with the same phase and frequency also. The reason why the flow resistance variate in time is that the inertia forces are greater than the viscous forces. Inertial forces are forces due to flow velocity while the viscous forces are the bonding forces between liquid molecules. The inertial force of the flow is getting stronger near pipe walls than viscous forces in turbulent flows. The difference between both forces are being stronger intermittently due to some imbalances exists in the flow so that the laminar flow stability are broken down then the flow becomes turbulent.

Viscous forces suddenly failed in the near-wall flow region across inertial forces and fluid vortices exists by this phenomenon which moves from the wall into the pipe flow core region while spinning its around. These eddy fluid clusters as well as carry heat and momentum together with, agitate and mixing the flow also. For this reason, the flow energy is converted to sensible heat in the flow by these vortex motions. Fig. 7 has shown the variations of pressures with the time at each taps including all the five pipe types at close Reynolds numbers. When these variations are examined, it can be seen that the pressure fluctuations are in the same phase, frequency and amplitude for all six tap locations.



Figure 7. Variation of pressures across the time at each tap locations of five pipe type flows at close Reynolds numbers

The amplitude of swing motion of water in the piezometer tubes is directly proportional to the flow resistance encountered in the piezometer hose. The amplitude of the swing motion will be lower in the hose of which the flow resistance is high. As can be seen from Fig. 3, the length of the piezometer hose used on tap 7 is about 1.6 times longer than others. So that, as can be seen in Fig. 8, the pressure variation at tap 7 is slightly different from the pressure variation at tap 6. It is seen that the amplitude of the tap 7 is lower than tap 6 as shown in Fig. 8. This is indicated by the root mean square (RMS) value of the amplitudes given in Table 2 in the last column. Whereas Table 2 has shown the RMS values of the pressure amplitudes in all tap locations of aluminium pipe at a given Reynolds number.

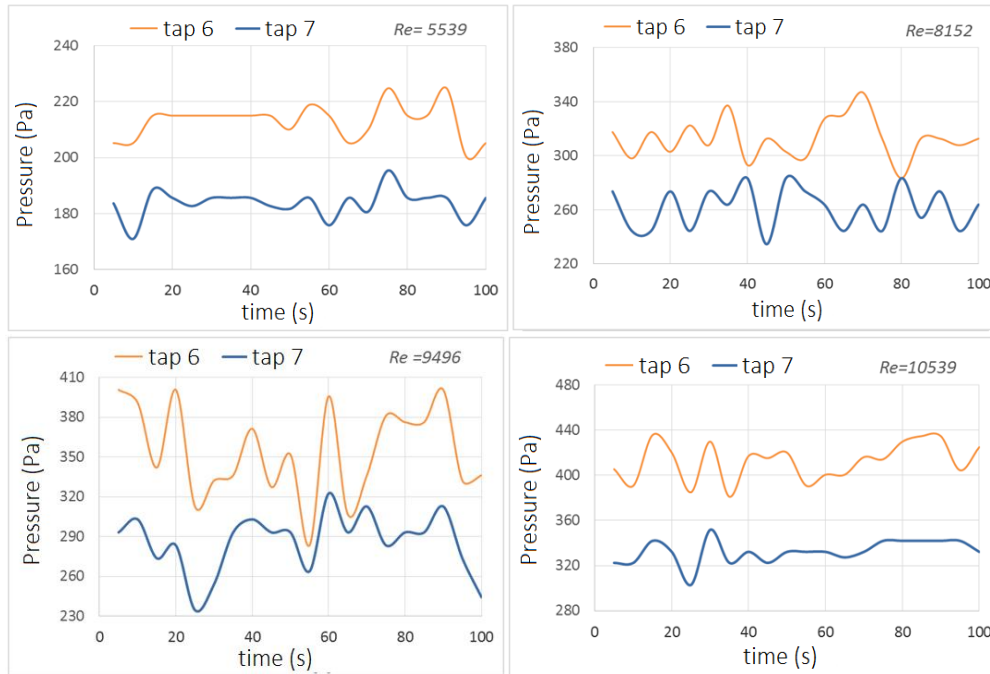


Figure 8. Comparison of pressure variations in pressure taps 6 and 7 at four different Reynolds numbers

Effective Static Pressure

In the pipe flow, for the variation of the pressure over the time, the amount of deviation from the average pressure value of the instantaneous pressure is called the pressure amplitude or fluctuate value. To find out whether the pressure amplitude is related to pipe diameter, roughness and Reynolds number, the pressure amplitude values can be calculated as below.

$$P' = |P - \bar{P}|$$

P' : pressure amplitude value

P : instantaneous pressure value

\bar{P} : time mean pressure value

The RMS values of the pressure amplitude which shows the time mean effective value are calculated as follows.

$$P'_{RMS} = \sqrt{\frac{\sum_{i=1}^N (P - \bar{P})^2}{N}}$$

Here, N is the time step number. 21 images has been taken from each camera recordings so the total time step must be $N = 21$. In Table 2, the pressure fluctuating values of all pressure taps are given for the Reynolds number of 5539 of aluminum pipe flow. Similar tables are prepared for other pipe types which is not given here. In Table 2, the RMS values of each tap are given in the last row. When the RMS value of tap 7, which is given in the last column, is observed it is seen that it is lower than the RMS values of other taps. As stated above, the longer the piezometer hose in the tap 7 is the reason. The longer the hose in the oscillation movement, the more friction creates resistance.

Tablo 2. Absolute deviations from the time averaged pressure values of the pressures at all taps and their time averages in the aluminum pipe flow

absolute pressure amplitude values P' (Pa) $Re=5539$							
t (s) / L (m)	0.2	0.3	0.4	0.5	0.6	0.7	1.7
5	3.567	6.058	6.106	5.911	2.296	7.768	0.049
10	10.406	9.966	9.038	10.797	12.067	7.768	12.751
15	2.296	2.736	3.664	3.860	2.589	2.003	4.837
20	2.296	2.736	3.664	3.860	2.589	2.003	1.905
25	0.636	0.196	0.244	1.026	2.296	2.003	1.026
30	3.273	2.736	3.664	5.814	3.566	2.003	1.905
35	4.250	4.690	3.664	3.860	3.566	2.003	1.905
40	2.296	2.736	1.710	1.026	2.589	2.003	1.905
45	4.250	4.690	3.664	3.860	2.589	2.003	1.026
50	2.296	2.736	1.710	1.026	2.296	2.883	2.003
55	4.250	4.690	4.642	5.814	2.589	5.911	1.905
60	0.636	0.196	1.221	1.026	2.589	2.003	7.865
65	15.292	14.852	6.106	10.797	12.067	7.768	1.905
70	10.406	9.966	6.106	5.911	2.296	2.883	2.980
75	14.021	14.461	8.550	8.745	12.360	11.773	11.676
80	0.636	0.196	0.733	1.026	2.589	2.003	1.905
85	4.250	4.690	3.664	5.814	2.589	2.003	1.905
90	18.906	14.461	11.481	13.630	12.360	11.773	1.905
95	15.292	14.852	15.877	10.797	12.067	12.653	7.865
100	5.521	5.081	6.106	5.911	7.182	7.768	1.905
P'_{RMS}	8.327	7.893	6.316	6.645	6.686	6.206	3,334

Table 3 has shown the RMS values of the pressure amplitudes which is determined from each taps on aluminium pipe at all Reynolds numbers studied. Similar tables are also prepared for other pipes which is not given here. RMS values of the tap 7 are not shown in the table since it has not the same fluctuation conditions with other taps. So it will be enough to use the inputs of the first six taps to determine the overall RMS values. When Table 3 is seen, it is seen that the RMS values of any tap are different at Reynolds numbers. When the variation of RMS value in each tap is examined across Reynolds, no any relation are observed between RMS and Reynolds numbers it can be said that RMS values do not depend on the Reynolds number. The last column in Table 3 shows the mean RMS values in each Reynolds numbers. In addition, an overall average value is taken from the mean tap RMS values as shown in the last row. These overall average RMS values are given in Table 4 for all pipe types.

Table 3. RMS values of the pressure amplitudes for aluminium pipe

Aluminium Pipe, P'_{RMS} (Pa)							
Re / L (m)	0.2	0.3	0.4	0.5	0.6	0.7	Mean
4572	0.004	0.932	1.357	1.047	0.003	0.349	0.615
5539	8.327	7.893	6.316	6.645	6.686	6.206	7.012
8152	15.105	15.119	16.074	15.453	15.404	14.735	15.315
9496	37.110	35.226	35.319	34.888	32.091	34.147	34.797
10539	16.053	18.329	17.691	15.785	18.300	16.651	17.135
11371	24.309	21.235	21.452	20.164	17.903	18.876	20.657
12172	24.209	24.282	25.814	25.768	24.173	24.548	24.799
13295	15.619	15.607	16.394	15.483	14.340	13.535	15.163
15712	15.127	10.904	19.012	15.625	14.028	14.109	14.801
18004	12.513	10.645	13.134	11.183	11.980	9.964	11.570
21043	10.798	9.523	9.892	9.661	8.726	7.584	9.364
	Overall Mean						15.56

Table 4. Overall mean RMS values of the pressure amplitudes for whole pipe types.

Overall RMS values				
Aluminium pipe (D=26mm)	Copper pipe (D=26mm)	Steel pipe (D=28mm)	Galvanised pipe (D=28mm)	Plastic pipe (D=21mm)
15.56	15.27	13.16	11.63	21.75

The overall average RMS values given in Table 4 were obtained from the flows in a certain numbers experimented in the Reynolds numbers between 2000 and 25000 for each pipe type. Even though the pipe flows were not provided at the same Reynolds numbers for each pipe type, the flows performed at a certain number have had nearly a uniform Reynolds distribution in the Reynolds range studied. Hence, due to the overall average values are obtained from the statistical values in the Reynolds numbers between 2000 and 25000, which is not important to be the same or not of the Reynolds numbers so that the comparisons can be made. In Table 4, the diameters of each pipe type are given in parentheses. The diameter of the plastic pipe is the smallest one however the overall average RMS value is seen the highest one. Similarly, when the RMS values are observed to be related to the pipe diameter, it is seen that the aluminum and copper pipe diameters are the same and their RMS values are close each other and iron and galvanized pipe have the same diameters also and their RMS values has been close to each other. Here it is seen that the overall RMS values are inversely proportional to the pipe diameter. The reason is that the flow velocity is higher in the small pipe diameter for the same Reynolds number considered. It is seen that the higher the flow velocity, the more the pressure amplitudes are affected. However to learn the effect of pipe roughness on RMS values, aluminium and copper pipes can be compared, since both have the same pipe diameters. Even though pipe diameter are the same the roughnesses are different as shown in Table 1. However, the overall average RMS values are very close to each other. So roughness can not be said to have much effect on the oscillation amplitude. So roughness can not be said to have much effect on the oscillation amplitude. As a result, the pressure fluctuation amplitudes seem to have an increasing relationship with flow velocity.

Conclusion

In this study, experimental water flows were performed for the Reynolds numbers ranged from 2000 to 25000 with five pipe types made of different materials. Pipe diameters and pipe surface roughness also is different. Approximately 12 different pipe flow rates were carried out evenly in the Reynolds number range studied. From the pipe inlet, seven pressure taps were drilled on the pipe at different locations longitudinal. The pressure in the pipe flows is measured by observing the water heights in the piezometer hoses inserted to these pressure taps. Measurements were time-dependent, so each pipe flow was recorded with camera for three minutes of time. Twenty one snapshots were obtained from each camera recordings at equal time intervals. The pressures at each tap locations are read from these snapshot pictures. These pressures are examined for any flow rate and it is seen that the pressures at each top locations fluctuate with time. When the pressures at all tap locations are compared to each other for any flow rate, it is seen that pressure values fluctuate with time in the same phase, frequency and amplitude. The time dependent RMS values of the turbulent pressures amplitudes were obtained. The RMS values of the pressure amplitudes, which is the amount of deviation from the time mean value, are obtained. When the variation of RMS values were examined across the Reynolds number, it was found that there was no relation with the Reynolds number. The same RMS values were found to be independent of the pipe surface roughness. An overall average value of the RMS values of all flow rates were obtained. In the Reynolds number range studied, it is seen that this is the largest in the small pipe diameter according to the overall average RMS value. The reason for this is that the velocity is being higher in the small pipe diameter for the same Reynolds number considered. Consequently, the flow velocity appears to have a significant impact on the pressure amplitudes

References

- Anslys Workbech, (2018) " CFX Help menu" Ansys student version
- Anselmet F. Ternat ,F. Amielh M. Boiron O. Boyer P. & Pietri L., 2009. "Axial development of the mean flow in the entrance region of turbulent pipe and duct flows".*Elsevier C. R. Mecanique*. 337, 573–584
- Kerswell, R. R., 2005, "Recent Progress in Understanding the Transition to Turbulence in a Pipe," Institute of Physics Publishing, Nonlinearity, 18, pp. R17–R44
- Özışık N., 1985. "HEAT TRANSFER: a basic approach", *MackGraw-Hill Book Co*, international edition
- Reynolds, O., 1883, "On the Dynamical Theory of Incompressible Viscous Fluids and Determination of the Criterion," *Philos. Trans. R. Soc. London*, 186, pp. 123–164.
- Willis, A. P., Peixinho, J., Kerswell, R. R., and Mullin, T., 2008, "Experimental and Theoretical Progress in Pipe Flow Transition," *Philos. Trans. R. Soc. London, Ser. A*, 366_1876_, pp. 2671–2684.
- White F.M., 2003. "Fluid Mechanics", 5th edition, *McGraw–Hill Book Co*, New York
- Zagarola, M.V., and Smits, A. J., 1998, "Mean-Flow Scaling of Turbulent Pipe Flow," *J. Fluid Mech.*, 373, pp. 33–79.
- Ghajar, A.J. and Tam, L.M. (1995) Flow Regime Map for a Horizontal Pipe with Uniform Wall Heat Flux and Three Inlet Configurations. *Experimental Thermal and Fluid Science*; 10:287-297
- Zanoun E.-S. and Egbers, C. (2016). Flow Transition And Development In Pipe Facilities Journal Of Engineering And Applied Science, Vol. 63, No. 2, PP. 141-155
- Zimmer F., Zanoun E.S. and Egbers C. (2011). "A study on the influence of triggering pipe flow regarding mean and higher order statistics". 13th European Turbulence Conference (ETC13) *Journal of Physics: Conference Series*, Volume 318, Section 3.

Author Information

Hasan Duz

Batman University, Tecnology Faculty, Automotive Engineering
Batman Üniversitesi, Batı Raman Kampüsü, Lojmanlar, Loj 3 No:12, Batman, Turkey
E-mail: hasan.duz@batman.edu.tr

Ahmet Beyzade Demirpolat

Fırat University, Eneering Faculty, Mechanical Engineering Department
Fırat Üniversitesi, Makine Mühendisliği Bölümü, Elazığ, Turkey

Numerical Investigation of the Transition Length at the Entrance Region of Pipe Flows

Hasan DUZ
Batman University

Ahmet Beyzade DEMIRPOLAT
Firat University

Abstract: In this study, the steady, incompressible and axis symmetric flows in the pipe entrance region has been simulated numerically for the Reynolds numbers between 1000 and 25000 and for the square edged pipe inlets. The developing boundary layer at the pipe entrance region first grows as laminar then disturbed to a turbulent state at downstream away of the inlet. From pipe inlet to a downstream distance where laminar to turbulent transition begins is called the transition length. Determination of the transition length has been significant for hydro and aeromechanics and yet it seems not to be defined clearly. The effects of wall surface roughness, pipe diameter and Reynolds numbers on transition length has been investigated numerically by covering transition and turbulent flow regimes too. On the purpose, water flows were simulated numerically including five different relative roughness. The numerical results obtained has shown that the transition length is the power function of the Reynolds number inverse proportionally. Likewise the numerical study has also shown that changing the pipe diameter but keeping the relative roughness the same has left no effect on the transition length. As an outcome, a numerical correlation which define the dimensionless transition length and well fitting the numerical values was derived as a function of Reynolds number.

Keywords: Entrance length, Pipe flow, Developing flow, Numerical

Introduction

In 1800, Osborne Reynolds has found the flows behaving as two different in the experiments he made then the flow is classified as laminar and turbulent. Laminar flow is a kind of flow that occur at low velocities and follow a regular movement whereas turbulent flow is a kind of flow that occurs at bigger velocities than low and is a kind of irregular and intermixed flow. He found the dimensionless Reynolds number to specify the flow type. Laminar flow is a stable flow and effects such as vibration, free stream turbulence and roughness disturb the flow stability and make the flow turbulent. It has been seen in many experiment that the flow can stay laminar when a sensitive flow condition was provided (Özışık M. Necati (1985), White F.M. (2003)). When Osborne Reynolds mix the flow at pipe entry to make turbulence, laminar flow lasted up to a Reynolds number of 2300 and when a sensitive flow condition was provided by not allowed to any turbulence exists it has been seen that laminar flow lasted up to a Reynolds number of 13000 in the experiments.

For the flows over a flat surface, flow first begins as laminar in the leading edge and a certain distance away from the inlet the flow stability is deteriorated and it become a turbulent flow structure. Figure 1 illustrate three stages of the fluid flowing over the inside surface of a pipe as being laminar, transient and turbulent. The flow distance from the pipe inlet to the location where the flow first disturb to turbulent is called the transition length (L_t). After transition length, a transitional flow region occur for a while then the flow becomes fully developed. The measured distance from inlet to where the flow to become full turbulent is called entrance length. It is seen in many experimental works that the flow distances is depend on the flow velocity, surface roughness, free stream turbulence level, surface vibrations, and heating and cooling processes (Minkowycz et al. (2009), Zanoun et al. (2009)). Though some empirical correlations are proposed for both flow distances through the

- This is an Open Access article distributed under the terms of the Creative Commons Attribution-NonCommercial 4.0 Unported License, permitting all non-commercial use, distribution, and reproduction in any medium, provided the original work is properly cited.

- Selection and peer-review under responsibility of the Organizing Committee of the Conference

experiments, a general solution to the problem is not still be clarified well due to many parameters effects on the flow.

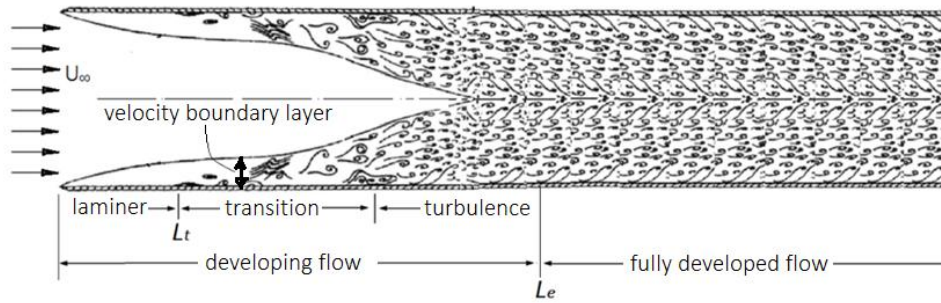


Figure 1. Developing and fully developed flow at pipe entrance

According to experimental studies, when a flow with high freestream turbulence level pass over a full roughly surface, transition length lasted up at $Re_t = 10^5$ but for a flow not contained any tubulence in the freestream pass and over a smooth flat surface it lasted up to $Re_t = 10^6$ as measured in the experiments (Özişik (1985)). In case pipe inside flow study, due to pipe diameter limit the flow peripheral , transition distance from laminar to turbulence is being different than the flows over flat surfaces. Fig. 2 has shown the flow development after pipe inlet. The velocity boundary layer that forms the result of the viscous effects from the pipe inlet, thickness of it increase along the inlet and since the thickness is limited by the pipe radius, the entire flow cross-section is filled with the boundary layer. From the pipe inlet, the viscous effects begin to change in the resulting velocity profile. This velocity profile changes along the flow until it become a constant velocity profile. The flow region where the velocity profile changes is called inlet flow or developing flow. The pipe flow, in which the velocity profile is along constant, is called the fully developed pipe flow. Different definitions are also available in the literature for fully developed pipe flow. For example, fully developed flow begins when such like two flow properties, wall shear stress or mean turbulent flow statistics reach the constant values (Anselmet et al. (2009), Patel&Head (1969)). Therefore, Zimmer et al. (2011) said that it should be required to define the fully developed flow as a flow that starts when the time-averaged turbulence flow statistics become constant. In the author's experimental study, it was reported that the developing flow distance is even longer when turbulence flow statistical values was measured.

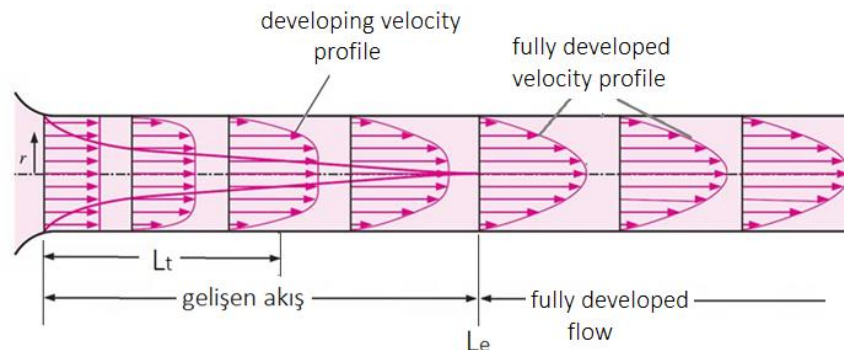


Figure 2. Variation of velocity profile along the developing and fully developed flow

Along the fully developed pipe flow, the wall shear stress and the friction factor are constant since the pressure drop is linear. The fully developed laminar or turbulent pipe flows are largely solved with theoretical and empirical relations, while the developing flow portion has still not been fully solved. In engineering applications, pipe-tank connections generally become conical (bell mouth), square edged and reentrant. while a sharp edged inlet produce much turbulence in the flow, bell mouth inlet produces minimal turbulence. The amount of turbulence goes to pipe at the inlet is effect on the transition and entrance lengths (Tam et al. (2013), Augustine (1988)). It is evident that the transition and inlet lengths with high turbulent inlet are shorter than with the low turbulent inlet. Table 1 gives the entrance lengths reported in experimental studies of pipe flows.

As shown in Table 1, the dimensionless entrance lengths (L_e / D) are reported for a large Reynolds number range for the turbulent flows. The experimental studies reported have also not been performed especially to measure entrance lengths, they are measured additionally in the experimental studies for different purposes. In most of these experimental studies, the pipe inlet connection type used is not reported. According to Table 1 the

inlet lengths vary from 25 to 80 diameters. It appears well from the Table 1 that the the empirical relations expressing the entrance lengths is also suggested. Anselmet et al (2009) has reported two empirical relation at high Reynolds numbers as given in Table 1 and also it appear that Augustine (1988) has suggested an empirical relation. It is seen in the literature that experimental studies on pipe flow are mainly aimed at finding the inlet lengths. Experimental studies to find transition lengths are rare. In this study, the transition lengths were investigated numerically in the Reynolds numbers range of $2 \times 10^3 - 25 \times 10^3$. The flow at the inlet of the pipe was chosen with a smooth velocity profile and at high turbulence intensity. The numerical results obtained are analysed and compared with empirical data. As an outcome, two numerical relation expressing the transition lengths are developed.

Numerical Pipe Flow

Firstly, in order to gain validation to numerical solution, an experimental study has been carried out with four pipe types made of different materials. Pipe types, relative roughness and pipe diameters are given in Table 2. Here it is aimed to see the effects of different relative roughness on flow conditions. The relative roughness of the tubes given in Table 2 was determined by the pressure differences measured in the fully developed flow region in the experiment.

Table 1. Dimensionless entrance lengths reported by the experimental studies

Dimensionless Entrance Length (L/D)		Reynolds Number	Author
Constant wall shear stress	Mean turbulent statistics		
80		-----	Osborne Reynolds
$L_e/D = 2.09 \times 10^{-8} * Re^{-1.66}$		5000-15000	Augustine (1988)
$L_e/D = 1.6 Re^{1/4}$		$10^5 - 10^6$	Anselmet et al. (2009)
$L_e/D = 4.4 Re^{1/6}$			
A long Empirical formula		$1,95 \times 10^5$	Salami (1986)
25 - 40		$3 \times 10^3 - 3 \times 10^6$	Nikuradse (1966)
30		$5 \times 10^4 - 5 \times 10^5$	Laufer (1954).
50 - 80		$10^3 - 10^4$	Patel & Head (1969)
70		$3 \times 10^4 - 1 \times 10^5$	Zanoun et al. (2009)
-----	72	175000	Perry & Abell (1978)
50	80	$1 \times 10^5 - 2 \times 10^5$	Doherty et al. (2007)
Not attain to 40		388000	Barbin&Jones (1963)
	70	$1.5 \times 10^5 - 8.5 \times 10^5$	Zimmer et al. (2011)

Table 2. Pipe type, Relative roughnesses and diameters

Pipe Type	Diameter	Relative roughness
	(mm)	ϵ / D
Aluminium pipe	26	0,0016
Copper Pipe	26	0,00016
Steel Pipe	28	0,0024
Galvanized Pipe	28	0,0026
PPRC pipe	21	0,00033

Static pressures were measured trough piezometres tubes fitted on pressure taps, which is welded to the holes drilled at seven different locations on the pipe. Pipe flows at each flow rate were recorded bya camera for three minutes. Time mean values of pressures are obtained for each location from each flow record. The pressure values obtained from the numerical flows made in the same parallel with the experiment are compared with the pressure values measured in the experiment in Fig.3.

Numerical Solution and Validation

Basically, fluid flows are defined by differential flow equations which is the results of the laws of mass, momentum and energy conservation. For this reason, the flow field in turbulent flows shows a continuous change with time temporarily and spatially. The time-dependent solution of a turbulent flow is difficult since it requires a solution to the time-dependent development of turbulence structures that is available in a wide range in the flow. The numerical method used to solve the time-dependent fundamental flow equations of a turbulent flow is called direct numerical simulation (DNS). The solution is not possible with today computers except that of very simple flows. Since solution is required very large mesh numbers and time steps.

Another method suggested for the solution of turbulent flow is to take the instantaneous effects of the flow to the time average effect. By this way, turbulent flows become time independent flows. The instantaneous drags existed by the turbulent structures against the flow form additional stresses in the time-averaged basic flow equations. These stresses are called Reynolds stresses or turbulent stresses. The time averaged conservation equations that forms in this way are called Reynolds averaged Navier-stokes equations (RANS). The only unknown in RANS equations is the Reynolds stresses. Therefore many turbulence models are developed to solve these Reynolds stresses. The solution of a turbulent flow with RANS equations is simple and the cost of numerical computation is very low in comparison to the DNS method.

In this study, turbulent pipe flows are solved via computer by applying finite difference numerical method to RANS equations. SST k-omega model are selected to solve the Reynolds stresses. To provide laminar to turbulent transition, Gamma-Theta model is selected. The pipe length has been selected long enough to cover the fully developed flow partly. Since the pipe flow is axis symmetrical, the flow area is limited to a small flow area sliced. The boundary conditions, fluid properties and flow type are defined in Table 3 below.

Table 3. Boundary conditions and flow field properties

Numerical properties	
<i>Flow state</i>	Steady-state, incompressible and isothermal flow
<i>Basic flow equations</i>	RANS Equations
<i>Turbulence model</i>	SST k-omega model
<i>Pipe inlet</i>	Smooth velocity and high turbulent intensity (T_U) = %7
<i>Pipe wall</i>	roughly
<i>Pipe outlet</i>	Open to atmosphere at gauge pressure
<i>fluid</i>	27 °C water

As shown in table 3, after setting up of boundary condition, flow and fluid properties, pipe flows are solved with CFX flow solver program. Numerical flows are kept parallel with experimental flows. As a result, the flow characteristics such as pressure, velocity, friction factor and wall shear stress were analyzed along the flow. Numerical and experimental values were compared in order to gain validity to numerical solution. The experimental and numerical values are compared in Fig 3 in terms of the pressure drop across the flow including all the flows of a pipe type. As shown in Fig. 3, experimental values and numerical values are agree well to each other. The mean and maximum deviations of the numerical values from the experimental ones are given in Table 4.

As can be seen in Table 4, numerical values of all pipe flows deviate from the experimental values by 7-9% about on average. The deviation amount is a tolerable one since it is natural to have such a detective. Because physical conditions such as fluid temperature can not be precisely determined and faults that occur in flow measurements and in static pressure readings in experimental runs are thought to be caused by these deviations. For this reason, flow characteristics are analyzed below using numerical data.

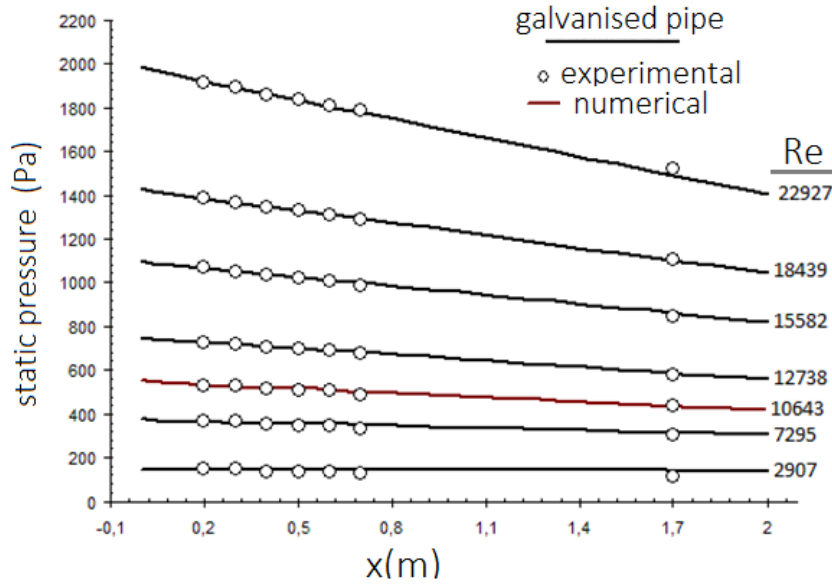


Figure 3. Comparison of numerical and experimental data in terms of pressure variation along the flow

Table 4. Percent deviation of numerical values from experimental data in terms of pressure variation along the flow

Deviation (%)	aluminium pipe	copper pipe	commercial steel pipe	galvanised pipe	Plastic pipe
maximum	±%20	±%24	±%36	±%35	±%18
average	%7.30	%7.70	%7.60	%9.40	%9

Numerical Analysis

Transition values must be obtained from the numerical solution so to analysis the transition distance. As the flow properties change at location where laminar to turbulence transition occur, the transition distance can be obtained from that flow characteristic which show the best in change at location. Variation of velocity, friction factor and wall shear stress in the transitional flow can be examined. Pressure variation along the pipe entrance is commomnly determined in experimental flows in order to find the transition distance. Since the wall shear stress or friction factor associated with the pressure variation change more distinctive therefore the transition distances can be obtained from the Darcy friction factor variations. The relationship between wall shear stress, pressure change and Darcy friction factor can be found by the static force balance on the Δx differential wall flow include pressure drop.

$$\tau_d = \frac{1}{4} \frac{D}{\Delta x} \Delta P = \frac{D}{4} \frac{\partial P}{\partial x} \tag{1}$$

$$\Delta P = f * \frac{\Delta x}{D} \frac{1}{2} \rho U^2 = f * \frac{\rho U^2}{2D} \quad \tau_d = \frac{1}{8} f \rho U^2$$

Where ΔP is the static pressure difference that occurs at the pipe flow portion with a thickness of Δx . U is the average flow velocity in the pipe and f is the Darcy friction factor. As can be seen, the wall shear stress and the friction factor are functions of the pressure gradient. Since the pressure drop is linear in the fully developed flow, the pressure gradient becomes constant so that the wall shear stress and the friction factor are also constant. Since the pressure drop in the developing flow region is parabolic, the shear stress and friction factor are variable here.

Figure 4 show the variation of the wall shear stress along the flow which is obtained from the numerical solution. As can be seen from the figure, wall shear stress has shown a parabolic change at the entrance of the pipe. This variation show the developing flow at pipe entrance. Wall shear stress is increasing after a minimum value. The reason why start to increase after a minimum is that the flow begins to gain turbulence. After a certain distance the shear stress will no longer change. Unchanged values sign to a fully developed flow. The

flow section where the wall shear stress no longer changes is called fully developed flow. Since many experimental studies show that the pressure drop is linear in the fully developed flow region, so that the wall shear stress is constant in this flow region. The location where the wall shear stress becomes minimum is the location where the laminar to turbulence is first begin to transit. For this reason, the transition distances are obtained from measuring the flow distances where the minimum values exists. For example in aluminum pipe, the variations of friction factors are shown in Fig.5 for different Reynolds numbers. On observing the friction factor curves in the Figure 5 it is seen that the minimum distance becomes shorter towards high Reynolds numbers. Here, the laminar flow region narrows and fully developed flow begins to occur at the short pipe distances. This shows that the transition distance is getting smaller towards high Reynolds numbers. The transition distances at each flow rate found from the numerical Darcy friction factor variations are given in Table 5.

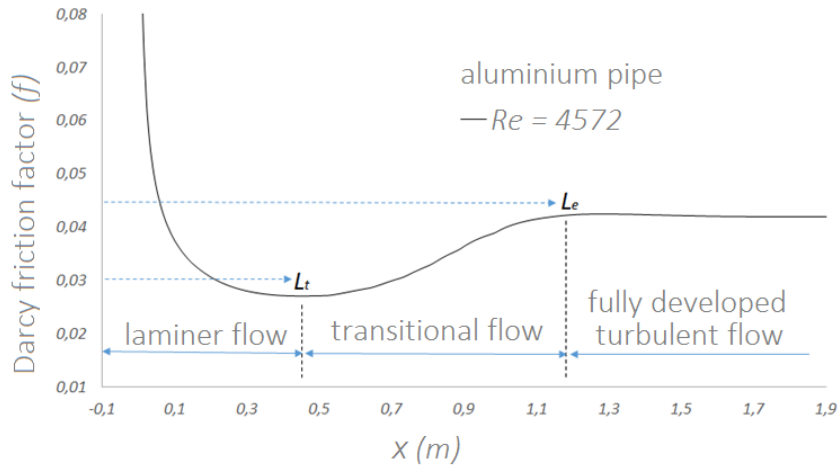


Figure 4. Variation of Darcy friction factor along the pipe flow

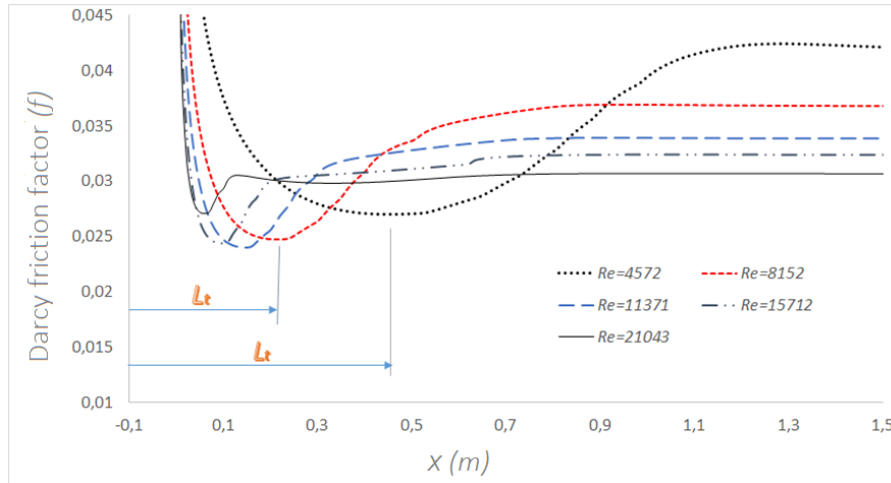


Figure 5. Variation of Darcy friction factor along the flow at different Reynolds numbers

Table 5. Numerical transition lengths obtained from the flows at different Reynolds numbers of five pipe types

Aluminium pipe										
Reynolds	4572	5539	8152	9496	11371	12172	15712	18004	21043	
$L_t(m)$	0,419	0,354	0,202	0,169	0,139	0,124	0,093	0,078	0,061	
Copper pipe										
Reynolds	3443	4326	5738	7785	9282	11079	13295	15856	18387	21077
$L_t(m)$	0,652	0,460	0,326	0,224	0,184	0,150	0,122	0,098	0,082	0,071

steel pipe											
Reynolds	3609	5422	7101	8722	10643	11906	13907	17257	19733	21688	23602
$L_t(m)$	0,611	0,356	0,252	0,192	0,156	0,132	0,110	0,084	0,071	0,060	0,050
galvanised pipe											
Reynolds	4559	7295	9553	10643	11977	14078	15582	18439	22927		
$L_t(m)$	0,449	0,234	0,180	0,150	0,130	0,109	0,094	0,072	0,051		
PPRC plastic pipe											
Reynolds	3691	4921	6890	8120	9843	12890	14458	17540	20979	24317	
$L_t(m)$	0,468	0,310	0,214	0,165	0,139	0,096	0,084	0,071	0,058	0,048	

When Table 5 is observed, it is seen that the transition values decrease with Reynolds number. The transition values of the plastic pipe flow are lower than other pipe flows. The only reason is that the flow velocity in the smaller pipe diameter is bigger than other pipes. Therefore, high flow velocity cause to laminar to turbulence transition becomes earlier. Since flow velocity is a very effective parameter on the flow stability to breakdown. The variation of the dimensionless values (L_t / D) of the numerical L_t values, obtained for each flow rate as shown in Table 5, are illustrated in Fig. 6. across Reynolds numbers. As shown in Figure 6, the variation of L_t / D values conform to an exponential function inversely proportional to the Reynolds number. When the dimensionless transition distances of five pipes are examined, it is seen that the effect of relative roughness on L_t values is seen in a level to negligible when compared to Reynolds number effect. Curve fitting operations were performed to derive a general relation to the variations of the dimensionless transition values given with Reynolds number. As a consequent, it is seen that the dimensionless L_t / D curves fit well with both relations given in Equ.2 and Equ.3.

$$\frac{L_t}{D} = 406429 \left[(\text{Re} - 2000)^{-1.215} - 2700 \text{Re}^{-2.2} \right] \quad (2)$$

$$\frac{L_t}{D} = 619062 \text{Re}^{-5/4} \quad (3)$$

As shown in Fig. 6, Equ. 2 has shown a deviation of $\pm 25\%$ in maximum and a deviation of $\pm 10\%$ in average from the non-dimensional numerical transition values. Equ. 3 has shown a deviation of $\pm 20\%$ in maximum and an deviation of $\pm 8\%$ in average from the numerical non-dimensional transition values. Both of the proposed equations also express well the dimensionless numerical transition values. In the numerical study, it is shown that the dimensionless transition values are very close to each other despite the use of pipes in different relative roughnesses. According to the experimental studies reported, the most effective parameter on the transition values is the Reynolds number, which is a representative to the flow velocity, and the free stream turbulence. In the numerical study, high turbulence level (7%) was entered at the pipe inlet. For this reason, the transition values found in this study will be shorter than for a low turbulence inlet, as long as the same pipe and Reynolds number are considered. Since the turbulence amount at the pipe inlet is being very effective on the laminar to turbulence transition. So in an inlet containing high turbulent intensity, the transition distances will be lower

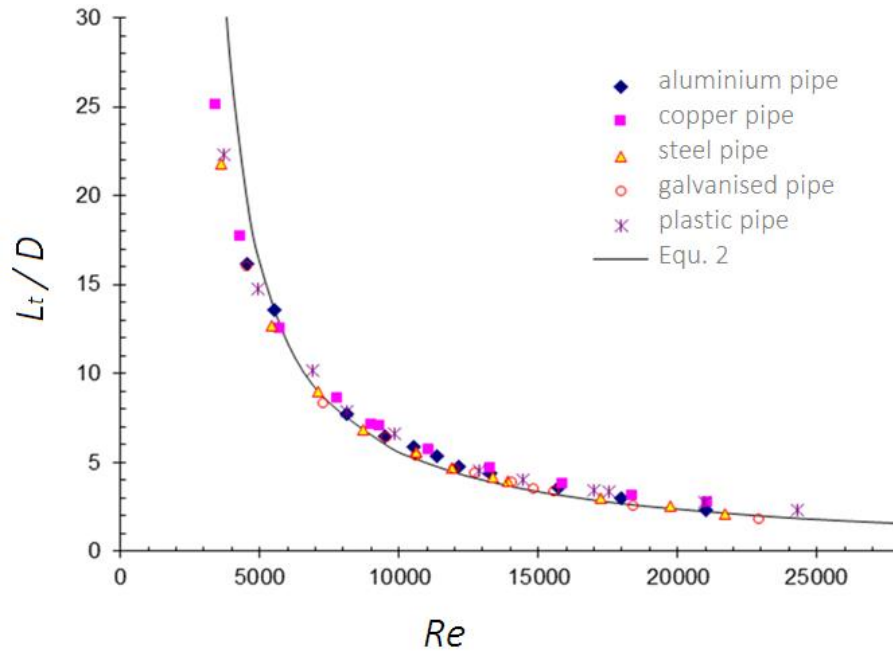


Figure 6. Variation of dimensionless transition lengths with Reynolds

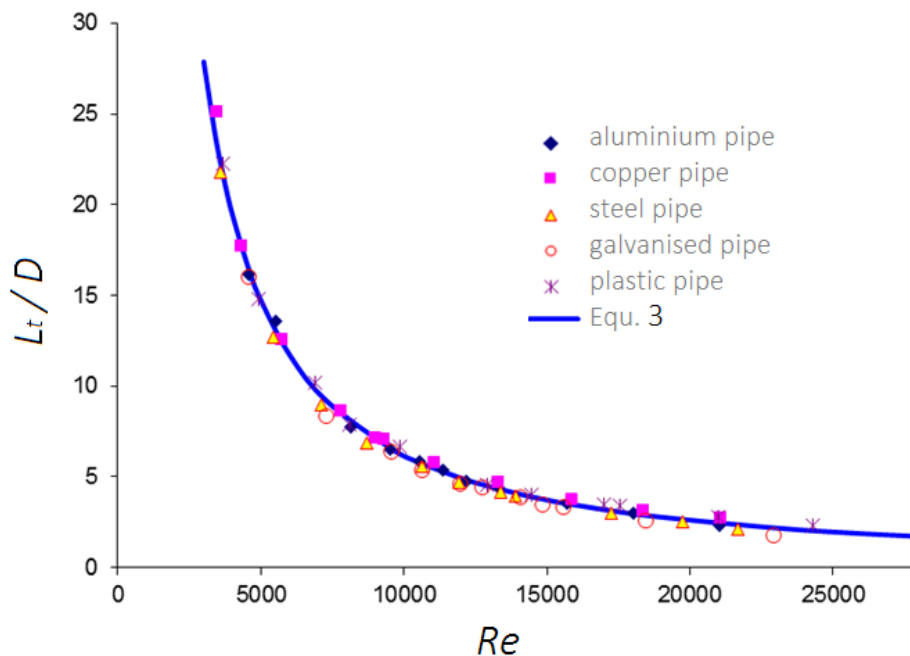


Figure 7. Numerical variation of transition lengths with Reynolds

Here, an additional numerical flow simulations were carried out to investigate the influence of relative roughness on the transition distance. Pipe diameters are changed while the relative roughness remained the same in all runs of the numerical flow simulations. Numerical flows were performed by using two different relative roughness values. The variation of the transition values, obtained from the new numerical solutions, with Reynolds numbers are shown in Fig. 8 dimensionlessly.

As shown in Fig. 8, it is seen that on observing the variation of the dimensionless transition values with Reynolds number, the values are fitted on each other for the diameters with the same relative roughness. It is seen that in Figure 8, the dimensionless transition distance in the pipes with high relative roughness is lower than in the pipes with low relative roughnesses. The difference seems slightly higher towards high Reynolds numbers. The transition values of both relative roughnesses in the same Reynolds numbers can be compared as a percentage. While it is seen that the dimensionless transition value at low relative roughness ($\epsilon / D = 0,00033$) is 6% higher than the transition value at high relative roughness ($\epsilon / D = 0,0026$) at $Re = 4000$, it is also seen

%4 at $Re = 8000$, %19 at $Re = 16000$ and %39 at $Re = 20000$. One reason for the shortened of the transition distance in the pipes where the relative roughness is high is that the roughness produce turbulence so that the laminer to turbulent transition exists earlier at short flow distances. The reason of the difference decreasing towards low Reynolds numbers is that may be the roughness not being effective on laminer flow or due to low velocity in low Reynolds numbers. So it seems that the relative roughness is being more effective at high Reynolds numbers.

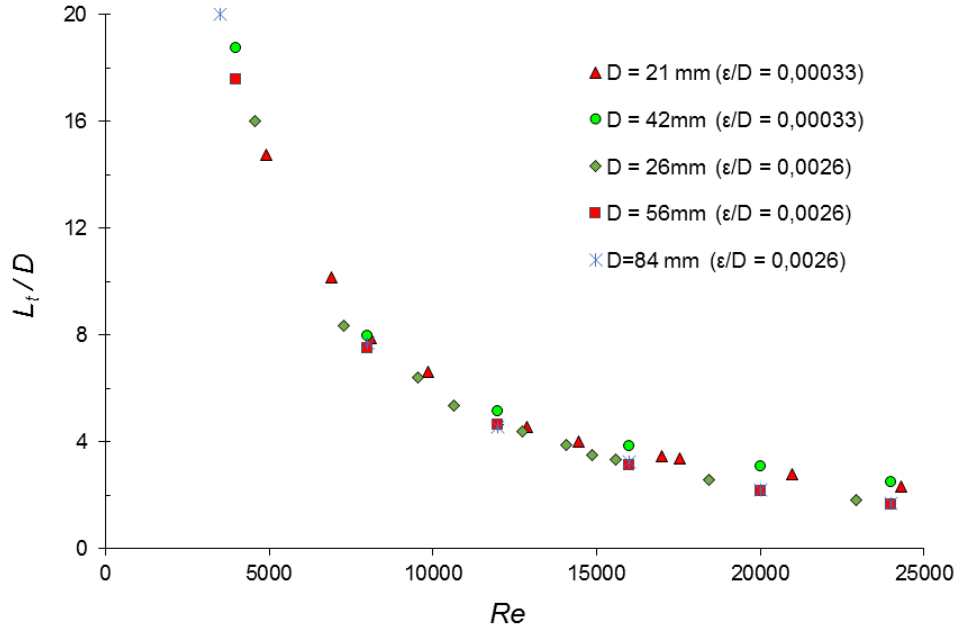


Figure 8. Variation of transition lengths across pipe diameters for the same relative roughnesses

As a result, as shown in Fig. 8, according to the numerical flow analysis made with the pipes in different relative roughnesses, the relative roughness does not seem to have much effect on the dimensionless transition lengths towards low Reynolds numbers however the effect is increased towards high Reynolds numbers. In Figure 8 according to the relative roughness change, it is seen that the difference in transition lengths increases towards high Reynolds numbers. It can be seen here that when the relative roughness increases, the transition distance is beginning to decrease. It is seen that of the pipe diameter variations in the same relative roughness are not effective on the transition values. As a result, it can be seen that in the numerical flow analyzes performed in the range of 3000 to 25000 Reynolds, the dimensionless transition values can be expressed by Equ. 2 and Equ. 3 being well agree.

Conclusion

In this study, the transition distance at which the transition from laminer to turbulence begins is analyzed in the range of $3000 < Re < 25000$ Reynolds number in the numerical flow simulations with different relative roughness pipes. Flow simulations are carried out with RANS equations. A high turbulence (7%) value was entered into the inlet flow, to resemble a sharp-edged pipe inlet.

Variation of dimensionless transition distance in flows with Reynolds number, relative roughness and pipe diameter were investigated.

- Transition distance is found as an exponential function of inverse proportion to the number of Reynolds numbers.
- The variation amount in the transition distance decreases towards high Reynolds numbers.
- The effect of roughness on the transition distance has been negligible in comparison to Reynolds effect. When the Reynolds number increases, the influence of the relative roughness variation on the transition distance is increased. The reason is that the roughness produces more turbulence when the flow velocity increases.
- The dimensionless transition distance has changed inverse proportionally with the relative roughness value and not changed when the pipe diameter is changed in the case the relative roughness value remained the

same. Due to the effect of relative roughness on the dimensionless transition distance is low the dimensionless transition distance is expressed as a function of the Reynolds numbers. As a result of curve fittings, it was seen that the variations of dimensionless transition distances with Reynolds number can be expressed in two relations, Eq. (2) and Eq. (3). Both equations estimate the numerical data with a mean error of 10%. Both of the proposed correlations here are limited to a sharp edged pipe inlet and in the Reynolds number range given in the study. In addition, the suggested correlations should be well supported by experimental data.

References

- Anselmet, F., Ternat, F., Amielh, M., Boiron, O., Boyer, P., & Pietri, L. (2009). Axial development of the mean flow in the entrance region of turbulent pipe and duct flows. *Comptes Rendus Mécanique*, 337(8), 573-584.
- Augustine, J. R. (1988). *Pressure Drop Measurements in the Transition Region for a Circular Tube with a Square-Edged Entrance* (Master's Thesis). Bachelor of Science in Mechanical Engineering. The University of Southwestern Louisiana Lafayette, Louisiana.
- Barbin, A. R., & Jones, J. B. (1963). Turbulent flow in the inlet region of a smooth pipe. *Journal of Basic Engineering*, 85(1), 29-33.
- Doherty, J., Ngan, P., Monty, J., & Chong, M. (2007, January). The development of turbulent pipe flow. In *16th Australasian Fluid Mechanics Conference (AFMC)* (pp. 266-270). School of Engineering, The University of Queensland.
- Minkowycz, W. J., Abraham, J. P., & Sparrow, E. M. (2009). Numerical simulation of laminar breakdown and subsequent intermittent and turbulent flow in parallel-plate channels: Effects of inlet velocity profile and turbulence intensity. *International Journal of Heat and Mass Transfer*, 52(17-18), 4040-4046.
- Nikuradse J (1966). Gestzmassigkeiten der turbulerten stromung in glatten rohren. Forschung auf dem Gebiet des Ingenieurwesens. Translated in NASA TT F-10, 359(3), 1932, 1-36.
- Laufer, J. (1954). The structure of turbulence in fully developed pipe flow. NACA Report, Washington, National Bureau of Standards.
- Ozisik, M. N. (1985). *Heat transfer: a basic approach*. New York: McGraw-Hill
- Patel, V. C., & Head, M. R. (1969). Some observations on skin friction and velocity profiles in fully developed pipe and channel flows. *Journal of Fluid Mechanics*, 38(1), 181-201.
- Perry, A. E., & Abell, C. J. (1975). Scaling laws for pipe-flow turbulence. *Journal of Fluid Mechanics*, 67(2), 257-271.
- Salami, L. A. (1986). An investigation of turbulent developing flow at the entrance to a smooth pipe. *International journal of heat and fluid flow*, 7(4), 247-257.
- Tam, H. K., Tam, L. M., & Ghajar, A. J. (2013). Effect of inlet geometries and heating on the entrance and fully-developed friction factors in the laminar and transition regions of a horizontal tube. *Experimental thermal and fluid science*, 44, 680-696.
- White, F. M. (2003). *Fluid Mechanics*. 5th edition, McGraw-Hill Book Co, New York.
- Zanoun, E. S., Kito, M., & Egbers, C. (2009). A study on flow transition and development in circular and rectangular ducts. *Journal of Fluids Engineering*, 131(6), 061204.
- Zimmer, F., Zanoun, E. S., & Egbers, C. (2011). A study on the influence of triggering pipe flow regarding mean and higher order statistics. In *Journal of Physics: Conference Series* (Vol. 318, No. 3, p. 032039). IOP Publishing.

Author Information

Hasan Duz

Batman University, Tecnology Faculty, Automotive Engineering
Batman Üniversitesi, Batı Raman Kampüsü, Lojmanlar, Loj 3 No:12, Batman, Turkey
E-mail: hasan.duz@batman.edu.tr

Ahmet Beyzade Demirpolat

Fırat University, Engineering Faculty, Mechanical Engineering Department
Fırat Üniversitesi, Makine Mühendisliği Bölümü, Elazığ, Turkey

The Eurasia Proceedings of Science, Technology, Engineering & Mathematics (EPSTEM), 2018

Volume 2, Pages 111-117

ICRES 2018: International Conference on Research in Education and Science

Organization of Practical-Research Works with "Black Box" Method

Nurgul SHUYUSHBAYEVA

Kokshetau State University named after Sh.Ualikhanov

Gulsinay ALTAYEVA

Kokshetau State University named after Sh.Ualikhanov

Nazgul TANASHEVA

Kokshetau State University named after Sh.Ualikhanov

Akbota MEIRMANOVA

Kokshetau State University named after Sh.Ualikhanov

Abstract: The ability to use basic formulas to improve students' knowledge of the physical Olympiad, knowledge of units of measure and their ability to influence logical and abstract thinking. Algorithms and necessary instructions are used to calculate the tasks. The period of application of knowledge in practice has a leading place in the learning process because comprehensive activities of pupils in the execution of tasks are carried out through a great mental work. The Olympiad tasks allow to use creativity and thus expand the scope of their application. It is necessary to take into account that students cannot do without realistic mental activities on the basis of the analysis of the theoretical and practical skills required for the release of the Olympiad tasks. The solution of experimental tasks selects the theoretical proof of its execution, the method of its solution, evaluates the process of measurements, estimates of errors and analysis of received results.

Keywords: Physics, Black box, Logical thinking, Experimental research work, Olympiad tasks

Introduction

Organization of experimental research in physics at school is one of the essential elements of developing student's creative abilities. Tasks require the use of physical laws in any particular situation. That's why experimental work is important in helping to clarify the students' knowledge, to see the different aspects of general laws. There is no practical value for knowledge without experiments [1-2].

The experimental-research work is based on the development of the deeper study of physical laws, intensification of motivation, persistence in achieving the goals, the desire for physics, the ability of self-education and self-comprehension.

During the physical experimental research work of students, the following features are formed:

- Searching - finding out skills, increasing enthusiasm for knowledge.
- Uses textbooks, teaching aids, various definitions, and works with many scientific books, self-study and self-improvement.
- Logical thinking skills are developed, and further identification and proof of attitudes are revealed.
- Self-study, self-education, self-evaluation, self-determination of the results of their work.
- They are convinced that success in experimental research work, success in creative activities, overcome difficulties in life, and the ability to take responsibility for their own work.

The importance of organizing experimental research work comprehends by modern physical phenomena for the formation of modern physics teachers. In turn, we have put forward a study of the technique of physical experiment using the "black box" method. This method is compact, ergonomic and environmentally friendly and easy to use. Let's talk about the black box method in organization of experimental research works:

- This is an Open Access article distributed under the terms of the Creative Commons Attribution-Noncommercial 4.0 Unported License, permitting all non-commercial use, distribution, and reproduction in any medium, provided the original work is properly cited.

- Selection and peer-review under responsibility of the Organizing Committee of the Conference

Method

1) In the circuit diagram shown in the figure 1, all voltmeters are identical and have a resistance of $R = 1.00 \text{ k}\Omega$. Find the readings of all voltmeters if an ideal source with voltage $\mathcal{E} = 9.00 \text{ V}$ is connected to them.

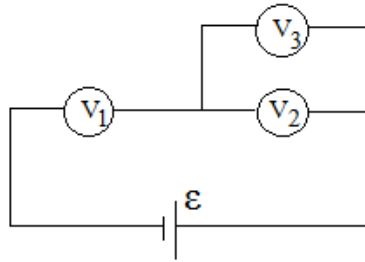


Figure 1. The circuit diagram

A black box is connected instead of one of the voltmeters (in the figure 2), the current-voltage characteristic of which have the form shown in the figure 3 below, where $U_0 = 1.00 \text{ V}$ and $I_0 = 1.00 \text{ mA}$. Further, assume that the voltage given by the source can be adjusted.

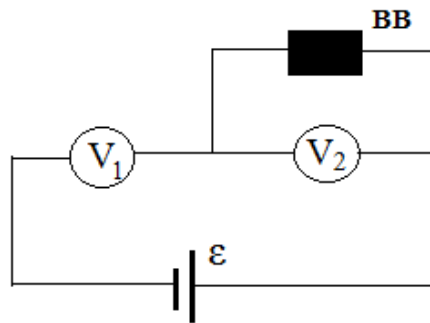


Figure 2. A black box is connected of the circuit

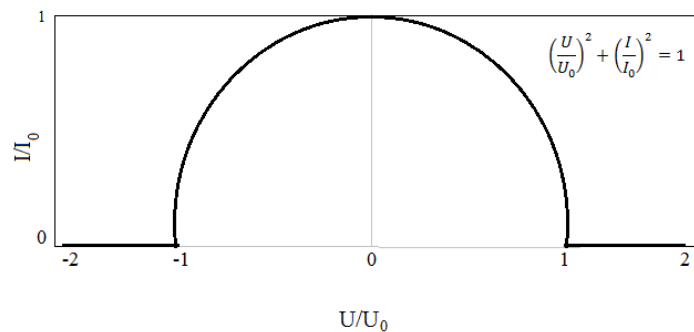


Figure 3. The current-voltage characteristic

- 2) Which element is necessary inside the black box.
- 3) Find the maximum power generated by the black box.
- 4) Find the voltage of the source \mathcal{E} , at which the black box generates maximum power. What are the voltmeter readings in this case?
- 5) Find the voltmeter readings when the source voltage is equal to zero.
- 6) Find the readings of the voltmeters when the source voltage is $\mathcal{E} = 3.00 \text{ V}$.
- 7) Find the source voltage at which the current in the black box is maximum.
- 8) Find the readings of the voltmeters at the source voltage equal to $\mathcal{E} = 2,10 \text{ V}$.
- 9) Maximum source voltage at which current is not equal to zero.

Results and Discussion

1) It is known that voltmeters show the voltage on themselves. The resistance of the voltmeters connected in parallel is

$$R_{11} = \frac{RR}{R+R} = \frac{R}{2}, \quad (1)$$

and the equivalent resistance of the circuit

$$R_{tot} = R + R_{11} = \frac{3}{2}R \quad (2)$$

The current which flows through the voltmeter V_1 is

$$I = \frac{\varepsilon}{R_{tot}}, \quad (3)$$

and hence the voltage across it is equal to

$$V_1 = I_{tot}R = \frac{2}{3}\varepsilon = 6V \quad (4)$$

Voltage across voltmeters V_2 and V_3 are equal to each other and constitute

$$V_2 = V_3 = \varepsilon - V_1 = \frac{1}{3}\varepsilon = 3V. \quad (5)$$

2) It follows from the current-voltage characteristic that at a voltage equal to zero, the current through the black box is not zero. This means that there is a power supply (battery) in the black box.

3) The power generated by the black box is equal to

$$P = IU \quad (6)$$

where

$$\left(\frac{U}{U_0}\right)^2 + \left(\frac{I}{I_0}\right)^2 = 1 \quad (7)$$

From the symmetry of expressions (5) and (6) it follows that the maximum power is reached when

$$U = \frac{U_0}{\sqrt{2}}, \quad I = \frac{I_0}{\sqrt{2}} \quad (8)$$

and is

$$P_{\max} = \frac{I_0}{2}U_0 = 0.5mW \quad (9)$$

4) Let the black box generate the maximum power, then the current in it and the voltage are given by the expression (8). The current flowing through the voltmeter V_2 is

$$I_2 = \frac{U_0}{\sqrt{2}R}, \quad (10)$$

and hence the current flowing through the voltmeter V_1 is

$$I_1 = I_2 + \frac{I_0}{\sqrt{2}} \quad (11)$$

Hence we find the voltage of the power supply

$$\varepsilon = \frac{U}{\sqrt{2}} + I_1R = U_0\sqrt{2} + \frac{I_0}{\sqrt{2}}R. \quad (12)$$

In this case, the voltmeter readings are equal

$$V_1 = I_1 R = \frac{U_0 + I_0 R}{\sqrt{2}} = 1.41V, \quad (13)$$

$$V_2 = \frac{U_0}{\sqrt{2}} = 0.71V. \quad (14)$$

5) Suppose that the voltage drop across the black box is U , and the current flowing through it is I . The current flowing through the voltmeter V_2 is

$$I_2 = \frac{U}{R} \quad (15)$$

and hence the current flowing through the voltmeter V_1 is

$$I_1 = I_2 + I \quad (16)$$

Hence the voltage of the power supply

$$\varepsilon = U + I_2 R = 2U + IR. \quad (17)$$

Thus, the current flowing through the black box depends on the voltage of the power supply according to the law

$$I = \frac{\varepsilon - 2U}{R} \quad (18)$$

For convenience, we rewrite relation (18) in dimensionless form

$$\frac{I}{I_0} = \frac{\varepsilon}{U_0} \frac{U_0}{I_0 R} - \frac{U}{U_0} \frac{2U_0}{I_0 R} \quad (19)$$

Simultaneously with the relation (19), there is a relation between U and I , expressed by the current-voltage characteristic

$$I = \begin{cases} I_0 \sqrt{1 - \left(\frac{U}{U_0}\right)^2} & \left| \frac{U}{U_0} \right| \leq 1 \\ 0 & \left| \frac{U}{U_0} \right| > 1 \end{cases} \quad (20)$$

Solving jointly (19) and (20) with $\varepsilon = 0$, we obtain

$$U = -U_0 \frac{1}{\sqrt{1 + \left(\frac{2U_0}{I_0 R}\right)^2}} \quad (21)$$

$$I = I_0 \frac{\frac{2U_0}{I_0 R}}{\sqrt{1 + \left(\frac{2U_0}{I_0 R}\right)^2}} \quad (22)$$

Thus, the voltmeter readings are equal

$$V_1 = -V_2 = U_0 \frac{1}{\sqrt{1 + \left(\frac{2U_0}{I_0 R}\right)^2}} = 0.45V \quad (23)$$

The corresponding graphical construction is shown in the figure 4 below, on which the straight line corresponds to equation (19).

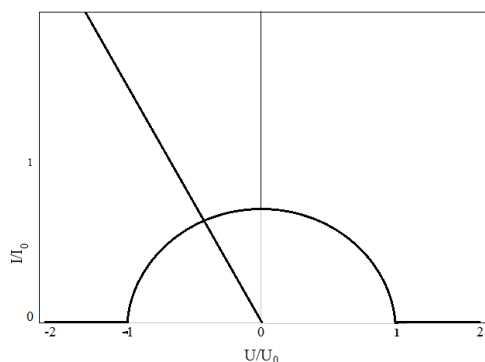


Figure 4. The current-voltage characteristic (the straight line corresponds to equation (19))

- 6) In the case of a voltage equal to $\mathcal{E} = 3 \text{ V}$, the construction yields the following figure 5

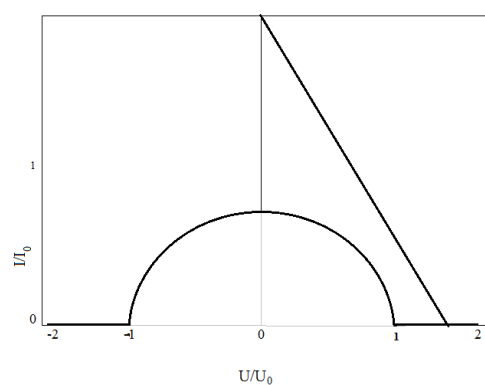


Figure 5. The current-voltage characteristic (voltage equal to $\mathcal{E} = 3 \text{ V}$)

from which it can be concluded that the current flowing through the black box is zero, and the voltage on it coincides with the voltage on the voltmeter:

$$V_2 = \frac{\mathcal{E}}{2} = 1.5V. \quad (24)$$

Hence the voltage across the voltmeter V_1 is

$$V_1 = \mathcal{E} - \frac{\mathcal{E}}{2} = \frac{\mathcal{E}}{2} = 1.5V. \quad (25)$$

- 7) The construction should give the following figure 6

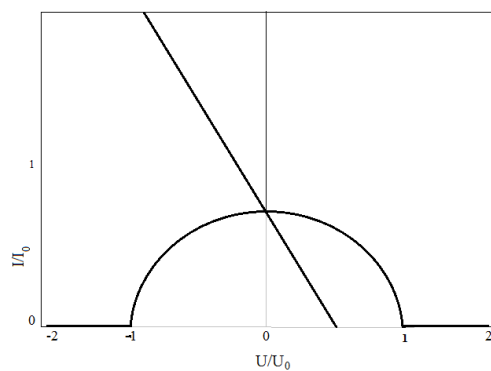


Figure 6. The current-voltage characteristic (voltage equal to $\mathcal{E} = 1 \text{ V}$)

from which we determine that the source voltage is equal to

$$\mathcal{E} = U_0 = 1V. \quad (26)$$

8) Solving jointly the system of equations (19) and (20), we obtain two roots

$$U = U_0 \frac{\frac{2\mathcal{E}U_0}{I_0^2 R^2} \pm \sqrt{1 + \frac{4U_0^2}{I_0^2 R^2} - \frac{\mathcal{E}_0^2}{I_0^2 R^2}}}{1 + \frac{4U_0^2}{I_0^2 R^2}} \quad (27)$$

This case corresponds to the construction shown in the figure7

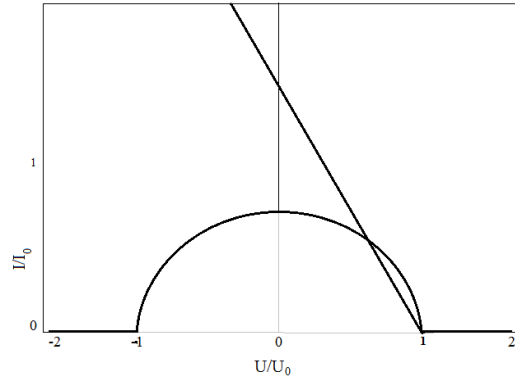


Figure 7. The current-voltage characteristic (the system of equations (19) and (20))

To a stable solution there corresponds a smaller of the roots, which is equal to

$$U = U_0 \frac{\frac{2\mathcal{E}U_0}{I_0^2 R^2} \sqrt{1 + \frac{4U_0^2}{I_0^2 R^2} - \frac{\mathcal{E}_0^2}{I_0^2 R^2}}}{1 + \frac{4U_0^2}{I_0^2 R^2}} = 0.69V \quad (28)$$

9) Not all points of intersection of line (19) and semicircle (20) correspond to stable values of current and voltage in the circuit. Let us determine which points are stable. Let the voltage on the black box increase by some small value δU , then the current through it decreases by a certain value of δI . The change in current through the voltmeter, which is connected in parallel to the black box, is equal to

$$\delta I_R = \frac{\delta U}{R}. \quad (29)$$

For the stability of the solution it is necessary to have a condition

$$-\delta I + \delta I_R > 0, \quad (30)$$

since in this case the current through the voltmeter V_1 increases, and this will cause a drop in voltage on the black box and voltmeter V_2

From (29) and (30) it follows that

$$\frac{\delta I}{\delta U} < \frac{1}{R}. \quad (31)$$

Condition (31) corresponds to line 1 in the figure 8, which is tangent to the circle and its slope to the x axis is $U_0 / I_0 R$.

Passing through the point of circle A straight line 2 from equation (19), we find the maximum voltage of the source

$$\varepsilon = \frac{U_0 + 2I_0R}{\sqrt{1 + \left(\frac{I_0R}{U_0}\right)^2}} = 2.12V. \quad (32)$$

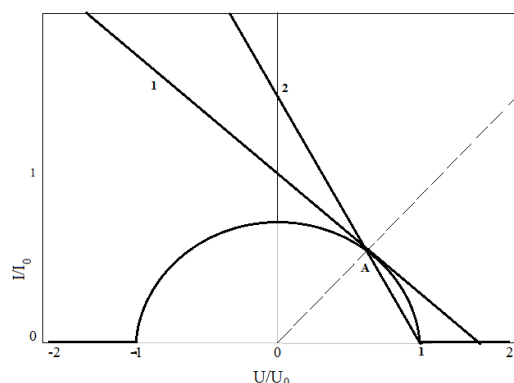


Figure 8. The current-voltage characteristic (the maximum voltage of the source)

Conclusion

Practical assignments can be used to introduce new concepts and formulas in the lesson, clarify the learning laws, and draw closer to the content of new materials. It is important to pay more attention to the ways in which it can be detected and not to pay attention to the ease or difficulty of the research. Thus, the student learns to work independently [2].

References

- Kamenetsky S.E., Puryshva N.S.. (2000). *Theory and methodology of teaching physics at school*. General issues. Ed. Moscow: "Academy".
- Shuyushbayeva N.N. (2011) *Methodical bases of solving the Olympiad tasks in physics*. Kokshetau, Keleshek Publishing House.
- Varlamov S.D., Zilberman A.R, Zinkovskii V.I. (2009) *Experimental tasks at the lessons of physics and physical olympiads*. - Moscow: MTsNMO.

Author Information

Nurgul Shuyushbayeva

Kokshetau State University named after Sh.Ualikhanov
Address: Republic of Kazakhstan, 020000, Kokshetau,
Campus №1 - 76 Abay street, the main campus
Contact e-mail: nn_shuish@mail.ru

Gulsinay Altayeva

Kokshetau State University named after Sh.Ualikhanov
Address: Republic of Kazakhstan, 020000, Kokshetau,
Campus №1 - 76 Abay street, the main campus

Nazgul Tanasheva

Kokshetau State University named after Sh.Ualikhanov
Address: Republic of Kazakhstan, 020000, Kokshetau,
Campus №1 - 76 Abay street, the main campus

Akbota Meirmanova

Kokshetau State University named after Sh.Ualikhanov
Address: Republic of Kazakhstan, 020000, Kokshetau,
Campus №1 - 76 Abay street, the main campus

Influence of Inclined Bed Channel on Characteristic of Flow for Step Broad-Crested Weirs

Saleh Jaafer SULEIMAN
Northern Technical University

Adnan ISMAEL
Northern Technical University

Abdulnaser AHMED
Northern Technical University

Sulaiman Jasim AL ZUBAIDY
Northern Technical University

Abstract: Influence of inclined bed channel on characteristic of flow for step broad-crested weirs was investigated experimentally. Discharge coefficient, water surface profile and Froude number were calculated experimentally. The results showed that water surface profiles were smooth and continues having a descending trend from the point of measurement taking the shape of the weir with a steep drop near the downstream face of the weir. Increasing effective head to crest height ratio (H_e/Y) and channel bed slope (S_o), increased the coefficient of discharge (C_D) up to 5%. Also it was found, that for small values of (Fr_2), the weir performance tends to the ideal .and with increase (Fr_2), the discharge coefficient (C_D) decrease for all weir models, because the discharge and the velocity heads increases. Empirical equation was developed on the basis of obtained results.

Keywords: Inclined bed channel, Step broad-crested weirs, Discharge coefficient

Introduction

The weir is an obstruction constructed across a river or stream in order to increase and control water head at the upstream of the weir or for water flow measurement. Weirs with different types considered as the most hydraulic structures which used in open channel flow. The authors [1] are studying the characteristics of square-edge and round-nosed, rectangular broad crested weir under free flow and submerged flow conditions and they found to be a function of the head of water at the upstream causing flow and the radius, of the upstream top corner. While others presented a method for predicting both subcritical and supercritical flow characteristics over drops and describe an empirical relation to roughly calculate the relative energy loss [2]. The Coefficients of Discharge calculated over a large broad – crested weir, two empirical equations were found depending on the geometry of the weir [3]. The single step broad crested weirs are more efficient than traditional weir and the maximum energy dissipation ratio in single step broad crested weirs was approximately (10%) higher than traditional weirs [4]. Square edge broad crested weir can be well improved and the discharge coefficient is increased by introducing an upstream face slope of 0.5H: 1V and this value of Slope are quite enough to give high values of discharge coefficient [5]. Hussein et al. [6] have been improved the coefficient of discharge in comparison with traditional weir due to adding a step to the broad crested weir. [7] and [8] giving design tables for a wide range of variables. Hussein et al. [9] studied the hydraulic efficiency of single step broad-crested weir was improved. Empirical equations for energy dissipation and discharge coefficient due to the effecting parameters were derived.

the main objective of research is to study the effect of channel slope on characteristics of flow for single step broad – crested weirs.

Experimental Setup

The experiments were achieving in channel is 12 m long, 0.5m width and 0.45 m depth as. The channel was pivoted with jacking station for normal inclination. Triangular sharp-crested weir installed in the inlet of the channel for measuring discharge as illustrated in figure 1. The flume was provided with point gauge installed on the rails to measure water surface.



Figure 1. Channel setup

Weir Models

Five weir models were manufactured and tested in which the downstream crest height and angle channel slope were varied . These models can be classified in to four groups based on the variation of channel slope (S_0) [group (1,2,3 and 4) ($S_0 = 0, 0.001, 0.002$ and 0.004)] . Each group included the testing of five models based on the variation of D/S weir height (Y_1) [model No.(1,2,3,4 and 5)($Y_1=(12,10,8,6$ and 4 cm)]. Details of the testing are shown in table (1) and Fig. (1) . All models were manufactured from thermos stone and well varnished to represent smooth surfaces . To ensure stability of water surface levels and uniform flow with very low turbulence, every model was placed on the bed of the laboratory flume at distance 3.5 m downstream from the flume inlet . Then the model was glued to the flume bed using an adhesive material applied to the boundary of the weir model to resist the overflowing water pressure and to prevent any possible leakage through the sides and bottom of the weir . After construction the testing program started by flowing different discharges to overtop the weir model. for each discharge , upstream water surface profile measurement were recorded by measuring the heads overall the grid points upstream the weir model . All measurements were conducted at the center line of the channel width. In each test, The measurements along the weir models were conducted under the free flow conditions. In all tests free-falling nappe at D/S step of models were fully aerated to prevent ventilation holes.

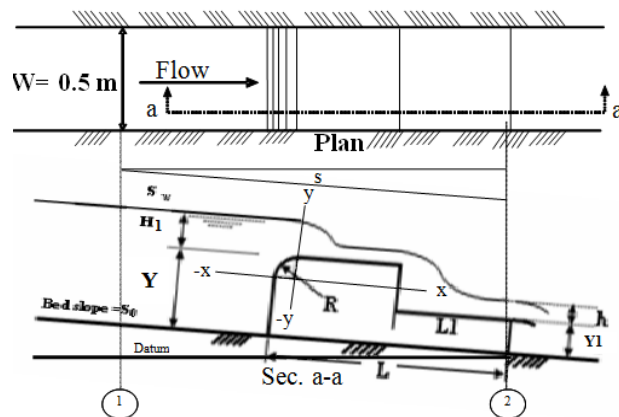


Figure 2. Locations of grid points for the water head measurements

Table 1. Details of the tested weir models

Model No.	Y/Y ₁	Slope	Run No.	He(cm)	Discharge Range (Q L/sec)	Range of C _D	Fr ₂
1	1	0	1 - 6	- 6.81 11.34	5.43 – 11.9	0.896 - 0.914	1.05-1.32
		0.001	7-12	5.67-10.81	4.17– 11.174	0.906- 0.921	1.08-2.04
		0.002	13-18	5.26-11.36	3.78 – 12.25	0.919 - 0.938	1.06 – 2.13
		0.004	19-24	5.37-11.61	3.97 – 12.88	0.936 - 0.955	1.08- 2.18
		0	25 - 30	4.34 -11.57	2.77 – 12.47	0.90 -0.929	1.07-1.56
2	1.2	0.001	31 - 36	5.57-11.04	4.11 -11.69	0.915 - 0.935	1.21-2.31
		0.002	37 - 42	5.47 - 11.27	4.06 -12.32	0.932 - 0.955	1.06-2.13
		0.004	43 - 48	5.58 - 11.52	4.27 -12.95	0.949 - 0.972	1.08-2.17
		0	49 - 54	4.95 - 10.5	3.41 -10.82	0.908 - 0.932	1.3-1.79
3	1.5	0.001	55 - 60	5.57 -11.47	4.14 -12.47	0.923 - 0.941	1.35 -2.33
		0.002	61 - 66	5.47 - 11.17	4.08 -12.25	0.935 - 0.963	1.18-2.3
		0.004	67 - 72	4.75 -11.61	3.35 -13.20	0.948 - 0.978	1.43-2.91
		0	73 - 78	4.24 - 11.59	2.72 -12.76	0.916 - 0.949	1.15-1.8
4	2	0.001	79 - 84	4.32 – 11.83	2.86 -13.24	0.934 - 0.954	1.31 – 2.76
		0.002	85 - 90	5.78 – 11.17	4.50 -12.35	0.948 -0.97	1.45-2.64
		0.004	91 - 96	5.89 – 11.63	4.75 -13.50	0.974 -0.998	1.3 – 2.49
		0	97 - 102	4.85 – 11.37	3.32 -12.32	0.91 -0.943	1.02-1.52
5	3	0.001	103 - 108	5.57 – 10.83	4.17 -11.51	0.93 -0.947	1.32-2.36
		0.002	109 - 114	6.51 – 10.85	5.37 -11.73	0.948 - 0.963	1.38- 2.17
		0.004	115 - 120	5.06 – 10.86	3.73 -11.99	0.961 - 0.983	1.41- 3.24

Water Surface Profiles

The experimental results of measurements of water surface profiles along the center line of the channel show a descending trend from the point of measurement taking the shape of the weir with a steep drop near the downstream face of the weir . Fig. (2,3&4) shows the dimensionless center line water surface profiles of Y/H_e versus X/H_e for all test runs of weir model No.(3)[$Y/Y_1=1.5$, $S_o =0.001$, 0.002 & 0.004] , where , H_e is the effective upstream head above crest and X is the horizontal distance measured from the upstream of the crest.

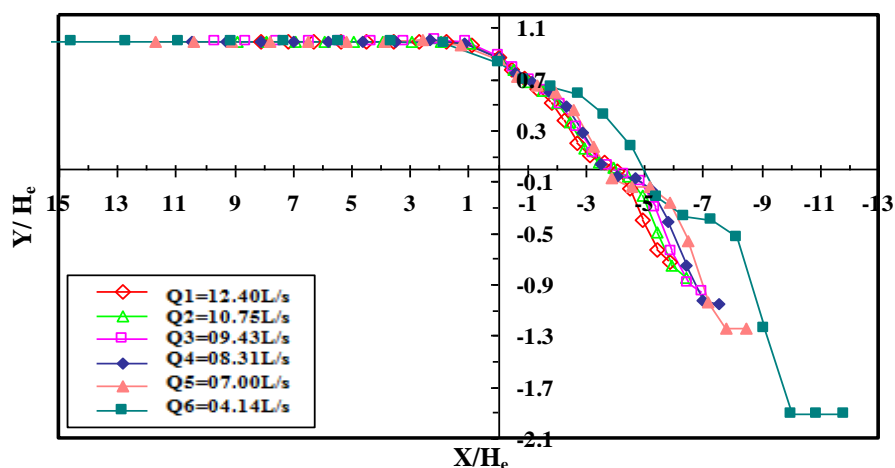


Figure 3. Relation between Y/H_e versus X/H_e for all runs of weir ($Y/Y_1=1.5$ and $S_0=0.001$)

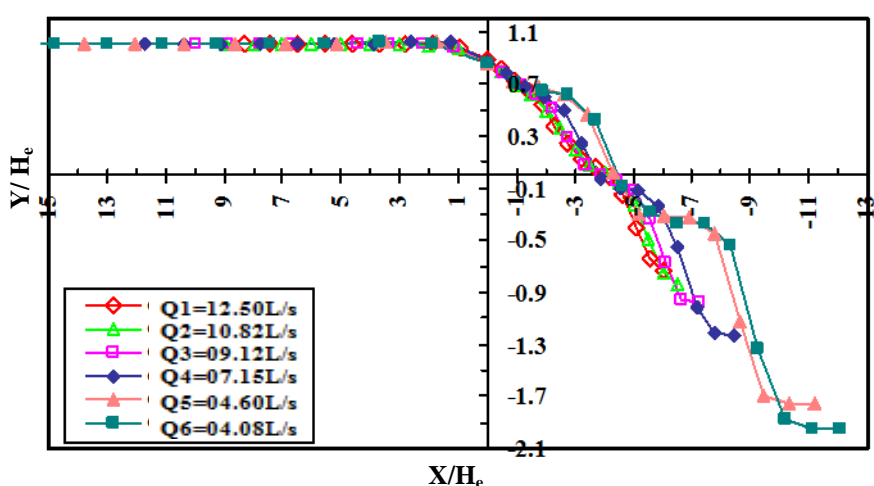


Figure 4. Relation between Y/H_e versus X/H_e for all runs of weir ($Y/Y_1=1.5$ and $S_0=0.002$)

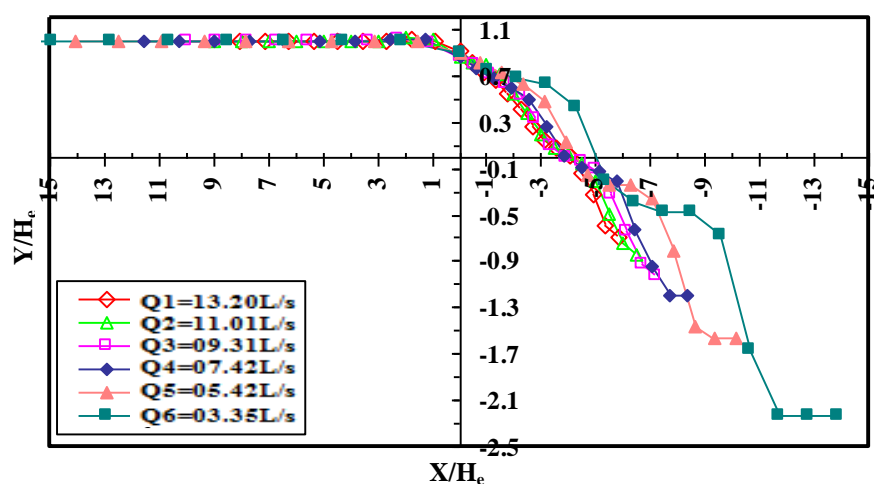


Figure 5. Relation between Y/H_e versus X/H_e for all runs of weir ($Y/Y_1=1.5$ and $S_0=0.004$)

The distance upstream crest at which the water surface profile became stable and parallel to the bed of channel for all weir models are shown in table (2) . These are the nearest locations where a point gauge should be located to measure upstream heads accurately.

Table 2. Distance upstream crest at which the water surface profile become stable and parallel to the bed of channel for all weir models

Weir height ratio (Y/Y ₁)	Bed slope of channel S _o =0.001	Bed slope of channel S _o =0.002	Bed slope of channel S _o =0.004
	Distance range	Distance range	Distance range
1	(1.9 - 8.19)H	(2.73 - 8.2)H	(3.8 - 8.56)H
1.2	(1.37 - 8.23)H	(1.83 - 8.3)H	(1.4 - 8.5)H
1.5	(1.8 - 7.9)H	(2.7 - 8.0)H	(2.7 - 8.0)H
2	(1.81 - 7.84)H	(1.85 - 8.0)H	(2.7 - 8.0)H
3	(1.9- 8.57)H	(2.86 - 8.57)H	(3.81 - 8.57)H

Theoretical Consideration

Dimensional Analysis

The broad crested models are based on the following assumptions: flow upstream of weir is steady, sub-critical and two dimensional; the effect of flow surface tension is eliminated. For rectangular broad crested weir assuming the critical flow on the weir crest [9]:

The relevant parameters in the study of single step broad-crested weirs come from the following groups:

- (A)- Fluid properties and physical constants : kinematics viscosity of water ν (m²/s) and the acceleration of gravity g (m/s²),
- (B)- Channel geometry : the bed slope of channel S_o (dimensionless),
- (C)- Weir geometry : radius of the upstream corner of the weir R (cm), upstream weir height Y (cm), downstream weir height Y_1 (cm), length of weir L (cm), length of d/s stepped weir L_1 (cm) and width of weir W (cm),
- (D)- Upstream flow properties : effective upstream head above crest including approach velocity head H_e (cm) , flow rate over the weir per unit width q_w (m²/s).

For a free flow over a single step broad-crested weir with rounded upstream corner, a functional relationship can be taking all the above parameters and written as follows.(see Fig(1)) :

$$f_1(q_w, H_e, Y, Y_1, L, L_1, W, R, \nu, g, S_o) = 0 \dots \dots \dots (1)$$

Since, L, L_1, W , and R . are fixed in this study then equation (1) can be rewritten as :-

$$f_2(q_w, H_e, Y, Y_1, \nu, g, S_o) = 0 \dots \dots \dots (2)$$

Using Buckingham Pi-theorem and after certain permissible manipulations, Eq.(2) becomes:

$$C_D = \frac{q_w}{\left(\frac{2}{3}\right)^{3/2} * (g)^{1/2} * (H_e)^{3/2}} = f_3\left(\frac{H_e}{Y}, \frac{Y}{Y_1}, R_e, Fr_2, S_o\right) \dots \dots \dots (3)$$

R_e = Reynolds number, and
 Fr_2 = Froude number.

Reynolds number will have very large values and hence its effect on C_D will be very little, therefore, R_e can be dropped and Eq.(3) can be rewritten as:

$$C_D = f_4 \left(\frac{H_e}{Y}, \frac{Y}{Y_1}, F_{r2}, S_o \right) \dots \dots \dots (4)$$

Factors Affecting on the Coefficient of Discharge

Effective Head to Crest Height of weir Ratio (H_e/Y)

a) When (Y/Y_1) constant:

The experimental results for all weirs showed that a relation between C_D , and (H_e/Y), for different angles of channel bed slope [$S_o = 0 , 0.001, 0.002 \& 0.004$] were shown in Figs.(5,6,7,8 & 9) , respectively. From these figures one may observe that for the same ratio (Y/Y_1) an increase in H_e/Y causes an increase in C_D , this could be made the over flowing process becomes easier , smooth and no nappe was visible.and also Fig.(8) show that weirs of upstream to downstream height ratio ($Y/Y_1=2$ give higher value of $C_D =0.985$ at $H_e/Y=0.7$ & $S_o = 0.004$) than those of [$(Y/Y_1=1,1.2,1.5 \& 3)$], ($C_D =0.949 ,0.962,0.968 \& 0.974$)] at the same value of (H_e/Y & S_o) above.

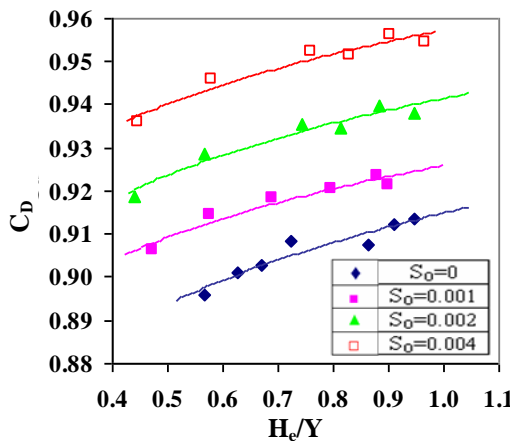


Figure 6. Relation between C_D versus H_e/Y for weirs of ($Y/Y_1=1$).

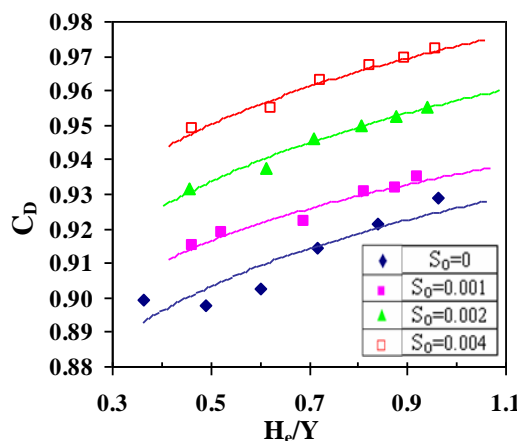


Figure 7. Relation between C_D versus H_e/Y for weirs of ($Y/Y_1=3$).

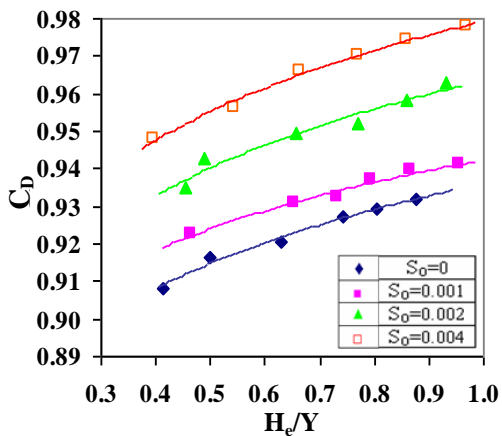


Figure 8. Relation between C_D versus H_e/Y for weirs of ($Y/Y_1=1.5$).

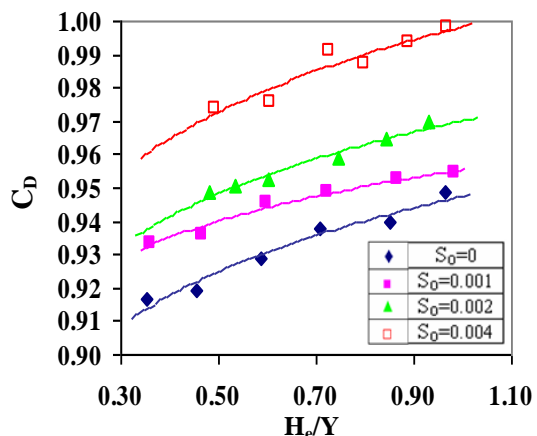


Figure 9. Relation between C_D versus H_e/Y for weirs of ($Y/Y_1=2$).

b) Bed slope of channel (S_o) constant

The experimental results for all weirs showed that there is a relation between the discharge coefficient (C_D), and upstream head to crest height of weir ratio (H_e/Y). At different upstream height to downstream height of weir ratio [$(Y/Y_1=1, 1.2, 1.5, 2 \text{ \& } 3)$] are shown in figs. (10, 11, 12 & 13), respectively. These figures showed that, an increase in H_e/Y value causes an increase in C_D value at the same bed slope of channel (S_o). This also could be attributed to the reason that as the head above crest increases the overflowing process becomes easier and continues.

From fig. (13) it is interesting to realize that weirs on the channel with angle of bed slope [$S_o = 0.004$] give higher values of $C_D = 0.99$ at $H_e/Y = 0.8$ & $(Y/Y_1 = 2)$ than those of weirs ($S_o = 0, 0.001 \text{ \& } 0.002$), ($C_D = 0.94, 0.955 \text{ \& } 0.962$) at the same value of $(H_e/Y \text{ \& } Y/Y_1)$ above.

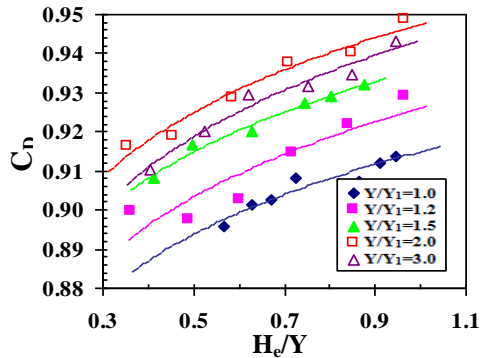


Figure 10. Relation between C_D versus H_e/Y for weirs of ($S_o=0$).

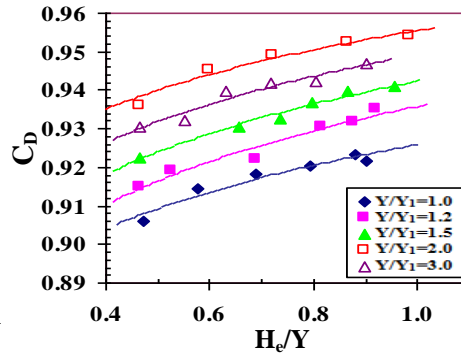


Figure 11. Relation between C_D versus H_e/Y for weirs of ($S_o=0.001$).

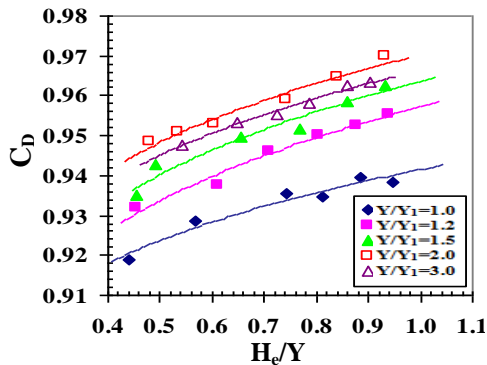


Figure 12. Relation between C_D versus H_e/Y for weirs of ($S_o=0.002$).

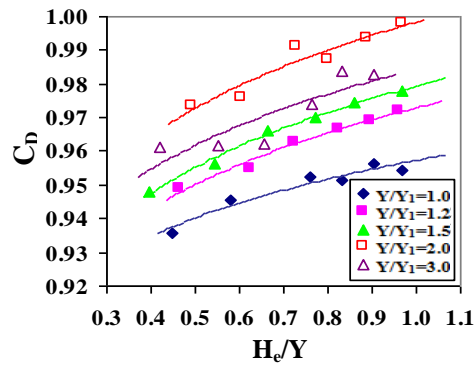


Figure 13. Relation between C_D versus H_e/Y for weirs of ($S_o=0.004$).

Froude Number (Fr_2)

The relation between discharge coefficient (C_D) and Froude number (Fr_2) at downstream for all weir models ($Y/Y_1=1, 1.2, 1.5, 2 \text{ \& } 3$), is shown in figs (15, 16, 17 & 18), respectively. It is clearly seen that for all small values of (Fr_2), the weir behaves almost ideally giving high values of (C_D) this behavior is explained that for small values of (Fr_2) the weir discharge is small and velocity head of the flow is very small, and the operating head is the same at every point along the crest being sensibly equal to the head in the approach channel. therefore, for small (Fr_2) values, the weir performance tends to the ideal. and as (Fr_2) increases, the discharge coefficient (C_D) decrease, because the discharge and the velocity heads increases; consequently, a large proportion of the crest operates under a head less than that in the approach channel with corresponding fall in performance.

From fig. (18) it is seen that weirs of ($Y/Y_1=2$ and $S_o = 0.004$) give higher values of C_D than weirs of [$(Y/Y_1=1, 1.2, 1.5 \text{ \& } 3)$, ($S_o = 0, 0.001 \text{ \& } 0.002$)] due to the effect of step.

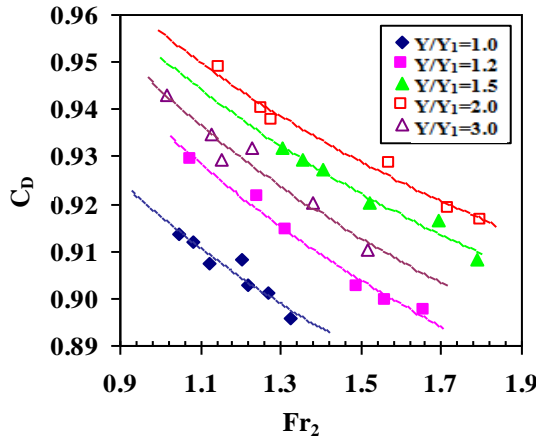


Figure 15. Relation between C_D versus Fr_2 for weirs of ($S_0=0$).

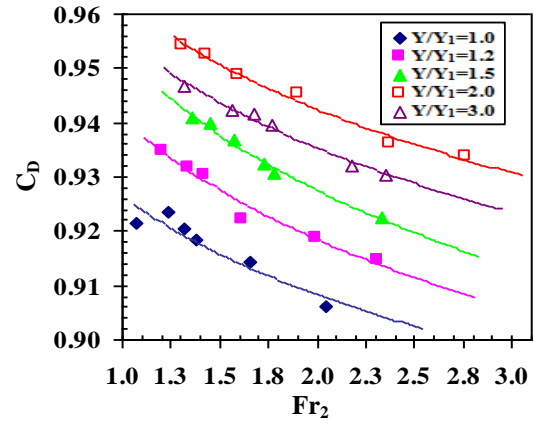


Figure 16. Relation between C_D versus Fr_2 for weirs of ($S_0=0.001$).

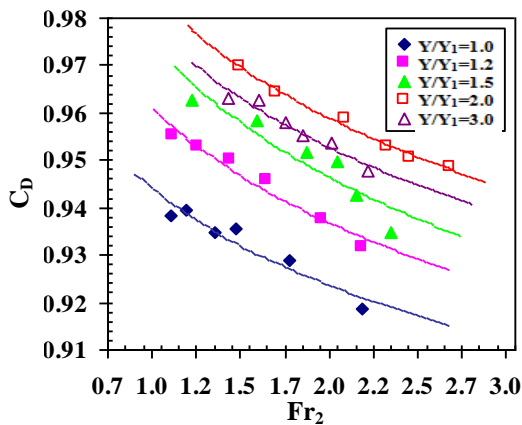


Figure 17. Relation between C_D versus Fr_2 for weirs of ($S_0=0.002$).

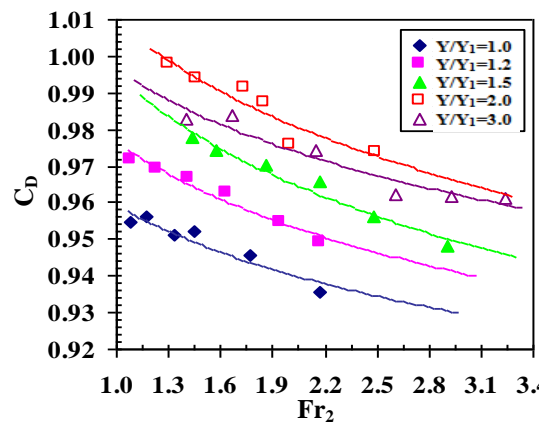


Figure 18. Relation between C_D versus Fr_2 for weirs of ($S_0=0.004$).

Angle Bed Slope of Channel (S_0)

One of the main objectives of this study is to determine the effect of bed slope of channel S_0 on discharge coefficient C_D . Therefore Fig.(14) shows the effects of S_0 on C_D for the weir models ratio $Y/Y_1=2$. and also may observe that C_D increases significantly with the increase of S_0 . The variation of average values of C_D with S_0 is shown in Fig.(14) indicating that the average value of C_D reaches the highest value when S_0 is equal to 0.004, this means that well the relation between discharge coefficient C_D and angle bed slope of channel S_0 is increases linearly.

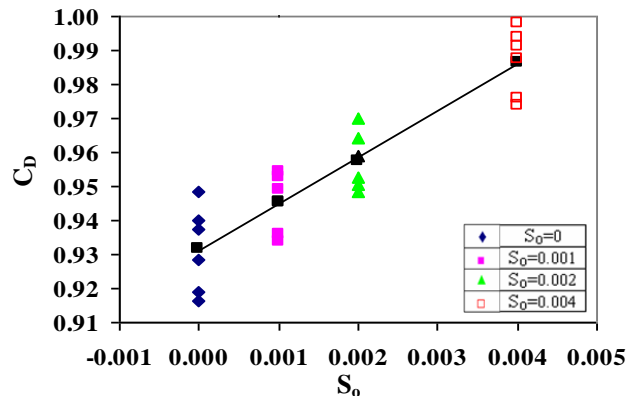


Figure 14. Relation between C_D versus S_0 for weirs of ($Y/Y_1=2$).

Empirical Expressions of Discharge Coefficient

Using (SPSS-20.0) was developed to correlate the coefficient of discharge C_D with a correlation coefficient =0.93. Empirical equation was developed on the basis of obtained results. equ (4)

$$C_D = 0.85 + \left[0.06 * \frac{H_e}{Y}\right] + \left[0.01 * \frac{Y}{Y_1}\right] + [0.008 * Fr_2] + [10.45 * S_o] \dots \dots \dots (5)$$

Figure 19 shows the relation between predicted versus observed values of C_D .

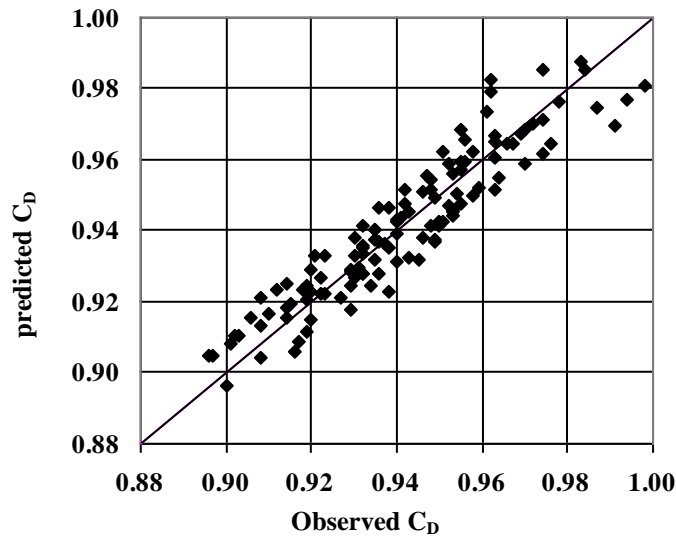


Figure 19. Relation between Predicted C_D versus observed C_D for all weir models.

Conclusions

With in the limits of the experimental data of the present investigation, the following main conclusions can be summarized as:

- 1-Traditional broad - crested weirs can be well improved when making it as an single step Broad– Crested Weirs. Also The value of (C_D) increases with the increase angle bed slope of channel(S_o) and increase of (Y/Y_1) values reaching its highest value when Y/Y_1 values reach 2.
- 2-For all weirs model one may observe that at the same ratio of (Y/Y_1)and at the same bed slope of channel(S_o) an increase in H_e/Y causes an increase in C_D .
- 3- Weir of ratio($Y/Y_1=2$ give higher value of $C_D =0.985$ at $H_e/Y=0.7$ & $S_o = 0.4$) than other weirs, Fig.(8). Also weir with bed slope ($S_o = 0.004$ give higher value of $C_D =0.99$ at $H_e/Y=0.8$ & $Y/Y_1=2$) than other weirs Fig.(13).
- 4-For weir model indicated that the average value of C_D reaches the highest value when S_o is equal to 0.004,and also the relation between C_D and S_o is increases linearly. Fig.(14)
- 5- For all weir models one may observe that when (Fr_2) increases , the discharge coefficient (C_D) decrease.
- 6- Empirical power expressions were obtained for single step broad–crested weirs to estimate discharge coefficient (C_D) in terms of effective head to crest height ratio (H_e/Y), upstream crest to downstream height ratio(Y/Y_1), Froude number (Fr_2) at downstream of the weir and bed slope of channel (S_o) with high correlation coefficients=0.933.

Acknowledgements or Notes

The Following Symbols are used in this Paper

C_D =dimensionless weir discharge coefficient ,

f1 to f4 =signify function of ,
g = acceleration due to gravity (m/s^2),
H1 = upstream head above crest(cm),
He = effective upstream head above crest(cm) ,
h = downstream head (cm),
L = weir length (cm),
L1 = length of d/s step weir (cm),
W = width of weir (cm),
Y = upstream weir height (cm),
Y1 = downstream weir height (cm),
q_w = flow rate over the weir per unit width (m^2/s) ,
R = radius of the upstream corner of the weir (cm),
R_e = Reynolds number (dimensionless),
Fr₂ = Froude number (dimensionless) at d/s,
S_o =Bed slope of channel (dimensionless),
ν = kinematics viscosity (m^2/s).

References

- Gogus , M. , Defne , Z. and Ozkandemir,V.,(2006). Broad-Crested Weirs with Rectangular Compound Cross Sections. *Journal of Irrigation and Drainage Engineering*, Vol.132, No.3, June, PP.272-280.
- Sarker, M .A. and Rhodes, D. G.,(2004). Calculation of Free-Surface Profile over a Rectangular Broad-Crested Weir. *Flow Measurement and Instrumentation*,Vol.15, Issue 4, August, PP.215-219.
- Gonzalez, C.A. and Chanson, H.,(2007). Experimental Measurement of Velocity and Pressure Distribution on a Large Broad-Crested Weir. *Flow Measurement and Instrumentation*,Vol.18,Issue 3-4,June-August,PP.107-113.
- Noori, B. M. and Juma ,I .A.,(2009). Performance Improvement of Broad Crested Weirs. *Journal of Al-Rafidain Eng. / Mosul University*, vol.17,no.2,pp.95-107.
- Al-Talib, A. N. J. (2007). *Laboratory Study of Flow Energy Dissipation Using Stepped Weirs* M. Sc . Thesis. Engineering College, University of Mosul. Iraq.
- Hussein H. , Juma I. and Shareef S. (2009). Flow Characteristics and Energy Dissipation Over Single Stepped Broad – Crested Weirs . *Journal Al- Rafidain Engineering*, College of Engineering University of Mosul. Iraq.
- Bos, M. G.; Replogle, J. A. and Clemmens , A. J. (1984). *Flow Measuring Flumes for Open Channel Systems*. John Wiley and Sons, Inc., New York, N.Y. .
- Boiten , W.,(2002). Flow Measurement Structures. *Flow Measurement and Instrumentation*, Vol.13, Issues 5-6, December, PP. 203-207 .
- Hussein, H.H., Juma, I.A.K., Shareef, S.J.S. (2011). Improving the hydraulic performance of single step broad-crested weirs, *Journal of Al-Rafidain Engineering, Mosul University*, 7 (1), 1-12.

Author Information

Saleh Suleiman

Engineering Technical College /Northern
Technical University
Mosul/Iraq
salehjafer@ntu.edu.iq

Adnan Ismael

Technical Institute /Northern
Technical University
Mosul/Iraq

Abdulnaser Ahmed

Technical Institute /Northern
Technical University
Mosul/Iraq

Suleiman AL Zubaidy

Technical Institute /Northern
Technical University
Mosul/Iraq

Investigation of Biological Properties of New 1-(2,6-Dimethylmorpholin-4-yl-metil)-3-alkyl(aryl)-4-[3-ethoxy-(4-benzenesulfonyloxy)-benzylidenamino]-4,5-dihydro-1*H*-1,2,4-triazol-5-ones

Gul OZDEMIR
Kafkas University

Muzaffer ALKAN
Kafkas University

Haydar YUKSEK
Kafkas University

Abstract: In this study, six new 1-(2,6-dimethylmorpholin-4-yl-methyl)-3-alkyl(aryl)-4-[3-ethoxy-(4-benzenesulfonyloxy)-benzylideneamino]-4,5-dihydro-1*H*-1,2,4-triazol-5-ones were obtained from the reactions of 3-alkyl(aryl)-4-[3-ethoxy-(4-benzenesulfonyloxy)-benzylideneamino]-4,5-dihydro-1*H*-1,2,4-triazol-5-ones with 2,6-dimethylmorpholine and formaldehyde. Characterization of new compounds obtained was carried out by IR, ¹H-NMR, ¹³C-NMR spectral data. Antibacterial properties of the synthesized novel compounds were evaluated by agar well method against *Escherichia coli*, *Pseudomonas aeruginosa*, *Staphylococcus aureus*, *Bacillus subtilis*, *Bacillus cereus* and *Klebsiella pneumoniae* strains.

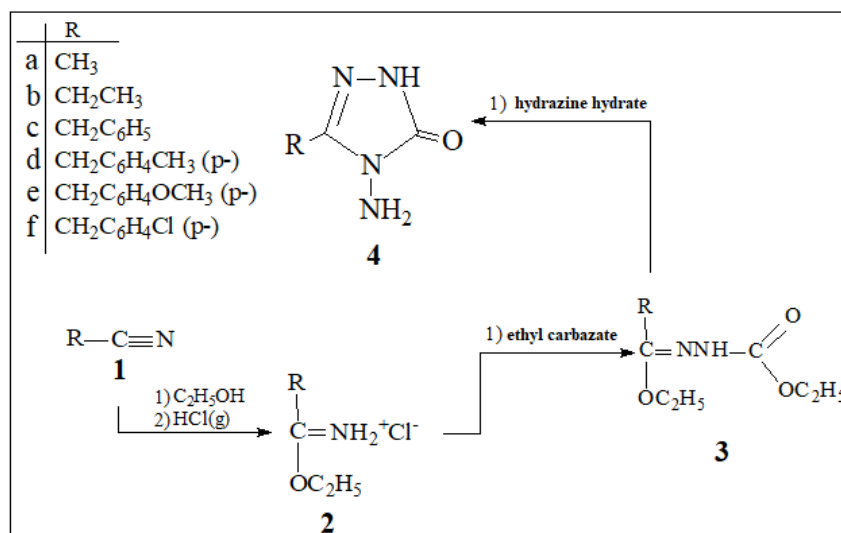
Keywords: 1,2,4-triazol-5-one, Schiff base, Mannich base, Synthesis, Antimicrobial activity

Introduction

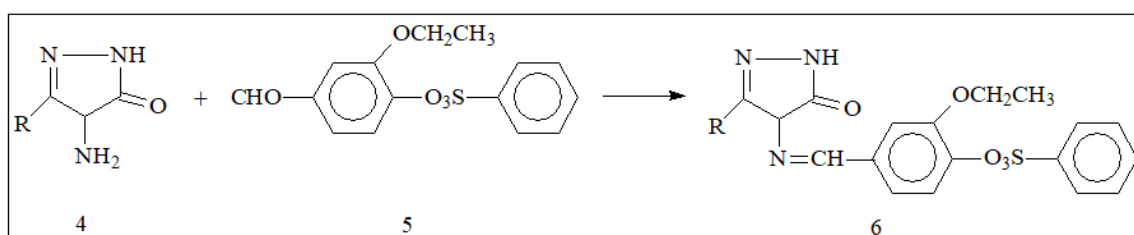
Biochemical properties of rings containing triazole ring or triazole derivative ring, which are important members of heterocyclic compounds, have a wide range of academic work (Ure, 2010; Manap, 2009; Kardaş, 2006). Recently, antitumor (Ikizler et al., 1998), anti-HIV, antihypertensive, diuretic properties (Gursoy et al., 2013; Yuksek et al., 2004; Yuksek et al., 2008), antimicrobial, antioxidant, antiinflammatory and pharmacological properties of the triazole ring, (Ikizler et al., 1997), antioxidants, antiinflammatory, anticonvulsant, antiparasitic, analgesic, antiviral and antibiotic effects of the triazole rings to have a broad spectrum of biological activities (Yukse, 2001; Ocak, 2004; GURSOY KOL et al., 2012) have been reported. In addition, several articles have been published concerning the synthesis of some N-arylideneamino-4,5-dihydro-1*H*-1,2,4-triazol-5-one derivatives.

Synthesis

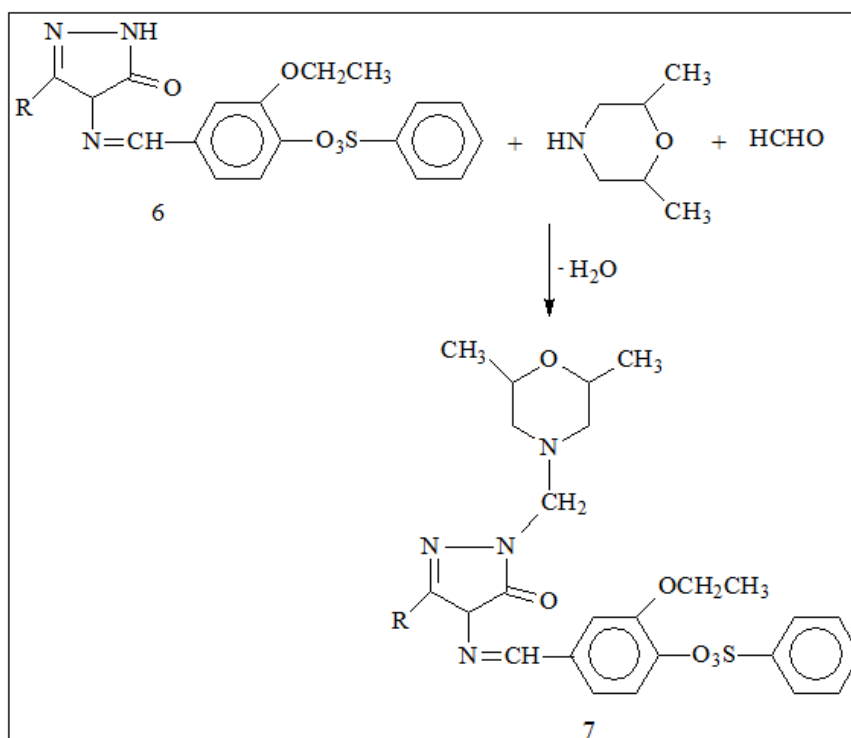
The Pinner method was used as an appropriate method for synthesizing the starting compounds used in the work (Pinner, 1892) (Equation 1). The compounds 4 obtained according to this method were reacted with 3-ethoxy-4-benzenesulfonyloxybenzaldehyde to provide synthesis of 6 type Schiff bases (Equation 2). Subsequently, six Mannich bases were synthesized (Equation 3) from the reactions of compounds 6 with 2,6-dimethylmorpholine and formaldehyde.



Equation-1



Equation-2



Equation-3

Method

Chemicals and Apparatus

Chemical reagents and all solvents used in this study were purchased from Merck AG, Aldrich and Fluka. Melting point was determined in open glass capillary using a Stuart melting point SMP30 apparatus and is uncorrected. The IR spectra were obtained on an ALPHA-P BRUKER FT-IR spectrometer. ^1H and ^{13}C NMR spectra were recorded in deuterated dimethyl sulfoxide with TMS as internal standard using a Bruker Ultrashield Plus Biospin spectrometer at 400 MHz and 100 MHz, respectively.

Synthesis of Compounds 7: The General Procedure

3-Ethoxy-4-hydroksibenzaldehyde (0,01 mol) dissolved in ethylacetate (20 mL) was treated with benzenesulphonyl chloride (0,01 mol) and to this solution was slowly added triethylamine (0.01 mol) with stirring at 0-5 °C. The process of stirring continued for 2 h, and then the mixture was refluxed for 3 h and filtered. The filtrate evaporated *in vacuo*, and the crude product was washed with water and recrystallized from ethanol to afford compound **5**. The corresponding compound **4** (0.01 mol) was dissolved in acetic acid (20 mL) and treated with 3-ethoxy-4-benzenesulphonyloksibenzaldehyde (0.01 mol). The mixture was refluxed for 2 h and then evaporated at 50-55 °C *in vacuo*. Several recrystallizations of the residue from ethanol gave pure compounds 3-alkyl(aryl)-4-[3-ethoxy-(4-benzenesulfonyloxy)-benzylidenamino]-4,5-dihydro-1*H*-1,2,4-triazol-5-ones **6** as crystals (Özdemir, 2016).

In the final step, the corresponding **6** type Schiff Base (5 mmol), 2,6-dimethylmorpholine (6 mmol) and formaldehyde (10 mmol) was refluxed 6 hours. Obtained mixture was filtered and crystallized from appropriate solvents and pure 7 type compounds were synthesized.

Spektral Data

Table 1. Spectral data of compound 7a

IR (KBr) cm^{-1}	$^1\text{H-NMR}$	$^{13}\text{C-NMR}$
1705 (C=O)	δ 1.03 (d, 6H, 2CH ₃ ; J:6.40 Hz)	10.94 (CH ₃)
1603, 1577 (C=N)	δ 1.10 (T, 3H, OCH ₂ CH ₃ ; J:6.40 Hz)	14.04 (OCH ₂ CH ₃)
1375 ve 1171 (SO ₂)	δ 2.01 (T, 2H, CH ₂ ; J:11.20 Hz)	18.92 (2CH ₃)
754 ve 695 (monosubstitue ring)	δ 2.31 (S, 3H, CH ₃)	55.57 (2CH ₂)
	δ 2.75 (d, 2H, CH ₂ ; J:10.40 Hz)	64.05 (OCH ₂ CH ₃)
	δ 3.50-3.55 (m, 2H, 2CH)	71.02 (2CH ₂)
	δ 3.83 (q, 2H, OCH ₂ CH ₃ ; J: 8.80 Hz)	112.91, 120.08, 124.30, 128.14,
	δ 4.54 (s, 2H, NCH ₂)	129.48, 133.59, 134.85, 135.12,
	δ 7.31 (d, 1H, ArH; J: 8.40 Hz)	139.58, 150.87 (ArC)
	δ 7.46-7.49 (m, 2H, ArH)	143.13 (Triazol C ₃)
	δ 7.67 (t, 2H,ArH; J: 8.00 Hz)	150.15 (N=CH)
	δ 7.83-7.85 (m, 3H, ArH)	150.00 (Triazol C ₅)
	δ 9.66 (s, 1H, N=CH)	

Table 2. Spectral data of compound 7b

IR (KBr) cm^{-1}	$^1\text{H-NMR}$	$^{13}\text{C-NMR}$
1673 (C=O)	δ 1.03 (d, 6H, 2CH ₃ ; $J=6.40$ Hz)	δ 10.01 (CH ₂ CH ₃)
1603, 1576 (C=N)	δ 1.11 (t, 3H, OCH ₂ CH ₃ ; $J=6.80$ Hz)	δ 14.03 (OCH ₂ CH ₃)
1373 ve 1159 (SO₂)	δ 1.21 (t, 3H, CH ₂ CH ₃ ; $J=7.60$ Hz)	δ 18.40 (CH ₂ CH ₃)
749 ve 696 (monosubstitue aromatic ring)	δ 2.00 (t, 2H, CH ₂ ; $J=10.80$ Hz)	δ 18.93 (2CH ₃)
	δ 2.72 (d, 2H, CH ₂ CH ₃ ; $J=7.60$ Hz)	δ 55.60 (2CH ₂)
	δ 2.75 (t, 2H, CH ₂ ; $J=12.40$ Hz)	δ 64.03 (OCH ₂ CH ₃)
	δ 3.51 – 3.54 (m, 2H, 2CH)	δ 65.50 (NCH ₂)
	δ 3.93 (q, 2H, OCH ₂ CH ₃ ; $J=7.20$ Hz)	δ 71.02 (2CH ₂)
	δ 4.55 (s, 2H, NCH ₂)	δ 112.95; 118.98; 124.33;
	δ 7.31 (d, 1H, ArH; $J=8.00$ Hz)	128.14(2C); 128.49(2C); 133.62;
	δ 7.46-7.49 (m, 2H, ArH)	134.86; 135.14; 139.58; 150;87
	δ 7.67 (t, 2H, ArH; $J=8.00$ Hz)	(ArC)
	δ 7.82-7.85 (m, 3H, ArH)	δ 146.84 (Triazol C ₃)
	δ 9.62 (s, 1H, N=CH)	δ 150.29 (N=CH)
		δ 153.03 (Triazol C ₅)

Table 3. Spectral data of compound 7c

IR (KBr) cm^{-1}	$^1\text{H-NMR}$	$^{13}\text{C-NMR}$
1708 (C=O)	δ 1.03 (d, 6H, 2CH ₃ ; $J=6.40$ Hz)	δ 14.03 (OCH ₂ CH ₃)
1587 (C=N)	δ 1.12 (t, 3H, OCH ₂ CH ₃ ; $J=6.80$ Hz)	δ 18.93 (2CH ₃)
1391 ve 1166 (SO₂)	δ 2.01 (t, 2H, CH ₂ ; $J=11.20$ Hz)	δ 30.94 (CH ₂ Ph)
850 (1,4-disubstitue aromatic ring)	δ 2.78 (d, 2H, ArH ₂ ; $J=10.40$ Hz)	δ 55.64 (2CH ₂)
760 ve 698 (monosubstitue aromatic ring)	δ 3.51 – 3.55 (m, 2H, 2CH)	δ 63.99 (OCH ₂ CH ₃)
	δ 3.80 (q, 2H, OCH ₂ CH ₃ ; $J=6.80$ Hz)	δ 65.60 (NCH ₂)
	δ 4.55 (s, 2H, CH ₂ Ph)	δ 71.01 (2CH ₂)
	δ 4.59 (s, 2H, NCH ₂)	δ 112.04; 120.68; 124.29;
	δ 7.28-7.32 (m, 6H, ArH)	128.14; 128.47(2C); 128.60(2C);
	δ 7.37-7.40 (m, 2H, ArH)	129.48(2C); 133.54; 134.86;
	δ 7.66 (t, 2H, ArH; $J=8.00$ Hz)	135.11; 135.71; 139.60;
	δ 7.81-7.85 (m, 3H, ArH)	150.81 (ArC)
	δ 9.61 (s, 1H, N=CH)	δ 144.86 (Triazol C ₃)
		δ 150.17 (N=CH)
		δ 152.45 (Triazol C ₅)

Table 4. Spectral data of compound 7d

IR (KBr) cm^{-1}	$^1\text{H-NMR}$	$^{13}\text{C-NMR}$
1709 (C=O)	δ 1.03 (d, 6H, 2CH ₃ ; $J=6.40$ Hz)	δ 14.03 (OCH ₂ CH ₃)
1589 (C=N)	δ 1.12 (t, 3H, OCH ₂ CH ₃ ; $J=6.80$ Hz)	δ 18.92 (2CH ₃)
1349 ve 1167 (SO₂)	δ 2.01 (t, 2H, CH ₂ $J=10.80$ Hz)	δ 20.56 (PhCH ₃)
849 (1,4-disubstitue aromatic ring)	δ 2.25 (t, 3H, PhCH ₃)	δ 30.55 (CH ₂ Ph)
763 ve 697 (monosubstitue aromatic ring)	δ 2.78 (d, 2H, CH ₂ $J=10.40$ Hz)	δ 55.65 (2CH ₂)
	δ 3.51 – 3.55 (m, 2H, 2CH)	δ 63.98 (OCH ₂ CH ₃)
	δ 3.81 (q, 2H, OCH ₂ CH ₃ ; $J=6.80$ Hz)	δ 65.50 (NCH ₂)
	δ 4.03 (s, 2H, CH ₂ Ph)	δ 71.00 (2CH ₂)
	δ 4.59 (s, 2H, NCH ₂)	δ 112.03; 120.68; 124.29;
	δ 7.10 (d, 2H, ArH; $J=8.00$ Hz)	128.14(2C); 128.48(2C);
	δ 7.20 (d, 2H, ArH; $J=8.00$ Hz)	129.03(2C); 129.47(2C);
	δ 7.30 (d, 1H, ArH; $J=8.00$ Hz)	132.57; 133.56; 134.84;
	δ 7.38-7.41 (m, 2H, ArH)	135.13; 135.87; 139.60;
	δ 7.67 (t, 2H, ArH; $J=8.00$ Hz)	150.81 (ArC)
	δ 7.81-7.85 (m, 3H, ArH)	δ 145.00 (Triazol C ₃)
	δ 9.62 (s, 1H, N=CH)	δ 150.17 (N=CH)
		δ 150.38 (Triazol C ₅)

Table 5. Spectral data of compound 7e

IR (KBr) cm^{-1}	$^1\text{H-NMR}$	$^{13}\text{C-NMR}$
1700 (C=O) ¹	δ 1.03 (d, 6H, 2CH ₃ ; $J=6.40$ Hz)	δ 14.03 (OCH ₂ CH ₃)
1612 ve 1576 (C=N)	δ 1.12 (t, 3H, OCH ₂ CH ₃ ; $J=6.80$ Hz)	δ 18.92 (2CH ₃)
1365 ve 1162 (SO ₂)	δ 2.00 (t, 2H, ArH; $J=11.20$ Hz)	δ 30.10 (CH ₂ Ph)
811 (1,4-disubstitue aromatic ring)	δ 2.77 (d, 2H, ArCH; $J=10.00$ Hz)	δ 55.02 (OCH ₃)
752 ve 688 (monosubstitue aromatic ring)	δ 3.51 – 3.55 (m, 2H, 2CH)	δ 55.65 (2CH ₂)
	δ 3.71 (s, 3H, OCH ₃)	δ 63.99 (OCH ₂ CH ₃)
	δ 3.82 (q, 2H, OCH ₂ CH ₃ ; $J=6.80$ Hz)	δ 65.50 (NCH ₂)
	δ 4.02 (s, 2H, CH ₂ Ph)	δ 71.01 (2CH ₂)
	δ 4.58 (s, 2H, NCH ₂)	δ 112.15; 120.60; 127.43;
	δ 6.86 (d, 2H, ArH; $J=8.40$ Hz)	128.14(2C); 129.47(2C);
	δ 7.23 (d, 2H, ArH; $J=8.80$ Hz)	129.68(2C); 133.57; 134.84;
	δ 7.31 (d, 1H, ArH; $J=8.00$ Hz)	135.13; 139.60; 150;82
	δ 7.40-7.43 (m, 2H, ArH)	151.12 (ArC)
	δ 7.67 (t, 2H, ArH; $J=8.00$ Hz)	δ 145.15 (Triazol C ₃)
	δ 7.83-7.85 (m, 3H, ArH)	δ 150.18 (N=CH)
	δ 9.62 (s, 1H, N=CH)	δ 150.47 (Triazol C ₅)

Table 6. Spectral data of compound 7f

IR (KBr) cm^{-1}	$^1\text{H-NMR}$	$^{13}\text{C-NMR}$
1705 (C=O)	δ 1.03 (d, 6H, 2CH ₃ ; $J=6.40$ Hz)	δ 14.04 (OCH ₂ CH ₃)
1577 (C=N)	δ 1.11 (t, 3H, OCH ₂ CH ₃ ; $J=6.80$ Hz)	δ 18.92 (CH ₃)
1373 ve 1162 (SO ₂)	δ 2.00 (t, 2H, CH ₂ $J=?$)	δ 30.29 (CH ₂ Ph)
749 ve 694 (1,3-monobsttue aromatic ring)	δ 3.51 – 3.55 (m, 2H, 2CH)	δ 55.62 (2CH ₂)
	δ 3.79 (q, 2H, OCH ₂ CH ₃ ; $J=6.80$ Hz)	δ 63.99 (O CH ₂ CH ₃)
	δ 4.11 (s, 2H, CH ₂ Ph)	δ 65.50 (NCH ₂)
	δ 4.55 (s, 2H, NCH ₂)	δ 71.02 (2CH ₂)
	δ 7.29 (d, 1H, ArH; $J=8.00$ Hz)	δ 112.10; 120.68; 124.30;
	δ 7.34 – 7.40 (m, 6H, ArH)	128.14(2C); 128.41(2C);
	δ 7.66 (t, 2H, ArH; $J=8.00$ Hz)	129.48(2C); 130.53(2C);
	δ 7.82 – 7.85 (m, 3H, ArH)	131.45; 133.49; 134.73;
	δ 9.62 (s, 1H, N=CH)	134.86; 135.10; 139.63;
		150.82 (ArC)
		δ 144.53 (Triazol C ₃)
		δ 150.17 (N=CH)
		δ 152.60 (Triazol C ₅)
		δ 162.27 (COO)

Antibacterial Properties

Antibacterial properties of the synthesized type 7 compounds against bacterial strains of *B. subtilis*, *B. cereus*, *P. aeruginosa*, *K. pneumoniae*, *S. aureus* and *E. coli* were investigated and the results are presented in Table 7.

Table 7. Antibacterial Properties of Compounds 7a-f

	<i>B. subtilis</i>	<i>B. cereus</i>	<i>P. aeruginosa</i>	<i>K. pneumoniae</i>	<i>S. aureus</i>	<i>E. coli</i>
7a	-	14	18	7	-	21
7b	-	10	12	7	8	17
7c	-	17	9	8	9	14
7d	-	12	14	7	11	18
7e	-	18	13	8	8	13
7h	-	14	17	9	7	20

0-5,5 mm negative effect; 5,5-10 mm (+) low effect; 11-16 (++) modarate effect; 17 and upper (+++) high effect (Perez et al., 1990; Ahmad et al., 1998)

Result and Discussion

There was no compound effect against *B. subtilis* strain. For *B. cereus*; compound 7b is at a low level, compound 7a, 7b, 7d and 7h is moderate and compounds 7c and 7e have a high level of activity. Different result obtained from *P. aeruginosa*. While compounds 7c-e were moderately active, compounds 7a and 7h had a high level of activity. All of the compounds have shown low effect for *K. pneumoniae*. For *aureus*, a gram-positive bacterium, while compounds 7a, 7b, 7c, 7e and 7f showed low activity, only compound 7d had moderate activity. The bacterium in which the highest activity was observed is *E. coli*. While compounds 7c and 7e were moderately effective, other compounds were highly active.

As a result, it has been concluded that the synthesized 7a-f type Mannich Some type of compounds acted at various levels against gram negative and gram positive bacteria. This situation draws attention to further research.

References

- Ahmad, I., Mehmood, Z., Mohammed, F., (1998). Screening of Some Indian Medicinal Plants for Their Antimicrobial Properties, *J. Ethnopharmacol.* 62 (1998), 183–193.
- Gürsoy-Kol, Ö., Yüksek, H., İslamoğlu, F., In-vitro Antioxidant and Acidic Properties of Novel 4-(5-methyl-2-thienylmethyleneamino)-4,5-dihydro-1H-1,2,4-triazol-5-one Derivatives. Synthesis and Characterization, *Revista de Chimie (Rev. Chim.) (Bucharest)*, 63(11); 1103-1111 (2012).
- Gürsoy-Kol, Ö., Yüksek, H., İslamoğlu, F., Synthesis and In-vitro Antioxidant Activities of Novel 4-(3-Methyl-2-thienylmethylene-amino)-4,5-dihydro-1H-1,2,4-triazol-5-one Derivatives with Their Acidic Properties, *J. Chem. Soc. Pak.*, 35(4); 1179-1190 (2013).
- Ikizler, A. A., İkizler, A., Yüksek, H., Serdar, M., “Antitumor Activities of Some 4,5-dihydro-1H-1,2,4-triazol-5-ones”, *Modelling, Measurement & Control C, AMSE* 133res, 57; 25-33 (1998).
- Ikizler, A.A., Uçar, F., Yüksek, H., Aytin, A., Yasa, I., Gezer, T., “Synthesis and Antifungal Activity of Some New Arylideneamino Compounds”, *Acta Pol. Pharm.*, 54 (2); 135-140 (1997).
- Kardaş, F., (2006). Synthesis, Potentiometric Titrations and Antioxidant Properties of Some Novel 3-Substituted-4-(4-methylthiobenzylideneamino)-4,5-dihydro-1H-1,2,4-triazol-5-one Derivatives, Master Thesis, Kafkas University, Institute of Science, Kars.
- Manap, S., (2009). Synthesis of some novel 3-alkyl (aryl) -4- (3,4-disubstituedbenzylideneamino)-4,5-dihydro-1H-1,2,4-triazol-5-one derivatives, Characterization of Their Structure, Investigation of Antioxidant and Acidity Properties, Master Thesis, Kafkas University, Institute of Science, Kars.
- Ocak, M., Yüksek, H., Kolaylı, S., Küçük, M., Ocak, Ü., Bahçeci, Ş., Alkan, M., Şahinbaş, E., Yıldırım, N., Antioxidant Properties of Some Schiff Bases Containing Triazole Ring, XVIII. International Chemistry Congress, Kars, 556 (2004).
- Özdemir, G. (2016), Synthesis of Some Novel 4- [3-ethoxy-4 (benzenesulfonyloxy) benzylideneamino] -4,5-dihydro-1H-1,2,4-triazol-5-one Derivatives, Characterization of Their Structure and Investigation of Some Properties, Master Thesis, Kafkas University, Institute of Science, Kars.
- Perez, C., Pauli, M., Bazerque, P. (1990). An Antibiotic Assay by Agar Well Diffusion Method, *Acta Biol. Med. Exp.* 15, 113–115.
- Pinner, A., (1982). *Die Imidoäther und Ihre Derivate*, 1. Auflage, Oppenheim, Berlin.
- Üre, S., (2010). Synthesis of Some 1-methyl-3-alkyl (aryl) -4- (3,4-dimethoxybenzylideneamino) -4,5-dihydro-1H-1,2,4-triazol-5-one to Characterization Structures and Investigation Antioxidant Properties, Master Thesis, Kafkas University, Institute of Science, Kars.
- Yüksek, H., Alkan, M., Çakmak, I., Ocak, Z., Bahçeci, Ş., Calapoğlu, M., Elmastaş, M., Kolomuç, A., Aksu, H., (2008). Preparation, GIAO NMR Calculations and Acidic Properties of Some Novel 4,5-dihydro-1H-1,2,4-triazol-5-one Derivatives with Their Antioxidant Activities, *Int. J. Mol. Sci.* 9: 12-32.
- Yüksek, H., Alkan, M., Ocak, Z., Bahçeci, S., Ocak, M., Ozdemir, M., (2004). Synthesis and Acidic Properties of Some New Potential Biologically Active 4-acylamino-4,5-dihydro-1H-1,2,4-triazol-5-one Derivatives” *Indian J.Chem.*, 43 (7): 1527-153.
- Yüksek, H., Bahçeci, Ş., Alkan, M.,(2001). Bazı 4-(4-hidroksibenzenilidenamino)-4,5-dihidro-1H-1,2,4-triazol-5-on Bileşiklerinin ve Asetil Türevlerinin Sentezi” XV. National Chemistry Congress, İstanbul, OK-P13 (2001).

Author Information

Gul Ozdemir

Kafkas University,
Department of Chemistry,
Kars, Turkey

Haydar Yuksek

Kafkas University,
Department of Chemistry,
Kars, Turkey

Muzaffer Alkan

Kafkas University,
Education Faculty
Kars, Turkey
muzafferalkan61@gmail.com

Synthesis and Antioxidant Activities of Some Novel 1-(Morpholine-4-yl-methyl)-3-alkyl(aryl)-4-(3-methoxy-4-isobutyryloxy)benzylideneamino-4,5-dihydro-1*H*-1,2,4-triazol-5-ones

Sevda MANAP
Kafkas University

Fevzi AYTEMIZ
Kafkas University

Haydar YUKSEK
Kafkas University

Abstract: In this study, 3-alkyl(aryl)-4-(3-methoxy-4-isobutyryloxy)benzylideneamino-4,5-dihydro-1*H*-1,2,4-triazol-5-ones (1) were treated with morpholine in the presence of formaldehyde according to the Mannich reaction to synthesize five novel 1-(morpholine-4-yl-methyl)-3-alkyl(aryl)-4-(3-methoxy-4-isobutyryloxy)benzylideneamino-4,5-dihydro-1*H*-1,2,4-triazol-5-ones (2). In addition, the antioxidant properties of compounds 2 were analyzed and evaluated using three antioxidant assays, including reducing power, free radical scavenging and metal chelating activity. For the measurement of the reductive ability, Fe^{3+} - Fe^{2+} transformation was investigated in the presence of compound using by the method of Oyaizu (1986). The hydrogen atoms or electrons donation ability of the synthesized compound was measured by DPPH \cdot using the method of Blois (1958). The chelating effect of ferrous ions by the compound was determined according to the method of Dinis, Madeira & Almeida (1994). BHT, BHA, EDTA and α -tocopherol were used as reference antioxidant compounds.

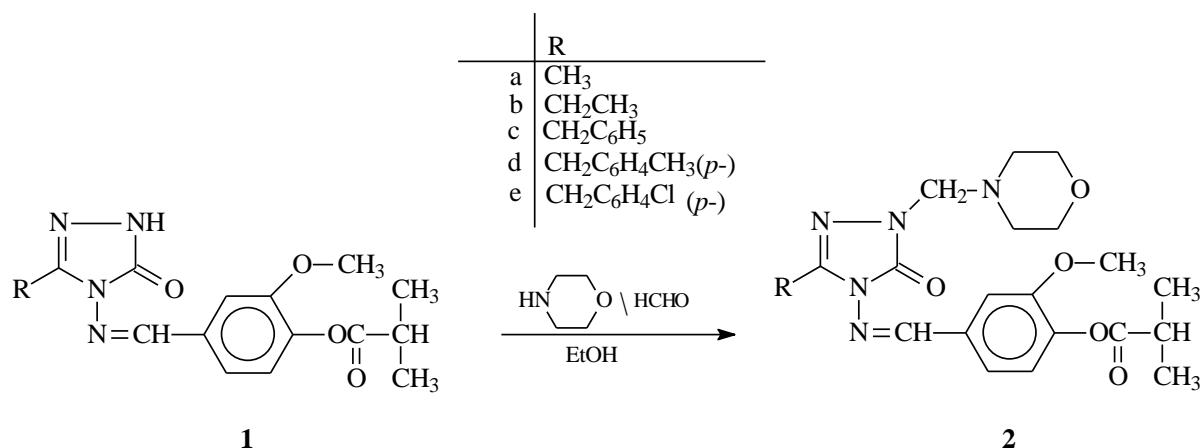
Keywords: 1,2,4-Triazol-5-one, Mannich base, Antioxidant activity

Introduction

1,2,4-Triazole and 4,5-dihydro-1*H*-1,2,4-triazol-5-one derivatives are reported to possess a broad spectrum of biological activities such as antitumor (Chen et al., 2016), antibacterial (Zhang et al., 2014), antioxidant (Chidananda et al., 2012), anti-inflammatory (El-Serwy, Mohamed, Abbas, & Abdel-Rahman, 2013), analgesic (Uzgören-Baran et al., 2012), antihypertensive and diuretic (Ali, Ragab, Farghaly, & Abdalla, 2011) properties.

Antioxidants are extensively studied for their capacity to protect organism and cell from damage that is induced by the oxidative stress. A great deal of research has been devoted to the study of different types of natural and synthetic antioxidant. A large number of heterocyclic compounds, containing the 1,2,4-triazole ring, are associated with diverse biological properties such as antioxidant, anti-inflammatory, antimicrobial and antiviral activity. External chemicals and internal metabolic processes in human body or in food system might produce highly reactive free radicals, especially oxygen derived radicals, which are capable of oxidizing biomolecules by resulting in cell death and tissue damage. Oxidative damages play a significantly pathological role in human diseases. Cancer, emphysema, cirrhosis, atherosclerosis and arthritis have all been correlated with oxidative damage. Also, excessive generation of reactive oxygen species (ROS) induced by various stimuli and which exceeds the antioxidant ability of the organism leads to variety of pathophysiological processes like inflammation, diabetes, genotoxicity and cancer (McClements & Decker, 2000).

In the present paper, the antioxidant activities of five new 1-(morpholine-4-yl-methyl)-3-alkyl(aryl)-4-(3-methoxy-4-isobutyryloxy)benzylideneamino-4,5-dihydro-1*H*-1,2,4-triazol-5-ones (**2**), which were obtained by the reactions of 3-alkyl(aryl)-4-(3-methoxy-4-isobutyryloxy)benzylideneamino-4,5-dihydro-1*H*-1,2,4-triazol-5-ones (**1**) with morpholine in the presence of formaldehyde (Scheme 1).



Scheme 1 Synthesized of compounds 2

Method

Chemicals and Apparatus

Chemical reagents used in this paper were bought from Merck AG, Aldrich and Fluka. Melting points were recorded in open glass capillaries using a Stuart SMP30 melting point apparatus and were not corrected. The infrared spectra were recorded on an Alpha-P Bruker FT-IR Spectrometer. ¹H and ¹³C NMR spectra were determined in deuterated dimethyl sulfoxide with TMS as internal standard using a Bruker Avance III spectrophotometer at 400 MHz and 100 MHz, respectively.

Synthesis of Compounds 4: The General Procedure

1-(morpholine-4-yl-methyl)-3-alkyl(aryl)-4-(3-methoxy-4-isobutyryloxy)benzylideneamino-4,5-dihydro-1*H*-1,2,4-triazol-5-ones (**2**) were synthesized by the reactions of 3-alkyl(aryl)-4-(3-methoxy-4-isobutyryloxy)benzylideneamino-4,5-dihydro-1*H*-1,2,4-triazol-5-ones (**1**) with morpholine in the presence of formaldehyde. The corresponding compound **1** (0.01 mol) was dissolved in 100 mL of ethanol followed by addition of morpholine (0.015 mol) and formaldehyde (0.02 mol). The reaction mixture was refluxed for 3 hours. After standing at room temperature overnight, the solid was filtered and crystallized from ethanol. The solid was recrystallized from the same solvent and purified by drying *in vacuo* to obtain pure compounds **2** as colourless crystals.

1-(Morpholine-4-yl-methyl)-3-methyl-4-(3-methoxy-4-isobutyryloxy)benzylideneamino-4,5-dihydro-1*H*-1,2,4-triazol-5-one (**2a**)

Yield: 76.9%, m.p. 136 °C. IR: 3067 (C=CH), 1762, 1691 (C=O), 1601, 1577 (C=N), 1237 (COO) cm⁻¹. ¹H NMR (DMSO-*d*₆): δ 1.24 (d, 6H, 2CH₃; *J*=7.20 Hz), 2.32 (s, 3H, CH₃), 2.58 (t, 4H, CH₂NCH₂; *J*=4.40 Hz), 2.84 (hept, 1H, CH; *J*=7.20 Hz), 3.56 (t, 4H, CH₂OCH₂; *J*=4.40 Hz), 3.84 (s, 3H, OCH₃), 4.54 (s, 2H, NCH₂), 7.23 (d, 1H, ArH; *J*=8.40 Hz), 7.46 (dd, 1H, ArH; *J*=8.40 Hz, 2.00 Hz), 7.59 (d, 1H, ArH; *J*=1.60 Hz), 9.69 (s, 1H, N=CH). ¹³C NMR (DMSO-*d*₆): δ 10.95 (CH₃), 18.73 (2CH₃), 33.18 (CH), 49.97 (CH₂NCH₂), 56.06 (OCH₃), 65.92 (NCH₂), 66.05 (CH₂OCH₂), [111.50; 120.69; 123.40; 132.13; 142.08; 151.32] (ArC), 143.12 (Triazole C₃), 150.23 (N=CH), 153.79 (Triazole C₅), 174.20 (COO). MS (70 eV): *m/z* (%): 118.11 (24), 129.09 (24), 132.13 (38), 418.13 (M+1, 100), 459.13 (6).

1-(Morpholine-4-yl-methyl)-3-ethyl-4-(3-methoxy-4-isobutyryloxy)benzylideneamino-4,5-dihydro-1H-1,2,4-triazol-5-one (2b)

Yield: 77.4%, m.p. 154 °C. IR: 3077 (C=CH), 1763, 1692 (C=O), 1611, 1578 (C=N), 1235 (COO) cm⁻¹. ¹H NMR (DMSO-*d*₆): δ 1.23 (d, 6H, 2CH₃; *J*=7.20 Hz), 1.24 (t, 3H, CH₂CH₃; *J*=6.80 Hz), 2.59 (t, 4H, CH₂NCH₂; *J*=4.40 Hz), 2.74 (q, 2H, CH₂CH₃; *J*=7.60 Hz), 2.84 (hept, 1H, CH; *J*=7.20 Hz), 3.56 (t, 4H, CH₂OCH₂; *J*=4.40 Hz), 3.84 (s, 3H, OCH₃), 4.55 (s, 2H, NCH₂), 7.23 (d, 1H, ArH; *J*=8.00 Hz), 7.46 (dd, 1H, ArH; *J*=8.00 Hz, 1.60 Hz), 7.58 (d, 1H, ArH; *J*=1.60 Hz), 9.69 (s, 1H, N=CH). ¹³C NMR (DMSO-*d*₆): δ 9.96 (CH₂C₃), 18.38 (C₃), 18.72 (2CH₃), 33.18 (CH), 49.98 (CH₂NCH₂), 56.03 (OCH₃), 65.96 (NCH₂), 66.03 (CH₂OCH₂), [111.52; 120.56; 123.40; 132.17; 142.07; 151.32] (ArC), 146.83 (Triazole C₃), 150.35 (N=CH), 153.75 (Triazole C₅), 174.19 (COO). MS (70 eV): *m/z* (%): 118.11 (12), 129.10 (44), 132.13 (28), 432.15 (M+1, 100).

1-(Morpholine-4-yl-methyl)-3-benzyl-4-(3-methoxy-4-isobutyryloxy)benzylideneamino-4,5-dihydro-1H-1,2,4-triazol-5-one (2c)

Yield: 72.6%, m.p. 131 °C. IR: 3068 (C=CH), 1758, 1696 (C=O), 1596, 1578 (C=N), 1246 (COO), 747 and 697 (monosubstituted benzenoid ring) cm⁻¹. ¹H NMR (DMSO-*d*₆): δ 1.24 (d, 6H, 2CH₃; *J*=7.20 Hz), 2.60 (t, 4H, CH₂NCH₂; *J*=4.40 Hz), 2.84 (hept, 1H, CH; *J*=7.20 Hz), 3.57 (t, 4H, CH₂OCH₂; *J*=4.40 Hz), 3.83 (s, 3H, OCH₃), 4.12 (s, 2H, CH₂Ph), 4.59 (s, 2H, NCH₂), 7.21 (d, 1H, ArH; *J*=8.00 Hz), 7.23-7.25 (m, 1H, ArH), 7.31-7.36 (m, 4H, ArH), 7.38 (dd, 1H, ArH; *J*=8.00 Hz, 1.60 Hz), 7.49 (d, 1H, ArH; *J*=1.60 Hz), 9.64 (s, 1H, N=CH). ¹³C NMR (DMSO-*d*₆): δ 18.72 (2CH₃), 31.05 (CH₂Ph), 33.17 (CH), 50.00 (CH₂NCH₂), 56.00 (OCH₃), 66.04 (NCH₂+CH₂OCH₂), [110.68; 121.22; 123.34; 132.11; 142.10; 151.29] (ArC), [126.77; 128.50(2C); 128,63(2C); 135.70] (ArC linked C-3), 144.91 (Triazole C₃), 150.24 (N=CH), 153.07 (Triazole C₅), 174.18 (COO). MS (70 eV): *m/z* (%): 118.11 (40), 129.10 (64), 132.13 (60), 494.20 (M+1, 100).

1-(Morpholine-4-yl-methyl)-3-p-methylbenzyl-4-(3-methoxy-4-isobutyryloxy)benzylideneamino-4,5-dihydro-1H-1,2,4-triazol-5-one (2d)

Yield: 72.8 %, m.p. 122 °C. IR: 3072 (C=CH), 1756, 1695 (C=O), 1613, 1579 (C=N), 1243 (COO), 860 (1,4-disubstituted benzenoid ring) cm⁻¹. ¹H NMR (DMSO-*d*₆): δ 1.24 (d, 6H, 2CH₃; *J*=6.80 Hz), 2.24 (s, 3H, PhCH₃), 2.59 (t, 4H, CH₂NCH₂; *J*=4.40 Hz), 2.84 (hept, 1H, CH; *J*=6.80 Hz), 3.57 (t, 4H, CH₂OCH₂; *J*=4.40 Hz), 3.84 (s, 3H, OCH₃), 4.06 (s, 2H, CH₂Ph), 4.58 (s, 2H, NCH₂), 7.12 (d, 2H, ArH; *J*=8.00 Hz), 7.21 (d, 1H, ArH; *J*=8.00 Hz), 7.23 (d, 2H, ArH; *J*=8.00 Hz), 7.39 (dd, 1H, ArH; *J*=8.40 Hz, 1.60 Hz), 7.50 (d, 1H, ArH; *J*=1.60 Hz), 9.64 (s, 1H, N=CH). ¹³C NMR (DMSO-*d*₆): δ 18.72 (2CH₃), 20.56 (PhCH₃), 30.65 (CH₂Ph), 33.17 (CH), 49.99 (CH₂NCH₂), 55.98 (OCH₃), 66.03 (NCH₂+CH₂OCH₂), [110.67; 121.23; 123.36; 132.13; 142.08; 151.28] (ArC), [128.52(2C); 129.07(2C); 132.57; 135.88] (ArC linked C-3), 145.06 (Triazole C₃), 150.24 (N=CH), 153.01 (Triazole C₅), 174.20 (COO). MS (70 eV): *m/z* (%): 118.11 (36), 129.10 (56), 132.13 (36), 508.21 (M+1, 100).

1-(Morpholine-4-yl-methyl)-3-p-chlorobenzyl-4-(3-methoxy-4-isobutyryloxy)benzylideneamino-4,5-dihydro-1H-1,2,4-triazol-5-one (2e)

Yield: 73.8 %, m.p. 125 °C. IR: 3062 (C=CH), 1763, 1697 (C=O), 1594, 1576 (C=N), 1245 (COO), 860 (1,4-disubstituted benzenoid ring) cm⁻¹. ¹H NMR (DMSO-*d*₆): δ 1.24 (d, 6H, 2CH₃; *J*= 7.20 Hz), 2.59 (t, 4H, CH₂NCH₂; *J*=4.40 Hz), 2.84 (hept, 1H, CH; *J*= 6.80 Hz), 3.57 (t, 4H, CH₂OCH₂; *J*= 4.40 Hz), 3.83 (s, 3H, OCH₃), 4.13 (s, 2H, CH₂Ph), 4.58 (s, 2H, NCH₂), 7.21 (d, 1H, ArH; *J*= 8.00 Hz), 7.36-7.42 (m, 5H, ArH), 7.49 (d, 1H, ArH; *J*=2.00 Hz), 9.65 (s, 1H, N=CH). ¹³C NMR (DMSO-*d*₆): δ 18.72 (2CH₃), 30.51 (CH₂Ph), 33.17 (CH), 49.97 (CH₂NCH₂), 56.01 (OCH₃), 66.03 (NCH₂), 66.09 (CH₂OCH₂), [110.77; 121.21; 123.37; 132.06; 142.13; 151.30] (ArC), [128.45 (2C); 130.58 (2C); 131.49; 134.70] (ArC linked C-3), 144.59 (Triazole C₃), 150.33 (N=CH), 153.24 (Triazole C₅), 174.19 (COO). MS (70 eV): *m/z* (%): 118.11 (48), 129.10 (84), 132.10 (48), 528.18 (M+1, 100).

Antioxidant Activity

Chemicals

Butylated hydroxytoluene (BHT), ferrous chloride, DPPH., α-tocopherol, 3- butylated hydroxyanisole (BHA), (2-pyridyl)-5,6-bis(phenylsulfonic acid)-1,2,4-triazine (ferrozine) and trichloroacetic acid (TCA) were obtained from E. Merck or Sigma.

Reducing Power

The reducing power of the compounds **2a-e** was determined using the method of Oyaizu (1986). Different concentrations of the samples (50-250 µg/mL) in DMSO (1 mL) were mixed with phosphate buffer (2.5 mL, 0.2 M, pH = 6.6) and potassium ferricyanide (2.5 mL, 1%). The mixture was incubated at 50°C for 20 min. after which a portion (2.5 mL) of trichloroacetic acid (10%) was added to the mixture, which was then centrifuged for 10 min at 1000 x g. The upper layer of solution (2.5 mL) was mixed with distilled water (2.5 mL) and FeCl₃ (0.5 mL, 0.1%), and then the absorbance at 700 nm was measured in a spectrophotometer. Higher absorbance of the reaction mixture indicated greater reducing power.

Free Radical Scavenging Activity

Free radical scavenging effect of the compounds **2a-e** was estimated by DPPH[•] by the method of Blois (1958). Briefly, 0.1 mM solution of DPPH[•] in ethanol was prepared, and this solution (1 mL) was added to sample solutions in DMSO (3 mL) at different concentrations (50-250 µg/mL). The mixture was shaken vigorously and allowed to stand at room temperature for 30 min. Then the absorbance was measured at 517 nm in a spectrophotometer. Lower absorbance of the reaction mixture indicated higher free radical scavenging activity. The DPPH[•] concentration (mM) in the reaction medium was calculated from the following calibration curve and determined by linear regression (R: 0.997):

$$\text{Absorbance} = 0.0003 \times \text{DPPH}^{\bullet} - 0.0174$$

The capability to scavenge the DPPH radical was calculated using the following equation:

$$\text{DPPH}^{\bullet} \text{ scavenging effect (\%)} = (A_0 - A_1/A_0) \times 100$$

where A₀ is the absorbance of the control reaction and A₁ is the absorbance in the presence of the samples or standards.

Metal chelating activity

The chelating of ferrous ions by the compounds **2a-e** and references was measured according to the method of Dinis et al., (1994). Briefly, the synthesized compounds (30–60 µg/mL) were added to a 2 mM solution of FeCl₂ (0.05 mL). The reaction was initiated by the addition of 5 mM ferrozine (0.2 mL), and then the mixture was shaken vigorously and left standing at room temperature for 10 min. After the mixture had reached equilibrium, the absorbance of the solution was measured at 562 nm in a spectrophotometer. All tests and analyses were run in triplicate and averaged. The percentage of inhibition of ferrozine-Fe²⁺ complex formation was given by the formula: % inhibition = (A₀ - A₁ / A₀) × 100, where A₀ is the absorbance of the control, and A₁ is the absorbance in the presence of the samples or standards. The control did not contain compound or standard.

Results and Discussion

Synthesis

In this study, the structures of five new 1-(morpholine-4-yl-methyl)-3-alkyl(aryl)-4-(3-methoxy-4-isobutyryloxy)benzylideneamino-4,5-dihydro-1H-1,2,4-triazol-5-ones (**2**) were identified by using IR, ¹H NMR, ¹³C NMR, and MS data.

Antioxidant Activity

The antioxidant capacities of five newly synthesized compounds **2a-e** were determined. Different processes have been used to identify antioxidant capacities. The processes used in the paper are clarified below:

Total reductive capability using the potassium ferricyanide reduction method

The reducing power of the compounds **2** was determined. The reductive capabilities of compounds are assessed by the extent of conversion of the Fe³⁺/ferricyanide complex to the Fe²⁺/ferrous form. The reducing powers of

the compounds were observed at different concentrations, and results were compared with BHA, BHT and α -tocopherol. The reducing capacity of a compound may serve as a significant indicator for its potential antioxidant activity (Meir, Kanner, Akiri, & Philosoph-Hadas, 1995). The antioxidant activity of a putative antioxidant has been attributed to various mechanisms, among which are prevention chain initiation, binding of transition metal ion catalyst, decomposition of peroxides, prevention of continued hydrogen abstraction, reductive capacity and radical scavenging (Yildirim, Mavi, & Kara, 2001). In this study, all of the amounts of the compounds showed lower absorbance than blank. Hence, no activities were observed to reduce metal ions complexes to their lower oxidation state or to take part in any electron transfer reaction.

DPPH Radical Scavenging Activity

The model of scavenging the stable DPPH radical model is a widely used method to evaluate antioxidant activities in a relatively short time compared with other methods. The effect of antioxidants on DPPH radical scavenging was thought to be due to their hydrogen donating ability (Baumann J, Wurn G & Bruchlausen V, 1979). DPPH is a stable free radical and accepts an electron or hydrogen radical to become a stable diamagnetic molecule (Soares J R, Dinis T C P, Cunha A P & Almeida L M, 1997). The reduction capability of DPPH radicals was determined by decrease in its absorbance at 517 nm induced by antioxidants. The absorption maximum of a stable DPPH radical in ethanol was at 517 nm. The decrease in absorbance of DPPH radical was caused by antioxidants because of reaction between antioxidant molecules and radical, progresses, which resulted in the scavenging of the radical by hydrogen donation. It is visually noticeable as a discoloration from purple to yellow. Hence, DPPH is usually used as a substrate to evaluate antioxidative activity of antioxidants (Duh P D, Tu Y Y & Yen G C, 1999). Antiradical activities of compounds and standard antioxidants such as BHT, BHA and α -tocopherol were determined by using DPPH method. Scavenging effect values of the compounds with BHT, BHA and α -tocopherol at different concentrations are respectively given Figures 1. The newly synthesized compounds which demonstrate increasing scavenging effect with growing concentration were plotted on the graphs.

The metal chelating effect of these compounds and references decreased in order of α -tocopherol > BHA > BHT > 4b, which were 74.9, 74.3, 65.8, 9.6 (%), at the highest concentration, respectively.

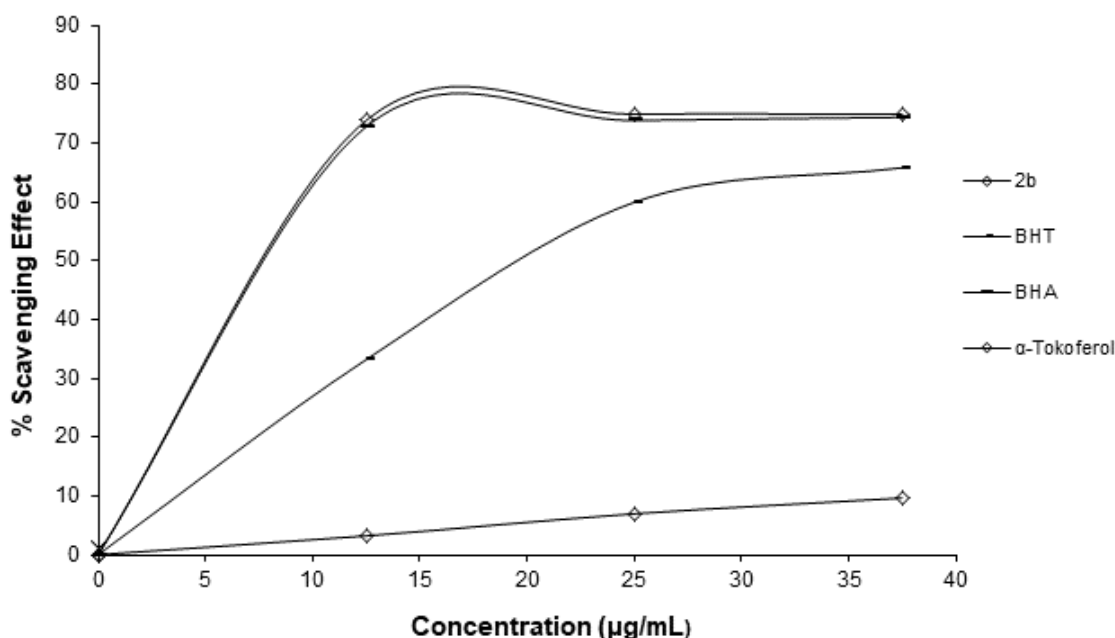
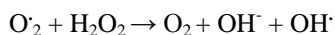


Figure 1. Scavenging effect of compounds 2b, BHT, BHA and α -tocopherol at different concentrations

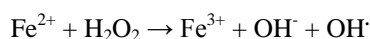
Ferrous ion chelating activity

The chelating effect towards ferrous ions by the compounds and standards was determined. Ferrozine can quantitatively form complexes with Fe^{2+} . In the presence of chelating agents, the complex formation is disrupted with the result that the red colour of the complex is decreased. Measurement of colour reduction therefore allows estimation of the chelating activity of the coexisting chelator (Yamaguchi F, Ariga T, Yoshimura Y &

Nakazawa H, 2000). Transition metals have pivotal role in the generation oxygen free radicals in living organism. The ferric iron (Fe^{3+}) is the relatively biologically inactive form of iron. However, it can be reduced to the active Fe^{2+} , depending on condition, particularly pH (Strlic M, Radovic T, Kolar J & Pihlar B, 2002) and oxidized back through Fenton type reactions with the production of hydroxyl radical or Haber-Weiss reactions with superoxide anions. The production of these radicals may lead to lipid peroxidation, protein modification and DNA damage. Chelating agents may not activate metal ions and potentially inhibit the metal-dependent processes (Finefrock, A. E., Bush, A. I., & Doraiswamy, P. M, 2003). Also, the production of highly active ROS such as O_2^- , H_2O_2 and OH is also catalyzed by free iron through Haber-Weiss reactions:



Among the transition metals, iron is known as the most important lipid oxidation pro-oxidant due to its high reactivity. The ferrous state of iron accelerates lipid oxidation by breaking down the hydrogen and lipid peroxides to reactive free radicals via the Fenton reactions:



Fe^{3+} ion also produces radicals from peroxides, even though the rate is tenfold less than that of Fe^{2+} ion, which is the most powerful pro-oxidant among the various types of metal ions (Calis I, Hosny M, Khalifa T & Nishibe S, 1993). Ferrous ion chelating activities of the compounds **2**, EDTA and α -tocopherol are respectively shown in Figures 2

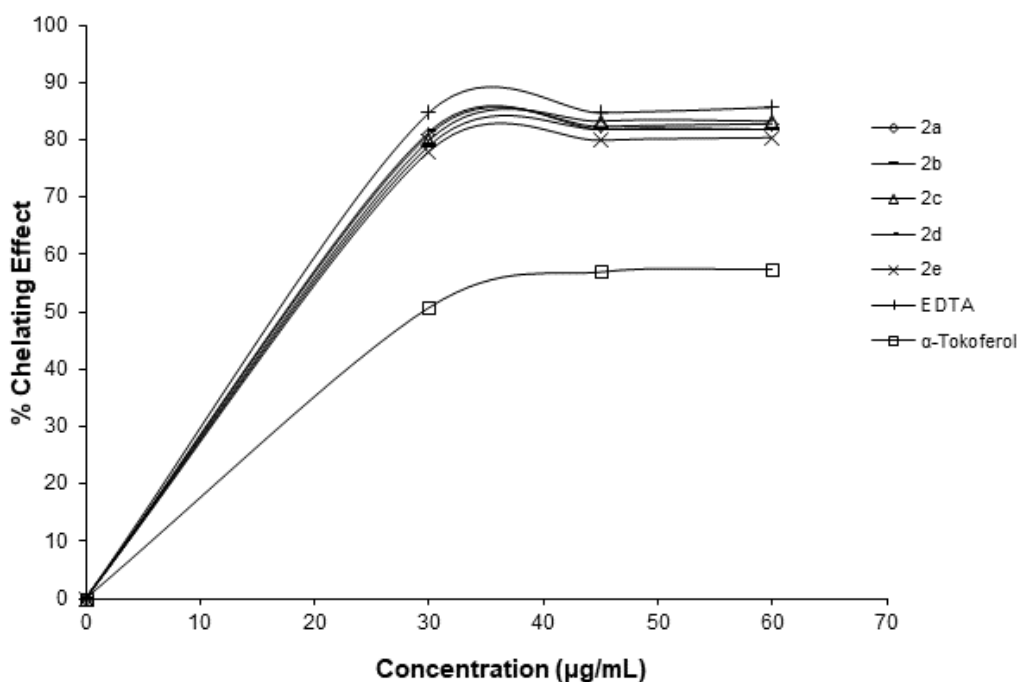


Figure 2. Metal chelating effect of the compounds 2a-e, EDTA and α -tocopherol on ferrous ions

In this study, metal chelating capacity was significant since it reduced the concentrations of the catalyzing transition metal. It was reported that chelating agents that form σ -bonds with a metal are effective as secondary antioxidants because they reduce the redox potential thereby stabilizing the oxidized form of metal ion (Gordon, M., H, 1990). The data obtained from Figures 2 reveal that the compounds demonstrate a marked capacity for iron binding, suggesting that their action as peroxidation protectors may be related to their iron binding capacity.

Conclusion

In this study, the structures of five new 4,5-dihydro-1H-1,2,4-triazol-5-one derivatives synthesized from the reactions of 1 type compounds with a benzaldehyde derivative were identified by using IR, ^1H NMR, ^{13}C NMR, and MS data. The newly synthesized compounds were screened for their antioxidant activities.

References

- Ali, K. A., Ragab, E. A., Farghaly, T. A., & Abdalla, M. M. (2011). Synthesis of new functionalized 3-substituted [1,2,4]triazolo [4,3-a]pyrimidine derivatives: potential antihypertensive agents. *Acta Poloniae Pharmaceutica*, 68(2), 237–47. Retrieved from <http://www.ncbi.nlm.nih.gov/pubmed/21485297>
- Baumann, J., Wurn, G., & Bruchlausen, V. (1979). Prostaglandin synthetase inhibiting O₂ – radical scavenging properties of some flavonoids and related phenolic compounds. *Naunyn-Schmiedebergs Archives of Pharmacology*, 308, R27.
- Blois, M. (1958). Antioxidant determinations by the use of a stable free radical. *Nature*, 181(4617), 1199–1200. <http://doi.org/10.1038/1811199a0>
- Calis I, Hosny, M., Khalifa T & Nishibe, S. (1993). *Phytochemistry*, 33, 1453.
- Chen, X., Shi, Y. M., Huang, C., Xia, S., Yang, L. J., & Yang, X. D. (2016). Novel dibenzo[b,d]furan-1H-1,2,4-triazole derivatives: Synthesis and antitumor activity. *Anti-Cancer Agents in Medicinal Chemistry*, 16(3), 377–386. <http://doi.org/10.2174/1871520615666150817115913>
- Chidananda, N., Poojary, B., Sumangala, V., Kumari, N. S., Shetty, P., & Arulmoli, T. (2012). Facile synthesis, characterization and pharmacological activities of 3,6-disubstituted 1,2,4-triazolo[3,4-b][1,3,4]thiadiazoles and 5,6-dihydro-3,6-disubstituted-1,2,4-triazolo[3,4-b][1,3,4]thiadiazoles. *European Journal of Medicinal Chemistry*, 51, 124–136. <http://doi.org/10.1016/j.ejmech.2012.02.030>
- Dinis, T. C. P., Madeira, V. M. C., & Almeida, L. M. (1994). Action of phenolic derivatives (acetaminophen, salicylate, and 5-aminosalicylate) as inhibitors of membrane lipid peroxidation and as proxyl radical scavengers. *Archives of Biochemistry and Biophysics*, 315(1), 161–169. <http://doi.org/10.1006/abbi.1994.1485>
- Duh, P. D., Tu Y Y & Yen, G. C. (1999). *Food Sci Technol-Leb*, 32, 269.
- El-Serwy, W. S., Mohamed, N. A., Abbas, E. M., & Abdel-Rahman, R. F. (2013). Synthesis and anti-inflammatory properties of novel 1,2,4-triazole derivatives. *Research on Chemical Intermediates*, 39(6), 2543–2554. <http://doi.org/10.1007/s11164-012-0781-9>
- Finefrock, A. E., Bush, A. I., & Doraiswamy, P. M. (2003). Current status of metals as therapeutic targets in Alzheimer's disease. *Journal of the American Geriatrics Society*. 51(8), 1143–1148. <http://doi.org/10.1046/j.1532-5415.2003.51368.x>
- Gordon M H, (1990). *Food Antioxidants* (Elsevier, London).
- McClements, D., & Decker, E. (2000). Lipid oxidation in oil-in-water emulsions: Impact of molecular environment on chemical reactions in heterogeneous food systems. *Journal of Food Science*, 65(8), 1270–1282. <http://doi.org/10.1111/j.1365-2621.2000.tb10596.x>
- Meir, S., Kanner, J., Akiri, B., & Philosoph-Hadas, S. (1995). Determination and involvement of aqueous reducing compounds in oxidative defense systems of various senescing leaves. *Journal of Agricultural and Food Chemistry*, 43(7), 1813–1819. <http://doi.org/10.1021/jf00055a012>
- Oyaizu, M. (1986). Studies on products of browning reaction. Antioxidative activities of products of browning reaction prepared from glucosamine. *The Japanese Journal of Nutrition and Dietetics*, 44(17), 307–315. <http://doi.org/10.5264/eiyogakuzashi.44.307>
- Soares, J. R., Dinis, T. C. P., Cunha, A. P., & Almeida, L. M. (1997). Antioxidant activities of some extracts of *Thymus zygis*. *Free Radical Research*, 26(5), 469–478. <http://doi.org/10.3109/10715769709084484>
- Uzgören-Baran, A., Tel, B. C., Sargöl, D., Öztürk, E. I., Kazkayas, I., Okay, G., Ertan, M., Tozkoparan, B. (2012). Thiazolo[3,2-b]-1,2,4-triazole-5(6H)-one substituted with ibuprofen: Novel non-steroidal anti-inflammatory agents with favorable gastrointestinal tolerance. *European Journal of Medicinal Chemistry*, 57, 398–406. <http://doi.org/10.1016/j.ejmech.2012.07.009>
- Yamaguchi, F., Ariga, T., Yoshimura, Y., & Nakazawa, H. (2000). Antioxidative and anti-glycation activity of garcinol from *Garcinia indica* fruit rind. *Journal of Agricultural and Food Chemistry*, 48(2), 180–185. <http://doi.org/10.1021/jf990845y>
- Yildirim, A., Mavi, A., & Kara, A. A. (2001). Determination of antioxidant and antimicrobial activities of *Rumex crispus* L. extracts. *Journal of Agricultural and Food Chemistry*, 49(8), 4083–4089. <http://doi.org/10.1021/jf0103572>
- Strlic, M., Radovic, T., Kolar, J., & Pihlar, B. (2002). *J Agr Food Chem*, 50, 6313.
- Yamaguchi, F., Ariga, T., Yoshimura, Y., & Nakazawa, H. (2000). *J Agr Food Chem*, 48, 180.
- Zhang, F., Wen, Q., Wang, S. F., Shahla Karim, B., Yang, Y. S., Liu, J. J., Zhang, W. M., Zhu, H. L. (2014). Design, synthesis and antibacterial activities of 5-(pyrazin-2-yl)-4H-1,2,4-triazole-3-thiol derivatives containing Schiff base formation as FabH inhibitory. *Bioorganic & Medicinal Chemistry Letters*, 24(1), 90–95. <http://doi.org/10.1016/J.BMCL.2013.11.079>

Author Information

Sevda Manap

Kafkas University,
Department of Chemistry,
Kars, Turkey
Contact e-mail: manapsevda@gmail.com

Fevzi Aytemiz

Kafkas University,
Department of Chemistry,
Kars, Turkey

Haydar Yuksek

Kafkas University,
Department of Chemistry,
Kars, Turkey

Synthesis and Potentiometric Titrations of 3-Alkyl(Aryl)-4-[3-etoxy-4-(4-methoxybenzensulfonyloxy)-benzylidenamino]-4,5-dihydro-1H-1,2,4-triazol-5-ones

Ozlem AKTAS YOKUS

Kafkas University

Murat BEYTUR

Kafkas University

Sevda MANAP

Kafkas University

Haydar YUKSEK

Kafkas University

Abstract: Determination of pK_a values of the active constituent of certain pharmaceutical preparations is important because the distribution, transport behaviour, bonding to receptors, and contributions to the metabolic behaviour of the active constituent molecules depend on the ionization constant. It is known that 1,2,4-triazole and 4,5-dihydro-1H-1,2,4-triazol-5-one rings have weak acidic properties, so that some 1,2,4-triazole and 4,5-dihydro-1H-1,2,4-triazol-5-one derivatives were titrated potentiometrically with tetrabutyl ammonium hydroxide (TBAH) in non-aqueous solvents, and the pK_a values of the compounds were determined. In this study, the first part of the study nine novel 3-alkyl(aryl)-4-[3-etoxy-4-(4-methoxybenzensulfonyloxy)-benzylidenamino]-4,5-dihydro-1H-1,2,4-triazol-5-ones were synthesized from the reactions of the corresponding 3-alkyl(aryl)-4-amino-4,5-dihydro-1H-1,2,4-triazol-5-ones with 2-ethoxy-4-formylphenyl 4-methoxybenzenesulfonate, which was obtained from the reaction of 3-ethoxy-4-hydroxybenzaldehyde with 4-methoxybenzenesulfonyl chloride by using triethylamine. The new compounds synthesized were also characterized by using IR and 1H -NMR, ^{13}C -NMR spectral data. The second part of the study, nine novel 3-alkyl(aryl)-4-[3-etoxy-4-(4-methoxybenzensulfonyloxy)-benzylidenamino]-4,5-dihydro-1H-1,2,4-triazol-5-ones were titrated potentiometrically with TBAH (tetrabutylammonium hydroxide) in four different non-aqueous solvents (isopropyl alcohol, tert-butyl alcohol, acetone and *N,N*-dimethylformamide) and graphs were drawn for all cases. The half neutralization potentials and pK_a values were determined by half neutralization method. The effects of solvents and molecular structure upon acidity were also discussed.

Keywords: Synthesis, 4,5-dihydro-1H-1,2,4-triazol-5-one, TBAH, pK_a , Half-neutralization method

Introduction

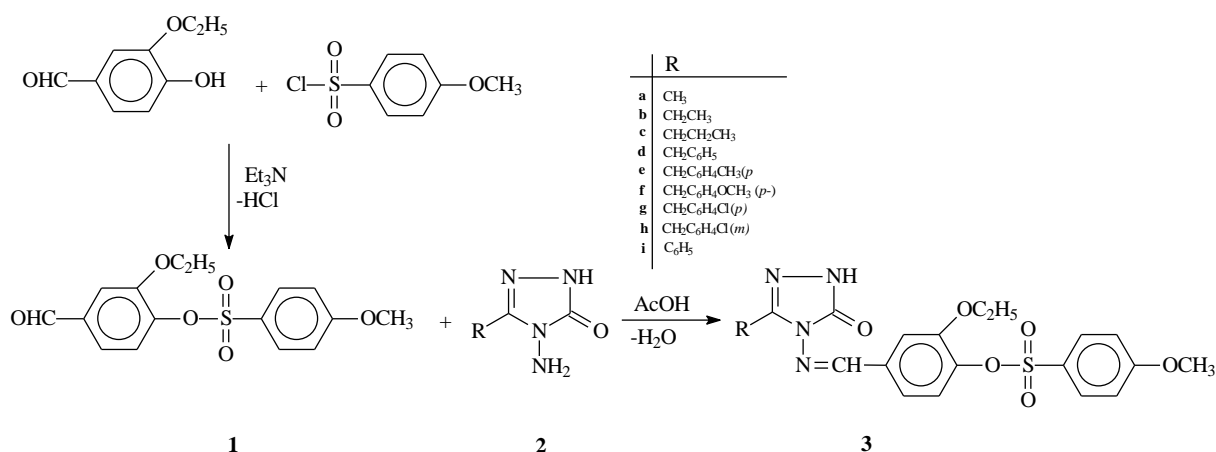
1,2,4-Triazole and 4,5-dihydro-1H-1,2,4-triazol-5-one derivatives are reported to possess a broad spectrum of biological activities such as antifungal, antimicrobial, hypoglycemic, antihypertensive, analgesic, antiparasitic, hypocholesteremic, antiviral, anti-inflammatory, antitumor and anti-HIV properties (Bhat, Bhat & Shenoy, 2001; Modzelewska-Banachiewicz et al., 2000; Varvaressou, 2000; Witkowski, 1973; Burzozowski, 1998; Katica et al., 2001; Wang, You & Xu, 1996; Ikizler, 1998; Demirbaş, 2001; Ulusoy, Gursoy & Otuk, 2001; Yüksek et al., 1997; Ikizler et al., 1997). In addition, several articles reporting the synthesis of some *N*-arylidenamino-4,5-dihydro-1H-1,2,4-triazol-5-one derivatives have been published (Ikizler et al., 1997; Ikizler et al., 1998; Ikizler & Yüksek, 1994; Bahçeci et al., 2002a; Bahçeci et al., 2002b). The acetylation and

- This is an Open Access article distributed under the terms of the Creative Commons Attribution-Noncommercial 4.0 Unported License, permitting all non-commercial use, distribution, and reproduction in any medium, provided the original work is properly cited.

- Selection and peer-review under responsibility of the Organizing Committee of the Conference

methylation of 4,5-dihydro-1*H*-1,2,4-triazol-5-one derivatives have also been reported (Yüksek et al., 1997; Bahçeci et al., 2002a; Bahçeci et al., 2002b; İkizler & Yüksek, 1993). On the other hand, it is known that 1,2,4-triazole and 4,5-dihydro-1*H*-1,2,4-triazol-5-one rings have weak acidic properties, so some 1,2,4-triazole and 4,5-dihydro-1*H*-1,2,4-triazol-5-one derivatives were titrated potentiometrically with tetrabutylammonium hydroxide in non-aqueous solvents, and the corresponding pK_a values of the compounds were determined (Bahçeci et al., 2002a; Bahçeci et al., 2002b; Yüksek et al., 2003; Yüksek et al., 2004; İkizler et al., 1988; İkizler & Erdoğan, 1988; İkizler et al., 1988).

This paper describes the synthesis of a series of novel 3-alkyl(aryl)-4-[3-ethoxy-4-(4-methoxybenzenesulfonyloxy)-benzylidenamino]-4,5-dihydro-1*H*-1,2,4-triazol-5-ones (**3**) from the reactions of 3-alkyl(aryl)-4-amino-4,5-dihydro-1*H*-1,2,4-triazol-5-ones (**2**) with 2-ethoxy-4-formylphenyl 4-methoxybenzenesulfonate (**1**) (Scheme 1). The starting compounds **2a-i** were prepared from the reactions of the corresponding ester ethoxycarbonylhydrazones with an aqueous solution of hydrazine hydrate as described in the literature (İkizler & Yüksek, 1994; İkizler & Ün, 1979). Furthermore, we also examined the potentiometric titrations of the synthesized compounds **3a-i** with tetrabutylammonium hydroxide (TBAH) in four non-aqueous solvents (isopropyl alcohol, *tert*-butyl alcohol, acetone and *N,N*-dimethylformamide) to determine the corresponding half-neutralization potentials (HNP) and the corresponding pK_a values. The data obtained from the potentiometric titrations were interpreted and the effects of molecular structure and solvents were studied (Bahçeci et al., 2002a; Bahçeci et al., 2002b; Yüksek et al., 2003; Yüksek et al., 2004; İkizler et al., 1988; İkizler & Erdoğan, 1988; İkizler et al., 1988; Gündüz, 1998).



Scheme 1: Synthesis of compounds of type 3

Method

Chemicals and Apparatus

In this study, a Jenway 3040 ion analyser pH meter equipped with an Ingold pH electrode was used for potentiometric titrations. For each compound titrated, a 0.001 M solution was separately prepared in each non-aqueous solvent. A 0.05 M solution of TBAH in isopropyl alcohol, which is widely used in the titration of acids, was used as titrant. The mV values obtained on the pH meter were recorded. Finally, the half-neutralization potential (HNP) values were determined by plotting the volume (mL) (TBAH)-mV graph.

Procedure for the synthesis of 2-ethoxy-4-formylphenyl 4-methoxybenzenesulfonate (1)

4-methoxybenzenesulfonyl chloride (10 mmol) was reacted with 3-ethoxy-4-hydroxybenzaldehyde (10 mmol) in ethyl acetate (100 mL). Then, triethylamine (20 mmol) was slowly added in the solution at stirring at 0-5 °C with magnetic stirring. After stirring for 2 hours at room temperature, it was refluxed for 3 hours and filtered. The crude product was crystallized several times in ethanol to afford compound **1**. Yield 93.75%. Mp: 61 °C. ¹H NMR (400MHz, DMSO-d₆, δ): 1.17 (t, 3H, OCH₂CH₃; *J*=6.80 Hz), 3.87 (s, 3H, OCH₃), 3.91 (q, 3H, OCH₂CH₃; *J*=6.80 Hz), 7.15-7.18 (m, 2H, ArH), 7.41 (d, 1H, ArH; *J*=8.40 Hz), 7.51 (d, 1H, ArH; *J*=1.60 Hz), 7.55 (dd, 1H, ArH; *J*=8.00 Hz, 1.60 Hz), 7.75-7.78 (m, 2H, ArH), 9.95 (s, 1H, CHO), ¹³C NMR (100MHz, DMSO-d₆, δ): 14.02 (OCH₂CH₃), 55.96 (OCH₃), 64.22 (OCH₂CH₃), 113.39; 114.69 (2C); 122.75; 124.48; 126.20; 130.28; 130.58, 135.79; 141.95; 151.24; 164.13 (Ar-C), 191.94 (2CHO).

General procedure for the synthesis of compounds 3a-I

2-ethoxy-4-formylphenyl 4-methoxybenzenesulfonate (**1**) (10 mmol) was dissolved in acetic acid (15 mL) and reacted with the corresponding compound **2** (10 mmol) to synthesize 3-alkyl(aryl)-4-[3-ethoxy-4-(4-methoxybenzenesulfonyloxy)-benzylidenamino]-4,5-dihydro-1*H*-1,2,4-triazol-5-ones and was refluxed for 1.5 hour. Then, the solution evaporated at 50-55 °C *in vacuo*. The residue was crystallized several times in ethanol and pure **3a-i** compounds were obtained as colorless crystals.

3-Methyl-4-[3-ethoxy-4-(4-methoxybenzenesulfonyloxy)-benzylidenamino]-4,5-dihydro-1*H*-1,2,4-triazol-5-ones (**3a**)

Yield 95.03%. M.p. 186°C. IR (KBr, ν , cm^{-1}): 3189 (NH), 1708 (C=O), 1579 (C=N), 1353 and 1196 (SO_2) 741 and 700 (1,4-disubstituted benzenoid ring). ^1H NMR (400 MHz, DMSO-d_6): δ 1.16 (t, 3H, OCH_2CH_3 , $J=7.20$ Hz), 2.27 (s, 3H, CH_3), 3.84-3.90 (m, 5H, OCH_2CH_3 + OCH_3), 7.15-7.17 (m, 2H, ArH), 7.27 (d, 1H, ArH, $J=8.00$ Hz), 7.43-7.47 (m, 2H, ArH), 7.74-7.77 (m, 2H, ArH), 9.67 (s, 1H, N=CH), 11.82 (s, 1H, NH). ^{13}C NMR (100 MHz, DMSO-d_6): δ 11.00 (CH_3), 14.08 (OCH_2CH_3), 55.94 (OCH_3), 64.07 (OCH_2CH_3), 112.74, 114.63 (2C), 119.99, 124.22, 126.32, 130.58 (2C), 133.59, 139.64, 150.96, 164.05 (Ar-C), 144.29 (triazole C_3), 151.15 (triazole C_5), 152.48 (N=CH).

3-Ethyl-4-[3-ethoxy-4-(4-methoxybenzenesulfonyloxy)-benzylidenamino]-4,5-dihydro-1*H*-1,2,4-triazol-5-ones (**3b**)

Yield 88.70%. M.p. 172°C. IR (KBr, ν , cm^{-1}): 3191 (NH), 1698 (C=O), 1593 (C=N), 1364 and 1199 (SO_2) 751 and 707 (1,4-disubstituted benzenoid ring). ^1H NMR (400 MHz, DMSO-d_6): δ 1.15 (t, 3H, OCH_2CH_3 , $J=7.20$ Hz), 1.20 (t, 3H, CH_2CH_3 , $J=7.60$ Hz), 2.68 (q, 2H, CH_2CH_3 , $J=7.60$ Hz), 3.84-3.89 (m, 5H, OCH_2CH_3 + OCH_3), 7.14-7.18 (m, 2H, ArH), 7.14 (d, 1H, ArH, $J=8.40$ Hz), 7.44 (d, 2H, ArH, $J=8.40$ Hz), 7.73-7.76 (m, 2H, ArH), 9.67 (s, 1H, N=CH), 11.85 (s, 1H, NH). ^{13}C NMR (100 MHz, DMSO-d_6): δ 9.96 (CH_2CH_3), 14.09 (OCH_2CH_3), 18.43 (CH_2CH_3), 55.96 (OCH_3), 64.04 (OCH_2CH_3), 112.80, 114.65 (2C), 119.86, 124.28, 126.31, 130.59 (2C), 133.63, 139.60, 150.96, 164.04 (Ar-C), 148.05 (triazole C_3), 151.28 (triazole C_5), 152.49 (N=CH).

3-*n*-Propyl-4-[3-ethoxy-4-(4-methoxybenzenesulfonyloxy)-benzylidenamino]-4,5-dihydro-1*H*-1,2,4-triazol-5-ones (**3c**)

Yield 83.33%. M.p. 163°C. IR (KBr, ν , cm^{-1}): 3172 (NH), 1697 (C=O), 1594 (C=N), 1368 and 1196 (SO_2) 748 and 690 (1,4-disubstituted benzenoid ring). ^1H NMR (400 MHz, DMSO-d_6): δ 0.97 (t, 3H, $\text{CH}_2\text{CH}_2\text{CH}_3$, $J=7.20$ Hz), 1.17 (t, 3H, OCH_2CH_3 , $J=7.20$ Hz), 1.69 (sext, 2H, $\text{CH}_2\text{CH}_2\text{CH}_3$, $J=7.60$ Hz), 2.60 (t, 2H, $\text{CH}_2\text{CH}_2\text{CH}_3$, $J=7.20$ Hz), 3.84-3.89 (m, 5H, OCH_2CH_3 + OCH_3), 7.15-7.17 (m, 2H, ArH), 7.28 (d, 1H, ArH, $J=8.00$ Hz), 7.43-7.46 (m, 2H, ArH), 7.73-7.77 (m, 2H, ArH), 9.67 (s, 1H, N=CH), 11.86 (s, 1H, NH). ^{13}C NMR (100 MHz, DMSO-d_6): δ 13.45 ($\text{CH}_2\text{CH}_2\text{CH}_3$), 14.07 (OCH_2CH_3), 18.92 ($\text{CH}_2\text{CH}_2\text{CH}_3$), 26.64 ($\text{CH}_2\text{CH}_2\text{CH}_3$), 55.95 (OCH_3), 64.02 (OCH_2CH_3), 112.85, 114.64 (2C), 119.79, 124.30, 126.32, 130.59 (2C), 133.63, 139.60, 150.94, 164.04 (Ar-C), 146.92 (triazole C_3), 151.21 (triazole C_5), 152.44 (N=CH).

3-Benzyl-4-[3-ethoxy-4-(4-methoxybenzenesulfonyloxy)-benzylidenamino]-4,5-dihydro-1*H*-1,2,4-triazol-5-ones (**3d**)

Yield 95.58%. M.p. 136°C. IR (KBr, ν , cm^{-1}): 3197 (NH), 1725, 1705 (C=O), 1580 (C=N), 1356 and 1199 (SO_2) 753 and 701 (1,4-disubstituted benzenoid ring). ^1H NMR (400 MHz, DMSO-d_6): δ 1.17 (t, 3H, OCH_2CH_3 , $J=6.80$ Hz), 3.84 (q, 2H, OCH_2CH_3 , $J=6.80$ Hz), 3.87 (s, 3H, OCH_3), 4.05 (s, 2H, CH_2Ph), 7.16 (d, 2H, ArH, $J=8.80$ Hz), 7.22-7.31 (m, 6H, ArH), 7.35-7.37 (m, 2H, ArH), 7.73-7.76 (m, 2H, ArH), 9.63 (s, 1H, N=CH), 11.12 (s, 1H, NH). ^{13}C NMR (100 MHz, DMSO-d_6): δ 14.07 (OCH_2CH_3), 31.15 (CH_2Ph), 55.06 (OCH_3), 66.00 (OCH_2CH_3), 111.93, 114.63 (2C), 120.53, 124.22, 126.28, 126.67, 128.41 (2C), 128.65 (2C), 130.60 (2C), 133.56, 135.82, 139.62, 150.90, 164.05 (Ar-C), 146.15 (triazole C_3), 151.14 (triazole C_5), 151.93 (N=CH).

3-*p*-methylbenzyl-4-[3-ethoxy-4-(4-methoxybenzenesulfonyloxy)-benzylidenamino]-4,5-dihydro-1*H*-1,2,4-triazol-5-ones (**3e**)

Yield 92.19%. M.p. 167°C. IR (KBr, ν , cm^{-1}): 3168 (NH), 1701 (C=O), 1575 (C=N), 1363 and 1197 (SO_2) 746 and 703 (1,4-disubstituted benzenoid ring). ^1H NMR (400 MHz, DMSO-d_6): δ 1.17 (t, 3H, OCH_2CH_3 , $J=7.20$ Hz), 2.24 (s, 3H, PhCH_3), 3.84 (q, 2H, OCH_2CH_3 , $J=6.40$ Hz), 3.87 (s, 3H, OCH_3), 3.99 (s, 2H, CH_2Ph), 7.09 (d, 2H, ArH, $J=8.00$ Hz), 7.14-7.19 (m, 4H, ArH), 7.26 (d, 1H, ArH, $J=8.80$ Hz), 7.37 (d, 2H, ArH, $J=8.40$ Hz),

7.73-7.76 (m, 2H, ArH), 9.62 (s, 1H, N=CH), 11.98 (s, 1H, NH). ¹³C NMR (100 MHz, DMSO-d₆): δ 14.08 (OCH₂CH₃), 20.55 (PhCH₃), 30.76 (CH₂Ph), 55.96 (OCH₃), 63.99 (OCH₂CH₃), 111.89, 114.63 (2C), 120.55, 124.23, 126.29, 128.52 (2C), 128.97 (2C), 130.60 (2C), 132.71, 133.58, 135.73, 139.62, 151.14, 164.05 (Ar-C), 146.29 (triazole C₃), 150.90 (triazole C₅), 151.86 (N=CH).

3-p-Methoxybenzyl-4-[3-etoxy-4-(4-methoxybenzensulfonyloxy)-benzylidenamino]-4,5-dihydro-1H-1,2,4-triazol-5-ones (3f)

Yield 90.24%. M.p. 151°C. IR (KBr, *v*, cm⁻¹): 3181 (NH), 1699 (C=O), 1577 (C=N), 1346 and 1198 (SO₂) 744 and 702 (1,4-disubstituted benzenoid ring). ¹H NMR (400 MHz, DMSO-d₆): δ 1.10 (t, 3H, OCH₂CH₃, *J*=6.80 Hz), 3.70 (s, 3H, *p*-OCH₃), 3.85 (q, 2H, OCH₂CH₃, *J*=6.80 Hz), 3.88 (s, 3H, OCH₃), 3.97 (s, 2H, CH₂Ph), 6.85 (d, 2H, ArH, *J*=8.40 Hz), 7.17-7.19 (m, 2H, ArH), 7.21-7.28 (m, 3H, ArH), 7.37-7.40 (m, 2H, ArH), 7.74-7.76 (m, 2H, ArH), 9.63 (s, 1H, N=CH), 11.96 (s, 1H, NH). ¹³C NMR (100 MHz, DMSO-d₆): δ 14.08 (OCH₂CH₃), 30.29 (CH₂Ph), 55.00 (*p*-OCH₃), 55.95 (OCH₃), 64.01 (OCH₂CH₃), 112.03, 113.86 (2C), 114.63 (2C), 120.67, 124.24, 126.30, 127.58, 129.72 (2C), 130.59 (2C), 133.59, 139.62, 151.15, 158.07, 164.05 (Ar-C), 146.45 (triazole C₃), 150.91 (triazole C₅), 151.96 (N=CH).

3-p-Chlorobenzyl-4-[3-etoxy-4-(4-methoxybenzensulfonyloxy)-benzylidenamino]-4,5-dihydro-1H-1,2,4-triazol-5-ones (3g)

Yield 95.58%. M.p. 181°C. IR (KBr, *v*, cm⁻¹): 3177 (NH), 1703 (C=O), 1576 (C=N), 1364 and 1198 (SO₂), 751 and 707 (1,4-disubstituted benzenoid ring). ¹H NMR (400 MHz, DMSO-d₆): δ 1.17 (t, 3H, OCH₂CH₃, *J*=7.20 Hz), 3.83 (q, 2H, OCH₂CH₃, *J*=7.20 Hz), 3.87 (s, 3H, OCH₃), 4.06 (s, 2H, CH₂Ph), 7.15-7.17 (m, 2H, ArH), 7.26 (d, 1H, ArH, *J*=8.00 Hz), 7.32-7.37 (m, 6H, ArH), 7.73-7.76 (m, 2H, ArH), 9.63 (s, 1H, N=CH), 12.01 (s, 1H, NH). ¹³C NMR (100 MHz, DMSO-d₆): δ 14.09 (OCH₂CH₃), 30.47 (CH₂Ph), 55.96 (OCH₃), 64.00 (OCH₂CH₃), 111.99, 114.63 (2C), 120.52, 124.24, 126.89, 128.35 (2C), 130.57 (2C), 130.60 (2C), 131.37, 133.51, 134.83, 139.65, 151.12, 164.05 (Ar-C), 145.80 (triazole C₃), 150.91 (triazole C₅), 152.08 (N=CH).

3-m-Chlorobenzyl-4-[3-etoxy-4-(4-methoxybenzensulfonyloxy)-benzylidenamino]-4,5-dihydro-1H-1,2,4-triazol-5-ones (3h)

Yield 92.85%. M.p. 175°C. IR (KBr, *v*, cm⁻¹): 3166 (NH), 1688 (C=O), 1575 (C=N), 1345 and 1166 (SO₂) 743 and 704 (1,4-disubstituted benzenoid ring). ¹H NMR (400 MHz, DMSO-d₆): δ 1.17 (t, 3H, OCH₂CH₃, *J*=7.20 Hz), 3.86 (q, 2H, OCH₂CH₃, *J*=6.80 Hz), 3.88 (s, 3H, OCH₃), 4.09 (s, 2H, CH₂Ph), 7.15 (d, 2H, ArH, *J*=8.80 Hz), 7.24-7.42 (m, 7H, ArH), 7.74 (d, 2H, ArH, *J*=8.80 Hz), 9.63 (s, 1H, N=CH), 12.03 (s, 1H, NH). ¹³C NMR (100 MHz, DMSO-d₆): δ 14.08 (OCH₂CH₃), 30.70 (CH₂Ph), 55.96 (OCH₃), 64.02 (OCH₂CH₃), 111.81, 114.62 (2C), 120.69, 124.20, 126.25, 126.73, 127.40, 128.74, 130.25, 130.61 (2C), 132.94, 133.50, 138.26, 139.66, 151.10, 164.05 (Ar-C), 145.64 (triazole C₃), 150.94 (triazole C₅), 152.04 (N=CH).

3-Phenyl-4-[3-etoxy-4-(4-methoxybenzensulfonyloxy)-benzylidenamino]-4,5-dihydro-1H-1,2,4-triazol-5-ones (3i)

Yield 94.73%. M.p. 217°C. IR (KBr, *v*, cm⁻¹): 3154 (NH), 1691 (C=O), 1575 (C=N), 1364 and 1196 (SO₂) 747 and 699 (1,4-disubstituted benzenoid ring). ¹H NMR (400 MHz, DMSO-d₆): δ 1.14 (t, 3H, OCH₂CH₃, *J*=6.80 Hz), 3.85 (q, 2H, OCH₂CH₃, *J*=6.80 Hz), 3.86 (s, 3H, OCH₃), 7.16 (d, 2H, ArH, *J*=8.80 Hz), 7.29 (d, 1H, ArH, *J*=8.40 Hz), 7.41-7.43 (m, 1H, ArH), 7.46 (d, 1H, ArH, *J*=2.00 Hz), 7.52-7.54 (m, 3H, ArH), 7.75-7.77 (m, 2H, ArH), 7.89-7.91 (m, 2H, ArH), 9.64 (s, 1H, N=CH), 12.40 (s, 1H, NH). ¹³C NMR (100 MHz, DMSO-d₆): δ 14.06 (OCH₂CH₃), 55.95 (OCH₃), 63.97 (OCH₂CH₃), 112.71, 114.66 (2C), 120.25, 124.39, 126.32, 126.53, 127.99 (2C), 128.47 (2C), 130.14, 130.58 (2C), 133.45, 139.77, 151.25, 164.05, (Ar-C), 144.58 (triazole C₃), 150.94 (triazole C₅), 154.77 (N=CH).

Results and Discussion

In this study, the structures of nine new 3-alkyl(aryl)-4-[3-etoxy-4-(4-methoxybenzensulfonyloxy)-benzylidenamino]-4,5-dihydro-1H-1,2,4-triazol-5-ones (**3**) were characterized with IR, ¹H NMR and ¹³C NMR spectral data. In order to determine the p*K*_a values of the compounds **3a-i**, they were titrated potentiometrically with TBAH in four non-aqueous solvents: isopropyl alcohol, tert-butyl alcohol, acetone and DMF. The mV values read in each titration were plotted against 0.05 M TBAH volumes (mL) added, and potentiometric

titration curves were obtained for all the cases. From the titration curves, the HNP values were measured, and the corresponding pK_a values were calculated.

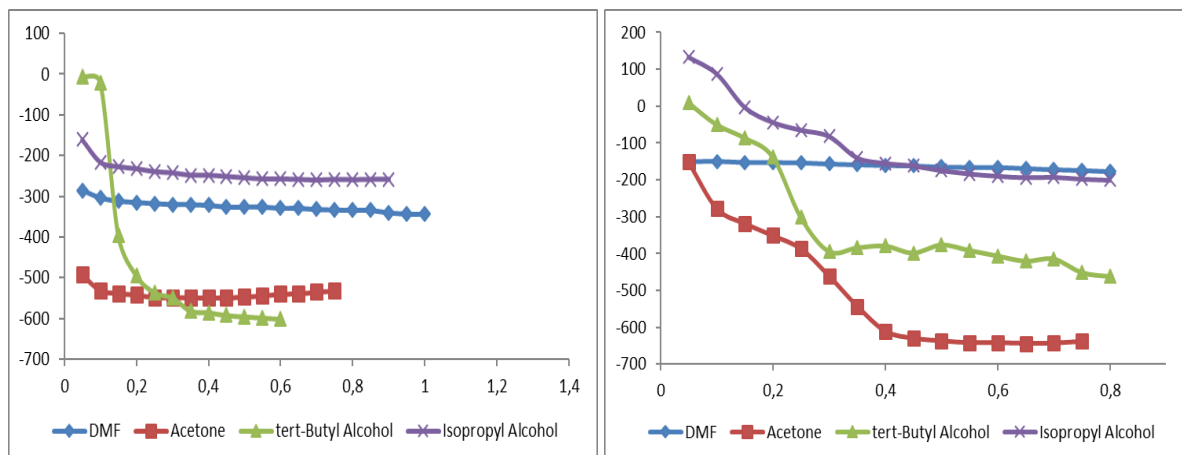


Figure 1. Potentiometric titration curves of 0.001 M solutions of compounds 3a and 3b titrated with 0.05 M TBAH in isopropyl alcohol, tert-butyl alcohol, DMF and acetone at 25 °C

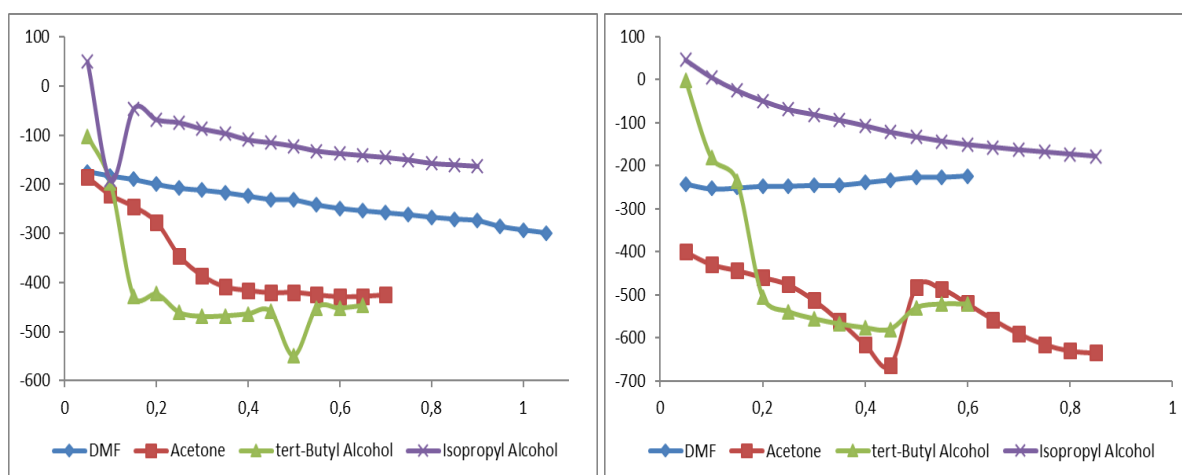


Figure 2. Potentiometric titration curves of 0.001 M solutions of compounds 3c and 3d titrated with 0.05 M TBAH in isopropyl alcohol, tert-butyl alcohol, DMF and acetone at 25 °C

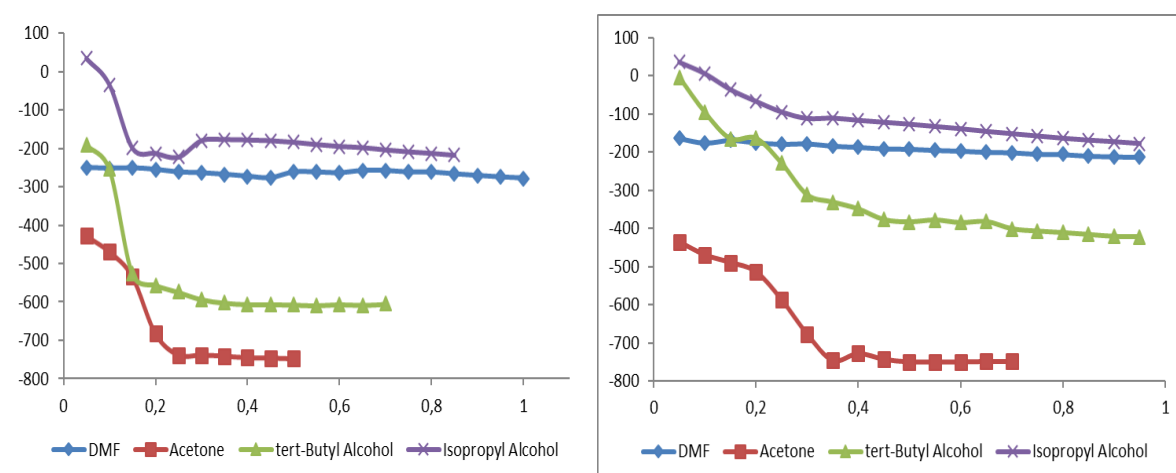


Figure 3. Potentiometric titration curves of 0.001 M solutions of compounds 3e and 3f titrated with 0.05 M TBAH in isopropyl alcohol, tert-butyl alcohol, DMF and acetone at 25 °C

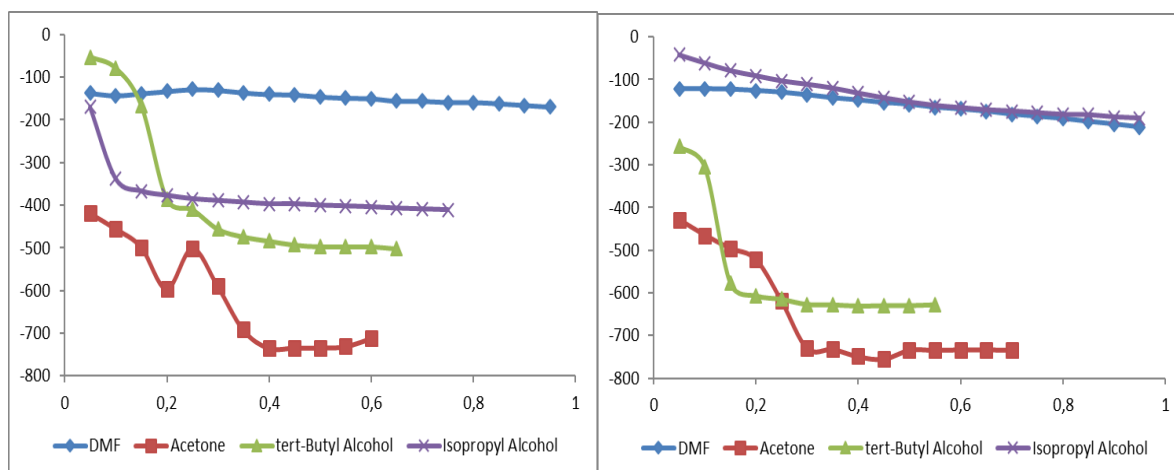


Figure 4. Potentiometric titration curves of 0.001 M solutions of compound 3g and 3h titrated with 0.05 M TBAH in isopropyl alcohol, tert-butyl alcohol, DMF and acetone at 25 °C

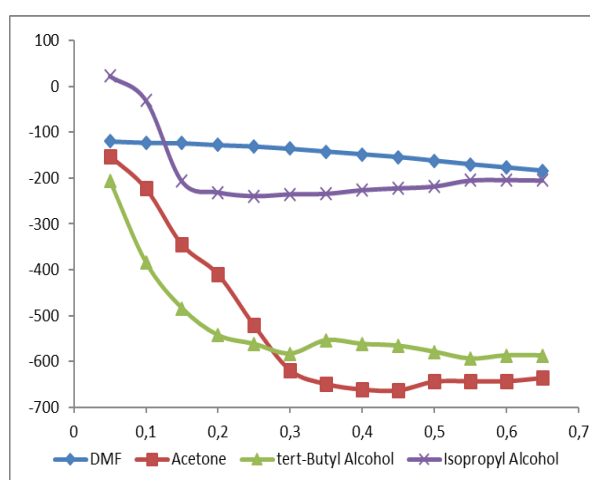


Figure 5. Potentiometric titration curves of 0.001 M solutions of compound 3i titrated with 0.05 M TBAH in isopropyl alcohol, tert-butyl alcohol, DMF and acetone at 25 °C

Table 1. The HNP and the corresponding pK_a values of compounds 3a-i in isopropyl alcohol, tert-butyl alcohol, DMF and acetone.

	DMF		Acetone		tert-butyl alcohol		isopropyl alcohol	
	pK_a	HNP	pK_a	HNP	pK_a	HNP	pK_a	HNP
3a	-	-	-	-	8,07	-14	-	-
3b	-	-	13,66	-335	8,95	-68	5,92	111
3c	-	-	11,97	-234	10,21	-150	-	-
3d	-	-	15,83	-459	10,77	-181	-	-
3e	-	-	16,03	-469	11,59	-222	7,23	34
3f	-	-	16,36	-490	10,41	-165	-	-
3g	-	-	16,50	-498	8,95	-66	-	-
3h	-	-	16,43	-496	12,65	-280	-	-
3i	-	-	12,8	-284	-	-	7,90	-4

The data obtained from the potentiometric titrations were interpreted, and the effect of the C-3 substituent in the 4,5-dihydro-1H-1,2,4-triazol-5-one ring as well as solvent effects was studied. As an example for the potentiometric titration curves for 0.001M solutions of compounds **3a-i** titrated with 0.05 M TBAH in isopropyl alcohol, tert-butyl alcohol, DMF and acetone are shown in Fig. 1-5.

When the dielectric permittivity of solvents is taken into consideration, the acidity order can be given as follows: DMF ($\epsilon = 36.7$) > acetone ($\epsilon = 36$) > isopropyl alcohol ($\epsilon = 19.4$) > tert-butyl alcohol ($\epsilon = 12$).

3a	: tert-butyl alcohol
3b	: isopropyl alcohol > tert-butyl alcohol > acetone
3c	: tert-butyl alcohol > acetone
3d	: tert-butyl alcohol > acetone
3e	: isopropyl alcohol > tert-butyl alcohol > acetone
3f	: tert-butyl alcohol > acetone
3g	: tert-butyl alcohol > acetone
3h	: tert-butyl alcohol > acetone
3i	: tert-butyl alcohol > acetone

When examined according to functional groups: The effect of the R functional groups on the distance from the acidic proton is very small. When the acidity of the compounds according to each solvent is examined;

N,N-dimethylformamid :-

Acetone : 3c > 3i > 3b > 3d > 3e > 3f > 3h > 3i

tert-Butyl alcohol : 3a > 3b = 3i > 3c > 3f > 3d > 3e > 3h

isopropyl alcohol : 3b > 3e > 3i

Conclusion

The synthesis, acidic properties and *in vitro* antioxidant evaluation of new 4,5-dihydro-1H-1,2,4-triazol-5-one derivatives are described. Design and synthesis of novel small molecules can play specifically a protective role in biological systems and in modern medicinal chemistry. Determination of pK_a values of the active constituent of certain pharmaceutical preparations are also important because of the distribution, transport behavior, bonding to receptors

References

- Bahçeci, Ş., Yüksek, H., Ocak, Z., Azaklı, A., Alkan, M., & Ozdemir, M (2002a). Synthesis and potentiometric titrations of some new 4-(benzylideneamino)-4,5-dihydro-1H-1,2,4-triazol-5-one derivatives in non-aqueous media. *Collect. Czech. Chem. Commun.* 67, 1215-1222.
- Bahçeci, Ş., Yüksek, H., Ocak, Z., Köksal, C., Ozdemir, M. (2002b). Synthesis and non-aqueous medium titrations of some new 4,5-dihydro-1H-1,2,4-triazol-5-one derivatives. *Acta Chim. Slov.* 49, 783-794.
- Bhat, A. R., Bhat, G. V., Shenoy, G. G. (2001). Synthesis and in-vitro antimicrobial activity of new 1,2,4-triazoles. *J. Pharm. Pharmacol.* 53, 267-272.
- Burzozowski, Z. (1998). Synthesis and anti-HIV activity of some new 2-mercapto-N-(1,2,4-triazol-3-yl)benzenesulfonamide derivatives containing the 1,2,4-triazole moiety fused with variety of heteroaromatic rings. *Acta Pol. Pharm.-Drug Res.* 55, 473-480.
- Demirbaş, A., Johansson, C. B., Duman, N., İkizler, A. A. Synthesis and biological activities of some new 4,5-dihydro-1H-1,2,4-triazol-5-ones. *Acta Pol. Pharm.-Drug Res.* 1996, 53, 117-121.
- Gündüz, T. (1998). *Susuz Ortam Reaksiyonları*, Gazi Büro Kitabevi Tic. Ltd. Şti: Ankara, Turkey.
- İkizler, A. A., Un, R. (1979). Reactions of ester ethoxycarbonylhydrazones with some amine type compounds. *Chim. Acta Turc.* 7, 269-290.
- İkizler, A. A., Erdoğan, Y. (1991). Determination of pK_a values of some benzylideneamino compounds in nonaqueous media. *Doğa-Tr. J. Chem.* 15, 337-344.
- İkizler, A. A., Yüksek, H. (1993). Acylation of 4-amino-4,5-dihydro-1H-1,2,4-triazol-5-ones. *Org. Prep. Proced. Int.* 25, 99-105.
- İkizler, A. A., Yüksek, H. (1994). Reaction of 4-amino-4,5-dihydro-1H-1,2,4-triazol-5-ones with 2,5-dimethoxytetrahydrofuran. *Collect. Czech. Chem. Commun.* 59, 731-735.
- İkizler, A. A., Uçar, F., Yüksek, H., Aytin, A., Yasa, I., Gezer, T. (1997). Synthesis and antifungal activity of some new arylideneamino compounds. *Acta Pol. Pharm.-Drug Res.* 54, 135-140.
- İkizler, A. A., İkizler, A., Yüksek, H., Serdar, M. (1998). Antitumor activities of some 4,5-dihydro-1H-1,2,4-triazol-5-ones. *Modelling, Measurement & Control C, AMSE Press 1*, 25-33.
- İkizler, A. A., Demibaş, A., Johansson, C. B., Çelik, C., Serdar, M., Yüksek, H. (1998). Synthesis and biological activities of some 4,5-dihydro-1H-1,2,4-triazol-5-one derivatives. *Acta Pol. Pharm.-Drug Res.* 55, 117-123.
- Katica, C.-R., Vesna, D., Vlado, K., Dora, G. M., Aleksandra, B., (2001). Synthesis, antibacterial and antifungal activity of 4-substituted-5-aryl-1,2,4-triazoles. *Molecules* 6, 815-824

- Modzelewska-Banachiewicz, B., Jagiello-Wojtowicz, E., Tokarzewska-Wielosz, E. (2000). Synthesis and biological activity of BIS-1,2,4-triazole and BIS-1,3,4-thiadiazole derivatives. *Acta Pol. Pharm.-Drug Res.* 57, 199-204.
- Ulusoy, N., GURSOY, A., OTUK, G. (2001). Synthesis and antimicrobial activity of some 1,2,4-triazole-3-mercaptoacetic acid derivatives. *II Pharmaco*, 56, 947-952.
- Varvaresou, A., Tsantili-Kakoulidou, A., Siatra-Papastaikoudi, T., Tiligada, E. (2000). Synthesis and biological evaluation of indole containing derivatives of thiosemicarbazide and their cyclic 1,2,4-triazole and 1,3,4-thiadiazole analogs. *Arzneim.-Forsch./Drug Res.* 50, 48-54.
- Yüksek, H., Demibaş, A., İkizler, A., Johansson, C. B., Çelik, C., İkizler, A. A. (1997). Synthesis and antibacterial activities of some 4,5-dihydro-1H-1,2,4-triazol-5-ones. *Arzneim.-Forsch./Drug Res.* 47, 405-409.
- Yüksek, H., Ocak, Z., Özdemir, M., Ocak, M., Bekar, M., Aksoy, M. (2003). A study on novel 4-heteroarylidenamino-4,5-dihydro-1H-1,2,4-triazol-5-ones. *Ind. J. Heterocycl. Chem.* 13, 49-52.
- Yüksek, H., Ocak, Z., Alkan, M., Bahçeci, Ş., Özdemir, M. (2004). Synthesis and determination of pK_a values of some new 3,4-disubstituted-4,5-dihydro-1H-1,2,4-triazol-5-one derivatives in nonaqueous solvents. *Molecules* 9, 232-240.
- Wang, Z., You, T., Xu, Y. (1996). Synthesis and biological activities of 2-substituted-5-(β-pyridyl)-2,3-dihydro-1,2,4-triazolo[3,4-b]-1,3,4-thiadiazoles. *Molecules* 1, 68-71

Author Information

Ozlem Aktas Yokus

Kafkas University,
Faculty of Education,
Kars, Turkey
Contact e-mail: ozak36@gmail.com

Murat Beytur

Kafkas University,
Department of Chemistry,
Kars, Turkey

Sevda Manap

Kafkas University,
Department of Chemistry,
Kars, Turkey

Haydar Yuksek

Kafkas University,
Department of Chemistry,
Kars, Turkey

Study of Some Biochemical Parameters and Fatty Acids Composition in Blood Serum of Women with Polycystic Ovary Syndrome

Abd-Alkream H.ISMAIL

Mosul University

Mohamed A.H.JASIM

Mosul University

Shaima a A.H.JASIM

Mosul University

Abstract: This study was designed to compare the level of some biochemical parameters and lipid fractions and percentage of fatty acids in serum of women with Polycystic ovary syndrome (PCOS), the study include (25) patients (females) who were diagnosed by ultrasonography, the sample collection is from Al-Bitol teaching hospital in Mosul city, the age is between (25-40) year and compared with (25) normal woman with same age were collected as control and measurement of a number of biochemical parameters in serum, as well as analysis and measurement of percentage of fatty acids in the fatty component of serum (cholesterol ester, phospholipids and triglyceride) by applying thin layer chromatography (TLC) and then re-esterification fatty acids and measurement percentage of fatty acids applying capillary gas chromatography (CGC). the result of this study show that there is a significant differences in the level of studied biochemical parameter and fatty acids percentage in patients compared with the control group.

Keyword: Biochemical parameters, Blood serum

Introduction

The polycystic ovary syndrome (PCOS) is considered as a common disease as it affect is about 30% of female all over the world (1). in which there is irregularity in menstrual cycle and it is lead to delay in pregnancy but it not cause infertility (2). The polycystic ovary syndrome is characterized by presence of small size follicles inside the ovary and specially under the external wall of ovary (3). the polycystic ovary syndrome is due to hormonal disturbance such as (LH, Estrogen and Dopamine) hormones (4) which lead to menstruation disturb and ovulation disturbance is usually accompany by hypertension, weight gain and hirsute in some areas of body specially the chin and chest (5). The polycystic ovary syndrome is probably a mixed group of related conditions, in it is full from there is hirsutism, amenorrhoea, infertility and ovarian abnormalities in the from of follicular cysts and a thickened capsule preventing ovulation (6). the condition may be discovered during investigations for infertility, breast development is usually normal but endometrial proliferation varies from the unstimulated state to hyperplasia (7).

Materials and Method

Samples Collection

In this study the blood samples were collected from patients after fasting period for (10-12) hours and (5) ml of blood from each subject was collected and serum was separated from it and then divided in to two parts: 1st part

- This is an Open Access article distributed under the terms of the Creative Commons Attribution-Noncommercial 4.0 Unported License, permitting all non-commercial use, distribution, and reproduction in any medium, provided the original work is properly cited.

- Selection and peer-review under responsibility of the Organizing Committee of the Conference

measurement of the following parameters glucose, total cholesterol(TC), high density lipoprotein cholesterol(HDL-C),triglyceride (TG),low density lipoprotein cholesterol (LDL-C) by enzymatic methods using kits(8,9), very low lipoprotein cholesterol(VLDL-C) was measurement theoretical(10) ,and phospholipids(PL) by colorimetric method (11).the 2nd part was stored at (-18)°c until measurement of fatty acids.

Extraction and Separation of lipids from Serum

Serum samples were treated with methanol and chloroform to extract lipids(10), lipids extract was separated into three parts cholesterol ester (CE),triglyceride(TG),phospholipids(PL)using thin layer chromatography (TLC).(11)

Transmethylation of Fatty Acids

In this study analysis and esterification of fatty acids by using tri-floro boron (BF₃) in Methanol(16%)(12).

Measurmeant of Percentage of Fatty Acids

Measurement of fatty acids in the three lipid fractions was performed by Capillary Gas Chromatography (CGC) Shimadzo 2010,column type TR-WAX, and length 30m, in industry center (Syria).

Statistical Analysis

Results were analyzed statistically for biochemical parameters and the percentage of fatty acids using *t*-test, $P < 0.05$ was considered statistically significant (13).

Results and Dissociation

Serum Glucose

The results showed that a significant increase in serum glucose in woman with Polycystic Ovary Syndrome(PCOS) compared with that control group as indicated in table (1) this increase may be due to insulin resistance which leads to increase serum glucose (14) or due to insulin metabolism defect (15) .This result is agreement with other studies(16,17).

Lipid Fractions

The results showed that a significant increase in total cholesterol (TC) in woman with (PCOS) compared with that of control group as indicated in table (1) this increase may be due to increase in (TC) synthesis as a result of insulin resistance in woman with (PCOS) (18).and the results showed that a significant decrease in (HDL-C) in patients comparison with control group as show in table (1) the cause of that may be due to close relationship to the elevated activity of plasma CETP(cholesterol ester transfer protein) which promotes the lipoprotein cholesterol of HDL to be transfered to other lipoprotein in patients (19).on the other hand, the results showed that there is significant increase in (LDL-C) may be due to defect in hepatic receptor (Apo B100) which plays an important role in increasing (LDL-C) through decreasing transport of (LDL-C) to hepatic tissue(20). But the results of (TG) and (VLDL-C) in patients showed insignificant results compared with control group as show in table (1),the same results were obtained in other new studies(21,22,23). whereas the results showed that a significant increase in (PL) this increases may be due to action of hepatic lipases which lead to abnormality metabolism of lipids specially phospholipids (24) and may cause of smoking which is play import role of increase (PL) in serum (25).

Table 1. Serum biochemical parameters from PCOS and control group

Biochemical Parameters	PCOS	Control	P value
mmol/l	25	25	
Glucose	6.86±1.65	4.35±0.23	<0.001
TC	6.83±1.30	4.67± 0.83	<0.001
HDL-C	0.87±0.20	1.41±0.21	<0.001
LDL-C	6.12 ±0.51	4.76±0.11	<0.001
TG	2.32±0.47	1.92±0.86	0.1
VLDL-C	1.04 ±0.08	0.86±0.03	0.12
PL	179± 11.54	165±9.87	<0.05

Values :Mean ± SD

Percentage of fatty acids:

The percentage of fatty acids was measured by using (CGC) through comparison of results with standard sample composed of (12) fatty acids, as indicated in fig(1): from the result analysis of standard sample of fatty acids and table (2)demonstrated a retention time (Rt) of these standard fatty acids.

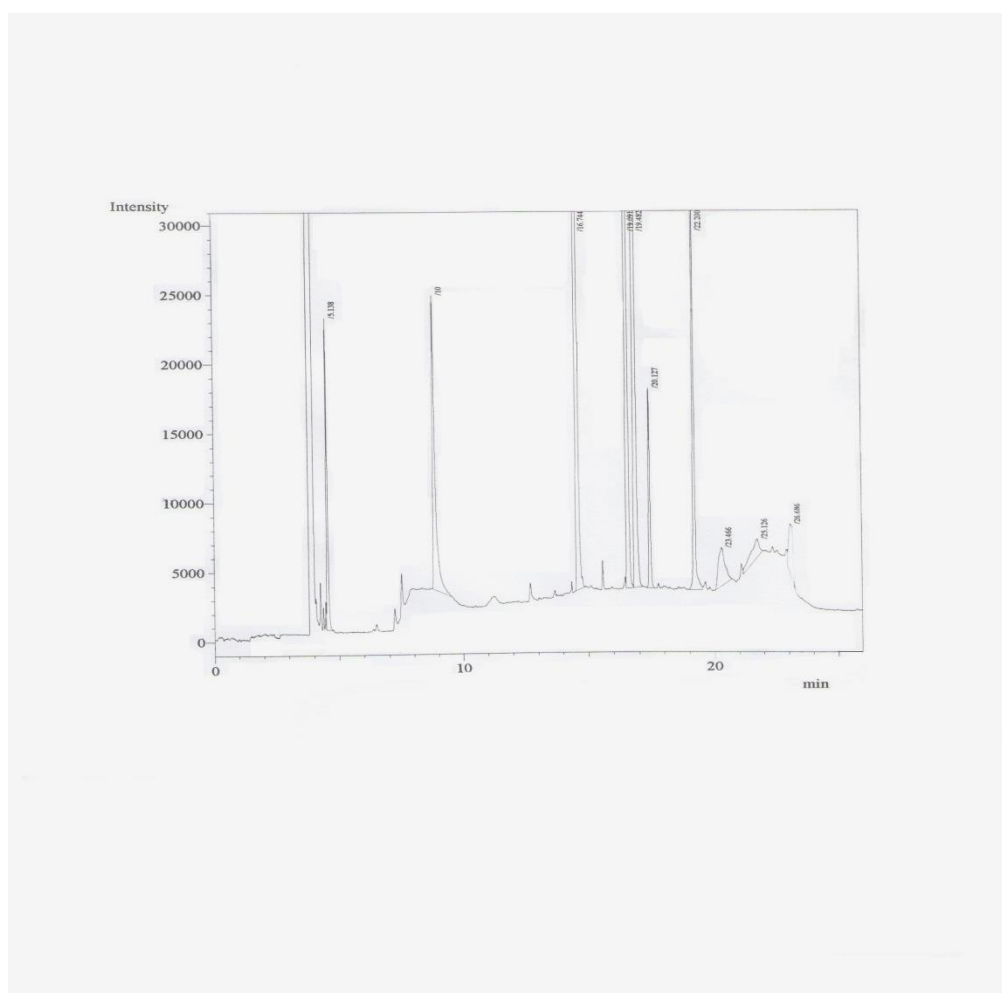


Figure 1. The CGC chart of (12) standard fatty acids

Table 2. Standard fatty acids

Standard fatty acids	Symbol	Retention time(min)
Capric acid	C10:0	4.900
Lauric acid	C12:0	5.138
Myristic acid	C14:0	8.500
Palmitic acid	C16:0	10.08
Palmitoleic acid	C16:1	16.74
Stearic acid	C18:0	19.09
Oleic acid	C18:1	19.48
Linoleic acid	C18:2	20.12
Linolenic acid	C18:3	22.20
Arachidonic acid	C20:4	23.46
Eicosapentaenoic acid	C20:5	25.12
Docosahexaenoic acid	C22:6	26.68

Percentage of fatty acids in (CE) part : Fig (2)

The results showed that a significant increases in percentage of total saturated fatty acids (SFA) in woman with (PCOS) in comparison with control group ,as show in table (3), this increasing may be due to abnormality in metabolism of fatty acids in patients (26).also a significant decrease in percentage of total monounsaturated fatty acids (MUFA) and a significant increase in percentage of total polyunsaturated fatty acids (PUFA) in this parts , this increasing may be due to insulin resistance in (PCOS) patients which leads to a big defect in enzymes action which leading to defect in percentage of unsaturated fatty acids (27).

Percentage of fatty acids in (TG) part: Fig (3)

The results showed that a significant increase in percentage of total (SFA) and total (MUFA) ,on the other hand a significant decrease in percentage of total (PUFA) in PCOS patients in compared with that of control group ,as shown in table (3), this may be due to some type of food(butter fat and hydrogenate vegetable oils) which leads to increase the risk factor of PCOS disease such as trans-fatty acid (28),or may be due to transport (Acetyl-CoA) from different metabolism pathway to pathway causes anabolism of fatty acids (29).

Percentage of fatty acids in (PL) part : Fig (4)

The results showed that a significant decrease in percentage of total (SFA) ,on the other hand a significant increase in percentage of total (MUFA) and (PUFA) in PCOS patients in comparison with control group ,as show in table (3),this decreasing or increasing may be due to defect in action of desaturation enzyme (Δ 9) desaturase and elongation enzymes (Δ 6),(Δ 5) in PCOS patients (30).

Table 3. Percentage of fatty acids composition of CE,PL,TG in serum PCOS woman and control group

Fatty acid	CE		PL		TG	
	control n 10	PCOS 5	control 10	PCOS 5	control 10	PCOS 5
SFA						
10:0	1.0±0.13	0.70±0.05	0.09±0.01	0.69±0.08	0.10±0.04	0.3±0.10
12:0	1.3±0.23	1.62±0.22	1.5±0.31	1.75±0.09	2.00±0.30	6.0±0.15*
14:0	0.56±0.10	1.36±0.30	0.38±0.1	2.95±0.18*	4.0±0.65	5.24±0.38
16:0	6.00±1.52	3.80±1.21*	10.25±2.8	2.43±0.89*	25.0±2.60	24.0±3.34
18:0	3.00±0.47	10.52±2.21*	10.01±1.3	11.75±1.87	5.25±1.24	7.25±0.9*
Total	11.86±2.45	18.00±3.99*	22.23±4.5	19.57±3.11*	36.35±4.83	42.8±4.9*
MUFA						
16:1	1.70±1.20	2.23±0.87	2.30±0.7	5.6±0.87*	3.50±0.35	7.28±1.2*

18:1	18.0±2.54	15.0±2.65*	8.30±1.44	9.26±2.11	20.24±1.24	18.9±1.8*
Total	19.70±3.74	17.23±3.52*	10.6±2.14	14.86±2.98*	23.74±1.59	26.18±3.*
PUFA						
18:2 n-6	20.0±2.43	22.0±3.32*	18.78±3.2	17.65±1.65	18.26±2.77	17.12±1.9
18:3 n-3	2.30±0.44	4.50±0.76*	2.10±0.98	5.74±2.43*	2.85±0.67	1.80±.55
20:4 n-6	6.80±1.77	10.23±1.83*	10.24±3.2	14.28±2.29*	4.85±0.55	3.24±.76
20:5 n-3	1.56±0.5	4.00±0.88*	2.85±0.34	5.56±1.20*	2.90±0.54	2.68±.21
22:6 n-3	2.38±0.91	5.00±0.67*	2.3±0.50	4.5±1.54*	6.65±0.88	2.56±1.3*
Total	33.04±6.0	45.73±7.46*	36.27±8.2	47.73±9.11*	35.51±5.41	27.4±4.7*
n-3	6.24±1.85	13.50±2.31*	7.25±1.82	15.8±5.17*	10.40±2.09	10.04±2.1
n-6	26.8±4.20	32.23±5.15*	29.0±6.40	31.93±3.94*	20.11±3.32	25.36±2.*

Values :Mean ± SD * : P value < 0.05

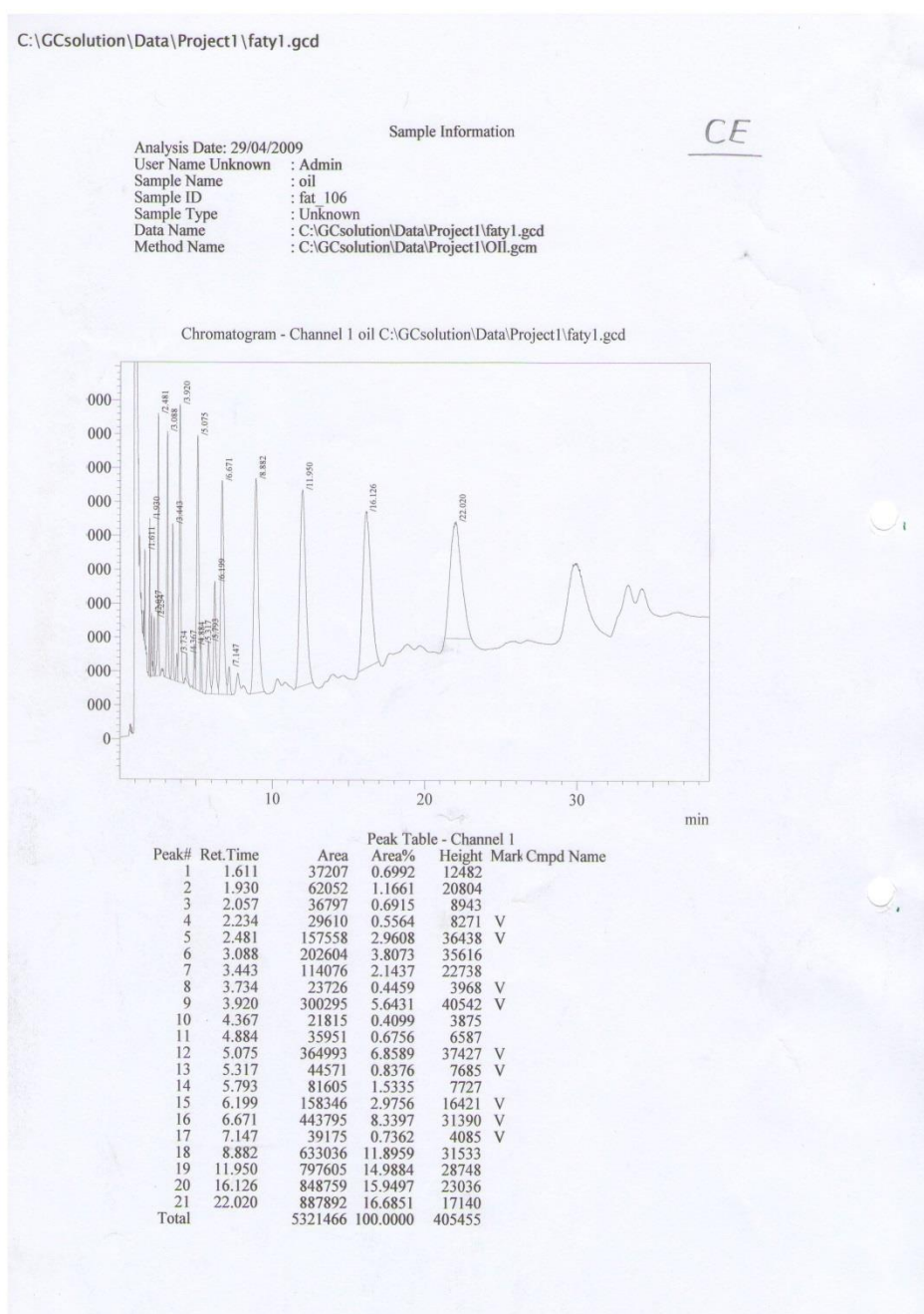


Figure 2. The CGC chart of fatty acids in CE part

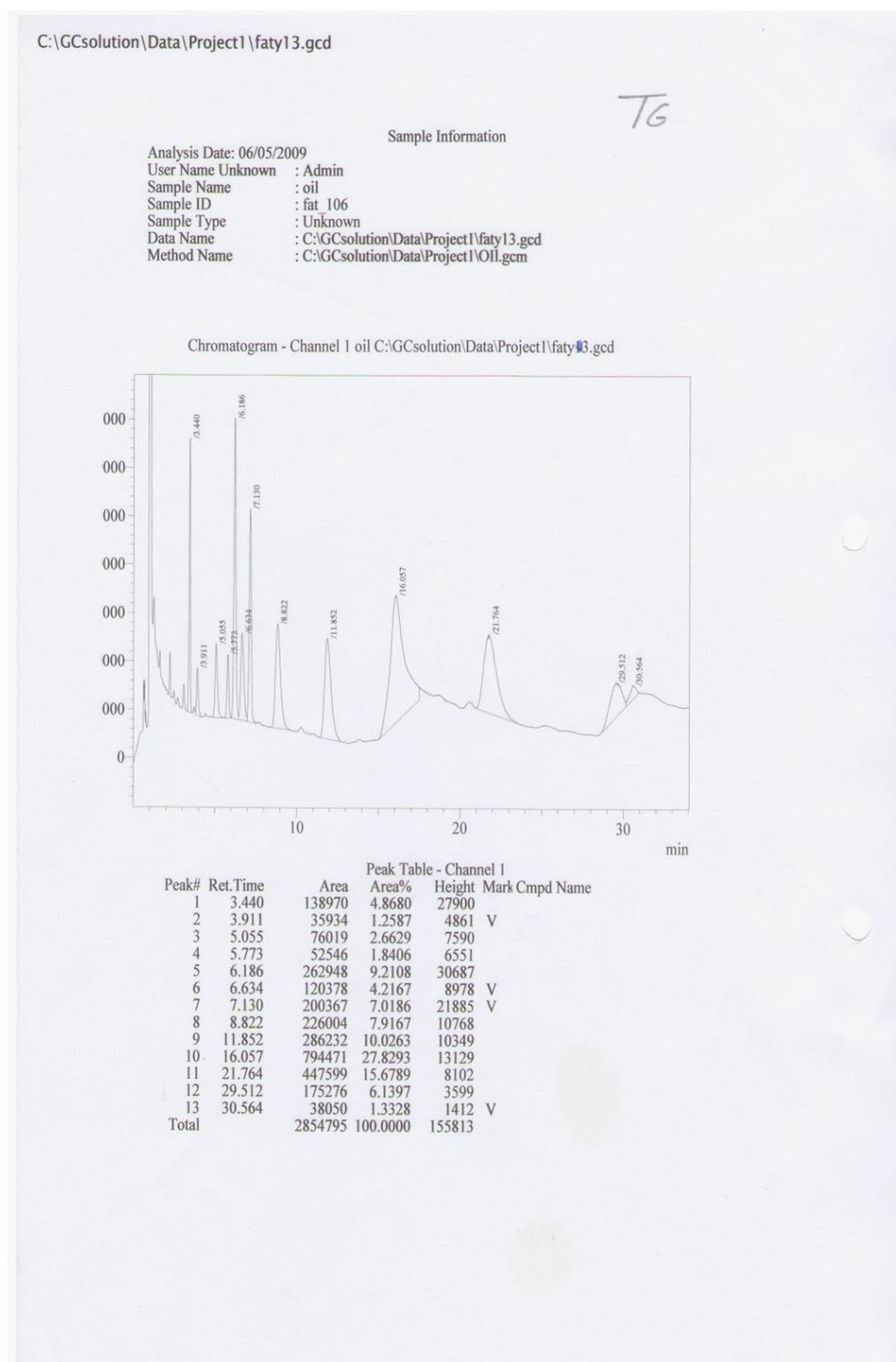


Figure 3. The CGC chart of fatty acids in TG part

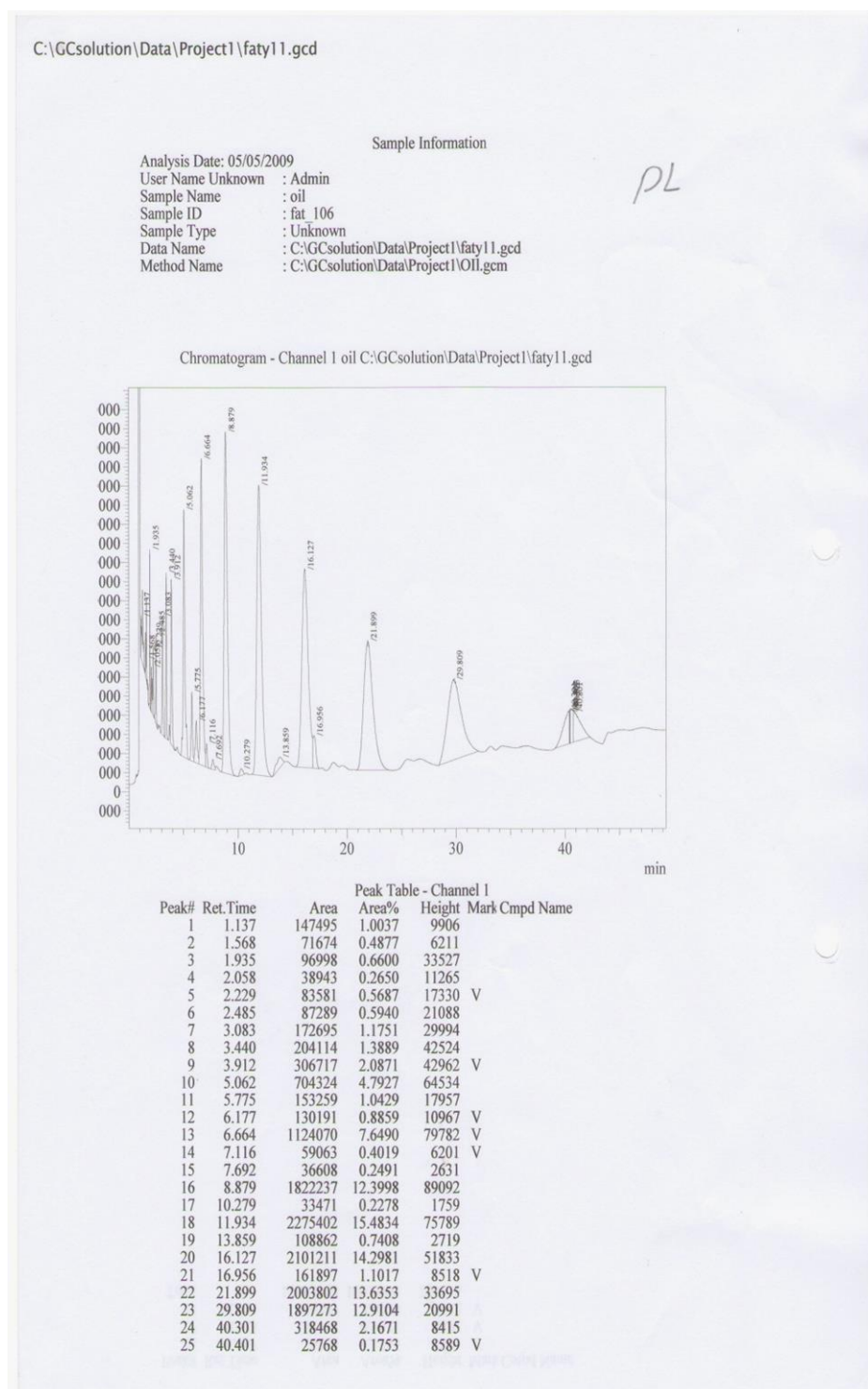


Figure 4. The CGC chart of fatty acids in PL part

References

- Desloover S. Ernst M. Use of metformin in polycystic ovary syndrome. *Annals of Pharmacotherapy* 35.(2001).
- Witchel S. Arslanian S. Ovarian responses to HCG stimulation .clin. *Endocrinal* 51 .(1999).
- Goldzieher J. Green J. Clinical and biochemical features of polycystic ovary disease . *fertile steril* 14 .(1993).

- Elting M. Korsen T. Schoemaker J. Woman with PCOS gain regular menstrual cycles when ageing . Hum. Report 15.(2000).
- Rai R. Backos M. Regan L. Polycystic ovaries and recurrent miscarriage .Hem .Report 15.(2000).
- Murray R., Grammar D. Harper's Biochemistry 25th ed .,Appleton and Lange, USA, (2000).
- Charnvises K. Weerakiet S. Wansumrith S. Acanthosis nigricans clinical predictor of abnormal glucose tolerance in Asian woman with PCOS. Gynecol. Endocrinol ,(2005).
- Burtis C, Ashwood E. Tiets Text Book of Clinical Chemistry.3rded. W.B.Saunders Com.:pp110-115.(1999)
- Kosnor G.M. Enzymatic determination cholesterol in HDL fraction .Clin.Chem.;22:665-670.(1976)
- Michael L, Edward P, Larry S. Clinical Chemistry .5th Williams &Wilkins. ; pp.288-292.(2005)
- Tietz N. Text Book of Clinical Biochemistry .W.B. Saunders Com. Philadelphia,USA;135-140.(1986)
- Ma J. Shahar E. Plasma fatty acids composition in middle-age adults. Am.J.Clin. Nutr.;62:564-571.(2005)
- Leonard T. Kathleen R. The ways and means of statistics. Harcourt Brace Jovanovich.;pp490-495. (1979)
- Dunaif A. Insulin resistance in PCOS. Ann. Acad. Sci 687.(1993).
- Peppard H. Marfori J. Nestler J. Prevalence of PCOS among woman with type 2 diabetes .Dia.Care 24.(2001).
- Marx T. Mehta A. Polycystic ovary syndrome: pathogenesis and termentover the short and long term. Clin.J.Medic.70.(2003).
- Dunaif A. Insulin resistance and the PCOS :mechanism and implications for pathogenesis .Endocrinol Rev.18.(1997).
- Ledingham J. Warell D. Concise oxford textbook of medicine .Oxford (2000).
- Juvonen T. Lajunen H. Polymorphisms CETP gene loci in woman with PCOS .J. lipids Res.36:804-812.(1995)
- Karen K. Kunt B. and Jan S. Transvascular LDL-C transport in patients with NIDDM. Arteriosclerosis;22:1168.(2002)
- Eduardas A. Nadežda L. Laura S. Multiple primary cancers: a case of successful treatment . acta medica lituanica. vol. 16. P. 47–51. (2009).
- Kapoor D. Jones T. Smoking and hormones in health and endocrine disorders . Euro. J. of Endocrinology. 152. 491–499 (2005).
- Anders C. E . A Geographical Analysis of Preventative Dietary Micronutrients :The Vancouver Island Hereditary Brest and Ovarian Cancer Research. Uni. of Victoria. (2004).
- Murray R. Gramner D and Rodweu W. Harper's Biochemistry 25th ed .Appleton and Lange ,USA :150-160.(1996)
- Al-Tamer Y. and Al-Juraisy A. Lipids component and fatty acid composition of Iraqi subjects who smoke and consume dairy products .Nurt. Metab. Cardiovasc. Dis.14:94-96.(2004)
- Mohr G. Kritz D. and Barret E. Plasma lipids and PCOS disease .Am. J .Epidemiol.,134:78-85.(1991)
- Scragg R. and Oliver J. Plasma lipids and insulin in PCOS disease. Br.Med.J.289:521-525.(1984)
- Cate S. and Helsu D. Trans fatty acids increase the risk factor of gallstone and PCOS disease .General Health News .(2005)
- Vessby B., Boberg M. and Andersson A. Desaturation and elongation of fatty acids and insulin action. Annals. of New York Academy of Sci., 967: 183-195.(2002)
- Shuo D. Kazuhisa U. and Ying F. The role and mechanism of fatty acids in some disease . Hepatobiliary pancreat Dis. Int.4:399-402.(2007)

Author Information

Abd-Alkream .H.Ismail

Department of Biology
College of Education
Mosul University, Mosul / Iraq
Contact E-mail:m.7186@yahoo.co.uk

Mohamed A.H.Jasim

Department of Chemistry College of Education
Mosul University, Mosul / Iraq

Shaima'a A.H.Jasim

Department of Physiology
Nineveh College of Medicine
Mosul University, Mosul / Iraq

Urea Containing Coated Cu and Zn: A Suitable Fertilizer for Healthier Growth of Rice and N-Uptake

Saima Kalsoom BABAR
Sindh Agriculture University

Mohammad Khanif B. YUSOP
Universiti Putra Malaysia

Innayatullah RAJPUR
Sindh Agriculture University

Naheed Akhtar TALPUR
Sindh Agriculture University

Abstract: Micronutrient deficiency is predominant globally hence a hurdle to achieve healthy crop growth and ultimately the yield. Malaysian acidic soils are also in same occurrence of micronutrient insufficiency because of subsidized (macronutrients) fertilizer performs. Repetitive fertilizer practices without retrieving nutrient contents in the soil may result on the growth and quality of rice. In this regard a pot experiment was organized on two soils; Kedah and Kelantan the main rice growing areas of Malaysia. The aim was to evaluate the effects of Cu and Zn coated urea on rice growth and N-uptake. Copper (at the rate of 3 & 5 kg ha⁻¹) Zn (at the rate of 7 & 10 kg ha⁻¹) as single and combined together, wrapped with coated and un-coated urea along with the suggested doses of NPK; 140, 70 and 70 kg ha⁻¹ respectively were applied. Application of coated urea in combination of Cu and Zn had positive effect on all the growth parameters, chlorophyll contents and N-efficiency in acidic soils. Mean comparison between treatments showed, the significant effect of combined (Cu and Zn) coated urea as compared to individual surface application of Cu and Zn. The growth parameters increment was recorded by 30-40% over control. Furthermore, the N, Cu and Zn contents in the soils along with chlorophyll contents in rice plants were also increased significantly ($p < 0.05$) in combined Cu and Zn coated urea applied soils over control. This increase in growth parameters is a confirmation of Cu and Zn coated urea application for better rice yield.

Keywords: Coated urea, Copper, Zinc, Paddy, Acidic soils

Introduction

The world's population with food and fiber demand is increasing at an alarming rate. It supposed to be 35% more population than the current 6.9 billion by the year 2050 (Ennis et al., 2011). Rice is the main staple food of the world's population. More than 50 percent people depend on this basic staple food. Therefore making it affordable for the poor is particularly decisive (Godfray et al., 2010). Among the leading 25 rice producing countries, Malaysia in one of them with an annual production 2.51 million metric tons (Stat). Rice known as a meal for the entire population in Malaysia too, but its production is limited to specifically designated areas. These designated areas called as granary areas of Malaysia which consisting on eight parts (Kamaruddin, et al., 2013). The Malaysia is still far behind the target of self- sufficiency in rice production. There are the numbers of factor affecting on Malaysia's self-sufficiency in rice production; among them the most commonly observed one is imbalance fertilizer practices. The application of NPK fertilizers along with intensive cultivation of high yielding varieties have been ultimately resulted in micronutrients deficiencies in soil and plants (Cakmak, 2002). Worldwide, the reports have proven inadequacy of Zn, Cu and Fe as compared to the rest of the other

- This is an Open Access article distributed under the terms of the Creative Commons Attribution-Noncommercial 4.0 Unported License, permitting all non-commercial use, distribution, and reproduction in any medium, provided the original work is properly cited.

- Selection and peer-review under responsibility of the Organizing Committee of the Conference

micronutrients. Rice is sensitive to micronutrients, deficiency of such nutrients in rice can cause drastic decline in production and become major constraints to productivity, durability and unremitting life of soils (Bell and Dell, 2008). Malaysian soils are acidic in nature and are expected to no deficiency for micronutrients. Rice farmers in the certain regions applied the subsidized fertilizer, virtually without micronutrient fertilizer application. However the facts have proven the micronutrients deficiency (zinc and boron) in Malaysia and the affirmative application of these micronutrients in the form of fertilizer have eventually enhance rice production (Hafeezullah, 2010; Saleem et al., 2010).

Micronutrients are involved in the number of indispensable processes in plant. In particular, micronutrients Cu and Zn are required for numerous essential progressions especially in cereals. Rice plant is unable to complete its biochemical processes, such as synthesizing of nucleotide and cytochrome; auxin metabolism and producing chlorophyll; as well as activating enzymes and maintenance of membrane integrity. The copper serves as effector, stabilizer and inhibitor, and also as catalyst of oxidation reaction in the plant. It is particularly important in N, proteins and hormone metabolism. At the same time, it is involved in photosynthesis and respiration a mechanism which ultimately affects pollen formation and fertilization (Dobermann and Fairhurst, 2000). Thus the current study was designed in such a manner, so can cover the important aspects of micronutrient coated fertilizer on the growth and N-uptake of rice plant. The objectives of this research are to compare the response of coated and un-coated urea with Cu and Zn on the growth components of rice and on N-efficiency along with its effect on micronutrients availability.

Method

The experiment was conducted in the glasshouse of Universiti Putra Malaysia on two different soil series. Cempaka (riverine alluvium) Kelantan, located on the latitude of 05-97370N and longitude of 102-29944, and Kuala Kedah (marine alluvium) Kedah located on the latitude of 06-13422N and longitude of 100.29527E on Global Positioning System (GPS). Twenty days old seedlings of rice variety MR-219 were transplanted in the pots. The pots were arranged in Randomizes Complete Block Design (RCBD) with three replications. Copper (Cu) and zinc (Zn) either alone or in the combinations were applied in the form of surface application and coated with urea.

Treatments detail

There were seventeen treatments used; control (without Cu and Zn application), Cu (3 kg ha⁻¹ and 5 kg ha⁻¹) in the form of CuSO₄, Zn (7 kg ha⁻¹ and 10 kg ha⁻¹) in the form of ZnSO₄ with and without coating of urea. The recommended doses of NPK in the form of urea, triple super phosphate, muriate of potash at the rate of 140, 70 and 70 kg ha⁻¹ has been applied. Each pot filled with the 10 kg of soil. The soil conditions were leveled before sowing. The big soil clods broken with hands in each pot and soil remained saturated for one week.

Observations

Plant growth parameters; plant height (cm), number of tillers plant⁻¹, number of panicle plant⁻¹, panicle length plant⁻¹, panicle weight (g), and nutrients contents were determined (Dobermann and Fairhurst, 2000). These observations were taken from each treatment with three imitates. Average of each parameter was elaborated for the further analysis.

Soil analysis

Soil texture was determined by the pipette method (Gee and Bauder, 1986). Soil pH examined in soil-water solution 1:1 (v/w) using PHM210 Standard pH meter (Jones Jr, 2001). Total N was determined by employing the Kjeldhal method (Bremner and Mulvaney, 1982). Soil available P was extracted by using Bray and Kurtz #2 (Bray and Kurtz, 1945). Ammonium extractable K (Hanway and Heidel, 1952) was assessed by flame photometry. Soil available Cu and Zn contents were obtained by using Mehlich-I (soil to water ratio 1:5, soil 5g and 25 mL of double acids; 0.05 N HCl and 0.025 N H₂SO₄) shaking time 15 minutes at 180 rpm used mechanical shaker, contents were determined on Atomic Absorption Spectrophotometer (Jones Jr, 2001).

Chlorophyll contents

A leaf chlorophyll content (SPAD) value was determined at middle of the growth period of rice plant. In this regard a portable chlorophyll meter (MINOLTATM SPAD-502) was adopted (Peterson, 1993) to record the values. From each treatment the youngest fully expanded leaf (YEL) pot⁻¹ was selected for the observation. The amount of the green color in the leaf tissue is illustrated by the SPAD readings which is associated with the actual chlorophyll content of the leaf tissue.

Plant analysis

To evaluate the nutrient contents in rice plants; one plant pot⁻¹ was selected at the middle growing stage of rice. Plant samples were properly washed with distilled water and dried on the room temperature, as the moisture contents dries up the samples were placed in the oven at 65°C for 48hours. Plant tissue samples were ground after they completely dries up. Determination of Cu and Zn was done with dry ashing method of plant analysis. In this regard 0.25 g of tissue (placing in furnace for 6 hours to make it in the ash form) was taken and added 2 mL of concentrated hydrochloric acid (HCl) and 10 mL of 20% nitric acid (20 mL HNO₃ + 100 mL of distilled water (D.W)) in to it. Samples were placed in water bath for one and half hour to let them dry. Then samples were diluted with D.W and the final volume made at 50 mL in volumetric flask. The filtered extract was analysed on Atomic Absorption Spectrophotometer. For N analysis, Kjeldhal procedure was followed (Jones Jr, 2001).

Statistical analysis

The data were statistically analyzed by using Statistix version 8.1. Analysis Of Variance (ANOVA) of Randomized Complete Block Design (RCBD) was carried out followed by the mean comparison of Tukey's range test at 5% level of confidence to estimate the treatments effect over control.

Results and Discussion

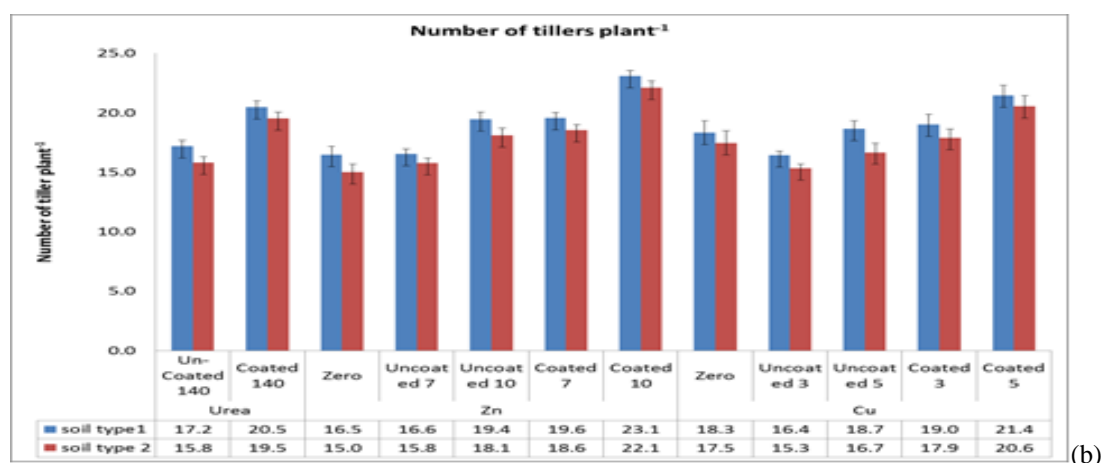
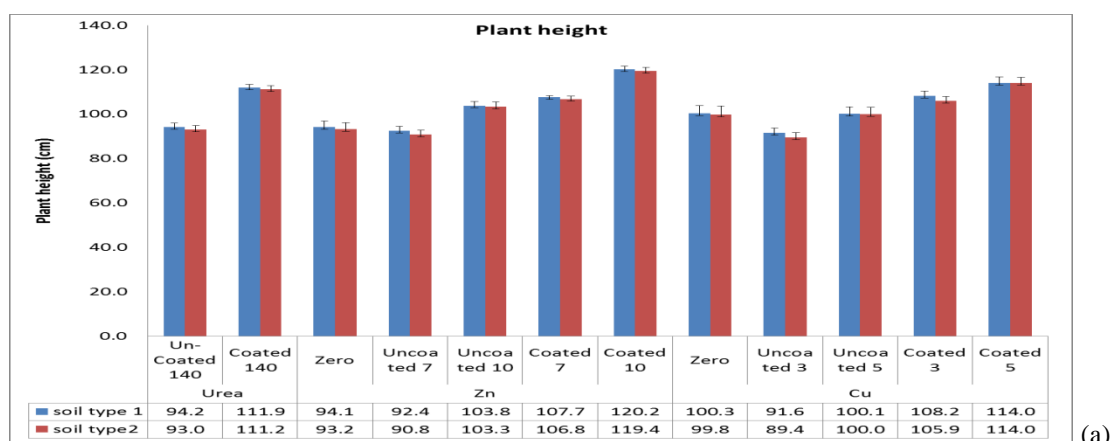
The soils from Kedah are generally derived from marine alluvium and Kelantan plains are derived from riverine alluvium. Both soils have distinct soil characteristics in terms of physical and chemical properties. The soil texture of riverine alluvium belt of Kelantan soil is mostly found loamy, whereas the marine belt from Kedah has more clay contents in their textural class. Micronutrients nonexistence have reported earlier in Kelantan plains (Soo, 1975) and similar conditions were found so in Kedah (Hafeezullah, 2010; Saleem et al., 2010). The results from the current research revealed the Cu and Zn deficiency in respective soils of Kelantan and Kedah (Table 1). Analysis of the other macronutrients found to be normal. The soil-1 represents soil series Chempaka (riverine alluvium) from Kelantan, whereas soil-2 characterizes the soil series Kuala Kedah (marine alluvium) Kedah in Table 1. The application of particular micronutrient (Cu and Zn) had positive effect on the growth and yield of rice and its quality (Liew et al., 2010). The role of zinc on cereals have already renowned and admitted. As rice is sensitive to Zn deficiency its application in the form of fertilizer significantly affects cereal's production. The deficiency of zinc may cause a drastic decline in the rice growth and yield (Alloway, 2004). Furthermore, an appropriate amount of micronutrients is decisive for the human health as well as for normal plant growth. Micronutrient Cu and Zn play an important role in the form of different mechanisms; as they regulate the enzymatic activities. Copper is required for the synthesis of lignin and act as a primal factor for N, protein and hormonal metabolism of plants. It serves as catalyst for photosynthesis, respiration, pollen formation and fertilization in rice (Dobermann and Fairhurst, 2000).

Table 1. Soil physical and chemical characteristics before planting rice
Soil Physical characteristics

Texture	Chempaka Clay loam	Kuala Kedah Silty clay
Soil Chemical Characteristics		
pH	5.12	5.29
Total N %	0.18	0.15
Extractable P mg kg ⁻¹	20.5	21.9
Exchangeable K cmol (+) kg ⁻¹	0.18	0.17
Zn mg kg ⁻¹	0.90	1.10
Cu mg kg ⁻¹	0.11	0.15

Effect of Cu and Zn Coated Urea on the Growth of Rice

Results showed that Cu and Zn coated urea significantly affected on all the growth parameters of rice along with the chlorophyll contents and nutrients uptake. It was manifested that the rice growth parameters in terms of plant height (cm), number of tillers plant⁻¹, number of panicles plant⁻¹, panicle length plant⁻¹ and panicle length panicle⁻⁵ positively responded towards Cu and Zn coated urea (Figure 1 (a to e)).



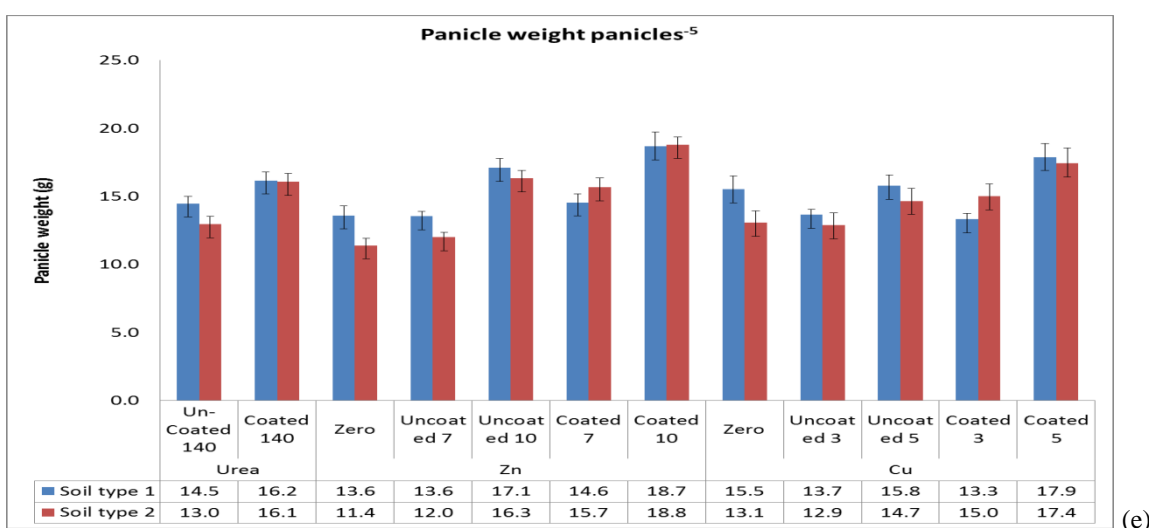
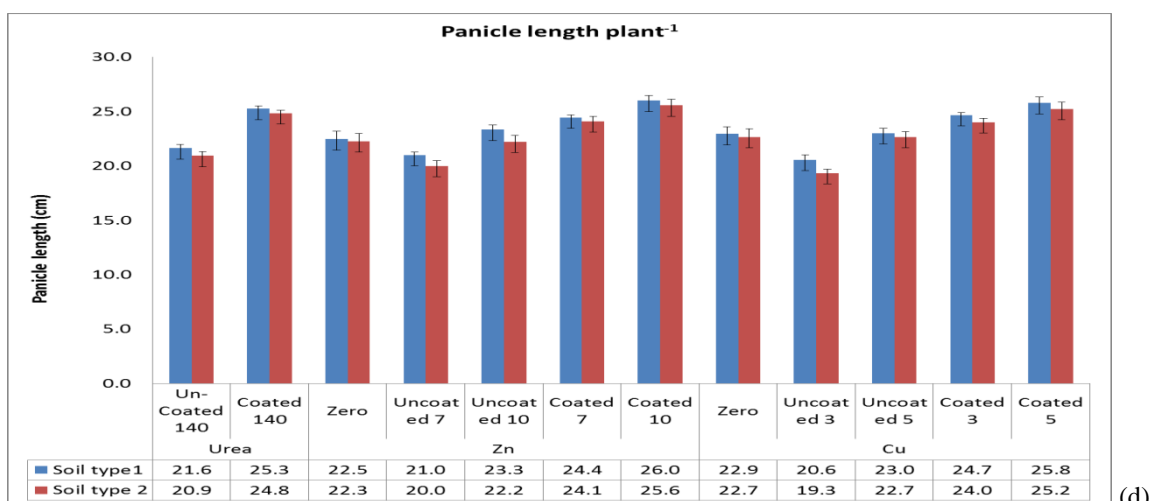
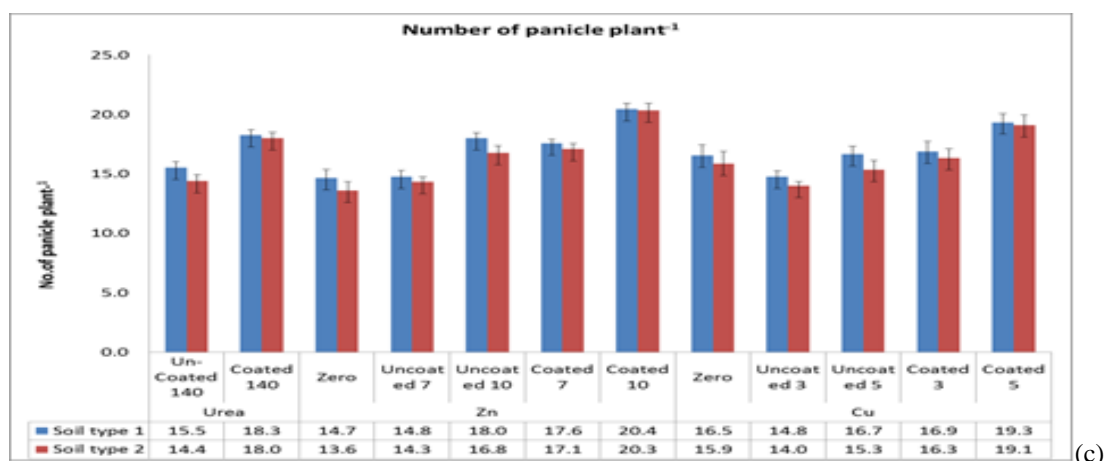


Figure 1. Effect of Cu and Zn coated urea on growth parameters of rice; (a) plant height (cm), (b) Number of tillers plant⁻¹, (c) Number of panicles plant⁻¹, (d) panicle length plant⁻¹, (e) panicle weight plant⁻¹.

Comparison between control and Cu and Zn (coated with urea and surface application) found significant difference among the various treatments. The results are in accordance with research conducted in Malaysia, where the researchers have applied combined Zn, Cu and Mo and individually. It was observed that the growth and yield of rice significantly affected with the application of combined micronutrients (Panhwar et al., 2015). The highest plant height (120cm) was observed from Cu and Zn coated urea. Significantly the higher number of tillers plant⁻¹ (23), number of panicle plant⁻¹ (21), panicle length plant⁻¹ (26cm) and panicle weight panicle⁻⁵ (19g) were recorded from combined Cu and Zn coated urea. The micronutrient either applied in single attribute

or in combined form can increased the growth and yield of rice. The current research has proven the progressive approach of Cu and Zn coated urea. Coating helps the fertilizer to dissolve gradually in the flooded rice soils. The synergetic influence of micronutrients can effect on the convenience of macronutrient in the soil. This action can enhance the photosynthetic activity of plant which eventually outcome with improved rice yield (Merrill and Watt, 1973). The results from the present studies are in the accordance with the research held on the role of Zn fertilizer on grain yield and some quality parameters in Iranian rice genotypes. Micronutrient application affected rice growth and interaction among micronutrients uptake, dispersal and application (Yadi, Dastan and Yasari, 2012). The special feature with the application of Zn was observed as antagonism with Fe (Imtiaz et al., 2010). The increment of Zn application in rice plant enhanced the availability of Zn and also the N-uptake (Wei, Shohag and Yang, 2012). Therefore, the highest mean values of growth and yield attributes can be possible from combined Cu and Zn application (Kumar et al., 2011) transplanting. Among the treatments, the higher values were found from the treatment that contains combination of Cu and Zn as compared to surface application of micronutrients and in an individual form. The mean values showed that the chlorophyll contents were ranged at 38.7 to 41.3 from the coated urea which is higher than the 35.8 recorded at uncoated micronutrients treatment.

Antioxidant and photosynthetic activities of higher plants can be affected by the presence of heavy metals. Soil and Plant Analyzer Development (SPAD) used as an indicator for assessing the chlorophyll contents of plant through leaves. The SPAD values were recorded lower in the control than the treatment contains Cu and Zn coated urea (Table 2). Combined Cu and Zn coated urea helped plants to absorb more N due to their synergistic effect and N-protein synthesis therefore, the chlorophyll increased with the application of combined Cu and Zn coated urea. The similar results were obtained in wheat crop, where micronutrients were applied with the variable rates of N, the SPAD values were improved (Shi et al., 2010).

Table 2. Effect of Cu and Zn coated urea on chlorophyll contents

	Treatments	Chlorophyll contents
Uncoated Urea	NPK (control)	33.833 g
	Zn10	35.667 f
	Zn7	34.000 g
	Cu5	36.500 ef
	Cu3	35.667 f
	Zn10+Cu5	37.667 de
	Zn7+Cu5	36.167 ef
	Zn10+Cu3	36.500 ef
	Zn7+Cu3	36.500 ef
Coated Urea	Zn10	40.167 b
	Zn7	38.500 cd
	Cu5	39.50 bc
	Cu3	38.333 cd
	Zn10+Cu5	41.833 a
	Zn10+Cu3	38.833 bcd
	Zn7+Cu5	38.833 bcd
	Zn7+Cu3	39.000 bcd

Means with the same letters in column are not significantly different from each other ($p>0.05$)

Factor	F-value	P-Value	HSD Value
Treatments	46.05	0.0000	1.617

Consequences of Cu and Zn coated urea on availability of N, Cu and Zn

The micronutrient contents along with N-uptake varied with treatment effect. The significant higher values of micronutrients were found from combination of Cu and Zn coated with urea (Table 3). The application of

micronutrient coated urea enhanced the N-uptake in rice plant. The concept behind the application of coated urea is slow release of urea in sub-merged conditions of rice soils. Hence the MNCU can minimize the nutrient losses and can able to provide the nutrients according to the need of the crop (Azeem et al., 2014). Zinc addition increased the Zn uptake in grain and straw, that simultaneously enhance the N-uptake (Wei et al., 2012). The results manifested that the MNCU enhance the nutrient uptake; Cu, Zn and N respectively.

Table 3 Nitrogen, Cu and Zn contents after application of Cu and Zn coated urea

Soil Chemical Characteristics	Soil1	Soil2
Total N %	0.25	0.23
Soil available Zn mg kg ⁻¹	2.50	2.25
Soil available Cu mg kg ⁻¹	1.51	1.65

Conclusion

The application of Cu and Zn coated urea in the combination along with the recommended doses of NPK significantly affected on the marine and riverine alluvium of Malaysian soils. All the growth parameters of rice plant, chlorophyll contents and nutrients availability increased with the application of combined Cu and Zn coated urea. Application of Cu and Zn coated urea can reduce the N-losses and enhanced its uptake. Consequently, there is a strong reasoning for the application of combined Cu and Zn coated urea, due to their synergetic effect with other nutrients in the flooded conditions of rice soils.

Recommendations

Controlled release urea can reduce N-losses by slowing its hydrolysis rate and enhance the N-contents. This experiment revealed that urea coated with Cu and Zn improved the efficiency of urea. Copper and Zn served dual role: 1) urease inhibitors and 2) essential micronutrients. Therefore, for obtaining the desired yields of rice, Cu and Zn coated urea should be applied in the rice soils across the world.

Acknowledgements

Authors are highly thankful to Higher Education Commission of Pakistan for the financial assistance to present this work at ICRES, Marmaris Turkey.

References

- Alloway, B. J. (2004). *Zinc in soils and crop nutrition*, International Zinc Association Brussels, Belgium.
- Azeem, B., Kushaari, K., Man, Z. B., Basit, A. and Thanh, T. H. (2014). Review on materials & methods to produce controlled release coated urea fertilizer. *Journal of Controlled Release* 181: 11-21.
- Bell, R. W. and Dell, B. (2008). *Micronutrients for sustainable food, feed, fibre and bioenergy production*, International Fertilizer Industry Association (IFA).
- Bray, R. H. and Kurtz, L. (1945). Determination of total, organic, and available forms of phosphorus in soils. *Soil Science* 59: 39-46.
- Bremner, J. and Mulvaney, R. (1978). Urease activity in soils. *Soil Enzymes* 501: 149-196.
- Cakmak, I. (2002). Plant nutrition research: Priorities to meet human needs for food in sustainable ways. In *Progress in Plant Nutrition: Plenary Lectures of the XIV International Plant Nutrition Colloquium*, pp. 3-24. Springer Netherlands.
- Dobermann, A. and Fairhurst, T. (2000). *Rice: nutrient disorders & nutrient management* (Vol. 1). Int. Rice Res. Inst.
- Ennis, S.R., Ríos-Vargas, M. and Albert, N.G. (2011). *The Hispanic population: 2010*, 4.
- Gee, G. W., Bauder, J. W. and Klute, A. (1986). Particle-size analysis. *Methods of soil analysis. Part 1. Physical and Mineralogical Methods*, 383-411.
- Godfray, H. C. J., Beddington, J. R., Crute, I. R., Haddad, L., Lawrence, D., Muir, J. F., Pretty, J., Robinson, S., Thomas, S. M. and Toulmin, C. (2010). Food security: the challenge of feeding 9 billion people. *Science* 327: 812-818.

- Hafeezullah, B. (2010). *Evaluation of Malaysian Rice Genotypes for Adaptability in Zinc Deficient Soil*, PhD Thesis, Universiti Putra Malaysia.
- Hanway, J. and Heidel, H. (1952). Soil analysis methods as used in Iowa state college soil testing laboratory. *Iowa Agriculture* 57: 1-31.
- Imtiaz, M., Rashid, A., Khan, P., Memon, M. and Aslam, M. (2010). The role of micronutrients in crop production and human health. *Pakistan Journal of Botany* 42: 2565-2578.
- Jones Jr, J. B. (2001). *Laboratory guide for conducting soil tests and plant analysis*, CRC press.
- Kamaruddin, R., Ali, J. and Saad, N. M. (2013). Happiness and its influencing factors among paddy farmers in Granary Area of Mada. *World Applied Sciences Journal* 28: 91-99.
- Kumar, M. and Babel, A. (2011). Available micronutrient status and their relationship with soil properties of Jhunjhunu Tehsil, District Jhunjhunu, Rajasthan, India. *Journal of Agricultural Science* 3 (2): 97-106.
- Liew, Y., Omar, S. S., Husni, M., Abidin, M. Z., and Abdullah, N. (2010). Effects of micronutrient fertilizers on the production of MR 219 rice (*Oryza sativa* L.). *Malaysian Journal of Soil Science* 14: 71-82.
- Merrill, A. and Watt, B. (1973). Agriculture Handbook No. 74. *Agricultural Research Service, United States Department of Agriculture*.
- Panhwar, Q. A., Naher, U. A., Radziah, O., Shamshuddin, J., Mohd Razi, I., Dipti, S. S. and Karabalei Aghamolki, M. T. (2015). Quality and antioxidant activity of rice grown on alluvial soil amended with Zn, Cu and Mo. *South African Journal of Botany* 98: 77-83.
- Peterson, T. A., Blackmer, T. M., Francis, D. D. and Schepers, J. S. (1993). G93-1171 Using a Chlorophyll Meter to Improve N Management. *Historical Materials from University of Nebraska-Lincoln Extension*, 1353.
- Saleem, M., Khanif, Y., Fauziah, I. C., Samsuri, A. and Hafeez, B. (2010). Boron Status of Paddy Soils in the States of Kedah and Kelantan, Malaysia. *Malaysian Journal of Soil Science* 14: 83-94.
- Shi, R., Zhang, Y., Chen, X., Sun, Q., Zhang, F., Römheld, V. and Zou, C. (2010). Influence of long-term nitrogen fertilization on micronutrient density in grain of winter wheat (*Triticum aestivum* L.). *Journal of Cereal Science* 51: 165-170.
- Soo, S. W. (1975). *Semi-detailed Soil Survey of the Kelantan Plain*, Ministry of Agriculture and Rural Development, Malaysia.
- Wei, Y., Shohag, M. and Yang, X. (2012). Biofortification and bioavailability of rice grain zinc as affected by different forms of foliar zinc fertilization. *PLoS one*, 7(9), e45428.
- Yadi, R., Dastan, S. and Yasari, E. (2012). Role of zinc fertilizer on grain yield and some qualities parameters in Iranian rice genotypes. *Annals of Biological Research* 3: 4519-4527.

Author Information

Saima Kalsoom Babar

Department of Soil Science,
Sindh Agriculture University Tandojam
70060, Pakistan
Contact e-mail: skbabar@sau.edu.pk

Mohd. Khanif B. Yusop

Department of Land Management
Universiti Putra Malaysia, 43400, Serdang, Selangor, Darul
Ehsan, Malaysia

Innayatullah Rajpar

Department of Soil Science, Sindh Agriculture University
Tandojam, 70060, Pakistan

Naheed Akhtar Talpur

Department of Soil Science, Sindh Agriculture University
Tandojam, 70060, Pakistan

Dormancy Breaking Studies of Dodder (*Cuscuta* spp.) was Problem in Greenhouse Tomato

Tamer USTUNER

Sütçü Imam University

Samet CAKIR

Sütçü Imam University

Abstract: Tomato cultivation was in the first place with 619.877 tons in the glass greenhouse in the Mediterranean region. Tomato production was ranked first with 437 tons while cucumber production ranked second with 48 tons in Kahramanmaraş (Anonymous 2015a). Many problems such as diseases, weeds and pests are encountered in greenhouse tomato cultivation. One of the most important of these problems is the weeds. One of the foreign weeds, Dodder (*Cuscuta* spp.) is a parasite plant and the most difficult to control. When you do not control with Dodder (*Cuscuta* spp.), economic loss occurs 100% in tomato yield and quality. It has been diagnosed that it is a dodder (*Cuscuta campestris* Yunck.) in tomato growing in the glass greenhouse of the Agriculture Faculties. Since the dodder seeds have dormancy, various attempts have been made to break this dormancy. Methods of breaking dormancy on dodder seeds; low temperature application was carried out at 3.5°C for 80 days, in deep freezer at -200°C for 24 hours, in pure water for 72 hours, kept at room temperature 26°C for 284 days and 1% Sulfuric acid (H₂SO₄) was applied to the seeds of the dodder for 3 minutes. From these applications dodder seed germination was observed only in sulfuric acid applications.

Keywords: Greenhouse tomato (F1 yaren tomato), Dodder, Dormancy and breaking methods

Introduction

Tomato is one of the most commercially produced vegetables in the world (Gaware et al. 2010). Total tomato production in the world has risen to over 159 million tons in 2015. Turkey, in tomato production in the world with 11.0034 million tons in China, India and the United States took place after the fourth (Anonymous 2015b). Mediterranean region in terms of greenhouse tomato production in Turkey with 619 877 tonnes in 1st, while cucumber production took place in 2nd with 328 889 tonnes. In Kahramanmaraş, greenhouse tomato production was ranked first with 437 tons while cucumber was ranked 2nd with 48 tons (Anonymous 2015a).

Feeding the rapidly increasing world population depends on sustainable growth of agricultural production, which depends not only on cultural practices such as selection of varieties, fertilization and irrigation but also on the protection of crops from pests and weeds. (Özer et al. 2001). Therefore, it is not possible to achieve the desired level of efficiency without controlling plant protection factors including disease, insects and weeds. Weeds in the most important plant protection factors are defined as plants that are grown in the place where the human beings do not want it (Uygur et al. 1984). Thanks to their competitiveness, allelopathic effects, vegetative and generative reproduction and genetic diversity, weeds can adapt to very different ecosystems and cause great productivity and quality losses in agricultural areas. It also affects culture plants with its parasitic effects and damages the cultivated plants by interfering with diseases and harmful organisms. By entering the competition of light and water with weeds, the weeds delay the ripening of the tomato juice. In addition, the nutrients such as nitrogen (N), phosphorus (P), potassium (K), magnesium (Mg) and iron (Fe) are consumed in the soil more than weeds in comparison to the tomatoes thus negatively affecting tomato yield and quality. Parasitic plants are plants that require a host vegetable in some part of their life. *Cuscuta* species (*Cuscuta* spp.) are, belonging to *Cuscuta* genus, *Convolvulaceae* family, *Solanales* team and plant kingdom,

- This is an Open Access article distributed under the terms of the Creative Commons Attribution-Noncommercial 4.0 Unported License, permitting all non-commercial use, distribution, and reproduction in any medium, provided the original work is properly cited.

- Selection and peer-review under responsibility of the Organizing Committee of the Conference

annual and complete parasitic plant. *Cuscuta* species are holo parasitic plants with white flowers that do not have leaf and chlorophyll. The yellow-orange 0.3 mm diameter strands attach themselves to the shoots and leaves of the host plants with houstonium, which satisfies all nutritional needs. A dodder species gives 3,000-25,000 seeds (Dawson 1984-1994, Fang et al. 1995).

Cuscuta (*Cuscuta* spp.) is a complete parasitic plant that surrounds the plant and prevents it from physiological activities such as sunning, aeration, development and growth, thus causing the crop plant to become weak and yield and quality decrease considerably. Dodder has been reported to damage the trunk and leaves of several dicotyledon plants, and sometimes monocotyledonous plants. It has also been found that a mature berry cultivated seed can survive for 10-20 years in the soil, replicating with seeds and plant parts. Technically, there are many ways to increase production in agricultural products. One of them is the ability to control weeds with modern plant protection methods. It has been reported that the weights and the prevalence levels of weeds' biology, ecology, relations with culture plants, and control methods of weeds should be well known (Özer 1993, Özer et al. 1998, Türe and Köse 2000).

Davis (1978) in a study conducted in Turkey, where the taxon *Cuscuta* 21, the two types of Kahramanmaraş was reported to spread naturally. Because it lives as a parasite, it causes the growth of the culture plant to be impaired, stopped or even killed. It prevents the activities such as growth and growth by wrapping the plants around (Lubenov 1985; Kadioglu 1992). According to the results of the researches on the spreads of host species of dodder and the hosts in Anatolia; The different three were found to be parasitic on culture plants. such as (*Cuscuta campestris* Yunck., (*C. approximata* Bab. and *C. monogyna* Vahl.) in addition to these, *C. arvensis* was also found and the hosts were found to be sugar beet, onion, clover and cottage vegetables (Nemli 1986). Cali et al. (1993) reported that dodder plays a role in the transport of some viruses by forming a bridge between diseased plants and healthy plants. In Anadolu, 55 hosts of *C. campestris* have been identified. It was determined that 27 of the plants, mostly grassy, are agricultural plants. The most common types are hosts of Dodder; *Beta vulgaris* L. (beet), *Medicago sativa* L. (clover), *Trifolium* spp. (onion), *Daucus carota* L. (carrot), *Pimpinella anisum* L. (anise), *Carum carvi* L. (cumin), *Vicia faba* L. (bean), *Capsium annuum* L. (pepper), *Allium cepa* L.), *Nicotiana tabacum* L. (tobacco), *Vicia sativa* L. (vetch), *Solanum melongena* L. (eggplant), *Cicer arietinum* L. (chickpea), *Asparagus officinalis* L. (asparagus), *Vitis vinifera* L. (grape), *Cucumis melo* L. (melon), *Solanum tuberosum* L. (potato), *Lycopersicon esculentum* Mill. (Tomato) and some ornamental plants (Nemli 1978, Parker and Riches 1993, Dawson et al. 1994). In the Isparta region, weeds, which are also a problem in tomatoes; *Chenopodium album*, *Portulaca oleraceae*, *Agropyron repens*, *Echinochloa crus-galli*, *Xanthium strumarium*, *C. campestris* and *Sinapis arvensis* (Yardımcı et al. 2000). Weed species that are problematic in Tokat province tomato planting areas; It has been reported that 49 species belong to 25 families. These species are *Convolvulus arvensis*, *Amaranthus retroflexus*, *E. crus-galli*, *Cyperus rotundus*, *P. oleracea*, *C. album*, *Sorghum halepense*, *Setaria viridis*, *Orobanch* spp., *Solanum nigrum* and *Cuscuta* spp. (Sirma et al. 2001). Single annual broadleaf in general in both field and greenhouse tomatoes in Turkey should constitute weed problem. Propolisamide, which is licensed in alfalfa and sugar beet together with cultural precautions in the domesticated Broomrape (*Orobanch* spp), dodder (*Cuscuta* spp.). Challenge, only chlorpromine is used, which is licensed in the Alfalfa. However, these herbicides are not licensed in domestication in our country (Günçan and Karaca 2014). 32 species belonging to 17 families were detected in the tomato surveys in the Lice district of Diyarbakır. In the region; *A. retroflexus* L. (4.63 plant/number m²), *C. arvensis* L. (4.09), *S. halepense* (L.) Pers. (4.06), *S. nigrum* L. (3.37), *E. colonum* (L.) Link. (3.04), *C. album* L. (1.88), *P. oleracea* L. (1.73), *E. crus-galli* (L.) P.B. (1.72) with holo parasitic plants, *Phelipanche ramosa* (L.) Pomel (3,73) and *Cuscuta* spp. (1.61) were detected high dense (Özaslan and Kendal 2014.).

It is stated that the lycopers with parasitic plant characteristics which cause the most economical damage by causing loss of yield in cultivated plants worldwide are most damaging to clover, clover, tomato, carrot, onion, sugar beet, potatoes, legumes, garlic, watermelon and pepper. It has also been reported that this harm occurring in cultivated plants varies between 50-90% in some cases (Nadler-Hassar and Rubin 2003, Lanini and Kogan 2005). There is a very large host mass. These families, Asteraceae, Convolvulaceae, Solanaceae, Fabaceae, Brassicaceae (Lian et al. 2006). Dodder cause 20-57% loss of crops in feed plants, while sugar beet yields decrease by 3.5-4 tons / ha (Aly et al. 2003). Konieczka et al. (2009) reported that it could cause 30-100% loss of product in carrot. Dodder also causes significant yield reductions in different cultivated plants, yield decreases were 60-65% in red berry, 86% in chickpea, 60-70% in alfalfa and 87% in lentil (Mishra 2009). There are over 200 varieties of 70 varieties all over the world (Costea and Stevanovic 2010).

C. campestris, which has a wide geographical distribution in the world, causes severe damage to carrots, clovers, sugar beets, onions, legumes, melons, watermelons, potatoes and many other cultivated plants (Dawson et al. 1994, Holm et al. 1997, Parker and Riches 1993, Press et al. 1990).

C. campestris has spread all over the world from North America. Dodder seen in such as Asian continent (Afghanistan, Bahrain, Bangladesh, China, India, Indonesia, Iran, Iraq, Israel, Japan, Kazakhstan, Korea, Kyrgyzstan, Malaysia, Pakistan, Qatar, Saudi Arabia, Syria, Taiwan, Turkey and Yemen), in Africa (Alabama, Arizona, California, Florida, Kansas, New Jersey, New York), Central America and the United States of America (Algeria, Cameroon, Egypt, Kenya, Libya, Uganda) In the Caribbean (Bahamas, Cuba, Jamaica), South America (Argentina, Chile), Europe; Austria, Belgium, Bulgaria, Cyprus, France, Germany, Greece, Italy, Romania, Slovakia, Spain, the United Kingdom and Oceania; Australia, Victoria, Fiji, New Zealand (Alfarhan 1994, Holm et al. 1997, Irum et al. 2011, Khan and Halim 1990, Gwoinget al. 2005, Lorenzi and Jeffery 1987, Morita, 1997, Parker and Wilson 1986, Parsons and Cuthbertson 1992, Racasens and Conesa 1990, Pier 2008, Yuncker 1932, Zerman and Saghir 1995, Zharasov et al. 2009).

Dodder prevalence of species that are expected to significantly across the world may lead to a significant loss of yield and quality of crops in Turkey. When assessed in these respects, it is of great importance to determine the levels of yield and quality in tomato production areas (*Cuscuta* spp). Bu amaçla, Yaren F1 Tomato planting and Küsküt (*Cuscuta* spp.) Plantations were planted in the planting area of the Kahramanmaraş Sütcü İmam University Agricultural Faculty in the greenhouse area. In this study, it was tried to remove the dormancy by applying the directions of breaking the dormancy to the seeds of the dodder.

Material and Method

Material

The materials of this research; Yaren F1 Tomato and Dodder (*C. campestris* Yunck.); under normal conditions, dodder seed kept at low temperature (at 3.5°C, -20 °C, Sulfuric acid (H₂SO₄), purified water and kept at room conditions (Figure 1, 2).



Figure 1. Yaren F1 tomato seedling in general



Figure 2. Sulfuric acid application to the dodder seed

Method

In Greenhouse Yaren F1 tomato trial pattern; Coincidence is planned according to trial design. Experimental design, 3 blocks and 6 blocks of each blot (Figure 4, 5). The size of the parcels is planned as 5x2 m. Each parcel has a margin of 2m between 1m blocks.

Each parcel is planned to have 4 rows and a row spacing of 45 cm and a row of 40 cm.

Planting Tomato Seedling

Tomatoes, peppers and eggplants in the summer vegetables group are one year in warm climates and several years in tropical climates. Tomato seedling was planted in places previously prepared with hand-hoe and then juice was given (Figure 3).



Figure 3. Greenhouse Yaren upper throat F1 fertilizing the roots of tomato seedlings

Determining aid intensity scale of dodder: Tomato scavenging rate by Tepe et al. (1997) as the 1-5 scale used is adapted by us on the basis of the tomato plants. Observational evaluations were made on the ground according to the following criteria for this:

- (1) No dodder,
- (2) Less dense (healthy tomatoes and no loss of yield)
- (3) Middle dense (visible damage to the tomato started)
- (4) Dense (significant loss of yield in tomatoes)
- (5) High dense (tomato plant is dead).

In this study, it was aimed to break down dormans with 6 different applications as the seeds of dodder seeds had dormancy. dodder seed collected from 2016 have been subjected to different applications such as;

1- Low temperature to one-dodder seed (3.5⁰C) application; Dodder seed collected from 2016 for 80 days (January 24 - 14 April 2017) duration 3.5⁰C refrigerator was maintained.

2- Dodder seed in the freezer (-20⁰C) application; Dodder seed collected from 2016 for 24 hours (15 April 2017) of the freezer.

3- Pure water application to dodder seed; Dodder seed collected from 2016 for 3 days (12-15 April 2017) of the purified water.

4- Kept at room temperature dodder seed; Dodder seeds collected from 2016 for a period of 284 days (from October 2016) at room temperature (26⁰C) was maintained.

5- Dodder seeds in 1% sulfuric acid (H₂SO₄) application; 2016 dodder seed collected from 3 minutes to a sulfuric acid was applied.

6- Dodder seeds in 1% sulfuric acid (H₂SO₄) application: Dodder seed collected from 2016 6 min with sulfuric acid was performed.

7- Control plot; There is no application in the control parseline.

Different applications to dodder seed (Table1);

Table 1. Greenhouse different dodder compliance test plan

I.Blok	N.T	L.T.	F.A.	P.W.A.	K	S.A(3dk)	S.A.(6dk)
II.Blok	L.T.	N.T	P.W.A.	F.A.	S.A(6dk)	K	S.A(3dk)
III.Blok	F.A.	K	S.A	N.T	L.T.	P.W.A.	C

Abbreviations:

N.T: Normal temperature application

S.A: Sulfuric acid application (3-6 min)

C: Control

L.T.:Low temperature application

F.A.:Freezer application

P.W.A.:Pure water application

Try Someone Different Dodder Compliance Plan in Pots

Yaren F1 test pattern tomatoes in pots;The coincidence is planned according to the trial design.Experimental design, 3 blocks and 6 rows of pots (Table 2).The length of the parcel is planned as 5x2 m.The side effects from each plot from 1m to 2m blocks share allowed. Each parcel is planned to have 6 rows of pots.

Minimum, maximum and average temperature values and average humidity values during the greenhouse tomato growing season are given in Table 3.

Table 2. Greenhouse minimum, maximum, average temperature, humidity and sunshine duration

PARAMETERS	April	May	June	July	August	September	October	November
Average minimum temperature (°C)	17,4	18,3	23,5	26,8	27,9	26,4	21,8	19,7
Average maximum temperature (°C)	32,1	33,0	38,7	39,3	40,5	32,7	30,6	23,5
Average temperature (°C)	24,75	25,65	31,1	33,0	34,2	29,5	26,2	21,6
Average Humidity (%)	70,9	74,6	59,3	60,1	63,4	58,4	54,7	46,2
Monthly total sunbathing time (Hour)	1735,2	188,1	196,5	197,4	199,6	185,3	170,8	162,5

In the greenhouse pot experiment cabin seedling planting and tuber planting are given in Figure 4.

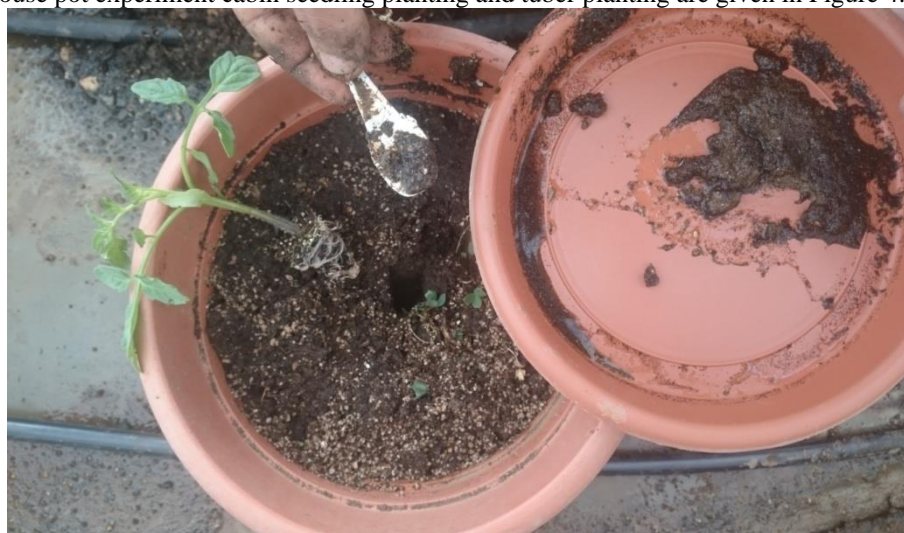


Figure 4. Dodder seed planting with soil and Yaren F1 tomato seedlings

Weeds that are Problematic in Tomato

Income at the beginning of the most irrigated crops during the growing period of tomato. For this reason weeding of weeds can be continuous in tomato growing. Weeds interfere with the tomato juice and nutrients in common and cause yield and quality deterioration.

Holo Parasitic Weeds

Dodder (*Cuscuta* spp.) Definition and Biology

Dodder (*Cuscuta* spp.) Cuscutaceae family and is located in a complete plant parasites (Yuncker, 1932). The plant is an orange-yellowish color, thready and leafless body. Flowers 2-3 mm long, pedicel (flower stalk), short from flower neck, flowers are collected in compact flower buds. Calyx lobes ovate or orbiculate, obtusely overlap each other. Staminal brackets, fibrillate (fringed), long corolla tubular. The stamens are shorter than the corolla lobes, the anthers are the average filament neck. The style is a fine, stigma-shaped round ball. Capsule 3.0-3.5 mm in diameter rounded, with permanent permanent corolla. The cycle of life is seen in three phases, namely the cycle of seed germination, the stage prior to host immobilization, and the stage of parasitic development (host development). In most species of dodder seed coat it is thick. Seeds remain dormant for 5-15 years in the soil. In order for the seeds to germinate, it is necessary to have the necessary soil in the soil.

During germination, the embryo is fed from the endosperm. When the nutrients in the endosperm are exhausted, the root will die and the filamentous body reaching a certain length enters the search for the host. If the host finds the host and keeps it, he will continue his life. It is known that the seeds need 3-5 weeks to grow on host germination. The body wrapped on the host end of the hour hand reaches dodder acting in the opposite direction. From the host-facing surface of the retained gland, the parasite develops hostile ecdysis, and these haustoria contact the host's floem and xylem. Thus the host takes the water, organic and inorganic substances necessary for his life.

Dodder Seed

Dodder seed brings several sayıdaöyle of from 3.000 to 25.000 is a yellow-brown seeds occurred (Figure 5). Seeds spilled on the ground are not capable of germinating immediately. Because the seedlings are very hard and thick structure also has dormancy. When the dormancy is broken and the host's hormone reaches the tohum, it can be germinated at optimum temperature and humidity. When the body emerging from the germinated seeds reaches the soil surface, it is held with forked shoot tips at the lowest branch of the host.



Figure 5. Overview of the dodder seeds

Dodder Root

Dodder does not have roots. The orange body is fed with nutrients from the seed embryo until it reaches the soil surface. When it reaches the surface of the soil, the host begins to feed on the hosts and branches of the host plant through the houstorium. For this reason, this weed lives on many host plants, especially tomatoes, as parasitic plants.

Dodder Stem

The dodder stems are threadlike and have no leaves. Therefore it does not contain chlorophyll. Hostorium is attached to the body and branches of host plants. They are full-parasitic clitoral plants without chlorophyll fed from their bodies by sending houstorium to the host transmission bunches (Figure 6).



Figure 6. After the exit of dodder host to the orientation of tomato roots

Tomatoes in pots in the greenhouse conditions completely diffused state dodder (Figure 7).



Figure 7. Domates saksı olgunlaşma evresindeki küskütün genel görünümü (12.06.2017)

Dodder plants cling to branches and tomatoes to the problem under field conditions are the result of feeding on the leaves of tomatoes is completely hostarium die (Figure 8).



Figure 8. The overall look of the death of dodder and tomato plants under field conditions (12.06.2017)

Dodder flowers

The flowers are small and are collected in the case of kimos flowers. The flower crown is white in color. In flowers, sepals are often combined; usually in five parts and rarely in four or three parts (Figure 9). The stamens are attached to the corolla tube, and most of the species are found in the staminal bracing under the stamens. The ovarium is two carpels, and each carpel has two seeds. The stylus may be combined or discrete, stigmatic, round, disc-shaped, or extended.

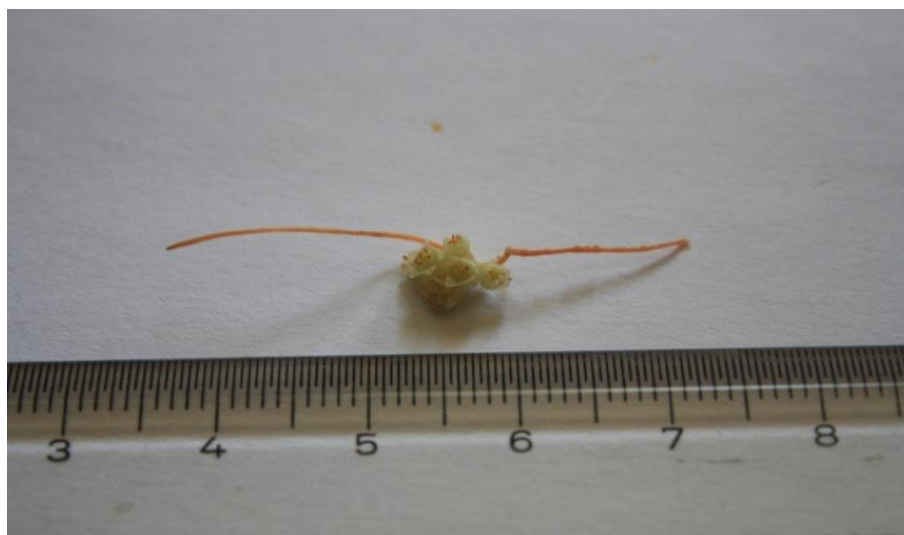


Figure 9. General view of the dodder flowers

Results

This dodder seed, have been identified by us as by examining the flowers and the body features *C. campestris* Yunck. Also in the parcel dodder density is calculated as 30.9. This result is evaluated intensively according to scale 1-5. It has been observed that tomato fruit yield and quality are not very effective when there is little or little density. It was observed that the duration of vegetation of chilled tomatoes was shorter than that of uninfected ones by 2 months. In addition, inflorescences in infected tomatoes were lower than those without infections. At the same time infected tomatoes fruit diameters were found to be lower. Infected tomato weights were found to be lower. It is not only effective in tomato color and moisture content.

Different applications have been made to remove the dormancy feature in the harsh greenhouse and field conditions that are a problem in Yaren F1 tomato production. To dodder seed dormancy breaking of dormancy aimed with 6 different applications. In the research, the seedlings collected from the year 2016 were subjected to different applications. These applications include; -3.5°C , which break the dormancy of -20°C and room temperature and held dodder seed germination was observed, although it is appropriate host. However, only 1% of these applications Sulfuric acid (H_2SO_4) for 3 minutes with the application made dodder seed germination was observed. only 1% of these applications Sulfuric acid (H_2SO_4) for 6 minutes with the application made dodder seed germination was observed. In this application, Sulfuric acid was observed to be completely dried within 3-4 days after reaching to the soil surface because the endosperm in the seed was damaged due to the thinning of the sultanate seed husk which had been kept in Sulfuric acid for 6 minutes. These seedlings are germinated but because the seed coat is too thin, the endosperm does not provide positive results because the nutrients present in the endosperm continue to develop and are not used to inject the seed into the host's body.

As a result, the dormancy of the seedlings can be broken by different methods. In this study, only 1% of these applications gave positive results for Sulfuric acid (H_2SO_4) for 3 minutes with the application.

Discussion

Different applications have been made to remove the dormancy feature in the harsh greenhouse conditions that are a problem in Yaren F1 tomato production. To dodder seed dormancy breaking of dormancy aimed with 6 different applications. These applications include; -3.5°C , -20°C and room temperature and held dodder seed germination was observed, although it is appropriate host. However, only 1% of these applications Sulfuric acid (H_2SO_4) for 3 minutes with 1% of these applications Sulfuric acid (H_2SO_4) for 6 minutes was applied on dodder seed. Only Sulfuric acid (H_2SO_4) for 3 minutes with the application made dodder seed germination.

In the other dormancy breaking methods; *C. campestris* (Lados 1999, Benvenuti et al. 2005), *C. trifolii* (Lados 1999), *C. monogyna* and *C. planiflora* (Salimi and Shahraeen 2000), *C. chinensis* (Marambe et al. 2002), *C. gronovii*, *C. umbrosa*, *C. epithimum* and *C. epilinum* have dormancy (Costea and Tardif 2006). However, the percentages of hard seeds at dispersal can vary from plant to plant *C. campestris* and *C. chinensis* (Marambe et al. 2002). In seeds of many species with PY, it serves as the environmental signal detector for germination and, once dormancy is broken, as the initial route of water entry into the seed (Baskin and Baskin 2000). However, a water gap has not been identified in the genus *Cuscuta* (Convolvulaceae), the only holoparasitic taxon with PY (Baskin et al. 2000). It probably does not have the capacity to change dormancy states, and as such cannot undergo dormancy cycling (Baskin and Baskin 2004). Meulebrouck et al. (2008) found that scarified seeds of *C. epithimum* require a period of cold stratification to break physiological dormancy (PD) of the embryo. Germination of *C. europea* seeds was not facilitated by mechanical scarification or by complete removal of the seed coat.

H_2SO_4 was used to break PY the entire seed coat was damaged (Liu et al. 1981). *Cuscuta campestris* seeds would not be exposed to such high concentrations of H_2SO_4 in nature. Therefore, acid scarification is not the natural way by which dormancy is broken in seeds of this species. Seeds of *C. australis* require a period >2 weeks of dormancy-breaking treatment to release them from dormancy, as found for seeds of clover species in Australia (Taylor 1981, Revell et al. 1999).

Only 17 % of non-treated *C. australis* seeds took up water, and thus only 17 % of the seeds germinated during a 6-d incubation period. However, all manually scarified seeds took up water rapidly and germinated. Thus, it is concluded that a high percentage (>80 %) of the fresh seeds of *C. australis* used in this study were physically dormant (Baskin and Baskin, 2004). Benvenuti et al. (2005) reported cycling of dormancy in initially physically dormant seeds of *C. campestris*. Their interpretation of dormancy cycling in this species seems to be that seeds cycle between PD and nondormancy (PD \leftrightarrow ND) after breaking of PY. Thus, we suggest that the cyclic pattern of germinability of *C. campestris* seeds may be explained by sensitivity cycling. Thus, seeds of *C. campestris* may have undergone cycling of sensitivity during burial in soil, and their dormancy-breaking requirements may have been fulfilled when they were incubated at 30°C . Hence, seeds showed a cyclic pattern of germination at 30°C . Sensitive seeds of *I. Lacunosa* respond quickly to dormancy-breaking treatment (Jayasuriya et al. 2008), requiring only 3 h at 35°C and RHs >90 % to become nondormant. Alebrahim et al. (2009) investigated the effects of sulfuric acid on the seeds of two different populations of the *Prosopis* strain (Borazjan and Kashmar). For the application of sulfuric acid, the seeds were placed in a 98% acid solution for 10, 20, 30, 40, 50 and 60 minutes. In the Borazjan and Kashmar populations, germination rates of 72.8-54.2% were observed after application of sulfuric acid, respectively. Pipinis et al. (2011) reported that in the control of *Cercis siliquastrum*

L. plant, there was a germination rate of 31-65% in the seeds subjected to sulfuric acid application (20 and 60 min) without any germination.

The results obtained in the study of dormancy-breaking in dodder seed and the results obtained in other investigators were found to be partially similar. Of course, this is because the time and dosage used in the methods are different.

References

- Alfarhan A.H. 1994. Taxonomic revision of the genus *Cuscuta* L. in Saudi Arabia. Arab Gulf Journal of Scientific Research, 12(1):99-107.
- Aly R., Westwood J. and Cramer C. 2003. Crop protection against parasites/pathogens through expression of sarcotoxin-like peptide. Patent No. WO02094008.
- Anonymous a 2015. Crop production statistics. www.tuik.gov.tr. (Access, January, 2017).
- Anonymous b 2015. <http://faostat.fao.org/site/567/DesktopDefault.aspx?PageID=567#ancor>, Acces: April 2015.
- Baskin J.M., Baskin C.C. 2000. Evolutionary considerations of claims for physical dormancy-break by microbial action and abrasion by soil particles. Seed Science Research. 10:409-413.
- Baskin J.M., Baskin C.C. 2004. A classification system for seed dormancy. Seed Science Research.14:1-16.
- Baskin J.M., Baskin C.C., Li X. 2000. Taxonomy, anatomy and evolution of physical dormancy in seeds. Plant Species Biology.15:139-152.
- Benvenuti S., Dinelli G., Bonetti A., Catizone P. 2005. Germination ecology, emergence and host detection in *Cuscuta campestris*. Weed Research. 45:270-278.
- Costea M., Tardif F.J. 2006. The biology of Canadian weeds. *Cuscuta campestris* Yuncker, *C. gronovii* Willd. ex Schult., *C. umbrosa* Beyr. ex Hook., *C. epithimum* (L.) L. and *C. epilinum* Weihe. Canadian Journal of Plant Science. 86:293-316.
- Costea M. and Stefanović S. 2010. Evolutionary history and taxonomy of the *Cuscuta umbellata* complex (Convolvulaceae): Evidence of extensive hybridization from discordant nuclear and plastid phylogenies. Taxon. 59:1783-1800.
- Calı S., Erdiler G. and Ekim T. 1993. Relationships between weeds and virus diseases in the alfalfa cultivation areas of Central Anatolia Region.Turkey I. Congress of Herbology,3-5 February 1993, Adana, 354-352.
- Davis, P.H., 1978. Flora of Turkey and East Aegean Islands. Edinburg University Press, Volume:1-10.
- Dawson J.H. 1984. Control of *Cuscuta* in alfalfa. In: Proc. 3 rd Internat. Sym. Parasitic Weeds, A review. p. 188-199. Aleppo, Syria.
- Dawson J.H., Musselman L.J., Wolswinkel P. and Dorr I. 1994. Biology and control of *Cuscuta*. Rev. Weed Sci. 1994. 6: 265-317.
- Fang R.C., Musselman L.J. and Plitmann U. 1995. *Cuscuta* In C.Y. Wu and P.H. Raven (eds.), Flora of China, Vol. 16. Science Press, Beijing, and Missouri Botanical Garden Press, St. Louis, pp. 322-325.
- Gaware T.J., Suta N. and Thorat B. N., 2010. Drying of Tomato Using Different Methods: Comparison of Dehydration and Rehydration Kinetics, Drying Technology, 28: 651-658.
- Gwoing L. MingYih C. and ChangSheng K. 2005. Morphological observation on floral variations of the genus *Cuscuta* in Taiwan. Taiwan, 50(2):123-130.
- Günçan, A. and Karaca, M. 2014. Weed control, Selçuk University Printing house. Page, 120.
- Holm L., Doll J., Holm E., Pançh J. and Herberger J. 1997. World Weeds: Natural Histories and Distribution. John Wiley & Sons, New York. 1129 pp.
- Jayasuriya K.M., Baskin J.M., Baskin C.C. 2008. Cycling of sensitivity to physical dormancy-break in seeds of *Ipomoea lacunosa* (Convolvulaceae) and ecological significance. Annals of Botany. 101:341-352.
- Kadioglu, İ. 1992. Dodder (*Cuscuta* spp.) and struggle. Herbology journal, Çukurova University Faculty of Agriculture Department of Plant Protection, 3 (5): 1-11.
- Khan M.S. and Halim M. 1990. *Cuscuta campestris* Yuncker - A new angiospermic record for Bangladesh. Bangladesh Journal of Botany, 19(1):103-105.
- Konieczka C.M., Colquhoun J.B. and Rittmeyer R.A. 2009. Swamp Dodder (*Cuscuta gronovii*) management in Carrot production, Weed Technology, 23: 408-411.
- Lados M. 1999. Effect of temperature, pH and host plant extract on the germination of *Cuscuta trifolii* and *C. campestris* seeds. Novenytermeles. 48: 367-376.
- Lanini W.T. and Kogan M. 2005. Biology and management of *Cuscuta* in Crops. Ciencia Investigation Agronomy. 32 (3), 127-141.

- Lian J.Y., Ye W.H., Cao H.L., Lai Z.M., Wang Z.M. and Cai C.X. 2006. Influence of obligate Parasite *Cuscuta campestris* on The community of its host *Mikania micrantha*. Weed Research. 46, 441-443.
- Lorenzi H.J. and Jeffery L.S. 1987. Weeds of the United States and their control. New York, USA; Van Nostrand Reinhold Co. Ltd., 355 pp.of its host *Mikania micrantha*. Weed Research. 46, 441-443.
- Lubenov Y. 1985. Harmful weeds is the source of life and death (Translated by B. Makaklı, M. Dinçer), Çağ Press, Ankara, 175 s.
- Marambe B., Wijesundara S., Tennekoon K., Pindeniya D., Jayasinghe C. 2002. Growth and development of *Cuscuta chinensis* Lam. and its impact on selected crops. Weed Biology and Management. 2:79-83.
- Meulebrouck K., Ameloot E., Van Assche J.A., Verheyen K., Hermy M. and Baskin C.C. 2008. Germination ecology of the holoparasite *Cuscuta epithimum*. Seed Science Research.18:25-34.
- Majd R., Aghaie P., Monfared E. K. and Alebrahim M. T. 2009. Evaluating of some treatments on breaking seed dormancy in mesquite. Available from: https://www.researchgate.net/publication/306323630_Evaluating_of_Some_Treatments_on_Breaking_seed_Dormancy_in_Mesquite [accessed Jun 29 2018].
- Mishra, J.S., 2009. Biology and management of Cuscuta species, Indian Journal of Weed Science, Volume:41,Issue:1 and 2; 1-11P.
- Morita H. 1997. Handbook of arable weeds of Japan. Tokyo, Japan: Kumiai Chemical Industry Co. Ltd., 128 pp.
- Nemli, Y. 1978. Morphological and Systematic Investigations of Cuscuta L. on Anatolian Species from Flowering Parasites, Associate Professor Thesis, Faculty of Agriculture of Ege University, Phytopathology and Agricultural Botanical Sector, Bornova- İzmir.
- Nemli Y. 1986. Dodder species (*Cuscuta* spp.) In cultural areas in Anatolia; Researches on distribution and hosts, Journal of Agricultural Faculty of Ege University, 23 (3):11-21.
- Nadler-Hassar T. and Rubin B. 2003. Natural tolerance of *Cuscuta campestris* to herbicides inhibiting amino acid biosynthesis. Journal of Weed Research, 43(5): 341-347.
- Özaslan C, Kendal E 2014. Determination of the weeds in production areas of Lice tomato, Iğdır University Journal, Inst. Sci. & Tech. 4(3): 29-34.
- Özer Z. 1993. Why weed (Herbology) science. Turkey 1.Herbology the proceedings of the congress, 3-5 February 1993. 1-7, Adana.
- Özer Z., Kadioglu İ., Önen H. and Tursun N. 1998. Herbology (Weed Science). Gaziosmanpaşa University Agricultural Faculty Publications No: 20, Tokat. 403 s.
- Özer Z., Kadioglu İ., Önen H., Tursun N. 2001. Herbology (Weed Science) Gaziosmanpaşa University Agricultural Faculty Publications, No: 20 Book serial number: 10 Tokat.
- Parker C. and Wilson A.K. 1986. Parasitic weeds and their control in the Near East. FAO Plant Protection Bulletin, 34(2): 83-98.
- Parker C. and Riches C.R. 1993. Parasitic weeds of the world: biology and control. CAB International, Wallingford, UK. 304 pp.
- Parsons W.T. and Cuthbertson E.G. 1992. Noxious Weeds of Australia. Melbourne, Australia: Inkata Press, 692 pp.
- Pier I. 2008. Pacific Islands ecosystems at Risk. USA: Institute of Pacific Islands Forestry. <http://www.hear.org/pier/index.html>.
- Pipinis E., Milios E., Smiris P. and Gioumousidis C. 2011. Effect of acid scarification and cold moist stratification on the germination of *Cercis siliquastrum* L. seeds. Turk J Agric For 35: 259-264.
- Racasens J. and Conesa J.A. 1990. Presence and spread of newly introduced weeds in crops in Catalonia. Actas de la Reunion de la Sociedad Espanola de Malherbologia, 307-315.
- Revell C.K., Taylor G.B., Cocks P.S. 1999. Effect of length of growing season on development of hard seeds in yellow serradella and their subsequent softening at various depths of burial. Australian Journal of Agricultural Research. 50:1211-1223.
- Salimi H. and Shahraeen N. 2000 Study on comparison of seed dormancy and germination of three species of dodder. Rostaniha. 1:33-36.
- Sırma M., Kadioglu İ. and Yanar Y. 2001. Important weed species detected in Tokat province tomato planting areas, frequency and density of occurrences. Herboloji magazine, Volume 4, Issue 1, Page,39-47.
- Taylor G.B. 1981. Effect of constant temperature treatments followed by fluctuating temperatures on the softening of hard seeds of *Trifolium subterraneum* L. Australian Journal of Plant Physiology. 8:547-558.
- Tepe I., Deveci M. and Keskin B. 1997. Investigate some alfalfa varieties of chestnut (*Cuscuta approximata* Bab.) on parasitization and damage levels. Turkey II. Reports of the Herbology Congress, 1-4 September 1997, İzmir, 355-360.
- Türe C. and Köse Y.B. 2000. A survey on the weed flour spreading in Eskişehir and some agricultural areas around it. Turkish Journal of Agriculture and Forestry 24: 327-331.

- Uygur F.N., Koch W. and Walte H. 1984. Plits, Introduction to weed science (course note) 1984 / 2 (1) Josef Margraf, Stuttgart.
- Yardımcı N., Özgönen H., Savaş H.S. and Erdoğan O. 2000. A study on determination of plant diseases and pests and weeds in Isparta region tomato growing. S.D.Ü. Science Institute journal, Volume (4):1, sayfa: 181-189.
- Yuncker T.G. 1932. The genus *Cuscuta*. Memoirs of the Torrey Botanical Club, 18:113-331.
- Zerman N. and Saghir A.R. 1995. The genus *Cuscuta* in Algeria. Arab Journal of Plant Protection, 13(2):69-75.
- Zharasov S.U. 2009. Field dodder in the south-east of Kazakhstan. Zashchita i Karantin Rastanii, No.1:30-32.
<http://www.z-i-k-r.ru>.

Author Information

Tamer Ustuner

Kahramanmaraş Sütcü Imam University, Faculty of
Agriculture, Department of Plant Protection, Avsar Campus,
Kahramanmaraş/Turkey
Contact e-mail: tamerustuner@ksu.edu.tr

Samet Cakir

Kahramanmaraş Sütcü Imam University, Faculty of
Agriculture, Department of Plant Protection, Avsar Campus,
Kahramanmaraş/Turkey

Investigation of a New Post Emergence Herbicide, Diquat Dipromide 200 g/l Against to Weeds in Peach Orchards in Black Sea Region

Tamer USTUNER
Sütçü Imam University

Ummet DIRI
Experts Agriculture Plant Protection Research & Engineering Ltd.

Abstract: In this study, Diquat 200 g/l herbicide was tested against to weeds causing damages in peach orchards of Samsun province in the Black Sea Region in 2017. The experiment was carried out in 9 blocks (6 doses of target herbicide+2 doses of reference herbicide+control) with 4 replicates in 2mx25m=50 m² parcels according to randomized blocks trial design. Herbicide effects in formed groups according to variance analysis with Tukey test (5%) in the JMP program were found to be different and significant, statistically. Weed density in peach gardens in Samsun region; shepard's purse (*Capsella bursa-pastoris*), bluegrass (*Poa annua*), sow thistle (*Sonchus oleraceus*), hooked bristlegrass (*Stellaria media*), brome grasses (*Bromus* spp.), Henbit deadnettle (*Lamium amplexicaule*), field marigold (*Calendula arvensis*) and pimpernel (*Anagallis arvensis*) was evaluated as being very intensive because it is more than 10 in m². In Post-emergence in peach gardens, Diquat dipromide (200 g/l) active ingredient herbicide was applied at the doses of 300, 400, 500, 600 and 1200 ml/da while Roundup Star Glyphosate Potassium Salt was applied at the doses of 300ml/da, respectively against to post-emergence weeds in peach orchards. Diquat dipromide (200 g/l) application at the dose of 300, 400, 500 ml/da was found ineffective against to both broad and narrow leaf weeds. At doses of only 600 and 1200 ml/da, the killing efficacy of herbicide was found at 90-100% both narrow and broad leaf weeds. For this reason, Diquat dipromide (200 g/l) was recommended as herbicide after discharge at a dose of 600 ml/da, which was found to be effective at 91.71% for eight weeds in the garden. Phytotoxic effect on peach trees was not observed at the dose of diquat dipromide 1200 ml/da.

Keywords: Peach, Weeds, Density, Post-emergence herbicide, Diquat dipromide

Introduction

Recent investigations have shown that weed competition can greatly reduce the growth, cropping and fruit quality of both young and mature fruit trees. A weed control programme to eliminate most or all weeds from fruit orchards is, therefore, important, particularly in high density plantings where high and regular fruit production and early capital return are so important.

Peach (*Prunus persica* L. Batsch) is a hard-seeded fruit species that can adapt to temperate and subtropical climate areas. The peach culture is based on 4000 years ago and is thought to be the motherland of East Asia and China. Peach [*Prunus persica* (L.) Batsch] is an important fruit crop cultivated on 1.54 million ha with an annual production of 20.27 million tonnes in the world (Faostat 2010). China is in the 1st place with 37.16% of peach production in the world. This is followed by EU countries with 26.20%. If Turkey is located in 10th place with 3.11% of production. According to TUIK data is obtained, in Turkey 642.720 tons of products per year from 16.300 million peach trees in Turkey. Peaches are mostly produced in the Marmara, Aegean, Black Sea and Mediterranean regions (Anonymous 2017a).

In different region of Turkey, The density is important of *Amaranthus retroflexus* L., *Anagallis arvensis* L., *Anthemis tinctoria* L., *Artemisia vulgaris* L., *Calendula arvensis*, *Capsella-bursa pastoris* (L.) Medik, *Carduus*

- This is an Open Access article distributed under the terms of the Creative Commons Attribution-Noncommercial 4.0 Unported License, permitting all non-commercial use, distribution, and reproduction in any medium, provided the original work is properly cited.

- Selection and peer-review under responsibility of the Organizing Committee of the Conference

spp., *Cerastium glomeratum* Thuill., *Chenopodium album* L., *Daucus carota* L., *Erodium* spp., *Euphorbia* spp., *Fumaria* spp., *Galium tricornutum* Dandy., *Geranium* spp., *Heiotropium europaeum* L., *Hibiscus trionum* L., *Lactuca serriola* L., *Malva* spp., *Matricaria* spp., *Medicago* spp., *Mentha arvensis* L., *Mercurialis annua* L., *Muscari* spp., *Papaver rhoeas* L., *Plantago* spp., *Portulaca oleracea* L., *Raphanus raphanistrum* L., *Ranunculus* spp., *Rumex* spp., *Scabiosa* spp., *Senecio vernalis* Waldst. and Kids., *Senecio vulgaris* L., *Silene colorata* Poir., *Sinapis arvensis* L., *Solanum nigrum* L., *Sonchus* spp., *Stellaria media* (L.) Vill., *Tribulus terrestris* L., *Trifolium* spp., *Urtica urens* L., *Verbena officinalis* L., *Veronica* spp., *Lamium orientale*, *Alopecurus myosuroides* Huds., *Avena* spp., *Bromus* spp., *Digitaria sanguinalis* (L.) Scop., *Echinochloa* spp., *Hordeum* spp., *Lolium* spp., *Phalaris* spp., *Poa* spp., *Setaria verticiliata* (L.) P. Beauv *Setaria viridis* (L.) P. Beauv, *Setaria glauca*, *Acroptilon repens* (L.) DC. , *Cirsium arvense* (L.) Scop., *Convolvulus arvensis* L., *Elymus repens*, *Cynodon dactylon*, *Cyperus rotundus* L. *Phragmites australis* and *Sorghum halepense* (Anonymous 2011, 2017b). In peach garden in India, *Urochloa maxima* (Jacq.) R. Webster, *Cynodon dactylon* (L.) Pers., *Cyperus rotundus* L., *Eleusine indica* (L) Gaertn., *Commelina benghalensis* L., *Chenopodium album* L., and *Parthenium hysterophorus* L. were the important weeds at the experimental site in the peach orchard during the investigations (Thakur et al. 2012). Among the herbicides, Diuron fb Glyphosate with the highest WCE (=weed control efficiency) (98.3%) did not differ significantly from Atrazine fb Glyphosate at 12 WAT (=weeks after treatment) in 2009. This was followed by Pendimethalin fb Glyphosate (96.0%), which did not differ significantly from Pendimethalin fb Paraquat or Atrazine fb Paraquat. Glyphosate appeared to be a better postemergence herbicide than Paraquat in terms of better WCE when used after Diuron and Atrazine. However, there was no significant difference between the two post-emergence herbicides when used after Pendimethalin. Diuron fb Glyphosate and Atrazine fb Glyphosate resulted in 100% WCE at 12 WAT in 2010, and it did not differ significantly from all the herbicide treatments, black polythene mulch, and straw mulch (8 cm). Pendimethalin and Atrazine reduced the weed biomass of bermuda grass compared with the weedy control at 6 WAT during both years but could not eradicate the weed (Tworkoski and Glenn 2001, Thakur et al. 2012, Hembree 2016). Richard (1998) has demonstrated that atrazine was not at all effective while Pendimethalin was less effective in controlling bermuda grass. Pendimethalin and Diuron treatments also failed to completely control benghal day flower, which was completely controlled by black polythene mulch and straw mulch at 6 WAT. Webster et al. (2006) also reported the poor efficacy of Diuron against tropical spiderwort (benghal dayflower). They found that Diuron at 1.68 kg/ha²¹ provided marginal control (73%) of tropical spiderwort at 6 WAT and the weed control percentage reduced further (36%) at lower Diuron rates. Atrazine also showed poor control of benghal dayflower at 6 WAT (MacRae et al. 2007).

Herbicidal activity was conducted at the request of company of herbicide with effective substance "Diquat dipromide 200 g/l" against the weeds which are problem in peach gardens.

Material and Method

The trial was established in Samsun (Carsamba- Köklük village) in the garden of Glohaven apricot variety at the age of 12. The planting gaps are 7x7 m in the garden where the experiment was carried out. It has been stated by the farmer in March to use Ammonium sulphate fertilizer per 3 kg/tree. Soil structure is loamy. Weeds which are found in dense area (density>10 in m²); *Capsella bursa-pastoris*, *Poa annua*, *Sonchus oleraceus*, *Bromus* spp., *Lamium amplexicaule*, *Calendula arvensis* and *Anagallis arvensis*. Ulug et al. (1993) was used in the identification of Turkish and scientific name in the identification of this weed.

Herbicides used in the trial and information about them are shown in Table 1.

Table 1. Information about the herbicides used in the herbicides test against weeds which are a problem in peachorchards in Samsun

Trade Name	Effective substance Name and%	Form.	Company	Using Dosage (Da)	
				Active Substance(g)	Preparation s (g)
EPİTAP SL	EPİTAP	SL	ETMA	60	300
“	“	“	“	80	400
“	“	“	“	100	500
“	“	“	“	120	600
“	“	“	“	140	700
“	“	“	“	160	800
**EPİTAP SL	“	“	“	320	1600
*Roundop Star	Glyphosate Potasyum salt 441 g/l	SL	Monsanto	132,3	300
*Roundop Star	Glyphosate Potasyum salt 441 g/l	SL	Monsanto	264,6	600

- ** Selectivity (phytotoxicity) dosage
- * Comparison Chemical

The experiment was carried out in 7 blocks (5 doses of trial herbicide+2 doses of control drug+control) and 4 replicates in $3 \times 12 = 36 \text{m}^2$ parcels according to randomized blocks trial design. Left was 1 m between the blocks, 1 m between the parcel is left as safety lane. Herbicide application was made on 17.09.2017, weeds were grown in 6-10 leaf period, fruit vegetable sweetening period. The medication was applied at a pressure of 3 atmospheres with a Matabi fixed pressure backpack sprayer. The spraying tool was fitted with a 2m work width, 6 Tee-jette nipple stimulation, 2m long boom. The calibration was made with 1.08 liters of land and 30 liters of water. The air was open and the temperature was measured at 22°C at the time of spraying.

Evaluation Time and Number

Before the experiment is established, weed species, development cycles and densities (numbers in m^2) were recorded (17.09.2017),

First evaluation: 7 days after herbicide application (24.09.2017),

Second evaluation: 21 days after herbicide application (08.10.2017): This count is based on evaluation of efficacy of medicines, and Table 2 in the results section is arranged according to this evaluation.

Third evaluation: 52 days after herbicide application (12.11.2017),

Fourth evaluation: 182 days after herbicide application was made evaluation (18.03.2017)

The phytotoxicity of the herbicides and the herbicidal effects of the herbicide were evaluated based on the observation and the percentages of the drugs were determined. In the control parcels, the weed in the square meter was recorded as number. By using variance analysis in the JMP program, groups of drugs were formed according to the Tukey (5%) test. Herbicide used in the trial; It has been observed carefully whether the phytotoxic effects on the culture plant have positive or negative effects on other pests, diseases and weeds and other organisms in the test area.

Results

Percentage effects of herbicides determined in the trial made against the weeds in peach orchards in Samsun (Carsamba-Köklük village) in 2017 are given in Table 2.

As can be seen from the examination of Table 2. Diquat dipromide 200 g/l against *Capsella bursa-pastoris*, *Poa annua*, *Sonchus oleraceus*, *Stellaria media*, *Bromus spp.*, *Lamium amplexicaule*, *Calendula arvensis* and *Anagallis arvensis*. The percentages on average were: 52.50, 30.00, 25.00, 22.50, 38.75, 40.00, 38.75 and 42.50 at 200 ml/da dose respectively; 77.50, 52.50, 52.50, 53.75, 57.50, 56.25, 61.25 and 61.25 at 300 ml/da dose; 93.75, 75.00, 76.25, 82.50, 81.25, 75.00, 80.00 and 78.75 at 400 ml/da dose; 95.00, 92.50, 91.25, 91.25, 90.00, 91.25, 90.00 and 92.50 at 600 ml/da dose; 100.00, 100.00, 100.00, 100.00, 100.00, 100.00, 100.00 and 100.00 at 1200 ml/da dose; Roundop Star used as a comparator in the dose of average dose per dose of 300 ml/d: 91.25, 92.50, 91.25, 91.25, 92.50, 91.25, 91.25 and 93.75 respectively. According to the statistical analysis, variance analysis was applied to the statistical JMP program, the groups according to the Tukey (5%) test are shown below (Table 2, 3).

According to the statistical analysis, variance analysis was applied to the statistical JMP program, the groups according to the Tukey (5%) test are shown below (Table 2,3).

Table 2. The effects of Misille 20 SL herbicide on the weed species in Peach orchards in Samsun

Herbicides	Doses (ml/da)	<i>Amaranthus</i> spp.	<i>Portulaca oleracea</i>	<i>Poa annua</i>	<i>Capsella bursa-pastoris</i>	<i>Anagallis arvensis</i>	<i>Setaria verticillata</i>	<i>Setaria viridis</i>	<i>Urtica urens</i>	<i>Solanum nigrum</i>	<i>Malva sylvestris</i>
Misille 20 SL	300	d	c	c	c	c	d	c	f	d	f
Misille 20 SL	400	c d	b	b	b	b	c	c	e	d	ef
*Roundop Star	300	c d	b	b	b	b	b	b	c	bc	c
Misille 20 SL	500	c b	b	a	b	a	b	b	d	c	e
Misille 20 SL	600	a b	a	a	a	a	a	a	cd	bc	d
Misille 20 SL	700	a	a	a	a	a	a	a	bc	ab	c
Misille 20 SL	800	a	a	a	a	a	a	a	ab	a	b
*Roundop Star	600	a	a	a	a	a	a	a	a	a	b
**Misille 20 SL	1600	a	a	a	a	a	a	a	a	a	a

** Phytotoxicity Dose * Comparison chemical

The herbicide used in the experiment showed a phytotoxic effect at 1600 ml/da on leaves of apricot plants.

Table 3. The effect of Misille 20 SL herbicide on the herbicide against weeds which is a problem in peach orchards in and phytotoxicity to culture plants.

Herbicides	Recurrent	Phytotoxicity	% effect to weeds										
			<i>Amaranthus</i> spp.	<i>Portulaca oleracea</i>	<i>Poa annua</i>	<i>Capsella bursa-pastoris</i>	<i>Anagallis arvensis</i>	<i>Setaria verticillata</i>	<i>Setaria viridis</i>	<i>Urtica urens</i>	<i>Solanum nigrum</i>	<i>Malva Sylvestris</i>	<i>Coryza canadensis</i>
Misille 20 SL (300 ml/da)	1	No	85	80	85	75	80	60	75	30	40	20	10
	2		80	70	85	80	85	55	65	40	45	30	10
	3		75	80	80	80	85	65	65	30	40	20	10
	4		85	80	85	70	80	60	60	40	30	20	10
	Average		81,25	77,50	83,75	76,25	82,50	60,00	66,25	35,00	38,75	22,50	10,00
Misille 20 SL (400 ml/da)	1	No	95	95	95	90	90	70	80	65	65	30	10
	2		90	95	95	90	95	80	75	55	60	40	20
	3		90	90	95	90	95	75	75	60	55	30	10
	4		90	90	90	90	95	85	80	55	55	30	10
	Average		91,25	92,50	93,75	90,00	93,75	77,50	77,50	58,75	58,75	32,50	12,50
Misille 20 SL (500 ml/da)	1	No	95	95	95	90	100	90	90	75	85	40	30
	2		95	95	100	95	100	90	95	80	85	50	20
	3		100	95	100	95	95	95	95	80	80	40	30
	4		95	95	100	95	100	90	90	85	80	50	20
	Average		96,25	95,00	98,75	93,75	98,75	91,25	92,50	80,00	82,50	45,00	25,00
Misille 20 SL (600 ml/da)	1	No	100	100	100	100	100	100	100	90	90	70	40
	2		95	95	100	95	100	95	95	90	90	65	45
	3		100	100	100	95	100	100	95	90	95	60	40
	4		100	100	100	100	100	95	100	90	95	65	30
	Average		98,75	98,75	100,00	97,50	100,00	97,50	97,50	90,00	92,50	65,00	38,75
20 SL (700)	1	Yok	100	100	100	100	100	100	100	95	95	80	50
	2		100	100	100	100	100	100	100	90	95	80	60
	3		100	100	100	100	100	100	100	95	100	85	55

	4		100	100	100	100	100	100	100	95	100	80	50
	Average		100,00	100,00	100,00	100,00	100,00	100,00	100,00	93,75	97,50	81,25	53,75
Misille 20 SL (800 ml/da)	1	No	100	100	100	100	100	100	100	95	100	90	80
	2		100	100	100	100	100	100	100	100	95	90	75
	3		100	100	100	100	100	100	100	100	100	90	70
	4		100	100	100	100	100	100	100	95	100	90	80
	Average			100,00	100,00	100,00	100,00	100,00	100,00	100,00	97,50	98,75	90,00
** Misille 20 SL (1600 ml/da)	1	No	100	100	100	100	100	100	100	100	100	100	95
	2		100	100	100	100	100	100	100	100	100	100	95
	3		100	100	100	100	100	100	100	100	100	100	100
	4		100	100	100	100	100	100	100	100	100	100	100
	Average			100,00	100,00	100,00	100,00	100,00	100,00	100,00	100,00	100,00	100,00
* Roundup Star (300 ml/da)	1	No	90	90	95	90	90	90	90	90	95	80	70
	2		95	95	95	90	95	95	90	95	95	70	80
	3		90	90	95	90	90	90	90	90	90	85	70
	4		90	95	95	90	95	90	95	90	90	85	75
	Average			91,25	92,50	95,00	90,00	92,50	91,25	91,25	91,25	92,50	80,00
* Roundup Star (600 ml/da)	1	No	100	100	100	100	100	100	100	100	100	90	90
	2		100	100	100	100	100	100	100	100	100	90	90
	3		100	100	100	100	100	100	100	100	100	95	90
	4		100	100	100	100	100	100	100	100	100	90	90
	Average			100,00	100,00	100,00	100,00	100,00	100,00	100,00	100,00	100,00	91,25
CONTROL	1	No	5	11	7	4	7	9	7	4	4	2	3
	2		4	15	9	5	6	12	4	5	3	4	2
	3		6	13	12	8	14	15	4	7	5	2	3
	4		3	10	10	5	13	9	6	8	2	2	2
	Average			4,50	12,25	9,50	5,50	10,00	11,25	5,25	6,00	3,50	2,50

** Phytotoxicity Dose * Comparison chemical

The numbers in the control refer to the weed of the weed in m²

Discussion

Samsun region in peach orchards; *Capsella bursa-pastoris*, *Poa annua*, *Sonchus oleraceus*, *Stellaria media*, *Bromus* spp., *Lamium amplexicaule*, *Calendula arvensis* and *Anagallis arvensis* were found to be intense. In peach orchards in different region of Turkey, The density is important of *A. retroflexus* L., *A. arvensis* L., *A. tinctoria* L., *A. vulgaris* L., *C. arvensis*, *C. pastoris* (L.) Medik., *Carduus* spp., *C. glomeratum* Thuill., *C. album* L., *D. carota* L., *Erodium* spp., *Euphorbia* spp., *Fumaria* spp., *G. tricornutum* Dandy., *Geranium* spp., *H. europaeum* L., *H. trionum* L., *L. serriola* L., *Malva* spp., *Matricaria* spp., *Medicago* spp., *Mentha arvensis* L., *Mercurialis annua* L., *Muscari* spp., *Papaver rhoeas* L., *Plantago* spp., *P. oleracea* L., *Raphanus raphanistrum* L., *Ranunculus* spp., *Rumex* spp., *Scabiosa* spp., *Senecio vernalis* Waldst. and Kids., *Senecio vulgaris* L., *Silene colorata* Poir., *Sinapis arvensis* L., *Solanum nigrum* L., *Sonchus* spp., *Stellaria media* (L.) Vill., *Tribulus terrestris* L., *Trifolium* spp., *Urtica urens* L., *Verbena officinalis* L., *Veronica* spp., *Lamium orientale*, *Alopecurus myosuroides* Huds., *Avena* spp., *Bromus* spp., *Digitaria sanguinalis* (L.) Scop., *Echinochloa* spp., *Hordeum* spp., *Lolium* spp., *Phalaris* spp., *Poa* spp., *Setaria verticiliata* (L.) P. Beauv. *S. viridis* (L.) P. Beauv., *S. glauca*, *Acroptilon repens* (L.) DC., *Cirsium arvense* (L.) Scop., *C. arvensis* L., *E. repens*, *C. dactylon*, *Cyperus rotundus* L. *Phragmites australis* and *Sorghum halepense* (Anonymous 2017). In terms of weed species and density, Our findings the same Anonymous (2017) in Turkey. In peach garden in India, *Urochloa maxima* (Jacq.) R. Webster, *C. dactylon* (L.) Pers., *C. rotundus* L., *Eleusine indica* (L.) Gaertn., *Commelina benghalensis* L., *C. album* L., and *Parthenium hysterophorus* L. were the important weeds at the experimental site in the peach orchard during the investigations (Majek et al. 1993, Thakur et al. 2012).

Three pre-emergence herbicides, oxyfluorfen, oxadiazon 0.75, 1.0, 1.25 litre (a.i.) ha⁻¹ and metolachlor 1.0, 1.5 and 2.0 litre (a.i.) ha⁻¹ were applied twice, in March and October (Chikoye et al. 2005.) The orchard was found to be manifested with 7 monocot and 23 dicots prominent weed species. All the treatments significantly reduced the weed population, dry weight of weed and nutrient depletion by weeds as compared to control (unweeded). In this respect, pre-emergence herbicide oxyfluorfen was found to be the most effective treatment for control of dicot weeds. Application of metolachlor and controlled both monocot and dicot weeds. The various weed control treatments had a non-significant effect on fruit yield, total soluble solids and acidity. The highest

fruit weight was obtained with oxyfluorfen followed by oxadiazon and oxyfluorfen. However, metolachlor proved to be most effective and economical treatment (Chatha and Chanana 2007). In the peach horticulture in North Carolina Parker and Meyer (1996) determined that peach tree growth was greater when grown in the presence of grass *Muhlenbergia schreberi*, *Eremochloa ophiuroides*, *Paspalum notatum*, in the Pacific Northwest per annual grass (Granatstein 2002, Vrbničanin et al. 2010). In the Peach orchard of India; *C. dactylon*, *C. rotundus*, *Bidens pilosa*, *Tridax procumbens*, *Acanthospermum hispidum* and *Lagasca mollis*, *Polygon plebejum*, *Euphorbia geniculata*, *Amaranthus viridis*, *P. oleracea*, *Oxalis* spp., *Mullugo pentaphylla*, *Digitaria marginata*, *Eleusine indica*, and *S. glauca* were found in important density (Sing and Rana 2016). In terms of weed species and density in the world, our findings seen partial same with other research.

The efficacy of the herbicide in the world and Turkey has found different results when examined. Because there are big differences in the world countries in terms of weed species, regional climate and soil characteristics. In the peach horticulture in California, There were several hundred weeds per square meter in the unfumigated area, consisting primarily of *Capsella bursa-pastoris* L., *S. arvensis* L., and *Medicago hispida* Gaertn., *S. media*, and *M. neglecta* Wallr. was found dense. An interrow tillage operation in early March removed most of the weeds between the herbicide-treated bands in the fumigated blocks but did little to relieve weed competition within the row in the unfumigated area. On March 15, 2007, all Preherbicide treatments, except sulfentrazone, substantially reduced total weeds in the tree rows compared with the no-herbicide control. Control with the Post-herbicide treatments was poor, but those treatments may not have reached full impact having been applied only 2 wk before the weed counts. Later observations suggested that POST-D flumioxazin and rimsulfuron also suppressed many of the weeds present (Hanson and Schneider 2008, Dayan et al. 2011). Gramoxone at 500 ppm, mixture or 2,4,5-T at 100 ppm and Gramoxone at 500 ppm controlled the shrubby weeds of *Rosa moschata*, *Rubus* spp. and *Berberis* spp. effectively. Weed control in peach orchards with the combination of dalaponat 10 kg/ha and 4-D at 1.0 kg/ha when applied in two split doses. Weed control with terbacilat 3.0 and 5.0 kg/ha. *Commelina nudifera*, *Ageratum conyzoides* and *Euphorbia hirtawere* controlled wellly 5.0 kg/ha Simazine and 3-5 kg/ha Atrazine (Abouzienna et al. 2008, Sing and Rana 2016).

Conclusion

C. bursa-pastoris, *P. annua*, *S. oleraceus*, *S. media*, *Bromus* spp., *L. amplexicaule*, *C. arvensis* and *A. arvensis* in the experiment of the weeds in the peach gardens in Samsun (Carsamba-Köklük village), at rates of 200 ml/da, 300 ml/da, 400 ml/da and 600 ml/da and 1200 ml/da, respectively, 200 ml/da: 52.50, 30.00, 25.00, 22.50, 38.75, 40.00, 38.75 and 42.50; 300 ml/da: 77.50, 52.50, 52.50, 53.75, 57.50, 56.25, 61.25 and 61.25; 400 ml/da: 93.75, 75.00, 76.25, 82.50, 81.25, 75.00, 80.00 and 78.75; 600 ml/da: 95.00, 92.50, 91.25, 91.25, 90.00, 91.25, 90.00 and 92.50; 1200 ml/da: 100.00, 100.00, 100.00, 100.00, 100.00, 100.00, 100.00 and 100.00, Roundup Star, used as a comparator, was found to be effective on average at average rates of 300 ml/d: 91.25, 92.50, 91.25, 91.25, 92.50, 91.25, 91.25 and 93.75 respectively.

C. bursa-pastoris, *P. annua*, *S. oleraceus*, *S. media*, *Bromus* spp., *L. amplexicaule*, *C. arvensis* and *A. arvensis*, which are in the 200, 300, and 400 ml/dose trial area of the EPITAP drug, they can not be used. However, it was found to be effective more than 90% at the dose at 600 ml/dose and 100% at 1200 ml/dose. Whereas, Roundup Star used as a control herbicide was 91.87 % at 300 l/dose effective against weeds in peach garden. No phytotoxic effects were observed in the peach gardens of all doses, including the dose of 1200 ml/da, which is comparable to the phytotoxicity of the trial herbicide used in the trial.

Statistically, the EPITAPH was included in the same group as the statistically significant dose-dependent dose at 600ml/da of the comparative drug Roundup Star at 300 ml/da.

As a result of these evaluations; EPITAP which at 600 ml/da dozen effective on *P. annua*, *S. oleraceus*, *S. media*, *Bromus* spp., *L. amplexicaule*, *C. arvensis*, *A. arvensis* and *C. bursa-pastoris* which is a problem in peach gardens that it can be used after these weed emergence. EPITAP can be recommended as post-emergence herbicide after emergence due to the effect it shows in in the peach orchards.

References

Abouzienna H.F., Hafez O.M., El-Metwally I.M., Sharma S.D., Singh M. 2008. Comparison of weed suppression and mandarin fruit yield and quality obtained with organic mulches, synthetic mulches, cultivation, and glyphosate. HortSci. 43:795-799.

- Anonymous 2011. Technical Instruction of Peach Integrated control, T.C. Food, Agriculture and Livestock Ministry, General Directorate of Agricultural Researches and Policies, Directorate of Plant Health Researches, 166p.
- Anonymous 2017a. Peach and Nectarine Integrated Control Technical Instruction. T.C. Food, Agriculture and Livestock Ministry, General Directorate of Agricultural Researches and Policies, Directorate of Plant Health Researches, 136P.
- Anonymous 2017b. Biological activity test report. Ministry of Agriculture and Rural Affairs Agricultural Research Institute, Publication No. 78, Samsun, Turkey.
- Chatha R.P.S. and Chanana Y.R. 2007. Studies on weed management in young peach orchards. *Indian Journal of Horticulture*, 64(3):300-303.
- Chikoye D., Udensi U.E. and Lum A.F. 2005. Evaluation of a new formulation of atrazine and metolachlor mixture for weed control in maize in Nigeria. *Crop Protect.*, 24: 1016-1020.
- Dayan F.E., Howell J., Marais J.P., Ferreira D. and Koivunen M. 2011. Manuka oil, a natural herbicide with preemergence activity. *Weed Sci.*, 59: 464-469.
- Faostat, 2010. Statistical database of the food and agricultural organization of the United Nations [Internet]. [cited 2012 May 12]. Available from: <http://www.faostat.fao.org>
- Granatstein D. 2002. Tree fruit production with organic farming methods. <http://organic.tfrec.wsu.edu/organicIFP/OrganicFruitProduction/OrganicMgt.PDF> (Accessed August, 2007).
- Hanson B.D. and Schneider S.A. 2008. Evaluation of weed control and crop safety with herbicides in open field tree nurseries. *Weed Technology*, 22: 493-498.
- Hembree K.J. 2016. Weedmanagement in established orchards. UC IPM Pest Management Guidelines: Apricot, UC ANR Publication, 3433.
- MacRae A.W., Mitchem W.E., Monks D.W., Parker M.L. and Galloway R.K. 2007. Tree growth, fruit size, and yield response of mature peach to weed-free intervals. *Weed Technology*, 21: 102-105.
- Majek B.A., Neary P.E., Polk D.F. 1993. Smooth pigweed interference in newly planted peach trees. *Journal of Product Agriculture*, 6: 244-246.
- Parker M.L., Meyer J.R. 1996. Peach tree vegetative and root growth respond to orchard floor management. *HortScience*, 31: 330-333.
- Richard E.P. 1998. Control of perennated bermuda grass (*Cynodon dactylon*) and Johnson grass (*Sorghum halepense*) in sugarcane (*Saccharum* spp. hybrids). *Weed Technology*, 12: 128-133.
- Singh R. and Rana S.S. 2016. Weed management of orchards. Available from: https://www.researchgate.net/publication/320426461_27Weed_management_of_orchards [accessed Apr 13, 2018].
- Thakur A., Singh H., Jawandha SK. and Kaur T. 2012. Mulching and herbicides in peach: Weed biomass, fruit yield, size, and quality. *Biological Agriculture & Horticulture*, 28 (4), 280-290.
- Tworkoski T.J. and Glenn DM. 2001. Yield, shoot and root growth, and physiological responses of mature peach trees to grass competition. *HortSci.*, 36: 1214-1218.
- Ulug E., Kadioglu İ. and Üremis İ. 1993. Some Features of weeds and Turkey.
- Vrbničanin S., Jovanović-Radovanov K. and Oparnica Č. 2010. Weed incidence in stone-fruit orchards: Plum, apricot and peach. *BiljniLekar*, 38(4/5), 277-299.
- Webster T.M., Burton M.G., Culpepper A.S., Flanders J.T., Grey T.L. and York A.C. 2006. Tropical spiderwort (*Commelina benghalensis* L.) control and emergence patterns in preemergence herbicide systems. *Journal of Cotton Sci.*, 10: 68-75.

Author Information

Tamer Ustuner

Kahramanmaraş Sütcü Imam University, Faculty of Agriculture, Department of Plant Protection, Avsar Campus, Kahramanmaraş/Turkey
Contact e-mail: tamerustuner@ksu.edu.tr

Ummet Diri

Experts Agriculture Plant Protection Research & Engineering Ltd. Adana/Turkey

Compact Wideband Lowpass Filter Based on Inverted Cascading Stubs

Emad S. AHMED

University of Technology

Jabbar K. MOHAMMED

University of Technology

Abstract: In this study, a new compact wideband lowpass filter was introduced. The proposed filter is developed by cascading two shapes of '4' open stubs back to back embedded on a microstrip line. This structure results in wide cutoff frequency and rejection band with improved scattering parameters. The filter utilized operating bands up to 4 GHz. Many useful wireless communication bands were allocated within this band, global system for mobile communications (GSM) bands (1.8, 1.9 and 2.1 GHz) and 2.4 GHz which is used for industrial, scientific and medical (ISM) band and wireless local area networks (WLANs) applications. The designed filter also covers the band 3.5 GHz widely used for worldwide interoperability for microwave access (WiMAX) applications. The frequency response of the filter shows good stopband characteristic and provides -3 dB cutoff frequency at 3.85 GHz. The return loss of the designed filter is -50.8 dB at 3GHz and the insertion loss is less than -0.18 dB along the passband. The proposed filter has been designed, analyzed, and optimized on a substrate with 10.8 dielectric constant and thickness of 1.27 mm using full wave Electromagnetic Simulator. The proposed filter is a compact size and the final optimized dimension of the simulated filter with the above features is only 20 mm × 15mm.

Keywords: Microstrip, Lowpass filter, WLAN applications, WiMAX, Wideband filter

Introduction

Microstrip filters are highly used in microwave systems due to their small size, easy of fabrication, low cost and light weight. Miniaturization in industry of mobile communication systems, motivate the researchers in continuing their filter design contributions with compact size that can be fitted easily inside the mobile phone. They try to design a simple microstrip miniaturized filter with sharp cut-off frequency and good attenuation characteristics that's needed in modern communication systems applications (Hong and Lancaster, 2001; Solanki and Sharma, 2015).

Mixers and oscillators are commonly use lowpass filters to suppress harmonics, noise and other undesired signals that exist in their operations. A novel small size microstrip LPF with a sharp edge passband and high attenuation within stop-band are proposed and presented in literature. In (Mohsen, Zahra F, and Mozghan, 2014), LPF was designed by combining the star-shaped resonator with the half ring-shaped stubs, this leads to a compact circuit size with sharp edge transition band. (Challal, Azrar and Vanhoenacker, 2012) proposed a wide stopband microstrip LPF based on quasi-triangular defected ground structure (DGS). This structure enhance the rejection of higher spurious and harmonics that is used in wideband applications. (Kim and Yun, 2005) use asymmetrical stepped microstrip structures to design LPF with good harmonic suppression. (Zakaria, Mutalib, Mohamad and Zainuddin, 2013) proposed a defected stripline structure to demonstrate a notch in bandpass filter constructed from the integration of lowpass and highpass filter. This notch was used to remove the undesired signals in the filter characteristics. (Seghier, Benabdallah, Benahmed, and Nouri, 2016) designed a composite microstrip bandpass filter with new techniques. The design utilized high-pass and low-pass structure embedding individually into each other. This technique was proposed to be used for ultra-wideband wireless communications. Optimization was used for tuning the passband performance of the proposed filter. The filter

- This is an Open Access article distributed under the terms of the Creative Commons Attribution-Noncommercial 4.0 Unported License, permitting all non-commercial use, distribution, and reproduction in any medium, provided the original work is properly cited.

- Selection and peer-review under responsibility of the Organizing Committee of the Conference

shows UWB characteristics with a good s-parameters in the range of 3GHz to 10GHz as well as sharpness rejection characteristics performance. A compact and wide stopband lowpass filter is presented in (Karthikeyan and Kshetrimayum, 2015). Two cascaded stages of open complementary split ring resonator (OCSRR) were used in the constructing of the LPF. DGS section using a shape of tapered dumbbell was placed under the resonators for the purpose of bandwidth enhancement. The rejection bandwidth covers the entire UWB spectrum.

Step impedance method with linear alternative too high or too low part characteristic impedance was used to design less complexity LPF. Good filter response characteristics can be achieved by changing length or width of the designed impedances. The lowpass filter is usually implemented either by series connected high-low stepped-impedance sections or by series-shunt stubs microstrip line sections. Microstrip is an easy method to design LPFs by alternating high impedance and low impedance sections of microstrip lines. Stepped impedance LPFs filters are popular because they are easier to design and take up less space than a similar lowpass filter using stubs (Omid and Arman, 2012; Garvansh and Arun, 2014; Shilpi. Pooja and Prasad, 2014; Abdel-Rahman, Verma, Boutejdar and Omar, 2004; Mathaei, Young and Jones, 1980; Niharika and Pankaj, 2012; Liew, Syed, Mohd, Yufridin and Lee, 2015; Packiaraja, Vinoyb, Ramesha and Kalghatgi, 2011).

In this paper, a wideband LPF using two inverted “4” shapes resonators of microstrip stubs of high-low impedances is presented. The resonators designed using high-low impedance sections transformed from lumped elements ladder LPF. A review of design technique to convert a lumped element LPF prototype into microstrip line circuits is presented. The design and synthesis of the proposed LPF has been presented. Substrate with dielectric constant 10.8 and thickness of 1.27 mm at 3.85GHz cut-off frequency have been used. The results of the optimized filter were obtained through full wave Electromagnetic Simulator.

Lumped Elements Lpf Design Review

The proposed LPF filter specifications are to pass 4 GHz frequency band with attenuation not less than -15 dB at 6 GHz and 3.85 GHz cut-off frequency. According to tables given in (Pozar, 2012), fourth order filter with maximally flat response will achieves the desired requirements of prototype LPF. The forth order values of these elements are: $g_0 = g_5 = 1$, $g_1 = g_4 = 0.7654$, $g_2 = g_3 = 1.8478$.

The lumped values of the LPF can be calculated from:

$$C_i = \frac{g_i}{Z_o \omega_c} \quad (1)$$

$$L_i = \frac{Z_o g_i}{\omega_c} \quad (2)$$

The circuit of maximally flat fourth order LPF is given in Fig.1 and the Lumped values after frequency and impedance scaling are given as: $C_1 = 0.63281$ PF, $L_2 = 3.81972$ nH, $C_3 = 1.52789$ PF, $L_4 = 1.58204$ nH.

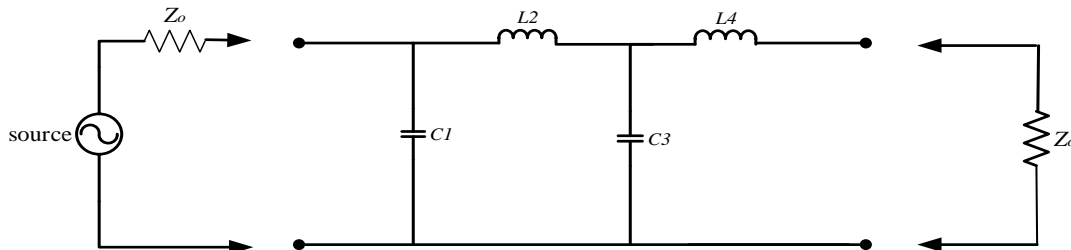


Figure 1. Maximally flat fourth order LPF equivalent circuit

The corresponding frequency and phase response are shown in Fig.2. It is clearly shown that the response is maximally flat with cut-off frequency at 3.85 GHz and stop frequency at 6 GHz with (-15) dB attenuation.

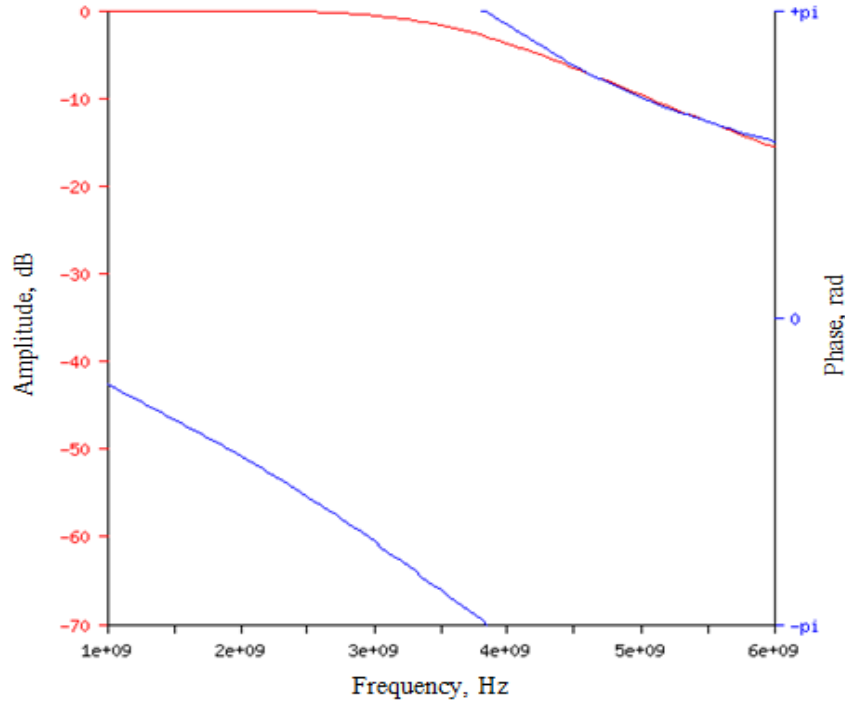


Figure 2. Frequency and phase responses of maximally flat of order N=4.

Distributed Model of the Proposed 4th Order LPF

The conversion of lumped element LPF to distributed microstrip model is done using low-high impedance transformation sections. The low impedance shunt stub will act as shunt capacitor and the high impedance series stub will act as series inductances. The source and load will terminated by 50 Ω impedances. The design and synthesis of the microstrip LPF with series-shunt stubs microstrip sections is achieved on substrate of 10.8 dielectric constant and 1.27 mm thickness. The highest characteristic impedance is assumed to be $Z_{high}=70 \Omega$ and the lowest impedance is $Z_{low}=52.5 \Omega$. The corresponding width of the shunt and series stubs are $W_C=1$ mm and $W_L=0.5$ mm respectively and the width of the input/output of 50 ohm port sections is $W_F=1.1$ mm. The initial guess of electrical length of series and shunt stubs can be calculated by:

$$\ell_{ci} = \frac{\lambda_{gc}}{2\pi} \sin^{-1}(2\pi f_c Z_{low} C_i) \quad \text{for } i = 1, 3 \quad (3)$$

$$\ell_{li} = \frac{\lambda_{gl}}{2\pi} \tan^{-1}\left(2\pi f_c \frac{L_i}{Z_{high}}\right) \quad \text{for } i = 2, 4 \quad (4)$$

$$\lambda_g = \frac{c}{f_r \sqrt{\epsilon_{eff}}} \quad (5)$$

Where c is the speed of light in free space, f_r is the resonance frequency and ϵ_{eff} is the effective dielectric constant given by:

$$\epsilon_{eff} = \frac{\epsilon_r + 1}{2} + \frac{\epsilon_r - 1}{2} \left[\left(1 + 12 \frac{h}{w}\right)^{-0.5} + 0.04 \left(1 - \frac{w}{h}\right)^2 \right] \quad (6)$$

Where h is the substrate thickness and w is the width of microstrip section. Using equations (3)-(6), and using $f_r=f_c$, then the initial guess of stubs length are:

$$l_{c1} = 3.7 \text{ mm}, l_{c3} = 4.9 \text{ mm}, l_{l2} = 4.2 \text{ mm}, l_{l4} = 2.4 \text{ mm}$$

Figure 3 shows the distributed microstrip LPF model transformed from fourth order maximally flat lumped elements LPF circuit.

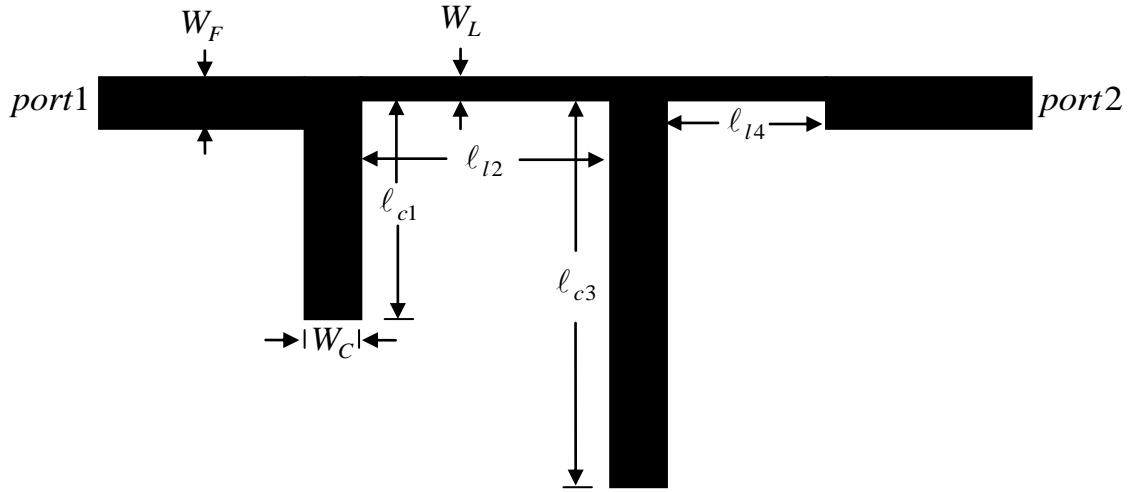


Figure 3. Filter configuration of transformed lumped elements of order N=4

The filter configuration shown in Fig.3 is analyzed using full wave Electromagnetic Simulator. Figure 4 shows the simulated frequency response of the distributed LPF model of Fig. 3. It is clearly shown that the cut-off and stop frequencies are 4.1 and 5.78 GHz respectively with 1.68 GHz transition band.

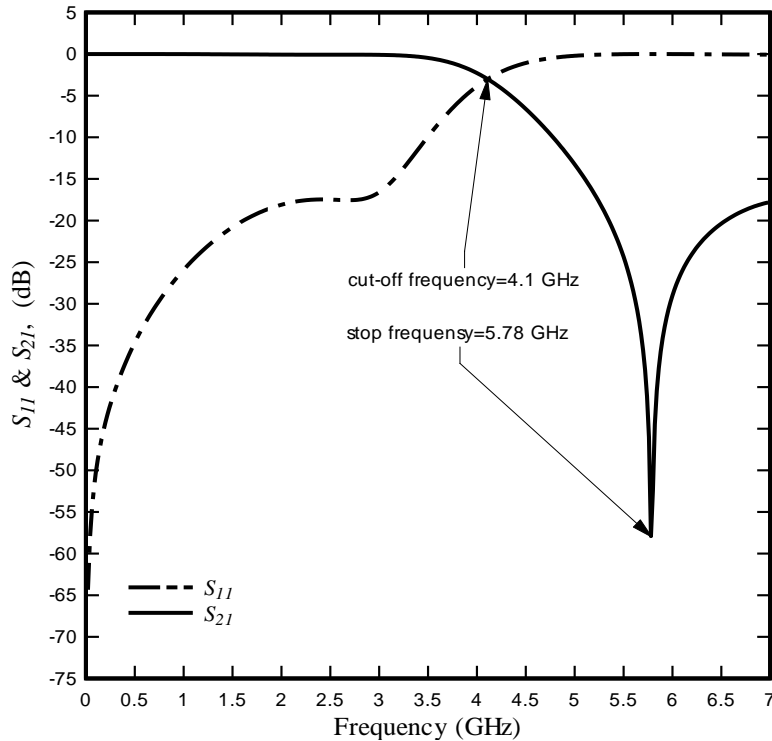


Figure 4. Frequency response of distributed microstrip LPF

Figure 4 show that the cut-off frequency of the distributed LPF transformed from lumped elements is shifted from the designed cut-off frequency 3.85 GHz to 4.1 GHz. The length of the series and shunt stubs can be optimized to tune the filter to the desired cut-off frequency.

Cascaded LPF Design and Simulation Results

To enhance the passband and stopband characteristics of the converted prototype LPF shown in Fig.3, two modified stages have been cascaded. The positions of the shunt stubs in each of the modified stage are vertically changed to form a shape of “4”. One of the “4” shapes is inverted and embedded back to back with the other as shown in Fig.5.

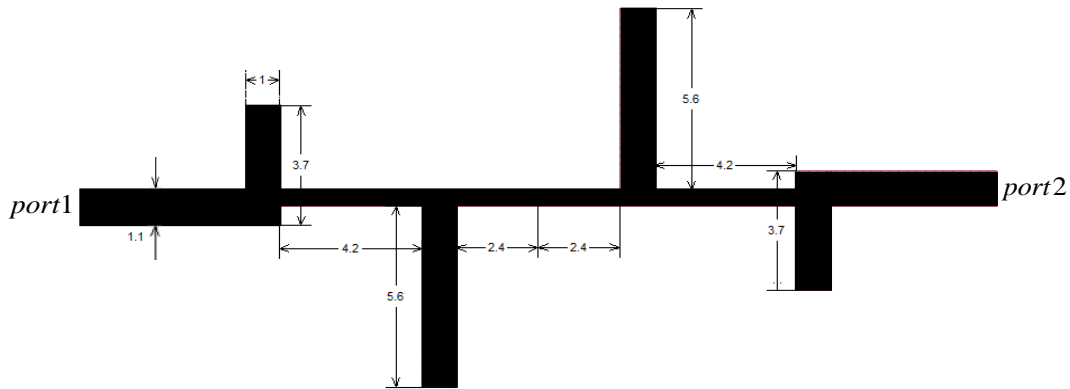


Figure 5. The proposed configuration of two stages of inverted “4” shapes LPF

The configuration of the proposed LPF presented in Fig.5 is built and simulated using full wave Electromagnetic Simulator. Figure 6 shows the simulated frequency response of the single stage and the modified two stages LPF. The proposed filter response has a Quasi-elliptical shape with sharp cut-off and small transition band. The cut-off frequency is 3.85 GHz and the stop frequency is at 4.78 GHz with attenuation -60.9dB followed by transmission zero of attenuation of -81.8 dB at 5.6 GHz.

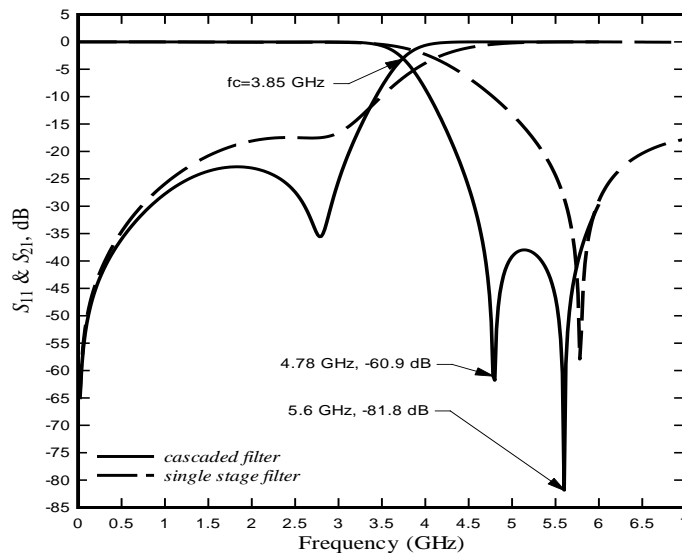


Figure 6. Frequency response of the designed LP filters: Single stage (dotted line), and cascaded two stages of inverted shapes of “4” (solid line)

Conclusion

In this paper a design procedures of fourth order lumped elements maximally flat LPF was presented. The order of the filter was selected according to the prototype LPF specifications. The transformed distributed microstrip LPF filter has small increment drift in the value of cut-off frequency, so the lengths of shunt stubs should be increased to overcome this drift. Quasi-elliptical frequency response can be achieved by cascading of two filter

stages. With proper selection of shunt stubs vertical positions, optimal pass, transition, and attenuation bands characteristics can be achieved.

References

- Abdel-Rahman A., Verma A. K., Boutejdar A., and Omar A.S. (2004). Control of bandstop response of Hi-Lo microstrip low-pass filter using slot in ground plane, *IEEE Trans. On microwave Theory and Tech.*, vol.52, pp. 1008 – 1013.
- Challal M., Azrar A. And Vanhoenacker D. J. (2012). A Novel Ultra-Wide Stopband Microstrip Low-Pass Filter for Rejecting High Order Harmonics and Spurious Response, *Proceedings of the 24th International Conference of Microelectronics ICM 2012*, December 17-20, Algeria.
- Garvansh, N. S. and Arun K. (2014). Design and Synthesis of Stepped Impedance Microstrip Line Low Pass Filter, *International Conference on Recent Trends in Engineering and Technology (ICRTIET-2014 Conference Proceeding)*.
- Hong J.-S and Lancaster M. J. (2001). *Microstrip Filters for RF/Microwave Applications*, John Wiley and Sons, Inc.
- Karthikeyan S. S., Kshetrimayum R. S. (2015). Compact and Wide Stopband Lowpass Filter Using Open Complementary Split Ring Resonator and Defected Ground Structure, *Radioengineering*, Vol. 24, No. 3, pp. 708-711.
- Kim I.-S. and Yun S.-W. (2005). Compact LPF using asymmetrical microstrip step impedance discontinuity for harmonic suppression, *IEEE Electronics Letters*, Vol. 41, No. 16.
- Liew H. F., Syed I. S. H, Mohd F.A. M. , Yufridin W. and Lee Y. S. (2015). A Review of Technique to Convert Low Pass Filter Into Microstrip Line Circuit, *ARPN (Asian Research Publishing Network) Journal of Engineering and Applied Sciences*, VOL. 10, NO. 16, pp. 7164-7174.
- Mathaei G.L., Young L. and Jones E.M.T. (1980), *Microwave Filter impedance matching networks and coupling structures*, Artech House, Dedham, Mass.
- Mohsen H, Zahra F, and Mozghan A. (2014). A Novel Compact Microstrip Low-pass Filter with a Wide Rejection-Band and Sharp Roll-Off using Star-Shaped Resonator. *ACES JOURNAL*, Vol. 29, No. 5.
- Niharika S. V. and Pankaj S. T. (2012). Design and Analysis of Stepped Impedance Microstrip Fractal Low Pass Filter, *International Journal of Electronics and Communication Engineering*. Volume 5, Number 5, pp. 603-607.
- Omid B. and Arman R. (2012). Design, Simulation and Construction a Low Pass Microwave Filters on the Micro Strip Transmission Line, *International Journal of Computer Theory and Engineering*, Vol. 4, No. 5, pp.784-787.
- Packiaraja D., Vinoyb K.J., Ramesha M., and Kalghatgi A.T. (2011). Design of compact low pass filter with wide stop band using tri-section stepped impedance resonator. *International Journal of Electronics and Communications (AEÜ)*, 65, pp.1012– 1014.
- Pozar D. M. (2012). *Microwave Engineering*, John Wiley & Sons, 4th edition.
- Seghier S., Benabdallah N., Benahmed N., and Nouri K. (2016). Design and Optimization of a Microstrip Bandpass Filter for Ultra Wideband (UWB) Wireless Communication, *International Journal of Information and Electronics Engineering*, Vol. 6, No. 4, pp. 230-233.
- Shilpi G., Pooja R, and Prasad R. K. (2014). Design & Optimization of Stepped Impedance Low Pass Filter using ADS Simulation tool at 5 GHz, *International Journal of Advanced Research in Computer Engineering & Technology (IJARCET)*. Volume 3, Issue 5, pp. 1813-817.
- Solanki A, and Sharma N. (2015). Design of Microstrip Low Pass Filter for L-Band Application, *International Journal of Electronics and Electrical Engineering*. Vol. 3, No. 3, pp.212-215.
- Zakaria Z., Mutalib M. A., Mohamad M. S. and Zainuddin N. A. (2013). Transformation of Generalized Chebyshev Lowpass Filter Prototype to Suspended Stripline Structure Highpass Filter for Wideband Communication Systems, *Proceeding of the 2013 IEEE International Conference on RFID Technologies and Applications*, 4 – 5 September, Johor Bahru, Malaysia.

Author Information

Emad S. Ahmed

Dept. of Comm. Eng., University of Technology,
Baghdad/Iraq
30029@uotechnology.edu.iq

Jabbar K. Mohammed

Dept. of Comm. Eng., University of Technology,
Baghdad/Iraq

The Preliminary Results for Atmospheric Parameters of the Candidate Ap Stars HD 90763 and HD 92728

Asli ELMASLI
Ankara University

Seyma CALISKAN
Ankara University

Kubraozge UNAL
Ankara University

Abstract: Chemical peculiar Ap stars show overabundances of some metals, such as strontium, chromium, europium, praseodymium, and neodymium. The rotations of these stars are much slower than those of normal A-type stars. Another characteristic of Ap stars is that they have stronger magnetic fields compared to classical A-type stars. We have selected the A-type stars HD 90763 and HD 92728 to derive their atmospheric parameters. Both stars' high-resolution spectra were obtained using the Coude Echelle Spectrograph mounted on the 1.5 m Russian-Turkish Telescope at the TÜBİTAK National Observatory, on the 23rd of February, 2017. The wavelength range of the spectra is from 3900 to 7900 Å. We followed the standard reduction procedures for both stars and normalised the order covering the hydrogen beta profile. We used ATLAS9 model atmospheres. The strontium 4215.519 Å line seen in the spectra of HD 90763 and the neodymium 5102.428 Å line of HD 92728 were compared to the same lines of the normal A-type star HD 187983. Sr line in HD 90763 and Nd line in HD 92728 are much stronger than those of the normal A-type star. Thus, we suggest that HD 90763 and HD 92728 may be chemically peculiar Ap star candidates.

Keywords: Ap stars, HD 90763, HD 92728

Introduction

A-type stars are remarkable objects in their unusual abundance pattern. Among them the chemically peculiar Ap stars are intermediate mass main sequence objects with strong magnetic fields.

The spectral classes of HD 90763 and HD 92728 are given by Cowley et al. (1969) as A1p (Sr) and A0Vs (Si). McDonald et al. (2012) computed the effective temperatures and luminosities using their infrared photometric data. The effective temperature and luminosity of HD 92728 are 9894 K and 61.6 L_{\odot} , the values are 9011 and 20.4 L_{\odot} for HD 90763. Martin et al. (2004) determined the atmospheric parameters of HD 92728, using the star's photometric data and high-resolution spectrum. They used ATLAS9 and BALMER9 codes for the analysis. The effective temperature, surface gravity, and microturbulence of HD 92728 were derived as 10250 K, 4.25, and 3.8 km/s. The projected velocity is 20 km/s. Mg and Fe abundances are given as 7.54 and 7.5 in the same study. We present the atmospheric parameters of HD 90763 and HD 92728 in this study.

Observations

The high-resolution spectra of HD 90763 and HD 92728 were obtained using the Coude Echelle Spectrograph mounted on the 1.5 m Russian-Turkish Telescope at the TÜBİTAK National Observatory, on the 23rd of

- This is an Open Access article distributed under the terms of the Creative Commons Attribution-Noncommercial 4.0 Unported License, permitting all non-commercial use, distribution, and reproduction in any medium, provided the original work is properly cited.

- Selection and peer-review under responsibility of the Organizing Committee of the Conference

February, 2017. The spectral wavelength range is from 3900 to 7900 Å with a resolution of 40,000. The observed stars properties as well as the observation log is presented in Table 1. The calibration frames (bias, flat fielding) and arc spectra (Th-Ar) were taken at the beginning of the observation run. We applied classical reduction procedures to the observed data by using IRAF code.

Table 1. The properties and observations log of HD 90763 and HD 92728

Star Name	RA [h m s]	DEC [° ' "]	Exposure Time [s]	S/N (@5000 Å)	v_{helio} [km s ⁻¹]	$v \sin i$ [km s ⁻¹]
HD 90763	10 28 43.96	-03 44 32.58 +57 11	4500	193	3.16 ± 2	38 ± 5.70
HD 92728	10 43 43.33	57.11	3600	193	-6.65 ± 2	25 ± 2.52

Atmospheric Parameters of HD 90763 and HD 92728

The initial model atmospheres of both stars were derived from narrow band Strömgren photometry. The surface gravity and effective temperature values were determined from the calibrations of Napiwotzki et al. (1993) using the uvbyβ data adopted from Hog et. al. (2000). These values are listed in Table 2, and were used for calculating the initial model atmosphere of the star with ATLAS9 code (Kurucz, 1993a; 2005; Sbordone et al., 2004).

Table 2. Initial atmospheric parameters of the target stars

Star Name	Strömgren		Johnson			References
	T_{eff} (K)	logg	T_{eff} (K)	logg	m_v m_b	
HD 90763	8315	3.99	8932	4.24	6.032 6.079	Hog et. al. (2000)
HD 92728	10011	3.96	10587	4.26	5.782 5.744	Hog et. al. (2000)

We produced synthetic H_{β} line profiles for these initial atmospheric parameters by using the SYNTHE code (Kurucz, 1993b; 2005). These synthetic H_{β} line profiles did not fit the observed spectrum of each star. Thereby, we refined the atmospheric parameters of both stars and generated new synthetic spectra. These new synthetic H_{β} line profiles were compared to the observed spectrum. A good agreement of the effective temperature was achieved for HD 90763 at 8900 K and for HD 92728 at 8900 K, while the surface gravity was fixed to 4.0 for both star.

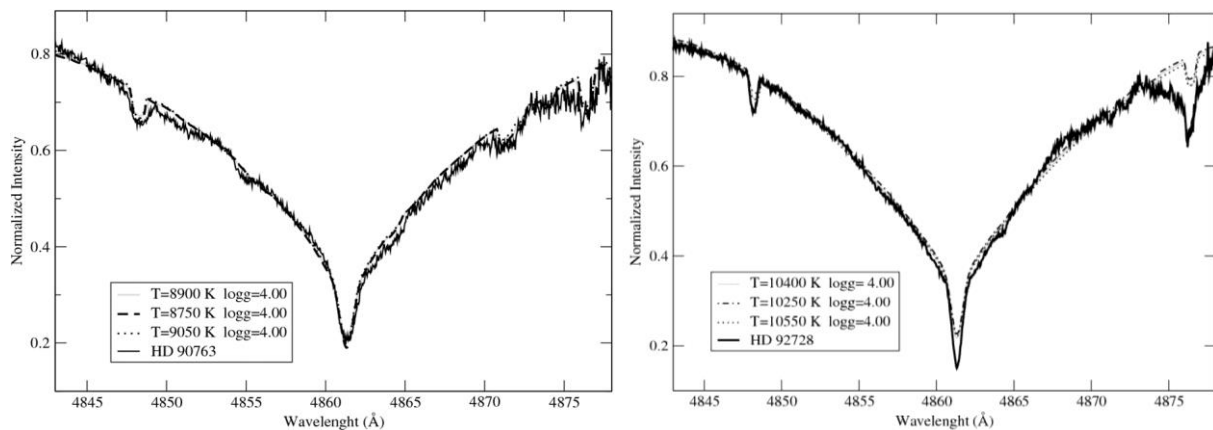


Figure 1. Synthetic and observed H_{β} profiles of HD 90763 and HD 92728

Metal Lines of HD 90763 and HD 92728

Among Ap stars some metallic lines such as strontium, neodymium, and praseodymium are abundant compared to the Sun. We searched for the Sr II at 4215.519 Å, Nd III at 5102.428 Å, and Pr II at 5129.54 Å ions in both of the stars observed spectra. The Sr II at 4215.519 Å line of HD 90763 can be seen in the left side of Figure 2. It is compared to the normal A-type star HD 187983. From this figure we can see that Sr is overabundant compared to the normal A-type star. The 4215.519 Å line of strontium in HD 92728 could not be seen on the spectra due to noise.

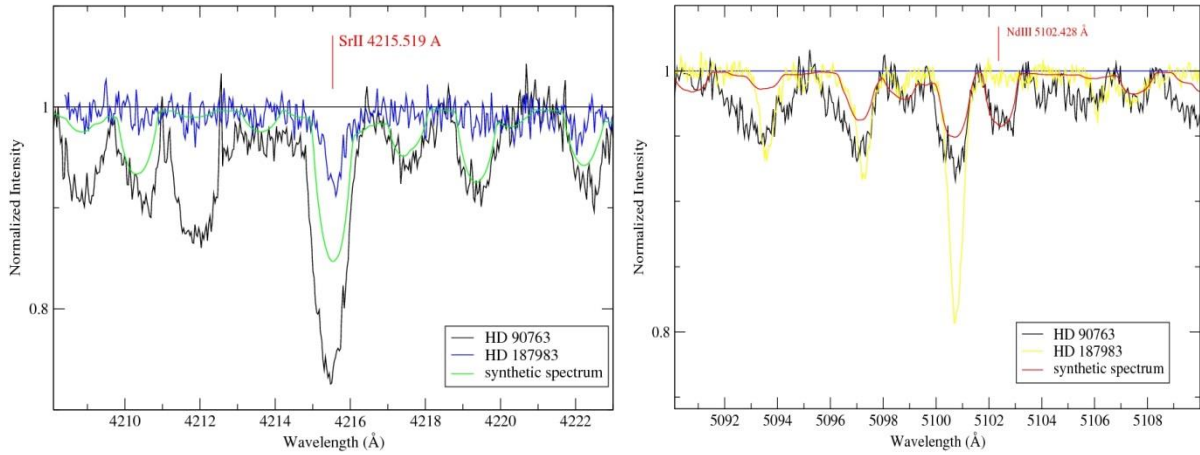


Figure 2. The strontium and neodymium atomic lines of HD 90763 are compared to a normal A-star (HD 187983).

In the observed spectrum of HD 92728, left figure of Figure 3, both strontium and praseodymium lines can be seen. The Pr II line at 5129.54 Å is not observed in HD 90763 spectrum. In the right figure in Figure 3 we compared the Nd III 5102.428 Å line with the normal A-type star HD 187983. This line in HD 90763 is stronger than that of the normal A-type star.

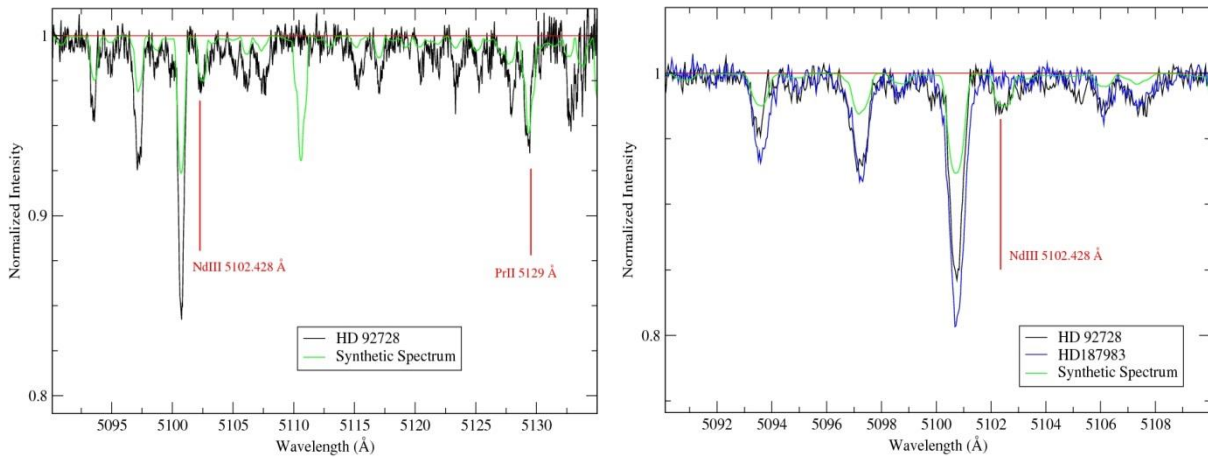


Figure 3. The neodymium and praseodymium atomic lines of HD 92728 (left). The Nd III ion at 5102.428 Å is compared to a normal A type star (HD 187983) spectra. The synthetic spectrum is given in solar abundance.

Conclusion

We derived the atmospheric parameters of HD 90763 and HD 92728 from their high resolution spectra obtained at the TÜBİTAK National Observatory. We searched for specific metallic lines, which are indicators of Ap stars, in the target stars spectra. In the spectra of each star we found the elements strontium, neodymium, and praseodymium. We compared these ions with a normal A-type star and saw that these elements are abundant in HD 90763 and HD 92728. We conclude that HD 90763 and HD 92728 may be Ap star candidates.

Acknowledgements

We thank to TÜBİTAK for a partial support in using T150 telescope with project number 14BR1150-671.

References

- Cowley, A., Cowley, C., Jaschek, M., Jaschek, C. (1969). A study of the bright A stars. I. A catalogue of spectral classifications. *Astronomical Journal*, 74, 375- 406.
- Hog E., Fabricius C., Makarov V.V., Urban S., Corbin T., Wycoff G., Bastian U., Schwekendiek P., Wicenc A. (2000). The Tycho-2 catalogue of the 2.5 million brightest stars. *Astronomy and Astrophysics*, 355, 27-30.
- Kurucz, R. L. (1993a). ATLAS9 Stellar Atmosphere Programs and 2 km/s grid. *Kurucz CD-ROM No. 13. Cambridge, Mass.: Smithsonian Astrophysical Observatory*, 1993.
- Kurucz, R. L. (1993b). SYNTHE Spectrum Synthesis Programs and Line Data. *Kurucz CD-ROM No. 18. Cambridge, Mass.: Smithsonian Astrophysical Observatory*, 1993.
- Kurucz, R.L., (2005). ATLAS12, SYNTHE, ATLAS9, WIDTH9, et cetera. *Mem. Soc. Astron. Ital. Suppl.* 8, 14
- Martin, J.C. (2004). The Origins and Evolutionary Status of B Stars Found Far from the Galactic Plane. I. Composition and Spectral Features. *The Astronomical Journal*, 128, 2474-2500.
- McDonald, I., Zijlstra A.A., Boyer M.L. (2012). Fundamental parameters and infrared excesses of Hipparcos stars. *Monthly Notices of the Royal Astronomical Society*, 427, 343-357.
- Napiwotzki, R., Schoenberner, D., Wenske, V. (1993). On the determination of effective temperature and surface gravity of B, A, and F stars using Stromgren UVBY beta photometry. *Astronomy and Astrophysics*, 268, 653-666.
- Sbordone, L., Bonifacio, P., Castelli, F., Kurucz, R. L. (2004). ATLAS and SYNTHE under Linux. *Memorie della Società Astronomica Italiana Supplement*, 5, 93.

Author Information

Asli Elmasli

Ankara University
Department of Astronomy and Space Sciences, Ankara
University, Tandoğan, Ankara 06100, Turkey
Contact e-mail: elmasli@ankara.edu.tr

Seyma Caliskan

Ankara University
Department of Astronomy and Space Sciences, Ankara
University, Tandoğan, Ankara 06100, Turkey

Kubraozge Unal

Ankara University
Department of Astronomy and Space Sciences, Ankara
University, Tandoğan, Ankara 06100, Turkey

Synthesis and Characterization of Osmium (III) Complexes with Substituted Nitrones

Khalaf I. KHALLOW
University of Mosul

Eman M.H. Al-BAYATE
University of Mosul

Abstract: New series of complexes of general formula $[\text{OsL}(\text{Cl})_2(\text{H}_2\text{O})_2] \cdot n\text{H}_2\text{O}$; where $\text{LH} = [\alpha\text{-}(2\text{-hydroxy-1-naphthyl)-N-(para-R-phenyl nitrone)}$, $n = \text{number of the crystallization water (0-6)}$ and $\text{R} = \text{H, Cl, Br, COCH}_3, \text{NHCOCH}_3, \text{NH}_2$ and CH_3 were synthesized. The complexes were synthesized from direct reaction of the osmium(III) chloride with ligand (L) in a molar ratio of 1:1 respectively. These complexes were characterized by several physical methods such as melting points, molar conductance and elemental analysis (CHN), magnetic moments as well spectral such as infrared and electronic spectral measurements. These studies revealed that the Ligand (L) was behaved as a bidentate, univalent and coordinated to the osmium(III) ion through the oxygen atoms of both, the hydroxyl and the nitrone groups, as well, the presence of two chloride ions and two aqua molecules to give the most probable octahedral geometry around each osmium ion in each complex. The elemental analysis (CHN) as well the infrared spectra showed the presence crystallization water molecules outside the coordination sphere. Their molar conductance measurements revealed the non-electrolytic behavior of the synthesized complexes.

Keywords: Osmium (III), Nitrone, Schiff base, Complexes

Introduction

Many researchers referred that nitrones have special interest due to the broad spectrum of their applications and their successful use as building blocks in different synthetic strategies. They utilized in organic synthesis (1,2), their function as inhibitor for corrosion of mild steel in organic acid media (3) and their uses as precursor for synthesizing compounds having antibacterial activities (4,5). As well, their combination with either alkenes or alkynes cyclo-addition were achieved leading to the formation of new C-C and C-O bonds (6). Besides, new methods of nitrone group activation both with nucleophilic reagent by radical cation formation and with electrophilic reagent by generating dipolar stabilized anions were explored (7). The use of nitrones as ligands was also explored by preparing a series of complexes with transition metal ions (8). They are also used as a suitable ligand for heme model as in metalloporphyrine nitrone complex which was characterized by X-ray crystal structure (9). Recent years have witnessed a renewing interest in their chemistry mainly due to the development of the methods of preparation and subsequent applications (10, 11). The shortages of the 5d metal ion complexes with nitrones has prompted us to synthesis and characterize a new series of substituted nitrones with osmium (III) chloride.

Experimental

1-Preparation of the ligands: The ligands were prepared according to the procedure in two steps (12) and the following procedure was adopted for the preparation of all the ligands in the present study :

Para-substituted nitrobenzene (0.10 mole) and ammonium chloride (0.10 mole, 5.34 g) were dissolved in (100 ml) of Ethanol, cooled to 10°C and (4.0 g) of zinc powder was added with stirring for 2 hrs. The mixture was filtered to get the hydroxylamine in the filtrate to which (0.07 mole) of 2-hydroxy-1-naphthaldehyde was added. The mixture was stirred for 20 hrs. in a dark place. The precipitate was filtered and washed several times with ether then dried. The following equations represent the methods for the prepared ligands with their melting points and crystallization solvents showed in Table(1).

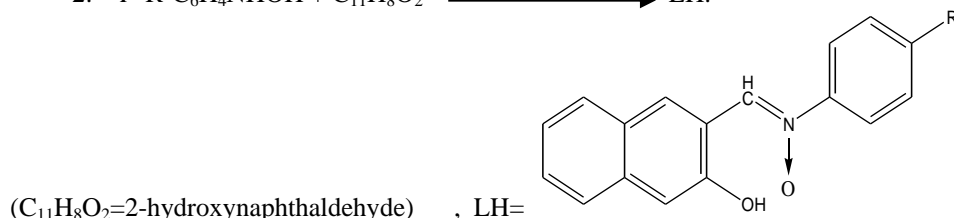
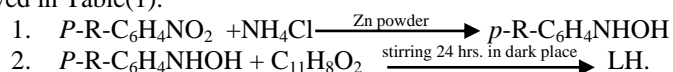


Table 1. The melting points and solvents for the prepared ligands

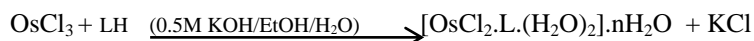
Ligands	R	M.p.°C	Solvent
L ₁	COCH ₃	178	Ethanol
L ₂	Br	65	Ethanol
L ₃	Cl	55	Ethanol
L ₄	CH ₃ CONH	140	Ethanol
L ₅	CH ₃	85	Acetone
L ₆	H	68	Ethanol
L ₇	NH ₂	214	Chloroform

2. Synthesis of the Complexes

A solution of (30 ml, 0.005 mole) of the corresponding ligand in hot ethanol was added to a stirred solution of (20 ml, 0.005 mole) of OsCl₃ in 25 ml of (60%) petroleum ether. A solution of (0.5 M) KOH was added till become alkaline (pH 7-9) and refluxed for 3hrs then cooled to the room temperature. The obtained solid was filtered, washed with ethanol and ether then dried.

Result and Discussion

The synthesized complexes were prepared according to the following equation:



n= 0-6 ; R= COCH₃, Br, Cl , CH₃ , H, NHC(=O)CH₃ and NH₂.

The elemental analysis and some of the physical properties of the prepared complexes are listed in Table (II). They were stable in the solid state and soluble in dimethylformamide (DMF) and dimethylsulfoxide (DMSO) at room temperature. The molar conductivity values in DMF at 10⁻³M were lying in the range (19-55) Ω⁻¹. mol¹.cm⁻¹ indicating the non- electrolytic behavior of all complexes (13) as shown in Table (II).

The coordination sites of the ligands with the osmium (III) ion had been determined by careful comparison of the infrared spectra of the synthesized complexes with that of parent ligands as shown in Table(III). The free ligands showed important spectra in the regions (1077-1215) , (1595-1599) and (1253-1356) attributed to ν(C-O) , ν(C=N) and ν(N→O) respectively. The naphtholic (C-O) spectra

were shifted to a lower values ($\Delta\nu=17-52$) when compared with the spectra of their complexes. This is interpreted as due to the linkage of the ligand with Os(III) ion through the oxygen atom of the naphtholic group(14,15). The azomethine (C=N) spectra were found unchanged or very slightly changed ($\Delta\nu=1-5$) comparing with that of the complexes and hence no indication of the coordination of the azomethine with the metal ion. Moreover, on comparison of the infrared spectra of the ligands and their complexes showed a significant shift toward a lower values by range (7-16) cm^{-1} in the nitron ($\text{N}\rightarrow\text{O}$) group suggesting the involvement of their oxygen atoms in the coordination with the osmium(III) ion(16). The presence of the coordinated and crystallization water molecules in the prepared complexes were indicated by existence of broad bands in the range (3421-3508) cm^{-1} , as it is not easy to distinguish between both types of water molecules since they appeared as a broad bands. As well, the coordinated water molecules in all complexes is indicated by existence of two somewhat weaker bands assigned as the OH rocking(ν) and wagging(ω) vibrations at (814-863) and (633-748) cm^{-1} respectively(17). The Os-Cl bond is usually appeared in the region 200-300 cm^{-1} and this region is beyond the limit of the apparatus. In the low frequency region, the spectra of the synthesized complexes Table(III) exhibited new bands which were not present in the corresponding ligands, were located at 435-588 cm^{-1} attributed to $\nu(\text{Os-O})$ stretching(18).

The electronic spectra of the synthesized complexes are tabulated in Table(IV) and showed three bands at (451-642), (402-445) and (362-399) nm as d-d transition which assigned to ${}^2\text{T}_{2g}\rightarrow{}^4\text{T}_{1g}$, ${}^2\text{T}_{2g}\rightarrow{}^4\text{T}_{2g}$ and ${}^2\text{T}_{2g}\rightarrow{}^2\text{A}_{2g}, {}^2\text{T}_{1g}$ in the octahedral environment respectively(19,20). The high intensity bands in the spectra of the synthesized complexes at (270-319) nm were assigned to the charge transfer absorption between the ligands and the osmium(III) ion(21).

The magnetic susceptibility measurements of the prepared complexes were lying in the range (1.54-1.99) B.M. are indicative of single electron per Os(III) ion suggesting their consistency with their octahedral arrangement(21).

In conclusion, the substituted nitron ligands, in the present study, behaved as bidentate, univalent ligands coordinated through the two oxygen atoms of, the naphtholic and nitron groups. The elemental analyses showed the existence of a number of crystallization water molecules outside the coordination sphere. The presence of two chloride ions and two coordinated water molecules besides the bidentate ligands gave the most probable octahedral geometry around Os(III) ion in each complex as depicted below :

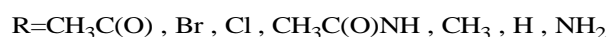
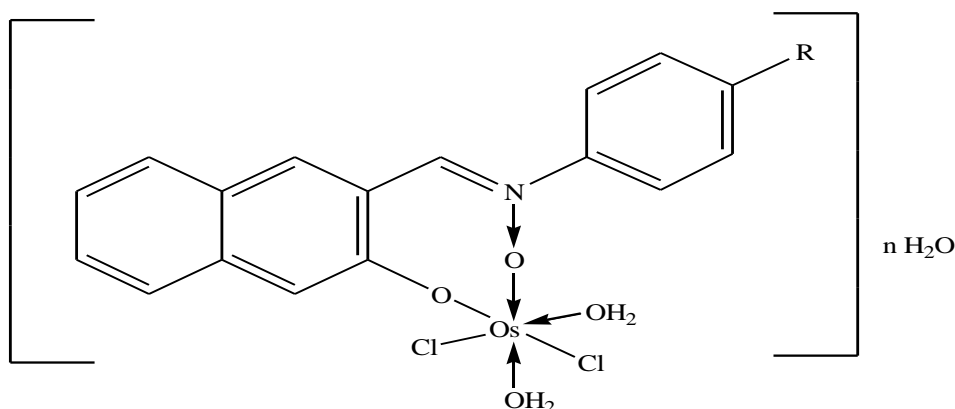


Table 2. Elemental analysis and physical properties of the synthesized complexes

Complexes	Color	M.p. °C	Elemental analysis			Λ_M (DMF)
			Calc./ (Found)			
			C	H	N	
[OsCl ₂ L ₁ (H ₂ O)]	Light olive	76-78	37.92 (38.09)	3.01 (3.68)	3.32 (3.81)	29
[OsCl ₂ L ₂ (H ₂ O) ₂]	Olive	66-68	31.99 (31.65)	2.37 (2.12)	2.19 (2.01)	42
[OsCl ₂ L ₃ (H ₂ O) ₂] ₂ 6H ₂ O	Olive	140-142	29.09 (27.92)	3.88 (2.16)	2.00 (2.44)	35
[OsCl ₂ L ₄ (H ₂ O) ₂] ₂ 3H ₂ O	Olive	96-98	34.03 (34.18)	3.76 (3.55)	4.18 (4.05)	37
[OsCl ₂ L ₅ (H ₂ O) ₂] ₂ 2H ₂ O	Olive	160-162	35.47 (34.78)	3.64 (3.27)	2.30 (2.09)	55
[OsCl ₂ L ₆ (H ₂ O) ₂] ₂ 4H ₂ O	Olive	242d	32.33 (31.98)	3.83 (3.36)	2.22 (2.11)	39
[OsCl ₂ L ₇ (H ₂ O) ₂] ₂ 2H ₂ O	Olive	260d	33.45 (33.01)	3.47 (3.13)	4.59 (4.31)	19

Table 3. Selected I.R. absorption bands of the ligands and their complexes

Compounds	ν C-O	ν C=N	ν N→O	ν Os→O	Coordinated water		
					ν (OH)	τ (OH)	ω (OH)
L ₁	1077	1595	1258	-----	-----	-----	-----
[OsCl ₂ L ₁ (H ₂ O) ₂]	1045	1590	1243	475	3445	861	740
L ₂	1105	1599	1356	-----	-----	-----	-----
[OsCl ₂ L ₂ (H ₂ O) ₂]	1071	1596	1345	586	3508	863	676
L ₃	1139	1597	1255	-----	-----	-----	-----
[OsCl ₂ L ₃ (H ₂ O) ₂] ₂ 6H ₂ O	1090	1596	1245	586	3421	827	675
L ₄	1163	1598	1346	-----	-----	-----	-----
[OsCl ₂ L ₄ (H ₂ O) ₂] ₂ 3H ₂ O	1146	1596	1333	588	34336	827	678
L ₅	1170	1599	1261	-----	-----	-----	-----
[OsCl ₂ L ₅ (H ₂ O) ₂] ₂ 2H ₂ O	1136	1594	1245	560	3444	817	645
L ₆	1163	1599	1253	-----	-----	-----	-----
[OsCl ₂ L ₆ (H ₂ O) ₂] ₂ 4H ₂ O	1139	1596	1246	435	3443	814	748
L ₇	1215	1598	1283	-----	-----	-----	-----
[OsCl ₂ L ₇ (H ₂ O) ₂] ₂ 2H ₂ O	1163	1596	1292	571	3450	829	659

Table 4. Electronic spectra and magnetic moments for the synthesized complexes

Complexes	${}^2T_{2g} \rightarrow {}^4T_{1g}$	${}^2T_{2g} \rightarrow {}^4T_{2g}$	${}^2T_{2g} \rightarrow {}^2A_{2g}, {}^2T_{1g}$	Charge Transfer	μ_{eff} (B.M.)
	$\lambda_{\text{max}}(\text{nm})$	$\lambda_{\text{max}}(\text{nm})$	$\lambda_{\text{max}}(\text{nm})$		
[OsCl ₂ L ₁ (H ₂ O) ₂]	467	442	395	319	1.71
[OsCl ₂ L ₂ (H ₂ O) ₂]	460	405	385	316	1.88
[OsCl ₂ L ₃ (H ₂ O) ₂] ₂ 6H ₂ O	---	445	395	337	1.99
[OsCl ₂ L ₄ (H ₂ O) ₂] ₂ 3H ₂ O	538	441	362	316	1.59
[OsCl ₂ L ₅ (H ₂ O) ₂] ₂ 2H ₂ O	620	431	392	288	1.68
[OsCl ₂ L ₆ (H ₂ O) ₂] ₂ 4H ₂ O	509	402	387	307	1.54
[OsCl ₂ L ₇ (H ₂ O) ₂] ₂ 2H ₂ O	529	445	397	270	1.91

References

- Breuer E., Aurich H.G. and Nielson A., (1989), *Nitrones, Nitronates and Nitroxides*, John Wiley & Sons, New York, 129.
- Wong E.H.H., Junkers T. and Kowolik C.b., (2011), Nitrones in synthetic polymer chemistry *Polymer Chemistry*, 2, 1008.

- Thiumalaikumar M. and Jegannathan . S., (2011), *Potugaliae Electrochimica Acta*, ,29910,1.
- Charaborty B., Chhetri .M.S. Chhetri S.Katley and .Samanta A ,(2010), *Ind. J. Chem.*, ,49B,209.
- Amutha C., Saravanan S. Saravanan,Dhandapani P.S., Muthusbramanian S. and Sivasubramanian .S, (2008), *Ind. J. Chem.*,47B,276.
- Dondas . H.A., Cumins .J.E., Grigg .R. and Thornton P, (2001), *Tetrahedron* ,57,7951.
- Grigorev I.A., (2009), *ARKIVOC*,(IV),136.
- Villamena F.A., Dickman .M.H and D.R.Christ ,(1998) , *Inorg. Chem .* , 37,1446.
- Lee J., Twamley .B. and Richter . G.B.Richter Addo (2002), *Chem.Commun.*,380.
- Kannan. S.,Usman A and .Fun H.K, (2002), *Polyhedron*,21(23),2403.
- Yavus S., Ozkan H., Colak N, and Yildirim Y. , (2011), *Molecules*, ,16,6677.
- West P.R. and Davis .G.C.Davis (1989), *J. Org. Chem.*, ,54,5176.
- Geary W.J.,(1974),*Chem.Abst*,75.
- Canpolat E, and Kaya M.,Turk , (2005), *J.Chem.*, 29,409.
- Mounika K, Anupama B, Pragathi J and Gyanakumari C, (2010), *J. Sci .Res.*, 2(3),513.
- Al-Allaf . T.A.K. and .Omer A.O.,(1993), *Pure and Applied Sciences*, 20,53.
- Ahmed .A.H, Omran .A.A, and El-Sherbiny G.M., (2006), *J. Appl. Res.*, 2(1),44.
- Nakamoto K,(1988) , *Infrared Spectra of Inorganic and Coordination Compounds*, 5th Ed, John Wiley & Sons,183.
- Sharma V.K.,Srivastava S ,and Srivastava A.(2007), *Bioinorg. Chem. and App.*, Hindawi Publishing Corporation,Article10.
- Chitilappilly P.S. and Yusuf K.K.M, (2008), *Ind. .J. Chem.*, 47A,848.
- El-Hindawy A.M., Al-Madfa .H.A, El-Bindary.A. , Abdul-Ghany S. andDiab .M,(1994), *Qatar Univ. Sci. .J.* ,14(C) ,80.

Author Information

Khalaf I. Khallow

Dept. of Chemistry
College of Education for Pure Sciences
University of Mosul, Iraq
Email: kikhallow@yahoo.com

Eman M.H. Al-Bayate

Dept. of Chemistry
College of Education for Pure Sciences
University of Mosul, Iraq

Effects of Light on Egg Performance and Behaviour in Japanese Quails (*coturnix coturnix japonica*)

Gokce Irem DEMIRCI DEMIRBAS
ISTEK Private Atanur Oguz Anatolian High School

Cuneyt KUBANC
Istanbul University

Abstract: Lighting period (photoperiod) is one of the most important environmental factors affecting on animals. Thus, we aimed to investigate the effect of lighting period on efficient production performance of Japanese quails under controlled environmental conditions via the egg yield and behavioural characteristics. 48 female and 12 male Japanese quails (*Coturnix coturnix japonica*) were randomly divided into two groups with two replicates. A scheduled lighting program was applied as 7 Light (L): 17 Dark (D), 6L:18D, 5L:19D, 4L:20D, 3L:21D for five-day periods along 25 days in total using a metal halide lamp with an intensity of light at 41.5 lx to the trial group. At the end of observation, 162 eggs without any damage were obtained from the birds exposed to scheduled lighting program whereas the mean number of damaged eggs/total number of eggs (DE/TE) ratio was 37% in control group exposed to normal daylight length. The number of damaged eggs was correlated with the total number of eggs ($p < 0.01$ vs. control) and egg weight ($p < 0.0001$) in trial group. Egg weight was also found to correlate with body weight ($p < 0.01$ vs. control). During observational experiments any significant difference was recorded in wing stretching, drinking and playing in both groups. However, birds exposed to shortened light headed for less feeding and laying ($p < 0.05$ vs. control) and had leaning to aggressive behaviours such as shouting or stridulating, feather and egg pecking and cannibalism. In conclusion, adding darkness to lighting program contributes energy saving with the equal or even improved production performance in aviaries.

Keywords: Behaviour, Egg production, Lighting program, Quail

Introduction

Commercial quail is one of the alternative sources for animal protein foods especially in underdeveloped countries. Therefore, Japanese quails are mostly kept in battery cages with the purpose of benefiting their eggs and meat (Jatoi et al 2013b). Production performance studies with broilers (Altan et al 1998), quails (Sarica 1998) and pheasants (Tepeli et al 2000) are mostly focused on feed intake, feed conversion ratio, egg quality, effects of various environmental conditions as light.

Light, as a powerful exogenous factor in control of many physiological and behavioural processes, is one of the most important environmental factors affecting broiler performance and physical activity (Olanrewaju et al 2006, Bayram & Özkan 2010, Ma et al 2013). Light intensity, colour and photoperiodic/scotoperiodic regimes have different effects on physical activities of broiler chickens (Olanrewaju et al 2006). In particular, manipulation of light intensity is a widely adopted management tool (Deep et al 2012) affecting broiler production, behaviour and welfare (Bayraktar et al 2012). Therefore, many light patterns have been applied so far, such as continuous lighting (Mahmud et al 2011, Jatoi et al 2013b), near-continuous lighting (Olanrewaju et al 2006, Bayraktar et al 2012), light and dark periods (Bayram & Özkan 2010, Schwean-Lardner et al 2012), intermittent lighting programs (Rahimi et al 2005, Olanrewaju 2006, Mahmud et al 2011, Jatoi et al 2013b, Ma et al 2013) different colours of light (Olanrewaju et al 2006) and various light sources (Ghuffar et al 2009) to rear broilers in numerous studies conducted in various countries. Mostly, broilers have been kept on a

- This is an Open Access article distributed under the terms of the Creative Commons Attribution-Noncommercial 4.0 Unported License, permitting all non-commercial use, distribution, and reproduction in any medium, provided the original work is properly cited.

- Selection and peer-review under responsibility of the Organizing Committee of the Conference

continuous or nearly continuous lighting schedule to maximize feed intake and grow rate (Rahimi et al 2005, Bayram & Özkan 2010 Schwean-Lardner et al 2012). In order to improve welfare and save energy alternative programs with shorter daylight lengths may be applied (Bayram & Özkan 2010). Many studies in different countries showed that different light regimens have significant effects on weight gain and disease problems (Mahmud et al 2011). For instance; birds exposed to near-continuous light had less feed efficiency, but showed higher mortality than birds exposed to longer dark period (Schwean-Lardner et al 2012). Therefore, most of the recent researches have headed for limited light regimens to improve production in broilers due to the low physical activity of birds during darkness (Mahmud et al 2011).

The purpose of this study is to investigate the effect of lighting period on production performance of Japanese quail under controlled environmental conditions. For integrative investigation of the effects of lighting period on the complex interrelation between production performance and lighting period, we measured egg yield and behaviour characteristics.

Method

All experiments in this study were approved by the institutional Animal Experimentation Committee of Istanbul University Cerrahpasa Medical School (31653:07.12.2006). Care and handling of the animals were in accordance with the guidelines for Institutional and Animal Care and Use Committees. The current study has been carried out in accordance with the Declaration of Helsinki.

Animals and Housing

Experiments were performed on 48 female, 12 male Japanese quails at 6-weeks of age with a mean± SEM body weight of 245.9±3.1 g. This research was carried out in two laboratories under same environmental conditions except light. Both laboratories' conditions were kept at 20°C±1 and relative humidity rate were adjusted as 37.4 %. Feed (quail pellet feed with 20 % Crude Protein and 2850 Kcal/kg Metabolic Energy) and water were provided ad libitum in all groups during the entire experimental period (Çoban et al 2008, Duve et al 2011).

Experimentation and Scheduled Lighting Program

48 female and 12 male Japanese quails (*Coturnix coturnix japonica*) were randomly divided into two groups. Birds in Group 1 served as trial group including 12 female and 3 male Japanese Quails (n=2) and exposed to scheduled lighting program as 7 Light (L):17 Dark (D), 6L:18D, 5L:19D, 4L:20D, 3L:21D for five-day periods along 25 days in total. A halogen lamp with 150 W was used to mimic the colour of daylight and photoperiod was provided with an intensity of light at 41.5 lx, calculated according to the formula (Özkaya 1972);

$$\Phi = (E_{on} \times S) / \eta$$

Where Φ is light flux, E_{on} is light intensity, S is illuminated area, η is performance of light. Calculation was confirmed with the lx meter of 4 in 1 Multifunction Environment Meter. Moreover, birds in Group 2 served as control including 12 female and 3 male Japanese quail (n=2) and exposed to normal day light length.

Measurements and Observations

Throughout the experimental protocol, the weight of individuals and their eggs in each group were daily measured with a high sensitive digital scale (Excell BH-600).

Eggs in every group were collected daily and the total, damaged and undamaged eggs were counted. Damaged egg ratio (%) was calculated as:

$$N_d/N_t$$

Where N_d is the number of damaged eggs, N_t is the number of total eggs.

For behavioural analysis, various types of behaviour patterns were classified as stretching, water drinking, feeding, playing, stridulating and egg-laying of individuals were observed during the entire protocol (Vercellino et al 2012, Vercellino et al 2013).

Statistical Analysis

Values were reported as mean \pm SEM. Statistical analysis was performed using GraphPad Prism version 5.0 for Windows (GraphPad Software, San Diego, CA, USA). Two-tailed Pearson Correlation Test was used to analyze the relationships between lighting periods, number of undamaged eggs, egg weight and body weight. A p-value of <0.05 was considered statistically significant.

Results and Discussion

Egg Performance

Total 162 eggs were obtained from the birds exposed to scheduled lighting program. None of them was found to be damaged. However, total 289 eggs were obtained from birds in control group and 108 of them were damaged. In control group, mean value of DE/TE ratio was 37 ± 3 % and mean value for egg weight was 11.97 ± 0.07 g. Minimum egg weight per day was 11.31 g and 12.63 g as maximum egg weight of group exposed to normal day light length. In trial group exposed to lighting program, minimum egg weight per day was 11.94 g, 12.89 g as maximum and mean value of egg weight was 12.34 ± 0.06 g (table 1). The total number of eggs was correlated with the number of damaged eggs in trial group ($p<0.01$ vs. control) but the effect was minor. The number of damaged eggs was also correlated with the egg weight ($p<0.0001$) (table 3).

Table 1 EW (g/individual/cage), BW (g/individual/cage), DE/TE, and EW/BW (%) ratio in two groups

	Control				Trial		
	DE/TE (%)	EW (g)	BW(g)	EW/BW	EW (g)	BW(g)	EW/BW
Min	10	11.31	249.2	0.04	11.94	240.20	0.04
Max	67	12.63	261.2	0.05	12.89	248.30	0.05
Mean	37 ± 3	11.97 ± 0.07	$255.3\pm0.53^{***}$	0.04	12.34 ± 0.06	245.3 ± 0.46	0.05

Body Weight

Birds exposed to lighting program in trial group had 240.2 g body weight per day as minimum and 248.3 g as maximum and 245.3 ± 0.5 g as mean value of body weight whereas 249.2 g as minimum, 261.2 g as maximum body weight and 255.3 ± 0.53 g ($p<0.0001$) as mean value for body weight in control group (table 1). The egg weight was correlated with body weight in the trial group ($p<0.01$) (table 2) and, EW/BW was found to be correlated with egg weight in both trial and control groups (table 2-3); but egg weight was not found to be correlated with the ratio in control group on contrary to trial group ($p<0.0001$) (table3). There was no correlation between body weight and the total number of eggs in both trial and control groups (table 2-3). However, number of damaged eggs in control group was significantly correlated with EW/BW ($p<0.0001$) (table 3).

Table 2. Correlation among TE, EW, BW and EW/BW in trial group

Trial	TE	EW	BW	EW/BW
TE		$p>0.05$	$p>0.05$	$p>0.05$
EW	$p>0.05$		$P=0.0086$ $r^2=0.26$	$p<0.0001$ $r^2=0.93$
BW	$p>0.05$	$p=0.0086$ $r^2=0.26$		$p<0.0001$ $r^2=0.50$
EW/BW	$p>0.05$	$p<0.0001$ $r^2=0.93$	$p<0.0001$ $r^2=0.50$	

Table 3. Correlation among TE, EW, BW and EW/BW in control group

Control	TE	DE	EW	BW	EW/BW
TE		P=0.01 r ² =0.23	p>0.05	p>0.05	p>0.05
DE	P=0.01 r ² =0.23		P<0.0001 r ² =0.55	p>0.05	P<0.0001 r ² =0.54
EW	p>0.05	P<0.0001 r ² =0.55		P=0.98 r ² =0.00003	P<0.0001 r ² =0.99
BW	p>0.05	p>0.05	p>0.05		p>0.05
EW/BW	p>0.05	P<0.0001 r ² =0.54	P<0.0001 r ² =0.99	p>0.05	

Behavioural Features

As behavioural features were compared between two groups; there was not a significant difference in wing stretching, drinking and playing in both groups (p>0.05). However, birds in trial group showed lesser feeding and egg laying and even no aggression behaviours such as shouting or stridulating (p<0.05 vs. control group) (figure 1).

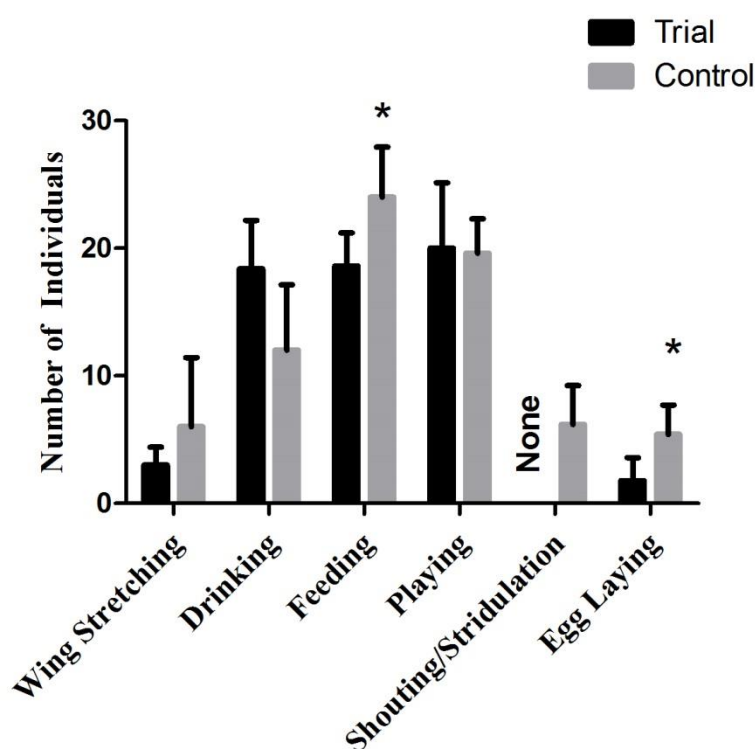


Figure 1. Behavioural features observed in trial and control groups

The results of the present study showed that the birds exposed to scheduled lighting program starting from 7h light and 17h darkness had the most production of egg during 5h light and 19h darkness applied. The most remarkable point of this finding was that the production performance of this group is 100% and the eggs obtained from these birds were all undamaged.

There are many factors affecting on egg performance such as diets, feeding time and method (Kocaman et al 2006), alternatives for feeding ingredients (Yıldırım & Öztürk 2013, Ertaş et al 2006, Tekeli et al 2005, Karaoğlu et al 2004, İpek et al 2003, Bozkurt et al 2001), cage density (Kum & Kocaoğlu-Güçlü 2006), age (Şeker et al 2005), body weight (Jatoi et al 2013a), egg weight, and heat stress (Ertaş et al 2006), besides light factors (intensity, colour, and photoperiod).

Results on production performance seem to be closer to Kocaman et al (2006) who previously reported a negative and significant correlation between the air content (CO₂) in aviaries and relative humidity and egg production. Moreover similar results were found by Nariç et al (2010), who determined that total number of eggs in selection group of their study as 107.92 with a peak performance value of 90.41%. Our results regarding to the number of eggs were also similar to small close-bred flocks in imported group of Jatoi et al (2013a); in mean egg weight were lower than the heavy close-bred flocks'. In another study of Jatoi et al (2013b) had the highest egg production in the group exposed to shorter lighting hours as in our research. When we compare the results with ours, we thought that the production performance may be increased as the lighting hours get shortened. Even, the egg weight of the shorter lighted group of Jatoi et al (2013b) is closer to the result of group exposed to standard lighting program in ours. Kum and Kocaoğlu-Güçlü (2006) applied just the opposite of our starting point for lighting program (17h light and 7h darkness) and got the results closer but lower than ours. Şeker et al (2005), Nazlıgül et al (2001), and Yıldırım & Öztürk (2013) applied 16 h light and 8 h darkness in their studies. As the results in egg weight of Yıldırım and Öztürk (2013) were closer to ours; the results of egg weight in Nazlıgül et al (2001) and Şeker et al (2005) were lower than our results.

İpek et al (2003) and Tekeli et al (2005) added Cu at limited levels to laying-hen diets and observed that this heavy metal had a positive effect on egg production and egg weight. İpek et al (2003) used Cu with Zn in diets. These heavy metals are important trace elements needed at very limited values in the organisms. So up to a limit value it is possible to say that adding these metals to pellet feed may affect in a positive way but must be careful to accumulation and harms of these elements in the organisms. For egg weight, we suggest applying shorter lighting program to hens rather than to adding these metals to their diets, because the results of our study were very closer to heavy metal applied ones (12.34 ±0.06 g).

Ertaş et al (2006) investigate the effect of mussel shell supplementation as calcium source on egg production and egg weight in heat-stressed layer Japanese quails and stated that supplementation of mussel shell to the diets improved egg production and egg weight. Mussels are the bio indicator organisms in aquatic ecosystems and this means they accumulate the aquatic pollution, mostly known heavy metals containing Cd, Cu, Pb, Zn, at very high concentrations. By adding the shells of these organisms to the fodder of laying-hens it is possible to say that food chain continues and the bioaccumulation gets higher and higher up to next organism. The result of this study is closer to our results in terms of egg weight; but lower than our production performance.

Bozkurt et al (2001) added zeolite to fodder at different levels and stated that this had a positive effect on DE/TE ratio. But the results of this study gave us an idea that adding zeolite to fodder and scheduled lighting as 5h lighting/19h darkness to quails may be applied to improve egg performance in aviaries. Because we had no damaged eggs if we add zeolite at a limited value with energy saving procedure this may also increase the production performance to up levels.

Karaoğlu et al (2004) and Bozkurt et al (2001) are the only studies that indicated the DE/TE ratio of their researches among the studies that we scanned through. Bozkurt et al (2001) added zeolite and Karaoğlu et al (2004) added sorghum at certain levels to fodder and noted that the ratios were 1.062 and 0.75 respectively. The two researches were closer to each other in production performance but lower than our results.

Ma et al (2013) investigated the effect of an alternative intermittent lighting program on production performance of laying-hens and their results for egg production seems to be lower than the results of this present study. The percentage of cracked eggs is higher than our investigation.

We noted the mean body weight as 245.3 g in trial group and 255.3 g in control cage. These findings are in same way as Bayraktar et al (2012), a study related with the effects of spot lighting on broiler performance, metal halide group of Ghuffar et al (2009); but far away from the findings of Altan et al 1998. The most interesting point related with body weight results is about the correlations between the parameters. We noticed that body weight was correlated with egg weight and the number of damaged eggs but not correlated with number of total eggs. So it is possible to say that egg parameters as numbers are not related with body weight, may be with feed intake and feed conversion ratio due to the relationship between these parameters and body weight.

According to the observational results we are able to say that long-term lighting period is one of the most important stress factors affecting on production performance in aviaries. In experimental group we noticed that the aggression behaviours as pecking feathers and eggs, preening, and cannibalism mostly between males were decreased, even not observed. We interpreted these results due to shortened lighting period. These results are in the same direction with the study of Wechsler and Schmid (1998). Gilani et al (2012) observed severe feather

pecking behaviour type in their experimental group, containing dark brooders. It is shown that the hormone melatonin caused the reduction of locomotor activity in vertebrates. Azpeleta et al (2010) demonstrated this situation in gold fish and showed that the dark period reduces locomotor activity, but when the lights on sense to feeding increased. After all these results of the existing researches, it is possible to say that adding darkness to lighting programs may result in equal or improved production performance and as a decrease in stress level. In previous studies it is stated that increasing the darkness period in lighting program may reduce leg problems and the risk of lameness, and ensure proper eye conditions. One of the negative implications of long scotoperiod is to be hunger due to low vision (Duve et al 2011). This may be the reason of reduction in feed intake and feed conversion ratio.

During darkness period, melatonin, one of pineal gland hormones, responsible for maintaining and regulating circadian rhythms in diurnal species, provides peak and is repressed by light during daylight. This hormone is produced in both pineal gland and retina in birds. Due to production in retina the effect of light predominated than the other environmental factors. In poultry rest and sleep primarily occur during scotoperiod but behaviours like feeding and drinking water mostly occur in day (Schwean-Lardner et al 2014). As Duve et al (2011) we observed feeding in trial group significantly less than control group. They noted that feeding activity was affected by both length and timing of scotoperiod. Similar findings were also noted in Schwean-Lardner et al (2014) in terms of feeding but also drinking. Bayram and Özkan(2010) observed that birds exposed to 16L:8D program turned to rest and sleep less than the other group but behaviours like drinking, pecking, preening were observed higher.

Conclusion

In conclusion, 5 h lighting 19h darkness lighting period is equal or even better production performance in terms of number of eggs and mean egg weight per individual in standard lighting programs used in aviaries. Adding darkness to lighting program helps to save energy with the equal or even improved production performance in aviaries. We hope that this study will be pioneer to the future studies on the relationship among melatonin, darkness period and aggression.

Acknowledgements

None of the authors have any conflict of interest and this study was supported by Istanbul University Scientific Research Projects Fund with the project number T-98/15122006. The authors kindly thank to Assoc. Prof. Dr. Uğur Aksu for his valuable comments on this manuscript.

References

- Altan, Ö., Altan, A. & Özkan, S. (1998). Değişik Aydınlatma Yöntemlerinin Etlik Piliç Performansı Üzerine Etkisi. *Tr. J. Vet. Anim. Sci.* 22:97-102.
- Azpeleta, C., Martinez-Alvarez, R.M., Delgado, M.J., Isorna, E. & De Pedro, N. (2010). Melatonin Reduces Locomotor Activity and Circulating Cortisol in Goldfish. *Horm. Behav.* 57:323-329.
- Bayraktar, S., Altan, A. & Seremet, C. (2012). The Effects of spot Lighting on Broiler Performance and Welfare. *J. Anim. Vet. Adv.* 11(8):1139-1144.
- Bayram, A. & Özkan, S. (2010). Effects of a 16-hour light, 8-hour dark Lighting Schedule on Behavioral Traits and Performance in Male Chickens. *J. Appl. Poult. Res.* 19:263-273.
- Bozkurt, M., Çubuk, M. Basmacıoğlu, H. & Alçiçek, A. (2001). Yumurta Tavuğu Karma Yemlerine İlave Edilen Doğal Zeolitin Yumurta Verimi ve Yumurta Kabuk Kalitesine Etkileri: Enerji ve Protein Düzeyi Dengelememiş Karmalara Doğal Zeolit İlavesi. *Hay. Üret.* 42(1):21-27.
- Çoban, O., Laçın, E. & Sabuncuoğlu, N. (2008). Effect of Some Parental and Environmental Factors on Some Reproductive Traits of Japanese Quails. *Ital. J. Anim. Sci.* 7:479-486.
- Deep, A., Schwean-Lardner, K., Crowe, T.G., Fancher, B.I. & Classen, H. L. (2012). Effect of Light Intensity on Broiler Behavior and Diurnal Rhythms. *Appl. Anim. Behav. Sci.* 136:50-56.
- Duve, L. R., Steinfeldt, S., Thodberg, K. & Nielsen, B. L. (2011). Splitting the Scotoperiod: Effects on Feeding Behaviour, Intestinal Fill and digestive transit time in Broiler Chickens. *Brit. Poultry Sci.* 52(1):1-10.
- Ertaş, O.N., Çiftçi, M., Güler, T. & Dalkılıç, B. (2006). Sıcaklık Stresi Altında Yetiştirilen Bildircinlerde Tatl Su Midyesi Kabuklarının Kalsiyum Kaynağı Olarak Kullanılma Olanakları Yumurta Verimi ve Bazı Kan Parametreleri Üzerine Etkisi. *Fırat. Üniv. Sağlık Bil. Derg.* 20(1):15-20.

- Gilani, A., Knowles, T.G.& Nicol, C.J. (2012). The Effect of Dark Brooders on Feather Pecking on Commercial Farms. *Appl. Anim. Behav. Sci.* 142:42-50.
- Ghuffar, A., Rahman, K., Siddique, M., Ahmad, F.& Khan, M.A. (2009). Impact of Various Lighting source (Incandescent, Fluorescent, Metal Halide and High Pressure Sodium) on the Production Performance of Chicken Broilers. *Pak. J. Agri. Sci.* 46(1):40-45.
- İpek, H., Yertürk, M.& Avcı, M. (2003). Yumurtlama Dönemindeki Bildiricim Karma yemlerine farklı Oranlarda Çinko ve Bakır İlavesinin Yumurta Verim Özellikleri ile Bazı Kan Parametreleri Üzerine Etkisi. *YYÜ. Vet. Fak. Derg.*, 14(1):65-68.
- Jatoi, A.S., Sahota, A.W., Akram, M., Javed, K., Jaspal, M.H., Hussain, J., Mirani, A.H.& Mehmood, S. (2013a). Effect of Different Body Weight Categories on the Productive Performance of Four Close-Bred Flocks of Japanese Quails (*Coturnix coturnix japonica*). *J. Anim. Plant. Sci.* 23(1):7-13.
- Jatoi, A.S., Khan, M.K., Sahota, A.W., Akram, M., Javed, K., Jaspal, M.H.& Khan, S.H. (2013b). Post-Peak Egg Production in Local and Imported Strains of Japanese Quails (*Coturnix coturnix japonica*) as Influenced by Continuous and Intermittent Light Regimens During Early Growing Period. *J. Anim. Plant Sci.* 23(3):727-730.
- Karaoğlu, M., Gül, M. Yörük, M.A., Esenbuğa, N., Macit, M., Turgut, L.& Bilgin, Ö.C. (2004). Farklı Fiziksel İşlem Görmüş Sorgumun (*Sorghum vulgare*) Yumurta Tavuğu Rasyonlarına Değişik Düzeylerde Katılmasının Yumurta Verimi Ve Kalitesi Üzerine Etkisi. *IV. Ulusal Zootekni Kongresi, 1-3 Eylül*, Cilt:1, 476-483, Isparta.
- Kocaman, B., Esenbuğa, N., Yıldız, A., Laçın, E.& Macit, M. (2006). Effect of Environmental Conditions in Poultry Houses on the Performance of Laying Hens. *IJPS.* 5(1): 26-30.
- Kum, E.& Kocaoğlu-Güçlü, B. (2006). Standart ve Sıkışık Kafes Yoğunluğunda Yetiştirilen Yumurta Tavuğu Karma Yemlerine Organik Asit İlavesinin Performansa Etkisi. *Sağlık Bilim. Der. (Journal of Health Sciences)*, 15(2):99-106.
- Ma, H., Li, B., Xin, H., Shi, Z.& Zhao, Y. (2013). Effect of Intermittent Lighting on Production Performance of Laying-Hen Parent Stocks. *ASABE Annual International Meeting, Kansas City, MO, July21-24*, 1-10.
- Mahmud, A., S., R.& Ali, I. (2011). Effect of Different Light Regimens on Performance of Broilers. *J. Anim. Plant Sci.* 21(1):104-106.
- Narınç, D., Aksoy, T.& Karabağ, K. (2010). Japon Bildiricimlerinde Canlı Ağırlığı Arttırmak İçin Gerçekleştirilen Kısa Dönemli Seleksiyonun Yumurta Verimine Etkisi. *I. Kümes Hayvanları Kongresi, Kayseri*.
- Nazlıgül, A., Türkyılmaz, K.& Bardakçioğlu, H.E. (2001). Japon Bildiricimlerinde (*Coturnix coturnix japonica*) bazı Verim ve Yumurta kalite Özellikleri Üzerinde Bir Araştırma. *Tr. J. Vet. Anim. Sci.* 25:1007-1013.
- Olanrewaju, H. A., Thaxton, J. P., Dozier III, W.A., Purswell, J., Roush, W.B.& Branton, S.L. (2006). A Review of lighting Programs for Broiler Production. *IJPS.* 5(4):301-308.
- Özkaya, M. (1972). Aydınlatma Tekniği. İTÜ Mühendislik-Mimarlık Fakültesi Yayınları:88, Teknik Üniversite Matbaası, Gümüşsuyu, İstanbul.
- Rahimi, G., Rezai, M., Hafezian, H.& Saiyazadeh, H. (2005). The Effect of Intermittent Lighting Schedule on Broiler Performance. *IJPS.* 4(6):396-398.
- Sarıca, M. (1998). Işık Rengi ve Aydınlatma Şeklinin Bildiricimlerin Büyüme ve Karkas Özelliklerine Etkileri. *Tr. J. Vet. Anim. Sci.* 22:103-110.
- Schwean-Lardner, K., Fancher, B.I.& Classen, H.L. (2012). Impact of Daylength on Behavioural output in commercial broilers. *Appl. Anim. Behav. Sci.* 137:43-52.
- Schwean-Lardner, K., Fancher, B.I., Laarveld, B.& Classen, H.L. (2014). Effect of Day Length on Flock Behavioural patterns and Melatonin Rhythms in Broilers. *Brit. Poultry Sci.* 55 (1):21-30.
- Şeker, İ., Kul, S., Bayraktar, M.& Yıldırım, Ö. (2005). Japon Bildiricimlerinde (*Coturnix coturnixjaponica*) Yumurta Verimi ve Bazı Yumurta Kalite Özelliklerine Yaşın Etkisi. *İstanbul Üniv. Vet. Fak. Derg.* 31(1):129-138.
- Tekeli, S.K., Öztürk, K.& Esen-Gürsel, F. (2005). Yumurtacı Tavukların Yemine Yüksek Dozda İlave Edilen Bakırın Yumurta Üretimi, Yumurta Kabuk Ağırlığı ve Yumurta Kabuk Kalınlığına Etkisi. *İstanbul Üniv. Vet. Fak. Derg.* 31(1): 179-185.
- Tepeli, C., Çetin, O., Kırıkçı, K., Yapar, K.& Yılmaz, R. (2000). Farklı Aydınlatma Sürelerinin Sülünlerin (P. colchicus) Bazı Verimleri Üzerine Etkileri. *Vet. Bil. Derg.* 16(1):97-102.
- Vercellino, R. do A., Moura, D.J. de, Maia, A. P. de A., Medeiros, B. B. L., Carvalho, T. R. M. de, Salgado, D. D. A.& Nääs, I. de A. (2012). Different Light Intensity on the Behavior and Welfare of Commercial Broiler Chicks. *Ninth International Livestock Environment Symposium, Valencia, Spain, July 8-12*, 1-6.
- Vercellino, R. do A., Moura D.J. de, Nääs, I. de A., Maia A.P. de A, Medeiros, B.B.L., Salgado, D.D.A.& Carvalho, T.R.M. de. (2013). The Influence of Side-Curtain Color on Broiler Chick Behavior. *Braz. J. Poult. Sci.* 15(3):173-179.

- Wechsler, B.& Schmid, I. (1998). Aggressive Pecking by Males in Breeding Groups of Japanese Quail (*Coturnix coturnix japonica*). *Brit. Poultry Sci.* 39:333-339.
- Yıldırım, A.& Öztürk, E. (2013). Damızlık japon Bildircını Rasyonlarında Soya Küşpesi Yerine Pamuk Tohumu Küşpesi İkamesinin Yumurta Verim ve Kalite Özelliklerine Etkisi. *TURJAF.* 1(1):44-50.

Author Information

Gokce Irem Demirci Demirbas

Istek Private Atanur Oğuz Anatolian High School
Balmumcu Mah. Gazi Umurpaşa Sk.
No:26 Balmumcu İstanbul 34349
Contact e-mail: demirci.gokce.irem@gmail.com

Cuneyt Kubanc

Istanbul University Faculty of Sciences,
Department of Biology,
Zoology Division, 34134,
Vezneciler, Istanbul/Turkey

Modeling Clustered Scale-free Networks by Applying Various Preferential Attachment Patterns

Gokhan KUTLUANA

Bartın University

Ilker TURKER

Karabük University

Abstract: Preferential attachment phenomenon is a key factor providing scale-free behavior in complex networks. In this study, we introduced various preferential attachment patterns applied in a growing Barabasi-Albert network, denoted by a factor α . We first generated networks under constant preferential attachment levels from 0 to 2, where 1 stands for linear preferential attachment. Then we performed network simulations under uniformly distributed random α condition, within the interval [0,2]. Although mean α is 1 for this setup, generated networks displayed greater clustering together with lower modularity and separation values compared to the setup with $\alpha=1$. We also performed similar network generation procedures with various distribution functions applied for α , each resulting random levels of preferential attachment. We achieved networks with power-law consistent degree distributions with γ coefficients between 2 and 3, together with improved clustering coefficients up to ~ 0.3 . As a result, scale-free network topologies featuring greater clustering levels compared to pure Barabasi-Albert model are achieved.

Keywords: Complex network modeling, Preferential attachment, Scale-free networks, Clustering coefficient

Introduction

Real networks diverge from random networks with their degree sequences and clustering property. Most real networks have power-law consistent degree distributions labeling them as *scale-free* (Albert & Barabási, 2002; Barabási & Albert, 1999). Scale-free networks promote generation of a small number of hubs together with numerous low-degree nodes, where the degree sequences of all nodes are consistent with a linear decaying character in a log-log scale of degree distribution (Clauset, Shalizi, & Newman, 2009; Newman, 2003). This distribution is mostly governed by the preferential attachment phenomenon, a key ingredient of most current network models that highly connected nodes increase their connectivity faster than their less connected peers (Jeong, Néda, & Barabási, 2003). In networks with preferential attachment, new nodes prefer connecting to more connected nodes instead of less connected ones. This generic mechanism has significant roles in real networks and have been subject of many studies of network analysis and modeling (Abbasi, Hossain, & Leydesdorff, 2012; Dereich & Mörters, 2009; Johnson, Faraj, & Kudravalli, 2014; Milojević, 2010; Poncela, Gómez-Gardenes, Floría, Sánchez, & Moreno, 2008).

Preferential attachment is said to be linear, if the connectivity of a node is linearly dependent to its degree. In some occasions, nodes in real networks display attachment levels with non-linear dependence to node degree. These behaviors are labeled as sub-linear or super-linear preferential attachment. The critical level of this attachment level is abstracted with an α parameter that is equal to 1 for linear preferential attachment, less than 1 for sub-linear and greater than 1 for super-linear attachment levels (Barabási, 2016). Networks with sub-linear preferential attachment levels display stretched exponential degree distribution, meaning fewer and smaller hubs compared to a scale-free network, and a concave degree distribution in a log-log scale. On the other hand, networks with super-linear attachment display convex log-log degree distributions, which lead to a hub-and-spoke topology as a result of “a winner-takes-all” dynamics (Barabási, 2016; Dereich & Mörters, 2011).

- This is an Open Access article distributed under the terms of the Creative Commons Attribution-Noncommercial 4.0 Unported License, permitting all non-commercial use, distribution, and reproduction in any medium, provided the original work is properly cited.

- Selection and peer-review under responsibility of the Organizing Committee of the Conference

Clustering is another key ingredient of real networks, captured with a coefficient indicating in what rate the neighbors of a given node are also neighbors of each other (Barabási, 2016; Newman, 2003). This coefficient is averaged over all nodes to present the level of average clustering of a network. Many modeling studies are conducted to capture both preferential attachment and clustering properties of real networks. These studies employ several mechanisms like triad-formation (Alstott, Klymko, Pyzza, & Radcliffe, 2016; Holme & Kim, 2002; Kim & Diesner, 2017), improving clustering of networks with arbitrary degree distributions (Bansal, Khandelwal, & Meyers, 2009; Colomer-de-Simon & Boguná, 2012; Herrero, 2015) and promoting connections between spatially close nodes (Manna & Sen, 2002; Türker, 2018; Xie, Ouyang, & Li, 2016; Xulvi-Brunet & Sokolov, 2002).

In this study, we aimed to achieve clustered scale-free network topologies by applying various preferential attachment levels including α parameters of constant values below and above 1, uniform distributed random α values, α values generated from some mathematical expressions like sinusoidal or sigmoid functions etc. The results of the corresponding models are presented in the next section. Although no strategy is employed for tuning clustering property, the results demonstrate that scale-free networks with improved clustering according to Barabasi-Albert network are achieved.

Method

We generated growing network models, based on Barabasi-Albert (BA) scale-free model (Albert & Barabási, 2002). The computational fashion followed to realize a BA network is illustrated in Fig. 1. For a new node just joining the network, connecting probability to an old node is directly proportional with the number of occurrences of the node ID in the edges array. This provides realization of linear preferential attachment phenomenon in a numerical fashion.

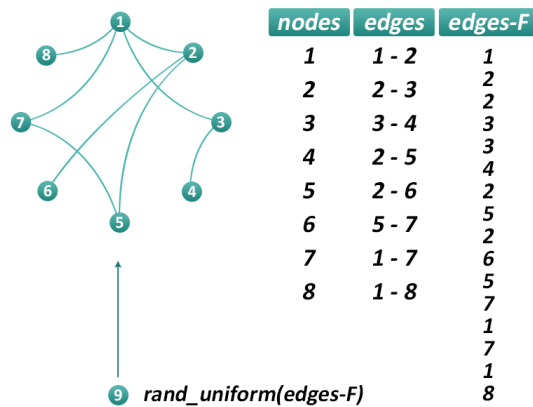


Figure 1. The computational method followed to achieve a BA network is illustrated. The new node (9) just joining the network chooses a node to connect from the flattened edges array (edges-F), with an index randomly generated from a uniform distribution. By the way, nodes have attachment probabilities proportional with their current degrees

Tuning Preferential Attachment

In the above-mentioned setup, the likelihood to connect to a node depends on that node's degree k . The functional form of preferential attachment can be approximated with Eq. 1.

$$\Pi(k) \sim k^\alpha \quad (1)$$

For networks with linear preferential attachment $\alpha = 1$, corresponding to linear dependence of Π with k . For any $\alpha > 0$, new nodes tend to make connections to more connected nodes over less connected ones. For $\alpha < 1$ (sub-linear preferential attachment) this bias is weak and insufficient to provide a pure scale-free degree distribution, rather resulting a stretched exponential distribution. On the other hand, for $\alpha > 1$, connecting to more connected nodes is promoted, resulting a structure that rich get richer than in a network with linear preferential attachment (Barabási, 2016). This behavior, labeled as super-linear attachment, exhibits a hub-and-spoke topology and a convex degree distribution in log-log scale.

We tuned the generated network models with this α parameter such that, the occurrence count of the ID of a node with degree k in the edges-F array is equal to k^α . For linear attachment, the ID of a node with degree 2 is repeated $2^1 = 2$ times in this array, corresponding to linear attachment as illustrated in Fig. 1. For α values resulting non-integer repeat counts, the result is rounded to the nearest integer. For instance, if $\alpha = 1.4$ and the degree of a node is 2, this count will be $2^{1.4} \sim 2.63$, therefore the node ID will be repeated 3 times in the edges-F array.

Results and Discussion

We first generated networks by setting constant α parameters within the interval [0-2] by incrementing 0.2 for each network setup. This procedure is applied to two sets of networks where the first is constructed with 1 links assigned for each new node and the second is constructed with 5 links assigned for each new node. This count of edges corresponds to the parameter m described in BA model in Ref. (Albert & Barabási, 2002).

We present the basic network parameters in Table 1 and 2 as follows. As seen from the tables, average path length displays monotone decaying trend for both setup. Modularity measure remains almost constant for α values up to 1.4, showing a steep decay for greater α values. This indicates that super-linear preferential attachment, resulting a hub-and-spoke topology avoids nodes to organize into modules. For the similar α interval, average clustering coefficient increases dramatically. As a result, networks emerge to get more clustered but less modular for super-linear attachment region.

Table 1. Results for networks generated with $m=1$ links per step and different preferential attachment levels (α). The last column corresponds to random α applied at each step of the growing network, from a uniform distribution between 0 and 2. Clustering coefficient results 0 for $m=1$ setup.

α	0	0,2	0,4	0,6	0,8	1	1,2	1,4	1,6	1,8	2	Rnd
Avg. Clustering C.	-	-	-	-	-	-	-	-	-	-	-	-
Avg. Path Length	10,7 6	10,5 6	9,36	8,52	8,13	7,21	5,66	3,05	2,22	2,03	2,02	6,35
Modularity	0,93 4	0,93 4	0,93 4	0,93 3	0,92 9	0,92 5	0,90 4	0,53 4	0,15 5	0,03 1	0,02 4	0,89 2

Table 2. Results for networks generated with $m=5$ links per step and different preferential attachment levels (α). The last column corresponds to random α applied at each step of the growing network, from a uniform distribution between 0 and 2.

α	0	0,2	0,4	0,6	0,8	1	1,2	1,4	1,6	1,8	2	Rnd
Avg. Clustering C.	0,01 5	0,01 7	0,01 8	0,01 9	0,02 6	0,04 3	0,08 5	0,21 1	0,60 3	0,75 9	0,72 4	0,07 7
Avg. Path Length	3,24	3,19	3,19	3,15	3,08 7	2,96 4	2,77	2,5	2,01	2	1,99	2,88
Modularity	0,28 2	0,28 5	0,29	0,28 8	0,27 8	0,28	0,26 3	0,25	0,19 3	0,15 2	0,10 6	0,27 2

A noteworthy output of these simulations is that, selecting α parameter from a uniform random distribution between 0 and 2 (with a mean of 1) results networks with greater clustering (~ 2 times) compared to networks with linear preferential attachment ($\alpha = 1$). Although they have the same expected α parameter, picking random α at each step emerges as a key factor for improving clustering in scale-free networks. These results also indicate that networks with improved clustering are observed for α values typically greater than 1.

We also present the degree distributions for these networks in Fig. 2 to consult the power-law consistencies. These plots indicate that, degree exponent decreases with increasing α parameter, since the super-linear preferential attachment results convex degree distributions. Visual inspection says that power-law fitting is not a suitable choice for α values greater than 1.4. On the other hand, degree distributions for both $\alpha=1$ and $\alpha=\text{rand}(0-2)$ scenarios result in power-law consistent distributions with exponents close to 2.7, whereas the network with randomized α setup with mean 1 exhibits approximately twice clustering coefficient compared to fixed $\alpha=1$. This result emerges as a phenomenon that random levels of preferential attachment plays a key role in improving clustering.

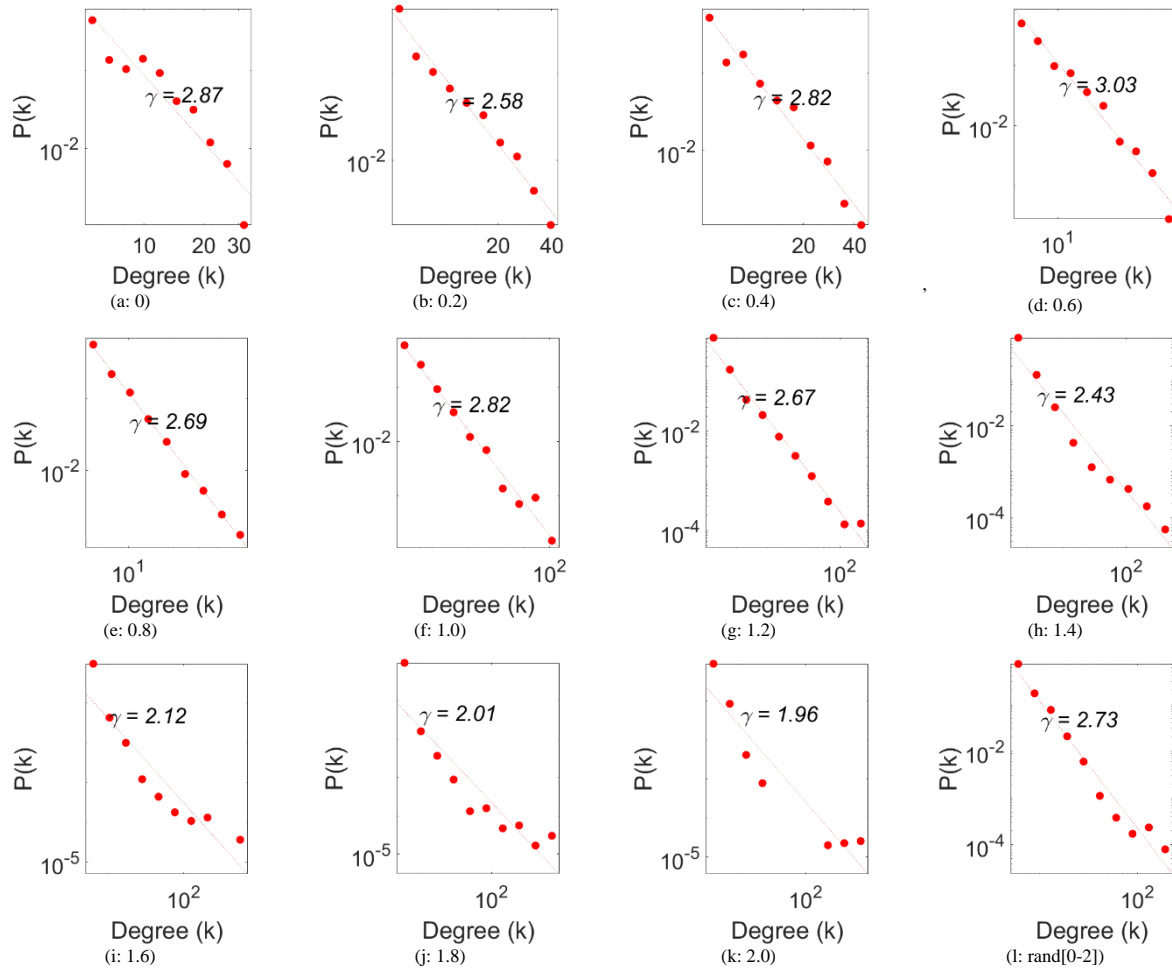



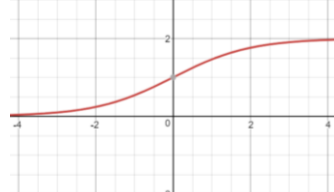


Figure 2. Log binned degree distributions for the networks generated with $m=5$ links per step and different preferential attachment levels (α), gradually increased from 0 (a), to 2 (k) with increment 0.2 at each plot. The last plot (l) corresponds to random α applied at each step of the growing network, from a uniform distribution between 0 and 2. Both axes are logarithmically scaled. Power-law fits with degree exponents are presented for each plot, after least-squared (LS) fitting performed.

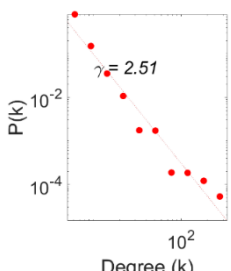
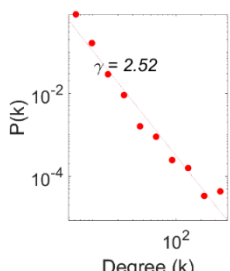
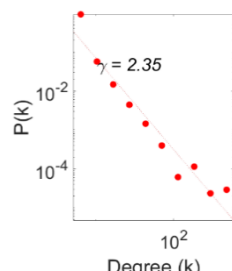
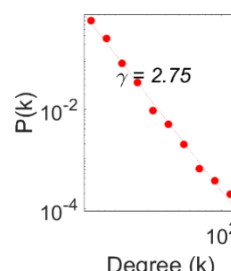
To further investigate the advantage of random α on clustering mentioned above, we applied four different patterns of random α generation procedures, as given in Table 3. As seen from the function plots, the first 3 functions are expected to generate α parameters with mean values greater than 1 (which will result in improved clustering). The last function is expected to produce symmetric α values around 1, but also promote α values rather closer to 0 and 2. All network generation procedures are performed with $m=5$ links per step, and 1000 steps of simulation.

Table 3. Functions applied for random α generation procedures. Uniform random numbers are generated within the interval given in the rightmost column, and the corresponding y values are used as random α at each step of a growing network.

Graph	Function	Applied Interval
	$y = 1 + e^{-x}$	[0,3]
	$y = 2 * \sin(x)$	[0, π]
	$y = 1.25 + e^{-x} \sin(x)$	[0, π]
	$y = \frac{2}{1 + e^{-x}}$	[-4,4]

Applying random level of preferential attachment at each step of growing network, we generated four network topologies. Generating uniform random numbers within the given intervals for each function, the generated y values are constituted for α at each step of edge generation. We present the results of network analysis for each setup in Table 4, together with the resulting degree distributions.

Table 4. Network parameters for the four different patterns of random preferential attachment. Corresponding degree distributions are also presented at the end of each column.

	$y = 1 + e^{-x}$	$y = 2 * \sin(x)$	$y = 1.25 + e^{-x}$	$y = \frac{2}{1 + e^{-x}}$
Avg. Clust. C.	0,1638	0,1856	0,3039	0,12
Avg. Path Length	2,5885	2,6250	2,3189	2,8
Degree Dist.				

As seen in Table 4, the first 3 functions promoting α values greater than 1, result in greater clustering and low separation, while the last function (a type of sigmoid function) generating symmetric α values around 1 yields less clustering but better consistency with power-law behavior. Although the first 3 distribution plots show

convex tendencies, they seem to be acceptable to be labeled as scale-free. The most deviated one from pure power-law consistency is the third one, which dominantly produces greater α values from 1.25. The last model with symmetric α distribution around 1 deviates from the uniformly generated α model in Table 2, by promoting α values rather close to 0 and 2. As a result, both networks have similar average path length values, while power-law consistencies and degree coefficients also seem to be identical. Additionally, the latter one seems to be more successful in improving clustering property (0.077 vs. 0.12). This result indicates that, beyond generating random α parameters symmetric around 1, promoting the values close to 0 and 2 also has a significant impact on improving clustering.

Conclusion

We applied various levels of fixed preferential attachment levels, together with random number generation processes at each step of wiring in growing BA-like networks. We first outlined that clustering coefficient and modularity measures are inversely proportional with the preferential attachment level. Picking random levels of preferential attachment (α) at each wiring procedure emerges as a key factor for improving clustering, while it preserves average path length. Picking α from a uniform distribution between 0 and 2 results in approximately improving clustering twice, while this improvement is three times for a sigmoid function symmetric around 1. We conclude these results that fixed level of preferential attachment may emerge as an inhibiting factor on clustering, in growing networks.

References

- Abbasi, A., Hossain, L., & Leydesdorff, L. (2012). Betweenness centrality as a driver of preferential attachment in the evolution of research collaboration networks. *Journal of Informetrics*, 6(3), 403-412.
- Albert, R., & Barabási, A. L. (2002). Statistical mechanics of complex networks. *Reviews of Modern Physics*, 74(1), 47-97. doi: 10.1103/RevModPhys.74.47
- Alstott, J., Klymko, C., Pyzza, P. B., & Radcliffe, M. (2016). Local rewiring algorithms to increase clustering and grow a small world. *arXiv preprint arXiv:1608.02883*.
- Bansal, S., Khandelwal, S., & Meyers, L. A. (2009). Exploring biological network structure with clustered random networks. *BMC bioinformatics*, 10(1), 405.
- Barabási, A. L. (2016). *Network Science*. Cambridge: Cambridge University Press.
- Barabási, A. L., & Albert, R. (1999). Emergence of scaling in random networks. *Science*, 286(5439), 509-512. doi: 10.1126/science.286.5439.509
- Clauset, A., Shalizi, C. R., & Newman, M. E. J. (2009). Power-Law Distributions in Empirical Data. *Siam Review*, 51(4), 661-703. doi: 10.1137/070710111
- Colomer-de-Simon, P., & Boguná, M. (2012). Clustering of random scale-free networks. *Physical Review E*, 86(2), 026120.
- Dereich, S., & Mörters, P. (2009). Random networks with sublinear preferential attachment: degree evolutions. *Electronic Journal of Probability*, 14, 1222-1267.
- Dereich, S., & Mörters, P. (2011). Random networks with concave preferential attachment rule. *Jahresbericht der Deutschen Mathematiker-Vereinigung*, 113(1), 21-40.
- Herrero, C. P. (2015). Ising model in clustered scale-free networks. *Physical Review E*, 91(5), 052812.
- Holme, P., & Kim, B. J. (2002). Growing scale-free networks with tunable clustering. *Physical Review E*, 65(2). doi: 10.1103/PhysRevE.65.026107
- Jeong, H., Neda, Z., & Barabási, A.-L. (2003). Measuring preferential attachment in evolving networks. *EPL (Europhysics Letters)*, 61(4), 567.
- Johnson, S. L., Faraj, S., & Kudaravalli, S. (2014). Emergence of Power Laws in Online Communities: The Role of Social Mechanisms and Preferential Attachment. *Mis Quarterly*, 38(3), 795-808.
- Kim, J., & Diesner, J. (2017). Over-time measurement of triadic closure in coauthorship networks. *Social Network Analysis and Mining*, 7(1), 9. doi: 10.1007/s13278-017-0428-3
- Manna, S. S., & Sen, P. (2002). Modulated scale-free network in Euclidean space. *Physical Review E*, 66(6), 066114.
- Milojević, S. (2010). Modes of collaboration in modern science: Beyond power laws and preferential attachment. *Journal of the Association for Information Science and Technology*, 61(7), 1410-1423.
- Newman, M. E. J. (2003). The structure and function of complex networks. *Siam Review*, 45(2), 167-256. doi: 10.1137/s003614450342480
- Poncela, J., Gómez-Gardenes, J., Floría, L. M., Sánchez, A., & Moreno, Y. (2008). Complex cooperative networks from evolutionary preferential attachment. *Plos One*, 3(6), e2449.

- Türker, İ. (2018). Generating clustered scale-free networks using Poisson based localization of edges. *Physica A: Statistical Mechanics and its Applications*, 497, 72-85. doi: <https://doi.org/10.1016/j.physa.2018.01.009>
- Xie, Z., Ouyang, Z., & Li, J. (2016). A geometric graph model for coauthorship networks. *Journal of Informetrics*, 10(1), 299-311.
- Xulvi-Brunet, R., & Sokolov, I. M. (2002). Evolving networks with disadvantaged long-range connections. *Physical Review E*, 66(2), 026118.

Author Information

Gokhan Kutluana

Bartın University
Health Services Vocational School

Ilker Turker

Karabük University
Faculty of Engineering, Computer Engineering Dept.
Contact e-mail: iturker@karabuk.edu.tr

Optimization the Combined Heat and Power Economic Dispatch problem using Harmony Search Algorithm

Fatima Zohra BENAYED

University of Science and Technology, Mohamed-Boudiaf

Lahouari ABDELHAKEM-KORIDAK

University of Science and Technology, Mohamed-Boudiaf

Mostefa RAHLI

University of Science and Technology, Mohamed-Boudiaf

Abstract: Recently, combined heat and power units, known as cogeneration, which produce both heat and electrical power, have played an increasing in different industries. In order to utilize CHP units more efficiently, economic dispatch problem is applied to determine the optimal combination of the power and heat outputs of system while satisfying heat and power demand and other constraints with minimum fuel cost. This problem is known as combined heat and power economic dispatch (CHPED). Due to complex characteristics, heuristic and evolutionary based optimization approaches have become effective tools to solve the CHPED problem. The problem which is used in this paper is non-linear, non-smooth and non-convex. Harmony Search Algorithm is applied to two tests with different characteristics. The obtained results demonstrate the efficiency of the proposed method in solving non-convex and non smooth problems, with considering and non considering the transmission loss and also with both equal and different initialization of the problem for the same CHP units.

Keywords: Combined heat and power (CHP), Cogeneration, economic dispatch (ED), Harmony Search algorithm (HS), Optimization

Introduction

The energy efficiency of the most efficient conventional power production unit is less than 60%, but the fuel efficiency of combined heat and power (CHP) production unit can be as much as 90% [1,3]. Beside its high efficiency, CHP results in the reduction of environmental pollutants (CO₂, SO₂, SO_x, and, NO_x emissions) by about 13–18% [2]. In order to utilize CHP units more efficiently, economic dispatch problem is applied to determine the optimal combination of the power and heat sources' outputs to satisfy heat and power demand of system and operational constraints. This problem is known as CHP economic dispatch (CHPED) problem and has attracted a lot of interests in recent years. Dual dependency of heat and power production in CHP units makes the CHPED problem a complicated optimization problem, which needs powerful optimization techniques to solve it. The CHPED problem will be more complex if the effects of the valve-point in cost function and system losses are taken into account. Considering valve-point effects make the CHPED problem non-convex. Hence, using gradient based classic optimization methods does not guarantee obtaining the optimal solution. Because non-convex CHPED problem has a lot of local optima and in most cases, classical methods find a relative optimum (or local optimum) that is closest to the starting point.

Stochastic search methods which are not based on the gradient of the objective function are used to solve constrained CHPED problem. These methods can give a good solution with reasonable computation time where the exact methods fail to produce a solution or they are too slow.

In this paper, the CHPED problem is solved using stochastic search method appealed Harmony Search algorithm (HS). This algorithm was inspired by the music improvisation process in which the musician searches for harmony and continues to polish the pitches to obtain a better harmony. The first time, Harmony Search algorithm was introduced by Geem et al in [4]. Here, the Harmony Search algorithm is applied to solve non-linear, non-convex and non-smooth CHPED problem with considering valve-point effects and system losses on a test system which consists of 7 units and also without considering the system losses on a test system consisting of 5 units with both equal and disparate initialization of the problem for same combined heat and power units.

Formulation of CHPED problem

The CHPED problem is to determine the power and heat of a unit production so that the system production cost is minimized while the power and heat demands and other constraints are satisfied. Mathematically; the problem is to minimize the following objective function [5].

$$\text{Minimize } F_{fuel} = \sum_{i=1}^{N_p} f_i(P_i) + \sum_{j=1}^{N_c} f_j(P_j, h_j) + \sum_{k=1}^{N_h} f_k(h_k) \quad (1)$$

Where N_p, N_c and N_h are the number of conventional thermal units, cogeneration units and heat-only units, respectively; h and P are the heat and electrical power output of unit, respectively. $f_i(P_i)$, $f_j(P_j, h_j)$ and $f_k(h_k)$ represent the fuel cost function of i -th power-only unit, fuel cost function of j -th cogeneration unit and fuel cost function of k -th heat-only unit, respectively[5].

Quadratic fuel cost function of power-only units may be written as:

$$f_i(P_i) = a_i(P_i^2) + b_i(P_i) + c_i \quad | \quad \$ \quad (2)$$

Where, a_i, b_i and c_i are the cost coefficients of the i -th power-only unit. In a practical generation unit, steam valve admission effects lead to the ripple in the production cost. In order to model this effect more accurately, a sinusoidal term is added to the quadratic cost function. Considering valve-point effects make the problem non-convex and non-differentiable. The unit cost function considering valve-point effects is represented as follows.

$$f_i(P_i) = a_i(P_i^2) + b_i(P_i) + c_i + |d_i \sin(e_i(P_i^{min} - P_i))| \quad \$ \quad (3)$$

Where, d_i and e_i are the cost coefficients for modeling the valve-point effects.

The production cost of cogeneration and heat-only units are defined as:

$$f_j(P_j, h_j) = a_j(P_j^2) + b_j(P_j) + c_j + d_j(h_j^2) + e_j(h_j) + f_j(P_j, h_j) \quad | \quad \$ \quad (4)$$

$$f_k(h_k) = a_k(h_k^2) + b_k(P_k) + c_k \quad | \quad \$ \quad (5)$$

Where, a_j, b_j, c_j, d_j, e_j and f_j are the cost coefficients of the j -th cogeneration unit; a_k, b_k and c_k represent the cost coefficient of k -th heat-only unit.

The objectives function of the CHPED problem, which is to be minimized, Subject to the equality and inequality constraints.

Equality Constraints

Heat and power balance constraints

$$\sum_{i=1}^{N_p} P_i + \sum_{j=1}^{N_c} P_j = P_D + P_L \quad | \quad MW \quad (6)$$

$$\sum_{j=1}^{N_c} h_j + \sum_{k=1}^{N_h} P_k = H_D \quad | \quad MWth \quad (7)$$

Where, P_D and H_D are total power and heat demands of system, respectively. P_L is the total active power transmission loss. Transmission losses of the system should be taken into account in order to meet the load demand exactly.

The B-coefficient method is one of the most commonly used by power utility industry to calculate the network losses. In this method the total active power transmission loss is expressed as a quadratic function of the unit power outputs that can be approximated in the following [6]:

$$P_L = \sum_{i=1}^{N_p+N_c} \sum_{j=1}^{N_p+N_c} P_i B_{ij} P_j \quad MW \quad (8)$$

Where, B_{ij} the loss coefficient for a network branch connected between buses i and j .

Inequality Constraints

Capacity limit constraints

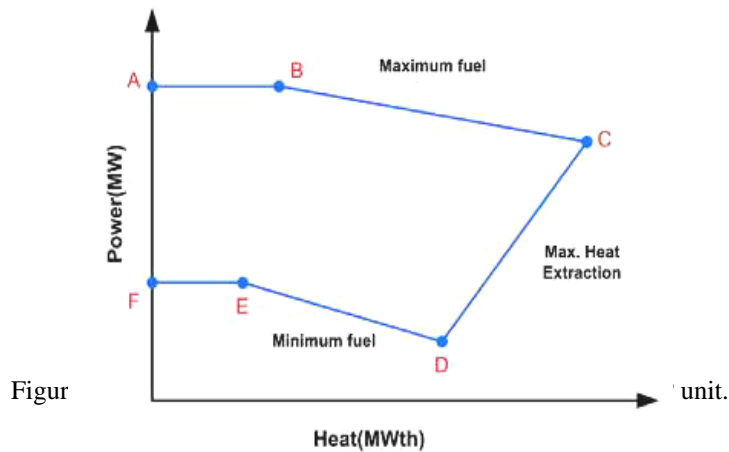
$$P_i^{min} \leq P_i \leq P_i^{Max} \quad i = 1, \dots, N_p \quad (9)$$

$$P_j^{min}(h_j) \leq P_j \leq P_j^{Max}(h_j) \quad j = 1, \dots, N_c \quad (10)$$

$$h_j^{min}(P_j) \leq h_j \leq h_j^{Max}(P_j) \quad j = 1, \dots, N_c \quad (11)$$

$$h_k^{min} \leq h_k \leq h_k^{Max} \quad k = 1, \dots, N_h \quad (12)$$

Where, P_i^{min} and P_i^{Max} are the minimum and maximum power outputs of i -th conventional unit in MW; $P_j^{min}(h_j)$, $P_j^{Max}(h_j)$, $h_j^{min}(P_j)$ and $h_j^{Max}(P_j)$, are the linear inequalities that define the feasible operating region of the j -th CHP unit; h_k^{min} and h_k^{Max} are also the minimum and maximum thermal outputs of the k -th heat-only unit. It is obvious that the heat production limits of CHP units are dependent to the unit power production and vice versa. The heat-power Feasible Operation Region (FOR) for a CHP unit is depicted in (Figure 1) [6]. The upper and lower bounds of heat and power units are restricted by their own generation limits [7].



Harmony Search Algorithm

Harmony Search. Firstly developed by Geem et al. in 2001, harmony search (HS) [4] is a relatively new meta-heuristic optimization algorithm, and it is based on natural musical performance processes that occur when a musician searches for an optimal state of harmony. The optimization operators of HS algorithm are specified as the harmony memory (HM), which keeps the solution vectors which are all within the search space; the harmony memory size HMS, which represents the number of solution vectors kept in the HM; the harmony memory consideration rate (HMCR); the pitch adjustment rate (PAR); the pitch adjustment bandwidth (bw).

In the HS algorithm, musical performances seek a perfect state of harmony determined by aesthetic estimation, as the optimization algorithms seek a best state (i.e. global optimum) determined by objective function value. It has been successfully applied to various optimization problems in computation and engineering fields [8].

The optimization procedure of the HS algorithm consists of steps 1–5, as follows:

Step 1: Initialize the optimization problem and algorithm parameters.

Step 2: Initialize the harmony memory HM.

Step 3: Improvise a new harmony from the HM.

Step 4: Update the HM.

Step 5: Repeat Steps 3 and 4 until the termination criterion has been satisfied.

The detailed explanation of these steps can be found in [4] which are summarized in the following:

Step 1. Initialize the optimization problem and HS algorithm parameters.

First, the optimization problem is specified as follow:

$$\text{Minimize } f(x) \text{ subject to } x_i \in X_i, \quad i = 1, \dots, N$$

Where $f(x)$ is the objective function, x is the set of each decision variable (x_i); X_i is the set of the possible range of values for each design variable (continuous design variables), that is, $x_{i \text{ lower}} \leq X_i \leq x_{i \text{ upper}}$, where $x_{i \text{ lower}}$ and $x_{i \text{ upper}}$ are the lower and upper bounds for each decision variable; and (N) is the number of design variables. In this context, the HS algorithm parameters that are required to solve the optimization problem are also specified in this step. The number of solution vectors in harmony memory (HMS) that is the size of the harmony memory matrix, harmony memory considering rate (HMCR), pitch adjusting rate (PAR), and the maximum number of searches (stopping criterion) are selected in this step. Here, HMCR and PAR are parameters that are used to improve the solution vector. In this context, both are defined in Step 3.

Step2. Initialize the harmony memory (HM).

The harmony memory (HM) is a memory location where all the solution vectors (sets of decision variables) are stored. In Step 2, the HM matrix, shown in (Eq.13), is filled with randomly generated solution vectors using a uniform distribution,

$$HM = \begin{bmatrix} x_1^1 & x_2^1 & \dots & x_{N-1}^1 & x_N^1 \\ x_1^2 & x_2^2 & \dots & x_{N-1}^2 & x_N^2 \\ \vdots & \vdots & \vdots & \vdots & \vdots \\ x_1^{HMS-1} & x_2^{HMS-1} & \dots & x_{N-1}^{HMS-1} & x_N^{HMS-1} \\ x_1^{HMS} & x_2^{HMS} & \dots & x_{N-1}^{HMS} & x_N^{HMS} \end{bmatrix} \quad (13)$$

Step3. Improve a new harmony from the HM.

A new harmony vector $x'=(x'_1, \dots, x'_N)$ is generated based on three rules: (a) memory consideration, (b) pitch adjustment, and (c) random selection. Generating a new harmony is called 'improvisation'. In the memory consideration, the value of the first decision variable (x'_1) for the new vector is chosen from any value in the specified HM range (x'_1, \dots, x_N^{HMS}). Values of the other decision variables (x'_2, \dots, x_N^{HMS}) are chosen in the same manner.

The HMCR, which varies between 0 and 1, is the rate of choosing one value from the historical values stored in the HM, while (1-HMCR) is the rate of randomly selecting one value from the possible range of values.

$$x'_i \leftarrow \begin{cases} x'_i \in \{x_i^1, x_i^2, \dots, x_i^{HMS}\} \text{ w.p. } (HMCR) \\ x'_i \in X_i \dots \dots \dots \text{ w.p. } (1 - HMCR) \end{cases} \quad (14)$$

After, every component obtained by the memory consideration is examined to determine whether it should be pitch-adjusted. This operation uses the PAR parameter, which is the rate of pitch adjustment as follows:

$$\text{Pitch adjusting decision for } x'_i \leftarrow \begin{cases} \text{Yes} & \text{with probability } PAR \\ \text{No} & \text{with probability } (1 - PAR) \end{cases} \quad (15)$$

The value of (1 - PAR) sets the rate of doing nothing. If the pitch adjustment decision for x'_i is yes, then x'_i is replaced as follows:

$$x'_i \leftarrow x'_i \pm r.bw \quad (16)$$

Where bw is an arbitrary distance bandwidth, r is a random number generated using uniform distribution between 0 and 1. In Step 3, HM consideration, pitch adjustment or random selection is applied to each variable of the New Harmony vector in turn.

Step4. Update the HM.

If the new harmony vector, (x'_1, \dots, x'_N) is better than the worst harmony in the HM, judged in terms of the objective function value, the new harmony is included in the HM and the existing worst harmony is excluded from the HM.

Step5. Repeat Steps 3 and 4 until the termination criterion has been satisfied.

The $HMCR$ and PAR parameters introduced in Step 3 help the algorithm find globally and locally improved solutions, respectively [8].

PAR and bw in HS algorithm are very important parameters in fine-tuning of optimized solution vectors, and can be potentially useful in adjusting convergence rate of algorithm to optimal solution. So fine adjustment of these parameters are of great interest.

Mahdavi and al. [9] proposed an improved harmony search algorithm that uses variable PAR and bw in improvisation step. The HS proposed in this work has exactly the same steps of classical HS with exception that Step 3, where the HS proposed dynamically updates PAR in which concepts from dispersed particle swarm optimization are adopted. The key difference between HS proposed and traditional HS method is in the way of adjusting PAR and bw to improve the performance of the HS algorithm and eliminate the drawbacks lies with fixed values of PAR and bw , HS algorithm proposed uses variables PAR and bw in improvisation step (Step 3). PAR and bw change dynamically with generation number as shown in (Figure. 2) and expressed as follow:

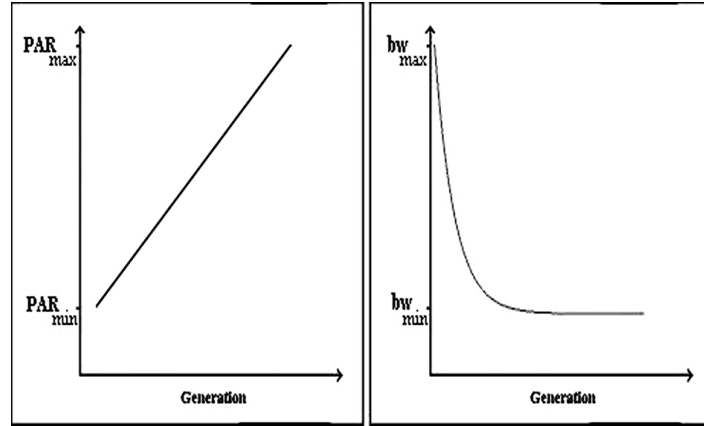


Figure 2. Variation of PAR and bw versus generation number

$$PAR(gn) = PAR_{min} + \frac{(PAR_{max} - PAR_{min})}{NI} \times gn \quad (17)$$

and

$$bw(gn) = bw_{max} \cdot \exp(c \cdot gn) \quad (18)$$

$$c = \frac{\ln\left(\frac{bw_{min}}{bw_{max}}\right)}{NI} \quad (19)$$

Where, PAR is pitch adjusting rate for each generation, PAR_{min} is minimum pitch adjusting rate, PAR_{max} is maximum pitch adjusting rate, NI is number of solution vector generations, gn is generation number. $bw(gn)$ is bandwidth for each generation, bw_{min} is minimum bandwidth, and bw_{max} is maximum bandwidth.

Case Study and Analysis of Optimization Results

In this paper the performance of proposed HS algorithm based CHPED problem is implemented using personal Matlab 7.1 program.

Two test systems are studied in this paper to show the effectiveness and validity of the proposed method. Test system 1 is selected from [10] and test system 2 was presented in [7]. Power outputs are in MW, heat outputs are in MWth and costs are in \$ in all of the tables and figures. Economic dispatch is obtained using Harmony search algorithm proposed and the results are compared with other algorithms. The parameters of harmony search proposed used in the above tests problems are Harmony memory size (HMS) =6, Harmony memory consideration rate (HMCR) =0.95, Minimum pitch adjusting rate (PAR_{min}) =0.45, Maximum pitch adjusting rate (PAR_{Max}) =0.95, the Minimum bandwidth (bw_{min}) =0.001, and the Maximum bandwidth (bw_{Max}) =0.1.

Test System 1

The proposed test system consists of one power-only unit, 2 CHP units and the heat-only unit. The feasible operating regions of the two cogenerations units are given in (figure 3) and (figure 4) [3]. The system power demand PD and the heat demand HD are 200MW and 115MWth, respectively.

Table 1. Cost function parameters of test system1

Power only unit Unit	a	b	c	d	e	f	P_{min}	P_{Max}
1	0	50	0	0	0	0	0	150
CHP units							Feasible region	coordinates $[P^C, H^C]$
2	0.0345	14.5	2650	0.030	4.2	0.031	[98.8,0], [81,104.8]	[215,180],[247,0]
3	0.0435	36.0	1250	0.027	0.6	0.027	[44,0],[44,15.9],[40,75]	[110.2, 135.6], [125.8,32.4], [125.8,0]
Heat only units							H_{min}	H_{Max}
4	0	23.4	0	0	0	0	0	2695.2

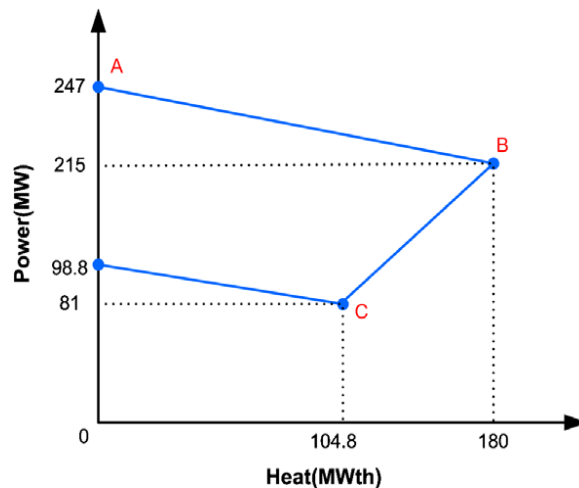


Figure 3. Feasible operation region for the cogeneration unit 2 for system1 and unit 5 for system2

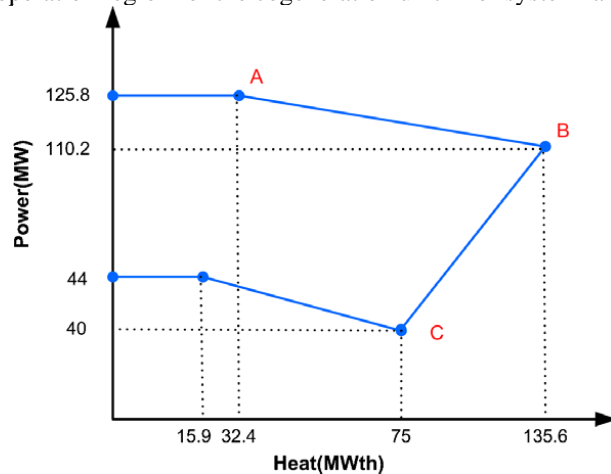


Figure4. Feasible operation region for the cogeneration unit 3 for system1 and unit 6 for system2

The results obtained by using the harmony search algorithm proposed is presented in table 2 and compared with the results obtained by various other techniques mentioned in the paper such as genetic algorithm (GA) [13], harmony search algorithm (HS) [3], augmented Lagrange Hopfield network (ALHN)[14], selective particle swarm optimization (SPSO) [12] and Proposed harmony search algorithm (EDHS)[11]. It is inferred from the table that the feasible optimum is 8526.9 \$.

Table 2. Comparison the best results of HS algorithm proposed for test system1 with other methods

Output	P1	P2	P3	H2	H3	H4	Cost
GA[13]	0	159.23	39.95	40.77	75.06	0	9267.2
HS[3]	0	160	40	40	75	0	9257.07
ALHN[14]	0	159.9994	40	39.9993	75	0	9257.05
SPSO[12]	0	159.7065	40	39.9097	75	0	9248.17
EDHS[11]	0	200	0	0	115	0	8606.07
<i>HS proposed</i>	2.8458	100.3939	43.1259	17.6107	76.5430	29.3301	8526.9

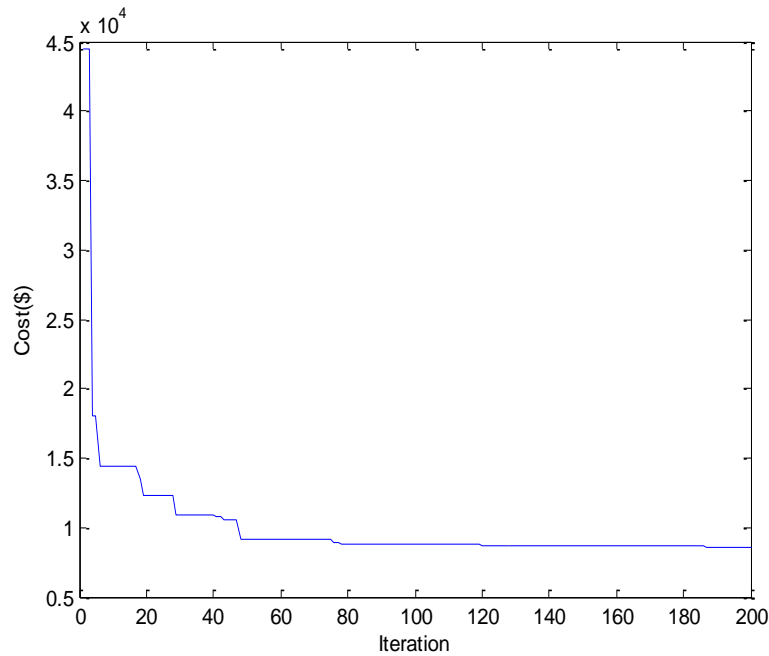


Figure 5. Convergence history the fuel cost according to the iterations of the test system 1

Test System 2

In this section a test system considering valve –point effects and transmission losses is considered to show the performance of the proposed algorithm. This system is consisted of 7 units, where units of 1-4 are power only units, units 5 and 6 are CHP units and unit 7 is heat-only unit. The cost function parameters of this case along with the feasible region coordinates of CHP units are presented in table 3.

Table 3. Cost function parameters of test system2

Power only units								
Unit	a	b	c	d	e		P _{min}	P _{Max}
1	0.008	2	25	100	0.042		10	75
2	0.003	1.8	10	140	0.04		20	125
3	0.0012	2.1	100	160	0.038		30	175
4	0.001	2	120	180	0.037		40	250
CHP unit	a	b	c	d	e	f	Feasible region	Coordinates [P ^c ,H ^c]
5	0.0345	14.5	2650	0.030	4.2	0.031	[98.8,0], [81,104.8]	[215,180],[247,0]
6	0.0435	36.0	1250	0.027	0.600	0.011	[44,0],[44,15.9],[40,75]	110.2,135.6], [125.8,32.4], [125.8,0]
Heat only unit								
	a	b	c				H _{min}	H _{Max}
7	0.038	2.0109	950				0	2695.2

The coefficients of the network loss matrix are provided in the following. The units of B-matrix elements are 1/MW.

$$B = \begin{bmatrix} 49 & 14 & 15 & 15 & 20 & 25 \\ 14 & 45 & 16 & 20 & 18 & 19 \\ 15 & 16 & 39 & 10 & 12 & 15 \\ 15 & 20 & 10 & 40 & 14 & 11 \\ 20 & 18 & 12 & 14 & 35 & 17 \\ 25 & 19 & 15 & 11 & 17 & 39 \end{bmatrix} * 10^{-7} \quad (20)$$

The obtained optimal dispatch using HS algorithm proposed is obtained and presented in table 4 and compared with the results obtained using Artificial Bee Colony (ABC) [15], Bee Colony optimization (BCO) [7], Group Search optimization (GSO) [16] and Gravitational search algorithm (GSA) [17]. The cost convergence of the proposed algorithm is presented in figure 6. It can be observed that HS proposed provides better results as compared to the results of the previous algorithms. The feasible optimum of the system stands at 9535.3 \$.

Table 4. Comparison the best results of HS algorithm proposed for test system2 with other methods

Method	P1	P2	P3	P4	P5	P6	H5	H6	H7	PL	Cost
ABC [15]	58.711 7	98.5398	112.6735	209.8158	81.00	40.00	23.1014	72.2437	54.6549	2.88	10314
BCO[7]	43.945 7	98.5888	112.9320	209.7719	98.80 00	40.00	12.0974	78.0236	59.879	8.03 84	10317
GSO[16]	45.618 8	98.5401	112.6727	209.8154	94.10 27	40.00 01	27.66	74.9987	47.3413	0.74 98	10094. 2670
GSA[17]	48.763 8	98.7469	112	208.5113	92.69 09	40	35.9704	75	39	-	9912.6 928
HS proposed	11.669 2	21.7849	30.8187	43.5728	97.36 60	44.25 95	16.3812	75.0674	32.9191	0.00 3	9535.3

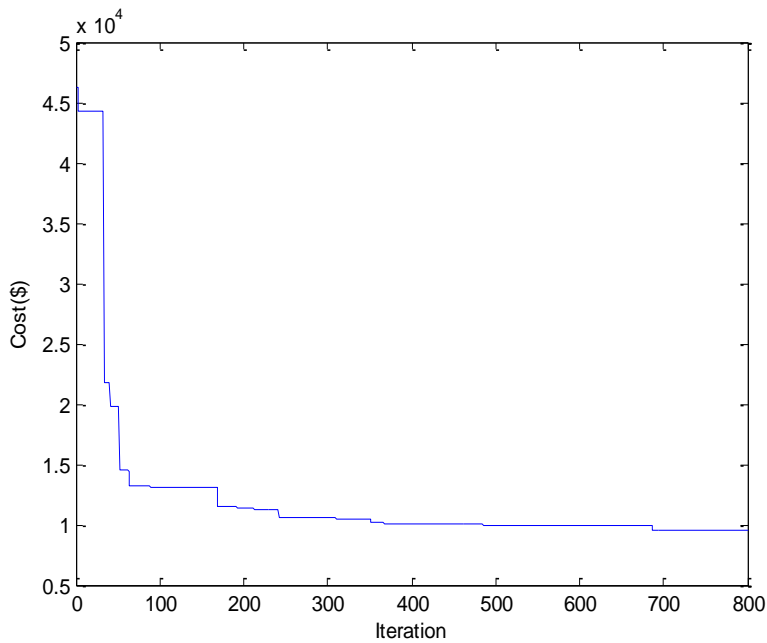


Figure 6. Convergence history the fuel cost according to the iterations of the test system 2

Conclusion

In this work harmony search algorithm proposed is used to solve CHPED problem. Two test cases with different characteristics are used to illustrate the proposed method. Valve-point effects, transmission losses, capacity limits and heat-power dependency constraints are considered in studied systems. As the results show, HS proposed has a significant decrease in cost of test system2, and test system 1, so the proposed method can be

used as an alternative method for solution of CHPED problems. As future work, CHP problem can be extended by considering more practical constraints like as heat losses, ramp rates and the electricity power load balance.

References

- Mohammadi-Ivatloo, B., Moradi-Dalvand, M., Rabiee, A., (2013). Combined heat and power economic dispatch problem solution using particle swarm optimization with time varying acceleration coefficients. *Electric Power Systems Research*, 95, 9-18.
- Karki, S., Kulkarni, M., Mann, M. D., Salehfar, H., (2007). Efficiency improvements through combined heat and power for on-site distributed generation technologies. *Cogeneration and distributed generation journal*, 22(3), 19-34.
- Vasebi, A., Fesanghary, M., and Bathaee, S.M. T., (2007). Combined heat and power economic dispatch by harmony search algorithm. *International Journal of Electrical Power and Energy Systems*, 29(10), 713-719.
- Geem, Z. W., Kim, J. H., Loganathan, G. V. (2001). A new heuristic optimization algorithm: harmony search. *Simulation*, 76(2), 60-68.
- Song, Y.H., Chou, C.S., Stonham, T.J., (1999). Combined heat and power economic dispatch by improved ant colony search algorithm. *Electric Power System Research*, 52, 115-121.
- Murugan, R., Mohan, M. R., (2012). Artificial Bee colony Optimization for the combined Heat And Power Economic Dispatch problem. *ARNP Journal of Engineering and Applied Sciences*, 7(5).
- Basu, M., (2011). Bee colony optimization for combined heat and power economic dispatch. *Expert Systems with Applications*, 38(11), 13527-13531.
- Lee, K.S., Geem, Z.W., (2005). A new meta-heuristic algorithm for continuous engineering optimization: harmony search theory and practice. *Computer Methods in Applied Mechanics and Engineering*, 194, 3902-3933.
- Coelho, L. D. S, Mariani, V.C., (2009). An improved harmony search algorithm for power economic load dispatch. *Energy Conversion and Management*, 50(10), 2522-2526.
- Guo, T., Henwood, M.I., Van Ooijen, M., (1996). An algorithm for combined heat and power economic dispatch. *IEEE Transactions on Power System*, 11, 1778-1784.
- Khorram, E., Jaberipour, M., (2011). Harmony search algorithm for solving combined heat and power economic dispatch problems, *Energy Conversion and Management*, 52, 1550-1554.
- Ramesh, V., Jayabarathi, T., Shrivastava, N., Baska, A., (2009). A novel selective particle swarm optimization approach for combined heat and power economic dispatch, *Electric Power Components and Systems*, 37, 1231-1240.
- Song, Y.H., Xuan, Q.Y., (1998). Combined heat and power economic dispatch using genetic algorithm based penalty function method. *Electrical Mach. Power Systems*, 26, 363-372.
- Dieu, V.N., Ongsakul, W., (2009). Augmented Lagrange Hopfield network for economic load dispatch with combined heat and power. *Electrical Power Components and Systems*, 37(12), 1289-304.
- Mohan, R.M.R., (2012). Artificial Bee Colony Optimization for the Combined Heat and Power Economic Dispatch problem. *ARNP Journal of Engineering and applied sciences*, 7(5).
- Basu, M., (2016). Group search optimization for combined heat and power economic dispatch. *Electrical Power Components and systems*, 78, 138-147.
- Beigvand, S.D., Abdi, H., La scala, M., (2016). Combined heat and power economic dispatch problem using gravitational search algorithm. *electrical power systems research*, 133, 160-172.

Author Information

Benayed Fatima Zohra

University of Science and Technology, Mohamed-Boudiaf
Faculty of Electrical Engineering, USTO, BP 1505, Oran
El M'naouer, Oran, Algeria
Contact e-mail: benayedf@yahoo.fr

Abdelhakem-koridak Lahouari

University of Science and Technology, Mohamed-Boudiaf
Faculty of Mechanical, USTO; BP 1505, Oran El
M'naouer, Oran, Algeria,

Rahli Mostefa

University of Science and Technology, Mohamed-Boudiaf
Faculty of Electrical Engineering, USTO, BP 1505, Oran
El M'naouer, Oran, Algeria

Voice Controlled Home Automation Design

Ahmet VATANSEVER

Trakya University

Hilmi KUSCU

Trakya University

Gurkan TUNA

Trakya University

Abstract: In recent years, in parallel with the advances in technology, home automation systems have started to offer more functions and been more sophisticated. Compared to the past, remotely controllable home automation systems have become much cheaper and are not luxurious anymore; hence more and more people nowadays use home automation systems to make their lives easier. Home automation systems especially play a key role for the elderly and disabled and offer convenient and flexible solutions for them. Since home automation systems allow the elderly and physically disabled to maintain their lives in a comfortable and secure environment, the aim of this study is to design a voice controlled home automation system. To design the proposed home automation system, firstly a prototype home has been built and then some devices have been placed in it. Then, by using a throat microphone, a set of voice commands has been defined in the voice recognition module. The designed home automation system works as follows. Basically the voice recognition module converts voice commands into digital signals, and then these digital signals are transmitted to the home automation system via a ZigBee-based communications module. The receiver of the ZigBee communications module receives the commands given by the transmitter and sends them to the microcontroller. Finally, the microcontroller analyzes the commands and performs the expected operations. Arduino Uno has been used as the microcontroller and EasyVR module has been used for voice recognition. The software of the home automation system has been developed in C using Arduino IDE.

Keywords: Home automation system, Voice recognition, Microcontroller, EasyVR, Arduino

Introduction

The elderly population has increased rapidly as a result of both developments in health services and rise in people's lifespan in Turkey and worldwide. As the elderly lead a long life, they need some help to live happily in their houses. Home automation is one of the major growing and progressing industries thanks to developing technology, which could be helpful for those people. Home automation systems make people's life easier, safer, more comfortable and more economical. Some of the home automation systems serve people who like luxury and sophisticated home automation platforms, on the other hand, others generally target elderly and handicapped people who only need some help. For example, old people or people with special needs who live alone at home may have troubles in using household appliances. Voice command system may help those people to open and close them.

Speech Recognition is a key component of novel home automation solutions. Basically, it is a kind of technology that provides the system to understand the words (not the meanings) given by speech (Bharambe, & Kodgire, 2016). Controlling an electronic device by voice provides both easy use and increase in efficiency and productivity. Voice recognition systems also help users do two or more tasks simultaneously while working on computers or other devices (Bharambe, & Kodgire, 2015).

- This is an Open Access article distributed under the terms of the Creative Commons Attribution-Noncommercial 4.0 Unported License, permitting all non-commercial use, distribution, and reproduction in any medium, provided the original work is properly cited.

- Selection and peer-review under responsibility of the Organizing Committee of the Conference

© 2018Published by ISRES Publishing: www.isres.org

This study aims to design a home automation system that responds to voice commands and allows controlling the on/off status of electrical devices like lamp, air conditioner, television and door in a house. The system allows controlling various devices using the following commands: “open the door”, “close the door”, “turn on the air conditioner”, “turn off the air conditioner”, “switch on the lights”, “switch off the lights”, “turn on the television”, “turn off the television”, “power on all the devices” and “power off all the devices”.

Method

The Structure of the System

A pair of Arduino Uno boards controls the implemented system. The XBee RF modules are used for wireless communications. One of them is a transmitter for transferring the signals and the other one is a receiver for getting the signals; and both are connected to the Arduino Uno card. The EasyVR module is used as the voice recognition card and EasyVR Commander which is graphical interface software of EasyVR module defines voice commands.

Figure 1 shows the flow diagram of the voice controlled home automation system. As can be seen from this flow chart, the voice command is firstly told by the user and these voice commands are transmitted to EasyVR module via throat microphone. Then, EasyVR module receives these voice commands and transforms them into digital signals using Analog Digital Converter (ADC). The next step is to compare voice commands to the ones recognized before, i.e. open the door, close the door, turn on TV, turn off TV etc... If they match, it transmits each letter value which is corresponding for commands as binary. This binary information is later received by ATmega328 microcontroller. After matching and comparison is finished here, transmitter sends information signals to XBee. These digital signals are taken by receiver XBee and binary values are sent to ATmega328 microcontroller. Microcontroller compares value serials to values here. Last, according to value serials, servo engines and leds accomplish the task here.

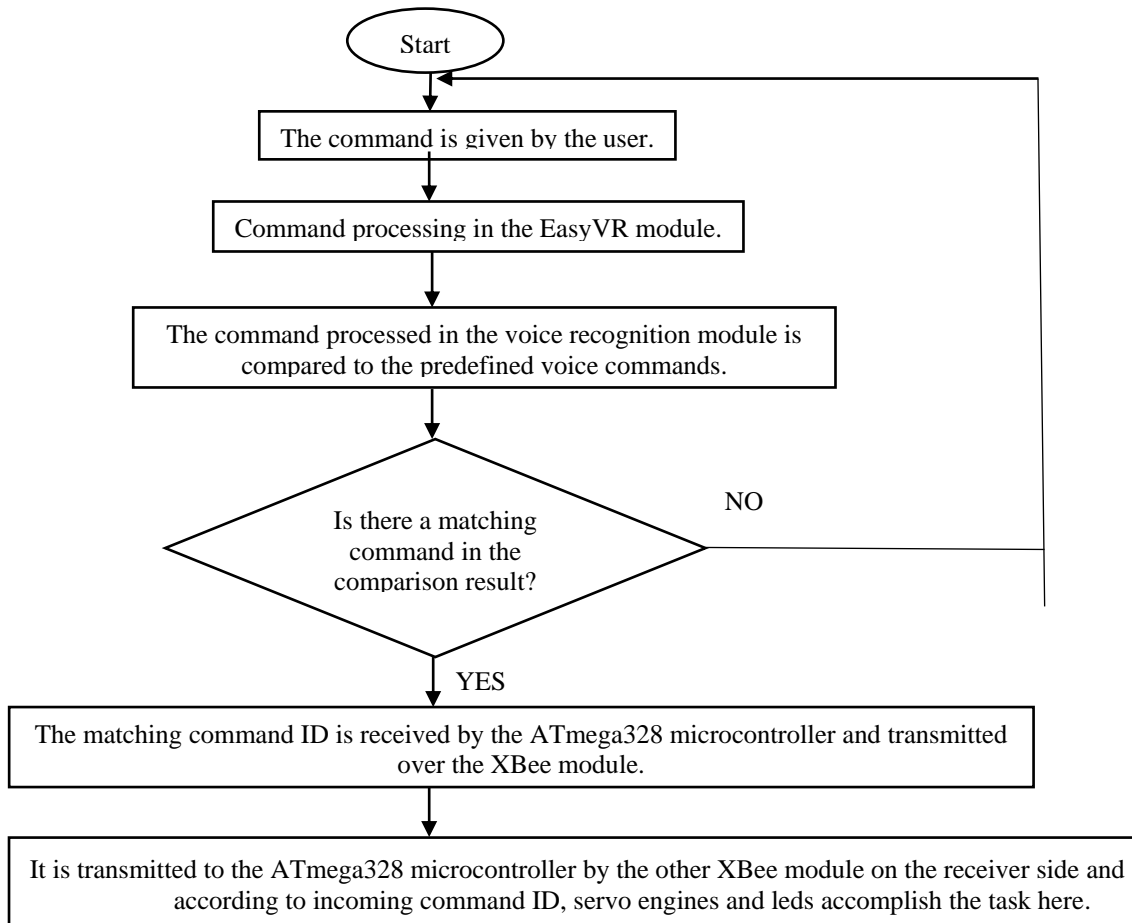


Figure 1. Flow chart of controlling the home automation system by voice

When the command “open the door” is issued by the user, servo engine placed under the door turns around with 90° angle, which enables the door to open. If the command “close the door” is given, servo engine moves to the starting point so the door closes. If “turn on the air conditioner”, “switch on the lights” and “turn on the television” commands are issued, the leds in the model which represents the appliances in the house are turned on. If “turn off the air conditioner”, “switch off the lights” and “turn off the television” commands are given, the leds are turned off. When “power on all the devices” command is given, television, air conditioner, and lamp is activated. If “power off all the devices” command is issued, television, air conditioner, and lamp is turned off.

Arduino Uno Microcontroller Card

Arduino, a ready-to-use electronic card, has a main microcontroller, pins to connect control units, and communication ports (Delebe, 2014). The Arduino Uno is a microcontroller board based on the ATmega328. There are 14 digital input/output pins, and 6 of them can be used as PWM output. Also, it has 6 analog input pins, 16 MHz crystal oscillator, a USB input, a power input, and reset button. The card consists of the necessary things to support microprocessor (Arduino Uno Datasheet, 2015). Figure 2 describes the front and back surface of Arduino Uno:

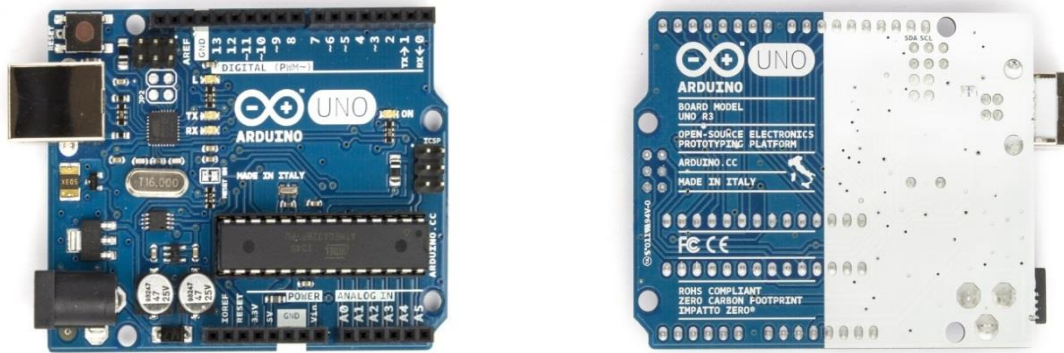


Figure 2. Arduino Uno microprocessor card

EasyVR Shield 2.0 Voice Recognition Card

EasyVR Shield 2.0 is a voice recognition shield developed for Arduino. It was designed to provide versatile, robust and cost effective solutions for various voice recognition applications. It is commonly used for voice controlled light switches, locks, curtains or kitchen appliances in home automation solutions (EasyVR User Manual, 2015). Figure 3 shows an EasyVR Shield 2.0 module.



Figure 3. EasyVR Shield 2.0

EasyVR Shield 2.0 Features

An EasyVR module consists of a set of built-in Speaker Independent (SI) commands for ready-to-run basic control functions. In addition, besides voice passwords, it supports 32 user-defined Speaker Dependent (SD) triggers or commands. An EasyVR 2.0 module contains SonicNet technology for wireless interactions between modules and other voice sources. In addition, it has both DTMF tone generation and simple and user friendly graphical user interface. It can be used on any host with standard UART interface powered with 3.3V-5V. There is serial communication protocol in order to program on host card. Headphone jack and microphone input are also available in addition to programmable LED to indicate feedback during recognition tasks (EasyVR User Manual, 2015).

ZigBee Technology

ZigBee, a new standard for wireless communications, enables low cost, low power, short range and low-data-rate wireless multi-hop networking technology standard (Masica, 2007). It forms a suitable baseline for sensors and control network based upon IEEE 802.15.4 (Kızıllırmak, 2012). It is widely accepted because of minimum power use, low-cost, secure, easy-to-install in implementations that are relatively low throughput size data transmitting like distant monitoring, control and distributed processing (Masica, 2007). Due to its advantages over competitive technologies, ZigBee is a very nice option for wireless voice applications (Öztaş, Belen, Kaya, & Kaya, 2011).

Digi XBee 2 Serial XBee-PRO ZigBee Modules

In this study, two XBee-PRO 63mW PCB antennas are used. These modules are wireless communications modules which enable to form low-power and high-cost sensor connections by using 802.15.4 and ZigBee communication protocols that work on 2.4 GHz ISM frequency band (Xbee Pro63mw Datasheet, 2016). In Table 1, technical features of XBee-PRO ZigBee (XBee PRO ZigBee Product Datasheet, 2016) modules are indicated.

Table 1. Technical specifications of Xbee-PRO ZigBee modules

Feature	Value
Indoor Range	90m
Outdoor Range	1600m
Transmit Power	63mW
Receiver Sensitivity (% 1per)	-101dBm
Serial Data Interface	UART, SPI
Configuration Method	API VEYA AT commands
Frequency Band	ISM 2.4 GHz
Data Rate	250kbps
Digital Input/Output	15
Supply Voltage	2.7-3.6V
IDS	PAN ID and addresses, cluster IDs and endpoints (optional)
Operating Temperature	-40 °C- +85 °C

Servo Motor

The servo motor is used to open or close the door. Tower Pro SG90 is a plastic and geared mini servo engine. It has small, light and high output power. Servo can be turned to 180⁰ (each way is 90⁰). Table 2 shows tower pro sg90 mini servo motor features.

Table 2. Tower pro SG90 mini servo motor features

Feature	Value
Operating Voltage	4.8 V - 6 V
Stall Torque	1.2kg / 42.3oz (4.8V) , 1.6 kg / 56.4oz (6.0V)
Operating Speed	0.1 s / 60°
Weight	9 g
Size	22 mm x 11,5 mm x 27 mm
Gear Box	Plastic

Throat Microphone

Throat microphone transmits voice with throat vibration. Therefore, the voice can be transferred clearly even in noisy environments. In order to convey voice commands into EasyVR voice recognition module, throat microphone with two sensors (shown in Figure 4) are used (Throat microphone two sensors datasheet, 2016).



Figure 4. Throat microphone with two sensors

Features of Microphone

- Sensitivity: 37.5+/-2dB @1kHz 2.2KΩ 3V 0dB=1v/pa
- Impedance: Max. 2.20kΩ @1kHz
- Directivity: Omni-directional frequency: 100Hz - 16000Hz
- Max. Operation Voltage: 10V
- Standard Operation Voltage: 3V
- Current Consumption: max. 0.5 mA
- S/N Ratio: Min. -56dB @1.1Khz

Hardware Implementation

Figure 5 shows the design of voice controlled home automation.

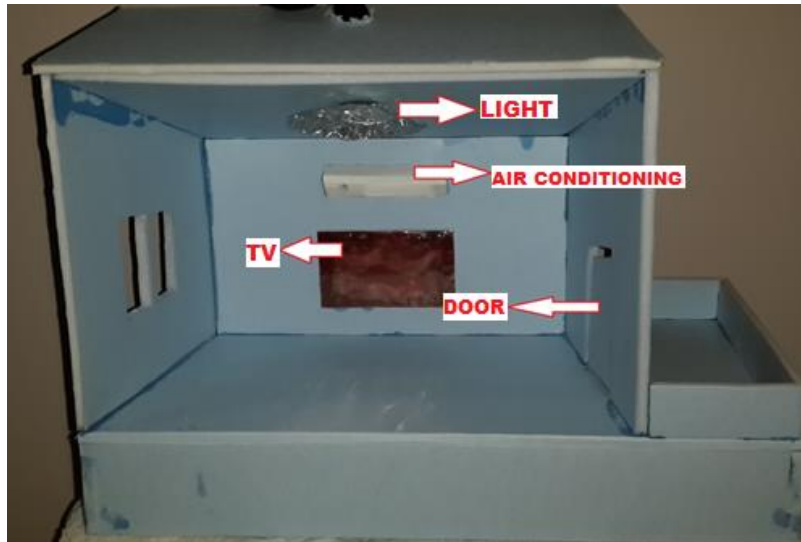


Figure 5. Design of the voice controlled home automation

Results and Discussion

Although home automation systems can be controlled using different methods, in this study, voice commands are used to control the designed home automation system. Because the system has been designed to help the elderly and physically disabled. 10 commands are used to control the devices connected to the home automation system. Commands can be given via throat microphone in both normal and noisy environments. Therefore, each command has been tested 10 times in both normal and noisy environments.

The results show that 95% of success rate has been reached in a normal environment and 94% of success rate has been reached in a noisy environment. It is clear from the results that the environment does not have such importance as throat microphone transmits the voice with throat vibration.

Table 3. The results of tests with throat microphone in normal environment

No	Commands	Number of tests	Accuracy
1	Turn on the air conditioner	10	10
2	Turn off the air conditioner	10	10
3	Switch on the lights	10	9
4	Switch off the lights	10	10
5	Turn on the television	10	9
6	Turn off the television	10	10
7	Open the door	10	10
8	Close the door	10	9
9	Power on all the devices	10	9
10	Power off all the devices	10	9

Table 4. The results of tests with throat microphone in noisy environment

No	Commands	Number of tests	Accuracy
1	Turn on the air conditioner	10	9
2	Turn off the air conditioner	10	10
3	Switch on the lights	10	9
4	Switch off the lights	10	10
5	Turn on the television	10	10
6	Turn off the television	10	9
7	Open the door	10	9
8	Close the door	10	10
9	Power on all the devices	10	9
10	Power off all the devices	10	9

In this research, the system responds to commands of only the researcher whose commands have been introduced before. It is not possible for unauthorized person to use the system. This system is speaker-dependent; however, it can also be developed as speaker-independent system.

One factor affecting voice recognition systems is noise or another voice in the environment. Other factors are the quality of the microphone used in the study and the distance between the microphone and the user. Voice recognition systems work effectively only when the user and the microphone is close to each other. For that reason, throat microphone with two sensors is preferred in this study. According to the tests, it is understood that even in noisy environment throat microphone can transmit the commands clearly. However, there is a drawback of throat microphone. It may cause sweating and itching on throat.

Conclusion

Considering the important role of home automation systems for the elderly and physically disabled, in this study a voice controlled home automation system has been designed. To implement the common functions of a typical home automation system, firstly a prototype home has been built and then some devices have been placed in it. Then the design of the voice recognition and communications modules has been realized using off-the-shelf components. Finally the software of the designed home automation system has been developed. Although in this study we have focused on controlling only four appliances, the overall functions of the designed system provided by the voice recognition system can be used for different purposes such as controlling wheelchairs and directing vehicles and mobile robots. Since the designed home automation system allows the elderly and disabled to control some devices remotely via voice, it can make their lives easier and more comfortable. The future work of this study consists of increasing the number of functions the designed system provides, and improving the voice recognition capabilities.

References

- Arduino Uno Datasheet (2015, June, 15). Retrieved form <http://arduino.cc/en/Main/ArduinoBoardUno>.
- Bharambe, D.V. & Kodgire, S.P. (2015). PSoC based isolated speech recognition system for voice controlled appliances. *International Journal of Advanced Research in Computer Engineering & Technology (IJARCET)*, 4(11), 4270-4272.
- Bharambe, D. & Kodgire, S.P. (2016). Speech recognition system for voice controlled devices. *International Journal of Latest Trends in Engineering and Technology* 6(3), 455-459.
- Delebe, E. (2014). *Projeler ile Arduino*. İstanbul: Kodlab Yayın Dağ.
- EasyVR User Manual (2015, June, 15) Retrieved form http://www.veear.eu/files/easyvr_user_manual_3_6.7.pdf.
- Kızılırmak, E. Y. (2012). *ZigBee İle Endüstriyel Vinç Kontrolü*. (Unpublished master dissertation). University of Hacettepe, Ankara, Turkey.
- Masica, K. (2007). Recommended practices guide for securing zigbee wireless networks in process control system environments. Retrieved from http://energy.gov/sites/prod/files/oeprod/DocumentsandMedia/Securing_ZigBee_Wireless_Networks.pdf.
- Öztaş, Ş., Belen, M. A., Kaya, İ., & Kaya, A. (2011). Zigbee teknolojisi kullanılarak kablosuz kafe otomasyon sistemi tasarımı. Symposium of Elektrik-Elektronik ve Bilgisayar, University of Fırat, Elazığ.
- Throat microphone two sensors datasheet (2016, June, 12) Retrieved from <http://tr.aliexpress.com/item/Clear-Transmission-Throat-Microphone-Air-Tube-Headset-with-2-Sensors-for-Yaesu-Portable-Radio-FT-10R/32276708707.html#extend>
- Xbee Pro63mw Datasheet (2016, June, 21). Retrieved form <http://www.robotistan.com/xbee-pro-63mw-pcb-anten-seri-2b-xbp24-bz7pit-004>.
- XBee-PRO ZigBee Product Datasheet (2016, June, 16). Retrieved form http://www.digi.com/pdf/ds_xbee_zigbee.pdf.

Author Information

Ahmet Vatansever

Trakya University

Edirne, Turkey

Contact e-mail: ahmetvatansever@trakya.edu.tr

Hilmi Kescu

Trakya University

Edirne, Turkey

Gurkan Tuna

Trakya University

Edirne, Turkey

A Comparison of the Performance of Classification Methods and Artificial Neural Networks for Electricity Load Forecasting

Gurkan TUNA

Trakya University

Ahmet VATANSEVER

Trakya University

Resul DAS

Firat University

Abstract: Electricity load forecasting plays a key role for utility companies. Short-term and medium-term electricity load forecasting processes allow the utility companies to retain reliable operation and high energy efficiency. On the other hand, long-term electricity load forecasting allows the utility companies to minimize the risks. Long-term forecasting also helps the utility companies to plan and make feasible decisions in regard to generation and transmission investments. Since there are commercial and technical implications of electricity load forecasting, the accuracy of the electricity forecasting is important not only to the utility companies but also to the consumers. In this paper, we carry out a performance evaluation study to evaluate the accuracy of different classification approaches for electricity load forecasting. As shown with the results of the performance evaluation study, some of the investigated approaches can successfully achieve high accuracy rates and therefore can be used for short-, mid-, or long-term electricity load forecasting.

Keywords: Load-Forecasting plan, Artificial neural networks, Regression analysis, Support vector machine, Prediction techniques

Introduction

Thanks to the understanding of the future consumption provided by electricity load forecasting, utility companies obtain many benefits. By carrying out electricity load forecasting, utility companies plan well for the future, determine the required resources to ensure uninterrupted power to the consumers, utilize the generating plants efficiently, decide easily the best time with the minimum impact for maintenance of the power systems, and minimize the risks via economically viable decisions for future investments (Weron, 2006; Suganthi, & Samuel, 2012; Hernandez et al., 2014).

One of the most important decisions that utility companies must make is whether in the near future they need more generating plants or not and if yes what the type, size and location of the generating plants will be. In this way, the utility companies will be able to determine areas with growing demand and generate the power near the load (Suganthi, & Samuel, 2012; Almeshaei, & Soltan, 2011). This also enables them to minimize the transmission and distribution infrastructures and reduce the associated losses.

Well-known prediction approaches such as artificial neural network models, and support vector machines and linear regression trees can be used for electricity load forecasting (Hastie, Tibshirani, & Friedman, 2009; Hernandez et al., 2014). An emerging approach for electricity load forecasting is the use of a combination of the well-known prediction approaches. Different from the existing studies, instead of focusing on the use of a prediction algorithm for electricity load forecasting, in this study we mainly focus on the performance comparison of the existing prediction algorithms used for electricity load forecasting. The dataset used in this

- This is an Open Access article distributed under the terms of the Creative Commons Attribution-Noncommercial 4.0 Unported License, permitting all non-commercial use, distribution, and reproduction in any medium, provided the original work is properly cited.

- Selection and peer-review under responsibility of the Organizing Committee of the Conference

study consists of the actual consumption of Ankara in Turkey and was obtained during the period from December 2011 to April 2013. The remainder of this paper is structured as follows. Section 2 reviews the prediction approaches used in this study. Discussion on the performance of the reviewed approaches is given in Section 3. Finally, this paper is concluded in Section 4.

Method

In this study, a dataset that consists of 12168 rows was obtained from Republic of TURKEY, Energy Market Regulatory Authority (EMRA) and used. The dataset consist of 12168 rows. Each row of the dataset consists of hour, day of week, month, year, temperature of Ankara, and electricity load. In the first step of the evaluation study, Linear Regression, Multilayer Perceptron and Support Vector Machines prediction techniques were preferred. After a pre-filtering step, the techniques were first implemented in WEKA (Waikato Environment for Knowledge Analysis) (<https://www.cs.waikato.ac.nz/ml/weka/>) and the accuracy of the techniques were compared. In parallel with the studies in the literature (Guerard, & Schwartz, 2010) correlation coefficient, one of the most commonly used indicators of forecasting accuracy, was used to compare the performance of the employed techniques. Correlation coefficient is basically a number between 0 and 1 and a measure of how well the predicted values from a forecast model fit with the real data (Guerard, & Schwartz, 2010). If the correlation coefficient is 0 or very low, there is not any relationship between the predicted values and the actual values. However, if the correlation coefficient is 1 or very high, there is strong relationship between the predicted values and actual values (Yan, & Su, 2009).

In the second step of the evaluation study, Artificial Neural Network was implemented in MATLAB (<https://www.mathworks.com/products/matlab.html>) for electricity load forecasting of Ankara. However, before carrying out the evaluation study, the dataset that consists of 12168 rows was first divided into training, validation and test datasets as listed in Table 1. Due to the required number of features, the number of hidden neurons was set to 5. Levenberg - Marquardt algorithm (Reynaldi, Lukas, & Margaretha, 2012) was preferred for the training phase.

Table 1. Percentages of training, validation and test phases for Ankara

Phase	Percentage (%)	Total Number of Rows
Training	70	8517
Validation	20	2434
Testing	10	1217

Results and Discussion

The first prediction technique used in the performance evaluation was Linear Regression (Yan, & Su, 2009). The results of Linear Regression technique for electricity load forecasting are listed in Table 2 and the forecasting errors are listed in Table 3. The second prediction technique used in the performance evaluation was Multilayer Perceptron (Popescu et al., 2009). The results of Multilayer Perceptron technique for electricity load forecasting are listed in Table 4 and the forecasting errors of Multilayer Perceptron technique are given in Table 5. Finally, the last technique used in the performance evaluation was Support Vector Machines (Steinwart, 2014). The results of Support Vector Machines technique for electricity load forecasting are listed in Table 6 and the forecasting errors of Support Vector Machines technique are listed in Table 7. As given by the results presented in Table 2, Table 4 and Table 6, when correlation coefficient is considered, Multilayer Perceptron technique achieved the highest forecasting accuracy.

Table 2. Classification results for Ankara when Linear Regression was employed

Term	Value
Correlation Coefficient	0.5955
Average Absolute Error	2650.1462
Root Mean Square Error	3299.8781
Relative Absolute Error	% 76.1906
Root Relative Squared Error	% 80.3389
Total Number of Rows	12168

Table 3. Error values for Ankara when Linear Regression was employed (Please note that only the first 10 rows were given.)

Row	Actual Value	Predicted Value (MW)	Error
1	26400	22937.41	-3462.59
2	24700	23254.628	-1445.372
3	23800	23546.02	-253.98
4	23400	23837.412	437.412
5	23300	24102.977	802.977
6	23700	24497.676	797.676
7	24300	24944.028	644.028
8	25700	25467.862	-232.138
9	29300	25965.868	-3334.132
10	31500	26515.528	-4984.472

Table 4. Classification results for Ankara when Multilayer Perceptron was employed

Term	Value
Correlation Coefficient	0.7225
Average Absolute Error	2370.6511
Root Mean Square Error	2990.0692
Relative Absolute Error	% 68.1553
Root Relative Squared Error	% 72.7962
Total Number of Rows	12168

Table 5. Error values for Ankara when Multilayer Perceptron was used (Please note that only the first 10 rows were given.)

Row	Actual Value (MW)	Predicted Value (MW)	Error
1	26400	24425.549	-1974.451
2	24700	24538.664	-161.336
3	23800	24692.135	892.135
4	23400	24897.205	1497.205
5	23300	25166.922	1866.922
6	23700	25489.836	1789.836
7	24300	25872.411	1572.411
8	25700	26325.012	625.012
9	29300	26888.114	-2411.886
10	31500	27782.122	-3717.878

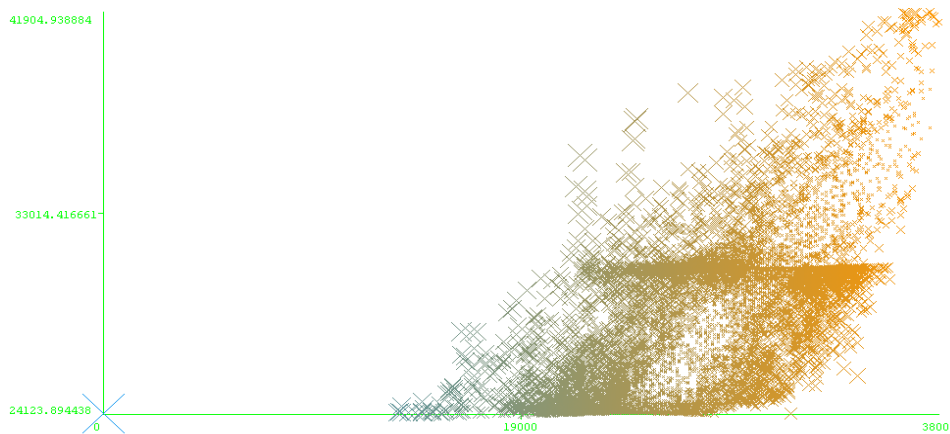


Figure 1. The actual values (X coordinate) vs predicted values (Y coordinate) when Multilayer Perceptron was employed

Table 6. Classification results for Ankara when Support Vector Machine was used

Term	Value
Correlation Coefficient	0.5938
Average Absolute Error	2640.5974
Root Mean Square Error	3310.1538
Relative Absolute Error	% 75.9161
Root Relative Squared Error	% 80.589
Total Number of Rows	12168

Table 7. Error values for Ankara when Support Vector Machine was used (Please note that only the first 10 rows were given.)

Row	Actual Value	Predicted Value (MW)	Error
1	26400	22673.061	-3726.939
2	24700	22994.054	-1705.946
3	23800	23283.813	-516.187
4	23400	23573.572	173.572
5	23300	23832.098	532.098
6	23700	24246.79	546.79
7	24300	24723.947	423.947
8	25700	25294.804	-405.196
9	29300	25834.428	-3465.572
10	31500	26436.517	-5063.483

An overview of forecasting results for Ankara is given in Figure 2. In this figure, the MSE value shows the average of the difference between the desired output and the current output of the artificial neural network. *R* represents the correlation between the actual values and the predicted values. Being the coefficient of correlation, *R* ranges from -1 to +1. If *R* is closer to +1 or -1, the two variables are related (Hastie, Tibshirani, & Friedman, 2009). On the other hand, if *R* is close to 0, it means that there is no relationship between the variables.

As shown in the error histogram shown in Figure 3, the target (actual) values are the values that the artificial neural network based model was expected to produce. The output values are values that the artificial neural network based model obtained. The error values show the margin between the target values and the output values. Results of the regression analysis for Ankara when Artificial Neural Network was employed are shown in Figure 4. The values of *R* and the results of the regression analysis show that the employed artificial neural network based model obtained satisfactory forecasting accuracy. To sum up, various statistical forecasting techniques can be used for electricity load forecasting if thousands of accurate data samples are available to be processed automatically.

	Samples	MSE	R
Training:	8517	3804642.77007e-0	8.81202e-1
Validation:	2434	3482206.47683e-0	8.91388e-1
Testing:	1217	3727131.82955e-0	8.73353e-1

Figure 2. An overview of forecasting results for Ankara

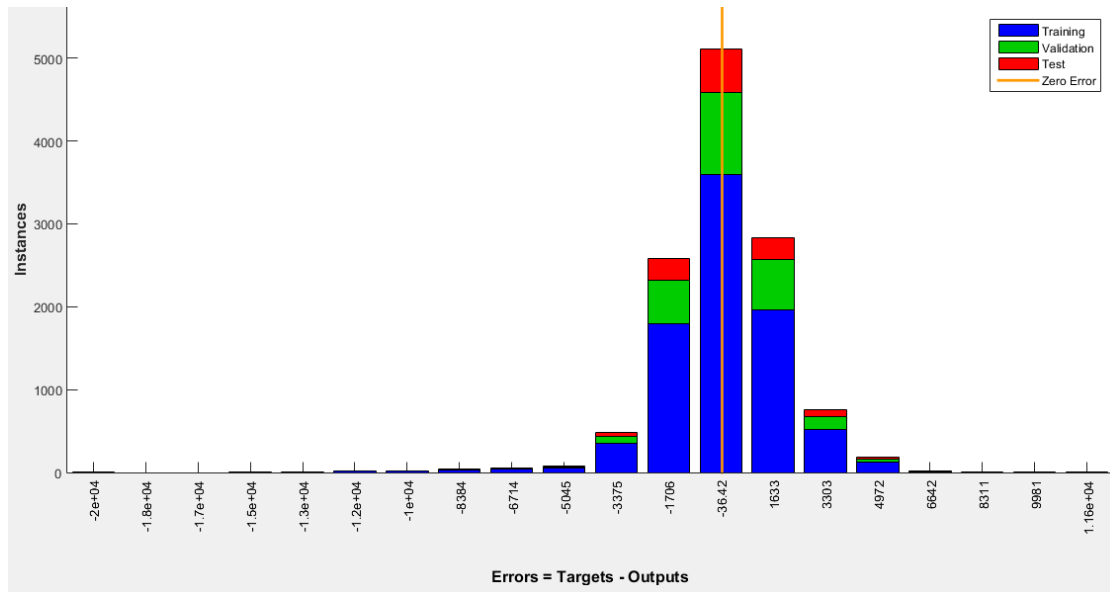


Figure 3. Error histogram for Ankara when Artificial Neural Network was employed

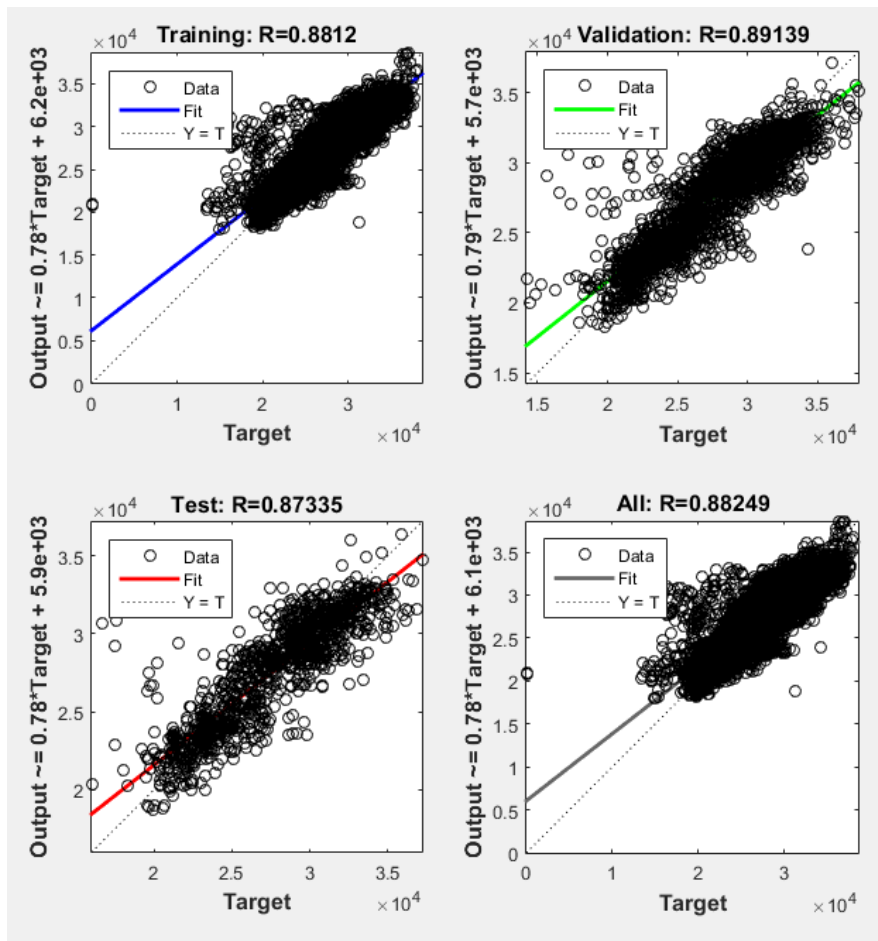


Figure 4. Results of the regression analysis for Ankara when Artificial Neural Network was employed

Conclusion

Electricity load forecasting is the predicting of electrical power required to meet the short-term, medium-term or long-term demand. It not only helps utility companies in their operation and management of the supply to their customers but also aids in planning on their capacity and operations so that all the customers can be supplied

reliably with the required energy. In addition, it is an important process that contributes to the efficiency and revenues for the utility companies. Considering all these benefits, in this paper, we realized a performance evaluation study to evaluate the accuracy of different classification approaches for electricity load forecasting. The results of the performance evaluation study show that electricity load forecasting can be realized successfully if careful analysis is made and a satisfactory dataset is available. The main limitation of this study is that since seasons and other factors may affect the way customers use the power, these factors should be taken into consideration for electricity load forecasting.

References

- Almehshaei, E., & Soltan, H. (2011). A methodology for Electric Power Load Forecasting. *Alexandria Engineering Journal*, 50(2), 137-144.
- Guerard, J. B., & Schwartz, E. (2010). *Quantitative corporate finance*. New York: Springer.
- Hastie, T. J., Tibshirani, R. J., & Friedman, J. H. (2009). *The elements of statistical learning: data mining, inference, and prediction*. Springer New York Inc., USA.
- Hernandez, L., Baladron, C., Aguiar, J. M., Carro, B., Sanchez-Esguevillas, A. J., Lloret, J., & Massana, J. (2014). A survey on electric power demand forecasting: Future trends in smart grids, microgrids and smart buildings. *IEEE Communications Surveys & Tutorials*, 16(3), 1460-1495.
- Popescu, M. -C., Balas, V. E., Perescu-Popescu, L., & Mastorakis, N. (2009). Multilayer perceptron and neural networks. *WSEAS Trans. Cir. and Sys.*, 8(7), 579-588.
- Reynaldi, A., Lukas, S., & Margaretha, H. (2012). Backpropagation and Levenberg-Marquardt Algorithm for Training Finite Element Neural Network. *Proceedings of the 2012 Sixth UKSim/AMSS European Symposium on Computer Modeling and Simulation (EMS '12)* (pp. 89-94).
- Steinwart, I. (2014). *Support vector machines*. Springer.
- Suganthi, L., & Samuel, A. A. (2012). Energy models for demand forecasting—A review. *Renewable and Sustainable Energy Reviews*, 16(2), 1223-1240.
- Weron, R. (2006). *Modeling and forecasting electricity loads and prices*. Chichester: Wiley & Sons.
- Yan, X., & Su, X. G. (2009). *Linear regression analysis theory and computing*. Singapore: World Scientific.
- <https://www.cs.waikato.ac.nz/ml/weka/>
- <https://www.mathworks.com/products/matlab.html>

Author Information

Gurkan Tuna

Trakya University
Edirne, Turkey
Contact e-mail: gurkantuna@trakya.edu.tr

Ahmet Vatansver

Trakya University
Edirne, Turkey

Resul Das

Firat University
Elazığ, Turkey

Molecular Investigation of Metallo- β -lactamase Encoding Gene in Nosocomial Carbapenem-Resistant Enterobacteriaceae in Iraqi Hospitals

Ahmed S. K. AL-KHAFAJI
University of Baghdad

Shaymaa Fadhel Abbas ALBAAAYIT
University of Baghdad

Omyma S. IBRAHEEM
University of Baghdad

Hawraa H. ABDUL-ILAH
University of Baghdad

Abstract: In recent years, there has been an increasing amount of evidence that nosocomial carbapenem-resistant Enterobacteriaceae pose a major public health threat. This study aims to uncover the association of multidrug-resistance related genes with increasing the rate of acquired hospital infections by Enterobacteriaceae pathogens. Enterobacteriaceae species (n=57) were detected in clinical specimens (n=45) obtained from patients with infected wounds and burns in 3 Iraqi hospitals. Carbapenem-resistant Enterobacteriaceae bacteria were investigated by antibacterial susceptibility tests. The Molecular investigation by PCR analysis showed that *Klebsiella pneumoniae* isolates (n=5) and *Escherichia coli* isolates (n=3) are carrying metallo- β -lactamase encoding gene (*bla_{IMP}*). It can be concluded that the expression of *bla_{IMP}* is considered among the main reasons of dominating resistance strains of Enterobacteriaceae pathogens and thus spreading nosocomial infection in Iraqi clinical centers. However, further molecular investigation is needed to overcome this resistance on molecular bases when treating.

Keywords: *bla_{IMP}*, Enterobacteriaceae, Nosocomial infection, Metallo- β -lactamase

Introduction

Recently, augmented multidrug-resistance among Enterobacteriaceae members has been considered as dreadful medical problem in Iraqi clinical centers (1), (2). Most of the cases with infected burns or wounds including post-operable wounds are administrated with intensive courses of different antibiotics of new generations. However, a number of those patients ended up with bacteremia or eventually septicemia (3).

Enterobacteriaceae represents a group of Gram-negative bacteria that colonise the intestine as either natural microbial flora or pathogens (4). However, various members belong to this family, such as, *Escherichia coli*, *Klebsiella pneumoniae*, *Serratia marcescens*, *Enterobacter spp.*, *Proteus spp.*, *Acinetobacter spp.*, are among the most common causes of nosocomial infection of burns and wounds (5), (6) Enterobacteriaceae pathogens are implicated in prevalence of antibiotic resistance to a wide range of β -lactam therapeutics utilized for treating Enterobacteriaceae related infection. The recent two decades have witnessed emergence of carbapenem-resistant Enterobacteriaceae (CRE) and, therefore, increasing CRE-related infections. This has led to poor prognosis of patients suffering from such infections when treating with β -lactams involving therapeutics and therefore increasing rate of morbidities and mortalities (7), (8), (9). There are four main groups of carbapenemases (beta lactamases); Class A carbapenemase (10), Class B carbapenemase (11), Class D β -lactamases (12) and carbapenem-hydrolyzing class D β -lactamases (13). Metallo- β -lactamase, which is encoded by *bla_{IMP}* (14). The

- This is an Open Access article distributed under the terms of the Creative Commons Attribution-Noncommercial 4.0 Unported License, permitting all non-commercial use, distribution, and reproduction in any medium, provided the original work is properly cited.

- Selection and peer-review under responsibility of the Organizing Committee of the Conference

reason behind emergence the antimicrobial resistance to carbapenems is that of utilizing carbapenems-related antibiotics to treat the strains producing β -lactamases, which can hydrolyze all β -lactams except such antibiotics and then emergence of new generations of strains that can resist this type of antibiotics (carbapenems) (15). The aim of present study is, therefore, to investigate the involvement of *bla*_{IMP} in prevalence of carbapenem-resistant Enterobacteriaceae in nosocomial infection in Iraqi hospitals.

Method

Specimen Collection

Specimens of infected burns or wounds including post-operable wounds were collected from three local hospitals based in Baghdad, Iraq. There was no need for ethical approval since the samples were autonomously collected from the hospitals' laboratories where the clinical microbiology investigation is routinely carried out. Individuals with infected burns and wound were sampled for four months during the period between January and April, 2018. Sampling of specimens was conducted using swab transporting media.

Bacterial Isolates

Fifty seven isolates of *Enterobacteriaceae* species were diagnosed by the routine automated method Vitek® 2 (BioMérieux, France). The isolates identified comprised 31 *Klebsiella pneumoniae*, 22 *Escherichia coli*, 2 *Enterobacter aerogenes*, 1 *Serratia marcescens* and 1 *Proteus mirabilis*.

Antibacterial Susceptibility

The antibacterial susceptibility tests were carried out for all bacterial isolates using disc diffusion method to identify the carbapenem-resistant Enterobacteriaceae (CRE), while the minimal inhibitory concentrations (MICs) identified by dilution method using Mueller-Hinton broth. For quality control of antibacterial susceptibility test, *E. coli* ATCC 25922 strain was employed.

PCR Detection

Candidate bacterial isolates, which resist or moderately resist imipenem, were subjected to detect *bla*_{IMP} gene by PCR technique using the primers F-5-CTACCGCAGCAGAGTCTTTG-3, R-5-AACCAGTTTTGCCTTACCAT-3 already designed and reported by Senda *et al* 1996 (16).

Results and Discussion

In the present study, three local hospitals based in Baghdad, Iraq were subjected to investigate the prevalence of nosocomial infection with the carbapenem-producing Enterobacteriaceae members. Total of fifty seven bacterial isolates were obtained from forty five clinical samples collected from different sites of body injuries (burn wounds, trauma and post-operable wounds). The specimen collection distributed according the hospital (fifteen from each) and within the same hospital according the type of injury (five from each). 26 of cases were female while the rest 19 were males. Their age ranged between 19-45 years old. 70% of bacterial isolates were obtained from burn specimens followed by trauma accounting for 25%, while the rest (5%) were isolated from post operable wounds.

The bacterial isolates manifested different patterns of response to the tested antibiotics; amikacin, ceftazidime, Cefixime, Cefmetazole, Cefotaxime, imipenem, Norfloxacin and Ampicillin with sulbactam (Table 1). Eight carbapenem-resistant Enterobacteriaceae isolates (five isolates of *Klebsiella pneumoniae* and three *Escherichia coli* isolates) were selected for PCR analysis based on imipenem MIC of 4 μ g/mL (Table 1). Such isolates are suspicious for production of carbapenemase (Patel *et al* 2017). Therefore, the *bla*_{IMP} gene was investigated in these isolates.

Table 1. Bacterial susceptibility of bla_{IMP}-expressing isolates

Bacterial isolates	Antibiotic MIC (µg/ml)							
	AN	CAZ	CFM	CMZ	CTX	IPM	NOR	SAM
<i>Klebsiella pneumoniae</i> isolates								
KP04	32	>128	>128	128	>128	16	>128	8
KP09	16	64	32	64	>128	16	64	8
KP16	16	>128	128	64	128	64	>128	64
KP18	32	32	>128	>128	64	32	16	4
KP22	16	128	32	>128	64	16	16	128
<i>Escherichia coli</i> isolates								
EC10	>128	>128	>128	>128	>128	128	>128	128
EC22	16	>128	64	128	>128	64	>128	64
EC50	32	128	>128	>128	>128	64	32	64

Abbreviations: AN, amikacin; CAZ, ceftazidime; CFM, Cefixime; CMZ, Cefmetazole; CTX Cefotaxime; IPM, imipenem; NOR, Norfloxacin; SAM, Ampicillin with sulbactam

To screen the resistant isolates, the Clinical Laboratory Standards Institute (CLSI) definition was adopted. CLSI defines Enterobacteriaceae as carbapenem-resistant if they have minimum inhibitory concentrations (MICs) of ≥ 4 µg/ml against imipenem (17).

The molecular investigation of carbapenem-resistant Enterobacteriaceae by PCR analysis showed that bla_{IMP} gene is carried by four isolates of *Klebsiella pneumoniae* (KP04, KP16, KP18 and KP22) in addition to all of the tested *Escherichia coli* isolates (EC10, EC22 and EC50) (figure 1). This may prove the implication of bla_{IMP} in increasing the antibiotic resistance in the examined isolates of hospital acquired infections in Iraq. Nevertheless, the molecular detection of the expression level of metallo-β-lactamase is crucial to solidify this observational evidence.

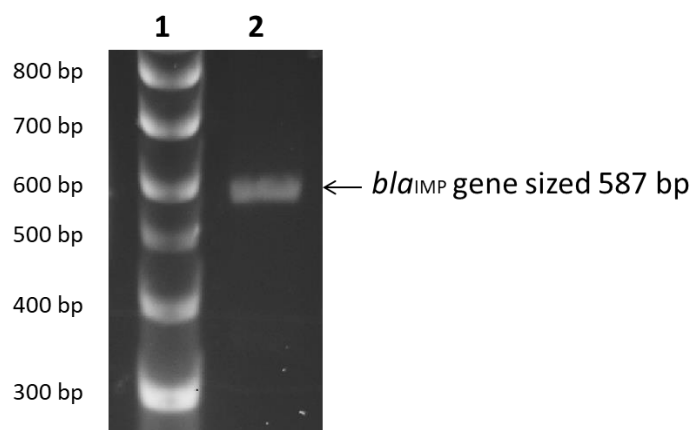


Figure 1: Representative gel electrophoresis photograph showing the amplified sequence of the bla_{IMP} detected in the imipenem resistant isolates. 1) HyperLadder II DNA marker. 2) Amplified DNA fragment of bla_{IMP} gene sized 587 bp.

Conclusion

In a 2013 US Centers for Disease Control and Prevention (CDC) report, carbapenem-resistant Enterobacteriaceae were listed as one of the three most urgent antimicrobial resistant threats. CREs received this highest threat level due to rapidly increasing global spread, propensity for multidrug resistance, and high mortality during blood stream infections (BSI) (18).

Carbapenem resistance in Gram-negative bacteria, especially when carbapenemases are involved, is the main contributing factor for multidrug resistance and usually the definitive step before pan drug resistance. Indeed, resistance to other last-resort drugs among carbapenemase producers may rapidly emerge when these agents are necessarily used in healthcare settings. Moreover, it has been shown that carbapenem-resistant Gram-negative nosocomial pathogens will continue to evolve accumulating more carbapenem-resistance mechanisms, or more than one carbapenemase-encoding gene (19). This will lead in many cases to increased carbapenem MICs ruling

out the best-to-date therapeutic choice against carbapenemase producers, which is the combined treatment including at least one carbapenem. The molecular investigation of such pathogens can be accurate and fast. Implementing of molecular detection of carbapenemase encoding genes in our hospital could bring huge benefits in terms of predicting the drug of choice to treat the related hospital acquired infection (20). Taking together our and other findings, it can be concluded that the emergence of Enterobacteriaceae nosocomial pathogens pose a foreseeable threat in Iraqi medical centers and, therefore, further molecular analysis is needed to conquer this resistance on expression level when treating.

Recommendations

1. Investigating the molecular mechanisms give rising emergence of Enterobacteriaceae producing carbapenemase may assist to explore how to eliminate spreading these nosocomial pathogens.
2. Employing carbapenemase encoding genes as biomarkers for predicting the antibacterial therapeutic regimens in Iraqi hospitals to reduce the mortalities associated with the antibiotics miss-use to treat Enterobacteriaceae-related nosocomial infections.

Acknowledgements

We would like to acknowledge Mariam J Nsaif (University of Baghdad, Collage of Science, Department of Biology) for her kind assistance in this work. This is a voluntary research work and has not been funded by any organization.

References

- Carattoli A. Resistance plasmid families in Enterobacteriaceae. *Antimicrobial agents and chemotherapy*. 2009;53(6):2227-38.
- Huang XZ, Frye JG, Chahine MA, Glenn LM, Ake JA, Su W, et al. Characteristics of plasmids in multi-drug-resistant Enterobacteriaceae isolated during prospective surveillance of a newly opened hospital in Iraq. *PloS one*. 2012;7(7):e40360.
- Church D, Elsayed S, Reid O, Winston B, Lindsay R. Burn wound infections. *Clinical microbiology reviews*. 2006;19(2):403-34.
- Guarner F. The intestinal flora in inflammatory bowel disease: normal or abnormal? *Current opinion in gastroenterology*. 2005;21(4):414-8.
- Azzopardi EA, Azzopardi E, Camilleri L, Villalpos J, Boyce DE, Dziewulski P, et al. Gram negative wound infection in hospitalised adult burn patients--systematic review and metanalysis. *PloS one*. 2014;9(4):e95042.
- Finley PJ, Norton R, Austin C, Mitchell A, Zank S, Durham P. Unprecedented Silver Resistance in Clinically Isolated Enterobacteriaceae: Major Implications for Burn and Wound Management. *Antimicrobial agents and chemotherapy*. 2015;59(8):4734-41.
- Patel G, Huprikar S, Factor SH, Jenkins SG, Calfee DP. Outcomes of carbapenem-resistant Klebsiella pneumoniae infection and the impact of antimicrobial and adjunctive therapies. *Infection control and hospital epidemiology*. 2008;29(12):1099-106.
- Borer A, Saidel-Odes L, Riesenber K, Eskira S, Peled N, Nativ R, et al. Attributable mortality rate for carbapenem-resistant Klebsiella pneumoniae bacteremia. *Infection control and hospital epidemiology*. 2009;30(10):972-6.
- Tischendorf J, de Avila RA, Safdar N. Risk of infection following colonization with carbapenem-resistant Enterobacteriaceae: A systematic review. *American journal of infection control*. 2016;44(5):539-43.
- Yang YJ, Wu PJ, Livermore DM. Biochemical characterization of a beta-lactamase that hydrolyzes penems and carbapenems from two *Serratia marcescens* isolates. *Antimicrobial agents and chemotherapy*. 1990;34(5):755-8.
- Pitout JD, Nordmann P, Poirel L. Carbapenemase-Producing Klebsiella pneumoniae, a Key Pathogen Set for Global Nosocomial Dominance. *Antimicrobial agents and chemotherapy*. 2015;59(10):5873-84.
- Donald HM, Scaife W, Amyes SG, Young HK. Sequence analysis of ARI-1, a novel OXA beta-lactamase, responsible for imipenem resistance in *Acinetobacter baumannii* 6B92. *Antimicrobial agents and chemotherapy*. 2000;44(1):196-9.
- Evans BA, Amyes SG. OXA beta-lactamases. *Clinical microbiology reviews*. 2014;27(2):241-63.

- Sidjabat HE, Townell N, Nimmo GR, George NM, Robson J, Vohra R, et al. Dominance of IMP-4-producing enterobacter cloacae among carbapenemase-producing Enterobacteriaceae in Australia. *Antimicrobial agents and chemotherapy*. 2015;59(7):4059-66.
- Nordmann P, Dortet L, Poirel L. Carbapenem resistance in Enterobacteriaceae: here is the storm! *Trends in molecular medicine*. 2012;18(5):263-72.
- Senda K, Arakawa Y, Ichiyama S, Nakashima K, Ito H, Ohsuka S, et al. PCR detection of metallo-beta-lactamase gene (blaIMP) in gram-negative rods resistant to broad-spectrum beta-lactams. *Journal of clinical microbiology*. 1996;34(12):2909-13.
- Hariharan P, Bharani T, Franklyne JS, Biswas P, Solanki SS, Paul-Satyaseela M. Antibiotic susceptibility pattern of Enterobacteriaceae and non-fermenter Gram-negative clinical isolates of microbial resource orchid. *Journal of natural science, biology, and medicine*. 2015;6(1):198-201.
- Maded JY, Haenni M, Nordmann P, Poirel L. Extended-spectrum beta-lactamase/AmpC- and carbapenemase-producing Enterobacteriaceae in animals: a threat for humans? *Clinical microbiology and infection : the official publication of the European Society of Clinical Microbiology and Infectious Diseases*. 2017;23(11):826-33.
- Meletis G. Carbapenem resistance: overview of the problem and future perspectives. *Therapeutic advances in infectious disease*. 2016;3(1):15-21.
- Rood IGH, Li Q. Review: Molecular detection of extended spectrum-beta-lactamase- and carbapenemase-producing Enterobacteriaceae in a clinical setting. *Diagnostic microbiology and infectious disease*. 2017;89(3):245-50.

Author Information

Ahmed S K Al-Khafaji

Department of Biology, College of Science, University of Baghdad
Al-Jadriya, Baghdad 10070, Iraq
Contact e-mail: alkhafaji72@gmail.com

Shaymaa Fadhel Abbas Albaayit

Department of Biology, College of Science, University of Baghdad
Al-Jadriya, Baghdad 10070, Iraq

Omyma S Ibraheem

Department of Biology, College of Science, University of Baghdad
Al-Jadriya, Baghdad 10070, Iraq

Hawraa H Abdul-Ilah

Department of Biology, College of Science, University of Baghdad
Al-Jadriya, Baghdad 10070, Iraq

Olive Pomace and Cherry Stones used as Biofuels

Andreja MARZI

Primary School and Kindergarten Ankaran

Abstract: The aim of the article is to show how to encourage students to deepen their knowledge and their enthusiasm for research. In this way we can also promote the popularization of science and technology as well as the identification of students talented in specific research areas. This article presents an example of writing a research assignment undertaken by students in the final year of primary school (class 9, i.e. age 14-15). During school lessons, we did not discuss biomass as fuel in detail, but we found the topic very interesting, which is why we decided that we would focus on it in our research paper. We live in the age of diminishing supplies of fossil fuels and consequently a growing interest in the renewable energy sources, including biofuels. Through research assignment, we wanted our students to learn more about the characteristics of biofuels which we haven't discussed in detail in class. Biofuel is a solid, liquid or gaseous fuel, obtained from a relatively recently deceased biological substance. In addition to looking for information in literature and electronic resources, we conducted experiments in which we measured how many degrees a particular quantity of water heats up by the burning of various fuels, and the amount of residue left after burning. The fuels we used were: pellets, briquettes, olive pomace, cherry stones, biodiesel, ethanol and sawdust. We established that different types of fuel emit, when burnt, different amounts of heat. Water heated up the most when burning ethanol, while it heated up the least when using biodiesel. Experiments showed that different fuels burn for different amounts of time, leaving a residue which depends on the type of fuel.

Keywords: Research assignment, Biofuels, Experimental work

Introduction

Renewable energy sources

The motives for using renewable energy resources have been changing throughout human history. In the initial phase of technological development renewable energy sources were the only source that people used. All activities depended on local and natural energy resources and building materials. The middle of the 19th century marked the beginning of the era of extensive use of fossil fuels and the development of technologies for their conversion into other forms of energy. At the end of the 20th century scientists started to warn people about the harmfulness of carbon dioxide, which is created in the process of burning fossil fuels. Calling people's attention to the need for fairer development in all regions of the world led to the formation of the theory of sustainable (and environmentally friendly) development. In this context, the efforts towards the use of renewable energy sources grew stronger.

What are renewable energy sources? We must understand that all sources of energy are derived from nature. Renewable sources are those sources that can be used again and again as they are available in plenty and are not going to perish anytime soon. They are sources of energy we obtain from constant natural processes such as the wind, solar radiation (solar power stations), water current in rivers or streams (hydroenergy), Earth's heat fluxes (geothermal energy), the tides and waves of the seas and oceans (tidal energy and wave energy), photosynthesis by which plants build biomass (wood, vegetable oils that we convert into biodiesel, bioethanol, biogas).

The main advantages of renewable energy sources include the fact that their use reduces the emissions of greenhouse gases; these energy sources are also free, they are durable and have a great potential. Renewable

- This is an Open Access article distributed under the terms of the Creative Commons Attribution-NonCommercial 4.0 Unported License, permitting all non-commercial use, distribution, and reproduction in any medium, provided the original work is properly cited.

- Selection and peer-review under responsibility of the Organizing Committee of the Conference

© 2018 Published by ISRES Publishing: www.isres.org

energy sources cannot be stored in nature except in the form of biomass and the heat of oceans. Thus we have to use various devices for storing the energy of renewable resources, which lessens their efficiency and makes their exploitation more expensive.

The second decade of the 21st century is a favourable time for further development of technologies linked to renewable energy sources. The European Union decided to pursue the objective of reducing greenhouse gases emissions by 40 percent by the year 2030. Using the existing technologies, this can be achieved through greater use of the energy from nuclear power plants or by expanding the use of renewable sources of energy in all forms: direct solar radiation and the energy of water, wind and biomass. In recent years, wood, other solid biofuels and renewable waste have presented the crucial part of renewable energy sources.

Figure 1 shows the primary production of energy from renewable sources in EU during the period 1990-2016.

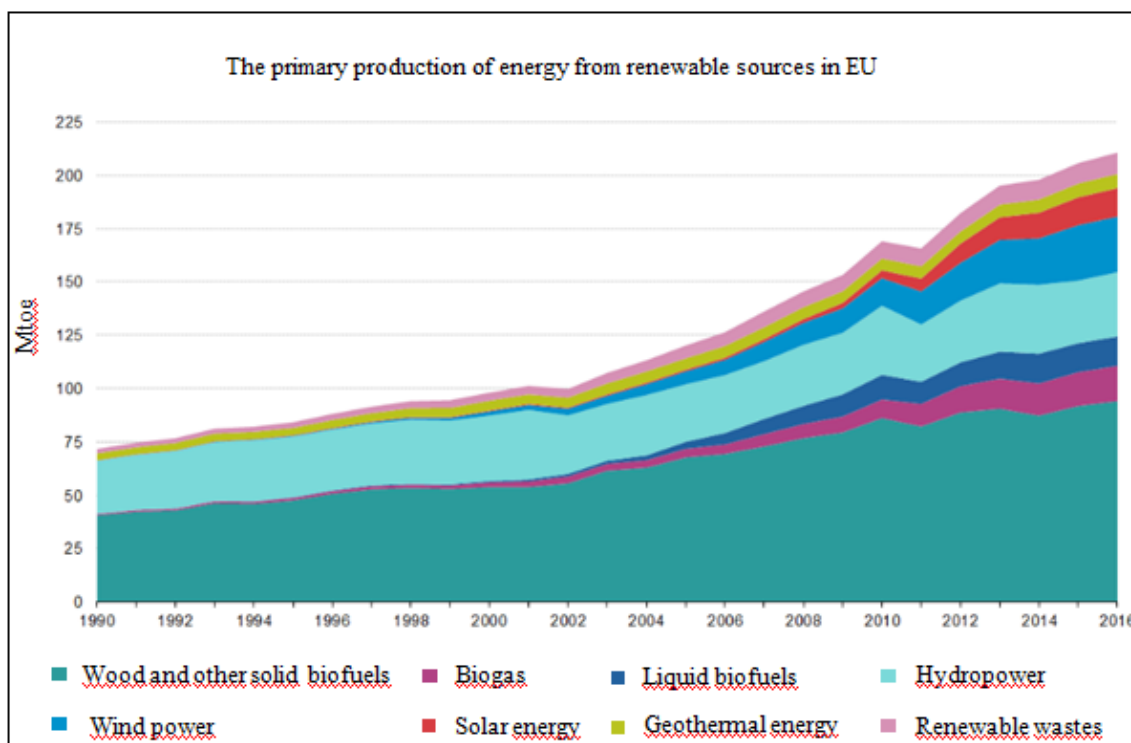


Figure 1. The final water temperature (source: eurostat)

Biomass and Biofuels

According to the *Directive on renewable energy resources*, biomass derives from different kinds of organic materials: energy crops (oil plants; plants containing sugar), wood, forest waste and agricultural waste, and biodegradable waste from households, fishery and industry.

Approximately 0,01 percent of solar energy received by the Earth is used for the production of organic matter in plants, but despite the low rate of energy recovery the binding of solar energy into biomass is one of the most important energy conversions. The contribution of biomass as regards covering the total energy needs of humanity is circa 14 percent. Among various kinds of biomass wood and scrap wood are used the most. The share contributed by other kinds of biomass such as agricultural waste (straw, animal manure), wood scrap from forest waste and the processing of wood as well as energy crops is growing.

Biomass can be used for heating, for generating electricity and producing biofuels. Fuels produced from biomass with the described procedures can be classified into three groups:

- solid biomass (wood biomass, agricultural crops);
- liquid biofuels (bioethanol, biodiesel) ;
- gases from biomass (biogas, wood gas, landfill gas).

Bioethanol is an alcohol which is nowadays produced by sugar fermentation, especially from corn and sugar cane, but also from corn stalks, prairie grasses, fast-growing trees, sawdust and algae. By using bioethanol we can reduce emissions of greenhouse gases by 22-56 percent (and even by 91 percent, by using cellulose ethanol – a fuel barely known to date). However, production of corn ethanol leads to a great consumption of fossil fuels and releases a lot of CO₂, so many scientists are currently in double mind as regards the processing of corn into fuel. For the time being it is mostly used as a complement to petrol.

Biodiesel is a methyl ester produced from biomass. It is formed through the esterification of vegetable oils and animal fats (usually canola, soya and oilseed rape). High quality biodiesel can be used in normal diesel engines, independently or in mixtures with diesel. Its use can reduce carbon dioxide emissions by 68 percent.

Olive pomace (pulp) is one of the more interesting biofuels, which can be completely dried and compressed into blocks that can be then used for heating. While olive pomace remains nearly unknown as a fuel in Slovenia, it is already being used as an energy resource in the Near and Middle East and some other parts of the world (Spain, Turkey).

Wood biomass is an ancient, but at the same time modern, environmentally friendly and familiar source of energy. If we want to keep waste gas emission below the permissible level, wood biomass needs to be treated in a suitable way and the heating devices (stoves) should be in working order.

Methods

Experimental work

Our essential research method was laboratory work. We precisely determined the experimental procedure and prepared the needed laboratory equipment. We decided that we would do our laboratory work at school, in Chemistry room, in the framework of Chemistry Club.

In the experimental part we tried to answer the following questions: how many °C do various fuels heat up a particular amount of water and what amount of residue is left after the burning of solid fuels.

Laboratory equipment

For our experiments we needed: an empty spirit burner, a laboratory balance, a stand and a gauze, a beaker, a holed aluminium container, a thermometer, a measuring cylinder and a stopwatch.

Fuels that were used

The fuels we used during our experimental work were the following: pellets, briquettes, sawdust, olive pulp (undried and dried for one hour at 105°C), cherry stones (undried and dried for one hour at 105°C), biodiesel, ethanol and fuel oil.

We decided to use olive pomace because we live in a region which is known for the production of olive oil and the locals use the leftovers of the process of pressing olives also at home as a fuel in central heating appliances. Cherry stones can also be used as a fuel.

The work procedure

We measured the amount of heat emitted during the burning of various fuels. We observed this indirectly, through measuring the temperature of water heated by the release of heat during the burning of a specific fuel.

On a piece of paper we weighed 20 g of solid fuel; we measured out 20 ml of liquid fuel with the help of a measuring cylinder. We put some old newspaper (0,9 g) and a combustion tablet (3 g) into the aluminium container, while the liquid fuel was poured into the burner. We put on protective glasses and continued with our work. On the lower stand we put a container with a solid fuel, or the burner with a liquid fuel, while we put a gauze and a beaker containing 50 ml of water on the upper stand. With the thermometer we measured the initial water temperature and noted it down. Then we ignited the combustion tablet and watched the burning process and the changes in water temperature. Temperature was read every 5 minutes. After all of the fuel burnt out, we noted the final water temperature and the total burning time. We also weighed the mass of the residue.

Results and Discussion

Final temperature of water after the burning of various fuels

The final temperature of water after burning of a particular fuel can be seen in the following diagram:

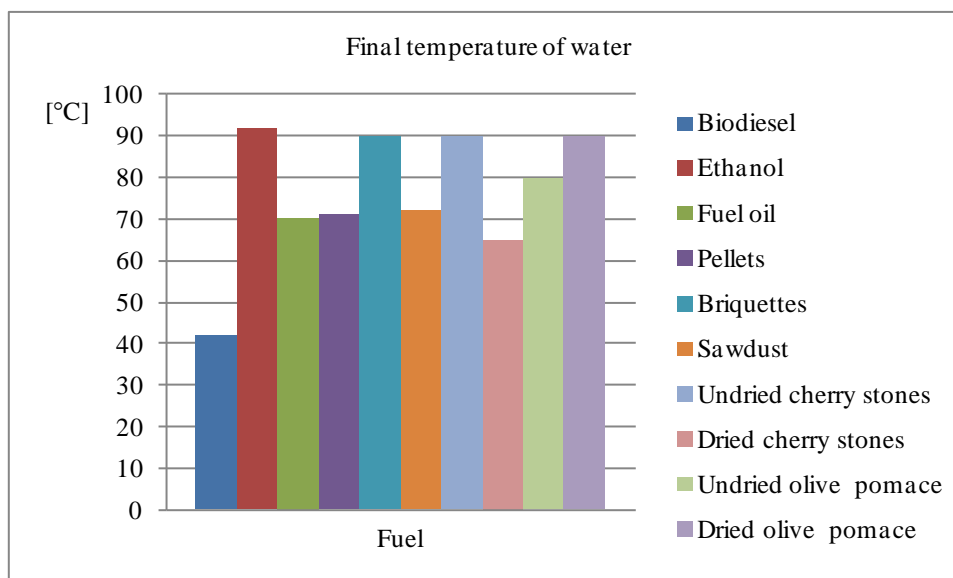


Figure 2. The final water temperature

Ethanol gave off the most heat during burning (the final water temperature being 92°C), while biodiesel produced the least heat (the final water temperature being 42°C). (see fig. 2)

Residue left after the burning of solid fuels

After weighing the residue left after burning, we arrived at the following findings. (see fig. 3)

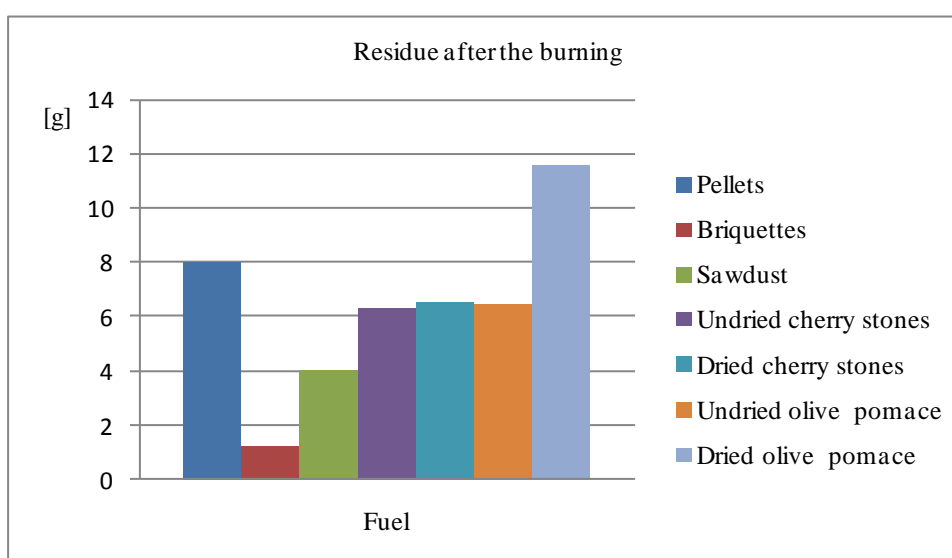


Figure 3. The residue after the burning of solid fuels

We found that briquettes burnt down almost completely - the amount of residue left after burning this fuel is the smallest. The greatest amount of residue is left after burning dry olive pomace (see fig.3).

Burning Time

The burning time of a particular fuel can be seen in the following table.

Table 1. Burning time of different fuels

Fuel	Burning time [min]
Biodiesel	35
Ethanol	23
Fuel oil	60
Pellets	23
Briquettes	16
Sawdust	18
Undried cherry stones	11
Dried cherry stones	14
Undried olive pomace	13
Dried olive pomace	13

Fuel oil burnt the longest (60 min and more), while undried cherry stones burnt for the shortest time (11 min). (Table 1)

Conclusion

The results of experiments showed us the following that different kinds of fuel emit different amounts of heat during burning (for example, the final temperature with biodiesel is 42°C, while the final temperature with ethanol is 92°C). Some substances take more time to burn, some less (for example, fuel oil burns for more than an hour, while undried cherry stones burn for eleven minutes). After the burning of all kinds of fuels we noticed a residue, even if only in the form of soot. Amongst all the samples, ethanol gave off the most heat. Each of the fuels used left a residue after burning, namely different amounts of soot and ash (for example, the burning of briquettes gave us 1,2 g of residue, while dry olive pomace left 11,6 g of residue).

This report presents an example of making a research paper in elementary school, which is not the same as proper research work. This is especially true when it comes to the originality of hypotheses that form the basis of research and the precision with which these are tested. Students upgrade their existing knowledge with a different, research-oriented approach which includes doing experiments and forming conclusions independently. In their work, students can deploy their creativity and critical thinking skills, especially in connection to trending topics and everyday subjects of their interest.

Teacher plays a significant role in directing and monitoring research work done by students of this age group. He or she needs to be equipped with good professional, psychological and didactic knowledge, he or she needs to be acquainted with the systematics of research work, and he or she also needs to be able to establish good relationships with students and between students.

References

- Činkole, Kristan, E. (2016). *Obnovljivi viri energije v Sloveniji: Prerez časa in prostora*. Ljubljana : Borzen.
- Kobal, E. (1989). *Raziskovanje je odkrivanje novega znanja*. Ljubljana: Državna založba Slovenije.
- Kolar, J. (1981). *Kako deluje?: Človekovo okolje*. Ljubljana: Tehniška založba.
- Koželj, B., Vuk, D. (1987). *Splošna ekologija z varstvom okolja*. Maribor: Založba Obzorja.
- Medved, S., Arkar, C. (2009). *Energija in okolje: obnovljivi viri energije*. Ljubljana: Zdravstvena fakulteta.
- Novak, P., Medved, S. (2000). *Energija in okolje: Izbira virov in tehnologij za manjše obremenjevanje okolja*. Ljubljana: Svet za varstvo okolja R Slovenije.
- Renewable energy (n.d.). In Eurostat Statistics Explained. Available from http://ec.europa.eu/eurostat/statistics-explained/index.php/Renewable_energy_statistics
- Use of energy from renewable sources. (2009). Directive 2009/28/EC of the European Parliament and of the Council of 23 April 2009 on the promotion of the use of energy from renewable sources and

amending and subsequently repealing Directives 2001/77/EC and 2003/30/EC. Retrieved from <http://eur-lex.europa.eu/legal-content/SL/TXT/PDF/?uri=CELEX:32009L0028&from=EN>
Zupančič M.(n.d.). *Biogoriva*. Agencija Republike Slovenije za okolje. Retrieved from <http://www.arso.gov.si/podnebne%20spremembe/poro%C4%8Dila%20in%20publikacije/>

Author Information

Andreja Marzi

Primary School and Kindergarten Ankaran
Regentova ulica 4, 6280 Ankaran, Republic of
Slovenia

Contact e-mail: andreja.marzi@osv-ankaran.si

Determination of Morphology and Allergenic Proteins of Pistachio (*Pistachia vera* L.) Pollens in Gaziantep

Gulay KASOGLU
Gaziantep University

Ibrahim Halil KILIC
Gaziantep University

Mehmet OZASLAN
Gaziantep University

Isik Didem KARAGOZ
Gaziantep University

Abstract: Allergens can be defined as antigens that stimulate specific IgE (Immunoglobulin E) antibody formation and react with it. In this study, the morphologies of *Pistachia vera* allergenic pollens belonging to Anacardiaceae family in South Eastern Anatolia were examined by light microscopy and pollens extracts were prepared from these species. The specimens used in morphological studies were obtained from Gaziantep University campus area. Slides of pollens were prepared according to Wodehouse (1935) method and the morphological characteristics of pollens were determined using microphotographs taken by light microscopy. Pollens crude extracts were obtained from the flora grown in this region. Extraction method established by Aytug et al. (1991) was used to prepare crude extracts from the collected pollens, 'Coca' solution was added extensively and sterile filtration technique was used for sterilization. BCA assay and absorbance measurements were used to determine the protein concentration. Standard curve was generated using concentrations and absorbance values of standard protein samples prepared at different concentrations (0, 1-1mg/ml). The protein concentration of the pollens extracts was calculated using the correct equation obtained from this curve. These crude extracts contain many major and minor allergens that can be used to diagnose allergic diseases. Due to the very high concentration of allergenic proteins in *P. vera*, it can be included in allergen kits. Moreover, allergy tests should be conducted to those living in this region. The results obtained from this study can both contribute to systematic studies and to the treatment of allergic diseases caused by these types of pollens.

Keywords: Pollen allergy, Pollen extract, *P. vera*, Pollen morphology

Introduction

It is noteworthy that allergic diseases are one of the major public health problems nowadays in most developed countries. Allergic reactions can occur in various organs in children, adults and almost all age groups. Allergic diseases have a significant impact on the health of the patients and their families and therefore affect their daily life activities. The incidence of allergic diseases in our country is rapidly increasing in the last years (1). Approximately 20% of the population in USA suffers from at least one form of allergy. It is the third most common chronic disease for children and the fifth leading chronic disease for all ages below 18 years (2).

Allergic diseases results from various sources of allergens. Pollens are one of the major aeroallergens that cause increased allergic sensitization and the associated symptoms (3). Pollens are produced in the male organ of the flower and then transported to the female organ for fertilization .In this process called pollination, pollens are mostly carried by insects and winds (4).

- This is an Open Access article distributed under the terms of the Creative Commons Attribution-Noncommercial 4.0 Unported License, permitting all non-commercial use, distribution, and reproduction in any medium, provided the original work is properly cited.

- Selection and peer-review under responsibility of the Organizing Committee of the Conference

Pollen allergenic proteins spreading in the atmosphere that enters the body through respiration, cause diseases such as allergic asthma and allergic rhinitis in humans (5, 6).

Identification of pollens in the atmosphere of the region is very important in the diagnosis and treatment of allergic diseases. For this purpose, pollen collection devices are used to detect atmospheric pollen (1). Recombinant or purified natural allergens are crucial in the study of the sensitization required during the selection of pollen vaccine suitable for the specific immunotherapy used in the treatment of allergic diseases. Most of the recombinant allergens react very well in immunoassays of specific IgE, and purified natural allergens may be a good alternative in this aspect. In some cases, natural allergens may react better than their recombinant counterparts. However, natural allergens are more advantageous in terms of high immunoreactivity (7).

Turkey has a very rich flora due to its wide varieties of geographical and climate features. Therefore, studies conducted in different regions should detect and identify pollens types prevalent in those regions. Pollens identification studies should be repeated at regular intervals taking into account that the plants are affected by environmental factors and the active pollens spreading on those areas should be determined. This process is important for evaluating and controlling the allergic discomfort of people living in or coming to the area. Furthermore, routine screening and identification studies of the prevalent pollens types in the region, can provide valuable information about which pollen groups should be included in allergic tests and treatment and these findings will also contribute to the medical field (1).

The identification of allergenic pollens of *P. vera* plant belonging to Anacardiaceae family and the determination of total protein values of pollens obtained from plants grown in South East Anatolia region in this study are taken as a base for further studies in the future. In the scope of the identification studies of different allergenic features of flora growing in different regions, this study can be a preliminary study for the researchers who will work on this field.

Method

Pollens samples of *P. vera* (pistachio) species investigated in the scope of this study were collected during pollination season from trees grown in forested areas in Gaziantep University campus in Gaziantep province. Species identification was performed by Dr. Hüseyin TEKİN from the Botany Department.

Fresh pollens were collected for extraction, morphological identification and allergenic proteins determination purposes. The pollens were collected at this time because the best time for pollen collection is immediately after the opening of the stamen containing the pollen sacs (8). Pistachios (*P. vera*) pollens was collected during its flowering time, dried and then passed through sterile sieves. After sieving, pollens were washed thoroughly with acetone to eliminate foreign particles. The washed pollens were covered with aluminum foil to protect them from light.

The pollens samples were analyzed using the light microscope according to Wodehouse method (9), and pollen diameter, exine thickness and aperture diameters were determined.

Extraction method described by Aytuğ B. et al. (1996) was performed to extract the active substances from pollens. Then, to determine the total protein concentration in the pollens extracts, the 'Bicinchoninic Acid (BCA)' assay was used according to the protocol of BCA Protein Macro Assay Kit (Serva Electrophoresis GmbH).

Results and Discussion

In this study, the morphology of *P. vera* allergenic pollens belonging to the Anacardiaceae family in South Eastern Anatolia was investigated under light microscopy. Pollens extracts were prepared from this species, then pollen diameter, aperture diameter and exine thickness were measured using microscopic photographs.

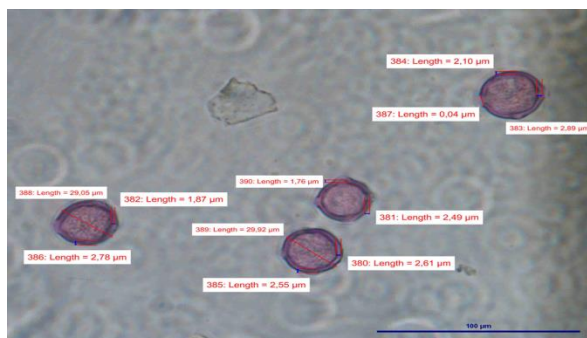


Figure 1. *Pistacia vera* pollens

The total protein concentration value measured in the prepared pollens extracts was 3739,601 µg/mL. This total protein concentration is thought to contain allergenic proteins in *P. vera* pollens.

Table 1. Total protein concentration values of *P.vera* pollens extracts measured by BCA assay

	Measurements	Mean	Standard deviation	Result
<i>P.vera</i> pure	3,289/3,476/3,977	3,578	0,291572	3739,601 µg/mL

Conclusion

In Turkey, pollens extracts kits used in the diagnosis and treatment of allergic diseases are mostly imported. The costs of these commercial allergen kits obtained through DNA technologies are very expensive. In addition, allergenic pollens have different properties in different areas, and therefore the use of these imported kits may be ineffective for the diagnosis of allergic reactions triggered by local pollens. For this reason, pollens extracts obtained from the local plants grown in this region is more useful for the diagnosis and treatment of people affected by allergies in this region. Moreover, the use of pollens extracts in which allergens can be isolated with high purity can be of advantage in allergic diseases diagnostic tests and treatment.

The crude extracts of plants used to diagnose allergic diseases contain many major and minor allergens. In the present study, crude extracts of *P. vera* containing allergens were prepared and that can be used as one of the components of allergens kits. Our results suggest that it is possible to include *P.vera* extracts in the allergy test panels performed on people living in this region. We believe that the use of domestic pollen extracts instead of imported pollen extracts will contribute to the diagnosis and treatment of allergic diseases as well as to the country's economy.

References

- Sapan N. Polenlerin alerjik hastalıklardaki önemi. Türkiye Klinikleri J Allergy-Special Topics 2011; 4(1): 1-4.
- Peebles RS, Church M and Durham SR. Principles of allergy diagnosis. Holgate S, Church M, Broide D, and Martinez F, ed. Allergy. 4th Ed. Elsevier 2012;129
- Behrendt H, Becker WF. Localization, release and bioavailability of pollen allergens: The influence of environmental factors. Current Opinion in Immunology 2001;13:709-15.
- Bıçakçı, A., & Tosunoğlu, A. (2017). The Influence of Environmental and Atmospheric Variables on Allergenic Pollen. Asthma Allergy Immunology, 14(3), 107-116.
- Spieksma, F.T.M., 1991, Regional European pollen calendars. In: D'Amato G, Spieksma, F.T.M, Bonini S editors, Allergenic pollen and pollinosis in Europe. Oxford: Blackwell Sci. Publ., 49–65.
- Ventura, M.T, Gelardi, M., Di Gioia, R., Buquicchio, R., Accettura, G., Tummolo, R. A. and et al., 2007, Statistical evaluation and parameters of phlogosis in patients sensitized to cypress, Journal of biological regulators and homeostatic agents, 21:41-8.
- Movérare, R., Everberg, H., Carlsson, R., Holtz, A., Thunberg, R., Olsson, P., ... & Högbom, E. (2008). Purification and characterization of the major oak pollen allergen Que a 1 for component-resolved diagnostics using ImmunoCAP®. International archives of allergy and immunology, 146(3), 203-211.
- Aytuğ B, Peremeci E. (1987). Pollen grains; pollinosis and pollen extracts. Journal of Faculty of Medicine I.U, 50, 163-170.

Wodehouse R.P. (1935). Pollen Grains. New York: McGraw-Hill.

Author Information

Gulay KASOGLU

Gaziantep University
Department of Biology 27310, Gaziantep, Türkiye
Contact e-mail: glykasoglu@gmail.com

Ibrahim Halil KILIC

Gaziantep University
Department of Biology 27310, Gaziantep, Türkiye

Mehmet OZASLAN

Gaziantep University
Department of Biology 27310, Gaziantep, Türkiye

Isik Didem KARAGOZ

Gaziantep University
Department of Biology 27310, Gaziantep, Türkiye

Molecular Characterization of Yogurt Bacteria Isolated from Beans and Lentils

Mesut CAY

Gaziantep University

Ibrahim Halil KILIC

Gaziantep University

Isik Didem KARAGOZ

Gaziantep University

Zeynep KOLOREN

Gaziantep University

Bekir Siddik KURT

Gaziantep University

Sami Serhat TONUS

Gaziantep University

Mehmet OZASLAN

Gaziantep University

Abstract: As yogurt and similar fermented dairy products have proved positive effects on human nutrition and health, its production and consumption are rapidly increasing all over the world. However, efforts continues to improve the production and quality of yogurt with various properties using new techniques. In Turkey production of yogurt form fermented milk is carried out using starter cultures imported from abroad. Lentil and bean were inoculated into milk without UHT to obtain a first culture. Yogurt production was carried out using milk without UHT in the first culture. Fresh pure culture was obtained from the produced yogurt and DNA's were isolated and stored. Molecular characterization was performed using 16s rRNA sequence analysis by next-generation sequencing and MALDI-TOF methods. In this study, we investigated whether or not the obtained bacteria are good candidates to be yogurt starter cultures. This study is a preliminary study for the researchers who will work in this field and will shed light to the scientific community.

Keywords: Lentil, Beans, Yogurt

Introduction

Nowadays yogurt made with various flavors and properties has become a valuable food with rapidly increasing consumption in almost every country. As yogurt and similar fermented dairy products have proved positive effects on human nutrition and health, its production and consumption are rapidly increasing all over the world. However, efforts continues to improve the production and quality of yogurt with various properties using new techniques (İşleten, 2006) In the Turkish Food Codex Communiqué on fermented milk products, yogurt is defined as the fermented dairy product in which the symbiotic cultures of *Streptococcus thermophilus* and *Lactobacillus delbrueckii* subsp. *bulgaricus* are generally used during fermentation process. Naturally, many different techniques are widely used for the production of yogurt from milk using lactic acid bacteria. The aim of this study was to identify the microorganisms isolated from beans (*Phaseolus vulgaris*) and lentil (*Lens*

- This is an Open Access article distributed under the terms of the Creative Commons Attribution-Noncommercial 4.0 Unported License, permitting all non-commercial use, distribution, and reproduction in any medium, provided the original work is properly cited.

- Selection and peer-review under responsibility of the Organizing Committee of the Conference

culinaris) and used in the production of yogurt using microbiological methods and to obtain preliminary data for industrial use of the identified strains.

Materials and Methods

Species identification of commercial legumes was carried out at the Botany Department of the Faculty of Science and Arts, Gaziantep University. Daily pasteurized milk (without Ultra-High Temperature) supplied from shopping malls was used for the production of yogurt.

Yogurt Production

Commercially available lentils and beans were inoculated into milk without UHT and incubated at 37 ° C for 24 hours. It was designated as the 1st product. The yoghurt was obtained by adding 20gr from the 1st product and inoculating it into 1 litre of milk. Yogurt production scheme is given in Figure 1.1. Produced yoghurts were stored at 4°C. In the 2nd day following storage, the produced yoghurts were diluted and seeded in the medium.

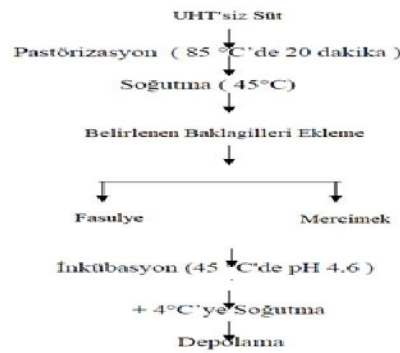


Figure 1.1 Yogurt production flowchart

Microbiological Analyzes of Yoghurt Samples

Under aseptic conditions, the produced yoghurt samples were homogenized by adding 10 g to 90 mL of sterile 0.1% (v/v) dilution solution of Yeast Sucrose Broth (YSB). Homogenization and subsequent dilutions were performed in a ratio of 1: 9. According to Wahr and Frank (2004), the produced yoghurt samples were seeded in MRS Agar and M17 Agar (Lee et al., 1974) (Figure 1.2), and after incubation, gram staining (Figure 1.3) and catalase assays (Table 1.1) were performed.

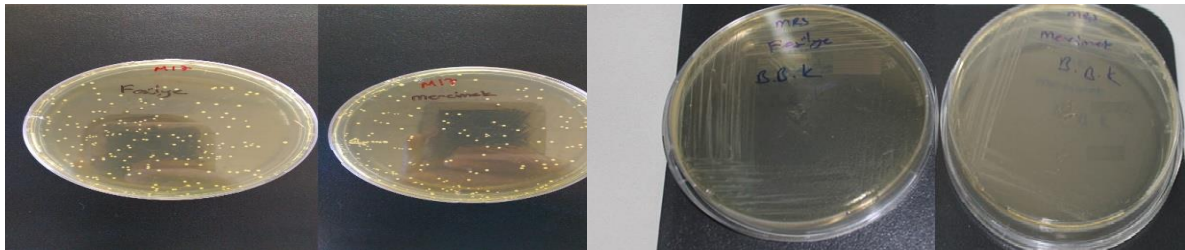


Figure 1.2 Development of microorganisms

Four isolates were isolated from the culture media and observed under microscope. These were short or long rod (Lactobacillus) or round or elliptical (Streptococcus) shaped and were gram-positive (+) when stained with gram stain. Two of the four isolates were of coccus morphology whereas the other two were of basillus morphology. All four isolates were gram positive.

MALDI-TOF Method

Morphological identification of the isolated bacteria was performed using Gram staining, catalase test and microscopic 100x oil immersion objective lense. Identification of the isolated bacteria using MALDI-TOF MS method was carried out in the Central Research Institute of Food and Feed Control Directorate,Bursa,Turkey.

Molecular Characterization of Lactic Acid Bacteria by 16S rRNA Method

Molecular identification of the four isolates isolated from the produced yogurts was confirmed by repeating the 16S rRNA gene sequence analysis method (Sanger et al., 1977) twice in Sentegen,Ankara.

Results

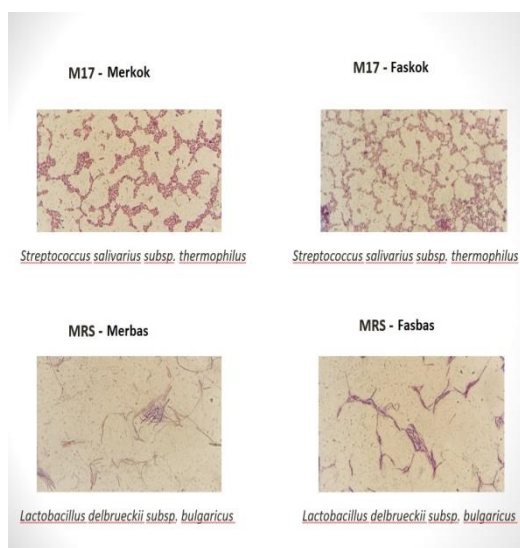


Figure 1.3 Gram staining results

Table 1.1 Catalase test results

Bacteria (M17)	Catalase test results
Merkok (Coccus-shaped bacteria isolated from Lentil)	-
Faskok (Coccus-shaped bacteria isolated from Beans)	-
Bacteria (MRS)	
Merbas (Basillus-shaped bacteria isolated from Lentil)	-
Fasbas (Basillus-shaped bacteria isolated from Beans)	-

Table 1.2 MALDI-TOF results

Number	Isolate code	Morphology/gram staining	MALDI-TOF MS identification results
1	Merkok (Coccus-shaped bacteria isolated from Lentil)	Coccus (+)	<i>Streptococcus thermophilus</i>
2	Faskok (Coccus-shaped bacteria isolated from Beans)	Coccus (+)	<i>Streptococcus thermophilus</i>
4	Merbas (Basillus-shaped bacteria isolated from Lentil)	Basillus (+)	<i>Lactobacillus delbrueckii</i>
5	Fasbas (Basillus-shaped bacteria isolated from Beans)	Basillus (+)	<i>Streptococcus mitis/oralis</i>

Table 1.3 16S rRNA sequence analysis results.

Number	Isolate code	Morphology/gram staining	16s rRNA identification results
1	Merkok (Coccus-shaped bacteria isolated from Lentil)	Coccus (+)	Streptococcus salivarius subsp. thermophilus
2	Faskok (Coccus-shaped bacteria isolated from Beans)	Coccus (+)	Streptococcus salivarius subsp. thermophilus
4	Merbas (Basillus-shaped bacteria isolated from Lentil)	Basillus (+)	Lactobacillus delbrueckii subsp. bulgaricus
5	Fasbas (Basillus-shaped bacteria isolated from Beans)	Basillus (+)	Lactobacillus delbrueckii subsp. bulgaricus

Discussion and Conclusion

Nowdays, the dairy industry is making great efforts to develop new production technologies and active marketing strategies that will add new flavors and improve health benefits of yogurt to meet consumer expectations and to increase the per capita milk consumption. Using standard yogurt culture; we aimed to improve physical, chemical, microbiological and sensory properties of yogurt and to introduce good candidates to be yogurt starter cultures. Taken together our results in general, through fermenting milk without UHT using two different legumes first yeast was obtained then yogurt was produced. All samples were gram positive (+) when stained with gram. It was observed that the colonies that were grown on M17 media were of coccus morphology while those grown on MRS media were of bacillus morphology. According to the results of identification by MALDI-TOF, Merkok- and Faskok-denoted isolates were identified as *Streptococcus salivarius* subsp. *thermophilus* whereas Merbas-denoted isolate was identified as *Lactobacillus delbrueckii* subsp. *bulgaricus* and Fasbas-denoted isolate was identified as *Streptococcus mitis/oralis*. According to the results of molecular identification using 16S rRNA gene sequence analysis Merkok- and Faskok-denoted isolates were identified as *Streptococcus salivarius* subsp. *thermophilus*, whereas Merbas- and Fasbas-denoted isolates were identified as *Lactobacillus delbrueckii* subsp. *bulgaricus*. In our study, we attempted to make robust characterization using 16S rRNA gene sequence analysis. In this study; Merkok- and Faskok-denoted isolates were similar strains whereas Fasbas-denoted isolate was identified as different strain. However, 16s rRNA gene sequence analysis has identified this strain as *Lactobacillus delbrueckii*. The contribution of these strains to the process of yogurt production may be a potential source of data for future studies. The newly identified strains will definitely make a positive contribution to the production of yogurt under controlled conditions and to the industrial use of strains. The results obtained in our study will constitute a database for researchers working with lactic acid bacteria and therefore the effort and time spent in the identification process will be spared.

References

- İşleten, M., 2006. Süt kaynaklı toz bileşenlerin yağsız yoğurdun kalite kriterleri üzerine etkisi. Çanakkale Onsekiz Mart Üniversitesi, Fen Bilimleri Enstitüsü, Gıda Mühendisliği Anabilim Dalı, Yüksek Lisans Tezi, Çanakkale
- Lee, S.Y., Vedamuthu, E.R. and Waham, C.J. 1974. An agar medium for the differential enumeration of yogurt starter bacteria. *J. of Milk, Food Tech.*, Vol. **37** (5); pp. 272-276.
- Sanger, F., Nicklen, S. and Coulson, A.R. 1977. DNA Sequencing with chainterminating inhibitors. *PNAS* 74(12), 5463-5467.
- Wahr, M.H. and Frank, J.F. 2004. *Lactic Acid Bacteria, Standart methods for the examination of dairy products* 17th Edition, NW, pp. 235-247, Washington.

Author Information

Mesut Cay

Gaziantep University
Department of Biology 27310, Gaziantep, Türkiye

Ibrahim Halil Kilic

Gaziantep University
Department of Biology 27310, Gaziantep, Türkiye
Contact e-mail: kilic@gantep.edu.tr

Mehmet Ozaslan

Gaziantep University
Department of Biology 27310, Gaziantep, Türkiye

Isik Didem Karagoz

Gaziantep University
Department of Biology 27310, Gaziantep, Türkiye

Zeynep Koloren

Gaziantep University
Department of Biology 27310, Gaziantep, Türkiye

Bekir Siddik Kurt

Gaziantep University
Department of Biology 27310, Gaziantep, Türkiye

Sami Serhat Tonus

Gaziantep University
Department of Biology 27310, Gaziantep, Türkiye

Manifestation of Ankylosing Spondylitis and Crohn`s Disease

Olena SULIMA

Dnipro City Hospital, Dnipropetrovsk, Ukraine

Volodymyr SULLYMA

SO "Dnipropetrovsk Medical Academy Ministry Health of Ukraine"

Abstract: Regional or granulomatous ileitis is a chronic bowel disease (Crohn's disease) that covers all the layers of the intestinal wall (transmural lesions), and sometimes spreads to the mesentery, regional lymph nodes affecting both the small and large intestines, but most often localized in the terminal section of a thin guts (regional, terminal ileitis). These diseases can be accompanied by damage to the peripheral joints, spine, or joints and spine. The clinical manifestations of the joint syndrome in both processes are the same. The pathogenesis of the intestinal process and joint damage has not been fully established, but it is believed that many mechanisms participate in it, and in particular, toxic, immune, autoimmune. In the blood of patients, antibodies to the cells of the intestinal mucosa, lymphocytotoxin antibodies, circulating immune complexes, in which, possibly, antigenic components of intestinal microbes, etc., are also present. In Crohn's disease, articular manifestations usually occur in childhood and adolescence. The development of peripheral arthritis in these diseases is usually not associated with the carriage of the histocompatibility antigen B27. Ankylosing spondylitis is more common in men than in women (3: 1). This disease usually develops in people who have HLA B27. Articular changes with regional ileitis occur more often in patients with other extraintestinal manifestations of the processes - with ulcers of the oral mucosa, exacerbate erythema nodosum, gangrenous pyoderma.

Keywords: Ankylosing spondylitis, Crohn's disease, Manifestation

Introduction

Regional or granulomatous ileitis is a chronic bowel disease (Crohn's disease) that covers all the layers of the intestinal wall (transmural lesions), and sometimes spreads to the mesentery, regional lymph nodes affecting both the small and large intestines, but most often localized in the terminal section of a thin guts (regional, terminal ileitis).

These diseases can be accompanied by damage to the peripheral joints, spine, or joints and spine. The clinical manifestations of the joint syndrome in both processes are the same. It is important to note that the course of ankylosing spondylitis (AS) varies greatly from person to person. So too can the onset of symptoms. Although symptoms usually start to appear in late adolescence or early adulthood (ages 17 to 45), symptoms can occur in children or much later in life.

The most common early symptoms of AS are frequent pain and stiffness in the lower back and buttocks, which comes on gradually over the course of a few weeks or months. At first, discomfort may only be felt on one side, or alternate sides. The pain is usually dull and diffuse, rather than localized. This pain and stiffness is usually worse in the mornings and during the night, but may be improved by a warm shower or light exercise. Also, in the early stages of AS, there may be mild fever, loss of appetite, and general discomfort. It is important to note that back pain from AS is inflammatory in nature and not mechanical. The pain typically becomes persistent (chronic) and is felt on both sides, usually lasting for at least three months. Over the course of months or years,

the stiffness and pain can spread up the spine and into the neck. Pain and tenderness spreading to the ribs, shoulder blades, hips, thighs, and heels is possible as well.

Note that AS can present differently at onset in some people. This tends to be the case in women more than men. Quoting Dr. Elaine Adams, "Women often present in a little more atypical fashion so it's even harder to make the diagnosis in women." For example, we have heard anecdotally from some women with AS that their symptoms started in the neck rather than in the lower back.

Varying levels of fatigue may also result from the inflammation caused by AS. The body must expend energy to deal with the inflammation, thus causing fatigue. Also, mild to moderate anemia, which may also result from the inflammation, can contribute to an overall feeling of tiredness.

Chronic inflammatory arthritis, a hallmark of several inflammatory rheumatic diseases, and inflammatory bowel disease are both life-long conditions, with substantial morbidity and even mortality. These diseases are highly prevalent—for example, chronic arthritis has a frequency of approximately 2%–3% within a given population. Interestingly, the co-existence of gut and joint inflammation was found to be prominent in spondyloarthritis, a family of interrelated rheumatologic diseases. Number of typical clinical and genetic characteristics, including peripheral arthritis (particularly of lower limb joints) as well as inflammation of the axial skeleton (e.g., spine). Moreover, different forms of may also affect other organs, such as the skin (psoriasis) or the eye (anterior uveitis), demonstrating the systemic nature of these diseases. Various subtypes have been described based upon clinical features, but any two may share important characteristics. The prototypical disorder of the family is ankylosing spondylitis (AS), which is characterized by prominent inflammation of the axial skeleton (spine, sacroiliac joints), although other joints may also be affected. Other diseases include infection-triggered reactive arthritis, some forms of juvenile idiopathic arthritis, arthritis in association with inflammatory bowel diseases (IBD), and some forms of psoriatic arthritis

Method

The pathogenesis of the intestinal process and joint damage has not been fully established, but it is believed that many mechanisms participate in it, and in particular, toxic, immune, autoimmune. In the blood of patients, antibodies to the cells of the intestinal mucosa, lymphocytotoxin antibodies, circulate immune complexes, in which, possibly, antigenic components of intestinal microbes, etc., are also present.

A recent study found a strong association between increased levels of an inflammatory marker in the gut and the subsequent development of Crohn's disease in those with existing ankylosing spondylitis.

Patients participating in the study were asked to provide stool and blood samples, as well as to complete a questionnaire at the beginning of the study, (to establish their baseline scores) and once again five years later at the follow up visit. Of the patients with ankylosing spondylitis initially enrolled in the study, 80% completed the study by returning for the follow up examination.

Researchers found that an elevated level of gut inflammation at the start of the study – as evidenced by increased levels of a protein called calprotectin in the stool – was a strong predictor of the development of Crohn's disease within five years.

The striking relationship between IBD and AS has been recognized for many years: up to 10% of IBD patients develop AS, and, vice versa, IBD commonly develops in patients primarily diagnosed with AS. As both have an important underlying genetic heritability, it has been suggested that the two diseases could have an overlapping set of predisposing genes. Strong evidence for this idea has been derived from the Icelandic genealogy database: it was shown that AS and IBD have a strong elevated cross-risk ratio in first- and second-degree relatives. However, the precise nature of the predisposing genes remained unknown for some time.

Results and Discussion

In Crohn's disease, articular manifestations usually occur in childhood and adolescence. The development of peripheral arthritis in these diseases is usually not associated with the carriage of the histocompatibility antigen B27. Ankylosing spondylitis is more common in men than in women (3: 1). This disease usually develops in people who have HLA B27. One particularly interesting aspect of the paper is the elucidation of a strong association with genes implicated in the Th17 pathway, a lymphocyte subset that has gathered much attention lately because of its prominent role in a variety of immune-mediated inflammatory disorders, including psoriasis

and CD. While the association of AS with the receptor for IL-23, which is implicated in the expansion and survival of Th17 cells, has been previously reported, Danoy and co-workers provide two additional links to the Th17 pathway. Firstly, they report a clear association with STAT-3, which is, amongst other things, implicated in IL-23R signal transduction. In addition, an association with the p40 subunit shared between IL-12 and IL-23 was revealed. It is intriguing that so many genes predispose to AS. The functional significance of these associations is, however, presently unclear. For example, some of the IL-23R single nucleotide polymorphisms associated with AS may confer either protection or susceptibility to the disease. Nevertheless, more than 30 years after the discovery of HLA-B27 as a strong heritability factor for AS, further evidence points to an important genetic susceptibility for adaptive immunity shared with CD.

Conclusion

Articular changes with regional ileitis occur more often in patients with other extraintestinal manifestations of the processes - with ulcers of the oral mucosa, exacerbate erythema nodosum, gangrenous pyoderma. However, one important limitation of the new study is the potential bias caused by subclinical bowel inflammation. Approximately two-thirds of patients suffering from AS, have microscopic signs of gut inflammation without any accompanying clinical gastrointestinal symptoms. In fact, mucosal alterations are one of the first signs of ongoing inflammation. Histologically, the gut inflammation can be divided into acute (mimicking a short-term and self-limiting bacterial enterocolitis) and chronic types (with altered intestinal architecture, blunted and fused villi, and influx by mononuclear cells), common in enterogenic-triggered reactive arthritis and AS patients, respectively. Furthermore, 10%–15% of these patients eventually develop IBD, particularly CD. This progression to overt CD is a very peculiar feature of the chronic type of inflammation where up to 20% of those that have chronic gut inflammation develop CD.

Thus, it is clear that more studies are needed linking the presence of subclinical gut inflammation in AS to the association of genes. Other items on the research agenda should include the functional significance of the identified gene polymorphisms in shaping the immune response and the potential interaction between the single nucleotide polymorphism of the various genes identified and their impact on clinical manifestation of disease. It is clear that exciting times lie ahead for this area of research.

References

- Braun J, Sieper J. Ankylosing spondylitis. *Lancet*. 2007;369:1379–1390. [PubMed]
- Jacques P, Elewaut D. Joint expedition: linking gut inflammation to arthritis. *Mucosal Immunol*. 2008;1:364–371. [PubMed]
- Mielants H, Veys EM, Cuvelier C, De Vos M, Goemaere S, et al. The evolution of spondyloarthropathies in relation to gut histology. II. Histological aspects. *J Rheumatol*. 1995;22:2273–2278. [PubMed]
- Thjodleifsson B, Geirsson AJ, Bjornsson S, Bjarnason I. A common genetic background for inflammatory bowel disease and ankylosing spondylitis: a genealogic study in Iceland. *Arthritis Rheum*. 2007;56:2633–2639. [PubMed]
- Danoy P, Pryce K, Hadler J, Bradbury LA, Farrar C, et al. Association of variants at 1q32 and STAT3 with ankylosing spondylitis suggests genetic overlap with Crohn's disease. *PLoS Genet*. 2010;6:e1001195. doi: [10.1371/journal.pgen.1001195](https://doi.org/10.1371/journal.pgen.1001195). [PMC free article] [PubMed]
- Barrett JC, Hansoul S, Nicolae DL, Cho JH, Duerr RH, et al. Genome-wide association defines more than 30 distinct susceptibility loci for Crohn's disease. *Nat Genet*. 2008;40:955–962. [PMC free article][PubMed]
- Burton PR, Clayton DG, Cardon LR, Craddock N, Deloukas P, et al. Association scan of 14,500 nonsynonymous SNPs in four diseases identifies autoimmunity variants. *Nat Genet*. 2007;39:1329–1337. [PMC free article] [PubMed]

Author Information

Olena Sulima

Dnipro City Hospital
Dnipropetrovsk, Ukraine
Contact e-mail: Olenasulima2@gmail.com

Volodymyr Sulyma

SO “Dnipropetrovsk Medical Academy Ministry Health of Ukraine”
Vernadskyj Street, 9, Dnipro, 49000, Ukraine

Treatment of Arthritis with Ulcerative Colitis

Olena SULIMA

Dnipro City Hospital, Dnipropetrovsk, Ukraine

Volodymyr SULLYMA

SO "Dnipropetrovsk Medical Academy Ministry Health of Ukraine"

Abstract: Arthritis, or joint inflammation, is the most common complication of ulcerative colitis. Twenty-five percent of people with ulcerative colitis suffer from it, and it is often found in young patients. In addition to joint pain, arthritis also causes swelling and stiffness (stiffness in the joint). With ulcerative colitis, arthritis can manifest itself in two different forms: Peripheral arthritis usually affects large joints of the hands and feet, including elbows, wrists, knees and ankles. Pain can "migrate" from one joint to another and last from a few days to several weeks. The more intense the inflammatory process in the colon, the more pronounced arthritis. To date, there are no special tests to confirm ulcerative colitis-associated arthritis. This diagnosis can be made only by eliminating other causes of pain in the joints. Fortunately, such peripheral arthritis usually does not cause a significant change in the function of the joint. Spondyloarthritis (arthritis of the intervertebral joints) causes pain and stiffness in the lower part of the spine and sacroiliac joints. In young people, these symptoms may appear much earlier than intestinal manifestations. Unlike peripheral arthritis, spondyloarthritis can lead to a significant deterioration in the function of the spine, as the amount of movement in the intervertebral joints decreases. Spondylitis usually appears at the age of about 35-45 years. In most cases, the symptoms of peripheral arthritis decrease with the disappearance of inflammation in the large intestine. After a course of drugs such as prednisolone or sulfasalazine, joint pain usually disappears. The use of Infliximab (Remicade®) for the treatment effectively reduces inflammation and swelling of the joints. Unlike peripheral arthritis, unfortunately, in spondyloarthritis there is no such clear relationship between the disappearance of signs of inflammation in the intestine and the disappearance of joint symptoms. In such patients, non-steroidal anti-inflammatory drugs (NSAIDs) are used to relieve pain and swelling of the joints. However, these drugs should be used under the supervision of a doctor, as they can provoke an exacerbation, since they irritate the intestinal mucosa. To prevent a decrease in the volume of movement in the joints it is very important to engage in exercise therapy.

Keywords: Arthritis, Ulcerative colitis, Treatment

Introduction

Arthritis, or joint inflammation, is the most common complication of ulcerative colitis. Twenty-five percent of people with ulcerative colitis suffer from it, and it is often found in young patients. In addition to joint pain, arthritis also causes swelling and stiffness (stiffness in the joint). With ulcerative colitis, arthritis can manifest itself in two different forms:

Peripheral arthritis usually affects large joints of the hands and feet, including elbows, wrists, knees and ankles. Pain can "migrate" from one joint to another and last from a few days to several weeks. The more intense the inflammatory process in the colon, the more pronounced arthritis. To date, there are no special tests to confirm ulcerative colitis-associated arthritis. This diagnosis can be made only by eliminating other causes of pain in the joints. Fortunately, such peripheral arthritis usually does not cause a significant change in the function of the joint.

Spondyloarthritis (arthritis of the intervertebral joints) causes pain and stiffness in the lower part of the spine and sacroiliac joints. In young people, these symptoms may appear much earlier than intestinal manifestations. Unlike peripheral arthritis, spondyloarthritis can lead to a significant deterioration in the function of the spine, as the amount of movement in the intervertebral joints decreases. Spondylitis usually appears at the age of about 35-45 years.

Introducing biosimilar infliximab for the treatment in rheumatology (rheumatoid arthritis and ankylosing spondylitis) and inflammatory bowel disease (ulcerative colitis) may reduce treatment costs associated with biologics. This study aimed to investigate the budget impact of adopting biosimilar infliximab in five European countries, considering that the budget impact includes the adoption of biosimilar infliximab and the availability of biologic alternatives such as vedolizumab, biosimilar etanercept, biosimilar rituximab, and other relevant factors.

Method

In this study, all adult patients receiving maintenance therapy with innovator infliximab in City Hospital and Department of Medical Academy were systematically switched to biosimilar infliximab. Effectiveness was assessed by the retention rate of biosimilar infliximab at the time of the third infusion. Sensitivity analyses for effectiveness included changes of disease activity parameters and infliximab trough levels between baseline and the last visit as well as the occurrence of adverse events leading to drug discontinuation. Factors associated with biosimilar infliximab discontinuation at the last visit were explored.

In most cases, the symptoms of peripheral arthritis decrease with the disappearance of inflammation in the large intestine. After a course of drugs such as prednisolone or sulfasalazine, joint pain usually disappears. The use of Infliximab (Remicade®) for the treatment effectively reduces inflammation and swelling of the joints. Unlike peripheral arthritis, unfortunately, in spondyloarthritis there is no such clear relationship between the disappearance of signs of inflammation in the intestine and the disappearance of joint symptoms.

An existing budget impact model was adapted to forecast the budget impact in the more countries. Respondents in a Delphi panel, conducted in 2015 and consisting of several leading rheumatologists and gastroenterologists from different nationalities, were asked to forecast uptake of biosimilar infliximab and estimate the proportion of patients eligible for a particular type of biological treatment, including biosimilar infliximab. Scenario analyses assessed the influence of various factors, including price reductions, on the budget.

Results and Discussion

In such patients, non-steroidal anti-inflammatory drugs (NSAIDs) are used to relieve pain and swelling of the joints. However, these drugs should be used under the supervision of a doctor, as they can provoke an exacerbation, since they irritate the intestinal mucosa.

A total of patients fulfilled the inclusion criteria, including rheumatoid arthritis, axial spondyloarthritis and inflammatory bowel diseases. The retention rate was 80% at the time of the third biosimilar infusion. Between baseline and the last visit, 20% patients discontinued biosimilar infliximab, mainly due to experienced inefficacy. No clinical or biological factors were associated with biosimilar discontinuation. No serious adverse events occurred. No change in objective disease activity parameters or infliximab trough levels was detected. Uptake of biosimilar infliximab was particularly expected for naïve patients; switching patients that already received other biologics was not expected much. Market shares after 5 years of biosimilar infliximab were 2% in rheumatology in countries and in gastroenterology ranged from 4% to 30%. Budgets were expected to decrease for rheumatologic diseases. For gastroenterology, budgets were expected to decrease in other countries. Budgets were expected to increase substantially, due to the introduction of vedolizumab in the studied period. Budget was expected to slightly increase for ankylosing spondylitis and ulcerative colitis. Savings in budget were expected in all countries, for all diseases, when larger price discounts on biosimilar infliximab were used.

Conclusion

To prevent a decrease in the volume of movement in the joints it is very important to engage in exercise therapy.

No changes in drug trough levels or objective parameters were observed after the systematic switch to biosimilar infliximab in a real clinical practice setting. Only changes in patient-reported outcomes were observed, suggesting attribution effects rather than pharmacological differences. This study has shown that only when price reductions are large enough (i.e., 50% or more), physicians indicated that they will prescribe biosimilars. Policy makers should ensure substantial price reductions and stimulate physicians to use biosimilar products, to obtain savings in healthcare budgets.

References

- Brodzsky V., Baji P., Balogh O., Péntek M. (2014). Budget impact analysis of biosimilar infliximab (CT-P13) for the treatment of rheumatoid arthritis in six Central and Eastern European countries. *Eur. J. Health Econ.* 15(Suppl. 1), S65–S71. 10.1007/s10198-014-0595-3 [[PMC free article](#)][[PubMed](#)] [[Cross Ref](#)]
- Cooksey R., Husain M. J., Brophy S., Davies H., Rahman M. A., Atkinson M. D., et al. . (2015). The cost of Ankylosing Spondylitis in the UK using linked routine and patient-reported survey data. *PLoS ONE* 10:e0126105. 10.1371/journal.pone.0126105 [[PMC free article](#)] [[PubMed](#)] [[Cross Ref](#)]
- Danese S., Gomollon F. (2013). Governing board and operational board of ECCO. ECCO position statement: the use of biosimilar medicines in the treatment of inflammatory bowel disease (IBD). *J. Crohns. Colitis* 7, 586–589. 10.1016/j.crohns.2013.03.011 [[PubMed](#)] [[Cross Ref](#)]
- Dignass A., Lindsay J. O., Sturm A., Windsor A., Colombel J. F., Allez M., et al. . (2012). Second European evidence-based consensus on the diagnosis and management of ulcerative colitis part 2: current management. *J. Crohns. Colitis* 6, 991–1030. 10.1016/j.crohns.2012.09.002 [[PubMed](#)][[Cross Ref](#)]
- Dörner T., Kay J. (2015). Biosimilars in rheumatology: current perspectives and lessons learnt. *Nat. Rev. Rheumatol.* 11, 713–724. 10.1038/nrrheum.2015.110 [[PubMed](#)] [[Cross Ref](#)]
- Fautrel B., Woronoff-Lemsi M. C., Ethgen M., Fein E., Monnet P., Sibilia J., et al. . (2005). Impact of medical practices on the costs of management of rheumatoid arthritis by anti-TNF α biological therapy in France. *Joint Bone Spine* 72, 550–556. 10.1016/j.jbspin.2004.12.009 [[PubMed](#)][[Cross Ref](#)]

Author Information

Olena Sulima

Dnipro City Hospital
Dnipropetrovsk, Ukraine
Contact e-mail: Olenasulima2@gmail.com

Volodymyr Sulyma

SO “Dnipropetrovsk Medical Academy Ministry Health of Ukraine”
Vernadskyj Street, 9, Dnipro, 49000, Ukraine

Cytotoxic Activity Against Cancer Cells of *Pistacia vera*

Basak SIMTICIOGLU

Gaziantep University

Ahmet CAKIR

Kilis 7 Aralık University

Ibrahim Halil KILIC

Gaziantep University

Mehmet OZASLAN

Gaziantep University

Isik Didem KARAGOZ

Gaziantep University

Abstract: *Pistacia vera* fruit, one of the leading products of today's sweet and snack sector, which has been seen in the history of the kingdom, are able to support daily nutritional needs and treatment of many diseases due to the phenolic and flavonoid content in the literature. Especially the studies on colon cancer and breast cancer are remarkable potential antitumoral activity of pistachio examined. The aim of this study is to examine in more detail the *P. vera* plant, in which we have previously tested the methanol-hexane extracts of the seed and the test and obtained positive results. As well as observing the cytotoxic activities of the plant extracts and active ingredients obtained from different parts on the lung cancer cells. After counting A549 and HUVEC cell lines which replicated in the medium, were added on 96 well plate. Then, different part of plants extract and 2 major active ingredients also added. Then MTT dye was applied and measured spectrophotometrically. *P. vera* extracts and active ingredients which studied cytotoxic activity research were found to be effective in all cell lines in general. Particularly *P. vera*'s remaining after the fruit parts, methanol extract which obtained from waste containing leaf and stem parts and PVK-1 active agent showed selective activity on normal cells and cancer cells, therefore we consider that it has a high therapeutic index. We believe that this plant should be imparted to sciences and health sector with further studies.

Keywords: *Pistacia vera*, Lung cancer, Cytotoxic activity, Phytotherapy

Introduction

Pistacia vera L. (Pistachio) also known as “the king of fruit” is a member of Anacardiaceae family and it grows on the Pistachio tree (Maskan & Karataş, 1999). The production of pistachio, which is the mainland Middle East, is mostly performed in Iran, USA, Turkey and Syria. *P. vera* fruit, one of the leading products in today's sweet and snack industry. It is also used to increase the nutrition, color and taste in the making of pasta, chocolate, baklava, ice cream and meat products (Tous & Ferguson, 1996; Yahia, 2011). For this reason, it is of great commercial importance.

In our country, *P. vera* is produced and consumed especially in the Southeast Anatolia and due to having numerous biological activities it helps to protect (Surh, 2003) and therapy (Kalkanci et al., 2007) a large variety diseases.

Pistachio nut plays an important role in healthy nutrition and reducing the risk of disease due to its rich protein, fat and fatty acids, vitamins, minerals and fiber content. It also contains important phytochemicals that can provide antioxidant support for cardiovascular and autoimmune diseases including carotenoids (β -carotene and lutein), γ -tocopherol and phenolic compounds such as phenolic acids, flavonoids, lignans, anthocyanins and proanthocyanidins (Bolling, Chen, McKay, & Blumberg, 2011).

Pistachio nut has rich content and because of this it is a potent source for therapeutic biological activator. For instance, studies by Sari and colleagues (2012) and Hosseinzadeh and colleagues (2010) have shown to have antioxidant activities of seed, testa, leaf and resin of *P. vera*. Also Halvorsen and colleagues (2006) indicated that *P. vera* is included among the top 50 foods with high antioxidant potential. In addition, studies on the anticancer activity of this plant have come to the forefront in recent years. In a study, phytosterols in pistachio have been reported to prevent the development of prostate cancer (Kashaninejad & Tabil, 2011) It has also been reported that Pistachio is a good source of gamma-tocopherol and may reduce the risk of lung cancer (Anonim, 2009). In the other studies, researches indicated that *P. vera* has been shown to play a therapeutic role on HepG2 hepatoma cell lines, MCF-7 human breast cancer cell line and colon carcinogenesis (Fathalizadeh et al., 2015; Gleis et al., 2017; Seifaddini pour, Farghadani, Namvar, Mohamad, & Abdul Kadir, 2018). (Kashaninejad & Tabil, 2011)

In this study, we investigated that some biological properties of *P. vera*. For this purpose, cytotoxic activities of seven extracts and two major metabolites from *P. vera* were studied by MTT method.

Method

Extracts and Major Metabolites of *P. vera*

We collected the plant samples in Campus of Gaziantep University. Seven extracts from different parts (hull, peduncle, leaf, leaf and peduncle together, seed coat) of *P. vera* by soxhlet apparatus. Then alcohols were removed by evaporation in the rotary evaporator. The extracts obtained were stored at + 4 °C until beginning of the experiment (Fakili, 2010).

In addition, two major metabolites from *P. vera* were isolated by Prof. Dr. Ahmet CAKIR from Kilis 7 Aralık University, Kilis, Turkey. Silica column chromatography was used and chloroform-ethyl acetate as mobile phase for the extraction. After this, obtained fractions were checked by thin layer chromatography (TLC). Their chemical characterizations were confirmed by FTIR, 1H-NMR, 13C-NMR, 1D-NMR and 2D-NMR.

Cell Lines

A549 (non-small cell lung cancer) and HUVEC (Human umbilical vein endothelial cell) cell lines was cultured at complete culture medium (DMEM) (Gibco company USA) as supplemented with 10% fetal bovine serum (FBS), 1% antibiotic solution (100 U/ml penicillin and 100 μ g/ml streptomycin) and then incubated at 37 °C in 5% CO² and humidity of 80% for cells attachment (Jin, Zhang, Kang, Wang, & Zhao, 2010). Prior to the cytotoxic activity study, cells were counted with hemacytometer.

Cytotoxic Activity Assay

Cell growth inhibitory assay was performed by MTT (3–4,5- dimethylthiazol-2,5 biphenyl tetrazolium bromide) method on A549 (non-small cell lung cancer) and HUVEC (Human umbilical vein endothelial cell) cell lines with various concentrations (6,25 –100 μ g/ml) for 48 h (Jin et al., 2010) After counting cell lines which replicated in the DMEM (Dulbecco's Modified Eagle Medium), were added on 96 well plate to be 5×10^3 in each well. Different part of plants extract and 2 major active ingredients also added in 5 different doses (6.25-100 μ g/ml) and then MTT dye was applied. After dissolving the formazan crystals formed, the color intensity was measured with a spectrophotometer at a wavelength of 570 nm. Viability rates of cells were determined using absorbance readings (Berridge, Herst, & Tan, 2005).

Viable cells were calculated by following formula:

$$\text{Viable cells (\%)} = (A_s / A_c) * 100$$

As: Absorbance of extraction sample treated cells
 Ac: Absorbance of control group (max viability)

Statistical Analysis

Data collected for assays and measurements were statistically analyzed as factorial experiments in a completely randomized design with at least three replications.

Results and Discussion

The % viability values obtained by colorimetric measurements of the MTT assay are shown on the graph (Figure1 and Figure 2). According to the graph of survival results of A549 lung cancer cell line (Figure 1), it was observed that leaf methanol, hull methanol extracts and PVK-X major component showed low cytotoxic activity, whereas peduncle methanol extract showed no effect. Peduncle acetone, leaf and peduncle together methanol, hull ethanol and hull ethyl acetate extracts were found to be effective in reducing the viability of cancer cells. In addition, PVK-I major component showed strong cytotoxic activity on the cells and completely killed the cancer cells.

According to % viability graph of HUVEC cell line (Figure 2), leaf methanol and hull ethanol did not show cytotoxic effect, also leaf + peduncle methanol extract and PVK-X compound showed low efficacy. Hull methanol, seed coat methanol and peduncle methanol extracts were reduced cell viability to half. As well as hull ethyl acetate, peduncle acetone extracts and PVK-I showed strong cytotoxic activity.

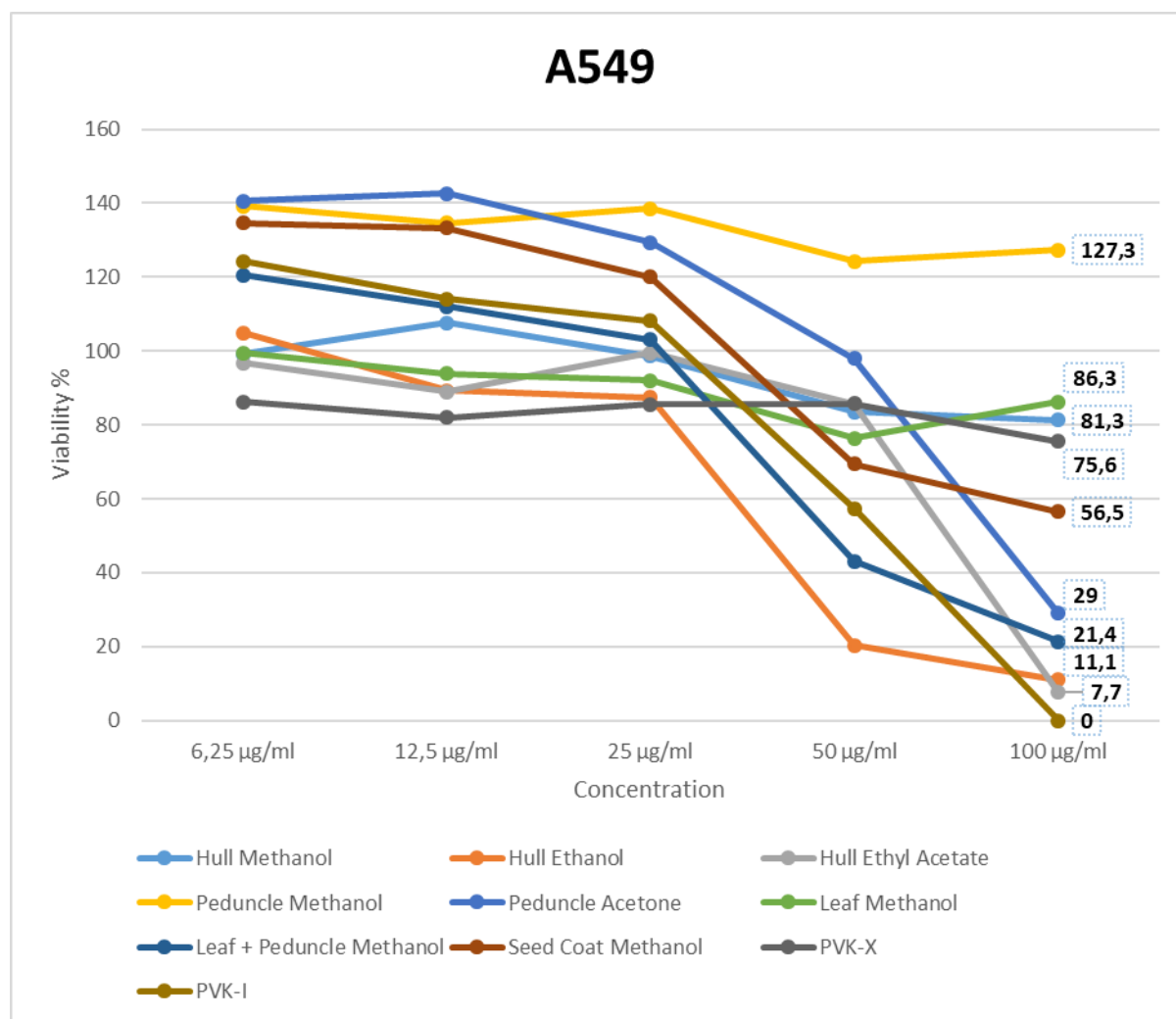


Figure 1. Cell Viability of A549

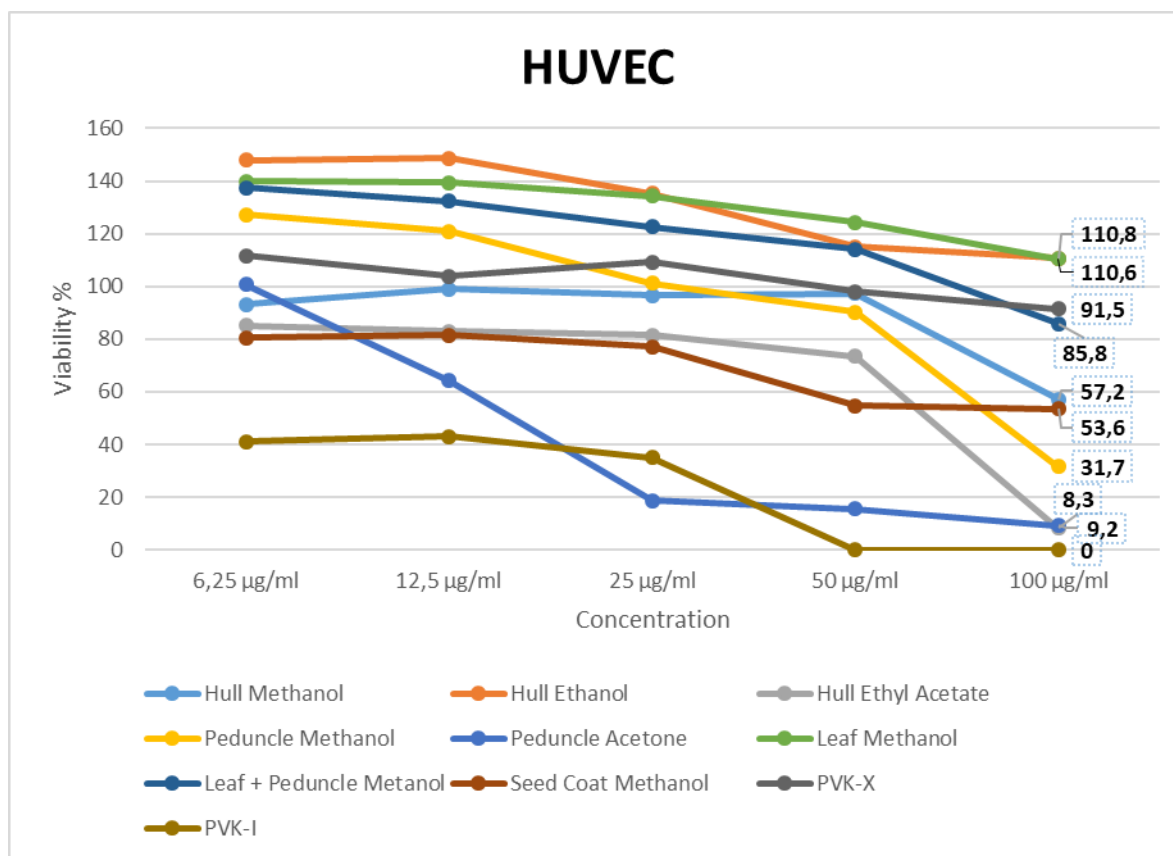


Figure 2. Cell Viability of HUVEC

Conclusion

Particularly, *P. vera*'s remaining after the fruit parts, methanol extracts which obtained from waste containing leaf, peduncle and hull parts showed selective activity on normal and cancer cells. The results of our study are similar to Fathalizadeh et al. (2015), Seifaddinipour et al. (2017) and Gleis et al. (2018)'s received. It also confirms the Anonim's hypothesis (Anonim, 2009).

Therefore, we consider that it has a high therapeutic index. In the direction of the results, we think that *P. vera* plant will contribute to the scientific world by foreground in the pharmacological sense. For this reason, we suggested that *P. vera* plant may be potential therapeutic herbaceous plant and it would be useful for the scientific world to evaluate it in with more detailed studies.

References

- Anonim. (2009). American Association for Cancer Research. "Pistachios may reduce lung cancer risk." *ScienceDaily*
- Berridge, M. V., Herst, P. M., & Tan, A. S. (2005). Tetrazolium dyes as tools in cell biology: New insights into their cellular reduction. In *Biotechnology annual review* (Vol. 11, pp. 127–152). [https://doi.org/10.1016/S1387-2656\(05\)11004-7](https://doi.org/10.1016/S1387-2656(05)11004-7)
- Bolling, B. W., Chen, C.-Y. O., McKay, D. L., & Blumberg, J. B. (2011). Tree nut phytochemicals: composition, antioxidant capacity, bioactivity, impact factors. A systematic review of almonds, Brazils, cashews, hazelnuts, macadamias, pecans, pine nuts, pistachios and walnuts. *Nutrition Research Reviews*, 24(02), 244–275. <https://doi.org/10.1017/S095442241100014X>
- Fakili, O. (2010). Türkiye'de Kekik Adı ile Anılan Bitkiler Konusunda Yapılan Çalışmaların Envanteri. Retrieved from <http://traglor.cu.edu.tr/objects/objectFile/2x5rCuOF-3082013-55.pdf>
- Fathalizadeh, J., Bagheri, V., Khorramdelazad, H., Kazemi Arababadi, M., Jafarzadeh, A., Mirzaei, M. R., ... Hajizadeh, M. R. (2015). Induction of apoptosis by pistachio (*Pistacia vera* L.) hull extract and its molecular mechanisms of action in human hepatoma cell line HepG2. *Cellular and Molecular Biology*

- (Noisy-Le-Grand, France), 61(7), 128–134. Retrieved from <http://www.ncbi.nlm.nih.gov/pubmed/26638894>
- Glei, M., Ludwig, D., Lamberty, J., Fischer, S., Lorkowski, S., & Schlörmann, W. (2017). Chemopreventive Potential of Raw and Roasted Pistachios Regarding Colon Carcinogenesis. *Nutrients*, 9(12), 1368. <https://doi.org/10.3390/nu9121368>
- Halvorsen, B. L., Carlsen, M. H., Phillips, K. M., Bøhn, S. K., Holte, K., Jacobs, D. R., & Blomhoff, R. (2006). Content of redox-active compounds (ie, antioxidants) in foods consumed in the United States. *The American Journal of Clinical Nutrition*, 84(1), 95–135. <https://doi.org/10.1093/ajcn/84.1.95>
- Hosseinzadeh, H., Abolghasem, S., Tabassi, S., Moghadam, N. M., Rashedinia, M., & Mehri, S. (2012). Antioxidant Activity of Pistacia vera Fruits, Leaves and Gum Extracts. *Health Services Iranian Journal of Pharmaceutical Research*, 11(3), 879–887. Retrieved from <https://www.ncbi.nlm.nih.gov/pmc/articles/PMC3813125/pdf/ijpr-11-879.pdf>
- Jin, S., Zhang, Q. Y., Kang, X. M., Wang, J. X., & Zhao, W. H. (2010). Daidzein induces MCF-7 breast cancer cell apoptosis via the mitochondrial pathway. *Annals of Oncology*, 21(2), 263–268. <https://doi.org/10.1093/annonc/mdp499>
- Kalkanci, N., Bagci, C., Davutoglu, V., Yaman, A., Tarakcioglu, M., & Aksoy, M. (2007). *Antepfistiğının Kan Kolesterol Seviyesi Üzerine Etkileri*. Tarım ve Köyişleri Bakanlığı. Retrieved from https://arastirma.tarim.gov.tr/afistik/Belgeler/Taranan_yayinlar/antepfistiğinin_kan_kolesterol_seviyesi_uzerine_etkileri_001.pdf
- Kashaninejad, M., & Tabil, L. G. (2011). Effect of microwave–chemical pre-treatment on compression characteristics of biomass grinds. *Biosystems Engineering*, 108(1), 36–45. <https://doi.org/10.1016/J.BIOSYSTEMSENG.2010.10.008>
- Maskan, M., & Karataş, Ş. (1999). Storage stability of whole-split pistachio nuts (*Pistachia vera* L.) at various conditions. *Food Chemistry*, 66(2), 227–233. [https://doi.org/10.1016/S0308-8146\(99\)00055-2](https://doi.org/10.1016/S0308-8146(99)00055-2)
- Sari, I., Baltacı, Y., Bağcı, C., Davutoglu, V., Erel, O., Celik, H., ... Aksoy, M. (2010). Effect of pistachio diet on lipid parameters, endothelial function, inflammation, and oxidative status: A prospective study. *Nutrition*, 26(4), 399–404. <https://doi.org/10.1016/J.NUT.2009.05.023>
- Seifaddini, M., Farghadani, R., Namvar, F., Mohamad, J., & Abdul Kadir, H. (2018). Cytotoxic Effects and Anti-Angiogenesis Potential of Pistachio (*Pistacia vera* L.) Hulls against MCF-7 Human Breast Cancer Cells. *Molecules*, 23(1), 110. <https://doi.org/10.3390/molecules23010110>
- Surh, Y.-J. (2003). Cancer chemoprevention with dietary phytochemicals. *Nature Reviews Cancer*, 3(10), 768–780. <https://doi.org/10.1038/nrc1189>
- Tous, J., & Ferguson, L. (1996). *Mediterranean Fruits*. In: *Progress in new crops*. ASHS Press, Arlington, VA.
- Yahia, E. (2011). *No Title and technology of tropical and subtropical fruits*. Oxford Cambridge Philadelphia New Delhi.

Author Information

Basak Simitcioglu

Gaziantep University
Department of Biology, Faculty of Arts and Sciences,
University of Gaziantep, 27310, Gaziantep, Türkiye
Contact e-mail: basaksimitcioglu@gmail.com

Ahmet Cakir

Kilis 7 Aralık University
Department of Biology, Faculty of Arts and Sciences,
University of Gaziantep, 27310, Gaziantep, Türkiye

Ibrahim Halil Kilic

Gaziantep University
Department of Biology, Faculty of Arts and Sciences,
University of Gaziantep, 27310, Gaziantep, Türkiye

Mehmet Ozaslan

Gaziantep University
Department of Biology, Faculty of Arts and Sciences,
University of Gaziantep, 27310, Gaziantep, Türkiye

Isik Didem Karagoz

Gaziantep University
Department of Biology, Faculty of Arts and Sciences,
University of Gaziantep, 27310, Gaziantep, Türkiye

Determination of Potential Allergenic Proteins and Morphogenic Proteins and Morphology of Linden (*Tilia cordata*), Anatolian oak (*Quercus ithaburensis*) and Birch (*Betula alba*) Pollens in Gaziantep

Ozlem ONMAN
Gaziantep University

Ibrahim Halil KILIC
Gaziantep University

Mehmet OZASLAN
Gaziantep University

Isik Didem KARAGOZ
Gaziantep University

Abstract: Allergic diseases are a major public health problem in the modern societies. Pollens dispersed through wind are one of the major aeroallergens. When they are released to atmosphere in sufficient amount, they can cause the development of diseases such as asthma, rhinitis, rhinoconjunctivitis etc. in allergically hypersensitive individuals. The spreading of pollens are influenced by their amount in the air, their structures, geographic areas and the climate. Therefore, the types of pollens that hypersensitive individuals who live in different regions are exposed to may differ and different allergic reactions may occur in affected individuals. The high amount of allergens in pollens enhance the sensitivity to pollens. Thus the research in region-specific plant species allergenic effects is very important. Pollens of linden (*Tilia cordata*), Anatolian oak (*Quercus ithaburensis*) and birch (*Betula alba*) are important allergen sources in Gaziantep province. Pollen allergens are water soluble, stable proteins or glycoproteins of molecular weight between 5-80 kD. A single pollen type usually contains several different allergens. Pollens from linden (*T. cordata*), Anatolian oak (*Q. ithaburensis*) and birch (*B. alba*) were collected during pollination period and their extracts were prepared. For identification of pollens morphology slides were prepared according to Wodehouse's method and images were taken under light microscope. Total concentrations of potential allergen proteins were determined from prepared pollen extracts using the BCA method. In this study, we aimed to prepare extracts of pollens from linden, Anatolian oak and birch widely grown in wooded areas of Gaziantep University for the study of allergens and their use for diagnosing allergic diseases.

Keywords: Allergic diseases, *Tilia cordata*, *Quercus ithaburensis*, *Betula alba*, Pollen extract

Introduction

Allergic diseases are a major health problem in most modern societies. According to the European allergy report, the seasonal prevalence of allergic rhinitis in Europe is 15% and the prevalence of asthma is 2.5-10%. Repeated exposure of the person to allergens is a precondition for developing allergic symptoms and causing the disease to occur. Sensitive individuals when repeatedly exposed to allergens they develop symptoms of type 1 allergic disease such as flushing, blistering, or eczema, rhinoconjunctivitis, sneezing or airway bronchoconstriction [1]. Biological particles in the air contain fungus spores, bacteria, viruses, algae, other particles of plants and of these the most prevalent component are pollens. These aeroallergens are responsible for the production of specific IgE antibody after allergic sensitization [2, 3]. Some properties show differences

- This is an Open Access article distributed under the terms of the Creative Commons Attribution-NonCommercial 4.0 Unported License, permitting all non-commercial use, distribution, and reproduction in any medium, provided the original work is properly cited.

- Selection and peer-review under responsibility of the Organizing Committee of the Conference

between pollens grains with potent allergenic effect and the other pollen grains such as pollen wall structure, the release and localization of the allergens, and the deposit substances in them [4]. Allergen extracts are biological mixtures containing a combination of different proteins, glycoproteins and polysaccharides, so it is difficult to obtain as pure substances. The use of recombinant allergens as a reference substances for major allergen measurements is required [5]. Most of the recombinant allergens react very well in immunoassays of specific IgE, and purified natural allergens may be a good alternative in this aspect. In some cases, natural allergens may even react much better than their recombinant counterparts. The advantage of natural allergens is that they often exhibit higher immunoreactivity than recombinant allergens produced in bacteria due to the fact that it may be difficult to achieve the proper folding of recombinants in the bacterial expression system. In addition, the natural allergens preparations often consist of different isoforms and isovariants panels bearing different IgE binding epitopes [6].

The pollen extracts obtained in this study were compared to commercial ones. In this study we aimed to compare pollen extracts of *Tilia cordata*, *Quercus ithaburensis* and *Betula alba* which were produced efficiently to commercial allergens used in diagnostic tests of allergic diseases (such as skin prick test, nasal provocation test) and to prepare pollen extracts to be used as an affordable domestic diagnostic tests for allergic diseases.

Method

Pollen samples of *Tilia cordata*, *Quercus ithaburensis*, and *Betula alba* species investigated in this study were collected during the pollination season from the trees grown in Gaziantep province. Species identification was performed by Dr. Hüseyin TEKİN from the Botany Department. Fresh pollens were collected for extraction, morphological identification and allergenic proteins determination purposes. For pollens extraction purpose, fresh pollens were collected at the time immediately after the opening of the stamen containing the pollen sacs. The collected pollens were dried, sieved and then washed thoroughly with acetone to eliminate foreign particles. The washed pollens were covered with aluminum foil to protect them from light. The prepared pollens samples were examined under the light microscope according to Wodehouse method [7], and pollen diameter, exine thickness and aperture diameters were measured. Extraction method described by Aytuğ B. et al. (1996) was performed to extract the active substances from pollens [8]. Then, to determine the total protein concentration in the pollens extracts, the sensitive 'Bicinchoninic Acid (BCA)' assay was used according to the protocol of the commercially available BCA Protein Macro Assay Kit (Serva Electrophoresis GmbH) [9].

Results and Discussion

Microscopic images of pollens obtained from *B.alba* species belonging to Betulaceae family, *T. cordata* species belonging to the Tiliaceae family and *Q. ithaburensis* species belonging to the Fagaceae are shown in Figures 1, 2 and 3. The total protein concentrations of pollens extracts prepared in the study were 1156,7067 µg/mL for *B. alba*, 1259,2826 µg/mL for *T. cordata* and 919,941 µg/mL for *Q. ithaburensis*.

The measurement results of the prepared pollen protein concentrations compared to the commercial pollen extracts (Allergopharma) used in the skin prick test are shown in Table 1. The pollens protein concentrations were 788,44242 µg/mL for *B. alba* species, 757,83781 µg/mL for *Q. insaburensis* species and 815,347 µg/mL for *T. cordata* species.



Figure 1. *Betula alba* pollens. Figure 2. *Quercus insaburensis* pollens. Figure 3. *Tilia cordata* pollens.

Table 1. Comparison between prepared pollen extracts and the commercial allergens

	Measurements	Mean	Standard Deviation	Results µg/ml
<i>B.alba</i> commercial	0,645/0,635/0,678	0,653	0,018373	788,44242
<i>Q.ithaburensis</i> commercial	0,611/0,619/0,637	0,622	0,010873	757,83781
<i>T.cordata</i> commercial	0,655/0,691/0,692	0,679	0,017211	815,34757

Conclusion

Recent studies have shown a significant increase in the number of individuals with allergic diseases caused by aeroallergens [2, 3]. Recombinant or purified natural allergens are crucial in the study of the sensitization patterns required during the selection of pollen vaccine for the specific immunotherapy used in the treatment of allergic diseases. The advantage of natural allergens compared to the recombinant allergens produced in bacteria is that they often exhibit higher immunoreactivity. Moreover, the use of pollens extracts in which natural allergens can be obtained with high purity can be of advantage in allergic diseases diagnostic tests and treatment. The results of the comparisons between the pollen extracts obtained in this study and the commercial allergens could play a key role in the identification of local allergens. We believe that with further detailed studies, domestic pollen extracts can be an alternative to imported commercial kits used in diagnostic tests of allergic diseases (such as skin prick test, nasal provocation test) and will contribute to health sector and science field.

References

- Behrendt, H., & Becker, W. M. (2001). Localization, release and bioavailability of pollen allergens: the influence of environmental factors. *Current opinion in immunology*, 13(6), 709-715.
- Cacciola, R. R., Sarva, M., & Polosa, R. (2002). Adverse respiratory effects and allergic susceptibility in relation to particulate air pollution: flirting with disaster. *Allergy*, 57(4), 281-286.
- D'amato, G. (2002). Environmental urban factors (air pollution and allergens) and the rising trends in allergic respiratory diseases. *Allergy*, 57(s72), 30-33.
- Çelenk, S. (2011). Bazı Polenler Neden Daha Allerjik?. *Turkiye Klinikleri Journal of Immunology Allergy Special Topics*, 4(1), 5-9.
- Heinzerling, L., Mari, A., Bergmann, K. C., Bresciani, M., Burbach, G., Darsow, U. & Bom, A. T. (2013). The skin prick test–European standards. *Clinical and translational allergy*, 3(1), 3.
- Movérare, R., Everberg, H., Carlsson, R., Holtz, A., Thunberg, R., Olsson, P., ... & Högbom, E. (2008). Purification and characterization of the major oak pollen allergen Que a 1 for component-resolved diagnostics using ImmunoCAP®. *International archives of allergy and immunology*, 146(3), 203-211.
- Wodehouse R.P. (1935). Pollen Grains. New York: McGraw-Hill.
- Aytuğ B. 1996. Polen Ekstrelerinin Hazırlanması. Yüksek Lisans Ders Notları.
- Walker J M. 2002. The Protein Protocols Handbook. Second edition. Humana Press.

Author Information

Ozlem Onman

Gaziantep University
Department of Biology, 27310, Gaziantep, Turkey
Contact e-mail: ozlemonman@gmail.com

Ibrahim Halil Kilic

Gaziantep University
Department of Biology, 27310, Gaziantep, Turkey

Mehmet Ozaslan

Gaziantep University
Department of Biology, 27310, Gaziantep, Turkey

Isik Didem Karagoz

Gaziantep University
Department of Biology, 27310, Gaziantep, Turkey

Detection of Eczema DISEASE by using Image Processing

Yasir Salam Abdulghafoor AL-KHAFAJI

University of Baghdad

Shatha K. MUALLAH

University of Baghdad

Muntaha R. IBRAHEEM

University of Baghdad

Abstract: Because very bad weather in Iraq like elevated temperature, Smokes, dust, also increase depopulation to bad environment and increase the number of displaced, diseases have increased significantly including dermatological diseases and the most common types is eczema as a result of bad nutrition, bacteria, soils, bad food, and others factors. Because of all these environmental factors, physiological, chemical factors and others factors, became very necessary to detect skin diseases specially eczema and treated it to avoid aggravation the disease with the help of biomedical engineers, with less cost, and to prevent disease from spreading when at that it will be difficult and take long time to be treated.. So the aim of research is take an image to the infection area then process this image by MATLAB in many ways to obtain an image that can help the doctors in their work to recognize the eczema and the rate of infection and make it easy to improve and safe people life. Three lesioned layers are selected in this study, face layer, hand layer and foot layer, the study showed that the foot layer is more comfortable for detection the eczema in this approach technique.

Keywords: Eczema, MATLAB, Image processing, Skin disease

Introduction

For last decade and until now the skin disease is one of the widely distributed diseases specially the “eczema” and this word means “to boil over,” which is a Greek word. The eczema looks like red, inflamed, itchy patches that occur during flare-ups. This disease comes in three stages mild, moderate, or severe. Its location in the body appears in different places, eczema can be developed on the face of children and babies (especially the cheeks and chin), but any part on the body may be infected by eczema and symptoms may be different from one child to the next [Nedorost and Susan T 2012]. The Eczema is a disease infected the old and the younger people, but it goes away as the child became older, also other conditions are affected in it like environment and the person's health history and it may be appears as a reflexes for infected with other disease. Its symptoms begin as red places, then it will rise in a tiny blisters filling with a clear fluid atop red. When the blisters burst, the reddish skin will weep and ooze. In advanced eczema, which named as a chronic eczema, the blisters are less appearance and less oozing instead the skin will appears more thick, and more elevated, and larger. Eczema always and in the most time is very itchy and its itching is disturbing and very needy for scraping it and itching it, there are many types of eczema. A severe one which named atop dermatitis and the long lasting form which named a chronic eczema.[Oranj.AP et al,2002]

At the same time a person may have more than one type of eczema, or may be one type depending on Triggers and symptoms and treatment, beside that at the patient conditions, and these types we talking about could be either “atopic dermatitis.”, or a chronic eczema. Therefore the importance is started here to

know which type or types that you are infected with, to know how to manage it and take the best medical care.

The Major Features of Eczema are

The basic features and symptoms of eczema in infant Pruritis, Rash and extensors, and flexural in bigger children, the appearance of symptoms depend on the type of eczema its chronically relapsing, and on family history of other atopic disease, Dryness also other common features that may be appear. Facial pallor, Allergic shiners, Pityriasis alba, Ichthyosis vulgaris, Keratosis pilaris, White dermatographism, Conjunctivitis, Keratoconus and cataracts, skin prick test positivity.

There is many types for eczema the best define for eczema is an inflammatory skin reaction to various exogenous and/or endogenous stimuli. Clinical presentation includes itching and severe rash which is appears in redness spots, scaling and papulo vesiculation. This is for general but it comes in steps depending in many features that we talked about before like the patient history, his age immunity the type of skin and many other features. Beside the basic types there are many other sub types: which is named as Eczema / Seborrheic dermatitis, atopic dermatitis, Dyshidrotic eczema , Discoid, nummular eczema / pompholyx, Contact dermatitis ,Varicose eczema , Asteatotic eczema[Agha HM et al,2016]. The specific causes of infected and cause eczema remains unknown, but it is believed that it happened and develop due to an environmental factors and a combination of hereditary (genetic) factors.

If a parent has had the disease eczema or another atopic disease, there children are more likely to develop it. And if both parent have an atopic disease, the chance increase further. The weather and other environmental factors especially the dust and strong sun light are also known to bring out the symptoms of Eczema. The major symptoms include: Irritant, Allergens, Microbes, Hot and cold temperature, Foods, Stress, and Hormones [McAlear et al, 2012]

The Treatments for eczema is treated depending on family physicians, but it is necessary to search for help from a health specialist since there are many causes of eczema and if we see there is no improving in healing.

The good careens for skin are the key if the eczema is mild, so the good care is all it need. If the eczema is from the severe type of eczema, it is definitely need to take medicine for it. So the basic steps for skin care are:

1-Soap and moisturizer. And Short, warm showers. Don't take very hot or very 2-long showers or baths. They can dry out your skin [Torley, D et al,2013].

3-Stress management. And 4-Get a humidifier.

For acute eczema the main treatment where there is significant weeping and oozing always herbal medicine is very perfect treatment in which using dilute solutions of vinegar or tap water and compress the area followed by evaporation. After that placing the infected part of the body in front of fan. As soon as the acute weeping has been shrinking, then treatment by steroid is not harmful and it could be an effective treatment. This treatment may be orally or by an injection (shot) [Kalliomäki, M et al 2010].

The medicines is differ depending on the case and the doctors the medicine used is one of several hormones may be get use and may be they not treat the case and some of these drugs are: Hydrocortisone, Antihistamines, Corticosteroids. The exposal patient to U.V therapy is an effective way. This may help if the skin condition is severe, to prevent eczema should avoid personal care products to allergy: skin contact with allergens such as soap, cosmetic, lotions, perfumes...ect, and Wear gloves when handling skin irritants. Wear cotton clothes control dust mite, maintain a home humidity level at 45-50% and at last avoid trigger foods [Torley, D et al.2013, Kalliomäki, M et al.2010].

Image Processing

Image processing is a software program in which it manipulating the image, and that for making an enhancement on the image and making it clearer and more understanding or to get some important information from it. So it is a type of signal processing when output may be image or characteristics or some image features and input is an image. The method of using image processing is one of the rapidly growing technologies in now days. It is considered a core or a center for research area within engineering and computer science.

Image processing basically includes the following three steps:

Input the image via image acquisition tools, then analyzing, handling and manipulating the image; and the final step is to get the Output which will be image or report based on the image analysis.

One of the best ways for dealing with Image processing can be simply done by using MATLAB software, Image Processing Toolbox in which this program MATLAB provides a global apps of workflow and algorithms for image analysis, processing, visualization, and developed algorithms. MATLAB provides performance of the image segmentation, image enhancement, noise reduction, geometric transformations, image registration, and 3D image processing.

Common image processing workflows can be automated by image Processing Toolbox apps. Segmentation of image data, compartment of image registration techniques and batch-process large data sets. The images, 3D volumes, and videos; adjust contrast; create histograms; and manipulate regions of interest can be explored (ROIs) by visualization functions and apps [F M Candocia.2006].

The best way for dealing with image processing is the manipulating and enhanced the image to achieve an aesthetic standard or supporting the reality. Anyway the translation between the human visual system and digital imaging devices can be definitely defined as a means of image processing. The world in the same manner cannot be perceived by the human visual system as digital detectors, additional noise and bandwidth restrictions are imposed with display devices [Y.L Kang etal.2004]. Because of all this, The development of the mathematical methods and algorithms to analyze and quantify biomedical data and cooperation it with other research for application of information analysis and visualization to biomedical research problems and development of the tools(in both hardware and software) our cooperation can be supported by giving the ability to analyze biomedical data to support the discovery and advancement of biomedical knowledge, these are considered the main goals of the image process technique [K. Wan etal.2004].

Methods and Algorithm

The algorithm consists of steps as shown below:

RGB to gray scale

Gray scale is an image in which the value of each pixel is a single sample, gray scale image are distinct from black and white images., A grayscale digital image is an image in which the value of each pixel is a single sample, that is, it gives only intensity information. The sort of these images, also known as black-and-white, are composed exclusively of shades of gray, changing from black to white , it's a white at the strongest intensity and black at the weakest .

Grayscale images are distinct from one-bit bi-tonal black-and-white images, these images have only two colors, black and white which in the context of computer imaging. In between. Grayscale, Grayscale images have many shades of gray , the result of measuring the intensity of light at each pixel in a single band of the electromagnetic spectrum are often the grayscale images ,and in such cases when only a given frequency is captured they are monochromatic proper. Grayscale images also can be synthesized from a full color image; see the section about converting to grayscale [Houcque.2005].

A (digital) color image is a digital image in which each pixel includes color information. For visually acceptable results, it is important to provide three samples (color channels) for each pixel, in some color space they are interpreted as coordinates. In computer display, The RGB color space is commonly used. In a color image each pixel has three values (or channels) and they measure the chrominance and intensity of light. The brightness information in spectral band is considered the actual information stored in the digital image data [Houcque.2005].

Converting RGB to gray scale

The main reason is that you either want to process the brightness information of an image, for example doing edge detection, or you want to do something with the color information, for example comparing if an object is colored in the same image as on another image. To do that you need to separate the brightness information from the color information, which is mostly done by using an RGB to gray scale. In the latter color spaces it is a lot easier to compare colors than in RGB.

*Therefore the processors prefer the gray scale more than the color space [T. Kumarm and K. Verma.2010].

Image Resizing

Resizing: This step is very important for increasing or decreasing the total number of pixel For standardization size of the image to avoid any error and to facilitate read and show the image in MATLAB. The scaling of images indicates to the resizing of a digital image digital imaging and in computer graphics . In video technology, the up scaling or resolution enhancement is known as the magnification of digital. The image can be scaled with no loss of image quality when an image is made up with scaling. A new image with a higher or lower number of pixels should be produced when scaling a raster graphics image, A visible quality loss is resulted from the decreasing the pixel number (scaling down). From the standpoint of digital signal processing [T. Kumarm and K. Verma.2010].

Image Denoising

When the image has a noise this noise can be considered a random variation of brightness or color information in images, and is usually an aspect of electronic noise. The sensor and circuitry of a scanner or digital camera are considered the main reasons of this noise. Image noise can be also produced in the unavoidable shot noise of an ideal photon detector and in film grain . Image noise adds spurious and extraneous information which is considered an undesirable by-product of image capture [M. Song et al.2010].
Types of image noise

1. Thermal Noise (additive Gaussian noise): Acquisition is considered the main sources of Gaussian noise in digital images e.g. poor illumination and/or high temperature, and/or transmission are considered the main reasons of the sensor noise .
 2. Shot noise (random counts, Poisson noise): A statistical quantum fluctuations, that is, variation in the number of photons sensed at a given exposure level, is considered the main cause of dominant noise in the darker parts of an image from an image sensor . This noise is known as photon shot noise. Shot noise has a root-mean-square value proportional to the square root of the image intensity [M. Song et al.2010].
 3. Salt-and-Pepper (replacement noise): An image containing salt-and-pepper noise will have dark pixels in bright regions and bright pixels in dark regions. This type of noise can be caused by analog-to-digital converter error [A. Gilat.2004].
 4. Anisotropic noise: Orientation in images can produce this type of the noise, Row noise or column noise can be effected on the image sensors to cause this noise [www.mathworks.com, July 2010].
- Image denoising is an important image processing task, the main properties of a good image denoising model is that it will remove noise while preserving edges [Lindsay MacDonald.2006].

Image filtering

Filters are using to remove the noise from the an image, convolution filters is considered a Linear filters , they can be represented using a matrix multiplication including some nonlinear operations such as thresholding and image equalization as is in the median filter[[Lindsay MacDonald.2006].
Image filtering is used to:- 1.Remove noise 2.Sharpen contrast 3.Highlight contours 4.Detect edge and other uses depending on the type of the filter[[Lindsay MacDonald.2006].

Median filter

Median filtering is used to remove the pepper and salts noise from the Images, it can be considered a nonlinear process. It is a very effective to remove the noise while preserving edges. The median filter works by replacing each value with the median value of neighboring pixels through the moving (pixel by pixel) in the entire image, "window" is a pattern of neighbors which slides, pixel by pixel over the entire image. The median value can be computed through the sorting all the pixel values from the window into numerical order, and then the pixel being considered will be replaced by the middle(median)pixel value[[Lindsay MacDonald.2006].

Image Enhancement

Image Enhancement: Is the process of digitally manipulating a stored image using software. The principle of image enhancement techniques is to process an image so that the result is more suitable than the original image.

The aim of image enhancement is to improve the interpretability of information in images for human viewers. Image enhancement techniques can be divided into:
1-spatial domain method which depends on pixels 2-Frequency domain method which depends on the Fourier transform.

Enhancement of (contrast): the contrast factor has the large importance for evaluation of the image equality, the contrast is resulted from the luminance diversity that reflected from two surfaces. Contrast makes an object distinguishable from other object and the background [Alan C.Bovik.2005].

Features extraction

Feature extraction means that the extraction of unique features from the processed lesion images. The complexity of classification problems in processed images can be reduced by this method. The affected area can be distinguished from background through a certain features like geometry and color.

Feature extraction has a very important role to increase the accuracy of the results in biomedical image processing, it is a necessary step to increase the quality of the processed image. However, to improve the quality of image, the image enhancement algorithm can be used to enhance the image, contrast, brightness adjustment [Joseph G etal.2006].

Image Segmentation

Is the process of dividing the image into several segments in order to change the representation image into form that is more meaningful and easy to analyze [M. Dalwadi.etal.2013].

*Steps of Segmentation by using K-means clustering are:-

Step (1): Image read.

Step (2): The image conversion from RGB color space to $L^*a^*b^*$ color space:-The image that we use it contain different color in order to distinguish these colors it is necessary to convert image from color space to $L^*a^*b^*$ space which consists of a luminosity layer L, chromaticity-layer a^* and chromaticity-layer b^* , All of the color information is in the a^* and b^* layers.

Step (3): Classify the colors in $a^* b^*$ space using K-mean clustering:-

Clustering is a method of dividing the data into a number of clusters, it used when the data is without defined groups ,the aim of this algorithm is to find groups in the used data, Then the image will be clustered into 3 clusters by using the Euclidean distance metric.

Step (4): create an array to store the results of the clustering and choose the clustering containing ROI which will be converted to gray scale and then create GLCM

ROI

It means the region of interest which is the region that contains the selected subset of samples within a set of data identified for a particular purpose[Nedorost and Susan T 2012]. In many application areas the concept of a ROI is commonly used. A region of interest (ROI) is a piece of an image in which the filtering process or other operation can be performed on. More than one ROI in a one entire image can be defined. [www.mathworks.com]

GLCM

The graye Level Coocurrence Matrix (GLCM) method is a way in which the second order statistical texture features can be extracted. A GLCM is a matrix in which the number of gray levels and the number of columns and rows are equal, in the image. The matrix element $A(a, b | \Delta c, \Delta d)$ of two pixels with relative frequency, these pixel are separated by a pixel distance $(\Delta c, \Delta d)$, this matrix of a given neighborhood is occurred, one with intensity 'a' and the other with intensity 'b' [P. Mohanaiah etal.2013].

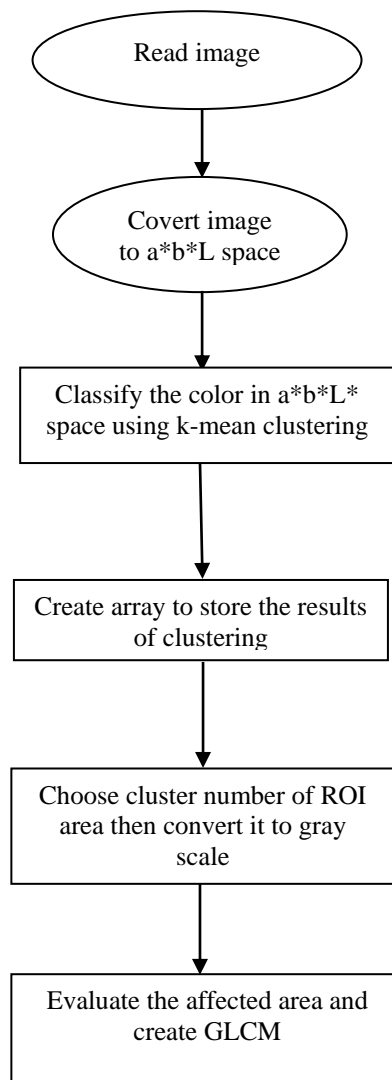


Figure 1. Block diagram of image segmentation

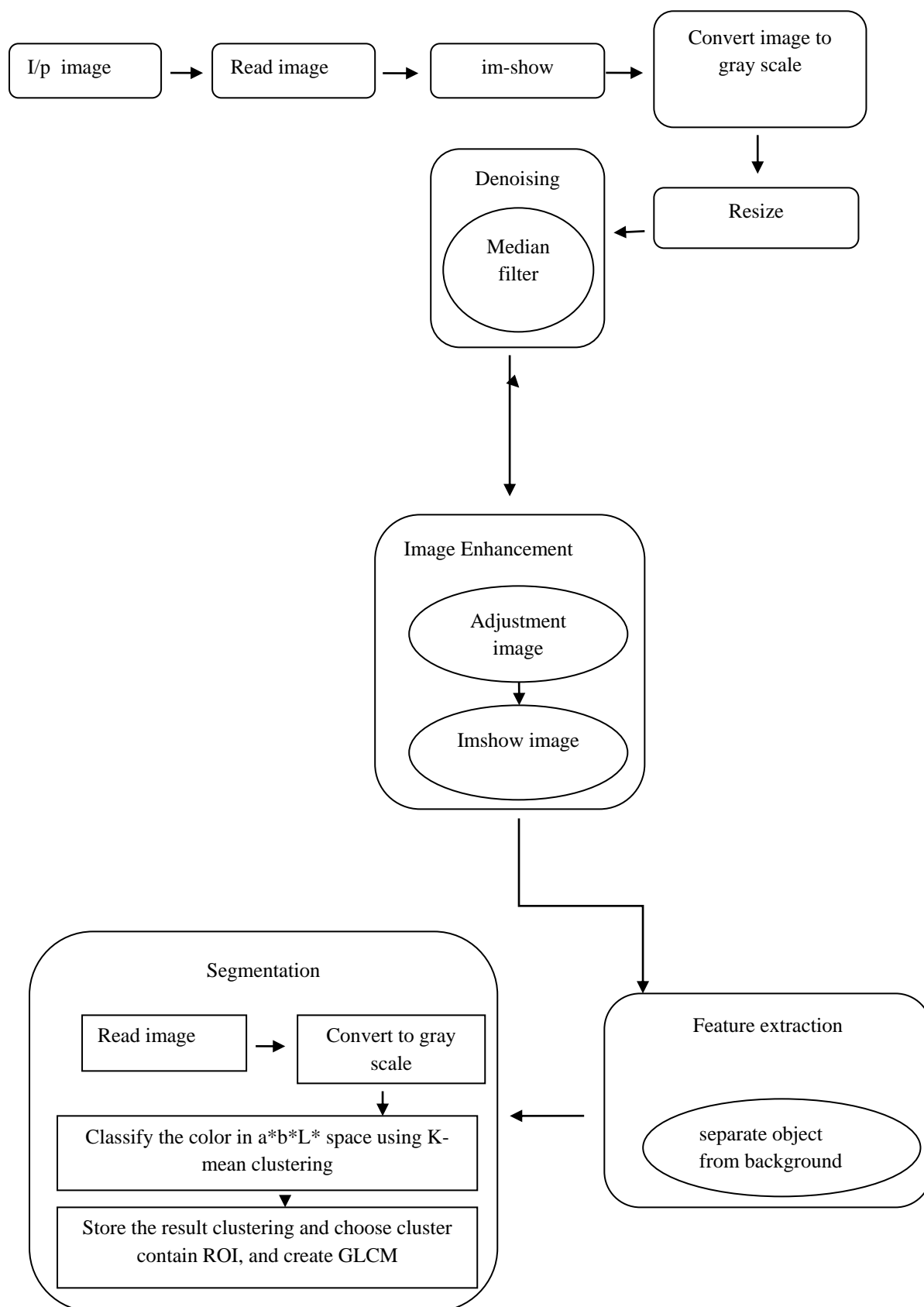


Figure 2. General block diagram of proposed technique

Results and Discussion

Approach technique was applied on three different skin layers, face, hand and foot layers were selected to detect and study the eczema disease on skin of these three different layers from the human body.

Three images of each layer were selected to use in this study, these images were taken from volunteers infected with Eczema, then these images were pre-processed by using image processing technique as shown in general block diagram of approach technique. After image process technique, image segmentation technique was applied on these image data by using K-mean clustering, then the cluster that has the region of interest (ROI) will be selected as shown in fig.1 and figure2.

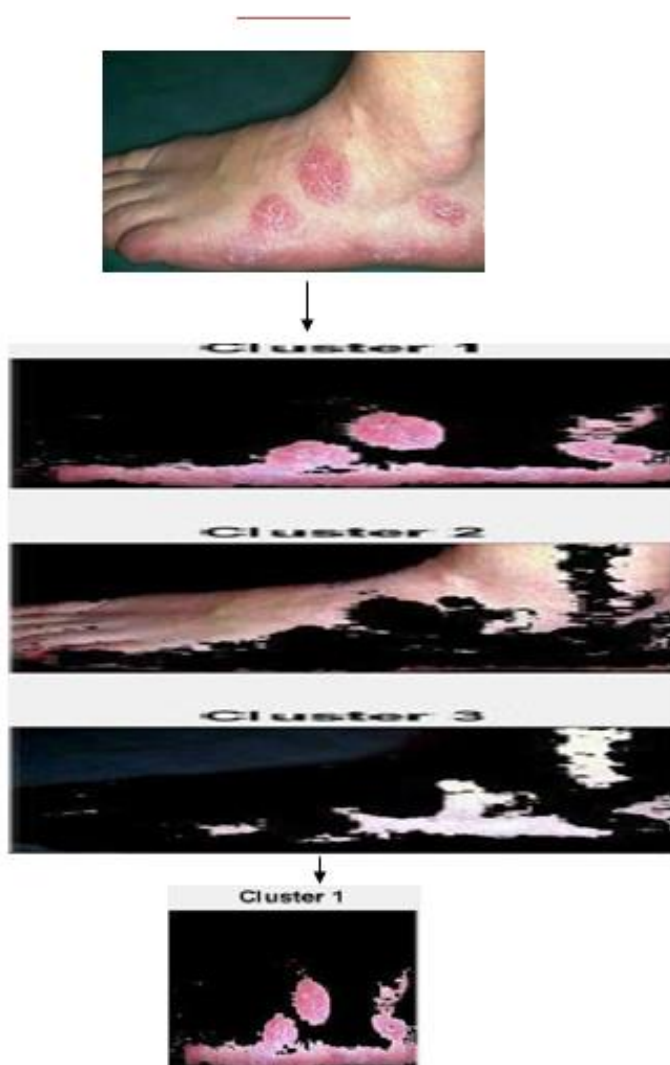


Figure 3. Choosing ROI cluster in the foot layer

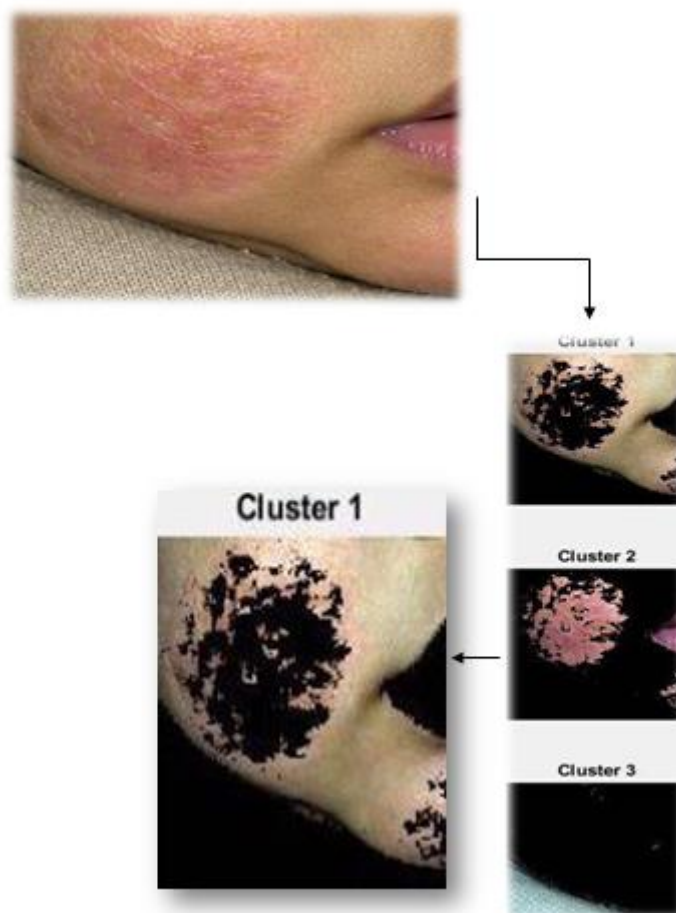


Figure 4. Choosing ROI cluster in the face layer

After choosing ROI cluster, the features of this cluster was extracted and calculated.

The main features extraction were selected to study as following

1. Affectedarea:It is the area of skin that containing the infection.
2. Contrast: is the difference between maximum and minimum pixel intensity in image.
3. Correlation: Refers to a linear shift time invariant relationship between any two neighbor pixels in the image.
4. Energy:Energy is defined based on a normalized histogram of the image. Energy shows how the gray levels are distributed. When the number of gray levels is low then energy is high.
5. Homogeniaty:Measure of similarity or uniformity of gray level with in region in the image.
6. Mean:Represents the average value of set of pixels .
- Standard deviation: Refers to how much variation exists from the mean value.
7. Entropy: Refers to how much information containing in the image
8. Variance: describe the probability distribution by measuring of how far a set of pixels is spreading out from the mean value.
9. Skewness: use to make a judgment in the surface of an image.
10. Kurtosis: It is often considered as a measure of sparsity of the image.

Fig (3, 4) shows the distribution of eczema in skin of face layer of different three persons.

Table-1 shows the results of feature extraction of infected skin in the face layer



Figure 5. Face Image after choosing cluster with ROI



Figure 6. Face Image after choosing cluster with ROI



Figure 7. Face Image after choosing cluster with ROI

Table 1. The results of features extraction of infected skin in the face layer

parameters	Fig(4.5)	Fig(4.6)	Fig(4.7)	Average value
Affected area	46.954	50.4558	54.9714	50.7937
contrast	0.9816	0.7996	0.9942	0.92513
correlation	0.8596	0.9280	0.9085	0.8987
energy	0.2846	0.2514	0.1999	0.2453
homogeneity	0.9288	0.9194	0.8977	0.9153
mean	56.0075	75.2324	83.7614	71.667
std	67.3785	80.9849	80.6263	76.3299
entropy	4.5385	4.8004	5.3139	4.2842
variance	4.1019e+03	5.0718e+03	5.5423e+03	4.905e+03
kurtosis	2.1574	1.6703	1.4004	1.7427
skewness	0.7461	0.4431	0.3697	0.5196

Fig (5,6,7) shows the distribution of eczema in skin of hand layer of different three persons. Table-2 shows the results of feature extraction of infected skin in the hand layer

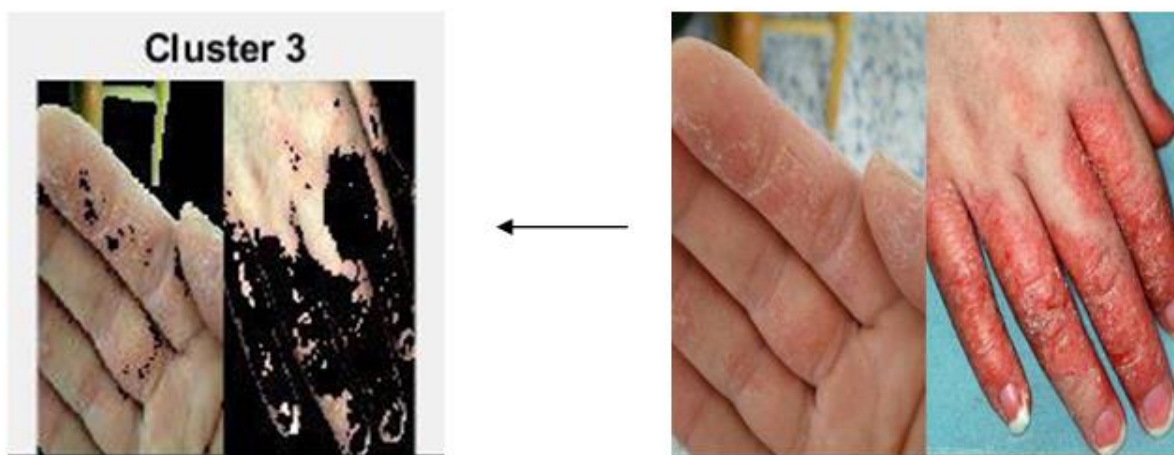


Figure 8. Hand Image infected with eczema

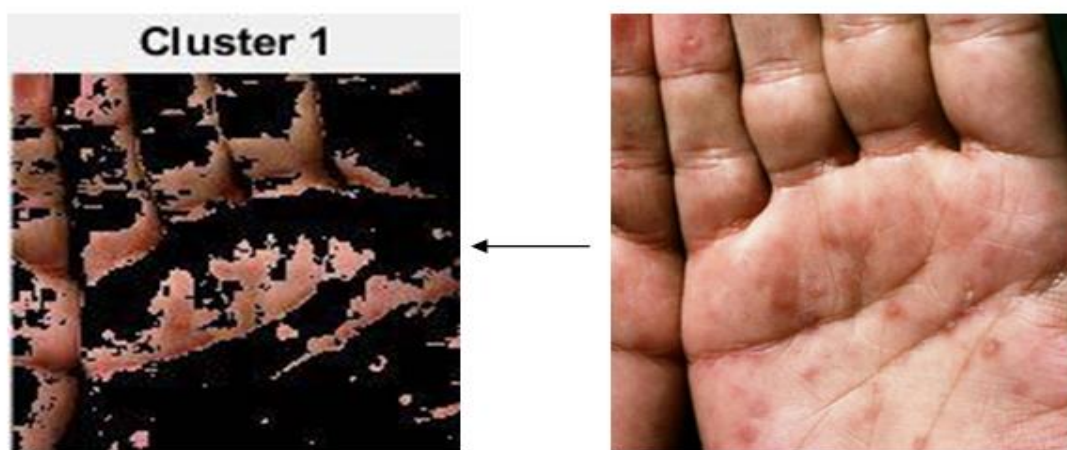


Figure 9. Hand Image infected with eczema

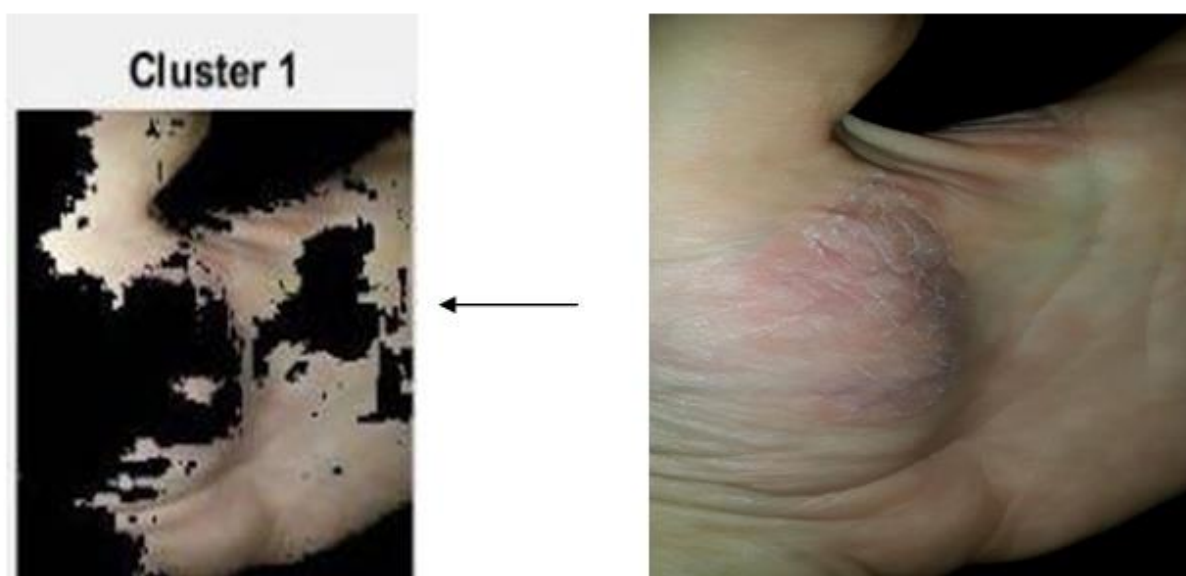


Figure 10. Hand Image infected with eczema

Table 2. Shows the results of feature extraction of infected skin in the hand layer

parameters	Fig.(4.8)	Fig.(4.9)	Fig.(4.10)	Average value
Affected area	64.698	17.5537	43.6859	41.9792
contrast	1.5935	0.8989	0.9932	1.1618
correlation	0.8697	0.8337	0.9235	0.8756
energy	0.1686	0.4307	0.3280	0.3091
homogeniaty	0.8724	0.9316	0.9464	0.9168
mean	11.7704	37.7889	80.8234	43.4609
std	90.3369	61.1987	92.5032	81.346
entropy	5.5609	3.4140	4.3994	4.4581
variance	5.4504e+03	3.2824e+03	7.9760e+03	5.5696e+03
kurtosis	1.3996	3.5058	1.4943	2.133
skewness	-0.1632	1.3592	0.4463	0.5474

Fig (8, 9, and 10) shows the distribution of eczema in skin of hand layer of different three persons.



Figure 11. Foot image after choosing cluster of ROI

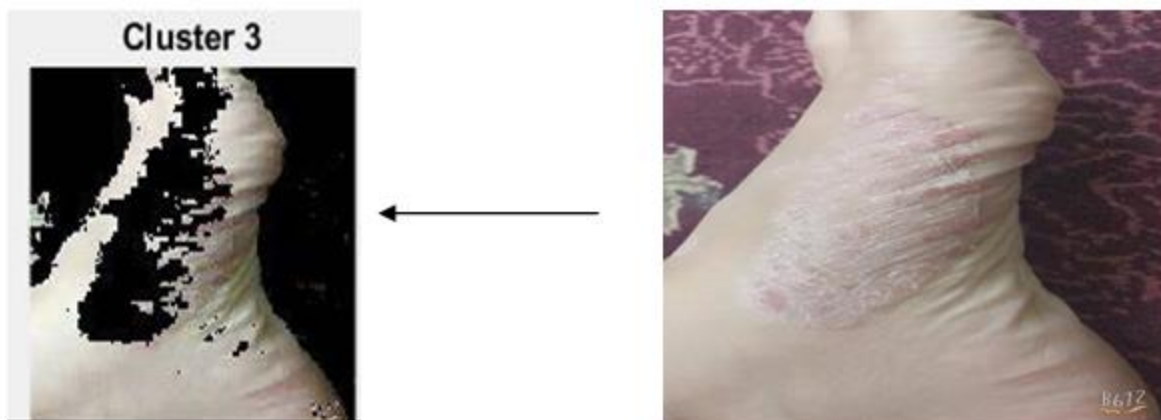


Figure 12. Foot image after choosing cluster of ROI



Figure 13. Foot image after choosing cluster of ROI

Table -3: Shows the results of feature extraction of infected skin in the foot layer

parameters	Fig(4.10)	Fig(4.11)	Fig(4.12)	Average value
Affected area	15.2881	14.653	15.0201	14.987
contrast	0.8342	0.5024	0.6409	0.6591
correlation	0.9412	0.9298	0.9182	0.9297
energy	0.2918	0.4031	0.5972	0.4307
homogeniaty	0.9546	0.9686	0.9550	0.9594
mean	83.3903	44.0921	37.2528	54.9117
std	91.3877	68.5514	73.6490	77.8627
entropy	4.5785	3.8074	2.3735	3.5864
variance	6.7652e+03	4.4708e+03	4.8297e+03	5.3552e+03
kurtosis	1.3870	3.2072	3.9967	2.8637
skewness	0.3603	1.2805	1.6356	1.0921

Fig (11, 12,13) shows the distribution of eczema in skin of hand layer of different three persons.

The average value of each feature in all layers was calculated to simplify study of results, it can be shown that the effected infected area in the face layer is larger than both hand and foot layer, also it can be shown that the hand layer is more contrast than both face and foot layers, the contrast of face layer is more than the foot layer. it is clearly that the foot layer is relatively more correlated than both face and hand layers, also the energy of foot layer is higher than both face and hand layers. The homogeneity of fool layer is relatively higher than both face and hand layers, it can be seen that the entropy in the face layer is relatively higher than both hand and foot

layers, also it can be shown that the variance and standard of deviation in the hand layer is higher than both face and foot layers, it obviously that the kurtosis in the foot layer is higher than the face and hand layers, it is clearly that the foot layer has a higher skewness than the hand and face layers

Conclusion

It can be concluded that the face layer is infected by eczema higher than the hand and foot layers because the skin of the face is more sensitive than the rest when it subjected to external environment factors and pollution, so the face layer image has a more entropy than the rest layers. The hand layer image has the best contrast but it's pixels data are spreading out over a large range of the value then it has a higher probability distribution than the rest layers, all layers have a high positive correlation but the foot layer is more correlated, the foot layer image has a low gray level but the best compressibility ,because a good homogeneity , the foot layer image has the better uniformity of gray level than the rest layers, the foot layer image has a longer and sharper peak distribution than the rest layers, the foot layer image has a good asymmetry of probability distribution than the rest layers, it can be concluded that the foot layer detection is more comfortable in this approach technique.

References

- A. Gilat. "MATLAB: An introduction with Applications". John Wiley and Sons, 2004.
- Agha HM, Asim SAA, Alam MZ, Wahid Z. "Frequency of different types of eczema in a tertiary care hospital". *Professional Med J*:23(1):060-064.2016.
- Alan C. Bovik Handbook of image and video processing, Academic press. ISBN 0-12-119792-1. 2005.
- F M Candocia, "A scale-preserving lens distortion model and its application to image registration", Florida Conference on Recent Advances in Robotics, FCRAR, Miami, May 25–26, 2006.
- Houcque. "Applications of MATLAB: Ordinary Differential Equations. Internal communication", Northwestern University, pages 1–12, 2005.
- Joseph G.pellegrino; In Joseph D.Bronzino.BME et al. "infrared camera characterization". 2006.
- K. Wan N. Maddage C.S. Xu "Characterization of dominant speech for automatic sports highlight generation" submitted to ICASSP 2004.
- Kalliomäki, M; Antoine, JM; Herz, U; Rijkers, GT; Wells, JM; Mercenier,. "Guidance for substantiating the evidence for beneficial effects of probiotics: prevention and management of allergic diseases by probiotics". *The Journal of Nutrition*. 140 (3): 713S–21S. 2010.
- Lindsay Mac Donald "digital Heritage". ISBN 0-7506-6183-6(2006).
- M. Dalwadi , D. Khandhar, K. Wandra, "Automatic Boundary Detection and Generation of Region of Interest for Focal Liver Lesion Ultrasound Image Using Texture Analysis", *International Journal of Advanced Research in Computer Engineering & Technology (IJARCET)*, ISSN: 2278 – 1323. Volume 2, Issue 7, July 2013.
- M. Song, D. Tao, C. Chan, X. Li, and C. Chen, "Color to gray: Visual cue preservation," *IEEE Trans. Pattern Anal., Machine Intel.*, vol. 32, no. 9, pp. 1537–1552, 2010.
- MATLAB and Simulink for Technical Computing, URL: <http://www.mathworks.com>, July 2010.
- McAleer, MA; Flohr, C; Irvine, AD . "Management of difficult and severe eczema in childhood". *BMJ (Clinical research ed.)*. 345: e4770. doi:10.1136/bmj.e4770.2012.
- Nedorost, Susan T. (2012). "Generalized Dermatitis in Clinical Practice". Springer Science & Business Media. pp. 1–3, 9, 13–14. ISBN 9781447128977. Archived from the original on 15 August 2016. Retrieved 29 July 2016.
- OranjAP ,Devilevs ACA ,kunzB,etal. Thomasks.Ra. 2002 "Handout on Health: Atopic Dermatitis (A type of eczema)". NIAMS. May 2013. Archived from the original on 30 May 2015. Retrieved 29 July 2016.
- P. Mohanaiah, P. Sathyanarayana, L. GuruKumar," Image Texture Feature Extraction Using GLCM Approach", *International Journal of Scientific and Research Publications*, Volume 3, Issue 5, ISSN 2250-3153, May 2013 .
- T. Kumarm, K. Verma ." A Theory Based on Conversion of RGB image to Gray image "International Journal of Computer Applications (0975 – 8887) Volume 7– No.2, 2010.
- Torley, D; Futamura, M; Williams, HC; Thomas, KS "What's new in atopic eczema? An analysis of systematic reviews published in 2010–11. *Clinical and experimental dermatology*". 38(5): 449–56.2013.
- www.mathworks.com/help/images/roi-based-processing.html.
- Y.L Kang J.H. Lim Q. Tian M.S Kankanhalli C.S Xu "Visual Keywords Labeling in Soccer Video" submitted to ICPR. 2004.

Author Information

Yasir Salam Abdulghafoor Al-khafaji

Alkawarizmi Collage of engineering / University of
Baghdad/ Biomedical dep. Iraq
E-Mail: yasir_bio@yahoo.com

Shatha K. Muallah

Alkawarizmi Collage of engineering /University of
Baghdad/ Biochemical dep. Iraq

Muntaha R. Ibraheem

Alkawarizmi Collage of engineering / University of
Baghdad/ Biomedical dep. Iraq

Central Automorphism Groups for Semidirect Product of p-Groups

Ozge OZTEKIN

Gaziantep University

Zeynep GURBUZ

Gaziantep University

Abstract: Let $\mathbb{Z}_{p^2} \rtimes_{\phi} \mathbb{Z}_p$ be the semi-direct product of \mathbb{Z}_{p^2} and \mathbb{Z}_p with respect to ϕ , (ϕ is homomorphism from \mathbb{Z}_p to automorphisms group of \mathbb{Z}_{p^2}). In this work, the group $\text{Aut}_C(\mathbb{Z}_{3^2} \rtimes_{\phi} \mathbb{Z}_3)$ of all central automorphisms of $\mathbb{Z}_{3^2} \rtimes_{\phi} \mathbb{Z}_3$ is studied and we determine the form of central automorphisms of $\mathbb{Z}_{3^2} \rtimes_{\phi} \mathbb{Z}_3$.

Keywords: P-group, Semi-direct product, Central automorphism

Introduction

Let G be a group. By $C(G)$, $\text{Aut}G$ and $\text{Inn}(G)$ we denote the center, the group of all automorphisms and the group of all inner automorphisms of G , respectively. An automorphism θ of G is called central automorphism if θ commutes with every inner automorphism, or equivalently, if $g^{-1}\theta(g)$ lies in the center of G for all g in G . The central automorphisms form a normal subgroup of $\text{Aut}(G)$ and we denote this group with $\text{Aut}_C(G)$. Also $\text{Aut}_C(G)$ is the subgroup of $\text{Inn}(G)$.

A p-group is a group in which every element has finite order, and the order of every element is a power of prime number p . The term p-group is typically used for a finite p-group, which is equivalent to a group of prime power order.

In literature, there are important studies about central automorphisms of p-groups [1], [2]. In [1] Adney and Yen has shown that if G is a finite purely non abelian group then $|\text{Aut}_C(G)| = |\text{Hom}(G/G', Z(G))|$. The automorphisms of direct and semidirect product of p-groups was given by Stahl in [3].

In this work our goal is to determine the central automorphisms of $\mathbb{Z}_{p^2} \rtimes_{\phi} \mathbb{Z}_p$ where $p=3$ and ϕ is homomorphism from \mathbb{Z}_p to automorphisms group of \mathbb{Z}_{p^2} .

Preliminaries

Definition. Let H and K be non-trivial finite groups and $\phi: K \rightarrow \text{Aut}(H)$ be a homomorphism. We define the operation \rtimes_{ϕ} as the following: Let $H \rtimes_{\phi} K$ be the set $\{(h, k): h \in H, k \in K\}$ on which it acts an operation $*$ as

$$(h_1, k_1) * (h_2, k_2) = (h_1 \cdot \phi(k_1)(h_2), (k_1 \cdot k_2))$$

We define $G \triangleq H \rtimes_{\phi} K$ as the semi-direct product of H and K with respect to ϕ .

Definition. An automorphism θ of G is called central automorphism if θ commutes with every inner automorphism, or equivalently, if $g^{-1}\theta(g)$ lies in the $C(G)$. The central automorphisms form a normal subgroup of $\text{Aut}(G)$.

Main Results

Theorem. Let ϕ be an automorphism of $\mathbb{Z}_p \rtimes_{\phi} \mathbb{Z}_p$ (p is odd number) where $\phi: \mathbb{Z}_p \rightarrow \text{Aut}(\mathbb{Z}_p)$ and $\phi(a)=1+pa$ then ϕ is defined by

$$\phi(a,b)=(a^i b^j, a^{pm} b)$$

where $i \in \mathbb{Z}_p, j, m \in \mathbb{Z}_p$ and $i \not\equiv 0 \pmod{p}$

Proof. REF.[3]

Theorem. $|\text{Aut}(\mathbb{Z}_p \rtimes_{\phi} \mathbb{Z}_p)| = p^3(p-1)$.

Proof. REF.[3]

For determining the central automorphisms of $\mathbb{Z}_3 \rtimes_{\phi} \mathbb{Z}_3$, first we find the $C(\mathbb{Z}_3 \rtimes_{\phi} \mathbb{Z}_3)$.

Lemma. $C(\mathbb{Z}_3 \rtimes_{\phi} \mathbb{Z}_3) = \{(0,0), (3,0), (6,0)\}$.

Proof. If $(a,b) \in C(\mathbb{Z}_3 \rtimes_{\phi} \mathbb{Z}_3)$ then for every $(c,d) \in (\mathbb{Z}_3 \rtimes_{\phi} \mathbb{Z}_3)$,

$$(a,b) * (c,d) = (c,d) * (a,b)$$

from this we get

$$(a+(1+3b)c, b+d) = (c+(1+3d)a, d+b).$$

a must be 0,3 or 6 and b must be 0 for the last equation to be provided for every $(c,d) \in (\mathbb{Z}_3 \rtimes_{\phi} \mathbb{Z}_3)$. Therefore $C(\mathbb{Z}_3 \rtimes_{\phi} \mathbb{Z}_3) = \{(a,0) | a=0,3,6\}$

Corollary. $C(\mathbb{Z}_3 \rtimes_{\phi} \mathbb{Z}_3) = \langle (3,0) \rangle$ and the order of $C(\mathbb{Z}_3 \rtimes_{\phi} \mathbb{Z}_3)$ is 3.

Theorem. Let θ be an automorphism of $\mathbb{Z}_3 \rtimes_{\phi} \mathbb{Z}_3$. If θ is central then it has the form

$$\theta(a,b) = (a \rightarrow a^{3k+1}, a^{3m} b)$$

where $k, m \in \mathbb{Z}_3$.

Proof. Let θ be an automorphism of $\mathbb{Z}_3 \rtimes_{\phi} \mathbb{Z}_3$. Then it has the form

$$\theta(a,b) = (a^i b^j, a^{pm} b) \quad (1)$$

where $i \in \mathbb{Z}_3, j, m \in \mathbb{Z}_3$ and $i \not\equiv 0 \pmod{3}$

If $\theta \in \text{Aut}_C(\mathbb{Z}_3 \rtimes_{\phi} \mathbb{Z}_3)$ then for all $g=(a,b) \in \mathbb{Z}_3 \rtimes_{\phi} \mathbb{Z}_3$, θ satisfy $g^{-1} * \theta(g) \in C(\mathbb{Z}_3 \rtimes_{\phi} \mathbb{Z}_3)$

By using the operation $*$ rule we get

$$g^{-1} * \theta(g) = (i(a+3ab) + j(b+3b^2) - a, 0).$$

For $(i(a+3ab) + j(b+3b^2) - a, 0) \in C(\mathbb{Z}_3 \rtimes_{\phi} \mathbb{Z}_3)$

$$(i(a+3ab) + j(b+3b^2) - a, 0) = 0, 3, 6$$

Therefore the conditions $(i=1, j=0)$, $(i=4, j=0)$ and $(i=7, j=0)$ satisfy this equation for all g . We put this conditions at (1) we get the general form of central automorphisms as:

$$\theta(a,b) = (a \rightarrow a^{3k+1}, a^{3m} b).$$

References

- J. E. Adney T. Yen, Automorphisms of p -groups, Illinois J. Math. 9(1965), 137-143.
 A. R. Jamali and H. Mousavi, On the central automorphism group of finite p -groups, Algebra Colloq. 9(1) (2002), 7-14.
 G. Saeden Stahl, J. Laine, G. Behm, On p -groups of low power order, Master Thesis, KTH, (2010).

Author Information

Ozge Oztekin

Department of Mathematics, Gaziantep University
 Contact e-mail: ozgedzozr@gmail.com

Zeynep Gurbuz

Department of Mathematics, Gaziantep University

Synthesis of Some Novel 3-Alkyl(Aryl)-4-[3-(2-furylcarbonyloxy)-4-methoxy-benzylidenamino]-4,5-dihydro-1*H*-1,2,4-triazol-5-one Compounds

Onur AKYILDIRIM
Kafkas University

Abstract: In this study, nine novel 3-alkyl(aryl)-4-[3-(2-furylcarbonyloxy)-4-methoxy-benzylidenamino]-4,5-dihydro-1*H*-1,2,4-triazol-5-one (3) compounds were synthesized from a reaction of type 1 compounds with 3-(2-furylcarbonyloxy)-4-methoxybenzaldehyde (2) which is obtained from a reaction of 3-hydroxy-4-methoxybenzaldehyde and furan-2-carbonyl chloride. The finally part contains that synthesis of new compounds. The structures of these novel compounds were characterized by using, IR, ¹H NMR and ¹³C NMR spectral data.

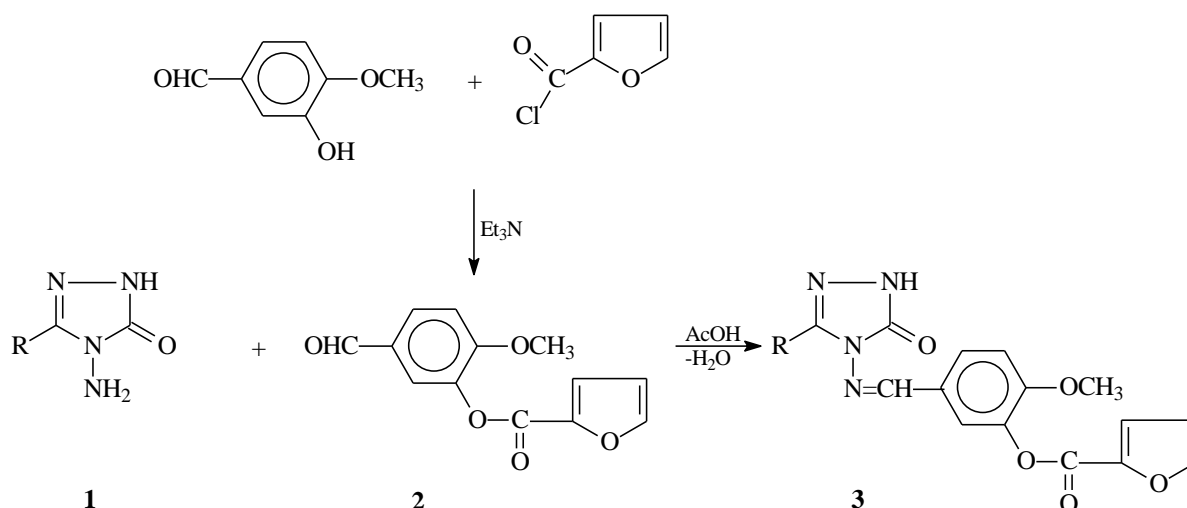
Keywords: 1,2,4-triazol, Schiff base, Synthesis

Introduction

1,2,4-Triazole and 4,5-dihydro-1*H*-1,2,4-triazol-5-one derivatives have been reported to possess a wide range of biological activities, such as anti-tumor (Chen et al., 2016), anti-bacterial (Zhang et al., 2014), anti-oxidant (Chidananda et al., 2012), anti-inflammatory (El-Serwy, Mohamed, Abbas, & Abdel-Rahman, 2013), analgesic (Uzgören-Baran et al., 2012), anti-hypertensive and diuretic (Ali, Ragab, Farghaly, & Abdalla, 2011) qualities.

In a recent study it has been reported that diaminobenzidine is a chemo-sensor which selectively displays fluorescent emission in the presence of zinc (II) (Kumar et al., 2017). In another study, it has been shown that a Schiff base of mesoporous SBA-15 which was modified by Fe₃O₄ nanoparticles removes Ce (III) ions from aqueous solutions in less than one minute (Dashtian et al., 2017). In a similar study, it has been reported that a novel colorimetric and fluorescent MMIP chemosensor based on Schiff base can detect some trace heavy and transition metal ions at high selectivity and sensitivity in an aqueous solution (Zhang et al., 2017).

In the present study, nine novel compounds 3-alkyl(aryl)-4-[3-(2-furylcarbonyloxy)-4-methoxy-benzylidenamino]-4,5-dihydro-1*H*-1,2,4-triazol-5-ones (**3a-i**) were synthesized from the reactions of 3-alkyl(aryl)-4-amino-4,5-dihydro-1*H*-1,2,4-triazol-5-ones (**1a-i**) and 3-(2-furylcarbonyloxy)-4-methoxybenzaldehyde (2) (Scheme 1).



1, 3	R
a	CH ₃
b	CH ₂ CH ₃
c	CH ₂ CH ₂ H ₃
d	CH ₂ C ₆ H ₅
e	CH ₂ C ₆ H ₄ .CH ₃ (<i>p</i> -)
f	CH ₂ C ₆ H ₄ .OCH ₃ (<i>p</i> -)
g	CH ₂ C ₆ H ₄ .Cl (<i>p</i> -)
h	CH ₂ C ₆ H ₄ .Cl (<i>m</i> -)
i	C ₆ H ₅

Scheme 1

Method

Chemicals and Apparatus

Chemical reagents and all solvents used in this study were purchased from Merck AG, Aldrich and Fluka. Melting point was determined in open glass capillary using a Stuart melting point SMP30 apparatus and is uncorrected. The IR spectra were obtained on an ALPHA-P BRUKER FT-IR spectrometer. ¹H and ¹³C NMR spectra were recorded in deuterated dimethyl sulfoxide with TMS as internal standard using a Bruker Ultrashield Plus Biospin spectrometer at 400 MHz and 100 MHz, respectively.

Synthesis of Compounds 3: The General Procedure

3-Hydroxy-4-methoxybenzaldehyde (0.01 mol) dissolved in ethyl acetate (20 mL) was treated with furan-2-carbonyl chloride (0.01 mol) and to this solution was slowly added triethylamine (0.01 mol) with stirring at 0-5 °C. The process of stirring continued for 2 h, and then the mixture was refluxed for 3 h and filtered. The filtrate evaporated *in vacuo*, and the crude product was washed with water and recrystallized from ethanol to afford compound **2**, mp 90 °C; IR: 2826 ve 2746 (CHO), 1743, 1688 (C=O), 1511, 1468 (C=C), 1283 (COO), 1178 (C-O, furan), 807 (1,4-disubstituted benzenoid ring) cm⁻¹. ¹H NMR (400 MHz, DMSO-d₆): δ 3.90 (s, 3H, OCH₃), 6.82 (t, 1H, ArH; *J*=3.60 Hz), 7.41 (d, 1H, Ar-H; *J*=8.40 Hz), 7.60 (dd, 1H, ArH; *J*=3.60 Hz, 0.40 Hz), 7.77 (d, 1H, Ar-H; *J*=2.00 Hz), 7.92 (dd, 1H, ArH; *J*=8.40 Hz, 02.00 Hz), 8.12 (s, 1H, Ar-H), 9.70 (s, 1H, CHO). ¹³C NMR (100 MHz, DMSO-d₆): δ 56.52 (OCH₃), 112.80, 113.13, 120.57, 123.23, 129.70, 130.35, 138.91, 142.49, 148.82, 153.53 (Ar-C), 156.05 (COO), 190.82 (CHO).

The corresponding compound **1** (0.01 mol) was dissolved in acetic acid (20 mL) and treated with 3-(2-furylcarbonyloxy)-4-methoxybenzaldehyde **2** (0.01 mol). The mixture was refluxed for 2 h and then evaporated at 50-55 °C in vacuo. Several recrystallizations of the residue from ethanol gave pure compounds 3-alkyl(aryl)-4-[3-(2-furylcarbonyloxy)-4-methoxy-benzylidenamino]-4,5-dihydro-1H-1,2,4-triazol-5-one **3** as colorless crystals.

3-Methyl-4-[3-(2-furylcarbonyloxy)-4-methoxy-benzylidenamino]-4,5-dihydro-1H-1,2,4-triazol-5-one (3a)

Yield: 97.22%, m.p. 221 °C. IR (KBr, ν , cm^{-1}): 3139 (NH), 1741, 1695 (C=O), 1610 (C=N), 1507, 1469 (C=C), 1266 (COO), 1163 (C-O, furan), 834 (1,4-disubstituted benzenoid ring) cm^{-1} .

3-Ethyl-4-[3-(2-furylcarbonyloxy)-4-methoxy-benzylidenamino]-4,5-dihydro-1H-1,2,4-triazol-5-one (3b)

Yield: 75.44%, m.p. 192 °C. IR (KBr, ν , cm^{-1}): 3161 (NH), 1743, 1699 (C=O), 1603 (C=N), 1510, 1469 (C=C), 1271 (COO), 1170 (C-O, furan), 834 (1,4-disubstituted benzenoid ring) cm^{-1} . ^1H NMR (400 MHz, DMSO- d_6): δ 1.20 (t, 3H, CH_3 ; $J=7.60$ Hz), 2.68 (q, 2H, CH_2 ; $J=7.60$ Hz), 3.86 (s, 3H, OCH_3), 6.82 (dd, 1H, Ar-H; $J=3.60$ Hz, 1.60 Hz), 7.34 (d, 1H, Ar-H; $J=9.20$ Hz), 7.60 (dd, 1H, Ar-H; $J=3.60$ Hz, 0.80 Hz), 7.74-7.76 (m, 2H, Ar-H), 8.12 (s, 1H, Ar-H), 9.66 (s, 1H, N=CH), 11.82 (s, 1H, NH). ^{13}C NMR (100 MHz, DMSO- d_6): δ 10.00 (CH_3), 18.45 (CH_2), 56.22 (OCH_3), 112.77, 113.12, 120.44, 121.01, 126.54, 128.27, 138.98, 142.62, 148.05, 151.41 (Ar-C), 148.72 (triazole C_3), 152.79 (N=CH), 153.53 (triazole C_5), 155.61 (COO).

3-n-Propyl-4-[3-(2-furylcarbonyloxy)-4-methoxy-benzylidenamino]-4,5-dihydro-1H-1,2,4-triazol-5-one (3c)

Yield: 72.60%, m.p. 199 °C. IR (KBr, ν , cm^{-1}): 3168 (NH), 1735, 1702 (C=O), 1588 (C=N), 1513, 1437 (C=C), 1270 (COO), 1174 (C-O, furan), 811 (1,4-disubstituted benzenoid ring) cm^{-1} . ^1H NMR (400 MHz, DMSO- d_6): δ 1.06 (t, 3H, $\text{CH}_2\text{CH}_2\text{CH}_3$; $J=7.60$ Hz), 1.68 (sext., 2H, $\text{CH}_2\text{CH}_2\text{CH}_3$; $J=7.60$ Hz), 2.64 (t, 2H, $\text{CH}_2\text{CH}_2\text{CH}_3$; $J=7.60$ Hz), 3.86 (s, 3H, OCH_3), 6.81 (dd, 1H, Ar-H; $J=8.00$ Hz, 1.60 Hz), 7.31 (d, 1H, Ar-H; $J=8.80$ Hz), 7.60 (m, 1H, ArH), 7.74-7.77 (m, 2H, Ar-H), 8.12 (m, 1H, Ar-H), 9.66 (s, 1H, N=CH), 11.82 (s, 1H, NH). ^{13}C NMR (100 MHz, DMSO- d_6): δ 13.42 ($\text{CH}_2\text{CH}_2\text{CH}_3$), 18.82 ($\text{CH}_2\text{CH}_2\text{CH}_3$), 26.62 ($\text{CH}_2\text{CH}_2\text{CH}_3$), 56.22 (OCH_3), 112.76, 113.15, 120.44, 121.07, 126.52, 128.19, 138.98, 142.62, 148.72, 153.53 (Ar-C), 146.89 (triazole C_3), 151.35 (triazole C_5), 152.90 (N=CH), 155.60 (COO).

3-Benzyl-4-[3-(2-furylcarbonyloxy)-4-methoxy-benzylidenamino]-4,5-dihydro-1H-1,2,4-triazol-5-one (3d)

Yield: 99.26%, m.p. 207 °C. IR (KBr, ν , cm^{-1}): 3135 (NH), 1740, 1698 (C=O), 1590 (C=N), 1509, 1467 (C=C), 1271 (COO), 1172 (C-O, furan), 813 (1,4-disubstituted benzenoid ring), 772 and 699 (monosubstituted benzenoid ring) cm^{-1} . ^1H NMR (400 MHz, DMSO- d_6): δ 3.85 (s, 3H, OCH_3), 4.05 (s, 2H, CH_2Ph), 6.82 (dd, 1H, Ar-H; $J=7.60$ Hz, 1.60 Hz), 7.20-7.22 (m, 1H, Ar-H), 7.25-7.31 (m, 5H, Ar-H), 7.60-7.61 (m, 1H, Ar-H), 7.70-7.73 (m, 2H, Ar-H), 8.12 (s, 1H, Ar-H), 9.61 (s, 1H, N=CH), 11.94 (s, 1H, NH). ^{13}C NMR (100 MHz, DMSO- d_6): δ 31.08 (CH_2Ph), 56.22 (OCH_3), 112.80, 113.13, 120.46, 121.24, 126.47, 126.64, 128.15, 128.35 (2C), 128.79 (2C), 135.83, 138.92, 142.60, 148.75, 153.53 (Ar-C), 146.22 (triazole C_3), 151.25 (triazole C_5), 152.48 (N=CH), 155.63 (COO).

3-p-Methylbenzyl-4-[3-(2-furylcarbonyloxy)-4-methoxy-benzylidenamino]-4,5-dihydro-1H-1,2,4-triazol-5-one (3e)

Yield: 99.29%, m.p. 214 °C. IR (KBr, ν , cm^{-1}): 3165 (NH), 1743, 1699 (C=O), 1591 (C=N), 1513, 1468 (C=C), 1272 (COO), 1174 (C-O, furan), 832 (1,4-disubstituted benzenoid ring) cm^{-1} . ^1H NMR (400 MHz, DMSO- d_6): δ 2.21 (s 3H, PhCH_3), 3.85 (s, 3H, OCH_3), 3.99 (s, 2H, CH_2Ph), 6.82-6.84 (m, 1H, Ar-H), 7.07 (d, 2H, Ar-H; $J=7.60$ Hz), 7.18 (d, 2H, Ar-H; $J=8.00$ Hz), 7.29 (d, 1H, Ar-H; $J=8.40$ Hz), 7.61-7.62 (m, 1H, Ar-H), 7.70-7.73 (m, 3H, Ar-H), 8.13-8.14 (m, 1H, Ar-H), 9.61 (s, 1H, N=CH), 11.94 (s, 1H, NH). ^{13}C NMR (100 MHz, DMSO- d_6): δ 20.52 (PhCH_3), 30.74 (CH_2Ph), 56.21 (OCH_3), 112.79, 113.10, 120.45, 121.18, 126.53, 128.53, 128.66 (2C), 128.91 (2C), 132.74, 135.68, 138.93, 142.63, 148.76, 153.51 (Ar-C), 146.33 (triazole C_3), 151.28 (triazole C_5), 152.31 (N=CH), 155.63 (COO).

3-p-Methoxybenzyl-4-[3-(2-furylcarbonyloxy)-4-methoxy-benzylidenamino]-4,5-dihydro-1H-1,2,4-triazol-5-one (3f)

Yield: 90.41%, m.p. 218 °C. IR (KBr, ν , cm^{-1}): 3171 (NH), 1746, 1690 (C=O), 1586 (C=N), 1508, 1436 (C=C), 1266 (COO), 1176 (C-O, furan), 809 (1,4-disubstituted benzenoid ring) cm^{-1} . ^1H NMR (400 MHz, DMSO- d_6): δ 3.68 (s, 3H, OCH₃), 3.85 (s, 3H, OCH₃), 3.97 (s, 2H, CH₂Ph), 6.81-6.85 (m, 3H, Ar-H), 7.20-7.23 (m, 2H, Ar-H), 7.30 (d, 1H, Ar-H; $J=8.40$ Hz), 7.61 (m, 1H, Ar-H), 7.71-7.75 (m, 3H, Ar-H), 8.13 (m, 1H, Ar-H), 9.61 (s, 1H, N=CH), 11.90 (s, 1H, NH). ^{13}C NMR (100 MHz, DMSO- d_6): δ 30.23 (CH₂Ph), 54.95 (OCH₃), 56.22 (OCH₃), 112.79, 113.14, 113.79 (2C), 120.45, 121.24, 126.51, 127.60, 128.18, 129.87 (2C), 138.94, 142.62, 148.76, 153.52, 158.05 (Ar-C), 146.52 (triazole C₃), 151.26 (triazole C₅), 152.47 (N=CH), 155.63 (COO).

3-p-Chlorobenzyl-4-[3-(2-furylcarbonyloxy)-4-methoxy-benzylidenamino]-4,5-dihydro-1H-1,2,4-triazol-5-one (3g)

Yield: 97.28%, m.p. 226 °C. IR (KBr, ν , cm^{-1}): 3124 (NH), 1747, 1702 (C=O), 1598 (C=N), 1514, 1470 (C=C), 1274 (COO), 1172 (C-O, furan), 826 (1,4-disubstituted benzenoid ring) cm^{-1} . ^1H NMR (400 MHz, DMSO- d_6): δ 3.85 (s, 3H, OCH₃), 4.06 (s, 2H, CH₂Ph), 6.82 (dd, 1H, Ar-H; $J=7.60$ Hz, 1.60 Hz), 7.28-7.34 (m, 5H, Ar-H), 7.60-7.61 (m, 1H, Ar-H), 7.68-7.73 (m, 3H, Ar-H), 8.12-8.13 (m, 1H, Ar-H), 9.62 (s, 1H, N=CH), 11.95 (s, 1H, NH). ^{13}C NMR (100 MHz, DMSO- d_6): δ 30.39 (CH₂Ph), 56.22 (OCH₃), 112.79, 113.12, 120.45, 121.21, 126.44, 128.28 (3C), 130.76 (2C), 131.36, 134.82, 138.94, 142.62, 148.76, 153.55 (Ar-C), 145.88 (triazole C₃), 151.23 (triazole C₅), 152.53 (N=CH), 155.62 (COO).

3-m-Chlorobenzyl-4-[3-(2-furylcarbonyloxy)-4-methoxy-benzylidenamino]-4,5-dihydro-1H-1,2,4-triazol-5-one (3h)

Yield: 89.04%, m.p. 208 °C. IR (KBr, ν , cm^{-1}): 3152 (NH), 1736, 1702 (C=O), 1590 (C=N), 1513, 1473 (C=C), 1276 (COO), 1161 (C-O, furan), 863, 756 and 709 (1,3-disubstituted benzenoid ring), 817 (1,4-disubstituted benzenoid ring) cm^{-1} . ^1H NMR (400 MHz, DMSO- d_6): δ 3.85 (s, 3H, OCH₃), 4.08 (s, 2H, CH₂Ph), 6.81-6.83 (m, 1H, Ar-H), 7.24-7.33 (m, 4H, Ar-H), 7.43 (m, 1H, Ar-H), 7.59-7.60 (m, 1H, Ar-H), 7.68-7.72 (m, 3H, Ar-H), 8.12-8.13 (m, 1H, Ar-H), 9.60 (s, 1H, N=CH), 11.90 (s, 1H, NH). ^{13}C NMR (100 MHz, DMSO- d_6): δ 30.72 (CH₂Ph), 56.23 (OCH₃), 112.77, 113.08, 120.40, 120.92, 126.44, 126.67, 127.51, 128.50, 129.04, 130.18, 132.88, 138.23, 138.99, 142.65, 148.73, 153.59 (Ar-C), 148.73 (triazole C₃), 151.22 (triazole C₅), 152.49 (N=CH), 155.59 (COO).

3-Phenyl-4-[3-(2-furylcarbonyloxy)-4-methoxy-benzylidenamino]-4,5-dihydro-1H-1,2,4-triazol-5-one (3i)

Yield: 97.50%, m.p. 227 °C. IR (KBr, ν , cm^{-1}): 3149 (NH), 1744, 1704 (C=O), 1609 (C=N), 1512, 1467 (C=C), 1272 (COO), 1180 (C-O, furan), 834 (1,4-disubstituted benzenoid ring) cm^{-1} . ^1H NMR (400 MHz, DMSO- d_6): δ 3.86 (s, 3H, OCH₃), 6.81 (dd, 1H, ArH; $J=3.60$ Hz, 1.60 Hz), 7.34 (d, 1H, Ar-H; $J=8.80$ Hz), 7.51 (d, 2H, Ar-H; $J=2.4$ Hz), 7.52 (d, 1H, Ar-H; $J=1.6$ Hz), 7.59 (d, 1H, Ar-H; $J=4.00$ Hz), 7.69 (d, 1H, Ar-H; $J=2.00$ Hz), 7.79 (dd, 1H, ArH; $J=8.80$ Hz, 2.00 Hz), 7.88-7.90 (m, 2H, Ar-H), 8.12 (d, 1H, Ar-H, $J=2.40$ Hz), 9.56 (s, 1H, N=CH), 12.36 (s, 1H, NH). ^{13}C NMR (100 MHz, DMSO- d_6): δ 56.27 (OCH₃), 112.78, 113.34, 120.48, 121.80, 126.20, 126.70, 127.86 (2C), 128.04, 128.50 (2C), 130.06, 138.93, 142.58, 144.54, 151.37 (Ar-C), 148.74 (triazole C₃), 153.75 (N=CH), 155.57 (triazole C₅), 156.17 (COO).

Results and Discussion

In this study, the structures of nine new 3-alkyl(aryl)-4-[3-(2-furylcarbonyloxy)-4-methoxy-benzylidenamino]-4,5-dihydro-1H-1,2,4-triazol-5-ones (**3a-i**) were characterized with IR, ^1H NMR and ^{13}C NMR spectral data.

References

- Ali, K. A., Ragab, E. A., Farghaly, T. A., & Abdalla, M. M. (2011). Synthesis of new functionalized 3-substituted [1,2,4]triazolo [4,3-a]pyrimidine derivatives: potential antihypertensive agents. *Acta Poloniae Pharmaceutica*, 68(2), 237-47. Retrieved from

- <http://www.ncbi.nlm.nih.gov/pubmed/21485297>
- Chen, X., Shi, Y. M., Huang, C., Xia, S., Yang, L. J., & Yang, X. D. (2016). Novel dibenzo[b,d]furan-1H-1,2,4-triazole derivatives: Synthesis and antitumor activity. *Anti-Cancer Agents in Medicinal Chemistry*, 16(3), 377–386. <http://doi.org/10.2174/1871520615666150817115913>
- Chidananda, N., Poojary, B., Sumangala, V., Kumari, N. S., Shetty, P., & Arulmoli, T. (2012). Facile synthesis, characterization and pharmacological activities of 3,6-disubstituted 1,2,4-triazolo[3,4-b][1,3,4]thiadiazoles and 5,6-dihydro-3,6-disubstituted-1,2,4-triazolo[3,4-b][1,3,4]thiadiazoles. *European Journal of Medicinal Chemistry*, 51, 124–136. <http://doi.org/10.1016/j.ejmech.2012.02.030>
- Dashtian, K., Zare-Dorabei, R. (2017). Synthesis and characterization of functionalized mesoporous SBA-15 decorated with Fe₃O₄ nanoparticles for removal of Ce(III) ions from aqueous solution: ICP-OES detection and central composite design optimization. *Journal of Colloid and Interface Science*, 494, 114–123. <http://dx.doi.org/10.1016/j.jcis.2017.01.072>
- El-Serwy, W. S., Mohamed, N. A., Abbas, E. M., & Abdel-Rahman, R. F. (2013). Synthesis and anti-inflammatory properties of novel 1,2,4-triazole derivatives. *Research on Chemical Intermediates*, 39(6), 2543–2554. <http://doi.org/10.1007/s11164-012-0781-9>
- Kumar, M., Kumar, A., Singh, M.K., Sahu, S.K., John, R.P. (2017). A novel benzidine based Schiff base “turn-on” fluorescent chemosensor for selective recognition of Zn²⁺. *Sensors and Actuators B: Chemical*, 241, 1218–1223. <http://dx.doi.org/10.1016/j.snb.2016.10.008>
- Uzgören-Baran, A., Tel, B. C., Sargöl, D., Öztürk, E. I., Kazkayas, I., Okay, G., Ertan, M., Tozkoparan, B. (2012). Thiazolo[3,2-b]-1,2,4-triazole-5(6H)-one substituted with ibuprofen: Novel non-steroidal anti-inflammatory agents with favorable gastrointestinal tolerance. *European Journal of Medicinal Chemistry*, 57, 398–406. <http://doi.org/10.1016/j.ejmech.2012.07.009>
- Zhang, F., Wen, Q., Wang, S. F., Shahla Karim, B., Yang, Y. S., Liu, J. J., Zhang, W. M., Zhu, H. L. (2014). Design, synthesis and antibacterial activities of 5-(pyrazin-2-yl)-4H-1,2,4-triazole-3-thiol derivatives containing Schiff base formation as FabH inhibitory. *Bioorganic & Medicinal Chemistry Letters*, 24(1), 90–95. <http://doi.org/10.1016/J.BMCL.2013.11.079>
- Zhang, S., Wu, X., Niu, Q., Guo, Z., Li, T., Liu, H. (2017). Highly selective and sensitive colorimetric and fluorescent chemosensor for rapid detection of Ag⁺, Cu²⁺ and Hg²⁺ based on a simple Schiff base. *Journal of Fluorescence*, 27, 729–737. <http://doi.org/10.1007/s10895-016-2005-y>

Author Information

Onur Akyildirim

Kafkas University,
Faculty of Engineering and Architecture
Department of Chemical Engineering
Kars, Turkey
Contact e-mail: onurakyildirim@gmail.com

Gaussian Calculations of 3-(*p*-Chlorobenzyl)-4-(3,4-Dihydroxybenzylidenamino)-4,5-Dihydro-1*H*-1,2,4-Triazol-5-One and *N*-Acetyl Derivative using B3lyp and HF Basis Sets

Gül KOTAN

Kafkas University, Kars Vocational School

Sule BAHCECI

Fatih Education Faculty, Karadeniz Technical University

Haydar YUKSEK

Kafkas University, Department of Chemistry

Abstract: 3-*p*-Chlorobenzyl-4-(3,4-dihydroxybenzylidenamino)-4,5-dihydro-1*H*-1,2,4-triazol-5-one (**1**) and 1-acetyl-3-*p*-chlorobenzyl-4-(3,4-dihydroxybenzylidenamino)-4,5-dihydro-1*H*-1,2,4-triazol-5-one (**2**) were described in the literature. In this study, these compounds were optimized by using the B3LYP/631G (d,p) and HF/631G (d,p) basis sets. IR absorption frequencies of analysed molecules were calculated by two methods. The veda4f program, was used in defining IR data, which were calculated theoreticall. ¹H-NMR and ¹³C-NMR isotropic shift values were calculated by the method of GIAO using the program package Gaussian G09. Experimental and theoretical values were inserted into the grafic according to equation of $\delta_{exp} = a + b \cdot \delta_{calc}$. The standard error values were found via SigmaPlot program with regression coefficient of a and b constants. The experimental and the obtained theoretical values were compared and found by regression analysis that are accurate. Furthermore, electronic, geometric and thermodynamic parameters, UV-Vis values, dipole moments, the HOMO-LUMO energy, total energy of the molecule, bond angles, bond lengths and mulliken charges from both methods were calculated.

Keywords: 4,5-Dihydro-1*H*-1,2,4-triazol-5-one, GIAO, HOMO-LUMO, UV-Vis

Introduction

1,2,4-Triazoles were reported to shown substantial antibacterial, antifungal and antihelmintic activities (Hardman et al., 1996; Gennaro et al., 1995; Richardson et al., 1984; Ammermann et al., 1991; Heindel et al., 1980). On the other hand, quantum chemical calculation methods have widely been used to theoretically predict the structural, spectroscopic, thermodynamic and electronic properties of molecular systems. The quantum chemical alculcation methods provide support for experimental structural and spectroscopic studies (Yüksek et al., 2005a; Yüksek et al., 2005b; Yüksek et al., 2008a; Yüksek et al., 2008b; Gökçe ve ark., 2013; Gökçe ve ark., 2014). In this study, we report the thereotical properties of Shiff bases containing 1,2,4-triazoles. All theoretical calculations investigated for the molecule were calculated with the Gaussian 09 quantum chemistry program (Frisch et al., 2009) on a equipped computer. Assential calculations were carried out using the Density Functional Theory (DFT) and Hatree Fock (HF) method with the restricted B3LYP (Kohn et al., 1996; Becke et al., 1993; Becke et al., 1988) level of theory, using 6-31G(d,p) basis sets, for all atoms. For this, firstly, 3-*p*-Chlorobenzyl-4-(3,4-dihydroxybenzylidenamino)-4,5-dihydro-1*H*-1,2,4-triazol-5-one (**1**) and 1-acetyl-3-*p*-chlorobenzyl-4-(3,4-dihydroxybenzylidenamino)-4,5-dihydro-1*H*-1,2,4-triazol-5-one (**2**) were optimized by using and 6-31G(d,p) two different basis sets (Frisch et al., 2009; Wolinski, Hilton & Pulay, 1990). Thus, the most stable form of the compound were determined. The optimized structures were used to calculation of the varied theoretical properties of the compound. Then, theoretical vibrational frequency were done in gas phase. Therefore, The veda4f program was used in defining IR data (Jamróz, 2004) which are multiplied with

- This is an Open Access article distributed under the terms of the Creative Commons Attribution-Noncommercial 4.0 Unported License, permitting all non-commercial use, distribution, and reproduction in any medium, provided the original work is properly cited.

- Selection and peer-review under responsibility of the Organizing Committee of the Conference

appropriate adjustment factors (Merrick et al., 2007) and result gave positive frequency values. This result, structure of compound were shown stable. Experimental data obtained from the literature (Bahçeci et al., 2002). The experimental and the calculated theoretical values were compared. The theoretical data obtained according to DFT/HF 6-31G(d,p) basis sets are formed using theoretical infrared spectrum. The experimental and theoretical IR spectra are given in Figs. 3. The ^1H and ^{13}C -NMR chemical shifts for the optimized molecular geometry of the molecule were calculated at B3LYP/6-31G(d,p) levels by using GIAO (the Gauge-Independent Atomic Orbital) (Pearson, 1989) approach in dimethyl sulfoxide (DMSO) solvent. Experimental and theoretical values were inserted into the graphic according to equation of $\delta_{\text{exp}} = a + b \cdot \delta_{\text{calc}}$. The standard error values were found via SigmaPlot program with regression coefficient of **a** and **b** constants. The temperature addicted thermodynamic parameters (thermal energies **E**, thermal capacity **CV**, entropy **S**) were calculated from the vibrational frequency calculations of the title compound in the gas phase using the DFT/HF 6-31G(d,p) level. In addition to the highest occupied molecular orbital (HOMO) and the lowest unoccupied molecular orbital (LUMO), bond lengths, mulliken charges, $E_{\text{LUMO}} - E_{\text{HOMO}}$ energy gap (ΔE_g), electronegativity (χ), electron affinity (A), global hardness (η), softness (S), ionization potential (I), chemical potential (Pi), electrophilic index (ω), Nucleophilic index (IP), total energy of the molecule, dipole moments were calculated.

Computational Details

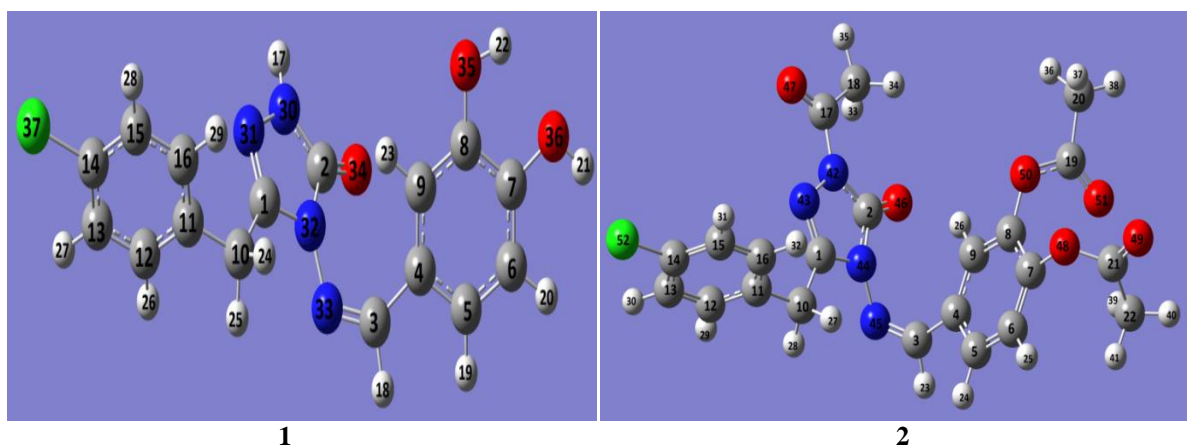


Figure 1. The Gausview structure of the molecules 1 and 2.

Table 1. The calculated and experimental ^{13}C and ^1H -NMR DMSO isotropic chemical shifts of the molecule 1 and 2 (δ/ppm)

No	Exp.	DFT	Differ.	DFT/ DMSO	Differ./ DMSO	HF	Differ.	HF/ DMSO	Differ./ DMSO
C1	145.71	152.07	-6.36	153.90	-8.19	145.10	0.61	147.93	-2.22
C2	154.57	148.46	6.11	149.59	4.98	147.33	7.24	148.56	6.01
C3	151.24	160.27	-9.03	161.83	-10.59	168.16	-16.92	171.09	-19.85
C4	124.57	133.21	-8.64	131.49	-6.92	120.99	3.58	119.38	5.19
C5	121.75	129.15	-7.40	131.01	-9.26	118.74	3.01	121.80	-0.05
C6	112.86	114.99	-2.13	117.17	-4.31	107.46	5.40	110.10	2.76
C7	145.71	147.88	-2.17	149.96	-4.25	138.88	6.83	140.35	5.36
C8	149.25	148.05	1.20	147.43	1.82	138.91	10.34	137.37	11.88
C9	115.53	119.55	-4.02	117.82	-2.29	116.97	-1.44	113.76	1.77
C10	30.35	42.55	-12.20	42.09	-11.74	27.32	3.03	26.87	3.48
C11	134.72	136.69	-1.97	137.87	-3.15	128.68	6.04	130.08	4.64
C12	130.69	134.13	-3.44	134.72	-4.03	127.12	3.57	127.52	3.17
C13	128.59	131.61	-3.02	131.83	-3.24	125.00	3.59	125.16	3.43
C14	133.31	145.93	-12.62	144.73	-11.42	133.21	0.10	131.64	1.67
C15	128.59	131.63	-3.04	131.74	-3.15	124.98	3.61	125.11	3.48
C16	130.69	135.10	-4.41	135.41	-4.72	127.55	3.14	127.82	2.87
H17	11.95	7.81	4.14	8.26	3.69	7.19	4.76	7.58	4.37
H18	9.42	8.51	0.91	8.69	0.73	8.89	0.53	9.15	0.27
H19	7.05	7.56	-0.51	7.86	-0.81	7.36	-0.31	7.82	-0.77
H20	6.82	7.29	-0.47	7.76	-0.94	7.10	-0.28	7.64	-0.82
H21	7.27	8.21	-0.94	8.16	-0.89	3.63	3.64	4.59	2.68

H22	9.42	4.41	5.01	5.53	3.89	4.78	4.64	5.10	4.32
H23	9.75	5.78	3.97	6.17	3.58	8.92	0.83	8.50	1.25
H24	4.02	4.37	-0.35	4.64	-0.62	3.06	0.96	3.43	0.59
H25	4.02	4.77	-0.75	4.85	-0.83	3.58	0.44	3.78	0.24
H26	7.32	8.08	-0.76	8.30	-0.98	7.74	-0.42	8.00	-0.68
H27	7.36	8.07	-0.71	8.22	-0.86	7.78	-0.42	7.95	-0.59
H28	7.36	8.12	-0.76	8.27	-0.91	7.72	-0.36	7.90	-0.54
H29	7.32	8.20	-0.88	8.42	-1.10	7.57	-0.25	7.84	-0.52
No	Exp.	DFT	Differ.	DFT/ DMSO	Differ./ DMSO	HF	Differ.	HF/ DMSO	Differ./ DMSO
C1	144.55	152.43	-7.88	155.13	-10.58	146.04	-1.49	149.88	-5.33
C2	153.24	149.18	4.06	149.76	3.48	147.89	5.35	148.44	4.80
C3	148.20	159.51	-11.31	161.85	-13.65	168.43	-20.23	171.56	-23.36
C4	131.85	136.67	-4.82	137.09	-5.24	123.69	8.16	124.66	7.19
C5	126.82	133.08	-6.26	134.87	-8.05	123.50	3.32	126.42	0.40
C6	122.36	127.27	-4.91	128.16	-5.80	118.83	3.53	120.15	2.21
C7	148.20	153.01	-4.81	152.13	-3.93	143.25	4.95	141.84	6.36
C8	142.35	148.57	-6.22	147.67	-5.32	137.51	4.84	135.74	6.61
C9	124.38	126.79	-2.41	127.23	-2.85	123.20	1.18	121.86	2.52
C10	30.92	41.91	-10.99	41.53	-10.61	27.22	3.70	26.82	4.10
C11	130.90	134.11	-3.21	136.17	-5.27	126.57	4.33	128.89	2.01
C12	130.90	133.52	-2.62	134.64	-3.74	126.85	4.05	127.56	3.34
C13	128.34	131.56	-3.22	131.86	-3.52	125.14	3.20	125.23	3.11
C14	133.95	146.73	-12.78	144.98	-11.03	134.20	-0.25	132.04	1.91
C15	128.34	132.10	-3.76	131.65	-3.31	125.44	2.90	125.16	3.18
C16	130.90	135.83	-4.93	135.81	-4.91	127.87	3.03	128.04	2.86
C17	165.90	164.99	0.91	167.77	-1.87	156.51	9.39	160.43	5.47
C18	23.48	32.39	-8.91	32.67	-9.19	21.15	2.33	21.38	2.10
C19	168.10	171.91	-3.81	173.78	-5.68	160.96	7.14	162.99	5.11
C20	20.29	28.21	-7.92	28.44	-8.15	17.65	2.64	17.82	2.47
C21	167.98	167.84	0.14	171.54	-3.56	156.93	11.05	161.19	6.79
C22	20.29	28.40	-8.11	28.71	-8.42	17.02	3.27	17.34	2.95
H23	9.58	8.76	0.82	9.03	0.55	9.08	0.50	9.39	0.19
H24	7.76	8.08	-0.32	8.44	-0.68	7.78	-0.02	8.28	-0.52
H25	7.45	7.98	-0.53	8.28	-0.83	7.68	-0.23	8.06	-0.61
H26	7.78	8.16	-0.38	8.38	-0.60	8.93	-1.15	8.78	-1.00
H27	4.17	4.63	-0.46	4.94	-0.77	3.10	1.07	3.53	0.64
H28	4.17	4.71	-0.54	4.87	-0.70	3.57	0.60	3.84	0.33
H29	7.43	7.99	-0.56	8.28	-0.85	7.71	-0.28	8.02	-0.59
H30	7.41	8.08	-0.67	8.22	-0.81	7.81	-0.40	7.96	-0.55
H31	7.41	8.23	-0.82	8.31	-0.90	7.80	-0.39	7.92	-0.51
H32	7.43	8.46	-1.03	8.63	-1.20	7.62	-0.19	7.88	-0.45
H33	2.50	3.34	-0.84	3.42	-0.92	2.91	-0.41	3.00	-0.50
H34	2.50	3.17	-0.67	3.17	-0.67	2.79	-0.29	3.03	-0.53
H35	2.50	2.63	-0.13	2.67	-0.17	2.37	0.13	2.39	0.11
H36	2.32	3.02	-0.70	3.23	-0.91	2.48	-0.16	2.73	-0.41
H37	2.32	2.63	-0.31	2.66	-0.34	2.71	-0.39	2.77	-0.45
H38	2.32	3.31	-0.99	3.37	-1.05	2.20	0.12	2.21	0.11
H39	2.32	3.24	-0.92	3.29	-0.97	2.28	0.04	2.29	0.03
H40	2.32	2.52	-0.20	3.15	-0.83	2.07	0.25	2.18	0.14
H41	2.32	2.95	-0.63	2.56	-0.24	2.21	0.11	2.59	-0.27

The optimized R^2 values of the compound 1: B3LYP/631G(d,p) (DMSO): ^{13}C : 0.9883, ^1H : 0.4533; HF/631G(d,p) (DMSO): ^{13}C : 0.9762, ^1H : 0.5872.

The optimized R^2 values of the compound 2: B3LYP/631G(d,p) (DMSO): ^{13}C : 0.9971, ^1H : 0.9883; HF/631G(d,p) (DMSO): ^{13}C : 0.9916, ^1H : 0.9862.

There is such a relationship between R^2 -values of the compound. Found standard error rate and a, b constants regression values were calculated according to formulæ $\text{exp} = a + b \cdot \delta$ calc Eq. These values for compound were

given in the table 2. Theoretical and experimental carbon and proton chemical shifts ratios between according to a, b ve R^2 values, linear a correlation were observed.

Table 2. The correlation data for chemical shifts of the molecules 1 and 2

		^{13}C				^1H			
		R	S. hata	a	b	R	S. hata	a	b
1	DFT	0.9878		1.0640	-	0.3445	2.1386	0.4761	4.2815
	HF		4.6218		13.0263				
2	DFT	0.9797	5.9515	0.9483	9.0500	0.5763	1.8616	0.6130	3.5978
	HF	0.9971	3.7293	1.0388	-	0.9883	0.4190	1.0287	-0.6739
	HF	0.9916	6.3450	0.9778	4.7248	0.9862	0.4539	0.9389	0.2417

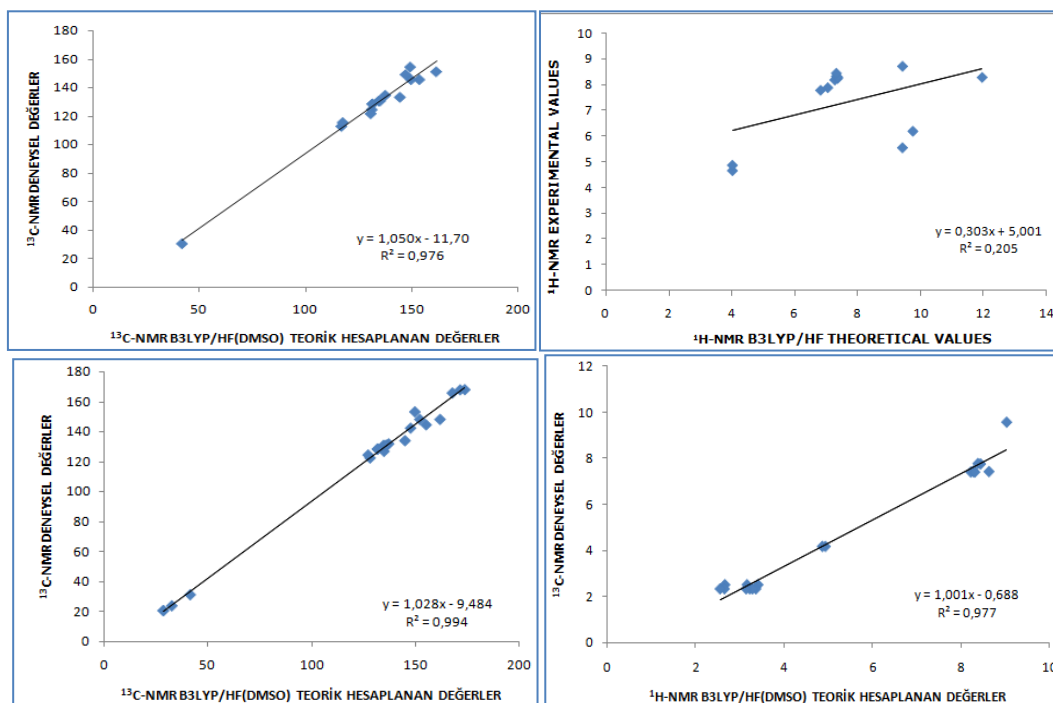


Figure 2. The correlation graphs for 6-31G(d,p) chemical shifts of the molecules 1 and 2

The Vibration Frequency of the Compound

Theoretically IR values were calculation veda 4f programme and scala values were obtain. IR spectrums were drawn with obtained values according to HF and DFT method. Theoretically IR values were compare with experimentally IR values. The result of this compare were found corresponding with each other of values. (Table 3).

 Table 3. Significant vibrational frequencies (cm^{-1}) of the molecules 1 and 2

Significant vibrational frequencies	Experimental (cm^{-1})		B3LYP/HF 6-31G(d,p)			
	IR(1)	IR(2)	DFT(1)	HF(1)	DFT(2)	HF(2)
$\nu\text{C}=\text{C}$	1570		1593	1620		
$\nu\text{C}=\text{N}$	1590,1580	1610,1590	1623	1717	1601	1701
$\nu\text{C}=\text{O}$	1715	1780,1760,1700	1773	1780	1773	1831
$\nu\text{C}-\text{H}$	3056		3091	3039		
$\nu\text{N}-\text{H}$	3150		3557	3555		
$\nu\text{O}-\text{H}$	3336		3643	3750		

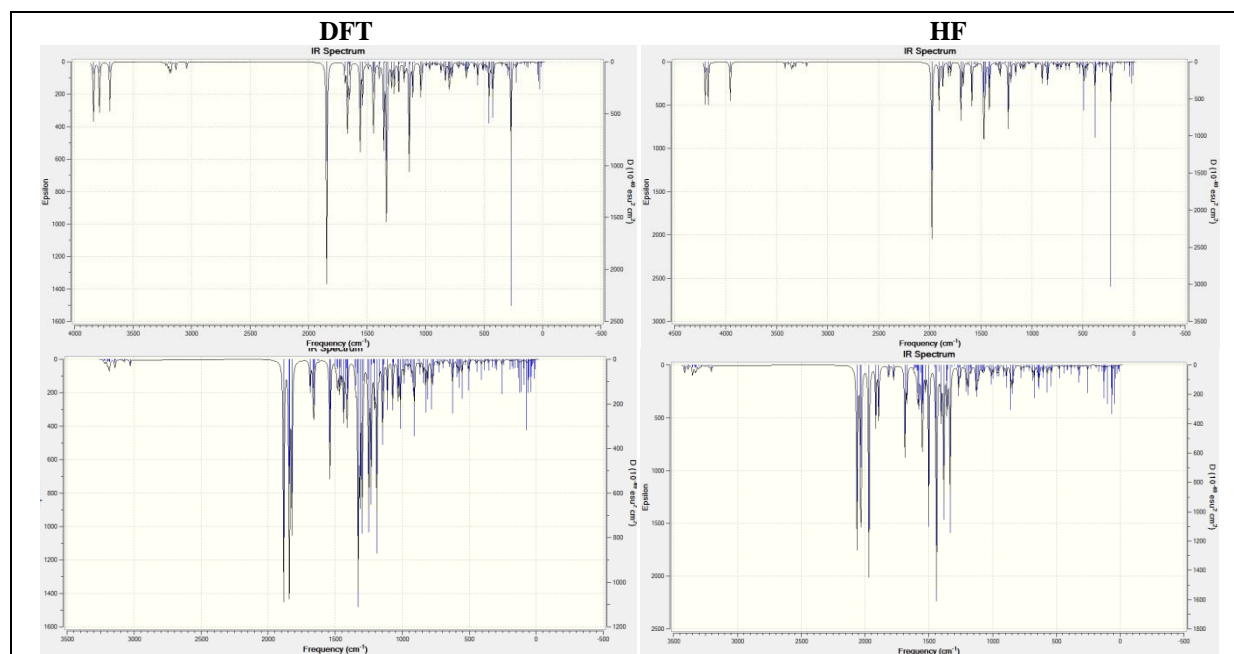


Figure 3. Experimental and theoretical IR spectrums and simulated of the molecules 1 and 2.

Table 4. The calculated bond lengths of the molecules 1 and 2

bond length 1	DFT	HF	bond length 1	DFT	HF	bond length 2	DFT	HF	bond length 2	DFT	HF
C(1)-N(31)	1.300	1.267	C(15)-H(28)	1.084	1.073	C(1)-N(43)	1.294	1.263	C(16)-C(11)	1.400	1.388
C(1)-N(32)	1.388	1.380	C(15)-C(16)	1.393	1.383	C(1)-N(44)	1.398	1.384	N(45)-C(3)	1.289	1.259
C(1)-C(10)	1.499	1.498	C(16)-H(29)	1.086	1.075	C(1)-C(10)	1.501	1.498	C(3)-H(23)	1.091	1.079
N(31)-N(30)	1.381	1.370	C(16)-C(11)	1.399	1.388	N(42)-N(43)	1.394	1.381	C(3)-C(4)	1.470	1.484
N(30)-H(17)	1.006	0.990	N(33)-C(3)	1.290	1.260	N(42)-C(17)	1.429	1.410	C(4)-C(5)	1.403	1.390
N(30)-C(2)	1.374	1.349	C(3)-H(18)	1.091	1.079	C(17)-O(47)	1.207	1.183	C(4)-C(9)	1.404	1.389
C(2)-O(34)	1.217	1.199	C(3)-C(4)	1.466	1.481	C(17)-C(18)	1.508	1.506	C(5)-H(24)	1.085	1.075
C(2)-N(32)	1.422	1.383	C(4)-C(5)	1.404	1.388	C(18)-H(33)	1.092	1.081	C(5)-C(6)	1.391	1.381
N(32)-N(33)	1.393	1.397	C(4)-C(9)	1.408	1.394	C(18)-H(34)	1.094	1.082	C(6)-H(25)	1.084	1.073
C(1)-C(10)	1.499	1.498	C(5)-H(19)	1.085	1.075	C(18)-H(35)	1.089	1.079	C(6)-C(7)	1.395	1.382
C(10)-H(24)	1.098	1.086	C(5)-C(6)	1.392	1.385	N(42)-C(2)	1.399	1.374	C(7)-O(48)	1.375	1.358
C(10)-H(25)	1.096	1.084	C(6)-H(20)	1.087	1.076	C(2)-O(46)	1.215	1.197	O(48)-C(21)	1.398	1.362
C(10)-C(11)	1.513	1.512	C(6)-C(7)	1.390	1.378	C(2)-N(44)	1.410	1.373	C(21)-O(49)	1.199	1.177
C(11)-C(12)	1.398	1.386	C(7)-O(36)	1.370	1.355	N(44)-N(45)	1.391	1.399	C(21)-C(22)	1.507	1.505
C(12)-H(26)	1.086	1.076	O(36)-H(21)	0.965	0.942	C(10)-H(27)	1.091	1.086	C(22)-H(39)	1.093	1.080
C(12)-C(13)	1.394	1.384	C(7)-C(8)	1.409	1.394	C(10)-H(28)	1.095	1.084	C(22)-H(40)	1.092	1.083
C(13)-H(27)	1.084	1.073	C(8)-O(35)	1.361	1.345	C(10)-C(11)	1.513	1.512	C(22)-H(41)	1.089	1.079
C(13)-C(14)	1.393	1.381	O(35)-H(22)	0.968	0.944	C(11)-C(12)	1.397	1.386	C(7)-C(8)	1.402	1.387
C(14)-Cl(37)	1.760	1.744	C(8)-C(9)	1.386	1.377	C(12)-H(29)	1.086	1.076	C(8)-O(50)	1.390	1.371
C(14)-C(15)	1.393	1.382	C(9)-H(23)	1.081	1.071	C(12)-C(13)	1.395	1.384	O(50)-C(19)	1.374	1.343
						C(13)-H(30)	1.084	1.073	C(19)-O(51)	1.207	1.184
						C(13)-C(14)	1.392	1.380	C(19)-C(20)	1.503	1.498
						C(14)-Cl(52)	1.759	1.743	C(20)-H(36)	1.092	1.083
						C(14)-C(15)	1.394	1.382	C(20)-H(37)	1.089	1.083
						C(15)-H(31)	1.084	1.073	C(20)-H(38)	1.094	1.079
						C(15)-C(16)	1.392	1.382	C(8)-C(9)	1.384	1.378
						C(16)-H(32)	1.085	1.075	C(9)-H(26)	1.082	1.071

Table 5. The calculated bond angles with B3LYP/HF 631G(d,p) of the molecule1 and 2.

	bond angles	B3LYP	HF		bond angles	B3LYP	HF
1	C(1)-N(31)-N(30)	104.314	104.822	27	H(28)-C(15)-C(16)	120.825	120.690
2	C(1)-N(32)-C(2)	107.989	107.670	28	C(14)-C(15)-C(16)	119.031	119.162
3	N(31)-C(1)-N(32)	111.741	111.506	29	C(15)-C(16)-H(29)	119.153	119.091
4	N(31)-N(30)-H(17)	120.090	120.790	30	H(29)-C(16)-C(11)	119.667	119.825
5	H(17)-N(30)-C(2)	124.717	125.429	31	C(1)-N(32)-N(33)	121.389	122.020
6	N(31)-N(30)-C(2)	114.513	113.416	32	N(32)-N(33)-C(3)	118.973	117.547
7	N(30)-C(2)-O(34)	130.513	129.838	33	N(33)-C(3)-H(18)	110.921	112.173
8	O(34)-C(2)-N(32)	128.522	127.998	34	H(18)-C(3)-C(4)	113.594	114.513
9	C(2)-N(32)-N(33)	125.612	123.480	35	C(3)-C(4)-C(5)	116.446	115.879
10	C(1)-C(10)-C(11)	113.794	113.863	36	C(3)-C(4)-C(9)	124.515	124.561
11	C(1)-C(10)-H(24)	108.475	107.910	37	C(4)-C(5)-H(19)	119.654	120.283
12	C(1)-C(10)-H(25)	107.581	107.738	38	H(19)-C(5)-C(6)	119.438	119.283
13	H(24)-C(10)-H(25)	105.470	106.127	39	C(4)-C(5)-C(6)	120.905	120.431
14	H(24)-C(10)-C(11)	110.273	110.340	40	C(5)-C(6)-C(7)	119.590	119.704
15	H(25)-C(10)-C(11)	110.868	110.524	41	C(5)-C(6)-H(20)	120.486	120.325
16	C(10)-C(11)-C(12)	120.708	120.683	42	H(20)-C(6)-C(7)	119.922	119.969
17	C(10)-C(11)-C(16)	120.780	120.724	43	C(6)-C(7)-O(36)	124.746	124.043
18	C(11)-C(12)-H(26)	119.647	119.863	44	C(6)-C(7)-C(8)	120.333	120.294
19	H(26)-C(12)-C(13)	119.148	119.046	45	C(7)-O(36)-H(21)	110.141	111.829
20	C(12)-C(13)-H(27)	120.818	120.664	46	O(36)-C(7)-C(8)	114.918	115.658
21	H(27)-C(13)-C(14)	120.185	120.190	47	C(7)-C(8)-O(35)	120.294	120.601
22	C(12)-C(13)-C(14)	118.996	119.146	48	C(8)-O(35)-H(22)	107.807	110.084
23	C(13)-C(14)-Cl(37)	119.473	119.563	49	O(35)-C(8)-C(9)	119.915	119.423
24	Cl(37)-C(14)-C(15)	119.512	119.512	50	C(8)-C(9)-H(23)	117.848	118.418
25	C(13)-C(14)-C(15)	121.077	120.925	51	H(23)-C(9)-C(4)	121.645	121.507
26	C(14)-C(15)-H(28)	120.145	120.148				

bond angles 2	B3LYP	HF	bond angles 2	B3LYP	HF
C(1)-N(43)-N(42)	105.214	105.578	N(42)-C(2)-O(46)	130.406	129.835
C(1)-N(44)-C(2)	108.033	107.757	C(2)-N(44)-N(45)	126.350	122.967
N(43)-C(1)-N(44)	111.945	111.768	N(44)-N(45)-C(3)	118.801	117.333
N(43)-N(42)-C(17)	119.321	119.327	N(45)-C(3)-H(23)	111.634	112.577
N(43)-C(1)-C(10)	126.535	126.852	H(23)-C(3)-C(4)	114.648	115.066
N(44)-C(1)-C(10)	121.460	121.342	C(3)-C(4)-C(5)	117.883	116.809
C(1)-C(10)-H(27)	107.932	107.654	C(3)-C(4)-C(9)	123.408	123.860
C(1)-C(10)-H(28)	107.437	107.596	C(4)-C(5)-H(24)	119.602	120.135
H(27)-C(10)-C(11)	110.428	110.437	H(24)-C(5)-C(6)	119.499	119.269
H(28)-C(10)-C(11)	110.713	110.525	C(4)-C(5)-C(6)	120.893	120.583
H(27)-C(10)-H(28)	105.314	106.180	C(5)-C(6)-H(25)	120.867	120.668
C(1)-C(10)-C(11)	114.550	114.088	H(25)-C(6)-C(7)	119.046	119.357
C(10)-C(11)-C(16)	121.075	120.719	C(5)-C(6)-C(7)	120.079	119.973
C(10)-C(11)-C(12)	120.339	120.573	C(6)-C(7)-O(48)	121.873	121.752
C(11)-C(12)-H(29)	119.755	119.959	C(7)-O(48)-C(21)	122.962	125.018
H(29)-C(12)-C(13)	119.047	119.011	O(48)-C(21)-O(49)	116.867	117.203
C(11)-C(12)-C(13)	121.198	121.030	O(49)-C(21)-C(22)	125.764	124.346
C(12)-C(13)-H(30)	120.783	120.656	C(21)-C(22)-H(39)	111.321	111.211
H(30)-C(13)-C(14)	120.231	120.203	C(21)-C(22)-H(40)	110.187	110.371
C(13)-C(14)-Cl(52)	119.502	119.557	C(21)-C(22)-H(41)	107.680	107.215
Cl(52)-C(14)-C(15)	119.459	119.502	H(39)-C(22)-H(40)	108.034	108.943
C(12)-C(13)-C(14)	118.987	119.141	H(40)-C(22)-H(41)	110.344	110.115
C(14)-C(15)-H(31)	120.130	120.149	H(39)-C(22)-H(41)	109.280	108.952
H(31)-C(15)-C(16)	120.671	120.671	O(48)-C(7)-C(8)	118.706	118.659
C(14)-C(15)-C(16)	119.142	119.180	C(7)-C(8)-O(50)	120.293	120.789
C(15)-C(16)-H(32)	119.132	119.071	C(8)-O(50)-C(19)	118.423	119.972
H(32)-C(16)-C(11)	119.806	119.925	O(50)-C(19)-O(51)	123.306	122.963
C(15)-C(16)-C(11)	121.057	121.003	O(51)-C(19)-C(20)	126.534	126.217
N(42)-C(17)-O(47)	119.616	119.760	C(19)-C(20)-H(36)	110.560	109.892
O(47)-C(17)-C(18)	124.610	123.550	C(19)-C(20)-H(37)	109.418	109.387
N(42)-C(17)-C(18)	115.766	116.690	C(19)-C(20)-H(38)	109.059	109.012
C(17)-C(18)-H(33)	111.249	110.996	H(36)-C(20)-H(37)	107.537	107.940
C(17)-C(18)-H(34)	111.158	111.020	H(37)-C(20)-H(38)	109.657	110.088
C(17)-C(18)-H(35)	107.208	106.956	H(36)-C(20)-H(38)	110.573	110.494
H(33)-C(18)-H(34)	106.425	107.064	C(8)-C(9)-H(26)	118.178	118.863
H(34)-C(18)-H(35)	110.221	110.382	H(26)-C(9)-C(4)	121.436	121.313

Frontier Molecular Orbital Analysis

Frontier molecular orbitals (FMO) (Figs. 4,5) determines the electric, electronic transitions, optical properties and kinetic stability (Fukui et al., 1952). HOMO-LUMO energy of compound was calculated using 6-31G (d,p)

level of theory. Using HOMO-LUMO energy gap electronegativity (χ), electron affinity (A), global hardness (η), softness (S), chemical potential (μ), ionization potential (I), chemical potential (Pi), electrophilic index(ω), Nucleophilic index (IP) for the compound was calculated. These all properties are calculated as follows (Parr, 1989; Parr et al., 1999; Özdemir et al., 2013):

$$\eta = (I - A)/2, \mu = -(I + A)/2, \chi = (I + A)/2, \text{Pi} = \chi, \omega = \mu^2 / 2\eta$$

In this formule, I and A symbolised ionization potential and electron affinity of the compound, which are virtually obtained from HOMO and LUMO energies. Where $I = -E_{\text{HOMO}}$ and $A = -E_{\text{LUMO}}$ showed as per Janak theorem (Janak, 1978) and Perdew et al. (Perdew et al., 1982). The HOMO-LUMO energy gap in compounds is 4.29; 11,18 e.v. All these parameters such as global hardness (η) chemical potential (μ), the global electrophilicity index (ω), electronegativity (χ), ionization potential (I), chemical potential (Pi), electrophilic index(ω), Nucleophilic index (IP) have been calculated for the target compound using 6-31G (d,p) basis set and are showed in Tables 6,7.

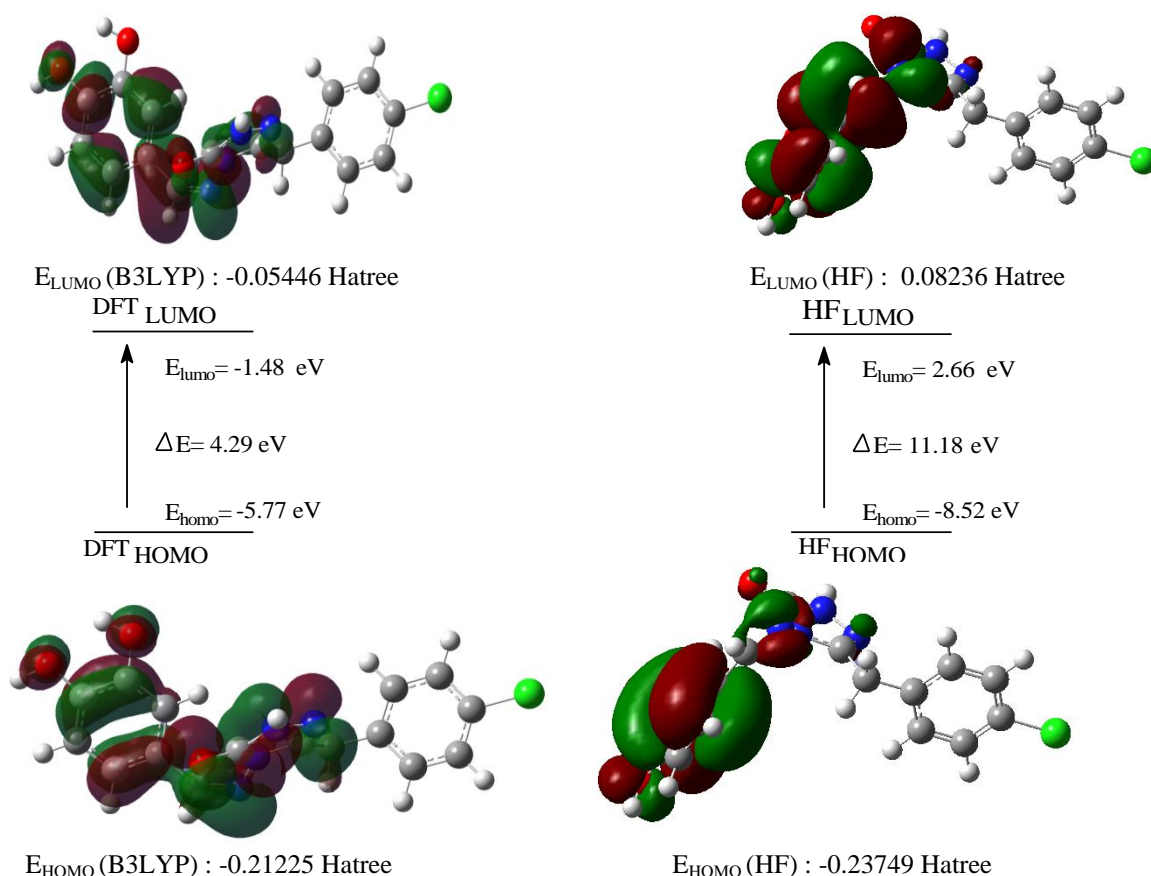


Figure 4. HOMO-LUMO energy calculated with DFT/HF 6-31G(d,p) levels of the molecule 1

Table 6. The calculated electronic structure parameters of the molecule 1

		Hatree	ev	kcal/mol	KJ/mol
	LUMO	-0,05446	-1,48189	-34,1738	-142,985
	HOMO	-0,21225	-5,77547	-133,188	-557,262
A	electron affinity	0,05446	1,48189	34,1738	142,985
I	ionization potential	0,21225	5,77547	133,188	557,262
ΔE	energy gap	0,15779	4,29358	99,0137	414,278
χ	electronegativity	0,133355	3,62868	83,6807	350,124
Pi	chemical potential	-0,133355	-3,62868	-83,6807	-350,124
ω	electrophilic index	0,000701517	0,01909	0,4402	1,84183
IP	Nucleophilic index	-0,01052104	-0,28628	-6,60199	-27,623
S	molecular softness	12,6751	344,898	7953,65	33278,4
η	molecular hardness	0,078895	2,14679	49,5068	207,139

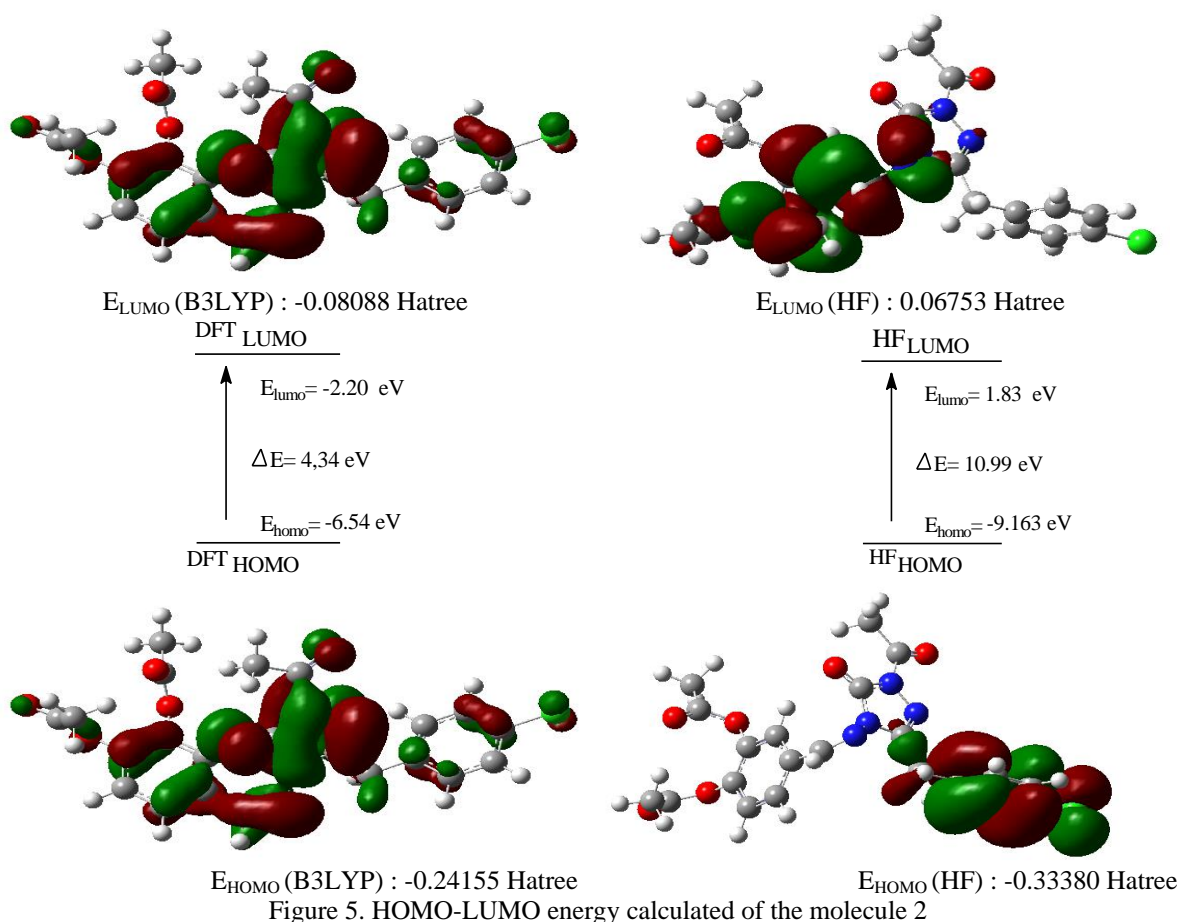


Table 7. The calculated electronic structure parameters of the molecule 2

	Hatree	ev	kcal/mol	KJ/mol
LUMO	-0,08088	-2,2008	-50,7524	-212,35
HOMO	-0,24155	-6,57274	-151,573	-634,19
A electron affinity	0,08088	2,2008	50,7524	212,35
I ionization potential	0,24155	6,57274	151,573	634,19
ΔE energy gap	0,16067	4,37194	100,821	421,839
χ electronegativity	0,161215	4,38677	101,163	423,27
Π chemical potential	-0,161215	-4,38677	-101,163	-423,27
ω electrophilic index	0,001043964	0,02841	0,65509	2,74093
IP Nucleophilic index	-0,01295121	-0,35241	-8,12692	-34,0034
S molecular softness	12,4479	338,715	7811,08	32681,9
η molecular hardness	0,080335	2,18597	50,4105	210,92

Thermodynamics Properties of Compound

Table 8. The calculated thermodynamics properties of the molecule 1.

	DFT	HF
Rotational temperatures (Kelvin)		
A	0.02986	0.01930
B	0.00363	0.00439
C	0.00353	0.00406
Rotational constants (GHz)		
A	0.62224	0.40219
B	0.07555	0.09141
C	0.07348	0.08467
Thermal Energies E (kcal/mol)		
Translational	0.889	0.889
Rotational	0.889	0.889
Vibrational	183.677	196.381
Total	185.455	198.159

Thermal Capacity CV (cal/mol-K)		
Translational	2.981	2.981
Rotational	2.981	2.981
Vibrational	73.753	68.087
Total	79.715	74.048
Entropy S (cal/mol-K)		
Translational	43.401	43.401
Rotational	35.785	35.889
Vibrational	81.320	75.340
Total	160.507	154.630
Zero-point correction (Hartree/Particle)	0.274631	0.296125
Thermal correction to Energy	0.295541	0.315786
Thermal correction to Enthalpy	0.296485	0.316730
Thermal correction to Gibbs Free Energy	0.220223	0.243260
Sum of electronic and zero-point Energies	-1522.105640	-1515.008945
Sum of electronic and thermal Energies	-1522.084730	-1514.989284
Sum of electronic and thermal Enthalpies	-1522.083786	-1514.988340
Sum of electronic and thermal Free Energies	-1522.160048	-1515.061810
Zero-point vibrational energy (Kcal/Mol)	172.33359	185.82126

Table 9. The calculated thermodynamics properties of the molecule 2

	DFT	HF
Rotational temperatures (Kelvin)		
A	0.01278	0.00903
B	0.00242	0.00261
C	0.00229	0.00235
Rotational constants (GHz)		
A	0.26638	0.18817
B	0.05035	0.05433
C	0.04782	0.04900
Thermal Energies E (kcal/mol)		
Translational	0.889	0.889
Rotational	0.889	0.889
Vibrational	260.146	277.814
Total	261.924	279.592
Thermal Capacity CV (cal/mol-K)		
Translational	2.981	2.981
Rotational	2.981	2.981
Vibrational	107.833	99.762
Total	113.794	105.724
Entropy S (cal/mol-K)		
Translational	44.332	44.332
Rotational	37.458	37.704
Vibrational	129.793	123.222
Total	211.583	205.257
Zero-point correction (Hartree/Particle)	0.386315	0.416320
Thermal correction to Energy	0.417402	0.445558
Thermal correction to Enthalpy	0.418346	0.446502
Thermal correction to Gibbs Free Energy	0.317816	0.348977
Sum of electronic and zero-point Energies	-1979.955917	-1970.231524
Sum of electronic and thermal Energies	-1979.924831	-1970.202287
Sum of electronic and thermal Enthalpies	-1979.923887	-1970.201343
Sum of electronic and thermal Free Energies	-1980.024417	-1970.298867
Zero-point vibrational energy (Kcal/Mol)	242.41655	261.24488

Table 10. The calculated mulliken charges datas of the molecule 1 and 2

1	DFT	HF	1	DFT	HF	2	DFT	HF	2	DFT	HF
C1	0.536	0.605	H18	0.086	0.156	C1	0.547	0.622	H27	0.142	0.163
C2	0.768	1.024	H19	0.331	0.361	C2	0.817	1.094	H28	0.152	0.179
C3	0.077	0.195	H20	0.336	0.371	C3	0.072	0.195	H29	0.092	0.160
C4	0.142	-0.098	H21	0.112	0.240	C4	0.131	-0.107	H30	0.111	0.180
C5	-0.140	-0.156	H22	0.134	0.161	C5	-0.122	-0.144	H31	0.113	0.181
C6	-0.128	-0.192	H23	0.149	0.176	C6	-0.113	-0.167	H32	0.097	0.161
C7	0.298	0.342	H24	0.094	0.161	C7	0.317	0.371	H33	0.154	0.168
C8	0.313	0.354	H25	0.110	0.178	C8	0.329	0.362	H34	0.160	0.157
C9	-0.117	-0.151	H26	0.109	0.177	C9	-0.123	-0.139	H35	0.136	0.161
C10	-0.321	-0.288	H27	0.093	0.160	C10	-0.322	-0.291	H36	0.148	0.160
C11	0.131	0.001	N28	-0.412	-0.543	C11	0.128	-0.001	H37	0.151	0.174
C12	-0.109	-0.138	N29	-0.341	-0.344	C12	-0.119	-0.139	H38	0.165	0.167
C13	-0.069	-0.112	N30	-0.438	-0.638	C13	-0.068	-0.110	H39	0.138	0.189
C14	50.094	-0.164	N31	-0.279	-0.274	C14	-0.093	-0.162	H40	0.184	0.142
H15	0.288	0.340	O32	-0.584	-0.681	C15	-0.071	-0.110	H41	0.150	0.175
H16	0.114	0.169	CI33	-0.028	-0.006	C16	-0.083	-0.121	N42	-0.423	-0.667
H17	0.093	0.162				C17	0.560	0.743	N43	-0.315	-0.286
						C18	-0.387	-0.409	N44	-0.462	-0.661
						C19	0.586	0.763	N45	-0.252	-0.258
						C20	-0.389	-0.414	O46	-0.520	-0.646
						C21	0.567	0.759	O47	-0.424	-0.511
						C22	0.418	-0.454	O48	-0.511	-0.671
						H23	0.128	0.181	O49	-0.414	-0.510
						H24	0.107	0.175	O50	-0.517	-0.667
						H25	0.116	0.184	O51	-0.450	-0.560
						H26	0.115	0.242	CI 52	-0.023	-0.001

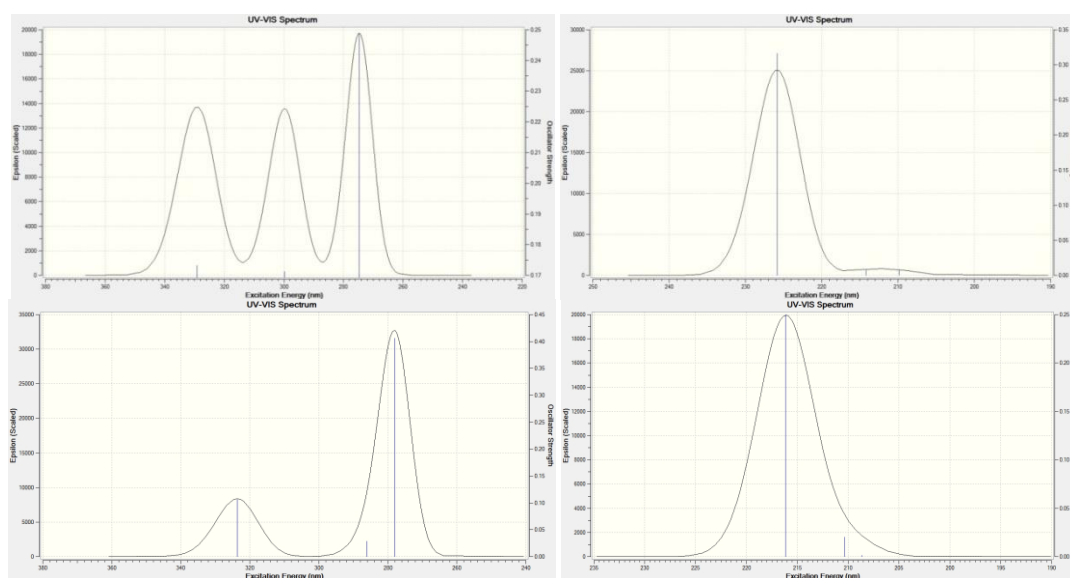


Figure 6. The UV-vis spectrum of the molecules 1 and 2

λ (nm)B3LYP/HF	Excitation energy (eV) B3LYP/HF	λ (nm)B3LYP/HF	Excitation energy (eV) B3LYP/HF
329.11/225.85	3.7673/5.4898	323.65/216.16	3.8308/5.7357
299.75/214.20	4.1362/5.7883	286.10/210.31	4.3336/5.8952
274.69/209.87	4.5137/5.9076	278.04/208.65	4.4592/5.9422

Table 11. The calculated dipole moments datas of the molecule

Dipole moments	B3LYP 1	HF 1	B3LYP 2	HF 2
μ_x	-1.4678	-0.6046	2.4975	2.7535
μ_y	-5.2882	-6.5842	-4.5046	-6.5222
μ_z	1.4558	1.9100	2.3302	2.3489
μ_{Toplam}	5.6779	6.8823	5.6532	7.4591

Table 12. The calculated total energy datas of the molecule

Energy	B3LYP	HF
1	-1522.380	-1515.305
2	-1980.342	-1970.647

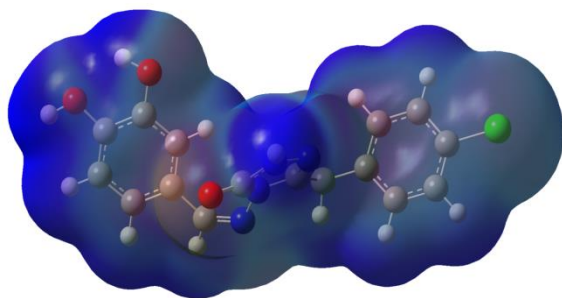


Figure 7. The total density of the molecule

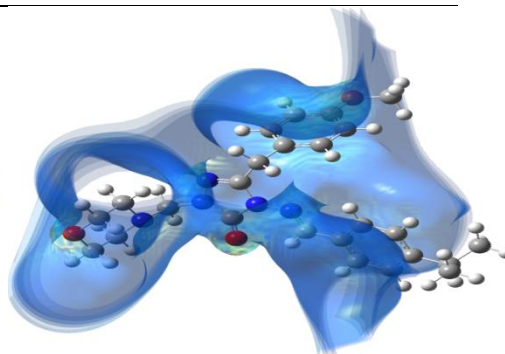


Figure 8. The MEP of the molecule

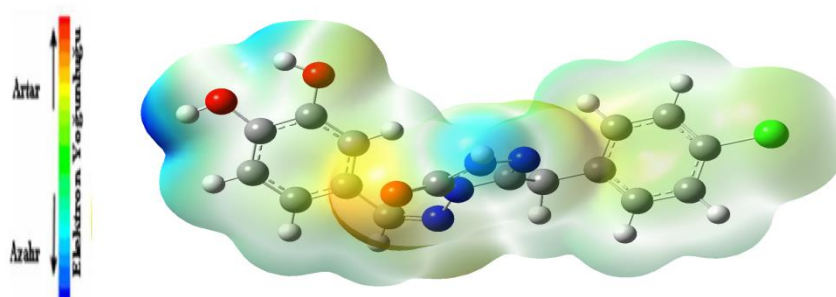


Figure 9. The ESP of the molecule

Conclusion

In this work, geometrical parameters and spectroscopic parameters such as IR, $^1\text{H-NMR}$ and $^{13}\text{C-NMR}$ spectra of molecule are calculated by Density Functional Theory (DFT) and Hartree-Fock (HF) methods with the 631G(d,p) basis sets of the program package Gaussian G09W. Obtained spectroscopic parameters are compared with experimental data. Otherwise, calculated theoretical properties of the compound according to two different basis sets were compared. In the result, the obtained data with B3LYP/HF 631G (d,p) basis sets were found to be closer to the experimental data. The chemical shifts in the calculations $^1\text{H-NMR}$ and $^{13}\text{C-NMR}$ and IR vibrational frequencies are found to be compatible with the experimental data. Theoretical and experimental carbon and proton chemical shifts ratios between according to R^2 and a, b values, linear a correlation were observed. The positive frequency in the IR data was found. This result, structure of compound were shown stable. In addition, the highest occupied molecular orbital (HOMO) and the lowest unoccupied molecular orbital (LUMO), bond lengths, mulliken charges, $E_{\text{LUMO}}-E_{\text{HOMO}}$ energy gap (ΔE_g), electronegativity (χ), electron affinity (A), global hardness (η), softness (σ), ionization potential (I), total energy of the molecule, thermodynamics properties (thermal energies (E), entropy (S), thermal capacity (CV), dipole moments were calculated B3LYP/HF 631G (d,p) basis sets.

References

- Hardman, J., Limbird, L., Gilman, A., Goodman and Gilman's (1996). The Pharmacological Basis of Therapeutics, 9th edn, p.988, McGraw-Hill, New York.
- Gennaro, A.R., Remington. (1995). The Science and Practice of Pharmacy, vol. II, Mack Easton, PA, p. 1327.
- Richardson, K., Whittle, P.J. (1984). Eur. Pat. Appl. EP 115 416; Chem. Abstr. 101 230544p.
- Ammermann, E., Loecher, F., Lorenz, G., Janseen, B., Karbach, S., Meyer, N. (1990). Brighton Crop Prot. Conf. Pests. Dis. 2 407; Chem. Abstr. 114 (1991) 223404h.
- Heindel, N.D., Reid, J.R. (1980). J. Heterocycl. Chem. 17 1087.
- Yüksek, H., Gürsoy, Ö., Çakmak, İ. and Alkan, M. (2005). Synthesis and GIAO NMR Calculation for Some New 4,5-Dihydro-1H-1,2,4-triazol-5-one Derivatives: Comparison of Theoretical and Experimental ^1H and ^{13}C Chemical Shifts Magn. Reson. Chem43 585-587.

- Yüksek, H., Çakmak, İ., Sadi, S., Alkan, M. and Baykara, H. (2005). Synthesis and GIAO NMR Calculations for Some Novel 4-Heteroarylidenamino-4,5-dihydro-1H-1,2,4-triazol-5-one Derivatives: Comparison of Theoretical and Experimental ¹H and ¹³C Chemical Shifts Int. J. Mol. Sci 6 219-229.
- Yüksek, H., Alkan, M., Bahçeci, Ş., Çakmak, İ., Ocağ, Z., Baykara, H., Aktaş, Ö. and Ağyel, E. (2008). Synthesis, Determination of pKa Values and GIAO NMR Calculations of Some New 3-Alkyl-4-(p-methoxybenzoylamino)-4,5-dihydro-1H-1,2,4-triazol-5-ones J. Mol. Struc 873 142-148.
- Yüksek, H., Alkan, M., Çakmak, İ., Ocağ, Z., Bahçeci, Ş., Calapoğlu, M., Elmastaş, M., Kolomuç, A. and Aksu, H. (2008). Preparation, GIAO NMR calculations and acidic properties of some novel 4,5-dihydro-1H-1,2,4-triazol-5-one derivatives with their antioxidant activities Int. J. Mol. Sci 9 12-32.
- Gökçe, H., Bahçeli, S., Akyıldırım, O., Yüksek, H. and Gürsoy-Kol, Ö. (2013). The Syntheses, Molecular Structures, Spectroscopic Properties (IR, Micro-Raman, NMR and UV-vis) and DFT Calculations of Antioxidant 3-alkyl-4-[3-methoxy-4-(4-methylbenzoxo)benzylidenamino]-4,5-dihydro-1H-1,2,4-triazol-5-one Molecules Letters in Organic Chemistry 10 (6): 395-441.
- Gökçe, H., Akyıldırım, O., Bahçeli, S., Yüksek, H. and Gürsoy-Kol, Ö. (2014). The 1-acetyl-3-methyl-4-[3-methoxy-4-(4-methylbenzoxo)benzylidenamino]-4,5-dihydro-1H-1,2,4-triazol-5-one Molecule Investigated by a Joint Spectroscopic and Quantum Chemical Calculations Journal of Molecular Structure DOI: <http://dx.doi.org/10.1016/j.molstruc.2013.10.044>, 1056-1057: 273-284.
- Frisch, M.J., Trucks, G.W., Schlegel, H.B., Scuseria, G.E., Robb, M.A., Mennucci, B., Petersson, G.A., Nakatsuji, H., Caricato, M., Li, X., et al. (2009). Gaussian 09, Revision C.01, Gaussian, Inc., Wallingford, CT.
- Kohn, W., Becke, A.D., Parr, R.G. (1996). Density functional theory of electronic structure, J. Phys. Chem. 100 12974-12980.
- Becke, A.D. (1993). Density-functional thermochemistry. III. The role of exact Exchange, J. Chem. Phys. 98 (7) 5648-5652.
- Becke, A.D. (1988). Density-functional exchange-energy approximation with correct asymptotic behavior, Phys. Rev. A 38 3098-3010
- Wolinski, K., Hilton, J.F. and Pulay, P.J. (1990). Am. Chem. Soc., 112, 512.
- Jamróz, M.H. (2004). Vibrational Energy Distribution Analysis: VEDA 4 program, Warsaw.
- Merrick, J.P., Moran, D., Radom, L. (2007). An Evaluation of Harmonic Vibrational Frequency Scale Factors. Journal of Physical Chemistry, 111 (45), 11683-11700.
- Bahçeci, Ş., Yüksek, H., Ocağ, Z., Köksal, C., Özdemir, M. (2002). "Synthesis and non-aqueous medium titrations of some new 4,5-dihydro-1H-1,2,4-triazol-5-one derivatives", Acta Chim. Slov., 49: 783-794.
- Pearson, R.G. (1989). Absolute electronegativity and hardness: applications to organic chemistry, J. Org. Chem. 54 1423-1430.
- Fukui, K., Yonezawa, T., Shingu, H.J. (1952). A molecular orbital theory of reactivity in aromatic hydrocarbons, J. Chem. Phys. 20 722-725.
- Parr, R., (1989). Density Functional Theory of Atoms and Molecules, Oxford University Press, New York.
- Parr, R., Szentpaly, L., Liu, S. (1999). Electrophilicity index, J. Am. Chem. Soc. 121 1922-1924.
- Ozdemir, N., Dayan, S., Dayan, O., Dinçer, M., Kalaycioglu, N. (2013). Experimental and molecular modeling investigation of (E)-N-{2[(2-hydroxybenzylidene)amino]phenyl} benzenesulfonamide Experimental and molecular modeling investigation of (E)-N-{2[(2-hydroxybenzylidene)amino]phenyl} benzenesulfonamide, Mol. Phys. 11 (6) 707-723.
- Janak, J.F. (1978). Proof that $\delta^2 E / \delta n_i^2 = \epsilon$ in density-functional theory, Phys. Rev. B 18 7165.
- Perdew, J.P., Parr, R.G., Levy, M., Balduz Jr, J.L. (1982). density-functional theory for fractional particle number: derivative discontinuities of the energy, Phys. Rev. Lett. 49 1691.

Author Information

Gul Kotan

Kafkas University Kars Vocational School
Kars, Turkey
Contact e-mail: gulkemer@hotmail.com

Sule BAHCECI

Fatih Education Faculty, Karadeniz Technical University,
Trabzon, Turkey

Haydar Yuksek

Kafkas University, Department of Chemistry
Kars, Turkey

Supplier Selection with Quality Function Deployment

Bahar OZYORUK
Gazi University

Abstract: Supply chain management (SCM) requires many complex decisions to be made while ensuring the movement of products, suppliers, producers, wholesalers, distributors, retailers, and ultimately, customers. Selection and evaluation of supplier is very important in these decisions. In order to complete the product design and production process of the products, the Quality Function Deployment (QFD) is widely used. However, this study can also be used in procurement decisions that are included in the production process, making it possible for managers to make the right decisions. In this study, contribution to the supplier selection process, which is the most important step in the management of the supply chain of Quality Function Deployment was investigated. In an enterprise that produces water treatment devices and water tanks, QFD assessed the supplier characteristics and decided to select the appropriate supplier. The provision of variable components of these suppliers will also be assessed separately. The results have been evaluated in terms of the company.

Keywords: Supplier selection, Quality function deployment QFD), Supplier ranking

Introduction

Supply Chain Management (SCM) is the management of all operations within the chain of business functions, processes and plans of these enterprises in order to enhance the performance of all enterprises within the supply chain. In this definition, it is emphasized that the operator should take into consideration suppliers as well, and the functions, processes and plans of the suppliers should be developed together with the enterprise. Because suppliers have positive or negative effects on the business (Mirmahmutoğulları, 2007).

The selection and valuation of the supplier is an important issue in the TCM. Incorporating customer requests into the development process of new products and services, thus enabling Quality Function Deployment to deliver products or services to the customer, higher quality, faster, and cheaper, can also provide improvements in procurement activities involved in the production process.(Akao, Y., 1990)

Quality Function Propagation (KFI), customer needs and needs; from product design to after-sales service is the best and cheapest way to reflect the method is known. At this point, KFI practitioners are able to provide higher profits by making customers more satisfied.

In this study, in order to improve the characteristics of the suppliers in the supply chain management, the contribution of the Quality Function Propagation method to the supplier selection process has been investigated. An example of how to use the quality function propagation method to improve supplier characteristics is given. It has been researched in the sample which properties of the suppliers to be improved should be improved.

Quality Function Deployment

Quality function deployment is a method that identifies customer needs, desires and expectations and develops products and services that are compatible with these needs, reducing the cost of product or service development, shortening total production time, increasing productivity and increasing customer satisfaction.

Stages of Establishing Quality House

The general structure of the quality house consists of 6 main parts.

1. Creation of Customer Parts
2. Creation and analysis of the planning matrix
3. Determination and Analysis of Quality Characteristics
4. Creation and Analysis of Relationship Matrix
5. Determination and Analysis of Technical Correlation
6. Determination of technical benchmarks and targets
7. Planning the Development Project Based on the Results

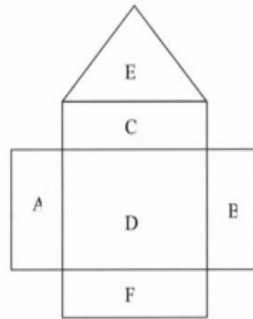


Figure 1. Basic parts of quality house

- A: The voice of the consumer
- B: Customer satisfaction levels
- A: Technical specifications
- D: Relationship matrix between the voice of the consumer and technical specifications
- E: Correlation between technical specifications (relationship)
- F: Comparison between competitive products and target values

Methods

In this study, it was tried to choose suppliers of an operator who produces lightning rod and earthing materials. In the study, "customer" was included as a "producer company" where the supplier company sold the products. It is aimed to examine and improve the supplier characteristics of 4 supplier firms (Cn) in supplying aluminum plates provided by the producer company in customer position. When determining the supplier characteristics, opinions of the 3 different procurement personnel who are working at the client firm and responsible for procuring the same group material were taken about the supplier companies. which features of the currently working suppliers should be improved.

In the first phase of the application, the producer company's purchasing authorities were interviewed and the main characteristics of the supplier's supplier were identified and given in Table 1. Relative importance ratings of supplier characteristics were calculated using 1-9 importance scoring, taking into account interviews with 3 acquirers in need. These values are presented in Table 2.

Table 1. Required features in the supplier

W ₁	The amount of returned material
W ₂	Price level
W ₃	Compliance with agreed delivery time
W ₄	Alternative distribution channels
W ₅	Term sale possibility
W ₆	Distance proximity
W ₇	Required certifications and experience

Table 2. Relative importance ratings

	1. buyer		2. buyer		3. buyer		Importance Grade (g _m)	
	crisp	fuzzy	crisp	fuzzy	crisp	fuzzy	crisp	fuzzy
W ₁	9	[8,9,9]	9	[8,9,9]	9	[8,9,9]	9	[8,0, 9,0, 9,0]
W ₂	9	[8,9,9]	8	[7,8,9]	8	[7,8,9]	8,3	[7,3, 8,3, 9,0]
W ₃	7	[6,7,8]	8	[7,8,9]	7	[6,7,8]	7,3	[6,3, 7,3, 8,3]
W ₄	5	[4,5,6]	4	[3,4,5]	6	[5,6,7]	5	[4,0, 5,0, 6,0]
W ₅	6	[5,6,7]	7	[6,7,8]	7	[6,7,8]	6,7	[5,6, 6,6, 7,6]
W ₆	8	[7,8,9]	6	[5,6,7]	7	[6,7,8]	7	[6,0, 7,0, 8,0]
W ₇	7	[6,7,8]	6	[5,6,7]	8	[7,8,9]	7	[6,0, 7,0, 8,0]

The companies and other companies that are frequently working in the present situation and expressed as C are potential suppliers. Opinions on the relational performance of this firm's products from three buyers were also taken according to scale 1-9 and presented in table 3. The C values in the chart indicate the target performance values for the supplier. This is determined by the experts.

Table 3. Relational comparison matrix

What is (W _m)	1. buyer				2. buyer				3. buyer				Customer Comparison Matrix (X)				e _j
	C ₁	C ₂	C ₃	C ₄	C ₁	C ₂	C ₃	C ₄	C ₁	C ₂	C ₃	C ₄	C ₁	C ₂	C ₃	C ₄	
W ₁	5	9	8	4	6	9	9	3	6	8	9	4	5,67	8,67	8,67	3,67	0,1423
W ₂	8	5	5	9	8	6	4	8	8	5	6	9	8,00	5,33	5,00	8,67	0,145
W ₃	6	8	9	5	5	8	8	4	6	9	8	3	5,67	8,33	8,33	4,00	0,1437
W ₄	3	8	8	3	4	7	7	2	5	8	7	3	4,00	7,67	7,33	2,67	0,1393
W ₅	8	7	8	6	9	6	6	4	7	7	7	5	8,00	6,67	7,00	5,00	0,1466
W ₆	9	8	9	3	9	8	8	2	8	9	8	1	8,67	8,33	8,33	2,00	0,1367
W ₇	7	8	8	6	8	9	8	5	6	9	8	5	7,00	8,67	8,00	5,33	0,1464

The final degree of importance for each supplier characteristic is calculated and normalized as shown in Table 4 below.

Table 4. Final importance ratings

What is (W _m)	Latest Importance Ratings		Scheduled Last Importance Ratings	
	crisp	fuzzy	crisp	fuzzy
W ₁	3,1445	[2,7951, 3,1445, 3,1445]	0,8216	[0,9390, 0,7189, 0,7189]
W ₂	1,9337	[1,6939, 1,9259, 2,0884]	0,5052	[0,3872, 0,4403, 0,4774]
W ₃	2,3704	[2,0364, 2,3596, 2,6828]	0,6193	[0,4655, 0,5394, 0,6133]
W ₄	1,828	[1,4624, 1,8280, 2,1936]	0,4776	[0,3343, 0,4179, 0,5015]
W ₅	1,3684	[1,1495, 1,3547, 1,5600]	0,3575	[0,2628, 0,3097, 0,3566]
W ₆	3,8274	[3,2807, 3,8274, 4,3742]	1,0000	[0,7500, 0,8750, 1,0000]
W ₇	1,7299	[1,4828, 1,7299, 1,9770]	0,4520	[0,3390, 0,3955, 0,4520]

Based on these values, according to their importance, they are listed as follows:

$$W_6 > W_1 > W_3 > W_2 > W_4 > W_7 > W_5$$

In this case, the sixth supplier feature should be the top priority. Subsequently, customer needs for supplier characteristics have been turned into engineering properties. Seven technical requirements have been identified by the client company in order to meet customer needs, taking into consideration the characteristics of the existing and potential supplier companies, and the increase or decrease of these values is specified in Table 5.

Table 5. First technical ratings for how to

how are (H _m)	First Technical Ratings (t _n)	Scheduled First Technical Ratings
H ₁	67,73	0,55
H ₂	122,11	1,00
H ₃	93,47	0,77
H ₄	94,03	0,77
H ₅	71,86	0,59
H ₆	88,58	0,73
H ₇	54,59	0,45

Based on these values, a sequence as follows according to importance ratings is obtained.
H₂> H₄> H₃> H₆> H₅> H₁> H₇

in order to be able to conduct competitive analysis in technical terms, the values of how all the supplier companies are evaluated are determined. These are presented in Table 6.

Table 6. Values and priorities

how are (H _m)	Measurement Unit	Technical Competitiveness	Priority Rating (zn)
H ₁	%	0,150	
H ₂	\$	0,149	
H ₃	gün	0,150	
H ₄	%	0,150	
H ₅	\$	0,132	
H ₆	km	0,124	
H ₇	yıl	0,145	

The appropriate order has been determined considering the Technical Competition Priority Grade, Target Value and Growth Rate.

H₆> H₂> H₃> H₄> H₅> H₁> H₇

In this case, it is understood that the first factor to be improved and given importance is the distance of the supplier company to the manufacturer. This will greatly assist transport costs, which increase the procurement cost in the supply chain, to reduce other delayed costs. Another important factor is the cost of purchasing the material. For this reason, the supplier firm must first take precautions to reduce the cost of product sales.

Results and Discussion

In this study, the purpose of supplier selection, contribution of quality spread function to supplier selection process was investigated. Work has also been supported by an application example that includes improving the

characteristics of existing suppliers to carry ongoing and regular material and information. It has been determined that the first factor that needs to be improved from the factors considered in the study is the distance of the supplier firm to the manufacturer and the other important factor is the purchase cost of the material.

References

- Akao, Y., 1990, Quality Function Deployment- Integrating Customer Requirement in Product Design, Productivity Press, Massachusetts, p. 60-61.
- Akbaba, A., "Quality Function Immersion Method and Application to Service Enterprises", Journal of Dokuz Eylül University Social Sciences Institute, Volume 2, No 3, 1-3, 2000.
- Bergquist, K., Abeyssekera, J., "Quality function deployment (QFD) - A means for developing usable products", International Journal of Industrial Ergonomics, 18 (4): 269-275 (1996).
- Bozkurt, R., "Quality in Service Industries" National Productivity Center Productivity Magazine Total Quality Special Issue, 2: 171-212 (1998).
- Mirmahmudoğulları, S., "The Use of Quality Function Spreading in Organizing Supplier Characteristics in the Supply Chain Management Process", M.Sc. Thesis, Gazi University Institute of Science and Technology, Ankara, 2007
- Özdemir, A., "Decision Models in Supplier Choice and an Application Test", Ph.D. Thesis, Anadolu University Institute of Social Sciences, Eskişehir, 2007
- Özel B., 'A Hierarchical Supplier Selection Model with Fuzzy Axiomatic Design Approach', M.Sc. Thesis, Gazi University Institute of Science, Ankara, 2007
- Sevük, A., 1998. An Example for Quality Function Expansion (QFD) Approach in Welding Electrodepositions. Tüsiad Kalder 7th National Quality Congress, Communiqués and Biographies, İstanbul, p. 133-160
- Seyhan, H., "An Investigation of Quality Function Spread and An Application", M.Sc. Thesis, Uludağ University, Institute of Science, Bursa, 2005
- Sohn, S. Y., "Quality function deployment to local traffic accident reduction", Accident Analysis & Prevention, 31 (6): 751-761 (1999).
- Taptık, Y., Keles, Ö., 1998, Quality War Tools, Kalder, İstanbul, p. 110-115

Author Information

Bahar Ozyoruk

Gazi University Faculty of Engineering, Eti Mh. Yükseliş
Sk. No: 5
Maltepe / Ankara.
Contact e-mail: bahar@gazi.edu.tr

Adsorption of Heavy Metals using Banana Peels in Wastewater Treatment

Leong KOK SENG

Polytechnic Tun Syed Nasir Syed Ismail

Abstract: Heavy metal contaminants are present in wastewater from many industries such as metal manufacturing, dye and paint, chemicals and fertilizer. Heavy metal removal has become the main priority for the environmental concern due to the toxic. Banana peels are a low-cost agriculture waste which could be used for the adsorption of heavy metals in wastewater. Hence, this study focused on the adsorption capabilities of dried banana peels powder under various conditions such as the effect of agitation speed, temperature and contact time for efficient adsorption rate by using agricultural waste adsorbents which is banana peel (treated by acid and alkali). Although banana is one of the most important commercial crops in the world, most of the edible parts are consumed for its nutrients purpose only rather than using adsorption properties. In that case, the banana peels are used in adsorption of heavy metals where it extract out the Cu and Pb from the waste water from the industries. The findings of this study will contribute to bridging up the gap in knowledge on the potential of using banana peels for promoting in the adsorption process and minimize the effect on the living things caused by the waste water released by the heavy industries. The results from the optimized method revealed the applicability of the method to environmental water samples. This study therefore confirms that banana peel is a promising adsorbent for the removal of heavy metals from industrial effluent.

Keywords: Wastewater

Introduction

Heavy metal contaminants are present in wastewater from many industries such as metal manufacturing, dye and paint, chemicals and fertilizer. Heavy metal removal has become the main priority for the environmental concern due to the toxic. Heavy metals can be a reason to human major health problem because they contain high level of toxicity. Heavy metals are also considered as trace elements because of their presence in trace concentrations in various environmental matrices (Asma et al. 2005).

Water pollution due to development in technology, continues to be of great concern. With increasing generation of heavy metals from technological activities, many aquatic environments face metal concentrations that exceed water quality criteria. Research has been designed to protect the environment, animal and humans. Metal production such as emissions have decreased in many countries due to strict legislation, improved cleaning or purification technology and altered industrial activities, in the recent years (Mridul & Prasad, 2013). Dissipate losses from consumption of various metal containing goods are of most concern, today and in the future. Therefore, regulations for heavy metal containing waste disposal have been tightened.

A significant part of the anthropogenic emissions of heavy metals ends up in wastewater. Major industrial include surface treatment processes contain elements such as cadmium, lead, manganese, copper, zinc, chromium, mercury, arsenic, iron and nickel, as well as industrial products that at the end of their life, are discharged in wastes. Heavy metals are highly dispersed in a wide variety of economically important minerals. They are released to the environment during mineral extraction process. Therefore, mining activities are considered as the primary anthropogenic source of heavy metals (Norton et al. 2004). Major urban inputs to waste water include household effluents, drainage water, business effluents, atmospheric deposition, and traffic related emissions, transported with storm water into the waste system.

Plant materials are mainly comprised of cellulose materials that can adsorb heavy metal cations in aqueous solution. Numerous waste biomass sources are available in nature in which adsorption properties have been reported e.g. rice husk, saw dust, tea and coffee waste, orange peel, peanut shells, activated carbon, dry tree leaves and barks (Asma et al. 2005; Kishore 2008). Out of the wide range of adsorbents, banana peel seems to be good adsorbent and can be used as valuable material for cleaning of water. Biosorbent prepared from banana peels has been reported for the removal of chromium, cadmium and copper ions from aqueous solution. Adsorption of heavy metal ions occur as a result of physiochemical interaction, mainly ion exchange or complex formation between metal ions and the functional groups present on the cell surface.

A material having the capacity or tendency to adsorb other substances or materials is known as an adsorbent. Biosorbents are materials from a biological source which can absorb some things especially pollutants. This biological origin product is of prime interest for the environmental scientist for environment friendly cleansing. Adsorption, ion exchange, and chromatography are sorption processes in which certain adsorbates are selectively transferred from one phase to another phase. Strong biosorbents behavior of certain micro-organisms towards metallic ions is a function of the chemical make-up of the microbial cells. This type of biosorbents consists of dead and metabolically inactive cells (Friis & Myers-Keith, 1986).

Method

Some research about adsorption of heavy metals using low-cost adsorbent carried out. The data was collected from some related topic in websites. The banana peels are selected as a low-cost adsorbent due to its characteristics. The research stated that banana peels contain nitrogen, sulphur, and carboxylic acids; the acids are responsible for the peels' ability to bind the toxic metals and remove them from the water. Because of the high number of these acids in the peels, not only can banana peels remove the contaminants, but they can do it just as well, and in some cases better, than more expensive technological options. Stock solutions (100ppm) and standard solution (5ppm) should be prepared for each copper and lead. The standard solution is prepared from the stock solution that had been done initially with a high concentration of copper and lead. The standard solutions are prepared by adding 1000 ml deionised water to 50 ml of stock solutions. Then, the preparation of solutions should be done with the correct concentration. Solutions that should be prepared are Ethanoic acid at 0.1mole concentrations and sodium hydroxide at 0.1 mole concentration. These solutions will be used in treating the banana peels by soaking the banana peel in the solutions separately for a better adsorption rate on the heavy metals.

Results and Discussion

The effect of temperature on adsorption of copper (II) and lead (II) was studied using different temperature in the range of 30°C to 50°C. Figure 1 shows an increase in percentage removal of copper and lead for treated banana peel with the increase in temperature. Maximum removals of copper were 27.74% for acid treated banana peel and 15.78% for alkali treated banana peel respectively. Therefore, the optimum lead removal efficiency for acid treated banana peels recorded at 40°C with removal percentage of 53.28% while for alkali treated banana peels at 30°C with 26.94%. Therefore, the optimum temperature was selected as 40°C for both treated banana peel in the removal of copper and lead. According to the bold result in table 2,3, and 4, it is the highest among the other even there is reading below it. Some of them are been bold at the first part. The reason for this phenomenon is because the bold part shows the highest reading and it reaches the maximum adsorption at that particular point. In additions, when the rate of the adsorption reaches its maximum point there won't be any adsorption process occurs. Moreover, the value of the adsorption also decreases but not so obvious but slightly due to the absent of the adsorption process.

Table 1. Percentage removal of Cu (II) on treated banana peel (Acid) at various temperature

Variables	Initial Concentration (5ppm)	Contact Time (min)	Temperature (°C)	Final Concentration (ppm)	Removal Percentage (%)
Beaker 1	5	30	30	3.744	25.12
Beaker 2	5	30	40	3.662	26.76
Beaker 3	5	30	50	3.613	27.74

Table 2. Percentage removal of Cu (II) on treated banana peel (Alkali) at various temperature

Variables	Initial Concentration (5ppm)	Contact Time (min)	Temperature (⁰ C)	Final Concentration (ppm)	Removal Percentage (%)
Beaker 1	5	30	30	4.649	7.02
Beaker 2	5	30	40	4.211	15.78
Beaker 3	5	30	50	4.239	15.22

Table 3. Percentage removal of Pb (II) on treated banana peel (Acid) at various temperature

Variables	Initial Concentration (5ppm)	Contact Time (min)	Temperature (⁰ C)	Final Concentration (ppm)	Removal Percentage (%)
Beaker 1	5	30	30	2.399	52.02
Beaker 2	5	30	40	2.336	53.28
Beaker 3	5	30	50	2.381	52.38

Table 4. Percentage removal of Pb (II) on treated banana peel (Alkali) at various temperature

Variables	Initial Concentration (5ppm)	Contact Time (min)	Temperature (⁰ C)	Final Concentration (ppm)	Removal Percentage (%)
Beaker 1	5	30	30	3.653	26.94
Beaker 2	5	30	40	3.801	23.98
Beaker 3	5	30	50	3.825	23.50

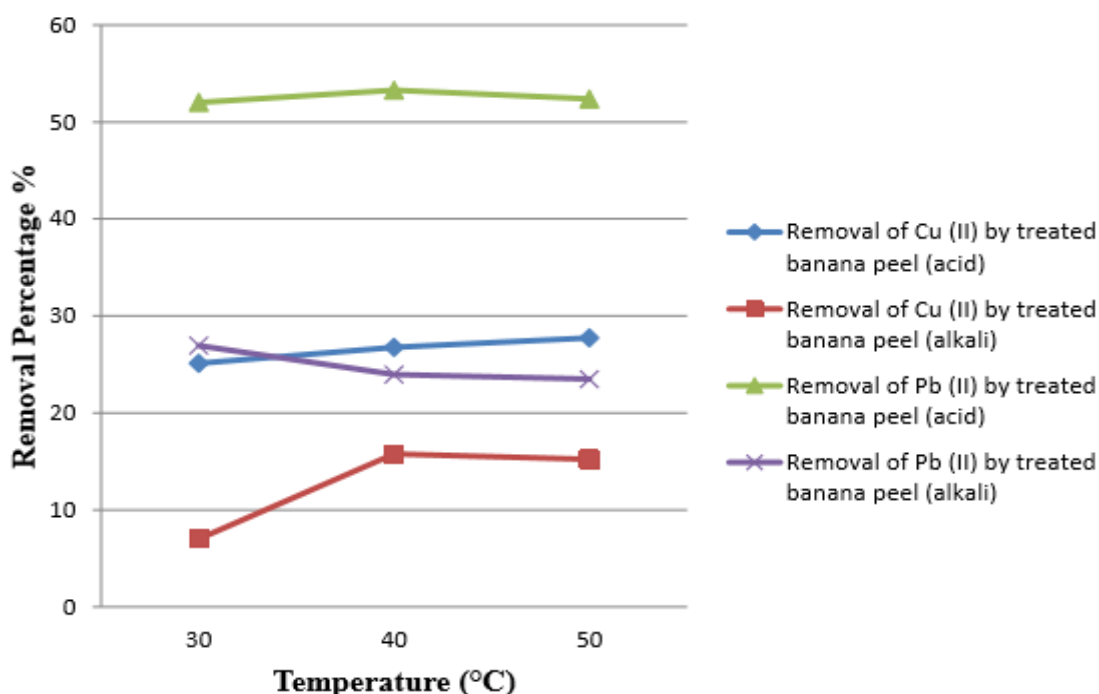


Figure 1. Percentage removal of Cu (II) and Pb (II) on treated banana peel at various temperatures

In Figure 2, it can be observed that agitation speed significantly affects the adsorption of copper (II) ion and lead (II) ion for both samples. The optimum copper removal efficiency for acid treated banana peels recorded at 100 rpm with removal percentage of 25.54% while for alkali treated banana peels at 150 rpm with 16.76%. The optimum lead removal efficiency for acid treated banana peels recorded at 50 rpm with removal percentage of 61.32% while for alkali treated banana peels at 100 rpm with 34.64%. It is proven that agitation speed plays an important role in adsorption efficiency.

Removal occurs only by the above layers and the under buried layers does not take part in the process as they have no contact with copper and lead. This indicates that shaking rate should be sufficient to assure that all the surface binding sites are readily available for copper and lead uptake. Agitation speed of 100 rpm was chosen as the optimum speeds for acid treated banana peels and alkali treated banana peels respectively. According to the

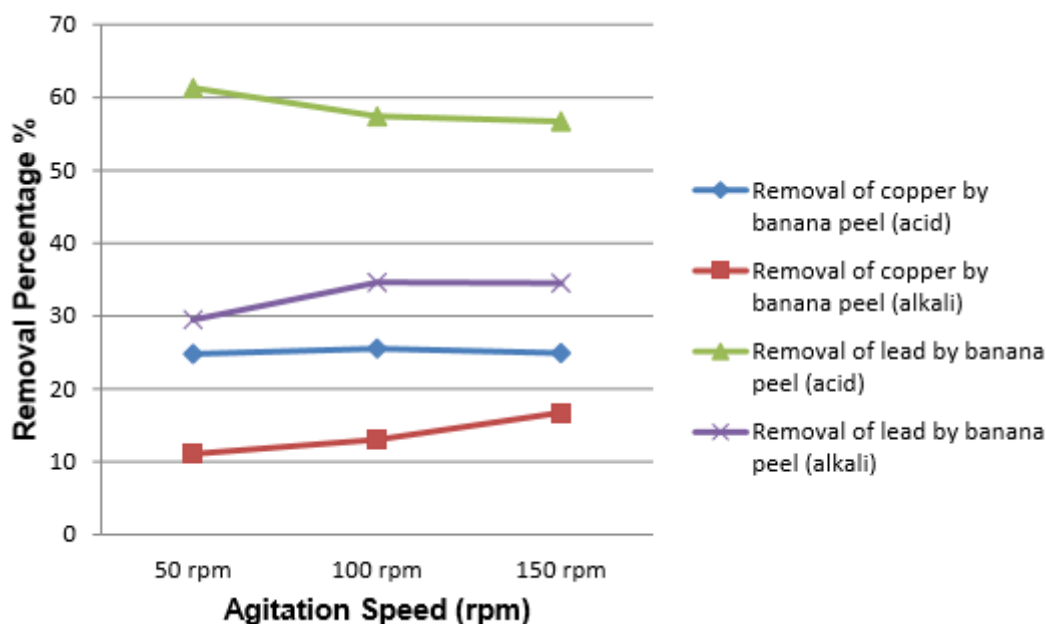
bold result in table 4.1(a), 4.1(c), 4.1(d), it is the highest among the other even there is reading below it. Some of them are been bold at the first part. The reason for this phenomenon is because the bold part shows the highest reading and it reaches the maximum adsorption at that particular point. In additions, when the rate of the adsorption reaches its maximum point there won't be any adsorption process occurs. Moreover, the value of the adsorption also decreases but not so obvious but slightly due to the absent of the adsorption process

Table 5. Percentage removal of Cu (II) on treated banana peel (Acid) at various agitation speed

Variables	Initial Concentration (5ppm)	Contact Time (min)	Agitation Speed (rpm)	Final Concentration (ppm)	Removal Percentage (%)
Beaker 1	5	30	50	3.759	24.82
Beaker 2	5	30	100	3.723	25.54
Beaker 3	5	30	150	3.753	24.94

Table 6. Percentage removal of Cu (II) on treated banana peel (Alkali) at various agitation speed

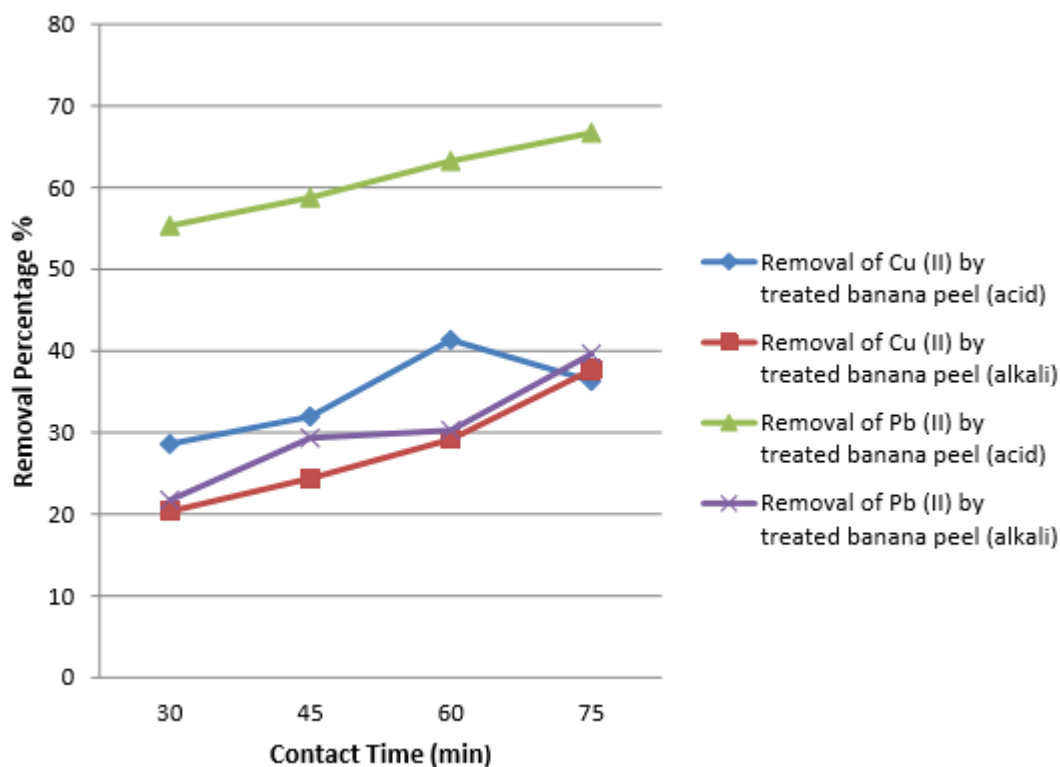
Variables	Initial Concentration (5ppm)	Contact Time (min)	Agitation Speed (rpm)	Final Concentration (ppm)	Removal Percentage (%)
Beaker 1	5	30	50	4.445	11.10
Beaker 2	5	30	100	4.347	13.06
Beaker 3	5	30	150	4.162	16.76



Based on Figure 4.3 the removal percentages for Cu (II) and Pb (II) on adsorbents are increasing as the contact time increase. The optimum contact time for acid treated banana peels in the removal of copper take place at 60th minutes with removal percentage of 41.36% while for alkali treated banana peels in the removal of copper take place at 75th minutes with removal percentage of 37.70%. In the removal of lead, the optimum contact time for acid treated banana peels take place at 75th minutes with removal percentage of 66.72% while for alkali treated banana peels take place at 75th minutes with removal percentage of 39.66%. The removal efficiency increased with increased of contact time for both samples. This can be attributed to the fact that more time becomes available for copper ions and lead ion to make an attraction complex with adsorbents.

Initial removal occurs immediately as soon as the copper or lead and adsorbents came into contact. But after some time, when some of easily available active site engaged, copper and lead needs time to find out more active sites for binding. Therefore, it is concluded that copper or lead and adsorbent should be contact for 75 minutes for acid and alkali treated banana peels respectively in order to get high removal percentage. According to the bold result in table 4.3(a), it is the highest among the other even there is reading below it. The reason for this phenomenon is because the bold part, which is the third beaker, it reaches the maximum adsorption at that particular point. In additions, when the rate of the adsorption reaches its maximum point there won't be any

adsorption process occurs. Moreover, the value of the adsorption also decreases but not so obvious but slightly due to the absent of the adsorption process.



Conclusion

In conclusion, the researchers had explained the promising parameters and either acid or alkaline should be used over a banana peel so that it can act as a better low cost adsorbent to adsorb heavy metals (copper (II) and iron (II)) from the industrial wastewater. The procedures can be applied in most of the heavy metal industries to treat their wastewater before the discharged it into the big sea where it might affect the humans back.

Recommendations

The present study can be used to conclude that non-hazardous agricultural waste materials such as banana peel is excellent substitutes for non-economic adsorbents such as activated carbon and silica for removal of heavy metals. Therefore, more studies and research should be done to enhance the adsorption capacity using these adsorbents. The effect of temperature, pH and adsorbent size should be studied as it can alter the adsorption rate and mechanisms. Furthermore, the effectiveness of these adsorbents on removal of other types of heavy metals such as iron (II) oxide and zinc could be explored.

References

- References and citations should be prepared in the latest APA (<http://owl.english.purdue.edu/owl/resource/560/02/>) format. References have to be cited in article text. See the references examples below.
- Angeli, E., Wagner, J., Lawrick, E., Moore, K., Anderson, M., Soderland, L., & Brizee, A. (2010, May 5). General format. Retrieved from <http://owl.english.purdue.edu/owl/resource/560/01/>
- Calfee, R. C., & Valencia, R. R. (1991). *APA guide to preparing manuscripts for journal publication*. Washington, DC: American Psychological Association.
- Duncan, G. J., & Brooks-Gunn, J. (Eds.). (1997). *Consequences of growing up poor*. New York, NY: Russell Sage Foundation.

- Harlow, H. F. (1983). Fundamentals for preparing psychology journal articles. *Journal of Comparative and Physiological Psychology*, 55, 893-896.
- Helfer, M. E., Kempe, R. S., & Krugman, R. D. (1997). *The battered child* (5th ed.). Chicago, IL: University of Chicago Press.
- Henry, W. A., III. (1990, April 9). Making the grade in today's schools. *Time*, 135, 28-31.
- Lastname, F. N. (Year). Title of dissertation. (Doctoral dissertation). Retrieved from Name of database. (Accession or Order Number)
- Lastname, F. N. (Year). Title of dissertation. (Unpublished doctoral dissertation). Name of Institution, Location.
- O'Neil, J. M., & Egan, J. (1992). Men's and women's gender role journeys: A metaphor for healing, transition, and transformation. In B. R. Wainrib (Ed.), *Gender issues across the life cycle* (pp. 107-123). New York, NY: Springer.
- Plath, S. (2000). *The unabridged journals*. K. V. Kukil (Ed.). New York, NY: Anchor.
- Schnase, J. L., & Cunniss, E. L. (Eds.). (1995). *Proceedings from CSCL '95: The First International Conference on Computer Support for Collaborative Learning*. Mahwah, NJ: Erlbaum.
- Schultz, S. (2005, December 28). Calls made to strengthen state energy policies. *The Country Today*, pp. 1A, 2A.
- Scruton, R. (1996). The eclipse of listening. *The New Criterion*, 15(30), 5-13.

Author Information

Leong Kok Seng

Polytechnic Tun Syed Nasir Syed Ismail

Malaysia

Contact: kokseng@ptsn.edu.my

The Eurasia Proceedings of Science, Technology, Engineering & Mathematics (EPSTEM), 2018

Volume 2, Pages 318-322

ICRES 2018: International Conference on Research in Education and Science

UDC 662.33 Experimental Determination of the Sulfur Content in the Shubarkol Coal

Tateyeva A.B.

Y.A.Buketov Karaganda State University

Baikenov M.I.

Y.A.Buketov Karaganda State University

Muratbekova A.A.

Y.A.Buketov Karaganda State University

Nesipbayev D.M.

Y.A.Buketov Karaganda State University

Nesipbayev B.M.

Y.A.Buketov Karaganda State University

Abstract: The sulfur content of the Shubarkol coal of the Karaganda coal basin was determined experimentally. The methods for determining the content of total sulfur, inorganic (sulfate) sulfur, inorganic (pyrite) sulfur are given.

Keywords: Shubarkol coal, Pyrite sulfur, Sulfate

Introduction

The combustion of coal is accompanied by evolution of sulfur compounds which corrode equipment as well as pollute the environment [1-4]. The coke sulfur worsens its quality as a metallurgical fuel, since in the blast furnace it goes into cast iron, giving it fragility and lowering the quality of the steel obtained from it.

According to the content of sulfur (S,%), coal is classified into: low sulfur –from 0,5 to 1,5; mid-sulfur –from 1,6 to 2,5; sulphurous from –2.6 to 4.0; high-sulfur coal more than 4,0

Determination of the total sulfur content.

The method is based on burning of the fuel sample with a mixture of magnesium oxide and sodium carbonate (Eshka mixture), by further dissolving the formed sulfates, on precipitating sulfate ions with barium chloride in a hydrochloric acid medium in the form of barium sulphate and on determination its weight.

Chemicals and Instruments

Muffle furnace with heating temperature up to 900 ° C.

The ceramic plate or is made of heat-resistant metal, length and width in accordance with the muffle working space the thick is 5 mm.

Porcelain crucibles in accordance with Standard 9147-59.

Glasses for weighing (boxes) in accordance with Standard 7148-70.

Hydrochloric acid in accordance with Standard 3118-67, diluted 1: 1.

- This is an Open Access article distributed under the terms of the Creative Commons Attribution-Noncommercial 4.0 Unported License, permitting all non-commercial use, distribution, and reproduction in any medium, provided the original work is properly cited.

- Selection and peer-review under responsibility of the Organizing Committee of the Conference

Mixture Eshka according to the Standard 5144-69.

Barium chloride according to the Standard 4108-65, a solution of 100 g / l.

Silver nitrate according to the Standard 1277-63, 3% solution, acidified with nitric acid.

Methyl orange (para-dimethylaminoazobenzenesulfonic acid sodium) according to the Standard 10816-64, 0.1% solution.

Materials and Methods

A sample of 0.5 g of coal (with a sulfur content up to 15% in fuel) is placed to a porcelain crucible in which 2 g of Eshka mixture is weighed with high accuracy, then are thoroughly mixed and another 1 g of Eshka mixture is added. The crucible with the fuel sample is placed in a preheated to 850 ± 25 ° C muffle furnace, pushing the plate into the zone of maximum heat for 3 minutes, and calcined at this temperature for 30 minutes.

The crucible with a sample of Shubarkol coal is placed in a cold muffle furnace, which is heated gradually, for at least 1 hour, to 850 ± 25 ° C. The calcination is continued at this temperature for 30-40 minutes.

Further, the mixture in the crucible are cooled, loosened and transferred to a 150 ml beaker, then 100 ml of hot water is added by washing the inner walls of the crucible and is heated to boiling. Provided that unburned coal particles are found that float to the surface, the burning of a new sample is repeated.

The solution above the precipitate is decanted through a filter into a 600 ml beaker.

The precipitate is washed three times with hot water, decanting the settled liquid in the same beaker. The precipitate is then transferred to a filter and washed thoroughly with a hot water jet from the wash-bottle. The total volume of the solution should not be more than 300 ml.

To the solution, is added 2-3 drops of methyl orange indicator and diluted 1: 1 of hydrochloric acid until the color of the indicator changes to pink. The solution is heated to boiling and 10 ml of a barium chloride solution is added in small portions with stirring. The solution with the precipitate of barium sulphate is aged for at least 30 minutes in a boiling water bath or on a sand bath at a temperature close to the boiling point.

The liquid that has settled in the beaker is filtered through a dense ashless filter, the precipitate is transferred to the same filter and washed with hot water until the chlorine ions are completely removed (sample with silver nitrate).

The filter with the precipitate is placed in the pre-calcined to constant weight crucible, slightly compacted, charred, without allowing the filter to ignite, and calcined in a muffle furnace at a temperature of 800 ± 25 ° C for 15-20 minutes. Then the crucible with the contents is cooled in air and weighed.

The content of total sulfur in the analytical sample of coal (S_{tot}) in percent is calculated by the formula:

$$S_{06}^a = \frac{(G1-G2)*0.1373*100}{G},$$

where, G1 is the mass of barium sulfate obtained by analyzing the test coal, g;

G2 is the mass of barium sulfate obtained in the control experiment, which should not exceed 0.005 g, g;

G - weight of coal, g;

0.1373 - coefficient of conversion of barium sulfate to sulfur.

Substituting the obtained values, we have:

$$S_{tot}^a = \frac{(0,024-0,005)*0,1373*100}{0,5} = 0,5$$

Determination of the Content of Inorganic (Sulfate) Sulfur

The method is based on dissolving the sulfates contained in the fuel in dilute hydrochloric acid, precipitating the sulfate ions with barium chloride in the form of barium sulphate and by weighing of the latter.

Chemicals and instruments

The apparatus and reagents specified at first experiment are used during this analyze, with the exception of the Eshka mixture, and in addition:

acid hydrochloric in accordance with Standard 3118-67, diluted 1: 7 and 1:20;

Ammonia water according to Standard 3760-64, diluted 1: 1;

water bromine, 3% solution.

Analysis Methods

A sample of 1 g coal is placed in a beaker, 100 ml of diluted 1: 7 hydrochloric acid is added, the solution is boiled for 10 minutes and filtered through a uncompact filter. The precipitate on the filter is washed 5-6 times with a dilute 1:20 hydrochloric acid solution.

1 ml of the bromine water is added to a filtrate (200-250 ml) and is boiled for 5 minutes, then is added dilute ammonia until precipitation formation. The solution is filtered through a filter. The precipitate on the filter is washed with hot water until disappearing of chloride ion (sample with silver nitrate). The filtrate is evaporated to a volume of 200-250 ml, 2-3 drops of a methyl orange indicator are added, then diluted 1: 1 with hydrochloric acid until the color of the indicator changes to pink, and then continues as indicated in 2.2.1.

Processing of Results

The content of sulfate sulfur in the analytical sample of coal (S_c) in percent is calculated by the formula:

$$S_c^a = \frac{(G1-G2) \cdot 0.1373 \cdot 100}{G},$$

where, G1 - mass of barium sulphate, obtained in the analysis of the test fuel, g;

G2 - is the mass of barium sulfate obtained in the control experiment, which should not exceed 0.005 g, g;

G - weight of coal, g;

0.1373 - coefficient of conversion of barium sulfate to sulfur.

The content of sulfate sulfur in the analytical sample of Shubarkol coal (S_c) is:

$$S_c^a = \frac{0,02 - 0,005 \cdot 0,1373 \cdot 100}{1} = 0,2$$

Determination of the Content of Inorganic (Pyrite) Sulfur

The method is based on the oxidation of pyrite sulfur with nitric acid to soluble sulfates and its determination by titrimetry on the pyrite iron.

Chemicals and Instruments

The apparatus and reagents specified at first experiment are used during this analyze, with the exception of the Eshka mixture, and in addition:

shaker;

acid hydrochloric in accordance with standard 3118-67, diluted 1: 7;

acid nitric according to the standard 4461-67, solution with a density of 1.2g / cm³;

hydrogen peroxide (perhydrol) according to standard 10929-64;

ammonia aqueous according to standard 3760-64;

potassium iodide in accordance with standard 4232-65, a solution of 200g / l;

sodium sulfate (sodium thiosulfate) according to standard 4215-66, 0.05 n solution;

starch, soluble according to standard 10163-62, freshly prepared solution of 10g / l.

Analysis Methods

A sample of Shubarkol coal with a mass of 1 g is placed in a beaker with a capacity of 300-500 ml, 100 ml of dilute hydrochloric acid are poured, covered with a watch glass, the contents are boiled for 10 minutes and filtered through a dense filter. The filter precipitate is washed 4-5 times with hot water. The filter with the precipitate is placed in a beaker in which the sample is treated with hydrochloric acid, 80 ml of nitric acid are added, mixed thoroughly and left for 24 hours.

For accelerated oxidation, the precipitate is placed in a flask with a capacity of 200-300 ml then 80 ml of nitric acid is added, the flask is closed with a well-fitted stopper and agitated on the shaker for 2 hours.

The insoluble residue is filtered onto a medium-density filter and is washed 7-8 times with hot water. The filtrate and washings are collected in a single beaker. If the filtrate is colored in a brown color, 3 ml of hydrogen peroxide is added and boiled to discoloration and termination of the release of bubbles. Further, to a boiling light filtrate, ammonia is poured into a stable weak odor and another 5 ml into excess. The precipitate of the iron oxide hydrate is filtered onto a medium-density filter and washed with hot water with a few drops of ammonia.

The precipitate on the filter is dissolved by hot dilute 1: 7 with hydrochloric acid and washed 5-6 times with hot water. The filtrate and washings are collected in a conical flask. The solution in the flask is neutralized with ammonia, adding it dropwise until a precipitate appears. Then 10 ml of diluted 1: 7 hydrochloric acid, 10 ml of potassium iodide solution are added to the solution, cover the flask with a watch glass and put in a dark place for 5 minutes. The formed out iodine is titrated with sodium thiosulfate before the color transition into a straw-yellow color, the starch solution is added and the titration is finished after the discoloration of the solution.

Processing of results.

The content of pyrite sulfur in the analytical coal sample (S_{ka}) in percent is calculated by the formula:

$$S_{ka}^a = \frac{n \cdot (V - V_1) \cdot 0.064 \cdot 100}{G},$$

where, n is the normality of the sodium thiosulfate solution;

V is the volume of sodium thiosulfate solution used for titration, ml;

V₁ is the volume of sodium thiosulfate solution used for titration in the control experiment, ml;

G - fuel sample, g;

0.064 - the amount of sulfur corresponding to 1 ml of a 1N solution of sodium thiosulfate, g.

The content of pyrite sulfur in the analytical sample of Shubarkol coal is:

$$S_{ka}^a = \frac{0.004 \cdot (5 - 2.5) \cdot 0.064 \cdot 100}{1} = 0.06$$

The content of organic sulfur in the analytical sample of coal (S_{opa}) in percent is calculated by the formula:

$$S_{opa}^a = S_{ob}^a - (S_c^a + S_{ka}^a),$$

where, S_{ob}^a - the total sulfur content in the analytical fuel sample, %;

S_c^a - content of inorganic (sulfate) sulfur in the analytical sample of coal, %;

S_{ka}^a - content of inorganic (pyrite) sulfur in the analytical sample of coal, %;

$$S_{opa}^a = S_{ob}^a - (S_c^a + S_{ka}^a)$$

The content of organic sulfur in the analytical sample of Shubarkol coal (S_{opa}) is:

$$0.5 - (0.2 + 0.06) = 0.26$$

High sulfur content in coals worsens their quality, causes a significant increase its cost and the risk of pollution of the environment with toxic sulfur oxides during energy use, and coking deterioration in the quality of coke and an increase in its consumption in the smelting of pig iron. For example, an increase in the sulfur content of coal by 0.1% leads to a decrease in the productivity of the blast furnace and an increase in the consumption of coke (by 1.8%). On the other hand, coals represent one of the main potential sources of raw sulfur. Desulfurization of coals is considered as a way of solving these two problems.

Reference

- State standard 30404-2013 (ISO-157:1996) /Топливо твердое минеральное. Solid mineral fuel. Determination of forms of sulfur/ 2013г
- Saranchuk V. I., Oshovsky V.V., Vlasova G. A.(2009) «Physical-chemical basics of fuel processing».
- Danilov A. P., Danilov S. A., Danilov I.A. (2010). Processing method of coal containing sulfur. Patent 2405026. /27.11.2010

Author Information

Tateyeva A.B.

Candidate of Chemical Sciences, Professor of the Chemical Technology and Petrochemistry Department
academician Y.A. Buketov
Karaganda State University
Universitetskaya street 28, Karaganda
Contact e-mail: almatateeva@mail.ru

Baikenov M.I.

Doctor of Chemical Sciences, Head of the Chemical Technology and Petrochemistry Department
academician Y.A. Buketov
Karaganda State University
Universitetskaya street 28, Karaganda

Muratbekova A.A.

Candidate of Chemical Sciences, Associate Professor of the Chemical Technology and Petrochemistry Department
The Karaganda State University of the name of academician E.A. Buketov
Universitetskaya street 28, Karaganda

Nesipbayev D.M.

Master student of the academician Y.A. Buketov
Karaganda State University
Universitetskaya street 28, Karaganda
The Karaganda State University of the name of academician E.A. Buketov
Universitetskaya street 28, Karaganda

Nesipbayev B.M.

Master student of the academician Y.A. Buketov
Karaganda State University
Universitetskaya street 28, Karaganda
The Karaganda State University of the name of academician E.A. Buketov
Universitetskaya street 28, Karaganda

Numerical Flow Analysis of The Variation of Central Axial Velocity Along The Pipe Inlet

Hasan DUZ

Batman University

Abstract: Due to no slip flow condition at the wall, the fluid enter the pipe with a smooth velocity start to develop along the flow to comply the zero velocity at the wall and maximum at the pipe center. After a certain distance where the development completed, the velocity profile becomes fully developed and no longer changes observed along the pipe flow. The region flow where the velocity profile develops is called developing flow or inlet flow and the region flow where the fully developed profile govern are called fully developed flow. Computation of the flow properties in the fully developed region can be enabled with various empirical theories, but the complex flow structure in pipe inlet region still has not been solved exactly. However It is quite important to know the flow behavior at the pipe inlet to compute the right pumping power especially in the fluid heating and cooling short pipe flow processes. the study performed, the steady pipe flows with Newtonian fluid were simulated numerically at low Reynolds numbers (ranged 1000 and 25000) covering the three flow regimes (laminar, transition and turbulence). High turbulence level and smooth velocity profile were assigned to the flow at pipe inlet. Turbulence flows were solved according to the time mean flow assumption. On the numerical results obtained, the variation of axial central velocity along the flow was examined for different relative roughnesses. Consequently, a numerical correlation which define the axial velocity and fit the numerical values well is proposed.

Keywords: Entrance length, Pipe flow, Developing flow

Introduction

Osborne Reynolds (1842-1912) has discovered laminar and turbulent flow behavior by injecting ink into glass-tubular flow in his experiments. At low flow velocities the ink followed a uniform flow path and not mixed to the flow along, while at high flow velocities the ink mixed with the flow over the entire cross section as in the move downstream. In the laminar flows, due to low flow velocity, fluid particles follows a smooth flow path, for this reason the laminar flows is smooth. Whereas in the turbulent flow, the instabilities in the flow cause the flow to get mixed in so that the fluid particles do not follow a uniform flow path. In general, all flows must be laminar, however some factors that degrade the flow stability, such as surface roughness, upstream turbulence, and heat transfer in the flow, force the flow to be turbulent. For this reason, if precise flow conditions are provided, all flows will remain laminar (Özışık, 1985). Turbulent flows include fluid clusters that are formed continuously near the wall and move during the flow while spin its around. These moving fluid clusters are called turbulent structures or swirl motions. These vortex structures form continuously near the wall, move, divide and disperse in the flow and eventually turn into sensible heat in the flow then disappears. They are responsible of the conversion of some of the mechanical energy into sensible heat energy. This describe why the energy loss is greater in turbulent flows. For example, especially for flows over a solid surface (flow through aircraft, turbine, and compressor blades) the flow being turbulent not only increases energy loss but also create vibration and noise in the flow. As a result, in addition to the viscous forces in the turbulent flow, there are also additional drag forces, so that the energy losses in turbulent flows are much higher than laminar flows of which viscous forces are dominated. For the flows over a flat surface, flow first begins as laminar in the leading edge and a certain distance away from the inlet the flow stability is deteriorated and it become a turbulent flow structure. Figure 1 illustrate three stages of the fluid flowing over the inside surface of a pipe as being laminar,

- This is an Open Access article distributed under the terms of the Creative Commons Attribution-Noncommercial 4.0 Unported License, permitting all non-commercial use, distribution, and reproduction in any medium, provided the original work is properly cited.

- Selection and peer-review under responsibility of the Organizing Committee of the Conference

transient and turbulent. The flow distance from the pipe inlet to the location where the flow first disturb to turbulent is called the transition length (L_t). After transition length, a transitional flow region occur for a while then the flow becomes fully developed. The measured distance from inlet to where the flow to become full turbulent is called entrance length. It is seen in many experimental works that the flow distances is depend on the flow velocity, surface roughness, free stream turbulence, surface vibrations, and heating and cooling processes (Minkowycz et al. (2009), Zanoun et al. (2009)). Though some empirical correlations are proposed for both flow distances through the experiments, a general solution to the problem is not still be clarified well due to many parameters effects on the flow.

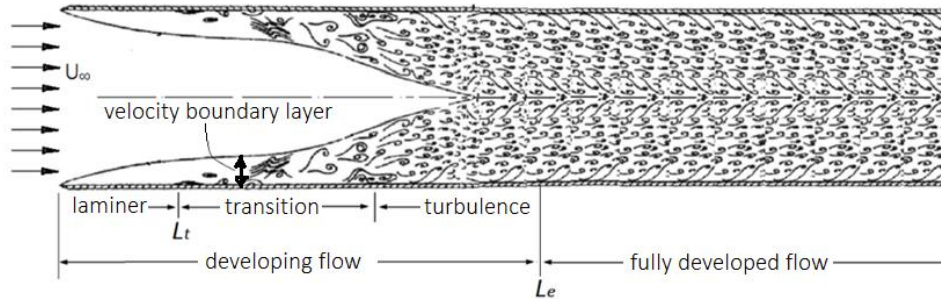


Figure 1. Developing and fully developed flow at pipe entrance

According to experimental studies, when a flow, contain high freestream turbulence level, pass over a full roughly surface, transition length lasted up at $Re_t = 10^5$ but for a flow not contained any turbulence in the freestream pass and over a smooth flat surface it lasted up to $Re_t = 10^6$ as measured in the experiments (Özişik (1985)). In case pipe inside flow study, due to pipe diameter limit the flow peripheral, transition distance from laminar to turbulence is being different than the flows over flat surfaces. Fig. 2 has shown the flow development after pipe inlet. The velocity boundary layer that forms as the result of the viscous effects from the pipe inlet, thickness of it increase along the inlet and since the thickness is limited by the pipe radius, the entire flow cross-section is filled with the boundary layer. From the pipe inlet, the viscous effects begin to change in the resulting velocity profile. This velocity profile changes along the flow until it become a constant velocity profile. The flow region where the velocity profile changes is called inlet flow or developing flow. The pipe flow, in which the velocity profile is along constant, is called the fully developed pipe flow. Different definitions are also available in the literature for fully developed pipe flow. For example, fully developed flow begins when such like two flow properties, wall shear stress or mean turbulent flow statistics reach the constant values (Anselmet et al. (2009), Patel&Head (1969)). Therefore, Zimmer et al. (2011) said that it should be required to define the fully developed flow as a flow that starts when the time-averaged turbulence flow statistics become constant. In the author's experimental study, it was reported that the developing flow distance is even longer when turbulence statistics measurements are based.

Along the fully developed pipe flow, the wall shear stress and the friction factor are constant since the pressure drop is linear. The fully developed laminar or turbulent pipe flows are largely solved with theoretical and empirical relations, while the developing flow portion has still not been fully solved. In engineering applications, pipe-tank connections generally become conical (bell mouth), square edged and reentrant. while a sharp edged inlet produce much turbulence in the flow, bell mouth inlet produces minimal turbulence. The amount of turbulence goes to pipe at the inlet is effect on the transition and entrance lengths (Tam et al. (2013), Augustine (1988)). It is evident that the transition and inlet lengths with high turbulent inlet are shorter than with the low turbulent inlet. Table 1 gives the entrance lengths reported in experimental studies of pipe flows.

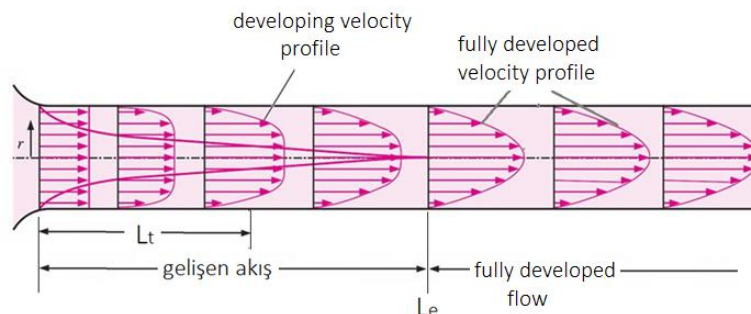


Figure 2. Variation of velocity profile along the developing and fully developed flow

Table 1. Dimensionless entrance lengths reported by the experimental studies

Dimensionless Entrance Length (L/D)			
Constant wall shear stress	Mean turbulent statistics	Reynolds Number	Author
80		-----	Osborne Reynolds
$L_e/D = 2.09 \times 10^{-8} * Re^{-1.66}$		5000-15000	Augustine (1988)
$L_e/D = 1.6 Re^{1/4}$		10 ⁵ - 10 ⁶	Anselmet et al. (2009)
$L_e/D = 4.4 Re^{1/6}$			
A long Empirical formula		1,95 x 10 ⁵	Salami (1986)
25 - 40		3x10 ³ - 3x10 ⁶	Nikuradse (1966)
30		5x10 ⁴ - 5x10 ⁵	Laufer (1954).
50 - 80		10 ³ - 10 ⁴	Patel & Head (1969)
70		3x10 ⁴ - 1x10 ⁵	Zanoun et al. (2009)
-----	72	175000	Perry & Abell (1978)
50	80	1x10 ⁵ - 2x10 ⁵	Doherty et al. (2007)
Not attain to 40		388000	Barbin&Jones (1963)
	70	1.5x10 ⁵ - 8.5x10 ⁵	Zimmer et al. (2011)

Numerical Study

Firstly, in order to gaining a validation to numerical solution, an experimental study has been carried out with four pipe types which is made of different materials. The selected pipe types, their relative roughness and pipe diameters are given in Table 2. Here it was aimed to see the effects of different relative roughness on flow conditions. The relative roughness of pipes, which is given in Table 2, was measured through the experimental work in which the pressure differences in the fully developed flow region is measured.

Static pressures were measured trough piezometres tubes fitted on pressure taps, which was welded to the holes drilled at seven different locations on the pipe. Pipe flows at each flow rate were recorded by a camera for three minutes. Time mean values of pressures are obtained for each pressure taps from each flow record. The pressure values obtained from the numerical flows, which are parallel to experiment, are compared with the pressure values of the experiment as shown in Fig.3.

Table 2. Pipe type, relative roughnesses and diameters

Pipe Type	Diameter (mm)	Relative roughness ϵ / D
Aluminium pipe	26	0,0016
Copper Pipe	26	0,00016
Steel Pipe	28	0,0024
Galvanized Pipe	28	0,0026
PPRC pipe	21	0,00033

Numerical Solution and Validation

Basically, fluid flows are defined by differential flow equations which is a results of mass, momentum and energy conservation. For this reason, the flow field in turbulent flows shows a continuous change temporarily and spatially. The time-dependent solution of a turbulent flow is difficult since it requires a solution of turbulence structures in time-dependent development that is available in the flow in a wide range. The numerical method used to solve the time-dependent fundamental flow equations of a turbulent flow is called direct

numerical simulation (DNS). The solution is not possible with today computers except that of very simple flows. Since solution is required very large mesh numbers and time steps.

An another method suggested for the solution of turbulent flow is to get the instantaneous effects of the flow into time average effect. By this way, turbulent flows become time independent flows. The instantaneous drags existed by the turbulent structures against the flow form additional stresses in the time-averaged basic flow equations. These stresses are called Reynolds stresses or turbulent stresses. The existed time averaged conservation equations are called Reynolds averaged Navier-stokes equations (RANS). Only unknown in RANS equations is the Reynolds stresses. Therefore many turbulence models are developed to solve these Reynolds stresses. The solution of a turbulent flow with RANS equations is simple and the cost of numerical computation is very low in comparison to the DNS method.

In this study, turbulent pipe flows are solved via computer by applying finite difference numerical method to RANS equations to each flow field point. SST k-omega model are selected to solve the Reynolds stresses. To provide laminar to turbulent transition, Gamma-Theta model is selected. The pipe length has been selected long enough to cover the fully developed flow partly. Since the pipe flow is axis symmetrical, the flow area is limited to a small flow area sliced. The boundary conditions, fluid properties and flow type are defined in Table 3 below.

As shown in table 3, after setting up of boundary condition, flow and fluid properties, pipe flows are solved with CFX flow solver program. Numerical flows are kept parallel with experimental flows. As a result, the flow characteristics such as pressure, velocity, friction factor and wall shear stress were analyzed along the flow. Numerical and experimental values were compared each other in order to gain validity to numerical solution. The experimental and numerical values are compared in Fig 3 in terms of the pressure drop along the flow including all flows of each pipe type. As shown in Fig. 3, experimental values and numerical values are in well agree. The mean and maximum deviations of the numerical values from the experimental ones are given in Table 4 also. As can be seen in Table 4, numerical values of all pipe flows has deviated from the experimental values about 7-9% in average. The deviation amount is a tolerable one since it is natural to have such a deviation. Because physical conditions such as fluid temperature can not be precisely determined and faults that occur in flow measurements and in static pressure readings in experimental runs are thought to be caused by these deviations. For this reason, flow characteristics are analyzed by means of numerical data as given below.

Table 3. Boundary conditions and flow field properties

	Numerical properties
<i>Flow state</i>	Steady-state, incompressible and isothermal flow
<i>Basic flow equations</i>	RANS Equations
<i>Turbulence model</i>	SST k-omega model
<i>Pipe inlet</i>	Smooth velocity and high turbulent intensity (T_U) = %7
<i>Pipe wall</i>	roughly
<i>Pipe outlet</i>	Open to atmosphere at gauge pressure
<i>fluid</i>	27 °C water

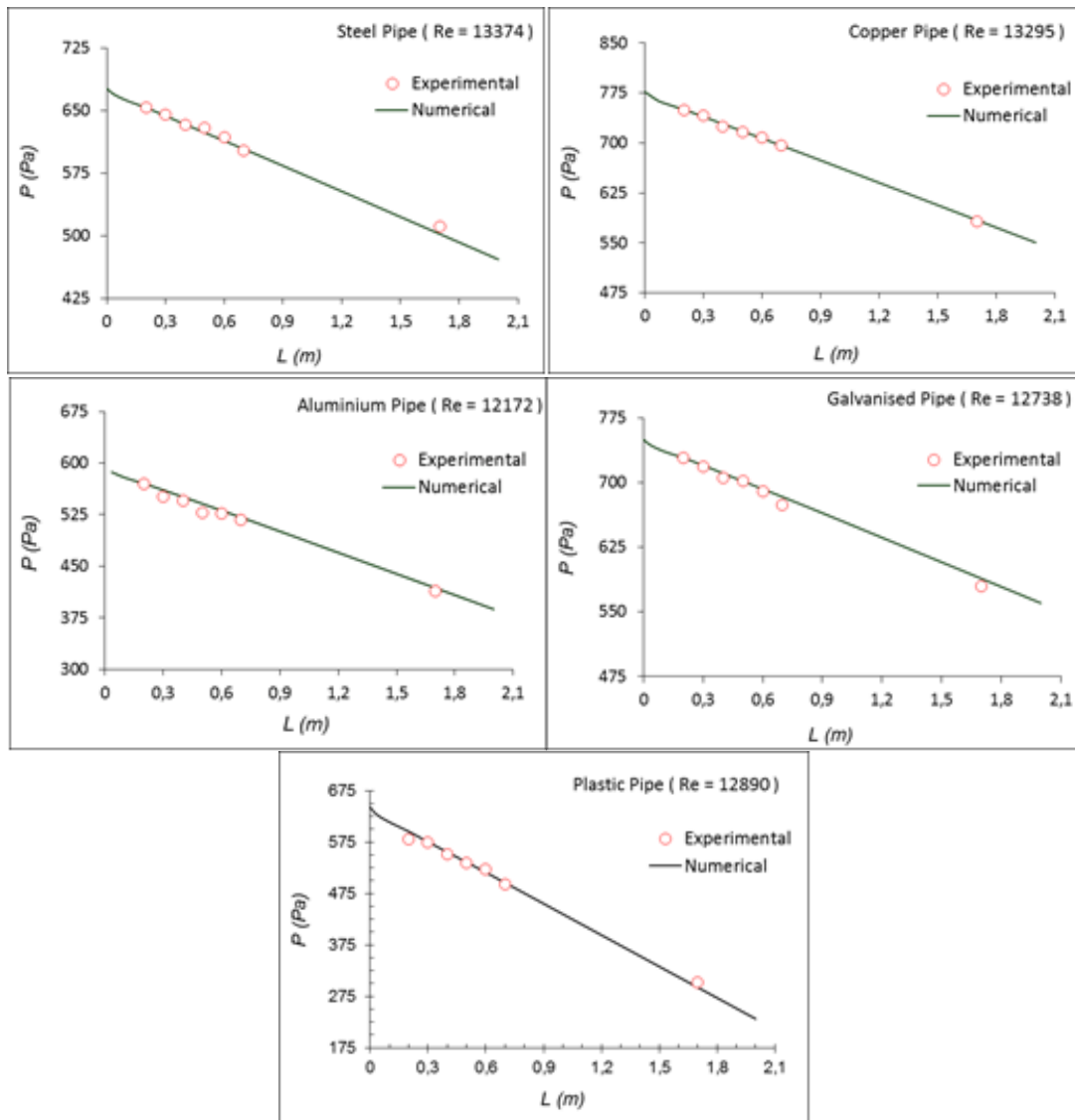


Figure 3. Comparison of numerical results with experimental data

Table 4. Percent deviation of numerical values from experimental data in terms of pressure variation along the flow

Deviation (%)	aluminium pipe	copper pipe	commercial steel pipe	galvanised pipe	Plastic pipe
maximum	±%20	±%24	±%36	±%35	±%18
average	%7.30	%7.70	%7.60	%9.40	%9

Numerical Analysis

In this section, the variation of central axial velocity in the pipe flows from the pipe inlet to fully developed flow is analyzed numerically. In this numerical study, pipe flows were performed with five pipe types at Reynolds numbers ranging from 2000 to 25000. The aim here is to examine the flow properties at low Reynolds numbered pipe flows where the transitional flow regime dominates. The uncertainty of the flow behavior, particularly at low Reynolds numbers, has led to prefer high Reynolds numbers in the design of heat exchangers pipe flows. In turbulent pipe flows with high Reynolds numbers, pressure losses are high and as well as energy consumption. Reducing fossil-based energy consumption for a cleaner environment has now become an obligation. In addition, reducing energy consumption also lowers the cost of energy consumption. The transition flow regime should be learned very well so that the designs of heat transfer also cover the low Reynolds numbered pipe flows. For this reason, more numerical and experimental studies are needed.

In this numerical study, a high turbulent flow presence at the conical pipe inlet is simulated along the downstream of the pipe flow. Therefore, a conical inlet and high turbulent free stream is the limitation of this numerical study. A conical pipe insert provide the inlet flow to be in a smooth velocity profile over the cross section. Therefore, a smooth velocity profile and a high turbulent level ($I = 7\%$) is assigned as input in the inlet boundary condition. The smooth velocity profile at pipe inlet begins to change along the pipe flow due the fluid does not slip on the inner pipe wall. As a result of velocity variations, a velocity boundary layer develops along the flow with an increasing in thickness permanently. The velocity in the boundary layer increases from zero in the wall normal direction and ends in increasing at the boundary of the boundary layer. The flow velocity outside the boundary layer increases to compansate the same flow rate at each section of the flow conduit. The developing boundary layer ends when its thickness increases along the flow and is equal to the pipe radius at a certain distance. By combining of the boundary layer thickness at the pipe center, the changed velocity profile convert to a fully developed laminar or turbulent velocity profile.

The variation of velocity profiles in the developing flow and in fully developed flow region are visualized. The numerical results obtained were analyzed and compared with experimental studies. Here, the velocity field are visualized with color contours and vectors. For example, the velocity variations on the central plane in the pipe flow is shown in Fig.4.

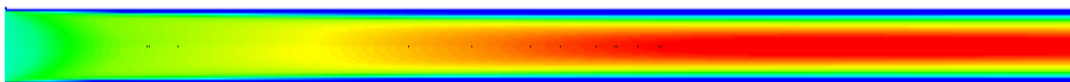


Figure 4. Display of the velocity distribution on the axial central plane by color contours

As shown in Fig. 4, the green color at the pipe inlet shows a low flow velocity, while the colours towards red show a high flow velocity. As can be seen the velocity colour varies from pipe inlet to a certain flow distance, but in the fully developed flow part, the colour of the velocity contour is unchanged. It also appears from the colour contour that the velocity decreases from the center line toward the pipe wall. The distribution of cross-sectional flow velocity at different downstream locations has been shown in the following figure. The state of velocity in the pipe flow can also be shown by vectors as shown in Fig. 5. In the Figure 5, the velocity at the pipe inlet ($x = 0$ m) is uniformly distributed. Downstream velocity vectors show that velocity profiles change along the flow. The velocity vectors at $x = 0.8$ m and $x = 1.2$ m appear to be the same, thus indicating the fully developed flow field. Comparisons of fully developed turbulent velocity profiles with experimental relationships and other experimental studies for all pipe flows are given in the following section.

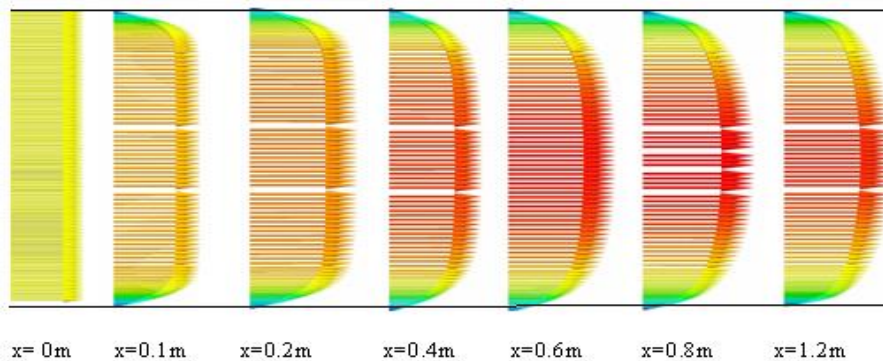
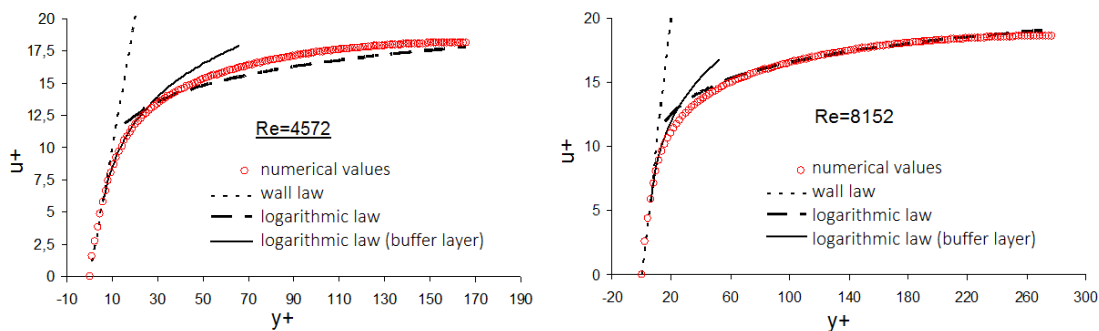


Figure 5. Cross-section velocity distribution vectors at different distances of the pipe



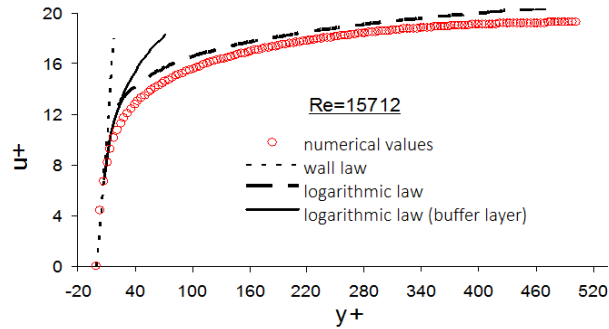


Figure 6. Comparison of dimensionless velocity profiles with empirical correlations at tree different Reynolds number flow of aluminium pipe aluminium pipe flows

Comparison with Empirical Correlations

In this section, velocity profiles obtained from the numerical study are compared with known empirical laws in order to provide the reliability of the numerical study. Due to fully developed flow conditions exists at 1.8m pipe location, The cross-section velocity profiles at that location have been used in comparisons. For example, velocity profiles of aluminium pipe flow at different Reynolds numbers are compared with the wall law and the logarithmic law in Fig.6. the wall law and logarithmic law are empirical relations that estimate the velocity variation in the sublaminar region and in the overlap region at high accuracy, respectively, in the fully developed turbulent pipe flow, In order to analyze the velocity variations in the numerical study, and to make sure that the resulting velocity profiles are correct, comparisons were made with those empirical relations

As shown in Fig. 6, the dimensionless velocity values in the fully developed flow are well agree with the wall law in the sublaminar flow region ($0 < y^+ < 5$). In this range, the wall law has shown an average deviation of 13% from the numerical values. In the case of $5 < y^+ < 30$, the numerical dimensionless velocity profiles deviate about $\pm 10\%$ in average from the logarithmic law curve in the buffer layer. Numerical dimensionless velocity has been well agree with logarithmic law in the dimensionless distances of $y^+ > 30$. Here, the logarithmic law values deviate from the numerical values of about 5% in the range of $30 < y^+ < 60$, about 3% in the range of $60 < y^+ < 300$ and about 4% in the range of $300 < y^+ < 600$.

When the dimensionless distances between $30 < y^+ < 600$ is considered, it show a deviation from the numerical values about 3.5% in the general average. As a result of above comparisons, it is seen that logarithmic law has much better in agreement with numerical values than buffer layer equation and wall law. The three relationships that have to be seen here are the empirical correlation and the numerical velocity profiles are in very good agreement with those empirical correlations. This reinforces the reliability of numerical study.

The dimensionless velocity data obtained from all flows of five pipe types which is performed in the Reynolds number range of 2000-25000 are compared with the wall law and the logarithmic law. As a result, it has been seen that well agreement are found in all Reynolds numbers. Table 5 shows the general average percent deviations of the empirical relations from the fully developed dimensionless velocity profiles covering all study data.

Table 5. General mean deviation percentages from numerical values of experimental correlations

	aluminium pipe	Copper pipe	Steel pipe	Galvanised pipe	Plastic pipe
Percent deviation- general average					
Wall law	$\pm 14\%$	$\pm 15\%$	$\pm 13\%$	$\pm 18\%$	$\pm 18\%$
Logarithmic law	$\pm 3\%$	$\pm 3\%$	$\pm 5\%$	$\pm 7\%$	$\pm 3\%$
Buffer layer Equation	$\pm 9\%$	$\pm 6\%$	$\pm 10\%$	$\pm 13\%$	$\pm 6\%$

According to the values given in Table 5, the logarithmic law is much better aligned with numerical values than the other two laws. It seems that the logarithmic law equation expressing the buffer layer is better aligned with the numerical values according to the wall law. The reason for the high deviation of the wall law is that the deviation to the dimensionless distances very close to the wall ($y^+ < 2$) begins to become high. The reason is that the pipes are rough. Because the wall law is generally in good agreement with the empirical values of the

smooth pipes. The above deviation percentages include comparisons up to 600 values of dimensionless distance. In the numerical study performed, the logarithmic law in the range of $30 < y^+ < 600$, the wall law in the range of $0 < y^+ < 5$ and the buffer layer equation in range of $5 < y^+ < 30$ is compared with the numerical dimensionless velocity values.

As a result, the fully developed velocity profiles in the numerical study are well adapted to the empirical relations. The comparison of numerical and empirical correlations here is intended to show the reliability of the numerical solution. According to these comparisons, the accuracy level of numerical study is obtained high.

Findings and Results

The reliability of numerical work is provided through comparisons of numerical data with experimental study in terms of pressure drop and with empirical relations in terms of fully developed velocity profiles. The numerical data in this case can be used to analyze the developing flow part in the pipe flow. By analyzing the axial velocity profiles obtained from the numerical studies, some important correlations can be obtained for the developing flow part. The variation in central axial velocity along the flow, which is obtained from the numerical simulation of the aluminum tube is shown in Fig. 7. The central axial velocity is accelerated to increase from pipe inlet to reach a maximum velocity in the downstream in order to meet the reduced flowrate due to the boundary layer developing effect.

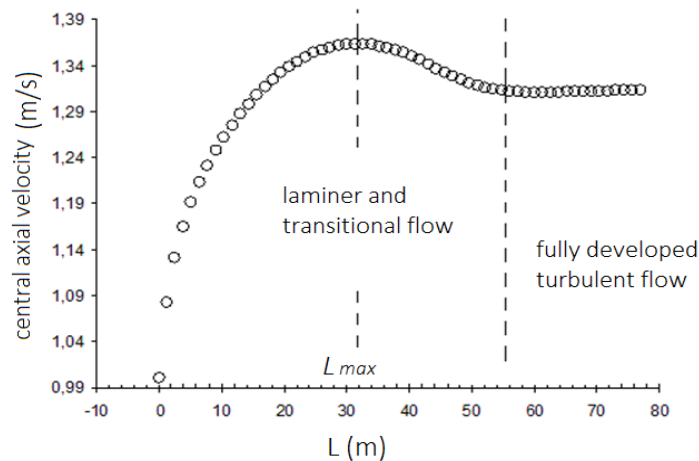


Figure 7. Variation of central axial velocity in Reynolds number of 4572 in the numerical aluminum pipe flow

As shown in Fig. 7, the axial velocity has shown a nonlinear increase from the pipe inlet towards peak point. At the peak point, the axial velocity reaches maximum and then decrease to a short distance to reach the unchanged values. The point at which the axial velocity has reached unchanged values is where the fully developed flow begins. In the fully developed flow section, two flow characteristics, such as axial velocity and pressure drop gradient, are no longer change throughout the flow. The flow point at which maximum velocity occurs is the flow point at which the boundary layer thickness combine at the pipe center. Here, fully developed flow occurs just beyond this point.

The transition distance to fully developed turbulence from pipe inlet can be determined from the observation of the variation of axial flow velocity, but the critical transition distance where laminar transit to turbulence from pipe inlet can not be determined as well the transition distance. In most experimental studies, axial velocity values are generally found to be maximum at a range of $30-40D$ in pipe diameters (Anselmet et.al. (2009)). In numerical studies with five pipe types, the dimensionless diameters (L_{max} / D) at which the central axial velocities are maximum are shown in Table 6 against the Reynolds number. When the dimensionless axial velocity values in the table are examined, it is seen that there is a rapidly decrease up to $Re=10000$ Reynolds number. After $Re > 10000$, it has passed to a low linear decrease of which the slope is low. The representation of L_{max}/D values given in Table 6 is shown on Fig. 8.

As shown in Fig. 8, L_{max} / D values has shown a rapid decline up to 10000 Reynolds numbers. From this Reynolds number, it has gone to a low linear drop which is low in slope. The following numerical relation is obtained as a result of curve fitting works for linear drops beginning from 10000 Reynolds number.

Table 6. Dimensionless L_{max}/D values where central axial velocity become maximum

aluminium pipe											
	4572	5539	8152	9496	10539	11371	12172	13295	15712	18004	21043
L_{max}/D	31.29	31.29	26.08	24.77	23.47	23.47	23.47	22.16	22.16	20.86	20.86
copper pipe											
	3443	4326	5738	7785	9002	9282	11079	13295	15856	18387	22084
L_{max}/D	37.81	32.59	29.99	26.08	24.77	24.77	23.47	23.47	22.16	22.16	
steel pipe											
Re	3609	5422	7101	8722	10643	11906	13374	13907	17257	19733	21688
L_{max}/D	36.32	31.48	27.85	24.21	23.00	23.00	21.79	21.79	20.58	20.58	20.58
galvanised pipe											
	2907	4559	7295	9553	10643	11977	12738	14078	14861	15582	18439
L_{max}/D	67.80	32.69	26.63	24.21	23.00	23.00	21.79	21.79	21.79	21.79	20.58
Plastic pipe											
	3691	4921	6890	8120	9842	12890	14458	16983	17540	20979	24317
L_{max}/D	33.90	32.28	27.44	25.83	24.21	22.60	22.60	22.60	22.60	22.60	20.98

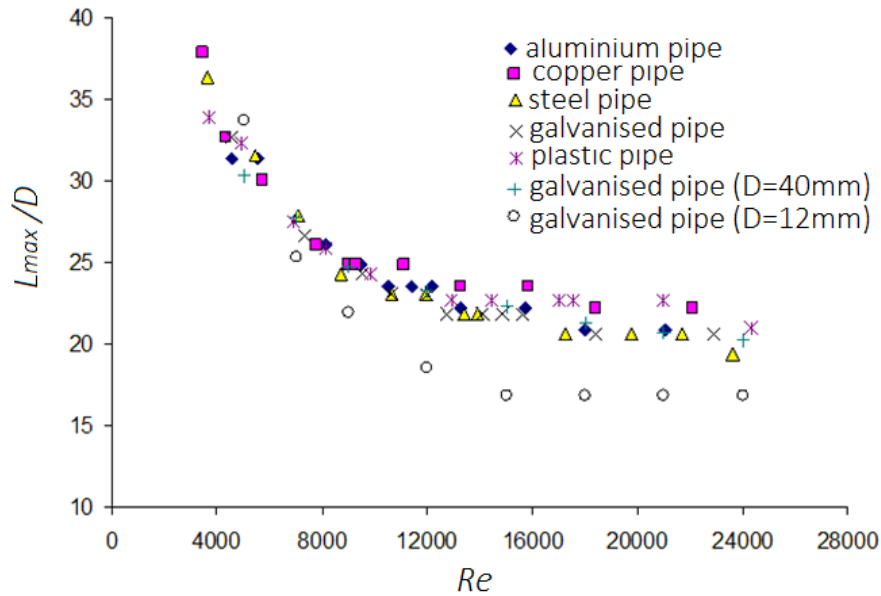


Figure 8. Variation of L_{max}/D values across Re for Maximum axial velocity

$$\frac{L_{max}}{D} = \frac{D^{0.2}}{\varepsilon^{0.06}} (28 - 0.00028Re) \quad Re > 10000 \quad (1)$$

In this numerical relation, the dimensionless diameter distance at which the axial velocity is maximum has been a function of the pipe diameter, roughness and Reynolds number. Diameter and roughness in this equation is just being a coefficient and it should be used their units in meter (m) in Equation. The correlation was found to deviate from the axial velocity values obtained from the entire numerical study by $\pm 8\%$ in maximum and $\pm 3.5\%$ in overall average. The estimated L_{max}/D values of the iron pipe and the galvanized pipe by Equ. (1) are shown in Fig. 9 below.

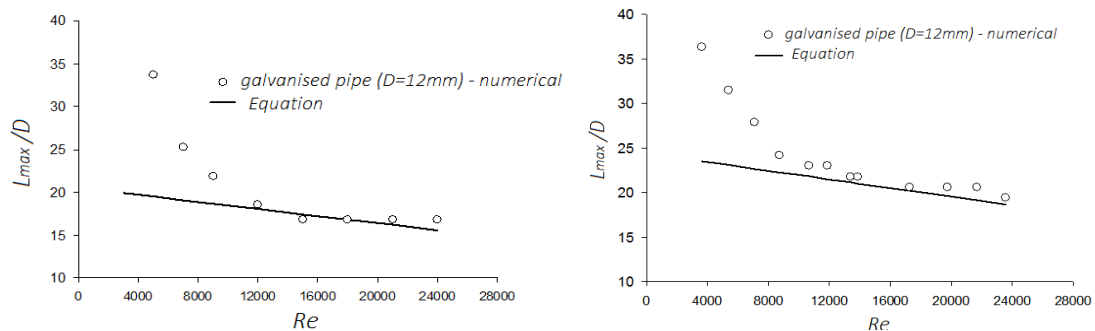


Figure 9. Estimation of L_{max}/D values where central axial velocity become maximum with Equ. (1) for galvanised and steel pipe flows

Conclusion

In this study, pipe flows in steady, incompressible and constant properties were simulated numerically in the Reynolds range of 2000-25000 for five pipe types with different relative roughness. In this study, pipe flows of steady, incompressible and constant properties were simulated numerically in the Reynolds numbers ranged between 2000 and 25000 by performing five pipe types in different relative roughness. In the solution of pipe flows, the RANS equations, which are time-averaged basic flow equations, were used. The SST k- ω model was used to include the turbulence effects into the stream. Flows were simulated with a lengthy pipe to cover the developing and fully developed flow region. Numerical results were compared with experimental work and other empirical velocity laws and it was seen that they fit very well. From the numerical results, the measured flow distances from the pipe inlet to flow point at which the central axial velocities were maximum were obtained. When the graphs of the variation of the axial velocity along the flow were analyzed, it was observed that the fully developed flow was slightly ahead of the flow point at which the axial velocity is maximum. The variation of the flow distances at which axial velocity is maximum was studied with Reynolds number and with different pipe types. Until $Re < 10000$, the dimensionless flow lengths exhibit a rapid and non-linear decrease. However, in the Reynolds range of $10000 < Re < 25000$, they show a drop in linear and at low slope. Variation of dimensionless flow lengths were investigated with pipe diameter, relative roughness and Reynolds number. As a result of curve fitting works, a numerical correlation including pipe diameter, relative roughness and Reynolds number effects and expressing dimensionless lengths in the range of $10000 < Re < 25000$ has been derived. The correlation was found to deviate by a maximum of $\pm 8\%$ and an overall average of $\pm 3.5\%$ from the axial velocity values obtained from the entire numerical study. The developing flow lengths can also be estimated by this relationship. However, the correlation can be suggested in the literature after testing with new experimental data.

References

- Anselmet, F., Ternat, F., Amielh, M., Boiron, O., Boyer, P., & Pietri, L. (2009). Axial development of the mean flow in the entrance region of turbulent pipe and duct flows. *Comptes Rendus Mécanique*, 337(8), 573-584.
- Augustine, J. R. (1988). *Pressure Drop Measurements in the Transition Region for a Circular Tube with a Square-Edged Entrance* (Master's Thesis). Bachelor of Science in Mechanical Engineering. The University of Southwestern Louisiana Lafayette, Louisiana.
- Barbin, A. R., & Jones, J. B. (1963). Turbulent flow in the inlet region of a smooth pipe. *Journal of Basic Engineering*, 85(1), 29-33.
- Doherty, J., Ngan, P., Monty, J., & Chong, M. (2007, January). The development of turbulent pipe flow. In *16th Australasian Fluid Mechanics Conference (AFMC)* (pp. 266-270). School of Engineering, The University of Queensland.
- Minkowycz, W. J., Abraham, J. P., & Sparrow, E. M. (2009). Numerical simulation of laminar breakdown and subsequent intermittent and turbulent flow in parallel-plate channels: Effects of inlet velocity profile and turbulence intensity. *International Journal of Heat and Mass Transfer*, 52(17-18), 4040-4046.
- Nikuradse J (1966). Gestzmassigkeiten der turbulerten stromung in glatten rohren. *Forschung auf dem Gebiet des. Ingenieurwesens*. Translated in NASA TT F-10, 359(3), 1932, 1-36.
- Laufer, J. (1954). The structure of turbulence in fully developed pipe flow. NACA Report, Washington, National Bureau of Standards.
- Ozisik, M. N. (1985). *Heat transfer: a basic approach*. New York: McGraw-Hill
- Patel, V. C., & Head, M. R. (1969). Some observations on skin friction and velocity profiles in fully developed pipe and channel flows. *Journal of Fluid Mechanics*, 38(1), 181-201.
- Perry, A. E., & Abell, C. J. (1975). Scaling laws for pipe-flow turbulence. *Journal of Fluid Mechanics*, 67(2), 257-271.
- Salami, L. A. (1986). An investigation of turbulent developing flow at the entrance to a smooth pipe. *International journal of heat and fluid flow*, 7(4), 247-257.
- Tam, H. K., Tam, L. M., & Ghajar, A. J. (2013). Effect of inlet geometries and heating on the entrance and fully-developed friction factors in the laminar and transition regions of a horizontal tube. *Experimental thermal and fluid science*, 44, 680-696.
- White, F. M. (2003). *Fluid Mechanics*. 5th edition, McGraw-Hill Book Co, New York.
- Zanoun, E. S., Kito, M., & Egbers, C. (2009). A study on flow transition and development in circular and rectangular ducts. *Journal of Fluids Engineering*, 131(6), 061204.

Zimmer, F., Zanoun, E. S., & Egbers, C. (2011). A study on the influence of triggering pipe flow regarding mean and higher order statistics. In *Journal of Physics: Conference Series* (Vol. 318, No. 3, p. 032039). IOP Publishing.

Author Information

Hasan Duz

Batman University, Tecnology Faculty, Automotive
Engineering, Turkey
Batman Üniversitesi, Batı Raman Kampüsü, Lojmanlar, Loj
3 No:12, Batman, Turkey
E-mail: hasan.duz@batman.edu.tr

Fuzzy Approaches to the Risk Assessment Methods for the Occupational Health and Safety

Murat GULBAY

Technical Sciences Vocational School, Gaziantep University

Abstract: Turkey's "Occupational Health and Safety Law" numbered as 6331 has been published in June 2012. According to the Occupational Health and Safety Law companies are categorized in three sections as Less Risky, Risky, and High Risky Companies. Based on this law, a regulation called "Occupational Health and Safety Regulation" has become operative and all of the companies compassed by this regulation are forced to prepare a risk assessment report in order to provide occupational health and safety, and increase their occupational health and safety levels. In the literature, there are about two hundreds of risk assessment methodologies. Among these methodologies, the mostly used ones are 5 by 5 L-type matrix method, Fine Kinney Method, and Hazard and Operability Analysis (HAZOP) which is proposed for the analysis of the risks in the chemical industry. These methods include strict lines and are not reflecting the practical issues of the real world applications. For this reason, these methods are to be adopted by the use of fuzzy logic. In this study, risk assessment methods used in the risk rating are evaluated and fuzzy approaches are proposed to provide more efficient and realistic results.

Keywords: Occupational health and safety, Fuzzy risk assessment, Fuzzy risk scores, Fuzzy 5x5 matrix method

Introduction

Risks are unavoidable in any activity. Over the years, risk management has gradually become an important part of work health and safety for each organization. To provide for a balanced and nationally consistent framework to secure the health and safety of workers and workplaces by protecting workers and other persons, providing for fair and effective workplace representation, encouraging unions and employer organizations to take a constructive role in promoting improvements in work health and safety practices, ensuring appropriate scrutiny and review of actions, providing a framework for continuous improvement, and maintaining and strengthening the national harmonization of laws relating to work health and safety Turkey's "Occupational Health and Safety Law" numbered as 6331 has been published in June 2012. Based on this law, a regulation called "Occupational Health and Safety Risk Assessment Regulation" has become operative and all of the companies compassed by this regulation are forced to prepare a risk assessment report in order to provide occupational health and safety, and increase their occupational health and safety levels. For this aim, all the companies are categorized in three sections as Less Risky, Risky, and High Risky Companies; and they are gradually forced to prepare a risk assessment report for their companies.

Risk assessment is the overall process of risk identification, risk analysis, and risk evaluation. In the literature, there are about two hundreds of risk assessment methodologies, such as Brainstorming, Delphi technique, Checklists, Preliminary hazard analysis (PHA), HAZard and OPERability study (HAZOP), Toxicity assessment, Structured "What-if" Technique (SWIFT), Scenario analysis (SA), Business impact analysis (BIA), Root cause analysis (RCA), Failure modes and effects analysis (FMEA), Fault tree analysis (FTA), Event tree analysis (ETA), Cause-consequence analysis, Cause-and-effect analysis, Decision tree analysis, Human reliability assessment (HRA), and Consequence/probability matrix methods. These methods include strict lines and are not reflecting the practical issues of the real world applications. For this reason, these methods are to be adopted by the use of fuzzy logic. In this study, 5x5 L-type matrix method is analyzed and a fuzzified 5x5 matrix type risk assessment method is proposed. In the next section, an overview of the 5x5 matrix method, also known as

- This is an Open Access article distributed under the terms of the Creative Commons Attribution-Noncommercial 4.0 Unported License, permitting all non-commercial use, distribution, and reproduction in any medium, provided the original work is properly cited.

- Selection and peer-review under responsibility of the Organizing Committee of the Conference

L-type matrix method, is presented. Then, a fuzzified 5x5 matrix method is proposed. Finally, a conclusion and future study recommendations are given.

5x5 Matrix Method for the Risk Analysis

It's a two-variable risk matrix whose variables are "consequence" and "likelihood" derived from the formal definition of the term "Risk" given by Turkey's "Occupational Health and Safety Law" numbered as 6331 and "Occupational Health and Safety Regulation". In this type of risk assessment matrix each variable is scored by the numbers between 1 and 5. The physical meaning of each score is given in the Table 1 and 2

Table 1. Scores for the variable "Consequence (C)"

Score (C)	Meaning
1	Slight (insignificant) effects
2	Minor effects
3	Moderate effects
4	Major effects
5	Severe effects

Table 2. Scores for the variable "Likelihood (L)"

Score (L)	Meaning
1	Rare
2	Unlikely
3	Possible
4	Likely
5	Almost certain

Risk score, R, for the method is defined as:

$$R = C \times L$$

It is clear that R ranges from 1 to 25. The resultant R can be interpreted as shown in Table 3.

Table 3. Overall risk scores for R

C \ L	1	2	3	4	5
1	1	2	3	4	5
2	2	4	6	8	10
3	3	6	9	12	15
4	4	8	12	16	20
5	5	10	15	20	25

Scores between 1 and 6 (green) may be interpreted as "Low Risks" that does not require taking precautions in the short time of period, while scores ranging from 8 to 12 may be identified as "Medium Risks" that require taking precautions in the short time of period. On the other hand, scores between 15 and 25 are called as "High (Critical) Risks" that results in taking precautions, immediately, as soon as possible. Detailed precautions for different levels of the overall risk scores are listed in Table 4.

Table 4. Preventive actions for different score levels of R.

Result (R)	Necessary Preventive Action
Cannot be tolerated (R=25)	Any ongoing activity must be immediately stopped. Work should not be started until the risk is reduced.
Important Risks (R=[15-20])	Any ongoing activity must be immediately stopped. After preventive measures are applied, work can be continued.
Moderate Risks (R=[8-12])	Risk mitigation measures should be applied. Work can be carefully continued.
Foldable Risks (R=[2-6])	Since the risk is low, there is no necessity to take preventive actions in the short term of period. However, existing controls should be continued.
Insignificant Risk (R=1)	Existing controls should be continued.

Fuzzified 5x5 Matrix Method for the Risk Analysis

Instead of using strict lines for scoring C and L, we may use fuzzy intervals to identify them. Minimum fuzzy interval for each score becomes [0,1], while its maximum is [4,5]. Namely, each score is identified by fuzzy interval numbers as [0,1], [1,2],[2,3], [3,4],[4,5]. Since the risk score R, is not only affected from two single and subjective measures it should be defined as an interval. The resultant score R can be obtained by using the the property for multiplication of the fuzzy intervals as:

$$[a,b] * [c,d] = [\min(ac, ad, bc, bd), \max(ac, ad, bc, bd)]$$

The minimum of R is [0,1] and the maximum is [16,25]. Representation of the C and L are shown in Tables 5 and 6, respectively.

Table 5. Fuzzy scores for the variable “Consequence (C)”

Score (C)	Linguistic Meaning
[0,1]	No work-hour loss. First aid is sufficient.
[1,2]	No work-day loss, no permanent effect. First-aid with outpatient treatment is required.
[2,3]	Results in Simple battery, simple personal injury. Treatment is necessary.
[3,4]	Causes serious personal injury. Long-term treatment is needed.
[4,5]	Causes to death, long-term disability or dismemberment

Table 6. Fuzzy scores for the variable “Likelihood (L)”

Score (L)	Linguistic Meaning
[0,1]	Very small, nearly never
[1,2]	Little, once in a year, in abnormal conditions
[2,3]	Medium, 3-5 times in a year
[3,4]	High, once in a month
[4,5]	Very high, every day to once in a week, in normal conditions

Finally, The resultant fuzzy R can be interpreted as shown in Table 7

Table 7. Overall fuzzy risk scores for R

L	[0,1]	[1,2]	[2,3]	[3,4]	[4,5]
C [0,1]	[0,1]	[0,2]	[0,3]	[0,4]	[0,5]
[1,2]	[0,2]	[1,4]	[2,6]	[3,8]	[4,10]
[2,3]	[0,3]	[2,6]	[4,9]	[6,12]	[8,15]
[3,4]	[0,4]	[3,8]	[6,12]	[9,16]	[12,20]
[4,5]	[0,5]	[4,10]	[8,15]	[12,20]	[16,25]

Table 8. Preventive actions for different score levels of fuzzy R

Fuzzy Risk Level, R	Action
[0,1] to [0,5]	Insignificant to tolerable: There is no need to plan further control processes, keep and control the existence of the current precautions/measures
[1,4] to [2,6]	Medium: New precautions necessary to reduce risk level
[3,8] to [6,12]	Important (serious): Start taking actions to reduce risk level as soon as possible, stop normal works, allow only risk prevention precautions/measures
[8,15] to [16,25]	Unbearable: Stop instantly. Act to reduce risk level. Never start any work until risk level is out of this level.

Preventive actions for different score levels of fuzzy R is illustrated in Table 8. If the company’s overall health and safety risk level with respect to its sector’s average, then when taking precautions the resultant R should be

considered as if it belongs to the one level higher. For example, if the company's overall health and safety risk level is low and R is decided as [6,12] which is categorized as "Important", then it can be seen as "Unbearable" in order to take the trigger effects of the other risks into consideration.

Results and Discussion

When determining risk scores for occupational health and safety, it is very difficult to score the variables and it is subjectively defined. Furthermore, reducing the risk score determination to only two parameters may not be correct and generally result in the loss of information due to its subjectivity. In order to handle this uncertainty in the parameters, a useful fuzzy 5x5 matrix type risk assessment method is proposed. It is more powerful than the classical 5x5 matrix type risk assessment methods and can be easily linked to the company's overall risk level.

Conclusion

The proposed fuzzified 5x5 matrix risk assessment method can be applied to the most of the companies. Using fuzzified risk levels and their corresponding actions allows better prevention of work injuries and/or occupational health and safety risks. It allows taking proactive actions and more powerful interpretations.

Recommendations

The same approach can be proposed for other risk assessment methods especially to the Fine-Kinney Method. Since it is not only two or three parameters which affect the risk score, the effect of the other parameters should be considered in the risk score determination.

References

- Occupational Health and Safety Law, <http://www.mevzuat.gov.tr/MevzuatMetin/1.5.6331.pdf>, Official Journal (30/06/2012, No: 28339)
Occupational Health and Safety Risk Assessment Regulation, Official Journal (29/12/2012, No: 28512)

Author Information

Murat Gulbay

Technical Sciences Vocational School, Gaziantep University, Turkey
Üniversite Bulvarı P.K. 27310 Şehitkamil / Gaziantep, TÜRKİYE
Contact e-mail: gulbay@gmail.com

Possible Problems in the Introduction in Ukraine of Medical Reform and the Practice of a Family Medicine Doctor

Volodymyr SULYMA

SO "Dnipropetrovsk Medical Academy Ministry Health of Ukraine"

Abstract: Currently, Ukraine is developing and phased implementation of medical reform, which involves the organization of work at the primary level of providing qualified medical help by a family medicine doctor. This reform can be accompanied by the development of possible medical and social and financial problems. The transfer of funding to the primary medical level and the possibility of allocating funds allocated to a specific number of residents assigned to a family medicine doctor can lead to the following problems:

1. The examination of patients only by a family medicine doctor in order to save the allocated financial resources and not performing complex laboratory and modern apparatus-instrumental additional researchers can lead to the establishment of an incorrect diagnosis, which will lead to the choice of the wrong treatment tactic and to the patient's serious condition, and in some cases and to death.
2. Treatment of patients only by a family medicine physician in order to save allocated financial resources and failing to consult with related specialists at the second and third levels of medical care, delay in hospitalization of patients to the hospital, may lead to the establishment of an incorrect diagnosis and the choice of the wrong treatment tactics, to a serious condition the patient, and to his death.

It is necessary to develop serious control conditions that will avoid the development of these problems when introducing medical reform in Ukraine.

Keywords: Medical reform, Problems, Family doctor

Introduction

The reform will start with primary care, that is, family doctors, physicians and pediatricians. Patients may apply to a family doctor, therapist or pediatrician, as soon as they feel the need for examination or treatment. In developed countries, primary care physicians without hospitalization resolve up to 80% of medical treatment using modern knowledge, basic equipment and most commonly used analyzes and medications.

All these services will be 100% covered by the state budget. A doctor will become a family agent in the health system. He will monitor health and fully provide primary diagnosis. For this, the doctor must be motivated, above all - financially.

From 2018, primary health care providers who have contracted with the National Health Service will start financing under the new model - an annual flat-rate payment for the maintenance of each patient with whom the doctors of the facility signed the contract. At the same time, the size of the payment for young people and the elderly will differ significantly in view of the increase in the number of appeals due to age characteristics.

It is important to remember that the primary link institution receives funds from patients and when they are healthy. The less they are ill, the less the doctor works, and the incomes are the same. So, we encourage doctors to take care of their patients. This model operates globally.

What Services Will Your Doctor Give You?

A primary care physician is a specialist who has all the information about the health of his patients. Because of this, he sees the relationship and can determine at what stage the intervention of a profile specialist is required.

Information about the patient's health will be contained in the electronic health system. Even when a citizen goes to another doctor, all information will be available.

The primary duty of the primary care physician is to prevent or detect early onset of the disease in a timely manner. And also to provide urgent help in acute conditions and sudden deterioration of health: high body temperature, acute and sudden pain, cardiac rhythm, bleeding, other conditions, diseases, poisonings and injuries in need of emergency care.

Method

Will this doctor treat the disease?

So. The primary care physician, in accordance with the protocol of treatment, examines the patient and assigns the necessary tests, most of which will be carried out immediately in the outpatient clinic. On the basis of the received information, the family doctor decides on the treatment of both acute and chronic conditions of the patient.

If necessary, the family doctor gives directions to profile specialists.

What else will be included in his duties?

- prevention of diseases at risk groups;
- vaccination;
- issuance of medical certificates and sick leave;
- Issuing recipes for the cost of the drug "Available medicines", including recipes for medicines for chronic patients.

In the villages of a family doctor, the local community chooses. Tariff wage rates for a primary care physician will be canceled. Rural communities will finally be able to substantially improve their primary care. By creating good conditions for life and work for a doctor, villagers will be able to invite promising specialists. A decent wage will be provided by the state.

Qualified doctors are ready to work in villages if, in addition to having a good salary, they will have accommodation with water and heating, equipped with a job and reimbursement of fuel costs for public transport.

If a small number of people live in a village, one family doctor can serve a few populated areas that are nearby. In this case, the doctor receives support from several local communities.

From 2020, the state will cover the examination, consultation and appointment of a doctor by a specialist or highly specialized medical establishment only upon referral from a primary care physician. As, according to statistics, the majority of appeals of citizens are within the competence of the family doctor without the involvement of a specialist or are in urgent calls.

A family doctor cannot write a referral to a particular specialist and / or a specific institution. He only indicates the profile of a highly specialized doctor. The patient independently decides where to contact him.

By 2020, to address the doctors of specialized or highly specialized medical institutions, patients can either on a direction, or on their own.

Results and Discussion

Primary reform does not cancel pediatricians. On the contrary, pediatricians will receive financial incentives under the same conditions as family doctors, since they are also primary care doctors. At the same time, the annual fixed payment for each child will be even higher than the average.

Like a family doctor, citizens can choose a pediatrician for their child separately. Or to serve the whole family in one family doctor. However, the Declaration on the choice of physician must be signed for each member of the family separately.

The pediatrician vaccinates children free of charge in accordance with the schedule of preventive vaccinations

When a citizen needs urgent specialized assistance, he or she addresses to any emergency facility. The treatment of life-threatening cases will be 100% covered by the state.

Reforming the model of financing of specialized medical care institutions will start in 2019 and the highly specialized - from 2020. By this time, the reform of the primary care system will take place and the necessary statistics will be collected in order to translate changes into the secondary and tertiary links. At the level of specialized and highly specialized assistance, the state will pay directly to the medical institution for each medical service provided for transparent and uniform tariffs for the whole country. The tariff will include all expenses: both for medicines, for equipment repair, and for the work of doctors.

Each year, the volume of services guaranteed by the state and tariffs will be approved by the Verkhovna Rada within the framework of the State Budget, this document will be called the program of medical guarantees. The first program of medical guarantees will be approved by 2020, when a new financing model will work at all levels. All tariffs will be reasonable and open.

This means that within the state-guaranteed healthcare package, the state will cover 100% of the cost of treatment, including expendable materials and medicines.

Conclusion

The transfer of funding to the primary medical level and the possibility of allocating funds allocated to a specific number of residents assigned to a family medicine doctor can lead to the following problems:

The examination of patients only by a family medicine doctor in order to save the allocated financial resources and not performing complex laboratory and modern apparatus-instrumental additional researchers can lead to the establishment of an incorrect diagnosis, which will lead to the choice of the wrong treatment tactic and to the patient's serious condition, and in some cases and to death.

Treatment of patients only by a family medicine physician in order to save allocated financial resources and failing to consult with related specialists at the second and third levels of medical care, delay in hospitalization of patients to the hospital, may lead to the establishment of an incorrect diagnosis and the choice of the wrong treatment tactics, to a serious condition the patient, and to his death.

It is important to remember that the primary link institution receives funds from patients and when they are healthy. The less they are ill, the less the doctor works, and the incomes are the same. So, we encourage doctors to take care of their patients. This model operates globally.

References

For materials:

офіційного сайту Верховної Ради України (rada.gov.ua)

Урядового порталу (www.kmu.gov.ua)

офіційного сайту МОЗ (moz.gov.ua)

Український медичний часопис (www.umj.com.ua)

Медсправа (www.medsprava.com.ua)

Здоровінфо (zdorov-info.com.ua)

BBC (www.bbc.com)

DW (www.dw.com)

Аптека (www.apteka.ua)

НВ (nv.ua)

Author Information

Volodymyr Sulyma

SO "Dnipropetrovsk Medical Academy Ministry Health of
Ukraine"

Vernadskyj Street, 9, Dnipro, 49000, Ukraine

Contact e-mail: Volodyasulyma2@gmail.com

First Results Surgical Treatment of Patients with Chronic anal Fissure Through Electric Welding of Biological Tissue

Volodymyr SULYMA

SO "Dnipropetrovsk Medical Academy Ministry Health of Ukraine"

Abstract: Existing methods of ectomy of chronic anal fissure is now accompanied by a fairly large number of postoperative complications such as pain syndrome, breach urine, bleeding, local edema, which leads to additional suffering patient, increases the cost of treatment. The aim is to study the results of treatment of chronic anal fissure through the use of electrocautery generator LigaSure (Covidien) for fissure and vessels that supply blood to them. After dilatation anal sphincters spend revision anal canal. Clip tighten chronic anal fissure from 0,5 to 2,0 cm from anal verge to 3,0 cm on deep recti on top and put on his stretched base, including vascular leg, bent electrode apparatus LigaSure. Spend electric welding grounds unit at intensity 2 or 3 LEDs, after which chronic anal fissure of the clip is removed without firmware vascular legs. Histological research after operation. Applying this method on treatment of 21 patients with a diagnosis of "Chronic anal fissure". Performance ectomy of chronic anal fissure using LigaSure, spread through small areas of damage and no sutures in the anal region, leads to a reduction of pain, no bleeding and swelling of tissue, accelerate wound healing, reduction of terms of treatment and temporary disability. This method is had trauma (zone 300-600 microns of tissue damage, early wound healing) and easy to use that can significantly improve the results of surgery and reduce the number of postoperative complications after ectomy of chronic anal fissure.

Keywords: Surgical treatment, Anal fissure, Electric welding

Introduction

An anal fissure is often caused by a hard or painful bowel movement, which damages the surrounding skin. A fissure can cause a severe or burning pain in or around anus, especially when open in bowels. This pain can last for a couple of hours. May also notice bright red blood on the toilet paper when wipe after a bowel movement.

The opening and closing of anus is controlled by internal (inside) and external (outside) anal sphincter muscles. May be control external anal sphincter, but not internal anal sphincter. If internal anal sphincter goes into spasm (tenses), this reduces the blood supply to fissure and stops it healing properly. A chronic anal fissure likely has the tear, as well as two separate lumps or tags of skin, one internal (sentinel pile) and one external (hypertrophied papilla). The fissure's location offers clues about its cause. A fissure that occurs on the side of the anal opening, rather than the back or front, is more likely to be a sign of another disorder, such as Crohn's disease. Recommended a surgical procedure called partial lateral internal sphincterotomy as the technique of choice for the treatment of anal fissures. In this procedure, the internal anal sphincter is cut starting at its distal most end at the anal verge and extending into the anal canal for a distance equal to that of the fissure.

The cut may extend to the dentate line, but not farther. The sphincter can be divided in a closed (percutaneous) fashion by tunneling under the anoderm or in an open fashion by cutting through the anoderm. The posterior midline, where the fissure usually is located, is avoided for fear of accentuating the posterior weakness of the muscle surrounding the anal canal. Additional weakness posteriorly can lead to what is called a keyhole deformity, so called because the resulting anal canal resembles an old fashioned skeleton key. This deformity promotes soilage and leakage of stool.

Existing methods of ectomy of chronic anal fissure is now accompanied by a fairly large number of postoperative complications such as pain syndrome, breach urine, bleeding, local edema, which leads to additional suffering patient, increases the cost of treatment.

The aim is to study the results of treatment of chronic anal fissure through the use of electrocautery generator LigaSure (Covidien) for fissure and vessels that supply blood to them.

Method

If you have a chronic anal fissure that is resistant to other treatments, or if your symptoms are severe, your doctor may recommend surgery. Doctors usually perform a procedure called lateral internal sphincterotomy, which involves cutting a small portion of the anal sphincter muscle to reduce spasm and pain, and promote healing. Studies have found that for chronic fissure, surgery is much more effective than any medical treatment. However, surgery has a small risk of causing incontinence.

Several surgeons have described procedures that stretch and tear the anal sphincters for the treatment of anal fissures. Though anal stretching often is successful in alleviating pain and healing the fissure, it is a traumatic, uncontrolled disruption of the sphincter. Ultrasonograms of the anal sphincters following stretching demonstrate trauma that extends beyond the desired area. Because only 70-80% of fissures heal and there is a 20% incidence of incontinence of stool, stretching has fallen out of favor.

Our recommendation: After dilatation anal sphincters spend revision anal canal. Clip tighten chronic anal fissure from 0,5 to 2,0 cm from anal verge to 3,0 cm on deep recti on top and put on his stretched base, including vascular leg, bent electrode apparatus LigaSure. Spend electric welding grounds unit at intensity 2 or 3 LEDs, after which chronic anal fissure of the clip is removed without firmware vascular legs. Histological research after operation.

Results and Discussion

Applying this method on treatment of 21 patients with a diagnosis of "Chronic anal fissure". Performance ectomy of chronic anal fissure using LigaSure, spread through small areas of damage and no sutures in the anal region, leads to a reduction of pain, no bleeding and swelling of tissue, accelerate wound healing, reduction of terms of treatment and temporary disability.

The choice of treatment remains difficult for the following reasons. Although surgery is highly efficacious and succeeds in curing the fissure in more than 90% of patients, in a systematic review of randomised surgical trials the overall risk of incontinence was about 10%. This was mostly incontinence to flatus, and there are no reports delineating the duration of this problem (is it permanent or transitory?) Publications describing treatment for incontinence after sphincterotomy for fissure are strikingly absent, implying a lack of need compared with other incontinent populations.

Medical treatment for chronic anal fissure, acute fissure, and fissure in children may therefore be applied with a chance of cure that is only marginally better than placebo. The risk of using such treatments is not great: mainly headache during the use of nitroglycerin ointment, without apparent adverse effect in the long term. Medical treatments can therefore be used in individuals wanting to avoid surgical treatment, and surgery can be reserved for treatment failures in adults with chronic typical fissure. Topical application of calcium channel blockers may be as effective as nitroglycerin ointment in the treatment of anal fissure, without the risk of headache, which many patients find unacceptably painful. Too few studies exist to establish this efficacy.

Would be advantageous if the risk of incontinence could be reduced after surgery or the success rate of medical treatments increased to that found in surgery, but with less risk of headache. The Cochrane reviews provide some direction here but not a quick fix. Anal stretch was found to have a significantly higher risk of incontinence than controlled sphincterotomy in surgical trials and a higher risk of treatment failure. Stretch should probably be abandoned in favour of partial internal sphincterotomy until a better operation is described. Among the medical treatments, calcium channel blockers applied topically caused fewer headaches and may be as efficacious as nitroglycerin ointment.

Traditional surgery that permanently weakens the internal sphincter is associated with a risk of incontinence. Medical therapies temporarily relax the internal sphincter and pose no such danger, but their limited efficacy has

led to displacement rather than replacement of traditional surgery. Emerging medical therapies promise continued improvement and new sphincter-sparing surgery may render traditional surgery redundant.

Conclusion

This method is had trauma (zone 300-600 microns of tissue damage, early wound healing) and easy to use that can significantly improve the results of surgery and reduce the number of postoperative complications after ectomy of chronic anal fissure.

References

- Feldman M, et al. Diseases of the anorectum. In: Sleisenger and Fordtran's Gastrointestinal and Liver Disease: Pathophysiology, Diagnosis, Management. 10th ed. Philadelphia, Pa.: Saunders Elsevier; 2016. <http://www.clinicalkey.com>. Accessed Sept. 17, 2015.
- Anal fissure. American Society of Colon and Rectal Surgeons. <https://www.fascrs.org/patients/disease-condition/anal-fissure-expanded-information>. Accessed Sept. 17, 2015.
- Wald A, et al. ACG Clinical Guideline: Management of benign anorectal disorders. American Journal of Gastroenterology. 2014; 109:1141.
- Perry WB, et al. Practice parameters for the management of anal fissures (3rd revision). Diseases of the Colon & Rectum. 2010; 53:1110.
- Nelson RL, et al. Non surgical therapy for anal fissure. Cochrane Database of Systematic Reviews. <http://onlinelibrary.wiley.com/doi/10.1002/14651858.CD003431.pub3/abstract>. Accessed Sept. 17, 2015.
- Breen E, et al. Anal fissure: Clinical manifestations, diagnosis, prevention. <http://www.uptodate.com/home>. Accessed Sept. 17, 2015.

Author Information

Volodymyr Sulyma

SO "Dnipropetrovsk Medical Academy Ministry
Health of Ukraine"
Vernadskyj Street, 9, Dnipro, 49000, Ukraine
Contact e-mail: Volodyasulyma2@gmail.com

A Design of Hybrid Expert System for Diagnosis of Breast Cancer and Liver Disorder

Aysegul ALAYBEYOGLU
Izmir Katip Celebi University

Naciye MULAYIM
Izmir Katip Celebi University

Abstract: It is certain that accurately and timely diagnosis of the diseases reduces the risk of morbidity and mortality of the disease. At that point, an expert system based on artificial intelligence techniques helps physicians or other healthcare professionals for diagnosis of it. In this study an expert system based on Firefly Algorithm is developed to diagnose both breast cancer and liver disorder. An experiential labour of the proposed system was managed using Indian Liver Patient Dataset and Breast Cancer Wisconsin (Original) Data Set received from UCI Machine Learning Repository sites. Standard statistical Metrics which are Negative Predictive Value, Positive Predictive Value, Specificity, Sensitivity, Precision, F_Measure and Accuracy are used to evaluate the performance of the proposed systems and simulation results show that the proposed system is 92% efficient in providing accurate diagnosis of Liver Disorder and 94.81% efficient in providing accurate diagnosis of Breast Cancer. C# programming language is used for the implementations of the system.

Keywords: Firefly algorithm, Expert system, Breast cancer, Liver disorder

Introduction

Expert System(ES)s are computer programs that are derived from AI [1] and is an intelligent interactional computer based decision tool that solves difficult and complex real life troubles and problems based upon information and notion of human experts in a particular fields [2]. Using friendly interfaces are important property of ESs and make them extremely interactional in nature and have access to complete, accurate and timely solving for these real life troubles and problems [3]. Medical practitioners can use computer devices to get help for systematizing, keeping and getting back of suitable medical knowledge to solve difficult states and these devices suggest them for favorable prognosis, diagnosis and therapeutic decision [4]. Computer technology can be used to cut down the ratio of mortality and minimize the waiting time to meet medical experts. Computer program developed by mimicking human intelligence could be used to help doctors in making timely and exact decisions considering patients' diagnosis [5].

Various intelligent systems have been developed to enhance more health service support and reduce cost of health expenses. These systems can behavior as an assistant which mimic human intelligence for patients and doctors [6- 8]. There are many studies which use artificial intelligent techniques in diagnosis of liver disorder and breast cancer. In [9], Naive Bayes classifier, Back propagation Neural Network algorithm, and Support Vector Machines Algorithms are used for liver disease diagnosis. In [10], support vector machine, a Bayesian and a k-nearest neighbour classifier is used for semi automatically segmented and quantified for diagnosis of liver disorders. In [11], a fuzzy expert system is developed for diagnosis of liver disorders. In [12], Support Vector Machine (SVM) and Naive Bayes are used to predict the liver disease. In [13], for prediction of liver disease, SVM and Random forest algorithms are compared. In [14], Artificial Neural Network (ANN) and Artificial Immune Algorithm (AIS) have been used to extract rules which have been trained for classification. Thus a set of rules is obtained for liver disorders. In [15], Breast cancer tumour is classified by using firefly algorithm to improve the parameters of local linear wavelet neural network. Support Vector Machine (SVM) is

- This is an Open Access article distributed under the terms of the Creative Commons Attribution-Noncommercial 4.0 Unported License, permitting all non-commercial use, distribution, and reproduction in any medium, provided the original work is properly cited.

- Selection and peer-review under responsibility of the Organizing Committee of the Conference

used to detect breast cancer for classifying in [16]. Breast cancer detection is achieved by using SVM combined with the feature selection technique in [17]. Lastly, Breast cancer datasets are tested with SVM algorithms and the results are compared with the results of other machine learning techniques in [18].

In this study, an expert system based on Firefly Algorithm is developed to diagnose breast cancer and liver disorder diseases. ILPD (Indian Liver Patient Dataset) has 583 patients' records and Breast Cancer Wisconsin (Original) Data Set has 699 patients' records, which are in UCI Machine Learning Repository site, are used for proposed system. Remainder of this paper is organized as follows: Section 2 presents the architecture of the proposed system, Section 3 presents the results of experimental study and the evaluations and lastly Section 4 presents the conclusion and recommendations.

Architecture and Interfaces of the Proposed System

The architecture of the proposed system for the diagnosis of liver disorders and breast cancer is shown in Figure 1. When the user enters knowledge of laboratory tests, the system infers results by using knowledge base and inference engine. Based on these, the system decides whether the patient is sick or not.

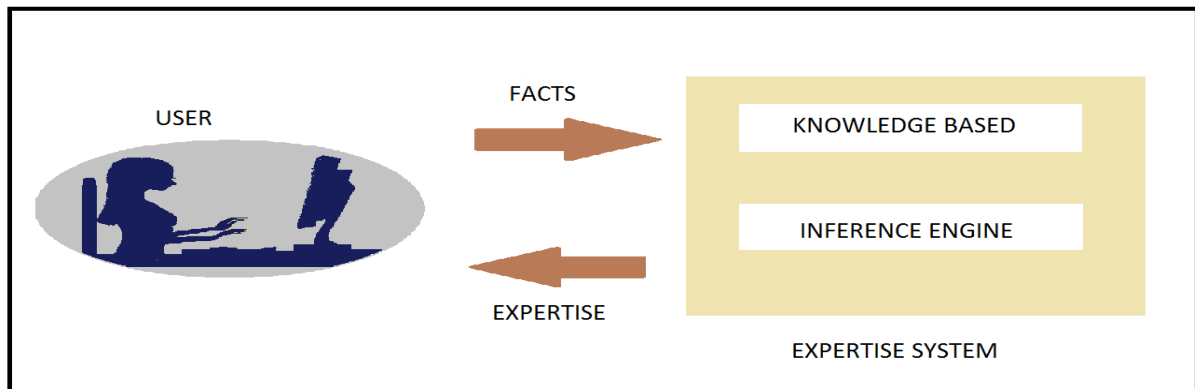


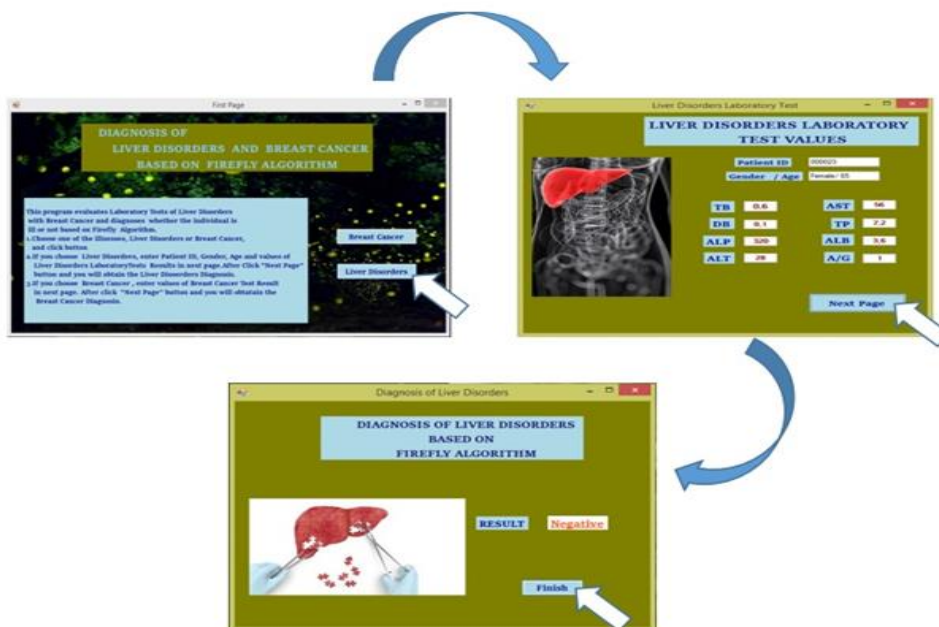
Figure 1. The architecture of the proposed system for the diagnosis of liver disorder and breast cancer

Interfaces of the Firefly algorithm based Hybrid Expert System

Designed interfaces are shown in Figure 2. First page gives information about usage of the system and presents choices for illnesses we can use in the system. If the user clicks Breast Cancer button, second page is opened and Breast Cancer Symptoms Results are entered by the user. When the Next Page button is clicked, Diagnosis of the Breast Cancer Symptoms Based on Firefly Algorithm is obtained as shown in Figure 2.a. If the user clicks Liver Disorders button, second page is opened and Patient ID, Gender, Age and Liver Disorders Laboratory Tests Results are entered as shown in Figure 2.b. When the Next Page button is clicked, Diagnosis of Liver Disorders Tests Results based on Firefly Algorithm is obtained.



(a) Firefly algorithm based expert system for Breast Cancer



(b) Firefly algorithm based expert system for Liver Disorders
 Figure 2. Interfaces of the proposed system

Simulation Results and Evaluations

In the proposed expert system, firefly algorithm is used for diagnosis of liver disorder and breast cancer detection. C# programming language is used for implementations. Some definitions of terminology and derivations from a confusion matrix and formulas are given below:

- **True positive (TP):** Sick people are accurately defined as sick,
- **False positive (FP):** Healthy people are inaccurately defined as sick,
- **True negative (TN):** Healthy people are accurately defined as healthy,
- **False negative (FN):** Sick people are inaccurately defined as healthy [19]

Table 1. Formulas and Parameters of CBR

$$Accuracy = \frac{TN + TP}{TN + TP + FN + FP}$$

$$Negative\ predictive\ Value = \frac{TN}{TN + FN}$$

$$Positive\ Predictive\ Value = \frac{TP}{TP + FP}$$

$$Specificity = \frac{TN}{TN + FP}$$

$$Sensitivity = \frac{TP}{TP + FN}$$

$$Precision = \frac{TP}{TP + FP}$$

$$F_Measure = 2 \times \frac{precision \times sensitivity}{precision + sensitivity}$$

Firefly Algorithm based Expert System for Liver Disorders

ILPD (Indian Liver Patient Dataset) which is in UCI Machine Learning Repository site has 583 patient records (2010). This data set comprises 416 liver patient registers and 167 non liver patient registers. In dataset, three number of patients have missing values and fourteen number of patients have the same data values. The data set is taken from north east of Andhra Pradesh, India. Chooser divides into two groups: liver patient or not. This

data set involves 441 male patient records and 142 female patient records. Any patient whose age surpasses 89 is written as being of age "90" [20]. There are 10 attributes that are age, gender, total Bilirubin, direct Bilirubin, total proteins, albumin, A/G ratio, SGPT, SGOT and Alkphos in dataset. In this study, last 8 laboratory tests results are used for diagnosis [20]. Table 2 shows attributes in ILPD Dataset and normal values of attributes.

Table 2. Attribute in ILPD Dataset and information of normal values of attributes [21].

Variable	Information (Normal Value)
Age	Age of the patient
Gender	Gender of the patient
TB	Total Bilirubin (0.22-1.0 mg/dl)
DB	Direct Bilirubin (0.0-0.2mg/dl)
Alkphos	Alkaline Phosphotase (110-310U/L)
SGPT	Alamine Aminotransferase (5-45U/L)
SGOT	Aspartate Aminotransferase (5-40U/L)
TP	Total Proteins (5.5-8gm/dl)
ALB	Albumin (3.5-5gm/dl)
A/G Ratio (LFT)	Albumin and Globulin Ratio (≥ 1)
SELECTOR	field used to split the data into two sets

In this study, 300 numbers of patient data are used to evaluate the system and to equilibrate the numbers of liver and non-liver patients. While number of positive liver disorder patient is 204, negative liver patient is 104. In Table 3, Liver Disorder Laboratory Test results can be seen according to the system based on firefly algorithm. As it can be obtained from Table 3, the system predicts accurately liver disorder test results of 188 number of patients which have liver disorders; it predicts inaccurately liver disorders test results of 16 number of patients. It can also be seen from the table that the system predicts accurately liver disorders test results of 88 number of patients which do not have liver disorders, it predicts inaccurately liver disorders test results of 8 number of them.

Table 3. Liver Disorder Laboratory Test results according to the system based on firefly algorithm

Liver Disorders Laboratory Test Results	Condition Positive	Condition Negative
Test Results Positive	True Positive (TP) = 188	False Positive (FP) = 8
Test Results Negative	False Negative (FN) = 16	True Negative (TN) = 88

As it is shown in Table 4, Negative predictive value is achieved 83.01%, Positive predictive value is achieved 95.91%, Sensitivity is achieved 92%, Specificity is achieved 84.16% and Accuracy (ACC) is achieved 92%. Positive predictive value 95.1% is significant because it gives a high confidence that its positive result is true. If sum of the sensitivity and specificity is higher than 170, it can be accepted that the system is useful and helpful as clinical investigation. In this study, the system determines condition as follows:

$$\text{Sensitivity} + \text{Specificity} = 92 + 84.16 = 176.16 > 170$$

Table 4. Simulation results and evaluations of liver disorder expert system

Negative Predictive Value	Positive Predictive Value	Specificity	Sensitivity	Precision	F_Measure	Accuracy
83.01	95.91	84.61	92	95.91	93.91	92

Figure 3 compares the values of real negative liver disorder and proposed system's negative liver disorder values in dataset. As it can be seen from the figure, the system achieves highly accurate predictions of Non-Liver Patients' Test Results values.

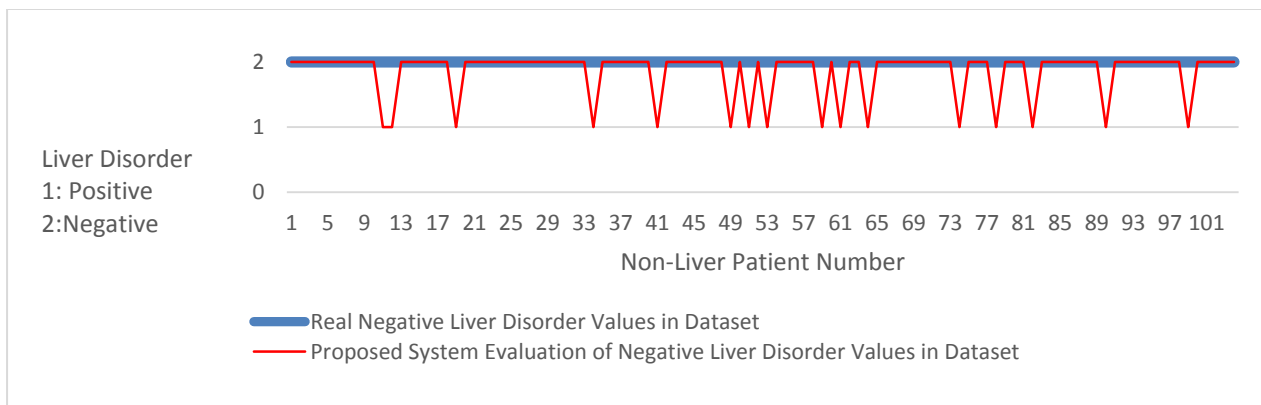


Figure 3. Comparison of real negative liver disorder values in dataset and proposed system’s negative liver disorders values in dataset

Figure 4 compares real positive liver disorder values in dataset and proposed system’s positive liver disorders values. It can be obtained from the simulation results that the system achieves highly accurate predictions of Liver Patients’ Test Results values.

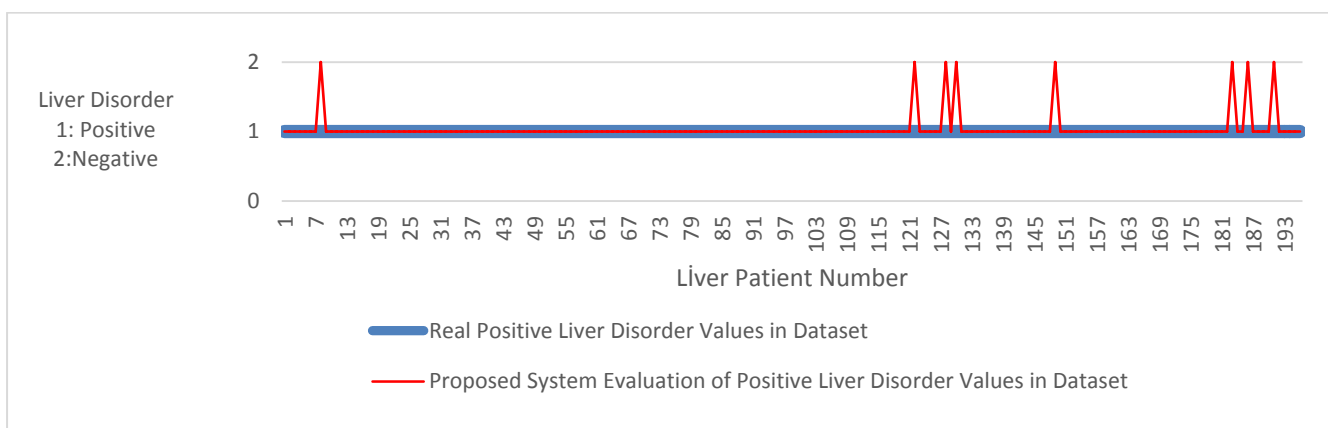


Figure 4. Comparison of real positive liver disorders value in dataset and proposed system’s positive liver disorders values

Firefly Algorithm based Expert System for Breast Cancer

Breast Cancer Wisconsin (Original) Data Set has 699 patients’ records which are used for evaluations of the proposed system. Specimens are obtained periodically. Therefore, the database represents this chronological grouping of the data set. Information of the dataset appears as below:

- Group 1: 367 instances (January 1989)
- Group 2: 70 instances (October 1989)
- Group 3: 31 instances (February 1990)
- Group 4: 17 instances (April 1990)
- Group 5: 48 instances (August 1990)
- Group 6: 49 instances (Updated January 1991)
- Group 7: 31 instances (June 1991)
- Group 8: 86 instances (November 1991)
-
- Total: 699 points (as of the donated database on 15 July 1992)

This data set comprises 241 number of malignant registers and 458 non benign registers. This breast cancer database is obtained from the University of Wisconsin Hospitals, Madison from Dr. William H. Wolberg [22].

There are 10 attributes in the dataset:

Attribute	Domain
1. Sample code number	id number
2. Clump Thickness	1 - 10
3. Uniformity of Cell Size	1 - 10
4. Uniformity of Cell Shape	1 - 10
5. Marginal Adhesion	1 - 10
6. Single Epithelial Cell Size	1 - 10
7. Bare Nuclei	1 - 10
8. Bland Chromatin	1 - 10
9. Normal Nucleoli	1 - 10
10. Mitoses	1 - 10
11. Class:	(2 for benign, 4 for malignant) [22]

In this study, patient Breast Cancer dataset by ignoring repetitive data is used for evaluating proposed system to equilibrate number of breast cancer and non-breast cancer. Number of Positive Breast cancer patient is 238 and negative liver patient is 225. In Table 5, Breast Cancer Laboratory Test results are given according to the system based on firefly algorithm. As it can be seen from the table, while the system predicts accurately breast cancer test results of 226 patients which have liver disorders, it predicts inaccurately liver disorders test results of 12 of them. It can also be obtained from the table that, the system predicts accurately liver disorders test results of 213 patients which do not have breast cancer, it predicts inaccurately liver disorders test results of 12 of them.

Table 5. Proposed system’s breast cancer laboratory test results

Breast Cancer Results	Condition Positive	Condition Negative
Test Results Positive	True positive (TP) = 226	False positive (FP) = 12
Test Results Negative	False negative (FN) = 12	True negative (TN) = 213

As it is shown in Table 6, Negative predictive value is achieved 83.01%, Positive predictive value is achieved 95.91%, Sensitivity is achieved 92%, Specificity is achieved 84.16% and Accuracy (ACC) is achieved 92%. Positive predictive value 95.1% can be accepted as significant because it gives a high confidence that its positive result is true. If sum of the sensitivity and specificity is higher than 170, it is said that the system is useful and helpful as clinical investigation. In this study, the system determines condition follows:

$$\text{Sensitivity} + \text{Specificity} = 92 + 84.16 = 176.16 > 170$$

Table 6. Simulation results and evaluations of breast cancer expert system

Negative Predictive Value	Positive Predictive Value	Specificity	Sensitivity	Precision	F_Measure	Accuracy
94.67	94.95	94.67	94.95	94.95	94.95	94.81

Figure 5 compares values of real negative breast cancer and the proposed system negative breast cancer values in dataset. It can be obtained from the figure that the system achieves highly accurate predictions of Non-Breast Cancer Patients’ Test Results values.

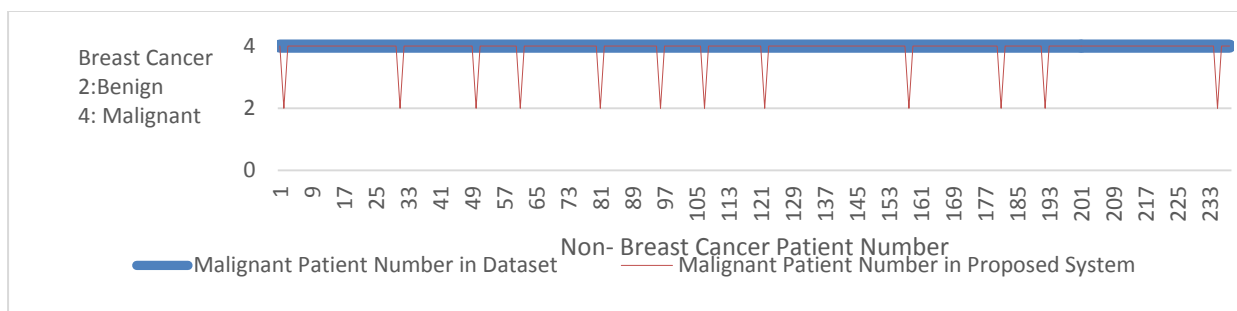


Figure 5. Comparison of real negative breast cancer values in dataset and proposed system's negative breast cancer values in dataset

Figure 6 compares the values of real positive breast cancer and the proposed system's positive breast cancer values. It can be obtained from the simulation results that the system achieves highly accurate predictions of Breast Cancer Patients.

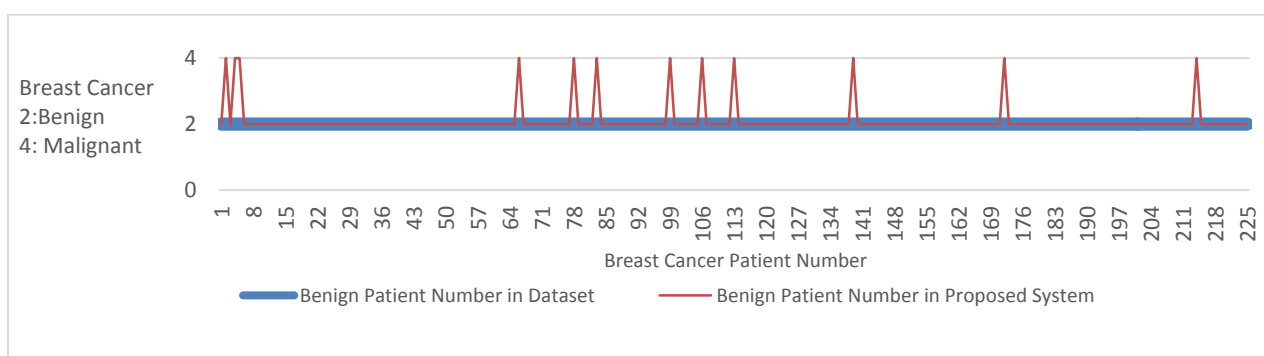


Figure 6. Comparison of the values of real positive breast cancer and proposed system's positive breast cancer.

Conclusion

In this study, an expert system is developed for the diagnosis of Breast cancer and Liver disorders. The expert system is driven by Firefly Algorithm. The system can be used by practitioners and touched health care personnel accurately and timely diagnosis of Liver Disorders and Breast Cancer irrespective of the position of the medical. The system can be useful for the hospitals which have insufficient number of doctors and medical personnel. It also can help to reduce a great number of patients who are waiting for to be checked by doctors [23]. The system which is based on firefly algorithm can be used to cut down the ratio of mortality and minimize the waiting time to meet medical experts. Computer program which is developed by mimicking human intelligence can be used to help doctors in making timely and exact decisions considering patients' diagnosis [5].

References

- Chair, E. F., Friedland ,P. E., Johnson, B. B., Nii H. P., Schorr, H., Shrobe, H.& Engelmores R. S., (May 1993), Knowledge-Based System in Japan, Expert Systems and Artificial Intelligence, JTEC(Japanese Technology Evaluation Center) Panel on.
- Samuel, O.W., Omisore, M.O. & Ojokoh, B.A., 2013 Elsevier Ltd., A web based decision support system driven by fuzzy logic for the diagnosis of typhoid fever.
- Durkin, J. J. (1994). Expert system design and development. New Jersey: Prentice-Hall.
- Szolovits, P., Patil, R. S., & Schwartz, W. B. (1988). Artificial intelligence in medical diagnosis. Journal of Internal Medicine, 108, 80–87.
- Ishak, W.H.W & Siraj ,F., (2002) . Artificial Intelligence in Medical Application: An Exploration. Health Informatics Europe Journal [Online].
- Ishak, W.H.W & Yamin, F.M., (2001). Artificial Intelligence in Decision-Making. Presented at National Conference on Management Science: New Paradigms for the Knowledge Economy (19-20 June), Universiti Putra Malaysia, Serdang, Selangor.

- Alexopoulos, E., Dounias, G. D., & Vemmos, K. (1999). Medical diagnosis of stroke using inductive machine learning. In *Machine learning and applications* (pp. 20–23). Chania, Greece
- Bourlas, P., Giakoumakis, E., & Papakonstantinou, G. (1999). A knowledge acquisition and management system for ECG diagnosis. In *Machine learning and applications: Machine learning in medical applications* (pp. 27–29). Chania, Greece.
- Ramana, B. V., Babu, M.S.P., & Venkateswarlu, N. B. (2011) A Critical Study of Selected Classification Algorithms for Liver Disease *International Journal of Database Management Systems (IJDMS)*, Vol.3, No.2, May.
- Ribeiro, R., Marinho, R., Velosa, J., Ramalho, F., & Sanches, J. M.,(2011) Diffuse liver disease classification from ultrasound surface characterization, clinical and laboratorial data, http://users.isr.ist.utl.pt/~jmrs/research/publications/myPapers/2011/2011_ibPRIA_RicardoRibeiro.pdf (Accessed 2.2. 2016)
- Neshat, M., Yaghibi, M., Naghibi, M.B., & Esmaelzadeh, A., (2008) Fuzzy Expert System Design for Diagnosis of liver disorders, *International Symposium on Knowledge Acquisition and Modeling*, 252 – 256, 978-0-7695-3488-6, IEEE.
- Vijayarani, S., & Dhayanand, Mr.S., Liver Disease Prediction using SVM and Naïve Bayes Algorithms (2015) *International Journal of Science, Engineering and Technology Research (IJSETR)* Volume 4, Issue 4, April .
- Gulia, A., Vohra, R., & Rani, P., (2014) Liver Patient Classification Using Intelligent Techniques, (*IJCSIT*) *International Journal of Computer Science and Information Technologies*, Vol. 5 (4), 2014, 5110-5115
- Kahramanli, H., & Allahverdi, N., (2009) , Mining Classification Rules for Liver Disorders. *International Journal Of Mathematics And Computers In Simulation* 1, 9-19
- Akay M.F., (2009) Support vector machines combined with feature selection for breast cancer diagnosis, Elsevier Ltd. All rights reserved, *Expert Systems with Applications* 36 3240–3247
- Medical News Today : Your source for health news since 2003. <http://www.medicalnewstoday.com/articles/37136.php?page=2> Accessed 01.02.2016.
- Breast Cancer Care (2001) <https://www.breastcancercare.org.uk/information-support/have-i-got-breast-cancer/what-breast-cancer>
- NHS Choices, <http://www.nhs.uk/Conditions/Cancer-of-the-breast-female/Pages/Introduction.aspx>, Accessed 02.02.2016.
- Sensitivity and specificity From Wikipedia, the free encyclopedia, https://en.wikipedia.org/wiki/Sensitivity_and_specificity, Accessed 10.02.2016
- The UC Irvine Machine Learning Repository, <http://archive.ics.uci.edu/ml/datasets/ILPD+%28Indian+Liver+Patient+Dataset%29> Accessed 12.10.2015.
- M.S.Prasad Babu & Somesh Katta , (2015), Artificial Immune Recognition Systems in Medical Diagnosis , *Software Engineering and Service Science (ICSESS)*, 6th IEEE International Conference on, 978-1-4799-8352-0, IEEE.
- The UC Irvine Machine Learning Repository, <http://archive.ics.uci.edu/ml/datasets/Breast+Cancer+Wisconsin+%28Original%29> Accessed 12.10.2015.
- Rong-Ho Lin. An intelligent model for liver disease diagnosis. *Artificial Intelligence in Medicine* 2009;

Author Information

Aysegul Alaybeyoglu

Izmir Katip Celebi University

Computer Engineering Department

Contact e-mail: aysegul.alaybeyoglu@ikc.edu.tr

Naciye Mulayim

Izmir Katip Celebi University

Biomedical Engineering Department

Appendix

Table 1.A Some of the training data set of 70 number of liver disorder patients

AGE	gender	TB	DB	TP	ALB	A/G	SGPT	SGOT	ALKPHOS	RESULT
52	Male	0.6	0.1	178	26	27	6.5	3.6	1.2	-1
66	Male	0.6	0.2	100	17	148	5	3.3	1.9	-1
55	Male	0.8	0.2	482	112	99	5.7	2.6	0.8	1
37	Male	0.8	0.2	147	27	46	5	2.5	1	1
61	Male	0.8	0.1	282	85	231	8.5	4.3	1	1
61	Male	0.8	0.2	163	18	19	6.3	2.8	0.8	-1
61	Male	0.8	0.2	192	28	35	6.9	3.4	0.9	-1
.
.

Table 2.A Some of the training data set of 60 number of breast cancer patients

Sample code number	Clump Thickness	Uniformity of Cell Size	Uniformity of Cell Shape	Marginal Adhesion	Single Epithelial Cell Size	Bare Nuclei	Bland Chromatin	Normal Nucleoli	Mitoses	Class:
1018099	1	1	1	1	2	10	3	1	1	-1
1223543	1	2	1	3	2	1	1	2	1	-1
1223793	6	10	7	7	6	4	8	10	2	1
654546	1	1	1	1	2	1	1	1	8	-1
654546	1	1	1	3	2	1	1	1	1	-1
1091262	2	5	3	3	6	7	7	5	1	1
1167439	2	3	4	4	2	5	2	5	1	1
850831	2	7	10	10	7	10	4	9	4	1
1105257	3	7	7	4	4	9	4	8	1	1
.
.
.

Investigation the Performance of Stream Water Wheel Turbines using CFD Techniques

Mohammad A. AL-DABBAGH
Northern Technical University

Abstract: A stream water wheel is a machine for converting the energy of moving water into power. It consists of a large metal wheel, with a number blades arranged on the outer rim which allows the wheel to be rotated by the water striking the blades. Water wheels were used since ancient as a primary source of power. It was used for irrigation, grain milling and supplying villages with water. In the present study, a stream water wheel turbine of 5 m in diameter is numerically simulated using ANSYS-CFX package under different flow conditions. The wake region behind the turbine is monitored where it influences on other turbines next to it. The simulation results have shown that in case of constructing a farm of wheel turbines, the streamwise span should not be less than 6 m. The stream wheel turbines works normally at a tip speed ratio TSR less than unity.

Keywords: Hydrokinetic turbines, Stream-water wheel turbine, Efficiency, CFD

Introduction

The water wheel was used as a primary source of power since ancient times (Denny 2004). It has been used for irrigation, grain milling and supplying villages with drinking water. It was considered as the first method that is used to replace the muscular effort of the humans and animals to perform a mechanical energy. The oldest water wheel, which is in a reserved panel of a mosaic is dating back to 4000 years BC, was built in Damascus (Institute of Technology – Baghdad – Iraq 2013) and another ancient one was found in Hama (Figure 1). The water power was used also in Mesopotamia and by Egyptians. They are harnessing energy from flux water by waterwheels giving revolving energy for different purposes (Schlager and Weisblatt 2006; Muller et al. 2007). Ancient Greeks, Chinese and Romans have also constructed great waterwheels to grind their grains. The Roman Architect Vitruvius already mentioned the stream wheels (Muller et al. 2007). At the end of the 18th century, about 500,000 watermills were working in Europe (Quaschnig 2010).



Figure 1. The water wheel that exists in Hama

Water wheels are categorized by the method that make water entering the turbine, relative to the wheel's axle (Figure 2). The overshot & pitch back water wheels are appropriate where there is water level difference of no more than 2 meters, often in connotation with a small basin. Breastshot and undershot wheels can be utilized with streams or high volume currents with big lakes (Paudel et al. 2013).

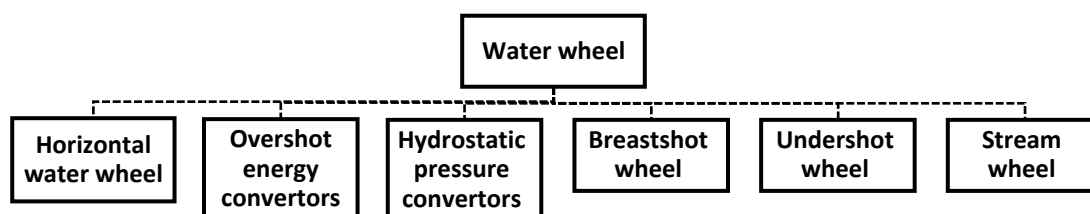


Figure 2. Water wheel classification

Many investigations have shown that water wheels are theoretically and economically promising choices for low head places with an efficiency range of 75-85% over changeable flow currents. Using a water wheel with big size chambers and low angular speeds aquatic life out of danger and the geometrical shape of the wheel provide well sediment passage and make it easier to floating the rubbish (Muller and Kauppert 2004). In addition, a strong and easy design of a water wheel leads to fewer works in constructing, working and repairing the structure, which result in less primary operation and maintenance prices (Woods et al. 2010). Table 1 shows specifications of different water wheels.

Table 1. Technical specifications of some water wheel turbines

Turbine type	Classification	Dimension (m)	Rated power (kw)	No. of blades	Working head (m)	Flow rate m ² /sec	Efficiency %
Horizontal water wheel		--	--	Multi	--	--	15-30
Overshot energy convertors	Overshot water wheel						
	Reversible water wheel	3-20	1.3-20	8-16	2.5-10	0.1-0.2	60-80
	Backshot water wheel						
Hydrostatic pressure convertors	Suspension water wheel						
	Back pres. Turbine Hydrostatic machine	0.8-5	2-12	Multi	1-2.5	0.5-0.6	60-90
Breastshot wheels	Sagebien wheel	4-8	5-200	Multi	0.75-5	0.35-0.65	50-75
Undershot wheel	Aqualienne wheel						
	Zuppinger wheel	2-4H	5-100	Multi	0.5 -3	0.5-0.95	35-76
Stream wheels	Poncelet wheel						
	Subcritical wheel	2-6	1.7-33	Multi	0.4-1.5	2.5-3.75	30-68
	Supercritical wheel						
	Deep water wheel						

Numerical Model

In the present study, because that the domain includes a rotating object, the wheel, a complex flow regime is expected to be occurred. The Reynolds stress-omega transport turbulence model is dependent as the powerful tool for analyzing the flow around and behind the structure. The occurrence of flow separation is maintained by this model. In addition, the complicated regimes represented by swirling and rotating fluids are treated well by this model. Because that this model treats the boundary layer near wall and be efficient for low Reynolds numbers besides the high ones, it is suitable for investigating the flow behavior in shallow streams where water wheel turbines work (Speziale et al. 1991; Biscarini et al. 2010; Chevallet et al. 2012). The basic equations representing the Reynolds stress- omega turbulence model are given as follow:

$$\frac{\partial}{\partial t}(\rho \overline{u'_i u'_j}) + \frac{\partial}{\partial x_k}(\rho u_k \overline{u'_i u'_j}) = -\frac{\partial}{\partial x_k} \left[\rho \overline{u'_i u'_j u'_k} + p'(\delta_{kj} u'_i + \delta_{ik} u'_j) \right] + \frac{\partial}{\partial x_k} \left[\mu \frac{\partial}{\partial x_k} (\overline{u'_i u'_j}) \right] - \rho \left[\overline{u'_i u'_k} \frac{\partial u_j}{\partial x_k} + \overline{u'_j u'_k} \frac{\partial u_i}{\partial x_k} \right] - \rho \beta (g_i \overline{u'_j \theta}) + p' \left(\frac{\partial u'_i}{\partial x_j} + \frac{\partial u'_j}{\partial x_i} \right) - 2\mu \frac{\partial u'_i}{\partial x_k} \frac{\partial u'_j}{\partial x_k} - 2\rho \Omega_k (\overline{u'_j u'_m} \varepsilon_{ikm} + \overline{u'_i u'_m} \varepsilon_{jkm}) + S_{user}$$

While the left side of the equation represents the summation of the local time derivative and the convection, the right side equals to the summation of molecular diffusion and pressure strain besides the user defined sources minus the turbulent diffusion, stress production, buoyancy production, dissipation and production by system rotation, respectively.

Model Setup

The present study involves investigation the performance of stream water wheel turbines. Simulation analyses are conducted using CFD techniques under two different flow velocities of 1.0 m s⁻¹ and 2.0 m s⁻¹. A wheel turbine with 12 blades is designed and placed at 5 m far from the inlet of a rectangular channel of 30 m length, 5 m height and 1 m width with a horizontal layout (Figure 3). The side walls are given a symmetry boundary condition and the bottom was smooth wall. The upper face of the domain is considered as free to atmosphere. The left face of the channel is considered as the channel entrance and given an inlet boundary condition while the right side, which is the channel outlet, was given a zero pressure. A clear water is used with a density of 998 kg m⁻³ and flowing with no any sediments.

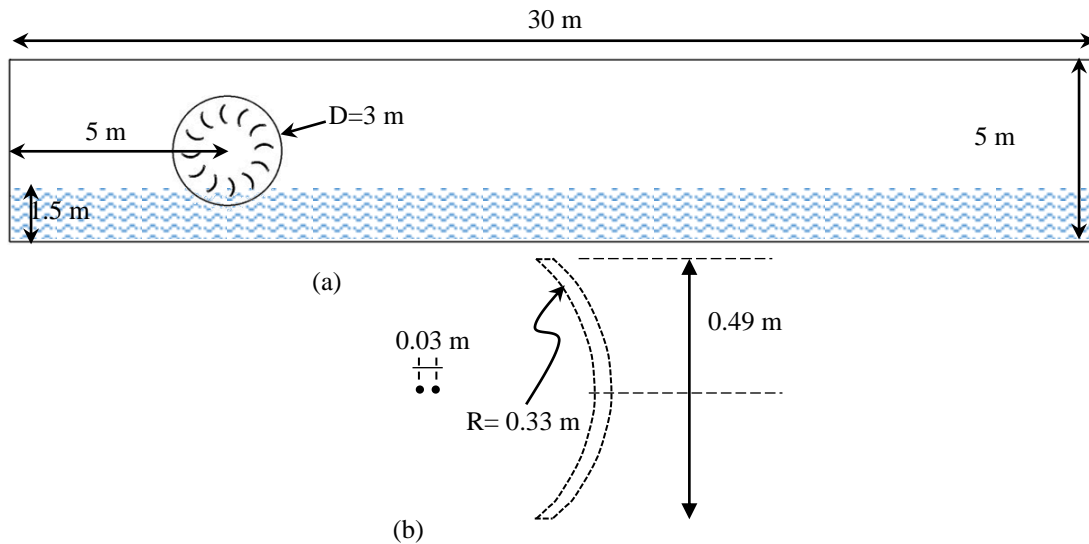


Figure 3. a. Channel domain and wheel position, b. blade's design

Meshing Process

In computational fluid dynamics simulation, the solution progress is constraint by mesh type and the refinement rate. When mesh elements are coarse, bad quality, the controlled volume will be instable and the solution progress will be diverged or may reach the end of the solution with high errors. This is attributed to that the output results from an element are dependent as input for the next element, so, when the element is coarse, large volume, no data will be available for some interested points inside. Therefore, the output results will be unsatisfied. Nevertheless, fine elements increase the rate of convergence and the simulation analysis progresses smoothly with low error residuals. Many types of mesh are provided by ANSYS package, which are tetrahedron, hex, prism and quadrilateral shapes. Each type serves a specific region where it is not recommended to use hex meshing for swept bodies while tetrahedron elements are good for moving or rotating machines. In the present study, the domain includes rotating object, therefore, triangle elements are used. Figure 4 shows the initial mesh in compare with the final mesh at the end of the simulation. It shows how the mesh becomes finer at the regions close to the blades while in the middle, the elements are coarse. This is attributed to that the entire region is free of water except some amounts which are lifted by the blades.

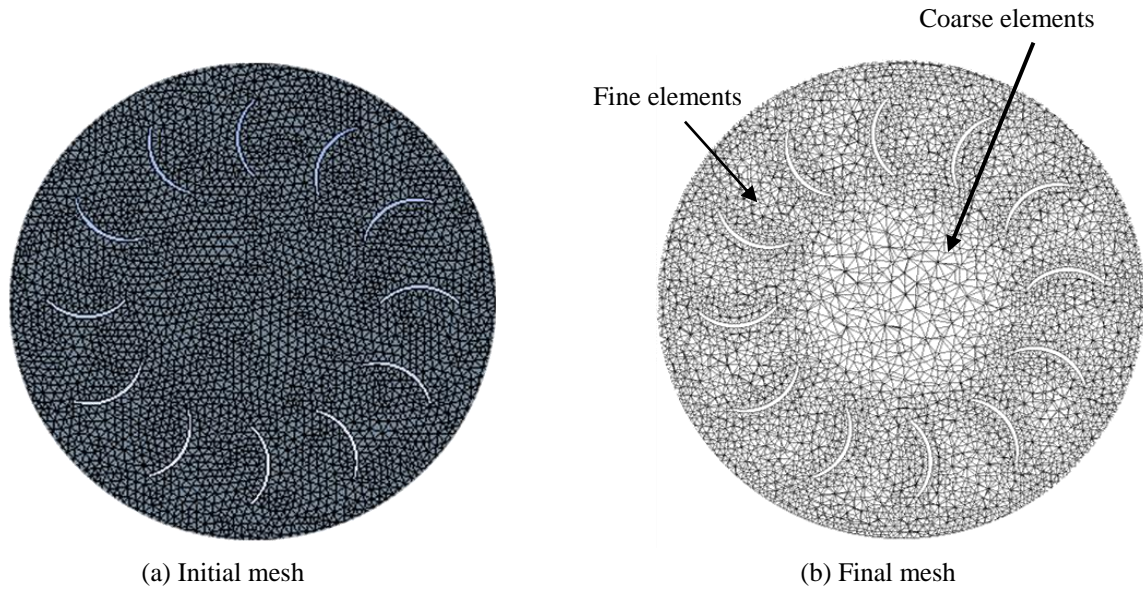


Figure 4. Initial and final mesh

Simulation Results

This study performs simulation analyses in order to investigate the flow pattern downstream stream water wheel turbines under different flow conditions. A constant number of blades is taken, which are 12 blades. The performance of the turbine is evaluated at different tip speed ratios. The tip speed ratio (TSR) is defined as the ratio of the rotational velocity of a turbine to the velocity of the flowing fluid. The TSR is considered as an important parameter should be taken into account to specify the optimum range of the angular velocity that gives a highest power value. (Cao 2011; Winchester and Quayle 2011; Niblick 2012; Syed Shah et al. 2013).

$$\lambda = \frac{\omega R}{v_{\infty}} \quad (1)$$

Where:

λ : tip speed ratio (TSR).

ω : angular speed of turbine.

R: turbine radius.

v_{∞} : free stream velocity.

The performance of the turbine is evaluated in terms of the power coefficient or the efficiency.

The turbine efficiency or the performance coefficient is a dimensionless parameter describing the performance of the turbine, which is determined as follow;

$$\eta = \frac{P_t}{P_w} = \frac{T\omega}{0.5\rho A v_{fluid}^3} \quad (2)$$

Where:

P_t : turbine power.

P_w : flowing water power.

T: torque developed by turbine shaft (N-m).

ω : angular velocity of the turbine (rads^{-1}).

ρ : water density (kgm^{-3}).

A: turbine's frontal cross-sectional area (m^2).

v_{fluid} : water velocity (m s^{-1}).

The simulation results have shown that performance of the wheel turbine under the two given velocities was the same. The water level raised up at the upstream side of the turbine due to flow resistance by the submerged body. For the given velocities, the flowing water downstream the turbine shows similar behavior. It is noticed that downstream the turbine at a distance of about 3 times the diameter of the wheel, the water level returns to

its initial case (Figures 5 and 6). The performance of the model is investigated at different tip speed ratios TSRs' where the turbine reached the maximum efficiency of about 0.15 at a TSR of about 0.42. At high TSR values, the turbine behaved similarly under the two given velocities where the efficiency was inversly proportional to the TSR values above 0.42 (Figure 7). Figure 8 shows the turbulence region at different velocities and rotational speeds in term of the water volume fraction.

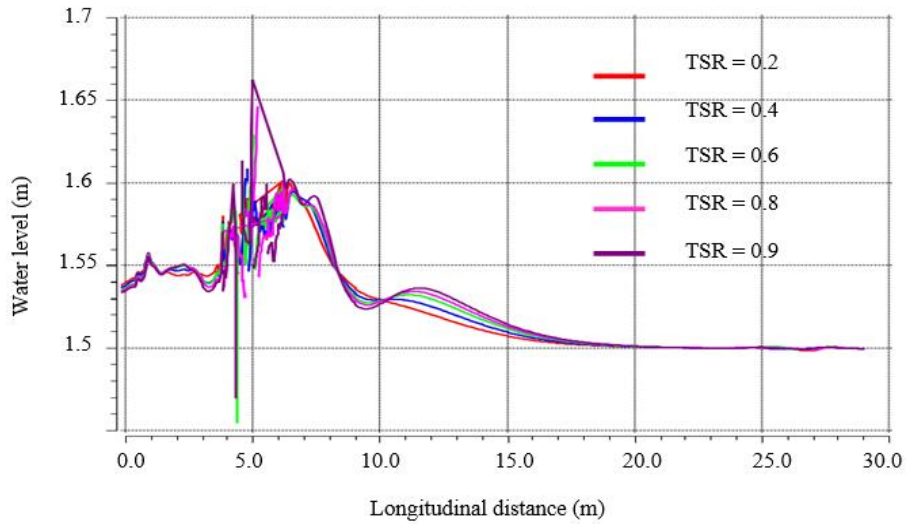


Figure 5. Water level at different distances along the channel at a flow velocity of 1.0 m s^{-1}

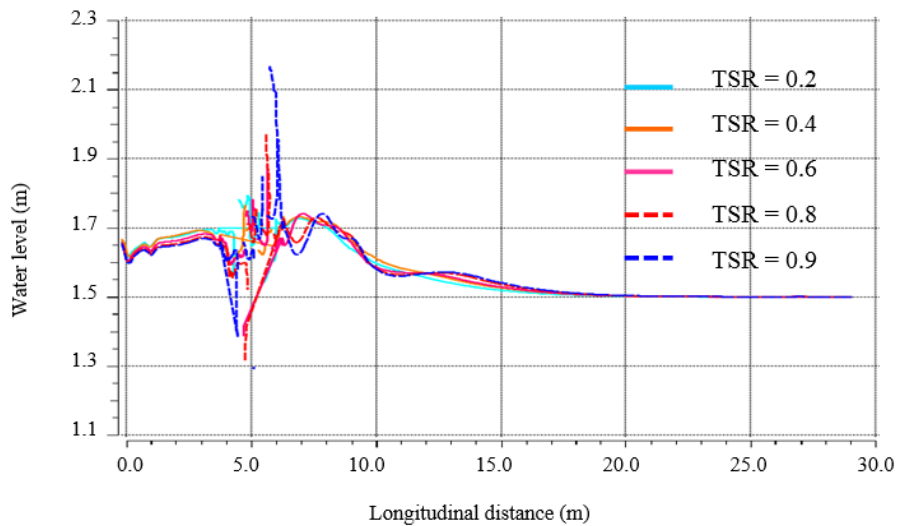


Figure 6. Water level at different distances along the channel at a flow velocity of 2.0 m s^{-1}

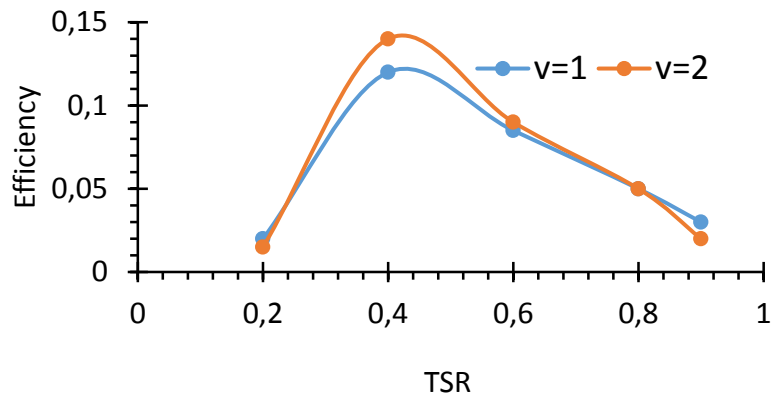


Figure 7. The turbine efficiency at different tip speed ratios

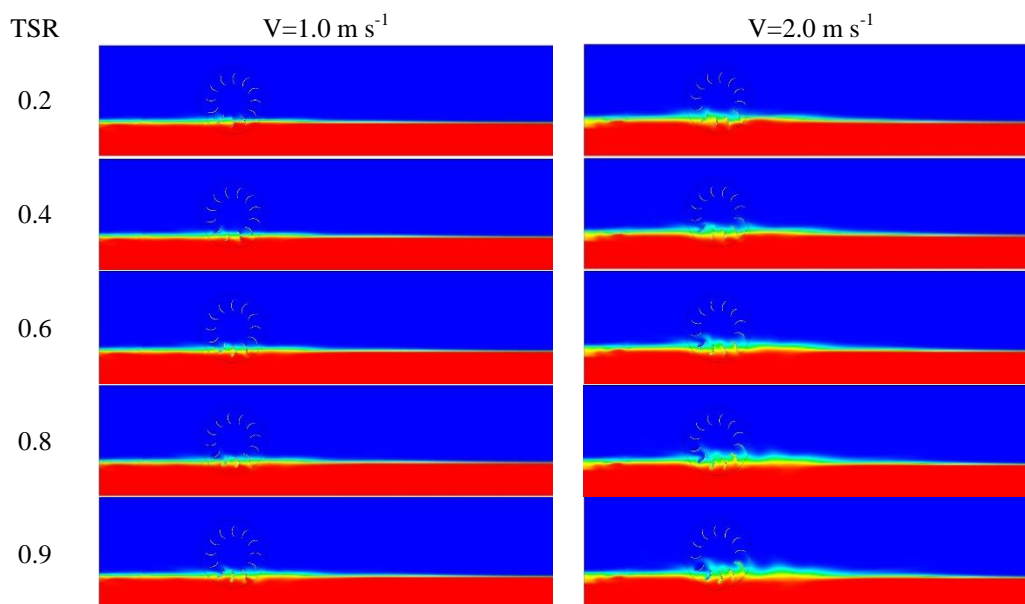


Figure 8. Water volume fraction under different flow conditions and TSRs'

Conclusions

In the present study, the performance of stream water wheel turbines is evaluated under different flow conditions. Computational fluid dynamics simulations analyses are conducted in order to investigate the suitable streamwise distance between the turbines. The simulation results have shown that in case of constructing a farm of stream water wheel turbines, the distance between the turbines should not be less than 3 times the diameter of the wheel. The flowing water behaved similarly at the two given velocities with high turbulence intensity for the maximum given velocity.

References

- Biscarini, C., Francesco, S. D. & Manciola, P. (2010). CFD modelling approach for dam break flow studies. *Hydrol. Earth Syst. Sci.*, Vol. 14, pp. 705–718.
- Chevallet, G., Jellouli, M. & Deroo, L. (2012). Democratization of 3D CFD hydraulic models: several Examples performed with ANSYS CFX. *SimHydro: New trends in simulation*. Sophia Antipolis.
- Denny M. The efficiency of overshoot and undershot water wheels. *European Journal of Physics*; 2004. 25: 193-202.
- Institute of Technology – Baghdad – Iraq, 2013.
- Muller G, Denchfield S, Marth R and Shelmerdine R. Stream wheels for applications in shallow and deep water. *Proceedings of 32nd IAHR Congress, Venice, Italy, Theme C2c, paper 291*; 2007.
- Muller G, Kauppert C. Performance characteristics of water wheels. *Journal of Hydraulic Research*; 2004a. 42(5):451-60.
- Paudel S, Linton N, Zanke UCE, Saenger N. Experimental investigation on the effect of channel width on flexible rubber blade water wheel performance, *Renewable Energy*; 2013. 52:1-7.
- Quaschnig V. *Renewable energy and climate change*. Singapore: Wiley; 2010.
- Schlager N, Weisblatt J, editors. *Alternative energy*. Vol.1.China: Thomson Gale; 2006.
- Speziale, C. G., Sarkar, S., & Gatski, T. B. (1991). Modeling the Pressure-Strain Correlation of Turbulence: An Invariant Dynamical Systems Approach. *J. of Fluid Mechanics*, Vol. 227, pp. 245-272.
- Woods G, Tickle A, Chandler P, Beardmore J, Pymm R. Peak power: Developing micro hydropower in the peak district, friends of the peak district, UK; 2010. Available at: <http://www.friendsofthepeak.org.uk/download/files/HYDRO/PEAKPOWERMainreportAppA.pdf>; 2010 [accessed: 30.09.12].

Author Information

Mohammad A. Al-Dabbagh

Northern Technical University, Technical Institute/ Mosul,
Department of water resources techniques
Mosul/ Iraq
Contact e-mail: mohamed.akram@ntu.edu.iq

Evaluation of Flow behavior over Broad-Crested Weirs of a Triangular Cross-Section using CFD Techniques

Mohammad A. AL-DABBAGH
Northern Technical University

Sulaiman D. AL-ZUBAIDY
Northern Technical University

Abstract: Weirs are barriers placed across a river and designed to control the flowing water in order to prevent floods, make waterways operable for inland navigation and measure flow discharge. Although there are many types of weirs, mainly used ones are sharp-crested, circular-crested (cylindrical), broad crested and ogee weirs. In the present study, triangular broad-crested weirs are numerically investigated under different flow conditions. Different interior angles of 90° , 100° , 110° and 120° are included for the opening of weirs. The flowing water over weirs is simulated using CFD techniques and evaluated at different flow regimes with inlet discharges of $0.012 \text{ m}^3 \text{ s}^{-1}$, $0.036 \text{ m}^3 \text{ s}^{-1}$ and $0.06 \text{ m}^3 \text{ s}^{-1}$. The simulation results have shown that the water level upstream the weir is inversely proportional to the opening angle, where an increment of 10° in the opening angle leads to a drop in water level about 1.5 cm. In addition, applying a discharge of $0.012 \text{ m}^3 \text{ s}^{-1}$, an uncovered region with water is created downstream the triangular broad-crested weirs, while the bed downstream of the rectangular broad-crested weir is covered with a thin layer of water at the same flow discharge. The aforementioned results are compared with a comparative data and show good agreement. By using triangular broad-crested weirs, it is important to measure the wake region and the hitting point of falling water downstream the weirs where this area must be strengthened well in order to resist water power and reduce the risk of drift.

Keywords: Weir, CFD, V-notch, Broad-Crested weir, Turbulence model

Introduction

Weirs are simple hydraulic structures used for flow measuring. They work as overflow dams to control water level in open streams (Lodomez et al. 2014). Weirs are classified according to the geometrical shape into different types such as rectangular, triangular, trapezoidal and cylindrical shapes. They are classified also according to the type of weir crest into two types, sharp-crested and broad-crested weirs (Hoseini et al. 2013). These structures are featured by their ease in design and low cost in maintenance. Investigating the flow behavior over weirs was interested by many researchers where many kinds of physical and numerical models are evaluated in term of their performance. Naghavi et al. (2011) evaluated experimentally and numerically the performance of circular weirs. Their results have shown that nappe separation significantly depends on the overflow discharge. Afshar and Hooman (2013) investigated experimentally and numerically the flow behavior over rectangular broad crested weirs. Computational fluid dynamics techniques are used with three turbulence models of RNG k- ϵ , standard k- ϵ and large eddy simulation LES in order to determine the water surface profile over the weir. The simulation results were agreed with the experimental work. Moreover, Namaee in (2014) studied numerically the performance of side weirs with an inclined ramp. He used ANSYS-FLUENT software with the standard k- ϵ turbulence model his results show that placing an inclined ramp decreases the lateral outflow. Yuce et al. (2015) have shown in the numerical study performed to evaluate the flow behavior over oblique cylindrical weirs that the flow over weirs is affected by the geometrical shape of the weir. They used CFD techniques with the SSG Reynolds stress turbulence model, where the simulation results have shown that the increasing the angle of obliqueness increases the flow velocity at the downstream face of the weir. In the

present study, the flow behavior over triangular broad-crested weirs is numerically investigated under different flow regimes using CFD techniques.

Numerical model

In fluid dynamics, the turbulence phenomena was the main subject considered by many researchers where it influences significantly on the hydraulic structures. Recently, different models have been developed in order to describe how the turbulence occurs. Each turbulence model used to describe a specific flow regime. Flow regimes of low turbulence are described by simple models such as k-ε and k-ω models while flow of high complexity, which includes rotating objects and large vortices, is described well by developed models such as Reynolds stress models. In the present study, because that no flow region of high complexity is expected, k-ε turbulent model is dependent to evaluate the flow behavior over rectangular and triangular broad-crested weirs (ANSYS user's guide).

The transport equations in the realizable k-ε model are:

$$\frac{\partial}{\partial t}(\rho k) + \frac{\partial}{\partial x_j}(\rho k u_j) = \frac{\partial}{\partial x_j} \left[\left(\mu + \frac{\mu_t}{\rho k} \right) \frac{\partial k}{\partial x_j} \right] + G_K + G_b - \rho \varepsilon - Y_M + S_k \quad (1)$$

and

$$\frac{\partial}{\partial t}(\rho \varepsilon) + \frac{\partial}{\partial x_j}(\rho \varepsilon u_j) = \frac{\partial}{\partial x_j} \left[\left(\mu + \frac{\mu_t}{\sigma_\varepsilon} \right) \frac{\partial \varepsilon}{\partial x_j} \right] + \rho C_1 S \varepsilon - \rho C_2 \frac{\varepsilon^2}{k + \sqrt{\nu \varepsilon}} + C_{1\varepsilon} \frac{\varepsilon}{k} C_{3\varepsilon} G_b + S_\varepsilon \quad (2)$$

Where

$$C_1 = \max \left[0.43, \frac{\eta}{\eta + 5} \right], \eta = S \frac{k}{\varepsilon}, S = \sqrt{2 S_{ij} S_{ij}} \quad (3)$$

Where; G_k , G_b are the turbulent kinetic energy created by mean velocity gradient and buoyancy, Y_M indicates the fluctuation in turbulence relative to the dissipation rate, σ_k and σ_ε represent the turbulent Prandtl numbers for kinetic energy and dissipation rate, S_k and S_ε are terms of user-defined source, C_1 and C_2 are constants.

Model Setup

In the present study, water flow over triangular broad-crested weirs is numerically investigated under different conditions. An open channel of 5 m length and 0.6 m width and 0.8 m height is included in the numerical models. Triangular broad-crested weirs with different opening angles are investigated under different flow regimes. The performance of weirs is evaluated under three different Froude numbers of 0.28, 0.85 and 1.4. The weir models are designed with four different opening angles of 90°, 100°, 110° and 120° (Figure 1). The triangular weirs are broad-crested with a length of 0.5 m and placed at 1.0 m from the inlet. The channel inlet and outlet were given a pressure inlet and pressure outlet, respectively. The channel sides, bottom and weir models were smooth walls. The upper face of the domain is subjected to atmospheric pressure (Figure 2).

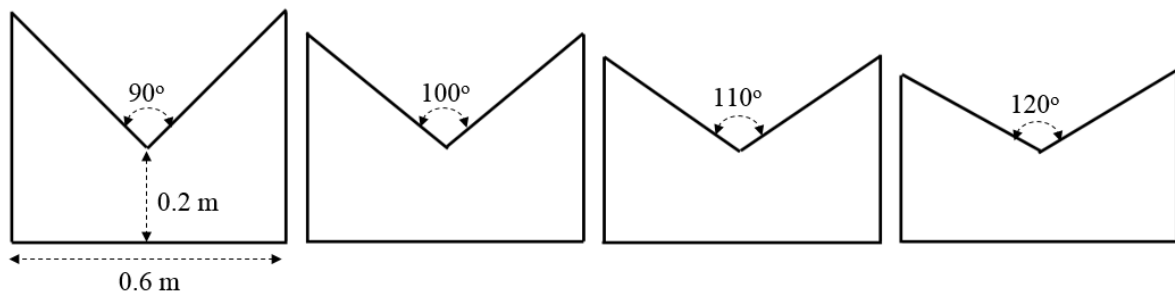


Figure 1. Triangular broad-crested weirs

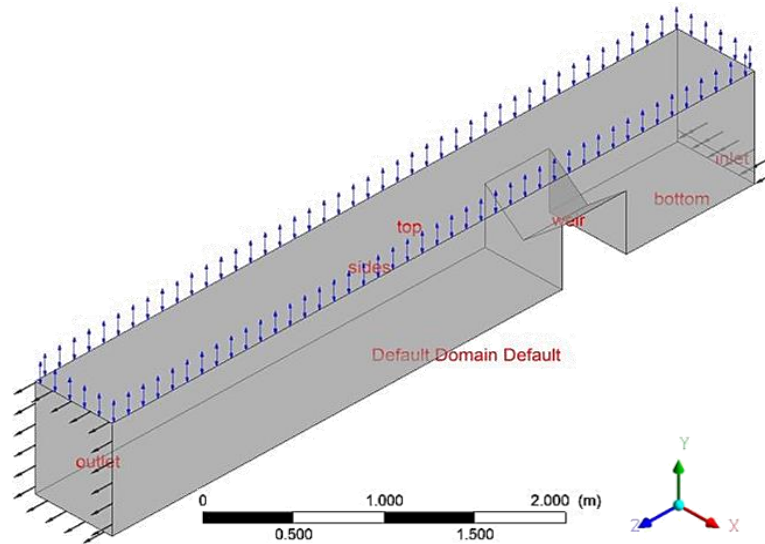


Figure 2. Channel domain and weir position

Simulation Results

In this study, computation fluid dynamics simulations have been performed in order to evaluate the flow behavior over triangular broad-crested weirs. A constant crest width of 0.5 m is used for triangular broad-crested models and the latter are designed with different opening angle of 90° , 100° , 110° and 120° . Three different Froude numbers are dependent to monitor the water level upstream the weir and the flow velocity downstream it.

Mesh Refinement

In CFD analyses, the solution progress is significantly depending on how the mesh is fine enough to avoid creation of folded elements. The accuracy of results is directly proportional to the mesh quality (Almohammadi et al. 2013). In the present study, the mesh refinement technique, which is provided by ANSYS package, is used in order to refine the mesh elements and reach the desired results (Yuce et al. 2015). Two levels of mesh refinement are performed for all models, where the refinement techniques senses turbulence regions, refines the elements depending upon the level of refinement as shown in figure 3.

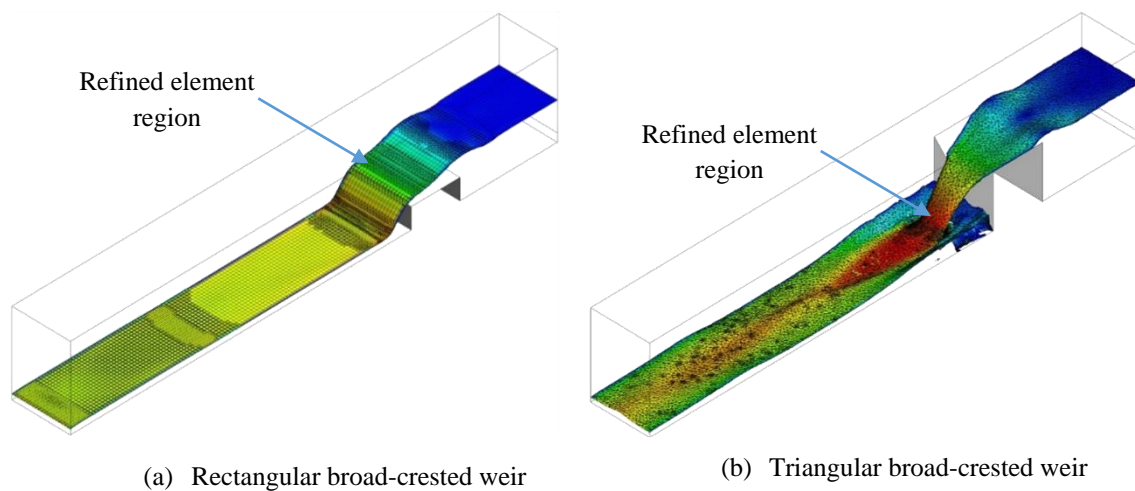


Figure 3. Mesh refinement

Effect of the Opening Angle

The simulation results have shown that when a flow discharge of $0.012 \text{ m}^3 \text{ s}^{-1}$ is given to the inlet, an uncovered region with water is created at the downstream side for all triangular broad-crested weirs (Figure 3.a). Nevertheless, providing the system with a discharge of $0.036 \text{ m}^3 \text{ s}^{-1}$ and $0.06 \text{ m}^3 \text{ s}^{-1}$ results in increasing the velocity of dropping water (Figure 3.b, c). Regarding the water level (h_u), the opening angle of triangular broad-crested weirs is inversely relative to water level upstream the weirs, whereas the opening angle of v-notch weirs increases 10° , the water level slightly decreases about 1.5 cm for the same discharge.

In the rectangular broad-crested weir, the simulation results have shown that there is no uncovered region with water is created at the downstream side and the water falls smoothly over the crest. The water level upstream the rectangular broad-crested weir was 0.27 m when a discharge of $0.012 \text{ m}^3 \text{ s}^{-1}$ is applied. Frequently, providing a discharge of $0.036 \text{ m}^3 \text{ s}^{-1}$ increases the water level at the upstream side about 0.04 m and also for the discharge of $0.06 \text{ m}^3 \text{ s}^{-1}$ (Figure 4).

Consequently, the pressure exerted by falling water (p_{dw}) with a discharge of $0.012 \text{ m}^3 \text{ s}^{-1}$ on the downstream side of the weir with an opening angle of 90° to 110° is increased about 120 Pa, in average, and about 43 Pa for the weir of 120° angle. In addition, increasing the discharge to $0.036 \text{ m}^3 \text{ s}^{-1}$ causes an increment in the pressure at the downstream bed about 2.4 KPa, 2.0 KPa, 1.5 KPa and 1.0 KPa for the weirs of 90° , 100° , 110° and 120° , respectively. Moreover, at a discharge of $0.06 \text{ m}^3 \text{ s}^{-1}$, the increment of the pressure was about 0.9 KPa, 0.98 KPa, 1 KPa and 1.1 KPa for the triangular broad-crested weirs of an opening angle of 90° , 100° , 110° and 120° .

The effective point that the falling water hits (x_e) is located on the bed downstream the weirs at a distance of about 0.66 m, 0.84 m and 0.83 for the three discharge of $0.012 \text{ m}^3 \text{ s}^{-1}$, $0.036 \text{ m}^3 \text{ s}^{-1}$ and $0.06 \text{ m}^3 \text{ s}^{-1}$, respectively (Table 1). The insignificant reduction in the location of hitting point downstream the v-notch weirs between the discharges $0.036 \text{ m}^3 \text{ s}^{-1}$ and $0.06 \text{ m}^3 \text{ s}^{-1}$, which is about 0.01 m, is attributed to the occurrence of overtopping flow where it decreases the distance of falling water downstream the weirs.

Regarding the rectangular broad-crested weir, the flowing water passed smoothly over the weir with low water head at the upstream side. These results are well agreed with the numerical study performed by Afshar and Hooman (2013) as shown in figure 5.

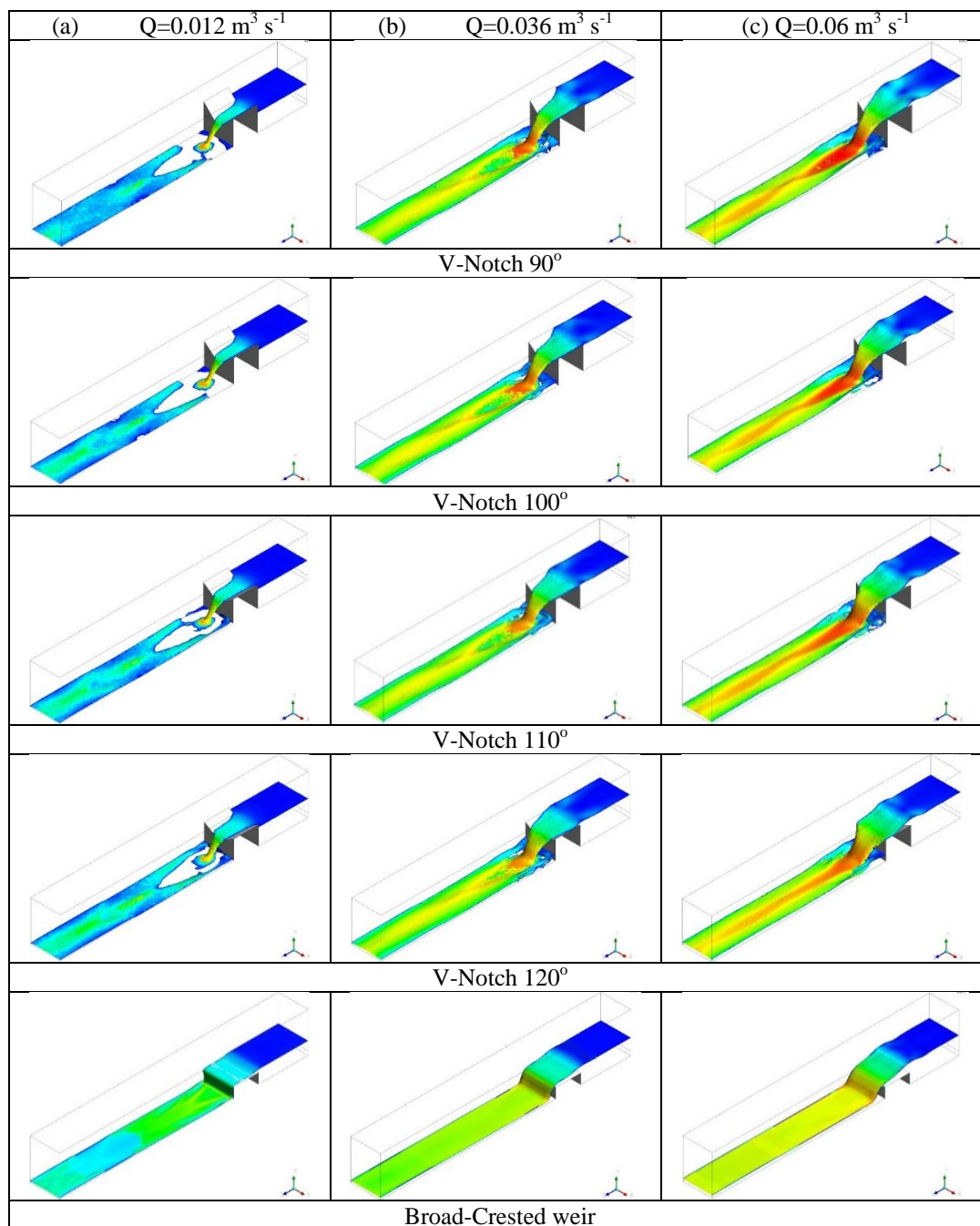


Figure 3. Water surface profile for different triangular broad-crested weirs

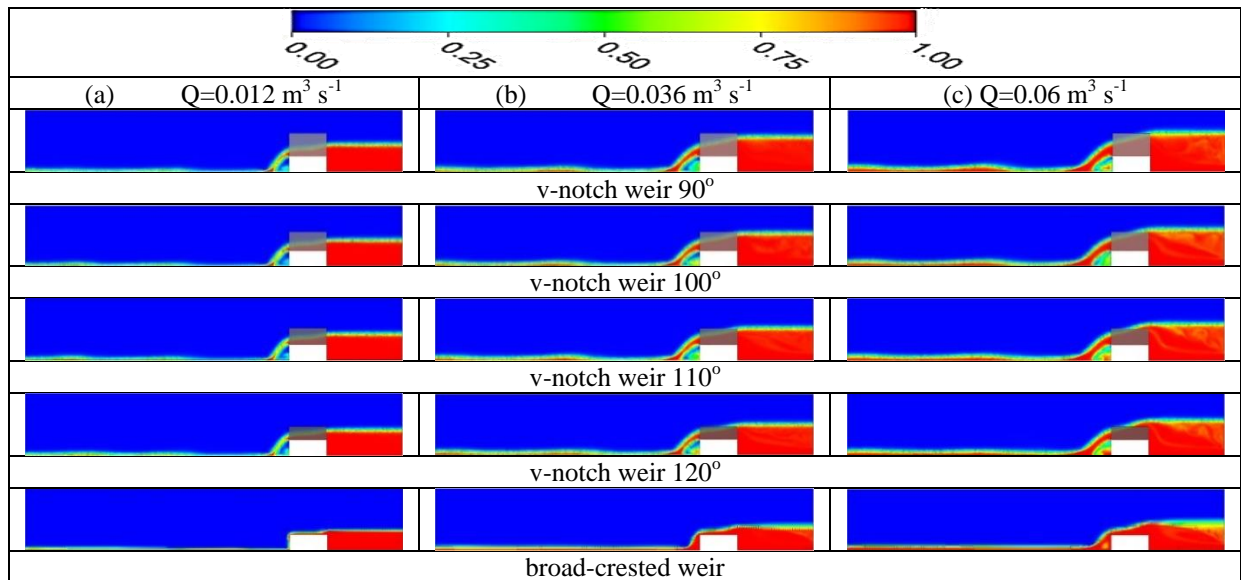


Figure 4. Water volume fraction at different flow conditions

Table 1. The simulation results

Variable	Rectangular broad-crested weir	triangular broad-crested weirs 90°	triangular broad-crested weirs 100°	triangular broad-crested weirs 110°	triangular broad-crested weirs 120°
h_u (m)	0.27	0.36	0.35	0.35	0.33
P_{dw} (Pa)	1428.28	519.824	629.989	757.163	800.05
x_e (m)	0.5	0.66	0.67	0.67	0.65
$Q=0.012 \text{ m}^3 \text{ s}^{-1}$					
h_u (m)	0.32	0.45	0.43	0.4	0.4
P_{dw} (Pa)	1357.9	2918.08	2565.91	2224.76	1828.94
x_e (m)	0.65	0.82	0.84	0.84	0.84
$Q=0.036 \text{ m}^3 \text{ s}^{-1}$					
h_u (m)	0.35	0.5	0.48	0.44	0.44
P_{dw} (Pa)	1884.54	3815.27	3547.65	3225.64	2949.83
x_e (m)	0.65	0.83	0.83	0.83	0.84
$Q=0.06 \text{ m}^3 \text{ s}^{-1}$					

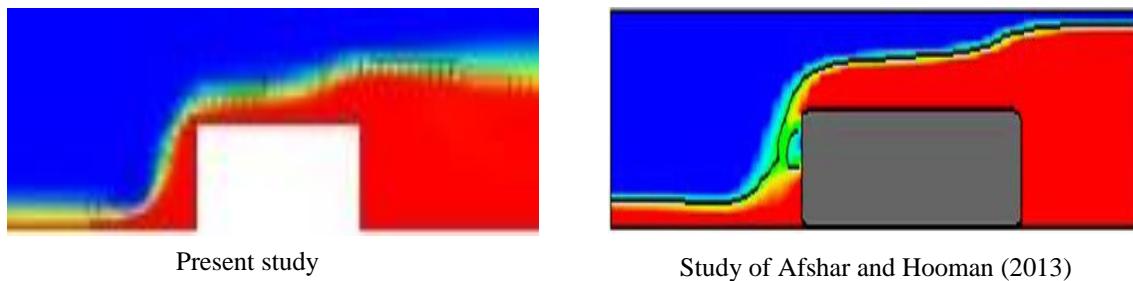


Figure 5. A comparison between the present study and the numerical analysis conducted by Afshar and Hoseini (2013) for the rectangular broad-crested weir

Conclusions

This study aims to evaluate the flow behavior over triangular broad-crested weirs under different flow conditions. The effect of opening angle of weirs is numerically investigated and compared with the behavior of rectangular broad-crested weirs. The simulation results have shown that the water level upstream the weir is inversely proportional to the opening angle, where an increment of 10° in the opening angle leads to a drop in water level about 1.5 cm. In addition, applying a discharge of $0.012 \text{ m}^3 \text{ s}^{-1}$, an uncovered region with water is created downstream triangular broad-crested weirs, while the bed downstream of the rectangular broad-crested weir is covered with a thin layer of water at the same flow discharge. Consequently, the pressure exerted by

falling water of $0.012 \text{ m}^3 \text{ s}^{-1}$ is less than other flow conditions. The difference in pressure exerted by falling water between the opening angles 90° and 100° , which is approximately similar to that between the opening angles 100° and 110° , was about 120 Pa. In addition, increasing the discharge to $0.036 \text{ m}^3 \text{ s}^{-1}$ causes an increment in the pressure at the downstream bed about 2.4 KPa, 2.0 KPa, 1.5 KPa and 1.0 KPa for the weirs of 90° , 100° , 110° and 120° , respectively. Moreover, at a discharge of $0.06 \text{ m}^3 \text{ s}^{-1}$, the increment of the pressure was about 0.9 KPa, 0.98 KPa, 1 KPa and 1.1 KPa for the v-notch weirs of an opening angle of 90° , 100° , 110° and 120° . By using triangular broad-crested weirs, it is important to measure the wake region and the hitting point of falling water downstream the weirs where this area must be strengthened well in order to resist water power and reduce the risk of drift.

Recommendations

The authors have recommended for future studies to use the same models included in the present study with curved corners and compare the results with the models of sharp edges. In addition, it is recommended to use different turbulence models under constant flow conditions, then compare the results among them.

References

- Afshar H. & Hooman H., (2013). Experimental and 3-D numerical simulation of flow over a rectangular broad-crested weir. *International Journal of Engineering and Advanced Technology*, 2, 6, pp. 214-219.
- Almohammadi, K., Ingham, D., Ma, L. & Pourkashan, M. (2013). Computational Fluid Dynamics (CFD) Mesh Independence Techniques for a Straight Blade Vertical Axis Wind Turbine. *Energy*, 58, 483–493.
- ANSYS user's guide
- Hoseini, S. H. Jahromi, S. H. M. & Vahid, M. S. R. (2013). Determination of Discharge Coefficient of Rectangular Broad-Crested Side Weir in Trapezoidal Channel by CFD. *International Journal of Hydraulic Engineering*, 2(4), 64-70. DOI: 10.5923/j.ijhe.20130204.02
- Lodomez, M., Ercicum, S., Dewals, B., Pirotton, M. & Archambeau, P. (2014). Comparison between Experimental and SPH Models over a Sharp-crested Weir. *The 5th International Junior Researcher and Engineer Workshop on Hydraulic Structures*. Spa, Belgium.
- Naghavi, B., Esmaili, K., Yazdi, J, & Vahid, F.K. 2011. An experimental and numerical study on hydraulic characteristics and theoretical equations of circular weirs. *Canadian Journal of Civil Engineering*, 38(12): 1327–1334. doi: 10.1139/111-092.
- Namaee, M. R. (2014). Numerical Investigation of a Side Weir with an Inclined Ramp. *World Applied Sciences Journal*, 31 (10): 1759-1766, 2014, DOI: 10.5829/idosi.wasj.2014.31.10.429
- Yuce, M. I., AL-DABBAGH, M. A. & AL-BABELY, A. H. (2015). Flow simulation over oblique cylindrical weirs. *Can. J. Civ. Eng.*, 42, 389–407. dx.doi.org/10.1139/cjce-2014-0157

Author Information

Mohammad A. Al-Dabbagh

Northern Technical University, Technical Institute/
Mosul, Department of water resources techniques
Mosul/ Iraq
Contact e-mail: mohamed.akram@ntu.edu.iq

Sulaiman AL-ZUBAIDY

Northern Technical University, Technical Institute/
Mosul, Department of water resources techniques
Mosul/ Iraq

Determination of the Morphological Characteristics of Scandaroon Pigeon Grown in the Central of Hatay Province (*Columba livia domestica*)

Hakan YILDIRIM

Mustafa Kemal University

Ugur DOGAN

Mustafa Kemal University

Tulay CIMRIN

Mustafa Kemal University

Abstract: Scandaroon pigeon know at the southeast and Hatay region in Turkey and is commonly raised in this area. This genotypewhich has different color varieties, has been cultivated by local people for centuries. This research was carried out in order to determine some morphological characteristics of scandaroon pigeons grown in the central of Hatay province. The study was conducted on a total of 224 pigeons (122 males and 102 females) reared in six different enterprises in 2016. Some morphological characteristics of pigeons were examined as coat color, marking, eye color, the number of wing and tail flight feathers. However, as a body morphometric characteristics; body weigh and length, trunk length, wing span and length, tail length, thoracic perimeter, chest width and depth, head length and width, beak length and depth, tarsus diameter were measured. In conclusion, in this study body weight and body morphological characteristics were found to be high in males and gender and age were effective on body characteristics

Keywords: Body morphometric characteristics, Morphological characteristics, Scandaroon pigeon

Introduction

The Scandaroon pigeon is a native genotype belonging to the subspecies of *Columba livia domestica*. Especially in the southeast region of Turkey it is growing. Baghdadi was also recognized by name in Turkey, which is an animal native to Iraq. This genotype found in the Hatay region is known as a squadron flyer pigeon (Işcen, Y., 2017).

These pigeons, with curved beak structure, have red colored feet. The nostrils are marked, the eyes are usually red, and the eyes are lint-free. In pure animals there is a backward color flow on the beak and it is called a mustache. Lay your neck and legs. It has been reported that live weights vary between 400-600g (Anonymous, 2016; Anonymous, 2018a).

This genotype with color varieties such as white, black, yellow, red and sky blue has a higher live weight than other pigeon breeds (Figure 1., 2., 3., 4., 5.).

The colors we call gray or ash become black belt. The so-called twin colored ones are made up of Red, Black, Yellow, and Gray colors on White. They are more popular than plain colors. At the bottom of their eyes is a patch (mustache) extending towards the gag. The Scandaroon pigeon is in the class of hard-haired pigeons and fast flying, the body and wings are strong (Anonymous, 2018b ; Anonymous, 2017).

Atasoy et al., (2013), cited the importance of locating breeds of locality in determining morphological characteristics of indigenous genotypes. This finding is important because it made with traditional methods of

- This is an Open Access article distributed under the terms of the Creative Commons Attribution-Noncommercial 4.0 Unported License, permitting all non-commercial use, distribution, and reproduction in any medium, provided the original work is properly cited.

- Selection and peer-review under responsibility of the Organizing Committee of the Conference

breeding pigeons in Turkey. Studies should be carried out to identify race characteristics by applying scientific methods and to determine race standards. For this reason, this study was carried out in order to determine the morphological characteristics of Iskenderun pigeons, which were extensively cultivated in the Hatay region.

Method

The research was carried out on 224 Scandaroon pigeons in total consisting of 122 males and 102 females in 6 separate enterprises in 2016 in Hatay. Operations are carried out by the same person in May, and measurements are taken according to age groups from animals. Pigeon ages were determined as 6-12, 13-36 and 37 months, using the business records.

The live weight was determined with a precision scale sensitive to 0.01 g.

Body length (between upper beak tip and longest tail wrist) is measured by a ruler.

Wing span (between the longest flying planes of the two wings) and its length (between the shoulder joint and the longest flying wing), trunk length (between two thighs and pgostyle end), tail length (between tail tail root and longest tail tail), thoracic perimeter (measured along the extreme end of the chest strap from under the two wings) was measured with the measurement strip.

The width of the chest (between the right and left inguinal cavity) and the depth (between the two chest vertebrae and the extreme end of the chest), head length (between upper beak tip and condyles occipitalus), head width (between the extreme points on the left and right of the head restraint), the length of the beak (between the upper beaked beak feather) and the depth (between the top and bottom of the middle part of the beak) and the diameter of the metatarsus (from the middle of the metatarsus bone) was measured by digital calipers. (Atasoy et.al., 2013; Özbaşer et al., 2016).

In the study pigeons with 5 color varieties were identified as white, black, red, partly yellow and sky blue according to feather colors (Figure 1., 2., 3., 4., 5). As a sign, the backward color flow was determined on the beak.

The general features of the Scandaroon pigeons are summarized as follows;

Size and carrying: Strong very high and proud bearing.

Head: long and narrow, without any angle or flat, arched, while the back of the head is well rounded and passing into the neck.

Eye: Large and fiery, dark colour in Whites and Pied, and in all other colors yellow-range.

Cere: bright red.

Beak: Very powerful, upper and lower mandibles of some thickness, well closed, and stumpy at the point, proceeding in shape to line of head, with forehead, skull and back part of the head forming more than a pure semi circle. Color, whitish-rose, except in blue, blue chequered, self-coloured birds, which may have a light horn-coloured beak.

Neck: long and bent, sharply curved. Thin at shoulders and breast slightly widening out.

Breast: Broad and strongly extended.

Back: Broad and somewhat arched, running powerfully to the tail.

Wing: Medium length, wide across and deep, lying very loose on body, sloping pointed to the rear resting on tail. Short primary flights.

Tail: short and well closed.

Lengs: Strong, featherless, red in colour (Anonymous, 2018a).

The morphological characteristics (body color, eye color, number of wing and number of wing and number of winged call) were expressed by the percentages of the statistical evaluation. The importance of the difference

between age and gender groups in the evaluation of body measurements was done by the General Linear Model method. Tukey test was applied to compare important groups (Dawson and Trapp, 2001).



Figure 1. White



Figure 2. Black



Figure 3. Yellow

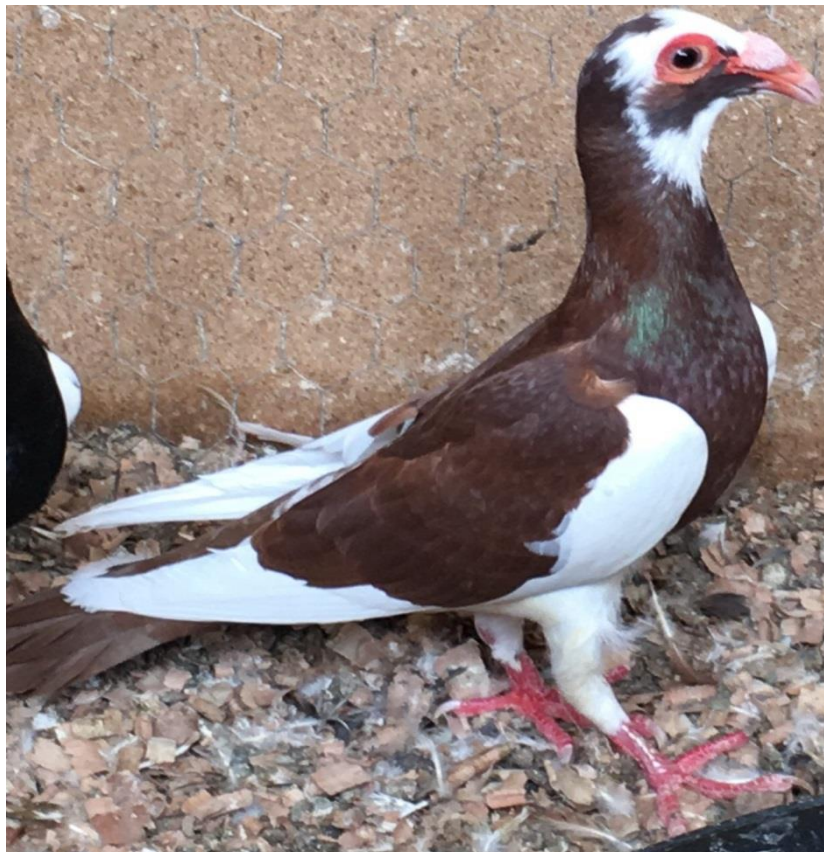


Figure 4. Red



Figure 5. Sky blue

Results and Discussion

Specified morphological characteristics are shown in Tables 1. and 2., and data on body characteristics are shown in Tables 3., 4., 5. and 6. In the head part, 13.53% of the marking, which is called as mustache and extending from the under eye to the gagged eye, was detected. The rate of those without sightseeing is 86.47%. The low rate of this structure, which is an important breeding feature in Scandaroon pigeons, can be explained by the fact that the genetic structure of the animal is not pure.

Table 1. Some morphological features in scandaroon pigeons

Color	Rate (%)	Marking	Rate (%)	Eye color	Rate (%)
White	15.21	Non marking	86.47	Red	95.17
Black	20.13	Mustache	13.53	Orange	4.83
Red	29.32				
Yellow	23.78				
Sky blue	11.56				
Total	100		100		100

Table 2. Some morphological features in scandaroon pigeons

Number of wing feather	Rate (%)	Number of tail feather	Rate (%)
12	89.26	12	53.78
13	7.54	13	23.17
14	3.2	11	11.73
		14	7.14
		10	4.18
Total	100		100

The effect of gender factor on all values except for beak length and shin diameter was found to be significant. Numbers were found high in male ($P < 0,001$, $P < 0,01$, $P < 0,05$) . Numbers were found high in male.

The statistically significant difference between age groups in terms of body weight, body length, trunk length, chest circumference, width and depth, head length and width and beak length indicates that the development of Scandaroon pigeons continues.

Atasoy et al (2013) obtained different results in terms of these properties. It is reported that these researchers did not have the age effect on these traits in the study of the tumbler pigeons.

This result can be explained by the fact that the Scandaroon pigeons were able to grow longer due to their squadron type pigeon group and having a larger body structure.

However, the effect of age and gender on the depth of the beak was found to be significant ($P < 0,05$), while age and gender were not affected by the length of the beak.

On the other hand, it has been determined that the effect of age on wing span and length and tail length is important ($P < 0,01$, $P < 0,05$, $P < 0,01$). This situation has a positive result for the ability to stay constant and stable.

While the effect of age and gender on the diameter of the shin is insignificant, a high value is obtained for this characteristic again in male.

Table 3. Body morphometric characteristics in scandaroon pigeons

	N	Live weight (g)	Body length (cm)	Trunk length (cm)	Wing span (cm)
P		**	*	*	**
Age (month)					
6-12	78	452.25±8.07c	39.79±0.34b	14.80±0.27b	70.36±0.21c
13-36	65	495.12±5.31b	40.54±0.21ab	15.50±0.13ab	71.41±0.34b
37 and over	81	520.24±6.50a	41.10±0.38a	16.11±0.18a	73.54±0.28a
P		**	*	*	**
Gender					
F	102	457.59±6.41b	39.50±0.55b	14.22±0.19b	70.15±0.28b
M	122	516.84±7.73a	41.13±0.38a	15.89±0.14a	72.64±0.33a
Total	224				
Average		496.21±6.08	40.31±0.48	15.05±0.16	71.40±0.27

- : Non significant, *: $P < 0,05$, **: $P < 0,01$, ***: $P < 0,001$

a,b,c : there is statistical variability between figures shown in different letters in the same column

Table 4. Body morphometric characteristics in scandaroon pigeons

	N	Wing length (cm)	Tail length (cm)	Thoracic perimeter (cm)	Chest width (mm)
P		*	**	*	*
Age (month)					
6-12	78	31.47±0.18b	13.32±0.11b	31.11±0.13b	55.30±0.45b
13-36	65	32.26±0.14ab	13.55±0.19ab	31.28±0.06b	56.51±0.43a
37 and over	81	32.64±0.15a	14.41±0.13a	32.42±0.14a	56.23±0.38a
P		**	*	*	*
Gender					
F	102	31.13±0.25b	13.26±0.17b	31.18±0.15b	55.17±0.39b
M	122	32.51±0.18a	14.31±0.13a	32.33±0.23a	56.30±0.48a
Total	224				
Average		31.82±0.18	13.78±0.14	31.75±0.29	55.75±0.36

- : Non significant, *: $P < 0,05$, **: $P < 0,01$, ***: $P < 0,001$

a,b,c : there is statistical variability between figures shown in different letters in the same column

Table 5. Body morphometric characteristics in scandaroon pigeons

	N	Chest depth (mm)	Head length (mm)	Head width (mm)
P		*	**	*
Age (month)				
6-12	78	68.16±0.42b	65.31±0.27c	27.54±0.15c
13-36	65	69.28±0.55a	66.47±0.38b	28.63±0.27b
37 and over	81	69.47±0.44a	68.32±0.28a	29.42±0.29a
P		*	***	*
Gender				
F	102	68.72±0.43b	65.27±0.28b	27.56±0.17b
M	122	69.25±0.49a	67.39±0.13a	28.31±0.13a
Total	224			
Average		68.99±0.38	66.33±0.18	27.93±0.18

- : Non significant, *: P<0.05, **: P<0.01, ***: P<0.001

a,b,c : there is statistical variability between figures shown in different letters in the same column

Table 6. Body morphometric characteristics in scandaroon pigeons

	N	Beak length (mm)	Beak depth (mm)	Tarsus diameter (mm)
P		-	*	-
Age (month)				
6-12	78	31.45±0.31	7.13±0.04b	3.42±0.09
13-36	65	31.57±0.29	8.67±0.05a	3.58±0.04
37 and over	81	31.45±0.13	8.34±0.03a	3.24±0.05
P		-	*	-
Gender				
F	102	31.21±0.27	7.83±0.04b	3.45±0.05
M	122	31.87±0.33	8.21±0.02a	3.53±0.08
Total	224			
Average		31.54±0.18	8.02±0.02	3.49±0.06

- : Non significant, *: P<0.05, **: P<0.01, ***: P<0.001

a,b,c : there is statistical variability between figures shown in different letters in the same column

Conclusion

In the study done body measurements were generally found to be high in men. However, it was found that body characteristics were influenced by sex and age P <0.001, P <0.01, P <0.05.

In traditional breeder conditions, Scandaroon pigeons differ in morphological and body characteristics. This is due to the random breeding of animals and the constant change of genetic structure, depending on the inadequate knowledge of breeders. It can be determined by the subjective assessment that the animals in the hands of the growers are not pure from morphological means.

Despite the fact that the qualitative properties are determined by a few genes and therefore the desired morphological properties are relatively more accurate, it is not possible to express this in the same manner for quantitative characters. Pure breeding is important for this accurate reflection of race characteristics.

The basic rule of pure breeding is to keep the individuals who hold the gene and gene combinations that determine the characteristics of the race belonging to the breed high in the structure. The determination of race characteristics at the molecular level (DNA analysis) and the selection methods and applications accordingly will increase the accuracy.

Recommendations

The Scandaroon pigeons need to be purified in terms of their genetic structure. For this purpose, it is essential to establish production stations in scientific sense. It is the universities and research institutes that will best accomplish this. Course and seminars can also be organized in order to increase the knowledge of traditional farmers.

Acknowledgements

I would like to thank the academics and farmers who helped me in the research.

References

- Anonymous (2016, March 14). Doğan güvercin. <http://doganguvercin.com/bagdatirk.htm>
- Anonymous (2017, March, 12). http://www.guvercin.info/irklar_iskenderun.php
- Anonymous (2018a, May 20). The Scandaroon, Part 2. <http://www.aviculture-europe.nl/nummers/09E05.pdf>
- Anonymous (2018b, May 16). http://www.kusvekuscudunyasi.com/arsiv/haber_detay.asp?haberID=778
- Atasoy, F., Erdem, E., & Hacan, Ö.G. (2013). Determination of Morphological Characteristics of Tumbler Pigeons in Province of Ankara (*Columba livia domestica*). *Ankara Univ. Vet. Fak. Derg.*, 60, 135-143
- Dawson, B. and Trapp, R. 2001. Basic and clinical biostatistics. Lange Medical Books/McGraw-Hill, New York
- İşçen, Y. (2017, January 10). <http://evcilguvercin.blogspot.com.tr/p/guvercin-yetistiriciligi-1.html> format.
- Özbaşer, F.T., Atasoy, F., Erdem, E., & Güngör, İ. (2016). Some Morphological Characteristics Squadron Flyer Pigeons (*Columba livia domestica*). *Ankara Univ. Vet. Fak. Derg.*, 63, 171-177

Author Information

Hakan Yıldırım

Mustafa Kemal University
Agriculture Faculty Animal Science
Hatay/Turkey
Contact e-mail: hakanyld@gmail.com

Ugur Dogan

Mustafa Kemal University
Agriculture Faculty Animal Science
Hatay/Turkey

Tulay Cimrin

Mustafa Kemal University
Agriculture Faculty Animal Science
Hatay/Turkey

A Critical Review of Major Nature-Inspired Optimization Algorithms

Julius Beneoluchi ODILI

Anchor University

A. NORAZIAH

Universiti Malaysia Pahang

Radzi AMBAR

Universiti Tun Hussein Onn

Mohd Helmy Abd WAHAB

Universiti Tun Hussein Onn

Abstract: Nature-inspired Algorithms are getting more and more popular in the past few decades owing to their amazing successes in solving a number of real-world optimization problems in different spheres of human endeavour ranging from the financial, medical and industrial to educational applications etc. Nature-inspired Algorithms (NAs) simulate the harmonious cooperation and competition in nature resulting in amazing solutions to seemingly impossible human problems. This paper examines ten nature-inspired techniques and their applications to different fields of human endeavour and concludes that the Nature-inspired Algorithms has enormous promise in the quest for greater human development through the harnessing of NAs' potentials for speeding-up of industrial processes, minimization of time, financial and computer resources required to obtain solutions to complex optimization problems etc. However, the study points out certain areas of concern in the development of the NAs, namely, the apparent lack of clear mathematical cum theoretical proofs of convergence of these algorithms, manual tuning of parameters and the recurring issue of experimenting with small-scale problems vi-a-vis the large and complex real-life problems.

Keywords: Nature-inspired algorithms, Metaheuristics, Trajectory-based, Population-based, Deterministic algorithms

Introduction

There has been an upsurge in the number of research studies in Artificial Intelligence and specifically in Nature-inspired Algorithms (NAs) in the past few decades. Such extensive studies have led to the design and development of several optimization algorithms such as the Great Deluge (Dueck, 1993), Hill Climbing (Selman & Gomes, 2006), Simulated Annealing (Kirkpatrick, Gelatt, & Vecchi, 1983), Particle Swarm Optimization (Kunna, Kadir, Jaber, & Odili, 2015), Artificial Bee Colony (Karaboga & Aslan, 2015), Bee Colony Optimization (Teodorović & Dell'Orco, 2005), Firefly Optimization (X.-S. Yang, 2009a). Before the birth of NAs, the deterministic algorithms such as the finite difference (Forsythe & Wasow, 1960), Raphson-Newton (Pletcher, Minkowycz, Sparrow, & Schneider, 1988), Nelder-Mead Simplex (Lagarias, Reeds, Wright, & Wright, 1998), Hook-Jeeves optimization methods (Aghamohammadi & Pourgholi, 2008) etc. were the dominant optimization algorithms for scientific investigations. The application areas of the NAs range from logistics (Vassiliadis & Dounias, 2009), image processing (Cuevas & Sossa, 2013), signature verification (Selman & Gomes, 2006), engineering designs (X.-S. Yang, 2005), financial applications (Brabazon, 2008), protein folding problems (Burke, Bykov, & Hirst, 2007) to business optimization (X.-S. Yang, Deb, & Fong, 2011) etc. The successful applications of NAs to these non-linear and complex optimization problems far above the performance of the deterministic models in terms of computational time used to achieve results and their

- This is an Open Access article distributed under the terms of the Creative Commons Attribution-Noncommercial 4.0 Unported License, permitting all non-commercial use, distribution, and reproduction in any medium, provided the original work is properly cited.

- Selection and peer-review under responsibility of the Organizing Committee of the Conference

capacity to obtain optimal or near-optimal solutions to complex optimization problems is a motivation for further research and this study in particular.

The success of NAs over the deterministic algorithms is as a result of the methodology applied by NAs in search for solutions to complex multimodal problems (X.-S. Yang, 2009b). Generally, NAs apply randomization mechanism which enable them construct solutions iteratively over a number of construction steps. Moreover, they are relatively simple algorithms in terms of their fitness updates and implementation strategies. For these reasons, the NAs are user-friendly. This recommends them to wide applicability by professionals in diverse research and application fields. Furthermore, NAs are general-purpose algorithms that can be applied to solve different kinds of problems. To achieve this, the primary requirement is the proper tuning of parameters to suit a particular problem at hand. This cannot be said of deterministic algorithms that are rather specialized, though capable of obtaining the optimal solutions.

The rest of this paper is organised thus: section two attempts a classification of NAs, highlighting the working of some of these algorithms and their areas of successful applications, strengths and weaknesses; section three discusses the findings of this review; section four draws conclusion on the study and section five acknowledges support for the study.

Classification of Nature-Inspired Metaheuristic Algorithms

A broad way to classify optimization algorithms is to identify them as either Stochastic or Deterministic, in terms of their solution dynamics (Venter, 2010). The deterministic algorithms were designed in such a way that they are able to obtain the optimal solution but their stochastic counterparts cannot guarantee the optimal results but could solve larger and more complex problems within a relatively short time. A popular general-purpose deterministic algorithm, for instance, is the DIRECT algorithm which makes use of Lipschitzian technique to identify promising sub-regions in the search space. (Olafsson, 2006). For the purpose of this paper, however, our interest is the stochastic optimization techniques which are usually nature-inspired. Nature inspired Algorithms (NAs) simulate nature's way of solving its own problems and this has opened a new vista in computer science.

Furthermore, NAs can be classified as Bio-inspired, Environment-based or Physics/Chemistry-based (Binitha & Sathya, 2012). As their name implies, Bio-inspired algorithms (BAs) are inspired by the biological processes of nature such as the behavior of plants and animals, evolutionary trends in nature and ecology. The Evolutionary algorithms arm of BAs, on the one hand, is broadly inspired by the Darwin theory of Evolution (Crawford & Krebs, 2013). Examples of the algorithms in this category are the Genetic Algorithm (Whitley, 1994), Evolutionary Strategies (Tyrrell, Hollingworth, & Smith, 2001), Genetic Programming (Banzhaf, Nordin, Keller, & Francone, 1998) etc. Another sub class of BAs is the Swarm-based algorithms which are inspired by the cooperative or competitive behavior of animals in our environment. Examples of the Swarm-based algorithms are the Particle Swarm Optimization (Kennedy, 2010), Ant Colony Optimization (Dorigo, Birattari, & Stützle, 2006) etc. The last subclass of BAs is the Ecology-based algorithms which are inspired by the natural ecosystem. Examples are the Biogeography-based Optimization (Simon, 2008), Invasive Weed Optimization (Mehrabian & Lucas, 2006), Symbiosis algorithms (Binitha & Sathya, 2012) etc. At this juncture, let us attempt taxonomy of the Nature-inspired algorithms. This effort is by no means exhaustive but will give a clearer picture of these optimization techniques (Please see Figure 1).

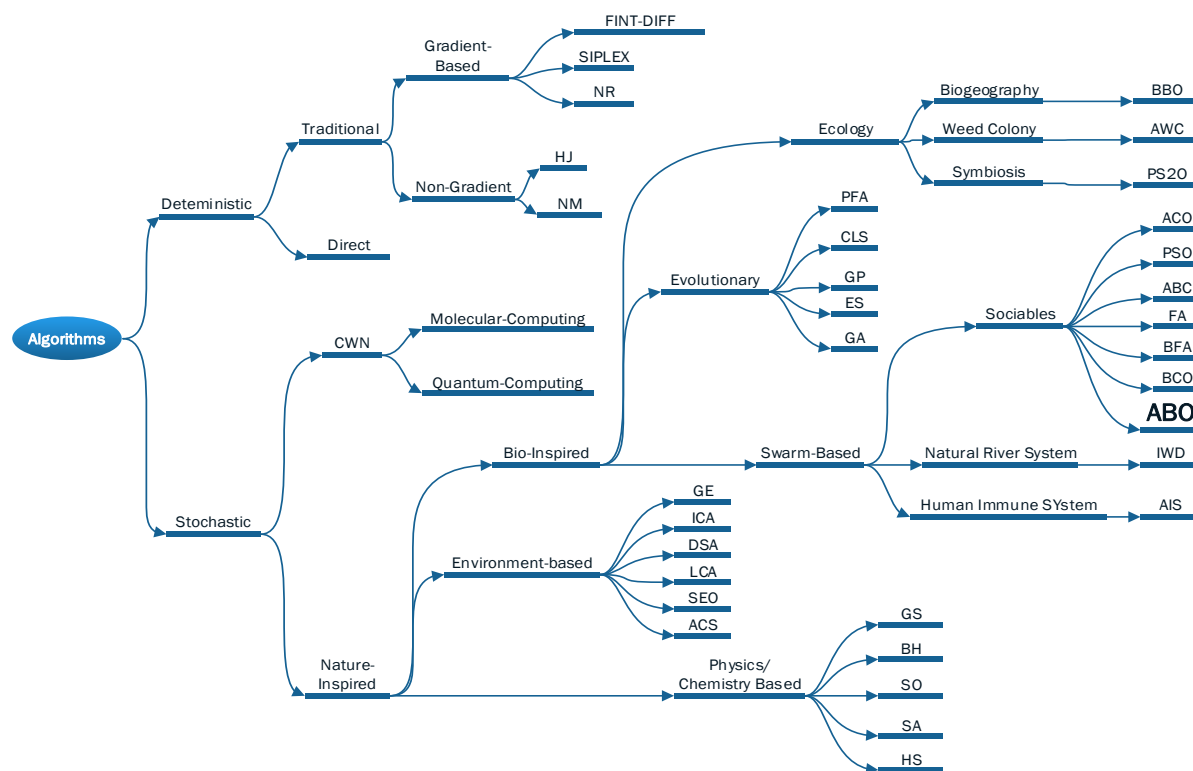


Figure 1. Taxonomy of algorithms

- | | |
|--|--------------------------------------|
| CWN=Computing with Nature | ACS= Ant Colony System |
| FINT-DIFF =Finite Difference | HJ= Hooke-Jeeves pattern |
| GA= Genetic Algorithm | NM= Nelder-Mead simplex |
| N.R = Newton-Raphson method | ES= Evolution Strategies |
| CLS= Classifier Systems | BBO= Biogeography-Based Optimization |
| GP= Genetic Programming | FA= Firefly Algorithm |
| LCA= League Championship Algorithm | PFA= Paddy Field Algorithm |
| DSA= Differential Search Algorithm | BCO= Bee Colony Optimization |
| ICA= Imperialist Competitive Algorithm | AWC= Artificial Weed Colony |
| GE= Grammatical Evolution | BFA=Bacteria Foraging Algorithm |
| GS= Gravitational Search | IWD= Intelligent Water Drop |
| BH= Black Hole | AIS= Artificial Immune System |
| SO= Spiral Optimization | ACO= Ant Colony Optimization |
| SA= Simulated Annealing | PSO= Particle Swarm Optimization |
| HS= Harmony Search | ABC= Artificial Bee Colony |
| ABO= African Buffalo Optimization | PS20= 2-Level PSO |
| SEO= Search Engine Optimization | |

Another way to classify Nature-inspired stochastic algorithms could be to categorize them as either population-based or trajectory-based (X.-S. Yang, 2009b). Population-based optimization techniques solve problems using a number of search agents which also result in obtaining a number of solutions in a particular iteration. Such population-based search algorithms are usually designed in such a way as to permit elitism which enables the algorithms to select the best solution amongst the several generated solutions. This way, these algorithms build solutions incrementally (Dorigo, Caro, & Gambardella, 1999). Population-based algorithms are sometimes, called exploration-based methods since they are exceptionally good in the diversification of the search space. An example of this is the GA which uses a set of strings (Whitley, 1994). So also is Particle Swarm Optimization that uses a number of agents or particles (Kennedy, 2010). On the other hand, Simulated Annealing, Great Deluge and Hill Climbing, Tabu Search etc. are trajectory-based and use a single agent that moves through the search space in a zigzag fashion as the iterations continue (Kennedy, 2010; Mirjalili, Mirjalili, & Lewis, 2014). In trajectory-based methods, the initial solution is, usually, obtained randomly and then improved upon iteratively. The difference between the Population-based and the Trajectory-based metaheuristics is primarily in the number of temporal solutions applied in an iteration of the search. While the

population-based methods use a number of agents and therefore, solutions, the Trajectory-based methods use a single search agent and, as such, generate a single solution per iteration.

Trajectory-based Algorithms

Trajectory-based algorithms start with a single solution and as the particular algorithm progresses; such a single solution is improved upon and replaced by the current solution. Some experts call them exploitation-based algorithms since they usually emphasize intensification of the search space (Manjarres et al., 2013). The search agent simply moves through the search space tracing the path to the optimal solution. This random movement through the solution space within the neighborhood of the current solution to another continues until the stopping criterion is reached which could be a maximum number of iteration or the satisfaction of some predefined stoppage criteria. The basic trajectory pseudocode has this format as in Fig.2:

1. *Generate initial solution* ($s(0)$)
2. $t := 0$
3. *While not Termination* ($s(t)$), *do*
4. *Explore neighborhood* $s'(t) := \text{SelectMove}(s(t))$;
5. *If* $\text{Move}(s'(t))$ *accepted, then*
6. $s(t) := \text{ApplyMove}(s'(t))$
7. *End if*
8. $t := t+1$
9. *End While*

Figure 2. Trajectory-based algorithms pseudocode

To help improve the efficiency in terms of time and quality of solutions of the Trajectory-based methods, experts introduced parallelism. The three popular parallel models in literature are the parallel multi-start, the parallel evaluation and parallel moves models (Alba, Talbi, Luque, & Melab, 2005)

- **Parallel multi-start model:** The parallel multi-start models, simply involve launching a number of trajectory-based searches with the aim of achieving robust solutions. These multi-start searches could work cooperatively or independently. Also, they could start from a particular point or from different points. They could use a similar or totally different parameters for their search (Mezmaz, Melab, & Talbi, 2006). A good example is the Kriging optimization method (Peri & Tinti, 2012)

- **Parallel moves model:** This uses a master-slave architecture that complies with the particular heuristic technique conducting the search. At the initial stage of the search, the master distributes the nodes among the slaves and at the expiration of the search; the slaves return their results to the master. This model basically speeds up the search as it is an imitation of population-based search, but this time under the harmonization of a master (Halambi et al., 2008). An example is the Panmictic Simulated Annealing (PSA) (Domínguez & Alba, 2011).

- **Parallel Move acceleration model:** This model evaluates each parallel move in a centralized place before subsequent moves are allowed. Some versions of this model permit such evaluation to be parallelized. Generally, parallelism has the disadvantage of low speed owing to much use of computer resources (Alba et al., 2005). Ethane Algorithm employs this technique. A major disadvantage of employing parallelism is the issue of huge computational cost that arises with such usage. Moreover, the application of parallelism is not a guarantee that the optimal solution will be achieved. (Domínguez & Alba, 2011)

It is pertinent to note that a number of trajectory-based search algorithms are available in literature. Some of the popular ones are the Simulated Annealing, Hill Climbing, Great Deluge algorithms.

Hill Climbing Algorithm

Hill Climbing (HC) searches for solution to problems in an iterative manner by first selecting an arbitrary solution and then tries to obtain better results/solutions by altering a single solution element (Hoffmann, 2010). If by this alteration, the new solution is better than then the previous, another alteration is made to another element of the newly-found solution until no improvement is possible on the solution. If, however, any alteration results in a poorer solution, then another alteration is made in the HC's efforts to obtain optimal

solution. The HC is different from similar algorithms like the Gradient Descent in that the Gradient Descent adjusts all the values of the present solution but the HC adjusts just one value/element of the present solution in the next iteration (Perkins, Lacker, & Theiler, 2003). The Hill Climbing pseudocode is presented in Figure 3:

```

1. PresentNode = startNode;
2. While (not termination) do
3.   For j = Neighbors of PresentNode)
4.     NextEval = -INF
5.     NextNode = NULL
6.     For all k in j
7.       If (EVAL(x) > nextEval)
8.         NextNode = k
9.       End if
10.    End for
11.  End for
12.  NextEval = EVAL (k)
13.  If nextEval <= EVAL (PresentNode)
14.    End if
15. End While
16. //Return present node if no better neighbors exist
17. Return PresentNode
18. PresentNode = nextNode;

```

Figure 3. Hill climbing pseudocode

In practical terms, HC is a kind of Depth-First search. However, unlike the Depth-First search method which outrightly rejects or accepts a solution, the HC uses a feedback mechanism which approximates the closeness or otherwise of the newly-found solution to determine the next direction of the search. Hill Climbing has been successfully applied to configure application servers (Xi, Liu, Raghavachari, Xia, & Zhang, 2004), Travelling Salesman's Problem (Selman & Gomes, 2006), signature verification (Galbally, Fierrez, & Ortega-Garcia, 2007) etc.

The HC has advantage over some other algorithms in that it uses very little computer resources in its search since it stores only the present solution. Moreover, HC is capable of returning fairly better results than other algorithms in a situation of unexpected interruption to the algorithms execution. Nevertheless, in addition to the problem of low speed in instances involving ridges, alleys or plateau, HC is prone to falling into local minima in non-convex functions.

Simulated Annealing

Simulated Annealing (SA) which models the heating and cooling processes of materials in metallurgical engineering was developed by Kirkpatrick, Gelatt and Vecchi (Kirkpatrick et al., 1983). The temperature is lowered gradually to ensure that the cooling process minimizes the system energy thereby making the metals very strong. In the cooling process, the algorithm starts with a random search at high temperature which becomes greedy descent until the temperature reaches zero. Randomness attribute helps Simulated Annealing escape local optima since greedy descent is prone to falling into local minima. Better results are usually obtained in lower temperatures than in higher ones.

In its search for solutions, SA assigns random values to random variables, at each move, then, it evaluates the acceptance probability to ascertain whether it is an improvement on the objective function (and that it does not increase the conflict); which is for a minimization problem, a lower objective value. However, sometimes the SA, with certain probability, accepts points that raise the objective function and in this way avoids being trapped in local minima, thus, ensuring global exploration. The acceptance probability ap is calculated using:

$$ap = e^{\left[-\frac{\Delta E}{kBT}\right]} \quad (1)$$

Here, ΔE represents the change energy, kB is the Boltzmann's constant, and T is the Temperature. Similarly, the change in the objective function Δf is directly related to the change in the Energy ΔE :

$$\Delta E = \gamma \Delta f \quad (2)$$

Here γ is a positive real constant. For effectiveness, an Annealing schedule which is sometimes linear and at other times geometric is chosen to systematically reduce the temperature as the algorithm progresses. The decrease of the temperature enables the SA to minimize the search scope and ensure early convergence.

SA has been applied to several problems, such as the Quadratic Assignment Problem, Job Shop Scheduling, Travelling Salesman's Problems, N-Queens problem, Artificial Neural Networks Training etc. (Ledesma, Aviña, & Sanchez, 2008). The pseudocode of the SA is presented in Figure 4.

```
1. Let  $x = x_0$ 
2. For  $y = 0$  to  $y_{max}$  :
3.    $T \leftarrow temperature(k\gamma/y_{max})$ 
4.   Select a neighbor randomly,  $x_{new} \leftarrow neighbor(x)$ 
5.   If  $P(E(s), E(x_{new}), T) \geq random(0, 1)$ , move to the new state
6.   End if
7. End for
8.  $x \leftarrow x_{new}$ 
9. Output: the final state  $x$ 
```

Figure 4. SA pseudocode

One of the biggest strengths of SA is her ability to escape being trapped in local minima with her tacit manipulation of the cooling temperature. However, SA is not very effective in a smooth energy landscape or in instances with few local minima. Moreover, SA has the problem of delay in arriving at quality solutions (Kumbharana & Pandey, 2013). This may be due to engaging in several evaluations of the cost function in each iteration.

The Great Deluge

The Great Deluge (GD) which was developed by G. Dueck is inspired by the activities of a person moving in different directions upwards a hill in times of a deluge in an attempt to avoid his/her feet being wet as the water level rises (Dueck, 1993). GD begins by assigning an initial value which is the same as the initial objective function to the parameter 'Level' and as the search progresses, this value is iteratively reduced. The algorithm accepts solutions that has lower (or at least, equivalent) values of the objective function than the present 'Level' (Mcmullan, 2007). A later version of GD accepts all downhill moves, thus, hybridizing GD with Hill Climbing to ensure greater efficiency. In implementing the GD, usually, an approximate solution J of the optimum solution is selected. Next a random value of *badness* K is chosen and used to evaluate the desirability or otherwise of the approximate solution.

The GD pseudocode is presented in Figure 5.

```

1. SolutGD ←Sol
2. SolutOptimalGD ←Sol
3. f(SolutGD) ←f(Sol)
4. f(SolutOptimalGD)←f(Sol)
5. Determine best rate of final solution, BestRate
6. Determine number of iterations, NumOfIterGD
7. Determine initial level: level ←f(SolutGD)
8. Determine decreasing rate ΔB = ((f(SolutGD)–BestRate)/(NumOfIterGD)
9. Determine iteration ←0
10. Determine not_improving_counter ←0, not_improving_length_GDA
11. Do while (iteration < NumOfIterGD)
12. Apply neighborhood structure Ni where i ∈ {1... K} on SolutGD, TempSolutGDi
13. Evaluate cost function f(TempSolGDi)
14. Seek the best solution among TempSolutGDi where i ∈ {1... K} call new solution SolutGD*
15. If (f(SolutGD*) < f(SolOptimalGD)) SolutGD ←SolutGD*
16. SolutOptimalGD ←SolutGD*
17. End if
18. If not_improving_counter ←0
19. Level = level - B
20. Else if (f(SolutGD*) ≤Level) SolutGD ←SolutGD*
21. End if
22. If not_improving_counter ←0
23. Else not_improving_counter++
24. End if
25. If (not_improving_counter == not_improving_length_GDA)
26. Level= level + random (0, 3)
27. Increase iteration by 1
28. End if
29. End do
30. Return SolutOptimalGD

```

Figure 5. Great deluge pseudocode

Please note that the higher the value of *badness* evaluation, the more undesirable solution J is. Another parameter *tolerance* is used to evaluate a number of factors leading to the choice of a new approximate solution J' that is a neighbor of J . The *badness* of J' is then calculated and the result is compared with parameter *tolerance*. If the output is better than *tolerance*, the GD is restarted recursively:

$$J := J' \quad (3)$$

However, if the output of J' is worse than *tolerance*, another neighbor J'' is selected for J and the process is then repeated until all the neighbors of J produce better results than *tolerance*, then the GD is terminated and J is then output as the solution.

So far, the application areas of the GD include examination, sports and course timetabling, patient admission problems (Kifah & Abdullah, 2015), protein structure prediction (Burke et al., 2007), facility layout problems (Nahas, Kadi, & El Fath, 2010) etc.

A close look at GD reveals that it is different from Hill-Climbing and Simulated Annealing because it accepts a candidate solution from the neighborhood. The GD permits the definition of the characteristics, for instance, processing time and processing region of the expected solution, of a search process in advance. These help to make GD much more efficient than some other algorithms such as Hill Climbing and Simulated Annealing (Burke, Bykov, Newall, & Petrovic, 2003). Nonetheless, GD has the disadvantage of falling into a local minima and this has led to the development of some variants of the algorithm (Mcmullan, 2007).

Population-based Metaheuristics

Generally, population-based methods utilize a set of decision vectors which is usually denoted by:

$$X = \{x_1, x_2, x_3, \dots, x_N\} \quad (4)$$

where

$$X_i = (x_{i1}, x_{i2}, \dots, x_{in}) \quad (5)$$

N represents the size of the population and n , the number of design variables in each decision vector (i.e. individuals in a population). Basically, population-based metaheuristics share a common structure made up of four main parts, namely, the main algorithm; an extension to deal with the constrained optimization problems; another extension to retain promising solutions and a part to halt the algorithm (stopping criteria). In most cases, the main algorithm has component tracks information among the population (crossover), another component that pushes the population forward for further exploration (sometimes called mutation in some methods) and the part that computes the best solution in each iteration (selection) (Chau, Kwong, Diu, & Fahrner, 1997). Based on the foregoing discussion, most population-based metaheuristics have a format similar to Figure 6:

- | |
|---|
| <ol style="list-style-type: none"> 1. 2. <i>Initialize population</i> 3. <i>Evaluate the objective function</i> 4. <i>Repeat</i> 5. <i>Evaluate the population quality</i> 6. <i>Apply the variation operator</i> 7. <i>Evaluate the objective function</i> 8. <i>Until termination condition</i> |
|---|

Figure 6. Population-based algorithms pseudocode

Most population-based techniques exploit some previous knowledge of the solution space and use this in the initialization phase to move the search agents towards the feasible region. In situations where this information is absent, the decision vectors are distributed uniformly within the search space. Examples of the population-based algorithms are the Genetic Algorithm, Firefly Algorithm, the African Buffalo Optimization algorithm etc.

Particle Swarm Optimization

Particle Swarm Optimization (PSO), which was developed by Kennedy and Eberhart is a simulation of the flocking of birds and schooling of fishes in search of food. PSO is a population-based, stochastic, global optimization technique specifically designed to be an easy-to-implement yet effective search optimization method (Kefi, Rokbani, Krömer, & Alimi, 2015). Since its development in 1995, PSO has been a very successful algorithm which has been applied to a wide range of application areas. The PSO models the velocity and positions of particles in their search for food. The position of each particles in PSO represents a solution to the problem. The algorithm makes use of five major parameters: the particles' velocity, their present position, the global best particles' position, the individual particle's knowledge of its previous best position achieved and the best position found by its neighbor. As the algorithm progresses, the particles update their position and velocity with each iteration until it reaches termination condition. Similarly, the PSO maintains an information repository that keeps track of the best achieved objective function values for each particle involved in the search process (Kefi et al., 2015)

PSO models the behavior of, for example, a swarm of birds searching for a food source. The entire particles converge on the best solution through the use of the information gathered by each particle, the neighboring particle as well as that obtained from the entire flock. The algorithm starts by initializing the particles in the search space, followed by updating the position and velocity of each particle in each iteration. Basically, the action steps in PSO algorithm are as follows:

1. Initialize particle
2. Do (Until termination)
3. For individual particle
4. Calculate fitness value
5. If fitness value is better than its overall best fitness value (pBest) since inception
6. Record the current value as its new pBest
7. End if
8. Select the particle that has the best fitness value in the swarm as the gBest
9. End for
10. For individual particle
11. Determine the individual particle's velocity using velocity equation
12. Update the individual particle's position using position equation until termination condition
13. End for
14. End do
15. Output the best result

Figure 7. PSO pseudocode

So far, PSO has been used successfully to address several problems ranging from complex nonlinear function optimization, communications and control applications, task assignment (Shi & Eberhart, 1999), antenna design, combinatorial optimization problems, biomedical and pharmaceutical applications, fault diagnosis etc. (Poli, 2007).

A critical assessment of the PSO algorithm, however, reveals that there are about 30 different variants of PSO presently (Langeveld & Engelbrecht, 2011). These great number of variants were developed in response to the observed weaknesses of the algorithm. Of this number, the classical PSO algorithm is relatively simple to implement and uses relatively fewer parameters than in some algorithms like the ACO (Pereira, 2011).

Furthermore, PSO is rather more efficient in its use of memory than the Evolutionary algorithms like the GA. In addition, PSO has the capacity for broad diversity in its search space since all the particles use the information obtained by the best particles either in the neighborhood or the overall best in each iteration to improve their positions and speed. This search mechanism of the PSO is different from that of GA, for example, because in the GA, worse solutions are discarded and the population only concentrates on the fittest individuals. It should be emphasized, nonetheless, that the PSO shares some similarities with Evolutionary algorithms like the Genetic Programming (GP), Evolutionary Strategies (ES) Evolutionary Programming (EP) and Genetic Algorithm (GA) through the initialization of solutions and the update of generations. Even though the PSO does not use evolution operators like crossover, mutation, recombination, inversion and selection, the particles in PSO are simply attracted by the best in the neighborhood or the global best as the case may be.

In all, PSO can be said to be an efficient and effective algorithm in searching continuous functions and in multimodal search environments. It has been successfully applied to solve the Travelling Salesman's Problems, PID tuning of Automatic Voltage Regulators, global optimization problems, computer networking problems, robotic applications, scheduling, signal processing (Odili & Kahar, 2016) etc. However, PSO uses several parameters such as the constriction factor, inertia weight, random numbers, social factors, neighborhood best, personal best, global best etc. and this affects the algorithm's speed and management of computer resources (Tanweer, Suresh, & Sundararajan, 2015).

Ant Colony Optimization

The Ant Colony Optimization (ACO) is one of the most popular metaheuristic algorithms in literature. The ACO algorithm designed by Marco Dorigo and Di Caro in 1999 as a modification of the Ant System by Marco Dorigo and Ant Colony System by Dorigo and Gambardella (Anwar, Salama, & Abdelbar, 2015). The ACO is a simulation of the random movements of ants in search of food. Once the ants discover a food source is, they pick particles of the food and on their way back to their nest, usually following a shorter route, deposits some amount of pheromones as a way of informing other ants of their discovery. As the neighboring ants receive the information by perceiving the scent of the pheromone, they will likely join the successful ant in the harvest of the food source. As these ants locate the food source, they, in turn, carry some fragments of the food and on their way back to the nest, drop pheromones as they further optimize the route of the initial ant. This process increases the pheromone concentration on the favorite 'shortest' route(s) and in that process attract other ants.

This harvest cycle continues and within a short while, the entire colony of ants are on the optimized route harvesting the food source to the safety of their nests. With time, changes are that the food source is either partially or totally exhausted, the pheromone concentration diminishes as the discouraged ants will no more drop pheromones. This serves as negative reinforcement as the route loses its attraction due to pheromone evaporation. This situation leads the ants to explore other areas (Wu, Xin, & Zhang, 2015).

The ACO basically is the modelling and simulation of ants' foraging behavior, brood sorting, nest building and self-assembling. The Algorithm has three main subroutines: ConstructAntSolutions, Pheromone Update and DeamonActions.

- (i) **ConstructAntSolutions:** This subroutine constructs the solution by stimulating the movement of artificial ants through adjacent states of a problem according to a transition rule and, thus, builds a solution iteratively.
- (ii) **Pheromone Update:** This subroutine performs pheromone update trails either through pheromone reinforcement or evaporation. The is achieved in two ways depending on the variant of the ACO one is working with: the pheromone update subroutine could be done at the end of each iteration or when the ants individually completes a solution.
- (iii) **DeamonActions:** This subroutine is optional depending on the problem being solved. It involves increasing the pheromone levels to select promising edges.(Kumbharana & Pandey, 2013)

In general, the ACO algorithm uses the following steps (Liu, Zhu, Ma, Zhang, & Xu, 2015):

1. Initialize pheromone values τ for all the edges in the graph.
2. For a start, all the edges should have equal amount of pheromone unless there exist some heuristic information favoring some edges that may lead to speedier convergence.
3. Construct a solution for each ant, $x = (1, 2, \dots, N)$
4. Update the pheromone values for each edge depending on the quality of solution.
5. End for
6. Go to Step 2 until stopping criterion is reached.
7. Output the best result

Figure 8. ACO pseudocode

So far, the ACO has proven to be effective in solving routing problems in computer and telecommunication networks, Sequential Ordering Problems, Travelling Salesman's Problems (Odili, 2013), Resource Constraint Project Scheduling, Subset problems, Machine Learning Problems, Vehicle routing, Proportional, Integral and Derivative parameters-tuning of Automatic Voltage Regulators, Stochastic optimization problems (Stützle, López-Ibáñez, & Dorigo, 2011) etc.

One of the strengths of the ACO is its flexibility in being hybridized with other heuristics or metaheuristics in a quest for greater efficiency. Moreover, it is robust in search situations where the graph is prone to dynamic changes. Also ACO performs well in distributed computing environments. However, it has the weakness of easily falling into premature convergence because its pheromone update is according to the present best path. Again, it uses several parameters that require proper tuning. Such parameters as pheromone quantity, pheromone update rule, evaporation rate, pheromone reinforcement rate etc and this affects the speed of the algorithm. (Gutjahr, 2003; Kumbharana & Pandey, 2013) .

Artificial Bee Colony Algorithm

The Artificial Bee Colony (ABC) which was inspired by the behavior of natural honey bee swarm was developed by Karaboga and Basturk in 2009 (Karaboga & Akay, 2009). The ABC categorizes bees into three, namely, scout bees, onlooker bees and employed bees. Scout bees are those that fly around the search place seeking solutions (food source). Similarly, onlooker bees wait in the nest expecting the report of the scout bees. On the other hand, employed bees refer to those bees that joins in the food source exploitation after watching the waggle dance of the scout bees. This classification is dynamic in that a scout bee could transform into an employed bee once it (the same scout bee) is involved in harvesting the food source and an onlooker bee at another stage. In this algorithm, the food source represents a solution to the optimization problem. The volume of nectar in a food source represents the quality (fitness) of the solution (Nozohour-leilabady & Fazelabdolabadi, 2015). Whenever the employed bees bring some nectar to the hive, they have three alternatives: return to get more nectar, accompany other dancing bee to a new site or simply stay back in the hive. The bees' decision is informed by a number of factors ranging from the quality and quantity of the available nectar at the food source, the distance of the food source to the hive and the number of employed bees harvesting the nectar

at that food source. The global search mechanism of the ABC depends of the random search capacity of the scout bees while the exploitation capacity of the algorithm is based on the activities of the employed and onlooker bees. This bee behavior can be replicated in some real life problems, such as in transportation and business applications (Pham et al., 2011).

In general, the pseudo code of the classical ABC (Nozohour-leilabady & Fazelabdolabadi, 2015) is:

1. *Initialize population with random solutions.*
2. *Evaluate fitness of the individual bees in the population.*
3. *While (stopping criterion is not reached), form new population.*
4. *Choose site(s) for the next neighborhood search.*
5. *Select bees for chosen locations to be searched ensuring that more bees are allocated to the best locations & evaluate fitness.*
6. *Choose the fittest bee from each patch for the next best harvesting site(s).*
7. *Assign remaining bees to search randomly and evaluate their fitness.*
8. *End While.*

Figure 9. ABC pseudo-code

The ABC has been successfully applied to solving a number of problems such as Travelling Salesman's Problems, accident diagnosis, reactive power optimization problems, radial distribution (Akay & Karaboga, 2015), training neural networks, wireless sensor networks, signal, image and video processing (Karaboga, Gorkemli, Ozturk, & Karaboga, 2014) etc.

Previous studies on the ABC has shown that it is very effective in feed-forward artificial neural networks training, in addition to the algorithm being very efficient in multidimensional search environments due to its capacity to get out of a local minimum with ease. However, studies on the Artificial Bee Colony are still not widespread (Karaboga, Akay, & Ozturk, 2007; Karaboga & Basturk, 2007; Karaboga & Ozturk, 2009) and there are several parameters to appropriately tune in order to get good results. Generally, the ABC is a slow algorithm.

African Buffalo Optimization

The African Buffalo Optimization algorithm was designed by Odili and Kahar in 2015 (Odili & Kahar, 2015a). It drew its inspiration from the random movement of the African buffalos deploying principally two distinct sounds (/waaa/ and /maaa/) to move around the diverse African landscape in search of grazing pastures (Odili & Kahar, 2015b). This algorithm harnesses the three main characteristics of the African buffalos that are responsible for their successful migration. These are their extensive memory represented by m'_k and w'_k in the algorithm; extensive communication represented by $bg - w_k$) and their personal intelligence, represented by $bp_k - w_k$. The ABO algorithm is presented in Figure 10

1. *Begin*
2. *Initialize the buffalos randomly within the search space;*
3. *While (until termination),*
4. *For j=1: n (n denotes the population),*
5. *Ascertain the buffalos' exploitation location:*
6. $mk' = mk + lp1(bg - wk) + lp2(bpk - wk)$
7. *Here wk =exploration move; where mk = exploitation move; bg = best buffalo with the best fitness; $lp1$ and $lp2$ represents the learning parameters; bpk , best location of buffalo k*
8. *Update the exploration fitness of buffalos:*
9. $wk' = (wk + mk) \lambda$
10. *Ascertain whether the bg is updating? Yes, go to 11. If No in 10 iterations, return to 2*
11. *End for*
12. *End while*
13. *Post best solution.*
14. *End*

Figure 10. ABO algorithm

The algorithm has not enjoyed wide application since it was first published. Some of the application areas include Mobile Ad-hoc Network (Hassan & Muniyandi, 2017), asymmetric travelling salesman's problem (Odili & Mohmad Kahar, 2016b), symmetric travelling salesman's problem (Odili, Mohmad Kahar, & Noraziah, 2016), strategic management, collision avoidance in electric fish, tuning of PID parameters of Automatic Voltage Regulators (Odili & Mohmad Kahar, 2016a) etc. Because of the limited applications so far, it is not very easy to evaluate the algorithm. In any case, the ABO has performed well in the areas of its application.

Firefly Algorithm

This population-based algorithm which was inspired by the flashing attitude of fireflies was developed by Xin-She Yang (Yeomans & Yang, 2014). In this algorithm, a number of fireflies work together to solve a problem through bioluminescent glowing that enables them to efficiently solve problems. The solutions to problems are modelled as a firefly whose flashes are proportional to the quality of solutions they represent. As a result, a brighter firefly attracts others colleagues and this aids further exploration of the search space. The four main characteristics of the algorithm include:

- (a) All fireflies are unisex, so they are attracted by a brighter colleague notwithstanding the sex
- (b) The brightness of a firefly is a function of the distance between the fireflies: the nearer they are to one another, the more the effect of the brightness of the brighter firefly and vice-versa.
- (c) If there is no brighter firefly than a particular firefly, the firefly without a brighter colleague, moves randomly
- (d) The landscape of the objective function affects the brightness of the firefly. The brightness of the firefly is proportional to the objective function in a maximization problem. The pseudo-code of the Firefly Algorithm is presented in Fig. 11:

1. Randomly place the bee to an empty solution
2. For each bee, execute the forward pass phase
3. Set $k=1$; k is a counter for constructive moves in the forward pass;
4. Determine all possible constructive moves;
5. End for
6. Select the next move using the roulette wheel;
7. $k = k + 1$; If $k \leq NC$ ($NC = \text{maximum number of counters}$),
8. Let the bees start the backward pass phase;
9. Sort the bees;
10. Let each bee decide, randomly, whether to continue its own exploration and become a recruiter, or to become a follower of bees with higher objective function value;
11. End roulette wheel
12. For every follower bee, choose (until termination) a new solution from recruiter bees using the roulette wheel
13. Repeat steps 7-11
14. Output the best result.

Figure 10.FFA pseudo-code

FFA has been successfully applied to Industrial Optimization, Image processing, Antenna design, Business optimization, Civil engineering, Robotics, Semantic web, Chemistry, Meteorology, Wireless sensor networks (Fister, Yang, & Brest, 2013) etc.

The FFA is believed to have least error percentage compared to many other metaheuristic algorithms such as the GA and the PSO. Moreover, it is relatively simple to implement and has proven to perform well in multi-modal search environments. It is quite close to the PSO except that it does not employ search velocities in its quest for solutions (X.-S. Yang, 2012). However, it has complicated fitness function and hugely depends on correct parameter setting to arrive at good solutions. Even though it obtains good results, the FFA is a slow algorithm. This may be due to the number of parameters that the algorithm uses in search of solutions.

Biogeography- Based Optimization

The BBO which was designed by D. Simon was inspired by the immigration and emigration between habitats by different species in nature (Simon, 2008). Using the values of the Habitat Suitability Index as the objective function, the BBO emphasizes communication between candidate solutions (habitats): the Low Habitat Suitability Index (LHSI) and the High Habitat Suitability Index (HHSI) which are features of each solution. Basically Habitat Suitability Index (HSI) of a solution is a measure of its fitness and this is dependent on the characteristic environmental features in that habitat. This algorithm obtains good solutions through regular interaction/communication and feature-sharing between the LHSI and the HHSI. Another very important parameter to the working of the BBO is the *mutation* parameter which, like the Genetic Algorithm, enables the algorithm to generate diversity and thus greater exploration (Simon, 2008). The BBO algorithm is presented in Figure 12.

```

1. Initialization: Initialize the population candidate solutions
2. While (not termination), do
3.   For each candidate solution, create emigration probability fitness of each
4.   candidate solution, with probability of (0, 1)
5.     For each candidate solution, create immigration probability
6.       For each individual specie, set independent variable index
7.       Using the set probabilistically criterion, determine whether to immigrate;
8.       If yes, then
9.         Using the created probabilistically choose the emigrating individual
10.      End if;
11.     End for
12.   End for
13. End while.
14. Consider the next independent variable index;
15. Probabilistically mutate to create another individual;
16. Consider the next individual;
17. Next generation
18. Repeat steps 2 and 3 until stopping criteria
19. Output best solution
    
```

Figure 12. BBO pseudocode

The BBO has been successfully applied to solve numerical problems, population distribution problems, Combined Heat and Power Economic Dispatch Problem etc. (Qu & Mo, 2011; Simon, Ergezer, & Du, 2009)

The BBO is an exploration-based algorithm and even though it adopts the mutation parameter of GA, it does not discard the previous population after a new Generation; rather, the BBO modifies the original population through migration. Similarly, the BBO depends on the evaluation of newly generated solution fitness to determine whether the species' rate of emigration or migration. However, BBO has been discovered to be rather weak in the migration and mutation stages, as such its overall performance is suspect (Alroomi, Albasri, & Talaq, 2013). BBO's ineffectiveness may possibly due to the use of several parameters that require proper tuning in order to get good results. Finally, the speed of the algorithm is suspect as a result of its use of several parameters.

Bee Colony Optimization

In this algorithm, a population of artificial bees conducts a search for the optimal solution(s). Each bee generates one solution to the problem (Karaboga & Basturk, 2007). The Bee Colony Optimization algorithm makes use of two alternating phases, namely, forward-pass phase and backward-pass phase. In the forward-pass phase, the bees explore the search space through a number of moves that construct or improve a solution and thereby creating a new solution. After arriving at this partial solution, the bees return to the nest to initiate the backward-pass phase where they communicate information about their newly-found solutions. They communicate the distance as well as the quality of the food source (solution) to the nest through a waggle dance. Based on the information collected at this phase, the bees (including the dancer) decide, with a certain probability, to abandon the newly-found solution and remain in the nest or to follow the dancing bee to the food source. This leads to the second forward-pass where the bees improve on the previously found solutions and after which they return to another backward-pass phase. These phases are performed repeatedly until a stopping criterion is reached.

The stopping criterion could be the maximum number of forward-/backward-pass phases, the maximum number of forward-/backward-phases without tangible improvement of the objective function or the arrival at the optimal solution. Basically, the pseudo-code of the Bee Colony Optimization algorithm is as in Fig. 13.

1. Randomly initialize the bees within the search space
2. For each bee, perform the forward-pass:
 3. Set $k=1$; k is a counter for constructive moves in the forward pass;
 4. Determine all possible constructive moves;
 5. Select one move using the roulette wheel;
 6. $k = k + 1$; If $k \leq NC$ ($NC =$ maximum number of counters),
 7. Return to step 2
8. End for
9. Let the bees start the backward-pass phase;
10. Based on the objective function value of each bee, sort the bees;
11. Let each bee decide, randomly, whether to continue its own exploration and become a recruiter, or to become a follower of bees with higher objective function value;
12. For every follower bee,
 13. Choose a new solution from recruiter bees using a roulette wheel;
 14. If the stopping criterion is not reached,
 15. Return to step 2
16. End if
17. End for
18. Output the best result.

Figure 13. BCO pseudo-code

Bee colony Optimization has been successfully applied to solving the Job Shop Problem, MANET- Routing Protocol, Generalized Assignment Problem, Engineering Optimization, Travelling Salesman's Problem, Numerical Assignment Problems etc. (Nagpure & Raja)

The mechanism that informs the decision of a bee to follow a particular dancer is not well established but it is rather vaguely considered that the decision to follow a particular bee is a function of the food source (Camazine & Sneyd, 1991). However, the abandonment phenomenon is of great benefit to the algorithm. That is to say that when the employed bees could not find the optimized solutions after some repetitions, they transform to the scout bees again and move in random paths to start searching for optimized solutions. This way, the solutions which are not optimized are abandoned and further searches are made for the global optimized points. This procedure helps the algorithm not to fall into a local optima or minima in a multi-dimensional search environment. As a result, it could be safe to say that the artificial bees use a combination of local and global searching methods to arrive at solutions.

It should, however, be observed that that the BCO has complicated fitness function. As such, obtaining good results is a function of proper setting of parameters such as minimum overshoot, rise time, steady state error and settling time in the state response. Moreover, it has been observed that Bee Colony algorithm is not as adaptive as ACO. Finally, BCO algorithm shows poor performance and remains inefficient in exploring search space because its search equation is significantly influenced by a random quantity which helps in exploration at the cost of exploitation of the search space (Babaeizadeh & Ahmad, 2014)

Findings

The development of several optimization algorithms, some of which have been described in this study, no doubt, has been of immense benefits to the scientific community in general and computer scientists, in particular (Di Caro, Ducatelle, Gambardella, & Dorigo, 2005; Giannakouris, Vassiliadis, & Dounias, 2010; Ridge a't, Kudcnko, & Kazakov'i, 2005; Wedde & Farooq, 2005; X.-S. Yang, 2009a). These algorithms have sped up industrial processes, minimized waste of time, money and computer resources. However, a critical look at these NAs indicates that there are no clear theoretical proofs of their workings. It is rather worrisome that in cases where there are results of convergence analysis as in the GA (Rudolph, 1994), these results are rather limited. Moreover, there are no clear mathematical proofs in most of these algorithms (Farmer, Guttman, & Thayer, 1993). As a result, there is need for deliberate research on the mathematical, theoretical and convergence evaluation of NAs. The research community will benefit maximally from NAs when the convergence conditions of NAs are clearer to the extent that the non- experts can easily understand.

Moreover, this study observes that that most application of NAs were concerned with relatively simple to medium-scale experimental cases involving scores of variables. It is not well established if these NAs can do as well in practical real-life situations that may involve hundreds or even thousands of variables. This should also be an area of further research investigation.

Furthermore, the application areas of the NAs are, to say the least, largely theoretical. Except in few situations like the practical Proportional, Integral and Derivative parameters-tuning of AVR and DC motors (Al Gizi, Mustafa, Al Zaidi, & Al-Zaidi, 2015; Meshram & Kanojiya, 2012) etc, most of the studies available in literature are more or less theoretical. The danger with such simulated studies is that it may not work appropriately in a real-life situation.

Finally, it is observed that most of the NAs still use manual setting of parameters. It will be better if the NAs employ dynamic setting of parameters in course of the algorithm execution. There have been a few studies employing dynamic parameter setting (Lobo, Lima, & Michalewicz, 2007; Schraudolph & Belew, 1992; B. YANG & ZHANG, 2004; Zielinski & Laur, 2007) but, we dare say, these studies are quite few and are basically at their infancy. The scientific community stands to benefit a lot more from NAs when the NAs employ dynamic parameter tuning.

Conclusion

This paper did a critical review of ten Nature-inspired optimization (NAs) techniques, picking three trajectory-based algorithms and seven population-based. The trajectory-based algorithms examined are the Simulated Annealing, the Great Deluge and the Hill Climbing. Similarly, the six population-based algorithms investigated in this study are the PSO, ACO, ABC, BCO, BBO ABO and the FFA. At the end of the critical analysis of these ten algorithms, it was observed that the NAs have made immense contributions to different aspects of human development: scientific, engineering, medical, business etc. Nevertheless, the study revealed that there is a general lack of clear mathematical and theoretical proof of convergence in most NAs. Moreover, the algorithms pay so much attention to problems with relatively less number of variables than that are common in practical day-to-day real-life industrial problems that has several hundreds, thousands and even millions of variables. There is, therefore, little or no guarantee that the same methodology used to obtain results in the small problems will produce same results in larger real-life environments. Furthermore, the studies are largely simulated with the possibility of not being as effective in real-life situations. It is, therefore, recommended that future research studies in NAs should place greater emphasis on experimentation with real-life situations, unravelling the mathematical and theoretical convergence analysis of the NAs, in addition to, focusing on problems with very large number of variables.

Finally, in terms of the algorithm design, it was observed that many of the NAs make use of several parameters leads to extensive use of computer resources and slow speed. The faster algorithms, according to this review, are usually those that deploy fewer parameters. This is in consonance with the recent drive for lean metaheuristic design deliberately avoiding the Frankenstein phenomena. Frankenstein phenomena refers to a situation where an optimization algorithm deploys several parameters in its search for solution to the extent that the individual contribution of each parameter is difficult to pinpoint (Sörensen, 2015; Sörensen & Glover, 2013). It is, therefore, recommended that algorithm designers should deploy only the number of parameters needed to obtain good solutions. This will enhance algorithm efficiency without compromising effectiveness.

Acknowledgment

The author appreciates the support of the Faculty of Computer Systems and Software Engineering, Universiti Malaysia Pahang, Kuantan 26300, Malaysia, for providing environment conducive for this research as well as the funding for this research under Grant 1403118. Our appreciation to Anchor University, Ayobo, Lagos, Nigeria and the Universiti Tun Hussein Onn, Malaysia for additional fundings.

Conflict of Interest

The author asserts that there exists no conflict of interest in the publication of this article.

References

- Aghamohammadi, M., & Pourgholi, M. (2008). Experience with SSFR test for synchronous generator model identification using Hook-Jeeves optimization method. *International Journal of System Applications, Engineering and Development*, 2(3), 122-127.
- Akay, B., & Karaboga, D. (2015). A survey on the applications of artificial bee colony in signal, image, and video processing. *Signal, Image and Video Processing*, 9(4), 967-990.
- Al Gizi, A. J., Mustafa, M., Al Zaidi, K. M., & Al-Zaidi, M. K. (2015). Integrated PLC-fuzzy PID Simulink implemented AVR system. *International Journal of Electrical Power & Energy Systems*, 69, 313-326.
- Alba, E., Talbi, E., Luque, G., & Melab, N. (2005). 4. Metaheuristics and Parallelism. *Parallel Metaheuristics: A New Class of Algorithms*. Wiley, 79-104.
- Alroomi, A. R., Albasri, F. A., & Talaq, J. H. (2013). Solving the Associated Weakness of Biogeography-Based Optimization Algorithm. *International Journal on Soft Computing*, 4(4), 1-20.
- Anwar, I. M., Salama, K. M., & Abdelbar, A. M. (2015). Instance Selection with Ant Colony Optimization. *Procedia Computer Science*, 53, 248-256.
- Babaeizadeh, S., & Ahmad, R. (2014). A Modified Artificial Bee Colony Algorithm for Constrained Optimization Problems. *Journal of Convergence Information Technology*, 9(6), 151.
- Banzhaf, W., Nordin, P., Keller, R. E., & Francone, F. D. (1998). *Genetic programming: an introduction* (Vol. 1): Morgan Kaufmann San Francisco.
- Binitha, S., & Sathya, S. S. (2012). A survey of bio inspired optimization algorithms. *International Journal of Soft Computing and Engineering*, 2(2), 137-151.
- Brabazon, A. (2008). *Natural computing in computational finance* (Vol. 1): Springer Science & Business Media.
- Burke, E., Bykov, Y., & Hirst, J. (2007). Great Deluge Algorithm for Protein Structure Prediction.
- Burke, E., Bykov, Y., Newall, J., & Petrovic, S. (2003). A time-predefined approach to course timetabling. *Yugoslav Journal of Operations Research ISSN: 0354-0243 EISSN: 2334-6043*, 13(2).
- Camazine, S., & Sneyd, J. (1991). A model of collective nectar source selection by honey bees: self-organization through simple rules. *Journal of theoretical Biology*, 149(4), 547-571.
- Chau, C., Kwong, S., Diu, C., & Fahrner, W. (1997). *Optimization of HMM by a genetic algorithm*. Paper presented at the Acoustics, Speech, and Signal Processing, 1997. ICASSP-97., 1997 IEEE International Conference on.
- Crawford, C., & Krebs, D. L. (2013). *Handbook of evolutionary psychology: Ideas, issues, and applications*: Psychology Press.
- Cuevas, E., & Sossa, H. (2013). A comparison of nature inspired algorithms for multi-threshold image segmentation. *Expert systems with applications*, 40(4), 1213-1219.
- Di Caro, G., Ducatelle, F., Gambardella, L. M., & Dorigo, M. (2005). AntHocNet: an adaptive nature-inspired algorithm for routing in mobile ad hoc networks. *European Transactions on Telecommunications*, 16(5), 443-455.
- Domínguez, J., & Alba, E. (2011). Ethane: a heterogeneous parallel search algorithm for heterogeneous platforms. *arXiv preprint arXiv:1105.5900*.
- Dorigo, M., Birattari, M., & Stützle, T. (2006). Ant colony optimization. *Computational Intelligence Magazine, IEEE*, 1(4), 28-39.
- Dorigo, M., Caro, G. D., & Gambardella, L. M. (1999). Ant algorithms for discrete optimization. *Artificial life*, 5(2), 137-172.
- Dueck, G. (1993). New optimization heuristics: the great deluge algorithm and the record-to-record travel. *Journal of Computational physics*, 104(1), 86-92.
- Farmer, W. M., Guttman, J. D., & Thayer, F. J. (1993). IMPS: An interactive mathematical proof system. *Journal of Automated Reasoning*, 11(2), 213-248.
- Fister, I., Yang, X.-S., & Brest, J. (2013). A comprehensive review of firefly algorithms. *Swarm and Evolutionary Computation*, 13, 34-46.
- Forsythe, G. E., & Wasow, W. R. (1960). Finite-difference methods for partial differential equations.
- Galbally, J., Fierrez, J., & Ortega-Garcia, J. (2007). Bayesian hill-climbing attack and its application to signature verification *Advances in Biometrics* (pp. 386-395): Springer.
- Giannakouris, G., Vassiliadis, V., & Dounias, G. (2010). Experimental study on a hybrid nature-inspired algorithm for financial portfolio optimization *Artificial Intelligence: Theories, Models and Applications* (pp. 101-111): Springer.
- Gutjahr, W. J. (2003). A converging ACO algorithm for stochastic combinatorial optimization *Stochastic algorithms: Foundations and applications* (pp. 10-25): Springer.

- Halambi, A., Grun, P., Ganesh, V., Khare, A., Dutt, N., & Nicolau, A. (2008). *EXPRESSION: A language for architecture exploration through compiler/simulator retargetability*. Paper presented at the Design, Automation, and Test in Europe.
- Hassan, M. H., & Muniyandi, R. C. (2017). An Improved Hybrid Technique for Energy and Delay Routing in Mobile Ad-Hoc Networks. *International Journal of Applied Engineering Research*, 12(1), 134-139.
- Hoffmann, J. (2010). A heuristic for domain independent planning and its use in an enforced hill-climbing algorithm *Foundations of Intelligent Systems* (pp. 216-227): Springer.
- Karaboga, D., & Akay, B. (2009). A survey: algorithms simulating bee swarm intelligence. *Artificial Intelligence Review*, 31(1-4), 61-85.
- Karaboga, D., Akay, B., & Ozturk, C. (2007). Artificial bee colony (ABC) optimization algorithm for training feed-forward neural networks *Modeling decisions for artificial intelligence* (pp. 318-329): Springer.
- Karaboga, D., & Aslan, S. (2015). *A new emigrant creation strategy for parallel Artificial Bee Colony algorithm*. Paper presented at the 2015 9th International Conference on Electrical and Electronics Engineering (ELECO).
- Karaboga, D., & Basturk, B. (2007). A powerful and efficient algorithm for numerical function optimization: artificial bee colony (ABC) algorithm. *Journal of global optimization*, 39(3), 459-471.
- Karaboga, D., Gorkemli, B., Ozturk, C., & Karaboga, N. (2014). A comprehensive survey: artificial bee colony (ABC) algorithm and applications. *Artificial Intelligence Review*, 42(1), 21-57.
- Karaboga, D., & Ozturk, C. (2009). Neural networks training by artificial bee colony algorithm on pattern classification. *Neural Network World*, 19(3), 279.
- Kefi, S., Rokbani, N., Krömer, P., & Alimi, A. M. (2015). *A New Ant Supervised-PSO Variant Applied to Traveling Salesman Problem*. Paper presented at the Hybrid Intelligent Systems: 15th International Conference HIS 2015 on Hybrid Intelligent Systems, Seoul, South Korea, November 16-18, 2015.
- Kennedy, J. (2010). Particle swarm optimization *Encyclopedia of Machine Learning* (pp. 760-766): Springer.
- Kifah, S., & Abdullah, S. (2015). An adaptive non-linear great deluge algorithm for the patient-admission problem. *Information Sciences*, 295, 573-585.
- Kirkpatrick, S., Gelatt, C. D., & Vecchi, M. P. (1983). Optimization by simulated annealing. *science*, 220(4598), 671-680.
- Kumbharana, N., & Pandey, G. M. (2013). A Comparative Study of ACO, GA and SA for Solving Travelling Salesman Problem. *International Journal of Societal Applications of Computer Science*, 2(2), 224-228.
- Kunna, M. A., Kadir, T. A. A., Jaber, A. S., & Odili, J. B. (2015). Large-Scale Kinetic Parameter Identification of Metabolic Network Model of E. coli Using PSO. *Advances in Bioscience and Biotechnology*, 6(02), 120.
- Lagarias, J. C., Reeds, J. A., Wright, M. H., & Wright, P. E. (1998). Convergence properties of the Nelder--Mead simplex method in low dimensions. *SIAM Journal on optimization*, 9(1), 112-147.
- Langeveld, J., & Engelbrecht, A. P. (2011). *A generic set-based particle swarm optimization algorithm*. Paper presented at the International conference on swarm intelligence, ICSI.
- Ledesma, S., Aviña, G., & Sanchez, R. (2008). Practical considerations for simulated annealing implementation. *Simulated Annealing*, 20, 401-420.
- Liu, J., Zhu, H., Ma, Q., Zhang, L., & Xu, H. (2015). An Artificial Bee Colony algorithm with guide of global & local optima and asynchronous scaling factors for numerical optimization. *Applied Soft Computing*, 37, 608-618.
- Lobo, F. G., Lima, C. F., & Michalewicz, Z. (2007). *Parameter setting in evolutionary algorithms* (Vol. 54): Springer Science & Business Media.
- Manjarres, D., Landa-Torres, I., Gil-Lopez, S., Del Ser, J., Bilbao, M. N., Salcedo-Sanz, S., & Geem, Z. W. (2013). A survey on applications of the harmony search algorithm. *Engineering Applications of Artificial Intelligence*, 26(8), 1818-1831.
- Mcmullan, P. (2007). An extended implementation of the great deluge algorithm for course timetabling *Computational Science-ICCS 2007* (pp. 538-545): Springer.
- Mehrabian, A. R., & Lucas, C. (2006). A novel numerical optimization algorithm inspired from weed colonization. *Ecological informatics*, 1(4), 355-366.
- Meshram, P., & Kanojiya, R. G. (2012). *Tuning of PID controller using Ziegler-Nichols method for speed control of DC motor*. Paper presented at the Advances in Engineering, Science and Management (ICAESM), 2012 International Conference on.
- Mezmez, M., Melab, N., & Talbi, E.-G. (2006). *Using the multi-start and island models for parallel multi-objective optimization on the computational grid*. Paper presented at the e-Science and Grid Computing, 2006. e-Science'06. Second IEEE International Conference on.
- Mirjalili, S., Mirjalili, S. M., & Lewis, A. (2014). Grey wolf optimizer. *Advances in Engineering Software*, 69, 46-61.
- Nagpure, H., & Raja, R. The Applications Survey on Bee Colony Optimization.

- Nahas, N., Kadi, D. A., & El Fath, M. N. (2010). *Iterated great deluge for the dynamic facility layout problem: CIRRELT*.
- Nozohour-leilabady, B., & Fazelabdolabadi, B. (2015). On the application of Artificial Bee Colony (ABC) algorithm for optimization of well placements in fractured reservoirs; efficiency comparison with the Particle Swarm Optimization (PSO) methodology. *Petroleum*.
- Odili, J. B. (2013). Application of Ant Colony Optimization to Solving the Traveling Salesman's Problem. *Science Journal of Electrical & Electronic Engineering, 2013*.
- Odili, J. B., & Kahar, M. N. M. (2015a). African Buffalo Optimization (ABO): a New Meta-Heuristic Algorithm. *Journal of Advanced & Applied Sciences, 03(03)*, 101-106.
- Odili, J. B., & Kahar, M. N. M. (2015b). Numerical Function Optimization Solutions Using the African Buffalo Optimization Algorithm (ABO). *British Journal of Mathematics & Computer Science, 10(1)*, 1-12.
- Odili, J. B., & Kahar, M. N. M. (2016). African Buffalo Optimization. *International Journal of Software Engineering & Computer Systems, 2*, 28-50. doi:<http://dx.doi.org/10.15282/ijsecs.2.2016.1.0014>
- Odili, J. B., & Mohamad Kahar, M. N. (2016a). African Buffalo Optimization Approach to the Design of PID Controller in Automatic Voltage Regulator System. *National Conference for Postgraduate Research, Universiti Malaysia Pahang, September, 2016*, 641-648.
- Odili, J. B., & Mohamad Kahar, M. N. (2016b). Solving the Traveling Salesman's Problem Using the African Buffalo Optimization. *Computational Intelligence and Neuroscience, 2016*, 1-12.
- Odili, J. B., Mohamad Kahar, M. N., & Noraziah, A., Odili Esther Abiodun (2016). African Buffalo Optimization and the Randomized Insertion Algorithm for the Asymmetric Travelling Salesman's Problems *Journal of Theoretical and Applied Information Technology, 87(3)*, 356-364.
- Olafsson, S. (2006). Metaheuristics. *Handbooks in operations research and management science, 13*, 633-654.
- Pereira, G. (2011). Particle Swarm Optimization. *INESCID and Instituto Superior Tecnico, Porto Salvo, Portugal, gpereira@gaips.inesc-id.pt, Verified email at gaips.inesc-id.pt, April, 15*.
- Peri, D., & Tinti, F. (2012). A multistart gradient-based algorithm with surrogate model for global optimization. *Communications in Applied and Industrial Mathematics, 3(1)*.
- Perkins, S., Lacker, K., & Theiler, J. (2003). Grafting: Fast, incremental feature selection by gradient descent in function space. *The Journal of Machine Learning Research, 3*, 1333-1356.
- Pham, D., Ghanbarzadeh, A., Koc, E., Otri, S., Rahim, S., & Zaidi, M. (2011). *The Bees Algorithm—A Novel Tool for Complex Optimisation*. Paper presented at the Intelligent Production Machines and Systems-2nd I* PROMS Virtual International Conference 3-14 July 2006.
- Pletcher, R., Minkowycz, W., Sparrow, E., & Schneider, G. (1988). Overview of basic numerical methods. *Handbook of Numerical Heat Transfer, 1-88*.
- Poli, R. (2007). An analysis of publications on particle swarm optimization applications. *Essex, UK: Department of Computer Science, University of Essex*.
- Qu, Z., & Mo, H. (2011). Research of hybrid biogeography based optimization and clonal selection algorithm for numerical optimization *Advances in Swarm Intelligence* (pp. 390-399): Springer.
- Ridge at, F., Kudcnko, D., & Kazakov'i, D. (2005). Moving Nature-Inspired Algorithms to Parallel, Asynchronous and Decentralised Environments. *Self-Organization and Autonomic Informatics (I), 1*, 35.
- Rudolph, G. (1994). Convergence analysis of canonical genetic algorithms. *Neural Networks, IEEE Transactions on, 5(1)*, 96-101.
- Schraudolph, N. N., & Belew, R. K. (1992). Dynamic parameter encoding for genetic algorithms. *Machine learning, 9(1)*, 9-21.
- Selman, B., & Gomes, C. P. (2006). Hill-climbing Search. *Encyclopedia of Cognitive Science*.
- Shi, Y., & Eberhart, R. C. (1999). *Empirical study of particle swarm optimization*. Paper presented at the Evolutionary Computation, 1999. CEC 99. Proceedings of the 1999 Congress on.
- Simon, D. (2008). Biogeography-based optimization. *Evolutionary Computation, IEEE Transactions on, 12(6)*, 702-713.
- Simon, D., Ergezer, M., & Du, D. (2009). *Population distributions in biogeography-based optimization algorithms with elitism*. Paper presented at the Systems, Man and Cybernetics, 2009. SMC 2009. IEEE International Conference on.
- Sörensen, K. (2015). Metaheuristics—the metaphor exposed. *International Transactions in Operational Research, 22(1)*, 3-18.
- Sörensen, K., & Glover, F. W. (2013). Metaheuristics *Encyclopedia of operations research and management science* (pp. 960-970): Springer.
- Stützle, T., López-Ibáñez, M., & Dorigo, M. (2011). A concise overview of applications of ant colony optimization. *Wiley Encyclopedia of Operations Research and Management Science*.

- Tanweer, M., Suresh, S., & Sundararajan, N. (2015). *Improved SRPSO algorithm for solving CEC 2015 computationally expensive numerical optimization problems*. Paper presented at the Evolutionary Computation (CEC), 2015 IEEE Congress on.
- Teodorović, D., & Dell'Orco, M. (2005). *Bee colony optimization—a cooperative learning approach to complex transportation problems*. Paper presented at the Advanced OR and AI Methods in Transportation: Proceedings of 16th Mini-EURO Conference and 10th Meeting of EWGT (13-16 September 2005).—Poznan: Publishing House of the Polish Operational and System Research.
- Tyrrell, A. M., Hollingworth, G., & Smith, S. L. (2001). *Evolutionary strategies and intrinsic fault tolerance*. Paper presented at the Evolvable Hardware, 2001. Proceedings. The Third NASA/DoD Workshop on.
- Vassiliadis, V., & Dounias, G. (2009). NATURE-INSPIRED INTELLIGENCE: A REVIEW OF SELECTED METHODS AND APPLICATIONS. *International Journal on Artificial Intelligence Tools*, 18(04), 487-516.
- Venter, G. (2010). Review of optimization techniques. *Encyclopedia of aerospace engineering*.
- Wedde, H. F., & Farooq, M. (2005). A performance evaluation framework for nature inspired routing algorithms *Applications of Evolutionary Computing* (pp. 136-146): Springer.
- Whitley, D. (1994). A genetic algorithm tutorial. *Statistics and computing*, 4(2), 65-85.
- Wu, Y., Xin, Y., & Zhang, Y. (2015). Application of ACO to Vehicle Routing Problems Using Three Strategies.
- Xi, B., Liu, Z., Raghavachari, M., Xia, C. H., & Zhang, L. (2004). *A smart hill-climbing algorithm for application server configuration*. Paper presented at the Proceedings of the 13th international conference on World Wide Web.
- YANG, B., & ZHANG, Z.-k. (2004). Dynamic Characteristic Parameter Setting Method for Human-simulated Intelligent Controller. *Information and Control*, 33(6), 670-673.
- Yang, X.-S. (2005). Engineering optimizations via nature-inspired virtual bee algorithms *Artificial Intelligence and Knowledge Engineering Applications: A Bioinspired Approach* (pp. 317-323): Springer.
- Yang, X.-S. (2009a). Firefly algorithms for multimodal optimization *Stochastic algorithms: foundations and applications* (pp. 169-178): Springer.
- Yang, X.-S. (2009b). Harmony search as a metaheuristic algorithm *Music-inspired harmony search algorithm* (pp. 1-14): Springer.
- Yang, X.-S. (2012). Nature-inspired metaheuristic algorithms: success and new challenges. *arXiv preprint arXiv:1211.6658*.
- Yang, X.-S., Deb, S., & Fong, S. (2011). Accelerated particle swarm optimization and support vector machine for business optimization and applications *Networked digital technologies* (pp. 53-66): Springer.
- Yeomans, J. S., & Yang, X.-S. (2014). Municipal waste management optimisation using a firefly algorithm-driven simulation-optimisation approach. *International Journal of Process Management and Benchmarking*, 4(4), 363-375.
- Zielinski, K., & Laur, R. (2007). *Adaptive parameter setting for a multi-objective particle swarm optimization algorithm*. Paper presented at the IEEE Congress on Evolutionary Computation, 2007. CEC 2007.

Author Information

Julius Beneoluchi Odili

Anchor University, Lagos
1-4, Ayobo Road, Ipaja, Lagos
Odili_julest@yahoo.com

A. Noraziah

Universiti Malaysia Pahang,
Gambang, Kuantan 26300, Malaysia

Radzi Ambar

Universiti Tun Hussein Onn, Malaysia
Batu Pahat, Johor, Malaysia

Mohd Helmy Abd Wahab

Universiti Tun Hussein Onn, Malaysia
Batu Pahat, Johor, Malaysia

Implementation Strategies for the Cuckoo Search and the African Buffalo Optimization for the Benchmark Rosenbrock Function

Julius Beneoluchi ODILI

Anchor University

A. NORAZIAH

Universiti Malaysia Pahang

Radzi AMBAR

Universiti Tun Hussein Onn

Mohd Helmy Abd WAHAB

Universiti Tun Hussein Onn

Abstract: The introduction of five benchmark global optimization test functions by De Jong has remained prominent in Mathematics and Computer Science for over three decades now. This paper examines the effect of the search population and the number of iterations of the Cuckoo Search and the African Buffalo Optimization in providing solutions to one of Dejong function, the Rosenbrock function, sometimes called Dejong2 function which is a unimodal non-separable function. The Rosenbrock function because of its deceptive flat landscape has proven to be a good test case for optimization algorithms since the flat surface provides very misleading information to search agents. After a number of experimental investigations using different iteration numbers and population, this study concludes that the CS provides better solutions but at a cost of more computer resources than the ABO. As a result, this study in harmony with the No Free Lunch Theorem concludes that if speed is the main consideration, the ABO is a better algorithm in solving the Rosenbrock (or a similar function), otherwise, the CS is a better choice.

Keywords: African buffalo optimization, Cuckoo search, Iteration, Rosenbrock, Search population

Introduction

Kenneth Dejong has become a very popular figure in the Mathematics and Computer Science, especially because of his noble contributions to the field of optimization search landscape. In his PhD thesis, Dejong introduced five benchmark optimization functions that are fast becoming effective testbed for several optimization search algorithms. The benchmark functions are the Sphere function, Rosenbrock function, Step function, Quartic function and Shekel Foxhole function. The five functions are presented in Figures 1-5 (De Jong, 1975).

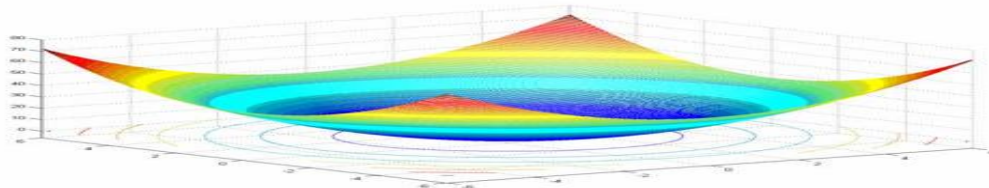


Figure 1. Sphere function (function, Accessed on 2nd May, 2018)

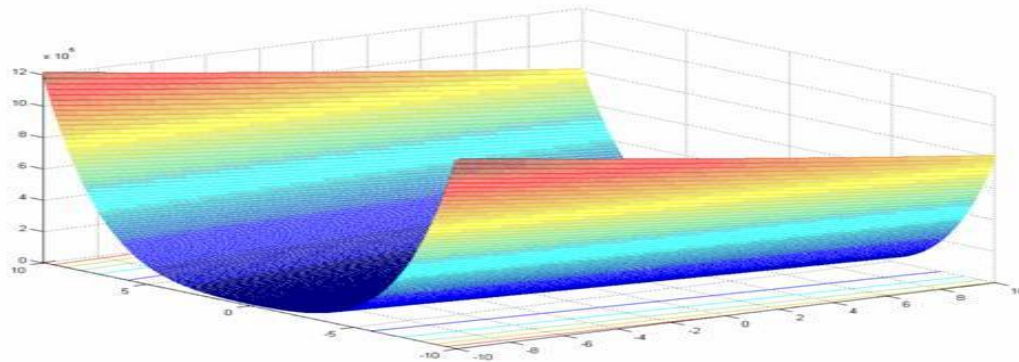


Figure 2. Rosenbrock function (Rosenbrock, Accessed on 2nd May, 2018)

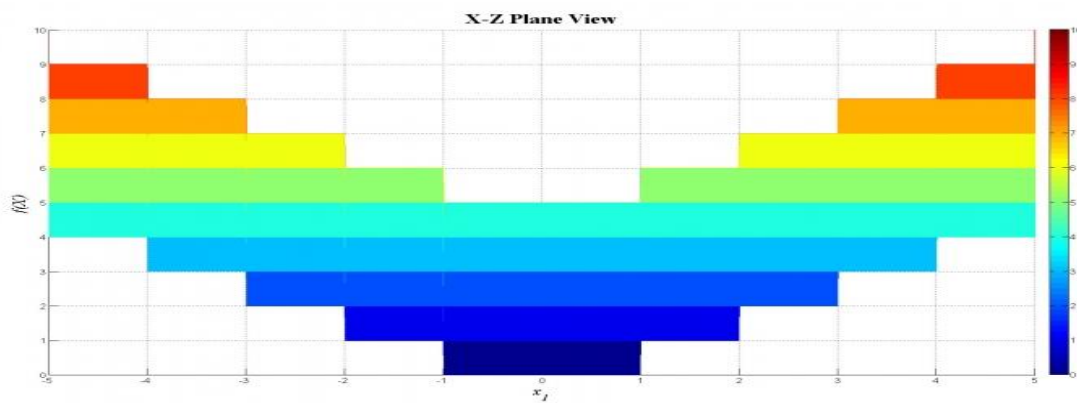


Figure 3. Step function accessed on 2nd May, 2018)

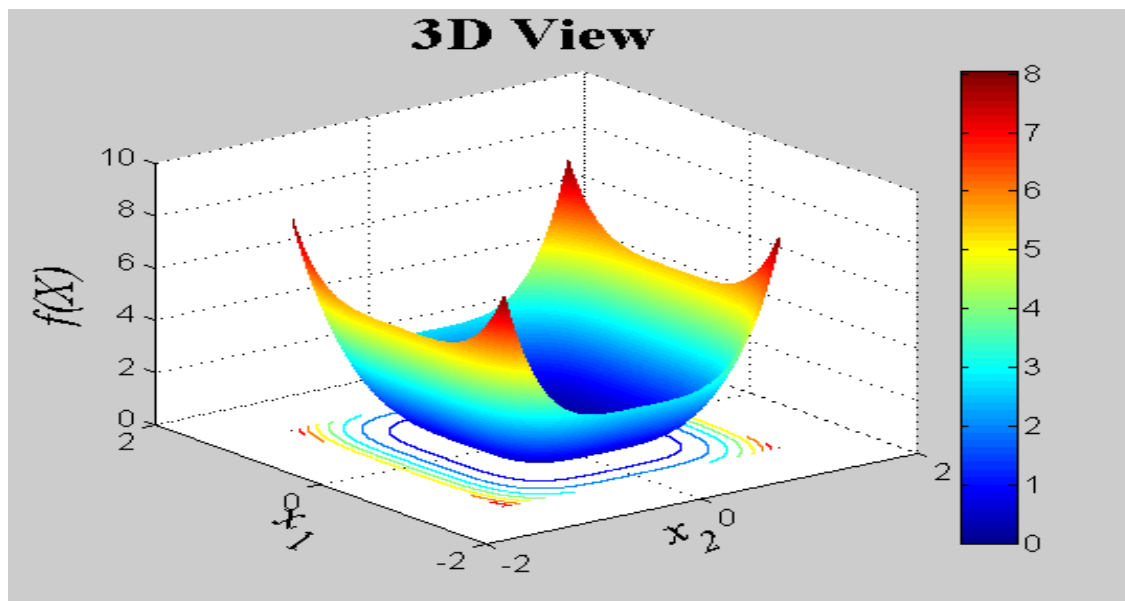


Figure 4. Quartic function

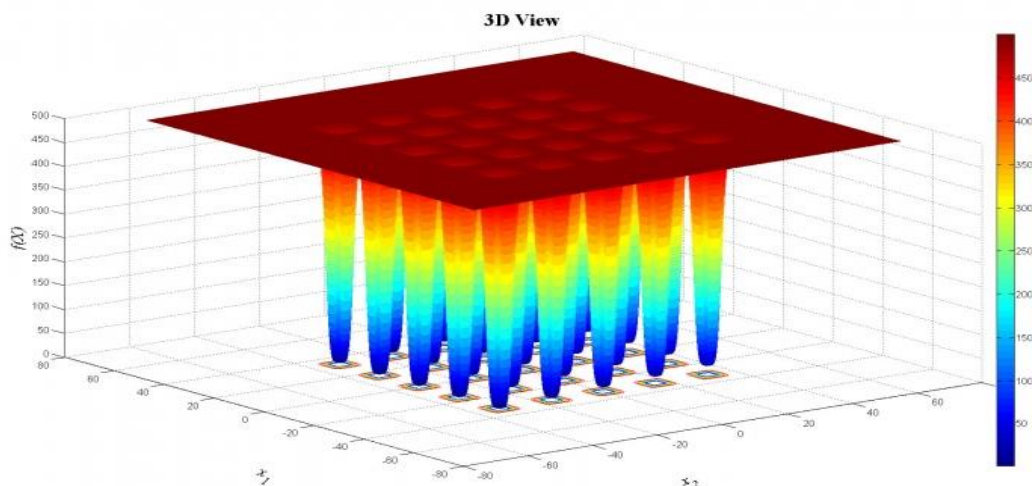


Figure 5. Shekel foxholes function

These functions represent different search landscapes ranging from monomodal Separable (Sphere, Quartic and Step function) Unimodal Non Separable (Rosenbrock) and Multimodal Non Separable (Shekel Foxhole)(Problems, Accessed on 11th February, 2017). A monomodal function has just a single minimum or optimum while a multimodal function has two or more optima or minima (Casini et al., 2012). Please note that by separable function we actually mean separable PDE (Partial Differential Equation) as opposed to ODE (Ordinary Differential Equation) (Odili and Kahar, 2015b). An ODE contains one or more functions of a particular independent variable and its derivatives (Kunna et al., 2015). Similarly, a separable PDE function is such that is divisible into a number of separate variables. That is to say such separable PDE can be re-written as a collection of f functions of just a variable. As such the separability of a function is akin to interrelation or epistasis among variables of a function (Visintin, 2012). Also, please recall that epistasis deals with the measurement of the contributions a gene in relation to other genes to the overall fitness of an individual (Sackton and Hartl, 2016).

In mathematics and computer science, it is believed that Non Separable functions are rather more difficult to optimize hence our interest in comparing the African Buffalo Optimization and the Cuckoo Search, two very effective and efficient algorithms, in solving the benchmark Rosenbrock function which is a non-separable function with particularly focus on the effect of the number of iteration and search populations in obtaining good solutions.

The rest of this paper is organized in the following ways: section two discusses the African Buffalo Optimization algorithm while section three examines the Cuckoo Search; section four is concerned with the experimental setting and discussion of results of the two algorithms in solving the benchmark Rosenbrock function and section five draws conclusions from the study.

Africa Buffalo Optimization

The ABO was designed in 2015 with inspiration from the harmonious herd management of African buffalos in their search for fresh green pastures in different parts of the African landscapes to satisfy their large appetites (Odili and Kahar, 2015a). The African buffalos manage their large herds using two vocalizations: the waaa (explore) and the maaa (exploit) vocalizations. With these two simple vocalizations, the buffalos are able to organize themselves out of harsh fruitless fields to very fertile and fruitful locations. The ABO has been successfully used to solve a number of optimization problems such as the symmetric Travelling Salesman's Problem (Odili and Mohmad Kahar, 2016b), asymmetric Travelling Salesman's Problem (Odili et al., 2015), Collision-avoidance in electric fishes, Strategic Management, PID Controller's parameters tuning of Automatic Voltage Regulators (Odili and Mohmad Kahar, 2016a)etc. The pseudocode of the ABO is presented in Figure 6.

1. Begin
2. Initialize the buffalos randomly within the search space;
3. While (until termination),
4. For j=1: n (n denotes the population),
5. Ascertain the buffalos' exploitation location:
6. $mk' = mk + lp1(bg - wk) + lp2(bpk - wk)$
7. Here wk =exploration move; where mk = exploitation move; bg = best buffalo with the best fitness; $lp1$ and $lp2$ represents the learning parameters; bpk , best location of buffalo k
8. Update the exploration fitness of buffalos:
9. $wk' = (wk + mk) \lambda$
10. Ascertain whether the bg is updating? Yes, go to 11. If No in 10 iterations, return to 2
11. End for
- 12.. End while
13. Post best solution.
14. End

Figure 6. Pseudocode of ABO

Cuckoo Search

The Cuckoo Search (CS) which was developed by X. Yang and S. Deb basically simulates the irresponsible attitude of the cuckoo bird to brood over their eggs until hatching (Yang and Deb, 2009). The cuckoo enjoys laying her eggs in the nests of other unwatchful birds (or other cuckoo species) in order to transfer the egg-brooding responsibilities to the host bird. If the host bird discovers the prank of the cuckoo, it either abandons the nest or throws away the cuckoo eggs(exploration). At other times, the host bird goes ahead to broods over and incubates the cuckoo eggs (exploitation). On its part, the cuckoo bird, with a certain probability, perfects her act by imitating the eggs of the host bird in order to perpetuate its fraud. In the CS, the eggs belonging to the host bird in a particular nest represents a solution to an optimization problem, while those of the cuckoo represents newer solutions. The overall aim of these two kinds of egg is to replace the older solutions with the newer ones (cuckoo's).

The CS has been applied successfully to solve a number of optimization problems, such as the wireless sensor networks, travelling salesman's problems, shortest path in distributed system document clustering, speech recognition, flood forecasting, job scheduling, image processing, classification task in health sector etc. with competitive outcomes (Kamat and Karegowda, 2014). The CS pseudocode (Agrawal et al., 2013) is presented in Figure 7

1. Begin
2. Objective function: $f(x)$ $x = (x_1, x_2, \dots, x_j)$
3. Ascertain the initial population of nests and distribute them randomly
4. While (until termination)
5. Generate randomly a cuckoo by Levy flight using
6. $X_{ij}(t + 1) = X_{ij}(t) + \alpha \text{Levy}(\lambda)$
7. Determine the cuckoo fitness
8. Choose a nest randomly among available host nests
9. If ($f_i > f_k$) then
10. Replace k by the new solution
11. End if
12. Abandon a fraction of the unfruitful nests and replace with newer ones
13. Keep the good solutions
14. Rank the good solutions and obtain the current overall best
15. End while
16. Output the best outcome
17. End

Figure 7. Cuckoo search pseudocode

Implementation Evaluation for Cuckoo Search and African Buffalo Optimization

In this paper the focus is unravelling the impact of the number of iterations as well as the search population needed to obtain the best outcome to the problem under investigation. The experiments were performed using MATLAB on a PC, 4GB RAM, Intel Duo Core i7 370 CPU @ 3.40GHz, 3.40GH running Windows 10. To make sure that the comparisons are fair, all experiments were implemented using MATLAB on the same PC. The buffalo population/nests are 10 and 50. Similarly, number of iterations are 10, 20, 100, 1000, 5000, and 10,000. The ABO parameters used for the experiments are $lp1=0.7$; $lp2=0.5$ and those of the CS are $pa=0.5$; $u=rand(size(s)) * \sigma$; $v= rand(size(s))$; $step = u./abs(v) .^ (1/\beta)$; $step\ size = 0.01 * step$. Each experiment was executed five times. The benchmark Rosenbrock function (Shi and Eberhart, 1999) is

$$f(x) = \sum [(100 x_i - x_{i+1})^2 + (x_i - 1)^2] \quad d-1 \quad i=1 \tag{1}$$

The optimal solution to the Rosenbrock function is:

$$f(x) = 0 \tag{2}$$

Table 1. Comparative search with 10 buffalos/nests

Iterations	ABO			CS				
	f_{min}	Average	Time (secs)	Average Time (s)	f_{min}	Average	Time (secs)	Average Time (s)
10	0.0359	0.0426	0.022	0.021	2.3080	0.5634	0.040	0.031
	0.0580		0.021		0.0013		0.031	
	0.0028		0.022		0.0329		0.033	
	0.1025		0.021		0.4738		0.034	
	0.0137		0.019		0.0012		0.018	
100	0.0018	0.0527	0.030	0.0542	$3.9731e^{-13}$	$5.0611e^{-13}$	0.172	0.163
	0.0018		0.059		$9.8137e^{-14}$		0.162	
	0.0031		0.060		$4.4142e^{-12}$		0.154	
	0.0308		0.059		$1.5596e^{-13}$		0.170	
	0.2259		0.063		$5.5449e^{-15}$		0.157	
1000	0.0011	0.0077	0.468	0.4650	$4.6147e^{-85}$	$4.4527e^{-78}$	1.565	1.5874
	0.0004208		0.455		$1.0024e^{-83}$		1.556	
	0.00065974		0.472		$4.2801e^{-78}$		1.563	
	0.0124		0.464		$4.2170e^{-69}$		1.600	
	0.0241		0.466		$8.1493e^{-75}$		1.653	
5000	$2.503e^{-07}$	$2.9357e^{-06}$	2.293	2.273	0	$2.4697e^{-320}$	8.118	7.9480
	$1.0443e^{-04}$		2.291		$3.0304e^{-318}$		8.086	
	$1.4071e^{-06}$		2.277		$4.3782e^{-318}$		7.867	
	$6.6688e^{-06}$		2.247		0		7.848	
	$3.0553e^{-05}$		2.258		$4.9407e^{-324}$		7.821	
10000	$1.8499e^{-05}$	$3.7547e^{-05}$	4.640	4.488	0	0	15.372	15.761
	$3.5446e^{-05}$		4.497		0		15.586	
	$2.8062e^{-05}$		4.421		0		15.683	
	$6.9589e^{-05}$		4.422		0		15.979	
	$3.6141e^{-05}$		4.458		0		16.183	

After a number of experiments, the simulation results of the CS and ABO searching with different populations of 10 and 50 nests/buffalos and different number of iterations ranging from 10 to 10,000 is presented in Table 1.

As can be seen in Table 1, at 10 iterations, the CS has an overall better than the ABO. It was only when the iteration was 10 that the ABO obtained a better result (mean: 0.0426 to CS's 0.5634) In all other instances of the run, the CS average results were better. This could be as a result of the ABO's combination of exploration fitness with exploitation fitness at each iteration resulting in faster convergence at a solution. However, in the other instances (that is, at iteration 100, 1000, 5000 and 10,000), the CS obtained better solutions.

Nonetheless, in terms of time taken to obtain good result, the ABO is the algorithm of choice. In 96% of the runs in Table 1, the ABO spent less time than the CS to obtain results. It was only in one instance that the CS converged earlier than the ABO and that was in the last run of iteration 10 (refer to the portion highlighted in

yellow ink). This fast speed of the ABO is a mark of the algorithm’s efficiency because time correlates with use of computer resources (Khompatraporn et al., 2005).

Table 2. Comparative search with 50 buffalos/nests

Iterations	ABO			CS				
	f_{min}	Average	Time (sec)	Average Time (s)	f_{min}	Average	Time (secs)	Average Time (s)
10	0.0101		0.063		0.1048		0.071	
	0.0518		0.052		1.1899		0.068	
	0.091	0.0357	0.051	0.051	0.0314	1.0334	0.068	0.0784
	0.013		0.037		2.9252		0.068	
	0.0127		0.052		0.9157		0.117	
100	0.0126		0.229		$4.1464e^{-14}$		0.172	
	0.0013		0.225		$6.8572e^{-14}$		0.162	0.163
	0.0044	0.0058	0.229	0.228	$2.6223e^{-16}$	$3.8376e^{-15}$	0.154	
	0.0036		0.230		$2.7811e^{-15}$		0.170	
	0.0069		0.227		$2.7811e^{-16}$		0.157	
1000	$6.1493e^{-05}$		1.981		$1.3143e^{-54}$		6.231	
	$6.1548e^{-05}$		1.986		$5.4190e^{-56}$		6.257	6.310
	$3.4435e^{-04}$	$4.4423e^{-04}$	2.056	2.032	$1.6071e^{-56}$	$2.2048e^{-55}$	6.364	
	$2.8068e^{-04}$		2.052		$1.0727e^{-55}$		6.384	
	$3.6573e^{-05}$		2.083		$1.6111e^{-54}$		6.313	
5000	$4.1663e^{-06}$		4.526		$6.8572e^{-161}$		26.775	
	$1.9063e^{-07}$		9.830		$2.6223e^{-169}$		25.366	30.042
	$2.7224e^{-05}$	$2.7808e^{-06}$	9.737	8.761	$2.7811e^{-165}$	$4.9646e^{-165}$	31.439	
	$1.6645e^{-05}$		10.012		$7.3016e^{-165}$		32.744	
	$3.4444e^{-06}$		9.702		$5.2609e^{-167}$		33.884	
10000	$7.8032e^{-06}$		20.117		$2.0759e^{-269}$		67.500	
	$5.9999e^{-07}$		20.734		$6.5280e^{-272}$		68.044	68.441
	$2.0300e^{-07}$	$4.1005e^{-06}$	19.853	20.237	$8.5684e^{-271}$	$5.3958e^{-272}$	68.585	
	$1.0420e^{-06}$		20.138		$8.2255e^{-269}$		70.631	
		20.341		$1.5813e^{-279}$		67.447		

Based on the results presented in Table 1, it may be safe to conclude that while the CS is a more effective algorithm in terms of obtaining optimal or near optimal solution to this particular problem (and by extension, other similar problems to the one) under investigation here, the ABO is a more efficient algorithm since the algorithm converges faster to a solution than the CS.

Furthermore, it is necessary to investigate the performances of both algorithms when a population of 50 search agents (buffalos or nests) are deployed to the search space. In the next set of experiments, 50 buffalo/nests population and different iterations numbers (10, 100, 1000, 5000 and 10,000) are used. The simulation outcome presented in Table 2.

The experimental output in Table 2 follows the trend in Table 1, that is, that the ABO converges faster than the CS. This can be seen in the results of using a population of 50 buffalos or nests when the iteration number is 10. The ABO obtained better result (mean: 0.0357 to CS’s 1.0334) due to ABO’s capacity for quicker convergence at a solution. As in the first set of experiments, from iteration 100, the tide turned in favor of the more effective CS (refer to Table 2).

Similarly, in terms of time taken to arrive at a solution, the ABO has an edge over the CS just like in the first set of experiments (refer to Table 1). It was only in iteration 100, that the CS had a faster speed than the ABO. In all other instances, the ABO converged faster at a solution, though in most instances, the ABO’s output is inferior to those of the CS. In fact, from iteration 1000 to 10,000, the ABO is, at least, three times faster than the CS. The reason for the ABO’s speed could be traceable to the Algorithm’s use of fewer parameters in its quest for solutions than the CS. The ABO being a parameter-less optimization algorithm uses just two controlling parameters, namely, the $lp1$ and $lp2$. The CS, on the other hand, uses a number of parameters such as pa, step, step size, sigma etc. Deploying several parameters in course of a search has the demerit of slowing down the speed of a search since the algorithm is bogged down by the parameter handling procedure (Sörensen, 2015).

Conclusion

This paper examines the effects of the population of search agents cum iteration number in solving the benchmark Rosenbrock function. The choice of these two comparative algorithms is as a result of their very good results in solving the optimization problems to which they have been deployed. Moreover, aside both algorithms being both recently designed population optimization search algorithms, the CS is a parameterized optimization search algorithm but the ABO is a parameter-less algorithm. A parameter-less algorithm does not require the tuning of individual parameters of a problem to obtain solutions, it simply uses the controlling parameters of the algorithm to solve any kind of problems it is confronted with. In the case of the ABO, the controlling parameters are the $lp1$ and $lp2$. The only two other examples of the parameter-less algorithms, in literature, are the Teaching Learning Based Optimization (TLBO) and the Jaya Algorithms. In the light of the differences and similarities of the CS and the ABO, therefore, it is necessary to investigate their capacities to solve different kinds of problems, hence this study.

After a number of experimental evaluations, it was discovered that in solving the benchmark Rosenbrock function (or a similar problem), the CS produced better outcome. The good results of the CS could be the problem-specific tuning of parameters. On the other hand, the ABO converges faster at a solution than the CS. This could be as a result of its use of fewer parameters, regular interactions among the buffalos coupled with straight-forward calculation of exploitation and exploration fitness of the buffalos.

Based on the foregoing, it may be safe to conclude that, in line with the No Free Lunch Theorem which states that there is no algorithm that is best to solve all problems, rather whatever is of interest to the practitioner/researcher may determine the choice of an optimization algorithm to solve a problem. In the problem under investigation here (the benchmark Rosenbrock function or a similar problem to it), if obtaining near-optimal solution at the shortest possible time is the utmost concern of the user, then the ABO is a better algorithm. Also, the main concern is obtaining a solution that is nearest to the optimal, then CS should be choice. Similarly, a nonprofessional user may prefer the ABO, being a parameter-less algorithm, because the user is saved the problem of parameter tuning.

Acknowledgement

The author appreciates the Faculty of Computer Systems and Software Engineering, Universiti Malaysia Pahang, for funding this study under Grant PGRS 1403118. Our appreciation to Anchor University, Ayobo,Lagos, Nigeria and the Universiti Tun Hussein Onn, Malaysia for additional fundings

Conflict of Interest

The author asserts that no conflict of interest exists in the publication of this manuscript

References

- Agrawal, S., Panda, R., Bhuyan, S. and Panigrahi, B. K. (2013) 'Tsallis entropy based optimal multilevel thresholding using cuckoo search algorithm', *Swarm and Evolutionary Computation*, 11, pp. 16-30.
- Casini, F., Vaunat, J., Romero, E. and Desideri, A. (2012) 'Consequences on water retention properties of double-porosity features in a compacted silt', *Acta Geotechnica*, 7(2), pp. 139-150.
- De Jong, K. A. (1975) 'Analysis of the behavior of a class of genetic adaptive systems'.
function, S. (Accessed on 30th January, 2017a) 'http://www-optima.amp.i.kyoto-u.ac.jp/member/student/hedar/Hedar_files/TestGO_files/Page1113.htm'.
- Function, S. (Accessed on 30th January, 2017b) '<http://www.al-roomi.org/benchmarks/unconstrained/n-dimensions/192-step-function-no-1>'.
- Kamat, S. and Karegowda, A. (2014) 'A brief survey on cuckoo search applications', *Int. J. Innovative Res. Comput. Commun. Eng.*, 2(2).
- Khompatraporn, C., Pintér, J. D. and Zabinsky, Z. B. (2005) 'Comparative assessment of algorithms and software for global optimization', *Journal of Global Optimization*, 31(4), pp. 613-633.

- Kunna, M. A., Kadir, T. A. A., Jaber, A. S. and Odili, J. B. (2015) 'Large-Scale Kinetic Parameter Identification of Metabolic Network Model of E. coli Using PSO', *Advances in Bioscience and Biotechnology*, 6(02), pp. 120.
- Odili, J. B. and Kahar, M. N. M. (2015a) 'African Buffalo Optimization (ABO): a New Meta-Heuristic Algorithm', *Journal of Advanced & Applied Sciences*, pp. 101-106.
- Odili, J. B. and Kahar, M. N. M. (2015b) 'Numerical Function Optimization Solutions Using the African Buffalo Optimization Algorithm (ABO)', *British Journal of Mathematics & Computer Science*, 10(1), pp. 1-12.
- Odili, J. B., Kahar, M. N. M., Anwar, S. and Azrag, M. A. K. 'A comparative study of African Buffalo Optimization and Randomized Insertion Algorithm for asymmetric Travelling Salesman's Problem'. *Software Engineering and Computer Systems (ICSECS), 2015 4th International Conference on: IEEE*, 90-95.
- Odili, J. B. and Mohamad Kahar, M. N. (2016a) 'African Buffalo Optimization Approach to the Design of PID Controller in Automatic Voltage Regulator System', *National Conference for Postgraduate Research, Universiti Malaysia Pahang*, September, 2016, pp. 641-648.
- Odili, J. B. and Mohamad Kahar, M. N. (2016b) 'Solving the Traveling Salesman's Problem Using the African Buffalo Optimization', *Computational intelligence and neuroscience*, 2016, pp. 1-12.
- Problems, B. (Accessed on 11th February, 2017) 'Benchmark Problems', <https://www.cs.cmu.edu/afs/cs/project/jair/pub/volume24/ortizboyer05a-html/node6.html>.
- Rosenbrock (Accessed on 30th January, 2017) '<http://www.cs.unm.edu/~neal.holts/dga/benchmarkFunction/rosenbrock.html>'.
- Sackton, T. B. and Hartl, D. L. (2016) 'Genotypic context and epistasis in individuals and populations', *Cell*, 166(2), pp. 279-287.
- Shi, Y. and Eberhart, R. C. 'Empirical study of particle swarm optimization'. *Evolutionary Computation, 1999. CEC 99. Proceedings of the 1999 Congress on: IEEE*, 1945-1950.
- Sörensen, K. (2015) 'Metaheuristics—the metaphor exposed', *International Transactions in Operational Research*, 22(1), pp. 3-18.
- Visintin, A. (2012) *Models of phase transitions*. Springer Science & Business Media.
- Yang, X.-S. and Deb, S. 'Cuckoo search via Lévy flights'. *Nature & Biologically Inspired Computing, 2009. NaBIC 2009. World Congress on: IEEE*, 210-214.

Author Information

Julius Beneoluchi Odili

Anchor University, Lagos
1-4, Ayobo Road, Ipaja, Lagos
Odili_julest@yahoo.com

A. Noraziah

Universiti Malaysia Pahang,
Gambang, Kuantan 26300, Malaysia

Radzi Ambar

Universiti Tun Hussein Onn, Malaysia
Batu Pahat, Johor, Malaysia

Mohd Helmy Abd Wahab

Universiti Tun Hussein Onn, Malaysia
Batu Pahat, Johor, Malaysia

Notes to the Question of Presenting the Theme of Special Solutions of Ordinary Differential Equations in a University Course

Irina ANDREEVA

Peter the Great St. Petersburg Polytechnic University

Abstract: As Sir Isaac Newton has said, laws of the Nature have been written in the language of Differential Equations. In particular, the classical theory of normal systems of Ordinary Differential Equations, supported by Cauchy theorems of existence and uniqueness of solutions, describes determined processes taking place in the Nature, technics and even in the society, i.e. such processes, for which a condition of a described system in an arbitrary fixed moment depends on its condition in any other moment. Solutions, describing such processes, are called the ordinary. But when the conditions of the Cauchy theorem are not satisfied, a situation totally changes. A point, in any neighborhood of which such conditions are not satisfied, may become for a system under consideration a point of non-uniqueness, a point of bifurcation. A solution of a system, each point of which appears to be a point of non-uniqueness, is called a special solution. A task of a full integration of a system demands finding of all its solutions, special solutions as well as ordinary ones. But this item shows us some gap in a special literature. This paper presents materials with the aim to fill this gap.

Keywords: Differential equations, Ordinary solution, Special solution, Bifurcations

Introduction

Let us consider a differential equation of the first order which is not resolved with respect to the derivative

$$F(x, y, y') = 0, \quad (1)$$

where F and $F'_{y'} \in C(D)$, $D \subset \mathbb{R}^3$ is a domain, and $F'_{y'}(x, y, y') \neq 0$ in any domain $U \subset D$, (otherwise in such a domain U function F will not depend on y' , and consequently equation (1) won't be a differential equation in U).

The *solution* of Eq. (1) is called any function belonging to the C^1 class (that means it must have a continuous derivative)

$$\varphi : I = \langle \alpha, \beta \rangle \rightarrow \mathbb{R},$$

(where I be an open, semi open or non-degenerate interval of the x axis), which is, being substituted into the Eq. (1) instead of y , transforms Eq. (1) into an identity with respect to x : $F(x, \varphi(x), \varphi'(x)) \equiv 0, x \in I$.

Any solution graph is called the *integral curve* of this equation.

A *region of definition* of Eq. (1) is called a set G belonging to an (x, y) plane, such as for any $p_0 = (x_0, y_0) \in G$ the equation

$$F(x_0, y_0, y') = 0 \quad (2)$$

has at least one solution $y' = y'_0, q_0 = (x_0, y_0, y'_0) \in D$.

Geometrically this means, that Eq. (1) sets in any point $p_0 \in G$ at least one tangential direction y'_0 for its integral curves. For the Eq. (1) the solutions of the Eq. (2) are called *allowable values* of y' in a p_0 point.

A *Cauchy problem* for the Eq. (1) is being formulated in the following way: we set a point $p_0 = (x_0, y_0) \in G$ and an allowed for it value $y' = y'_0$; it's necessary to find a solution φ of the Eq. (1), satisfying conditions

$$\varphi(x_0) = y_0, \varphi'(x_0) = y'_0. \quad (3)$$

A point $q_0 = (x_0, y_0, y'_0)$ is called the *initial point* of the solution φ and of the integral curve corresponding to this solution $y = \varphi(x)$.

Conditions (3) are called the *initial conditions* (or the *initial data*) for the solution φ . The solution of the Cauchy problem is called *unique*, if for every two of its solutions $\varphi_1(x), x \in I_1, \varphi_2(x), x \in I_2, \exists \delta > 0 : \varphi_2(x) \equiv \varphi_1(x)$ for $x \in I_1 \cap I_2 \cap (x_0 - \delta, x_0 + \delta)$. In an opposite case such a solution is called *nonunique*.

A solution of Eq. ($y = \varphi(x), x \in I$, is called *ordinary (special)*, if for each its point $q_0 = (x_0, y_0, y'_0) = (x_0, \varphi(x_0), \varphi'(x_0))$ the solution of a Cauchy problem Eq. (1), Eq. (3) is *unique (non-unique)*.

An integral curve of the Eq. (1) is called *ordinary (special)*, if it represents a graph of an *ordinary (special)* solution.

A point $p_0 = (x_0, y_0) \in G$ is called a *point of uniqueness for Eq. (1)*, if for each allowed for it value $y' = y'_0$ a solution of the Cauchy problem Eq.(1), Eq. (3) is unique or doesn't exist. In the opposite case it's called for eq. (1) a *point of non-uniqueness*.

The relation

$$\Phi(x, y, C) = 0 \quad (4)$$

where C means an arbitrary constant, is called a *general integral* for Eq. (1) on a set $G' (\subset G)$, if for every point $p_0 = (x_0, y_0) \in G'$ and any allowed for it value $y' = y'_0$ it implicitly defines a unique solution of the Cauchy problem.

Using a general integral (4) of the Eq. (1), we sometimes are able to find the special integral curves which lie in G' , as envelopes of a family of curves defined with this integral.

The Sufficient Attribute of the Envelope

As it was shown by V. Zalgaller (1975) and A. Andreev, I. Andreeva (2002), the following theorem takes place.

Theorem 1.

Let

$$\Phi(x, y, C) = 0, \Phi \in C^2(D), (D \in \mathbb{R}^3 - \text{a domain}), \quad (5)$$

be a family of curves, depending on a parameter $C \in I = (a, b)$ and covering the set G at the (x, y) plane, $G \times I \subset D$. Let $\Phi'_y(x, y, C) \neq 0$ in $G \times I$.

If the system of equations

$$\Phi(x, y, C) = 0, \quad \Phi'_C(x, y, C) = 0, \quad (x, y, C) \in GxI, \quad (6)$$

has a solution of C^1 – class

$$y = \psi(x), \quad C = C(x), \quad x \in J, \quad (7)$$

and $C'(x) \neq 0$ on every interval $J' \subset J$, then a curve $y = \psi(x)$, $x \in J$, is an envelope of a family of curves (5), which is tangential in every its point $(x_0, \psi(x_0))$ to a curve of this family $\Phi(x, y, C(x_0)) = 0$.

Corollary 1.

Let $\Phi(x, y, C) = 0$, where $C \in I = (a, b)$ is an arbitrary constant, be a general integral of the Eq. (1) on a G set. If for a family of curves (4) the conditions of the Theorem 1 are satisfied, and consequently this family of curves has an envelope $y = \psi(x)$, $x \in J$, then such an envelope appears to be a special integral curve for the Eq. (1).

A Proof.

An envelope of a family of integral curves of the Eq. (1) always is an integral curve for the Eq. (1) itself. The same time every point of it is a point of non-uniqueness, consequently it always appears to be a special integral curve for the Eq. (1).

Conclusions

The next stages of a consideration of the theme contain the thorough study of the algebraic and common non-algebraic cases including the parametrical integration of the equations. (A. Andreev, I. Andreeva, 2002). This study leads to formulating and proof of attributes of existing of the special solutions (I. Andreeva, 2003).

Recommendations

The article presents a review of data and results, which are insufficiently represented in general educational literature.

Methods of investigation may be useful for applied studies of ordinary differential equations having special solutions.

The paper may be interesting for researchers (A. Andreev, I. Andreeva, 2017) as well as for students and post-graduate students.

Acknowledgements or Notes

The Author expresses a deep gratitude to Professor Dr. Alexey Andreev, the Department of Differential Equations, St. Petersburg State University, for important and useful advice and support.

References

- Andreev, A.F., & Andreeva, I.A. (2002). On a Question of Parametric Integration of Differential Equations. *Vestnik St. Petersburg University: Ser.1. Mathematics, Mechanics, Astronomy*, 4, 3- 10.
- Andreeva, I.A. (2003). *Higher Mathematics. Special Solutions of Differential Equations of the First Order*. St. Petersburg: SPbPU Publishing House.
- Andreev, A.F., & Andreeva, I.A. (2017). Investigation of a Family of Cubic Dynamic Systems. *Vibroengineering Procedia*, 15, 88 – 93. DOI: 10.21595/vp.2017.19389.
- Zalgaller, V.A. (1975). *A Theory of Envelopes*. Moscow: Nauka.

Author Information

Irina Andreeva

Peter the Great St. Petersburg Polytechnic University

195251 St. Petersburg, Polytechnicheskaya, 29.

Russian Federation

Contact e-mail: irandr2@gmail.com

A Literature Survey on Green Supplier Selection

Bahar OZYORUK
Gazi University

Abstract: In today's supply chain, we have to deal with many complex decision problems. Under appropriate circumstances, appropriate decision problems must be solved. In recent years, as in many fields of work, the increase in environmental awareness in the manufacturing sector and the legal obligations imposed have influenced decisions made by many manufacturers. The green strategies dealt with have become a new competitive tool for companies. Firms have been aiming to increase their productivity and profitability with green applications. In this study, the criterias to be considered in choosing the green supplier, which is the most important group of the green supply chain, have been examined and classified. It has been explained how suppliers should improve their working conditions for these criteria that are sensitive to the environment. In which sectors, which green criteria are mentioned in the foreground. It is explained that the obligations of the law regulatory authorities bring to what sectors.

Keywords: Green supplier, Green supply chain

Introduction

The supply chain, starting with goods movement and ending up to the point of consumption, is a network of interconnected and collaborative organizations (Handfield and Ernest, 1999) that controls, manages and develops the flow of materials and information to meet customer expectations. Figure 1 shows this structure.



Figure 1. Structure of the Supply Chain

Supply chain management has been influential in expanding and expanding businesses into new markets. Organizations have come to a stronger position in the market they owned over time. As a result, production and consumption showed a rapid increase. The increase of education and consumption brought many problems together. With the increase in consumption, the wastes generated after use have seriously threatened human health and the ecological balance of the world.

Green Supply Chain

Businesses have developed the concept of "Green Supply Chain Management" by incorporating environmental elements and social responsibility into the classical supply chain management. The organization, procurement,

- This is an Open Access article distributed under the terms of the Creative Commons Attribution-Noncommercial 4.0 Unported License, permitting all non-commercial use, distribution, and reproduction in any medium, provided the original work is properly cited.

- Selection and peer-review under responsibility of the Organizing Committee of the Conference

production and logistics functions are also designed to include environmental awareness (Simpson and Power, 2005). Green supply chain;

- ▶ Addresses the environmentally sensitive approach to products throughout their lifecycle.
- ▶ the product; is the production of the waste by minimizing the harm to the environment after it has been consumed until it is consumed as raw material.
- ▶ Enables production to be achieved by having environmental and quality certificates.

Green supply chain management systems; declining sources of raw materials, waste of landfills, increased environmental pollution such as pollution has become an important competitive factor. (Shang, Lu and Li, 2010). Firms are aiming to increase their productivity and profitability with green applications and they want to minimize the negative effects on the environment and create awareness.

Green Supplier

Businesses are faced with many suppliers that they provide various raw materials and services. Choosing the best suppliers for businesses and the evaluation of these suppliers is as complex as it is important.

Companies have to pay more attention to environmental management because of environmental issues such as global warming. Therefore, in choosing suppliers, they prefer the firm that best matches the environmental goals of the operator, not the supplier that gives the most reasonable price. From this point of view, the evaluation and selection of suppliers in the green supply chain will be differentiated and important. We will try to develop long-term relationships with suppliers. Suppliers, who are the first people in the green supply chain, have quite a big deal.

Green supplier choice approach; monitoring of suppliers based on environmental performance, and cooperation with green suppliers that meet only environmental standards (Arimura et al., 2011).

In the selection of green suppliers, they are detailed with sub criteria based on the main criteria of green design, green production, green image, green storage and environment management system. For example, under the main criteria of green supplier selection, recycled products, reduced use of hazardous materials, and cooperation with customers for economic design can be defined. Sub criteria can be defined within other main criteria.

Green Supplier Selection Literature Survey

In studies of the green supply chain and the green supply chain components, it is clear that the interest in the concept of 'green' is increasing and the environmental elements are added to each of the traditional supply chain components. As a result of the research, the literature on the green supply chain is presented in Table 1.

Table 1. Literature on green supplier selection

RESEARCHERS	YEAR	NAME	DISCUSSED CRITERIA
Joseph Fiksel	1996	Environmental Design: Creating Efficient Products and Processes	Pollution prevention, environmental management, total quality management, design
C.R. Carter ve J.R. Carter	1998	Organizational Determinants of Environmental Procurement: The First Evidence from the Consumer Products Industry	Distribution channels, environmental procurement, structural equality models and supply chain management
Benita M. Beamon	1999	Green Supply Chain Design	Supply chain, logistics, environment, environmental management strategy
F. Boons	2002	Green Products: Framework for Product Chain Management	Material reduction, product substitution, recycling
Devashish Pujari, Gillian Wright, Ken Peattie	2003	Green and Competitive Impact on Environmental New Product Development Performance	Customer satisfaction, product life cycle, post-use application design, senior management support, environmental product policy
Samir K. Srivastava	2007	Green Supply Chain Management: A Literature Review	Design, green production, reverse logistics, energy management, recycling
Sinem Büyüksaatçi	2009	Green Supply Chain Management and an Application	Air pollutant rate, photochemical smoke incident frequency, change in surface water level, algae growth
Jamal Fortes	2009	Green Supply Chain Management: A Literature Review	Green design, recycling, green production, reverse logistics
Deniz Peker	2010	Green Supply Chain Management in Enhancing Environmental Performance	Green procurement, green design, recycling, green distribution, business association
Joseph Sarkis, Qinghua Zhu, Kee-Hung Lai	2010	Organizational Theoretical Review of Green Supply Chain Management Literature	Environmental performance, economic performance, operational performance
Anil S. Dube, Dr.R.R. Gawande	2011	Green Supply Chain Management: A Literature Review	Product life cycle, green design, reverse logistics, green production
Nevzat Korkankorkmaz	2012	A Research on Lean and Green Supply Chain Management	Senior management support, relations with suppliers, relations with customers, lean practices, environmental management system
Esen Andiç, Öznur Yurt, Tunçdan Baltacıoğlu	2012	Green Supply Chains: Potential Applications and Markets Efforts to Turkey	Green supply chains environmental issues, focus groups waste management reverse logistics
Nadine Kafa, Yasmina Hanı, Abederrahman El Mhamedı	2013	Sustainability Performance Measurement for Green Supply Chain Management	Green procurement, green design, green production, green distribution, reverse logistics
Wenge Zhu, Yuanjie Hekristina	2017	Green Product Design in Competitive Supply Chains	Yeşil ürün marjinal maliyeti, yoğun yeşil ürün, yeşil ürün geliştirme, yeşil tedarik zinciri tasarımları
Sarkis, J.	2018	Sustainable green supply chain	Grene product
Nasrollahi	2018	The impact of social media applications on the green supply chain	Structural equation model (206 firms)

Results and Discussion

The ability of the supply chain to demonstrate its expected performance depends on the correct choice of the supplier regarding the supply chain first supplier. It is also valuable to work with environmentalists. In this study, studies carried out in the literature with emphasis on green suppliers are examined. These studies are presented in a table form for review.

Recommendations

In this study, the criteria affecting the selection of green suppliers can be included in the optimization methods so that firms can better manage the decision making process.

Conclusion

In the literature survey, it is observed that in recent years the importance of green procurement selection has increased in the historical development process. Limited resource utilization and environmental practices are expected to be even more dramatic in the coming years

References

- Andiç, E., Yurt, Ö., Baltacıoğlu, T. (2012). Green supply chains: Efforts and potential applications for the Turkish market. *Resources, Conservation and Recycling*, 58, 50– 68.
- Arimura, T. H., Darnall, N. and Katayama, H. (2011). Is ISO14001 a gateway to more advanced voluntary action? The case of green supply chain management. *Journal of Environmental Economics and Management*, 61, 170-182.
- Beamon, B. (1999). Designing the green supply chain. *Logistics Information Management*, 4(12), 332-342.
- Büyüksaatçi, S. (2009). Yeşil Tedarik Zinciri Yönetimi ve Bir Uygulama, Yüksek Lisans Tezi, İstanbul Üniversitesi Fen Bilimleri Enstitüsü Endüstri Mühendisliği Anabilim Dalı, İstanbul.
- Carter, C. R. and Carter, J. R. (1998). Interorganizational determinants of environmental purchasing: Initial evidence from the consumer products industries. *Decision Sciences*, 29(3), 659-684.
- Dube A., Gawande, Dr. R. R. (2011). Green supply chain management – A literature review. *International Journal of Computer Applications*, 0975 – 8887.
- Fiksel, J. (1996). *Design for environment: Creating ecoefficient products and processes*. NewYork: McGraw-Hill.
- Fortes, J. (2009). Green supply chain management: A literature review. *Otago Management Graduate Review*, 7, 51-62.
- Handfield, R., Ernest, L., Nichols, Jr. (1999). *Introduction to supply chain management*. NewJersey: Prentice Hall.
- Kafa, N., Hanı, Y., El Mhamedı A. (2013). Sustainability performance measurement for green supply chain management. 6th IFAC Conference on Management and Control of Production and Logistics The International Federation of Automatic Control. Center for Information Tecnology Renato Archer , Fortaleza, Brazil.
- Korkankorkmaz, N. (2012). Yalın ve Yeşil Tedarik Zinciri Yönetimine İlişkin Bir Araştırma, Yayımlanmamış Yüksek Lisans Tezi, Gebze Yüksek Teknoloji Enstitüsü, Kocaeli.
- Mahdi Nasrollahi (2018)The Impact of Firm's Social Media Applications on Green Supply Chain management
- Peker, D. (2010) Çevresel Performansın Geliştirilmesinde Yeşil Tedarik Zinciri Yönetimi, Yüksek Lisans Tezi, Uludağ Üniversitesi Sosyal Bilimler Enstitüsü İşletme Anabilim Dalı Üretim Yönetimi ve Pazarlama Bilim Dalı, Bursa.
- Pujari, D., Wright, G., Peattie, K. (2003). Green and competitive influences environmental newproduct development performance. *Journal of Business Research*, 56, 657– 671.
- Sarkis, J. (2017). Greener manufacturing and operations: From design to delivery and back, *International Journal of Operations & Production Management* 25 (5), 449-468
- Sarkis, J., Zhu, Q., Lai, K. (2010). An organizational theoretic review of green supply chain management literature. *International Journal of Production Economic* ,130, 1-15
- Shang, K., Lu, C., Li, S. (2010). Ataxonomy of green supply chainmanagement capability among electronics-related manufacturing firms in Taiwan. *Journal of Environmental Management*, 91, 1218-1226.

- Srivastava, S. K. (2007). Green supply-chain management: A state-of-the-art literature review. *International Journal of Management Reviews*, 9(1), 53-80..
- Zhu, Q., Sarkis, J., and Lai, K. (2008). Green supply chain management implications for closingthe loop. *Transportaion Research*, 1-18.
- Zhu, W., He Y. (2017). Green product design in supply chains under competition. *European Journal of operational Research*, 258, 165–180.
- Wu, C., Barnes, D., (2016). An integrated model for green partner selection and supply chain construction. *Journal of Cleaner Production*, 112(3), 2114–218

Author Information

Bahar Özyörük

Gazi University Faculty of Engineering, Eti Mh. Yükseliş
Sk. No: 5, Maltepe / Ankara, Turkey
Contact e-mail: bahar@gazi.edu.tr

Development of A Diagnostic Expert System (FDD-Expert) for Woven Fabric Defects

Berkay BARIS

Kırklareli University

E.Serdar GUNER

Kırklareli University

H.Ziya OZEK

Namik Kemal University

Abstract: A variety of computer aided techniques have been proposed to help solving diagnostic problems in different disciplines. Commonly known as expert systems, approaches, undertaking distinct formalisms for modelling domain knowledge, include: rule-based and frame-based systems or semantic and neural networks. Explanatory mechanisms are more easily implemented with rule-based systems and graphical models making these preferred solutions to the diagnostic problem. Since the pioneering work by Feigenbaum (DENDRAL, 1971) theory and utility of expert systems have progressively evolved, and accompanied by the appearance of various expert systems development tools. In textile industry, expert systems are generally used to increase production, improve quality and reduce costs. This paper describes Fabric Defect Diagnosing System (FDD-EXPERT), an expert system in the domain of fabric defects. Fabric defect is known as an undesirable fault in the fabric which deteriorates the quality fabric and makes it inferior. FDD-EXPERT contains 173 different defects based on TS471 ISO8498 Woven Fabric Description of defects with additional 47 defects. Defects depicted in this domain are classified based upon their similarity of appearance, multiple attributes relevant to effect upon visual quality and sources of defects. Possible reasons for each defect and remedial solutions are also included. A rule-based knowledge domain and inference engine is generated in PROLOG. User friendly interface of the system is developed through Visual Basic (VB.Net). It is a combination of logic and declarative programming. This diagnostic system may be utilised as problem solving and training tool by novice operators or as a supplementary knowledge for expert operators.

Keywords: Fabric defect, Diagnostic expert system, Prolog

Introduction

Expert systems have found broad acceptance in various technical, medical and social disciplines over the decades. They may be used in a wide area of applications to solve problems related to: Analyzing, Classification and Interpreting; Diagnosing and Debugging; Monitoring and Control; Design, Planning and Prediction; and Training and Instruction. Practical expert systems within each of these application areas do exist (Frenzel, 1988). An expert system is a knowledge-based system emulating expert thought to solve significant problems in a particular domain of expertise. It is a computer program which uses explicitly represented knowledge and computational inference techniques to imitate a human expert in a specific domain (Grimson and Patil, 1987).. Therefore, expert systems usually have two major components: a knowledge base and an inference strategy. The knowledge base incorporates a collection of facts and rules.

Failure diagnosis has become increasingly important for industrial automation and a variety of fault / defect detection. Therefore various diagnosis techniques have been developed for the diagnostic problem in technical

processes. These techniques include model-based approaches, knowledge based approaches, qualitative simulation based approaches, neural network based approaches and classical multivariate statistical techniques..

In this paper, an expert system has been developed for diagnosing woven fabric defects. In general, textile materials are highly varied by nature, and the effect of variation or unevenness is likely to generate some faults or defects in manufacturing process. Consequently, occurrence of defects resulting from hundreds of different reasons are inevitable. The identification of a wide range of defects and solutions to eliminate them is very important as it directly relates to productivity and quality. The use of expert knowledge in this area for an expert system has been the focus of this work.

Review of Expert Systems for Fault Diagnoses

In the late 1960's to early 1970's, expert systems began to emerge as a branch of Artificial Intelligence. Domain specific knowledge was used as a basis for the development of the first intelligent systems in various domain. One of the best references for all the early systems was published Feigenbaum (1981). In the 1980's, expert systems emerged from the laboratories and developed commercial applications due to the powerful new software for expert systems development as well as the new possibilities of hardware . During the period 1985-1995 expert systems were very much popular topic in artificial intelligence developments due to the attention in knowledge management issue (Angeli, 2010). After 1995 expert system applications appeared to decline as stand-alone systems and their technology embedded in mainstream of information technology. New expert systems was set to combine symbolic with numerical information or with other artificial intelligence techniques to produce more effective systems.

The Expert System is one of the well-known reasoning techniques that is utilized in diagnosis applications domain. According to an MIT report by Scherer and White (1989), the first diagnostic expert systems for technical fault diagnosis were developed in the early 1970's. Since then numerous systems have been built. Several researchers combine numerical with qualitative methods the last few years and various methodologies have been proposed for the combination of knowledge-based techniques. Surveys of early diagnostic expert systems for technical processes were provided by Tzafestas (1986) and Scherer and White (1989) and by Liao (2005). Early diagnostic expert systems were rule based and used empirical reasoning whereas new model based expert systems use functional reasoning. The utilization of Expert systems for the supervisory systems used in the automatic control of the industrial processes are reviewed by Alexandra (1998). Some concepts related to the problem of supervision and diagnosis, as well as the functions and principles associated are also presented.

Diagnostic expert systems have also found application in network conditions. Web-based expert systems are based on traditional expert systems technology, rule-based and case based reasoning primarily (Kumar & Mishra, 2010). They incorporate client-server architectures and web browser-based interfaces (Grove 2000; Duan et al 2005).

The application of expert system in the field of textiles is also common to take advantage of knowledge-based computer programs in order to solve diversified and complicated problems based on human expertise. Development of expert systems in textile industry is focused on to increase production, improve quality and reduce costs. The common application purposes of the expert systems are:

- design or configuration of a textile product and clothing or a process
- diagnosing fabric, garment, machine or process faults
- quality detection in various processes

Examples of early expert systems which were developed for applications in the textile industry cover various operations such as diagnosing defects in the bleaching of cotton fabrics (Günther, 1989), predicting a wool dyeing recipe (Frei & Walliser, 1989 – 1991), finishing (Texperto) (Frei and Poppenwimmer 1992), pad-steam dyeing (Bafarex) (Lange et al, 1992), the colour matching process (Smart-Match) (Karamantscheva 1994; Datacolor International 1997), controlling the dyeing process (Viviani 1996).

An intelligent diagnosis system capable of tracing possible breakdown causes of fabric defects is applied to fabric inspection processing by Lin and his colleagues (1995). In addition to the basic expert system, a diagnosis system developed using fuzzy set theory was also integrated. The system, using the Turbo C program, can act as an expert consultant for operators tracing the causes of breakdowns at any time, and the expert system, developed in an artificial intelligence language PROLOG, can provide the operator with a knowledge

base for further consultation in fabric inspection. It was reported that, thanks to intelligent diagnosis system, even a new operator lacking expertise or skill in the weaving engineering field can still easily determine causes of fabric defects in a fraction of a second and then eliminate them. The results of experiments on various diagnostic cases was proved to be satisfactory by performance. This system was further developed by Lin (2009) by using a search mechanism based on genetic algorithm which can help find the correct solution (i.e., upper boundaries and lower ones) to the inverse fuzzy equation.

Dlodlo and colleagues (2007) developed a hybrid expert system architecture to support yarn fault diagnosis. The system has used a combination of rule-based and case-based techniques to achieve the diagnosis. Chung-Feng and his colleagues (2014) published a work on diagnosing single or double fault conditions of significant process parameters based on the spinline tension signal in meltspinning process.

A review of applications of expert systems into various areas of coloration and textile industry has been presented by Goodarz and his colleagues (2010). Shim (2009) has developed a knowledge-based diagnostic expert system to troubleshoot issues in the coloration of polyester materials as the most widely used synthetic fibre. The study was accomplished in four stages: selection of a suitable ES development tool, knowledge acquisition, design and development of appropriate modules and finally testing and evaluation of the system. An expert system for troubleshooting of faults encountered in ink jet printing of cotton substrates is developed by Kalav (2012). An analysis and selection of the most encountered faults in ink jet printing, the processes, which start with cotton production and end at fixation, are examined. Thirteen symptoms are selected as the most encountered problems in ink jet printing of cotton substrates. In addition, sixty-one causes are suggested as the possible causes of thirteen symptoms. The system is reported as a useful tool for troubleshooting of ink jet printing of the cotton substrates.

A hybrid intelligent classification model as a size recommendation expert system is proposed in a recent work Shahrabi, Hadavandi and Salehi (2013). Three stages for developing a hybrid intelligent classification system based on data clustering and probabilistic neural network (PNN) are proposed. In the first stage, the clustering algorithm is used for specifying the sizing chart. In the second, the resulting sizing chart is used as a reference for developing a new intelligent classification system by using a PNN and the accuracy of the proposed model is evaluated by using the Iranian male's body type data set at the last stage. It is proved that experimental results show that the proposed model has a good accuracy and can be used as a size recommendation expert system to specify the right size for the customers.

A Case-Based Reasoning method was proposed in a recent study (Perez, et al. 2017) to complement the results of the finite element simulation, mathematical modelling and neural networks methods. The analysis of textile designs or structures includes the use of mathematical models to simulate the behaviour of the textile structures (yarns and fabrics). The Finite Element Method has largely facilitated the prediction of the behaviour of that textile structure under mechanical loads. Artificial Neural Networks for classification problems is claimed to be a very effective tool as a quick and accurate solution.

A recent work (Sawatwarakul, Joines, and Shamey, 2015) introduces the design and development of a diagnostic expert system for the dyeing of protein fibres. The system is designed to aid in the identification of root causes of problems with a view to enabling users to arrive quickly at remedial solutions. The performance of the system was reported as highly satisfactory. This diagnostic system is proposed to teach students and to be utilised by novice colourists as a problem-solving tool, and also to be employed as a supplementary knowledge resource by seasoned dyers.

Expert System Structure

The Expert System is a knowledge-based system that consists of two main modules: the knowledge base and the inference engine. It is an intelligent computer program that uses knowledge and inference procedures to solve problems that are difficult enough to require significant human expertise for their solution. Expert systems usually have a knowledge acquisition module and an explanation module as extra components. A typical expert system for fault recognition is shown in Figure 1.

A typical Expert System consists of three components: an inference engine, a knowledge base and a working memory. Declarative descriptions of expert-level information, necessary for problem solving, are stored in the knowledge base. The inference engine solves a problem by interpreting the domain knowledge stored in the knowledge base (Nabiyev, 2002). The inference engine also records the facts about the current problem in a

special purpose workspace, called working memory. The working memory may also include modules for a natural language communication with the user, a reasoning explanation interface as well as an automated knowledge acquisition tool.

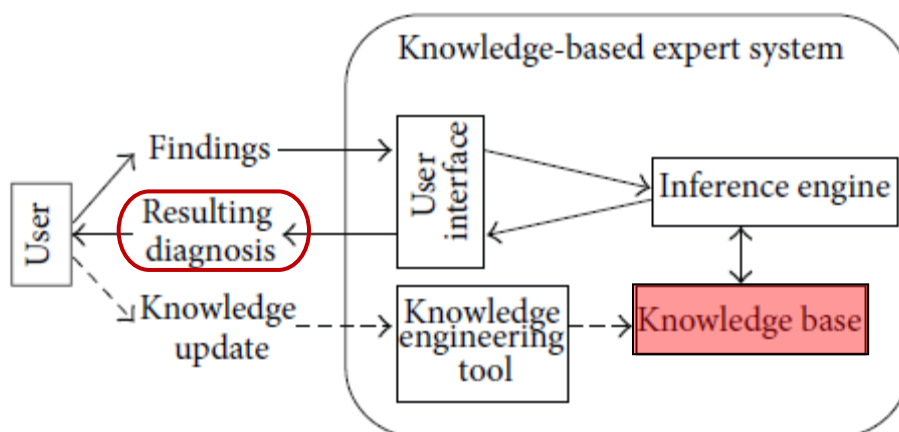


Figure 1. Basic structure and components of a diagnostic expert system

Expert systems approach undertaking distinct formalisms for modelling domain knowledge which includes rule-based and frame-based systems or semantic and neural networks. Rule-based programming is one of the most commonly used techniques for developing expert systems. A rule-based expert system consists of a set of rules that can be repeatedly applied to a collection of facts (Soe & Paing, 2008). The following concepts are essential to rule-based systems:

- Facts represent circumstances that describe a certain situation in the real world.
- Rules represent heuristics that define a set of actions to be executed in a given situation.

There is a basic distinction between derivations and production rules. Derivation rules have the form if <condition> then <conclusion>, whereas production rules conclusion, in derivation rules, is abstract: it consists of deriving logical consequences from certain conditions.

Explanatory mechanisms are more easily implemented with rule-based systems and graphical models making these preferred solutions to the diagnostic problem

Defects in Woven Fabrics

Textile manufacturing operations involve a series of processes towards to converting textile fibres into yarn, fabric, finished fabric and clothing. In consideration of huge variation in physical properties of textile fibres, especially natural fibres, textile materials are likely to display various distinctions. The degree of variation is also increased by the nature of converting processes. This is one of the dominant reasons for occurrence of defects in textiles.

In general, defect is defined as an imperfection that impairs worth or utility. It may be absence of something necessary for completeness or perfection or a non conformity. ISO/IEC 9126 distinguishes between a “defect” and a “nonconformity”, a defect being the nonfulfillment of intended usage requirements, whereas a nonconformity is the nonfulfillment of a requirement. In a product more than one defect may be present and a relatively small number of minor defect may be acceptable to the customer.

Woven fabrics are produced by interlacing of two sets of straight yarns by means of weaving technique. The weaving technique is the intersection of warp and weft yarns which cross and interlace at right angles to each other in accordance with a given pattern. The lengthwise yarns are known as warp yarns and width wise yarns are known as weft or filling yarns and the fabric produced is known as woven fabric. A number of faults are likely to occur in fabric during the course of weaving process.

A Fabric defect is any abnormality in the fabric that hinders its acceptability by the consumer. Fabric faults or defects, are responsible for considerable amount of defects found by the garment industry. An automated defect detection and identification system enhances the product quality and results in improved productivity to meet both customer demands and to reduce the costs associated with off quality. This fact makes the identification

and remedy of defects in fabric manufacturing very critical issue. . Due to the increasing demand for quality fabrics in global competition , high quality requirements are today greater since customer has become more aware of poor quality problems. To avoid rejection of fabric, it is necessary to avoid defects otherwise, price of fabric is likely to be reduced by 45%-65% due to the presence of a number of defects. This fact is one of the driving factors of development of an expert system for defect diagnosis.

Several characteristics of woven fabrics are determined by the raw materials used, manufacturing technique employed, constructional parameters selected and finishing sequence adopted. However, variation in raw materials or lack of control over pre-treatment processes and application of in appropriate wet processing technology leads to the development of defects in finished fabrics. Fabric defect is a fault or lack that spoils the effective use of fabric.

There are different kind of fabric defects as many as 173 . The causes of each defect may be different or similar factors which are apparent at different departments or stages of the entire manufacturing process i.e. from spinning, winding and warping, sizing and others. The quality of the fabric at a weaving loom is determined by the entire sequences of operations from weaving preparatory to weaving. In case of a finished fabric, source of faults are also due to inappropriate setting or parameters in operations of pre-treatments, dyeing, printing and finishing

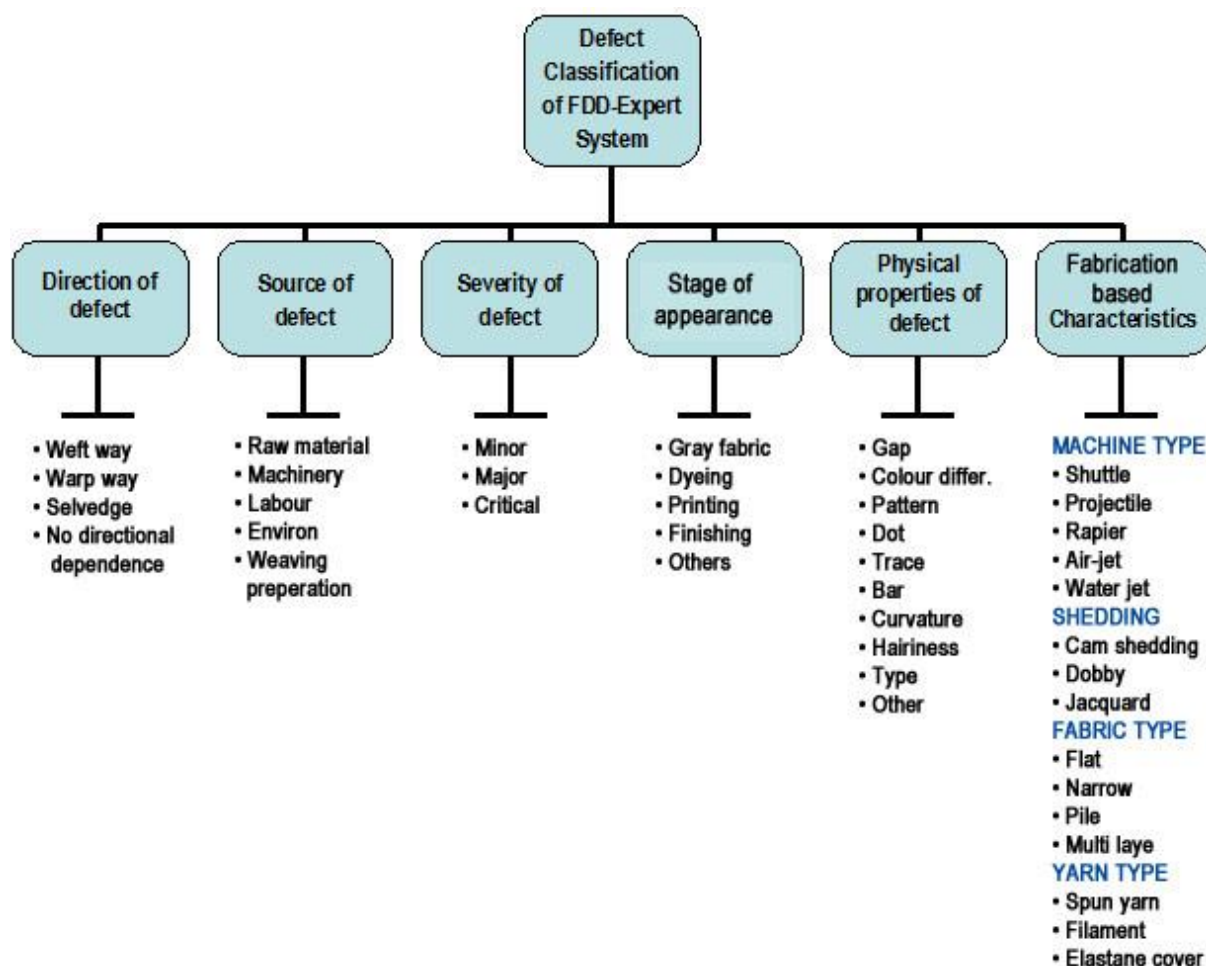


Figure 2. The list of attributes assigned to characterise woven fabric defects

Therefore, an appropriate classification system of defects considering each process in relation to the manner in it affects the subsequent process, should be developed. Woven fabric defects are identified to characterise several aspects with relevant attribute values. The characteristics for distingusiing defects are given as follows:

- The direction of defect
- The source of defect
- The severity (impact) of defect
- The stage of appearance

- Physical properties of defect
- Fabrication based characteristics
- Dimensions of defect

Defects are classified in accordance with attributes assigned to each characteristic class. The list of defect classification for the FDD-Expert is given in Fig.2.

Development of the FDD-Expert System

The development phases of the expert system is given in Fig. 3. The expert system is called as FDD-Expert to denote Fabric Defect Detection. The requirements of the system are:

- to define and explain possible woven fabric faults
- to reach defects by the standard defect names as well alternative names used in industry
- to make clear distinctions between all defects
- to enable user to diagnose the causes of any defect
- user friendly
- accessible defect picture archive
- tracing forward and backward between the source of fault and defect
- systematic list of solutions for remedial actions
- search engine for faults

FDD-Expert system is structured to accomplish all the requirements with a rich archives of default photographs. The expert system developed in this study is in a rule-based structure. The rule base of the system was extracted by employing the Formal Concept Analysis (Ganter and Wille, 1999) method. The first step of this method is determining the formal objects and the attributes associated with these formal objects. In the second step, the formal objects are clustered using their largest common attribute sets. The clusters that emerge in this way are called "formal concepts". A formal concept represents a set of objects with certain common characteristics in a specific domain.

In order to apply the Formal Concept Analysis method on the fabric faults domain, first the defects and their descriptive characteristics are represented in a structured way on a table. In this table each fabric defect is specified by its visual cues which are the formal attributes for this domain. In the next stage, the Formal Concept Analysis algorithm was applied to reveal the clusters of fabric faults, which are the formal concepts. The structure of relationship is given in Fig.4. In this study, a parallel and recursive algorithm in the FCALGS library (Krajca et al., 2008) was used for applying Formal Concept Analysis.

The most important advantage of using Formal Concept Analysis on this expert system is that fabric defects with common features can be easily grouped and presented to the user, without the obligation of providing all properties of a specific fabric defect. Formal concepts revealed by using fabric defects and their visual characteristics are automatically converted into Prolog syntax. Prolog is a general purpose logic programming language and is especially used in artificial intelligence programming. In Prolog, as a declarative programming language, program structures are coded as facts and rules in the knowledge base. Automatic deductions can be extracted through this knowledge base by a logic interpreter. Allowing automatic logical deductions from facts and rules, Prolog provides an elegant way of developing expert systems.

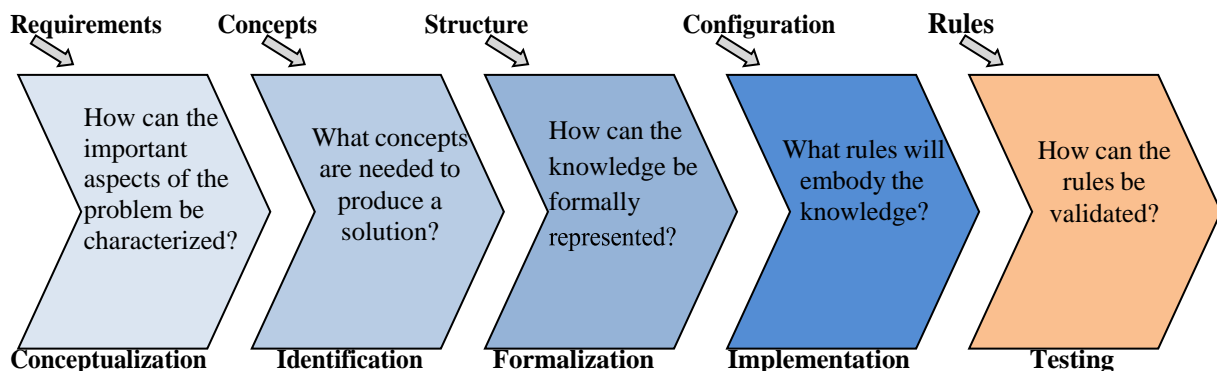


Figure 3. Development phases for expert system building

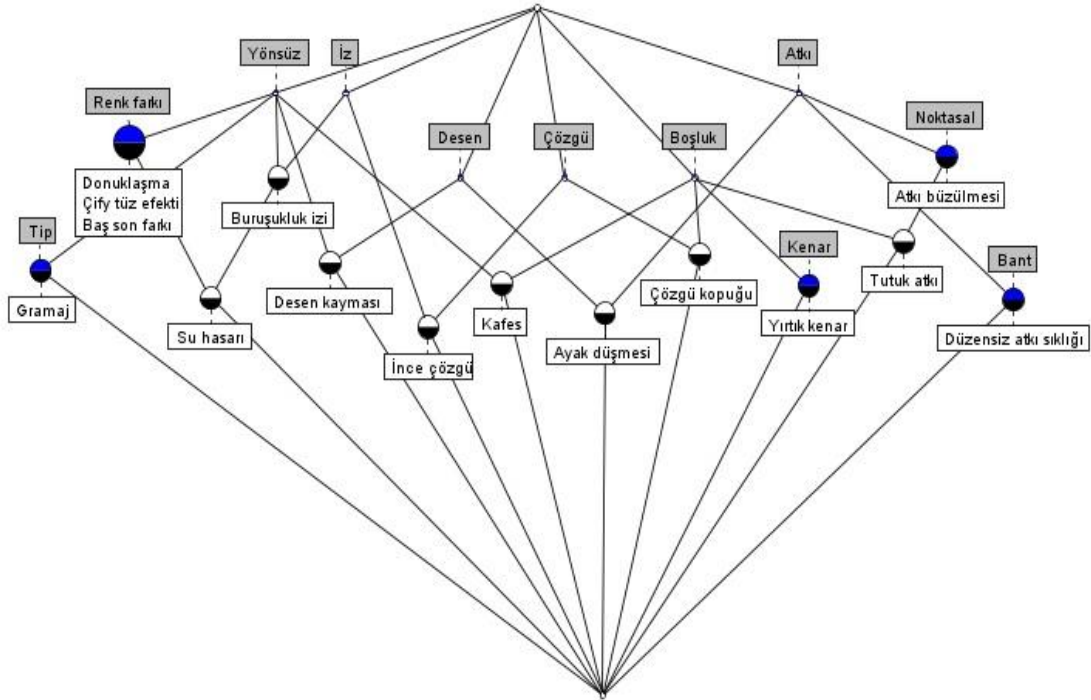


Figure 4. Conexp lattice relationship diagram for Formal Concept Analysis of defects and their attributes

For the domain at hand, the concepts extracted by using the Formal Concept Analysis are converted to Prolog syntax by coding both the fabric fault clusters and their attributes as list structures in the form of facts. In order to implement this rule-based programming infrastructure, SWI-Prolog (Wielemaker et al., 2012), which is an open source Prolog distribution, was used in this study. The modules that constitute the background part of the expert system have been made user-friendly by developing a screen to allow the user for selecting the visual cues for fabric faults. The user is able to see both the possible causes of a defect and solutions for remedy on the same screen, by simply selecting the visually identified cues.

Analysis and Findings

According to the proposed framework, the defects of woven fabrics are classified in terms of characteristics. The interface of expert system with dialogue panels makes the search and diagnosing process easier and quicker. The opening scree of the system is given in Fig. 5. User is expected to select or mark apparent characteristics of any defect on the basis of attribute values. There are six groups of characteristics to enable the user to outline any defect. These defect attributes or cues are basic and simple criteria to prevent any subjectivity.

The development of the defect database are carried out in collaboration with 5 large scale weaving mill. Their expertise knowledge on defining faults and finding appropriate solution are separately collected and integrated into the database.

The FDD expert system is capable of tracing the defect even with one characteristic. But the more attributes selected, the quicker the diagnosing of defects. The first characteristic to be marked is likely to be the direction of the defect. This selection brings the list of all relevant defects. Then selection of a characteristic for physical appearance of the defect shortens the list with defects having two common characteristics. The selection of fabrication based characteristics such as the machine type, yarn type or fabric type appear to enhance the diagnosing ability of the system. User may select any defect from the list of possible defects, to see specific causes for that particular defect as seen in Fig.6. In order to see the possible ways of eliminating or remedying the source of defect, that specific cause has to be marked. It is also possible to use a search engine to reach any defect in the database.

Berkay Barış - Tez Proje

Hatanın Yönü

Atkı

Çözgü

Kenar

Rasgele

Hatanın

Boşluk

Renk Farkı

Desen

Noktasal

İz

Bant

Tip

Eğrilik

Türlenme

Diğer

Hatanın Belirdiği

Ham Kumaş

Boyama

Baskı

Diğer İşlem

Dokuma Makinesi

Mekikli

Mekikçili

Kancalı

Hava Jetli

Su Jetli

Kamlı

Armürlü

Jakarlı

Kumaş Türü

Standart

Dar Dokuma

İlmekli

İnlük Türü

Kesik Elyaf

Filament

Elastanlı

Fantezi

Seçili Özelliklerden Hatayı Bul

Arama:

İçeren hataları getir

Olası Hatalar

Seçilen Hatanın Açıklaması

Seçilen Hata İçin Alternatif Adlar

ISO Kodu:

Şiddet:

Seçilen Hatanın Resmi

Nedenleri dokuma makinesi tipine göre kısıtla

Seçilen Hata İçin Olası Nedenler

Seçilen Neden İçin Çözüm Yolu

Bu sebepten kaynaklanan diğer hataları gör

Figure 5. Opening screen picture of the FDD expert system

Berkay Barış - Tez Proje

Hatanın Yönü

Atkı

Çözgü

Kenar

Rasgele

Hatanın

Boşluk

Renk Farkı

Desen

Noktasal

İz

Bant

Tip

Eğrilik

Türlenme

Diğer

Hatanın Belirdiği

Ham Kumaş

Boyama

Dokuma Makinesi

Mekikli

Mekikçili

Kumaş Türü

Standart

Dar Dokuma

İnlük Türü

Kesik Elyaf

Filament

Elastanlı

Fantezi

Seçili Özelliklerden Hatayı Bul

Arama:

İçeren hataları getir

Nedenleri dokuma makinesi tipine göre kısıtla

Olası Hatalar

- Yay atkı - Gıf yay atkı
- Atkı eğriliği
- Kalın yer - İnce yer
- Atkı bandı
- Duruş izi, başlangıç yeri
- Koyu renk, makine duması
- Asılı atkı**
- Atkıda tarak kesigi
- Syrılmış atkı
- Kopuk atkı, düşük atkı
- Eksik atkı
- Atkı büzülmesi
- İlmeklenmiş atkı
- Kanşık atkı
- Atkı abrası

Seçilen Hatanın Açıklaması

Kumaş yüzeyinde çok sayıda atkı ilmeği bulunması veya iplik kopuğunun olmadığı küçük bir üçgen şekilde açıklık bulunması.

Seçilen Hata İçin Alternatif Adlar

Tutuk atkı

ISO Kodu:

Şiddet:

Seçilen Hatanın Resmi

Nedenleri dokuma makinesi tipine göre kısıtla

Seçilen Hata İçin Olası Nedenler

Tefe vuruşu esnasındaki bir bekleme anında belirgin bir çözgü düğümüne veya kumaş yüzeyindeki bir

Seçilen Neden İçin Çözüm Yolu

İlgili işlemin talimatnamesi gözden geçirilmelidir ve dokumacılar uyarılmalıdır, gerekirse düğüm atma eğitimi verilmelidir.

Bu sebepten kaynaklanan diğer hataları gör

Figure 6. The list of defects relevant to weft way direction and causes and solution for a specific defect

The quality inspection operators and department managers of the five weaving mill are asked to test the FDD expert. They have used the system for diagnosing certain defects and defects specific to their mill. The majority of 177 defects have been tested. The performance of the expert system on the basis of user friendliness, correctness of the knowledge, accessibility to the root causes and remedial solution was found satisfactory.

419

Conclusion

This study was focused on development of an expert system for diagnosing defects based on a systematic defect classification. The systematic classification of defects on the base of various characteristics has been one of the important outputs of the work. On may say that it is the most important stage to develop a reliable database. The potential sources of faults and possible solutions to eliminate that fault and the resultant defect are also included in the database under systematic and standard headings. The expected impact of this database is to offer a standard terminology and a systematic fault tracing methodology for industrial users. The trials with the developed expert system proved that the expert system Works efficiently and a useful detect diagnosis and remedy tool in case of rarely seen defects. It is also found useful for training of fabric inspection operators as well as weaving loom fixers.

Acknowledgements

The authors are grateful for the financial support of the Scientific and Technological. Research Council of Turkey (TÜBİTAK) ARDEB under the project grant No:116M064.

References

- Alexandra, A A (1998) Using Expert Systems for Fault Detection and Diagnosis in Industrial Applications, Technology Showcase: JOAP International Condition Monitoring Conference, Mobile, Alabama, USA.
- Angeli, C. (2010) Diagnostic Expert Systems: From Expert's Knowledge to Real-Time Systems Ch. 4 of Advanced Knowledge Based Systems: Model, Applications & Research (Eds. Sajja & Akerkar), Vol. 1, pp 50 – 73.
- Chung-Feng J K, Chang-Chiun, H, Tzen-Chin G, Chien-Chun L and Tsann-Tay T, (2014). Recognition of fault process conditions based on spinline tension in melt spinning, Textile Research Journal, 2014, Vol. 84(14) pp.1549–1557
- Datacolor International (1997). Tintoria, 11 (1997) 89.
- Duan, Y, Edwards, J. S. & Xu, M. X. (2005). Web-based expert systems: benefits & challenges. Elsevier, Information & Management 42, pp. 799–811.
- Dlodlo, N, Hunter, L, Cele, C, Metelerkamp, R, Botha, A F (2007). A Hybrid Expert Systems Architecture for Yarn Fault Diagnosis, Fibres & Textiles in Eastern Europe April / June 2007, Vol. 15, No. 2 (61)
- Fan, J, Hunter L, (1998), A worsted fabric expert system, Part I: System development. Text. Res. J. 68:9(1998), pp. 680-686.
- Feigenbaum, E. (1981). *Handbook of Artificial Intelligence*: Heuris Tech Press, W. Kaufman Inc.
- Fiber Organon (2012) (online: <http://www.fibersource.com/feb/feb3c.htm>; Access: March 2018.
- Frei G and Walliser R (1989), Textilia, 65 pp.20.
- Frei G and Walliser R (1991). J.of Society of Dyers and Colorist, 107 pp.147–149.
- Frei G and Poppenwimmer K, (1992), Textilveredlung, 27 (1992) pp.276.
- Frenzel, L E, (1988) "Understanding Expert Systems", Howard W. Sams and Company, Indianapolis.
- Ganter, B., & Wille, R. (1999). Formal Concept Analysis. Mathematical Foundations. Berlin: Springer.
- Goodarz, M, Tehran, A, Malek, R M, Mazaheri, F M (2010). Review of Expert Systems in the Coloration and Textile Industry, Journal of Color Sci. Tech. of the Institute for Color Science and Technology. 4 (2010), pp. 41-53.
- Grimson, E.L. and Patil, R.S. (1987) *AI in the 1980s and Beyond*, MIT Press, Cambridge, MA.
- Grove, R. F. (2000). Internet-based expert systems. Expert Systems 17, pp. 129–136.
- Günther R, (1989). L'Ind. Text., 1197 (1989) 78.
- Kalav, B. (2012), Pamuklu Kumaşların İnk Jet Baskısında Bilgi Tabanlı Uzman Sistem Kullanarak Problem Belirleme Ve Giderme, Ph.D Thesis, İTÜ Fen Bilimleri Enst. İstanbul.
- Karamantscheva I (1994). Textilveredlung, 29 pp.29.
- Krajca, P., Outrata, J., & Vychodil, V. (2008). Parallel recursive algorithm for FCA. In CLA (Vol. 2008, pp. 71-82).
- Kumar, S and Mishra R B (2010). Web-based expert systems and services, The Knowledge Engineering Review, Vol. 25:2, 167–198. & Cambridge University Press.
- Lange A, Nahr U and Schurmann K (1992), Textilveredlung, 27 pp.268.
- Liao, S. H. (2005) Expert system methodologies and applications – a decade review from 1995 to 2004, Expert Systems with Applications, 28, pp. 93–103.
- Lin, J-J, Lin, C-H and Tsai I S, (1995). Applying Expert System and Fuzzy Logic to an Intelligent

- Diagnosis System for Fabric Inspection, Textile Research Journal Vol 65 (12) pp. 697–709.
- Lin, J-J, (2009). A Genetic Algorithm-based Solution Search to Fuzzy Logical Inference for Breakdown Causes in Fabric Inspection, Textile Research Journal Vol 79(5):pp. 394–409
- Nabiyev, V. 2012. Yapay Zeka, (4.Baskı) Ankara, Seçkin Yayıncılık.
- Pérez, J P, Arrieta, A G, Encinas, A H and Queiruga-Dios, A (2017), Manufacturing processes in the textile industry. Expert Systems for fabrics production, ADCAIJ: Advances in Distributed Computing and Artificial Intelligence Journal Regular Issue, Vol. 6 (1), pp. 41-50.
- Sawatwarakul, W, Joines, J and Shamey, R (2015), A diagnostic expert system for the dyeing of protein fibres, Society of Dyers and Colourists, Coloration Technology, 131, pp.389–395.
- Schere, W. and White, C. 1989. A Survey of Expert Systems for Equipment Maintenance and Diagnostics. In Knowledge-based system Diagnosis, Supervision, and Control ed. Tzafestas, S. Plenum Publishing Inc.
- Shahrabi J, Hadavandi E, Salehi E M (2013) "Developing a hybrid intelligent model for constructing a size recommendation expert system in textile industries", International Journal of Clothing Science and Technology, Vol. 25 Issue: 5, pp.338-349.
- Shamey R and Sawatwarakul W (2014), Text. Progress, 46 (2014) 323.
- Sawatwarakul W, (2014) A diagnostic expert system for the dyeing of protein fibers. PhD Dissertation (Raleigh, NC: North Carolina State University.
- Shim, W S (2009). A diagnostic expert system for the coloration of polyester materials. PhD Dissertation, North Carolina State University, Fiber and Polymer Science Raleigh, North Carolina, USA.
- Soe, S M M and Paing, M P, (2008) Design and Implementation of Rule-based Expert System for Fault Management, World Academy of Science, Engineering and Technology 24 2008 pp.34-40.
- Tzafestas, S.G. (1986) Knowledge engineering approach to system modelling, diagnosis, supervision and control, Proceedings of the IFAC Symposium on Simulation of Control Systems, I. Troch, P. Kopacek and F. Breiteneker (eds), Oxford: Pergamon, pp.15–22.
- Viviani F, (1996). Riv. Tecnol. Tessil., 5 p.138.
- Watkins P, (1992) Luxury Fibres: Rare Materials for Higher Added Value (London/New York: Economist Intelligence Unit.
- Wielemaker, J., Schrijvers, T., Triska, M., & Lager, T. (2012). Swi-prolog. *Theory and Practice of Logic Programming*, 12(1-2), 67-96.

Author Information

Berkay Baris

Kırklareli University
Lüleburgaz Vocational High School Keprtepe Mevkii
Lüleburgaz, Kırklareli

E.Serdar Guner

Kırklareli University
Faculty of Engineering, Dept. Of Software Engineering
Yazılım Mühendisliği Bölümü, Kayalı Yerleşkesi, Kırklareli

H.Ziya Ozek

Namik Kemal University
Corlu Faculty of Engineering, Dept. of Textiles Engineering
Corlu Tekirdag
Contact e-mail: zozek@nku.edu.tr

Lean Innovation Approach in Industry 5.0

Banu OZKESER

Koluman Otomotiv Endüstri A.Ş.

Abstract: It's no doubt that industry 4.0 takes a big part in our daily lives. Mobile phones, touch pad, flipped classrooms can be important examples of how we use the digital life. However, in the near future not only the knowledge and digital life but also robots behaving like a human will cover a huge time. Since, people start to get in collaboration with industry 4.0. In other words, this means that industry 5.0 is coming. Within this fact, keeping innovation in a lean form gets more importance. Complex projects make the innovation be far and far away. Thus, lean approach in innovation management makes the applications of industry 5.0 be smooth. Value management is a good solution as a method in this approach. In this paper, r&d projects' processes in industry 5.0. platform are taken into account with lean innovation approach. Therefore, the sub-processes, which do not carry value into the product, are eliminated. Simplicity is based in the lean innovation logic. Hence, every step should be thought as a bridge whether gaining value or not.

Keywords: Industry 5.0., Innovation, Lean approach, Value management, Collaboration

Introduction

Most of the companies are aware of the valuable synergies by getting together lean management approach and industry 4.0. This double interaction, which is called lean industry 4.0., starts to leave its place to the lean industry 5.0 as the time passes. Since, the man meets machine in this new world.

The usage of robotics in production has been rising since the 1960s, while they were first introduced as a part of Industry 3.0. Robots grew up especially in the automotive field in which they were used primarily for welding processes so as to get the bodies together. As demands matured, robots started seeing use in other different fields, like logistics, medicine and food industries. Additionally, 2006 was the first year when more robots were used outside the automotive industry than inside. Nowadays, robots are used not only in huge facilities, but also more affordable and easy-to-use collaborative robots – in small and medium-sized businesses.

The advantages of robotic automation consists of the following;

- a) Robots develop the consistency of service/product quality and manufacturing line flow, corresponding the demand for high-quality outputs at lower cost
- b) They present to save workers from having dangerous tasks at work
- c) Robots have the capability of generating data on process quality to optimize both a company and production processes
- d) Because robots cost the same everywhere in the world, they can help companies reshore manufacturing jobs that have been transferred to low-cost labor countries and level the playing field in general

Owing a car between 1970s and 90s usually involved selecting a make and model at a car – perhaps ordering a car in a particular color and with certain extras. Granted, this is a lot of choice compared to what Henry “as long as it’s black” Ford had to offer (i.e., Industry 2.0). But it’s nothing like “configuring” a car online today. Today, car buyers have so many options to choose from, that any given buyer has a good chance of ending up with a car that at least appears to neighbors, co-workers and so on as one of a kind. Driven by a desire to make affordable, high-quality products that at least give the appearance of uniqueness, today’s mass customization is largely enabled by Industry 4.0 technologies – including internet connections between dealership ordering systems,

- This is an Open Access article distributed under the terms of the Creative Commons Attribution-Noncommercial 4.0 Unported License, permitting all non-commercial use, distribution, and reproduction in any medium, provided the original work is properly cited.

- Selection and peer-review under responsibility of the Organizing Committee of the Conference

supply chain systems, and even the robots on the car factory floor. The customer makes choices from a growing list of options. This set of choices is configured and packed in just the right order. The truck arrives at the car factory at just the right minute. And the forklifts deliver the parts straight to the assembly line station where the customer's "unique" car appears.

On the other hand, industry 5.0 products/services, which collaborates of man and machine, empower people to realize the basic human urge to express themselves. These personalized products can also be called as the human touch. The customers demand most and pay most for are products that bear the distinctive mark of human care and craftsmanship. Products like these can only be made through human involvement – human engagement. These consumers accept technology – they don't mind if automation, for example, is a part of the production processes. However, they crave the personal imprint of human designers and craftspeople, who produce something special and unique through their personal effort. In other words, this is called personalization.

Consequently, industry 5.0 is a return to pre-industrial production, but one that is enabled by the most advanced technologies out there.

Literature

In literature review of this paper, industry 5.0 and lean innovation are taken into consideration in two other steps.

Industry 5.0

Industry 5.0 is a digital transformation of the existing era. There are many documents regarding to the massive benefits from Industry 4.0 and it is no doubt that industry 4.0 is the bringing together of robots, interconnected devices and fast networks of data within a factory environment, basically to make the factory more productive and to execute the routine tasks that are best done by robots and not best done by humans. (<https://www.raconteur.net/business/manufacturing-gets-personal-industry-5-0>)

It can be said that the industrial revolution was born between the centuries 18th and 19th centuries. It was a time during which rural and agrarian societies in both America and European countries became industrial and urban. Prior to the Industrial Revolution, production was done in people's homes, using hand tools or hand-made. Especially, iron and textile industries, along with the improvement of the steam engine, has got serious roles in the Industrial Revolution, which also saw improved systems of transportation, communication and finance. It's a well-known fact that industrialization resulted a huge volume and various of produced goods. It resulted in often grim employment and living conditions for the poor and working classes, too. (<https://www.history.com/topics/industrial-revolution>)

Finally, it can be taken into consideration as industry 5.0 is a future, also it means that the change processes directing towards closer cooperation between human and machines. (<https://medium.com/@michael.rada/industry-5-0-definition-6a2f9922dc48>)

Table 1. History of Industrial Revolution

Era	
1.0	1780-Mechanisation Industrial production based on machines powered by water and steam
2.0	1870-Electrification Mass-production using assembly lines
3.0	1970-Automation Automation using electronics and computers
3.5	1980-Globalisation Offshoring of production to low-cost economies
4.0	Today-Digitalisation Introduction of connected devices, data analytics and artificial intelligence technologies to automate processes further
5.0	Future-Personalisation Industry 5.0 is focused on the cooperation between man and machine, as human intelligence works in harmony with cognitive computing.

<https://www.raconteur.net/business/manufacturing-gets-personal-industry-5-0>

Lean Innovation Approach

Over the past years, the speed of innovation has been continuously increasing. The time span between subsequent product relaunches has shortened drastically (Adick, 2008). To keep their market share, companies are forced to bring products to market at an ever-increasing speed while at the same time the number of product variants is rising. In many markets, such as the automotive industry, this has led to a microsegmentation of markets. Companies offer a higher variety of products with a lower sales volume per product variant (Morgan, 2006).

The term “Lean” as a basic trend of organizing business operations was invented in 1990 by Womack et al. in “The Machine that Changed the World”. In automotive field, Womack et al. investigated differences in performance between leading western and Japanese automobile manufacturers. They made comparisons about rates, plant productivities, lead-times and found that the Japanese manufacturers clearly outperformed their western competitors in all measures. For example, American and European producers required on average 25.1 and 36.2 hours to produce a car respectively. On the other hand, Japanese car companies needed a time of only 16.8 hours while at the same time achieving a lower defect rate (Womack, 1990).

Although production was only one of the areas investigated in the “Machine that Changed the World”, the large differences in manufacturing performance pointed out in the study attracted the largest interest. In their effort to explain the productivity gap, Womack et al. particularly investigated the Toyota Production System (TPS). They found that its underlying principles differed significantly from traditional ways of mass manufacturing employed by the western car manufacturers. Since, as the authors found, Toyota was able to do “more and more with less and less” Womack et al. baptized the concept “Lean Manufacturing” (Womack, 1994).

Despite their close connection, the roots of the Toyota Production System go back much further than the term “Lean Manufacturing”. The fundamentals of the TPS were laid in the 1950s when in the Post-World War II era Toyota was forced to manufacture a wide range of different models for small-volume markets (Leung, 2014), (Womack, 1990). Based on these experiments and the experience he had gathered when visiting plants mainly in the US, he developed a production system which was characterized by a particularly high flexibility. The principles and methods developed at Toyota were refined over the years and extended to include its suppliers

(Oke, 2015). Though the basic ideas had been published by Shigeo Shingo, called “Study of the Toyota Production System” in 1980, the new taxonomy developed by Toyota remained largely unknown in the western world until the beginning of the 90’s of the 20th century (Womack, 1990).

Today, lean principles have spread well beyond their origin in automotive manufacturing in two major dimensions. Initially, Lean principles have been adapted by a variety of different sectors (Shen, 2012), (Green, 1998). Concepts like Lean Construction or Lean Healthcare which apply Lean in domains other than automotive are – although still in a nascent stage – gaining increasing attention. Secondly, in the last years there has been a growing awareness that the application of Lean to the area of manufacturing is by no means sufficient. Lean rules are increasingly implemented from a lifecycle perspective, in corporate support functions as well as in leadership processes by following the notion of the “Lean Enterprise” (Womack, 2003), (Morgan, 2006).

Method

Value Management

When collaboration between man and machine is thought with lean innovation approach, sources are going to be much more important than before. Since; time, raw-material, human resources, finance etc. should be implemented more carefully. In this point, finding the pivot point in relation to costs and risks, must be completed. In other words, eliminating the waste points makes us earn value. Therefore, value management may be thought as an approach in lean innovation management.

Value management was presented to analyse optional materials for the aim of selecting the one that provided same, better, or best function at the least cost. Value management was conceived and practised at the early stage of project conceptualisation as a result of the need for innovation, novelty and advancement of existing practice. There are various aspects of different values from different participants, however the aim of value management implementation is to unify these differences in order to achieve the project’s stated goals using minimum resources.

The key principle of value management is to compare the analysis results of all alternatives. It also means that the more options there are and the more detailed explanation can be available about their backgrounds, the better the ability of the value management team to brainstorm and identify the best alternative, using the principle of function and cost. One of the costs regarding to value management is that of collecting information, cost (initial, annual, running, maintenance), lifespan, and the physical characteristics of elements or components to facilitate deliberation by team members.

The Society of American Value Engineers (SAVE) has adopted the term ‘value engineering’ as observed from their name and public reports published by the body over time. This implies that the term has metamorphosed from ‘value analysis’ initially proposed by Lawrence Miles during the World War II to ‘value engineering’ in the United States of America. Published materials from the United Kingdom (UK) have adopted ‘value management’ to describe the process. The Institute of Value Management (IVM), a similar one, is also tasked with the responsibility of controlling the process of the discipline in the UK. Authors affiliated with the USA, especially those from countries that adopt American English, prefer the term ‘value engineering’ while those from regions and countries with links to the UK and adopt British English usually use the term ‘value management’.

Value planning is the first phase and an approach of value management that is associated with achieving project value during the planning stages of a project. For instance, in construction this is associated with value at the early stage, namely, conception, inception, feasibility, viability, and other planning-related activities of the project. Value planning can be thought as a branch of value control and they are both derived from the principle of cost planning and cost control, which are common terms for management of developmental projects.

Value control indicates a direct link to cost control which is not the same as value management, justifying the reason why the term is not common among value management experts, analysts, or researchers. Value analysis is associated with the post-construction or completion phase, indicating that the practice is related to the value of completed project. This is inclusive of the use and re-use stages of a project.

The most well-known definition of lean principles passes through some major ones depending on value management. The first Lean principle – and the basis for all following principles – is to specify the value as defined by the customer of the particular enterprise. As it’s pointed out that providing the wrong good or service

in the right way is muda” (Womac, 19). Therefore, a company has to thoroughly analyze the needs of its customers and clarify which value the organization plans to deliver. Secondly, both identifying and mapping the Value Stream. The value stream shows all phases required to make product/service. Identifying value stream and the way value is realized, establishes when and how decisions are to be made. The key technique behind value stream is process mapping for a very specific reason: that of understanding how value is framed into the product from client’s point of view.

For a company confronted with a heterogeneous set of customers, specifying value is not a straight-forward task. While one customer might value a low price of a product, other customers might favor a high quality, a good performance, fast delivery or extraordinary service. Therefore, the appropriate value proposition of a company will strongly depend on the market segment it targets and strategic considerations on how it wants to position itself. Customer value for a company pursuing a penetration strategy will naturally differ from customer value as perceived by a producer of premium goods.

Results and Discussion

Finally, lean approach implementation requires a much more balanced approach of simultaneously minimizing waste (HR, Money etc..) and maximizing value. Applying lean principles to product/service development may play an important role in fostering innovation and long-term organizational learning. It is so important to find out the right balance between defining norms as guidelines and giving engineers the freedom to pursue unconventional solutions, otherwise this has negative consequences for organizational learning and innovation.

Conclusion

The effective planning and management of value assets is essential. This can be achieved by the systematic management of all decision processes taken through out. This paper has been prepared for showing the economic need to achieve more efficient and effective infrastructure asset reconfiguration. What is clear is that lean management can be an important tool and has the potential to deliver integration. Lean approach still has a strong currency within the most of the fields; however, it is being applied in isolated knowledge pockets with no integrated view of how Lean processes and lean assets and design can be applied together in a whole system and multidisciplinary lean approach.

Further work may be needed by different industry practitioners, researchers and scientists to develop new integrated lean project and asset management approaches that can be used by supply chains , planners and approaches.

Recommendations

The method, value management, was taken into account so as to compare optional materials in order to arrive at the best function one at the lowest possible overall cost. This paper revealed that the concept of value management was first introduced to lean approach for industry 5.0. However, it may be implemented in other fields. Due to the varying information and different levels of operation of the implementation, value management is the most common one of all. As advantages as the practice has been in projects, there may be some risks, undoubtedly.

In addition to this, The direct and indirect costs of conducting the exercise should also be identified. The aim of this paper is to frame on the knowledge for subsequent future studies about lean approach or industry 5.0. For instance, value management as a discipline, can be utilized while preparation of interface between industry 5.0 and implementation field.

References

Adickes H, Amoscht J, Bong A, Deger R, Hieber S, Krappinger R, Lenders M, Post P, Rauhut M, Rother M: Lean Innovation: Auf dem Weg zur Systematik. In: Aachener Werkzeugmaschinen-Kolloquium (Ed.): *Wettbewerbsfaktor Produktionstechnik – Aachener Perspektiven*. Aachen: Apprimus Verlag, 2008.

- Green, S. D., & Moss, G. W. (1998). Value management and post-occupancy evaluation: Closing the loop. *Facilities*, 16(1/2), 34–39.
- Jay, C. I., & Bowen, P. I. (2015). Value management and innovation: A historical perspective and review of the evidence. *Journal of Engineering, Design and Technology*, 13(1), 123–143.
- Karunasena, G., Rathnayake, R. M., & Senarathne, D. (2016). Integrating sustainability concepts and value planning for sustainable construction. *Built Environment Project and Asset Management*, 6(2), 125–138.
- Kelly, J., & Male, S. (2006). Value management. In J. Kelly, R. Morledge, & S. Wikinson (Eds.), *Best value in construction* (pp. 77–99). London: Blackwell.
- Kelly, J., Male, S., & Graham, D. (2014). *Value management of construction projects*. Oxford: Wiley.
- Leung, M.-Y., & Yu, J. (2014). Value methodology in public engagement for construction development projects. *Built Environment Project and Asset Management*, 4(1), 55–70.
- Liu, G., & Shen, Q. (2005). Value management in China: Current state and future prospect. *Management Decision*, 43(4), 603–610.
- Male, S. (2002). A re-appraisal of value methodologies in construction. *Construction Management and Economics*, 11(2002), 57–75.
- Miles, L. D. (1972). *Techniques for value analysis and engineering* (2nd ed.). New York: McGraw-Hill.
- Morgan JM: High performance product development: A systems approach to a Lean Product Development process. *Department of Industrial and Operations Engineering*. Michigan: University of Michigan, 2002.
- Morgan JM, Liker JK: *The Toyota Product Development System: Integrating People, Process, and Technology*. New York, Productivity Press, 2006.
- Oke, A. E. & Ogunsemi, D. R. (2011). Value management in the Nigerian construction industry: Militating factors and the perceived benefits. In *Proceedings of the Second International Conference on Advances in Engineering and Technology* (pp. 353–359). Faculty of Technology, Makerere University, Uganda.
- Oke, A. E., & Ogunsemi, D. R. (2013). Key competencies of value managers in Lagos state, Nigeria. In S. Larry & S. Agyepong (Eds.), *Proceedings of 5th West Africa Built Environment Research (WABER) Conference* (pp. 773–778). Ghana: Accra.
- Oke, A. E., Aghimien, D. O., & Olatunji, S. O. (2015). Implementation of value management as an economic sustainability tool for building construction in Nigeria. *International Journal of Managing Value and Supply Chains*, 6(4), 55–64.
- Palmer, A., Kelly, J. & Male, S. (1996). Holistic appraisal of value engineering in construction in United States. *Construction Engineering and Management*, 324–326.
- Perera, S., Hayles, C. S., & Kerlin, S. (2011). An analysis of value management in practice: The case of Northern Ireland's construction industry. *Journal of Financial Management of Property and Construction*, 16(2), 94–110.
- Shen, G. Q., & Yu, A. T. (2012). Value management: Recent developments and way forward. *Construction Innovation*, 12(3), 264–271.
- Shen, Q., & Liu, G. (2004). Applications of value management in the construction industry in China. *Engineering, Construction and Architectural Management*, 11(1), 9–19.
- Short, C. A., Barrett, P., Dye, A., & Sutrisana, M. (2008). Impacts of value engineering on five capital arts projects. *Construction Management and Economics*, 35(3), 287–315.
- Society of American Value Engineers. (2015). What is value engineering? Retrieved May 27, 2016, from <http://www.value-eng.org/>.
- The College of Estate Management. (1995). Value engineering. Retrieved May 12, 2016, from <http://www.cem.ac.uk/postalcourses>.
- The Institute of Value Management. (2015). What is value management? Retrieved May 12, 2016, from http://www.ivm.org.uk/what_vm.htm.
- Womack, J. P., & Jones, D. T. (1997). Lean thinking—banish waste and create wealth in your corporation. *Journal of the Operational Research Society*, 48(11), 1148–1148.
- Womack JP, Jones DT: *Lean Thinking. Banish Waste and Create Wealth in Your Corporation*. 2. Edition. New York: Simon and Schuster, 2003.
- Womack JP., Jones, DT, Roos, D: *The Machine That Changed The World: Based On The Massachusetts Institute of Technology 5-Million-Dollar 5-Year Study On The Future Of The Automobile*. New York: Macmillan, 1990.
- Womack JP, Jones DT: From Lean Production to the Lean Enterprise. *Harvard Business Review*. 1994; 72: 93–93.
- Yekini, A. A., Bello, S. K. & Olaiya, K. A. (2015). Application of value engineering techniques in sustainable product and service design. *Science and Engineering Perspectives*, 10(Sept), 120–130. Retrieved May 1, 2018, <https://www.raconteur.net/business/manufacturing-gets-personal-industry-5-0>

Retrieved May 1, 2018, (<https://www.history.com/topics/industrial-revolution>)

Retrieved May 1, 2018, (<https://medium.com/@michael.rada/industry-5-0-definition-6a2f9922dc48>)

Author Information

Banu Ozkeser

Koluman Otomotiv Endüstri A.S.

R&D Center

Sahin mah Sait Polat Bulvari No:386/C Mersin/Turkey

Contact e-mail: banuozkeser@gmail.com

Extraction of Heavy Metals using Dithizone Method on Seawater

Leong KOK SENG

Polytechnic Tun Syed Nasir Syed Ismail

Abstract: Research conducted is related to the preparation and characterization of dithizone method based on extraction of cadmium, lead and zinc trace metals from seawater samples. Inorganic metals or ions can act back with dithizone to produce colourful coordination. The dithizone reagent is highly sensitive to the presence of heavy metals such as plumbum (Pb), cadmium (Cd) and zinc (Zn) as designated in this study. Inorganic metals or ionic can react with dithizone to produce colored coordination compounds. The resulting dithizoneate may be extracted with an organic solvent such as carbon tetrachloride (CCl₄). This study also involves steps such as adjusting the pH value in order to produce the dithizoneate metal product we need. In this study, metal powders were dissolved in seawater samples and extracted with dithizone to enhance the detection and extraction facilities. We analyze trace metals carried out by plasma atomic emission spectroscopy (ICP-OES) to see the efficiency of dithizone extraction methods into seawater samples used. Dithizone extraction method used in extracting Pb element indicates a good performance.

Keywords: Dithizone

Introduction

Malaysia is a country surrounded by the sea, it also has many beautiful beaches. However, the issue of environmental pollution is quite alarming as Malaysia is a developing country. Environmental pollution is caused by the acts of some selfish and irresponsible parties who have dispersed toxic waste into the water without being processed. The act has polluted the water resources and hunted seawater. Wastes of the industrial sector such as fuel contain high heavy metals. As we know, heavy metals are very difficult to get rid of and will continue to be contaminated in our body after we take sea life such as shellfish, fish and others (Jong et al. 2010).

Seagrasses have been known to generally play an important role in the sea in general. Fermentation metals such as iron (Fe) and cadmium (Cd) are very important for the growth of phytoplankton, iron (Fe) are also used in chlorophyll production processes in biogeochemical cycles of marine life, copper (Cu), cadmium (Cd) and lead (Pb) toxic in some circumstances (Lee et al. 2011). Photogravure is an important element in marine life, but traceable metal data on a scale globally is very limited due to difficulties in sampling and analysis. This incident is due to the very low concentration of metals (10^{-9} to 10^{-12} mol L⁻¹) compared to the high salt matrix in sea water. Thus, trace metal analysis requires a pre-concentration process with purification prior to detection such as solvent extraction followed by trace metal qualification using plasma atomic emission spectroscopy (ICP-OES).

There are various methods of extraction of metals from water, but the method of extracting metals from seawater is the most difficult extraction due to disturbances such as chloride ions, high salt concentrations and so on in sea water. In addition, the method of extraction of seepage metal from seawater involves measures or work that is quite complicated and requires much labor, long allocated time and large quantities of seawater samples. In this study, trace metal extraction was performed using the dithizone method. Inorganic metals or ionic can react with dithizone to produce colored coordination compounds. This dithizone reagent is highly sensitive to the presence of heavy metals such as lead (Pb), cadmium (Cd) and zinc (Zn) as provided in this study. This resulting dithizoneate can be extracted with organic solvents such as carbon tetrachloride (CCl₄). This study also involves measures such as adjusting the pH values so as to produce the dithizoneate metal

- This is an Open Access article distributed under the terms of the Creative Commons Attribution-Noncommercial 4.0 Unported License, permitting all non-commercial use, distribution, and reproduction in any medium, provided the original work is properly cited.

- Selection and peer-review under responsibility of the Organizing Committee of the Conference

products we need. For example, when analyzing zinc (Zn) metal, by adjusting the pH value to 4.0 - 5.5, zinc (Zn) will react with dithizone to produce zinc dithizonate. The metal alloys are defined as toxic metals due to the presence of elements Pb, Cd, As, Ti, and U elements. In the water symbol there are various metals such as Cr, Ni, Mn, Co, Fe and Zn (Alloway 1990). Most of these metals do not affect the environment when present in small quantities. However, however, if it is present in excess quantities, it is said to be toxic because of the contamination effect it will carry. Trace metals or heavy metals will have an impact even within a short period of time, as well as chronic consequences on aquatic life as well as animals or humans that consume the aquatic life. Heavy metals are difficult to decompose and will accumulate in our body such as tissue organisms. The properties of these toxic metals will continue to occur in our bodies, and will cause very serious effects such as causing a person to infect chronic or carcinogenic diseases. In this study, trace metals aimed at being extracted are cadmium (Cd), lead metal (Pb) and zinc metal (Zn).

Method

Preparation of Standard Solution Dithizone

30 mg dithizone dissolved in 1000 mL of chlorophyll. Solution dithizone shaken until no visible sedimentation under volumetric flask. It then added 5.0 mL of ethanol before being stored in the laboratory refrigerator under 12 ° C. Before use, incorporate 5.0 mL of HNO₃ into the solution and shake to avoid precipitate the volumetric glass flask.

There are many types of standard methods that have been used in determining the concentration of heavy metals in seawater samples. However, only a few studies have been able to effectively extract the traceable metal and the results of this study are more pronounced than seawater. Among such studies were carried out by Lim and Shahru (2002), made using the Cadmium method, the hydronium method. Both methods are an ideal method for assessing the content of heavy metals. However, both methods require a considerable length of time and complicated measures. Additionally, these methods involve high risk reagents besides requiring high costs of either cost or maintenance costs.

In this study, metal extraction traction was carried out using the dithizone method. Dithizone or known as diphenylthiocarbazone or 1,5- diphenylthiocarbazone is a compound containing sulfur (S) and a good ligament. Dithizone is prepared with dithizone's reaction to react with various metals such as lead (Pb) and cadmium (Cd) and produce colored complexes. With the pH value adjustment, the results for the determination of heavy metals such as lead (Pb), cadmium (Cd) and zinc (Zn) will be easier and faster. For example, when conducting zinc (Zn) metal analysis, by adjusting the pH value to 4.0 - 5.5, zinc (Zn) will react with dithizone to produce zinc.

Results and Discussion

Table 1 and figure 1 show the percentage of zinc metal extraction and the concentration of zinc metal which is stirred by using 10 mL of 5.0 ppm Zn (NO₃)₂ and 10.0 ppm Zn (NO₃)₂ and diluted solution. It can be seen that the extraction method of dithizone for 10.0 ppm of Zn (NO₃)₂ solution using distilled water can obtain the highest concentration of trace metal, which is 0.615 mg / L with the highest extraction percentage of 30.8%. Meanwhile, extraction by sea water obtained the lowest concentration of trace metals for 10.0 ppm of Zn (NO₃)₂ solution was 0.349 mg / L with 17.5% percentage of recovered extraction.

This condition occurs due to the suitability of pH value which is less suitable for Zn metal. The pH value of the buffer provided was impaired by the addition of acetic acid during the experiment as the production of Zn was required to have a relatively low pH adjustment of 2.5 - 3.0. This incident is also due to the loss of most Zn metal during solvent evaporation through spinning evaporation and drying before being sent to ICP-OES. Zn (1040.15 K) has a lower boiling point compared to Pb (2022.15 K) and Cd (1180.15 K) under 1.0 atm pressure. This feature shows Zn is a more volatile metal and is easily lost during heated.

Table 1. Percentage of zinc metals extracted using dithizone method

Type	Extraction (%)	
	5ppm	10ppm
Distilled Water	30.0	30.8
Artificial Seawater	28.9	21.9
Seawater	21.4	17.5

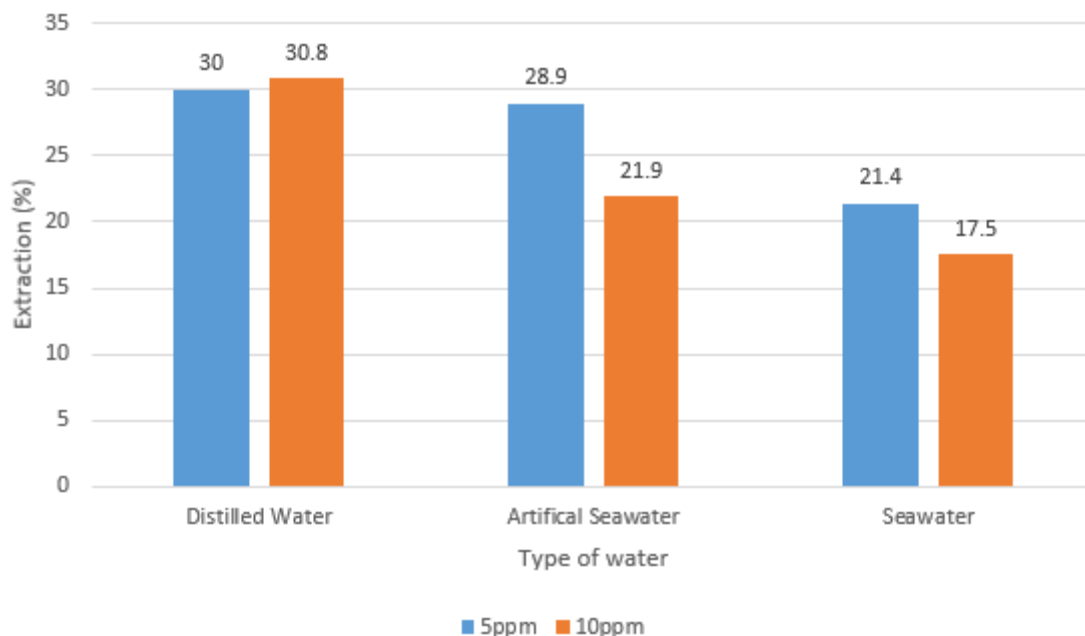


Figure 1. Comparison of percentage of zinc metal extraction using 5.0 ppm and 10.0 ppm Zn (NO₃)₂ solution

Table 2 and Figure 2 show the percentage of cadmium metal extraction and the concentration of cadmium metal which is displaced by using 10 mL of standard solution of 5.0 ppm Cd (NO₃)₂ and 10.0 ppm Cd (NO₃)₂ with diluted solution. Cadmium metal is the most successful traceable metal to be extracted from water samples using the method of treatment. Overall, we can see that the method is highly sensitive to the cadmium metal through the percentage of metal extraction obtained is the highest among the three trace metals. The highest extraction of metals is 10.0 ppm Cd (NO₃)₂ solution using distilled water, which is 1.835mg / L. It is also the closest percentage of extraction to the perfect, by 99.2%. The lowest percentage of extraction is by extraction by natural sea water, ie 70.7% or 1.414 mg / L recovered using 10.0 ppm of Cd (NO₃)₂ solution used with 0.0707mg Cd extracted from 0.10005mg as entered early research.

This incident occurs due to the pH value in the solution during titration, which is about 3.0 corresponding to cadmium metal according to Table 1. According to Lohan et al study, the pH value is very important for the recovery of trace metals where the effectiveness of the extraction percentage is 99.2%. In addition, cadmium metal element contamination can be determined through this analysis through a percentage of metal extraction as high as 84.3% for 5.0 ppm and 70.7% for 10.0 ppm standard metal solution for water blank types. Air blank means no added oceans in the sample. The contamination is likely to come from the contamination of the instrument which is the contamination of the rotating evaporator or in the beaker during the solvent drying process.

Table 2. Percentage of cadmium metals extracted using dithizone method

Type	Extraction (%)	
	5ppm	10ppm
Distilled Water	90.4	99.2
Artificial Seawater	87.0	82.9
Seawater	84.5	82.7

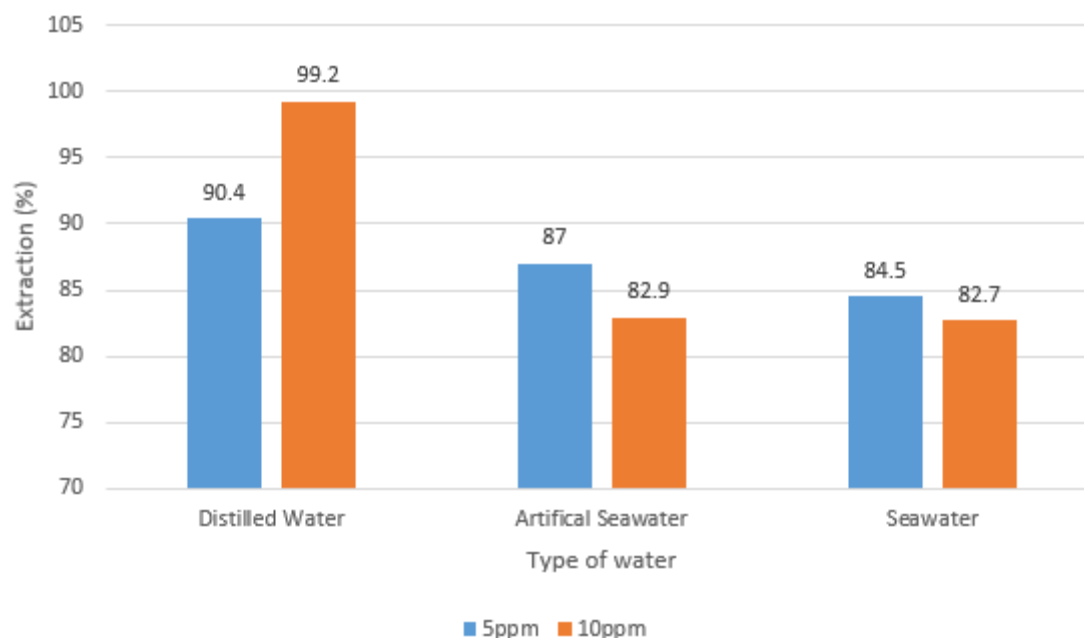


Figure 2. Comparison of percentage of cadmium metal extraction using 5.0 ppm and 10.0 ppm Cd (NO₃)₂

Table 3 and figure 3 shows the percentage of extraction and concentration of the extracted metal for Pb (NO₃)₂ by using 5.0 ppm and 10.0 ppm of the standard Pb (NO₃)₂ solution in 10.0 ml. The percentage of metal extraction and the concentration of extraction metal against the trace metals using artificial sea water samples was higher than the extraction of trace metals using seawater samples. For Pb elements, artificial sea water sample has reached 66.2% effectiveness of metal recovery with 5.0 ppm of standard metal solution and reached 62.6% for 10.0 ppm of standard metal solution. The percentage of metal extraction is low due to the presence of large ion disruption of ion chloride and salt matrix in water, thus affecting the effective extraction of the method. Dithizone extraction method used in extracting lead element indicates a good performance.

Table 3. Percentage of lead metals extracted using dithizone method

Type	Extraction (%)	
	5ppm	10ppm
Distilled Water	74.6	79.8
Artificial Seawater	66.2	62.6
Seawater	61.8	55.8

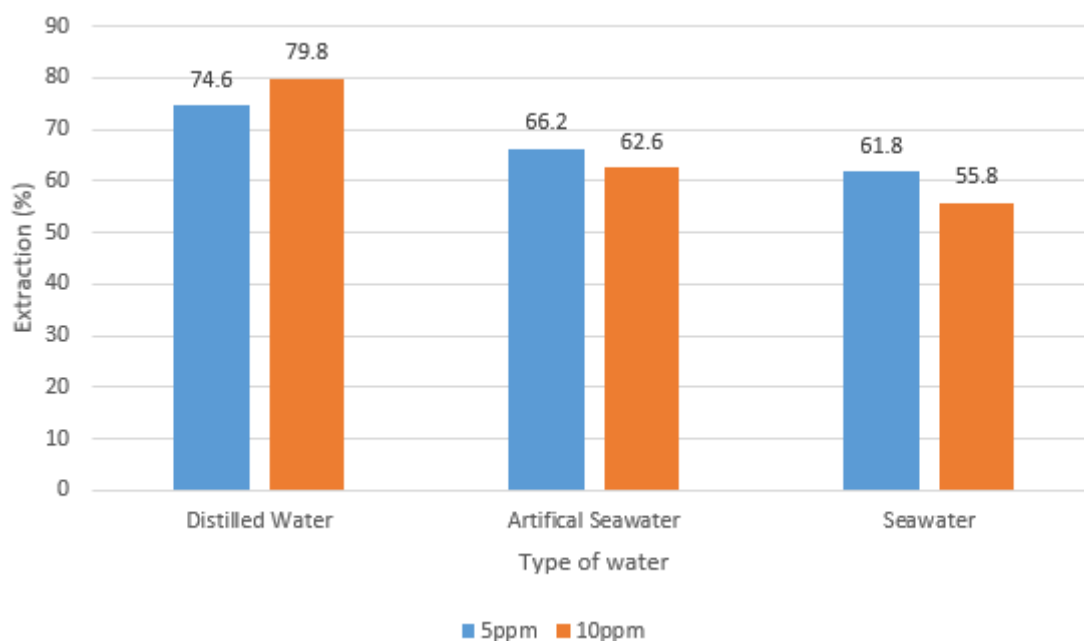


Figure 3. Comparison of percentage of lead metal extraction using 5.0 ppm and 10.0 ppm $Pb(NO_3)_2$

Conclusion

Studies show that simple extraction methods such as dithizone can produce trace metals from seawater samples with ICP-OES determination. This method only uses about 180 - 220 mL of sea water sample volume for each concentration of a standard metal solution, for 5.0 ppm with 10.0 ppm. This study also shows that the simultaneous analysis potential of some elements (Cd, Pb and Zn) can be carried out through spiking extraction on samples by using several standard solutions. This method can be useful for the analysis of large quantities of trace metals. This is because this method can be used to measure the analysis of various elements by simply using a small sample volume. This can help in the collection of samples, sample storage and analysis on samples become easier. Given more attention to the pH value analyzed, it is believed that the reading or value of the extracted trace metal concentration for each element obtained from the experiment is further enhanced. Using the dithizone method, the extracted metal concentration was 1.414 mg / L for Cd, 0.038 mg / L for Pb and 0.473mg / L for Zn.

Recommendations

Revision of chemicals and radar tools and instruments such as pH meter, rotary evaporation machine used is very important. Ensure that the chemicals and equipment used are always in good condition to improve the effectiveness of the analysis and also save time allocated. The provided standard solutions should not be used for more than 2 weeks. It should be provided every 2 weeks to improve the sensitivity and reagent selection of metal elements. In this way, contamination and elemental contamination can be avoided, the extraction decision can be reversed.

References

- Satyanarayanan M., Balaram V., Gnaneshwar T., Dasaram B., Ramesh S. L., Ramavati Mathur dan Drolia R. K.. 2006. Determination of trace metals in seawater by ICP-MS after preconcentration matrix separation by dithiocarbamate complexes. *Indian Journal of Marine Sciences* (36): 71-75.
- Hiraide M., Yoshida Y dan Mizuike A. 1976. Flotation of traces of heavy metals coprecipitated with aluminium hydroxide from water and seawater. *Anal. Chim. Acta* (81): 185-189.
- Sturgeon R. E. dan Berman S.S.. 1980. Preconcentration of trace metals from seawater for determination by graphite furnace atomic-absorption spectrometry. *Talanta* (27): 85-94.

- Danielsson L.G., Magnusson B., Westerlund S. dan Zhang K.. 1982. Trace metal determination in estuarine waters by electrothermal atomic absorption spectrometry after extraction with dithiocarbamate complexes from freon. *Anal. Chim. Acta (144)*: 183-188.
- Sachhsenberg S., Klenrike Th., Krumbein W. E. dan Zeeck E., 1992. A back extraction procedure method: Rapid determination of metals in seawater matrices. *Fresenius J. Anal. Chem (342)*: 163-166.
- Jan T. K. dan Young D. R.. 1978. Determination of microgram amounts of some transition metals in seawater by methyl isobutyl ketone-nitric acid successive extraction and flameless atomic absorption spectrophotometry. *Anal. Chem. (50)*: 1250-1253.
- Wu J. dan Boyle E. A.. 1997. Low blank preconcentration technique for the determination of lead, copper and cadmium in a small volume seawater by isotope dilution ICPMS. *Anal. Chem. (69)*: 2464-2470.
- Chandrasekhar K., Chary S. N., Kamala C. T. dan Apama V. 2003. Determination of trace metals in seawater by induced coupled mass spectrometry with preconcentration on silica-immobilized 8-hydroxyquinoline. *Anal Chem. (57)*: 2907-2911.
- Jong M. L., Edward A., Boyle A., Yolanda Echegoyen-Sanz, Jessica N., Fitzsimmons, Ruifeng Zhang dan Richard A. Kayser. 2010. Analysis of trace metals (Cu, Cd, Pb, and Fe) in seawater using single batch nitrilotriacetate resin extraction and isotope dilution inductively coupled plasma mass spectrometry. *Anal. Chim. Acta. (686)*: 93-101.
- Mark L. Wells dan Kenneth W. Bruland. 1998. An improved method for rapid preconcentration and determination of bioactive trace metals in seawater using solid phase extraction and high resolution inductively coupled plasma mass spectrometry. *Marine Chemistry (63)*: 145-153.
- Tessier A., Campbell P. G. C. dan Bisson M.. 1979. Sequential extraction procedure for the speciation of particulate trace metals. *Analytical Chemistry (51)*: 844-851.
- Antun Kucak dan Maja Blanusa. 1998. Comparison of two extraction procedures for determination of trace metals in soil by atomic absorption spectrometry. *Arh hig rada toksikol (49)*: 327-334.
- Bert L. Vanllee dan John G. Gibson. 1948. An improved method for the determination of small quantities of zinc in blood and tissue samples. *Microdetermination of Zinc in Blood.:* 435-449.

Author Information

Leong Kok Seng

Polytechnic Tun Syed Nasir Syed Ismail
Malaysia
kokseng@ptsn.edu.my

On the Solution of the Generalized Symmetric Woods-Saxon Potential in the Dirac Equation

Bekir Can LUTFUOGLU
Akdeniz University

Abstract: In this work, we present a solution to the Dirac equation that is coupled with vector and scalar generalized symmetric Woods-Saxon potential energy in one plus one space-time. The chosen potential energy has a flexible structure to examine four different physical problems. The potential energy can be a barrier or well depend on being attractive or repulsive. Furthermore, the included surface effects can be attractive or repulsive. Therefore, in one class a potential barrier occurs with a pocket or an extra barrier nearby the effective radius. Similar effects occur in the potential well whether the surface effects are repulsive or attractive. Here we use the usual two-component approach. We obtain the solutions in hypergeometric function form.

Keywords: Dirac equation, Scalar and vector potential energies, Generalized symmetric, Woods-Saxon potential energy

Introduction

In 1928, only after two years of the introduction of the second order Klein-Gordon equation [Klein 1926], Dirac declared the first order relativistic wave equation [Dirac 1928]. Basically, Dirac equation describes the dynamics of spin half particles and possesses results in the high accuracy of the fine details of the hydrogen spectrum. The time passed but its fashion did not pass, and it is still in used to describe the natural laws in many areas in physics [Lee 2009, Hosseinpour 2017].

In 1954, Woods and Saxon introduced a potential energy alternative to the square barrier, later will be called with their names (WSP), to calculate the differential cross section of elastically scattered protons from medium or heavy nuclei [Woods & Saxon 1954]. The potential energy obtained its fame with the highly accurate results especially in nuclear [Brandan et al 1997], atom and molecule physics [Costa et al. 1999] within relativistic [Bayrak et al. 2015, Rojas et al. 2005] and non-relativistic [Zaichenko et. Al 1976] approaches. Besides those studies, Satchler declared a more generalized form of the WSP, namely GSWP, by introducing the surface interactions in addition to the core effects. [Satchler 1983].

In one dimension we investigate the symmetric form of the GSWP (GSWSP) energy is given form

$$V(x) = \Theta(-x) \left[\frac{-V_0}{1 + e^{-\alpha(x+L)}} + \frac{W e^{-\alpha(x+L)}}{(1 + e^{-\alpha(x+L)})^2} \right] + \Theta(x) \left[\frac{-V_0}{1 + e^{\alpha(x-L)}} + \frac{W e^{\alpha(x-L)}}{(1 + e^{\alpha(x-L)})^2} \right]$$

Here, $\Theta(x)$ denotes the step function. The GSWSP energy has three common parameters with WSP energy. V_0 , α , L are the strength, the slope and the effective distance of the potential energy.

Recently, we studied the GSWP energy within non-relativistic [Lütfüoğlu, Akdeniz, Bayrak 2016] and relativistic approaches [Lütfüoğlu, Lipovsky, Kriz 2018, Lütfüoğlu 2018]. Furthermore, we analyzed the comparison of the WSP and GSWP in terms of thermodynamic functions [Lütfüoğlu Commun.Theor. Phys. 2018]. Finally, we used the GSWP energy to obtain energy spectra by solving Schrödinger and Klein-Gordon equations and discussed the results in the statistical mechanic point of view [Lütfüoğlu Can. J. Phys. 2018].

In this paper, we investigate the solution of the Dirac equation within the presence of scalar and vector GSWSP energy. In method section we derive the Dirac equation. We discuss the solution in the Results and Discussion section.

Method

We use analytical algebraic methods to solve the Dirac equation in the natural units.

Dirac Equation

We start with the non-interacting Dirac equation

$$\left(i\gamma^\mu \frac{\partial}{\partial x^\mu} - m\right)\Psi(x, t) = 0.$$

Here, m is the mass of the particle. We couple an external potential which describes the interaction via the four momentum and mass.

$$\left[\gamma^\mu \left(i \frac{\partial}{\partial x^\mu} - eA_\mu\right) - (m + gV_s)\right]\Psi(x, t) = 0.$$

Here, e and g are coupling constants. In 1+1 dimension, the four-vector A_μ has two components, namely time and spatial components. We propose a nonzero time component and call it as the vector potential. Furthermore, we choose the spatial component as zero. Moreover, we take Pauli matrices σ^3 and $i\sigma^1$ instead of the gamma matrices. Since the GSWSP energy does not depend on time, we can separate the wave function into time and space functions.

$$\Psi(x, t) = \psi(x)e^{-iEt}$$

Then, we substitute them into the Dirac equation and we find

$$\left[\sigma^3(E - eA_0) - \sigma^1 \frac{d}{dx} - (m + gV_s)\right]\psi(x) = 0.$$

We choose the external potential to be equal to GSWSP energy with equal magnitude. Then, we decompose the Dirac spinor, into upper $u_1(x)$ and lower $u_2(x)$, spinors as

$$\psi(x) = \begin{pmatrix} u_1(x) \\ u_2(x) \end{pmatrix}.$$

and we obtain coupled first order equations

$$\begin{aligned} \frac{du_2(x)}{dx} &= [(E - V(x)) - (m + V(x))]u_1(x), \\ \frac{du_1(x)}{dx} &= [-(E - V(x)) + (m + V(x))]u_2(x). \end{aligned}$$

We follow the path that was introduced in the book of Flügge [Flügge 1974]

$$\begin{aligned} \phi(x) &= u_1(x) + i u_2(x), \\ \chi(x) &= u_1(x) - i u_2(x). \end{aligned}$$

After some algebra we obtain

$$\frac{d^2\phi(x)}{dx^2} + \left[(E - V(x))^2 - (m + V(x))^2 + i \frac{d}{dx} V(x)\right]\phi(x) - K(x)\phi(x) = 0,$$

$$\frac{d^2\chi(x)}{dx^2} + \left[(E - V(x))^2 - (m + V(x))^2 - i \frac{d}{dx} V(x) \right] \chi(x) - L(x)\chi(x) = 0.$$

Here

$$K(x)\phi(x) = \frac{\frac{d}{dx}V(x)}{m + V(x)} \left[\frac{d}{dx} - i(E - V(x)) \right] \phi(x),$$

$$L(x)\chi(x) = \frac{\frac{d}{dx}V(x)}{m + V(x)} \left[\frac{d}{dx} + i(E - V(x)) \right] \chi(x).$$

Chabab et al. showed that these terms can be ignored when the strength of interaction is very small to the mass term [Chabab et al. 2016].

Results and Discussion

Since GSWSP energy is symmetric, we study only negative region. Moreover, we examine the solutions only for one of the composite spinors, $\phi(x)$. All results can be extended. We apply the following transformation

$$z = [1 + e^{-\alpha(x+L)}]^{-1},$$

and we find that the GWSP energy and its derivative become

$$V(x) \xrightarrow{\text{yields}} -(V_0 - W_0)z - W_0z^2,$$

$$\frac{d}{dx}V(x) \xrightarrow{\text{yields}} \alpha z(z-1)[(V_0 - W_0) + 2W_0z].$$

Then we obtain a dimensionless differential equation as follows.

$$\left[\frac{d^2}{dz^2} + \left(\frac{1}{z} + \frac{1}{z-1} \right) \frac{d}{dz} - \frac{\epsilon^2}{z^2(z-1)^2} + \frac{C^2}{(z-1)^2} + \frac{D^2}{z(z-1)} + \frac{F^2}{z-1} \right] \phi_L(z) = 0,$$

Here, we abbreviate the following terms:

$$\epsilon^2 = \frac{m^2 - E^2}{\alpha^2},$$

$$C^2 = \frac{2(E + m - i\alpha)W_0 + i\alpha V_0}{\alpha^2},$$

$$D^2 = \frac{(2E + 2m - i\alpha)V_0 + (E + m - i\alpha)W_0}{\alpha^2},$$

$$F^2 = \frac{2iW_0}{\alpha},$$

One can obtain the general solution with the ansatz

$$\phi_L(z) = z^\mu (z-1)^\nu f(z),$$

It is a very well-known result that such differential equations yield to be a hypergeometric differential equation. Therefore, we obtain the function $f(z)$ in terms of Gauss hypergeometric functions ${}_2F_1$. Here, we avoid discussing the results in details since it is going to be published in a separate paper.

Conclusion

In this work, we discuss the solution of the Dirac equation when it is coupled with vector and scalar GSWSP energy in 1+1 dimension. We obtain that the resulting wave function is expressed in terms of Gauss ${}_2F_1$ hypergeometric functions.

Acknowledgements

The author thanks to the organization committee for being very kind and helpful not only during the meeting ICRES 2018 but after too. This work was supported by The Scientific Research Projects Coordination Unit of Akdeniz University. Project Number is FBA-2018-3471.

References

- Bayrak, O. & Aciksoz, E.. (2015). Corrected analytical solution of the generalized Woods-Saxon potential for arbitrary ℓ states. *Phys. Scr.*, 90, 015302.
- Brandan, M. E. & Satchler, G. R.. (1997). The interaction between light heavy-ions and what it tells us, *Phys. Rep.*, 285, 143–243.
- Chabab, M., El Batoul, A., Hassanabadi, H., Oulne, M., & Zare, S.. (2016). Scattering states of Dirac particle equation with position-dependent mass under the cusp potential. *Eur. Phys. J. Plus*, 131(11).
- Costa, L.S., Prudente, F. V., Acioli, P. H., Soares Neto, J. J. & Vianna, J. D. M.. (1999). A study of confined quantum systems using the Woods-Saxon potential, *J. Phys. B: At., Mol. Opt. Phys.*, 32, 2461–2470.
- Dirac, P. A. M.. (1928). The quantum theory of the electron, *Proc. Roy. Soc.* A117, 610-628.
- Flügge, S.. (1974). *Practical Quantum Mechanics*. Berlin: Spinger.
- Hosseinpour, M., Andrade, F.M., Silva, E.O., & Hassanabadi, H. (2017). Scattering and bound states for the Hulthén potential in a cosmic string background. *Eur. Phys. J. C*, 77: 270.
- Klein, O.. (1926). Quantentheorie und fünfdimensionale Relativitätstheorie, *Z. Phys.*, 37, 895-906.
- Lee, D. -H.. (2009). Surface states of topological insulators: The dirac fermion in curved two-dimensional spaces. *Phys. Rev. Lett.*, 103, 196804.
- Lütfüoğlu, B. C., Akdeniz, F.& Bayrak, O.. (2016). Scattering, bound, and quasi-bound states of the generalized symmetric Woods-Saxon potential, *J. Math. Phys.*, 57, 032103.
- Lütfüoğlu, B. C.. (2018). Comparative Effect of an Addition of a Surface Term to Woods-Saxon Potential on Thermodynamics of a Nucleon, *Commun. Theor. Phys.*, 69, 23-27.
- Lütfüoğlu, B. C.. (2018). Surface interaction effects to a Klein-Gordon particle embedded in a Woods-Saxon potential well in terms of thermodynamic functions, *Can. J. Phys.*, 96, 843-850.
- Lütfüoğlu, B. C, Lipovsky, J. & Kriz, J..(2018) Scattering of Klein-Gordon particles in the background of mixed scalar-vector generalized symmetric Woods-Saxon potential, *Eur. Phys. J. Plus*, 133, 17.
- Lütfüoğlu, B. C.. (2018). An investigation of the bound-state solutions of the Klein-Gordon equation for the generalized Woods-Saxon potential in spin symmetry and pseudo-spin symmetry limits, *Eur. Phys. J. Plus*, 133, 309.
- Rojas, C. & Villalba, V. M. (2005). Scattering of a Klein-Gordon particle by a Woods-Saxon potential, *Phys. Rev. A*, 71, 052101.
- Satchler, G. R.. (1983). *Direct Nuclear Reaction*. Oxford: Oxford University Press.
- Woods, R. D. & Saxon, D. S.. (1954). Diffuse Surface Optical Model for Nucleon-Nuclei Scattering, *Phys. Rev.*, 95, 577-578.
- Zaichenko, A. K.& Ol'khovskii, V. S.. (1976) Analytic solutions of the problem of scattering by potentials of the Eckart class, *Theor. Math. Phys.*, 27, 475–477.

Author Information

Bekir Can Lutfuoglu

Akdeniz University
Faculty of Science, Department of Physics, 07058 Campus,
Antalya, Turkey.
+90 242 310 23 13
+90 242 227 89 11 (Fax)
Contact e-mail: bclutfuoglu@akdeniz.edu.tr

Investigation Methods for a Family of Cubic Dynamic Systems

Irina ANDREEVA

Peter the Great St. Petersburg Polytechnic University

Abstract: A broad family of differential dynamic systems is considered on a real plane of their phase variables x, y . The main common feature of systems under consideration is the follows: every particular system includes two equations with polynomial right parts of the third order in one equation and of the second order in another one. These polynomials are mutually reciprocal in the following understanding: their decomposition into forms of lower order does not contain common multipliers. The whole family of such dynamic systems has been split into subfamilies according to numbers of different multipliers in the abovementioned decomposition and depending on an order of sequence of different roots of polynomials. Every subfamily has been studied in a Poincare circle using especially developed investigation methods. As a result all possible for the dynamic systems belonging to this family phase portraits have been revealed and described. There appeared to exist more than 200 different topological types of phase portraits in a Poincare circle. The obtained results have a scientific interest as well as a methodical and educational one.

Keywords: Dynamic systems, Differential equations, Poincare circle, Phase portraits

Introduction

A differential dynamic system is interesting as a mathematical model of a phenomenon or a process, where statistical events (fluctuations) may be disregarded. Main characteristics of a dynamic system are: its initial state and a law of its transition to a different state. A totality of all possible (admissible) states for a given dynamic system is called a phase space of it.

The two fundamentally different categories of dynamic systems are: systems with continuous time and systems with discrete time. For cascades (dynamic systems with discrete time) their behavior is described as a sequence of states of a system. For flows (dynamic systems with continuous time) a state of a system is defined for each time point on a real (or an imaginary) axis. Flows and cascades are studied in the topological and the symbolic dynamics.

All types of dynamic systems (the both - with discrete and with continuous time) are commonly described using an autonomous system of differential equations. Such a system is defined in a certain domain. In that domain it satisfies the conditions of the Cauchy theorem of existence and uniqueness of solutions of differential equations. In this model singular points of differential equations will correspond to the positions of equilibrium of dynamic systems. Also periodical solutions of differential equations will correspond to dynamic systems' closed phase curves.

A global task of the dynamic systems theory is an investigation of curves which are defined by differential equations. It's necessary to split a phase space into trajectories and study a limit behavior of them. That means to find out equilibrium positions and make their classification; reveal attracting and repulsive manifolds (attractors and repellers, or the so-called sinks and sources).

Notions of the greatest importance in the theory of dynamic systems are: the notion of stability of equilibrium states, i.e. an ability of a system to remain near an equilibrium state under satisfactory small changes of initial data - or on a certain manifold - for an arbitrary long period of time; and the notion of a roughness of a system (preserving of a considered system's properties under some small changes of the model itself). A rough dynamic

- This is an Open Access article distributed under the terms of the Creative Commons Attribution-Noncommercial 4.0 Unported License, permitting all non-commercial use, distribution, and reproduction in any medium, provided the original work is properly cited.

- Selection and peer-review under responsibility of the Organizing Committee of the Conference

system preserves its qualitative character of motion despite of (satisfactory small) changes of its parameters. Special research methods described in this paper we consider effective; they may be useful for investigation of applied dynamic systems having polynomials in their right parts.

A bit of History

Studies of normal autonomous second-order differential systems with polynomial right parts were inspired by the great French mathematician-encyclopedist Jules Henri Poincare (April 29, 1854 – July 17, 1912). Jules H. Poincare (together with David Hilbert) is considered as one of the very last mathematicians, who were able to keep in mind all results in all areas of contemporary for them mathematics and mechanics. Poincare has created the topology, the qualitative theory of differential equations, he has developed new methods in celestial mechanics, also he has laid the mathematical foundations of the theory of relativity, etc.

Jules Poincare has revealed, that normal autonomous second-order differential system (having polynomial right parts) allows in principle its full qualitative investigation on an extended arithmetical plane $\bar{R}_{x,y}^2$ (A. Andronov and other authors, 1973).

Being inspired by Poincare's studies, next generations of mathematicians – followers, including contemporary scientists, have successfully studied some kinds of such systems. Among those, for example, are the quadratic dynamic systems (A. Andreev, I. Andreeva, 1997); systems, containing nonzero linear terms; cubic homogeneous systems; dynamic systems having nonlinear (of the odd degrees 3, 5, 7) homogeneous terms (A. Andreev, I. Andreeva, 2007), which have a center or a focus in a singular point O (0,0) (A. Andreev and other authors, 2017), and some additional systems' types.

The Article Subject Matter

We describe in the present paper results of the research of an extended family of dynamic systems on a real (arithmetical) plane x, y

$$\frac{dx}{dt} = X(x, y), \quad \frac{dy}{dt} = Y(x, y), \quad (1)$$

for which $X(x, y), Y(x, y)$ are reciprocal forms of x and y , X be a cubic, and Y be a square form, such as $X(0,1) > 0, Y(0,1) > 0$.

Our aim is to obtain and describe in a Poincare circle (A. Andreev, I. Andreeva, 2017) all types of phase portraits, possible – and different in the topological meaning - for the Eq. (1) systems, as well as to indicate special criteria of every portrait's appearance, close to coefficient criteria.

We follow the developed by Henri Poincare method of consecutive mappings: at first we perform a central mapping of a plane x, y (from a center (0, 0, 1) of a sphere Σ), augmented with a line at infinity ($\bar{R}_{x,y}^2$ plane) on a sphere $\Sigma: X^2 + Y^2 + Z^2 = 1$ with identified diametrically opposite points.

The first Poincare transformation helps us to do this:

$$x = \frac{1}{z}, \quad y = \frac{u}{z} \quad (u = \frac{y}{x}, \quad z = \frac{1}{x})$$

The Eq.(1) system this mapping transforms into a system, which in the Poincare coordinates

$$u, z \text{ after a time change } dt = -z^2 d\tau \text{ looks like}$$

$$\frac{du}{d\tau} = P(u)u - Q(u)z, \quad \frac{dz}{d\tau} = P(u)z,$$

where $P(u) \equiv X(1, u)$ and $Q(u) \equiv Y(1, u)$ are reciprocal polynomials.

Secondly we use an orthogonal mapping of a lower enclosed semi sphere of a sphere Σ to a circle $\bar{\Gamma}: x^2 + y^2 \leq 1$ with identified diametrically opposite points of its boundary Γ . This is achieved with the help of the second Poincare transformation.

The second Poincare transformation

$$x = \frac{v}{z}, \quad y = \frac{1}{z} \quad \left(v = \frac{x}{y}, \quad z = \frac{1}{y} \right)$$

also unambiguously maps a phase plane $R^2_{x,y}$ onto a Poincare sphere Σ with the diametrically opposite points identified, considered without its equator, and every Eq.(1) system the second Poincare transformation converts into a system, which in the coordinates τ, v, z looks like:

$$\frac{dv}{d\tau} = -X(v, 1) + Y(v, 1)vz, \quad \frac{dz}{d\tau} = Y(v, 1)z^2.$$

The circle $\bar{\Omega}$ and the sphere Σ are correspondingly called in this process the Poincare circle and the Poincare sphere (A. Andronov and other authors, 1973).

Main Notation Basic Definitions

$\varphi(t, p), p = (x, y)$ – a fixed point := a solution (a motion) of an Eq.(1) system with initial data $(0, p)$.

$L_p : \varphi = \varphi(t, p), t \in I_{max}$, - a trajectory of a motion $\varphi(t, p)$.

$L_p^{+(-)}$:= +(-)- a semi trajectory of a trajectory L_p .

O -curve of a system := its semi trajectory $L_p^s (p \neq O, s \in \{+, -\})$, adjoining to a point O under a condition that $st \rightarrow +\infty$.

$O^{+(-)}$ - curve of a system := its O -curve $L_p^{+(-)}$.

$O_{+(-)}$ -curve of a system := its O -curve, adjoining to a point O from a domain $x > 0 (x < 0)$.

TO -curve of a system := its O -curve, which, being supplemented by a point O , touches some ray in it.

A nodal bundle of NO -curves of a system := an open continuous family of its TO -curves L_p^s , where $s \in \{+, -\}$ is a fixed index, $p \in A, A$ - a simple open arc, $L_p^s \cap A = \{p\}$.

A saddle bundle of SO -curves of a system, a separatrix of the point O := a fixed TO -curve, which is not included into some bundle of NO -curves of a system.

E, H, P - O -sectors of a system: an elliptical, a hyperbolic, a parabolic ones.

A topological type (T-type) of a singular point O of a system := a word A_O consisting of letters N, S (a word B_O consisting of letters E, H, P), which describes a circular order of bundles N, S of its O -curves (of its O -sectors E, H, P) when traversing the point O in the «+»-direction, i. e. counterclockwise, starting with some of them.

$$P(u) = X(1, u) \equiv p_0 + p_1 u + p_2 u^2 + p_3 u^3, \\ Q(u) = Y(1, u) \equiv a + bu + cu^2$$

Note 1. For each Eq.(1) system:

- 1) a topological type (T-type) of a singular point O in its form B_O is naturally to obtain from its T-type in the form A_O , and backwards (we have to find both forms);
- 2) the real roots of a polynomial $P(u)$ (polynomial $Q(u)$) are actually the angular coefficients of isoclines of infinity (isoclines of a zero);
- 3) while listing the real roots of the system's polynomials $P(u), Q(u)$, altogether or separately, we number the roots of each polynomial in an ascending order.

Investigation of a Singular Point O (0, 0). Topological types of it

For finding of all O -curves and splitting of their totality into the bundles N, S , we apply the method of exceptional directions of a system in the point O (A. Andronov and other authors, 1973). In accordance with this manuscript, an equation of the exceptional directions for the point O of the Eq.(1) system must be written as

$$xY(x, y) \equiv x(ax^2 + bxy + cy^2) = 0.$$

The following cases can be implemented for it:

- 1) if $d \equiv b^2 - 4ac > 0$ this equation defines simple straight lines $x = 0$ and $y = q_i x$, $i = 1, 2$, $q_1 < q_2$.
- 2) if $d = 0$ this equation defines the straight line $x = 0$ and the double straight line $y = qx$, $q = -\frac{b}{2c}$.
- 3) if $d < 0$ – only a straight line $x = 0$.

Theorem 1. Words A_0 and B_0 defining a T-type of a singular point $O(0, 0)$ of the Eq.(1) system:

- 1) if $d > 0$ depending on signs of values $P(q_i)$, $i = 1, 2$, have forms, indicated in a Table 1,
- 2) if $d = 0$ depending on signs of values q and $P(q)$ - forms, indicated in a Table 2,
- 3) if $d < 0$ a form: $A_0 = S_0 S^0$, $B_0 = HH$

(A. Andreev, I. Andreeva, 2007, 2008, 2009, 2010, 2017).

Table 1. T-type of a singular point in the case of $d > 0$ ($r = \overline{1,6}$).

r	$P(q_1)$	$P(q_2)$	A_0	B_0
1, 4	+	+	$S_0 S_+^1 N_+^1 S_+^0 N_-^1 S_-^2 = S_0 S_+^1 N S_-^2$	PH^2
2	-	-	$S_0 N_+^1 S_+^1 S_+^0 S_-^1 N_-^2 = N S_+^2 S_+^0 S_+^1$	PH^2
3, 6	-	+	$S_0 N_+^1 N_+^1 S_+^0 S_-^1 S_-^2$	$PEPH^3$
5	+	-	$S_0 S_+^1 S_+^2 S_+^0 N_-^1 N_-^2$	H^3PEP

Table 2. T-type of the singular point $O(0, 0)$ in the case of $d = 0$.

q	$P(q)$	A_0	B_0
+	+	$S_0 S_+ N_+ S^0$	H^2P
-	-	$S_0 N_+ S_+ S^0$	PH^2
+	-	$S_0 S^0 S_- N_-$	H^2P
-	+	$S_0 S^0 N_- S_-$	PH^2
0	+	$S_0 S_+ N S_-$	H^2P
0	-	$N S_+ S^0 S_-$	PH^2

Note 2. It is necessary to explain the meaning of some new symbols appeared in the statement of the Theorem 1. A symbol S_0 (a symbol S^0) means a bundle S , adjoining to the point $O(0, 0)$ from the domain $x > 0$ along a semi axis $x = 0, y < 0$, when $t \rightarrow +\infty$ (along a semi axis $x = 0, y > 0$, when $t \rightarrow -\infty$).

A lower sign index «+» or «-» of every bundle N or S , different from S_0 and S^0 , indicates whether the bundle consists of \mathcal{O}_+ -curves or of \mathcal{O}_- -curves.

Upper index 1 or 2 of every bundle indicates whether its O -curves adjoining to the point O along a straight line $y = q_1 x$ or along a straight line $y = q_2 x$.

In the Table 2, lines 5, 6, a bundle N doesn't have a lower sign index, because it contains both \mathcal{O}_+ -curves and \mathcal{O}_- -curves simultaneously.

Corollary 1. It's possible to deduce from the Theorem 1, that Eq.(1) systems on the $R^2_{x,y}$ plane do not have limit cycles.

Really, a limit cycle could surround a singular point $O(0,0)$, and in that case the Poincare index of such a singular point should equal to 1 (A. Andronov and other authors, 1973). But let us use the Bendixon's formula for the index of an isolated singular point of a smooth dynamic system. It looks like the follows:

$$I(O) = 1 + \frac{\vartheta - k}{2},$$

where $\vartheta(k)$ is a number of elliptical (hyperbolic) O -sectors of the system. Bendixon's formula and our Theorem 1 say, that Poincare index $I(O) = 0$ for the singular point $O(0, 0)$ of every Eq.(1) system.

Corollary 2. For the singular point $O(0, 0)$ of the Eq.(1) system eleven different topological types are possible. Their further analysis give: for every Eq.(1) system a singular point $O(0, 0)$ has not more than four separatrices (in fact 2, 3 or 4 of them).

Infinitely Remote Singular Points (IR-points)

Further we study infinitely remote singular points of Eq.(1) system.

Topological types of IR-points $O_i(u_i, 0) \neq O_o(0, 0), i = \overline{1, m}$, of Eq.(1) systems are given in the

Theorem 2. Let a real number $u_i (\neq 0)$ be a root having the multiplicity $k_i \in \{1, 2, 3\}$ of a polynomial $P(u)$ of the Eq.(1) system. In this case a value $g_i = P^{(k_i)}(u_i)Q(u_i) \neq 0$ and words A_i^\pm , which determine the T-types of IR-points $O_i^\pm(u_i, 0)$ of such a system, depending on the value of k_i and signs of numbers u_i and g_i , have forms indicated in the Table 3.

Table 3. T-types of IR-points $O_i^\pm(u_i, 0), i \in \{1, \dots, m\}$.

u_i	k_i	g_i	A_i^+	A_i^-
+(-)	1, 3	+	$N_+(N_-)$	$S_-(S_+)$
+(-)	1, 3	-	$S_-(S_+)$	$N_+(N_-)$
+(-)	2	+	$S_-N_+(\emptyset)$	$\emptyset(N_-S_+)$
+(-)	2	-	$\emptyset(N_-S_+)$	$S_-N_+(\emptyset)$

Corollary 3. For the IR-points of the Eq.(1) systems only finite number, namely 13 of different T-types can appear. The further study of them indicates, that IR-points of each Eq.(1) system may have only m separatrices: one separatrix per each singular point $O_i(u_i, 0), i = \overline{1, m}$.

Note 3. In the tables 3 and 4 a lower sign index «+» or «-» of every bundle N or S , indicates whether the bundle adjusts to the point O_i^+ (or to the point O_i^-) from the side $u > u_i$ or from the side $u < u_i$ of the isocline $u = u_i$.

Different Subfamilies of an Eq.(1) Family of Dynamic Systems

Further we shall discuss special subfamilies of different order, which must be naturally distinguished depending on particular form of the decompositions of their polynomial right parts into multipliers of lower degrees. They need individual investigation and show different results of it, surely having also some common features.

Systems Containing 3 and 2 Multipliers in their Right Parts

Here we discuss Eq. (1) systems with decompositions of forms $X(x, y), Y(x, y)$ into real forms of lower degrees including 3 and 2 multipliers correspondingly:

$$X(x, y) = p_3(y - u_1x)(y - u_2x)(y - u_3x), Y(x, y) = c(y - q_1x)(y - q_2x), \quad (2)$$

where $p_3 > 0, c > 0, u_1 < u_2 < u_3, q_1 < q_2, u_i \neq q_j$ for each i and j .

The investigation method demands the following actions.

Basic notation and main concepts

$P(u), Q(u)$ – system’s polynomials P, Q :

$$P(u) := X(1, u) \equiv p_3(u - u_1)(u - u_2)(u - u_3), Q(u) := Y(1, u) \equiv c(u - q_1)(u - q_2).$$

$RSP(RSQ)$ – be an ascending sequence of all real roots of the polynomial $P(u) (Q(u))$, $RSPQ$ – be an ascending sequence of all real roots of both polynomials $P(u), Q(u)$.

A Double Change (DC)-transformation let’s call a double change of variables: $(t, y) \rightarrow (-t, -y)$. A Double Change transformation converts a system into another dynamic system, where signs and numberings of roots of $P(u)$,

$Q(u)$, and also the direction of motion upon trajectories with the increasing of t are reversed. We call a pair of different Eq. (2) systems mutually inversed in relation to a DC-transformation, if such a transformation converts one system in this pair into another member of the given pair, and call them independent of a DC-transformation otherwise.

Naturally, 10 diverse types of $RSPQ$ may appear for an arbitrary Eq. (2) system, due to $C_5^2 = \frac{5!}{2!2!} = 10$.

Using the DC-transformation of Eq. (2) systems we can conclude: six of them appear to be independent in pairs. But each of the rest four systems has the mutually inversed one among the first six dynamic systems.

Now we assign a specific number $r \in \{1, \dots, 10\}$ to each one of different $RSPQ$'s of the Eq. (2) systems in such a way that $RSPQ$ $r = \overline{1,6}$ will be independent in pairs, but $RSPQ$ sequences numbered with $r = \overline{7,10}$ will be mutually inversed to $RSPQ$'s having numbers $r = \overline{1,4}$.

The following notion is important.

An r -family of the Eq. (2) systems := the totality of systems (belonging to the Eq. (2) family) having the $RSPQ$ number r .

Via the common plan we research families of Eq. (2) systems with numbers $r = \overline{1,6}$. For families numbered with $r = \overline{7,10}$, we receive data using the DC-transformation of families, $r = \overline{1,4}$.

Here is a sequential plan of investigations for every given Eq. (2) family.

Step 1. We draw up a list of singular points of systems in a Poincare circle $\overline{\Omega}$. They are: a point $O(0, 0) \in \Omega$ and points $O_i^\pm(x_i, 0) \in \Gamma$, $i = \overline{0,3}$, $x_0 = 0$. For every certain point in the list we apply the notions of a saddle (S) and node (N) bundles of adjacent to this point semi trajectories, of a separatrix of this singular point, and of its topodynamical type (TD – type).

Step 2. Divide the whole family into subfamilies with numbers $s = \overline{1,7}$. For each given subfamily find topodynamical types of singular points as well as separatrices of them.

Step 3. Reveal the separatrices' behavior for all singular points of systems $\forall s \in \{1, \dots, 7\}$. The important questions are: a question of uniqueness of continuation of every given separatrix from a small neighborhood of a singular point to all the lengths of it; a question of a mutual arrangement of all separatrices in a Poincare circle Ω . We have answered this questions for all families of considered systems.

Step 4. Depict phase portraits belonging to systems of a given family and describe criteria of each portrait existence.

Investigation results for these subfamilies looks like the follows.

Systems belonging to the family number $r=1$ have 25 different types of phase portraits.

Families number 2 and 3: there exist 9 types of phase portraits per each family.

Families 4 and 5: there are 7 types of phase portraits per each one.

Systems belonging to the family number $r=6$ show us 36 different topological types of phase portraits.

Thus we conclude, that 93 different types of phase portraits in a Poincare circle exist in a total for the Eq. (2) systems. At the first glance there are lots of possibilities. But keep in mind, please: every chosen subfamily includes an uncountable number of differential dynamic systems.

Other Possible Types of Right Parts

Here we enlist other variants of decompositions of polynomials in right parts of our dynamic systems. All those types we've fully investigated and described.

1. Systems, for which decompositions of forms $X(x, y)$, $Y(x, y)$ into real multipliers of lowest degrees contain two multipliers each:

$$X(x, y) = p(y - u_1 x)^{k_1} (y - u_2 x)^{k_2}, \quad Y(x, y) = q(y - q_1 x)(y - q_2 x), \quad (3)$$

where $p, q, u_1, u_2, q_1, q_2 \in \mathbb{R}$, $p > 0, q > 0, u_1 < u_2, q_1 < q_2, u_i \neq q_j$ for each $i, j \in \{1, 2\}$, $k_1, k_2 \in \mathbb{N}$, $k_1 + k_2 = 3$.

It's naturally to distinguish two classes of Eq. (3) -systems. The A class contains systems with $k_1 = 1, k_2 = 2$, and the B class contains systems with $k_1 = 2, k_2 = 1$.

2. Systems containing 3 and 1 different multipliers in right parts.

$$\frac{dx}{dt} = p_3(y - u_1 x)(y - u_2 x)(y - u_3 x), \quad \frac{dy}{dt} = c(y - q_1 x)^2, \quad (4)$$

$p_3 > 0, c > 0, u_1 < u_2 < u_3, q (\in \mathbb{R}) \neq u_i, i = \overline{1, 3}$.

3. Systems containing 2 and 1 different multipliers in right parts.

$$\dot{x} = p_0 x^3 + p_1 x^2 y + p_2 x y^2 + p_3 y^3 \equiv p_3 (y - u_1 x)^2 (y - u_2 x), \quad (5)$$

$$\dot{y} = x^2 + bxy + cy^2 \equiv c(y - qx)^2,$$

where $p_3 > 0, c > 0, u_1 < u_2, q (\in \mathbb{R}) \neq u_{1,2}$.

Conclusion

This paper presents the results of the original investigation project. Its global aim is to reveal and describe all phase portraits in a Poincare circle different in the topological sense, which are possible for the broad and extended family of dynamic differential systems. All those portraits have been successfully constructed in the two forms - in the descriptive (as a table) and in the graphical ones.

The second aim of this work was to develop, successfully apply and describe certain new effective methods of investigation (A. Andreev, I. Andreeva, 2007, 2010, 2017).

Recommendations

The article presents a theoretical work, but above mentioned new methods of investigation may be useful for applied studies of dynamic systems of the second order with polynomial right parts. The work may be interesting for researchers as well as for students and post-graduate students.

Acknowledgements

This work would never be done without a great and immeasurable contribution of Professor Dr. Alexey Andreev, the Department of Differential Equations, St. Petersburg State University.

References

- Andronov, A.A., Leontovich, E.A., Gordon, I.I., & Maier, A.G. (1973). *Qualitative theory of second-order dynamic systems*. New York, NY: Wiley.
- Andreev, A.F., & Andreeva, I.A. (1997). On limit and separatrix cycles of a certain quasiquadratic system. *Differential Equations*, 33 (5), 702 – 703.
- Andreev, A.F., & Andreeva, I.A. (2007). Local study of a family of planar cubic systems. *Vestnik St. Petersburg University: Ser. I. Mathematics, Mechanics, Astronomy*, 2, 11- 16. DOI: 10.3103/S1063454107020021, EID: 2-s2.0-84859730890.
- Andreev, A.F., Andreeva, I.A., Detchenya, L.V., Makovetskaya, T.V., & Sadovskii, A.P. (2017). Nilpotent Centers of Cubic Systems. *Differential Equations*, 53(8), 1003 - 1008. DOI: 10.1134/S0012266117080018, EID: 2-s2.0-85029534241.

- Andreev, A.F., & Andreeva, I.A. (2007). Phase flows of one family of cubic systems in a Poincare circle. I. *Differential Equations and Control*, 4, 17-26.
- Andreev, A.F., & Andreeva, I.A. (2008). Phase flows of one family of cubic systems in a Poincare circle. II. *Differential Equations and Control*, 1, 1 - 13.
- Andreev, A.F., & Andreeva, I.A. (2008). Phase flows of one family of cubic systems in a Poincare circle. III. *Differential Equations and Control*, 3, 39 - 54.
- Andreev, A.F., & Andreeva, I.A. (2009). Phase flows of one family of cubic systems in a Poincare circle. IV₁. *Differential Equations and Control*, 4, 181 - 213.
- Andreev, A.F., & Andreeva, I.A. (2010). Phase flows of one family of cubic systems in a Poincare circle. IV₂. *Differential Equations and Control*, 4, 6- 17.
- Andreev, A.F., & Andreeva, I.A. (2017). Investigation of a Family of Cubic Dynamic Systems. *Vibroengineering Procedia*, 15, 88 – 93. DOI: 10.21595/vp.2017.19389.

Author Information

Irina Andreeva

Peter the Great St. Petersburg Polytechnic University
195251 St. Petersburg, Polytechnicheskaya, 29.
Russian Federation
Contact e-mail: irandr2@gmail.com

Importance of Smart Energy Management Algorithm in Renewable Energy Sources Integrated Energy Storage Unit

Yagmur KIRCICEK
Karabük University

Ahmet AKTAS
Istanbul Gelişim University

Mehmet OZKAYMAK
Karabük University

Abstract: The main problem in adding Renewable Energy Sources (RES) to electric power systems is that the energy generated from these sources is often unstable and volatile, depending on the climatic conditions. When the sun shines very well from the solar energy, a high amount of electricity can be produced on a cloudless day. In wind energy, when the wind speed is above a certain value, electricity is obtained with high efficiency and most importantly the energy production values change continuously according to the climatic conditions (solar brightness, wind speed etc.). This disadvantage of the RES can be eliminated by adding an energy storage unit to the established power generation system. Energy storage unit is required to be controlled by a smart energy management algorithm in the case of storage of energy overload of the energy storage unit, energy storage unit in case of load demand, and possible working conditions such as providing end user benefit by taking the RES. In this way, the energy demand of the customer will be met in a stable, high quality and continuous manner without a power loss in the system to be formed. In addition, the smart energy management algorithm raises the power quality factor in the electric grid, thus preventing frequency fluctuations, voltage fluctuations and other problems. Smart energy management control for distributed network infrastructures, together with being an indispensable unit, constitutes the most important part of the smart network concept. In this study, the importance of smart energy management algorithm in RES, which includes energy storage system, includes the contributions to the smart grid infrastructure and the benefits provided to the end user.

Keywords: Energy storage, Renewable energy resources, Smart energy management algorithm, Smart grids

Yenilenebilir Enerji Kaynakları Entegre Enerji Depolama Birimi'nde Akıllı Enerji Yönetimi Algoritmasının Önemi

Özet: Yenilenebilir Enerji Kaynaklarının (YEK) elektrik sistemlerine eklenmesi konusundaki asıl sorun, bu kaynaklardan üretilen enerjinin iklim koşullarına bağlı olarak genellikle istikrarsız ve değişken olmasıdır. Güneş çok iyi parladığında güneş enerjisinden, bulutsuz bir günde yüksek miktarda elektrik üretilebilir. Rüzgar enerjisinde rüzgar hızı belirli bir değerin üstünde olduğunda, yüksek verimlilikle elektrik elde edilir ve en önemlisi enerji üretim değerleri iklim koşullarına (güneş parlaklığı, rüzgar hızı vb.) göre sürekli değişir. YEK'nın bu dezavantajı, kurulu güç üretim sistemine bir enerji depolama birimi eklenerek ortadan kaldırılabilir. Enerji depolama ünitesinin, enerji depolama ünitesinin enerji yükünün depolanması, yük talebi durumunda enerji depolama ünitesinin depolanması ve son kullanıcı faydasının sağlanması gibi olası çalışma koşullarında akıllı enerji yönetim algoritması tarafından kontrol edilmesi gerekmektedir. YEK, böylelikle, müşterinin enerji talebi, oluşacak sistemde güç kaybı olmaksızın, kararlı, yüksek kaliteli ve sürekli bir şekilde karşılanacaktır. Ek olarak, akıllı enerji yönetimi algoritması elektrik şebekesindeki güç kalitesi faktörünü yükselterek frekans dalgalanmalarını, voltaj dalgalanmalarını ve diğer problemleri önler. Dağıtık ağ altyapıları için akıllı enerji yönetimi kontrolü, vazgeçilmez bir birim olmanın yanı sıra akıllı ağ konseptinin en önemli bölümünü oluşturmaktadır. Bu çalışmada, enerji depolama sistemini içeren YEK'da akıllı enerji yönetimi algoritmasının önemi, akıllı şebeke altyapısına ve son kullanıcıya sağlanan faydalara katkıları içermektedir.

Anahtar Kelimeler: Enerji depolama, Yenilenebilir enerji kaynakları, Akıllı enerji yönetimi algoritması, Akıllı şebekeler

Giriş

Yenilenebilir enerji kaynakları (YEK), fosil yakıtlara alternatif bir kaynak olarak sunulmaktadır. Yenilenebilir enerji kaynaklarından en yaygın olarak kullanılan sistemler, güneş ve rüzgâr kaynaklı sistemlerdir. Bu yenilenebilir enerji kaynakları çevre dostu ve sürdürülebilir bir yapıya sahip olduklarından kullanım oranı

giderek artmaktadır. Güneşin en parlak olduğu durumda fotovoltaik (FV) sistemler kararlı bir şekilde elektrik enerjisi üretirken, bulutlu ve akşam saatlerinde elektrik üretimi durmaktadır. Rüzgâr enerji sistemleri de aynı şekilde rüzgâr hızına bağlı olarak üretim gerçekleştirmektedir.

Yenilenebilir enerji kaynaklarının bu kararsız ve kesintili yapısı enerjinin sürekliliği konusunda önemli problemler ortaya çıkarmaktadır. Böylece YEK'ten üretilen enerji, genel enerji talebi ile örtüşmemektedir.

Bundan dolayı kullanıcılar tarafından enerjinin talep edilmediği ve YEK'ten üretilen tepe enerji miktarının çok olduğu durumda enerji depolama sistemlerinin önemi ortaya çıkmaktadır. Yenilenebilir enerji sistemleri depolama birimleri ile birlikte kullanılırsa, üretilen enerji depolanarak kullanıcılar için enerjinin sürekliliği sağlanmış olmaktadır. Böylelikle enerji depolama sistemleri kullanılarak YEK'e bağlı yük talebi sürekli olarak karşılanabilmektedir.

Bir akıllı mikro şebeke yapısı için enerji depolama sistemi oldukça önemlidir. Şebekedeki yüklerin doğru çalışmasını sağlamak için kullanılan enerji depolama sistemi aynı zamanda güç kalitesini de yükseltebilir. Enerji depolama uygulamaları ile çıkış gücü, iklim şartlarına bağlı değişen rüzgâr türbinleri, yalnız gündüz çalışabilen ve hava şartlarına göre değişen güneş enerji sistemleri gibi yenilenebilir enerji sistemlerinden kaynaklanan güç değerlerindeki değişim/dalgallılıkla başa çıkılabilir. Yenilenebilir enerji temelli akıllı mikro şebeke kavramı, kaynaklardan faydalanmanın ve fosil yakıt tüketiminin azaltılmasında iyi bir yoldur. Enerji depolama uygulamalarının kullanımı, yüklere kaliteli güç sağlanması için mikro şebekelerin kullanılmasıyla zorunlu hale gelmektedir. Mikro şebekelerde; şebekeye bağlı ve izole/ada modu olarak adlandırabileceğimiz iki işletme modu vardır. İzole/ada modu işletme süresince enerji depolama biriminin temel sorumluluğu enerji dengesinin sağlanmasıdır. Şebekeye bağlı mod süresince amaç yenilenebilir enerji kaynaklarının kesintili ve yük dalgalanmasının şebekeyi etkilemesinin/yayılmasının önlenmesidir. Tek tip bir enerji depolama ile yenilenebilir güç kullanan mikro şebekede bu işlevlerin tümü etkili/verimli bir şekilde gerçekleştirilemez. Fotovoltaik gibi kesintili yapıdaki yenilenebilir enerji kaynakları; yüksek enerji yoğunluklu depolama kullanımını gerektirmektedir. Aynı zamanda yükteki hızlı/ani değişimler/dalgalanmalar yüksek güç yoğunluklu depolama kullanımı ister. Bu tez çalışmasında önerilen batarya ve ultrakapasitörden oluşan HEDS, yüksek enerji ve yüksek güç yoğunluğuna sahip bir birleşik enerji depolama birimi olarak tasarlanmıştır. Bu hibrit yapı akıllı mikro şebeke uygulamaları için enerji depolama sistemlerinin gerçekleştirilmesinde oldukça gelecek vaat eden bir seçenektir [Castillo, A. & Kousksou, T.].

YEK'te enerji depolama birimlerinin kullanımı yaygın olarak artmakla birlikte bu sistemlerin kontrolü büyük önem kazanmaktadır. Sistemlerde bulunan birimlerin artmasıyla birlikte bu birimlerin kontrolü kullanıcı ve sistem güvenliği için vazgeçilmez bir unsur haline gelmektedir. Şebeke altyapısı, son kullanıcı ve diğer birimler arasındaki kontrollü haberleşme hem sistem verimi hem de sistem kararlılığını arttırmak için akıllı enerji yönetim algoritmalarının geliştirilerek kullanılmaktadır.

Yenilenebilir Enerji Kaynaklarında Enerji Depolama Birimlerinin Kullanılması

Mikro şebeke uygulamaları ve yenilenebilir enerji kaynaklarından güç üretiminin yaygınlaşmasıyla birlikte artan güç talebini karşılamak için enerji verimliliğinin yanında gerekli enerji tamponu olarak görev yapacak sistemler ve verimli enerji depolama sistemleri oldukça önem kazanmıştır. Günümüzde su pompalama, bataryalar, sıkıştırılmış hava, volanlar, ultrakapasitörler gibi bir çok enerji depolama teknolojileri şebekeyi kontrol etmek için kullanılmaktadır [Eyer, J. & Rajasekharan, J.]. Enerji depolama sistemleri, net yük değişimlerini izlemek, gerilim ve frekansı sabitlemek, tepe yükleri karşılamak, güç kalitesini iyileştirmek, yenilenebilir enerji kaynaklarının (güneş, rüzgâr vb.) entegrasyonunu kesin bir şekilde desteklemek amacıyla ve elektrikli araçlarda kullanılmaktadır [Denholm, P. & Diaz, G. F. & Connolly, D. & Quan, X.].

Dağıtık üretimde güneş ve rüzgâr gibi yenilenebilir enerji kaynaklarının şebekeye bağlantısı günümüzde oldukça önem kazanmıştır. Mikro şebekelerde dağıtık üretimlerin hızlı bir şekilde artması kurulu üretim kapasitesinin yüzdesinde artışa neden olmuştur. Fakat bu enerji kaynaklarının dalgalı ve kesintili doğası, elektrik şebekesinin çalışması ve kararlılığını önemli şekilde etkileyen güç akışında dalgalanmalara neden olmaktadır [Roberts, B. P.]. Bu problemleri çözmek için, süper iletken manyetik enerji depolama, ultrakapasitör enerji depolama, volan enerji depolama gibi gelişmiş teknoloji temelli kısa süreli dağıtık enerji depolama sistemleri mikro şebekede şebeke ve yük arasındaki anlık karşılaştırmayı dengelemek için alternatif potansiyel çözümler olarak bulunmaktadır [Wei, Z. & Tan, X.].

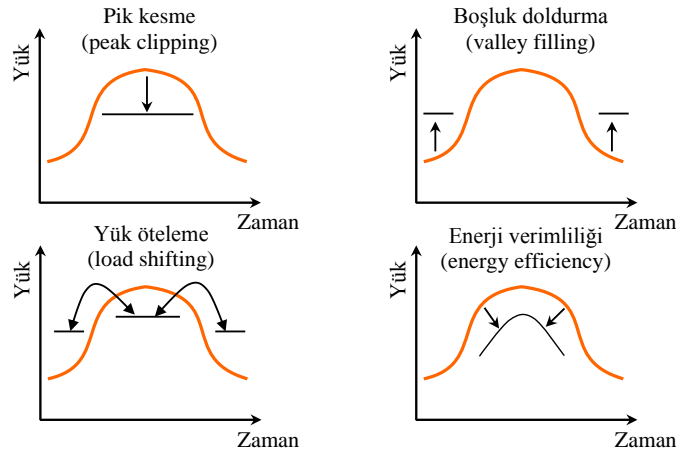
Birden fazla enerji depolama sistemi birbirini tamamlayıcı performans özellikleri ile birlikte kullanıldığında ortaya çıkan sistem bir hibrit enerji depolama sistemi olmaktadır. Bataryalar maliyet bakımından en uygun enerji depolama teknolojilerinden biridir. Ancak bataryaların anlık güç dalgalanmalarını karşılamak amacıyla enerji tamponu olarak kullanılması mümkün olmasa da, bu durumda kullanım ömründe ciddi oranda azalma

olmaktadır. Bir ultrakapasitörde enerjinin depolanması, bataryadaki gibi bir elektrokimyasal süreç yerine statik yüklenme ile yapıldığından bataryaya göre daha yüksek güç yoğunluğuna sahiptir. Bu yüzden daha iyi güç ve enerji performansı sağlamak için bu iki depolama cihazını birleştirmek oldukça avantajlı olmaktadır. Batarya ve ultrakapasitör, akım veya gücün uygun şekilde ikisi arasında paylaşılması ile aynı anda şarj veya deşarj olabilirler. Batarya şarj veya deşarj modlarının ikisinde de baskın olabilir. Hibrit enerji depolama sisteminde iki depolama elemanı arasında güç paylaşımı için farklı kontrol yöntemleri geliştirilmiştir [Wu, H. & Khajepour, J. & Moore, A. T.].

Bir mikro şebekenin en önemli özelliği, gerekli durumlarda çok hızlı bir şekilde ana şebekeden ayrılabilmesi, ada modunda işletmeye geçebilmesi ve gerektiğinde de ada modundan tekrar şebekeye bağlı duruma geçebilmesidir. Bu durumda mikro şebeke yüklerin enerji ihtiyacını dinamik olarak yüklerden gelecek bilgiye ihtiyaç duymaksızın sağlayabilmelidir. Bu durum sistemde enerji depolama birimleri kullanmayı gerektirmektedir. Kontrol yöntemi açısından bakıldığında şebeke bağlı durum ile şebekeden bağımsız durumlarda farklı kontrol stratejileri uygulanması gerekmektedir. Şebeke bağlantılı durumda şebeke, gerilim ve frekans için referans değerleri sağlamaktadır. Ancak şebekeden bağımsız duruma geçildiğinde mikro şebeke, yük talebi ile üretim dengesini sağlaması gerektiği gibi, gerilim ve frekans referans değerlerini de kendi içerisinde oluşturmak durumundadır. Bu şekilde farklı iki işletme modu ve her farklı işletme modu için farklı kontrol stratejisi ihtiyacı modlar arası geçiş işlemlerinin başlıca zorluklarıdır. Ayrıca asıl endişe gerektiren nokta ada işletme modundan şebekeye bağlı moda geçiş işlemidir, çünkü ada modunda kullanılan referans değerler ile şebeke bağlı moda kullanılan referans değerler farklı olmaktadır [Damjanovic, N.].

Çalışma modlarına karar verecek ve belirlenen çalışma modu için referans değerlerin üretilmesini sağlayan bir akıllı enerji yönetim algoritma birimi gerekmektedir. Sistemin şebekeye bağlantı noktasından alınacak sinyaller ile şebeke bağlı mod veya ada modu çalışma modlarına karar verilir. Şebekeye bağlı çalışma modunda mikro şebeke, güç üreticisi olarak çalışır. Şebeke bağlı mod için; pik kesme (peak clipping), boşluk doldurma (valley filling), enerji verimliliği (energy efficiency) durumları vardır. Bu durumlar yalnız şebeke bağlı çalışma modu için geçerlidir. Şebekeden bağımsız, ada modu çalışmasında yük öteleme (load shifting) esastır. Akıllı enerji yönetim algoritmasının kullanıldığı ve dinamik yük kontrol uygulamalarının yapıldığı örnek grafikler Şekil 1'de verilmektedir [Pires, V. F.].

Pik kesme, sistemdeki pik yüklerin azaltılmasıdır. Yük kontrol yönetiminin klasik yollarından biridir. Pik kesme modu kullanıcı tercihli ve kullanıcı tarafından değerleri tanımlanan bir moddur. Kullanıcı şebekeden sürekli beslenmesi gereken bir talep yük değeri tanımlar ve bu yük değerini aşan fazladan yük oluştuğu durumlarda bu fazla yüklerin enerjisi şebekeden çekilmez, yenilenebilir kaynaklardan veya depolanmış enerjiden sağlanır.



Şekil 1. Dinamik yük kontrol uygulamalarına örnek grafikler

Boşluk doldurma, yük kontrol yönetiminin ikinci klasik şeklidir. Boşluk doldurma, pik olmayan zaman dilimleri için yükler oluşturmayı kapsamaktadır. Bu durum özellikle bir zaman periyodundaki yük faktörünün (baz yükün pik yüke oranı) arttırmak için, sonradan yararlanılabilecek enerji depolanması gibi yüklerin devreye alınması ile sağlanmaktadır.

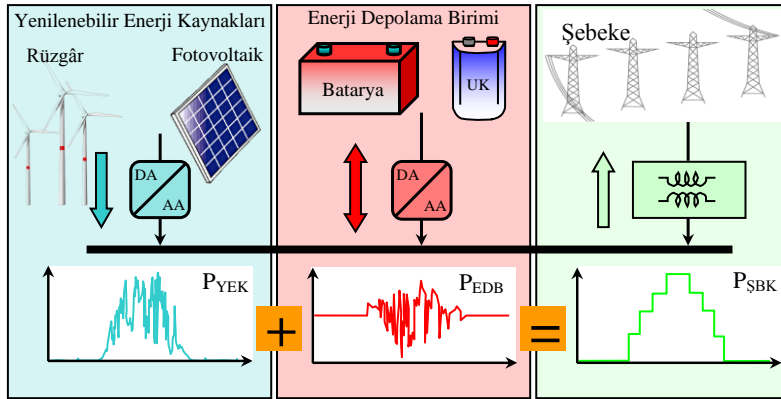
Yük öteleme, yük kontrol yönetiminin son şeklidir. Bu yaklaşım, yüklerin pik saatlerden pik olmayan saatlere ötelenmesini içermektedir. Bu sayede pik talebin karşılanması için gereken üretim tarafı düzenlemelerinin önüne geçilebilecektir. Enerji verimliliği, yük kontrol yönetimi kapsamında değerlendirilebilmektedir. Genellikle kullanılan cihazın teknolojik ya da kullanımsal özelliklerine göre ortaya çıkan bir değişim durumudur. Tüketicinin konfor şartlarını azaltmadan bir hizmet için harcanan birim enerjinin azaltılması, dolayısıyla da yük şeklinin aşağı yönde ötelenmesidir. Tüketiciler ve tedarikçiler yük şeklini değiştirmek için bağımsız hareket

edebilir. Fakat talep tarafı etkileşimi, tedarikçiler ve tüketiciler arasında iki taraflı kazanç sağlayan bir birlikteliği hedeflemektedir [Wu, D.].

Dağıtık üretim şebeke yapıları, akıllı ve mikro şebekelerin bir parçası olmaya başlamıştır. Elektrik güç sisteminde son yıllarda yaşanan gelişmeler, dağıtım seviyesinden güç sistemine bağlanan enerji üretim birimlerini ve enerji depolama birimlerini teşvik eder durumdadır. Bu uygulamalar birlikte ele alındığında dağıtık üretim birimleri olarak tanımlanırlar. Dağıtık üretim birimi olarak uygulanabilecek yeni teknolojiler ticari olarak pazarlanıp uygulanmaya başlamış olmakla birlikte bu sistemlerin şebekeye entegrasyonu, daha verimli kullanılabilmesi ve maliyetlerin azaltılabilmesi adına çeşitli çalışmalar sürmektedir. Dağıtık üretim birimlerine örnek olarak mikro türbinler, yakıt hücreleri, fotovoltaik sistemler, rüzgâr türbinleri, dizel jeneratörler, gaz türbini sistemleri sayılabilir.

YEK sistem entegrasyonunda depolama uygulaması, doğrudan YEK sistem ile bir bütün olarak şebekeye bağlanabildiği gibi, YEK sistem kurulumlarının yoğunlaştığı bölgelerde, merkezi veya dağıtık olarak bağımsız depolama birimleri şeklinde şebekeye bağlanmaları da mümkündür. Bu seçeneklerin tümünde YEK sistem kaynaklı şebeke riskleri önlenilebilir.

Öncelikle depolama ile YEK sistem güç çıkış grafiğinin daha düzgün bir karakter edinmesi sağlanabilir. Belirli limitler üzerindeki güç depolanabilir ve belirli limitler altında kalan güç değerleri için deşarj sağlanabilir böylece YEK sistem ve depolama birimi çıkışında belli bir aralık içerisinde daha düzgün bir güç eğrisine ulaşılabilir. Bu şekilde ani dalgalı güç yapısının şebeke üzerinde yaratacağı olumsuz etkiler bastırılabilir. Şekil 2’de YEK enerji üretim sistemi ve enerji depolama sisteminin akıllı enerji yönetim algoritmasıyla birlikte kullanılmasının sonucu sistemin şebekeye yapmış olduğu olumlu etki verilmektedir [Wu, D.].



Şekil 2. YEK, enerji depolama sistemi ve akıllı enerji yönetim algoritmasının şebekeye etkisi

YEK’e örnek olarak FV sistemleri, çevre dostu yapıları, basit, bakım gerektirmeyen, masrafsız işletme imkânları ile geleceğin güç sistemleri içerisinde vazgeçilmez güç kaynakları olarak yerini almışlardır. Şebeke yapısı, yoğunlukta olan yük karakteri, öncelikli ihtiyaçlar ve enerji üretim birimlerinin karakteristikleri gibi konular iyi incelenerek planlanacak dağıtım bölgeleri içerisinde; ihtiyaca en uygun şekilde cevap verebilecek özellikte farklı enerji depolama uygulamaları tesis edilmesi kaçınılmaz görünmektedir. Geleceğin dağıtık üretim temelli akıllı şebekelerinin en önemli anahtar unsurlarından biri enerji depolama uygulamaları olarak görülmektedir. Enerji depolama uygulamalarının yaygınlaşmasının önündeki en büyük engel maliyetleridir. Ancak FV sistem kurulum maliyetlerinin giderek düşmesi ile yaygınlığı artan küçük güçlü konut tipi FV sistem uygulamaları içerisine entegre edilebilen depolama uygulamalarının teşvik edilmesi sağlanabilirse, depolama uygulamalarının yaygınlaşması ve bahsedilen faydalara ulaşım çok daha ekonomik bir yoldan elde edilecektir. Çünkü bu tarz uygulamalarda kablo tesisatı, haberleşme, kontrol sistemi, güç elektroniği düzenekleri, işçilik vs gibi maliyetler FV sistem ve depolama uygulaması için ortak olmaktadır [Marzband, M.].

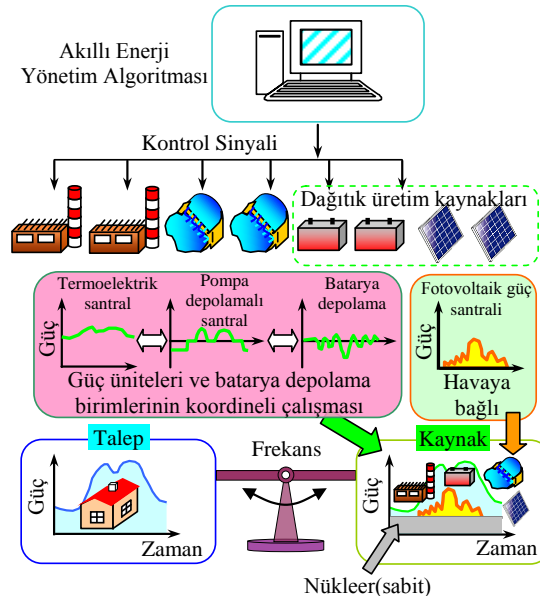
Kritik yüklerin kesintisiz bir şekilde beslenmesini garanti altına alabilmek için, enerji depolama sistemlerinin akıllı enerji yönetim sistemleri ile kontrol edilmesi gerekmektedir. Mikro şebekenin başarılı bir şekilde yönetilmesi, arıza ve bozucu etkilerin meydana geldiği durumlarda depolama sistemlerinin uygun kontrolü ve işletilmesi ile mümkündür. Elektronik olarak birbirine bağlı mikro kaynaklar, düşük atalet ve şebekenin kesintiye uğramadan sürdürülebilmesi bakımından avantajlıdır. Depolama sistemleri bu durumu destekler nitelikte, düşük gerilimli geçici durumlar oluştuğunda, motor kalkışlarında ve diğer kısa süreli aşırı yüklenme durumlarında, özellikle ada modu işletmesinde mikro kaynaklara yardımcı olmaktadır. Enerji depolama sistemleri genellikle doğru akım (DA) gerilim kaynaklarıdır. Bu yüzden alternatif akım (AA) kaynak olarak kullanmak için mutlaka DA/AA çeviriciler kullanılmalıdır. Depolama sistemleri yük talebindeki değişikliklere anında cevap verebilmelidirler. Bu nedenle yerel akıllı enerji yönetim algoritma birimleri tarafından kontrol edilmelidirler. Ultrakapasitör gibi bazı depolama kaynakları yüksek güç yoğunluğuna sahip olmalarına rağmen

kısa zamanda deşarj olurlar. Volan gibi bazı depolama kaynakları ise düşük güç yoğunluđuna sahip olsalar bile uzun bir süre enerji sağlayabilirler [Nguyen, H. K.].

Yenilenebilir Enerji Kaynaklarında Akıllı Enerji Yönetim Algoritmasının Önemi Ve Faydaları

Akıllı enerji yönetim uygulamaları özellikle akıllı şebeke işlevselliikleri ve dağıtık üretim prensibinin uygulanabilmesi konusunda YEK entegrasyonu için anahtar çözüm niteliğindedir. YEK entegrasyonunda depolama uygulamaları tampon görevi üstlenerek YEK çıkış gücündeki deđişimin sınırlanmasını sağlayabilir. Akıllı enerji yönetim algoritması enerji üretimi ile tüketim arasında dengeli işletme sağlayarak, frekans regülasyonu yapar. Rüzgâr ve güneş kaynaklı yenilenebilir enerji üretim birimlerinde çıkış gücü gün içerisindeki hava şartlarına bađlı olarak kısa süreli ani deđişimler gösterebildiđi gibi mevsimsel şartlara bađlı olarak da uzun süreli deđişimler de gösterebilmektedir. Bu güç dalgalanmalarının her türünün önlenmesine yönelik uygun karakteristik yapıya sahip enerji depolama sistemlerini akıllı enerji yönetimiyle birlikte gerçekleştirmek mümkündür. Kısa süreli ani güç salınımlarının bastırılması için batarya, volan, ultrakapasitör gibi enerji depolama teknolojileri kullanılabilirdiđi gibi uzun dönemlere etki eden mevsimsel deđişimleri yönetebilmek için de pompalı hidroelektrik enerji depolama, sıkıştırılmış hava ile enerji depolama gibi farklı uygulamalar tercih edilebilmektedir. Çok daha etkin bir depolama karakteristiđi sağlamak üzere çeşitli depolama uygulamalarının bir arada kullanıldığı hibrit enerji depolama sistemleri de uygulanabilmektedir. Bu tarz hibrit enerji depolama uygulamalarından olan ultrakapasitör ve batarya birleşiminden oluşan sistemler özellikle rüzgâr türbinleri veya FV sistemlerin ürettiđi ani deđişim gösteren dalgalı güç çıkışının düzenlenmesi bakımından gelecek vaat etmektedir. Enerji depolama uygulamalarının faydaları ve kullanım alanlarına genel bir bakış açısı oluşturulmasına yönelik verilen bu bilgiler doğrultusunda ilerleyen bölümlerde enerji depolama teknolojilerinin uygulama alanları ve işletme prensipleri daha detaylı açıklanarak sağlanabilecek faydalar her uygulama konusu sonunda değerlendirilmektedir [Thounthonga, P.].

Dağıtık enerji depolama olarak tarif edilen uygulama, elektrik dağıtım sistemi içerisine dağıtık şekilde ve son tüketicilere yakın konumlarda yerleştiren enerji depolama sistemlerinden oluşmaktadır. Bir veya birkaç büyük kapasiteli depolama birimi yerine dağıtım bölgesinde bu şekilde küçük güçlü çok sayıda depolama sistemi kullanılması daha verimli olabilmektedir. Bu sistem geleceğin akıllı şebekeleri ve enerji piyasası için oldukça uygun bir zemine oturmaktadır, modüler, akıllı, dağıtık sistem olarak akıllı şebeke konseptine uygun özelliktedir. Bu sistem özellikle şebeke işletmecileri tarafından uygulanması halinde dağıtım sistemleri için oldukça önemli bileşenler olabilmektedir [Pincetia, P.].



Şekil 3. YEK'te kullanılan akıllı enerji yönetim algoritmasının kontrol altyapı topolojisi

Akıllı enerji yönetim algoritmalarının YEK sistemlerinde kullanılması birçok muhtemel kombinasyon durumuna bakarak çalışmasıyla oldukça fazla fayda yaratabilmektedir. Güçlü, hızlı cevap yeteneđi olan, esnek bir karar altyapı mekanizmasıyla dinamik davranışları kompanze eden bir kontrol birimidir. Ayrıca bu sistemin özellikle önemli bir işlevi olarak, şebeke güç kalitesi şartlarının sağlanmasına, kararlılık ve güvenilirlik sağlanmasına hizmet edebilir. Tepe talep deđerlerine depolamadan hizmet sağlanması ve bu enerji ihtiyacını talebin düşük olduđu aralıkta elde etmesi sayesinde yükselen talep deđerlerine cevap verebilmek için gereken muhtemel iletim ve dağıtım tesisi yatırımlarının ertelenmesini sağlayabilir. Yine akıllı enerji yönetim algoritması, YEK entegrasyonu konusunda önemli bir görev üstlenebilir. Özellikle dağıtım şebekelerine bađlı

çatı tipi dağıtık FV sistemlerin yaygınlaşması halinde veya benzer şekilde dağıtım şebekesinde bulunan rüzgâr türbinleri olması halinde bu kontrol sistemlerinin şebekede oluşturdukları güç dalgalanması ve güç kalitesi problemlerinin önlenmesinde dağıtık enerji depolama yöntemi ile enerji arz ve talep dengesinin sağlanması, YEK dalgalılık etkilerinin bastırılması konularında başarılı bir etki gösterebilmektedir. Şekil 3'te YEK'te kullanılan akıllı enerji yönetim algoritmasının kontrol altyapı topolojisi verilememiştir. Akıllı enerji yönetim algoritması bütün sistemdeki alt birimleri ayrı ayrı kontrol ederek kullanıcıya kaliteli uygun fiyatlı enerjinin verilmesini sağlamaktadır.

Son tüketici uygulaması olarak akıllı enerji yönetim algoritması, elektrik faturalarından tasarruf amaçlı kullanılmaktadır. Çok zamanlı tarife uygulanan elektrik faturalarında tasarruf sağlayabilmek için şebeke tarife değerlerine ve sürelerine uygun ayarlanmış enerji depolama birimleri içeren akıllı enerji yönetim sistemleri ile tarifenin ucuz olduğu aralıklarda depolanan enerjinin, tarifenin pahalı olduğu ve talep değerinin yükseldiği zamanlarda kullanılması sağlanabilir, böylece faturada tasarruf sağlanabilmektedir. Bu ekonomik faydanın yanı sıra depolama sisteminin sunduğu kesintisiz güç kaynağı özelliği ile de enerji sürekliliği sağlanabilmektedir. Özellikle endüstriyel ve ticari tüketiciler için uygulanan sözleşme gücü ve güç aşımı durumlarında ödenen ceza bedellerinin önlenmesinde yine depolama uygulamalarından yararlanılabilir, böyle bir uygulamada güç aşımına sebep olan tepe güç talepleri depolama biriminden sağlanarak şebekeden fazla güç çekilmesi önlenmiş olur. Gerek konut yüklerinde gerekse endüstriyel ve ticari yüklerde, yukarıda bahsedilen şekilde depolama uygulamaları YEK kullanımı ile entegre şekilde daha etkin sonuçlar sağlayabilmektedir [Dash, V.].

Sonuçlar

YEK'te yaşanan teknolojik gelişmelerle beraber, elektrik güç sistemi tamamıyla bir değişim geçirmektedir. Bu değişimin hedefleri; temiz ve yenilenebilir enerji potansiyelinin en yüksek oranda değerlendirilmesi, tüketicilere daha güvenilir ve kaliteli enerji sağlanması, akıllı enerji yönetim sistemlerinin kullanılması ile ölçüm, denetim, işletme, bakım işlemlerinin daha başarılı bir şekilde gerçekleştirilmesi, sistemde yaşanan arızalar ve kesintilerin önlenmesi olarak sayılabilir.

Elektrik tarifesindeki farklılara göre depolama ve deşarj sağlanarak elektriğin ucuz olduğu aralıkta şarj sağlayıp, elektriğin pahalı olduğu aralıkta tüketicilere depolanmış enerjiyi sunabilmesi akıllı enerji yönetim algoritmasının en büyük avantajlarından biridir.

Eğer depolama sistemi, güç elektroniği veya güç dönüştürücü yapısına sahipse; akıllı enerji yönetim algoritması depolama birimini de devreye alarak güç kalitesi kontrolü yapar, gerilim ve reaktif güç düzenlemesine imkân veren bir araç olarak da işletebilir. Bu şekilde güç kalitesi şartlarının önemli bir bileşeni olan gerilim kararlılığı sağlanabilir. Şebeke tarafında oluşan değişken ve ani yük geçiş durumları meydana geldiğinde akıllı enerji yönetim algoritmasının hızlı tepkisiyle birlikte güç ve gerilim dalgalanmalarının önüne geçilmektedir.

Teşekkürler

Bu çalışma TÜBİTAK tarafından 117E767 nolu proje kapsamında desteklenmektedir.

Kaynakça

- Castillo, A., Gayme, D. F., (2014). "Grid-scale energy storage applications in renewable energy integration: A survey", *Energy Conversion and Management*, 87, 885-894.
- Connolly, D., (2010). "A Review of Energy Storage Technologies for the Integration of Fluctuating Renewable Energy", PhD Thesis, University of Limerick, Department of Energy Engineering, Ireland.
- Damnjanovic, N., (2011). "Smart Grid Functionality of a PV- Energy Storage System", Master Thesis, University of South Florida, Department of Electrical Engineering, USA.
- Dash, V., Bajpai, P., (2015). "Power management control strategy for a stand-alone solar photovoltaic-fuel cell-battery hybrid system", *Sustainable Energy Technologies and Assessments*, 9, 68-80.
- Denholm, P., Ela, E., Kirby, B., (2010). "Milligan M., The role of energy storage with renewable electricity", *National Renewable Energy Laboratory, NREL/TP-6A2-47187*, 6-44.
- Diaz, G. F., Sumper, A., Gomis, B. O., Villafafila, R., (2012). "A review of energy storage technologies for wind power applications", *Renewable and Sustainable Energy Reviews*, 16, 2154-2171.
- Eyer, J., Corey, G., (2010). "Energy storage for the electricity grid: Benefits and market potential assessment guide", *Sandia National Laboratories, SAND2010-0815*, 1-160.

- Khajesalehi, J., Hamzeh, M., Sheshyekani, K., Afjei, E., (2015). "Modeling and control of quasi Z-source inverters for parallel operation of battery energy storage systems: Application to microgrids", *Electric Power Systems Research*, 125, 164-173.
- Kousksou, T., Bruel, P., Jamil, A., Rhafiki, T. E., Zeraouli, Y., (2014). "Energy storage: Applications and challenges", *Solar Energy Materials & Solar Cells*, 120, 59-80.
- Marzband, M., Parhizi, N., Savaghebi, M., Guerrero, J. M. (2016). "Distributed smart decision-making for a multimicrogrid system based on a hierarchical interactive architecture", *IEEE Transactions on Energy Conversion*, 31(1), 637-648.
- Moore, A. T., (2012). "Design, Implementation and Evaluation of A Microgrid in Island and Grid Connected Modes With A Fuel Cell Power Source", Master Thesis, University of Western Ontario, Electrical and Computer Engineering, Canada.
- Nguyen, H. K., Song, J. B., Han, Z., (2015). "Distributed Demand Side Management with Energy Storage in Smart Grid", *IEEE Transactions on Parallel and Distributed Systems*, 26(12), 3346-3357.
- Pincetia, P., Vantia, M., Broccab, C., Carnesecchib, M., Macera, C. P., (2015). "Design criteria for a power management system for microgrids with renewable sources", *Electric Power Systems Research*, 122, 168-179.
- Pires, V. F., Romero, E., Vinnikov, D., Roasto, I., Martins, J. F., (2014). "Power converter interfaces for electrochemical energy storage systems-A review", *Energy Conversion and Management*, 86, 453-475.
- Rajasekharan, J., Koivunen, V., (2014). "Optimal Energy Consumption Model for Smart Grid Households With Energy Storage", *IEEE Journal of Selected Topics in Signal Processing*, 8(6), 1154-1166.
- Roberts, B. P., Sandberg, C., (2011). "The role of energy storage in development of smart grids", *Proceedings of the IEEE*, 99(6), 1139-1144.
- Tan, X., Li, Q., Wang, H., (2013). "Advances and trends of energy storage technology in Microgrid", *International Journal of Electrical Power & Energy Systems*, 44(1), 179-191.
- Thounthonga, P., Chunkag, V., Sethakul, P., Sikkabut, S., Pierfederici, S., Davat, B., (2011). "Energy management of fuel cell/solar cell/supercapacitor hybrid power source", *Journal of Power Sources*, 196, 313-324.
- Quan, X., Dou, X., Wu, Z., Hu, M., Yuan, J., (2016). "Harmonic voltage resonant compensation control of a three-phase inverter for battery energy storage systems applied in isolated microgrid", *Electric Power Systems Research*, 131, 205-217.
- Wei, Z., Garrett, D., Butkowski, J., Yang, W., (29-31 May 2012). "Overview of distributive energy storage systems for residential communities", *IEEE EnergyTech*, Cleveland, Ohio.
- Wu, D., Tang, F., Dragicevic, T., Vasquez, J. C., Guerrero, J. M., (2015). "A control architecture to coordinate renewable energy sources and energy storage systems in islanded microgrids", *IEEE Transactions on Smart Grid*, 6(3), 1156-1166.
- Wu, D., Tang, F., Dragicevic, T., Vasquez, J. C., Guerrero, J. M., (2014). "Autonomous active power control for islanded AC microgrids with photovoltaic generation and energy storage system", *IEEE Transactions on Energy Conversion*, 29(4), 882-892.
- Wu, H., Wang, S., Zhao, B., Zhu, C., (2015). "Energy management and control strategy of a grid-connected PV/battery system", *International Transactions on Electrical Energy Systems*, 25(8), 1590-1602.

A Reliability Test Track Assessment of a Light Commercial Vehicle by Index Method

Arif Senol SENER
İstanbul Gelişim University

Abstract: One of the most important parameters of a product's quality concept is its failure frequency and warranty costs during the warranty period; Product tests conducted in the process of reliability. For product test of a vehicle, the manufacturers require mathematically determined special test tracks and / or routes of fatigue effect. In this study Turkish customers' car usage was determined by questionnaire method. For Turkey road's characteristic, the data is collected with a vehicle equipped with sensors in Turkey. Data elaboration and detailing were executed on the raw data. The 3-sided Rain-flow method was used to evaluate the signals obtained from the strained parts. Despite that 2 axes Level-Crossing method was preferred for the non-stressed components such as gear change ratio, breaking quantity etc. Data of Turkish mission profile belong to each sensor were handled by multiplying elaborated signals with Turkish customer automotive usage. An accelerated test track for the warranty period corresponding to the fatigue effect of the Turkish customer profile using the fatigue life effects weighted average method was established near the manufacturer. The usage results of passenger cars produced in European countries and customer usage results of the light commercial vehicle produced in Turkey were compared.

Keywords: Automotive usage, Test track, Fatigue life analysis, Cycle counting, Weighted average index

Hafif Ticari Araçların Endeks Yöntemi İle Güvenilirlik Testi Pisti Değerlendirmesi

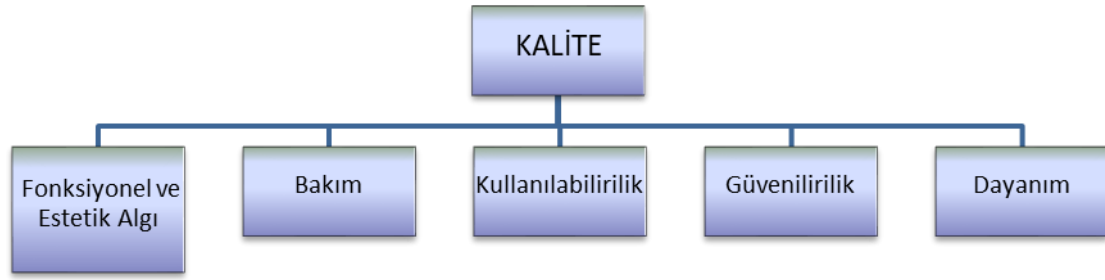
Özet: Bir ürünün kalite konseptinin en önemli parametrelerinden biri, garanti süresi boyunca arıza sıklığı ve garanti maliyetleridir (Güvenilirlik sürecinde yapılan ürün testleri). Bir aracın ürün testi için, üreticiler matematiksel olarak belirlenmiş özel test izlerini ve / veya yorulma etki yollarını gerektirir. Bu çalışmada Türk müşterilerin araç kullanımı anket yöntemi ile belirlenmiştir. Türkiye yolunun karakteristiği için, veriler Türkiye'deki sensörlerle donatılmış bir araç ile toplanmaktadır. Ham veriler üzerinde veri detaylandırma ve detaylandırma gerçekleştirilmiştir. Gerdirilmiş parçalardan elde edilen sinyalleri değerlendirmek için 3 taraflı yağmur akışı yöntemi kullanıldı. Buna rağmen, 2 eksenli seviye çaprazlama yöntemi, vites değiştirme oranı, kırılma miktarı, vb. gibi gerilmeden geçirilen bileşenler için tercih edilmiştir. Türk misyon profiline ait veriler, her bir sensöre ait detaylandırılmış sinyalleri Türk müşteri otomotiv kullanımı ile çarparak ele alınmıştır. Türk müşteri profilinin yorulma etkisine karşılık gelen garanti süresi için hızlandırılmış bir test pisti, yorulma ömrü etkilerini kullanarak ağırlıklı ortalama yöntemini üretici firmanın yanında oluşturmuştur. Avrupa ülkelerinde üretilen binek otomobillerin kullanım sonuçları ve Türkiye'de üretilen hafif ticari aracın müşteri kullanım sonuçları karşılaştırılmıştır.

Anahtar Kelimeler: Otomotiv kullanımı, Test yolu, Yorulma ömrü analizi, Döngü sayımı, Ağırlıklı ortalama endeks

Giriş

Günümüzde, otomobil kalite parametrelerinden biri olan güvenilirlik; daha tasarım sürecinde bir çok matematiksel hesaplarla her bir parça için atanan güvenilirlik hedefleri (garanti maliyetleri ve arıza sıklığı) otomobil ticari olarak satışa sunulmadan önce deneyler ve bir çok testler vasıtasıyla doğrulanıp aracın öngörülen toplam güvenilirlik hedefini sağlamasıyla amacına ulaşmaktadır.

Aracın tasarım sürecinden, ürünün piyasaya sunulana kadar ki zaman aralığında bir çok testler; prototip tesleri, banko testleri, yeterlilik testleri, kabin testleri, üretim süreç kontrol testlerinin yanısıra ürün garanti maliyetlerini ve ürün garanti süreci arıza sıklığını içeren güvenilirlik yol testleri yapılır.



Şekil 1. Kalite kavramının parametreleri

Şekil 1 de kalite kavramını oluşturan parametreler gösterilmiştir. Kalite kavramının parametrelerinden biri olan güvenilirlik ve dayanıklılık, uzun km kullanımında ortaya çıkar. Öyleki günümüzde bazı firmalar güvenilirlik hedefini 2 yıl 100.000 km ile sınırlandırırken diğer bazı firmalar ise 5 yıl 150.000 km olarak tahdit etmişlerdir. Bu nedenle, bir otomobilin güvenilirlik ve dayanıklılık testi sonuçlarının müşteri kullanımına bağlı olarak elde edilmesi müşteri kullanımında uzun süreç gerektirmektedir [Huizinga, A.T.M.J.M et.all]. Bir aracın servis ömrü, güvenilirlik ve emniyet süreçlerinin belirlenmesi, araç yapılarının tasarım süreci için hayati önem taşımaktadır [Grubisic, V., DreBler, K et.all]. Araç mühendisliğinin amacı, bir taraftan çok kısa olan bu geliştirme döngüsünde güvenlik ve güvenilirlik gibi iki özelliği düşünürken, diğer taraftan düşük maliyetli ve hafif tasarımı bir araya getirip diğer firmalarla rekabet etmektir.

Bu nedenle otomobil firmaları özellikle fonksiyonel testlerden biri olan güvenilirlik yol testlerini, ürün piyasaya sunulmadan çok kısa bir zaman aralığında yaparak tesbit edebileceği proses ve proje hatalarını kısa zamanda gidererek o projedeki hata sıklık miktarını ve proje maliyetini düşürüp hem müşterileri şikayetlerini azaltırken hemde ürün proje maliyetlerini ve hata sıklığının azalmasını amaçlar [Dodson B., and Schwab, H.,].

Bir parçanın dayanıklılığını etkileyen başlıca parametreler malzeme, geometri ve yük spektrumunun bir fonksiyonu olan taşıtın çalıştığı pazardaki müşteri kullanımınıdır [Grubisic, V, Bishop, N. W. M. and Sherratt, F]. Çalışmadaki yük koşulları, bir ürünün ve bileşenlerinin servis ömrü için büyük önem taşımaktadır [Grubisic, V]. Bir araç ve parçalarının ömür tahminini ve hasar görmemiş zamanı etkileyen yük spektrumu aracın satıldığı pazardaki güvenilirlik gereksinimlerini de hesaba katan müşteri profilini referans alan yol testleri ve bilgisayar sanal analizleri ile hesaplanarak belirlenmelidir [Bishop, N. W. M. and Sherratt, F].

Son zamanlarda, araçların ömrü boyunca yük spektrumunu belirlemek için yaygın olarak kullanılan yöntemler müşteri kullanım metodlarıdır [Case Study, Şener, Ş. A, Pizzari, V, Marchesani, Mainieri, G.et.all, Fantacchiotti, M. and Vianello, M]. Müşteri profilini oluşturma çalışmalarından birini Brezilya ve İtalya pazarı için FIAT şirketi tarafından yapılmıştır. Yeni araç modellerinin geliştirilmesi için kullanılan standart bir yorulma test pisti Brezilya ve Türkiye’de yoktur. FIAT şirketi frekans bazlı yorulma ömrünü temel alan müşteri kullanımını da hesaba katan Brezilya yolları ile İtalyan yolları ve ayrıca özel test parkuru etkilerini esas alarak araçların yorulma testleri ve temsili yük profilini çıkarma çalışmaları yaparak karşılaştırmalar gerçekleştirilmiştir [D’Aprile, F].

Bir başka çalışmada FIAT şirketi Ritmo 60 ve Tipo1372 için bir metoduyla diğer bir müşteri kullanımı araştırmasını kara kutu (Balack Box) metoduyla gerçekleştirmiştir [Marchesani, Mainieri, G.et.all]. Bir başka çalışmada ise FIAT şirketi, cihazlarla donatılmış bir Punto aracıyla bir B segment aracında Türk müşteri profilini belirlemek için 1997’de yapmıştır [Pizzari, V].

Bu makalede, Türkiye’de üretilen bir Hafif Ticari Araç (HTA) ın güvenilirlik testleri için araştırma ve geliştirme sürecinde gerekli olan Türkiye Profili 200.000 km (Mission Profile; MP) ve Hızlandırılmış Güvenilirlik Test Parkuru’nu (HGTP) 20.000 km ağırlıklı ortalama metoduna göre nasıl tasarlanabileceği ve uygulanabileceği yöntem, süreçler ve ilgili sonuçlar verilmiştir.

Metod

Bir araç yada parçanın hızlandırılmış yorulma testi için, taşıtın normal kullanım şartlarında karşılaştığı bütün yük değerlerine karşılık gelen temsili bir yük spektrumu kullanılmalıdır. Bir parçanın kullanım ömrü genellikle kullanım sırasında yükleme koşullarından etkilenir. Tasarım-proses doğrulama ve güvenilirlik testi için temsili bir yük spektrumu oluşturulması gerekmektedir [Grubisic, V]. Son zamanlarda, bir aracın müşteri kullanımını belirlemek için müşteri kullanımını esas alan anket ve kara kutu adında iki yöntem kullanılmaktadır [Case Study, Şener, Ş. A, Pizzari, V, Marchesani, Mainieri, G.et.all].

Karakutu Metodu

Bu yöntem, gönüllü sürücülerin araçlarının veri toplama cihazları ve sensörleriyle donatılarak uzun bir süre seyahat esnasında verilerinin kaydedilmesi esasına dayanmaktadır. Kaydedilen veriler düzenli olarak periyodik bir şekilde araç üreticisi tarafından sabit bir diske kaydedilerek boşaltılır. Bu metodla veri toplama yaklaşık üç yıl zaman almaktadır. Tüm ölçümlerden sonra veriler istatistiksel olarak değerlendirilerek araç kullanım özellikleri sayısal olarak raporlandırılır [Marchesani, Mainieri, G.et.all, Fantacchiotti, M. and Vianello, M].

Anket Metodu

Anket metodu, araç kullanımı vb. bilgileri toplamak için aynı segment araçların müşterilerine telefonla anket yapılarak araç kullanım bilgileri ve benzeri diğer bilgileri elde etmeyi esas almaktadır [Grubisic, V, Mainieri, G.et.all, Paul, P. K, et.all]. Anket ölçüm sonuçlarının değerlendirilmesi sonucunda, cihaz ve sensörlerle donanımlı bir araç ve/veya birkaç araç ile bir yol testi simülasyonu yapılır. Yol testi sırasında veriler, değişik manevraların yapıldığı ve değişik yol profillerinde (şehir içi, şehirlerarası, dağlık alanlar, kırsal alanlar vb.) ve otomobil yük şartlarında bir test şoförü veya farklı şoförler kullanılarak toplanır [Mainieri, G.et.all, Şener, Ş. A, Pizzari, V, Marchesani, C. et.all]. Toplanan ham sinyaller yol sınıflarına ve yük koşullarına göre sınıflandırıldıktan sonra veri işleme yapılır. Veri işleme bitmiş sinyaller 2 yada 3-boyutlu matris aralıklarında istatistiksel sinyal sayma metodlarıyla işleminden geçirilir.

Müşteri kullanımı, araç yükü ve yol tipi ile düzenlenerek her bir sensor için 200.000 km lik bir MP oluşturur. Metodoloji; eğer aynı girdiler tekrarlanabilirse, aynı hasarın oluşacağına dayanır. [Mainieri, G.et.all]. MP bulunması nın ardından aynı yorulma etkisini yaratacak hızlandırılmış test parkuru veya test bankosunda yapılacak testler için yeni yol sinyalleri oluşturulur. Eğer aynı girişler sağlanırsa, çeşitli formların matris hesabı, yol uyarma sinyallerinin karışımının değerlendirilmesi için bir model sağlayacak ve test uzunluğunu veya test süresini optimize edecektir.

$$E [Y1] + F [Y2] + G[Y3] + + Z [Yn] = [D] \quad 1$$

Burada E, F, G, ... Z, test verilerinin çarpanlarıdır. [Y1], [Y2], ... [Yn] test ölçümlerinin matrisleridir ve [D] müşteri hedef ölçümlerinin toplam matrisidir. Bu şekilde Y1 yolunun zamanı, Y2 yolu zamanı, D hasar etkisini verene kadar devam edecek kadar açıktır [Mainieri, G.et.all].

Uygulama

Türk Müşteri Profilinin Tanımlanması-Anket Uygulaması

Diğer yöntemlerle karşılaştırıldığında düşük maliyetli, hızlı veri toplanabilmesi ve veri değerlendirme esnekliği sağlanmasından dolayı bu çalışmada "Anket" metodu seçilmiştir. Bir HTA'in Türkiye'deki müşteri kullanımı profili, üretici firma bayilerinin desteğiyle Türk müşterilerine yüz yüze uygulanan bir anket ile geliştirilmiştir.

Türk Müşteri Profilinin Tanımlanması -Yol Test Haritasının Belirlenmesi

Türkiyede yol karakteristiklerinin sensörlerle toplanabilmesi için ve Türk müşterisini temsil eden test güzergahının oluşumu;

- a- Bölgelere ve illere göre HTA'nın satış yüzdeleri,
- b- Üretici firmanın daha önceki model deneyimlerine göre arıza frekansı ve cinsi,
- c- Türkiye iklim koşulları,
- d- Türkiye coğrafyası özellikleri referans alınarak elde edilmiştir.
- e- Türkiye yol tipleri

referans alınarak Türkiye test güzergahı oluşturulmuş ve 4 sınıfa ayrılmıştır; şehir içi kullanımı için İstanbul ve Bursa'da, dağlık yollar için genelde Karadeniz bölgesinde, sıcak iklim ve kavisli yol koşulları içeren şehirlerarası yollar için Akdeniz'de, Orta Anadolu'daki yollar ise yüksek irtifalar, sıcaklıklar ve kentler arasındaki uzak mesafeler ile karakterize edilmiştir. Böylece veri toplama işlemleri için belirlenmiş güzergah yollardan veri toplamak için oluşturulmuştur [Oelmann, B, Şener, A. S].

Türk Müşteri Profiline Tanımlanması –MP Saptamak İçin Veri Toplama

PVeri ölçümleri sensörlerle donatılmış bir araçla normal sürücülerin otomobillerini kullandıkları yollarda uzman bir test şoförü ve bir mühendis tarafından araç tam yükte genelde sürücüleri takip ederek belirlenmiş olan test güzergahında veriler toplanmıştır.

Veri İşleme

Yorulma dış yükleri, doğrudan zamana bağlı olarak ölçülmez. Bunun yerine, aracın bazı parçalarında sensörlerle dış yüklerin reaksiyonları ölçülür [Grubisic, V]. Spike (sıçramış sinyal) analizi, frekans analizi, filtreleme, aritmetik işlemler ve istatistiksel sayım işlemi gibi işlemler ham veriler üzerinde yapılmıştır [NCode, MSC. Software GmbH nSoft 5.2].

Spike Analizi

Veri toplama sırasında, çevresel ve fiziksel faktörlerden dolayı ortaya çıkan bazı spike lar görsel ve istatistiksel yöntemlerle ortadan kaldırılmıştır [NCode, MSC. Software GmbH nSoft 5.2].

Filtreleme

Yorulma analizleri için aracın süspansiyon parçalarının frekans aralığı 40 Hz ve 60 Hz arasındadır. Yol simülasyonu için genellikle 100 Hz üzerindeki uyarımın ihmal edilebileceği kabul edilmektedir [Şener, Ş. A, Pizzari, V, NCode, MSC. Software GmbH nSoft 5.2]. 100 Hz üzerindeki frekansı yüksek düşük genlikli sinyaller, yorulma analizleri için anlamlı değildir ve bir alçak geçiren filtre ile orijinal veriden çıkarılmıştır [Şener, Ş. A, Pizzari, V, MSC. Software GmbH nSoft 5.2].

Aritmetik İşlemler

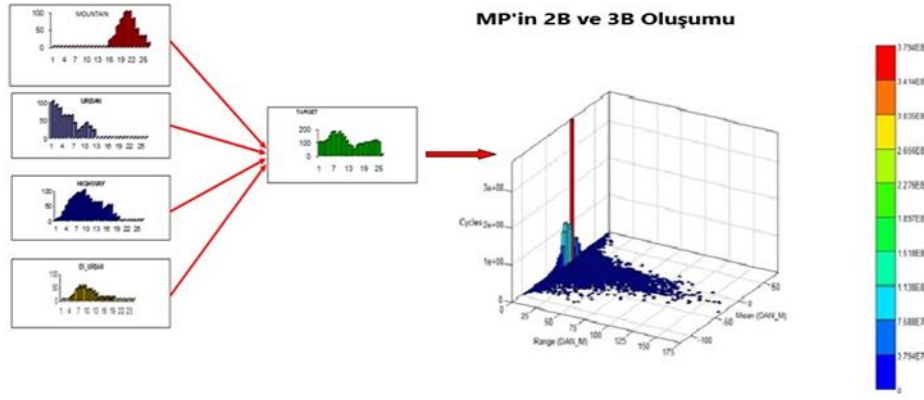
Araç yol testinin başlama zamanına kadar elde edilen veriler yorulma ömrünün hesaplanmasında yararlı olmadığından orijinal sinyallerden çıkarılmıştır [MSC. Software GmbH nSoft 5.2].

Yol Uyarma Sinyallerinin İstatistiksel Sayımı

Zamana bağlı sinyaller karşılaştırma için zamandan bağımsız olarak eşdeğer bir değere dönüştürülmelidir. Bu dönüşüm stres gören parçalara ortalama gerilmeyi de hesaba katan 3 boyutlu yağmur - akma istatistiksel sayma metodu, stres görmeyen parçalar için ise 2 boyutlu seviye – sayma istatistiksel sayım metodları uygulanarak gerçekleştirilmiştir [MSC. Software GmbH nSoft 5.2- Bishop, N.].

Hedef MP Oluşturma

Her bir yol verisi mesafe ve zaman açısından farklı olduğundan dolayı bu sinyallerin yorulma etkilerini mukayese edebilmek amacıyla her bir veri 1000 km'lik sinyale dönüştürülmüştür. 1000 km verilerin sinyallerinin karşılaştırılmasından sonra, sinyaller MP değerini oluşturmak için çeşitli yol tiplerine (şehir, şehirlerarası, dağ ve otoyol) göre sınıflandırılarak ekstrapolasyon yapılmıştır. Sınıflandırılmış 200.000 km MP verileri, anket sonuçlarından elde edilen Türk müşteri kullanım yüzdesi ile çarpılıp olarak yol sınıflarının tümünü içeren her bir fiziksel büyüklük için bir MP oluşturulmuştur. Şekil 2, MP tahrik mili burulma verilerine ait 3B histogramını göstermektedir [Mainieri, G.et.all, Şener.Ş.A., Pizzari, V.]



Şekil 2. Tahrik şaftı MP (200 000 km) Rain-flow 3D diyagramı [Şener.A.Ş.]

MP'nin Simülasyonu

Türk MP her bir sensör için oluşturulduktan sonra, aynı test aracıyla Bursa'daki otomobil fabrikasının civarında yorulma etkinliği ağır olan yollardan çeşitli sürüş koşullarında ve manevralarda test ölçümleri yapılarak kayıt edilmiştir. Daha sonraki adımda toplanan yol sinyalleri 1000 km ye normalize edilerek birbirleri arasında karşılaştırmalar yapılmıştır. Yorulma etkileri ağır olan parkurlar seçilmiştir ve 20.000 km ye ekstrapole edilmiştir. Bursa civarında toplanan veriler yol kullanım yüzdeleri ile çarpılarak 20.000 km'lik HGTP simülasyon verisi ağırlıklı ortalama metodu kullanılarak her bir sensör için oluşturulmuştur.

Deneyel Verilen Ağırlıklı Ortalama Metoduna Göre Benzeşiminin Kurulması

Ağırlıklı Ortalama Metodunun Tanımı

Kullanılan ağırlıklı ortalama metodu büyük veri demetlerinin çok sayıda tekrarı olup ancak sonlu bir sayıda seçilen veriler için kullanılır. Ağırlıklı ortalama yöntemi kavramı matematikten gelmektedir ve ortalama, çeşitli nicelikleri birlikte ekleyerek elde edilen sonuç olarak tanımlanabilir. Daha sonra bu toplam sayısının nicelik sayısına bölünmesiyle elde edilebilmektedir [Pizzari, V, Xie, S. X et. all]. Bu çalışmada, her bir sensörden elde edilen verileri, 2 boyutlu seviye sayma ve 3 boyutlu rain-flow matrisleri ile oluşturulmuştur [Pizzari, V. MSC. Software GmbH nSoft 5.2, ASTM standard]. Bu matris değerleri her bir veri için ayrı ayrı bir bilgisayar yazılımına yerleştirilmiş ve daha sonra her bir sensöre ait veriler, her güzergâhın indeksini hesaplamak ve aynı zamanda her bir değer grafiklerinin çizilmesi için, Denklem 2, 3 ve 4 kullanılarak çevrimler ve aralıklar hesaplanmıştır [Pizzari, V.].

$$TS = \sum_{i=1}^n S_i = S_1 + S_2 + S_3 + \dots + S_n \quad 2$$

$$SPK = \frac{TS}{TK} \quad 3$$

$$OI = \frac{\sum_{i=1}^n x_i \cdot S_i}{TS} \quad 4$$

Burada;

TS = Toplam çevrim

SPK = Km deki çevrim

OI = Ortalama Index

x_i = Fiziksel büyüklüğün aralığı

S_i = x_i aralığındaki çevrim adedi

TK = Toplam Km

MP ve HGTP Arasında Yorulma Yollarının Hesaplanması ve Oluşturulması

Bir yol benzetimi (simülasyonu) için araçtan mutlaka alınması gereken önemli parametreler;

- araç süspansiyonunun dikey kuvvetlerin karakteristiği
- araç süspansiyonuna yatay kuvvetlerin
- araç burulma karakteristiği
- araç gövdesine boylamasına kuvvetlerin karakteristiği
- araç gövdesine yanal kuvvetin karakteristiği

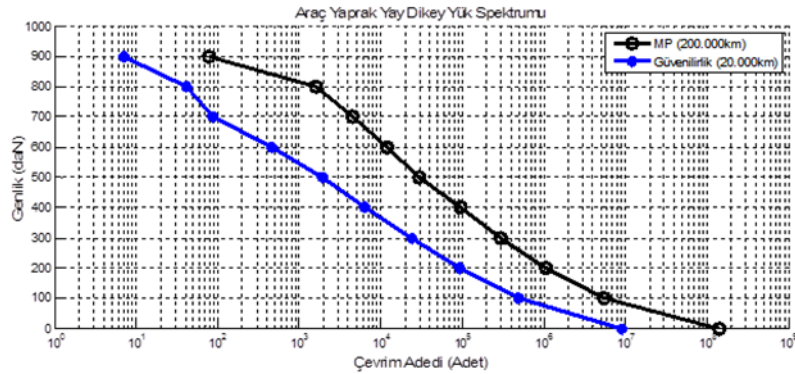
vites deęişim oranı karakteristięi
frenleme karakteristięi [Şener.Ş.A., Pizzari, V.].

Ortalama aęırlıklı indeks metoduna gre, iki yolun her ne kadar birbirini yorulma aısından simule ettięi eęrilerin birbirlerini yakınsamasının yanında her bir yolun aritmetik ortalama indeks deęerlerinin karşılaştırılması ile tespit edilir [Pizzari, V].

Sonuçlar ve Tartışmalar

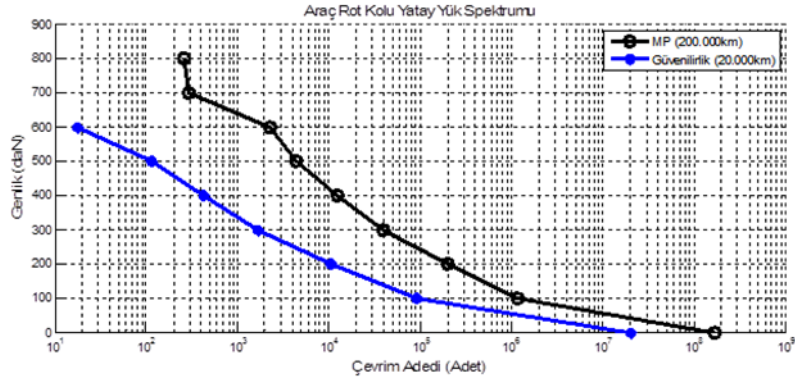
Bu alıřmada, Trkiye'de retilen bir HTA'nın Trk mřterisi ara kullanımı oranları ile Trk mřterilerinin HTA kullanımı amacı belirlenmiřtir. Bir Avrupa lkesi HTA ara kullanımı oranları ile elde edilen Trk mřterisi kullanımı oranı mukayese edildięinde řehir ii srř oranının Avrupa lkesindeki HTA tipik bir kullanımdan iki katı olduęu tespit edilmiřtir [Şener.Ş.A., Pizzari, V]. Trk mřterisi iin HTA kullanımının birinci amacının İřten –İře olduęu tespit edilmiřtir [Şener.Ş.A.].

MP ve HGTP benzeřim eęrileri rainflow ve seviye sayma metodlarına gre eęrilerinin benzeřimleri ile bu verilerin indeks deęerleri hesaplanarak sırasıyla ardı ardına Őekil 3'ten Őekil 9' a kadar verilmiřtir.



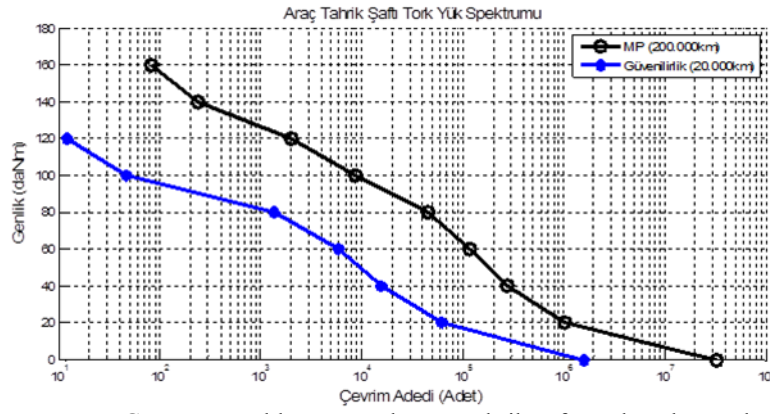
Őekil 3. MP ve HGTP gzergahları arasında yaprak yay dikey yk spektrumunu karşılaştırması

Őekil 3'te MP ve HGTP yollarındaki araa ait dikey yk verilerinin karşılaştırılması sunulmuřtur. Grafikten de grleceęi zere, her iki yolda birbirlerine ykler aısından olduka iyi bir korelasyon kurulmuřtur.



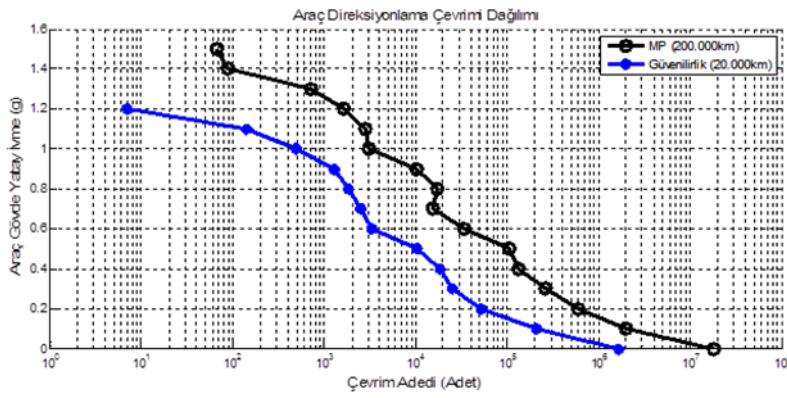
Őekil 4. MP ve HGTP gzergahları arasında direksiyon rod kolu yatay yk karşılaştırması

Őekil 4'da, MP ve HGTP gzergahları arasında virajlama ve sollama nedeniyle oluřan tekerlek yanal yklerinin eęrileri verilmiřtir. MP yk deęerleri zellikle byk yklerde 700-800 daN arasında HGTP den yksek olmasının nedeni Trkiye parkurundaki yolların zellikle Kař-Finike arasında ok daha aęır bir yol ve viraj etkisine sahip olduęu ngrlmektedir. Dięer yklerde ise her iki gzergah da birbirine iyi bir řekilde korele etmektedir.



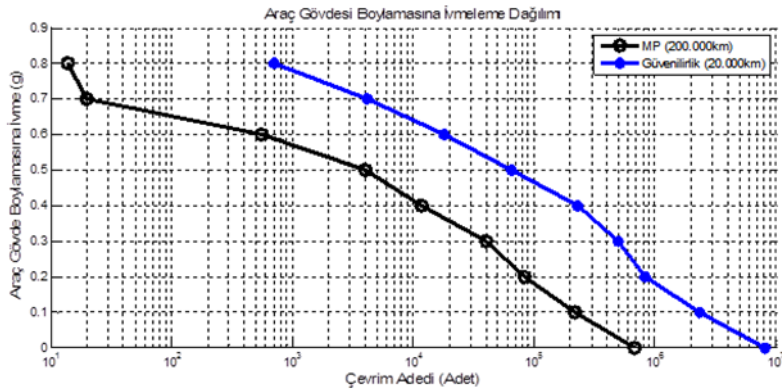
Şekil 5. MP ve HGTP güzergahları arasında araç tahrik şaftının burulma yük dağılımı

Şekil 5’de MP ve HGTP güzergahları arasında mukayeseli tahrik şaftı burulma eğrisi sunulmuştur. Grafiklerden görüldüğü gibi HGTP eğrileri MP değerine göre farklı bir şekilde az yakınsamaktadır. Bunun sebebi MP’de kullanılan İstanbul şehir içi araç kullanımında trafik sıkışıklığı sebebi ile oluşan durma ve kalkmadan dolayı olduğu gözlenmektedir [Şener,Ş.A.].



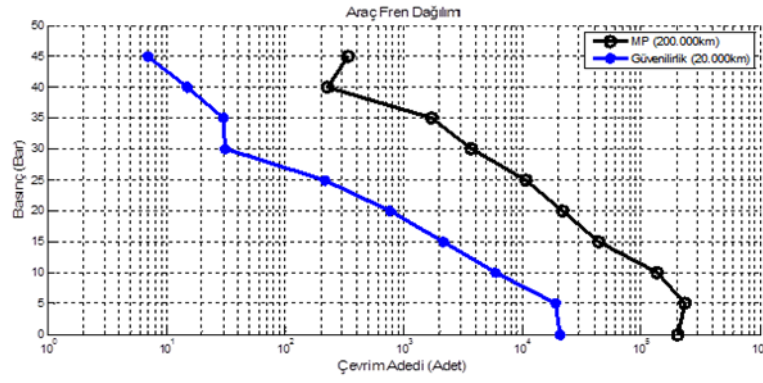
Şekil 6. MP ve HGTP güzergahları arasında araç kasası yatay ivmelenme verileri yük spektrumları mukayesesi

Şekil 6’de MP ve HGTP güzergahları arasında virajlama ve direksiyon manevralarından dolayı oluşan yanıl ivme yük spektrumları verilmiştir. Grafiklerden görüldüğü gibi, 0.7-1.3 g arasında birbirine oldukça yakınsamışken buna karşın 0.6 g civarında MP çevrim adedi HGTP verilerinden az bir şekilde daha fazladır.



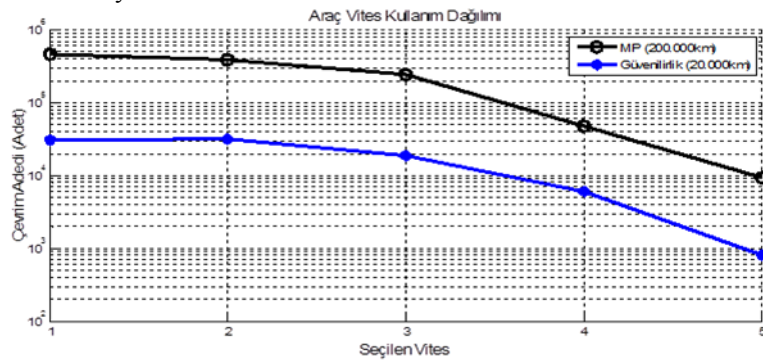
Şekil 7. MP ve HGTP güzergahları arasında araç kasası boylamasına ivmeleme yük spektrumunu mukayesesi

Şekil 7’de MP ve HGTP güzergahları arasında durma ve kalkmadan, frenlemeden ve yolların sinüzoidal eğiminden dolayı araç kasasında oluşan boylamasına ivmeleme yük spektrumu dağılımı verilmiştir.



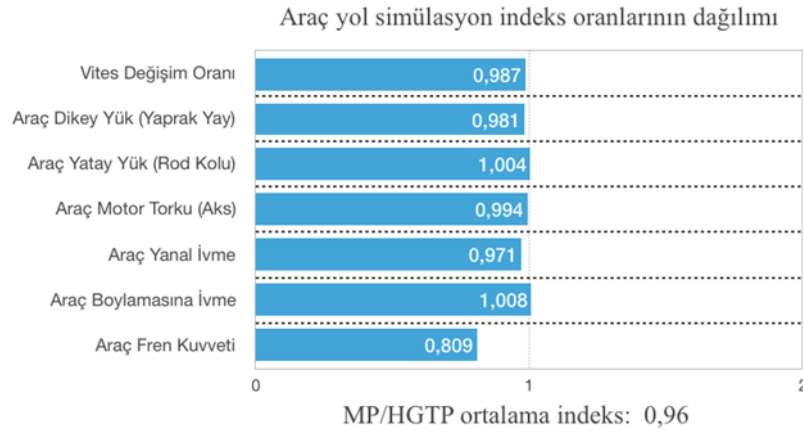
Şekil 8. MP ve HGTP güzergahları arasında araç frenleme yük spektrumunu mukayesesi.

Şekil 8 da MP ve HGTP güzergahları arasında fren basıncı ve fren adetleri yük spektrumunu dağılımı mukayeseli olarak verilmiştir. HGTP güzergahındaki yük spektrumunu verileri MP güzergahındaki fren çevrim değerine yeterince kadar yakınsamamıştır. Bunun nedeni MP güzergahında kullanılan şehir içi yolunda İstanbul şehir içi verilerininin HGTP güzergahında kullanılan şehir içi güzergahı verilerine göre çok aşırı bir şekilde dur ve kalk manevraları içermesinden dolayıdır.



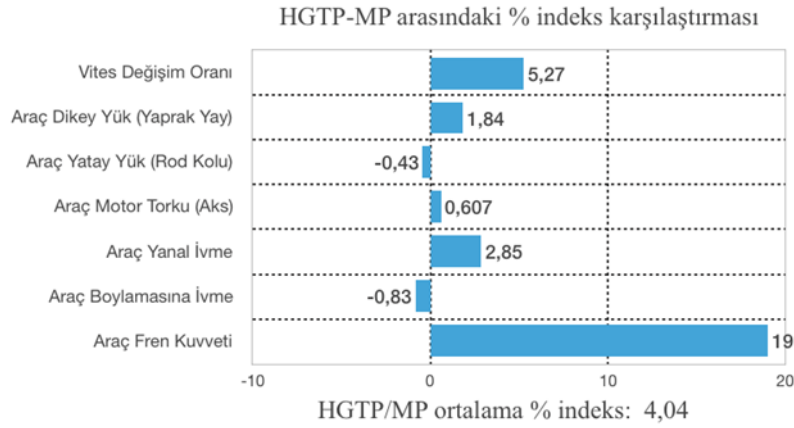
Şekil 9. MP ve HGTP güzergahları arasında araç vites değişim oranı yük spektrumunu mukayesesi

Şekil 9'de MP ve HGTP güzergahlarında araç vites değişim oranları yük spektrumunu verilmiştir. Bu grafik çevrim adetleri açısından değerlendirildiğinde MP güzergahındaki yük miktarı özellikle 4. vites oranına kadar çok daha ağırdır. Bunun nedeni MP güzergahında kullanılan İstanbul şehir içi trafiğinin çok miktarda dur ve kalk manevrası içermesinden kaynaklanmaktadır.



Şekil 10. MP ve HGTP güzergahları arasındaki indeks oranlarının dağılımı

Şekil.10'da MP global indeks değerleri ile HGTP indeksleri arasında ki dağılımı gösterilmektedir. Grafikten görüldüğü gibi iki yol güzergahı arasında iyi bir korelasyon elde edilmiştir. Ortalama indeks değeri yaklaşık 1 değerinde olup, ayrıca indekslerin dağılımı dengeli bir şekilde olduğu görülmektedir. HGTP indeks değeri MP indeks değerinden çok küçük miktarda daha ağırdır.



Şekil 11. MP ve HGTP güzergahlarının % genel indeks mukayesesi

Şekil.11'de MP 200.000 km ve HGTP 20.000 km % genel indeks oranlarının mukayeselerini vermektedir. Grafikte görüldüğü gibi 20.000 km HGTP genel ortalama indeks değerinin MP 200.000 km genel ortalama % indeks oranı olarak yaklaşık % 4 daha ağır bir parkur olduğu tespit edilmiştir [Pizzari, V].

Türk sürücülere özgü bir HTA araç için MP karakteristik verisi geliştirilmiştir. Her bir sensor için matematiksel bir MP (200.000 km) ağırlıklı ortalama metoduna göre oluşturulmuştur.

Yeni modellerin geliştirilmesinde kullanılacak olan güvenilirlik testleri için bir yorulma test parkuru, üretici firma yakınların da bir HTA için HGTP hesaplanarak tasarlanmıştır.

Bu çalışma kritik yük aralıkları saptanmış ve bundan sonraki model araba geliştirilmesinde kullanmak için arşivlenmiştir.

Tavsiyeler

Fren adedi ve vites değişim oranı farkını ilgili otomobil üretici firma ürün geliştirme sırasındaki yorulma testleri sırasında normal yol güzergahlarına ilave olarak fabrika içinde uygun bir alanda ilave manevralarla bu farkı gidermeleri sonucunda eğriler tamamıyla birlerine yakınsamaları sağlanmış olacaktır.

Teşekkürler

Bu araştırmaya katkılarından dolayı TOFAŞ A.Ş. ye teşekkür ederim.

Kaynaklar

- ASTM Standard E 1049-85, Philadelphia, USA 1997.
- Bishop, N., (1995). Analytical Fatigue Life Assessment of Vibration Induced Fatigue Damage . MSC World Users Conference, Universal City, CA.
- Bishop, N. W. M., Sherratt, F., (2000). Finite Element Based Fatigue Calculation, NAFEMS International Association for the Engineering Analysis Community, USA DOI:10.1111/j.1460-2695.1990.tb00604.
- D'Aprile, F., (2001). Structural characterization of a vehicle on a rig test versus different road profiles: analysis of experimental results. ATA-TORINO-. 54:7/8, 251-261.
- Dodson B., Schwab, H., (2006). Practitioner's guide to accelerated and reliability testing, ISBN-10 0-7680-0690-2 ISBN-13978-0-7680-0690-2.
- DreBler, K., Speckert, M., Müller, R., Weber. C., (2009). Customer loads correlation in truck engineering, Berichte des Fraunhofer ITWMNr. 151, F200812198 ISSN 1434-9973.
- Fantacchiotti, M., Vianello, M., (1994). Gradual improvement of the vehicle reliability up to the target value, FIAT Auto SpA Design Engineering Department, 4th International Conference, 1-5.
- Grubisic, V., (1986). Criteria and methodology for lightweight design of vehicle components, Fraunhofer-Institut für Betriebsfestigkeit(LBF), Darmstadt, Germany, DOI:10.4271/850367.
- Grubisic, V., (1994). Determination of load spectra for design and testing, International Journal of Vehicle Design.15 8-26.
- Huizinga, A.T.M.J.M., Van Ostajen, M.A.A., Slingeland. G.L., (2002). A practical approach to virtual testing in automotive engineering, Journal of Engineering Design, 13, 33-47

- Mainieri, G.; Ensor, D.F. 1999. Case Study - Complete Customer Usage Profiling Example Raw Data through Track Correlation to Accelerated Rig Drive in '4' Days., Iveco (Italy) - nCode (UK). Available from internet:<http://web.mscsoftware.com/support/library/conf/auto00/p05500.pdf>.
- Marchesani, C., Parmigiani, F., Vianello, M., (1979). Integrated method to define the mission profile of a passenger car, FIAT Auto SpA, 45-54, Italian.
- MSC. Software GmbH nSoft 5.2 User Manuel 1999.
- nCode (1998). International Inc.&MSC Software Corporation: User manuel MSC Corporation, Los Angles, USA.
- Oelmann, B., (2002). Determination of load spectra for durability approval of car drive lines, Fatigue and Fracture of Engineering Materials and Structures 25 1121-1125 DOI:10.1046/j.1460-2695.2002.00604.
- Paul, P. K., Dunga, R. K., Verma, A., Minakar, A: V., Raju, S., (2001). Techniques for accelerated design validation of tractor chassis, SAE Paper. 1, 1-50 DOI:10.4271/2001-26-0050.
- Pizzari, V., (04 February 1998). Turkish Mission Profile Research Segment B Vehicle, Turkish Instructions Prot. No.1, Arese, Direction of Technical Development Vehicle Reliabilityand Terreni Laboratory Test Measurements, Study Report, Italian.
- Şener, Ş. A., (2003). Fatigue life determination of the leaf spring on the light commercial vehicle according to Turkish Mission Profile (in Turkish), Istanbul, Turkey.
- Şener, A. S., (2014). Finite element based vehicle component fatigue life assessment according to a customer usage profile, Materials Testing. 56, 198-207, DOI:10.3139/120.110543.
- Şener, A. S., (2016). Fatigue life assessment of the driving shaft of a LCV by FEA using customer correlation data Materials Testing. 58:4, 325-332, DOI.10.3139/120.110861H.
- Xie, S. X., Liao, D., Chinchilli, V. M., (2001). Measurement Error Reduction Using Weighted Average Method for Repeated Measurements from Heterogeneous Instrument Environmetrics 12, 785-790 (DOI:10.1002/env.511).

Analysis of Thinning Zones and Pres Parameters of A Car Exhaust to be Produced by Deep Drawing of Sheet Metal

Erdal OZTURK
Gaziantep University

Murat GULBAY
Gaziantep University

Abstract: Deep drawing is a method of manufacturing cups and similar deep geometries by giving a plastic form to the sheets through a die. The most important problems observed in the parts produced by deep drawing method are irregularity of sheet metal thickness, thinning errors in certain places, cracking and shrinkage. Production without performing necessary analyses against the faults and designing the mold with respect to the results is problematic and may cause in material and time losses. In this study, a car exhaust to be produced by deep drawing is designed with CATIA program and analysis of thinning zones as well as optimal press parameters are performed by AutoForm program. According to the results of the analysis, the design of the car exhaust is optimized for mass production. In this way, defective parts will be avoided to increase product quality and extend functionality and product life. The study will also provide a guidance for pre-production analysis of other products that can be produced with deep drawing.

Keywords: Sheet metal processing, Sheet metal production fault analysis, Deep drawing

Sac Metal Derin Çekme Yöntemiyle Üretilen Araba Egzozunun İnceleme Noktalarının ve Pres Parametrelerinin Analizi

Özet: Derin çekme, sac levhalara bir kalıp yardımı ile plastik bir form vererek, kap ve benzeri derin geometrilerin üretilmesi için kullanılan bir yöntemdir. Derin çekme yöntemiyle üretilen parçalarda gözlenen en önemli problem, sac kalınlığının düzensizliği, belirli yerlerde incelleme hataları, çatlama ve büzülme olmasıdır. Hatalara karşı gerekli analizleri yapmadan üretim yapmak ve sonuçlara göre kalıbı tasarlamak problemlili olacağı gibi malzeme ve zaman kayıplarına da neden olabilir. Bu çalışmada, derin çekme ile üretilecek bir araba egzozu, CATIA programı ile tasarlanmakta ve incelleme bölgelerinin analizi ile AutoForm programı ile yapılarak optimum pres parametreleri belirlenmiştir. Analiz sonuçlarına göre, araba egzozunun tasarımı seri üretim için optimize edilmiştir. Bu sayede ürün kalitesini arttırmak, işlevselliği ve ürün ömrünü uzatmak suretiyle kusurlu parçaların üretimi önlenebilecektir. Çalışma aynı zamanda derin çekme ile üretilebilecek diğer ürünlerin üretim öncesi analizi için bir rehber olacaktır.

Anahtar Kelimeler: Sac metal şekillendirme, İnceleme bölgeleri, Sonlu elemanlar analizi

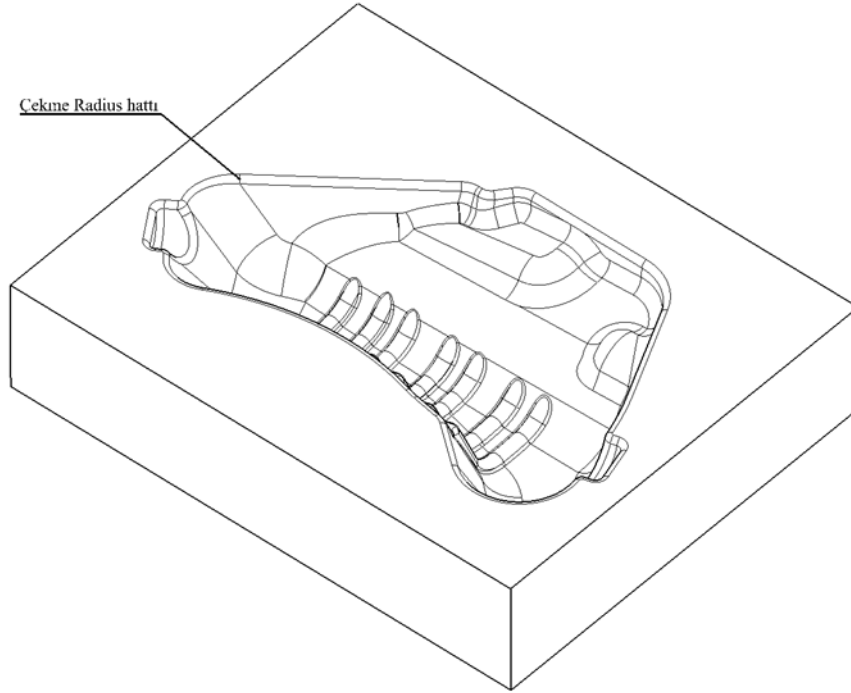
Giriş

Sac metal derin çekme şekillendirmede en çok karşılaşılan problemlerden biri baskı esnasında sac levhada meydana gelen incelmelerdir. İncelmenin fazla olduğu bölgelerde çatlama ve yırtılmalar meydana gelmektedir. Baskı esnasında yırtılmaya sebep olacak etkenlerden biri de dişi kalıp üzerindeki çekme radiusüdür. Çekme radiusünün tespiti sac şekillendirmede önemli parametrelerden biridir. çekme radiusünün istenenden küçük olması sac parçada yırtımlara, büyük olması ise dalgalanma ve kırılmaya sebep olmaktadır. Bu çalışmada farklı çekme radius değerlerinin ürün üzerindeki etkileri analiz edilmiştir.

Bu çalışmada sac levha malzemesi olarak derin çekmeye uygun Erdemir Dx54d+Z sac levhası seçilmiş, sac kalınlığı 1.2 mm alınarak dişi kalıp üzerindeki farklı çekme radius değerleri verilmek suretiyle analizler gerçekleştirilmiştir. Bu analizler sonucunda uygun çekme radius değeri belirlenerek yırtılmanın önüne geçilmiş, incelleme bölgeleri minimum seviyeye getirilmiş ve gerekli pres parametreleri belirlenmiştir.

Sac Metal Derin Çekme Yöntemiyle Üretilen Egzoz Sacının Farklı Çekme Radius Değerlerine Göre Tasarımı Ve İnceleme Bölgelerinin Optimizasyonu

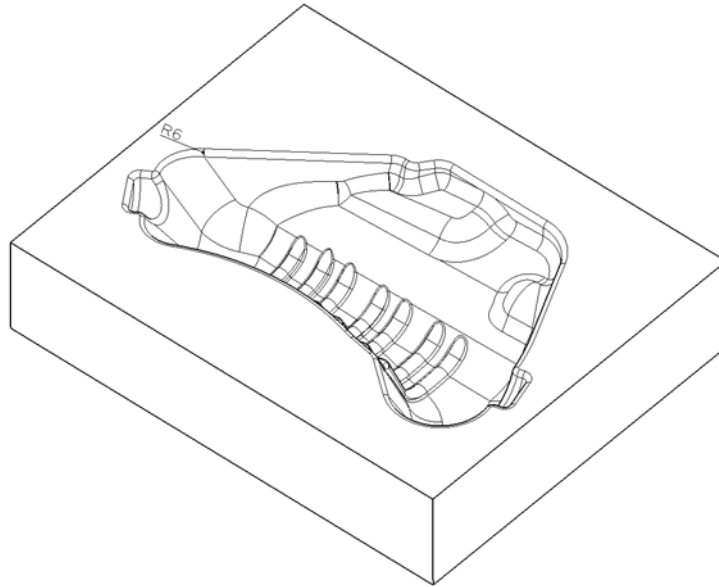
Şekil-1’de görülen araba egzoz sacının dişi kalıp üzerindeki çekme radüs hattının, 6 mm, 16 mm ve 8 mm olan tasarımları için Autoform programında ayrı ayrı incelme bölgeleri ve pres parametrelerinin analizi gerçekleştirilmiştir.



Şekil 1. Dişi kalıpta çekme radüsü

a) 6 mm Çekme Radüsü İçin İncelme Bölgeleri Analizi

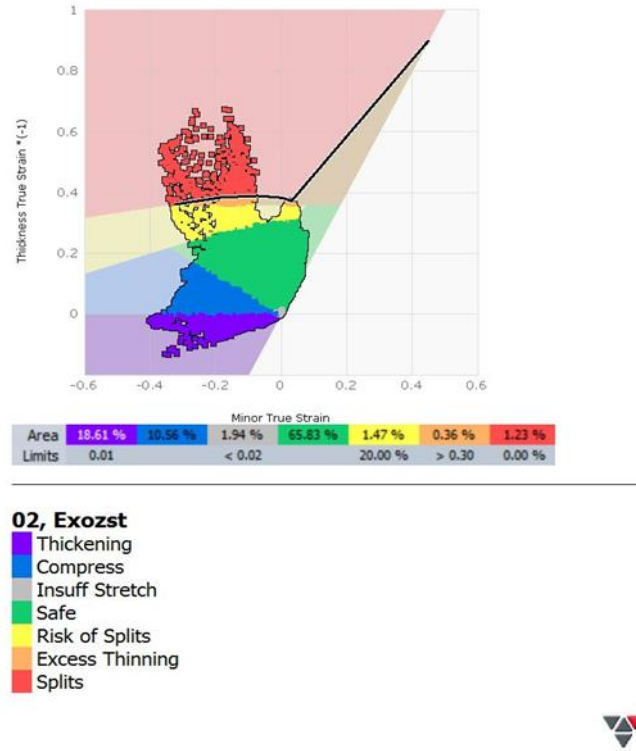
Şekil-2’de gözüktüğü gibi çekme radüs hattı 6 mm olarak tasarlanmış ve analizi yapılmıştır.



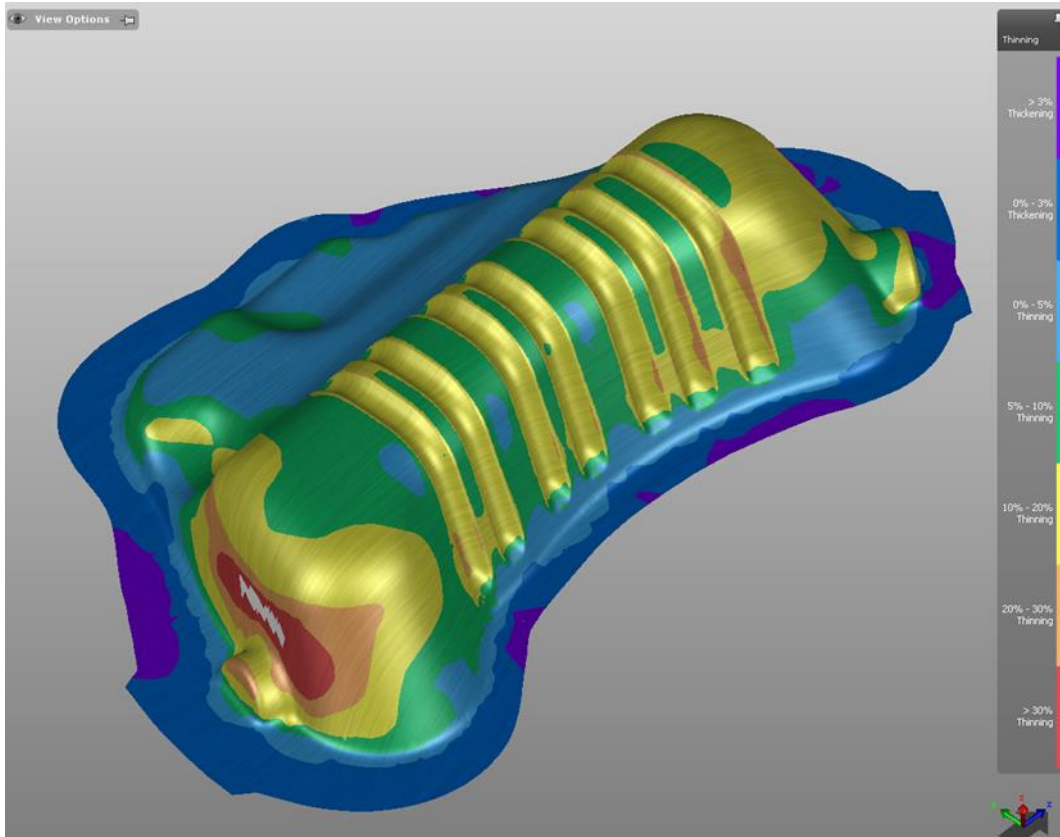
Şekil 2. 6 mm çekme radüsü için dişi kalıp çizimi

Diyagram 1’de analiz sonuçlarından elde edilen incelme bölgeleri limit diyagramı verilmiştir. Şekil-3’te gözüktüğü gibi 6 mm çekme radüs değeri verildiğinde kırmızı bölgeler oluşmuş ve sac parçada yırtılma meydana gelmiştir.

Thinning Limit Diagram



Diyaqram 1. 6 mm çekme radüsü için incelve bölgeleri limit diyaqramı

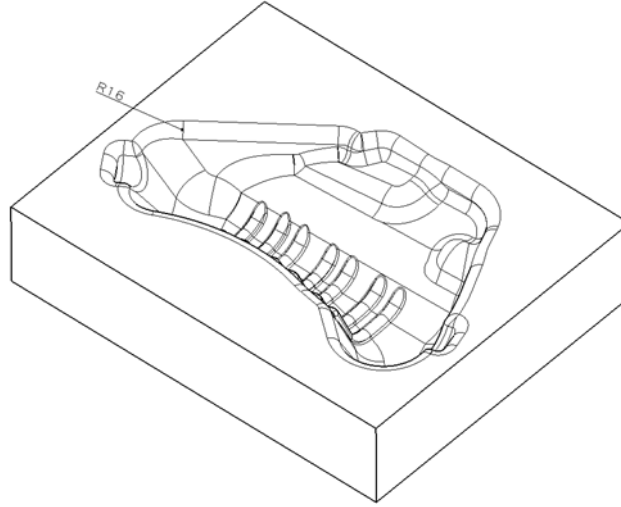


Şekil-3 6 mm çekme radüsü için oluşacak ürün ve incelve yüzdeleri

Şekil-3'te görüldüğü gibi 1.2 mm sac kalınlığındaki levhanın analiz sonucunda renk bölgeleri oluşturarak bu bölgede yüzde olarak incelmeler verilmiştir.

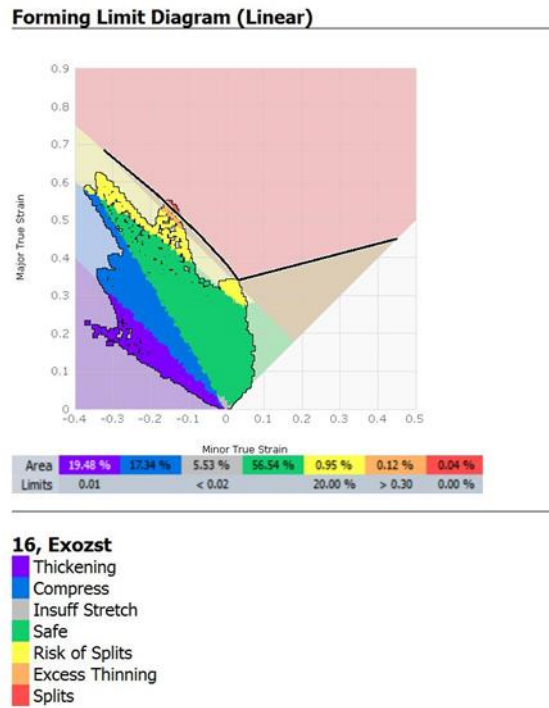
b) 16 mm Çekme Radüsü İçin İncelme Bölgeleri Analizi

Şekil-4'te gözüktüğü gibi çekme radüsü hattı 16mm olarak alınmış ve sonuçlar analiz edilmiştir.

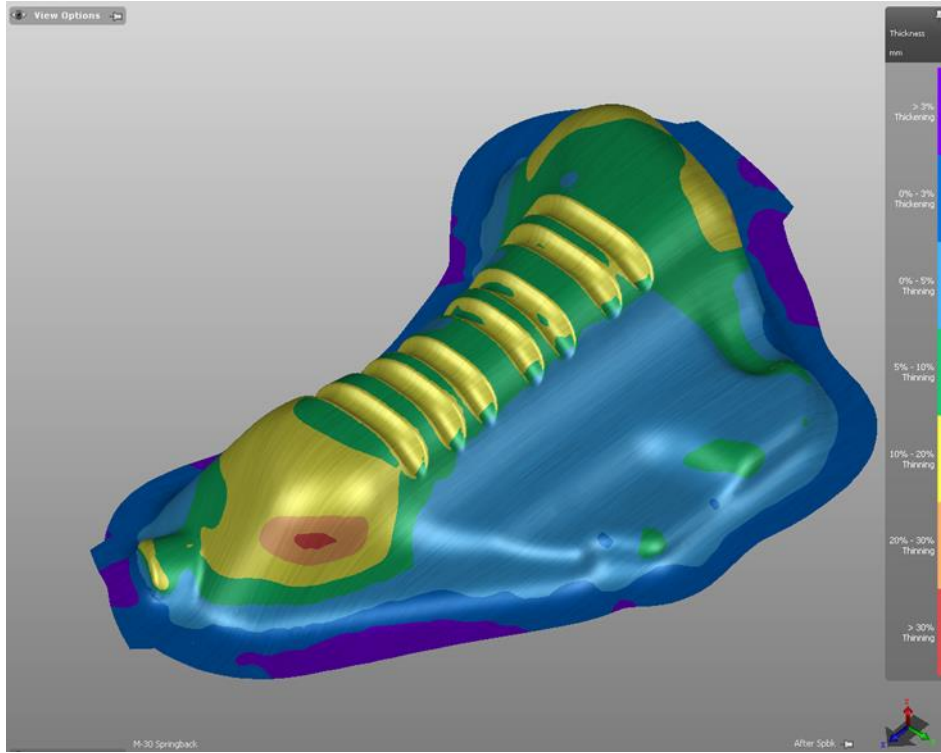


Şekil 4. 16 mm çekme radüsü için dişi kalıp çizimi

Diyagram-2 ve Şekil-5'te gözüktüğü gibi 16 mm çekme radüsü değeri verildiğinde kırmızı bölgeyi bir miktar geçerek yırtılma meydana gelmiştir.



Diyagram-2 16 mm çekme radüsü için incelme bölgeleri limit diyagramı

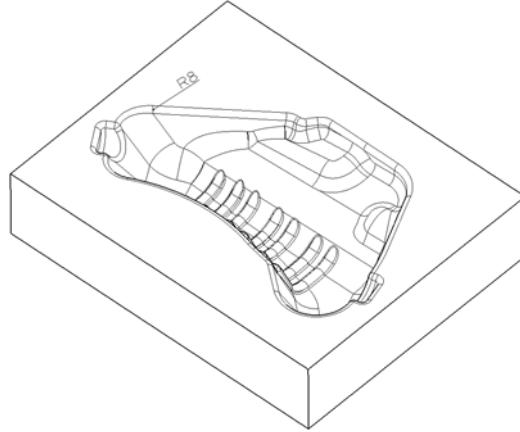


Şekil-5 16 mm çekme radüsü için oluşacak ürün ve incelme yüzdeleri

Şekil-5'te gözüktüğü gibi 1.2 mm sac kalınlığındaki levhanın analiz sonucunda renk bölgeleri oluşturularak bu bölgede yüzde olarak incelmeler verilmiştir. Radüs büyük olduğundan dolayı kırışmaya sebep olmuş ve bunun sonucunda bir miktar yırtılma meydana gelmiştir.

c) 8 mm Çekme Radüsü İçin İncelme Bölgeleri Analiz

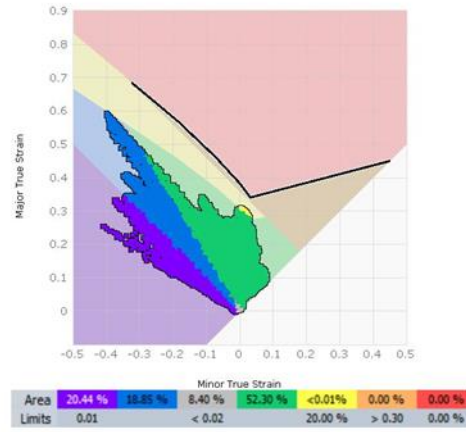
Şekil-6'de gözüktüğü gibi çekme radüs hattı 8 mm olarak tasarlanmış ve sonuçlar analiz edilmiştir.



Şekil 6. 8 mm çekme radüsü için dişi kalıp çizimi

Diyagram-3 ve Şekil-7'de gözüktüğü gibi 8 mm çekme radüs değeri verildiğinde yırtılma bölgesini geçmediği görülmektedir.

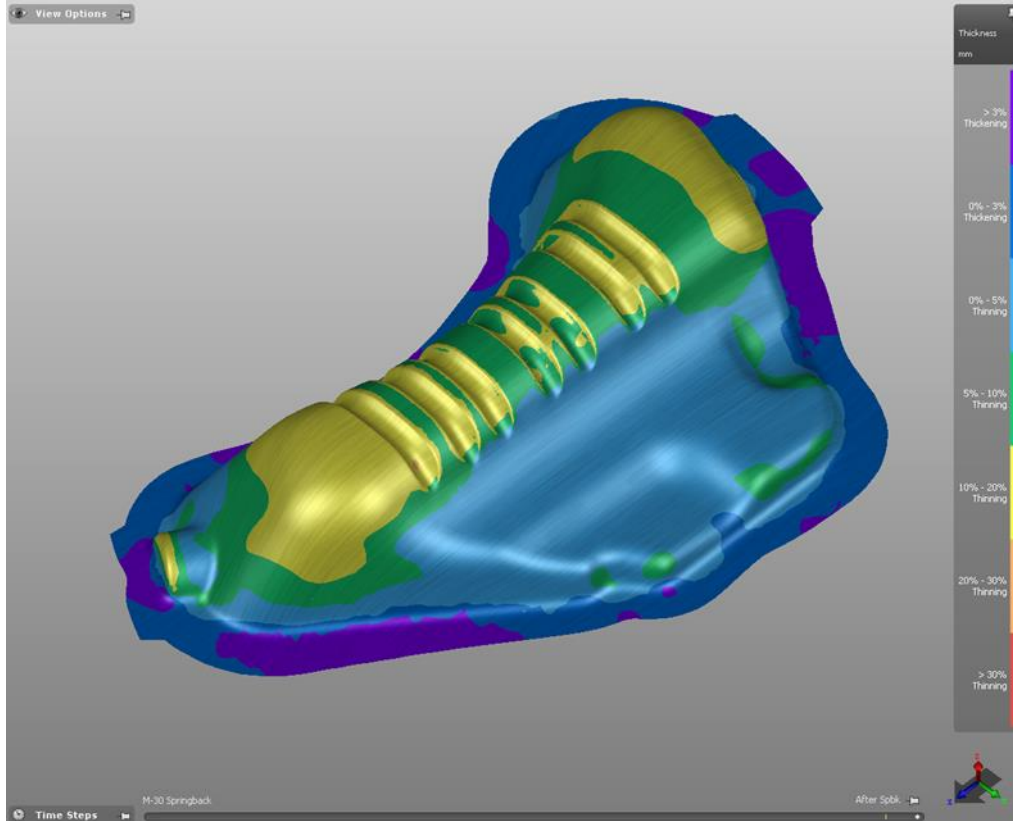
Forming Limit Diagram (Linear)



- 03, Exozst**
- Thickening
 - Compress
 - Insuff Stretch
 - Safe
 - Risk of Splits
 - Excess Thinning
 - Splits



Diyagram 3. 8 mm çekme radüsü için incelmeye bölgeleri limit diyagramı



Şekil-7 8 mm çekme radüsü için oluşacak ürün ve incelmeye yüzdeleri

Şekil-7'de gözüktüğü gibi 1.2 mm sac kalınlığındaki levhanın analiz sonucunda renk bölgeleri oluşturularak bu bölgede yüzde olarak incelmeler verilmiştir. Analiz sonuçlarından kırmızı bölgeler oluşmadığı ve incelmelerin en fazla sarı bölgelerde kalınlığı %10-%20 arasında olduğu gözükmektedir.

d) Analiz Sonuçlarının Değerlendirilmesi

Analiz sonuçlarında da gözüktüğü gibi çekme radüsü 6 mm olarak tasarlandığında yırtılma bölgelerinin en fazla olduğu, çekme radüsü 16 mm olduğunda ise kırışma bölgelerinin fazla olduğu ve bir miktar yırtılmanın olduğu gözlenmiştir.

Burada yırtılmanın hiç olmadığı incelme noktalarının en düşük olduğu çekme analiz sonuçları 8 mm radüs ile sağlanmıştır.

8 mm Çekme Radüsü İçin Pres Parametrelerinin Analizi

Analiz sonucunda elde edilen sonuçlar Şekil-8'de verilmiştir. Buna göre çekme radüsü için oluşacak ürün üst basıncı maksimum 1949.8 kN, alt basıncı ise 800 kN olarak belirlenmiştir.



Şekil-8 Pres parametrelerinin analiz sonucu

Sonuçlar

Bu çalışmada derin çekme yöntemi ile üretilmek üzere tasarlanan bir araba eksozu ele alınarak incelme bölgelerinin analizi farklı çekme radüsleri için incelenmiştir. 3 farklı radüse ait tasarım için AutoForm Programı ile incelme bölgeleri analiz edilmiş ve en uygun üretimin (incelme ve kırışmanın gözlemlenmediği) 8 mm radüse ait tasarım ile yapılması sonucuna varılmıştır. Ayrıca bu tasarıma ait pres parametreleri de analiz edilerek hatasız bir ürün üretimi için ön çalışmalar tamamlanmıştır.

Kaynaklar

- Çavuşoğlu, O , Gürün, H . (2014). Deformasyon hızının dp600 ve dp780 sac malzemelerin mekanik özelliklerine ve derin çekme işlemine etkilerinin incelenmesi. Gazi üniversitesi mühendislik-mimarlık fakültesi dergisi, 29 (4), . Doi: 10.17341/gummfd.76140
- Fırat, M., Kaftanoğlu, B., Eser, O., (2008). “Sheet metal forming analyses with an emphasis on the springback deformation”, Journal of Materials Processing Technology, 196 (1-3): 135-148.
- Esener, C. (2006). “AA5754 malzemesinin derin çekme işleminde baskı plakasının etkisinin teorik ve deneysel olarak incelenmesi” (Yüksek Lisans Tezi), Karabük Üniversitesi FBE, Karabük, 13-65.
- Gürün, H., (2008). “Derin çekme kalıplarındaki parametrelerin deneysel olarak incelenmesi ve bulanık mantık ile tahmini”,(Doktora Tezi), Gazi Üniversitesi FBE, Ankara.
- Erdir, S., (1995). “Profilli derin çekmede hata analizi ve alınabilecek önlemler”, (Yüksek Lisans Tezi), Yıldız Teknik Üniversitesi FBE, İstanbul, 77-85.
- AutoForm R7 <https://www.autoform.com/en/>

Artistic Reflections of Urban Wastes in Contemporary Turkish Pictures

Ayşe Şahin Öztürk
Necmettin Erbakan University

Ömer Tayfur Öztürk
Necmettin Erbakan University

Abstract: The birth of painting, which draws the technical and plastic bases of contemporary Turkish art from the West, is established on the late Ottoman period and the first years of the Republic. The first examples of modern Turkish painting were photographic works and then impressionism in the style of the period. The late reflections of this trend in the process of development in the western continuation were seen in Turkey. The development of painting in Turkey after the 1940s gained momentum and accelerated the development line to catch the line in the West. The socially realistic paintings reflect the artistry around many different styles, currents and subjects. In this diversity, the artists who are called socially realistic, the society that combines the form and the iconography in art became the language of the world. This idea has been preserved in the art of painting, the shell that we can call the style changed eventually. There are many elements that enable society to connect with art. The laborers who work at the point of raising the awareness of the arts, their heavy working conditions always have a big and important place in the art of social content. One of the important problems brought by the urbanization in the cities that are growing with the increase of the human population together with the modern city life is the household waste, in other words, our garbage. In this work, the pictures about the domestic waste and the environmental change in the city life in social life are examined. As a result, the reflections of these colorful and various squares in art were evaluated.

Keywords: Art, Artistic Reflections, Urban Wastes, Turkish Pictures

Çağdaş Türk Resminde Kentsel Atıkların Sanatsal Yansımaları

Özet: Çağdaş Türk resmi olarak adlandırılan teknik ve plastik temellerini Batı'dan alan resim anlayışının doğuşu Osmanlı'nın son dönemlerinde ve Cumhuriyetin ilk yıllarında temellenmiştir. Modern Türk resminin ilk örneklerini dönemin üslubu içerisinde fotografik çalışmalar ve daha sonra izlenimcilik oluşturmuştur. Devam eden süreç içerisinde Batı da gelişen bu akımların devamının geç yansımaları Türkiye'de de görülmüştür. Türkiye'de resim sanatının gelişim süreci 1940'lı yıllardan sonra Batı'daki çizgiyi yakalamak için ivme kazanmış ve gelişim çizgisini hızlandırmıştır. Toplumsal gerçekçi resimler birçok farklı tarz, akım ve konu çevresinde sanata yansımıştır. Bu çeşitlilik içerisinde toplumsal gerçekçi diye adlandırılan sanatçılar, sanatta biçimi ve ikonografiyi birleştirmiş toplumun sanattaki dili olmuşlardır. Resim sanatında bu fikir korunmuş, neticede tarz diye adlandırabileceğimiz kabuk değişmiştir. Toplumun sanatla bağını sağlayan birçok öge vardır. Toplumun sanatla bilinçlendirme noktasında çalışan emekçiler, onların ağır çalışma şartları toplumdaki yerleri her zaman toplumsal içerikli sanatta büyük ve önemli bir yere sahiptir. Modern şehir hayatıyla birlikte insan nüfusunun artmasıyla büyüyen şehirlerde kentleşmenin getirdiği önemli problemlerden biri de evsel atıklar, bir başka deyişle çöplerimizdir. Bu çalışmada: toplumsal hayatın içindeki şehir hayatındaki evsel atıklar ve çevresel dönüşümünü konu alan resimler incelenmiştir. Sonuç olarak elde edilen bol renkli ve çeşitli bu karelerin sanatta ki yansımaları değerlendirilmiştir.

Anahtar Kelimeler: sanat, kentsel atıklar, Türk resim sanatı

Giriş

Çağdaş Türk resmi olarak adlandırılan teknik ve plastik temellerini Batı'dan alan resim anlayışının doğuşu Osmanlı'nın son dönemleri ve Cumhuriyetin ilk yıllarında temellenmiştir. Modern Türk resminin ilk örneklerini dönemin üslubu içerisinde fotografik çalışmalar, daha sonra ise izlenimcilik oluşturmuştur. Batı da gelişen bu akımların devamının geç yansımaları Türkiye'de de görülmüştür. Türkiye'de resim sanatının gelişim süreci 1940'lı yıllardan sonra Batı'daki çizgiyi yakalamak için ivme kazanmış ve gelişim çizgisini hızlandırmıştır.

Resmin sanatının ana dili biçim dili olmasına karşın onun plastik değerlerine hiçbir şey katmayan, ikonografi biliminin irdelediği sembolik anlatım dili de vardır. Modernizm öncesi sanat daha çok anlatım dilini, modernizm sanatı biçim dilini, modernizm sonrası sanat eserleri de her iki dili birden kullanır (Huntürk, 2011: 15). Toplumun sanatla bağını sağlayan toplumsal temalar birçok farklı tarz, akım ve konu çevresinde sanata yansımıştır. Sanatçılar, sanatta biçimi ve ikonografiyi birleştirmiş toplumun sanattaki dili olmuşlardır.

Toplumun sanatla bağına sağlayan birçok öge vardır. Toplumun sanatla bilinçlendirme noktasında çalışan emekçiler, onların ağır çalışma şartları toplumdaki yerleri her zaman toplumsal içerikli sanatta büyük ve önemli bir yere sahiptir. Modern şehir hayatıyla birlikte insan nüfusunun artmasıyla büyüyen şehirlerde kentleşmenin getirdiği önemli problemlerden biri de evsel atıklar, bir başka deyişle çöplerimizdir.

Türkiye’de evsel ve ticari atık miktarının yaklaşık 20 milyon tonu bulunduğu, kişi başına yılda yaklaşık 187 kilogram özellikle üzerinde durduğumuz evsel atık ürettiğimiz tahmin edilmektedir. Evsel atıklarımızın % 20’lik kısmı geri dönüşüm malzemeleri olan ambalaj atıkları % 60’lik kısım ise organik atıklar ve % 20’lik kısım ise kirli atıklar oluşturmaktadır. (<http://www.terabook.org/proje/evsel-atiklarin-geri-donusumu-projesi/>).

Toplumun büyük bir kısmı gündelik yaşantısında farkında olmasa da bu çöp diye adlandırdığımız atıklardan hayatını kazanan insanlar vardır ve bunların sosyal yaşantısı ciddi bir olgudur. Bu iş grubunda çalışan emekçilerin ambalaj atıklarını geri kazandırarak topluma ve çevreye kazandırdıkları faydalardan söz edecek olursak; Kentimizin katı atık depolama alanına giden çöp miktarı azalması, neticede çevremizin korunmasını sağlaması. Çöpün taşınması ve depolanmasını kolaylaştırmak, Hammadde kullanımını azaltarak, doğal kaynaklarımızı korumak, %95’lere varan oranlarda enerji tasarrufu sağlamak, Küresel ısınmayı yavaşlatmak sayılabilir (www.cankaya.bel.tr). Bahsi geçen bu olgudan hareketle sanatını oluşturan veya bu atıklarla sanatsal objeler meydana getiren sanatçılar ve eserleri, çağdaş Türk resmi içinde önemli bir yere sahip görülmektedir.

Bu araştırmada gelişen şehir hayatı ile artan evsel atıkların önemi ve bu atıkların gerek çevresel dönüşümünü konu alan gerekse bu atıklardan malzeme olarak faydalanan sanatçıların eserleri konu alınmıştır. Kentsel bu atıkların sanata yansımaları örnekleriyle incelenmiştir.

Kentsel Atık, tüketim toplumunun oluşum süreci – sanat

Avrupa’da 18. ve 19. yüzyıllarda yeni buluşların üretime olan etkisi ve buhar gücüyle çalışan makinelerin makinalaşmış endüstriyi doğurması, bu gelişmelerin de Avrupa’daki sermaye birikimini arttırması Sanayi Devrimi ya da Endüstri Devrim’ini doğurmuştur.

Tüketim toplumunun oluşum sürecini ele alırken Sanayi Devrim’ini ve bunu hazırlayan nedenleri inceleyerek başlamak en doğru yöntem olacaktır. Sanayi Devrim’ini hazırlayan nedenlere kısaca değinecek olursak: Hızlı nüfus artışı 16. yüzyıldan başlayarak Avrupa’nın nüfusunun hızla artması, tarımdaki gelişmeler bu sektördeki nüfus ihtiyacını azaltarak bu nüfusun kentlere göç etmesine neden olmuştur. Böylece kent sanayisine hazır işgücü oluşmuş, yaşam düzeyi yükselmiş. Eskiden lüks sayılan şeker, kahve, çay gibi mallar artık orta sınıf ve alt sınıflar için doğal bir gereksinme olmaya başlamıştır. Bu da dolaylı olarak tüketim malı talebini arttırmıştır. Böylece tüketim toplumunun temelleri atılmıştır (http://tr.wikipedia.org/wiki/Sanayi_Devrimi 11/10/2014).

Sanayi devrimiyle başlayan ve insan hayatını kolaylaştıran teknolojik buluşlar, yenilikler, beraberinde, kapitalizmi ve çılgınca tüketim anlamına gelen tüketim kültürünü getirmiştir. Bu çılgınca tüketim, doğal olarak atık sorununu gündeme taşımış, baş edilmesi zor bir hale dönüşen atıklar, doğanın yapısını bozarken, görsel bir kirlilik de yaratmıştır.

Sanat, toplumsal ve bilimsel değişimlerden her dönem etkilenmiş, hatta ona göre şekillenmiştir. Sanayi devrimiyle başlayan, teknoloji ürünlerinin getirisi, doğanın halledilemez sorunsalı atık da, sanatçı duyarlılığı taşıyan çok sayıda insanın ilgisini çekmiş eserlerinde gerek araç olarak, gerekse direkt kullanmışlardır

Teknolojinin ürünü atıkların doğaya terk edilmesi çoğu sanatçının ilgisini çekmiş gerek onları toplayarak eserlerini oluşturmuşlar, gerekse de bir fotoğrafa dönüştürüp gözler önüne sermişlerdir.

Çağdaş Türk Sanatının Gelişimi ve Toplumsal İçerikli Sanat

Toplumsal sanat, toplumsal gerçekçi resim denildiğinde konusunu birey ve toplumdaki alan, gerçeği tüm çıplaklığı ile yansıtan resimdir. Toplumsal sorunlara karşı izleyiciye belli mesajlar iletmek isteyen toplumsal gerçekçiler dönemin ekonomik ve siyasi bunalımlarına tepki verir ve düzelmesi için resimler yaparak seslerini ve eleştirilerini duyurmak isterler (Arda, 2007: 36).

Türkiye de batılı anlamda resim eğitiminin başlangıcı olarak, Mühendishane-i Berri Hümayun’un ders programına resim derslerinin konulduğu 1795 tarihi kabul edilmektedir.

II. Abdülhamid tahta geçtikten sonra, Osman Hamdi Bey resim ve mimarlık alanında eğitim vermesi amacıyla 1883 yılında kurulan Sanayi-i Nefise'nin kuruluş çalışmalarını da yürüterek başına geçmiştir.

Osman Hamdi, bilimsel ve araştırmacı bir tavırla figürü ilk ele alan sanatçı olarak “*Sanatın amacı doğayı doğru taklit etmektir*” düşüncesiyle hareket etmiştir. Bu durum Osman Hamdi'nin sanatında bir çelişki yaratmış, bir dönem Batı taklidi bir dönem toplumsal gerçekçi resimleri ile ikilem içinde kalmıştır (Ersoy, A, 1997,54).

1908-1909 yıllarına kadar süregelen bu gelişmelerden Osmanlı Ressamlar Cemiyeti'nin kuruluşuna kadarki geçen dönem Türk resminde erken dönem olarak değerlendirilir.

Osmanlı Ressamlar Cemiyeti, 1921 yılında “*Türk Ressamlar Cemiyeti*”, 1926 Yılında “*Türk Sanayi-i Nefise Birliği*” daha sonra ise “*Güzel Sanatlar Birliği*” adı altında faaliyetlerini sürdürmüştür.

1914 Çallı Kuşağı: Çağdaş Türk resminin temeli Osmanlı Ressamlar Cemiyeti ile atılmış, çağdaş sanat akımlarına geçiş yine bu cemiyetle sağlanmıştır. Zira 1910'da bu cemiyet mensubu sanatçıların çoğu sanat eğitimi almaları amacıyla yurtdışına gönderilmiştir. Bu sanatçılar daha sonra I. Dünya Savaşı başlayınca yurda dönmüşlerdir, toplumsal anlayışta izlenimci resim yapmışlardır.

Çallı Kuşağı sanatçılarından bazıları Sanayi-i Nefise'ye hoca olarak, sanat anlayışlarını bu yolla yayarken, onların öğrencilerinden bir grup 1925 yılında sanat öğrenimi için Paris'e gönderilmiştir, 1928 yılında tekrar yurda çağrılmışlardır. Yurda dönüş yaptıktan sonra Müstakil Ressamlar ve Heykeltıraşlar Birliği adıyla anılan grubu oluşturmuşlardır. Ortak bir sanat anlayışı tanımayan birlik üyeleri farklı tarzlarda resimler yapmışlardır.

Genç Cumhuriyetin onuncu yılı olan 1933'te ise Müstakillerden ayrılan bir grup sanatçı “*D Grubu*” adıyla anılan grubu kurmuştur. Osmanlı Ressamlar Cemiyeti, Güzel Sanatlar Birliği ve Müstakil Ressamlar ve Heykeltıraşlar Birliğinden sonra, kurulan dördüncü ressamlar birliği olması nedeniyle alfabenin dördüncü harfi olan “*D*” den ismini almıştır (Candan, 2004:40). Bu grup ile toplumsal içerikli figür resmi sekteye uğramış yerine dönemin getirdiği yeni akımlar almıştır. Bu sentezin dışına çıkan sadece Turgut Zaim olmuştur.

1936 yılında akademi hocalarının değiştirilmesi, 1937 yılında Leopold Levy'nin resim atölyesi şefliğine getirilmesi, Levy'nin Türk kültür ve geleneksel sanatlarına büyük bir ilgi duyması ve bunu her fırsatta dile getirmesiyle çevresinde büyük bir etki yaratmış ve öğrencilerini de bu felsefe doğrultusunda etkilemiştir.

Bunun sonucunda Leopold Levy'nin atölyesinde çalışan öğrencilerden bir kısmı 1940'larda Yeniler Grubu adıyla birleşmişler ve etkinliklerini sürdürmüşlerdir. Yeniler'le, ilk kez Türkiye'de bir sanat grubu belirli bir görüş etrafında birleşmiştir. Yeniler, Türk resminin gerçek kimliğine kavuşabilmesi için; memleket yaşantısından alınan konuların yine konuya uygun bir üslupla işlenmesi gerektiğini savunmuşlar ve ulusal yerel bir sanat anlayışı sergilemişlerdir. (Giray, 1994: 46). Toplumsal gerçekçi resim anlayışı tekrar yeniler ile tuvalde vücut bulmuştur.

Yeniler Grubu 1940'lı yıllardan 1960'lı yıllara kadar resim sanatına figüratif ve toplumsal gerçekçi bir anlayış getirmişlerdir. Toplumun sorunlarıyla birebir ilgilenen grup üyeleri tüm sosyal gerçekleri halkın sıkıntılarını eserlerine yansıtmışlardır (Arda, 2007:40).

1950'ler: Türkiye de sanayileşmenin başlaması ile toplumun yaşantısında değişiklikler olmuş ve köyden kente göçler yaşanmıştır. Yaşanılan bu değişimi eserlerine yansıtan Nedim Günsür ve Neşet Günal Anadolu insanının yaşam gerçeklerini konu almışlardır (Doğan, 2003: 33).

Nedim Günsür gibi Paris'te Andre Lhote ve Fernand Leger atölyelerinde çalışmış, toplumsal gerçekçi anlayışta verdiği yapıtlarla ve yetiştirdiği öğrencilerle Türk resim sanatında yerini kanıtlamış diğer sanatçı da Neşet Günal (1923-2002)'dir. Günal, anıtsal yapıdaki biçimleriyle, eserlerinde kırsal kesimin geri kalmışlığını ve durağanlığını anlatır.

1960'lara gelindiğinde Türkiye de; Avrupa'da 1960'larda çıkan yeni figürasyon eğilimi Batı'da olduğu gibi, Dışavurumcu- Sürrealist ve Toplumsal Eleştirel Gerçekçi anlatımlarla kendini göstermiştir. İnsanın içsel yaşamı yönünde gelişen yeni bakış açısının yanı sıra toplumsal eleştirel gerçekçi sanat görüşünün de yeniden gündeme gelmesini sağlamıştır (Doğan, 2003: 39).

Bu eğilim içerisinde 1960'larda hicivsel ve mizahi anlatımıyla Cahit Burak, iri yüzlü kadın portreleriyle Nuri İyem, kent insanının yaşamından sahneler yansıtan Neşe Erdok, toplumdaki sıkışık kalmış insanların yabancılaşmasını, yalnızlığını, zevk alemlerini insanı ürperten bir anlatımıyla Mehmet Güler yüz söylenilebilir.

Toplumsal gerçekçi – eleştirel gerçekçi resim anlayışında eser üreten diğer sanatçılar olarak Osman Oral, İsmail Altınok, Hüseyin Bilişik, Duran Karaca, Kayıhan Keskinok, Mehmet Güler, Yalçın Gökçebağ, Veysel Günay ve Mehmet Başbuğ'u sayabiliriz.

1980'lerde ortaya çıkan Yeni Dışavurumculuk, dünyada ve Türkiye'de aynı anda görülmüştür. 1970'li yıllardaki sosyo-politik baskıların ve teknolojinin gelişmesinin sonucu oluşan varoluşçuluk düşüncesiyle beraber gelişmiştir. İnsan psikolojisine ve bireyselliğe önem veren varoluşçu düşünce, insanı ezen düzene, kişiliğini sindirmeye çalışan topluma karşı koyar. Bireyin kendini tanımasını, baskıdan kurtularak kişiliğini yaratmasını amaçlayarak topluma yabancılaşmasını ve yalnızlaşmasını engellemeye çalışır (Arda, 2007:51).

Türkiye'de Yeni Dışavurumculuk akımı içerisinde Cihat Aral, Nedret Sekban, Kasım Koçak, Seyyit Bozdoğan, Hüsnü Koldaş gibi sanatçılar söylenilebilir.

1980'lerden dünyayı vuran ekonomik kriz ile birlikte etkisini arttıran Yeni Dışavurumculuk ve bunun yanı sıra teknolojik gelişmelerle kitle iletişim araçlarının yaygınlaşması, akabinde internet yayıncılığı ile toplumsal olayların ve sanat olaylarının hızlı etkileşimine yol açmıştır. Sanatçılar resimlerinde figüratif dışavurumlar ve biçimi bozan dışavurumları ile sanatlarını göstermişlerdir.

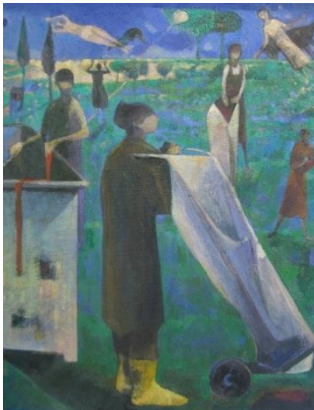
Sosyal, ekonomik, kültürel ve politik parçalanmalarına yabancı kalamayan sanatçılar ise, içsel duygularını dışa vurmaya ve olanları sorgulamaya başlamışlardır. Türkiye'nin gündeminde yer alan olayları kendi bakış açılarıyla farklı teknik ve anlatımlarıyla, konu çeşitliliği içerisinde yansıtan sanatçılar, figüratif resim sanatına ve toplumsal gerçekçi resmin gelişmesine katkılarda bulunmuşlardır. Zamanın aynası niteliğindeki bu işlerin her biri, toplumun yaşadığı olayları tek tek gözler önüne sermekte ve sanat yoluyla insanlara yol göstermektedir (Arda, 2007: 58).

Kentsel Atıkları Toplumsal İçerikli Ele Alan Sanatçılar

Cihat Aral

Sanatçı çöpten hayat bulan insanları, çöpün getirisiyle hayatını sürdürmeye çalışan insanları ele alarak toplumsal duyarlılığını göstermektedir. Aral, ifadeyi güçlendiren renk ve biçim bozmalarıyla 2002'de "Çöp İnsanları" ismini verdiği bir dizi çalışma üretir. Yaşamını çöpten çıkaran insanların dramını seyirciye aktarır. İnsanın modernleşen kent dokusu içindeki karmaşık yaşamını, ışık yansımalarının, gölgelerin oluşturduğu bir mekân içinde gösterir. Çöp toplayan insanları ile toplumsal yapıyı anlatmak istediğini söyleyebiliriz.

Resim 1:



Eser adı: Çöp İnsanları

Ölçüleri: Bilinmiyor

Tekniği: Tv.Yb

Tarihi: 2008

Cihat Aral bu eserinde açık kompozisyon düzeninde bir kurgu oluşturmuştur. Eser de dikey figür yapıları ile dinamik bir yapı oluşturulmuş bu yapı resmi üst kısımdan kesen yatay ufuk çizgisi ile zıt formların dengesi üzerine bir kurgu yaratılmıştır. Sağ latta duran ve ön plana çıkan çöp arabası ve buut formlarıyla resme diyagonal bir hareket katılmıştır. Resim yüzeyine perspektif gözetilerek dengeli yerleştirilmiş çöp toplayan insanlar ile ritmik hareket katılmıştır.

Resim yüzeyinde mavi- yeşil tonlar kullanılarak figürlerin ritmik hareketliliği durgunlaştırılmıştır. Buz rengi donuk yüzlerle çalışan insanların psikolojik durumlarına gönderme yapan sanatçı çöplerin renkli formlarıyla resimde dengeyi sağlamıştır.

Toplumsal bir olguyu ve insanların kent hayatının zorlukları içerisinde hayat mücadelelerini anlatan resim toplumsal gerçekçi anlayışta yapılmıştır.

Resim 2:



Eser adı: Çöp Toplayıcıları
Ölçüleri: 92.00 x 130.00 cm
Tekniği: Tv.Yb
Tarihi: 2005

Resim açık kompozisyon örneğine göre kurulmuştur. Grup grup tuval üzerine yerleştirilen figürler resme hareketlilik katmış ve sanatçı bu gruplamayla resimde boşluk doluluk dengesini sağlamıştır. Figürlerin dikey duruşu ufuk çizgisinin yataylığıyla zıtlık ve denge sağlanmıştır. Turuncu sarı tonlardaki zemin rengi soğuk mavi buz rengi tonlarındaki figürlerle resmin renk dengesi sağlanmıştır.

Çöp toplayan insanların zorlu yaşam şartları altında çalışmalarını anlatan eserde insanların yüzleri donuk buz renginde boyanması ile insanların psikolojik durumları anlatılmaya çalışılmıştır.

Resim kurgusal ve uslupsal özellikler açısından incelendiğinde biçimsel açıdan güçlü sosyal gerçekçilik akımına özgü niteliklerde olduğunu görmekteyiz.

Resim 3:



Eser adı: Karda Çöpçüler
Ölçüleri: 70.00x100.00 cm.
Tekniği: Tv.Yb
Tarihi: 2009

Resim açık kompozisyon düzenine göre kurulmuştur. Grup grup tuval üzerine yerleştirilen ağaçlar resme hareketlilik katmış ve sanatçı bu gruplamayla resimde boşluk doluluk dengesini sağlamıştır. Ağaçların resmi yarıdan ikiye yatay olarak kesmesi ve diyagonal biçimde kesmesiyle eserde bilinçli parçalanmalar oluşturulmuştur. Ağaçların dikey duruşu ufuk çizgisinin yataylığıyla zıtlık ve denge sağlanmıştır. Ağaç sıralarının kompozisyon üzerinde sağ üst köşeye doğru birleştiği noktada çöp arabasıyla çöp toplayan insanlar vurgulanmış ve kompozisyonun can alıcı etkin noktası olduğu anlatılmak istenmiştir.

Çöp toplayan insanların zorlu yaşam şartları altında çalışmalarını anlatan eserde zeminin beyaz mavi tonlarda işlenmesi karlı hava şartlarının yanı sıra psikolojik olarak yapılan işin zorluğuna da dikkat çekmektedir. Çöpler içerisinde çalışan insanların yalnızlığı eserde şiddetle vurgulanmıştır.

Resim kurgusal ve uslupsal özellikler açısından incelendiğinde biçimsel açıdan güçlü ve sosyal gerçekçilik akımına özgü niteliklerde olduğu anlaşılmaktadır.

Şükriye Göçer



Sanatçı çöp toplayan insanı ele alarak, doğa ve çevrede gözlemlediklerini renklerle bütünleştirmektedir.

Resim 4:

Eser adı: Eskici
Ölçüleri: 50x80 cm.
Tekniği: Tv.Yb
Tarihi: Bilinmiyor

Resim kapalı kompozisyon düzenine göre kurulmuştur. Resimde yatay kompozisyon elemanları olarak konak yol ve duvar yer alırken eserde orta alanda yer alan hurdacı figürü dikey duruşuyla zıtlık oluşturmaktadır. Renkçi bir anlayışta yapılan resimde hurdacı figürünün üzerindeki kabanının siyah tonlarda ele alınması ile dikkatleri üzerine çekmesi sağlanmıştır.

Eserde figürün rahat duruşunun yanı sıra siyah tonlarda bir elbise ile yorumlanması ve yoğun bir yük altında yorgun bir duruşla ele alınması resmin arka planda adeta hurdacının psikolojik durumuna atıf yapmakta.

Çöp toplayan insanların zorlu yaşam şartları altında çalışmalarını anlatan eserde zeminin beyaz mavi tonlarda işlenmesi karlı hava şartlarının yanı sıra psikolojik olarak yapılan işin zorluğuna da dikkat çekmektedir. Çöpler içerisinde çalışan insanların yalnızlığı eserde şiddetle vurgulanmıştır.

Resim kurgusal ve üslup özelliği açısından incelendiğinde izlenimci anlayışta yapılmış ve sosyal gerçekçilik akımına özgü niteliklerde olduğu anlaşılmaktadır.

Sonuç

Türkiye’de Batı’lı anlamda resim sanatının 200 yılı aşkın süredir devam eden serüveni içerisinde sanatçılar toplumun sorunlarını kendi benliklerinde yoğurup tuvallerine aktarmışlardır. 1980’lerden sonra yeniden parıldayan “Yeni Dışavurumculuk” akımı ile toplumsal gerçekler sanatçı tarafından vurgu yapılan, önemsetilen tarihe bir not olarak kalacak değerler olarak yansıtılmıştır ve yansıtılmaya devam edecektir.

Nüfusun artması şehirleşmenin getirmiş olduğu yaşam kavgaları yaşamın soğuk yüzü insanları toplumsal gerçeklere uzaklaştırmıştır. Bazı insanın yaşamında ardında bıraktıklarından bazıları yaşamını idare ettirmeye çalışmaktadır. Bu noktada sanatçı duyarlılığıyla evsel atıklardan topladıkları ambalaj atıkları ile yaşamını sürdüren insanların hayatlarını ele alan sanatçı onların yaşam gerçeklerini anlatmaya devam etmektedir.

Kaynakça

- ARDA, Zuhale, (2007). “Sanat Eğitimi ve Ressam Aydın Ayan’ın Resimlerine Estetik Bir Yaklaşım”, Konya: Selçuk Üniversitesi, (Yayınlanmamış Doktora Tezi).
- CANDAN, Latife Esra, (2004). “Cumhuriyetin İlanından Günümüze Türk Resminde Köy ve Köy Yaşantısının Resim Eğitimine Katkısı”, Konya: Selçuk Üniversitesi, (Yayınlanmamış Yüksek Lisans Tezi).
- DOĞAN, Fatma, (2003), “Türk Resim Sanatında Toplumsal Gerçekçi Eğilimler”, Yüksek Lisans Tezi, Eskişehir
- ERSOY, Ayla, (Ocak/Şubat 1997). “Karşılıklı Etkileşim İçinde Türk ve Batı Sanatı”, Türkiye de Sanat Plastik Sanatlar dergisi, Sayı:27, s:54.
- GİRAY, Kıymet, (Mart/Nisan 1994). “Türk Resminde Liman Sergisi, Yeniler Grubu ve Leopold Levy”, Türkiye de Sanat Plastik Sanatlar Dergisi, Sayı:13, s:46-47.
- HUNTÜRK, Özi, (2011).” Heykel ve Sanat Kuramları”, İstanbul: Kitabevi Yayınları

Web Kaynakları:

- <http://www.terabook.org/proje/evsel-atiklarin-geri-donusumu-projesi/>
- www.cankaya.bel.tr
- http://tr.wikipedia.org/wiki/Sanayi_Devrimi 11/10/2018

Interpainting As A Creating Method in Digital Illustration: Reinterpretations from Movie Scenes

Öğr. Gör. Erdinç ÇAKIR
Necmettin Erbakan Üniversitesi

Dr. Öğr. Üyesi Mahmut Sami ÖZTÜRK
Necmettin Erbakan Üniversitesi

Arş. Gör. Mevlüt ÜNAL
Necmettin Erbakan Üniversitesi

Dr. Öğr. Üyesi Mehmet SUSUZ
Necmettin Erbakan Üniversitesi

Abstract: Interpainting is used to quote a contemporary artwork or to describe reinterpreted works of art. It is inevitable that the interaction is in every field as well as in the field of art. Photography has changed our art and perception style in XIX. Century. As the photography gives birth to the cinema, digital illustrations are a good example of the relationship between technology and art in the meaning that new artistic works will be produced from the cinema. Even though the canvases are not replaced by computer screens yet fully benefit greatly from the computer or technology when designing the work of many artists. In a similar way to artworks that have been re-interpreted dozens or even hundreds of times such as Leonardo da Vinci's Mona Lisa, it is quite possible today to produce new artworks from cinemas. Besides it is still a matter of debate whether digital arts are art or not today, the intensive use of digital illustrations has contributed positively to the elimination of these debates. In the study, some examples of digital illustrations that worked directly from movie scenes or indirectly referencing to films will be examined.

Keywords: Interpainting, Digital Illustration, Cinema.

Dijital İllüstrasyonda Bir Yaratma Biçimi Olarak Resimlerarasılık: Sinema Sahnelerinden Yeniden Üretim

Özet: Resimlerarası terimi bir sanat eserinden alıntı yapılarak ya da yeniden yorumlanan sanat eserlerini tanımlamak için kullanılmaktadır. Etkileşimin her alanda olduğu gibi sanat alanında da olması kaçınılmazdır. XIX. yüzyılda fotoğraf, sanatı ve algılama biçimimizi değiştirmiştir. Dijital teknolojik yenilikler, özellikle bilgisayarda sanatı etkilemiştir. Fotoğrafın sinemayı doğurması gibi, sinemadan yeni sanatsal işler üretilmesi anlamında, dijital illüstrasyonlar teknoloji ve sanat arasındaki ilişkiye iyi bir örnek teşkil etmektedir. Tuvallin yerini bilgisayar ekranı henüz tam olarak almamış olsa bile birçok sanatçı işini tasarlarken bilgisayardan veya teknolojiyen faydasıyla faydalanmaktadır. Leonardo Da Vinci'nin Mona Lisa'sı gibi onlarca hatta yüzlerce kez yorumlanan sanat eserlerine benzer bir şekilde sinemadan da yeni işler üretilmesi günümüzde oldukça olağandır. Dijital sanatların sanat olup olmadığı hala tartışma konusu olduğu günümüzde dijital illüstrasyonların çok yoğun olarak kullanımı bu tartışmaların giderilmesine olumlu katkı sağlamaktadır. Çalışmada, doğrudan sinema film sahnelerinden çalışılmış ya da dolaylı olarak filme gönderme yapan dijital illüstrasyon örnekleri incelenecektir.

Anahtar Kelimeler: Resimselarasılık, Dijital İllüstrasyon, Sinema.

Dijital Sanat ve İllüstrasyon

Elektronik ortamda üretilmiş sanat eserlerini dijital sanat olarak tanımlayabiliriz. Genellikle bu üretimler bilgisayar destekli olmakla birlikte, ışık, ses, kamera, telefon aracılığı ile oluşturulmuş olabilir. Birçok sanatsal üretim yöntemi (video ve ses gibi) aynı anda kullanılabilen dijital sanat, bu anlamda klasik sanata meydan okumakta kendi metodlarını geliştirmektedir. Dijital sanatların meydan okumalarına karşın hala tartışılıyor olması ise henüz çok yeni olması ve tam olarak kendi kurallarını/kuralsızlığını oluşturamamasından kaynaklanmaktadır. Teknolojinin hızla gelişmesi, sanatçının bu gelişmelerin dışında kalamaması, sanatçıların

kendini ifade etme isteklerinin bir sonucu olarak, dijitali sanatın bir konusu bazende bir parçası olmasını sağlamıştır.

Bununla birlikte dijital sanatın çoğaltılabilir ve yeniden üretilebilir olması, sanatın biricik olma özelliğine saldırı olarak da değerlendirilebilmektedir. Dijital sanat, kendi içerisindeki tüm bu çatışmalar ve çelişkilerle birlikte, sanata yeni anlamlar yüklemektedir (Atan, Uçan, & Bilsel, 2015)

İllüstrasyon "Fransızca illustration "resimleme, renklendirme, nakış" sözcüğünden alıntıdır. Fransızca sözcük Latince illustratio "1. aydınlatma, 2. resimleme, renklendirme, nakış" sözcüğünden alıntıdır. Bu sözcük Latince illustrare "aydınlatmak, parlatmak" fiilinden +(tion ekiyle türetilmiştir. Latince fiil Latince lustrum "parıltı" sözcüğünün isimden türetilmiş fiilidir (Nişanyan Sözlük, 2018).

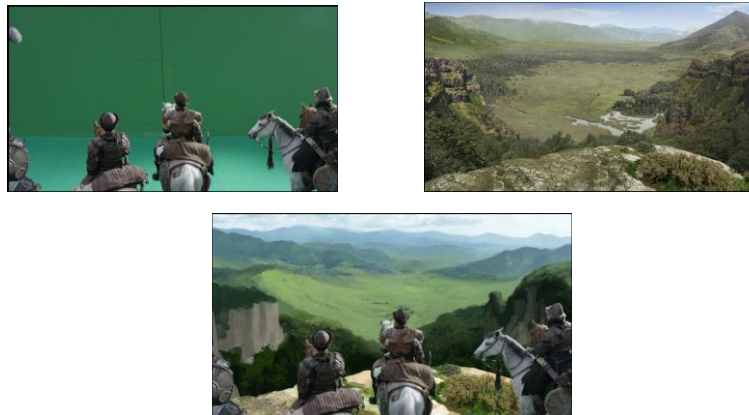
Dijital illüstrasyonu, vektörel tabanlı programlar (Adobe Illustrator, Corel Draw vb. Programlar) ve piksel tabanlı programlarda (Adobe Photoshop, Art Rage, Procreate, Corel Paint, Gimp vb.) üretilen işler olarak iki ana bölümde inceleyebiliriz. Vektörel tabanlı üretimler matematiksel formüller gibi sonuçları değişmeyen yani işin boyutu değişse de görüntü kaybının olmamasını sağlayan bir yapıdadır. Piksel tabanlı programlar ise görüntü boyutunun sergilenecek veya baskı alınacak boyutta ya da ona yakın boyutlarda işin başında karar verilmesi gereken programlardır. Piksel tabanlı üretimler ise işlev açısından daha esnek yapıda olmalarına karşın yanlış boyutlarda çalışılması veya önceden küçük çalışılıp daha sonra işin büyük ebatlarda baskı alınması durumlarında pikselleşme denilen ve normalde işte görmememiz gereken karelerin görülmesi problemi ortaya çıkabilen uygulamalardır. Dijital illüstrasyonun gerçek gücü tablet aracılığı ile katlanarak artmıştır. Tablet kullanan sanatçı bir kalem aracılığı ile kağıda çizim yapar gibi bir ekran üzerine veya ekrana bağlı bir aparat ile çizimi ekranda takip ederek istediği illüstrasyonu dijital ortamda rahatlıkla oluşturmaktadır.

Sanat ve teknoloji birbirlerini etkileyen kavramlar olmakta ve sanat, teknoloji ile birlikte değişmektedir. Genel anlamda sanatın bilgisayar teknikleriyle yeniden oluşumu, dijital sanatı doğurmuştur. Dijital sanat, disiplinler arası yakınlaşmaya neden olmuş, sanat, tasarım ve teknoloji birlikte ifade gücü bulmaya başlamıştır. (Atan, Uçan, & Bilsel, 2015)

Özellikle dijital teknolojiye yönelik yeni vaatler ve olanaklar, geleneksel sanata meydan okuyarak, yeni biçimsel sunumların oluşmasına neden olurken, yeni anlatım biçimlerini de doğurmuştur. (Özel Sağlamtimur, 2010)

Sinema ve Resim/İllüstrasyon Arasındaki Etkileşim

Sinema ve resim sanatı incelendiklerinde bazı yönlerden farklılaşsa da birçok yönden benzerlikler göstermektedir; özellikle de estetik özellikler bakımından ışık, renk, kompozisyon gibi temel özelliklerde çok fazla benzeşmektedir. Ayrıca birçok resmin(fotoğrafın) arka arkaya oynatılması sonucu sinemanın oluşması, bu argümanı oldukça desteklemektedir. Sinema tarihine baktığımızda bilgisayar desteğinin ve özel efektlerin olmadığı zamanlarda resim olarak bizzat kendisinin, günümüzde ise Mat Boyama (Matte Painting) denilen illüstrasyon/foto manipülasyon ile genellikle arka planda mekan oluşturmanın maliyetli veya mümkün olmadığı hayali mekanlarının oluşturulmasının gerektiği durumlarda gerçeklik yaratmak için kullanılan çalışmalar sinemanın bir parçası olmuş, olmaya da devam etmektedir. Bu açıdan sinema resmi/illüstrasyonu alıntılanmış, kendi sanatının bir parçası haline getirmiştir.



Resim 1: Atılğan Aşıkuzun 2014 "Diriliş Ertuğrul"

Geçmiş veya gelecek temalı yapılan yada kurgu ürünü olan bir filmin mat boyama sahneleri gerçekçi bir şekilde boyandığı kadar yaşanmışlık etkiside vermelidir. Bu sayede oluşturulan ütopyik sahne normalde var olmasada, kurgulanmış olduğu evrende alışılmış ve normalmiş gibi bir izlenim verilmesi durumunda daha etkili olacaktır (Armutçu, 2016).

Burada kendinin parçası haline getirilen resim/illüstrasyon alıntılanan ünlü bir sanat eseri ya da sinema filminden bağımsız bir sanat eseri olmamakla beraber benzer özelliklere değinilmesi karşılıklı etkileşimin algılanması açısından önemlidir. Sinemadan bağımsız olarak değerlendirildiğinde ise bu işler dijital sanat olarak sınıflandırılacak nitelikli işlerdir.

Sinemadan Dijital İllüstrasyonlar Yaratma

Aktulum görsel alıntıyı “en az iki resim (ya da bir resim ile bir başka sanatsal biçim) arasındaki resimlerarasılık (ya da göstergelerarasılık) sürecini başlatan yöntem” olarak tanımlamaktadır. *Alıntı, bir yöntem olarak resmin benimsenmiş bir özelliği olarak neredeyse her dönemde kullanılmıştır. Gerçekten de şu ya da bu resim, başka resimler yanında başka sanatsal biçimler olarak alıntılanarak varlığını sürdürülebilmektedir (Atakulum, 2016).* Sinema önce mat boyama ile kendi nesnesi yaptığı mekan ya da obje resimlerini yeniden dijital illüstrasyon üretimi ile yeni resmin tekrar objesi haline getirmektedir.

Alıntılama yöntemini veya kendine mal etme işini en fazla ve iyi yapan sanatçıların başında Picasso’yu sayabiliriz. *Picasso, “Avignonlu Kızlar” ve “Guernica” gibi eserleriyle kübist akımının temsilcilerinden biri olarak tanınmaktadır. Sanatçının eserlerini incelediğimizde geometrik çözümlerinin arkasındaki biçim ve imgeler oldukça tanıdık gelmektedir. Bunun nedeni sanatçının, hayranı olduğu diğer sanatçıların eserlerinden alıntulamalar yaparak eserlerini üretmesidir. Batı sanatının kanonlaşmış eserlerine olan bu ilgi yalnızca Picasso’da yoktur. Avrupa’da eğitim gören ve yerleşen Latin-Amerikalı sanatçıların çeşitli alıntılama yöntemleri kullanarak ürettikleri eserlerde Avrupalı sanatçıların izleri görülmektedir. Sanatçılar, usta sanatçıların eserlerini yeniden resmetmelerinde saygı duymakla beraber sanatsal açıdan kendilerini geliştirmek, özgün bir üslup oluşturmak ve sanatsal kimliklerini edinmek amacını gütmektedirler. (Atakulum, 2016)*



Resim 2: Diego Velazquez, *Las Meninas*, 1656, 318x276 cm



Resim 3: Pablo Picasso, *Las Meninas*, 1957, 194x260 cm

Klasik dönemde sanatçıların eserlerinin başkaları tarafından gravürlerinin yapıp yinelenmesi, Modernizmde sanatçıların, eski dönem usta sanatçıların çalışmalarını kopya ederek sanatsal unsurları öğrenmeye başlamaları ve kendi yorumları ile yeniden resmetmeleri, Postmodernizm ve günümüzde eleştirel bakış açıları ile çeşitli alıntılama yöntemleri kullanılmaktadır (Erdoğan, 2018).



Resim 4: Leonardo da Vinci, Mona Lisa 16.yy.



Resim 5: Marcel Duchamp, L.H.O.O.Q 1919

Modern sanatın önemli temsilcilerinden sayılan Johannes Kahrs'ın eserlerinde tv, film ekran görüntülerini kendi eserlerinin konusu yapmıştır. Bu görüntüleri kendi resminin konusu yaparken bazen ikonik isimleri olduğu gibi alırken bazen de görüntünün üzerinde oynamalar yaparak orijinali ile anlamını koparır.

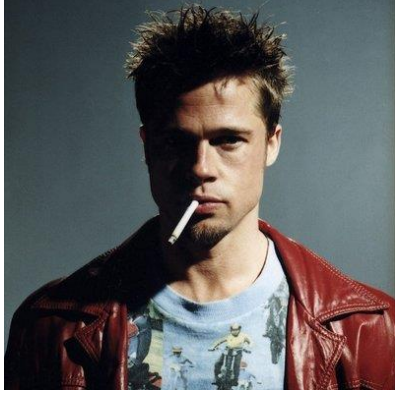


Resim 6: Untitled (jesus aged 43), 2015



Resim 7: Untitled (monkey man), 2015

Sinema günümüz dünyasında özellikle Hollywood bağlamında bakıldığında çok büyük bütçelerin ve en yeni tekniklerin kullanıldığı bir sektördür. Durum böyle olunca ortaya çıkan işler genellikle hayranlık uyandıracak etkili işler olmaktadır. Bu hayranlık uyandıran işler birçok sanatçıyı ya da sanatçı adayını etkileyip yeniden üretim yapma konusunda teşvik etmektedir.



Resim :8 Orijinal Karakter.



Resim :9 Sergio Mechoulam, 2014.



Resim 10: tyroneG, 2013

Yukarıdaki resimlerde 8 nolu resimde orijinal karakteri filmdeki haliyle görüyoruz, Resim 9 ve Resim 10 ise aynı karakterin aynı sahne görüntüsünden farklı çalışmaların yapıldığını görmekteyiz. Burada sanatçılar filmdeki karakterle kurdukları ilişki veya kendi tarzları doğrultusunda eserler yaratmaktadırlar. Dijital sanatçıların paylaşım yaptıkları birçok site mevcut, bu sitelerde aramalar yapıldığında ya da Google üzerinden görsel arama yapıldığında aynı resmin başka versiyonlarına da ulaşmak mümkün.

Taklit ve yineleme ile birlikte artan kavram yığınları içindeki karmaşayı çözmek zor olsa da genel itibariyle benzer anlamlar taşımaktadırlar. Alıntılamaı bir şemsiye terim olarak düşünüldüğünde bu kavramlar, eski eserlerin üsluplarını ve/veya imgelerini farklı bağlamlarda yeniden resmetmek/üretmek amacıyla kullanılan alıntılama yöntemleri olarak aralarındaki küçük değişikliklerle birbirinden ayrılmaktadırlar (Erdoğan, 2018).

Aslında alıntı her yerde vardır. Edebiyatta da vardır, resimde ya da müzikte de. Latince sözü burada anmak gerekiyor: “Non nova, sed nove”, yani yeni bir şey yok, yeni bir sunuluş biçimi var. Resimdeki biçem, izlek ya da düzenleme daha önce yapılanın yeni bir sunuluş biçimi gibi bir anlama varma da olası (Doğan, 2018).



Resim 11: Donnie Darko (Afiş Alternatifi)



Resim 12: Donnie Darko (Sinema Salonu Sahnesi Açı 1)

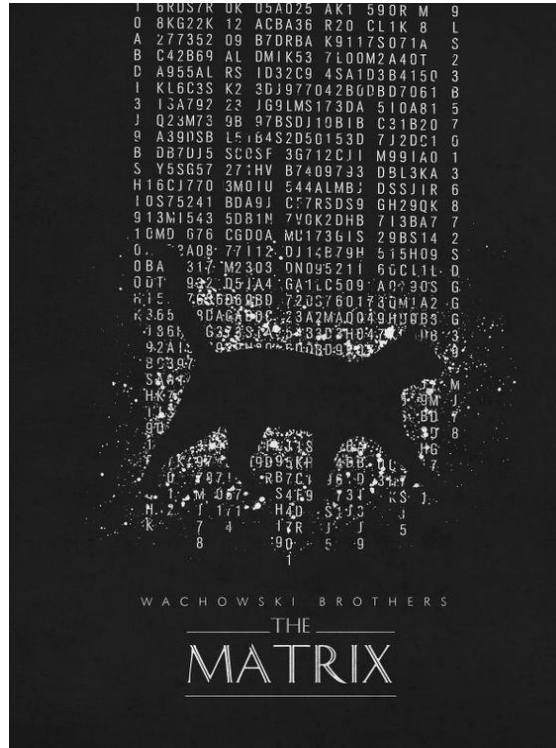


Resim 13: Donnie Darko (Sinema Salonu Sahnesi Açı 2)

Yukarıdaki alternatif afiş olarak tasarlanmış Donnie Darko filmine ait afiş, dijital illüstrasyon olarak filmin ilgili sahnelerinden esinlenerek çalışılmıştır. Resim 11'deki sahne Donnie Darko filmi izleyen herkesin hatırlayabileceği bir sahnenin yorumlanmış halidir. Resim 12'de filmin ana karakterlerinin boş bir sinema salonunda otururken arka plandan görmekteyiz. Filmin orijinalinde bu kurgunun aynısı görmüyoruz, resim 12 ve 13'deki planlardan görülen karakterler oturma düzenine göre tekrar yorumlanarak afiş (illüstrasyon) oluşturulmuştur.



Resim 14: Matrix I (Orijinal Film Sahnesi)



Resim 15: Matrix I (Afiş Alternatifi)

Resim 15'deki Matrix afişi olarak tasarlanan illüstrasyon filmin çok kısa bir anında görünen, ancak filmin önemli sahnelerinden olmakla beraber, sadece 1-2 saniyelik bir görüntünün yorumlanmasıyla oluşturulmuş ve muhtemelen izleyen kişi çok dikkatli değilse afiş ile film arasındaki bağlantıyı kurmakta zorlanacağı bir sahnedir üretilmiştir. Filmde kedinin geçtiği mekan afişe alınmamış, filmin ana konusu sayılabilecek kod fikri afiş illüstrasyonunun ana fikrini oluşturmuş, nesne olarak kedi seçilmiştir. Filmi çok iyi bilenlerin bile fark etmeyebileceği fark ise filmin orijinalinde kedi sağdan sola doğru yürümekte iken, afiş tasarımında soldan sağa doğru yürümektedir. Bu çalışma da daha çok fikrinsel olarak yola çıkılmıştır.



Resim 16: Yüzüklerin Efendisi III, 2003 – Kralın Dönüşü (Orijinal Sahne)



Resim 17: Evankart, 2014

Resim 16'deki Yüzüklerin Efendisi, Bölüm III (Kralın Dönüşü), filmin ana karakterlerinden Aragorn'un Palantir denilen bir cam küre ile Sauron ile yüzleşmesini gördüğümüz orijinal sinema versiyonunda görmediğimiz daha sonra yayınlanan DVD vb dijital ortamlarda eklenen uzatılmış versiyona ait olan bir sahnedir. Resim 17'te bu sahnenin dijital olarak çalışıldığı görülmekte. Sanatçı filmdeki sahneyi birebire yakın bir kompozisyonla almakla birlikte renk tercihinde kendi yorumunu katarak sahnenin etkisini arttırmış, daha zıt renkler tercih ederek, aynı zamanda arka plandaki bulanıklık artırılarak soyut bir mekan izlenimi ile birlikte, dramatik etkiyi arttırmıştır. Film 2003 yapımı olmasına rağmen 2014 yılında bile bilinirliği yüksek hayran kitlesi günümüzde bile artan bir yapım olması sebebiyle yeniden üretimin konusu olmaya devam etmiştir.



Resim 18: Leon-Aşkın Gücü, 1994 (Orijinal Sahne)



Resim 19: Lee Stevensen, 2014



Resim 20: Alex, 2014

Yukarıda resim 18’de gördüğümüz filmin orijinal sahnesi yine birçok sanatçı tarafından farklı tarzlarda ele alınmıştır. Resim 20’de sanatçı figürleri yorumlamadan olduğu gibi aktarmayı tercih ederken arka planı soyutlamıştır. Resim 19’da sanatçı kompozisyonu olduğu gibi alırken karakterler ve mekanı kendi tarzı ile yorumlamıştır.

Günümüzde tüm dünyaca tanınmış bir eserin alınıp yeniden yorumlanması fikri herkesçe bilinen bir sanat eserinin gücünden faydalanma kabul görme bazense öncekini reddetme konusunda sanatçı/tasarımcıya yardımcı olmaktadır.

Sonuç ve Öneriler

Resimlerarasılık geçmişten günümüze birçok sanatçı/sanatçı adayının dönem dönem başvurduğu bir yöntemdir. Bu yöntemin en geniş kullanım alanlarından biri olan dijital illüstrasyon kendine yeni konu bulma konusunda sinemayla adeta sınırsız bir kaynak bulmuştur.

Sanat eseri nedir; tanımında zaman zaman dayatılan “tek ve benzersiz” olma sözü sanat tarihine bakınca bazen esnetilen bir şey konumunda olduğu tespiti yanlış bir tespit olmaz. Birçok resmin yeniden yorumlandığı veya alıntılандığı bilinen bir gerçektir. Asıl soru alıntılanan iş özünden ne kadar ayrılmakta ve ortaya çıkan iş ne kadar özgün bir sanat eseri olarak karşımıza çıkmaktadır. Dijital sanatın, sanat eseri olarak hala tartışılır olduğu günümüzde ne yazık ki bunun cevabı net olarak vermek oldukça güçtür. İster öğrenme, isterse de yapan ustaya saygı biçiminde olsun alıntı yapma birçok farklı teknikle hala günümüzde de devam etmektedir.

Yeniden üretimin konusu olan filmlere genel olarak bakıldığında sinema severler tarafından sinema tarihinde mihenk taşı olmuş, yüksek bir hayran kitlesine sahip bilinirliği yüksek filmlerin tercih edildiği görülmektedir. Bu tercihte nelerin etken olduğu araştırılmaya muhtaç bir konu olmakla birlikte; daha çok ve kolay beğenilme, kolay kabul görme gibi etkenlerin sanatçıları bu yönetime yönlendirdiği düşünülebileceği gibi sadece sevdiği içinde tercih sebebi olabilir. Ancak sebep ne olursa olsun, sanatçıların birçoğu alıntılama yaptığını, kaynağı göstermeden bu yöntemi kullanmakta ve çoğu zaman Picasso ya da Marcel Duchamp kendi eserlerini imzalamaktadırlar.

Sanat eseri üretirken kullanılan tekniğin ne olduğunu bakılmaksızın çıkan işlerin özgünlüğü, yarattığı duygulara bakılması gerekliliği ortaya çıkmaktadır. Resimsel alıntı bir öğrenme biçimi olarak kesinlikle kullanılmalı, teknik öğrenirken böylece kompozisyon, ışık, perspektif gibi temel konularda referans alınarak öğrenme pekiştirilmelidir.

Kaynakça

- Özel Sağlamtimur, Z. (2010). Dijital Sanat. *Anadolu Üniversitesi Sosyal Bilimler Dergisi*, 10(3), s. 213-238. (2018, Nisan 24). Mayıs 2018 tarihinde Nişanyan Sözlük: <http://www.nisanyansozluk.com/?k=illüstrasyon&view=annotated> adresinden alındı
- Armutçu, B. (2016, Haziran 3). *MATTE PAINTING TEKNİĞİNDE UYGULAMA SORUNLARININ İNCELENMESİ VE ÇÖZÜM ÖNERİSİ*. Mayıs 2018 tarihinde Yükseköğretim Kurulu Başkanlığı Tez Merkezi: tez.yok.gov.tr adresinden alındı
- Atakulum, K. (2016). *Resimsel Alıntı*. Konya: Çizgi Kitabevi.
- Atan, A., Uçan, B., & Bilsel, Ç. (2015). Dijital Sanat Uygulamaları Üzerine Bir İnceleme. (26), s. 1-14.
- Doğan, G. (2018, Nisan 10). *GÖSTERGELERARASILIK: RESİMDE BAŞKASINDAN ESİNLENME NE ORANDADIR? ELEŞTİRİDEN ÇÖZÜMLEMEYE RESİM VE PLASTİK SANATLAR*. Mayıs 2018 tarihinde <https://dogangunay.blogspot.com>: <https://dogangunay.blogspot.com/2017/04/resimsel-aliti-konusunda-bildiklerimiz.html> adresinden alındı
- Erdoğan, Y. (2018, Nisan 20). *Pablo Picasso'nun Eserlerinde Resimsel Alıntılama Yöntemi Olarak Kendine Mal Etme*. Mayıs 2018 tarihinde <http://www.academia.edu>: [http://www.academia.edu/34162455/Yeliz_ERDOĞAN-Pablo_Picassonun_eserlerinde_resimsel_alıntılama_yöntemi_olarak_kendine_mal_etme_APPROPRIATION_AS_METHOD_OF_PICTORIAL_QUOTATION_IN_THE_PABLO_PICASSO_S_ARTWOR](http://www.academia.edu/34162455/Yeliz_ERDOĞAN-Pablo_Picassonun_eserlerinde_resimsel_alıntılama_yöntemi_olarak_kendine_mal_etme_APPROPRIATION_AS_METHOD_OF_PICTORIAL_QUOTATION_IN_THE_PABLO_PICASSO_S_ARTWORK) K adresinden alındı

Author Information

Erdinç Çakır

Necmettin Erbakan Üniversitesi
Abdülaziz Mahallesi, Abdülmümin Sokak, No:16, Meram,
KONYA/TÜRKİYE
ecakir@konya.edu.tr

Mahmut Sami ÖZTÜRK

Necmettin Erbakan Üniversitesi
Abdülaziz Mahallesi, Abdülmümin Sokak, No:16, Meram,
KONYA/TÜRKİYE
msozturk@hotmail.com.tr

Mevlüt ÜNAL

Abdülaziz Mahallesi, Abdülmümin Sokak, No:16, Meram,
KONYA/TÜRKİYE
mevlutunal@konya.edu.tr

Mehmet SUSUZ

Abdülaziz Mahallesi, Abdülmümin Sokak, No:16, Meram,
KONYA/TÜRKİYE
msusuz@konya.edu.tr

Presence of Semiotics in The Current Curricula of Institutions Providing Art Education

Dr. Öğr. Üyesi Mehmet SUSUZ
Necmettin Erbakan Üniversitesi

Dr. Öğr. Üyesi Mahmut Sami ÖZTÜRK
Necmettin Erbakan Üniversitesi

Dr. Öğr. Üyesi Mine Ülkü ÖZTÜRK
Necmettin Erbakan Üniversitesi

Abstract: As it is known, the art phenomenon has been exposed to changes and transformations on the axis of values of "form-content and purpose" from the human history to the day. But despite these changes and transformations, art has maintained the "communication medium" between artist (sender) and viewer (receiver). In particular, the "chaos environment" that has taken its toll during world wars has changed the present structure of the art inevitably. The change and transformation that started with Dadaism led the changes in understanding of art after 1950. In this process, the thesis of 'The End of Art and After the End of Art' were suggested. In the post modernism period, which started with the end of Modernism, the appearance of the very 'contentive (intellectual)' dimension rather than the 'form' dimension of the works of art brings the problems to the point of the meaning of art. Especially during this period, the artists presented the audience by putting codes and cyphers in the artistic forms that they were fed from the socio-cultural textures. Semiotics is key to the emergence of these codes and cyphers and should not be disregarded. Today, it is known that arts education institutions are not making full use of the advantages of 'semiotics'. In many parts of the Faculty of Fine Arts in our country, the concept of Contemporary Art is taught to students in the theoretical sense. Art criticism is used at the point of analysis of the artistic productions that have emerged. The current analysis methods used in Art Criticism courses are being discussed in terms of being sufficient about analyzing the contemporary art forms that are content (concept) oriented rather than form. For many years many art educators have pointed out that the institutions of arts education should include semiotics in the curriculum.

Keywords: Art, Art Education, Contemporary Art, Semiotics

Sanat Eğitimi Veren Kurumların Mevcut Ders Programlarında Göstergebilimin Varlığı

Özet: Bilindiği üzere sanat olgusu insanlık tarihiyle başlayıp günümüze kadar 'biçim-içerik ve amaç' değerleri ekseninde değişim ve dönüşümlere maruz kalmıştır. Fakat bu değişim ve dönüşümlere rağmen sanat, sanatçı (gönderici) ile izleyici (alıcı) arasında 'iletişim aracı' olma özelliğini korumuştur. Özellikle dünya savaşları sürecinde meydana gelen 'kaos ortamı' sanatın da mevcut yapısında değişimi kaçınılmaz kılmıştır. Dadaizm ile başlayan sanattaki değişim ve dönüşüm 1950 sonrası sanat anlayışlarına yön vermiştir. Bu süreçte 'Sanatın Sonu ve Sanatın Sonundan Sonra' tezleri ortaya atılmıştır. Modern sanata tepki olarak ortaya çıkan sanat anlayışları sanat eserinin 'biçimden' çok 'içeriksel (düşünsel / fikirsel)' boyutunu ön plana çıkartmıştır. Bu durum, ortaya çıkan sanat eserlerinin anlamlandırılması noktasında problemleri gün yüzüne çıkartmıştır. Özellikle bu dönemde sanatçılar, sosyo-kültürel dokulardan beslenerek biçimlendirdikleri sanatsal formlara şifre ve kodlar yerleştirerek izleyiciye sunmuştur. Bu şifre ve kodların ortaya çıkartılabilmesinde, göstergebilimin önemi göz önünde bulundurulmalıdır. Günümüzde, sanat eğitimi veren kurumlarda 'göstergebilimin' olanaklarından yeterince faydalanılmadığı yaygın kanıdır. Ülkemizdeki Güzel Sanatlar Fakültelerinin birçok bölümünde, Çağdaş Sanat kavramı öğrencilere teorik anlamda öğretilmektedir. Ortaya çıkan sanatsal üretimlerin çözümlenmesi noktasında ise 'Sanat Eleştirisi' dersinden yararlanılmaktadır. Sanat Eleştirisi dersinde kullanılan mevcut çözümlenme yöntemlerinin, biçimden çok içeriğin (kavramsal boyutun) ön plana çıktığı çağdaş sanat formlarının çözümlenmesi noktasında yeterliliği tartışılmaktadır. Uzun yıllardır birçok sanat eğitimcisi sanat eserini merkeze alıp inceleyen göstergebilimin, sanat eğitimi veren kurumların ders programlarında olması gerektiğini ifade etmektedir.

Anahtar Kelimeler: Sanat, Sanat Eğitimi, Çağdaş Sanat, Göstergebilim.

Giriş

“Güzel sanatlar eğitimi sürecinde sanat eğitimi alan bireylere uygulamalı çalışmalar yanında, sanat yapıtını oluşturan göstergeleri okuyup anlamlandırabileceği, kendine özgü yapısını kavrayabileceği eleştirel, kültürel ve estetik ile ilgili bilgi ve deneyim kazandırılmaya çalışılır” (Batu, 2014: 115). Sanat eğitimi, teoriğin ve pratiğin birleşiminden oluşur. Güzel sanatlar eğitimi veren kurumların ders müfredatlarında uygulamaya yönelik atölye derslere ek olarak birçok teorik ders bulunmaktadır. Bu teorik derslerin bazılarını belirtecek olursak; Sanat Tarihi, Çağdaş Dünya Sanatı, Kavramsal Sanat, Güncel Sanat, Mitoloji, Sanat Sosyolojisi, Sanat Psikolojisi, Türk Resim Sanatı, Türk Sanatı Tarihi, Sanat Felsefesi, Sanat Ontolojisi, Görsel Kültür, Modern Sanat, Postmodernizm, Sanat ve Pazarlama, Medya Okuryazarlığı, ...vb.. Güzel Sanatlar Fakültelerinin bünyesinde yer alan bölümlerin ders müfredatlarında yer alan teorik derslerin yoğunluğunun en önemli nedeni olarak, sanatın başlangıcından geldiği noktaya kadar ki süreçte geçirmiş olduğu değişim ve dönüşümlerin sosyo-kültürel etkenlerinin sanatçı, sanat eseri ve izleyici ekseninde değerlendirilmesi olarak ifade edilebilir.

Sanat eğitiminde, “...bir öğrencinin sanat tarihinin tüm gerçeklerini bilmesi (sanatçıların doğum ve ölüm tarihleri, terim ve süreçlerin tanımları, hatta sanatın psikolojisi), fakat buna karşılık, bir sanat eseri gördüğünde onu ayırt edememesi ve sanat eserinin estetik değerlerini iyi-kötü ayrıştırıramaması mümkündür” (Read, 2018: 127-128). Her ne kadar sanat eğitimi sürecinde öğrenciye birçok teorik ders veriliyor olsa da, bu dersler sanat eserlerinin çözümlenebilmesine yönelik bilgi ve beceriyi öğrenciye kazandırma noktasında yeterli olmadığı söylenebilir.

Öğrencilere, sanat eserlerini analiz edebilmelerine yönelik bilgi, “...görsel iletişim, imge ve yorumları, semiyotik, sanat eleştirisi, sanat yapıtı çözümlemesi gibi farklı adlandırmalar altındaki derslerle verilmeye çalışılmaktadır” (Batu, 2014: 115).

“İnsan zihni üretkendir, zihinsel enerji ne denli yoğun ise insan o denli düşünce üretir. İnsanın en yetkin zihinsel etkinliği olan düşünme soyuttur. Somuta dönüşmesi için sesle, yazıyla ya da biçim ve renklerle hareketlerle anlatılması gerekir. Bu anlatım biçimleri, yani resim, müzik, yazın, tiyatro vb. etkinlikler, insanın soyut düşüncelerini somutlaştırmaktadır” (Etike, 1995: 11). “Görsel sanatlarda 1960’lı yıllardan bu yana pop, kavramsal, performans, enstalasyon ve çevresel sanatların büyük bir kısmı da güzel sanat sisteminin kutupsallıklarına karşı direnmekte ve sanatla hayatı yakınlaştırmaya çalışmaktadır” (Shiner, 2013; 388). Sanatın, başlangıcından günümüze kadar ki süreçte değişen ve dönüşen yapısı, ortaya çıkan sanat eserlerinin anlamlandırılması sürecinde bazı zorlukları ortaya çıkartmıştır. Her ne kadar sanatçı soyut düşüncelerini sanat eserinde somutlaştırıyor olsa da, alıcı (izleyici) eserde kullanılan göstergelerin gerçek hayattaki göstergelerle olan benzerliği ölçüsünde sanat eserini değerlendirme sürecine girer. İzleyici, sanatçının kullandığı kod ve şifreleri tespit edip ortaya çıkartmaya çalışır. 1950 sonrası ortaya çıkan sanat anlayışları (Kavramsal Sanat, Arazi Sanatı (Land Art), Yoksul Sanat (Arte Povera), Süreç Sanatı, Fluxus, Happening (Oluşumlar), Performans Sanatı, Video Sanatı, vb.) , sanatın bilindik yapısından farklı değerleri ortaya çıkartmıştır. Ortaya çıkan bu durum, sanat eserlerinin bilindik yöntemlerle anlamlandırılmasını zorlaştırmıştır. Özellikle bu süreçte sanat eserlerinin çözümlenebilmesi için, bilindik sanat eleştirisi yöntemlerine ek olarak farklı disiplinlere de ihtiyaç duymuşlardır. Bu noktada “sanat eserini merkeze alıp nesnel ölçütlerle değerlendiren göstergebilimsel yaklaşımlardan faydalanılmasının gerekliliği” ortaya çıkmıştır.

Sanat Eğitiminde Göstergebilimin Önemi

“Göstergebilim anlamlama bilimidir. Göstergebilimsel çözümleme bir okuma eylemidir, anlamlı bir metin içinde içerik düzleminde yüzeyden derine doğru inerken, ima edilen anlamları görür. Bunu yaparken de varolan yapıyı geçici olarak ayrıştırır, bozar ve yeniden kurar” (Parsa ve Olgundeniz, 2014: 104). “Yazınsal ya da görsel söylem çözümlemelerinde, göstergenin türü değişir fakat işlevi değişmez. Göstergebilim yöntemiyle, dilsel göstergelerin ya da görsel göstergelerin birbirine eklenmesiyle betimlenerek sözcede anlamın oluşmasını sağlayan temel ulamlar ortaya konur” (Altınbüken, 2014: 240). Fransız göstergebilimci Roland Barthes, 1964 tarihinde Panzani makarnalarının reklam fotoğrafını incelemiştir. Bu çalışmasında “Barthes resimde görünen nesnelere, algılanan renklerin betimlemesini yaptıktan sonra resmin içerdiği bildirileri ekin bağlamında çözümler”. Félix Thürlemann ise, 1979’da Paul Klee’nin üç tablosunun analizini yapmıştır. “Thürlemann resimde anlamın oluşumu gibi karmaşık bir sürecin aslında yalın karşıtlıklar üzerine kurulu olduğunu göstermiş...”tir (Öztokat, 1998: 254).

“Kültür ve sanat alanlarındaki gelişmelerin bugün eğitim-öğretim alanında değerlendirilip örgütlenmesinde artık bilinen klasik bilim disiplinleri yetersiz kalmaktadır. Bu nedenle birçok Batı ülkeleri ve Amerikan üniversiteleriyle başka ülkelerin güzel sanatlar fakültelerinde ya da güzel sanatlar eğitimi veren yükseköğretim

kurumlarında, sanat tarihi dersi yerine ya da sanat tarihi dersine paralel olarak sanat bilimi dersleri okutulmakta veya kuramsal alanda yeni açılımlar getiren daha geniş sanat bilimi program örgütlenmelerine gidilmektedir” (Akdeniz, 2006: 43). “1960 yılından sonra sanat eğitiminde, ruhbilim’in etkisinin azalmaya, bunun yerine de başta toplumbilim olmak üzere, göstergebilim, güdümbilim ve diğerlerin etkisinin artmaya başladığı görülür. Bu durumda, sanat eğitiminin yeniden gözden geçirilmesi, yeni kavram, yöntem ve kuramlara göre derslerin yapılandırılması gerekmiştir. ...” (Özen, 2005: 34).

“Sanatçı üretirken özgürdür, ürettiklerinin anlaşılıp, anlaşılmaması onu bağlamaz. Kendi dünyasında özgürdür, yaratır, ürettiklerinin kendi dışındaki diğer insanlarca tüketilmesi sorunu ve bu sorunun çözümlenmesi onun sorumluluğunda değildir, ya da ne kadar sorumluluğundadır, ya da kimin ve kimlerin sorumluluğundadır?” (Etike, 1995: 17). “...Kavramsal Sanat’tan sonra gelişen resim, resmin söyleyecek sözünün bitmediğini kanıtlamaktadır. Resim, yalnızca kendi içine kapanarak teknik sorunlarla ilgilenmeyi sürdürmemiştir. Kavramsal Sanat’tan da dersini alarak yoluna devam etmiştir” (Giderer, 2003: 175). Özellikle aydınlanma çağıyla başlayan ‘sanat ortamında özgürleşme hareketleri’ sanatçıların eser üretme süreçlerinde aktif konuma geçirmiştir. Bu dönemde sanatçı, gerçek dünyadan beslenerek zihninde kurguladığı/tasarladığı imgeleri somutlaştırma ihtiyacı hisseder. Etike’nin de ifade ettiği gibi “Sanatçı üretirken özgürdür, ürettiklerinin anlaşılıp, anlaşılmaması onu bağlamaz”. Özellikle Dünya Savaşlarından sonra ortaya çıkan kaos ortamında toplamlar, ellerinde bulunan bazı değerleri sorgulama ihtiyacı hissetmişlerdir. bu değerlerden bir tanesi de ‘modernizm’ kavramıdır. Sanatın birçok alanında modernizme karşı tepkiler ortaya çıkmıştır. Bu tepkilerin sonucu olarak ‘postmodern’ süreç ortaya çıkmıştır. ‘Postmodernizm’ kavramının günümüzde yeterince algılanmadığı söylenebilir. Sanatta özellikle Marcel Duchamp’ın hazır nesnelere sanata dâhil etmesi ve özellikle 1950 sonrası ortaya çıkan sanat anlayışlarının bilindik sanat formlarından farklılık göstermesi sanatın algılanabilmesini zorlaştırmıştır. Bu dönemde sanatçı hiç olmadığı kadar özgürdür. İsteddiği malzemeyi kullanarak istediği formlarda ve istediği mekânlarda eserini ortaya koyabilir. Fakat bu dönemde ortaya çıkan sanat eserlerinde biçimden çok fikrin ön plana çıkması, sanatçıların ‘mesaj’ kaygısını ortaya çıkarttığı söylenebilir.

“...resim bir yanıyla bir şeyi açığa çıkaran, diğer yanıyla ise bir şeyi saklayan bir durumdur” (Günay, 2014: 125). “Bir resmin okunmasında, yögrumsal ve görüntüsel göstergeler arasındaki bağıntılar çözümlenerek derin yapıda yer alan anlam alanları ortaya çıkarılır” (Altınbükten, 2014: 241). “...Sanat göstergelerinde şifrelenmiş içeriğin alıcı yönünden gerektiği gibi çözülüp anlaşılması için, sanatçının kullanmış olduğu kod anahtarının onun elinde de olması gerekir” (Ziss, 2011: 100). Resim ya da farklı bir sanat eserinin çözümlenebilmesinin koşulu olarak, Ziss’in de ifade ettiği gibi, sanatçının eserini biçimlendirirken esere yerleştirdiği kod ve şifrelerin izleyiciler tarafından doğru bir şekilde tespit edilmesine bağlıdır. Eserin tam anlamıyla analiz edilebilmesi için betisel düzeydeki tespitlerin ötesinde izleksel düzeyin de ortaya çıkartılması gerekir. Bu süreci gerçekleştirecek olan eleştirinin alanında bilgi sahibi olması gerekir. Göstergebilim, sanat eğitimi alan bireylerin sanat eserlerini analiz edebilme becerilerini geliştirmede etkin kullanılacak bir disiplin olarak görülebilir.

Sanat Eğitimi Veren Kurumların Mevcut Ders Programlarında Göstergebilimin Varlığı

Ülkemizde çok sayıda Güzel Sanatlar Fakültesi bulunmaktadır. Bu fakültelerin dört yıllık ders programlarında, bünyesinde birçok görüntüsel göstergeyi barındıran sanat eserlerinin çözümlenmesine/anlamlandırılmasına yönelik farklı dersler yer almaktadır. Süreç itibarıyla sanatın dinamik yapısı bilindik sanatsal formların ötesinde, alışılmışın dışında sanat eserlerini ortaya çıkartmıştır.

“Sanatların bütününde artık eskisinden farklı gözlemi ve işlemeyi gerektiren fiziksel bir yan vardır; bu fiziksel yanın kendini çağdaş bilimin ve uygulamaların etkilerine daha fazla kapayabilmesi olanaksızdır” (Benjamin, 2013: 50). “Günümüz sanatıyla ilgili sorunlardan birisi sanatı anlamlandırmak ve değerlendirmek gibi görünüyor” (Şahin, 2016: 84). Biçimden öte kavramları ön plana çıkartan bu sanatsal formların çözümlenmesinde bilindik sanat eseri analiz yöntemlerinin yetersiz kaldığı genel kanıdır. Özellikle 1970’li yıllardan itibaren sanat eserlerinde yer alan görüntüsel göstergelerin çözümlenmesinde göstergebilimden faydalanılmıştır. Bu çalışmada, ülkemizdeki bazı üniversitelerin Güzel Sanatlar Fakültelerinin dört yıllık ders programlarında ‘göstergebilim’in ne ölçüde yer aldığı tespit edilmesi amaçlanmaktadır. Elde edilen bilgi ve bulgulara aşağıdaki tabloda belirtilen üniversitelerin ders bilgi paketlerinden ulaşılmıştır.

Üniversite	Fakülte	Bölüm	Ders Adı	Seçmeli/ Zorunlu
Afyon Kocatepe Üniversitesi	Güzel Sanatlar Fakültesi	Resim	Gösterge Bilime Giriş	S

		Sinema ve Televizyon	Göstergebilime Giriş	S
		İç Mimarlık ve Çevre Tasarımı	İç Mekan Tasarımında Gösterge Bilim	S
Çankırı Karatekin Üniversitesi	Güzel Sanatlar Fakültesi	Grafik Tasarımı	Grafik Tasarım`da Göstergebilim	Z
		Sinema ve Televizyon	Göstergebilim	Z
Gaziantep Üniversitesi	Güzel Sanatlar Fakültesi	Grafik Tasarım	Göstergebilim	Z
		Sinema Tv	Göstergebilim	Z
Marmara Üniversitesi	Güzel Sanatlar Fakültesi	Endüstri Ürünleri Tasarımı	Gösterge Bilim	S
		Film Tasarımı	Gösterge Bilim	S
		Fotoğraf	Gösterge Bilim	S
		Grafik	Gösterge Bilim	S
		Heykel	Gösterge Bilim	S
		İç Mimarlık	Gösterge Bilim	S
		Resim	Gösterge Bilim	S
		Seramik ve Cam	Gösterge Bilim	S
		Sinema ve Televizyon	Gösterge Bilim	S
		Tekstil	Gösterge Bilim	S
Necmettin Erbakan Üniversitesi	Güzel Sanatlar Fakültesi	Resim	Göstergebilim	S
Ordu Üniversitesi	Güzel Sanatlar Fakültesi	Sinema ve Televizyon	Göstergebilim	Z
		Resim	Göstergebilime Giriş I	S

Sonuç

“...güzel sanatların öğretimi, eleştirisi ve tarihine tahsis edilen disiplinler de değişmektedir” (Shiner, 2013; 399). Çağdaş sanat sürecinde ortaya çıkan sanatsal formların çözümlenmesinde bilindik sanat eleştirisi yöntemlerinin tam anlamıyla yeterli olacağını söylemek hatalı olur. Bu durumun en önemli nedenleri arasında, sanatın geçirmiş olduğu değişim ve dönüşümler gösterilebilir. 1910’larda başlayan nesnenin sanata eklenmesi, sonraki süreçlerde ortaya çıkan sanat anlayışlarına temel oluşturmuştur. Shiner’ın ifadeleri ışığında, sanat eğitimi veren kurumlarda öğretimin daha etkin şekilde sürdürülebilmesi için, ders müfredatlarının yeniden gözden geçirilerek, gerekli görülen değişikliklerin ve güncellemelerin yapılması gerekmektedir.

Ülkemizdeki üniversitelerin internet sayfalarındaki ders bilgi paketlerine bakıldığında, Güzel Sanatlar Fakültelerinin bünyesindeki bölümlerin birçoğunun dört yıllık ders müfredatında ‘göstergebilim’ dersinin olmadığı görülmüştür. Bazı bölümlerin ders müfredatlarında yer alan ‘Sanat Eleştirisi, Sanat Eseri Analizi, vb. derslerin içeriklerinde ‘göstergebilim’in kısmen eklendiği görülmüştür. Fakültelerin bazı bölümlerinde göstergebilim ‘seçmeli’ bazılarında ise ‘zorunlu’ ders olarak müfredatta yer almaktadır.

Özellikle sanat eğitiminde öğrenciler, gerek teorik derslerde gerekse uygulama derslerinde yoğun şekilde görüntüsel göstergelerle karşılaşmaktadır. Bu süreçte öğrenciler, nitelikli bir sanat eğitimi alabilmeleri noktasında karşılaştıkları görüntüsel göstergeleri anlamlandırabilmeleri için gerekli bilgileri almaları gerekir. Öğrencilerin sanat eserlerini çözümleyebilmeleri için eserin üretiliş sürecindeki sanat anlayışlarından, kullanılan teknik ve malzemelerden öte eserlerin üretildiği dönemdeki toplumların sosyo-kültürel yapılarının da iyi bir

şekilde analiz edilmesi şarttır. Bunun ortaya çıkartılabilmesi için, sanatçının esere yerleştiği kod ve şifrelerin doğru olarak tespit edilmesi gerekmektedir. Bu noktada sanat eğitimi veren kurumların, “sanat eserlerini merkeze alıp nesnel ölçütlerle çözümleyen ‘göstergebilim’ disiplininden faydalanmaları gerekmektedir”.

Sanatın dinamik yapısı alışlagelmişin dışında farklı sanat eserlerini karşımıza çıkartmaktadır. Bu durum var olan sanat eseri çözümleme yöntemlerini yetersiz bırakabilir. Dolayısıyla, kullanılan çözümleme yöntemlerinin güncellenmesi gerekmektedir. Araştırmacılar; çok sayıda tez, makale, vb. bilimsel çalışmalarda sanat eğitimi veren kurumların göstergebilimden yeterince faydalanmadığı ve “çağdaş sanat eseri çözümleme yöntemi olarak ‘göstergebilim’in sanat eğitimi veren kurumların ders müfredatlarında olması gerektiğini belirtmişlerdir”. Göstergebilimin ders müfredatlarında yer alması, bu dersi verebilecek nitelikli öğretmenlere olan ihtiyacı da ortaya çıkartmaktadır.

Kaynakça

- Akdeniz, Halil. (2006), “Sanat Bilimi ve Sanatsal Uygulamalar (Sanatçı Eğitimi)”, s.s. 39-44, Sanat Eğitiminde Sanat Biliminin Rolü, Yayına Hazırlayanlar: Prof. Dr. İnci SAN - Doç. Dr. Ayşe ÇAKIR İLHAN, Naturel Yayınları: Ankara, 1. Baskı, ISBN: 975-6422-26-2.
- Altınbükten, Buket. (2014), “Göstergebilim Yöntemiyle Görsel Sözce Çözümlemesi”, İletişim Araştırmalarında Göstergebilim- Yazınsaldan Görsele Anlam Arayışı, Literatürk Academia: Konya, s.s. 239-257.
- Batu, Bengü. (2014), “Sanat Yapıtı Eleştirisinde Karşılaşılan Sıkıntılar ve Göstergebilimsel Çözümleme Yöntemi”, Süleyman Demirel Üniversitesi Güzel Sanatlar Fakültesi Hakemli Dergisi ART-E Mayıs-Haziran’14 Sayı:13 ISSN 1308-2698, s.s. 114-128.
- Benjamin, Walter. (2013), “Pasajlar”, Tekniğin Olanaklarıyla Yeniden Üretilbildiği Çağda Sanat Yapıtı, Çev. Ahmet Cemal, Kazım Taşkent Klasik Yapıtlar Dizisi, Yapı Kredi Yayınları: İstanbul, 10. Baskı.
- Danto, Arthur C.. (2014), “Sanatın Sonundan Sonra - Çağdaş Sanat ve Tarihin Sınır Çizgisi”, Çev. Zeynep Demirsü, Ayrıntı Yayınları: İstanbul, 2. Baskı.
- Etike, Serap. (1995), “Sanat Eğitimi Yazıları”, İlke Kitabevi Yayınları: Ankara: 1. Baskı.
- Giderer, Hakkı Engin. (2003), “Resmin Sonu” ,Ütopya Yayınevi: Ankara.
- Günay, Veli Doğan. (2014), “Doğrulama Ulamı Bağlamında Sanat Yapıtında Doğru Ya Da Yanlış”, İletişim Araştırmalarında Göstergebilim- Yazınsaldan Görsele Anlam Arayışı, Literatürk Academia: Konya, s.s.111-134.
- Kuspit, Donald. (2014), “Sanatın Sonu”, Çev. Yasemin Tezgiden, Metis Yayınları: İstanbul, 4. Baskı.
- Özen, Dinçer. (2005), “Sanatta Gelişim Kuramları”, (3. Bölüm: Çocuğun Sanatsal Gelişimi), OKUL ÖNCESİ RESİM ÖĞRETİMİ, Ünite Yazarları: Doç. Bedri KARAYAĞMURLAR (Ünite: 1, 2, 4, 5), Yard. Doç. Doç. Dinçer ÖZMEN (Ünite: 3, 8, 9), Yard. Doç. Nurettin ŞAHİN (Ünite: 6, 7, 10), Anadolu Üniversitesi Açıköğretim Fakültesi Okulöncesi Öğretmenliği Lisans Programı, T.C. Anadolu Üniversitesi Yayını No: 1419, Açıköğretim Fakültesi Yayını No: 764: Eskişehir, 4. Baskı.
- Öztokat, Nedret. (1998), “Göstergebilim ve Plastik Sanatlarda Çözümleme”, 14-16 Mayıs 1998 Mersin Üniversitesi XII. Dilbilim Kurultayı Bildirileri, s.s. 253-258.
- Parsa, Alev Fatoş; Olgundeniz, Seda Sünbül. (2014), “İletişimde Göstergebilim ve Anlamlandırma Sürecini Örneklerle Değerlendirme”, İletişim Araştırmalarında Göstergebilim- Yazınsaldan Görsele Anlam Arayışı, Editör: Ahmet Güneş, Literatürk Academia: Konya, s.s.89-109.
- Read, Herbert. (2018), “sanat ve toplum”, Çev. Elif Kök, Hayalperest Yayınevi: İstanbul, 1. Baskı.
- Shiner, Larry. (2013), “Sanatın İcadı- Bir Kültür Tarihi”, Çev. İsmail Türkmen, Ayrıntı Yayınları: İstanbul, 3. Baskı.
- Şahin, Hikmet. (2016), “Modern Sanatta Geleneğin Reddi”, Akademik Sanat; Sanat, Tasarım ve Bilim Dergisi, Kış Winter 2016, s.s. 77-85, (Kaynak: <http://dergipark.gov.tr/download/article-file/275271> Erişim Tarihi: 30.04.2018).
- Ziss, Avner. (2011), “Estetik Gerçekliği Sanatsal Özümsemenin Bilimi”, Çev. Yakup Şahan, Hayalbaz Kitap: İstanbul, 2. Baskı.

Afyon Kocatepe Üniversitesi / Güzel Sanatlar Fakültesi
<https://obs.aku.edu.tr/oibs/bologna/start.aspx?gkm=0331388163548531107322343110834464388083328538784322234432344443551537703767921462197311153111235600363782199322343779835350343883442833225388883330021613735737336> Erişim Tarihi: 02.04.2018).

Çankırı Karatekin Üniversitesi / Güzel Sanatlar Fakültesi
<http://bbs.karatekin.edu.tr/AkademikBirimler.aspx?birim=15> Erişim Tarihi: 05.04.2018).

Gaziantep Üniversitesi / Güzel Sanatlar Fakültesi

[http://bbs.bim.gantep.edu.tr/\(S\(rgqgomkv2e1qjh1haynudvzh\)\)/Default.aspx?path=3_3_3](http://bbs.bim.gantep.edu.tr/(S(rgqgomkv2e1qjh1haynudvzh))/Default.aspx?path=3_3_3) Erişim Tarihi: 03.04.2018).

Marmara Üniversitesi / Güzel Sanatlar Fakültesi
<http://meobs.marmara.edu.tr/Program/programlar-hakkinda-bilgi/lisans-915002>
Erişim Tarihi: 03.04.2018).

Necmettin Erbakan Üniversitesi / Güzel Sanatlar Fakültesi
<https://obs.erbakan.edu.tr/oibs/bologna/start.aspx?gkm=0801388003110137798322303775634404377983732233291366903444835600> Erişim Tarihi: 06.04.2018).

Ordu Üniversitesi / Güzel Sanatlar Fakültesi
<http://bologna.odu.edu.tr/dereceprogramlari/1> Erişim Tarihi: 06.04.2018).4404377983732233291366903444835600 Erişim Tarihi: 06.04.2018).

Author Information

Mehmet SUSUZ

Abdulaziz Mahallesi, Abdülmümin Sokak, No:16, Meram,
KONYA/TÜRKİYE
msusuz@konya.edu.tr

Mahmut Sami ÖZTÜRK

Necmettin Erbakan Üniversitesi
Abdulaziz Mahallesi, Abdülmümin Sokak, No:16, Meram,
KONYA/TÜRKİYE
msozturk@hotmail.com.tr

Mine Ülkü ÖZTÜRK

Necmettin Erbakan Üniversitesi
Abdulaziz Mahallesi, Abdülmümin Sokak, No:16, Meram,
KONYA/TÜRKİYE
mineozturk@erbakan.edu.tr

GRAPHIC DESIGNER PROFILE AND PROFESSIONAL COMPETENCE ANALYSIS

Doç.Dr.Mustafa KINIK
Necmettin Erbakan Üniversitesi

Dr. Öğr. Üyesi Mahmut Sami ÖZTÜRK
Necmettin Erbakan Üniversitesi

Abstract: Individuals start their education process with great dreams and expectations when choosing their profession. Curriculum programs of educational institutions may not always meet the sectoral demands. Or the student can not be able to complete his / her education process with the target outcomes. Graphic design field is favoured , popular and has high expectations in postgraduate life. In this study, graphic designer profile, who works in the sector, were analyzed according to the designers views and occupational competences were analyzed according to the views of agency managers and owners. In this context, analysis of the data were done according to the questionnaires applied to 53 designers and 15 agency managers who provide graphic design services in Ankara province. From this point of view, the research is a descriptive study in the general survey model. A questionnaire including of 24 questions to the participatory designers and 15 questions to the managers was applied. According to findings; it has been revealed that a large majority of graphic designers working on the Ankara advertising market are postgraduate designers, their working schedules are very likely to each other, the softwares they use are similar and they don't have too much problems about payments and work disciplines. But they can't have time for social and educational activities because of the density of working hours. According to the opinions of agency owners, although the designers have a sufficient level of designing run and workflow, they are not particularly good at the process of printing and post-printing

Keywords: Graphi Designer, Advertising Industry, Designer Profile, Professional Qualification

GRAFİK TASARIMCI PROFİLİ VE MESLEKİ YETERLİLİK ANALİZİ

Özet: Bireyler, mesleklerini tercih ederken büyük hayaller ve beklentilerle eğitim süreçlerine başlarlar. Eğitim kurumlarının müfredat programları her zaman sektör taleplerini karşılayacak nitelikte olmayabilir. Ya da öğrenci eğitim sürecini hedeflenen kazanımlarla tamamlayamayabilir. Grafik tasarım alanı tercih edilen, sevilen ve mezuniyet sonrası iş yaşamında beklentileri yüksek olan bir branştır. Bu araştırmada; sektörde çalışan grafik tasarımcı profili tasarımcıların, mesleki yeterlikler ise ajans yönetici ve sahiplerinin görüşleri doğrultusunda analiz edilmiştir. Bu bağlamda Ankara ilinde grafik tasarım hizmeti veren 53 tasarımcı ve 15 ajans yöneticisine uygulanan anketlerden elde edilen verilerin analizleri yapılarak gerçekleştirilmiştir. Bu bakımdan araştırma genel tarama modelinde betimsel bir araştırmadır. Katılımcı tasarımcılara 24, yöneticilere 15 sorudan oluşan bir anket uygulanmıştır. Elde edilen bulgulara göre; Ankara reklam piyasasında çalışan grafik tasarımcılarının büyük bir çoğunluğunun üniversite mezunu olduğu, çalışma saatlerinin birbirine yakın olup benzer tasarım programları kullandıkları, ücret ve iş disiplini konusunda çok fazla sorun yaşanmadığı, çalışma saatlerinin fazla olmasından dolayı sosyal ve eğitsel etkinliklere zaman ayıramadıkları sonucuna varılmıştır. Ajans sahiplerinin görüşlerine göre tasarımcıların, tasarlama süreci ve iş akışı konusunda kısmen yeterli düzeye sahip olmalarına karşın özellikle baskı ve baskı sonrası süreç konusunda yeterli olmadıkları sonucuna ulaşılmıştır

Anahtar Kelimeler: Grafik Tasarımcı, Reklam Sektörü, Tasarımcı Profili, Mesleki Yeterlilik.

Giriş

Bilimsel ve teknolojik gelişmelerin yaşamamızı bütünüyle etkilediği bu yüzyılda teknolojik açıdan yaşanan gelişmeler, yaşamın içinden bir alan olması nedeniyle grafik tasarım alanına da yakından ilgilendirmektedir.

Bireyler, mesleklerini tercih ederken büyük hayaller ve beklentilerle eğitim süreçlerine başlarlar. Eğitim kurumlarının müfredat programları her zaman sektör taleplerini karşılayacak nitelikte olmayabilir. Ya da öğrenci eğitim sürecini hedeflenen kazanımlarla tamamlayamayabilir. Grafik tasarım alanı tercih edilen, sevilen ve mezuniyet sonrası iş yaşamında beklentileri yüksek olan bir branştır. Temel problemlerden biri ve belki de en önemlisi, çocukluk ve gençlik döneminde başlayarak yaşam boyu devam eden, hayatları boyunca kullanacakları

bir yeterliliğin araştırma, sorgulama, öğrenme becerilerini nasıl kazanıp kullanacağıdır. Bunu kullanan ve uygulayan insan refaha ve gelişen bir toplumsal statüye kavuşabilir.

Grafik tasarım, bir düşünce ürünüdür, bir gerekliliktir, bir gereklilikten doğmuştur, bir bilinç vardır. Yeni yapılan tasarım bütünüyle kendi kanunlarını yaratır. Kendine has, kendine özgü orijinalliktedir. Yani yeni bir şeydir. O ana kadar yaratılanlardan bazen daha iyi, bazen daha kötüdür. Ama daima yenidir (Odabaşı, 2006).

Grafik tasarımcı büroda; çoğu zaman bilgisayar karşısında, film stüdyolarında, fotoğraf stüdyolarında, ajanslarda, genellikle zamana karşı yarışarak çalışmak durumundadır. Tasarımcılar öncelikle çalıştıkları kurumlarda grafik tasarımcı veya sanat yönetmeni yardımcısı olarak işe başlarlar. Yaratıcılıkları, mesleki başarıları ve deneyimleri doğrultusunda; sanat yönetmeni, daha sonra da sanat yönetmenleri ve metin yazarlarından oluşan yaratıcı grubun başında yaratıcı yönetici olabilirler (Megep, 2007).

Ulusal Mesleki Yeterlilik Kurumu birçok alanda mesleki yeterlilik çalışmaları yapmıştır. Grafik tasarım alanıyla ilgili direkt bir çalışma olmamakla birlikte, “Web ve Çoklu Ortam Geliştiricisi” ve “Endüstriyel Reklamcı” alanlarında mesleki yeterlilikler çalışılmış ve Resmi Gazetede yayınlanmıştır.

Buna göre endüstriyel reklamcı; meslek, endüstriyel reklamcı (Tabelacı) Ulusal Meslek Standardı 5544 sayılı Mesleki Yeterlilik Kurumu (MYK) Kanunu ile anılan Kanun uyarınca çıkartılan 19/10/2015 tarihli ve 29507 sayılı Resmi Gazete’de yayımlanan Ulusal Meslek Standartlarının ve Ulusal Yeterliliklerin Hazırlanması Hakkında Yönetmelik ve 27/11/2007 tarihli ve 26713 sayılı Resmi Gazete ‘de yayımlanan Mesleki Yeterlilik Kurumu Sektör Komitelerinin Kuruluş, Görev, Çalışma Usul ve Esasları Hakkında Yönetmelik hükümlerine göre MYK’nın görevlendirdiği Açık hava Reklamcıları Derneği tarafından hazırlanmış, sektördeki ilgili kurum ve kuruluşların görüşleri alınarak değerlendirilmiş, ve MYK Metal Sektör Komitesi tarafından incelendikten sonra MYK Yönetim Kurulunca onaylanmıştır (Ulusal Meslek Standardı, 2017).

Web ve Çoklu Ortam Geliştiricisi, ulusal meslek standardı 5544 sayılı Mesleki Yeterlilik Kurumu (MYK) Kanunu ile anılan Kanun uyarınca çıkartılan “Ulusal Meslek Standartlarının Hazırlanması Hakkında Yönetmelik” ve “Mesleki Yeterlilik Kurumu Sektör Komitelerinin Kuruluş, Görev, Çalışma Usul ve Esasları Hakkında Yönetmelik” hükümlerine göre MYK’nın görevlendirdiği İstanbul Ticaret Odası (İTO) koordinasyonunda YASAD Yazılım Sanayicileri Derneği ve TÜBĞİDER Bilişim Sektörü Derneği tarafından hazırlanmıştır (Ulusal Meslek Standardı, 2017).

Aynı yönetmelikte, web ve çoklu ortam tasarımcı çalışma ortamı ve koşullar şu şekilde belirtilmektedir: Web ve Çoklu Ortam Geliştiricisi, genelde kapalı alanlarda, iyi aydınlatılmış, havalandırılmış, termal konfor koşulları ve uygun gürültü düzeyinde, ofis ergonomisine uygun hazırlanmış ortamlarda ayakta veya oturarak çalışır. Çalışma ortamı ve koşulları alt sektörlere göre farklılıklar gösterir (Ulusal Meslek Standardı, 2017).

Günümüzde grafik tasarım mesleği çalışanları yani grafik tasarımcılar, web ve çoklu ortam tasarımcıları ile aynı çalışma ortamlarında hizmet verirler. Hatta bu alanda çalışan tasarımcıların büyük bir çoğunluğunu grafik eğitimi almış grafik tasarımcılar oluşturur. Tasarım alanında hizmet veren reklam ajanslarının büyük oranda çalışma koşullarını meslek standartları çerçevesine uydurdukları görülmektedir.

Eğitim sistemi, öğrenciye dönük bir sistem olarak, öğrencinin sürekli aktif olduğu, araştırdığı, sorguladığı bir ortam yaratarak istenilen bu düzeyin oluşmasını sağlamaktadır. Eğitim iyi bir yaşam standardının oluşmasında en önemli ve en temel kıstaslardan biridir. Bundan en çok etkilenen branşlardan biri de hiç kuşkusuz grafik tasarımıdır.

Grafik tasarım bir mesajı iletme, düşünceyi görselleştirmek ve en iyi yalın bir biçimden hedef kitleye anlatma amacıyla olan önemli bir yaratıcı süreçtir. İyi bir tasarım için çevreyi olayları iyi algılamak ve yorumlamak özellikle bu alan için oldukça önemlidir.

Doğru, gerçekçi ve tam bir algılama içinde çok iyi gözlem yapmak, araştırmak, görmek, bilgilenmek kısacası hem grafik alanından hem de diğer alanlardan beslenmek oldukça önemlidir. Bunun içinde entelektüel, araştıran, okuyan, sorgulayan ve kendini sürekli geliştiren bireyler yetiştirilmesi zorunludur. Bu araştırmanın genel amacı Sektörde çalışan grafik tasarımcıların var olan profilini ortaya koyarak ajans sahipleri tarafından mesleki yeterliliklerinin ne olduğunu ortaya çıkarmaktır.

Bu araştırmada aşağıdaki sorulara cevap aranmıştır:

- Sektörde çalışan grafik tasarımcıların Üniversitelerde hangi alanlardan mezun olmuşlardır?
- Grafik tasarım sektörünü seçmelerindeki nedenler nelerdir?
- Grafik tasarım alanı ile ilgili ne kadar bilgi ve yeterliliğe sahipler?

- Kendilerini mesleki anlamda nasıl yeniliyorlar?
- İş süreci iş takibi konusunda seviyeleri ne durumdadır?
- Müşteri ile iletişim kurabilme becerileri nasıldır?

Yöntem

Araştırmada; sektörde çalışan grafik tasarımcı profili tasarımcıların, mesleki yeterlikler ise ajans yönetici ve sahiplerinin görüşleri doğrultusunda analiz edilmiştir. Bu bağlamda Ankara ilinde grafik tasarım hizmeti veren 53 tasarımcı ve büyük ve küçük ölçekli 15 ajansın yöneticisine uygulanan anketlerden elde edilen verilerin analizleri yapılarak gerçekleştirilmiştir. Bu bakımdan araştırma, genel tarama modelinde betimsel bir araştırmadır.

Katılımcı tasarımcılara 24, yöneticilere 15 sorudan oluşan bir anket uygulanmıştır. Anket katılımcılara internet aracılığıyla ulaştırılmış, survey sistemi kullanılarak mail yoluyla iletilmiş ve sonuçlar alınmıştır.

Bulgular ve Yorum

Bilimsel ve teknolojik gelişmelerin yaşamamızı bütünüyle etkilediği 21. Yüzyılda teknolojik gelişmelerin hızla ilerlemesi ve yaşamın içinden bir alan olması nedeniyle grafik tasarım alanına da yakından ilgilendirmektedir.

Grafik tasarım bir mesajı iletme, düşünceyi görselleştirmek ve en basit biçimden hedef kitleye anlatma amacıyla olan önemli bir yaratıcı süreçtir. İyi bir tasarım için çevreyi olayları iyi algılamak ve yorumlamak özellikle bu alan için oldukça önemlidir. Doğru, gerçekçi ve tam bir algılama içinde çok iyi gözlem yapmak, araştırmak, bilgilenmek kısacası hem grafik alanından hem de diğer alanlardan beslenmek oldukça önemlidir. Entelektüel bir yapıya ve araştırmacı, sürekli okuyan, gezen ve gören bir tasarımcılar olunması gerekir. Bu tarz eğitim dışı faaliyetlerin Ülkemizde tasarım alanında eğitim sürecinde ya da iş hayatında ne derece yapılabildiği hakkında kesin bir şey söylemek mümkün değil.

Çalışmanın örneklemini oluşturan, Ankara ilinde büyük, orta ve küçük ölçekli ajanslarda çalışan ve ankete katılan 53 tasarımcıdan 30'u kadın 23'ü erkektir. 20 ile 46 yaş arasındaki anket katılımcıların %54.72'lik kesimi üniversite mezunu olup yine bir çoğunluğu yüksek lisans ve doktora yapmaktadır. Bu da bize gittikçe alan eğitiminin önemini hatta lisans eğitiminden sonra da lisansüstü eğitimine önem verildiğini göstermektedir. Ankete katılanların % 13.21'i lise mezunu olup uzun süredir sektörde çalışmaktadır.

Grafik tasarım ile ilgili bir okuldan mezun olan katılımcıların % 29.27'si grafik eğitiminin muhakkak alınması gerektiği düşüncesinde olup % 26.83'ü okullarda yeterli sanatsal bilgiyi aldığı görüşündedir. Grafik tasarımdan mezun olmayıp sektörde çalışan kişilerin % 50.00'si grafik tasarım eğitimi almadan da bu mesleğin yapılacağı düşüncesindedir.

Sektörde çalışma sürelerine baktığımızda ankete katılan 53 kişiden 22'si yani % 41.51'i 5 ile 10 yıl arasında bu alanda çalışmaktadır. Sektörde çalışanların ve ankete katılanların % 69.23'ü 9.00- 18.30 arası normal mesai yapmaktadır. Buda bize Ankara piyasasındaki çalışma saatlerinin birbirine yakın olduğunu göstermektedir. İşyeri memnuniyet derecesine baktığımızda ise şöyle bir tablo ortaya çıkmıştır:

Tablo 1. Tasarımcıların çalıştıkları iş yeri memnuniyetlerine dair bulgular:

Çalıştığınız iş yerinden ne derece memnunsunuz?	f	%
Oldukça memnunum	23	44.23
Kısmen memnunum	24	46.15
Memnun değilim	5	9.62

Katılımcı tasarımcıların iş yeri memnuniyetlerine ilişkin soruya, yaklaşık % 90'ının memnun olduğunu görmekteyiz. İş yerinden memnun olmayan % 9.62'lik kesimin % 24.56'sı ücretten dolayı % 14.04'ü iş yeri disiplini % 12.28'i ise çalışılan ortamda bulunan birtakım eksikliklerden dolayı iş yerinden memnun değildir. Tasarım yaparken teknolojiden faydalanma şekli konusunda ankete katılan katılımcıların % 34.62'si tamamen bilgisayar programlarının özelliklerinde faydalanarak ve hazır tasarımları değiştirerek ve geliştirerek iş ürettikleri ortaya çıkmıştır. Çoğu katılımcının eskiz yapmadığı görülmektedir.

Hedef kitleyi göz önünde bulundurarak tasarım yapma konusunda; ankete katılanların % 71.15'i hedef kitle analizlerinin daha önceden yapılmış olduğu ve bu bilgiler ışığında tasarım yapıldığını belirtmiştir. Müşteri tasarımı beğenmediği takdirde ise yine katılımcıların % 92 gibi büyük bir çoğunluğu müşterinin fikirlerini alarak tasarımı tekrardan revize etmektedir. Buradan şu anlaşılmaktadır ki müşteri fikirleri göz önünde bulundurulmuş çalışmalarda tasarımcı operatör gibi çalışmakta, özgün tasarımlar üretememektedir. Programlar bilgisi hakkında sorular yönelttiğimiz katılımcıların bir kısmı üniversite döneminde bilgisayar olmadığı için okul döneminde program öğrenmeyip, sektör hayatında programları kullanmışlardır. Üniversite döneminde program öğrenenler ise genelde hep benzer programlar üzerinde durmuşlardır. Genel olarak Ankara piyasasında çalışan tasarımcılar Freehand, Adobe İllüstrator, Adobe Photoshop, Adobe Indesign, Corel Draw gibi programları öğrenmiş ve yine piyasada aynı programları kullanarak en çok da Adobe serisinin güncel sürümlerini takip etmektedir.

Mesleki anlamda tasarımcıların kendilerini nasıl yenilediklerini, beslediklerini görmek amaçlı yaptığımız anket sonucu şu şekilde olmuştur (Tablo 2):

Tablo 2. Tasarımcıların kendilerini mesleki anlamda nasıl yenilediklerine dair bulgular:

Kendinizi mesleki anlamda nasıl yeniliyorsunuz?	f	%
Çalıştığım yerin meslek içi eğitimlerine katılıyorum.	7	7.61
Kendi imkânlarımı kullanarak çeşitli kurslara/seminerlere/sergilere katılıyorum.	23	25.00
Kitaplardan ve İnternet'teki kaynaklardan faydalanıyorum.	42	45.65
Üye olduğum meslek örgütlerinin/derneklerin düzenlediği etkinliklere katılıyorum.	7	7.61
Akademik çalışmalarımı sürdürüyorum.	10	10.87
Kendimi yenileyemiyorum.	3	3.26

Teknolojinin gelişmesiyle birlikte internet ortamının varlığı ve çalışanların zaman sıkıntısından dolayı ankete katılanların % 45.65'lik kesimi kendilerini internet ortamından faydalanarak geliştirdiği görülmektedir. Tasarımcıların çoğu kendilerini yenilemek için kitaplardan faydalanmamakta, fakat süreli yayınların bazılarını takip etmektedirler. Tasarımcıların çoğu internet kaynaklarından faydalanırken alanıyla ilgili görsellerin, vektörlerin ve tasarımların olduğu birçok internet sitesinden haberdar ve bunları kullanmaktadır.

Sektörde çalışan tasarımcılar grafik tasarım mesleğinin yanı sıra alanıyla ilgili başka yan dallarla da ilgilenmekte ve yapmaktadır. Örneğin ankete katılanların % 22'lik gibi bir kısmı yaygın bir aktivite olan fotoğrafçılıkla ilgilenmekte olup, % 16.98'i tipografi, % 12.58'i illüstrasyon ve % 10.06'sı ise animasyon ile ağırlıklı olarak ilgilenmektedir.

Tasarımcılar, kendini geliştirme açısından süreli yayınlardan bazılarını bilmekte ve takip etmektedir. En çok takip edilen ve satın alınan dergi ise güncel bir dergi olan Grafik Tasarım dergisi olup % 33.08'lik gibi bir kesimi bunu almaktadır. Bunun peşinden sırası ile Photoshop Magazine ve Media Cat okunan dergiler arasındadır. Katılımcıların büyük bir çoğunluğu yabancı süreli yayını takip etmemektedir.

Alanıyla ilgili yapılan etkinliklere katılma açısından ankete katılan tasarımcıların % 44.23'ü yapılan etkinliklerde haberdar olup, zaman açısından sıkıntı yaşadıkları için çok fazla bu etkinliklere katılamamaktadır. Ancak yine benzer yoğunlukta grupta vakit buldukça bu etkinliklere katılarak kendilerini geliştirmektedir. Ankara piyasasında faaliyet gösteren ajansların yöneticilerine tasarımcılar hakkındaki genel görüş ve mesleki yeterlilik düzeyleriyle ilgili olarak sorular neticesinde ortaya çıkan sonuçları ise şu şekildedir:

Tablo 3. Ajans yöneticilerinin, çalışanların verilen bir işi iyi planlayıp, uygulayıp, istenilen zamanda tamamlayıp tamamlayamadıklarına dair görüşleri:

Verilen bir işi iyi planlayıp, uygulayıp, istenilen zamanda tamamlayabiliyor.	f	%
Kesinlikle katılmıyorum	2	13.33
Katılmıyorum	0	0.00
Kararsızım	1	6.67
Katılıyorum	9	60.00
Kesinlikle katılıyorum	3	20.00

Yukarıdaki sonuçlara baktığımızda katılımcı yöneticilerin yaklaşık % 80'lik tasarımcıların kendisine verilen bir işi iyi bir şekilde organize edip, planlayıp, uygulayıp, istenilen zamanda tamamlayabildiklerini ifade etmişlerdir. Yine bu katılımcıların %60'ı konuyla ilgili özgün tasarımlar yapabilmektedir demişlerdir.

Tablo 4. Ajans yöneticilerinin, tasarımcıların yaptıkları tasarımların uygulanabilir olmasına dair görüşleri:

Yaptığı tasarımların uygulanabilir olmasına dikkat ediyor.	f	%
Kesinlikle katılmıyorum	1	6.67
Katılmıyorum	2	13.33
Kararsızım	3	20.00
Katılıyorum	7	46.67
Kesinlikle katılıyorum	2	13.33

Ankete katılan yöneticilerin % 46.67'si tasarımcıların yaptığı tasarımların uygulanabilir olduğunu, % 33.33'lük oranda tasarımcıların yaptığı işin maliyetine dikkate alarak tasarımlarını yapmakta olduklarını düşünmektedir. Ajans yöneticilerinin büyük bir oranda ortak görüşü tasarımcıların hedef kitleye ve müşteriye uygun tasarım yaptıkları şeklindedir. Yine ajans yöneticileri tasarımcıların hedef kitleye ve müşteriye uygun tasarım yaptıkları fikirlerinde ortak bir görüşe sahiptir.

Masaüstü yayıncılık konusunda %53.33 lük katılımcı, tasarımcıların bu bilgiye sahip olduğu görüşünde olup, şuan çalışmakta olan personelinin web ve interaktif yayıncılık konusunda da tasarımcıların yeterli bilgi ve deneyim de olduğunu düşünmektedirler.

Tablo 5. Ajans yöneticilerinin çalışanların matbaa konusundaki bilgi yeterliklerine dair görüşleri:

Matbaa konusunda gerekli bilgiye sahiptir	f	%
Kesinlikle katılmıyorum	3	20.00
Katılmıyorum	0	0.00
Kararsızım	5	33.33
Katılıyorum	7	46.67
Kesinlikle katılıyorum	0	0.00

Ajans yöneticilerinin % 46.67'si, bünyelerinde çalışan tasarımcıların gerekli matbaa bilgi ve tecrübesine sahip olduğu düşüncesindedirler. Katılımcıların % 33.33'lük bir kısmı çalışanların alanıyla ilgili teknolojik gelişmeleri takip ettiği düşüncesindedir. Bunlara örnek olarak tasarımcıların alanıyla ilgili kullandıkları programların güncel sürümlerini takip etmelerini verebiliriz. Aynı zamanda yine aynı değerdeki kesim bahsettiğimiz gibi programların güncel sürümlerini de takip etmektedir.

İletişim kurma becerilerine baktığımızda tasarımcıların, ajans yöneticilerinin ortak görüşü şu şekildedir: Tasarımcıların müşteri, işveren ve diğer personel ile sağlıklı bir iletişim kurabildikleri konusunda hem fikirdirler. Bunun yanı sıra bünyesinde çalışan tasarımcıların işyeri tutum ve kurallarına uyan, ekip çalışmasına uyum sağlayan ve kesinlikle katıldıkları ortak değer olan ofis elemanlarını doğru ve etkili bir biçimde kullanmaları konusunda ortak görüşündedirler.

Sonuç

Ankara reklam piyasasında uzun süredir çalışan ve gözle görülebilir bir şekilde kadın tasarımcıların da yoğun olduğu sektörde tasarımcıların çoğu farklı ajans ortamlarında çalışsa da benzer saatlerde mesai yapmaktadır. Çoğu bu mesleği sevdiğinden bu işi yapmakta ve geneli de lisans mezunu düzeyindedir. Ücret, iş yeri disiplini gibi küçük sorunlar dışında pek bir sıkıntı yaşamadan ajans ortamında memnun bir şekilde çalışmaktadır. Hemen hemen çoğunun görüşü grafik tasarım özel bir yetenek, yaratıcılık ve eğitim gerektirmekte olup grafik eğitiminde sanatsal ve teknik bilginin alındığı görüşü savunulmaktadır.

Günümüzde internet ortamının hızla ilerlemesiyle birlikte tasarımcılar süreli yayınlardan bir iki tanesini takip etmekte genellikle kendini geliştirmek için internet ortamından faydalanmaktadır. Bunun yanı sıra tasarımcılar örnek alacağı, esinleneceği alanıyla ilgili web sitelerini takip etmektedir. Ayrıca yine büyük bir kısım alanının yanı sıra fotoğrafçılıkla birlikte tipografi, illüstrasyon afiş tasarımı gibi konulara da ilgi duymaktadır. Ankete katılan tasarımcılardan büyük bir kısmı alanıyla ilgili yapılan seminer, konferans sergi gibi etkinliklerden haberdar olup iş yoğunluğundan birçoğunun bu etkinliklere katılmadığını, bir kısmının da vakit buldukça bunlara katıldığını görmekteyiz.

Sektörde faaliyet gösteren ajanslardaki ajans yöneticileriyle tasarımcıların mesleki yeterlilikleriyle ilgili yapılan değerlendirmeye göre; genel anlamda tasarımcıların çoğu masaüstü yayıncılık konusunda iyi bir düzeyde olup müşteriye uygun, özgün tasarımlar yaptıklarını düşünüyorlar. Fakat maliyet ve uygulanabilirlik konusunda tasarımcıların ufak sorunlar yaşadığı düşüncesindedirler.

Bünyelerinde çalışan tasarımcıların matbaa bilgisine sahip olduklarını web ve interaktif yayıncılık konusunda yine bir takım eksikleri olduklarının görüşündedirler. Bunun yanı sıra firmada çalışan tasarımcılar, alanıyla ilgili teknolojik gelişmeleri kısmen takip edip uygulamaktadırlar. İletişim becerileri açısından değerlendirme sonuçlarına baktığımızda ise çalışan tasarımcıların çoğu hem kendi çevresinde hem işveren ile hem de müşteri ile sağlıklı, olumlu bir iletişim kurduğunu düşünülmektedir. Sektörde çalışan grafik tasarımcılara ve ajans yöneticilerine yöneltilen sorular neticesinde elde edilen sonuçlarına dayanarak ortaya çıkan bulgular ışığında şu önerileri sunabiliriz:

Sadece kitap ve internet kaynağının her ne kadar yaygın olsa da çok fazla yaratıcılığı geliştirmedeği görüşünden yola çıkarak tasarımcıların etkinliklere daha çok vakit ayırması için düzenlenmeler yapabilmeli, gerekirse ajans sahipleri bünyesindeki personelin mesleki gelişimleri için bu tür etkinlikleri takip edip görev olarak tasarımcıları yönlendirmelidir. Daha başarılı ve bilgili olmanın önemini göz önünde tutularak grafik eğitiminin hem kişinin kendisi için hem de ajans statüsü için önemli olduğu düşünülmeli ve kişiler desteklenmelidir. Okullarda daha çok teknik bilgi verilmeli ve yeni mezun grafik tasarımcıların sektör adaptasyonları göz önünde bulundurularak müfredat programalar düzenlenmelidir. Tasarımcılar farklı mecralara yönelik tasarımcı ihtiyacını göz önünde bulundurarak, farklı alanlarda kendini geliştirmelidir. Ajans sahipleri mesleki yeterlilikleri açısından bünyesinde çalışan elemanın her daim yanında olmalı, desteklemeli, gerektiğinde fikirlerine başvurup yönlendirmelidir.

Kaynakça

..... (26 Şubat 2013). Ulusal Meslek Standardı, Resmi Gazete: Sayı: 28571 (Mükerrer)

..... (1 Kasım 2017). Ulusal Meslek Standardı, .Resmi Gazete: Sayı: 30227 (Mükerrer)

Atan, A. (2006). Resimli Resim Sözlüğü. Asil Yayın Dağıtım: Ankara

Barnard, M. (2002). Sanat, Tasarım ve Görsel Kültür. Ütopya Yayınevi: Ankara.

Becer, E. (1997). İletişim ve Grafik Tasarımı. Dost Yayınları: Ankara.

Odabaşı, A, H. (2006). Grafikte Temel Tasarım. (3. Baskı) İstanbul: Yorum Yayınları.

Yanık, H. (2008). Masaüstü Yayıncılık. Muka Matbaacılık. İstanbul.

<http://megep.gov.tr>

<http://www.truity.com/career-profile/graphic-designer>, (Erişim tarihi:7 Aralık 2015)

Author Information

Mustafa KINIK

Necmettin Erbakan Üniversitesi
Abdulaziz Mahallesi, Abdülmümin Sokak, No:16, Meram,
KONYA/TÜRKİYE
mkinik@erbakan.edu.tr

Mahmut Sami ÖZTÜRK

Necmettin Erbakan Üniversitesi
Abdulaziz Mahallesi, Abdülmümin Sokak, No:16, Meram,
KONYA/TÜRKİYE
msozturk@hotmail.com.tr

Researching of Using Konya Ladik Red Clay as A Raku Glaze. International Conference on Research In Education and Science

Dr. Öğr. Üyesi Azize Melek ÖNDER
Necmettin Erbakan Üniversitesi

Dr. Öğr. Üyesi Mine Ülkü ÖZTÜRK
Necmettin Erbakan Üniversitesi

Abstract: In this study; it is aimed to investigate the use of contemporary ceramic technology in the production of grapes by raking the soil from the soil. Starting from this aim, working on the Ladik red hair taken from the Konya region. The clay was applied on the low grade casting slurry which is white in color. At the same time, 30-60% of Sileen was added to the Kile to give some kind of mildew. Plaques were observed by baking in an electric oven environment. To increase the texture and color scale, 1-3% of colorant oxide was added to the clay and tested under the same firing conditions.

Keywords: Ladlic, Red clay, Ceramic, Raku firing.

Ladik Konya Kırmızı Kilinin Raku Sırısı Olarak Kullanılabilirliğinin Araştırılması

Özet: Bu çalışmada; günümüz seramik teknolojisinden yararlanılarak, toprağın doğadan alındığı hali ile raku sırısı üretiminde kullanılmasının araştırılması amaçlanmıştır. Bu amaçtan yola çıkılarak, Konya yöresinden alınan Ladik kırmızı kili üzerinde çalışılmıştır. Kil, pişme rengi beyaz olan düşük dereceli döküm çamuru üzerine uygulanmıştır. Kile aynı zamanda %30-60 arasında Sülyen ilave edilerek bir miktar sırsı özellik kazandırılmıştır. Plakalar elektrikli fırın ortamında pişirilerek gözlenmiş, olumlu sonuç verenler raku pişirimi uygulanmıştır. Doku ve renk skalasını genişletmek amacıyla kile %1-3 arasında renklendirici oksit ilave edilmiş ve aynı pişirim şartlarında denenmiştir.

Anahtar Kelimeler: Ladik, Kırmızı Kil, Seramik, Raku Pişirimi.

Giriş

Raku bir seramik pişirim tekniğidir ve kökeni 16. yüzyılda Japonya kültürüne dayanmaktadır. Japon raku çay kâseleri ilk kez geleneksel çay seremonilerinde kullanılmıştır (Genç-Taçyıldız: 2012, 43).

Raku sırlarının düşük sıcaklıklarda eriyebilme özelliğine sahip olmasının yanı sıra estetik açıdan seramikte bıraktığı olumlu etki sebebi ile seramik sanatçıları tarafından tercih edilen bir teknik olmuştur (Çobanlı: 2018, 23).

Çalışma kapsamında Konya iline bağlı Ladik ilçesinden alınan kırmızı kil temizlendi, öğütüldü. Raku sırısı olabilmesi için içerisinde Sülyen ilave edilerek Esc-1 döküm çamuru (1000-1030 Co'de pişirilen, Eczacıbaşı'nın ürettiği döküm çamuru markası) üzerine uygulandı. Denemelerde oksidasyonlu ve redüksiyonlu pişirme yöntemlerinin her ikisi de kullanıldı. Denemeler ilk aşamada 1000 Co'de elektrikli fırınlarda pişirimleri yapıldı. Daha sonra Raku fırınında aynı sıcaklık sağlanarak denemeler gerçekleştirildi. Renk skalasını genişletmek amacıyla elde edilen oranlara %1-3 kırmızı demir oksit, bakır oksit, mangan oksit, kobalt oksit ve krom oksit ilave edildi.

Bu çalışma; ham seramik yüzeyler üzerinde daha önce kullanılmamış herhangi bir kil ve bilinen oksitler kullanılarak raku sırısı hazırlamak, elde edilen sonuçlardan kullanılabilir yeni raku sırlarına ulaşabilmek amacıyla yapılmıştır.

Deneysel Uygulamalar

Kullanım ihtiyacı doğrultusunda ortaya çıkan seramik, zaman içerisinde işlevselliği yanında sanatın bir parçası olarak karşımıza çıkmaktadır. İşlevselliğini artırmak için geliştirilen teknik, araştırmalar ve uygulamalar sanatsal

oluşum sürecinde seramik sanatçısının anlatımını zenginleştirmiş ve yeni arayışların oluşmasına zemin hazırlamıştır (Canduran, 2005: 33).

Bu çalışmada yapılan deneysel uygulamaların amacı; doğada farklı renk ve görünüme sahip killerden bir tanesinin alarak raku sırtı hazırlamak ve içerisine renklendirici oksitler, ergiticiler katarak renk ve doku çeşitliliği sağlayabilmektir.



Resim 1: Deneysel Uygulamalarda kullanılacak Ladik kili

Deneysel çalışmalar kapsamındaki sanat eseri uygulamalarında, Resim 1 de görülen, Konya ilinin Ladik ilçesinden alınan kil kullanılmıştır. Bulunan kil ilk aşamada hiçbir ergitici madde kullanılmadan deney plakaları üzerine uygulanmış, 900, 1000, 1100°C sıcaklıktaki fırınlarda pişirilerek denenmiştir. En uygun pişirme sıcaklığı olarak 1000°C kabul edilmiştir.

Deneysel çalışmalar kapsamında sanat eseri uygulamalarında kullanılabilen kil ve ergitici oranları araştırılmış, yapılan literatür araştırması sonucunda sülyen kullanımına karar verilmiştir. Yine literatür bilgileri doğrultusunda kile % 30 ile % 60 arasında sülyen ilave edilmiştir. Kil ve sülyen belli bir sıraya göre tartıldıktan sonra 60 dakika süre ile 100 gr.'lık jet değirmende öğütülmüş, öğütme işlemi bitiminde 100' MESH lık eleklerden geçirilmiştir (Resim 2, Resim 3, Resim 4).



Resim 2: Killerin tartılması



Resim 3: Kilin değirmenden çıkmış hali



Resim 4: Kilin kapa aktarılması

Uygun kuruma düzeyine gelen ESC-1 Döküm çamuru üzerine (Resim 5), hazırlanan karışım uygulanmıştır (Resim 4). Deneme örnekleri önce elektrikli fırın ortamında pişirilmiştir. Bu ortamdan olumlu sonuç alınan örnekler yeniden hazırlanıp, pişirme ortamını karşılaştırmak amacıyla raku tekniği kullanılarak indirgen ortamda pişirilmiştir (Resim 6).



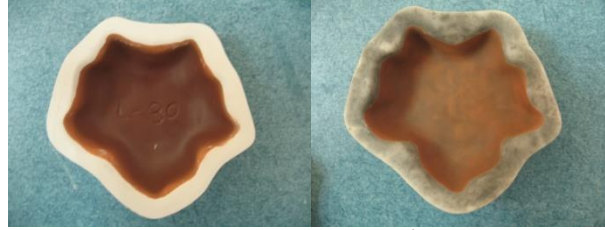
Resim 5: ESC-1 Döküm çamuru denemeleri



Resim 6: Uygulanan astarların fırınlanması

Kilin doğal rengi ile sürdürülen çalışmalarına, yeni bir boyut kazandırmak ve geniş bir renk paletine ulaşmak amacı ile renk veren oksitler kullanılmıştır. Bunun için ilk aşamada olumlu sonuç alınan L-55 sülyen seçilerek, içerisine kırmızı demir oksit, bakır oksit, mangan oksit, kobalt oksit ve krom oksit ilaveleri yapılmıştır. İlave edilen oksitlerin ortamda aktif olmaları (Kilin kendine has rengini fazla değiştirmemesi) istenmediğinden % 1 ve % 3 oranlarında karıştırılmış, karışım 60 dakikalık sürede, 100 gr'lık jet değirmen kullanılarak yapılmıştır. Denemeler tek pişirim olarak yapılmıştır.

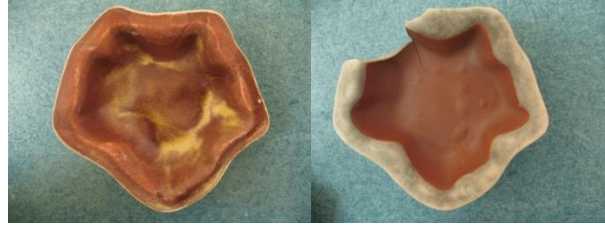
Ladik Kilinin Renklendirici Katılmamış Halleri



Oksidasyonlu Ortam

İndirgen Ortam (Raku)

Resim 7: ESC-1 Döküm Çamuru - %30 Sülyen – Ladik kili (L-30)



Oksidasyonlu Ortam

İndirgen Ortam (Raku)

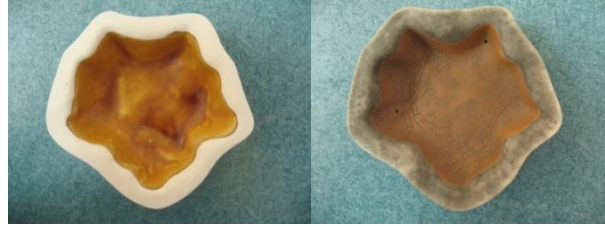
Resim 8: ESC-1 Döküm Çamuru - %50 Sülyen – Ladik kili (L-50)



Oksidasyonlu Ortam

İndirgen Ortam (Raku)

Resim 9: ESC-1 Döküm Çamuru - %55 Sülyen – Ladik kili (L-55)



Oksidasyonlu Ortam

İndirgen Ortam (Raku)

Resim 10: ESC-1 Döküm Çamuru - %60 Sülyen – Ladik kili(L-60)

Elde edilen örneklerden çıkan sonuçlar aşağıda verilmektedir.

- ESC-1 Döküm çamuru kullanılan bünyelerde;

Raku sırtı olarak hazırlanan L-30, L-50, L-55, L-60 Sülyen denemelerinin sonuçlara istenilen düzeydedir. Bu kilin sülyen ile karışımı sonucunda kil rengini kaybetmemiştir. Sadece kil resim 9'daki raku denemesinde soluklaşmış olduğu görülmüştür. Bu kil Oksidasyonlu pişirmede daha parlak, Raku pişiriminde ise mat bir görünüm elde edilmiştir.

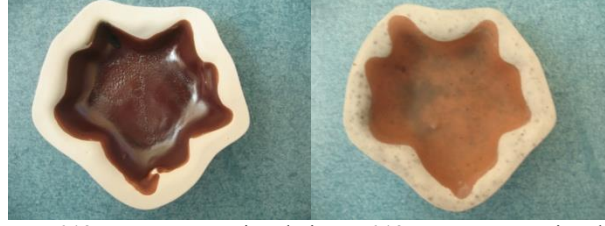
Ladik Kilinin Renklendirici Katılmış Haller



%1 Kırmızı Demir Oksit
Oksidasyonlu Ortam

%1 Kırmızı Demir Oksit
İndirgen Ortam (Raku)

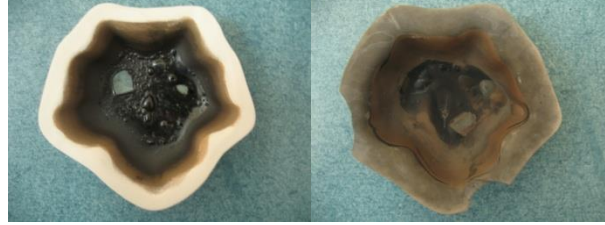
Resim 11: ESC-1 Döküm Çamuru - %55 Sülyen – Ladik Kili (L-55)



%3 Kırmızı Demir Oksit
Oksidasyonlu Ortam

%3 Kırmızı Demir Oksit
İndirgen Ortam (Raku)

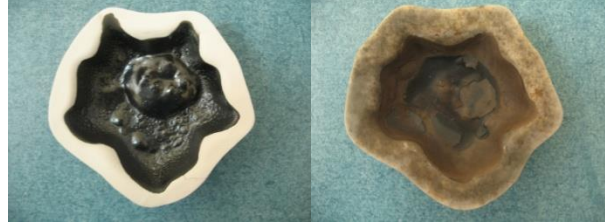
Resim 12: ESC-1 Döküm Çamuru - %55 Sülyen – Ladik Kili (L-55)



%1 Kobalt Oksit
Oksidasyonlu Ortam

%1 Kobalt Oksit
İndirgen Ortam (Raku)

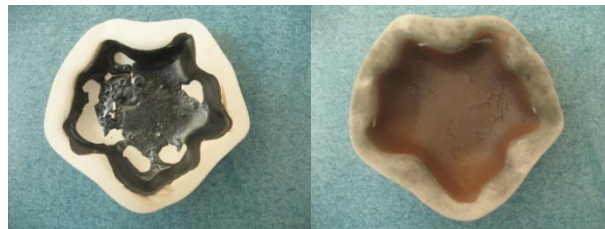
Resim 13: ESC-1 Döküm Çamuru - %55 Sülyen – Ladik Kili (L-55)



%3 Kobalt Oksit
Oksidasyonlu Ortam

%3 Kobalt Oksit
İndirgen Ortam (Raku)

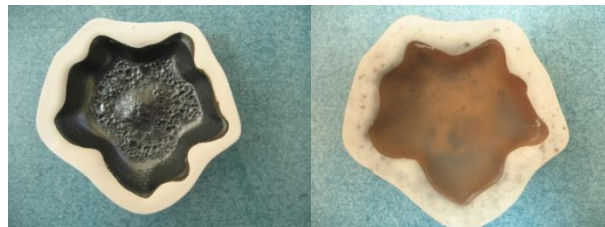
Resim 14: ESC-1 Döküm Çamuru - %55 Sülyen – Ladik Kili (L-55)



%1 Mangan Oksit
Oksidasyonlu Ortam

%1 Mangan Oksit
İndirgen Ortam (Raku)

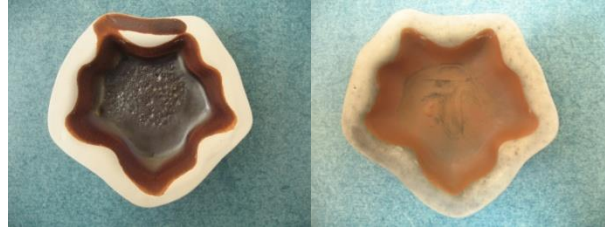
Resim 15: ESC-1 Döküm Çamuru - %55 Sülyen – Ladik Kili (L-55)



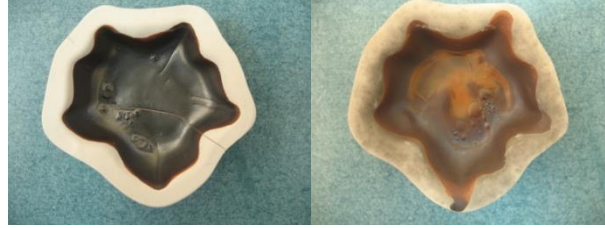
%3 Mangan Oksit
Oksidasyonlu Ortam

%3 Mangan Oksit
İndirgen Ortam (Raku)

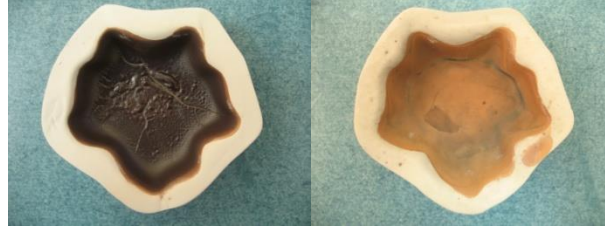
Resim 16: ESC-1 Döküm Çamuru - %55 Sülyen – Ladik Kili (L-55)



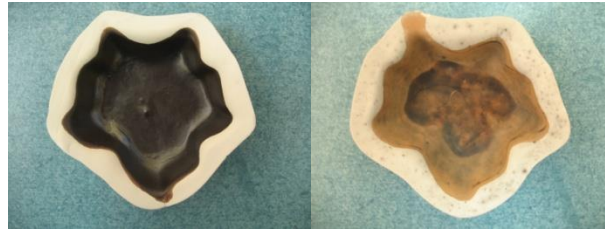
%1 Bakır Oksit Oksidasyonlu Ortam %1 Bakır Oksit İndirgen Ortam (Raku)
Resim 17: ESC-1 Döküm Çamuru - %55 Sülyen – Ladik Kili (L-55)



%3 Bakır Oksit Oksidasyonlu Ortam %3 Bakır Oksit İndirgen Ortam (Raku)
Resim 18: ESC-1 Döküm Çamuru - %55 Sülyen – Ladik Kili (L-55)



%1 Krom Oksit Oksidasyonlu Ortam %1 Krom Oksit İndirgen Ortam (Raku)
Resim 19: ESC-1 Döküm Çamuru - %55 Sülyen – Ladik Kili (L-55)



%3 Krom Oksit Oksidasyonlu Ortam %3 Krom Oksit İndirgen Ortam (Raku)
Resim 20: ESC-1 Döküm Çamuru - %55 Sülyen – Ladik Kili (L-55)

Çalışmalara yeni bir boyut kazandırmak ve geniş bir renk paletine ulaşmak amacı ile renk veren oksitlerden yararlanılmıştır. Bunun için elde edilen denemelerden Raku sırası olabilecek L-55 sülyen seçilmiştir. Bunlarının içerisine seramik sanatçıları tarafından çokça kullanılan bazı oksitler ilave edilmiştir. Bu oksitler kırmızı demir oksit, bakır oksit, mangan oksit, kobalt oksit ve krom oksit olarak belirlenmiştir.

L-55 Sülyen kullanılarak yapılan oksit karışımlarında renk değişimleri görülürken, astarın kalın kullanıldığı yerlerde kavlamalar oluşmaktadır. Aynı zamanda L-55 sülyen + oksit karışımı astarlarda, özellikle oksidasyonlu ortamda pişirilmesi sonucunda camlaşmalar görülmektedir.

Sonuç

Denemeler, literatürde yer alan bilgilerden yararlanılarak gerçekleştirilmiş, çalışma koşullarına uyarlanmış ve bunlara bazı değişiklikler getirilmiştir. Deneme sonuçlarından edinilen gözlemler aşağıda sıralanmaktadır;

-Denemelerde elde edilen örnekler gözlemlendiğinde oksitasyonlu ortamdaki pişirimlerde camlaşma görülmüş, indirgen ortamda yapılan pişirimlerde astarimsı bir görünüm almıştır.

-Hazırlanan raku sırlarının bünyeye olduğunda daha kalın sürülmesi elde edilen sırların oksitli ortamlardaki pişirimlerde camlaşmasına, indirgen ortamdaki pişirimlerde ise yine astarimsı bir görünüm elde edilmesini sağlamıştır.

-Raku sırları Esc-1 döküm çamuru üzerine uygulanarak tek pişirim yapılmıştır. Tek pişirimlik sırlar iki pişirim yapılan sırlara göre daha kırılğan olduğu tespit edilmiştir. Buna rağmen uygulama aşamasında ürünlerde ciddi bir problem yaşanmamıştır.

-Hazırlanan raku sırları bünye ile uyum göstermiştir. Kil miktarı artıkça raku sırında camlaşma azalmış ve sırat bir görünüm almıştır. Yapılan denemeler gözlemlendiğinde, istenilen hedefe ulaşılmıştır.

Günümüz seramik sanatında oldukça pahalı bir malzeme olan raku sırlarını imkân doğrultusunda yapabilmek hedeflenmiş ve ulaşılmıştır. Bu doğrultuda rastgele seçilen Lâdik kırmızı kili seramik çalışmalarda kullanılabilir olduğu kanıtlanmıştır. Bu seramikle uğraşan kişilerin kolayca ulaşabileceği, ekonomik bir malzeme olması ve sanatçıya farklı bakış açıları sunabilmesi bakımından da önemlidir.

Bu çalışmada verilmek istenen sonuç, tek bir kil ile çalışıldığında bile, neredeyse sonsuz seçeneklerde yeni astar ya da sırlar elde edilebildiğidir. Bu çalışmanın sonunda deneysel olarak elde edilen veriler, ileride bu alanda yapılacak çalışmalar için bir kaynak ve eksikliğin giderilmesi için bir veri niteliği taşımaktadır.

Kaynakça

- Canduran, Kaan (2005). Tuz Sırlarında Renkli Astar Uygulamaları. Hacettepe Üniversitesi Sosyal Bilimler Enstitüsü. Yayınlanmamış Yüksek Lisans Tezi.
- Çobanlı, Z. (2018). Raku. <https://earsiv.anadolu.edu.tr/xmlui/bitstream/handle/11421/1025/109413.pdf?sequence=1&isAllowed=y> s.13-30.
- Soner, G.-E. Taçyıldız, (2012). “Farklı Bünyeler Üzerinde Raku Sırlarının Araştırılması”, Anadolu Üniversitesi Sanat ve Tasarım Dergisi, Cilt 3, Sayı: 3, Eskişehir, s.41-49.

Author Information

Azize Melek Önder

Necmettin Erbakan Üniversitesi
Abdülaziz Mahallesi, Abdülmümin Sokak, No:16, Meram,
KONYA/TÜRKİYE
Melektolasa1@yahoo.com

Mine Ülkü ÖZTÜRK

Necmettin Erbakan Üniversitesi
Abdülaziz Mahallesi, Abdülmümin Sokak, No:16, Meram,
KONYA/TÜRKİYE
mineozturk@erbakan.edu.tr

Contributions of Archaeological Site Findings to Art Education and Art Practices

Dr. Öğr. Üyesi Mine Ülkü ÖZTÜRK
Necmettin Erbakan Üniversitesi

Abstract Although the recorded history does not provide a record to let us watch the thousands of years of life's progress, the meaning of the past may be obtained by following the trails in crafted items. There are many common tracks between the understanding towards production in the ancient era which was created as an ornament and then adopted to life, and the work of today's artists who have an esthetic concern and a struggle to produce more. Vanishing societies have left their legacies to their successors in the forms of worn out records. These findings not only shape the future, but also bring us the remnants of the life in the past. An artwork cannot express or reflect the texture of the nature or the beliefs belonging to another land. In this study, the objective is to study the form in archaeological findings and use these esthetic marks hidden in the details in the works of these initial life forms in their modern applications during their education. Now Art is able to speak a common language with numerous creations and formations and to transfer the records of past formations to artists' work and discoveries by adding a diverse selection of samples into their areas and lives.

Keywords: Art Education, Archaeology, Site, Çatalhöyük.

Arkeolojik Sit Buluntularının Sanat Eğitimi ve Pratiklerine Katkısı

Özet: Binlerce yıllık hayat serüveninin izlene bilecek tekrar bir kaydı yoktur, ancak üretilenlerin izinden geçmişin anlamı ortaya çıkartılabilir. Eski çağ insanının güzelleştirme çabasıyla yarattığı ve yaşamına uyarladığı üretme anlayışı; bugünkü sanatçının estetik kaygısıyla üretim çabası arasında ortak izler görülür. Bir şekilde son bulan toplumlar, kendi kültürlerini bir sonraki toplumlara bırakıp, tortulanan bu kayıtları geleceğe bırakmışlardır. Bu bulgular geleceğe yol verdiği gibi, bizlere geçmişin yaşamsal izlerini de taşır. Toprak üzerinde doğan gelişen sanat ürünü, o toprakta yaşamayan doğa varlıklarını, yerleşmemiş inançları; ne konu edebilir ne kendi dokusu içinde kendi boyasına uygun olarak gösterebilir. Bu bağlamda yapılan araştırmada öğrencilerin eğitimi süresince; arkeolojik eserlerdeki biçimi incelemesi ve bu ilk yaşam formlarının detayında saklı olan estetik izleri görerek kendi çağdaş uygulamalarında bunları uygulaması amaçlanmıştır. Bundan sonra Arkeoloji ve sanat; farklı örneklerle kendi alanlarına hayatlar katarak, yeni oluşumların kayıtlarını, çalışmalarına ya da keşiflerine aktarabilecek, sayısız oluşumların ve yaratıların ortak dilini oluşturabileceklerdir.

Anahtar Kelimeler: Sanat Eğitimi, Arkeoloji, Sit, Çatalhöyük.

Giriş

Tarihsel süreçte, her toplumun kendine özgü bir sanatı vardır. Nerede bir insan topluluğu varsa, orada yaşamı gerekli kılan yaşamın yanı sıra sezginin, bilinçaltının, içgüdüsellüğün bir etkisi olarak, sanat edimi daima kendisini göstermiştir.

Öznel olan durumun dışa dönüşmesi, somutlaşması ve başkalarına anlatması insan için önemli bir gereksinimdir. Daha kapsamlı bir anlayış ve deyimle sanat; insanın insan olma yazgısı ve koşulunu yenme, kendini aşabilme çabasıdır (Kınay, 1993). Çağdaş yaşamın ortaya çıkardığı tarihsel, toplumsal ve kültürel bir dönüşümün ürünü olarak teknoloji ve tüketim kültürü; yeni bir araştırma alanı olarak doğarken aradan geçen zaman içinde sosyal bilimlerin değişen doğası ve disiplinlerarasılığın öne çıktığı bir dönemde daha geniş ve daha kuşatıcı bir çalışma çerçevesine oturtulması gerekmektedir.

Kültürel mirasa sahip çıkmanın, modern toplumla ve bu toplum içinde çağdaş kentin kültürel aktarım alanlarında üretilen, yaratılan, yaşatılan sanatsal formlarla yakından ilişkili olduğunu; moderniteyi ve günümüzde küresel dünyanın kültürel kodlarını anlama süreci açısından da önemli olduğunu söyleyebiliriz. Bu bağlamda eğitim kurumlarına çok iş düşmektedir. Öğretim elemanının öğrenciye öncelikle bizi biz yapan kültürel mirasımıza sahip çıkma bilincini aşılması gerekmektedir. Yapılacak olan örnek sanat uygulamaları

kültürel mirasın anlaşılması ve korunmasına yönelik lisans eğitim alanında gerçekleştirilen olumlu adımlardan biri olacaktır.

Geleneksel ile çağdaş olanın sınırlarının çok iyi belirlenmesi, yeni ürünler elde edelim derken, tarihi ve kültürel mirasımızın dejenere edilmesi ya da kimliksiz bir üretime geçilmesine de müsaade edilmemelidir (Kahveci, 1998:392).

Kültürel değerlerimize sahip çıkmak, onların ışığında farklı teknik ve materyallerle yeniden yorumlamak ve yeni eserler sunmak sanat eğitiminin dolaylı bir görevidir. Bugünün değerlerini yaşadığı toprakların geçmişle özleştirmek, onlardan beslenmek; Sanat öğrencilerini neolitik çağa dair tarihi buluntularla geçmişe doğru fantastik bir yolculuğa çıkararak o dönemi anlama ve yeni estetik nesnelere oluşturma sürecine kaynak olacaktır. Bu uygulamalar sayesinde korunması gerekli kültür varlıkları ve alanlarının, bu evrensel değerlerin gelecek kuşaklara bırakılması sağlanabilir.

Kültür Varlığı ve Arkeoloji

İnsanın nasıl düşündüğü, duyduğu, yaptığı, istediği; insanın kendine nasıl baktığı, özünü nasıl gördüğü; değerlerini, ülkülerini, isteklerini nasıl düzenlediği işte bütün bunlar geçmişten getirdiği tarihsel kültürün öğeleridir.

Tarihin bir başka değeri ise bireylere kimlik duygusu katması, içinde buldukları toplumun ve insanoğlunun kültürel mirasını anlamasına yardımcı olmaktır. Birey ve toplum kendi kimliğini, sahip olduğu tarihi süreç sayesinde kazanır. (Aktaran; Kaya, 2009:71). Uygur'a (1996:17) göre; "kültür", insanın ortaya koyduğu, içinde insanın var olduğu tüm gerçeklik demektir. Öyleyse; kültür doğanın insan eliyle evcilleştirme ve ehlileştirme sürecine dair maddi ve manevi her türlü bileşenlerin toplamıdır. Kültür durağan değildir, kültür içgüdüsel olarak nesilden nesile aktarılan değerler-normlar-kurumlar-eserlerin kümülatifidir (toplamıdır).

Tarih Öncesi ve Tarihi Devirlere ait bilim, kültür, din ve güzel sanatlarla ilgili veya Tarih Öncesi ya da Tarihi Devirlerde sosyal yaşama konu olmuş, bilimsel ve kültürel açıdan özgün değer taşıyan yer üstünde, yer altında veya su altındaki bütün taşınır ve taşınmaz varlıklara, "Kültür Varlıkları" denir.

Taşınmaz Kültür Varlıklarına örnek olarak; kaya mezarlıkları, ören yerleri, akropol ve nekropoller; kale, hisar, burç, sur, tarihi kışla, kümbet, türbe, köprü, han, hamam, harabeler, sarnıç, tersaneler, medrese tekke, zaviye, arasta, bedesten gibi yapılar sayılabilir (Madran,2009:8). eski olmayan yakın tarihte inşa edilmiş bir yapı, taşıdığı özellikler nedeniyle eskilik vasfı aranmaksızın kültür varlığı olarak kabul edilmiştir. Tanımda geçen bir diğer unsur "nitelik" unsurudur. Bir taşınmazın kültür varlığı sayılabilmesi için, onun sosyal yaşama konu olmuş "bilim, kültür, din ve güzel sanatlarla ilgili" maddi ya da manevi bir "değer" taşıması gerektirir. Bu değerleri ortaya çıkaracak olan ise tarih, ilahiyat, sosyoloji, arkeoloji, sanat tarihi gibi bilim dallarıdır.

Sit Kavramı

Sit kavramı ile ilk yasa 1930'da Fransa'da çıkmıştır. Yasada "Site" olarak geçen terim, özel anlam taşıyan, doğal, kültürel ya da bilimsel ilginçlikleri olan mekân parçaları olarak tanımlanmaktadır (Özsoy, 1988). Korunacak özellikleri olan doğal, insan yapısı ya da her ikisinin ortak ürünü olan alanlara sit denilmektedir. Özelliklerine göre sit çeşitleri ise; doğal, tarihi, arkeolojik, kentsel gibi isimlerle sınıflandırılmaktadır (Bildiş, 2006:12).

Korunması Gerekli Taşınmaz Kültür ve Tabiat Varlıklarının Tespit ve Tescili Hakkında Yönetmelikte ve Kültür ve Tabiat Varlıklarını Koruma Yüksek Kurulu ilke Kararlarında, unsurlarından hareketle yapılmış bir sit türü tanımı bulunmamaktadır. Sit türleri ve derecelendirme çoğunlukla alanda yapılabilecek müdahalelerden hareketle belirlenmiştir. Aynı şekilde sit türleri arasındaki farklılık ve çakışma hali de belirginleşmemiştir. Konunun daha iyi anlaşılabilmesi için, kültür ve tabiat varlıklarını koruma mevzuatı içinde (Kanun, Yönetmelik, ilke Kararı vb.) geçen sit türlerini ve derecelerini aşağıdaki gösterildiği şekilde tasniflemek mümkündür. (Koç, 2007).

Sit Türleri ve Dereceleri:

1.Kültürel Sitler

- Tarihi sit

- Kentsel sit

- Arkeolojik Sit (1.Derece/2.Derece/3.Derece)
- Kentsel Arkeolojik sit
- 2.Dođal Sitler (1.Derece/2.Derece/3.Derece)

Arkeoloji Bilimi

Arkeoloji dünya üzerinde insan elinden çıkmış maddi nitelikli her türlü malzemeyi, kalıntıyı ya da genel anlamda insana dair bir üretim aşamasının sonucu olarak ortaya çıkmış ürün niteliğindeki tüm olguları içinde barındıran “kültürel miras” kavramını nitelik, nicelik, neden ve sonucu bakımından arařtıran bir bilim dalıdır.

Türkçede ise arkeoloji sözcüğünün karşılığı olarak kazıbilim kullanılsa da terminolojik olarak kullanımı itibariyle yaygınlık kazanmamıştır. Bunun sebebi ise arkeolojik buluntuya ulaşmak için uygulanan kazma eyleminin bir amaç değil söz konusu bilimsel disiplinin ihtiyaç duyduğu verileri elde etmek için kullanılan bir araç oluşudur.

Gerçek anlamda arkeoloji, insanı ve onun değişimlerini anlamaya çalışır. Bu noktada gerçek arkeoloji nesneyi ve onun değişimini ya da gelişimini tanımlamaya çalışan kazı biliminden farklılık gösterir. Arkeoloji ile antika, değerli eser, koleksiyon gibi kavramların neredeyse özdeşleştirilmesi ise mevcut halde arkeoloji biliminin ortaya koyduğu temel verilerin niteliği ile ilgilidir. Ancak “değerli eser” arkeoloji biliminin ulaşmak istediği gerçekten amaç değil, geçmişe dair var olanı çözümlenmek ve anlamlandırmak için kullanılan bir yan ürün yada enstrümandır (Özdoğan, 2004:1-11).

Arkeoloji bilimsel bir disiplin olarak ilk kez 15. ve 16. yüzyıllarda Avrupa’da ortaya çıkmıştır. Bunun da nedeni Rönesans hümanistlerinin Antikçağ sanat yapıtlarına ilgi duymaya başlaması ve üst sınıf aristokratların özgün ve değerli kalıntılara karşı yoğun ilgisidir. Bu bakış açısına bağlı olarak bir değerlendirmede bulunulduğunda Rönesans ile birlikte Avrupa ve Kuzey Amerika’nın sadece kendi tarihiyle ilgili değil farklı bölgelerde yaşayan birçok topluluğa dair izleri arkeolojik arařtırmalar kapsamında incelediği görülmektedir (Özdoğan, 2006: 29).

Sanat Eğitiminde Kullanımına Yönelik Uygulama Modeli

Sanat en basit tanım ve deyimle; bir form oluşturma yeti(qualifications), yetenek(talent) ve becerisidir(skills). İnsan, sonsuz sayıda farklı formlar üreten doğa karşısında, yetenek ve becerisiyle yaratıcı (kreativ) sürece ortak olmaktadır.

Kişinin öznel iç görüşü, imgeleri, düşünceleri ve duyguları sanat ile görselleşir. Bu çok öznel olan durumun dışa dönüşmesi, somutlaşması ve başkalarına anlatması insan için önemli bir gereksinimdir. Daha kapsamlı bir anlayış ve deyimle sanat; insanın insan olma yazgısı ve koşulunu yenme, kendini aşabilme çabasıdır (Kınay, 1993).

Sanatın insan yaşamına dair bütün gerekliliği ve zorunluluğu, insanoğlunun sahip olduğu tüm kapasiteleri sanatsal yetiye dönüştürme noktasında eğitimle ilişkilendirilmiştir. Genel anlamda eğitim dendiğinde yaşam boyu süren, insanın bilgi, beceri, yargı güçlerini geliştirmeyi de içine alan insan yetiştirme akla gelir.

Bu bağlamda, tarih bilinciyle öğrencilerin donatılması kültürel mirasın farkında olmasını sağlayacağı gibi, arkeolojik buluntular da artistik çalışmalara yeni bir perspektif açacaktır.

Yapılabilecek olan çalışmaların kazanımları öğrencilere kendi kültürünü ve farklı kültürel örüntüleri çok yönlü ve hoşgörülü bir yaklaşımla tanıma, benzerlik ve farklılıkları anlama, karşılıklı anlayış ve duygudaşlık geliştirme olanağı sunacaktır. Kültürel miras olan arkeolojik form ve nesnelerin, kültürel ve sanatsal yaratıcılığın yeni özgün yaratmalarının esin kaynaklarından biri olduğu düşünülmektedir.

Öğretim Tasarımı Hazırlık İşlem Basamakları:

Program Stratejilerinin Belirlenmesi

Eğitim süresince öğrencilerin; biçim inceleme, bakma ve görme arasındaki farkı anlama; Eski yaşam buluntularındaki saklı estetiği keşfederek farklı materyallerle güncel sanat pratikleri oluşturmak amaçlanmalıdır. Öğretim stratejisi olarak süreç boyunca katılımcı öğrencilerin tamamına yönelik ortak bir ders yapısından çok,

grupla ve bireysel öğretim tekniklerine ağırlık verilerek ve bireye özel yöntemlerle eğitim sunulması düşünülmeli ve uygulama sürecinde buna özen gösterilmelidir.

Özellikle uygulama çalışmalarında deneysel öğrenme projelerinin etkin öğrenmeyi destekleyecek önemli unsurlar olduğu öngörülmelidir. Projeler, katılımcıların belirleyecekleri alan ve konularda yürütülen uygulamalardan oluşmalıdır.

Ön Bilgi ve Hazır Bulunuşluk Tespiti

Çalışmanın bu bölümünde örneklem olarak seçilen öğrencilerin arkeolojik sitler ve buluntuları üzerine bilgileri ölçülmeli, çalışma öncesi hazırbulunuşluk bilgilerinin ne olduğu anlaşılmalıdır.

Öğrenme Etkinlikleri ve Değerlendirme

Lisans düzeyi öğrencilere yönelik olarak planlanıp yürütülecek bu eğitim /araştırma sürecinde eğitmen; bir yandan öğrenme ve iletişim etkinliklerini yönetip, yönlendirirken; diğer yandan süreci gözleyip, değerlendirerek programı daha etkin kılma çabaları sürdürmelidir. Bu bağlamda çalışma konusunun öğrencilere planlı bir şekilde anlatılabilmesi için arkeolojik sit ve buluntuları üzerine arkeoloji uzmanı desteği alınabilir.

Ders kapsamında belirlenen sunum etkinlikleriyle, öğrencilerin geçmişe ait nesnelere buluşması sağlanmalı, böylece öğrenciler geçmişe merak etmeye yönlendirilmelidir. Öğrenciler için merakla başlayan uygulamalar onların müzede gerçekleşecek olan öğrenme sürecine güdülenmelerine yardımcı olacaktır ve çalışma sürecinde aktif olmalarını destekleyecektir. Daha sonra müzede gerçekleştirilen anlatımlar; öğrencilerin bilişsel, duyuşsal ve sosyal becerilerini geliştirerek tarihsel bilgilerini yapılandırma tutumu içerisine girmelerini sağlayacaktır.

Müze Gezisi

Öğrencilerin görseller üzerinden gördükleri buluntuları müzede yerinde görmeleri önemlidir. Çalışma sürecinde kullanılacak hangi eser ve örneklerin bulunduğu tespit edilerek, gerekli doküman hazırlanmalıdır. Geziler sonrası devam eden haftalarda yapılan gezilerin kritikleri yapılmalı, gördükleri eserler üzerinde değerlendirmelerde bulunulmalıdır. Öğrencilerin dikkatlerini çeken eserler ve üzerinde çalışabilecekleri buluntular yorumlanmalıdır.

Tasarım ve Uygulama İşlem Basamakları:

Hazırlık ve Tasarım Aşaması

Plastik sanatlar uygulamalarında tasarım öncesi dönem oldukça karmaşık duygu yoğunluğunun yaşandığı bir süreçtir. Bu zaman diliminde zihinde problemlerden sonuca ulaşmak için yaşanan yoğun bir süreç söz konusudur.

Tasarlamada karşılaşılan en büyük güçlük geleceği tahmin için mevcut bilgilerden yararlanılmasıdır. Tahminlerin doğruluğu derecesinde başarılı bir sonuca ulaşılır

Ön Eskiz ve Tasarım

Öğrencilerin sit ve buluntuları hakkında yaptıkları araştırmalar sonucunda çalışılacak dönemde yapılan ve eski eserler olarak kabul edilen bu eserlerin günümüze sentezlemeleri istenmelidir. Öğrencilerden yapacakları çalışmalara yönelik tasarımlarını stilize ederek modern, işlevsel ve dekoratif amaçlı nasıl ve ne şekilde kullanabileceklerini göstermek amaçlı ön eskizleri ve çalışmalarını nasıl yapmayı planladıklarına dair küçük bir sunum dosyası hazırlanmalıdır. Yapılan eskizler doğrultusunda her öğrenciye tasarımda kullanacağı malzemeler tanıtılmalı, teknikler anlatılmalı ve uygulamalar hakkında bilgiler verilmelidir. Bu bilgilendirmeler sonucunda öğrenciyle istişare edilerek yapılacak çalışmanın ön eskizleri seçilmelidir. Sonrasında seçilen eskizlerin son özgün tasarımları hazırlanabilir.

Malzeme Temini Materyal Seçimi

Bu aşamada hangi sanat alanında uygulama yapılacaksa ona uygun malzeme ve materyal seçimi yapılmalıdır. Uygulama dersi ve hedeflerine yönelik içerikler oluşturulabilir.

Uygulama ve Değerlendirme

Ders içeriğine göre planlama ve hazırlığı yapılan malzeme içeriği belirlenen çalışma bu aşamada pratiğe dökülecektir. Uygulama süreçleri için zaman planlamaları yapılmalıdır. Süreç sonucunda oluşturulan içeriler sanat eleştirisi bağlamında öğrencilerce eğitimci ile değerlendirilmeli, sanat okuma etkinlikleri düzenlenmelidir.

Sonuç

Tarihi oluşturan bulgular kültürel bir belleğe hizmet eder. Bu bellek tarihsel süreçte insanın yaşamı anlamlandırma egemen kılma çabasını kaydeder. İnsan yarattıkça düşünür. Düşündükçe yaratıcı eylemini sürdürerek gelişir. Tarihsel geçmişe ayna tutan bu nesnelere ister üretilen eşya olsun, ister sanat yapıtı olsun o dönem tarihinin yaşamını tüm gerçekliğiyle çarpıtmadan ortaya koyar. Sanat nesnesi bir yanda doğduğu kültürel coğrafyanın özelliklerini diğer yandan da yaratıcısının kimliğini taşır.

Bir arkeoloğun tikel bir buluntudan tüme varma çözümlemesi-yaşamsal veri ve sosyal bir gerçekliğe (realiteye) ulaşma çabasıyla; bir sanatçının eserindeki plastik çözümleme çabasıyla aynı şeydir. Sanatçı yaratıcı süreçte etkilendiği faktörleri birer veri kaynağı olarak kullanıp eserini oluşturur. Yaratıcı edimler tek bir olguya hizmet eder. Oda insanın var olma nedenine bağlı olarak karşı koyamadığı üretime dürtüsüdür. Bu dürtünün yol açtığı olgu, bilme, bilgilendirme ve belgeleme iç güdüsüdür. Belirsiz, tehlikeli ve riskli konular yaratıcı bireyler için sınırsız bir çekim kaynağı ve cazibe merkezidir. Hem sanatçı hem de arkeolog bu cazibe merkezini keşfetme dürtüsüyle artistik bir serüvene çıkar. Sanatçının bilinçaltı etkileri sosyo-kültürel yaklaşımı, sanatında ne ölçüde açığa çıkarsa, bir arkeoloğun keşfettiği tarihsel sırda benzer şekilde açığa çıkar. Arkeoloğun kazısına başlarken duyduğu keşfetme heyecanı sanatçının heyecanı birbirine benzer. Bu bağlamda yapılan çalışmalarda öğrencilerin eğitim süresince; arkeolojik buluntudaki biçimi inceleme, bakma ve görme arasındaki farkı anlama eski yaşam formlarının detayında saklı olan estetik izi görebilme ve de kendi çağdaş uygulamalarında bunları uygulaması amaçlanmalıdır.

Sanatı yönlendiren önemli çıkış noktalarından biri olan arkeolojik buluntular yalın ve güçlü anlatımıyla sanat tarihinde ekspresyonizm ve kübizm gibi akımların ortaya çıkmasını sağlamıştır. Bundan dolayı günümüzde arkeolojik buluntuların hala keşfedilememiş yönleri yeni bir estetik için çıkış kaynağı olabilir. Bu perspektifle sanat eğitimi önemli bir misyon üstlenmektedir. Ülkemiz ve dünya örneği açısından bakıldığında; öğrencilerin ulaşabilecekleri birçok arkeolojik buluntu her coğrafya da mevcuttur. İfade ettiği anlam yüküyle, tarihe tanıklık eden arkeolojik buluntuları yeni nesillere tanıtmak kültürel mirası korumak adına da önemlidir.

References

- Bildiş, Aslıhan. (2006). Kentsel Koruma Bağlamında Eski Kentlerin Geliştirilmesine Yönelik Bir Araştırma; Tokat-Zile Örneğinde İrdelemeler. Yüksek Lisans Tezi, YILDIZ TEKNİK ÜNİVERSİTESİ Fen Bilimleri Enstitüsü, İstanbul
- Kahveci, Mücella. (1998). Prof. Dursun Yıldırım Armağanı Pars Yılı, Ankara.
- Kaya, Ramazan. (2009). Tarih Öğretim Yöntemleri, Prof. Dr. Demirel M. Yrd. Doç. Dr. Turani.(Editörler). Tarih Öğretiminin Amaçları. Birinci Baskı. Ankara. s. 69-135.
- Kınay, Cahid. (1993). Sanat Tarihi. T.C. Kültür Bakanlığı Yayınları, Ankara: Gaye Matbaacılık.
- Koç, Zeynel. (2007). Türkiye’de Taşınmaz Kültür Varlıkları ve Mali Teşvikleri. Doktora Tezi. MARMARA ÜNİVERSİTESİ, Sosyal Bilimler Enstitüsü, İstanbul.
- Madran Emre. (2009). Taşınmaz Kültür Varlıklarının Korunması ve Onarımına İlişkin Temel İlkeler El Kitabı. 12/4, Antalya: Mimarlar Odası Antalya Şubesi Yayınları
- Özdoğan, Mehmet. (2004). Arkeoloji Politikaları Avrupa'nın Sınırları. Atlas Dergisi, 141 Dergi İçi Eki, 1-11. İstanbul: Doğan Burda Dergi Yayıncılık.
- Özdoğan, Mehmet. (2006). Türk Arkeolojisine Tarihsel Süreç İçinde Bir Bakış. Ü. Yalçın, C. Pulak ve R. Slotta (Ed.), Uluburun Gemisi 3000 Yıl Önce Dünya Ticareti. (s.29-47). Bochum: Deutsches Bergbau Museum Bochum Yayınları.

Özsoy, Füsün. (1988). Kentsel Sit Bölgelerindeki Koruma Kararları Ve Koruma Bölgelerinde Kentsel Tasarım Disiplini.Yüksek Lisans Tezi, MİMAR SİNAN GÜZEL SANATLAR ÜNİVERSİTESİ Fen Bilimleri Enstitüsü, İstanbul.

Uygur, Mermi. (1996). Kültür Kuramı. İstanbul: Yapı Kredi Yayınları

Author Information

Mine Ülkü ÖZTÜRK

Necmettin Erbakan Üniversitesi
Abdülaziz Mahallesi, Abdülmümin Sokak, No:16, Meram,
KONYA/TÜRKİYE
mineozturk@erbakan.edu.tr

Existing Aesthetic Problems Based on The Restorations of Stone Works of The Ancient Period in The Side Museum

Ömer Tayfur ÖZTÜRK
Necmettin Erbakan University

Abstract: Many archaeological data that have remained daily from ancient periods come from stone works. Many works made of marble, which have an important place in the stone works, are now being exhibited in museums and ruins. It is inevitable to undertake a number of repairing, completing, cleaning and conserving works in the process between the exposition of these works made of marble, which are mostly related to the excavation contents and being exhibited in the museum. The studies on the antique stone artifacts found in the archaeological excavations that have been going on since 1947 in and around the Side Antique City near the town of Manavgat in Antalya province are examined. Preservation and restoration works on ancient Greek and Roman stone artifacts restored by Dietmar Friese, preserved in the museum, were examined and the aesthetic problems of the sculpture display and repair were questioned. This study examines the changes in the existing aesthetic problems over the years as a result of the restoration of the antique stone artifacts found in Side Museum.

Existing Aesthetic Problems, Restorations of Stone Works, Ancient Period, Side Museum

Side Müzesinde Bulunan Antik Dönem Taş Eserlerin Restorasyonları Neticesinde Mevcut Estetik Problemleri

Özet: Antik çağlardan günümüze kalan birçok arkeolojik veri düşünüldüğünde günümüze kadar en çok ulaşılmış olanlar şüphesiz taş eserlerdir. Taş eserler içerisinde önemli bir yere sahip olan mermerden yapılmış birçok eser bugün müzeler ve öğrenim yerlerinde teşhir edilmektedirler. Çoğunluğu kazı içeriklerine bağlı, mermerden yapılmış bu eserlerin gün yüzüne çıkarılıp müzede teşhir edilmeleri arasındaki süreçte bir takım onarım, tamamlama, temizleme ve korumaya yönelik çalışmalar yapılması kaçınılmaz olmaktadır. Antalya ili Manavgat ilçesi yakınlarında yer alan Side Antik Kentinde ve çevresinde 1947 yılından beri devam etmekte olan arkeolojik kazı çalışmalarında bulunan ve müzeye getirilen Antik Dönem taş eserler üzerindeki çalışmalar incelenmiştir. Müzede korunmakta olan Dietmar Friese tarafından restore edilmiş olan Antik Yunan ve Roma dönemi taş eserler üzerinde bugüne kadar yapılmış olan koruma ve onarım çalışmaları incelenmiş, incelemeler sonucunda heykellerin teşhir ve onarımında ne gibi estetik problemlerinin olduğu sorgulanmıştır. Bu çalışma Side Müzesi'nde bulunan Antik Dönem taş eserlerin restorasyonları neticesinde mevcut estetik problemleri yıllar içerisinde hangi değişimleri gösterdikleri incelenmiştir.

Giriş

Restorasyon, sanatsal değeri olan bir eseri, tarihi belge, kültür ve sanat objesi olarak ömrünü uzatmak amacıyla yapılan bilimsel ve teknik müdahalelerin toplamıdır. Müze envanterine girmiş veya girme durumu olan eserler için restorasyon yapmak veya yaptırmak başta idari sorumluların, eseri kazı yaparak topraktan veya denizden çıkarıp bulan arkeologların ve müzecilerin görevidir.

Kültür varlıklarının uzun yıllarca toprak altında kalmalarından dolayı birtakım tahribatlar ve deformasyonlar oluşmaktadır. Fakat basit yöntemlerle bile giderilebilecek hasarlar ihmaller neticesinde artarak ilerlemektedir. Bu konuda en büyük problem finansal sorunlardır. Bu yüzden müzelerimizde bakım onarım çalışması yapabilecek yetişmiş eleman sayısı yok denecek kadar azdır. Bu ve benzeri sorunlardan dolayı gerek öğrenim yerleri gerek müzeler ve bahçelerinde tutulan eserler son demlerini yaşamaktadır. Eserlerin toprak altında kalmaları koruma açısından daha olumlu bir sonuç doğuracaktır. Fakat toprak altında kalsalardı geçmiş tarih, kültür tarihi ve mirası bilimsel olarak ortaya konamazdı (Özgan, 2013: 11).

Arkeoloji biliminde eserlerin gün yüzüne çıkarılması kadar çıkarıldıktan sonraki safhalar da eserlerin durumu ve arkeoloji bilimi açısından da büyük önem arz etmektedir. Ayrıca eserler üzerinde yapılan çalışmalarda koruma onarım hatalarının da saptanması sonraki yapılacak çalışmalarda bu hataların tekrarını önlemede ve eserlere geri dönüşümsüz hasarları önlenmesine yardımcı olacaktır.

1960'lı yıllarda bulunmuş olan ve Side Müzesi koleksiyonuna dahil edilen eserlerin, daha sonra teşhir edilmek üzere dönem şartları içerisinde kimin işlem yaptığı bilinmemekle birlikte, eserler bir takım onarımlarla teşhire hazırlanmıştır. Bu onarımda, onarım yapan kimisenin teknik bilgileri doğrultusunda inşaat demiri, su borusu, çimento ve akemi kullanılarak eserler teşhire hazırlanmıştır. Onarım şekillerinden dönemin şartları, teknik bilgilerinin ancak bu yeterliliği sağlayabildiği anlaşılmıştır.

Aradan geçen uzun süreç sonunda, Müze koleksiyonuna giren ve teşhir edilmekte olan eserler doğal hava şartları asit yağmurları ve rüzgarla birlikte gelen toz, yüksek nem ve eser bünyesindeki tuzlar, vb. birçok sorunla toprak altından çıktığı durumdan gerek görsel olarak gerek sağlamlık olarak daha kötü bir noktaya gelmiştir.

Bölgenin ortalama bağıl nem oranları kışın %90, yazın ise %80 civarındadır. Yazları sıcak ve yağışsız bir iklimle sahip olan Side sahil kenti olması nedeniyle yüksek nem oranlarına sahiptir. Taş yapılar ve heykellerin korunması açısından nem ve tuzlu toprak koruma şartlarını ağırlaştırmaktadır.

2004 yılında uzun zamandır bölgede yaşayan ve kazıların başladığı yıllardan beri bölgeyle ve buluntularla ilgilenen ve eserleri müzeye kazandıran arkeologlarla bağlantısı olan *Alman Heykeltıraş Dietmar Friese*, Müze bünyesindeki kazılarda görev yapan belediye işçilerinden taş ustası Beyzade Yaycıoğlu ile birlikte eserler üzerinde koruma onarım çalışmalarına başlamıştır. Side Müzesi Müdür Vekili Arif Küçükçoban'ın da desteğiyle iki yılda 79 eser, ekip tarafından onarılmıştır.

Araştırmadan anlaşıldığı üzere elde edilen veriler; en sıkıntılı görünen heykellerden başlamak suretiyle 2004-2007 yılları arasında 79 eser üzerinde restorasyon çalışması yapıldığını göstermektedir. Müze içerisinde ve dışarısında sergilenen, bir kısmı depolarda muhafaza edilen bu eserlere yapılan müdahaleler, sağlamlaştırma ve temizleme üzerine uygulamalardır. Birkaç eserde tamamlama çalışması yapılmıştır. Müze bünyesinde kurulan restorasyon atölye binasında yapılan çalışmalarda görsel verilere dayanılarak kararlar verilmiştir.

Günümüz şartlarında, müzeciliğin de bilinçlenmesiyle birlikte sergileme şartları iyileştirilmiş ve iyileştirilmeye devam etmektedir. Eserler için en büyük sıkıntıların gözlemlendiği yerler özellikle depolar ve bahçe alanı olmuştur. Araştırma kapsamında yapılan değerlendirmeler ve incelemeler daha sonra yapılacak restorasyonlar için eksikliklerin giderilmesi açısından kaynak olacaktır.

Araştırmada: yapılan heykel restorasyonlarının Türkiye'de onarım ve müzecilik açısından önemi itibariyle restorasyonun kavram ve kuramına, eserlerin bulunduğu ve teşhir edildiği Side müzesi ve restorasyon atölyesi hakkında bilgilere, taşlarda bozulmalar ve sağlamlaştırılmasına yer verilmiştir. Sonuç olarak eserler üzerinde yapılan müdahaleler araştırılıp görsel analizleri yapılarak, mevcut eksikliklere öneriler getirilmiştir.

1. Restorasyon Kavramı

Tarih ve kültür açısından önem arz eden özgünlük değeri olan, toplum tarafından beğenilen veya değer taşıyan taşınır ve taşınmaz eserlerinin korunması ve geleceğe aktarılmasını amaçlayan meslek dalına restorasyon denilmektedir. Restorasyon, rölove, restitüsyon ve koruma- onarım gibi işlemleri içerir. Teknik tanım olarak restorasyon sanatsal değeri olan bir eserin veya yapının, özgün olan bütün değerleriyle birlikte, bir kültür ve tarih belgesi olarak ömrünün uzatılmasını sağlayan teknik müdahalelerin tümüne denilebilir (Kuban, 2000:9). Uygulama esnasında en uygun ve en az müdahaleyi, oluşturulan protokoller tarafından kararlar alınarak uygulama işlemi gerçekleşir. Esere en ufak bir müdahale belgelenecek arşivlenir.

Dünyadaki teknik ve teknolojik ilerlemeye bakıldığında zaman geçmişte eserler üzerine yapılan müdahaleler bilinmezken veya kayıt altına alınmazken, artık her müdahale arşivlenerek kayıt altına alınmaktadır. Her arşiv geçmişte geleceğe bağlamaktadır. Konservasyon: objelerin maddesel ve teknolojik özellikleri kadar, yapısını ve taşıdığı dekoratif öğelere özgün niteliklerine bağlı kalarak korumak, bozulmasına yol açan nedenleri ve etkenleri açığa çıkarmak, en uygun ve en etkili koruma yöntem ve malzemelerini saplayarak bunları objelere uygulamak, fiziksel ve estetik bütünlüğü aslına bağlı kalarak sağladıktan sonra stabil haldeki objeyi sergileme veya depolama için hazırlamaktır (<http://odogan.com/mimar/restorasyon-rolove-restitusyon-konservasyon-nedir.html> 15/12/2013). Tarihsel kültürel değer taşıyan objeler onu bulan elinde bulunduran müzeci veya koleksiyonerin değeri değil toplumun bir değeri sayılmalı ve yapılacak müdahale de konservatör bu noktayı dikkate almalıdır. Topluma ve gelecek nesillere olan sorumluluk bilincini taşımalıdır. Eserin maddi değeri ve kimin malı olduğu noktasından ziyade, konservatörün elinde bağımsız korunması önemlidir.

2. Side Müzesi'nin Tarihesi ve Koleksiyonu

Side Müzesi Manavgat İlçesi'ne bağlı Side Beldesi'ndedir. Manavgat'a 8 km. uzaklıktadır. Roma Dönemine ait agoranın karşısında bulunan, M.S 5-6.yüzyıldan kalma antik agoranın hamamı 1960- 1961 yıllarında restore edilerek müze haline getirilmiştir. (Ekler: Resim 1)

Müzedeki sergilenen eserlerin büyük bir bölümü, Prof. Dr. Arif Müfid Mansel tarafından,1947-1967 yılları arasında Side antik kentinde yapılan kazılarda, çıkarılan buluntulardır. Müze'de, Hellenistik, Roma ve Bizans Dönemi; yazıtlar, silah kabartmaları, Roma Döneminde yapılmış Grek orijinallerinin kopyası olan heykeller, torsolar, lahitler, portreler, ostotekler, amphoralar, sunaklar, mezar stelleri, sütun başlıkları ve sütun kaideleri sergilenmektedir.

Side bölgesinde gerek mimaride ve gerekse heykeltıraşlıkta farklı cinsten mermerlerin kullanıldığı bilinmektedir. Ancak analiz yapılmadığı için çıplak göz ve tecrübe ile bu üç mermer tipinin tercih edildiği söylenebilir.

Yapılacak analizlerle heykel üretiminde farklı tipte mermerlerin de kullanılmış olduğu gözler önüne serilecektir. Bu yüzden heykel yapımında Prokonnesos, Attika ve Dokimeion'dan getirilen mermerler kullanılmış, yerel taşlardan da traverten, kireçtaşı, konglomera gibi taşlar tercih edilmiştir.

3. Taşlarda Bozulma Türleri

Doğada uzun süre atmosfer koşullarının etkisinde kalan doğal taşlar, yapısına ve ortam koşullarına bağlı olarak fiziksel ve kimyasal özelliklerini kaybetmeye başlarlar. Sonuç olarak bozulmaya doğru bir gidiş başlar. Taş malzemelerinde bozulma; genellikle dışta başlayıp içte devam eden, malzemenin direncinin azalması, kırılabilirlik ve porozitesinin artması ve malzeme kaybı ile ortaya çıkan değişimdir. Değişimler bozulmalar biçiminde ortaya çıkarlar. Bozulma, malzemenin dayanma kapasitesinin azalmasını ve bozulmaya neden olan koşulları belirtir (Yıldırım, 2010: 76). Ayrışma, bozulma veya yaşlanma, yıpranma sürecine girmiş taşın evresel değişimi, masif (yoğun) ve sağlamdan başlayarak tanelenmeye, ufalanmaya ve dökülmeye dönüşüncüye kadar devam etmektedir.

Doğal taşların bozulma durumu literatürde geniş ölçüde çalışılmasına rağmen her özel durum, eserin bulunduğu mevkiisi, konumu gibi yerel faktörlerden yüksek oranda etkilenmektedir (Benedetti ve diğ., 2008: 155). Her konservasyon müdahalesinin doğru bir biçimde programlanması için, bozuma mekanizması ve derecesi, belirlenmiş nedenlerin tanımlanması, taşın türü ve özellikleri çok önemlidir (Alessandrini ve diğ., 1982: 8).

Taşlarda bozulma türleri aşağıda maddeler halinde incelenmiştir.

Kirlilik: Hem estetik açıdan hem kayaca zarar vermesi açısından kayacın kendi orijinal yüzeyinden farklı her türlü yabancı birikime kirlilik denir. Koruyucu nitelik gösteren kirlilik oluşumlarının (patina gibi) korunması, kayaca zarar veren kirlilik oluşumlarının ise kayacın ömrünü azaltmasından dolayı temizlenmesi gerekir (Dal, 2005: 73).

Kabuklanma: Ana kayaç yüzeyinden gözle görülebilecek kadar ayrılabilen yüzeyde kimyasal olarak biriken yabancı maddelerden oluşmuş bir tabakadır. Kimyasal ve fiziksel yapısı kısmen ya da tamamen kendisini oluşturan doğal yapı kayaçlarından farklıdır. Yağmur suyu ve havadaki karbondioksit, karbonat bileşimli kireçtaşlarını eriterek bikarbonat oluşturmaktadır. Bu durum, kalınlığı giderek artan kalsiyum karbonat çökmesine yol açar. Benzer şekilde, havada bulunan SO₂, suyun varlığında kalsit içerikli taşla reaksiyona girerek suda çözünebilen alçıtaşı oluşumundan olur bu yapıda yüzeylerde kabuklanmalara ve zamanla dökülmelere yol açmaktadır (Kloppman ve diğ., 2006:437). Bunlardan en yaygın görülün ise siyah kabuklanmadır. Siyah bölge kabuk oluşumu, hava kirliliği nedeniyle atmosferde oluşan asitlerin mermerin ana maddesi olan kalsiti alçıya dönüştürmesi ve bu bağlayıcı tabaka üzerinde havadaki partiküllerinin birikmesiyle ortaya çıkan siyah renkli tabakalar şeklinde görülmektedir (Giavarini ve diğ., 2008:914). Oluştukları alanlarda orijinal yüzey tabakalarının kaybına yol açarlar (Şener, 2000: 55).

Ufalanma: Kumlanma görülen taş yüzeyleri, is veya toz birikimi nedeniyle griden koyu siyaha kadar renk alırlar. Kalınlıkları 1 mm civarındadır. Karbonatlı taşlarda oluşan kumlanma sonucu taşların köşeleri yuvarlaklaşır.

Aşınma: Sürtünmeye bağlı oluşan ve taşın hacmindeki küçülmelere yol açan bozulma türüdür (Şener, 2000: 61). Kumtaşı gibi yumuşak yapı taşlarda, agresif maddeler ihtiva eden su gevşek dokulu olan taş yüzeyini zamanla eritebilir ve büyük boşluklar meydana getirebilir, sonuçta eriyerek yok olurlar (Akçaözöğlü ve diğ., 2008: 298).

Oyuk Oluşumu: Zayıf dirençli mineral yapıdaki volkanik kökenli kayaçlarda, minerallerin ayrışması ile çakıl taşı, aglomera, iri kavkılı ve killi kireçtaşı gibi tortul kökenli kayaçlarda ise, zamanla yapılaşma direncinin kaybolması sonucu, iri tanelerin yerinden çıkması ile kayaç üzerinde gelişigüzel oyuklar ve boşluklar oluşmaktadır (Yıldırım, 2007:12).

Çatlak-Kırık Oluşumu: Deprem, ısı genişlemeleri gibi nedenler ile birlikte malzemenin niteliklerini kaybetmeleri sonucu taşın çekme veya basınç dayanımı aşıldığı zaman çatlaklar meydana gelmektedir. Çatlaklar taşların birleşim yerlerinde oluşabileceği gibi, taşın bünyesinde de görülebilmektedir (Akçaözöğlü ve diğ., 2008: 299).

Parça kopması: Taşlarda parça kopmaları tuz etkileri, donma ve montaj malzemelerinin korozyona uğraması ve genişlemesiyle oluşur (Akçaözöğlü ve diğ., 2008: 299). Taş yüzeylerindeki dökülmelerle oluşan yuvalar ve genişleyen derzler estetik açıdan görünümü olumsuz etkileyen bir durumdur (Şener, 2000: 65).

Tuzlanma: Su ile temas eden taşta kendi yapısında olan veya çevresindeki malzemelerde bulunan tuzlar hareketlenmekte ve kuruma olan yerlerde beyaz çiçeklenmelere, taşta kabuklaşma, tozlaşma, oyuk şeklinde vs. bozulmalara yol açabilmektedir (Doehne ve Price, 2010: 11).

Yapraklaşma: Yapraklaşma, yüzeyin pullar ve ince yapraklar ya da daha geniş ve kalın tabakalar halinde kabarması ve dökülmesidir. Yapraklaşma çiçeklenme ve ufalanmada olduğu gibi daha çok nemin yoğunlaştığı bölgelerde meydana gelmektedir. Yapraklaşma tüm biçimleriyle taş malzemedeki önemli ölçüde parça kayıplarına yol açan bir bozulma türüdür (Şener, 2000: 67).

Biyolojik Patina: Yapılarda ve daha çok nemin yoğun olduğu bölgelerde görülmektedir. Bu tür oluşumlar yüzeyde yeşil renkli bir tabaka oluştururlar ve oyukların oluşmasına neden olabilmektedir. Mikro bitkiler yüzey yapısının bozulmasına, mikro çatlakların büyümesine yol açmaktadır. Likenler, taş yüzeyinin hemen altında nem tutarak, iyon değişimi ve asit salgılaması nedeni ile taşlara zarar verirler (Surt, 2011: 3; Caneva ve Salvadori, 1988: 23).

4. Taş Eserlerde Sağlamaştırma

Taş eserlerde bozulmayı mümkün olduğu kadar azaltmak veya durdurmak değişken atmosferik koşullara karşı taşın direnci artırılarak fiziksel özelliklerinin geliştirilmesini sağlamak sağlamaştırmanın ana hedefidir. Eserlerin korunması kimyasal koruyucu maddelerle olduğu kadar, çevre koşullarının iyileştirilmesi mümkündür. Kimyasal maddelerle koruma uygulaması zarar verici etkenlerin başka yollarla önlenemediği durumlarda kullanılmaktadır (Tulgar, 2007:10).

Sağlamaştırma, farklı nedenlerle mekanik güç olarak zayıflamış ve yüzey kaybına uğramış ya da uğrama olasılığı yüksek olan kısımlarının mekanik özelliklerini arttırmak ve bu kısımların taşın sağlam tabakasına yapışmasını sağlamak amacıyla taşların yüzeyinden derinlerine emdirilerek yapılan işlemdir. Sonuç olarak sağlamaştırılacak malzemenin mekanik özellikleri ve kimyasal bozulmalara karşı dayanıklılığı artırılmış, gözenekliliği ve su emme kapasiteleri azaltılmış olacaktır (Tulgar, 2007: 22 ; Mosquera ve diğ., 2002: 185). Sağlamaştırıcı, sağlamaştırma değerinin yanı sıra taş ile uyumluluğu, nem transferi üzerine etkisi, taş gözenekliliği üzerine etkisi, uzun süre dayanıklılığı, nüfuz derinliği ve görünümü üzerine etkisi ile ilişkin bazı basit performans gereksinimlerini de sağlayabilmelidir (Öztürk, 1992: 54).

Sağlamaştırma, teşhis, temizleme, ön sağlamaştırma, sağlamaştırma, yüzey koruma ve bakım da dahil olmak üzere bir dizi işlemin bir parçasıdır. Uygulamaların en az on yıl ve üzeri etkili olması beklenmekte ve yapının periyodik bakım programlarında, sağlamlık durumunun kontrolüne bağlı olarak yüzey koruyucuları değiştirilerek yenilenmelidir.

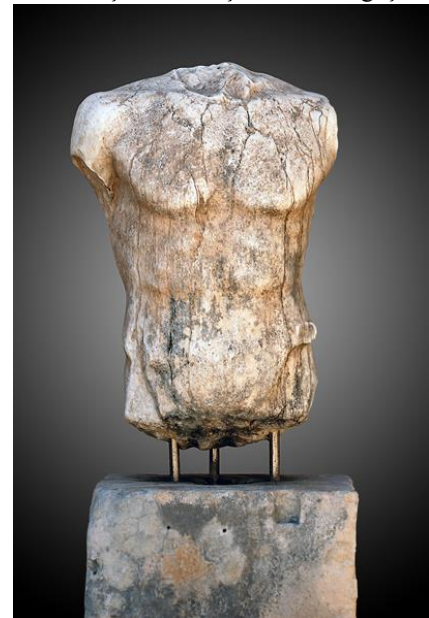
Sağlamaştırıcının Görünüm Üzerinde Etkisi: Sağlamaştırıcı taşın dokusunda, renginde ve yansımada işlemin başlangıcında veya dış ortamda maruz bırakıldıktan sonra taşın yüzeyinde film tabakası oluşturmamalı, renk, doku değişikliği ve lekelenme yapmamalıdır.

Sonuç

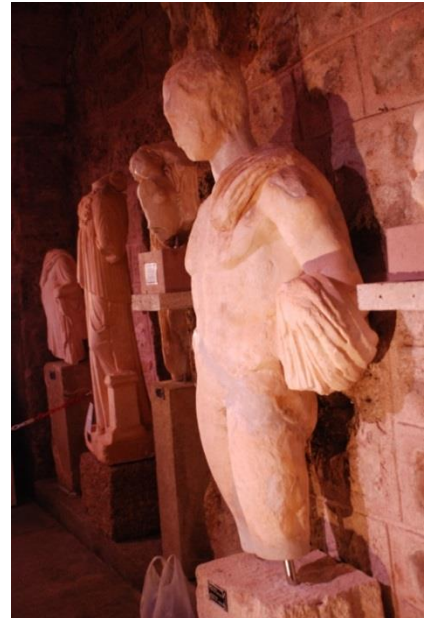
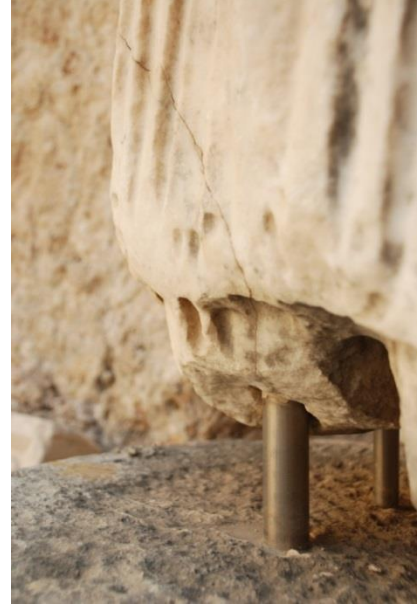
Side Antik çağda anılan adıyla, Pamfilya Antik Dönemden M.S. 10.yy. sonlarına kadar önemli bir liman kenti olmuştur. Halkı büyük bir yangın sonucu Antalya'ya göç etmiştir. Dönemin önemli bir liman kenti olan bölge zengin bir sanatsal eser ve mimari eser kaynağı barındırır. Osmanlının son dönemlerinde Girit'in elden çıkması ile birlikte Girit'ten göç eden Müslüman halk bu bölgeye yerleştirilmiş ve şimdilerde bilinen köy kurulmuştur. İlerleyen süreç içerisinde bölge turizm açısından önem kazanmaya başlamış ve bir turizm merkezi olmuştur. Şiddetli depremlerle terk edilen ve önemini yitiren merkez tekrar önem kazanmaya ve merkez olmaya başlayınca içinde barındırdığı ve yüzyıllarca bağrında sakladığı tarih Side'yi tekrar ilgi odağı yapmıştır. Tabi bunun tarihsel mirasın korunması açısından geri dönülmez zararları da olmuştur, olmaktadır.

1946 yılında Arif Müfit Mansel başkanlığında ve Jale İnan'ında aralarında bulunduğu araştırmacıların, bölgede araştırmalara başlaması ile bölge tarihi gün yüzüne çıkmıştır, bu çalışmalar beraberinde koruma ve onarım problemini doğurmuştur. Bu noktada sponsor desteğiyle Antik kent içerisinde bulunan Bizans Hamamı'nın yıkılmış çatı örtüsü tekrar beton yapı ile örtülmüş ve Müze'ye dönüştürülmüştür. Dönemin imkanları ve bilgi beceri sahibi olan uzmanlaşmış diye tanımlanabilecek kişi veya kişilerce, Arkeolojik kazı alanından getirilen nadide eserler müzede teşhir öncesi dönemin anlayışı içerisinde restore edilerek teşhir edilmiştir. Aradan geçen uzun süreç sonunda Müze Müdür Vekili Arif Küçükçoban ve uzun yıllar bölgede ikamet etmiş olan Alman Heykeltıraş Dietmar Friese'in katkılarıyla müzede eserler tekrar koruma onarıma alınmıştır. Daha önceki süreçlerde eserlerin korunması konusunda Müze'ye danışmanlık yapan Dietmar Friese 2004 yılından 2006 yılına kadar kayıtlı ve izinli 79 eseri restore etmiştir. Titiz ve itinalı çalışma prensibiyle kendi yetiştirmiş olduğu belediye kadrosunda olan taş ustası Beyzade Yayıoğlu ile birlikte yine dönemin imkanlarını zorlayarak en iyiyi, usulüne uygun olarak yapmış, yapmaya çalışmıştır. Bu süreçte Dietmar ihtiyacı olan Restorasyon Atölyesini (laboratuar da denilebilir) kurmuş ve Türkiye de İstanbul merkez laboratuarından sonra müze bünyesindeki tek restorasyon atölyesini kurmuştur.

Yapılan restorasyonların incelenmesi sonucunda varılan sonuçlar aşağıda maddeler halinde açıklanmıştır.



- Eserlerde bahçe şartların da sergileme koşulları göz önüne alındığında açık hava şartlarından ve topraktan kaynaklanan siyah lekelenmeler gözlemlenmektedir. Aciliyeti olan eserlerdeki yüzey deformasyonları restoratör tarafından temizlenerek sertleştirilmiştir, fakat birçok eserin yüzey temizliği ve yüzey sağlamlaştırması yapılmamış, yapılamamıştır. Yüzey temizliği açısından teknik malzeme sağlanılarak tekrar eserler ele alınmalıdır.
- Side bölgesinin coğrafi konumundan dolayı değişken yüksek bağıl nem oranları, eserlerin topraktan ve deniz den çıktıkları göz önüne alınırsa mevcut eserler tekrar analiz edilmeli ve tuzsuzlaştırma çalışması yapılmalıdır. Çünkü tuz tarihi eserler için büyük tahribata, eserlerin kristalleşmesine ve çatlakların artmasına ve genişlemesine yol açmaktadır.
- Daha önceki dönemlerde yapılmış olan restorasyon malzemelerinin başarılı bir şekilde temizlenmiş, fakat sağlam olduğu kanaatiyle dokunulmayan pimler ve yüzey kirlerinin aradan geçen süreç içerisinde tekrar ele alınması gerekmektedir.
- Restoratör, restorasyon yapmış olduğu tarihlerde yazmış olduğu raporlarda eserlerin röntgen cihazıyla çatlak ve kırık kontrollerinin yapılması gerektiğini belirtmiştir. Bugünkü teknolojik gelişmeler ışığında dijital termal kameralar ile taşın yüzey sertliği, kılcal çatlakların derinliği, eserin iç bölgelerindeki çatlak ve korozyonlar tespit edilebilmektedir. Yüksek maliyeti olmayan bu teknoloji ile eserlerin tarama ve analizleri yapılmalı. Sonuçlara göre gerekli tedbirler alınmalıdır.
- Restoratör çağın gelişimine göre kabul görmüş test ve analizleri yapılmış malzemeler ile heykeller üzerine deklükler açmış ve pimlerini montaj yapmıştır. Yapmış olduğu restorasyon ekolü krom çelik pim ve eseri taşıyabilecek bir kaide sistemini öngörmektedir. Sistemin eleştiri alan tarafı eser üzerinde kalıcı deliklerin açılması ve her onarımda daha fazla eserin tahrip olmasında neden olabilmesidir. İkinci bir mevzu da eser sarsıntı alması durumunda pimlerin bağlantı noktalarında çatlamlara yol açabilmesidir, bunun örnekleri yapılan restorasyonlarda gözlemlenmektedir. Bu sistem bugün cam elyaf polimer karışımı pimlere yerini bırakmıştır. Sertliği ve dayanımının yanı sıra esnekliği de olan bu pimler ileriki süreçte yapılabilecek restorasyonlarda kendini gösterecektir. Eserleri çelik veya başka pimler ile sergilemek yerine modern teknolojinin sağladığı imkanlarla eseri ayakta tutabilecek başkibir sistem kurulabilir.
- Heykellerin birçoğu kırık ve parça halinde olmasından dolayıdır ki kaidersiz ve teşhir durumunda kendini ayakta tutacak bir desteğe ihtiyaçları vardır. Bu noktada eserleri ayakta tutacak, her eser için ayrı ayrı ölçümleri yapılmış, tasarlanmış kaidelere ihtiyaç vardır. Kaide seçimi önemli bir konudur. Onarılan eserlerin, buldukları ortamdaki insan kaynaklı hasarlara ve deprem gibi afetlerden kaynaklanan hasarlara karşı en öncelikli korumaları kaideleri olacaktır. Bununla birlikte paha biçilemeyen değerdeki eserlerin altına değersiz görünümlü ve estetikten yoksun bir kaide koymak tarihe ve sanata yapılacak bir haksızlık- saygısızlık olacaktır. Burada restoratörün maddi olanakları dâhilinde en iyiyi araması ve uygulaması gerekmektedir.
- Eserlere yapılan kaidelerin montajında sabit pim kullanılması ileriki dönemlerde yapılacak olan başka onarımlarda değiştirilmesi düşünüldüğünde sorun teşkil edecektir. Kaide montajında yivli sistemler veya geçmeli pim sistemleri kullanılması daha uygundur. Bu sistem ile kaide de zemine veya duvara montaj yapılmalı ki çalınma riski, taşıma, çarpma ve afet durumlarında eser minimum zarar görmeli
- Heykel sanatının üç boyutlu olması ve tasarım ilkelerinin içerisinde zaman ilkesi (izleyicinin eser ile görsel iletişim süresi) göz önünde tutulması teşhire hazırlamada ve sergilemede dikkate alınması gereken bir olgudur. Eserlerin onarımları tamamlandıktan sonra müze içerisinde tanzim edilmesine kadar restoratörün görev ve sorumlulukları arasındadır. Heykeller teşhir edilirken her yönden okunmasını, algılanmasını sağlayacak teşhir düzeninde yerleştirilmesi gerekmektedir.
- Teşhir edilen eserlerin aydınlatılmasında kullanılacak aydınlatma cihazlarının eserin korunması açısından uygunluğuna dikkat etmek gerekmektedir. Bunun yanı sıra müzelerin sanat eserlerinin teşhir edildiği galeriler olması nedeniyle eserlerin estetik duruşları ve tanıtılmasında aydınlatmanın büyük önemin vardır. Aydınlatma konusunda gerek görüldüğü takdirde restorasyon projesi hazırlanırken iç mimariden yardım



alınabilir. Bu konudaki yapılan arařtırmalarda ülkemizdeki restore edilen eserlerin tanziminde müzeciliğin zamanın şartlarına ge ayak uydurduėu sylenilebilir.

Sonuç olarak Side Mze’sinde Dietmar Friese’in yapmış olduėu alıřma Arkeolojinin gn yzne ıkardığı eserlerin koruma ve onarımı konusunda Trkiye de rnek teřkil edecek bir cesaret ve sorumluluk bilincidir. Son zamanlarda mimari alanda yapılmakta olan Restorasyon projelerine ok sık rastlanmakta, fakat mzelerimizin depolarında yok olmaya mahkum edilen eserlerin de topluma kazandırılması gerekmektedir. Mzelerimizin iinde, depolarında kazı alanlarındaki depolarda saklanan eseler iin keřke toprak altında kalsaydı yorumlarını yapmak veya yaptırtmak kendimize yapılmış byk bir haksızlıktır. Side Mzesi rneėi bu konuda rnek alınması gereken bir bařarıdır.

KAYNAKA

Akazoėlu, S., Akazoėlu, K. ve zcan, F. (2008). “Eski Eserlerde Meydana Gelen Tas Bozulmalarının Adana’da rneklenmesi”, *ukurova niversitesi Mhendislik ve Mimarlık Fakltesi Dergisi*, Sayı: 23, No: 1, s.297-305.

Ahunbay, Z. (2011). *Tarihi evre Koruma ve Restorasyon* (6. Baskı). İstanbul: YEM Yayın

Alessandrini, G., Sala, G., Biscontin, G. ve Lazzarini, L. (1982). “The Arch of Peace in Milan”. 1St Researches on Stone Deterioration, International Institute for Conservation of Historic and Artistic Works, *Studies in Conservation*, Sayı: 27, No:1, s.8-18.

Benedetti, D., Bontempi, E., Pedrazzani, R., Zacco, A. Ve Depero, L. E. (2008). “Transformation in Calcium Carbonate Stones: Some Examples”, *Phase Transitions*, Sayı:81, No: 2–3, s.155–178.

Bingl, I. (2000). Trkiye’de Konservasyonun Tarihi, *I Ulusal Tařınabilir Kltr Varlıkları Konservasyonu ve Restorasyonu Kolokyumu*, 6-7 Mayıs 1999, Ankara: Ankara niversitesi Basımevi, 9-16.

Dal, M. (2005). *Edirne’de Dolomitik Yapı Kayalarının Tahrip Őekilleri ve Restorasyon Yntemleri*”, Trakya niversitesi Fen Bilimleri Enstits, yayınlanmamış Yksek Lisans Tezi, Edirne.

Doehne, E. ve Price, C. (ED.) (2010). *Stone Conservation: An Overview Of Current Research*, 2nd Ed, USA: Getty Conservation Institute.

Giavarini, C., Santarelli, M.L., Natalini, R., Freddi, F., (2008). “A Non-linear Model of Sulphation of Porous Stones: Numerical Simulations and Preliminary Laboratory Assessments”, *Journal of Cultural Heritage*, 9: 14: s.914- 922.

Kloppmann, K., Vergès-Belmin, V., Gosselin, C., Rolland, O., Bromblet, P., Vallet, J.M., Dotsika, E. (2006). “Isotope (sulphur, oxygen, boron) tracing of internal or external origin of sulphates involved in the degradation of French stone monuments (BOS project)” *Safeguarded cultural heritage- Understanding and viability for the enlarged Europe 7th European Commission Conference* 31/05-3/06 2006,1: (s.437- 440), Sauveur

Kkten Ersoy, H. (1999). Trkiye’deki İki Senelik Konservasyon ve Restorasyon Eėitiminin Sorunları ve zm nerileri, *I Ulusal Tařınabilir Kltr Varlıkları Konservasyonu ve Restorasyonu Kolokyumu*, 6-7 Mayıs 1999, Ankara: Ankara niversitesi Basımevi, 17-22.

Kuban, D. (2000). *Tarihi evre Korumanın Mimarlık Boyutu* (1. Baskı). İstanbul: YEM Yayın

zgan, R. (2013). *Roma Portre Sanatı II*. (1. Baskı) İstanbul: Ege Yayınları.

ztrk, I. (1992). *Alkoxysilanes, Consolidation of Stone and Earthen Building Materials*, A Thesis in The Graduate Program in Historic Preservation, Pennsylvania.

Sirt, E. (2011). *Evaluation Of Biodeterioration In Nemrut Mount Monument and Temple of Augustus By Using Various Techniques*, A Thesis Submitted To The Graduate School Of Natural And Applied Sciences Of Middle East Technical University, Ankara.

Őener, Y.S., (2000). *Kayseri İl Merkezindeki Seluklu Trbelerinde Mevcut Korunma Durumlarının Tespiti*, Ankara niversitesi Sosyal Bilimler Enstits Sanat Tarihi Blm, Yayınlanmamış Doktora Tezi, Ankara.

Tulgar, S. (2007). *Sultanahmet rme Dikilitař’ta Ayrıřmaların Teřhisi ve nerilen Korunma Yntemleri*, İstanbul niversitesi Sosyal Bilimler Enstits, Yayınlanmamış Yksek Lisans Tezi, Ankara

Yıldırım, N. (2007). *Kiretařlarında Tuzların Yıkıcı Etkilerinin Arařtırılması*, İstanbul Teknik niversitesi Fen Bilimleri Enstits, Yayınlanmamış Yksek Lisans Tezi, İstanbul.

Yıldırım N. (2010). “Dolmabahçe Sarayının Yapı Malzemeleri Üzerinde Suda Çözünebilir Tuzların Etkileri, *Restorasyon Konservasyon Çalışmaları*, İstanbul Büyükşehir Belediyesi KUDEP, 6, 70-86.

İnternet Kaynakları

<http://odogan.com/mimar/restorasyon-rolove-restitusyon-konservasyon-nedir.html> 15/12/2013

http://korumaveonarim.org/index.php?option=com_content&view=article&id=66:tuerkiyede-koruma-ve-onarmn-geliimi&catid=38:makaleler&Itemid=5902/02/13



INTERNATIONAL SOCIETY FOR RESEARCH IN
EDUCATION AND SCIENCE

www.isres.org

IOWA STATE
UNIVERSITY



GAZIANTEP
UNIVERSITY

EVMS
Eastern Virginia Medical School



<http://www.icres.net>

International Conference on Research in Education & Science
April 28 - May 01, 2018 • MARMARIS/TURKEY